



IMPERIAL INSTITUTE  
OF  
AGRICULTURAL RESEARCH, PUSA







THE  
LONDON, EDINBURGH, AND DUBLIN  
PHILOSOPHICAL MAGAZINE  
AND  
JOURNAL OF SCIENCE.

CONDUCTED BY

SIR OLIVER JOSEPH LODGE, D.Sc., LL.D., F.R.S.  
SIR JOSEPH JOHN THOMSON, O.M., M.A., Sc.D., LL.D., F.R.S.  
JOHN JOLY, M.A., D.Sc., F.R.S., F.G.S.  
RICHARD TAUNTON FRANCIS, F.R.S.E.

AND

WILLIAM FRANCIS, F.L.S.

---

"Nec araneorum sane textus ideo melior quia ex se fila gignunt, nec noster  
vilior quia ex alienis libamus ut apes." JUST. LIPSA. *Polit. lib. 1. cap. 1.* Not.

---

VOL. V.—SEVENTH SERIES.

JANUARY—JUNE 1928.

---

LONDON:

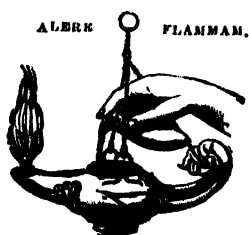
TAYLOR AND FRANCIS, RED LION COURT, FLEET STREET.  
SOLD BY SMITH AND SON, GLASGOW;—RODGES, STEELE, AND CO., DUBLIN;—  
AND THEVE J. BOUTHAU, PARIS.

"Meditationis est perscrutari occulta ; contemplationis est admirari  
perspicua . . . . Admiratio generat quæstionem, quæstio nvestigationem,  
investigatio inventionem."—*Hugo de S. Victore.*

---

—“Cur spirent venti, cur terra dehiscat,  
Cur mare turgescat, pelago cur tantus amaror,  
Cur caput obscura Phœbus ferrugine condât,  
Quid toties diros cogat flagrare cometas,  
Quid pariat nubes, veniant cur fulmina cœlo,  
Quo micet igne Iris, superos quis conciat orbes  
Tam vario motu.”

*J. B. Pinelli ad Mazonium.*



# CONTENTS OF VOL. V.

(SEVENTH SERIES).

NUMBER XXVII.—JANUARY 1928.

	Page
Mr. H. W. Swift on Operational Factors in Orifice Flow . . . . .	1
Dr. Balth. van der Pol and Dr. M. J. O. Strutt on the Stability of the Solutions of Mathieu's Equation. . . . .	18
Mr. R. C. J. Howland on the Calculation of the Periods of Circular Membranes and Disks. . . . .	39
Mr. C. R. Soderberg on the Practical Application of the Theory of Vibrations to Systems with several Degrees of Freedom . . . . .	47
Mr. P. K. Mitra on the Emission of Positive Electricity from Hot Tungsten in Mullard Radio Valves . . . . .	67
Mr. J. Kunz: A Note on Hamilton-Jacobi's Differential Equation in Dynamics. . . . .	79
Mr. J. P. Baxter on the Combustion of Carbonic Oxide.—Part I. . . . .	82
Mr. S. B. Gates on the Torsion-Flexure Oscillations of a System of Two Connected Beams . . . . .	97
Mr. A. Eagle on the Relations between the Fourier Constants of a Periodic Function and the Coefficients determined by Harmonic Analysis . . . . .	113
Dr. J. H. J. Poole on the Action of Heat on Pleochroic Halos. (Plates I. & II.) . . . . .	132
Dr. T. Takamine and Mr. T. Suga on the Reversal of Helium Lines. (Plate III.) . . . . .	141
Prof. F. H. Newman on the Spectrum of Ionized Sodium . . . . .	150
Miss F. M. Chambers: Notes on the Resonances of a Violin . . . . .	160
Dr. J. Taylor on the Intensities of Forbidden Multiplets. . . . .	166
Dr. Hume-Rothery on the Classification of Metallic Substances. . . . .	173
Prof. J. S. Townsend and Mr. R. H. Donaldson on Electrodeless Discharges . . . . .	178
Sir J. J. Thomson on Waves associated with Moving Electrons. . . . .	191
Mr. I. Vogel on the Calculation of the Equivalent Conductivity of Strong Electrolytes at Infinite Dilution.—Part II. (i.) Methyl Alcoholic Solutions. (ii.) The Effect of Temperature on the Con- stants in the Equation $A_0 = A + BC^n$ . . . . .	199
Mr. Sven Fagerberg on Interference between Grating-Ghosts. (Plate IV.) . . . . .	204
Dr. H. Jeffreys on the Earth's Thermal History . . . . .	208
Prof. J. Joly on the Earth's Thermal History . . . . .	215
Messrs. H. Beutler and B. Josephy on Double Excitation of Upper Levels in the Mercury Atoms by Collisions of the Second Kind. . . . .	222

	Page
Notices respecting New Books :—	
The Nature of the World of Man.....	223
Proceedings of the Geological Society :—	
Dr. J. A. Douglas and Mr. W. J. Arkell on the Stratigraphical Distribution of the Cornbrash: 1.—The South-Western Area.	224

---

### NUMBER XXVIII.—FEBRUARY.

Prof. F. Ehrenhaft and Dr. E. Wasser on New Evidence of the Existence of Charges smaller than the Electron.—(a) The Micro-magnet; (b) The Law of Resistance; (c) The Computation of Errors of the Method .....	225
Prof. J. L. Synge and Mr. A. J. McConnell on Riemannian Null-Geometry .....	241
Dr. R. D. Kleeman on the Constant of Mass Action .....	263
Mr. A. L. Johns and Prof. E. J. Evans on the Conductivities of some Dilute Amalgams at various Temperatures .....	271
Prof. E. A. Milne on the Angular Velocity of a Rigid Body .....	289
Mr. C. H. Bosanquet on the Capillary Rise of Liquids in Wide Tubes .....	296
Dr. C. H. Johnson on a Method of Measuring the Radiant Heat emitted during Gaseous Explosions .....	301
Mr. W. E. Benham: A Study of the Rectification Efficiency of Thermionic Valves at Moderately High Frequencies. ....	323
Prof. A. Petrowsky on the Problem of a Hidden Polarized Sphere. .	334
Prof. A. Ogg on the Crystal Structure of the Isomorphous Sulphates of Potassium, Ammonium, Rubidium, and Cæsium. (Plates V. & VI.) .....	354
Prof. D. A. Wells on Energy Distribution among Secondary Electrons from Nickel, Aluminium, and Copper .....	367
Messrs. J. Okubo and H. Hamada on Metallic Spectra excited by Active Nitrogen. (Plate VII.) .....	372
Mr. V. I. Vaidyanathan on the Diamagnetic Susceptibilities of Gases at Low Pressures .....	380
Dr. W. H. McCurdy on the Fine Structure of Mercury Lines. (Plate VIII.) .....	386
Mr. E. Remes on some Approximate Formulæ for the Numerical Integration of Differential Equations. (Analysis and generalization of a method given by H. T. H. Piaggio.) .....	392
Mr. J. P. Den Hartog on the Lowest Natural Frequency of Circular Arcs .....	400
Mr. T. Lewis on the Results of Classical Wave Mechanics obtained by using the Methods of Relativity Mechanics. ....	408
Messrs. A. Fage and F. C. Johansen on the Structure of Vortex Sheets .....	417
Mr. T. Thorkelsson on the Geyser Theory .....	441
Dr. J. H. J. Poole: Note on the Formation of Pleochroic Halos in Biotite .....	444
Mr. J. Taylor: A Reply to the Paper "Ionization by Collision." ...	445
Mr. G. Herzberg on Cathode Rays in the Electrodeless Ring-Discharge .....	446
Notices respecting New Books :—	
Abstracts of Theses, Science Series, Vol. III. ....	448

---

NUMBER XXIX.—MARCH.

Mr. E. Tyler on Vortices behind Aerofoil Sections and Rotating Cylinders .....	449
Dr. L. Silberstein: Contribution to the Theory of Photographic Exposure .....	464
Dr. E. T. Paris on the Coefficient of Sound-absorption measured by the Reverberation Method .....	489
Prof. C. V. Raman and Mr. K. S. Krishnan: A Theory of Light-Scattering in Liquids .....	498
Mr. J. Thomson on the Influence of Charged Metallic Points on the Spark Discharge .....	513
Prof. S. S. Bhatnagar and Mr. C. L. Dhawan on an Extension of Langevin's Theory of Atomic Magnetism to Molecules constituting Electronic Isomers .....	536
Miss D. M. Hirst and Prof. W. B. Morton: Supplementary Note on the Parallel-plate Condenser in Two Dimensions .....	545
Dr. K. C. Kar, Messrs. R. Ganguli and S. C. Laha on the Acoustics of Strings struck by a Hard Hammer .....	547
Dr. H. D. H. Drane on making very Sensitive Helical Springs from Quartz Fibre .....	559
Mr. H. P. Walmsley on Oscillatory Ionization Currents from Clouds of Cadmium-Oxide Particles. (Plate IX.) .....	561
Mr. N. A. de Bruyne: Some Experiments on the Auto-Electronic Discharge. (Plate X.) .....	574
Mr. E. J. Irons on the Effect of Constrictions in Kundt's Apparatus and the End Corrections of a Partially-stopped Tube. (Plate XI.) .....	580
Mr. D. O. Jones and Prof. E. J. Evans on the Magnetic Rotary Dispersion of Methyl and Propyl Alcohols .....	593
Prof. S. B. Mali on the Properties of Dry Liquids .....	609
Mr. L. J. Sivian on a Modification of the Rayleigh Disk Method for measuring Sound-Intensities .....	615
Dr. R. D. Kleeman on the Differential Equations of a Reacting Mixture .....	620
Prof. S. Chapman on Approximate Theories of Diffusion Phenomena .....	630
Dr. T. J. Fa. Bromwich: A Note on the Problem of the "Mass" of a Moving Electron .....	636
Mr. F. F. P. Bisacre on the Relativistic Rule for Equipartition of Energy. (Further note.) .....	639
Mr. W. E. Benham on Theory of the Internal Action of Thermionic Systems at Moderately High Frequencies.—Part I. ....	641
Drs. H. H. Poole and J. H. J. Poole on the Thermal Instability of the Earth's Crust .....	662
Dr. R. D. Kleeman on the Absolute Zero of the Externally Controllable Entropy and Internal Energy of a Substance and a Mixture .....	668
Notices respecting New Books:—	
Prof. E. L. Ince's Ordinary Differential Equations .....	668
Mr. P. Doig's An Outline of Stellar Astronomy .....	669
Proceedings of the Geological Society:—	
Prof. D. I. Mushketov on the Alai and Trans-Alai chains in Southern Turkestan, north of the Pamirs .....	670
Mr. C. W. Osman on the Granites of the Scilly Isles, and their Relation to the Dartmoor Granites .....	671

## NUMBER XXX.—APRIL.

Mr. W. R. Dean on the Stream-line Motion of Fluid in a Curved Pipe. (Second Paper.)	673
Prof. J. S. Townsend and Mr. S. P. MacCallum on Electrical Properties of Monatomic Gases	695
Dr. G. Green on some Problems in the Conduction of Heat	701
Mr. L. G. H. Huxley on the Corona Discharge in Helium and Neon	721
Dr. D. H. Bangham on Chemical Dynamics in a Rigidly Coherent Phase	737
Mr. W. H. Brooks on Sign Conventions applied to Flexing Problems	749
Mr. W. E. Dawson on a Simple Method for Determining the Orientation and Structure of Crystals with X-Rays	756
Prof. C. V. Raman and Mr. K. S. Krishnan: A Theory of the Birefringence induced by Flow in Liquids	769
Lieut.-Col. K. E. Edgeworth on Frequency Variations of the Triode Oscillator. A Note on Mr. D. F. Martin's Paper	783
Mr. L. Bastings on Coefficient of Absorption in Lead of the $\gamma$ -Rays from Thorium C' and Radium C	785
Dr. W. N. Bond and Miss D. A. Newton on Bubbles, Drops, and Stokes' Law. (Paper 2.)	794

## NUMBER XXXI.—MAY (SUPPLEMENT).

Prof. W. M. Hicks on the Sæcular Changes in Electronic Orbits in a Magnetic Field	801
Messrs. L. G. Carpenter and L. G. Stoodley on the characteristic Infra-Red Vibrations of certain Crystals of the Rock-Salt Type	823
Prof. A. Press: An Extension of Dulong and Petit's Law to Gaseous Compounds and Mixtures	832
Dr. H. P. Robertson on Relativistic Cosmology	835
Dr. R. S. Bartlett on the Resistance of Sputtered Films	848
Mr. E. W. B. Gill on Space-Charge Effects	859
Mr. J. P. Andrews: A Contribution to the Theory of Torsional Oscillations in Plastic Solids	865
Mr. J. S. Rogers on the Mobilities of the Positive Ions formed by Alpha Rays in Air, Hydrogen, and Helium	881
Mr. M. J. O. Strutt on the Distribution of Temperature in Alternating Current Conductors	904
Prof. A. Petrowsky on the Problem of a Hidden Polarized Sphere. (Part II.)	914
Prof. A. Petrowsky on the Problem of a Hidden Polarized Sphere. (Part III.)	927
Mr. S. F. Grace on Oscillatory Motion of a Viscous Liquid in a long straight Tube	933
Prof. E. F. Burton and Mr. A. Pitt on a New Method of Conductivity Measurement by means of an Oscillating Valve Circuit	939
Dr. J. W. Woodrow on the Ultra-violet Absorption Spectrum of Cod-Liver Oil	944
Dr. E. K. Sandeman on Multiple Reactive Gears	946
Mr. J. J. Manley on the Capillary Action of Mercury in the Absence of Gas-Grown Skins. (Plates XII.-XIV.)	958
Dr. R. T. Dunbar on Apparent Irregularities in Experiments with heterogeneous X-ray Beams, with special reference to the J-Phenomenon	962

	Page
Dr. Ann C. Davies and Miss R. N. Moss on the Cause of the Loss of Thermionic Activity of Thoriated Tungsten Filaments under certain Voltage Conditions .....	989
Notices respecting New Books:—	
Prof. A. H. Compton on X-rays and Electrons .....	1011
Mr. L. B. Loeb on the Kinetic Theory of Gases .....	1011
Proceedings of the Geological Society:—	
Dr. E. Greenly on the Lower Carboniferous Rocks of the Menaian Region of Carnarvonshire: their Petrology, Succession, and Physiography. With Palæontological Notes by Dr. S. Smith .....	1012
Mr. G. M. Lees on the Geology of South-Eastern Arabia ....	1013
Prof. J. K. Charlesworth on the Glacial Retreat from Central and Southern Ireland .....	1014
Dr. C. A. Matley on the Pre-Cambrian Complex and Associated Rocks of South-Western Lleyrn (Carnarvonshire). With a Chapter on the Petrology of the Complex by Dr. E. Greenly .....	1015

NUMBER XXXII.—MAY.

Prof. L. Wertenstein on the Purification of Radon .....	1017
Mr. G. C. Laurence on the Ranges of the Alpha-Particles of Uranium I. and II. ....	1027
Dr. K. G. Emel�us and Miss N. M. Carmichael on the Primary Dark Space of a Geissler Discharge .....	1039
Prof. D. M. Bose on Magnetism and the Structure of some Simple and Complex Molecules .....	1048
Prof. A. W. Porter on the Positions of X-Ray Spectra as formed by a Diffraction Grating .....	1067
Prof. T. M. Lowry on the Electronic Theory of Valency.—Part V. The Molecular Structure of Strong and Weak Electrolytes: (a) Complete Ionization .....	1072
Mr. W. E. Deming: Note on the Diffusion of Hydrogen through Iron .....	1081
Mr. W. D. Flower on the Emission of Particles from Hot Platinum in Air at Atmospheric Pressure. (Plate XV.) .....	1084
Mr. S. C. Biswas: A Note on the Predicted Ionization Potential of Niton .....	1094
Prof. H. A. Zinszer on the Shadowgraph Method as applied to a Study of the Electric Spark. (Plates XVI. & XVII.) .....	1098
Prof. W. Clarkson on the Presence of Charges at an Electrode Surface .....	1104
Prof. W. Mohammad and Mr. S. B. L. Mathur on the Fine Structure of the Spectrum Lines of Thallium in the Ultra-violet ....	1111
Dr. A. A. Robb on a Curious Optical Theorem and its Geometrical Basis .....	1114
Messrs. H. A. Thomas and G. W. Warren: An Optical Method of Measuring Small Vibrations .....	1125
Messrs. J. W. Woolcock and D. M. Murray-Rust: Note on the Construction of a Valve Oscillator for use in Conductivity Measurements .....	1130
Mr. J. W. Woolcock and Sir Harold Hartley on the Activity Coefficients of Hydrogen Chloride in Ethyl Alcohol .....	1133



## NUMBER XXXIII.—JUNE.

Dr. W. H. Watson on the Fluorescent Secondary X-Radiation and the J-Phenomenon .....	1145
Prof. C. G. Barkla: Note on Modified Scattered X-Radiation and Super-Position .....	1164
Dr. R. K. Schofield on Cohesion and Intermolecular Repulsion ..	1171
Prof. J. C. Hubbard and Mr. A. L. Loomis on the Velocity of Sound in Liquids at High Frequencies by the Sonic Interferometer .....	1177
Prof. R. D. Kleeman on Changes that may take place in the Interatomic Internal Energy according to Thermodynamics, and Catalytic Action .....	1191
Mr. G. D. Preston on the Crystal Structure of $\alpha$ -Manganese. (Plates XVIII. & XIX.) .....	1198
Mr. G. D. Preston on the Structure of $\beta$ -Manganese. (Plate XX.)	1207
Messrs. S. S. Bhatnagar, D. L. Shrivastava, K. N. Mathur, and R. K. Sharma on Tesla Luminescence Spectra of the Halogens. (Plate XXI.) .....	1226
Prof. V. O. Knudsen on the Measurement of Sound-absorption in a Room .....	1240
Mr. L. Woollard on Cavitation in Screw Propellers .....	1258
Notices respecting New Books:—	
Messrs. E. S. Hedges and J. E. Myers's The Problem of Physico-Chemical Periodicity, with a foreword by Prof. F. G. Donnan .....	1258
Dr. A. W. Stewart's Recent Advances in Organic Chemistry..	1259
Dr. T. M. MacRobert's Spherical Harmonics. An Elementary Treatise on Harmonic Functions with Applications .....	1260
Mr. E. Ower's The Measurement of Air Flow .....	1260
Mr. D. M. Turner's History of Science Teaching in England..	1261
Proceedings of the Geological Society:—	
Miss H. K. Cargill, Dr. L. Hawkes, and Miss J. A. Ledebor on the Major Intrusions of South-Eastern Iceland .....	1261
Dr. F. B. A. Welch on the Geological Structure of the Central Mendips .....	1263
Index .....	1264

## PLATES.

- I. & II. Illustrative of Dr. J. H. J. Poole's Paper on the Action of Heat on Pleochroic Halos.
- III. Illustrative of Dr. T. Takamine and Mr. T. Suga's Paper on the Reversal of Helium Lines.
- IV. Illustrative of Mr. S. Fagerberg's Paper on Interference between Grating-Ghosts.
- V. & VI. Illustrative of Prof. A. Ogg's Paper on the Crystal Structure of the Isomorphous Sulphates of Potassium, Ammonium, Rubidium, and Cæsium.
- VII. Illustrative of Messrs. J. Okubo and H. Hamada's Paper on Metallic Spectra excited by Active Nitrogen.
- VIII. Illustrative of Dr. W. H. McCurdy's Paper on the Fine Structure of Mercury Lines.
- IX. Illustrative of Mr. H. P. Walmsley's Paper on Oscillatory Ionization Currents from Clouds of Cadmium-Oxide Particles.
- X. Illustrative of Mr. N. A. de Bruyne's Paper on some Experiments on the Auto-Electronic Discharge.
- XI. Illustrative of Mr. E. J. Irons's Paper on the Effect of Constrictions in Kundt's Apparatus and the End Corrections of a Partially-stopped Tube.
- XII.-XIV. Illustrative of Mr. J. J. Manley's Paper on the Capillary Action of Mercury in the Absence of Gas-Grown Skins.
- XV. Illustrative of Mr. W. D. Flower's Paper on the Emission of Particles from Hot Platinum in Air at Atmospheric Pressure.
- XVI. & XVII. Illustrative of Prof. H. A. Zinszer's Paper on the Shadowgraph Method as applied to a Study of the Electric Spark.
- XVIII & XIX. Illustrative of Mr. G. D. Preston's Paper on the Crystal Structure of  $\alpha$ -Manganese.
- XX. Illustrative of Mr. G. D. Preston's Paper on the Structure of  $\beta$ -Manganese.
- XXI. Illustrative of Messrs. S. S. Bhatnagar, D. L. Shrivastava, K. N. Mathur, and R. K. Sharma's Paper on Tesla Luminescence Spectra of the Halogens.

# ERRATUM.

Page 20 (line 5 from end), Jan. 1928, after the sentence: "By Floquet's Theorem, the general solution of equation 4 has the form":

write the formula

$$A . e^{j\mu t} \Phi(t) + B . e^{-j\mu t} . \Psi(t),$$

instead of

$$A . e^{\mu t} \Phi(t) + B . e^{-\mu t} . \Psi(t).$$

THE  
LONDON, EDINBURGH, AND DUBLIN  
PHILOSOPHICAL MAGAZINE  
AND  
JOURNAL OF SCIENCE.

[SEVENTH SERIES.]

JANUARY 1928.

1. *Operational Factors in Orifice Flow.*

By H. W. SWIFT, M.A., B.Sc.\*

THE volumetric rate of flow through an orifice is commonly expressed in the form

$$Q = C_d \cdot a \sqrt{2gH},$$

where  $a$  is the area of the orifice,  $H$  the effective head, and  $C_d$  the coefficient of discharge. The usefulness of the quantity  $a\sqrt{2gH}$  as a basis of comparison lies in the facts that it is easily calculated from simple observations, and that for most practical purposes the value of the coefficient  $C_d$  is tolerably constant.

This coefficient itself is merely a convenient name for the product of certain other factors or coefficients which can be more directly attributed to physical causes and are therefore of primary importance in scientific inquiry. These factors are: the coefficient of contraction  $C_c$ , which arises from the fact that the discharging jet forms a vena contracta; the coefficient of velocity  $C_v$ , due to the fact that this jet has a velocity less than that theoretically due to the change in pressure; and with compressible fluids the "attenuation factor"  $C_a$ , which allows for the fact that the volume of such a fluid when measured at its initial density is less than that of an incompressible liquid due to attenuation at reduced pressures.

The values of these contributory factors depend on a large

\* Communicated by the Author.

number of conditions, which may generally be attributed either to the nature of the fluid in use or to the artificial configuration of the apparatus and the fashioning of the orifice itself. The effects of the physical properties of the fluid have been treated to some extent on a rational basis \* and fairly completely by experiment, and the effects of constructional factors are also known empirically † for most cases of practical importance. There are, however, certain conditions of flow which may affect the registration of an orifice to an important extent, and which are not directly attributable to hydraulic or constructional conditions but rather to the imposed conditions of operation. It is proposed here to consider the effects of three phenomena which may be classified as operational factors : Turbulence, Cavitation, Pulsating flow.

#### TURBULENCE.

In problems concerning uniform flow in pipes it is generally accepted that there is no need to pay quantitative regard to the degree of turbulence in the flow, this being implied in the value of the Reynolds number. Some caution is required, however, in applying this principle to other types of flow, for in obtaining the experimental evidence on which it is at present based, precautions were taken to suppress turbulence as far as possible—in fact, the conditions were those of “minimum turbulence.” In orifice flow it is found over a wide useful range that when similar precautions are taken the phenomena of flow can be explained in terms of the viscosity criterion which corresponds to the Reynolds number ; but these conditions are not easy to reproduce in experiment, still less in practical applications, so that acceptance of the Reynolds number as the sole criterion in uniform pipe-flow does not establish for it a *prima facie* claim under the different conditions which prevail in orifice flow. This case must be decided on independent evidence.

The supposed similarity between the conditions of pipe and orifice flow seems to be based largely on work carried out independently in Australia ‡ and America §, as a result of which it has been maintained that the coefficient of discharge (for water) diminishes as the head increases until a

\* Phil. Mag. Oct. 1926, p. 852.

† Muller, Z. V. D. I. lii. p. 285 ; Gaskell, Proc. Inst. C. E. cxvii. p. 243 ; Hodgson, Proc. Inst. C. E. cciv. p. p. 131.

‡ Bilton, Proc. Vict. Inst. Eng. ix. p. 27.

§ Judd and King, Am. Soc. Adv. Sci. 1906.

head of the order of 18 inches is reached, and that above this "critical head" the conditions become essentially turbulent and the coefficient remains constant at a "normal" value which is dependent on the size of orifice and on that alone. Against this must be set the evidence of almost all other workers\* in this field, who have obtained systematic changes in the coefficient at values of the Reynolds number far above that suggested as critical. The present author has himself been unable to obtain independent evidence of any critical change, but has found it possible (if no precautions are taken, easy) to obtain clear indications of turbulence with almost any head and orifice, and to a varying degree. The fact that all experimenters find it necessary to take steps to avoid turbulence is itself evidence that the Reynolds number is not always a sufficient criterion.

In considering the effects of turbulence, therefore, it is thought necessary to adopt a separate criterion, even if there are no means of evaluating it, and the simplest form appears to be the ratio  $\frac{l}{\epsilon}$ , where  $l$  stands for the linear dimensions of the apparatus and  $\epsilon$  is representative of the dimensions of the eddy system†. It is to be remarked that in general the degree of turbulence will increase as the statistical size of the eddies decreases (as, indeed, appears to be the case in pipe flow), and therefore as the value of the criterion increases.

Supposing in the first instance that turbulence alone is operative, we may express the total loss of head in the contracting jet by means of the equation

$$H_r = \frac{V^2}{2g} \cdot \alpha\tau,$$

where  $\tau = f\left(\frac{l}{\epsilon}\right)$ , and may be defined as the "intensity of turbulence."

Under these conditions the coefficient of velocity is given by  $C_v = (1 + \alpha\tau)^{-\frac{1}{2}}$ , and for practical purposes  $= 1 - \frac{\alpha\tau}{2}$  nearly, showing that it falls short of unity by an amount simply proportional to the "intensity of turbulence."

\* Cf. Hamilton Smith, 'Hydraulics,' ch. iii.; Dempster Smith and Walker, Proc. I. Mech. E. 1928, p. 23.

† It is what may be termed accidental as opposed to systematic turbulence which is here under discussion. Conditions which give rise to systematic vertical motion are clearly not amenable to such simple treatment, though they are generally found to cause increased discharge from a sharp-edged orifice.

In order to examine rationally the consequence of changes in the coefficient of contraction, we shall assume that the loss of head incurred by the fluid in its motion up to that surface, normal to the stream-lines, which contains the bounding curve of the orifice, may be written

$$h_z = \frac{v^2}{2g} \cdot b\tau,$$

where  $v$  is "representative" of the velocity at this surface. Following, then, the line of argument advanced in an earlier paper for the case of viscous resistance \*, we are led to an analogous expression for the coefficient of contraction :

$$C_c = C_0 + b\tau(1 - C_0)(2 - C_0),$$

and so for the coefficient of discharge:

$$C_d = C_0 + b\tau(1 - C_0)(2 - C_0) - C_0 \frac{a\tau}{2}.$$

It appears, therefore, that turbulence will tend to increase the area of the jet at the same time that it reduces the velocity of discharge. The resultant effect on the coefficient of discharge depends on the comparative values of  $a$  and  $b$ . If for descriptive purposes we take  $a=b$ , then the coefficient will vary according to the relation

$$C_d = C_0 + a\tau(2 - \frac{1}{2}C_0 + C_0^2),$$

and the changes so produced for various values of  $C_0$  are plotted in fig. 1. From this it seems likely that for Borda and sharp-edged orifices turbulence will cause an increase in the discharge under normal hydraulic conditions, while for rounded orifices it will definitely give rise to a diminution.

The special case of the Borda mouthpiece admits of no doubt when considered in view of the forces causing discharge; turbulence, or indeed any form of fluid friction, must give rise to a progressive increase in the coefficient of discharge so long as the mouthpiece continues to "run free."

For each form of orifice we are led to the conclusion that turbulence acting alone will effect a change in the coefficient which is proportional to the intensity of turbulence, and the coefficient will be constant if and only if this intensity remains constant.

Supposing, now, that it is possible for turbulent and viscous resistance to operate together, it is easy to apply the argument advanced above and to show that the resulting change in the

\* Phil. Mag. Oct. 1926, p. 867.

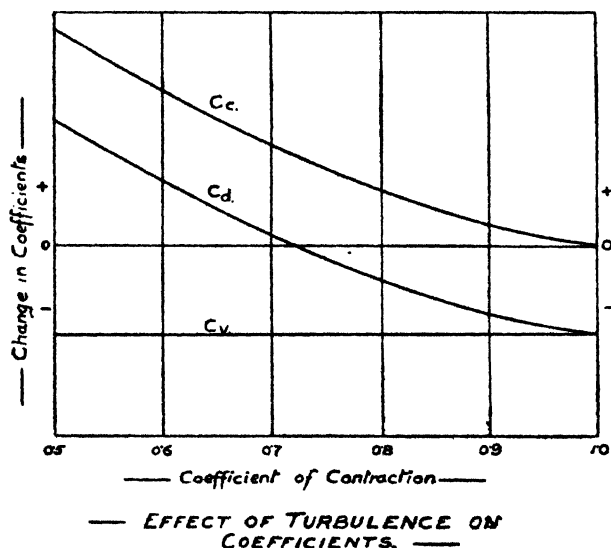
coefficient is the same as if the separate effects were superposed, so that

$$C_d = C_0 + c_1\eta + c_2\tau.$$

If it be further supposed that the two types of resistance are independent, then turbulence will still give rise to a change in the coefficient, as modified by viscous effects, which is dependent simply on its "intensity"  $\tau$ .

The joint operation of turbulence and viscosity is a matter for appeal to experiment. In fig. 2 are shown results obtained by timing the fall in level of water in a tank 3 feet in diameter as it discharged through a sharp-edged orifice  $\frac{1}{4}$  inch in diameter mounted in the base. In one case the water was

Fig. 1.

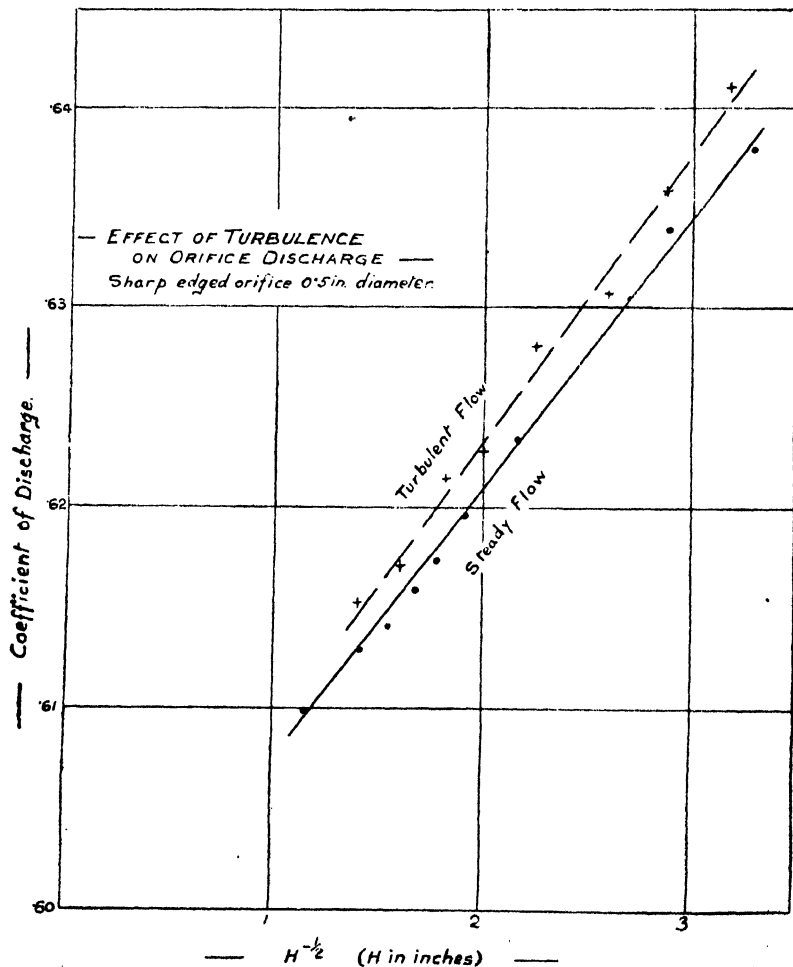


allowed to become still before discharge was commenced; in the other, turbulence was maintained artificially throughout discharge by unsystematic stirring as uniform in degree as possible. The results show that with the sharp-edged orifice used turbulence causes a definite increase in the discharge, but does not give rise to a constant coefficient. The changes in the coefficient are, in fact, systematically identical with those obtained under quiescent conditions, showing an increase which, although variable, has a mean value of about 0.5 per cent. When the same tank was emptied under naturally turbulent conditions (i. e. without waiting for the water to still before commencing discharge), the results



were similar, but showed a smaller increase of about 0.3 per cent. over the steady values. Determinations made at constant heads of 12 and 6.5 inches under artificially turbulent conditions showed on the average increases of 0.5, and 0.6 per cent. respectively. Tests with an orifice

Fig. 2.



1.0 inch diameter under a falling head gave an average rise of 0.4 per cent. in the coefficient with artificial turbulence. Under conditions of initial natural turbulence, a vortex formed at heads between 40 and 50 inches and deprived the results of any comparative value.

These experiments confirm the view that turbulence in orifice flow requires a separate criterion; they show definitely that turbulence and viscosity may be operative at the same time, and afford evidence that under the conditions of hydraulic discharge their effects may be superposed. Since the turbulence artificially maintained in these tests was considerably greater than that likely to be encountered in practice, the results give also some idea of the maximum effect likely to be introduced by turbulence in orifices of the sizes used.

The importance of turbulence will be determined by the ratio  $\frac{l}{\epsilon}$ . As a general rule, it is to be expected therefore that for a given eddy system the effects of turbulence will increase with the dimensions of the orifice, though the somewhat rough methods of the experiments just described do not give any indication of this. In the same way the statistical dimensions of the eddies will become smaller as the velocity and head increase; so that these conditions also are likely to make turbulence more important. In practice, moreover, turbulence is by nature inconstant; and since fluctuations in its intensity will be reproduced in the discharge, it is to be expected that conditions which predispose to turbulence will also give rise to variable registration. Furthermore, the factors which increase the importance of turbulence are those also which reduce the effect of the viscosity criterion  $\eta$ . Hence it is to be expected that with greater heads, larger orifices, and lower viscosities the results of experiments will be less consistent, and that under the conditions of approach normally met the coefficient of discharge may apparently cease to vary systematically. These systematic variations, due to the effects of viscous resistance and other causes, should, however, become evident when precautions are taken to eliminate the effects of turbulence.

The apparent constancy of the coefficient of discharge in the experimental work on which the "critical head" theory is based, may be fairly attributed to turbulent conditions in approach and to the accidental errors of experiment which might easily mask the small variations in the coefficient with large orifices and great heads. In point of fact, the expected change in the coefficient for a 2-inch orifice due to viscosity is only .01 between heads of 2 and 100 feet, which is of the same order as the irregular variations in the results of the experiments referred to. Moreover, in some

of these experiments\* it is stated that turbulence "was very noticeable at high heads"; while Dempster Smith†, who worked over a similar range, was able to maintain a clear glass-like surface and also a continuously falling coefficient.

An interesting fact which seems further to justify the similar treatment given above to viscous and to turbulent resistance was made evident in experiments by the author with a partially rounded orifice. This orifice was devised, by trial and error, of such a form that decrements in the coefficient of velocity due to viscous resistance were almost exactly balanced by corresponding increments in the coefficient of contraction, so that a virtually constant coefficient of discharge was maintained with water over a considerable range of heads and temperatures. It was found that the discharge from this orifice was also practically unaffected by turbulence in approach. When tested under a falling head between levels of 55 and 5 inches, the times recorded were : quiescent at 14° C., 1149·9 secs. ; quiescent at 63° C., 1151·4 secs. ; turbulent at 14° C., 1150·2 secs.

#### CAVITATION.

The registration of an orifice or similar form of meter may be affected to a considerable extent by the existence of a low pressure at the vena contracta. If the velocity at this point is high, the pressure may become correspondingly so low as to give rise to cavitation.

As the pressure of a liquid free from dissolved gases is reduced, no effect of hydraulic interest occurs until it reaches the vapour-pressure corresponding to the temperature of the liquid. At this point evaporation takes place and the constitution of the mixture passing the vena contracta is not easily determinable. Under these circumstances, of course, meters of the orifice type cease to have any value. In practice it will usually be easy to avoid such a state of affairs, though it may arise, for example, if a venturimeter is employed with hot water under a low static head.

A disturbing condition of greater practical interest arises from the presence of dissolved gases in the liquid passing through the meter. As the pressure of such a solution is reduced, the solubility of the gases is diminished according to Henry's law ; and if the pressure falls below that at which

\* Judd and King, *loc. cit.*

† Proc. I. Mech. E. 1923.

the solution becomes saturated, the excess gases will be set free and cavitation will occur. This effect will be further complicated by the partial evaporation of the liquid itself in the gas so liberated. This condition, though it may occur at a considerably higher pressure than that at which mass evaporation takes place, is not, as will appear, likely to become important in the case of a sharp-edged orifice, which owing to inferior pressure recovery is seldom employed in a pipe under large differential heads; but it is quite easy to produce in certain types of venturimeter, and its effect can then be estimated with some measure of confidence.

Suppose in the first instance that the water passing through a meter was saturated with (3 per cent. by volume of) air at atmospheric pressure. At an absolute pressure  $p$  inches of mercury the proportion of air remaining in solution will be  $\frac{p-v}{30}$ , where  $v$  is the vapour-pressure at the temperature which obtains. Hence the volume of air set free per unit volume of water is  $\frac{3}{100} \left(1 - \frac{p-v}{30}\right) \frac{30}{p-v}$ , measured at the existing throat-pressure. Hence the fraction  $k$  of the throat area actually occupied by water will be given by

$$\frac{1}{k} = 1 + \frac{9}{10} \left( \frac{1}{p-v} - \frac{1}{30} \right),$$

and the coefficient of discharge  $C$  becomes modified to  $C'$ , where

$$\frac{C'}{C} = \sqrt{\frac{m^2 - 1}{\frac{m^2}{k^2} - 1}},$$

$m$  being the ratio of pipe to throat areas.

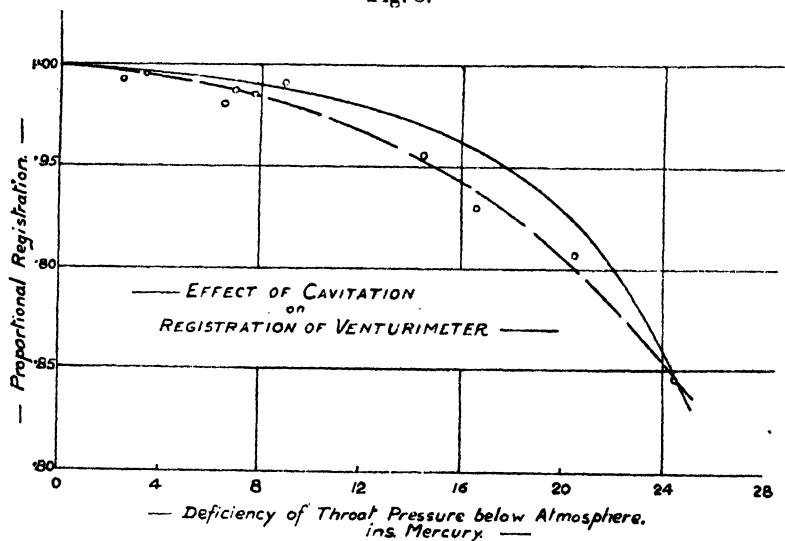
The changes represented by this expression, when applied to the case of a venturimeter for which  $m=9$ , delivering water at a temperature of about  $23^\circ \text{C}$ ., are indicated by the full line in fig. 3. Results deduced from a series of tests under these conditions are shown by points and the dotted line in the same figure.

In these tests a venturimeter was employed mounted in a six-inch pipe-line at the end of a straight length of upwards of forty diameters. At the entry to this length was a branch containing a six-inch valve which allowed more or less of the water to be bye-passed to waste. About the same distance beyond the venturi tube, there was mounted in the pipe a glass section, and just beyond this a delivery valve through which the water passed to a triangular notch meter. Water

was supplied from a turbine pump. It will be seen that by manipulating the delivery and bye-pass valves the rate of discharge and the pressure at the throat at the venturimeter may be varied independently. In the tests quoted it was clearly the best course to maintain a tolerably constant rate of flow at various throat-pressures in order to eliminate variations due to other causes in the coefficient either of the venturimeter or notch.

The differential pressure tubes were led from the lower parts of the annular rings at the entry and throat of the venturi tube, and a continual fall was maintained to the gauge itself. The pressure lead from the venturi throat to the

Fig. 3.



absolute pressure gauge was similarly taken from the lower part of the throat, and correction was made for differences of level. Freedom from air-locks was tested before and after each experiment.

As was to be expected, particularly at the higher vacua, the venturimeter readings were unsteady, and there was a certain amount of oscillation in the gauge-tubes. Nevertheless, the results are in general agreement with the theoretical values, and show that a more or less systematic diminution in the coefficient occurs at low throat-pressures, and that this may under certain circumstances be very considerable. During the tests at the lower pressures cavitation was distinctly audible at the throat of the meter, and bubbles

of air were visible in the water at the glass section of the pipe some forty diameters beyond.

In the equation given above, the effect of any value of  $k$  is greater for small than for larger values of  $m$ , but in practice low pressures are more likely to occur with high values of  $m$ . For example, with a pipe velocity of 5 feet per second the necessary static head in the pipe just above the venturimeter to ensure that the pressure at the throat shall not fall below atmospheric is 31 feet with a pipe to throat ratio of 9 and less than 6 feet with a ratio of 4. Cavitation is therefore only likely to arise to any considerable extent in practice when a meter of rather large pipe to throat ratio is installed near the open end of a pipe-line, and since modern design tends to favour small values of this ratio, cavitation is becoming less and less significant. Moreover, since the numerical case cited above refers to complete saturation of the water at atmospheric pressure, it gives a limiting value beyond which the correction for water is never likely to rise, and shows that this correction is quite small unless the throat-pressure is much below atmospheric.

There appear to be no previously published results against which these conclusions can be checked. The corrections proposed are scarcely effective, for example, under the conditions quoted by Gibson \*, which refer to throat-pressures in no case more than 18 inches of water below atmospheric. The discussion will, of course, only apply provided air-locks are eliminated in the gauge and its connexions, and non-observance of this condition has probably been responsible for more inaccurate registration in practice than has cavitation at the throat itself. The presence of air-locks is, of course, fatal to consistent metering.

### PULSATING FLOW.

For the measurement of a flow subject to fluctuations of short period, the orifice operates under a disadvantage inherent in any form of meter whose registration depends on a differential pressure not directly proportional to the rate of flow. This disadvantage arises not from irregularities at the orifice itself or changes in the actual coefficient of discharge, but from the means which have to be employed to measure the rapidly changing pressure difference. In order to obtain satisfactory readings it is necessary to damp out the oscillation of the fluid column in the gauge and its connexions; and

\* Proc. Inst. C. E. cxix. p. 391.

unless special and rather elaborate methods are employed, the mean value of the pressure so determined is representative not of the average ( $\bar{q}$ ), but of the "root mean square" ( $q$ ) rate of flow through the orifice.

In order, therefore, to compute the true mean rate of flow, it is necessary to multiply by the factor  $\frac{\bar{q}}{q}$  the rate of flow deduced from the mean value of the pressure difference. The value of this factor will, of course, depend upon the form of the pulsations and upon the frequency of their recurrence, and can only be calculated when these are known.

#### a. *Liquid Flow.*

In the case of liquid flow entirely confined by solid boundaries, the value of this factor can usually be determined with reasonable accuracy from the known conditions at the source of pulsation, since these will as a rule be exactly reproduced at the orifice.

For a flow curve consisting of sinusoidal arcs, such as might be produced by a two-throw single-acting pump without an air vessel, the value of the factor is easily found to be  $\frac{\sqrt{8}}{\pi} = 0.90$  approx., and is therefore of importance. For a three-throw single-acting pump, on the other hand, the factor differs from unity by one part in 1200 only, so that no correction is necessary.

The single-ram pump without air vessel gives a discharge curve of the same individual form as the two-throw, but the pulses are intermittent. It is easily shown that the factor for any such intermittent flow may be obtained from the "form factor" (the factor obtained from the wave-form itself) by the use of an "intermittency factor"  $\sqrt{k}$ , where  $k$  is the ratio of the duration of the pulse to the period of the complete cycle.

For if  $Q$  is the rate of flow at any instant, and  $t_0$  the period of the complete cycle, we may write

$$\frac{\bar{q}}{q} = \frac{\frac{1}{t_0} \int_0^{t_0} Q dt}{\left[ \frac{1}{t_0} \int_0^{t_0} Q^2 dt \right]^{1/2}},$$

and since each of these integrals is unchanged in value except during the portion  $kt_0$  of the period, this expression

may be written

$$\frac{\frac{1}{kt_0} \int_0^{kt_0} Q dt}{\left[ \frac{1}{kt_0} \int_0^{kt_0} Q^2 dt \right]^{\frac{1}{2}}} \sqrt{k} = f \cdot \sqrt{k},$$

where  $f$  is the "form factor."

Hence in the simple case of a single-ram pump the ratio

$$\frac{q}{Q} = \frac{\sqrt{8}}{\pi} \cdot \sqrt{\frac{1}{2}} = 0.636.$$

In practice, of course, it is seldom necessary to measure the discharge of such a pump without an air vessel, and an efficient air vessel will greatly reduce the importance of the correction. For example, a continuous sinusoidal fluctuation

$$Q = q_0 + q_1 \sin \omega t$$

gives a factor \*

$$\left( 1 + \frac{1}{2} \cdot \frac{q_1^2}{q_0^2} \right)^{\frac{1}{2}},$$

showing that the correction is less than 1 per cent. so long as the amplitude of these fluctuations does not exceed 40 per cent. of the mean rate of flow.

#### b. Gaseous Flow.

The effect of fluctuations on the registration of an orifice passing a gas or vapour is not amenable to such simple treatment. The instantaneous rate of flow at different points of the system is dependent not only on the changes at the source of pulsation, but also on the elastic properties of the fluid and on the damping effect of capacity and friction between the points of measurement and imposed pulsation.

Theoretical treatment of the effect of capacity for a given impressed wave-form leads to differential equations which can only be solved by a method of trial and error, all the more troublesome in that each trial involves a step-by-step integration †. In this treatment the impressed wave-form is usually a matter of some uncertainty, and such effects as friction and mass acceleration cannot well be taken into account. The results themselves are therefore to be regarded as essentially approximate, and can more usefully be employed to determine the precautions necessary to keep the correction within defined limits rather than to compute this correction

\* Gibson, P. R. S. Edin. xxxiii. p. 108.

† Hodgson, Inst. C. E. Sel. Pap. xxxi. p. 18.



when large. For this purpose a fairly simple method of treatment may be applied.

### 1. *Instantaneous Pulses.*

For a given mean rate of flow  $\bar{q}$  the effect of pulsation is clearly greatest when the whole quantity passing during a complete cycle is discharged into or out of the system instantaneously, and precautions which enable satisfactory registration to be made under these conditions may be regarded as safe in all cases.

In the discussion which follows we shall suppose that the gas after passing the orifice enters a "receiver" of volume  $V$  from which it is drawn in pulses, by an engine for example.

Assume that the pressure  $p_0$  upstream of an orifice remains sensibly constant, and that the density of the gas is then  $\rho_0$ . If the pressure and density in the receiver are  $p$  and  $\rho$  at any moment, the mass rate of flow through the orifice is given by

$$\frac{dm}{dt} = \rho_0 a_0 \sqrt{\frac{2(p_0 - p)}{\rho_0}},$$

where  $a_0$  is the effective area of the vena contracta. The effect of compressibility, if not negligible, may under all conditions of practical metering be allowed for sufficiently by a correction to  $a_0$  corresponding to the mean pressure difference  $\Delta p$ .

The throttling effect of the orifice will for a permanent gas\* give nearly isothermal conditions in any adequate receiver, and it follows that

$$\frac{\rho_0}{\rho} = \frac{p_0}{p},$$

so that the pressure in the receiver varies according to the relation

$$\frac{dp}{dt} = \frac{p_0 a_0}{V} \sqrt{\frac{2(p_0 - p)}{\rho_0}}.$$

Writing the volumetric rate of flow as  $q$ , we find

$$\frac{dq}{dt} = -\frac{p_0 a_0^2}{\rho_0 V},$$

which gives a linear relation between the rate of flow and time:

$$q = q_1(1 - \tau t),$$

where  $q_1$  is the initial value of  $q$ —i. e., the rate of flow

\* This argument cannot, of course, be maintained for steam, but the results are not likely to be greatly at variance.

immediately after the instantaneous discharge from the receiver—and  $r = \frac{p_0 a_0^2}{\rho_0 V q_1}$ .

Provided the period of fluctuation  $t_0$  is not so great that the pressures  $p$  and  $p_0$  equalize, the value of the ratio

$$\frac{\bar{q}}{q} = \frac{\left(1 - \frac{r}{2} t_0\right)}{\left(1 - r t_0 + \frac{r^2}{3} t_0^2\right)^{\frac{1}{2}}}$$

which is within 2 per cent. of unity so long as  $r t_0 < \frac{1}{2}$ , and within 1 per cent. when  $r t_0 < \frac{2}{3}$ .

When the conditions are such that  $r t_0 = \frac{1}{2}$ , the final rate of flow is one-half the initial, so that  $\bar{q} = \frac{3}{4} q_1$ , and the volume of the receiver necessary to give these conditions is

$$V = \frac{3}{2} \cdot \frac{p_0 a_0^2 t_0}{\rho_0 \bar{q}} = \frac{3}{4} Q \cdot \frac{p_0}{\Delta p},$$

where

$Q$  is the total discharge per cycle,

$\Delta p$  is for practical purposes the mean pressure difference across the orifice.

The capacity so determined may be regarded as adequate to reduce pulsation effects to 2 per cent. under the most unfavourable conditions of supply, and if the capacity is as great as  $Q \frac{p_0}{\Delta p}$  the discrepancy will be less than 1 per cent. On the other hand, if the capacity is much less than these values the pulsation effect will be considerable. A capacity of  $\frac{3}{4} Q \frac{p_0}{\Delta p}$ , for instance, gives an "error" of over 13 per cent. If the capacity is still less than this, there will be a period during each cycle over which there will be no flow from the orifice, and the "intermittency factor"  $\sqrt{k}$  will then operate. It is more satisfactory, however, to prevent than to remedy such conditions in practice.

## 2. Intermittent Pulses; constant rate.

In order to obtain corresponding results for flow in which the pulses are not instantaneous but occupy a measurable part of the cycle, we shall consider next a flow which at the source of pulsation takes the form indicated by  $A_1 O B_1 C_1 C_2$  in fig. 4, having a constant rate  $O$  during the fraction  $k$  of the period  $t_0$  and ceasing over the remainder of the cycle.

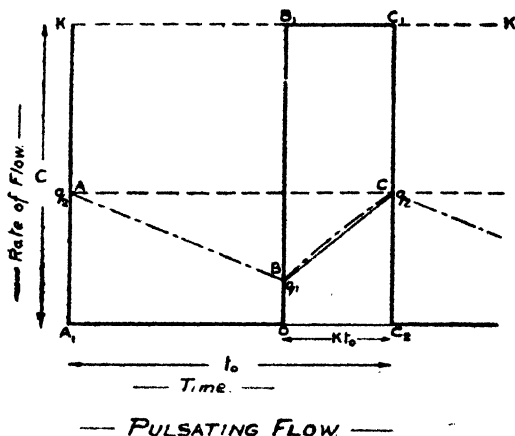
During these intervals the rate of flow at the orifice changes according to the linear law already considered. While discharge from the receiver is taking place at the rate  $C$ , the equation of flow through the orifice is

$$q = a_0 \sqrt{\frac{2(p_0 - p)}{\rho}},$$

where  $p$  satisfies the equation

$$\frac{dp}{dt} = \frac{p_0}{V}(q - C).$$

Fig. 4.



The solution of these equations is

$$C \log \frac{C - q}{C - q_1} + (q - q_1) + \frac{p_0 a_0^2}{\rho_0 V} t = 0,$$

showing that  $q$  approaches logarithmically the value  $C$  from its initial value  $q_1$ .

The variations in flow through the orifice during a cycle will therefore follow the line  $ABC$  in fig. 4, in which  $AB$  is a straight line and  $BC$  a logarithmic curve asymptotic to  $KK$  and of such a form that the areas  $A_1ABO$  and  $BB_1C_1C$  are equal. By direct integration and manipulation it can be shown that the ratio

$$\left(\frac{\bar{q}}{q}\right)^2 = k \frac{Q_0}{Q},$$

where  $Q_0$  is the volume of gas passing the orifice while delivery is taking place,  
 $Q$  is the total discharge per cycle.

In cases where the effect of pulsation is small, which are in fact those under consideration, the arc BC will be but slightly curved, and either of two approximations may be employed to determine the necessary receiver capacity.

a. If we assume that the arc BC is parabolic, we obtain for the area between the arc and chord BC an expression which finally reduces to

$$a = \frac{1}{12} \cdot \frac{1-k}{C} x_0^3,$$

where

$$x_0 = \frac{p_0 a_0^2}{\rho_0 V} t_0.$$

Hence

$$\left(\frac{\bar{q}}{q}\right)^2 = \frac{k \times \text{total area under ABC}}{\text{OBCU}_2} = \frac{t_0(q_1 + q_2) + 2a}{t_0(q_1 + q_2) + 2\frac{a}{k}};$$

and using the approximate expression for  $a$ , we find

$$\begin{aligned} \left(\frac{\bar{q}}{q}\right)^2 &= 1 - \frac{1}{12} \left( \frac{p_0 a_0^2 t_0^2}{\rho_0 V Q} \right)^2 (1-k)^2 \\ &= 1 - \frac{1}{48} \left( \frac{Q}{V} \cdot \frac{p_0}{\Delta p} \right)^2 (1-k)^2 \text{ nearly,} \end{aligned}$$

and the ratio  $\frac{\bar{q}}{q}$  is within 2 per cent. of unity so long as  $V \geq \frac{3}{4} Q \frac{p_0}{\Delta p} (1-k)$ .

b. If we use the fact that the ratio  $\frac{\bar{q}}{q}$  is not greatly different from that obtained when the rate of flow through the orifice follows the lines AB, BC, then by a simple integration we find

$$\frac{\bar{q}}{q} = \frac{1 - \frac{r_1 t_0}{2}}{\sqrt{1 - r_1 t_0 + \frac{r_1^2 t_0^2}{3}}},$$

where

$$r_1 = \frac{p_0 a_0^2}{\rho_0 V q_2} (1-k),$$

a result similar to that obtained for instantaneous pulses but with  $r(1-k)$  written in place of  $r$ . The correction for fluctuation becomes less than 2 per cent. when  $r t_0 (1-k) < \frac{1}{2}$ , and this condition is satisfied when  $V \geq \frac{3}{4} Q \frac{p_0}{\Delta p} (1-k)$ , as above.

3. *Intermittent Pulses; variable rate.*

For a periodic demand on the receiver which is both intermittent and variable, the solution, as mentioned above, is troublesome, and at the best only leads to approximate results; particularly so when the exact wave-form is a matter of uncertainty. It is not difficult, however, to obtain a simple expression for the receiver capacity which will assure reasonably accurate registration.

Suppose the demand per cycle is  $Q$  and the maximum rate of flow  $q_m$  at the source of pulsation. Then the conditions with any normal wave-form are more favourable than those which would obtain if the whole demand  $Q$  were absorbed at a uniform rate  $q_m$ , with idle intervals. The receiver capacity necessary to reduce the correction to a given value under these hypothetical conditions would therefore be ample under the actual conditions of operation; and since the value of this capacity can be easily estimated, it would appear to afford a useful criterion in metering practice. This capacity is given by

$$V = \frac{3}{4} Q \frac{p_0}{\Delta p} \left(1 - \frac{q}{q_m}\right)$$

to give a correction less than 2 per cent., and similarly by

$$V = Q \frac{p_0}{\Delta p} \left(1 - \frac{q}{q_m}\right)$$

to give a correction less than 1 per cent.

It will be found that these values are consistent with solutions obtained for special cases by Hodgson\*, using step-by-step integration.

II. *On the Stability of the Solutions of Mathieu's Equation.*

By BALTH. VAN DER POL, D.Sc., and Dr. M. J. O. STRUTT, E.I.†

THE movement of a particle in a field of force, the force being direct or inversely proportional to the elongation, is determined by the equation :

$$\frac{d^2x}{d\tau^2} + \omega_0^2 \cdot x = 0. \quad . \quad . \quad . \quad . \quad . \quad (1)$$

In the case where the force is inversely proportional to the elongation, we have

$$\omega_0^2 > 0,$$

\* *Loc. cit.* p. 14.

† Communicated by the Authors.

and the movement is of purely periodic type. On the other hand, if the force is directly proportional to the elongation, we have

$$\omega_0^2 < 0,$$

and the movement may be called unstable, as in general the elongation increases indefinitely with time.

If the force is a periodic function of the time with angular frequency  $p$ , the equation is :

$$\frac{d^2x}{d\tau^2} + (\omega_0^2 + \alpha_0^2 \cdot \cos p\tau) \cdot x = 0. \quad . \quad . \quad (2)$$

The three parameters occurring in this equation may simply be reduced to two parameters :

$$\frac{d^2x}{dt^2} + (\omega^2 + \alpha^2 \cdot \cos t) \cdot x = 0, \quad . \quad . \quad (3)$$

with

$$t = p \cdot \tau,$$

$$\omega \cdot p = \omega_0,$$

$$\alpha \cdot p = \alpha_0.$$

The equation with a frictional term, assuming friction to be proportional to velocity, may be reduced to equation (3) by a well-known simple transformation.

The equation (3) is of the type generally known as *Mathieu's differential* <sup>(1)\*</sup> equation.

In astronomy this equation has also been called after Lindstedt <sup>(2)</sup> and after Gylden <sup>(2)</sup>.

If, instead of the term

$$\alpha^2 \cdot \cos t,$$

we have a general Fourier series

$$\begin{aligned} F(t) = & \omega^2 + A_1 \cos t + A_2 \cos 2t + A_3 \cdot \cos 3t + \dots \\ & + B_1 \sin t + B_2 \sin 2t + B_3 \sin 3t + \dots, \end{aligned}$$

so that equation (3) becomes of the form

$$\frac{d^2x}{dt^2} + x \cdot F(t) = 0, \quad . \quad . \quad . \quad (4)$$

where  $F(t)$  is a function of  $t$  with period  $2\pi$ , the equation (4) is called *Hill's equation*.

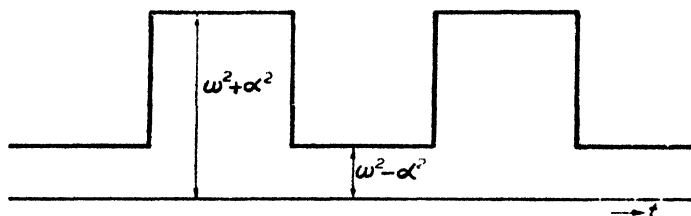
\* These numbers refer to the bibliography at the end of the paper.

As a special form of equation (4), we have

$$\frac{d^2x}{dt^2} + x \cdot \left[ \omega^2 + \frac{4}{\pi} \alpha^2 (\cos t - \frac{1}{3} \cos 3t + \frac{1}{5} \cos 5t - \dots) \right] = 0, \quad (5)$$

so that the "ripple" in the force, acting on the particle under consideration, has the form of fig. 1. The equation (4) and its special forms (3) and (5) occur in several

Fig. 1.



problems, of which we only mention the most important ones, viz. :—

- (1) The movement of a pendulum, the support of which is moved up and down with a frequency  $p/2\pi$  <sup>(3)</sup>;
- (2) the oscillations of locomotive mechanisms <sup>(4)</sup>;
- (3) the movement of a stretched string, the tension of which is varied periodically <sup>(5)</sup>;
- (4) the propagation of waves in stratified media <sup>(6)</sup>;
- (5) the propagation of electromagnetic disturbances in cables of periodic structure (pupin-coils);
- (6) the theory of modulation in wireless <sup>(7)</sup>;
- (7) the theory of superregeneration <sup>(8)</sup>;
- (8) the theory of astronomic perturbations <sup>(9)</sup>;
- (9) the production of electric currents by periodically varying the properties of circuits <sup>(10)</sup>;
- (10) the oscillations of membranes with elliptic boundary <sup>(11)</sup>;
- (11) the eddy currents in elliptic cylinders <sup>(12)</sup>;
- (12) the diffraction of light by elliptic cylinders <sup>(13)</sup>;
- (13) the oscillations of strings with periodic mass-distribution.

By Floquet's theorem <sup>(1)</sup>, the general solution of equation (4) has the form

$$A \cdot e^{\mu t} \cdot \Phi(t) + B \cdot e^{-\mu t} \cdot \Psi(t),$$

where A and B are constants of integration,

$\Phi$  and  $\Psi$  are periodic functions of  $t$  with period  $2\pi$ ,

$\mu$  a coefficient independent of  $t$ , generally called "exposant caractéristique."

After this theorem, if

$$F(t)$$

is an arbitrary solution of equation (4), we have

$$F(t+2\pi) = \sigma \cdot F(t).$$

Now three cases may arise :

$$(a) \quad |\sigma| > 1,$$

$$(b) \quad |\sigma| < 1,$$

$$(c) \quad |\sigma| = 1.$$

Case (a) represents a movement of unstable type; case (b) is of stable type; and case (c) is of unstable type.

It is to be noted that we call a movement stable if both solutions of equation (4) are of stable type, and unstable, if at least one of the solutions is of unstable type. From this definition it is already clear that there are more unstable possibilities than stable ones.

The first purpose of this paper is to fix the boundaries in the  $(\alpha^2, \omega^2)$ -plane between the stable modes of movement and the unstable ones. Moreover, the instability itself will be dealt with quantitatively.

In the literature the rules given for the stability of movement represented by equation (3), are partly contradictory <sup>(2)(14)(15)</sup>. This point makes it desirable to state clearly the conditions under which the solutions of (3) are stable.

Analytically equation (5) may be attacked in the simplest way, so that we shall first consider this case. A solution of equation (5) was already given by E. Meissner <sup>(4)</sup> for the case :

$$\omega^2 > \alpha^2 > 0.$$

The coefficient  $\sigma$  can be found in the following way:—

Let  $f$  and  $\phi$  be two independent solutions of equation (4), and let  $F$  also be a solution, then

$$F(t) = a_1 \cdot f(t) + a_2 \cdot \phi(t).$$

Now we have

$$F(t+2\pi) = \sigma \cdot F(t) = a_1 \cdot (t+2\pi) + a_2 \cdot \phi(t+2\pi),$$

where

$$f(t+2\pi) = a \cdot f(t) + b \cdot \phi(t),$$

$$\phi(t+2\pi) = c \cdot f(t) + d \cdot \phi(t).$$



Then if we assume :

$$\begin{aligned}\phi(0) &= 0, & \phi'(0) &= 1, \\ f(0) &= 1, & f'(0) &= 0\end{aligned}$$

we have :

$$\begin{aligned}a &= f(2\pi), & c &= \phi(2\pi), \\ b &= f'(2\pi), & d &= \phi'(2\pi),\end{aligned}$$

and

$$F(t+2\pi) = \alpha_1(af+b\phi) + \alpha_2(cf+d\phi).$$

Hence

$$\begin{aligned}\alpha_1 a + \alpha_2 c &= \sigma \cdot \alpha_1, \\ \alpha_1 b + \alpha_2 d &= \sigma \cdot \alpha_2, \\ \frac{\alpha_1}{\alpha_2} &= -\frac{c}{a-\sigma} = -\frac{d-\sigma}{b}. \quad . \quad . \quad . \quad (6)\end{aligned}$$

From the differential equation it follows that :

$$f \cdot \phi' - \phi \cdot f' = \text{constant},$$

and in our case

$$f \cdot \phi' - \phi \cdot f' = 1 = a \cdot d - b \cdot c. \quad . \quad . \quad . \quad (7)$$

From equations (6) and (7) we conclude :

$$\sigma^2 - \sigma(a+d) + 1 = 0,$$

or

$$\sigma = \frac{a+d}{2} \pm \sqrt{\left(\frac{a+d}{2}\right)^2 - 1} \quad \text{and} \quad \frac{a+d}{2} = \cos 2\pi\mu. \quad (7')$$

Hence

$$\sigma = e^{\pm 2\pi j\mu}, \quad j = \sqrt{-1}.$$

The three different possibilities of movement, mentioned above, are now expressed by :

- (a)  $|\cos 2\pi\mu| \geq 1$  : unstable,
- (b)  $|\cos 2\pi\mu| < 1$  : stable (indifferent),
- (c)  $|\cos 2\pi\mu| = 1$  : unstable.

Case (c) constitutes the limiting case of (a) and (b).

Now, in the case of a rectangular "ripple," with which we will first deal, we may consider two intervals, corresponding to fig. 1 :

$$(I.) \quad \text{from } t = 0 \text{ till } t = \pi : \frac{d^2 x}{dt^2} + (\omega^2 + \alpha^2) \cdot x = 0,$$

$$(II.) \quad \text{from } t = \pi \text{ till } t = 2\pi : \frac{d^2 x}{dt^2} + (\omega^2 - \alpha^2) \cdot x = 0.$$

In either of the two intervals the sine and cosine solutions may be immediately written down and we have the boundary

condition between the interval-solutions, that  $x$  and  $\frac{dx}{dt}$  be continuous at the boundary. These conditions, together with those for  $t=0$ , enable us to determine the four constants of integration and hence the complete solution.

From this complete solution we easily calculate

$$\cos 2\pi\mu = \frac{1}{2}[f(2\pi) + \phi'(2\pi)]$$

and find :

(I.) for  $\omega^2 > \alpha^2 > 0$  :

$$\cos 2\pi\mu = \cos x_1 \cos x_2 - \frac{1}{2}\left(\frac{x_1}{x_2} + \frac{x_2}{x_1}\right) \sin x_1 \sin x_2,$$

(II.) for  $\omega^2 < \alpha^2$  :

$$\cos 2\pi\mu = \cos x_1 \cosh x_3 - \frac{1}{2}\left(\frac{x_1}{x_3} - \frac{x_3}{x_1}\right) \sinh x_3 \sin x_1, \quad \dots (8)$$

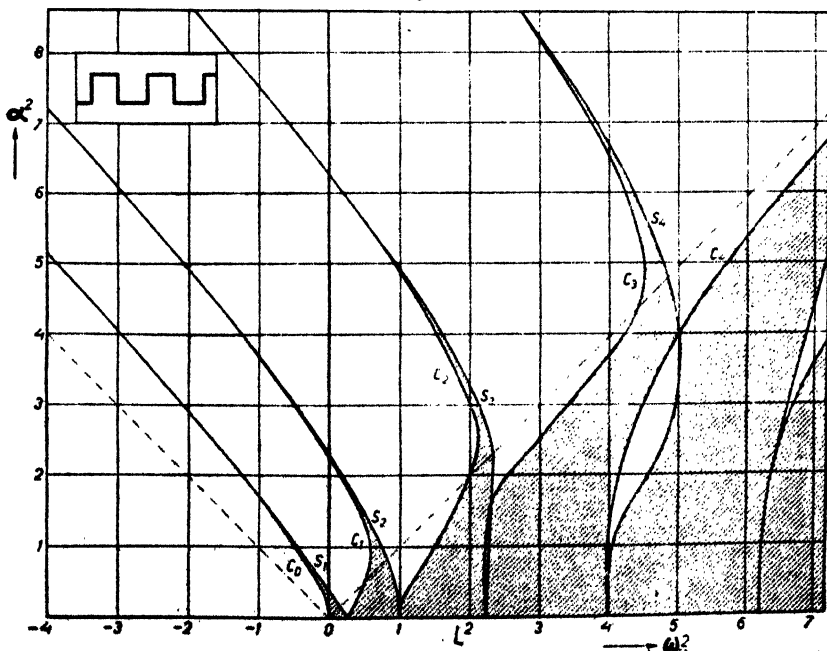
where

$$x_1^2 = \pi^2(\omega^2 + \alpha^2),$$

$$x_2^2 = \pi^2(\omega^2 - \alpha^2),$$

$$x_3^2 = \pi^2(\alpha^2 - \omega^2).$$

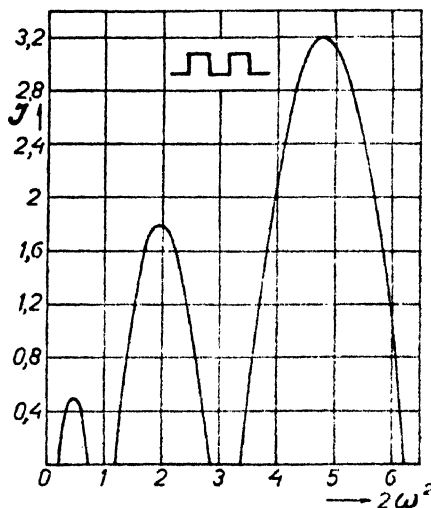
Fig. 2.



From the equations (8) we may plot curves (fig. 2) in the  $(\alpha^2, \omega^2)$ -plane, constituting the boundaries between the

regions of unstable (white in fig. 2) and of indifferent (shaded in fig. 2) (stable) movement. We may consider the diagram thus obtained as a plane, and may imagine the value of  $I = \cos 2\pi\mu - 1$  plotted perpendicularly on this plane above the regions of unstable movement. Thus a three-dimensional representation is obtained, in which the plane (sea) constitutes the region of indifferent movement and the mountains cover the regions of instability, the height of them at every point being a measure for the instability at that point.

In fig. 2 *a* a cut through the unstable mountains has been made along the line under  $45^\circ$  in the first quadrant of fig. 2.

Fig. 2 *a*.

Three special cases of equations (8) will now be considered separately.

(I.) *Small ripple*:  $\frac{|\alpha^2|}{\omega^2} \ll 1$ .

We easily deduce from the first one of equations (8) :

$$\cos 2\pi\mu = \cos 2\pi\omega - \frac{1}{2} \frac{\alpha^4}{\omega^4} \sin^2 \pi\omega. \quad (9)$$

Thus it is seen that the unstable areas starting from the points ( $\alpha^2=0$ ;  $\omega=\frac{1}{2}, \frac{3}{2}, \frac{5}{2} \dots$ ) are of greater instability in the neighbourhood of the  $\omega^2$ -axis than the unstable regions starting from the points ( $\alpha^2=0$ ;  $\omega=1, 2, 3 \dots$ ).

$$(II.) \text{ Fast ripple : } \begin{aligned} |\alpha^2| &<< 1, \\ |\omega^2| &<< 1, \\ |\alpha^2| &> |\omega^2|. \end{aligned}$$

In this case we deduce from the second equation (8) :

$$\cos 2\pi\mu = 1 - 2\pi^2\omega^2 - \frac{1}{8}\pi^4\alpha^4. \quad . \quad . \quad (10)$$

Hence, if  $\omega^2 > 0$ , the movement must be stable; but if  $\omega^2 < 0$ , we may either have a stable or unstable movement, the boundary between these two regions being given by

$$-\omega^2 = \frac{\pi^2}{12}\alpha^4. \quad . \quad . \quad . \quad (11)$$

Thus, the curve  $C_0$  of fig. 2 is given by equation (11) in the neighbourhood of  $\alpha^2 = \omega^2 = 0$ .

(III.) *Large ripple* (and  $\omega^2$  negative) or  
*Asymptotic behaviour* of the boundary-lines for

$$\begin{aligned} \alpha^2 &>> 1, \\ |\omega^2| &>> 1. \end{aligned}$$

In this case we deduce from the second equation (8) :

$$\frac{\omega^2}{\alpha^2} = \cos \pi \sqrt{\left(1 - \frac{\omega^2}{\alpha^2}\right)}. \alpha^2. \quad . \quad . \quad . \quad (12)$$

From equation (12) it follows that all boundary-lines tend asymptotically to straight lines under  $45^\circ$  in the second quadrant of our diagram (fig. 2).

In general, from this diagram we may make the following deductions:—

(I.) The unstable states of motion cover a larger area than the stable ones. This corresponds to the conclusion made from general considerations, that there are more possibilities of unstable movement than of stable movement.

(II.) Below the dotted line under  $45^\circ$  in the first quadrant of fig. 2 the motion is in general stable, the stable areas being cut by relatively small unstable ones. In this case ( $\alpha^2 < \omega^2 > 0$ ) the ripple (fig. 1) does not touch the zero line, and the coefficient of  $x$  (being proportional to the elastic force) in equation (5) remains always positive. *Thus without ripple we should have a stable movement, and the ripple under certain conditions may make the movement unstable.*

(III.) Above and to the left of the  $45^\circ$  line mentioned in the foregoing case, we have, in general, unstable motion, and the unstable areas of fig. 2 are separated by small stable areas. Moreover, the instability increases considerably with

the distance from the aforesaid line, attaining a maximum under  $45^\circ$  in the second quadrant of fig. 2 and in infinity.

To the right of the line  $\omega^2=0$  of fig. 2 the motion would without ripple have been of stable type, and thus the instability is exclusively due to the ripple.

(IV.) In the region to the left of the aforesaid line the motion is unstable without ripple, and the ripple has thus the effect of stabilization.

Physically this case may be realized by a reversed pendulum, which can be stabilized by a fast up and down movement of the lower end<sup>(3)</sup>. We may infer from fig. 2 that this stabilization ceases, however, if the ratio of the amplitude of the ripple to the length of the pendulum exceeds a certain magnitude. This has been verified by experiment; a reversed pendulum of length approximately equal to the amplitude of the movement of the support is, with a slow ripple-frequency, stable, but, after increasing the frequency of the ripple, becomes unstable again.

(V.) If  $\omega^2$  be negative and  $|\omega^2| > \alpha^2$ , the coefficient of  $x$  in equation (5) is always negative. Thus, the curvature of the solution in the  $(x, t)$ -plane being always of one sign, motion cannot be stable, as  $x$  increases indefinitely with  $t$ . Hence, below the  $45^\circ$  line in the second quadrant of fig. 2 no stable areas can exist.

Now that the general properties of motion represented by equation (5) have been discussed, we shall proceed to consider Mathieu's equation (3).

The analysis leading to equations (6), (7), and (7') is valid also in this case.

Let, again,

$$\frac{a+d}{2} = \cos 2\pi\mu,$$

then

$$\sigma = e^{\pm j \cdot 2\pi \cdot \mu}; \quad j = \sqrt{-1}.$$

One can easily show that  $\mu$  can only be real or purely imaginary, but can never be complex.

Thus fig. 3 shows  $\mu$ , as given by

$$2\pi\mu = \arccos \frac{a+d}{2},$$

$$i. e. \text{ when } \left| \frac{a+d}{2} \right| > 1, \text{ then } 2\pi j\beta = \arccos \frac{a+d}{2},$$

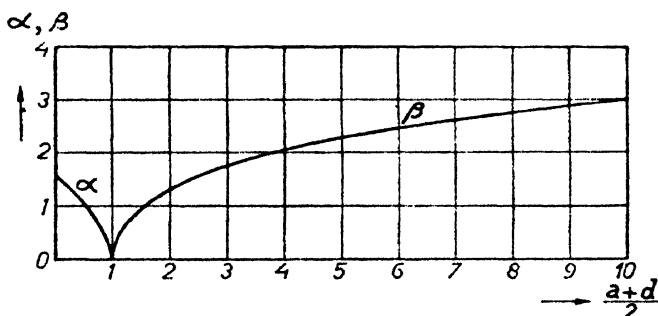
$$\text{and when } \left| \frac{a+d}{2} \right| < 1, \text{ then } 2\pi\alpha = \arccos \frac{a+d}{2},$$

where  $\alpha$  and  $\beta$  are plotted as ordinates in fig. 3.

Thus the three cases correspond respectively to

- (a)  $|\cos 2\pi\mu| > 1$  or  $\mu = \text{imaginary}$  : unstable,
- (b)  $|\cos 2\pi\mu| < 1$  or  $\mu = \text{real}$  : stable,
- (c)  $|\cos 2\pi\mu| = 1$  or  $\mu = 0$  or  $\frac{1}{2}$  : unstable.

Fig. 3.



In case (c) the general solution has no longer the form given by Floquet's theorem, but becomes <sup>(16)</sup>

$$A \cdot \Phi(t) + B \cdot t \cdot \Psi(t),$$

$\Phi$  and  $\Psi$  being functions with period  $2\pi$  in  $t$ .

Thus this case generally corresponds to an unstable movement, the movement being, however, of stable type if  $B=0$ , which depends on the initial conditions.

Equation (3) being a special form of Hill's general equation, we may apply Hill's analysis to equation (3) also.

Two independent solutions of equation (3) may be obtained in the form :

$$e^{i\mu \cdot t} \sum_{-\infty}^{\infty} b_n e^{int} \quad . \quad . \quad . \quad . \quad . \quad (13)$$

and

$$e^{-j\mu t} \sum_{-\infty}^{\infty} b_n e^{-jnt} \quad . \quad . \quad . \quad . \quad . \quad (14)$$

Substituting (13) or (14) into the differential equation and equating coefficients of equal powers of  $e$  to zero, we obtain a determinantal expression, which constitutes an equation for  $\mu$  :

$$\Delta(\mu) \equiv \begin{vmatrix} \dots & \dots & \dots & \dots & \dots & \dots & \dots & \dots & \dots \\ \dots & 0, & \frac{\alpha^2}{2[\omega^2-(\mu+1)^2]}, & 1, & \frac{\alpha^2}{2[\omega^2-(\mu+1)^2]}, & 0, & 0, & 0, & 0 \dots \\ \dots & \dots, & 0, & 0, & \frac{\alpha^2}{2[\omega^2-\mu^2]}, & 1, & \frac{\alpha^2}{2[\omega^2-\mu^2]}, & 0, & 0, & 0 \dots \\ \dots & \dots, & 0, & 0, & 0, & \frac{\alpha^2}{2[\omega^2-(\mu+1)^2]}, & 1, & \frac{\alpha^2}{2[\omega^2-(\mu+1)^2]}, & 0, & 0, \dots \end{vmatrix} =$$

Hill has shown that this equation may be written :

$$\sin^2 \pi \mu = \sin^2 \pi \omega \cdot \Delta(0), \quad \dots \quad (16)$$

whence

$$\Delta(0) = [\Delta(\mu)]_{\mu=0}.$$

Now, if  $\mu$  is given a fixed real value, the determinantal equation (15) corresponds to an equation between  $\omega^2$  and  $\alpha^2$ . Moreover, any real value of  $\mu$  corresponds to a periodic solution of equation (3).

Thus, for any real value of  $\mu$ , the expressions (13) and (14), together with the determinantal equation (15) between  $\alpha^2$  and  $\omega^2$ , are periodic solutions of Mathieu's equation (3), in which  $\omega^2$  and  $\alpha^2$  are related by equation (15). The coefficients  $b_n$  in the expressions (13) and (14) are determined by the set of equations :

$$[\omega^2 - (\mu + n)^2] \cdot b_n + \frac{\alpha^2}{2} \cdot (b_{n-1} + b_{n+1}) = 0.$$

We shall call the expressions (13) and (14) for any real  $\mu$ , defined as above, respectively :

$$\text{and} \quad \left. \begin{aligned} Me^{(I)} &= e^{j\mu t} \sum_{-\infty}^{\infty} b_n \cdot e^{jnt} \\ Me^{(II)} &= e^{-j\mu t} \sum_{-\infty}^{\infty} b_n \cdot e^{-jnt} \end{aligned} \right\} \dots \quad (17)$$

Now, by combining the functions (17), we obtain

$$\begin{aligned} Ce &= \frac{1}{2}(Me^{(I)} + Me^{(II)}) = \sum_{-\infty}^{\infty} b_n \cdot \cos(\mu + n)t \\ &= b_0 + \sum_1^{\infty} (b_n + b_{-n}) \cdot \cos(n + \mu)t, \quad \dots \quad (18) \end{aligned}$$

and

$$\begin{aligned} Se &= \frac{1}{2j}(Me^{(I)} - Me^{(II)}) = \sum_{-\infty}^{\infty} b_n \cdot \sin(n + \mu)t \\ &= \sum_1^{\infty} (b_n - b_{-n}) \sin(n + \mu)t. \quad \dots \quad (19) \end{aligned}$$

The functions (18) and (19) will further be called *generalized Mathieu Functions*. Corresponding to the fact that the differential equation (3) contains 2 parameters, any Mathieu function will be defined by two numbers—an index and the value of  $\alpha^2$  assigned to the function. The value of  $\omega^2$  is then determined from equation (15).

The index is determined by making

$$b_n + b_{-n} = 1$$

in equation (18), thus defining  $Ce_{2(n+\mu)}(\alpha^2, t)$ , and by making

$$b_n - b_{-n} = 1$$

in equation (19), thus defining  $Se_{2(n+\mu)}(\alpha^2, t)$ .

Hence, we have the generalized Mathieu functions :

$$Ce_{2(n+\mu)}(\alpha^2, t) \quad \text{and} \quad Se_{2(n+\mu)}(\alpha^2, t). \quad . \quad . \quad (20)$$

If

$$\mu = 0 ; \frac{1}{2},$$

we have Mathieu functions of integral degree,

$$Ce_m(\alpha^2, t) \quad \text{and} \quad Se_m(\alpha^2, t), \quad . \quad . \quad . \quad (21)$$

whereas the generalized Mathieu functions (20) may also be of fractional degree.

In the literature most attention has been given to Mathieu functions of integral degree, as these functions occur in several boundary problems in physics<sup>(1)</sup>, but Mathieu functions of fractional degree have only been considered very seldom<sup>(17)</sup>.

According to the definition given above, the determinantal equation (15) for any real value of  $\mu$  gives a relation between  $\omega^2$  and  $\alpha^2$ , which is represented by a curve in the  $(\alpha^2, \omega^2)$ -plane. The curves corresponding to the totality of all real values of  $\mu$  cover the whole stable (indifferent) motion area of the  $(\alpha^2, \omega^2)$ -plane. Thus, if we could draw all these curves, we would immediately have solved the first problem which presents itself, viz., the conditions of stable motion.

In any point of one of these curves, for which

$$\mu \neq 0 \text{ or } \frac{1}{2},$$

we have at the same time a solution  $Ce_{2(n+\mu)}(\alpha^2, t)$  and  $Se_{2(n+\mu)}(\alpha^2, t)$ , so that the general solution is

$$A \cdot Ce_{2(n+\mu)}(\alpha^2, t) + B \cdot Se_{2(n+\mu)}(\alpha^2, t).$$

If

$$\mu = 0 \text{ or } \frac{1}{2},$$



the general solution along the curves, represented by equation (15), can no longer be of the aforesaid form, but must be either <sup>(18)</sup> :

$$A \cdot Se_m(\alpha^2, t) + B \cdot \Phi_m(\alpha^2, t),$$

where  $\Phi_m(\alpha^2, t)$  is a function which contains  $t$  explicitly (before some of the terms with sine) and which thus is non-periodic and even, or

$$A \cdot Ce_m(\alpha^2, t) + B \cdot \Psi_m(\alpha^2, t),$$

where  $\Psi_m$  is a function of the same character as  $\Phi_m$  but odd

Hence, from the points of the  $\omega^2$ -axis, corresponding to

$$\mu = 0 \text{ or } \frac{1}{2},$$

and with the aid of equation (15), two curves for constant  $\mu$  can be drawn, these points being double points.

We can easily see, from equation (16), where these double points are to be found in the  $(\omega^2, \alpha^2)$ -plane.

The two corresponding values of  $\mu$  are zero and  $1/2$ . If  $\mu$  is zero, then for  $\alpha^2 \rightarrow 0$ ,

$$\Delta(0) = 1,$$

and we have from (16) :

$$\omega = 0, 1, 2, 3 \dots$$

Fig. 4.

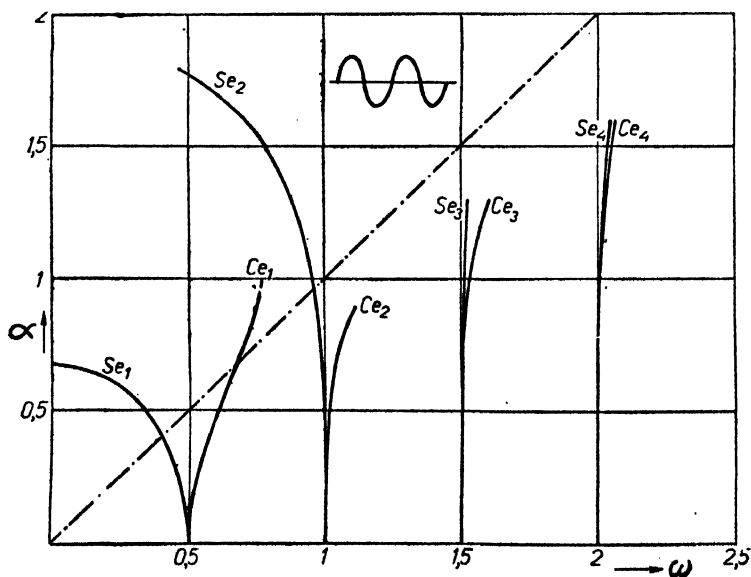


Fig. 5.

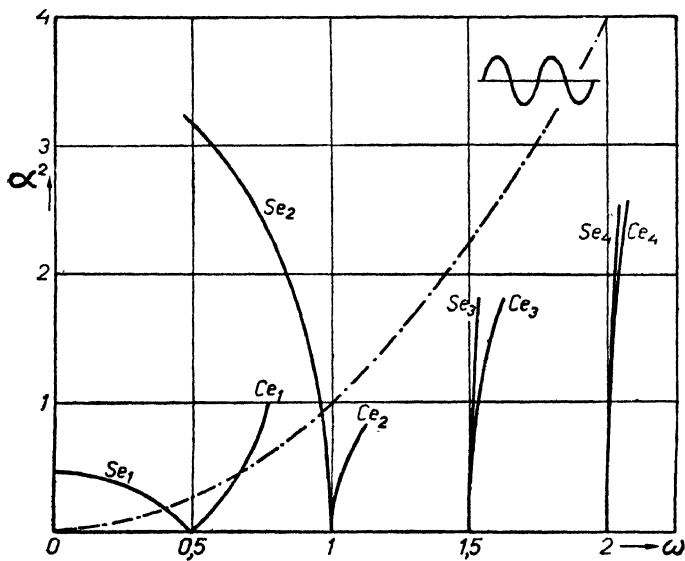


Fig. 6.

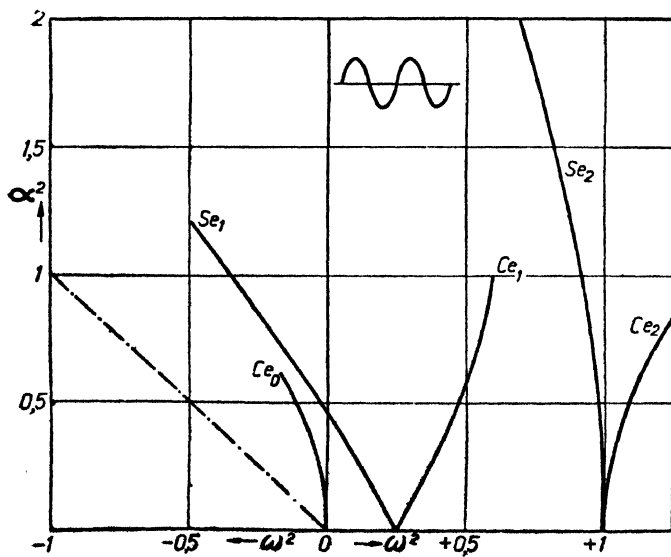


Fig. 7

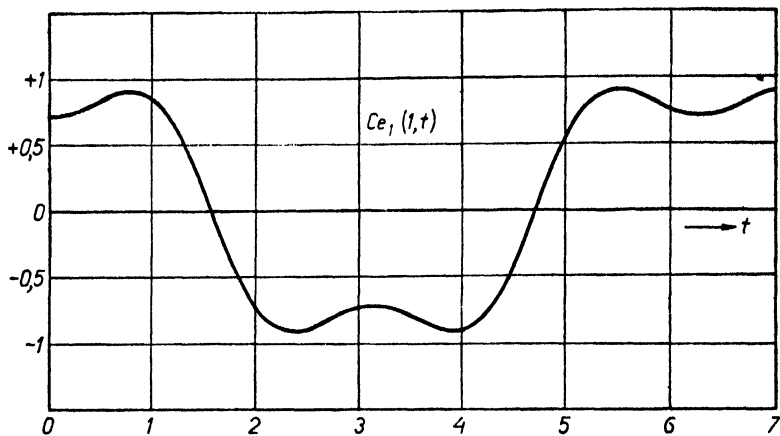
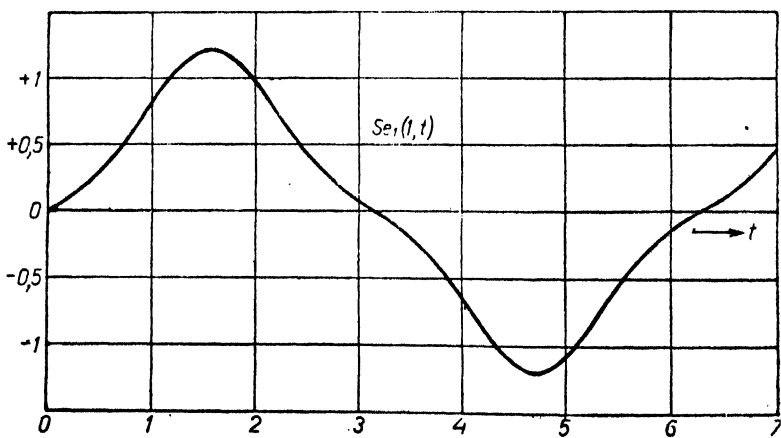


Fig. 8<sup>3</sup>



If  $\mu = 1/2$ , and again for  $\alpha^2 \rightarrow 0$ , (16) yields

$$1 = \sin^2 \pi \omega$$

or

$$\omega = \frac{1}{2}, \frac{3}{2}, \frac{5}{2} \dots$$

Numerically, the Mathieu Functions of integral and of fractional order, which reduce to

$$[Ce_m(\alpha^2, t)]_{\alpha^2 \rightarrow 0} = \cos \frac{m}{2} t$$

and

$$[Se_m(\alpha^2, t)]_{\alpha^2 \rightarrow 0} = \sin \frac{m}{2} t,$$

are easily derived by the method followed \*<sup>(11)</sup> by Mathieu.

We obtain the series (with Mathieu) :

$$\begin{aligned} Ce_1(\alpha^2, t) = & \cos \frac{t}{2} - \frac{\alpha^2}{4} \cos \frac{3t}{2} + 4\alpha^4 \left( \frac{\cos \frac{5t}{2}}{192} - \frac{\cos \frac{3t}{2}}{64} \right) \\ & - 8\alpha^6 \left( \frac{\cos \frac{7t}{2}}{9216} - \frac{\cos \frac{5t}{2}}{1152} + \frac{\cos \frac{3t}{2}}{1536} \right) \\ & + 16\alpha^8 \left( \frac{\cos \frac{9t}{2}}{737280} - \frac{\cos \frac{7t}{2}}{49152} + \frac{\cos \frac{5t}{2}}{24576} \right. \\ & \left. + \frac{11 \cos \frac{3t}{2}}{36864} \right) + \dots, \quad \dots \quad (22) \end{aligned}$$

with

$$\omega^2 = \frac{1}{4} + \frac{\alpha^2}{2} - \frac{\alpha^4}{8} - \frac{\alpha^6}{32} - \frac{\alpha^8}{384} + \frac{11\alpha^{10}}{4608} + \dots \quad (23)$$

The curve represented by equation (23) has been plotted as ( $Ce_1$ ) in figs. 4, 5, and 6, and the curve (22) in fig. 7 for  $\alpha^2 = 1$ .

$$\begin{aligned} Ce_2(\alpha^2, t) = & \cos t + 2\alpha^2 \left( -\frac{\cos 2t}{12} + \frac{1}{4} \right) + \frac{4\alpha^4}{384} \cos 3t \\ & - 8\alpha^6 \left( \frac{\cos 4t}{23040} + \frac{43 \cos 2t}{13824} + \frac{5}{192} \right) \\ & + 16\alpha^8 \left( \frac{\cos 5t}{2211840} + \frac{287 \cos 3t}{2211840} \right) \\ & + 32\alpha^{10} \left( \frac{-\cos 6t}{309657600} - \frac{41 \cos 4t}{16588800} + \frac{21059 \cos 2t}{79626240} \right. \\ & \left. + \frac{1363}{221184} \right) + \dots, \quad \dots \quad (24) \end{aligned}$$

with

$$\omega^2 = 1 + \frac{5}{12} \alpha^4 - \frac{763}{3456} \alpha^8 + \frac{1002419}{4976640} \alpha^{12} + \dots \quad (25)$$

\* Mathieu has given series which, as far as we are aware, are best suited for numerical calculations.

The curve given by equation (25) has been plotted as curve  $Ce_3$  in figs. 4, 5, and 6.

$$\begin{aligned} Ce_3 = & \cos \frac{3}{2}t + 2\alpha^2 \cdot \left( -\frac{\cos \frac{5}{2}t}{16} + \frac{\cos \frac{7}{2}t}{8} \right) + 4\alpha^4 \left( \frac{\cos \frac{7}{2}t}{640} + \frac{\cos \frac{9}{2}t}{64} \right) \\ & + 8\alpha^6 \cdot \left( \frac{-\cos \frac{9}{2}t}{46080} - \frac{7 \cos \frac{5}{2}t}{20480} + \frac{\cos \frac{7}{2}t}{1024} \right) \\ & + 16\alpha^8 \cdot \left( \frac{\cos \frac{11}{2}t}{2^{14} \cdot 3^2 \cdot 5 \cdot 7} + \frac{17 \cos \frac{7}{2}t}{2^{15} \cdot 3^2 \cdot 5} - \frac{\cos \frac{5}{2}t}{2^{14}} - \frac{\cos \frac{3}{2}t}{2^{12}} \right) \\ & + \dots, \dots \dots \dots (26) \end{aligned}$$

with

$$\omega^2 = \frac{9}{4} + \frac{\alpha^4}{16} + \frac{\alpha^6}{32} + \frac{13\alpha^8}{5120} - \frac{5\alpha^{10}}{2048} + \dots \dots \dots (27)$$

The curve given by equation (27) has been plotted as  $Ce_3$  in figs. 4 and 5.

$$\begin{aligned} Ce_4 = & \cos 2t + 2\alpha^2 \cdot \left( -\frac{\cos 3t}{20} + \frac{\cos t}{12} \right) + 4\alpha^4 \cdot \left( \frac{\cos 4t}{960} + \frac{1}{192} \right) \\ & + 8\alpha^6 \cdot \left( \frac{-\cos 5t}{80640} - \frac{13 \cos 3t}{96000} + \frac{11 \cos t}{17280} \right) \\ & + 16\alpha^8 \cdot \left( \frac{\cos 6t}{10321920} + \frac{23 \cos 4t}{6048000} - \frac{1}{92160} \right) \\ & - 32\alpha^{10} \cdot \left( \frac{\cos 7t}{1857945600} + \frac{53 \cos 5t}{1032192000} + \frac{4037 \cos 3t}{2419200000} \right. \\ & \quad \left. + \frac{439 \cos t}{62208000} \right) + \dots, \dots \dots (28) \end{aligned}$$

with

$$\omega^2 = 4 + \frac{\alpha^4}{30} + \frac{433\alpha^8}{216000} - \frac{189983\alpha^{12}}{1360800000} + \dots \dots \dots (29)$$

The curve given by (29) has been drawn as curve  $Ce_4$  in figs. 4 and 5.

$$\begin{aligned} Se_1 = & \sin \frac{t}{2} - \frac{\alpha^2}{4} \sin 3 \frac{t}{2} + 4\alpha^4 \cdot \left( \frac{\sin \frac{5}{2}t}{192} + \frac{\sin \frac{3}{2}t}{64} \right) \\ & - 8\alpha^6 \cdot \left( \frac{\sin \frac{7}{2}t}{9216} + \frac{\sin \frac{5}{2}t}{1152} + \frac{\sin \frac{3}{2}t}{1536} \right) \\ & + 16\alpha^8 \cdot \left( \frac{\sin \frac{9}{2}t}{737280} + \frac{\sin \frac{7}{2}t}{49152} + \frac{\sin \frac{5}{2}t}{24576} - \frac{11 \sin \frac{3}{2}t}{36864} \right) + \dots, \end{aligned}$$

with

$$\omega^2 = \frac{1}{4} - \frac{\alpha^2}{2} - \frac{\alpha^4}{8} + \frac{\alpha^6}{32} - \frac{\alpha^8}{384} - \frac{11\alpha^{10}}{4608} + \dots \dots \dots (30)$$

$$\omega^2 = \frac{1}{4} - \frac{\alpha^2}{2} - \frac{\alpha^4}{8} + \frac{\alpha^6}{32} - \frac{\alpha^8}{384} - \frac{11\alpha^{10}}{4608} + \dots \dots \dots (31)$$

The curve (31) is found as curve  $Se_1$  in figs. 4, 5, 6, and the curve (30) for  $\alpha^2=1$  in fig. 8.

$$Se_2 = \sin t - \frac{\alpha^2}{6} \sin 2t + \frac{\alpha^4}{96} \sin 3t \\ + 8\alpha^6 \cdot \left( \frac{-\sin 4t}{23040} + \frac{5 \sin 2t}{13824} \right) \\ + 16\alpha^8 \cdot \left( \frac{\sin 5t}{2211840} + \frac{37 \sin 3t}{2209140} \right) \\ + 32\alpha^{10} \cdot \left( \frac{-\sin 6t}{309657600} + \frac{11 \sin 4t}{33177600} - \frac{289 \sin 2t}{79626240} \right) + \dots, \\ \text{with} \quad \dots \quad (39)$$

$$\omega^2 = 1 - \frac{\alpha^4}{12} + \frac{5\alpha^8}{3456} - \frac{289 \alpha^{12}}{4976640} + \dots \quad (33)$$

The curve (33) is drawn as curve  $Se_2$  on figs. 4, 5, and 6.

$$Se_3 = \sin 3 \frac{t}{2} + 2\alpha^2 \cdot \left( -\frac{\sin \frac{5}{2}t}{16} + \frac{\sin \frac{t}{2}}{8} \right) + 4\alpha^4 \cdot \left( \frac{\sin \frac{7}{2}t}{640} - \frac{\sin \frac{t}{2}}{64} \right) \\ + 8\alpha^6 \cdot \left( \frac{-\sin \frac{9}{2}t}{46080} - \frac{7 \sin \frac{5}{2}t}{20480} + \frac{\sin \frac{t}{2}}{1024} \right) \\ + 16\alpha^8 \cdot \left( \frac{\sin \frac{11}{2}t}{2^{14} \cdot 3^2 \cdot 5 \cdot 7} + \frac{17 \sin \frac{7}{2}t}{2^{15} \cdot 3^2 \cdot 5} + \frac{\sin \frac{5}{2}t}{2^{14}} + \frac{\sin \frac{t}{2}}{2^{12}} \right) \\ + \dots, \quad \dots \quad (34)$$

with

$$\omega^2 = \frac{9}{4} + \frac{\alpha^4}{16} - \frac{\alpha^6}{32} + \frac{13\alpha^8}{5120} + \frac{5\alpha^{10}}{2048} + \dots$$

The curve (35) is drawn as curve  $Se_3$  in figs. 4 and 5.

$$Se_4 = \sin 2t + 2\alpha^2 \cdot \left( -\frac{\sin 3t}{20} + \frac{\sin 2t}{12} \right) + \frac{\alpha^4}{240} \sin 4t \\ - 8\alpha^6 \cdot \left( \frac{\sin 5t}{80640} + \frac{13 \sin 3t}{96000} - \frac{\sin t}{4320} \right) \\ + 16\alpha^8 \cdot \left( \frac{\sin 6t}{10321920} + \frac{23 \sin 4t}{6048000} \right) \\ + 32\alpha^{10} \cdot \left( \frac{-\sin 7t}{1857945600} - \frac{53 \sin 5t}{1032192000} + \frac{293 \sin 3t}{2419200000} \right. \\ \left. + \frac{397 \sin t}{124416000} \right) + \dots, \quad (36)$$

36 Drs. B. van der Pol and M. J. O. Strutt on the  
with

$$\omega^2 = 4 + \frac{\alpha^4}{30} - \frac{317}{216000} \alpha^8 + \frac{4507}{85050000} \alpha^{12} + \dots \quad (37)$$

The curve given by (37) has been drawn as  $Se_4$  in figs. 4. and 5.

The series of  $Se$  can be obtained from those of  $Ce$  by changing  $\frac{t}{2}$  in  $\frac{\pi}{2} - \frac{t}{2}$  and  $\alpha^2$  in  $-\alpha^2$ .

In general, we have:

$$\begin{aligned} Ce_g = & \cos \frac{g}{2} t + 2\alpha^2 \cdot \left[ \frac{-\cos(g+2) \cdot \frac{t}{2}}{4(g+1)} + \frac{\cos(g-2) \cdot \frac{t}{2}}{4(g-1)} \right] \\ & + 4\alpha^4 \left[ \frac{\cos(g+4) \cdot \frac{t}{2}}{32(g+1)(g+2)} + \frac{\cos(g-4) \cdot \frac{t}{2}}{32(g-1)(g-2)} \right] \\ & + 8\alpha^6 \cdot \left[ \frac{-\cos(g+6) \cdot \frac{t}{2}}{2^7 \cdot 3 \cdot (g+1)(g+2) \cdot (g+3)} \right. \\ & \quad - \frac{(g^2+4g+7) \cos(g+2) \cdot \frac{t}{2}}{2^7 \cdot (g+1)^3 \cdot (g-1) \cdot (g+2)} \\ & \quad + \frac{(g^2-4g+7) \cos(g-2) \cdot \frac{t}{2}}{2^7 \cdot (g-1)^3 \cdot (g+1) \cdot (g-2)} \\ & \quad \left. + \frac{\cos(g-6) \cdot \frac{t}{2}}{2^7 \cdot 3 \cdot (g-1)(g-2)(g-3)} \right] \\ & + 16\alpha^8 \cdot \left[ \frac{\cos(g+8) \cdot \frac{t}{2}}{2^{11} \cdot 3 \cdot (g+1) \cdot (g+2)(g+3)(g+4)} \right. \\ & \quad + \frac{(g^3+7g^2+20g+20) \cdot \cos(g+4) \cdot \frac{t}{2}}{2^8 \cdot 3 \cdot (g+1)^3 \cdot (g-1)(g+2)^2 \cdot (g+3)} \\ & \quad + \frac{(g^3-7g^2+20g-20) \cdot \cos(g-4) \cdot \frac{t}{2}}{2^8 \cdot 3 \cdot (g-1)^3 \cdot (g+1) \cdot (g-2)^2 \cdot (g-3)} \\ & \quad \left. + \frac{\cos(g-8) \cdot \frac{t}{2}}{2^{11} \cdot 3 \cdot (g-1)(g-2)(g-3) \cdot (g-4)} \right] \\ & + \dots, \dots, \dots, \dots, \dots, \dots, \dots, \dots, \quad (38) \end{aligned}$$

with

$$\begin{aligned} \omega^2 = & \frac{g^2}{4} + \frac{4\alpha^4}{2 \cdot (g^2-1)} + \frac{(5g^2+7)16\alpha^8}{32(g^2-1)^3 \cdot (g^2-4)} \\ & + \frac{(9g^6+22g^4-203g^2-116)}{2(g^2-1)^5 \cdot (g^2-4)^2 \cdot (g^2-9)} \cdot \alpha^{12} + \dots \quad (39) \end{aligned}$$

Formulæ (38) and (39) may be applied whenever  $g \neq 1, 2, 3, \text{ or } 4$ .

It is easily seen that the formulæ for  $Ce$  are obtained from those for  $Se$  by changing  $\alpha^2$  into  $-\alpha^2$  and  $\frac{t}{2}$  into  $\frac{\pi}{2} - \frac{t}{2}$ .

Furthermore, from the general formula for  $\omega^2$  it is obvious that as long as  $g$  is not an integer the curve in the  $\omega^2, \alpha^2$ -plane corresponding to  $Se_g$  is the same as that corresponding to  $Ce_g$ . Only if  $g$  is equal to an integer the two curves separate, including between them an area of instability.

Considering figs. 4, 5, and 6 generally and comparing them with fig. 2, it is seen that *the general character of the unstable regions is the same in the case of a sinusoidal ripple as in the case of a rectangular ripple.*

Mathieu functions of integer order are orthogonal, viz.:

$$\begin{aligned} \int_0^{4\pi} Ce_g \cdot Se_k \cdot dt &= 0, \\ \int_0^{4\pi} Ce_g \cdot Ce_k \cdot dt &\neq 0 \text{ if } k = g, \\ &= 0 \text{ if } k \neq g, \\ \int_0^{4\pi} Se_g \cdot Se_k \cdot dt &\neq 0 \text{ if } k = g, \\ &= 0 \text{ if } k \neq g. \end{aligned}$$

Mathieu functions of fractional degree have the property of orthogonality in a similar manner:

$$\begin{aligned} \int_0^{4\pi/s} Ce_s \cdot Se_{k+s} \cdot dt &= 0, \quad \left( \begin{array}{l} k = \text{integer} \\ s = \text{fraction} \end{array} \right) \\ \int_0^{4\pi/s} Ce_s \cdot Ce_{s+k} \cdot dt &\neq 0 \text{ if } k = 0, \\ &= 0 \text{ if } k \neq 0, \\ \int_0^{4/\pi s} Se_s \cdot Se_{s+k} \cdot dt &\neq 0 \text{ if } k = 0, \\ &= 0 \text{ if } k \neq 0. \end{aligned}$$

Similar relations have already been obtained by E. G. Poole<sup>(17)</sup>.

Mathieu functions enable us to solve the Mathieu equation in any region of stable movement. In the regions of unstable movement, however, they are no longer valid.

A method for obtaining the value of  $\mu$  and the solution of equation (3) in these regions has been given by E. T. Whittaker<sup>(1)</sup>. The series given by him ends with  $\alpha^8$  and so enables us to find the solution numerically for about the same values of  $\alpha$  as the series of Mathieu given above.

Various other methods of attack have been given for



equation (3), but the methods mentioned above have been the most successful numerically hitherto.

From the similarity of the diagrams representing the regions of stable and unstable movement of equations (3) and (5), we may expect that all the boundary lines between these regions also for equation (2) cut the  $\alpha^2$ -axis for large values of  $\alpha^2$  at points corresponding to

$$\alpha = n + \frac{1}{2},$$

where  $n=1, 2, 3$ , etc.

Finally, these boundary lines tend to straight lines under  $45^\circ$  in the second quadrant of fig. 2, the stable regions being rather large *below* the  $45^\circ$  line in the first quadrant and very small relatively to the unstable regions *above* and to the left of the aforesaid line. Thus there seems to be little doubt that the general behaviour of the solutions of the Mathieu equation will be similar to the behaviour, fully described above, of the case where the ripple is rectangular instead of sinusoidal.

### *Bibliography.*

- (1) Whittaker & Watson, 'Modern Analysis,' 2nd ed. p. 405.
- (2) Lindstedt, *Mémoires de la Académie de St. Petersbourg*, xxi. No. 4.  
H. Poincaré, 'Méthodes nouvelles de la Mécanique céleste,' ii. p. 229.  
F. Tisserand, 'Traité de Mécanique céleste,' iii. p. 1.
- (3) A. Stephenson, Proc. Manchester Phil. Soc. lii. p. 8 (1908).  
Balth. van der Pol, *Physica*, 1925, p. 157.  
Lord Rayleigh, 'Theory of Sound,' i. p. 82 (1926).  
G. Hamel, *Math. Ann.* lxxiii. p. 371 (1912).
- (4) E. Meissner, 'Schweizer Bauzeitung,' 1918, p. 95.
- (5) Lord Rayleigh, 'Theory of Sound,' i. p. 81 (1926); Scientific Papers, ii. p. 188.
- (6) Lord Rayleigh. 'Scientific Papers,' iii. p. 1.
- (7) R. Carson, Proc. Inst. Rad. Eng. 1922, p. 62.
- (8) H. Armstrong, Proc. Inst. Rad. Eng. 1922, p. 244.
- (9) *E.g.*, C. L. Charlier, 'Mechanik des Himmels,' i. p. 22.  
H. Poincaré, 'Leçons de Mécanique céleste,' ii.
- (10) Lord Rayleigh, 'Scientific Papers,' iii. p. 10.  
Balth. van der Pol, 'Experimental Wireless' (1926).
- (11) E. Mathieu, 'Cours de Mathématique physique,' p. 122 (1873).
- (12) M. J. O. Strutt, *Ann. d. Phys.* lxxxiv. (1927).
- (13) B. Sieger, 'Dissertation Würzburg' (1909).
- (14) A. Liapounoff, *Annales Faculté de Sciences de Toulouse*, 2nd ser. ix. p. 406.
- (15) F. Tisserand, *Bulletin Astronomique*, ix. p. 102 (1892).
- (16) H. Poincaré, 'Méthodes nouvelles de la Mécanique céleste,' i. p. 67.
- (17) P. Humbert, 'Fonctions de Mathieu et de Lamé,' p. 35 (1926. Gauthiers-Villars).

E. G. C. Poole, Proc. London Math. Soc. xx. p. 374 (1922).

Physical Laboratory of the  
Philips' Glowlampworks Ltd, Eindhoven.  
September 20th, 1927.

III. *On the Calculation of the Periods of Circular Membranes and Disks.* By R. C. J. HOWLAND, M.A., M.Sc., University College, London\*.

*Introductory.*

THE theory of the vibrations of a uniform circular membrane was given by Poisson † and Clebsch ‡. The vibrations of a circular disk were considered by Kirchhoff §. Both theories are fully expounded by Rayleigh ||, who gives also a method for calculating the effect on the periods of slight deviations from uniformity ¶.

The vibrations of some types of non-uniform membranes have been discussed by Routh \*\*, using the method of conformal transformation. A solution in Bessel functions for the symmetrical modes of a type of loaded membrane has been given by R. N. Ghosh ††. For a special kind of non-uniform disk, solutions in power series are obtainable ††. Apart from these special cases, only approximate methods have been used for determining the periods of non-uniform membranes and disks. Rayleigh's method of an assumed mode §§ has been applied successfully to disks ||| and to spinning disks ¶¶, and the Ritz method of minimum energy \*\*\* may also be used. It is, however, not always easy to find a suitable assumed mode, and a wrong assumption may lead to very large errors †††.

In a recent paper by the present writer ††† it was shown that very good values for the periods of bars may be obtained through the medium of an integral equation §§§.

\* Communicated by the Author.

† *Mém. de l'Académie*, viii. (1829).

‡ 'Theorie der Elasticität fester Körper' (1862).

§ *Crelle*, xl. p. 51 (1850).

|| 'Theory of Sound,' chapters ix. and x. (2nd ed. revised 1926).

¶ *Ibid.* pars. 208 and 221.

\*\* 'Some Applications and Conjugate Functions,' *Proc. Lond. Math. Soc.* xii. p. 73 (1881).

†† "On Indian Drums," *Phil. Mag.* ser. 6, xlv. pp. 315-316.

‡‡ Prescott, 'Applied Electricity' (London, 1924), par. 338.

§§ 'Theory of Sound,' par. 88.

||| Prescott, *loc. cit.* pars. 340 *et seq.*

¶¶ Lamb and Southwell, *Proc. Roy. Soc. A*, vol. xcix. pp. 272-280 and Southwell, *ibid.* vol. ci. pp. 133-152. Also Stodola, *Schweiz. Bauz.* vol. lxiii. pp. 251, 271 (1914).

\*\*\* Ritz, *Crelle*, 1903, or *Ges. Werke*, Paris, 1913.

††† Cf. the paper by Southwell cited above.

‡‡‡ *Phil. Mag.* ser. 7, iii. pp. 674-694 (1927).

§§§ A different method of treating the integral equation is given by Schwerin, *Zeit. Tech. Phys.* viii. p. 264 (1927).

It is here shown that the same method may be applied to find the periods of circular membranes and disks. It is theoretically capable of any required degree of accuracy, but it will be seen that, for the higher modes, accuracy can only be attained by laborious calculations.

*The Integral Equation.*

The membranes and disks considered may be of variable thickness, density, and rigidity. The vibrations may be controlled by either rigidity or tension or by both acting together, and the method of support is indifferent. It is supposed, however, that the density, rigidity, and tension, if variable, are functions only of the distance from the centre, *i. e.* there is circular symmetry. This is to be true also of the mode of support, but need not be true of the mode of vibration.

Let  $(r, \theta)$  be polar coordinates in the plane of the membrane or disk, the pole being at the centre. On a circle of radius  $\alpha$  apply a transverse force of magnitude  $\cos n\theta$  per unit length,  $n$  being an integer. The deflexion due to this at any point  $(r, \theta)$  will be written

$$K_n(r, \alpha) \cos n\theta,$$

where  $K_n(r, \alpha)$  is a function whose form depends on the density, rigidity, tension, and mode of support.

In a vibration with  $n$  nodal diameters, the frequency being  $\lambda$ , the deflexion may be written

$$w = w_n(r) \cos n\theta \cos 2\pi\lambda t,$$

and the mass-acceleration per unit length of a ring of mean radius  $\alpha$  and breadth  $\delta\alpha$  is

$$-4\pi^2\lambda^2 m(\alpha) \cdot w_n(\alpha) \cdot \cos n\theta \cos 2\pi\lambda t \cdot \delta\alpha,$$

$m$ , the mass per unit area, being also a function of the radius vector only.

It follows from d'Alembert's Principle that, if the mass accelerations are reversed and regarded as static forces, they will produce a deflexion identical with the actual instantaneous deflexion. The deflexion due to the reversed mass-accelerations on the ring of breadth  $\delta\alpha$  is

$$4\pi^2\lambda^2 m(\alpha) \cdot w_n(\alpha) \cdot \cos n\theta \cdot \cos 2\pi\lambda t \cdot \delta\alpha \cdot K_n(r, \alpha).$$

Integrating this and equating the result to the actual

deflexion, we have, after removing the common factors,

$$w_n(r) = 4\pi^2\lambda^2 \int_0^a m(\alpha) w_n(\alpha) K_n(r, \alpha) d\alpha, \quad (1)$$

in which  $a$  is the radius of the boundary\*.

*The Approximate Equation for the Frequencies.*

Applying to the integral in (1) the trapezoidal rule with  $\nu$  intervals, and remembering that, from its definition,  $K_0(r\alpha)$  is identically zero, we obtain the linear equation

$$w_n(r) = \frac{4\pi^2\lambda^2 a}{\nu} \sum_{q=1}^{\nu} \beta_q m\left(\frac{qa}{\nu}\right) w_n\left(\frac{qa}{\nu}\right) K_n\left(r, \frac{qa}{\nu}\right), \quad (2)$$

where

$$\left. \begin{aligned} \beta_q &= 1, & q \neq \nu, \\ \beta_{\nu} &= \frac{1}{2}. \end{aligned} \right\} \quad (3)$$

In (2) let  $r$  take successively the values

$$\frac{a}{\nu}, \quad \frac{2a}{\nu}, \quad \dots, \quad \frac{\nu a}{\nu},$$

and write

$$\left. \begin{aligned} w_n\left(\frac{qa}{\nu}\right) &= w_q, & m\left(\frac{qa}{\nu}\right) &= m_q, \\ K_n\left(\frac{pa}{\nu}, \frac{qa}{\nu}\right) &= k_{pq}. \end{aligned} \right\} \quad (4)$$

Then

$$w_p = \frac{4\pi^2\lambda^2 a}{\nu} \sum_{q=1}^{\nu} \beta_q m_q k_{pq} w_q, \quad (5)$$

$p = 1, 2, 3, \dots, \nu.$

Eliminating the  $w$ 's, we have for  $\lambda^2$  the equation of degree  $\nu$ :

$$\begin{vmatrix} m_1 k_{11} - \mu, & m_2 k_{12}, & \dots, & \frac{1}{2} m_{\nu} k_{1\nu} \\ m_1 k_{21}, & m_2 k_{22} - \mu, & \dots, & \frac{1}{2} m_{\nu} k_{2\nu} \\ \dots & \dots & \dots & \dots \\ m_1 k_{\nu 1}, & m_2 k_{\nu 2}, & \dots, & \frac{1}{2} m_{\nu} k_{\nu\nu} - \mu \end{vmatrix} = 0, \quad (6)$$

where

$$\mu = \frac{\nu}{4\pi^2\lambda^2 a}. \quad (7)$$

When the rim is fixed, the last column of the determinant is missing and the degree of the equation reduces to  $\nu - 1$ .

\* For the theory of this type of equation see Whittaker and Watson, 'Modern Analysis,' 3rd ed., par. 11.23.

*Determination of  $K_n(r, \alpha)$  for the Membrane.*

The deflexion of a stretched membrane under a given system of transverse force depends only on the tension. It is therefore possible to give general formulæ, independent of the variations in density or thickness of the material. These will enter into the equation for the periods only through the factors  $m_g$ .

If the membrane is stretched to a tension  $T$  and is acted upon by a transverse force of magnitude  $P \cos n\theta$  per unit area,  $P$  being any function of  $r$ , the deflexion  $w$  is given by the equation

$$\nabla^2 w + \frac{P}{T} \cos n\theta = 0,$$

or, writing

$$w = w_n \cos n\theta,$$

$$\frac{d^2 w_n}{dr^2} + \frac{8}{r} \frac{dw_n}{dr} - \frac{n^2}{r^2} w_n = -\frac{P}{T},$$

which may conveniently be written as

$$\frac{1}{r^{n+1}} \frac{d}{dr} \left\{ r^{2n+1} \frac{d}{dr} \left( \frac{w_n}{r^n} \right) \right\} = -\frac{P}{T}. \quad (8)$$

To identify  $w_n$  with  $K_n(r, \alpha)$ , let  $P$  be zero except when  $r = \alpha$ , while

$$\lim_{\epsilon \rightarrow 0} \int_{\alpha-\epsilon}^{\alpha+\epsilon} P dr = 1.$$

Then

$$\int_0^r P r^{n+1} dr = 0 \quad \text{if } r < \alpha, \\ = \alpha^{n+1} \quad \text{if } r > \alpha,$$

and a first integration of (8) gives

$$\frac{d}{dr} \left( \frac{w_n}{r^n} \right) = \frac{A}{r^{2n+1}} \Big| - \frac{\alpha^{n+1}}{T r^{2n+1}}.$$

In this equation and in all that follows the terms to the left of the vertical bar apply to the whole membrane; those to the right of the bar apply only for  $r > \alpha$ .

Integrating again,

$$\frac{w_n}{r^n} = \frac{A'}{r^{2n}} + B \Big| - \frac{\alpha^{n+1}}{T} \int_{\alpha}^r \frac{dr}{r^{2n+1}},$$

$$\text{or} \quad w_n = \frac{A'}{r^n} + B r^n \Big| - \frac{r^{2n} - \alpha^{2n}}{2n T \alpha^{n-1} r^n}.$$

If the membrane is complete,  $A'$  must be zero. If it is fixed at the rim, we have also

$$B = \frac{a^{2n} - \alpha^{2n}}{2nT\alpha^{n-1}a^{2n}}.$$

Hence

$$\left. \begin{aligned} K_n(r, \alpha) &= \frac{a^{2n} - \alpha^{2n}}{2nT\alpha^{2n}\alpha^{n-1}} \cdot r^n, \quad r < \alpha, \\ K_n(r, \alpha) &= \frac{a^{2n} - r^{2n}}{2nT\alpha^{2n}r^n} \cdot \alpha^{n+1}, \quad r > \alpha. \end{aligned} \right\} \dots \dots (9)$$

In the above integration it has been assumed that  $n$  is not zero. The formulæ for  $n=0$  are

$$\left. \begin{aligned} K_0(r, \alpha) &= \frac{\alpha}{T} \log \frac{\alpha}{r}, \quad r < \alpha, \\ K_0(r, \alpha) &= \frac{\alpha}{T} \log \frac{\alpha}{r}, \quad r > \alpha. \end{aligned} \right\} \dots \dots (10)$$

*Calculation of  $K_n(r, \alpha)$  for the Disk.*

If

$2h$  = thickness of disk,

$I = 2h^3/3$ ,

$E$  = Young's Modulus,

$\sigma$  = Poisson's Ratio,

$E' = E/(1 - \sigma)$ ,

the deflexion due to a transverse force of magnitude  $p$  per unit area is determined by the equation

$$\nabla^2(I\nabla^2 w) = \frac{p}{E'} \dots \dots (11)*$$

From the general assumption of symmetry,  $I$  is a function of  $r$  but not of  $\theta$ ;  $E'$  will be supposed constant. Writing  $p = P \cos n\theta$ , where  $P$  has the same meaning as before, we have

$$\left( \frac{d^2}{dr^2} + \frac{1}{r} \frac{d}{dr} - \frac{n^2}{r^2} \right) I \left( \frac{d^2}{dr^2} + \frac{1}{r} \frac{d}{dr} - \frac{n^2}{r^2} \right) w_n = \frac{P}{E'}. \quad (12)$$

Now, if  $\chi$  is any function of  $r$ , we may write

$$\left( \frac{d^2}{dr^2} + \frac{1}{r} \frac{d}{dr} - \frac{n^2}{r^2} \right) \chi = \frac{1}{r^{n+1}} \frac{d}{dr} \left\{ r^{n+1} \left( \frac{d\chi}{dr} - n \frac{\chi}{r} \right) \right\}. \quad (13)$$

and

$$\left( \frac{d^2}{dr^2} + \frac{1}{r} \frac{d}{dr} - \frac{n^2}{r^2} \right) \chi = r^{n-1} \frac{d}{dr} \left\{ \frac{1}{r^{n-1}} \left( \frac{d\chi}{dr} + n \frac{\chi}{r} \right) \right\}. \quad (14)$$

\* Prescott, 'Applied Elasticity,' p. 394.

$$\chi = I \left( \frac{d^2}{dr^2} + \frac{1}{r} \frac{d}{dr} - \frac{n^2}{r^2} \right) w_n,$$

we therefore obtain the following two first integrals of (12),

$$\begin{aligned} \frac{d\chi}{dr} - n \frac{\chi}{r} &= \frac{A}{r^{n+1}} \left| + \frac{1}{E'} \left( \frac{\alpha}{r} \right)^{n+1} \right|, \\ \frac{d\chi}{dr} + n \frac{\chi}{r} &= B r^{n-1} \left| + \frac{1}{E'} \left( \frac{r}{\alpha} \right)^{n-1} \right|, \end{aligned}$$

whence, by subtraction,

$$\begin{aligned} 2n \frac{I}{r} \left( \frac{d^2}{dr^2} + \frac{1}{r} \frac{d}{dr} - \frac{n^2}{r^2} \right) w_n &= B r^{n-1} \\ &\quad - \frac{A}{r^{n+1}} \left| + \frac{1}{E'} \left\{ \left( \frac{r}{\alpha} \right)^{n-1} - \left( \frac{\alpha}{r} \right)^{n+1} \right\} \right|. \end{aligned}$$

Again applying (13) and (14) to obtain first integrals, we find

$$\begin{aligned} 2n \left( \frac{dw_n}{dr} - n \frac{w_n}{r} \right) &= \frac{C}{r^{n+1}} + \frac{B}{r^{n+1}} \int_a^r \frac{r^{2n+1}}{I} dr \\ &\quad - \frac{A}{r^{n+1}} \int_a^r \frac{r}{I} dr \left| + \frac{1}{E' r^{n+1}} \int_a^r \left( \frac{r^{2n+1}}{\alpha^{n-1}} - \alpha^{n+1} r \right) \frac{dr}{I} \right| \end{aligned}$$

and

$$\begin{aligned} 2n \left( \frac{dw_n}{dr} + n \frac{w_n}{r} \right) &= D r^{n-1} + B r^{n-1} \int_a^r \frac{r}{I} dr \\ &\quad - A r^{n-1} \int_a^r \frac{dr}{I r^{2n-1}} \left| + \frac{r^{n-1}}{E'} \int_a^r \left( \frac{r}{\alpha^{n-1}} - \frac{\alpha^{n+1}}{r^{2n-1}} \right) \frac{dr}{I} \right|. \end{aligned}$$

Again subtracting,

$$\begin{aligned} 4n^2 w_n &= D r^n - \frac{C}{r^n} + B \left( r^n \int_a^r \frac{r}{I} dr - \frac{1}{r^n} \int_a^r \frac{r^{2n+1}}{I} dr \right) \\ &\quad + A \left( \frac{1}{r^n} \int_a^r \frac{r}{I} dr - r^n \int_a^r \frac{dr}{I r^{2n-1}} \right) \left| + \frac{1}{E'} \left[ r^n \int_a^r \left( \frac{r}{\alpha^{n-1}} \right. \right. \right. \\ &\quad \left. \left. \left. - \frac{\alpha^{n+1}}{r^{2n-1}} \right) \frac{dr}{I} - \frac{1}{r^n} \int_a^r \left( \frac{r^{2n+1}}{\alpha^{n-1}} - \alpha^{n+1} r \right) \frac{dr}{I} \right] \right|. \quad (15) \end{aligned}$$

When  $n=0$ , this result must be modified, since (14) now becomes identical with (13) and must be replaced by

$$\left( \frac{d^2}{dr^2} + \frac{1}{r} \frac{d}{dr} \right) \chi = \frac{1}{r \log r} \frac{d}{dr} \left\{ r \log r \frac{d\chi}{dr} - \chi \right\}. \quad (16)$$

Carrying out the integration as before, we get in place of (15)

$$w_0 = A \left( \log r \int \frac{r \log r}{I} dr - \int \frac{r (\log r)^2}{I} dr \right) + B \left( \log r \int \frac{r}{I} dr - \int \frac{r \log r}{I} dr \right) + C \log r + D \left| + \frac{\alpha}{E'} \left[ \log r \int \frac{r}{I} \log \frac{r}{\alpha} dr - \int \frac{r}{I} \log r \log \frac{r}{\alpha} dr \right] \right. \quad \dots \quad (17)$$

From (15) and (17), when  $I$  is known as a function of  $r$ , the form of  $K_n(r, \alpha)$  corresponding to any given boundary conditions may be determined.

### Numerical Results for Uniform Membrane.

The degree of accuracy attainable by the method outlined above is conveniently illustrated by using the method to calculate the periods of a uniform membrane. The method of calculation is sufficiently obvious, and only the results will be given. In Table I.,  $n$  is the number of nodal diameters,  $s$  the number of nodal circles of the mode of vibration. Five of the periods have been calculated with  $\nu$ , the number of intervals, varying from 4 to 6. The correct values of the periods are added for comparison. When  $\nu=6$  the equation for  $\mu$  is of degree 5; the calculation is then a little long. It will be seen that, for the mode having both a nodal diameter and a nodal circle, more than six intervals would be required to give an accurate result. With  $\nu=8$  or 9 the labour of calculation would be very great, but not prohibitive.

The values obtained are all too small. The errors increase, for a constant value of  $\nu$ , both with  $s$  and with  $n$ .

TABLE I  
Values of  $\lambda \sqrt{T/ma^2}$ .

		$\nu=4.$	$\nu=5.$	$\nu=6.$	True value.
$n=0 \dots$	$\begin{cases} s=0 \\ s=1 \end{cases}$	0.38 0.81	0.38 0.85	0.38 0.86	0.38 0.88
$n=1 \dots$	$\begin{cases} s=0 \\ s=1 \end{cases}$	0.59 0.98	0.595 1.03	0.60 1.06	0.61 1.12
$n=2 \dots$	$s=0$	0.75	0.78	0.79	0.82



## 46 Calculation of Periods of Circular Membranes and Disks.

### Results for Uniform Clamped Disk.

For a uniform disk clamped at the rim and of radius  $a$ , (17) will be found to lead to

$$\left. \begin{aligned} K_0(r, a) &= \frac{\alpha}{8EI} \left\{ \frac{(a^2 - \alpha^2)(a^2 + r^2)}{a^2} - 2(r^2 + \alpha^2) \log \frac{a}{\alpha} \right\}, & r < \alpha, \\ K_0(r, a) &= \frac{\alpha}{8EI} \left\{ \frac{(a^2 + \alpha^2)(a^2 - r^2)}{a^2} - 2(r^2 + \alpha^2) \log \frac{a}{r} \right\}, & r > \alpha. \end{aligned} \right\} \quad (18)$$

From these and (6) it is easy to calculate the fundamental frequency. Using four intervals, we find

$$\lambda = 1.67 \sqrt{EI/ma^4}.$$

With six intervals the coefficient is 1.64. The true value is 1.63.

The convergence to the true value is here rather slower than for the membrane, and this will be found to be the case in general. The accurate calculation of the higher frequencies therefore requires a large number of intervals. But this is compensated by the fact that the modes with nodal circles have much higher frequencies than the corresponding modes with only diametral nodes, and are, in consequence, seldom of importance. If only the modes without nodal circles are to be calculated, it is only necessary to find the highest root of equation (6), while it is known that the other roots are comparatively small. Under these circumstances it is unnecessary to calculate all the coefficients.

Consider, for example, a vibration with one nodal diameter. From (15) we obtain

$$\left. \begin{aligned} K_1(r, a) &= \frac{r}{4EI} \left[ \alpha^2 \log \frac{a}{\alpha} - \frac{a^2 - \alpha^2}{4a^4} \{ 2a^2\alpha^2 + (a^2 - \alpha^2)r^2 \} \right], & r < \alpha, \\ K_1(r, a) &= \frac{\alpha^2}{4EIr} \left[ r^2 \log \frac{a}{r} - \frac{(a^2 - r^2)}{4a^4} \{ 2a^2r^2 + (a^2 - r^2)\alpha^2 \} \right], & r > \alpha. \end{aligned} \right\} \quad (19)$$

With five intervals, and writing  $\mu = \frac{2500 EI'}{4\pi^2 \lambda^2 m a^4}$ , a slight

modification of (7), the equation for  $\mu$  becomes

$$\begin{vmatrix} 0.8990 - \mu, & 1.8088, & 1.6151, & 0.6578 \\ 0.4522, & 2.5592 - \mu, & 2.6158, & 1.1212 \\ 0.1795, & 1.1626, & 2.3877 - \mu, & 1.1958 \\ 0.0411, & 0.2803, & 0.6726, & 0.6872 - \mu \end{vmatrix} = 0$$

or  $\mu^4 - 6.533 \mu^3 - 7.483 \mu^2 - 4.30 \mu - 0.61 = 0. \quad (20)$

Of this equation the highest root is 5.262, leading to  $\lambda = 3.47 \sqrt{EI/ma^4}$ . The correct coefficient is 3.38. If (20) is deprived of its last term and the highest root is again calculated, the result is 5.266 and the value of  $\lambda$  is scarcely altered. If the last two terms of (20) are removed, the higher root of the resulting quadratic is 5.051, which leads to a coefficient 3.52. The approximation has been worsened by only  $1\frac{1}{2}$  per cent. Now, even with  $\nu$  as high as 8 or 10, it is a simple matter to calculate the first three terms in the equation. The result is a quadratic from which the value of  $\lambda$  will usually be obtainable within about 2 per cent.\*

IV. *On the Practical Application of the Theory of Vibrations to Systems with several Degrees of Freedom.* By C. RICHARD SODERBERG, Research Engineer, Westinghouse Electric & Mfg. Co., Power Eng. Dept., East Pittsburgh, Pa., U.S.A.†

## I. INTRODUCTION.

THERE are numerous engineering problems to which the general theory of vibrations can be applied profitably, but the rigorous treatment involves somewhat laborious arithmetical calculations, and is therefore often replaced by more or less unreliable methods of approximation. The author has in mind, particularly, the frequently occurring problems of determining the whirling speeds in multiple bearing machines, the critical speeds for torsional oscillations in line shafting with several masses, and various problems of similar nature encountered in foundation studies.

Ordinarily these problems are treated with sufficient accuracy by the determination of an approximate value for

\* For further examples of calculations of this kind see the Author's paper cited above and also a paper entitled "The Vibrations of Frames," Selected Eng. Papers, No. 47, Inst. C.E., 1927.

† Communicated by R. V. Southwell, M.A., F.R.S.

the fundamental principal frequency, but the rapid development of high-speed machinery in large units has brought about the necessity for considering the higher modes of motion as well. In turbo-generators, for example, the large units are now constructed in such a manner that the second mode of oscillation of the rotor is of more vital importance than the fundamental, because it is more apt to conflict with the operating speed.

The following will describe a method for the expansion and the solution of the system determinant, which the author has used for a considerable time in his engineering activity, and which he has found useful on account of the symmetry of the expressions involved.

The method does not involve any new principles of fundamental character. It depends primarily upon the writing of the determinantal equation in a definite form from which a set of preliminary solutions, corresponding to a set of arbitrary modes of vibration, are obtained. The correct solutions are then centred around these preliminary solutions, the transformation being carried out by a graphical process. The fundamental properties of this particular form of the determinantal equation arise from the fact that the unknown occurs only in the principal diagonal, and as inverse squares of the frequencies.

The empirical formula proposed by Dunkerley, for the calculation of whirling speeds in shafts\*, represents an approximation of the relations set forth below. A considerable portion of the literature on the subject has been devoted to discussions of the validity and the degree of approximation of the Dunkerley formula. The present treatment has been suggested, to a considerable extent, by the relations employed by these authors †.

## II. ESTABLISHING THE DETERMINANTAL EQUATION.

In order to illustrate the methods by which the determinantal equation can be brought to the desired form, we shall consider the most important of the major engineering problems—namely, the determination of whirling speeds in

\* Philosophical Transactions, vol. clxxxv. p. 279 (1894).

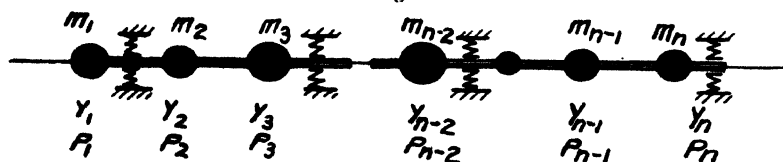
† E. Hahn, *Schweizerische Bauzeitung*, p. 191, Nov. 9, 1918: "Note sur la vitesse critique des arbres et le Formule de Dunkerley." Professor Hahn's treatment for whirling speeds differs but slightly from the present method. See also H. H. Jeffcott, *Proc. Roy. Soc.* vol. xcv. p. 106 (1918); R. C. Howland, *Phil. Mag.* vol. xlix. p. 1131 (1925); H. H. Jeffcott; *Phil. Mag.* p. 689 (April 1927).

multiple bearing arrangements, the determination of natural frequencies for torsional oscillations of line shafting with concentrated masses, and the determination of natural frequencies in mechanical systems of a more general type, such as are encountered in machine foundations, buildings, etc.

### 1. Whirling Speeds in Shafts.

Consider first the problem of whirling speeds in rotating shafts. The problem for shafts mounted in two bearings has been thoroughly investigated, and it is a well-known fact that the solution resolves itself into the determination of the natural frequencies of lateral vibrations. We shall consider the problem in a somewhat more general form, and refer to the system illustrated in fig. 1.

Fig. 1.



Lateral Vibrations of a System of Concentrated Masses on Elastic Shaft in Multiple Bearings.

Let there be  $n$  masses  $m_1, m_2, \dots, m_n$ , which can be treated as distinct mass concentrations, interspersed with flexible, massless, stretches of shafting. This generalization may at first appear too extensive, but anyone familiar with the practical aspects of the problem will agree that there are very few of the systems encountered in practical problems that cannot be satisfactorily replaced by a system of concentrated masses on a weightless shaft. Bearing supports, flexibly connected to a rigid foundation reference, are introduced in an arbitrary order between these masses.

The action of the bearing supports depends upon the combined elasticity of the oil film and the bearing pedestals. In the ordinary problems of whirling motion it is usually permissible to neglect the masses of the bearing supports. However, there are no serious difficulties in taking them into account. The elasticity of the bearing pedestals may be considered as known, although it may be necessary to resort to static tests for its determination. The elasticity of the oil film presents the most uncertain part of this problem; and here it must be stated that further investigations are necessary before a fully reliable method for taking this

effect into account can be evolved. The available investigations on the subject \* seem to indicate, however, that the oil film may, within certain limits, be considered as a spring of approximately constant flexibility. This conclusion is based on the fact that the motion of a rigid shaft in the oil film can be represented by linear differential equations.

In order to avoid excessive complications, it is assumed that the vibrations take place in one plane. Assuming a rotor structure of uniform flexibility in all directions, this is strictly permissible only when the flexibility of the bearing supports is the same for the vertical and the horizontal directions. This is usually not the case, because the flexibility of the bearing supports is frequently several times greater for horizontal motion than for vertical motion. However, the results obtained by treating the horizontal and vertical vibrations as independent motions seem to agree very well with experimental results.

Most engineering problems also permit the neglect of the gyroscopic forces; and where these terms are of importance, it is usually possible to apply a suitable correction.

Thus we may consider lateral vibrations of a system of masses, mechanically connected by a shaft of known elastic properties; this shaft is connected at certain points to a rigid foundation by mechanical members of known elasticity.

The differential equations of motion for this system are most easily established from the behaviour of the system under static loads  $P_1, P_2, \dots, P_n$ , acting at the mass concentrations in the plane of motion. If  $y_1, y_2, \dots, y_n$  represent the static displacements at the mass concentrations, the condition of static equilibrium appears in the following form:

$$\left. \begin{aligned} y_1 &= \alpha_{11} P_1 + \alpha_{12} P_2 + \dots + \alpha_{1n} P_n \\ y_2 &= \alpha_{21} P_1 + \alpha_{22} P_2 + \dots + \alpha_{2n} P_n \\ &\vdots \\ y_n &= \alpha_{n1} P_1 + \alpha_{n2} P_2 + \dots + \alpha_{nn} P_n \end{aligned} \right\} \quad (1)$$

The establishing of these equations is a problem of statics which never offers serious difficulties, although the expressions for the influence factors  $\alpha$  may take complicated forms. Ordinarily the "moment method," where the bending moments at the supports are selected as statically indeterminate factors, leads most quickly to the result. For almost all engineering problems it is necessary to resort to

\* Stodola, *Schweizerische Bauzeitung*, May 28, 1925. Hummel, *V.D.I. Forschungs Arbeiten*, Heft 287.

graphical constructions for determining the elastic properties of the individual spans.

Now, to obtain the differential equations of motion we change these static forces into inertia forces, and the static deflexions  $y$  into dynamic displacements—that is,

$$P_1 = -m_1 \ddot{y}_1; P_2 = -m_2 \ddot{y}_2; \dots; P_n = -m_n \ddot{y}_n. \quad (2)$$

The determinantal equation, from which the principal frequencies are determined, is obtained by putting

$$y_1 = A_1 \sin \omega t; y_2 = A_2 \sin \omega t; \dots; y_n = A_n \sin \omega t, \quad (3)$$

which, when introduced into the differential equations of motion, give the following condition for the independence of the integration constants  $A^*$ :

$$\begin{vmatrix} 1 - \alpha_{11}m_1\omega^2, & -\alpha_{12}m_2\omega^2, & \dots, & -\alpha_{1n}m_n\omega^2, \\ -\alpha_{21}m_1\omega^2, & 1 - \alpha_{22}m_2\omega^2, & \dots, & -\alpha_{2n}m_n\omega^2, \\ \dots & \dots & \dots & \dots \\ -\alpha_{n1}m_1\omega^2, & -\alpha_{n2}m_2\omega^2, & \dots, & 1 - \alpha_{nn}m_n\omega^2. \end{vmatrix} = 0. \quad (4)$$

Now divide each column of this determinant by

$$-\alpha_{11}m_1\omega^2, -\alpha_{22}m_2\omega^2, \dots, -\alpha_{nn}m_n\omega^2,$$

respectively, and put

$$X_1^2 = \frac{C^2}{\alpha_{11}m_1}; X_2^2 = \frac{C^2}{\alpha_{22}m_2}; \dots; X_n^2 = \frac{C^2}{\alpha_{nn}m_n}, \quad (5)$$

$$\xi^2 = \frac{1}{C^2\omega^2}, \quad (6)$$

where  $C$  is an arbitrary constant. Then the determinant appears in the following form:

$$\begin{vmatrix} 1 - \xi^2 X_1^2, & \frac{\alpha_{12}}{\alpha_{22}}, & \dots, & \frac{\alpha_{1n}}{\alpha_{nn}}, \\ \frac{\alpha_{21}}{\alpha_{11}}, & 1 - \xi^2 X_2^2, & \dots, & \frac{\alpha_{2n}}{\alpha_{nn}}, \\ \dots & \dots & \dots & \dots \\ \frac{\alpha_{n1}}{\alpha_{11}}, & \frac{\alpha_{n2}}{\alpha_{22}}, & \dots, & 1 - \xi^2 X_n^2. \end{vmatrix} = 0. \quad (7)$$

This is the form of the determinantal equation to which the simplified treatment will be applied.

\* Howland, Phil. Mag. p. 513, March 1927, describes a method for obtaining the determinantal equation by means of the integral equation and graphical integration, which appears useful for many problems where the systems are not readily subdivided into distinct mass concentrations.

If the coupling terms were all zero, the quantities  $X_1, X_2, \dots, X_n$  would represent the principal frequencies of the system—that is, they would then be the  $n$  positive roots in  $\frac{1}{\xi}$  of the equation (7). The units in which these frequencies are expressed depend upon the constant  $C$ ;  $C=1$  expresses the quantities as circular frequencies,  $C=\frac{1}{2\pi}$  as cycles per second, and  $C=\frac{30}{\pi}$  as cycles per minute. There will be no ambiguity in retaining the symbol  $\omega$  for the principal frequencies expressed in any of these units.

It has been found convenient to give these quantities a certain significance, even in those cases when the coupling terms are not zero. In the following they will be denoted as *component frequencies*. In many practical problems they represent rough approximations to the principal frequencies, in which cases they correspond to a set of quasi-principal modes of motion. However, the conception is in no way limited by the degree of approximation.

The chief function of these component frequencies is to furnish a convenient medium for expressing the principal frequencies. All the terms in equation (7) are non-dimensional, so that any convenient set of units may be used for expressing the component frequencies; the roots in  $\omega$  will then appear in the same units. The constants  $\alpha$  are usually very small numbers and, for this reason, inconvenient to carry along in the expansion of the determinant. This objection is eliminated by the form (7) because it contains only ratios of quantities of the same order. Of equal importance is the fact that the determinant is expressed in terms of elastic constants, the masses appearing only through the component frequencies. The advantage of this point will appear in connexion with the expansion and solution of the determinant.

## 2. *Torsional Vibrations in Shafts.*

Consider next the problem of determining the natural frequencies in torsion of a shaft carrying  $n+1$  mass concentrations (fig. 2). The positions of the bearings and their elastic properties do not enter into this problem.

We shall denote the rigidities of the shaft elements (in twisting moment per radian deflexion) by  $k_1, k_2, \dots, k_n$ . The moments of inertia of the masses, with respect to the axis of the shaft, will be denoted by  $m_1, m_2, \dots, m_{n+1}$ . Denoting by





54 Mr. Soderberg : *Practical Application of the Theory of*  
 where the inertia constants  $\alpha$  have the values :

$$a_{pp} = \frac{\sum_1^p m \sum_1^{n+1} m}{\sum_1^{n+1} m}, \quad . . . . . (12)$$

$$a_{pq} = a_{qp} = \frac{\sum_1^p m \sum_{q+1}^{n+1} m}{\sum_1^{n+1} m} \text{ when } p < q. \quad . . . (13)$$

It is evident from this result that the principal constants  $a_{pp}$  are made up from an imaginary system with *two* rigid masses :  $\sum_1^p m$  on the left of  $\theta_p$ , and  $\sum_{p+1}^{n+1} m$  on the right of  $\theta_p$ . The coupling constants  $a_{pq}$  are made up from an imaginary system with *three* rigid masses:  $\sum_1^p m$  on the left of  $\theta_p$ ,  $\sum_{p+1}^q m$  between  $\theta_p$  and  $\theta_q$ , and  $\sum_{q+1}^{n+1} m$  on the right of  $\theta_q$ , only the outer elements entering into  $a_{pq}$ . The notations are such that  $a_{pq}$  is formed for  $p < q$ , and  $a_{pq} = a_{qp}$ . These conclusions are easily verified by developing the equations for a system with three masses. Thus the quasi-principal modes of vibrations are obtained by dividing the system into all possible combinations of three-mass systems\*.

The determinantal equation for this system can now be written in the form :

$$\begin{vmatrix} k_1 - a_{11}\omega^2, & -a_{12}\omega^2, & \dots, & -a_{1n}\omega^2, \\ -a_{21}\omega^2, & k_2 - a_{22}\omega^2, & \dots, & -a_{2n}\omega^2, \\ \dots & \dots & \dots & \dots \\ -a_{n1}\omega^2, & -a_{n2}\omega^2, & \dots, & k_n - a_{nn}\omega^2. \end{vmatrix} = 0. \quad (14)$$

By dividing each column by

$$-a_{11}\omega^2, \quad -a_{22}\omega^2, \quad \dots, \quad -a_{nn}\omega^2,$$

respectively, and putting

$$X_1^2 = C^2 \frac{k_1}{a_{11}}; \quad X_2^2 = C^2 \frac{k_2}{a_{22}}; \quad \dots; \quad X_n^2 = C^2 \frac{k_n}{a_{nn}} \quad . \quad (15)$$

and

$$\xi^2 = \frac{1}{C^2 \omega^2}, \quad . . . . . (16)$$

\* This representation of the general torsion problem has been used by Zerkowitx and Wydler. See Hans Wydler, 'Dreheschwingungen in Kolbenmaschinenanlagen,' Julius Springer, 1922.

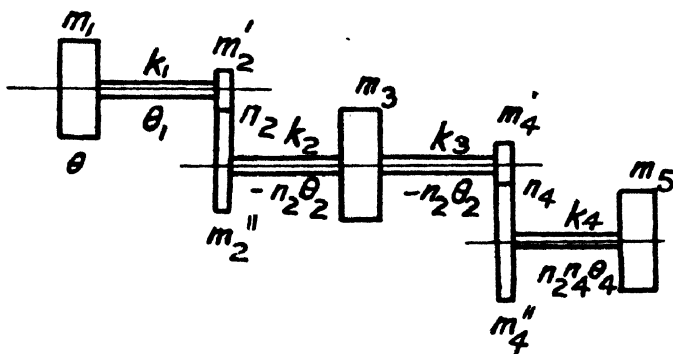
we now obtain

$$\begin{vmatrix} 1 - \xi^2 X_1^2, & \frac{a_{12}}{a_{22}}, & \dots, & \frac{a_{1n}}{a_{nn}}, \\ \frac{a_{21}}{a_{11}}, & 1 - \xi^2 X_2^2, & \dots, & \frac{a_{2n}}{a_{nn}}, \\ \dots & \dots & \dots & \dots \\ \frac{a_{n1}}{a_{11}}, & \frac{a_{n2}}{a_{22}}, & \dots, & 1 - \xi^2 X_n^2. \end{vmatrix} = 0. \quad (17)$$

This determinant is identical in form with (7), but the constants  $a$  now refer to the mass configuration, while the shaft constants  $k$  appear only through the component frequencies  $X$ .

An important variation of the torsion problem occurs in those cases where the different sections of the shaft are connected by gears. Fig. 3 is an example of such a system,

Fig. 3.



Torsional Vibrations of a System of Concentrated Masses on Gearing Sections of Elastic Shaft.

where the mass  $m_2'$  is geared to  $m_2''$  by a gear ratio  $n_2$ , and the mass  $m_4'$  is geared to  $m_4''$  by a gear ratio  $n_4$ . It will be found that the treatment of systems of this type is identical with that of the simple system, by virtue of the fact that it is always possible to replace the geared system by a simple direct-connected system. The correspondence is best shown by evaluating the kinetic and potential energies for the

56 Mr. Soderberg : *Practical Application of the Theory of* system in fig. 3. With the notations suggested in fig. 3 it is found that

$$T = \frac{1}{2}m_1\dot{\theta}^2 + \frac{1}{2}(m_2' + n_2^2m_2'')(\dot{\theta} + \dot{\theta}_1)^2 + \frac{1}{2}m_3n_2^2(\dot{\theta} + \dot{\theta}_1 + \dot{\theta}_2)^2 + \\ + \frac{1}{2}(m_4' + n_4^2m_4'')n_2^2(\dot{\theta} + \dot{\theta}_1 + \dot{\theta}_2 + \dot{\theta}_3)^2 + \\ + \frac{1}{2}m_5n_2^2n_4^2(\dot{\theta} + \dot{\theta}_1 + \dot{\theta}_2 + \dot{\theta}_3 + \dot{\theta}_4)^2, \quad \dots \quad (18)$$

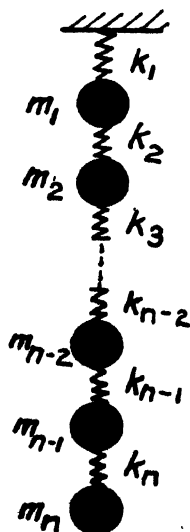
$$V = \frac{1}{2}k_1\theta_1^2 + \frac{1}{2}k_2n_2^2\theta_2^2 + \frac{1}{2}k_3n_2^2\theta_3^2 + \frac{1}{2}k_4n_2^2n_4^2\theta_4^2; \quad \dots \quad (19)$$

from which expression it is evident that the determinantal equation will obtain the form (17). It is merely necessary to modify the inertia and the shaft constants in an appropriate manner. The most reliable method for this modification is obtained by writing the expressions for  $T$  and  $V$  before the determinant (17) is formed.

### 3. *Vibrations in other Configurations.*

Considering, finally, the general types of systems encountered in engineering problems, it is usually possible to apply either one of the treatments given above.

Fig. 4.



Example of Mechanical System.

Fig. 4 illustrates a frequently re-occurring system, where  $n$  masses are connected in series by springs. This system is merely a general case of that shown in fig. 2, and it is so

simple that it is hardly necessary to outline the steps which lead to the determinantal equation. It is worthy of note, however, that the determinantal equation for this system may be made to take the form (7), where all terms, outside of the principal diagonal, are expressed through the elastic constants of the springs. In order to obtain this form, it is merely necessary to select as coordinates the absolute displacements of the masses, and either apply the method given for fig. 1 or write the Lagrangian equations in the usual manner. It is found that the constants  $\alpha$  take the values:

$$\alpha_{pp} = \sum_1^p \frac{1}{k} \quad . \quad . \quad . \quad . \quad . \quad . \quad . \quad (20)$$

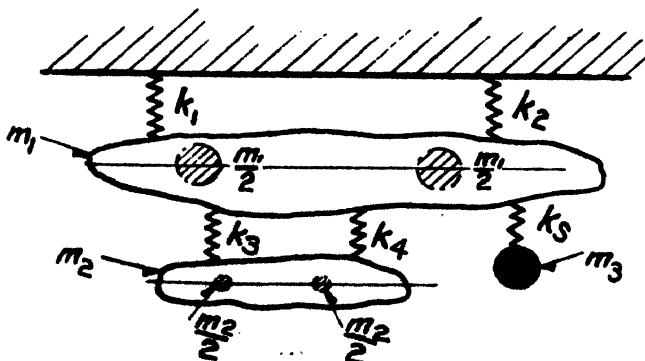
and  $\alpha_{pq} = \alpha_{qp} = \sum_1^p \frac{1}{k} \quad \text{when } p < q. \quad . \quad . \quad . \quad (21)$

The determinantal equation may also be written in such a manner that all terms, outside of the principal diagonal, are expressed through the masses (equation 17). In order to obtain this form, it is merely necessary to select as coordinates the relative displacements of the masses and write the Lagrangian equations of motion. The constants  $\alpha$  take the values:

$$\alpha_{pp} = \sum_p^n m \quad . \quad . \quad . \quad . \quad . \quad . \quad . \quad (22)$$

and  $\alpha_{pq} = \alpha_{qp} = \sum_p^n m \quad \text{when } p < q. \quad . \quad . \quad . \quad (23)$

Fig. 5.



Example of Mechanical System.

Fig. 5 illustrates another type of system which frequently occurs in studies of machine foundations. The masses  $m_1$

and  $m_s$  are assumed to vibrate with small amplitudes in the plane of the paper, the possible displacements being along the directions of the springs, so that this particular system has five degrees of freedom. This type of system may also be made to yield a determinantal equation of either the form (7) or (17). In the former case the absolute displacements of the equivalent masses, and in the latter case the extensions of the springs, are taken as coordinates.

### III. SOLUTION OF THE DETERMINANTAL EQUATION.

It is seen, therefore, that the determinantal equation for any of those systems which we have considered, and which constitute the major portion of important engineering problems, may be written in the form

$$\begin{vmatrix} 1 - \xi^2 X_1^2 & \frac{a_{12}}{a_{22}} & \dots & \frac{a_{1n}}{a_{nn}} \\ \frac{a_{21}}{a_{11}} & 1 - \xi^2 X_2^2 & \dots & \frac{a_{2n}}{a_{nn}} \\ \dots & \dots & \dots & \dots \\ \frac{a_{n1}}{a_{11}} & \frac{a_{n2}}{a_{22}} & \dots & 1 - \xi^2 X_n^2 \end{vmatrix} = 0, \quad (24)$$

where the constants  $a$  may be either elastic constants or inertia constants.  $\xi$  represents the inverse value of the principal frequencies to be determined, and the quantities  $X$  represent the component frequencies, obtained by considering certain obvious modes of oscillation. They may or may not constitute close approximations to the principal frequencies, and the process of the solution may be considered as a process of converting the component frequencies  $X$  into principal frequencies.

Expanding the determinant in descending powers of  $\xi$ , we obtain

$$\begin{aligned} & (-1)^n \left[ \xi^{2n} - \xi^{2n-2} \sum_{p=1}^n \frac{1}{X_p^2} + \xi^{2n-4} \sum_{p=1}^n \sum_{q=1}^n \frac{D_{pq}}{X_p^2 X_q^2} - \right. \\ & \left. - \xi^{2n-6} \sum_{p=1}^n \sum_{q=1}^n \sum_{r=1}^n \frac{D_{pqr}}{X_p^2 X_q^2 X_r^2} + \dots - \frac{D}{X_1^2 X_2^2 \dots X_n^2} \right] = 0, \quad (25) \end{aligned}$$

where the summations are extended over the possible permutations of  $n$  terms, each permutation taken once only.



is useful, even when the roots are to be evaluated by solving equation (29). The form of the constants  $S$  is so uniformly symmetrical that there are no difficulties in evaluating them directly from the determinant, nor, in many cases, from the expressions for the static equilibrium, or the kinetic and potential energy.

However, the main advantage of this method of expansion lies in the fact that it is possible to derive a simple graphical method for constructing the roots from the quantities  $S$ . This method will be explained successively for two, three, and several degrees of freedom.

For systems with two degrees of freedom we have

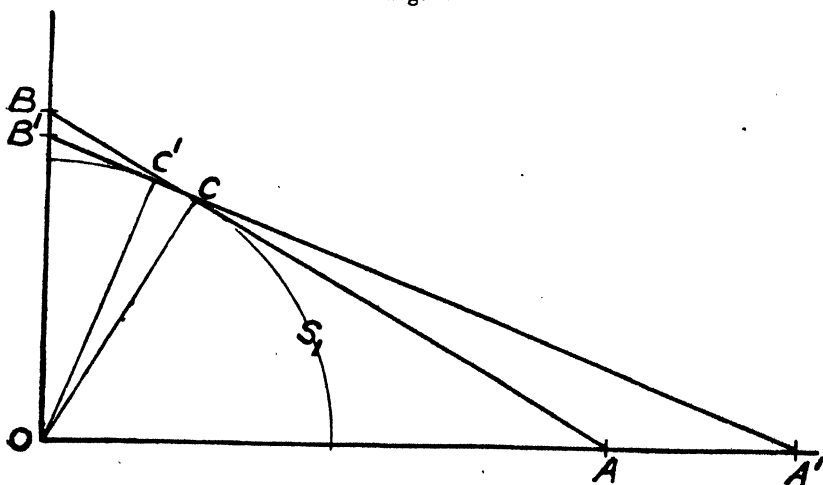
$$\frac{1}{\omega_1^2} + \frac{1}{\omega_2^2} = \frac{1}{X_1^2} + \frac{1}{X_2^2} = \frac{1}{S_1^2}, \quad \dots \quad (30)$$

$$\frac{1}{\omega_1^2 \omega_2^2} = \frac{D}{X_1^2 X_2^2} = \frac{1}{S_2^2}, \quad \dots \quad (31)$$

where

$$D = \begin{vmatrix} 1, & \frac{a_{12}}{a_{22}}, \\ \frac{a_{21}}{a_{11}}, & 1, \end{vmatrix} \dots \dots \dots (32)$$

Fig. 6.



Converting Component Frequencies into Principal Frequencies  
for Systems with Two Degrees of Freedom.

Now, if  $X_1 = OA$  and  $X_2 = OB$  are set off along the axes of a rectangular system of coordinates (fig. 6), we find immediately, from equation (30), that the perpendicular  $OC$

to the diagonal AB is equal to  $S_1$ . It is evident that the diagonal A'B', which corresponds to the principal frequencies  $\omega_1 = OA'$  and  $\omega_2 = OB'$ , lies at the same distance from O, so that it is a tangent to the circle  $S_1$ . Consequently, the component frequencies are converted into principal frequencies by rolling the diagonal AB on the circle  $S_1$  until its position satisfies equation (31), when its length is increased to  $A'B' = \frac{AB}{\sqrt{D}}$ . This gives a satisfactory con-

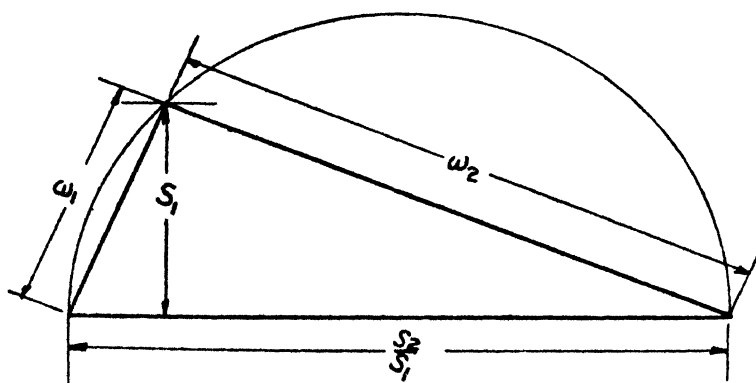
ception of the manner in which the component frequencies differ from the principal frequencies. If, for example,  $X_2$  is much smaller than  $X_1$ , it will change very slightly, even if the coupling factor  $\sqrt{D}$  is far from unity, while  $X_1$  will change considerably. In all cases the lowest of the component frequencies is lowered while the upper is raised.

For practical purposes it is more convenient to use a somewhat modified form of the construction. By dividing equation (31) into (30), we obtain

$$\omega_1^2 + \omega_2^2 = \frac{S_2^2}{S_1^2} \dots \dots \dots (33)$$

Thus, if we draw a semicircle on the base line  $\frac{S_2}{S_1}$  (fig. 7),

Fig. 7.



Graphical Construction of the Principal Frequencies for Two Degrees of Freedom.

and intersect this semicircle by a line parallel to the diameter at a distance  $S_1$ , the latter will give a point which determines the correct values of  $\omega_1$  and  $\omega_2$ .

In spite of the fact that the solution for two degrees of freedom is easily obtained by solving a quadratic equation,



it has been found worth while to use this graphical method, particularly in cases where the solution must be obtained a great number of times for different modifications of the same system.

Considering next a case with three degrees of freedom, we have

$$\frac{1}{\omega_1^2} + \frac{1}{\omega_2^2} + \frac{1}{\omega_3^2} = \frac{1}{X_1^2} + \frac{1}{X_2^2} + \frac{1}{X_3^2} = \frac{1}{S_1^2}, \quad (34)$$

$$\frac{1}{\omega_1^2 \omega_2^2} + \frac{1}{\omega_1^2 \omega_3^2} + \frac{1}{\omega_2^2 \omega_3^2} = \frac{D_{12}}{X_1^2 X_2^2} + \frac{D_{13}}{X_1^2 X_3^2} + \frac{D_{23}}{X_2^2 X_3^2} = \frac{1}{S_2^2}, \quad (35)$$

$$\frac{1}{\omega_1^2 \omega_2^2 \omega_3^2} = \frac{D}{X_1^2 X_2^2 X_3^2} = \frac{1}{S_3^2}, \quad (36)$$

where

$$D = \begin{vmatrix} 1, & \frac{a_{12}}{a_{22}}, & \frac{a_{13}}{a_{33}} \\ \frac{a_{21}}{a_{11}}, & 1, & \frac{a_{23}}{a_{33}} \\ \frac{a_{31}}{a_{11}}, & \frac{a_{32}}{a_{22}}, & 1, \end{vmatrix}; \quad D_{12} = \begin{vmatrix} 1, & \frac{a_{12}}{a_{22}} \\ \frac{a_{21}}{a_{11}}, & 1, \end{vmatrix}; \quad (37)$$

$$D_{13} = \begin{vmatrix} 1, & \frac{a_{13}}{a_{33}} \\ \frac{a_{31}}{a_{11}}, & 1, \end{vmatrix}; \quad D_{23} = \begin{vmatrix} 1, & \frac{a_{23}}{a_{33}} \\ \frac{a_{32}}{a_{22}}, & 1, \end{vmatrix}$$

Using a representation similar to the one shown on fig. 6 for a three-dimensional system of coordinates, it is evident that the three component frequencies are converted into principal frequencies by rolling the diagonal plane ABC on the sphere  $S_1$  until it is changed into the plane A'B'C', satisfying equations (35) and (36).

The practical solution by graphical construction corresponds to the one given in fig. 7, and is carried out in the following manner.

Dividing equation (36) into (35), we obtain

$$\omega_1^2 + \omega_2^2 + \omega_3^2 = \frac{S_3^2}{S_2^2} \quad (38)$$

Substituting from equations (34) and (36) in (35), the latter may be written in the following form :

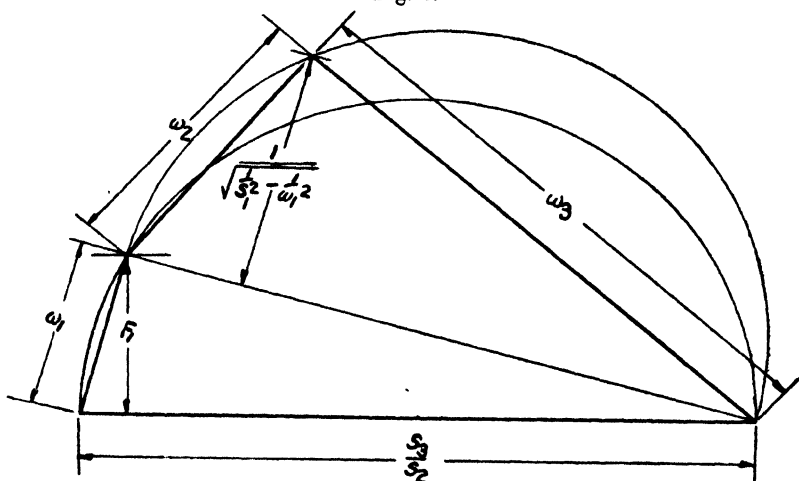
$$\frac{1}{\omega_1^2} + \frac{1}{\omega_2^2 + \omega_3^2} = \frac{1}{S_2^2 \left[ \frac{1}{S_1^2} - \frac{1}{\omega_1^2} \right]} = \frac{1}{p_1^2}, \quad (39)$$

so that

$$p_1 = S_2 \sqrt{\frac{1}{S_1^2} - \frac{1}{\omega_1^2}} \quad \dots \quad (40)$$

Now, drawing a semicircle on the base line  $\frac{S_2}{S_2}$  (fig. 8), we try several values of  $\omega_1$  (starting with a value slightly

Fig. 8.



Graphical Construction of the Principal Frequencies for Three Degrees of Freedom.

above  $S_1$ ) in equation (40) until the graphical construction yields a value of  $\omega_1$  equal to the assumed value, when  $\omega_1$  is established. The remaining chord in the semicircle now has the length  $\sqrt{\omega_2^2 + \omega_3^2}$ , and the remaining frequencies are obtained by drawing a new semicircle over this distance and intersecting it at a distance equal to

$$\frac{1}{\sqrt{\frac{1}{S_1^2} - \frac{1}{\omega_1^2}}},$$

which has already been established in finding  $\omega_1$ .

The construction for three degrees of freedom is thus characterized by one operation based on cut and trial, and a second on straightforward construction. Naturally, it is also possible to obtain all three roots by cut and trial, but this method possesses no marked advantage over the solution of the cubic.

No attention has been given so far to the order in which the roots are obtained. Naturally it is not always necessary that the roots appear in the order of magnitude as shown on fig. 8. This feature is of no consequence, as long as the result consists of a polygon  $\omega_1 - \omega_2 - \omega_3$ , closed by the base line  $S_3/S_2$ .

The process just given for three degrees of freedom establishes a pattern which can be followed for any number of roots. The number of cuts and trials is always two less than the number of roots.

In the general case, with  $n$  degrees of freedom, we have  $n$  equations, giving the relations between the inverse squares of the frequencies in terms of the quantities  $S_1, S_2, \dots, S_n$ . The two last equations can be combined into

$$\sum_{p=1}^n \omega_p^2 = \frac{S_n^2}{S_{n-1}^2}, \quad \dots \quad (41)$$

which establishes the base line  $S_n/S_{n-1}$ . Now, if we want to solve for a certain root  $\omega_1$ , we obtain the corresponding perpendicular from the base line  $p_1$  by rearranging the  $(n-1)$ th equation into

$$\begin{aligned} & \frac{1}{\omega_1^2} + \frac{1}{\sum_{p=2}^n \omega_p^2} \\ &= \frac{1}{S_{n-1}^2 \left\{ \frac{1}{S_{n-2}^2} - \frac{1}{\omega_1^2} \left[ \frac{1}{S_{n-3}^2} - \frac{1}{\omega_1^2} \left( \dots - \frac{1}{\omega_1^2} \left( \frac{1}{S_1^2} - \frac{1}{\omega_1^2} \right) \right) \right] \right\}}; \end{aligned} \quad (42)$$

that is,

$$p_1 = S_{n-1} \sqrt{\frac{1}{S_{n-2}^2} - \frac{1}{\omega_1^2} \left[ \frac{1}{S_{n-3}^2} - \frac{1}{\omega_1^2} \left( \dots - \frac{1}{\omega_1^2} \left( \frac{1}{S_1^2} - \frac{1}{\omega_1^2} \right) \right) \right]}. \quad (43)$$

When the root  $\omega_1$  is found a new base line is obtained, and a new set of constants  $t$ , corresponding to  $S$ , are immediately given. It is evident that

$$\frac{1}{t_1^2} = \frac{1}{S_1^2} - \frac{1}{\omega_1^2}, \quad \dots \quad (44)$$

$$\frac{1}{t_2^2} = \frac{1}{S_2^2} - \frac{1}{\omega_1^2} \left( \frac{1}{S_1^2} - \frac{1}{\omega_1^2} \right), \quad \dots \quad (45)$$

$$\frac{1}{t_{n-2}^2} = \frac{1}{S_{n-2}^2} - \frac{1}{\omega_1^2} \left[ \frac{1}{S_{n-3}^2} - \frac{1}{\omega_1^2} \left( \dots - \frac{1}{\omega_1^2} \left( \frac{1}{S_1^2} - \frac{1}{\omega_1^2} \right) \right) \right]. \quad (46)$$

These constants were all established in the process of finding  $\omega_1$ .

The perpendicular to the new base line, which determines  $\omega_2$ , is now given by

$$p_2 = t_{n-2} \sqrt{\frac{1}{t_{n-3}^2} - \frac{1}{\omega_2^2} \left[ \frac{1}{t_{n-4}^2} - \frac{1}{\omega_2^2} \left( \dots - \frac{1}{\omega_2^2} \left( \frac{1}{t_1^2} - \frac{1}{\omega_2^2} \right) \right) \right]}. \quad \dots (47)$$

As soon as  $\omega_2$  is given, a new base line is drawn, and a new set of constants  $u$  are determined in the same manner. The process is repeated until only  $\omega_{n-1}$  and  $\omega_n$  remain; these are obtained directly by intersecting the corresponding semicircle by the perpendicular

$$p_{n,n-1} = \frac{1}{\sqrt{\frac{1}{S_1^2} - \sum_{p=1}^{n-3} \frac{1}{\omega_p^2}}}. \quad \dots (48)$$

Certain general conclusions as to the approximate magnitude of the roots are obtained from the semi-principal frequencies and from the equations (28). It is evident from the first equation, which is nothing but the usual Dunkerley formula, that no root can be smaller than  $S_1$ ; in the case of a large number of roots,  $S_1$  will have a value very near to the lowest. Similarly, there can be no root greater than  $S_n/S_{n-1}$ , but the largest root is usually considerably below this value.

The question of accuracy of the result is of paramount importance. It is evident that the construction suffers from accumulation of errors for the higher roots. The author has found that, with reasonably careful drawing work on letter-size paper, the accuracy is quite sufficient for practical purposes, at least up to five or six roots. It is a general feature of most practical problems that only a few of the lower roots are of practical interest, so that it is not believed that the lack of accuracy will prohibit the use of the method for ordinary analysis of practical problems.

The major part of the arithmetical work is involved in the evaluation of the determinants and the subsequent calculation of the factors  $S$ . One of the most important advantages of the method lies in the circumstance that the determinants may usually be made to express either the elastic properties or the inertia properties of the system. In most engineering problems it is a question of obtaining a series of solutions for different magnitudes of the various elements. Sometimes it is required to find a suitable set of elastic properties for a given set of inertia, whilst at other times (perhaps more rarely) it may be desired to find a suitable set of masses for a given set of elastic constants. In such cases, and they constitute the most important and

most fruitful aspect of vibration analysis, it is possible to arrange the analysis so that the evaluation of the determinants is carried out once only, while the adjustment of the system is expressed by variations in the component frequencies.

#### IV. NUMERICAL EXAMPLES.

Figs. 9 and 10 have been given as examples of calculations for two representative cases.

Fig. 9 is a calculation of the whirling speeds of a turbine generator mounted in three bearings. The calculation has been carried out both for the case of perfectly rigid bearings and for the case of a practical set of values for the bearing flexibilities. In this problem it is possible to replace the system by three concentrated masses. The turbine spindle is comparatively short, so that the frequencies corresponding to its second mode of motion are very high. For this reason it is sufficiently accurate to represent it as a single mass,  $m_3$ . The generator rotor, on the other hand, is comparatively long, and here it is necessary to consider its second mode of motion. As a matter of interest, this particular rotor was analysed because the whirling speed corresponding to the second mode of motion of the generator rotor comes quite close to the operating speed (3600 R.P.M.).

The bearing flexibilities  $\delta$  have values of the same order as those found on similar installations, and they represent bearing conditions which can be approximated only by a very robust design.

The influence factors  $\alpha$  have been determined by graphical analysis of the actual rotor shaft. The positions of the equivalent masses were found by computing the radius of gyration of the middle body \*. It is of interest to note that for rotors of this type the treatment suggested by Rodgers gives results in close agreement with more rigorous methods for the determination of the second whirling speed, as given by Stodola†.

The calculation is self-explanatory. It is evident from the results that the bearing flexibility assumed does lower the fundamental critical speed an appreciable amount.

Fig. 10 is an example of a calculation of critical frequencies for torsion in a system of five masses. This example was selected from a Diesel electric ship drive.

These diagrams were drawn on base lines of about 6 inches in length, and the accuracy is, in all cases, well within 1 per cent. of the true values obtained by arithmetical computation.

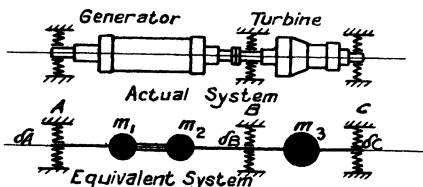
\* See Rodgers, *Phil. Mag.* p. 122, July 1922.

† Stodola, *'Dampf und Gasturbinen,'* p. 386.



FIG. 9.—Calculation of Whirling Speeds.

Calculation of Whirling Speeds in Three-bearing Machine.



Properties of the System.

Masses Lb.	Flex. Brg. Inches/Pound.	System Constants—Rigid Brgs. Inches/Pound.		System Constants—Flex. Brgs. Inches/Pound.	
$m_g = 8000$	$\delta_A = 1 \times 10^{-6}$	$a_{11} = 1.370 \times 10^{-6}$	$a_{12} = a_{21} = 1.014 \times 10^{-6}$	$a_{11} = 1.770 \times 10^{-6}$	$a_{12} = a_{21} = 1.232 \times 10^{-6}$
$m_g = 8000$	$\delta_B = 1$ "	$a_{22} = 1.024$ "	$a_{12} = a_{21} = -.0933$ "	$a_{22} = 1.174$ "	$a_{12} = a_{21} = -.0796$ "
$m_g = 10700$	$\delta_C = 1$ "	$a_{33} = .1418$ "	$a_{23} = a_{32} = -.1888$ "	$a_{33} = .1930$ "	$a_{23} = a_{32} = -.1024$ "

Calculations for Rigid Bearings.

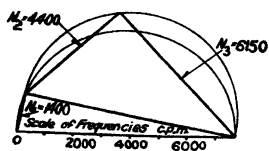
Comp. Freq.		Determinants.				Trials for $N_1$ .			
$X_p$ c.p.m.	$\frac{1}{X_p}$	$D_{pq}$	$\frac{D_{pq}}{X_p^2 X_q^2}$	D.	$\frac{D}{X_1^2 X_2^2 X_3^2}$	Term.	1st Trial.	2nd Trial.	3rd Trial.
$X_1 = 1789$	$.318 \times 10^{-6}$	$D_{11} = .266$	$.0195 \times 10^{-12}$	...	...	$N_1$	1450	1400	
$X_2 = 2068$	.233 "	$D_{12} = .955$	.0129 "	$D = .2208$	$.0007 \times 10^{-12}$	$\frac{1}{S_1} - \frac{1}{N_1^2}$	$.1143 \times 10^{-6}$	$.0782 \times 10^{-6}$	
$X_3 = 4810$	.043 "	$D_{23} = .868$	.0088 "	...	...	$P_1$	1670	1375	
$\Sigma \frac{1}{X_p^3} = .589 \times 10^{-6}$		$\Sigma \frac{D_{pq}}{X_p^2 X_q^2} = .0412 \times 10^{-12}$		.....		$N_1$	1700	1400	
$S_1 = 1305$		$S_2 = 4.93 \times 10^6$		$S_3 = 37.80 \times 10^9$		$S_2/S_3 = 7690$ $N_1 = 1400$			

Calculation for Flexible Bearings.

Comp. Freq.		Determinants.				Trials for $N_1$ .			
$X_p$ c.p.m.	$\frac{1}{X_p}$	$D_{pq}$	$\frac{D_{pq}}{X_p^2 X_q^2}$	D.	$\frac{D}{X_1^2 X_2^2 X_3^2}$	Term.	1st Trial.	2nd Trial.	3rd Trial.
$X_1 = 1875$	$.405 \times 10^{-6}$	$D_{12} = .268$	$.0291 \times 10^{-12}$	...	...	$N_1$	1300	1260	1265
$X_2 = 1931$	.268 "	$D_{13} = .981$	.0233 "	$D = .2633$	$.00162 \times 10^{-12}$	$\frac{1}{S_1} - \frac{1}{N_1^2}$	$.140 \times 10^{-6}$	$.0710 \times 10^{-6}$	$.1031 \times 10^{-6}$
$X_3 = 4120$	.059 "	$D_{23} = .964$	.0151 "	...	...	$P_1$	1445	1025	1235
$\Sigma \frac{1}{X_p^3} = .732 \times 10^{-6}$		$\Sigma \frac{D_{pq}}{X_p^2 X_q^2} = .0675 \times 10^{-12}$		.....		$N_1$	1500	1060	1268
$S_1 = 1170$		$S_2 = 3.85 \times 10^6$		$S_3 = 24.85 \times 10^9$		$S_2/S_3 = 6450$ $N_1 = 1265$			

Graphical Constructions.

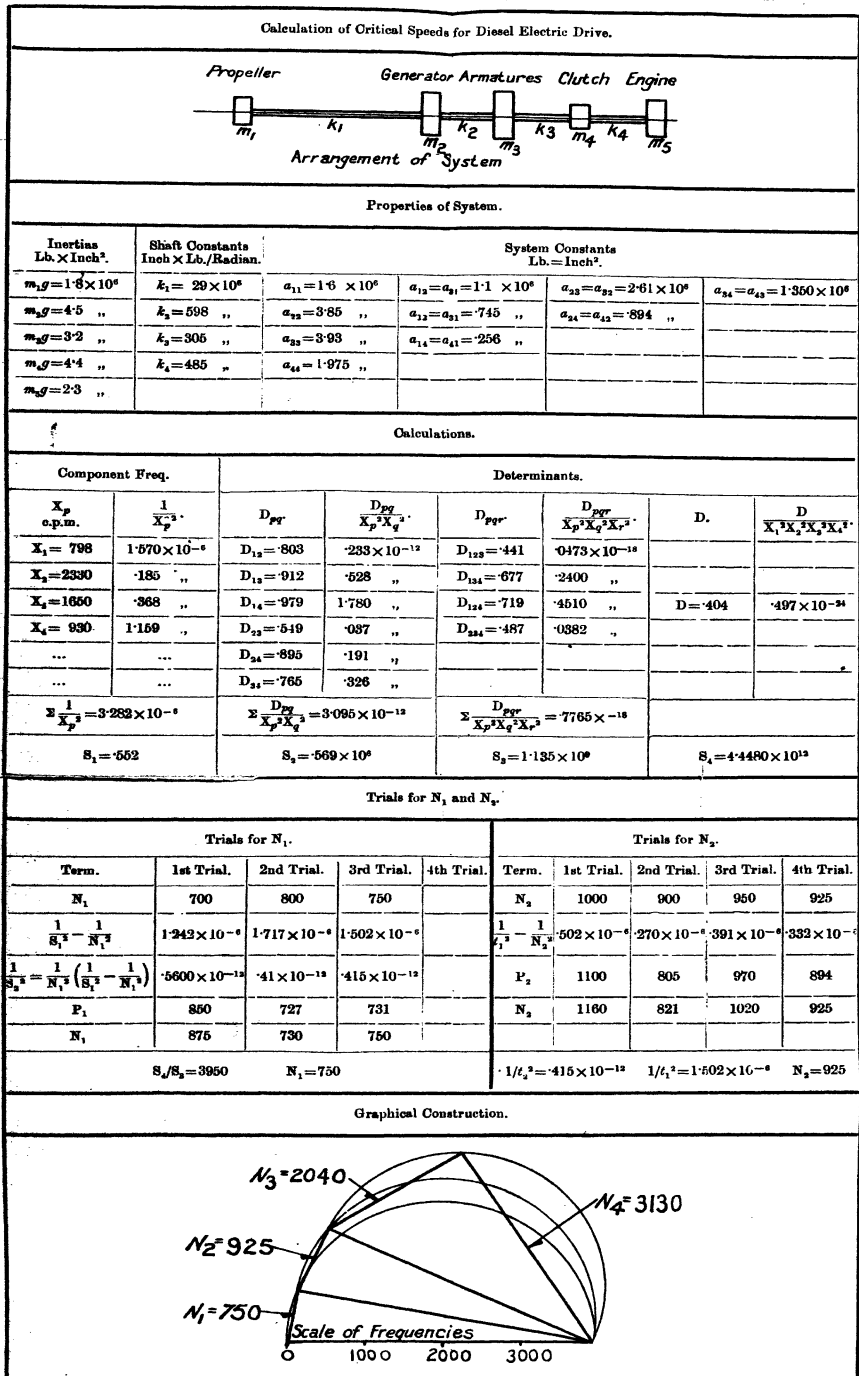
For Rigid Bearings



For Flexible Bearings



Fig. 10.—Example of Calculation of Natural Frequencies for Torsional Vibrations.







V. *On the Emission of Positive Electricity from Hot Tungsten in Mullard Radio Valves.* By PHANINDRA KUMAR MITRA, M.Sc.\*

**I**N a recent paper † Prof. W. A. Jenkins has shown that there is a copious emission of positive electricity from a hot tungsten wire which forms the anticathode of a Coolidge Tube at a very high temperature (beginning from about  $2000^{\circ}\text{C.}$  to  $3500^{\circ}\text{C.}$ , i. e., up to the melting-point of tungsten). The present investigator worked on the same lines, but with Mullard radio valves instead of with Coolidge tubes, partly because of the high price of Coolidge tubes and partly because with Mullard radio valves different types of cathodes of various sizes could be used with advantage. The present paper is an account of the variation of positive emission (i.) with temperature, (ii.) with applied potential difference; and (iii.) of growth and (iv.) decay of positive emission current with time under various conditions.

The arrangement of apparatus is, however, different from that used by Prof. Jenkins. In his arrangement he balanced the difference of potentials between the ends of a hot tungsten wire against the E.M.F. of a 2-volt storage cell, and knowing the current flowing through the tungsten wire, calculated its resistances when different currents were flowing through it. But in the present case an arrangement exactly similar to that used by Richardson ‡ has been made. The hot wire forms the fourth arm of a Wheatstone's bridge, two resistance boxes being made the first two arms, while a wire of low temperature-coefficient placed in a constant-temperature oil-bath forms the third arm of the bridge. The arrangement is shown below.

P, Q are two resistance boxes from which resistances of the order of  $10,000^{\omega}$  are generally unplugged. R is a non-inductive wire resistance of low temperature-coefficient placed in an oil-bath at constant temperature. T is a sensitive thermometer which shows any variation in temperature of the bath. The bath is placed on a vessel V provided with water-cooling arrangement. S is the tungsten anode of a Mullard radio valve, while C is made the cathode.  $G_1$  is a galvanometer of the order of  $10^{-8}$  ampere per 1 mm. division. X is a set of batteries of 12 2-volt accumulators. It supplies the heating current, as well as the current necessary for Wheatstone's net arrangement. P, Q being moderately

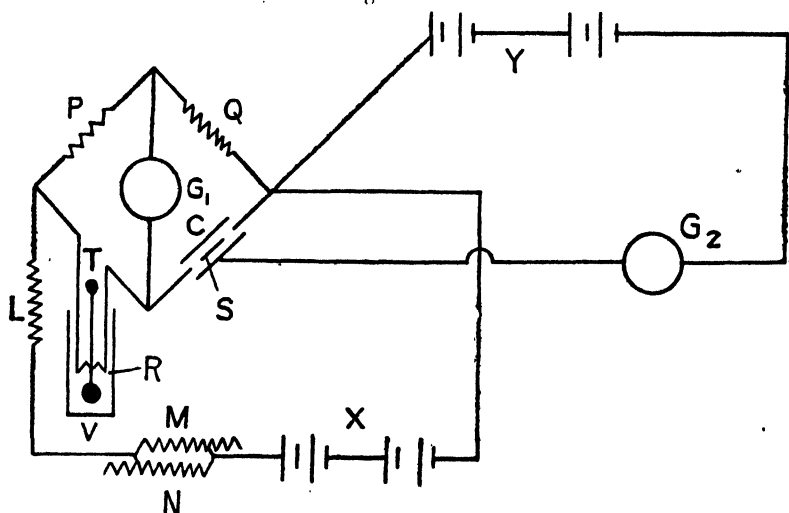
\* Communicated by Prof. S. N. Bose, M.Sc.

† Phil. Mag. (6) xlvii. p. 1025.

‡ Richardson, 'Emission of Electricity from Hot Bodies,' p. 16.

high resistances, the major part of the current passes through R and S. L is a resistance in the battery circuit for adjustment of current; while M, N, two resistances joined in parallel, are meant for fine adjustment of current.  $G_1$  is a very high-sensitivity galvanometer of the order of  $10^{-10}$  ampere per 1 mm. division used to measure the positive emission current. Y is a set of Exide batteries from which voltage from 2 to 200 could be easily and conveniently applied. The positive terminal of Exide batteries is joined with the anode, while the negative one is joined through the high-sensitivity galvanometer with the cathode of the radio valve.

Fig. 1.



In working with this high-sensitivity galvanometer, very great difficulty was experienced in eliminating the leak. In moist weather, even without the application of any voltage at all, a deflexion too great to remain on the scale was sometimes observed. To avoid leakage, the two sets of batteries had to be placed on two different tables, which in their turn were made to stand on ebonite blocks. The working tables as well were insulated by standing them on ebonite blocks. Every individual piece of apparatus was placed on blocks of paraffin wax for the purpose of insulation. Even with these precautions inclement weather affected the arrangement so much that carrying out experiments was out of the question.

# I. Variation of Positive Emission with Temperature.

Keeping the applied voltage constant, the heating current was gradually increased in steps, the positive emission current in each case was determined directly by the deflexion of the high-sensitivity galvanometer, while the balancing-point in the Wheatstone's net was obtained at each successive step by the low-sensitivity galvanometer. Thus the resistances of the tungsten filament could be determined as different currents flowed through it. Its initial resistance being known, temperatures of the filament could be calculated with the help of Langmuir's data\*. Experiments were carried out with valves U 30 Nos. 311 and 312, as well as with U 150 No. 72 and U 250 No. 15. With the first two tubes the initial resistances of the filament could be easily determined, while with the last two the initial resistances could not be accurately known, as the resistances of leads were appreciable and could not be determined without breaking the tubes altogether. Table I. shows the data for the first two tubes. The initial resistance of the first tube was 0.1480 ohm, while that of the second was 0.1481 ohm.

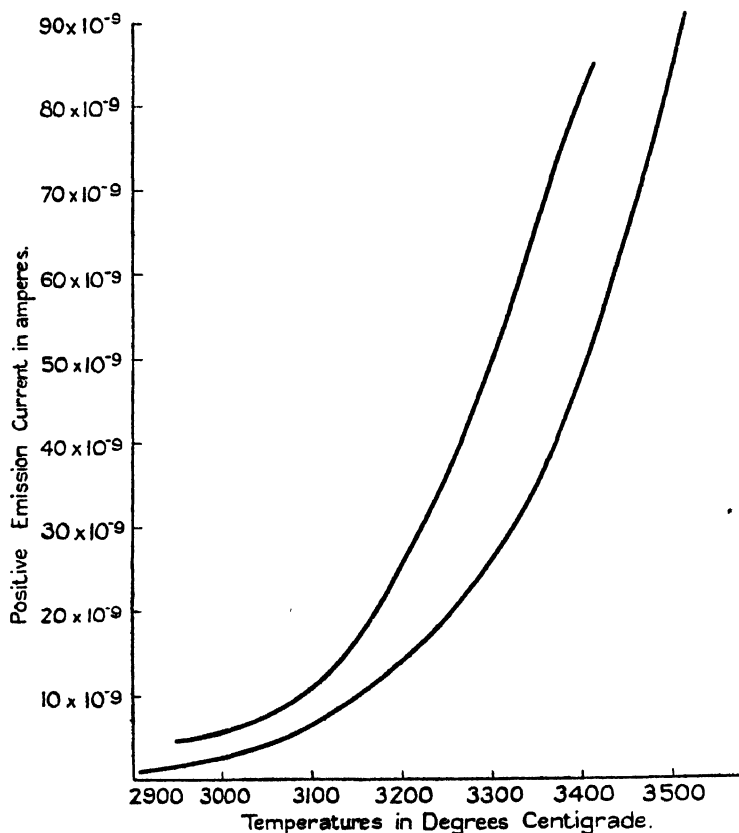
TABLE I.

Tube U 30 No. 311.			Tube U 30 No. 312.		
Resistance of Filament.	Temperature of Filament.	Positive Emission, in amperes.	Resistance of Filament.	Temperature of Filament.	Positive Emission, in amperes.
2.593 <sup>ω</sup>	2946° C.	4.5 × 10 <sup>-9</sup>	2.552 <sup>ω</sup>	2908° C.	1 × 10 <sup>-9</sup>
2.687	3033	7.5 "	2.651	2984	2.5 "
2.768	3108	10 "	2.711	3054	4 "
2.813	3152	16 "	2.834	3150	9.75 "
2.841	3180	21 "	2.949	3280	22.75 "
2.872	3207	27.5 "	3.004	3334	32.25 "
2.899	3235	34 "	3.053	3382	40 ,
2.942	3277	43.5 "	3.094	3420	54 "
2.967	3300	49 "	3.146	3472	71.5 "
3.010	3343	63 "	3.194	3517	92.5 "
3.089	3414	85 "	—	—	—

From fig. 2 it will be seen that emissions from each tube are very nearly similar, and that they increase very rapidly with temperature, more rapidly than linear relation would indicate.

\* Phys. Rev. (2) vii. p. 815.

Fig. 2.



## II. Variation of Positive Emission with Voltage.

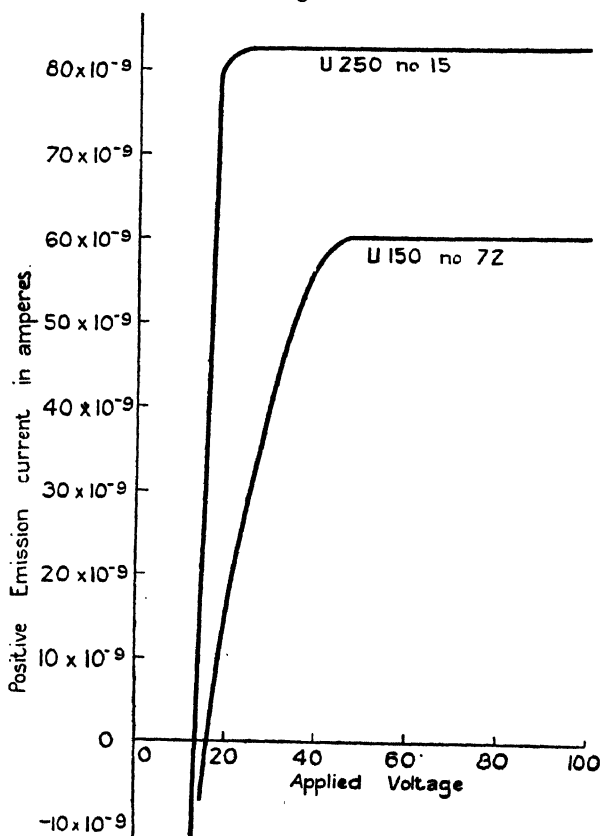
Keeping the heating current constant with the help of adjustable resistances, the applied voltage was successively increased from 2 to 100. With the valve tube U 150 No. 72, an applied voltage below 14 was not sufficient to completely resist the electron current. Even with 14 volts an electron current of  $7.5 \times 10^{-9}$  ampere was obtained. With the application of 16 volts and upwards there was a gradual rise of positive emission current. With tube U 250 No. 15 an applied E.M.F. below 12 volts was not found sufficient to resist the electron current, and even with 12 volts there was an electron current of  $46 \times 10^{-9}$  ampere. With the application of 14 volts and upwards there was a gradual increase of positive emission current. Table II. shows the data giving



the relation between the applied E.M.F. and the positive emission current for the tubes U 250 No. 15 and U 150 No. 72.

It will be readily seen from fig. 3 that a saturation value of the positive emission current is attained with a voltage of 42 with tube U 150 No. 72, while with tube U 250 No. 15

Fig. 3.



the saturation value of the current is attained with the application of 22 volts only. It should be noted, however, that with Coolidge tubes practically no saturation current was obtained.

### III. Growth of Positive and Negative Emission Currents with time.

In these experiments, an E.M.F. sufficient to produce the saturation value of the positive emission current was applied

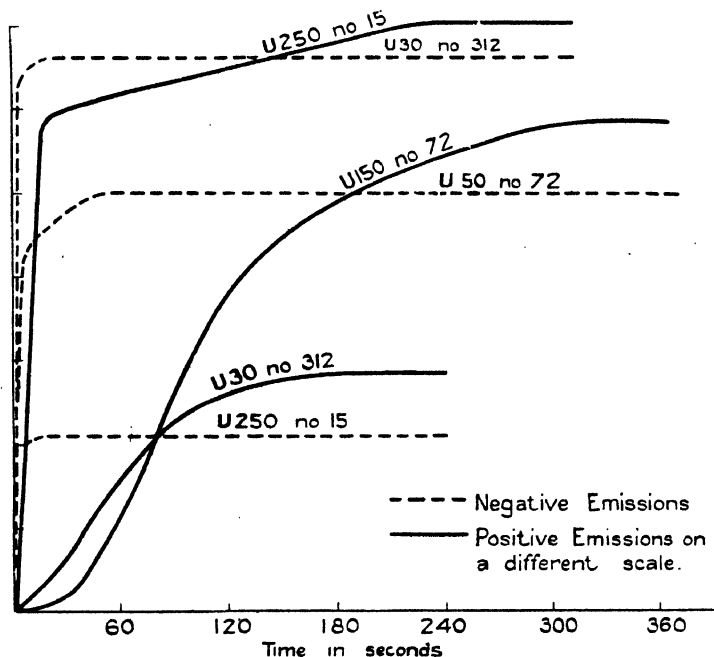
TABLE III.—Experiments with three valves: U 30 No. 312, U 250 No. 15, U 150 No. 72.

Time.	Tube U 30 No. 312. Potential applied, 36 volts.		Tube U 250 No. 15. Potential applied, 24 volts.		Tube U 150 No. 72. Potential applied, 54 volts.	
	Positive Emission Current, in amperes.	Negative Emission Current, in amperes.	Positive Emission Current, in amperes.	Negative Emission Current, in amperes.	Positive Emission Current, in amperes.	Negative Emission Current, in amperes.
5 sec. ....	$2.5 \times 10^{-10}$	$64 \times 10^{-5}$	0	$20 \times 10^{-5}$	0	$42 \times 10^{-5}$
15 sec. ....	7.5	66	$177.5 \times 10^{-10}$	21	$2.5 \times 10^{-10}$	45
30 sec. ....	20	66	180	21	5	48
45 sec. ....	33	66	182.5	21	20	50
1 min. ....	47.5	66	185	21	35	50
1 min. 30 sec. ....	70	66	190	21	80	50
2 min. ....	77.5	66	195	21	115	50
2 min. 30 sec. ....	82.5	66	200	21	135	50
3 min. ....	85	66	202.5	21	145	50
3 min. 30 sec. ....	85	66	207.5	21	155	50
4 min. ....	85	66	210	21	160	50
5 min. ....	—	—	210	21	170	50
6 min. ....	—	—	210	21	175	50
7 min. ....	—	—	—	—	175	50



at first and then the heating current was switched on and kept constant. Table III. and fig. 4 show the relation between the positive or negative emission current with time. It will be seen from fig. 4 that while the negative emission current attains its full value in less than half a minute, it requires from 3 to 6 minutes for the positive emission current to reach its maximum value.

Fig. 4.



#### IV. Decay of Positive Emission Current with time.

The applied potential difference was maintained constant, and was sufficient to produce saturation. The heating current was also kept constant. Tables IV., V., and VI. contain the experimental data showing the decay of positive emission current with time. Figs. 5, 6, and 7 show the characteristic curves for the decay of positive emission current. It will be noticed that the precise form of the current-time curves varies from one specimen of the wire to another. It depends on the previous treatment of the wires as well. The rate of decay is greater at a high temperature than at a low one. The current decays rapidly at first and

TABLE IV.

Type: U 500.

Potential difference applied, 64 volts.

Number of Tube. }	32.	37.	40.
Time, in minutes.	Positive Emission Current, in amperes.	Positive Emission Current, in amperes.	Positive Emission Current, in amperes.
0 .....	$56 \times 5 \times 10^{-10}$	$125 \times 5 \times 10^{-10}$	$182 \times 5 \times 10^{-10}$
5 .....	57 "	123 "	167 .. "
10 .....	54 "	120 "	158 "
20 .....	47 "	115 "	136 "
30 .....	—	112 "	126 "
40 .....	37.5 "	—	—...
45 .....	—	102 "	109 .. "
60 .....	32.5 "	95 "	98 "
90 .....	28 "	87 "	—.....
120 .....	25 "	78.5 "	79 "
180 .....	22 "	—	67.5 "
210 .....	—	69 "	—
240 .....	—	—	62.5 "

TABLE V.

Type of Valve: U 250.

Potential difference applied, 57 volts.

Number of Tube. }	15.	101.	102.	105.	108.
Time, in minutes.	Positive Emission, in amperes.	Positive Emission, in amperes.	Positive Emission, in amperes.	Positive Emission, in amperes.	Positive Emission, in amperes.
0 .....	$129 \times 5 \times 10^{-10}$	$81.5 \times 5 \times 10^{-10}$	$113 \times 5 \times 10^{-10}$	$113 \times 5 \times 10^{-10}$	$71.5 \times 5 \times 10^{-10}$
5 .....	—	79 "	113 "	108 "	56 "
10 .....	—	74.5 "	108 "	101 "	50 "
15 .....	133 "	—	—	—	—
20 .....	—	67.5 "	98.5 "	90 "	41 "
30 .....	121 "	62.5 "	90.5 "	82 "	30 "
45 .....	113 "	55.5 "	83 "	75 "	24 "
60 .....	103 "	49.5 "	76.5 "	69 "	21.5 "
90 .....	90 "	40.5 "	67.5 "	59 "	19.5 "
120 .....	79 "	34.5 "	59.5 "	49 "	15.5 "
150 .....	—	29.5 "	—	—	13.5 "
180 .....	64 "	26.5 "	43 "	34.5 "	12.5 "

TABLE VI.

Type of Tube : U 150.

Potential difference applied 67 volts.

Number of tube. } Time, in minutes.	72. Positive Emission, in amperes.	128. Positive Emission, in amperes.	137. Positive Emission, in amperes.
0 .....	$69 \times 5 \times 10^{-10}$	$83 \times 5 \times 10^{-10}$	$55.5 \times 5 \times 10^{-10}$
5 .....	69 "	82.5 "	53 "
10 .....	68 "	80.5 "	50.5 "
20 .....	64.5 "	77 "	46.5 "
30 .....	61 "	75.5 "	43.5 "
45 .....	57 "	73 "	40 "
60 .....	54 "	71 "	37 "
90 .....	48 "	69 "	33.5 "
120 .....	44 "	68 "	30.5 "
150 .....	40 "	—	—
188 .....	38 "	65 "	27 "

TABLE VII.

Type of Valve : U 250 No. 110.

Applied potential difference 67 volts.

Time.	Positive Emission, in amperes.
0 ..	$232 \times 5 \times 10^{-10}$
5 min. ....	225 "
10 min. ....	216 "
20 min. ....	189 "
30 min. ....	164 "
45 min. ....	143 "
1 hr. ....	127 "
1 hr. 30 min. ...	104 "
2 hrs. ....	90.5 "
3 hrs. ....	74 "
4 hrs. ....	61 "
5 hrs. ....	53 "
—	—
21 hrs. ....	29 "
24 hrs. ....	26 "
29 hrs. ....	23 "
—	—
46 hrs. ....	18 "
49 hrs. ....	17.5 "
54 hrs. ....	17 "

# *Electricity from Hot Tungsten in Mullard Radio Valves. 77*

then more slowly, approaching a constant value  $i_0$ . It should be noted, however, that  $i_0$  is not, strictly speaking, a constant.

Fig. 5.

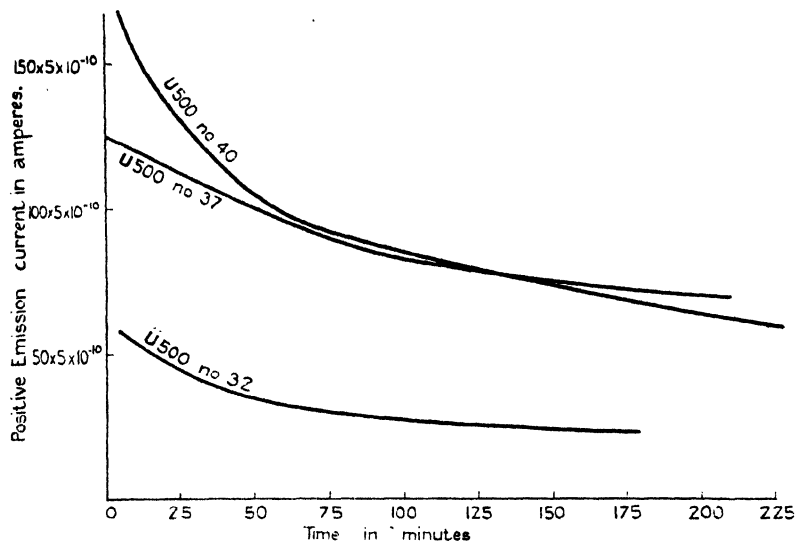
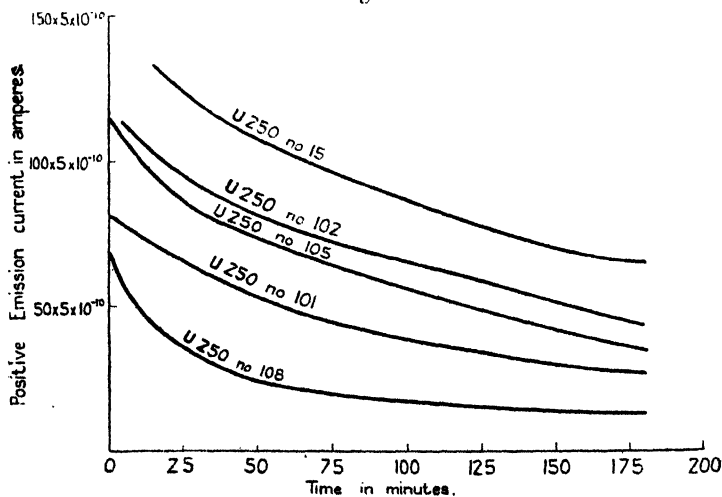


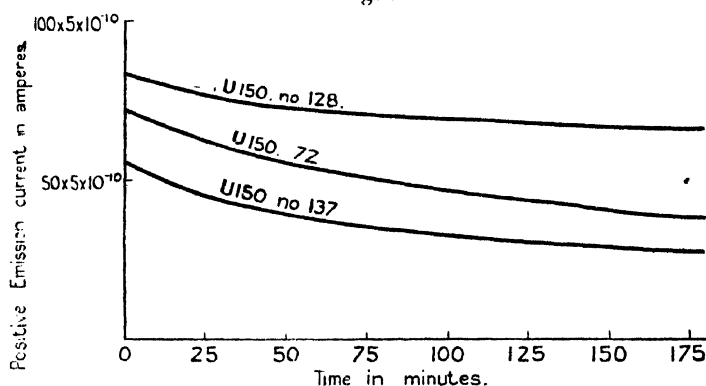
Fig. 6.



It also decays with time, but very slowly in the same general way. Table VII. shows the decay of positive emission

current with time with valve U 250 No. 110. It will be seen that a current goes down in the first stage from 232 to 53 in course of five hours, while in the second stage it goes down from 29 to 23 in eight hours, whereas in the final stage it goes down from 18 to 17, *i. e.*, only one division in course of eight hours. The decay in the first stage is very rapid, namely 179 in five hours, or about 36 divisions per hour. In the second stage it is about 0.75 division per hour; while in the last stage the decay is extremely slow, namely 0.12 division per hour.

Fig. 7.



As with a Coolidge tube, previous treatment of the valve plays a considerable part in the initial emission of positive electricity. It has been found that the application of the negative potential for about three hours with valve U 150 No. 72 increases the initial positive emission to twice its normal value. The experiment was made in the following way:—It was seen from the previous experiments that with the application of 54 volts there was a positive emission of about 32 divisions, and this positive emission decayed extremely slowly, so that we might reckon it as practically steady; now the applied potential was reversed, and this state of things continued for three hours; then, again, the potential was reversed. The initial positive emission current was now found to be about 60 divisions, but it decayed very rapidly. The following table shows this decay with time.

Tube U 150 No. 72. Potential applied, 54 volts.

Time.	Positive Emission Current, in amperes.
2 sec. ....	$60 \times 5 \times 10^{-10}$
5 sec. ....	40 "
15 sec. ....	35 "
30 sec. ....	34 "
45 sec. ....	33 "
1 min. ....	32 "
1 min. 30 sec. ....	32 "
2 min. ....	32 "
2 min. 30 sec. ....	32 "
3 min. ....	32 "

The theoretical aspects of this kind of positive emission current, which can be detected only at a very high temperature, will, it is hoped, be more fully discussed in a future paper.

VI. *A Note on Hamilton-Jacobi's Differential Equation in Dynamics.* By JAKOB KUNZ\*.

THE fundamental importance of the differential equation of the title in the new quantum mechanics makes it desirable to obtain that equation in various, and if possible simple, ways. In the following note I wish to derive the differential equation of Hamilton-Jacobi directly from Euler's differential equation of the calculus of variation.

Let

$$f = f(x, y_1, y_2, \dots y_n, y_1', y_2' \dots y_n')$$

be a function of an independent variable  $x$  and  $n$  dependent variables  $y_1, y_2 \dots y_n$ , independent among themselves, and let

$$y_1' = \frac{dy_1}{dx}, \quad y_n' = \frac{dy_n}{dx}.$$

Then the integral

$$I = \int f(x, y_1, y_2 \dots y_n, y_1', y_2' \dots y_n') dx$$

becomes an extremum if the following differential equations

\* Communicated by the Author.

80 Prof. J. Kunz : *A Note on Hamilton-Jacobi's*  
of Euler are satisfied :

$$\left. \begin{aligned} \frac{\partial f}{\partial y_1} - \frac{d}{dx} \left( \frac{\partial f}{\partial y_1'} \right) &= 0 \\ \frac{\partial f}{\partial y_2} - \frac{d}{dx} \left( \frac{\partial f}{\partial y_2'} \right) &= 0 \\ \vdots \\ \frac{\partial f}{\partial y_n} - \frac{d}{dx} \left( \frac{\partial f}{\partial y_n'} \right) &= 0 \end{aligned} \right\} \dots \dots (1)$$

In most of the classical examples of the calculus of variation it happens that  $f$  is explicitly independent of  $x$ , so that  $\frac{\partial f}{\partial x} = 0$ ; then the differential equations (1) can be put in another form, so that one integration can be carried out directly. Let us consider

$$\begin{aligned} & \frac{d}{dx} \left( f - y_1' \frac{\partial f}{\partial y_1'} - y_2' \frac{\partial f}{\partial y_2'} \dots - y_n' \frac{\partial f}{\partial y_n'} \right) \\ &= \frac{\partial f}{\partial x} + \frac{\partial}{\partial y_1} y_1' + \frac{\partial}{\partial y_2} y_2' + \dots + \frac{\partial f}{\partial y_n} y_n' \\ & \quad - y_1'' \frac{\partial f}{\partial y_1'} - y_2'' \frac{\partial f}{\partial y_2'} - \dots - y_n'' \frac{\partial f}{\partial y_n'} \\ & \quad - y_1' \frac{d}{dx} \frac{\partial f}{\partial y_1'} - y_2' \frac{d}{dx} \frac{\partial f}{\partial y_2'} - \dots - y_n' \frac{d}{dx} \frac{\partial f}{\partial y_n'} \end{aligned}$$

or

$$\begin{aligned} & \frac{d}{dx} \left( f - y_1' \frac{\partial f}{\partial y_1'} - y_2' \frac{\partial f}{\partial y_2'} - \dots - y_n' \frac{\partial f}{\partial y_n'} \right) - \frac{\partial f}{\partial x} \\ &= y_1' \left( \frac{\partial f}{\partial y_1} - \frac{d}{dx} \frac{\partial f}{\partial y_1'} \right) + y_2' \left( \frac{\partial f}{\partial y_2} - \frac{d}{dx} \frac{\partial f}{\partial y_2'} \right) + \dots \\ & \quad + y_n' \left( \frac{\partial f}{\partial y_n} - \frac{d}{dx} \frac{\partial f}{\partial y_n'} \right). \dots (2) \end{aligned}$$

If the equations (1) are satisfied, then the equation (2) reduces to

$$\frac{d}{dx} \left( f - y_1' \frac{\partial f}{\partial y_1'} - y_2' \frac{\partial f}{\partial y_2'} - \dots - y_n' \frac{\partial f}{\partial y_n'} \right) - \frac{\partial f}{\partial x} = 0. \quad (3)$$

and if  $\frac{\partial f}{\partial x} = 0$ , then the first integration gives

$$f - y_1' \frac{\partial f}{\partial y_1'} - y_2' \frac{\partial f}{\partial y_2'} \dots - y_n' \frac{\partial f}{\partial y_n'} = \text{constant.} \quad (4)$$

Now we consider a general mechanical system, of  $n$  degrees of freedom, whose potential energy  $E_p$  is only a function of the generalized coordinates  $q_1 \dots q_2 \dots q_n$ , and whose kinetic energy depends on the same coordinates and is a quadratic function of the generalized velocities

$$q_1' = \frac{dq_1}{dt}, \quad q_2' = \frac{dq_2}{dt} \dots q_n' = \frac{dq_n}{dt},$$

so that Euler's identity holds as follows:

$$\sum_{i=1}^n q_i' \frac{\partial f}{\partial q_i'} = 2E_k. \quad (5)$$

Now we put  $f = E_k - E_p$ , write  $t$  instead of  $x$ ,  $q$  instead of  $y$ , and obtain from the equations (1), changing the signs:

$$\frac{\partial E_p}{\partial q_1} - \frac{\partial E_k}{\partial q_1} + \frac{d}{dt} \frac{\partial E_k}{\partial \frac{dq_1}{dt}} = 0,$$

$$\frac{\partial E_p}{\partial q_2} - \frac{\partial E_k}{\partial q_2} + \frac{d}{dt} \frac{\partial E_k}{\partial \frac{dq_2}{dt}} = 0,$$

$$\dots$$

$$\frac{\partial E_p}{\partial q_n} - \frac{\partial E_k}{\partial q_n} + \frac{d}{dt} \frac{\partial E_k}{\partial \frac{dq_n}{dt}} = 0.$$

These are the equations of Lagrange. From the equations (2), on the other hand, we obtain

$$\frac{d}{dt} \left[ (E_k - E_p) - \frac{dq_1}{dt} \frac{\partial E_k}{\partial \frac{dq_1}{dt}} - \dots \frac{dq_n}{dt} \frac{\partial E_k}{\partial \frac{dq_n}{dt}} \right] - \frac{\partial (E_k - E_p)}{\partial t} = 0, \quad (6)$$

or by Euler's identity, and putting  $E_k + E_p = E$ , the total energy:

$$\frac{dE}{dt} + \frac{\partial (E_k - E_p)}{\partial t} = 0, \quad (7)$$

or

$$E + \frac{\partial}{\partial t} \int_{t_0} (E_k - E_p) dt = 0.$$



If we put  $S = \int_{t_0}^{t_1} (E_k - E_p) dt$ , then we obtain the differential equation of Hamilton-Jacobi :

$$E + \frac{\partial S}{\partial t} = 0. \quad . \quad . \quad . \quad . \quad . \quad (8)$$

If  $\frac{\partial f}{\partial t} = \frac{\partial (E_k - E_p)}{\partial t} = 0$ , then we obtain from (4),

$$E_k - E_p - 2E_k = \text{constant},$$

or

$$E_k + E_p = E = \text{constant},$$

which is the principle of conservation of energy.

### *Summary.*

The mechanical equations of Lagrange, of Hamilton-Jacobi, and the principle of conservation of energy have been derived from Euler's differential equation of the calculus of variation.

VII. *On the Combustion of Carbonic Oxide.*—Part I. By J. P. BAXTER, B.Sc., James Watt Research Fellow, University of Birmingham\*.

### *Introduction.*

IN an earlier paper (Harrison and Baxter, Phil. Mag. Jan. 1927) two methods of investigating gaseous combustion in a closed sphere were described. The first consisted in measuring the relative rise in temperature at a point during the explosion, as indicated by a platinum resistance thermometer, using an Einthoven String Galvanometer as the recording device; and the second of actually measuring the flame-velocity, using two or more fine wires as the means of recording the passage of the flame.

The first of these methods was applied to a number of

\* Communicated by Professor F. W. Burstall, M.Sc., M.A., M.Inst.C.E. M.I.Mech.E.

explosive mixtures, and the following conclusions were arrived at:—

- (a) The combustion of dry carbon monoxide probably takes place in two ways—firstly by direct oxidation, and secondly by the intervention of water-vapour.
- (b) The addition of extremely small traces of hydrogen produces a great acceleration in the speed of combustion, and may alter the method of combustion.

With a view to further investigating the above points, it was decided to carry out a series of measurements on explosions of carbon monoxide and air into which small regulated amounts of water-vapour, hydrogen, and other impurities would be introduced.

For this purpose a particularly pure supply of carbon monoxide is required, and owing to the size of the apparatus the gas must be available on a large scale. The department has for some years possessed a plant for the generation of carbon monoxide on a semi-works scale, so in 1926 Mr. Harrison and the author redesigned this apparatus, eliminating all metallic portions and constructing the reaction side entirely in silica and glass. The gas can now be made 99·8 % pure, the impurity being air, though during compression into cylinders the air impurity may go up to 2 %. The important point is that the gas, so far as we can tell, contains no hydrogen.

#### *The Effect of Water-vapour on Carbon-monoxide Explosions.*

In 1884, H. B. Dixon published a series of investigations on the action of water-vapour on the carbon-monoxide oxygen reaction. He showed that the mixture  $2\text{CO} + \text{O}_2$ , when dried over phosphorus pentoxide, would not combine when sparked in a eudiometer. He also showed that the addition of traces of dry carbon dioxide, cyanogen, air, nitrous oxide, and carbon bisulphate did not cause combination to occur, but traces of water-vapour, ether, pentane, hydrogen chloride, and hydrogen sulphide caused ignition to take place with ease.

Later he measured detonation velocities in the theoretical carbon-monoxide oxygen mixture containing different quantities of water-vapour, and showed that a maximum velocity was reached in the mixture containing 5·6 % water-vapour. Further increase above this value caused a slow decrease in flame-velocity.

Many workers investigated the possibility of igniting dry carbon-monoxide oxygen mixtures, and many theories have been put forward to explain the action of the water-vapour. Recent work by Prof. Bone and his co-workers seems to have established definitely that the direct oxidation of carbon monoxide in flames does take place, but that the presence of water or hydrogen compounds greatly facilitates the combustion. Quantitative measurements on this subject have also been made by R. W. Fenning, using a pressure indicator in a closed vessel, and by Garner and Johnson, who measured the infra-red emission from the flames of wet and dry carbon monoxide.

The present work, of which this is the first part, will endeavour to compare the action of hydrogen, in combination with a number of different elements, on the carbon-monoxide reaction. For this purpose it is intended to measure flame-velocities both directly and by means of a pressure indicator to be described later, and also to compare the time-temperature curves obtained as described in the previous paper. At the start, mixtures with air instead of with oxygen will be used, as these give lower flame-velocities, which are therefore more accurately measured, and also because at the same time it is intended to carry out measurements on the possible "activation of nitrogen" at low pressures.

### *The Hygroscopic Condition of the Gases.*

Although this paper deals only with explosions at one atmosphere initial pressure, the whole of the external apparatus to the sphere is designed to work up to ten atmospheres, as it is intended ultimately to reach this pressure.

The percentage of water-vapour in the gases is regulated by a system of saturation at a given temperature. It is also possible to use "dry" gases which have been passed slowly up a long column of calcium chloride

The saturators consist of steel tubes eight inches long and three and a half inches in diameter, with the ends closed by screwed steel caps, making a gas-tight joint. The gas enters at the bottom through a small diameter (2 mm.) steel pipe, silver soldered through the wall of the saturator, and then enters the water through a number of very fine holes drilled in the sides of the tube. A series of baffles are arranged which ensure the bubbles being well broken up and thoroughly saturated. At the top of the saturator is the

gas outlet with control valve, leading directly to the explosion sphere, and for the pressures used so far a sealed mercury in glass pressure-gauge for the regulation of the pressure inside the saturator.

The whole of this apparatus is immersed in a large water thermostat fitted with two efficient stirrers. An electric immersion heater is controlled by a thermostat regulator of fairly conventional design, the regulator break being connected with a two-volt battery and a quick break relay which operates the main heater. This thermostat has an error not exceeding one-half a degree centigrade.

During the process of filling the sphere the pressure in the saturator is kept constant at the pressure at which the sphere will ultimately be filled, so that the water-vapour content is accurately regulated.

### *The Pressure Indicator.*

As a great deal of constant volume explosion work has been carried out in the past by means of the average pressure determinations, it has been thought desirable to fit a pressure indicator to the sphere for comparison purposes.

One of the latest types of Prof. Burstall's optical indicators has been fitted, modified in such a way as to enable it to be used for sphere work. The diaphragm used is of the flat type, with one corrugation round the circumference. It is of nickel chrome steel, and is machined out of the solid to cut down hysteresis effects. The optical system is of the standard type, except that an oil dashpot device has been arranged to rotate one of the mirrors during the explosion, thus giving a curve recording pressure against time. A time marker, consisting of a small synchronous motor driven by a standard vibrating bar, is arranged to interrupt the source of light every one hundredth of a second, thus giving a suitable time record on the plate. The indicator has been accurately calibrated on the standard mercury column erected for that purpose in the department.

### *The Recording Circuit.*

For velocity measurements the recording circuit is the same as described in the previous paper. Normally two recording wires are used, one one inch from the spark, and the other one inch from the walls. The distance between

the wires is six inches. It is the average flame-velocity over this distance which is measured. Investigations of the way the flame travels over this space have shown that there is a steady diminution in velocity as the flame approaches the walls. This may be due to the increase in initial pressure of the unburnt gas caused by the combustion taking place near the centre, in accordance with the results of Newey and Crowe, who showed that, with increase in initial pressure from one to ten atmospheres, there was a decrease in flame-velocity. On the other hand, the increase in temperature produced by this compression should cause a greater flame-velocity. There is, however, no doubt that a steady diminution in velocity does take place as the flame spreads out over the sphere. In the present case, however, it is the average speed over a length of six inches in a direction inclined at forty-five degrees to the horizontal which is measured and used for purposes of comparison.

For the relative temperature measurements the thermometer as used before has been improved by the addition of a pair of compensating leads which balance out any resistance changes in the supports. It may be stated here that this thermometer gives almost identical results as the one originally used, showing that the effect of the leads, if any, is exceedingly small. The actual recording wire is of platinum-iridium alloy one and a half thousandths of an inch in diameter.

*Flame-velocities with varying Mixture-strength  
and Moisture-content.*

A series of determinations were carried out to discover if the alteration in moisture-content produced comparable effects with different mixture-strengths.

The flame-velocities were measured over the available range of mixture-strengths, with water-vapour contents of .88, 1.2, and 1.6 %, and also with gases slowly dried over calcium chloride. The results are set out in Table I.

These velocities are plotted against mixture-strength in fig. 2. There is no immediately apparent relationship between flame-velocity and moisture-content, the relationship varying with the mixture-strength.

A comparable set of results over a larger range of moisture-content are shown in Table II. and fig. 1. These are arbitrary velocities calculated from the pressure time-

records on the assumption that the flame reaches the wall at the time of maximum pressure. This is not strictly justified, and it is interesting to note that the curves, while similar, are definitely not of the same form, the greatest divergence being in the case of the dry mixtures.

In figs. 3 to 4 are set out a number of relative-temperature time curves, obtained with the compensated thermometer as previously described. Fig. 3 shows the progressive effect of addition of moisture to the  $2\text{CO}_2 + \text{O}_2 + 4\text{N}_2$  mixture. The general shape of the curve persists, but the time to reach maximum temperature is steadily reduced. The curve fig. 3 (a) is of interest for the somewhat violent temperature oscillations which follow the maximum. Similar changes are apparent on several other curves, and when explosions at higher pressures than these are fired, the oscillations become increasingly noticeable. It was thought that these might be caused by pressure oscillations set up inside the sphere; and to test this a microphone was designed which should record high-frequency pressure-changes over a very small area. It consists of a hollow phosphor-bronze cylinder three inches long by one inch in diameter, carrying at one end a small steel diaphragm three-eighths of an inch in diameter and five thousandths thick. Rigidly attached to the inside of this is a light coil of 40-gauge enamelled wire, arranged so that it can move freely over the head of an electro bar magnet. The leads for the existing coil for the magnet and those from the recording coil are conveyed outside the sphere inside the rods which support the protective casing. An exciting current of half an ampere is used, and the recording coil is connected directly to the Einthoven string galvanometer. When arranged so that the recording diaphragm is in the position usually occupied by the thermometer, a series of pressure oscillations are recorded of identical frequency with the temperature oscillations shown by the thermometer; thus proving the origin of these changes.

Figs. 4 to 9 show the temperature curves for a number of different mixture-strengths containing different amounts of water-vapour.

Fig. 10 shows a reproduction of the pressure curves from the Burstall Optical Indicator for the mixture  $2\text{CO} + \text{O}_2 + 4\text{N}_2$  with increasing moisture-content. It is noticeable that, as the time of attainment of maximum pressure decreases, the rate of subsequent cooling tends to increase.

It is not proposed to enter into any further discussion of these results at present, as the work is being continued along the lines of investigating the action of traces of hydrogen and also other compounds of hydrogen, and a general consideration of results is better left until a later paper.

In connexion with the assumption that the combustion of carbon monoxide takes place in two ways, a direct, and an indirect involving the action of water-vapour or some similar body, some interesting analysis has been carried out on the burned gases from the mixtures used in these explosions by the author's colleague Mr. L. E. Winterbottom, who has estimated the oxides of nitrogen produced during the reaction. His results are given at the end of this paper. It will be seen that, as the water-vapour content of the gases increases, the amount of oxides of nitrogen formed decreases very considerably. An increase in moisture-content causes more rapid cooling of the burned gases; and if the nitrogen oxides were the product of a purely thermal change, one would expect them to increase rather than decrease with the addition of water-vapour.

If, however, they are produced as a result of the direct oxidation of carbon monoxide, then the dry gases will favour a maximum yield, and wet gases favouring the indirect oxidation will give a reduced yield of nitrogen oxides. This is in agreement with Bone's figures for oxides of nitrogen produced at high pressures, which are generally recognized as favouring the direct oxidation.

### *The Estimation of Oxides of Nitrogen.*

During the combustion of carbon monoxide and oxygen in the presence of nitrogen, oxidation of the nitrogen may also occur. Bone has shown that as much as 3 per cent. of NO is formed during the combustion of a mixture  $2\text{CO} + 3\text{O}_2 + 2\text{N}_2$  at 75 atmospheres original pressure.

In the present research it is proposed to investigate the formation of oxides of nitrogen at low pressures—covering a range from one atmosphere to ten atmospheres original pressure.

The method of estimating small amounts of oxides of nitrogen has been arrived at after considerable experiment, and is essentially a micro-Kjeldhal estimation.

The combustion products, after stirring, are drawn from the explosion sphere by means of a Geryk vacuum pump through a series of absorption tubes containing concentrated potassium-hydroxide solution. Formation of potassium nitrite and potassium nitrate takes place—with nitrite in excess—as established by Le Blanc\*.

TABLE I.

Percentage of CO.	Percentage of N <sub>2</sub> .	Percentage of O <sub>2</sub> .	Percentage of H <sub>2</sub> O.	Flame-velocity. cm./sec.
21.0	63.2	15.8	{ Dry over } { CaCl <sub>2</sub> . }	59
26.0	59.2	14.8	—	73
30.0	56.0	14.0	—	75.
34.0	52.8	13.2	—	77
40.0	48.0	12.0	—	75
48.0	41.6	10.4	—	72
59.0	32.8	8.2	—	52
15.0	68.0	17.0	.88	50
23.0	61.0	15.4	—	95
27.5	58.0	14.5	—	132
29.0	56.8	14.2	—	138
34.0	52.8	13.2	—	165
40.0	48.0	12.0	—	180
45.0	44.0	11.0	—	170
58.0	33.6	8.4	—	127
19.0	64.8	16.2	1.2	85
23.4	61.2	15.3	—	115
29.0	56.8	14.2	—	160
38.0	49.6	12.4	—	197
45.0	44.0	11.0	—	170
63.0	29.6	7.4	—	120
20.0	64.0	16.0	1.6	135
27.5	58.0	14.5	—	190
34.0	52.8	13.2	—	220
40.0	48.0	12.0	—	235
48.0	41.6	10.4	—	220
62.0	29.6	7.4	—	160



After oxidation of the nitrite to nitrate the potassium nitrate is estimated by a micro-modification of Jodlbauer's\* method of estimating nitrates. This micro-Kjeldahl method has given consistent results, using direct titration in one hundredth normal solutions. Smaller quantities of ammonia in the distillate may necessitate the use of a colorimetric method for its estimation, but these colour-matching methods have not given accurate results in preliminary experiments.

TABLE II.

Per-centage of CO.	Per-centage of N <sub>2</sub> .	Per-centage of O <sub>2</sub> .	Per-centage of H <sub>2</sub> O.	Maximum pressure.	Time to reach max. pressure.	Calculated velocity.
27.0	58.4	14.6	<div style="display: inline-block; vertical-align: middle;"> <div style="text-align: center;">Dry over CaCl<sub>2</sub>.</div> </div>	88 lb	.38 sec.	0 cm./sec.
20.0	64.0	16.0		70	1.0	23
35.0	52.0	15.0		92	.30	89
48.0	41.6	10.4		84	.30	89
40.0	48.0	12.0		92	.24	95
58.0	33.6	8.4	—	88	.40	57
28.0	57.6	14.4	.88	100	.19	121
36.0	51.2	12.8	.88	97	.15	154
21.0	63.2	15.8	.88	86	.42	55
43.0	45.6	11.4	.88	100	.14	164
56.0	35.2	8.8	.88	90	.19	121
48.0	41.6	10.4	1.2	95	.12	194
42.0	46.4	11.6	1.2	100	.11	208
31.0	55.2	13.8	1.2	104	.13	177
24.0	60.8	15.2	1.2	92	.19	121
18.0	75.6	16.4	1.2	58	.72	32
36.0	51.2	12.8	1.2	100	.12	194
63.0	29.6	7.4	1.2	72	.19	121
30.0	56.0	14.0	3.1	104	.09	255
40.0	48.0	12.0	3.1	100	.08	290
19.0	64.8	16.2	3.1	85	.19	121
30.0	56.0	14.0	4.4	105	.07	330

\* *Z. anal. Chem.* xxvii. p. 92.

TABLE III.

Fig.	No.	Percentage of CO.	Percentage of N <sub>2</sub> .	Percentage of O <sub>2</sub> .	Percentage of H <sub>2</sub> O.
3.	a .....	30	56	14	·88
	b .....	30	56	14	Dry.
	c .....	30	56	14	1·2
	d .....	30	56	14	3·1
	e .....	30	56	14	4·4
4.	a .....	40	48	12	Dry.
	b .....	20	64	16	—
5.	a .....	27	58·4	14·6	Dry.
	b .....	48	41·6	10·4	—
6.	a .....	21	63·2	15·8	·88
	b .....	43	45·6	11·4	·88
7.	a .....	28	57·6	14·4	·88
	b .....	56	35·2	8·8	·88
8.	a .....	24	60·8	15·2	1·2
	b .....	42	46·4	11·6	1·2
9.	a .....	31	55·2	13·8	1·2
	b .....	48	41·6	10·4	1·2
10.	a .....	30	56	14	4·4
	b .....	30	56	14	3·1
	c .....	30	56	14	1·2
	d .....	30	56	14	·88
	e .....	30	56	14	Dry.

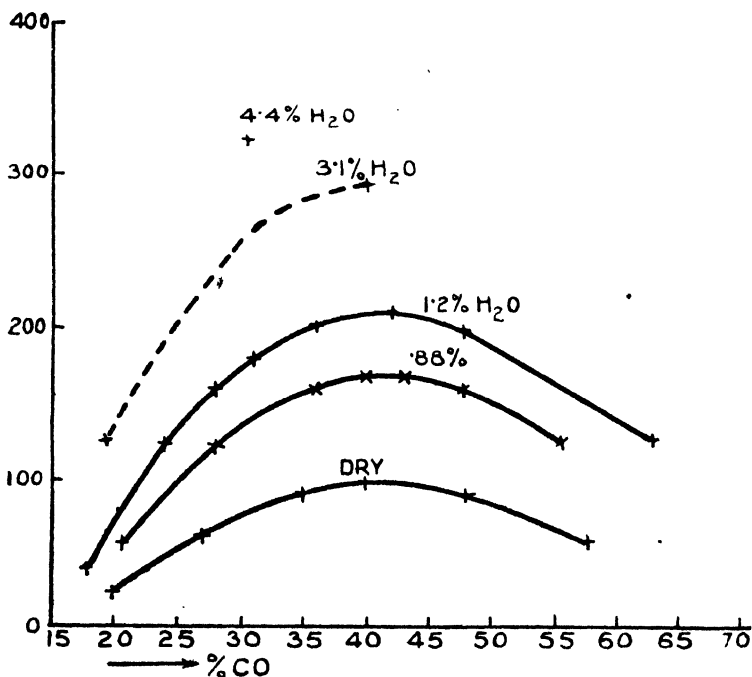
Experiments at one atmosphere original pressure have been conducted, and the effect on NO formation of

- (a) Percentage of CO in the unfired mixture.
- (b) Percentage of H<sub>2</sub>O in the unfired mixture has been ascertained.

It is evident that formation of NO is favoured in a weak mixture—where excess of oxygen is present.

The presence of water-vapour has a very pronounced effect on oxidation, an addition of 1.2 per cent. of  $H_2O$  to a dry 20-per-cent. mixture, for instance, halves the amount of nitrogen oxidation.

Fig. 1.



It is hoped to continue the research with special reference to—

- (1) Effect of small quantities of hydrogen on NO formation.
- (2) Formation of NO in CO-O mixtures containing small quantities of nitrogen.
- (3) Effect of addition of oxygen to a constant mixture of nitrogen and carbon monoxide.

Fig. 2.

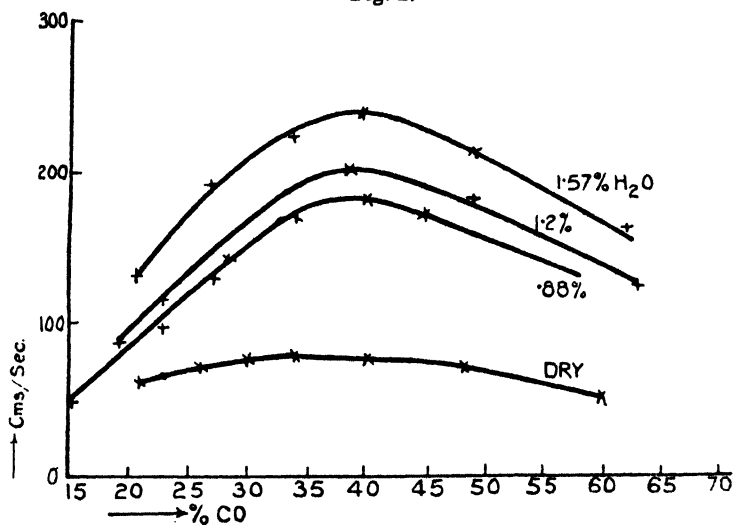


Fig. 3.

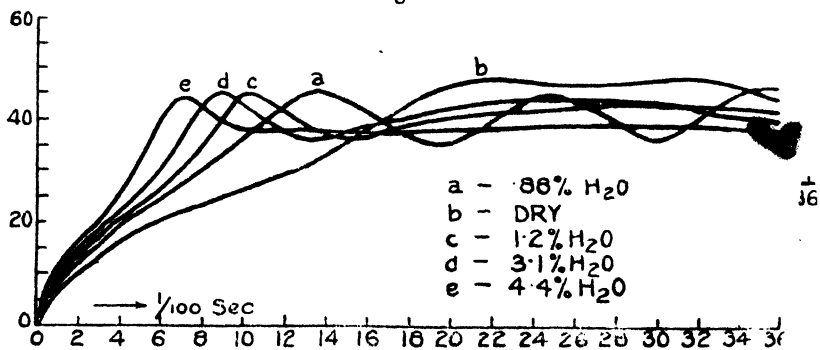


Fig. 4.

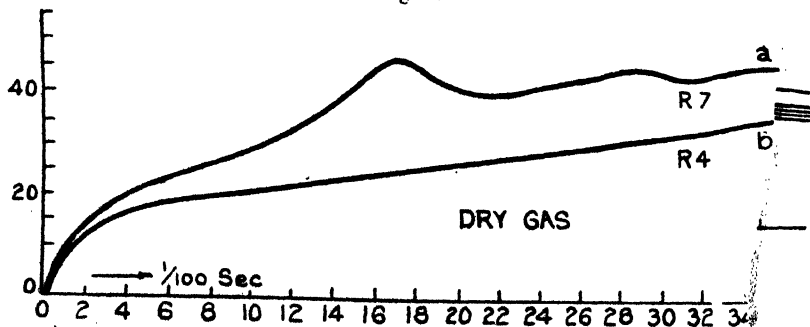


Fig. 5.

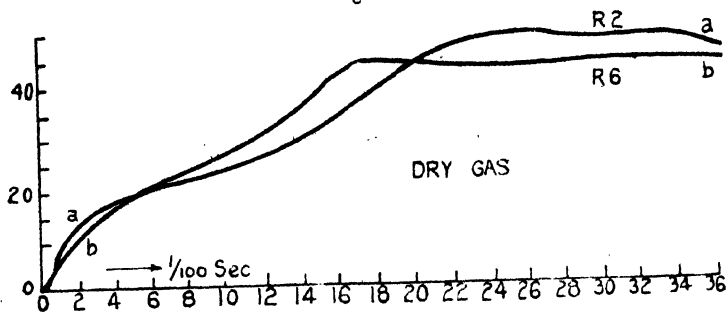


Fig. 6.

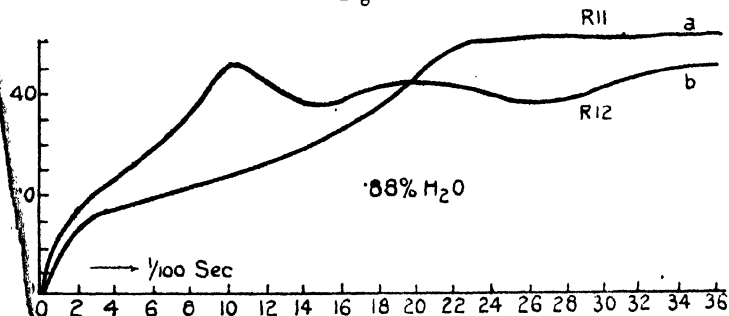


Fig. 7.

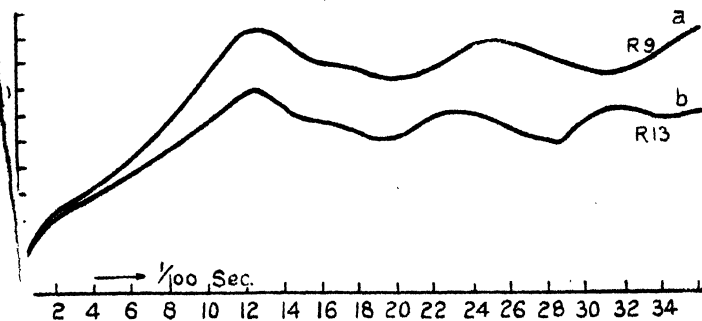


Fig. 8.

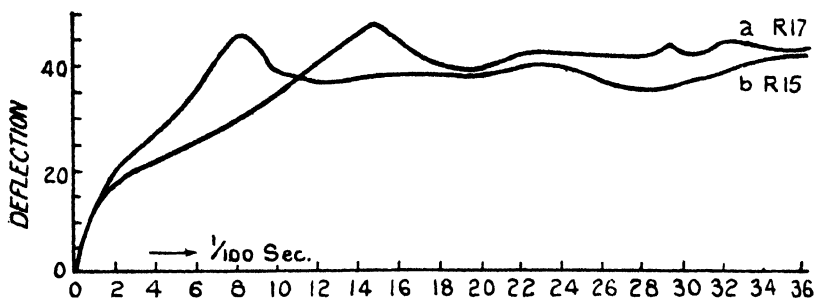


Fig. 9.

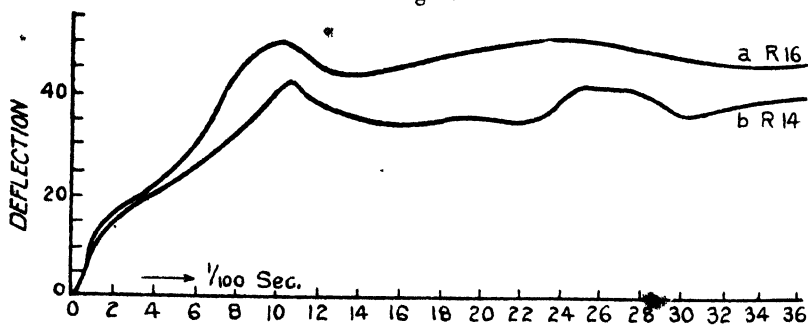


Fig. 10.

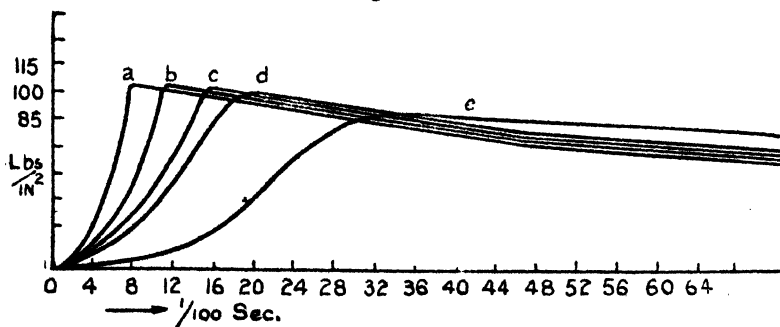
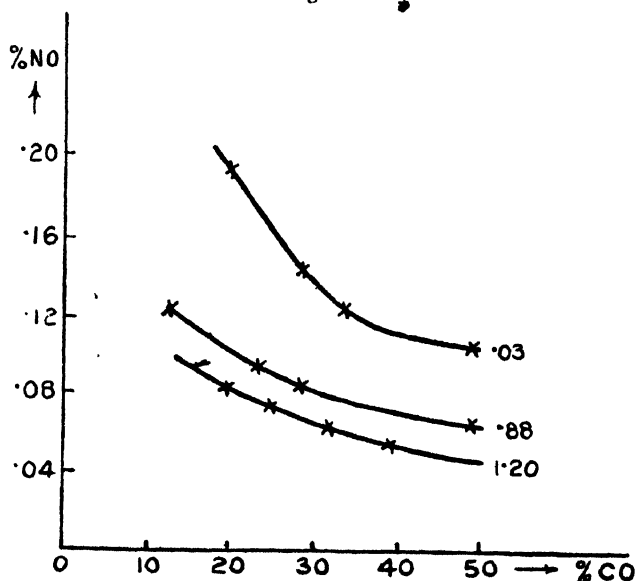


TABLE IV.

Percentage of CO.	Percentage of N.	Percentage of O.	Percentage of H <sub>2</sub> O.	Percentage of NO.
27	58.4	14.6	.03	.14
19	64.8	16.2	.03	.19
35.5	51.6	12.9	.03	.12
48	41.6	10.4	.03	.10
13	70.4	7.6	.88	.12
45	44	11	.88	.06
27.6	58	14.5	.88	.08
23	61.6	15.4	.88	.09
38.3	49.6	12.3	1.2	.05
24.6	60.4	15.1	1.2	.07
19.0	64.6	16.2	1.2	.08
31	55.2	13.6	1.2	.06

Fig. 11.



In conclusion, the author wishes to express his gratitude to Professor Burstall for much helpful advice, and to Mr. Pickering, of Birmingham University, for invaluable assistance in the construction and assembling of the apparatus required. He also thanks the Department of Scientific and Industrial Research for a grant which has defrayed the expenses of the research.

VIII. *The Torsion-Flexure Oscillations of a System of Two Connected Beams.* By S. B. GATES, M.A.\*

1. **T**HE ordinary theory of the independent flexural and torsional oscillations of bars applies in strictness only to movement of the system *in vacuo*, since only the elastic and inertia forces are included. If the oscillation takes place in a fluid medium, the fluid reactions provide another system of forces which may or may not be negligible compared with those usually considered. If the system as a whole has a large rate of translation through the fluid, it is probable that the fluid reactions during the oscillation become important. For instance, it may be necessary to retain the aerodynamic forces when considering the vibration of an elastic component of an aeroplane in flight. A type of elastic hydrodynamic problem is thus presented which assumes some importance in aeronautics, and has not hitherto received much study. One important consequence of the retention of the fluid reaction is that the independence of the flexural and torsional oscillations is destroyed. Thus if  $z$  is the displacement of the central line and  $\theta$  the twist of the beam, the equations to be solved are of the form :

$$\frac{d^2 z}{dt^2} + a^2 \frac{d^4 z}{dx^4} + f(z, \theta) = 0,$$

$$\frac{d^2 \theta}{dt^2} - b^2 \frac{d^2 \theta}{dx^2} + \phi(z, \theta) = 0,$$

where  $f(z, \theta)$  and  $\phi(z, \theta)$ , representing the fluid reactions, will usually comprise terms proportional to  $\frac{dz}{dt}$ ,  $\frac{d\theta}{dt}$ , and  $\theta$ .

The exact solution of these equations is of the form :

$$z = \sum \sum \alpha e^{\lambda x} e^{\mu t},$$

$$\theta = \sum \sum \beta e^{\lambda x} e^{\mu t},$$

and if we proceed in the usual way to find the admissible values of  $\lambda$  and  $\mu$ , we are led to a cubic equation in  $\lambda^2$ , the coefficients being, of course, functions of  $\mu$ . It appears to be very difficult to proceed algebraically with the exact solution beyond this stage.

2. It seems, therefore, that the problem of the related

\* Communicated by R. V. Southwell, M.A., F.R.S.



flexural and torsional oscillations of a long beam under the action of "external" forces imposed by the surrounding fluid is a complex and difficult one. There is, however, an elastic system of simpler type which, under certain simplifying assumptions, yields an exact algebraic solution, and this has features of practical and theoretical interest which may be put on record. We shall consider two long beams or spars of equal length and constant, but not necessarily the same, cross-section, each encastred at one end and free both to deflect in a direction perpendicular to the line joining the fixed ends and to twist about its central line. The spars are continuously connected along their length by connexions flexible enough to allow them to execute the prescribed motion. This system is supposed to oscillate in a fluid medium which gives rise to reactions of the type specified in the preceding paragraph. The following assumptions are made:

- (a) All stresses in the connexions are neglected.
- (b) The torsional rigidity of each spar is neglected, so that the torsional rigidity of the whole system arises solely from the flexural rigidity of the spars.

The centre of mass of a cross-section of this system, which in its undisplaced position is perpendicular to the spars, has a velocity parallel to the direction of motion of each spar, and the cross-section is twisting under the difference of the deflexions of the two spars. Hence the system may be regarded as a single "beam" of elongated cross-section which is executing combined flexural and torsional oscillations. Under the restrictions (a) and (b) the tractions across this section are supposed to be concentrated at the two spar centres and to consist of shear forces due to the separate deflexion of each spar. It is not necessary to assume that every dimension of this cross-section is small compared with the length of the spars.

On the practical side the system here contemplated represents an attempt to abstract the essential elastic features of a more or less flat rectangular structure, like an aeroplane wing, which is built up on two spars each encastred at one end. It is obvious that the strength of such a structure will reside principally in its spars, and also that large torsional rigidity of the spars themselves is not in general necessary to ensure torsional stiffness of the whole structure. Thus the assumptions (a) and (b) above, which have been introduced to bring the problem within the scope of an exact solution, are not such as to vitiate entirely its application to

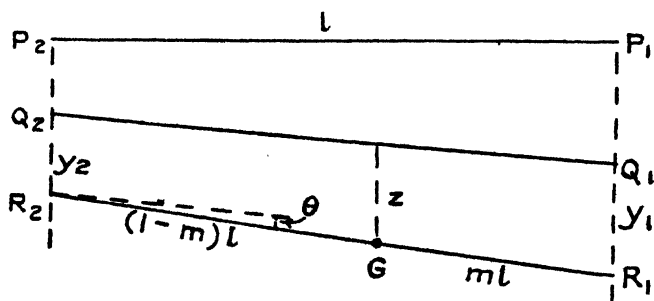
such subjects as the vibration of a cantilever monoplane wing in a stream of air.

3. Proceeding with the problem under the above assumptions, the following is the notation:—

- $x$  coordinate along a spar.
- $x=0$  at encastred end.
- $x=r$  at free end.
- $l$  distance between spar centres.
- $m$  the centre of mass of a cross-section of the structure divides  $l$  in the ratio  $m : 1-m$ .
- $y_1, y_2$  deflexions of the spar centres at section  $x$ , measured from their equilibrium positions.
- $z$  deflexion of centre of mass of section at  $x$ , measured from its equilibrium position.
- $\theta$  twist of section  $x$ , measured from its equilibrium position.
- $M$  mass of structure per unit of  $x$ .
- $I$  moment of inertia of structure, per unit of  $x$ , about an axis through the centre of mass of a section and parallel to the spars.
- $B_1, B_2$  flexural rigidities of spars.
- $f(z, \theta)$  component of fluid reaction parallel to  $z$ , per unit of  $x$ .
- $\phi(z, \theta)$  moment of fluid reaction about centre of mass of section per unit of  $x$ .

Fig. 1.

Diagram illustrating the motion of a section of the structure.



- $P_1, P_2$  are the spar centres at the encastred end  $x=0$ .
- $Q_1, Q_2$  are the spar centres at section  $x$  in equilibrium.
- $R_1, R_2$  are the spar centres at section  $x$  during the oscillation.
- $G$  is the centre of mass of section  $x$ .

A section of thickness  $dx$  is in motion under shear forces at  $R_1$  and  $R_2$  and the fluid reactions. Resolving parallel to  $z$  and taking moments about  $G$ , we have, remembering that all coordinates are measured from the equilibrium position of the section :

$$M dx \cdot \frac{d^2 z}{dt^2} = -B_1 \frac{d^4 y_1}{dx^4} dx - B_2 \frac{d^4 y_2}{dx^4} dx + f dx,$$

$$I dx \cdot \frac{d^2 \theta}{dt^2} = -ml \left( B_1 \frac{d^4 y_1}{dx^4} dx \right) + (1-m) l \left( B_2 \frac{d^4 y_2}{dx^4} dx \right) + \phi dx.$$

Since

$$y_1 = z + m l \theta,$$

$$y_2 = z - (1-m) l \theta,$$

we eliminate  $y_1, y_2$  to obtain :

$$M \frac{d^2 z}{dt^2} = -B_1 \left( \frac{d^4 z}{dx^4} + ml \frac{d^4 \theta}{dx^4} \right) - B_2 \left( \frac{d^4 z}{dx^4} - (1-m) l \frac{d^4 \theta}{dx^4} \right) + f,$$

$$I \frac{d^2 \theta}{dt^2} = -ml B_1 \left( \frac{d^4 z}{dx^4} + ml \frac{d^4 \theta}{dx^4} \right) + (1-m) l B_2 \left( \frac{d^4 z}{dx^4} - (1-m) l \frac{d^4 \theta}{dx^4} \right) + \phi.$$

If, as is generally the case, the fluid reactions due to the oscillation are the sums of terms in  $\frac{dz}{dt}$ ,  $\frac{d\theta}{dt}$ , and  $\theta$ , we may write :

$$f = -M \left( a_1 \frac{dz}{dt} + b_1 \frac{d\theta}{dt} + c_1 \theta \right),$$

$$\phi = -I \left( a_2 \frac{dz}{dt} + b_2 \frac{d\theta}{dt} + c_2 \theta \right).$$

The equations of motion now reduce to :

$$\left. \begin{aligned} \frac{d^2 z}{dt^2} + \alpha_1 \frac{d^4 z}{dx^4} + \beta_1 \frac{d^4 \theta}{dx^4} + a_1 \frac{dz}{dt} + b_1 \frac{d\theta}{dt} + c_1 \theta &= 0 \\ \frac{d^2 \theta}{dt^2} + \alpha_2 \frac{d^4 \theta}{dx^4} + \beta_2 \frac{d^4 z}{dx^4} + a_2 \frac{dz}{dt} + b_2 \frac{d\theta}{dt} + c_2 \theta &= 0 \end{aligned} \right\}, \quad (1)$$

where

$$\alpha_1 = \frac{B_1 + B_2}{M},$$

$$\beta_1 = \frac{l[mB_1 - (1-m)B_2]}{M},$$

$$\alpha_2 = \frac{l^2[m^2B_1 + (1-m)^2B_2]}{I},$$

$$\beta_2 = \frac{l[mB_1 - (1-m)B_2]}{I}.$$

4. To solve equations (1) we assume in the usual way :

$$z = g(x)e^{\mu t},$$

$$\theta = h(x)e^{\mu t}.$$

Then, writing D for  $\frac{d}{dx}$ , the equations for  $g$  and  $h$  are :

$$(\alpha_1 D^4 + \mu^2 + a_1 \mu)g + (\beta_1 D^4 + b_1 \mu + c_1)h = 0,$$

$$(\beta_2 D^4 + \mu a_2)g + (\alpha_2 D^4 + \mu^2 + b_2 \mu + c_2)h = 0.$$

Hence, if  $g = Ae^{\lambda x}$ ,  $h = Be^{\lambda x}$ , we have :

$$A(\alpha_1 \lambda^4 + \mu^2 + a_1 \mu) + B(\beta_1 \lambda^4 + b_1 \mu + c_1) = 0,$$

$$A(\beta_2 \lambda^4 + a_2 \mu) + B(\alpha_2 \lambda^4 + \mu^2 + b_2 \mu + c_2) = 0,$$

whence

$$k = \frac{B}{A} = - \frac{\alpha_1 \lambda^4 + \mu^2 + a_1 \mu}{\beta_1 \lambda^4 + b_1 \mu + c_1} = - \frac{\beta_2 \lambda^4 + a_2 \mu}{\alpha_2 \lambda^4 + \mu^2 + b_2 \mu + c_2}. \quad (2)$$

Thus a solution of equation (1) is :

$$\left. \begin{aligned} z &= \sum \sum A e^{\lambda x} e^{\mu t} \\ \theta &= \sum \sum k A e^{\lambda x} e^{\mu t} \end{aligned} \right\}, \quad \dots \dots \dots (3)$$

where  $k$  is given by equation (2), and one relation between  $\lambda$  and  $\mu$ , given by the last equality in (2), is found to be :

$$\begin{aligned} (\alpha_1 \alpha_2 - \beta_1 \beta_2) \lambda^8 &+ \{ (\alpha_1 + \alpha_2) \mu^2 + (a_1 b_2 - \beta_1 \alpha_2 + \alpha_2 a_1 - \beta_2 b_1) \mu \\ &+ (\alpha_1 c_2 - \beta_2 c_1) \} \lambda^4 + \mu^4 + (a_1 + b_2) \mu^3 \\ &+ (a_1 b_2 - a_2 b_1 + c_2) \mu^2 + (a_1 c_2 - a_2 c_1) \mu = 0. \quad (4) \end{aligned}$$

This, being a quadratic in  $\lambda^4$ , allows of further progress. It may be noticed that retention of the torsional stiffness of the spars would introduce a term  $\frac{d^2 \theta}{dx^2}$  in the second equation of (1), and thence terms in  $\lambda^6$  and  $\lambda^3$  in (4).

This would destroy the possibility of an algebraic solution.

5. The second equation which, with (4), will determine all the admissible values of  $\lambda$  and  $\mu$  in (3), is to be found from the end conditions of the spars.

Since the spars are encastred at  $x=0$  and free at  $x=r$ , we have :

$$y_1 = \frac{dy_1}{dx} = y_2 = \frac{dy_2}{dx} = 0 \text{ at } x=0,$$

and  $\frac{d^2 y_1}{dx^2} = \frac{d^3 y_1}{dx^3} = \frac{d^2 y_2}{dx^2} = \frac{d^3 y_2}{dx^3} = 0$  at  $x=r$ ,

for all values of  $t$ .

These lead to

$$\left. \begin{aligned} z = \frac{dz}{dx} = \theta = \frac{d\theta}{dx} = 0 \text{ at } x=0, \\ \text{and } \frac{d^2 z}{dx^2} = \frac{d^3 z}{dx^3} = \frac{d^2 \theta}{dx^2} = \frac{d^3 \theta}{dx^3} = 0 \text{ at } x=r, \end{aligned} \right\} \quad (5)$$

for all values of  $t$ .

If for a value of  $\mu$  which is admissible in (3) the roots of (4) are  $\lambda_1, \lambda_2, \dots, \lambda_8$ , and if the constants  $A$  are  $A_1, A_2, \dots, A_8$ , the conditions (5) require that:

$$\left. \begin{aligned} \sum_{n=1}^8 A_n &= 0 \\ \sum k_n A_n &= 0 \\ \sum \lambda_n A_n &= 0 \\ \sum k_n \lambda_n A_n &= 0 \\ \sum \lambda_n^2 e^{r\lambda_n} A_n &= 0 \\ \sum k_n \lambda_n^2 e^{r\lambda_n} A_n &= 0 \\ \sum \lambda_n^3 e^{r\lambda_n} A_n &= 0 \\ \sum k_n \lambda_n^3 e^{r\lambda_n} A_n &= 0 \end{aligned} \right\} \dots \dots \dots (6)$$

Elimination of the ratios  $A_1:A_2:\dots:A_8$  from the eight equations (6) leads to an eighth row determinantal equation involving  $\lambda$  and  $\mu$ . This, together with (4), suffices to determine all the admissible values of  $\lambda$  and  $\mu$ .

Finally, the single constant  $A$  which is undetermined by (6) for given values of  $\lambda$  and  $\mu$  must be found from the conditions at  $t=0$ . This completes the formal solution of the problem.

#### 6. Reduction of the Determinantal Equation.

The roots of equation (4) are given by  $\lambda^4 = \lambda_1^4$  and  $\lambda^4 = \lambda_2^4$ , where  $\lambda_1^4$  and  $\lambda_2^4$  are complex in general. Hence the roots are

$$\pm \lambda_1, \quad \pm i\lambda_1, \quad \pm \lambda_2, \quad \pm i\lambda_2,$$

and it is clear from the expression (2) for  $k$  that those roots with suffix 1 will have a single value of  $k$ , say  $k_1$ , associated with them, and that a single  $k_2$  will be associated with those of suffix 2.

The determinant arising from (6) is therefore :

$$\begin{vmatrix}
 1 & 1 & 1 & 1 & 1 & 1 & 1 \\
 k_1 & k_1 & k_1 & k_1 & k_2 & k_2 & k_2 \\
 \lambda_1 & -\lambda_1 & i\lambda_1 & -i\lambda_1 & \lambda_2 & -\lambda_2 & i\lambda_2 \\
 k_1\lambda_1 & -k_1\lambda_1 & ik_1\lambda_1 & -ik_1\lambda_1 & k_2\lambda_2 & -k_2\lambda_2 & ik_2\lambda_2 \\
 \lambda_1^3 e^{r\lambda_1} & \lambda_1^3 e^{-r\lambda_1} & -\lambda_1^3 e^{ir\lambda_1} & -\lambda_1^3 e^{-ir\lambda_1} & \lambda_2^3 e^{r\lambda_2} & \lambda_2^3 e^{-r\lambda_2} & -\lambda_2^3 e^{ir\lambda_2} \\
 k_1\lambda_1^2 e^{r\lambda_1} & k_1\lambda_1^2 e^{-r\lambda_1} & -k_1\lambda_1^2 e^{ir\lambda_1} & -k_1\lambda_1^2 e^{-ir\lambda_1} & k_2\lambda_2^2 e^{r\lambda_2} & k_2\lambda_2^2 e^{-r\lambda_2} & -k_2\lambda_2^2 e^{ir\lambda_2} \\
 \lambda_1^3 e^{r\lambda_1} & -\lambda_1^3 e^{-r\lambda_1} & -i\lambda_1^3 e^{ir\lambda_1} & i\lambda_1^3 e^{-ir\lambda_1} & \lambda_2^3 e^{r\lambda_2} & -\lambda_2^3 e^{-r\lambda_2} & -i\lambda_2^3 e^{ir\lambda_2} \\
 k_1\lambda_1^3 e^{r\lambda_1} & -k_1\lambda_1^3 e^{-r\lambda_1} & -ik_1\lambda_1^3 e^{ir\lambda_1} & ik_1\lambda_1^3 e^{-ir\lambda_1} & k_2\lambda_2^3 e^{r\lambda_2} & -k_2\lambda_2^3 e^{-r\lambda_2} & -ik_2\lambda_2^3 e^{ir\lambda_2}
 \end{vmatrix}$$

This may be reduced without much difficulty to the form :

$$(k_2 - k_1)^4 \cdot F(r\lambda_1) \cdot F(r\lambda_2),$$

where

$$F(r\lambda) = \lambda^6 \begin{vmatrix} 1 & 1 & 1 & 1 \\ 1 & -1 & i & -i \\ e^{r\lambda} & e^{-r\lambda} & -e^{ir\lambda} & -e^{-ir\lambda} \\ e^{r\lambda} & -e^{-r\lambda} & -ie^{ir\lambda} & ie^{-ir\lambda} \end{vmatrix}$$

$$= 16i\lambda^6 (\cosh r\lambda \cos r\lambda + 1).$$

Thus, omitting constant factors, the second equation for the determination of  $\lambda$  and  $\mu$  is

$$(k_1 - k_2)^4 \lambda_1^6 \lambda_2^6 (\cosh r\lambda_1 \cos r\lambda_1 + 1) (\cosh r\lambda_2 \cos r\lambda_2 + 1) = 0, \quad \dots (7)$$

where  $\lambda_1^4, \lambda_2^4$  are the roots of (4).

It is notable that the equation

$$\cosh r\lambda \cos r\lambda + 1 = 0$$

is that which determines the modes in the flexural oscillations of a single long beam encastred at one end and fixed at the other.

### 7. Discussion of the Modes.

It thus appears that if  $\lambda_1^4, \lambda_2^4$  are the roots of (4), admissible solutions arise in the following cases :—

- (1)  $\cosh r\lambda_1 \cos r\lambda_1 + 1 = 0,$
- (2)  $\cosh r\lambda_2 \cos r\lambda_2 + 1 = 0,$
- (3)  $k_1 = k_2,$
- (4)  $\lambda_1 = 0,$
- (5)  $\lambda_2 = 0,$

or when two or more of these conditions are simultaneously satisfied. Of these, the first two furnish the main part of the solution, the others requiring, in general, the satisfaction of special relations between the constants of the system.

*Cases (1) and (2).*

If  $z$  is a root of  $\cosh z \cos z + 1 = 0$ , then  $-z, iz$ , and  $-iz$  are roots, but there are no complex roots\*.

\* This may be proved analytically by pedestrian methods, or appeal can be made to the fact that the equation governs the flexural oscillations of a uniform cantilever bar, a motion which is necessarily pure harmonic, since it is not subject to dissipation of energy. (Rayleigh, 'Sound,' i. §§ 173, 175.)

The positive real roots are the infinite series :

$$1.875, 4.69, 7.85, 11.00, 14.14, 17.28 \dots,$$

approximating to  $(n + \frac{1}{2})\pi$  when  $n$  is large.

The method of constructing the modes which arise from this equation is therefore as follows:—If  $r\lambda_1$  takes any one of these values, the corresponding values of  $\mu$ , four in general, are obtained by substitution of  $\lambda_1^4$  in equation (4). With any one of these values of  $\mu$ ,  $\lambda_2^4$  is now obtained from (4) and the corresponding mode will be

$$\left. \begin{aligned} z &= (A_1 \cosh \lambda_1 x + A_2 \sinh \lambda_1 x + A_3 \cos \lambda_1 x + A_4 \sin \lambda_1 x \\ &\quad + A_5 \cosh \lambda_2 x + A_6 \sinh \lambda_2 x + A_7 \cos \lambda_2 x + A_8 \sin \lambda_2 x) e^{\mu t} \\ \theta &= \{ k_1 (A_1 \cosh \lambda_1 x + A_2 \sinh \lambda_1 x + A_3 \cos \lambda_1 x + A_4 \sin \lambda_1 x) \\ &\quad + k_2 (A_5 \cosh \lambda_2 x + A_6 \sinh \lambda_2 x + A_7 \cos \lambda_2 x + A_8 \sin \lambda_2 x) \} e^{\mu t} \end{aligned} \right\}, \quad (8)$$

where  $\mu$ ,  $\lambda_2$ , and the constants may be complex.

In general  $\lambda_2$  will not satisfy  $\cosh r\lambda \cos r\lambda + 1 = 0$ , but will be a function of the constants of the system.

It will be noticed that from a single solution of  $\cosh z \cos z + 1 = 0$  there arise four different solutions of the type (8), since with each of the four values of  $\mu$  associated with  $\lambda_1$  there will be a different  $\lambda_2$ . If there is a pair of complex values of  $\mu$ , the two corresponding solutions will, of course, combine to give a single real mode.

Hence, of any mode of this series, part takes the same form as in the problem of the single beam encastred at one end, and depends only on the length of the beam and the end conditions, while the other part depends on the arrangement of the two-beam system and the external forces.

Case (3).  $k_1 = k_2$

In any mode which satisfies this condition we shall have

$$\begin{aligned} z &= f(x) e^{\mu t}, \\ \theta &= C f(x) e^{\mu t}, \end{aligned}$$

where  $C$  is a constant, and it is evident that the corresponding mode of the deflexions  $y_1, y_2$  of the spars will be of this form. Thus any mode of this class is characterized by the relation

$$y_1/y_2 = \text{constant.}$$

To investigate the possibility of such modes we must



return to equation (2), in which, putting  $k_1=k_2=k$ , we have :

$$k(\beta_1\lambda_1^4 + b_1\mu + c_1) + \alpha_1\lambda_1^4 + \mu^2 + a_1\mu = 0,$$

$$k(\beta_1\lambda_2^4 + b_1\mu + c_1) + \alpha_1\lambda_2^4 + \mu^2 + a_1\mu = 0,$$

$$k(\alpha_2\lambda_1^4 + \mu^2 + b_2\mu + c_2) + \beta_2\lambda_1^4 + a_2\mu = 0,$$

$$k(\alpha_2\lambda_2^4 + \mu^2 + b_2\mu + c_2) + \beta_2\lambda_2^4 + a_2\mu = 0.$$

Subtracting the second from the first and the fourth from the third of these equations, we have

$$(k\beta_1 + \alpha_1)(\lambda_1^4 - \lambda_2^4) = 0$$

and

$$(k\alpha_2 + \beta_2)(\lambda_1^4 - \lambda_2^4) = 0,$$

whence it follows that either

$$\lambda_1^4 = \lambda_2^4 \quad . \quad . \quad . \quad . \quad . \quad . \quad (a)$$

or

$$\left. \begin{aligned} k\beta_1 + \alpha_1 &= 0 \\ k\alpha_2 + \beta_2 &= 0 \end{aligned} \right\} \quad . \quad . \quad . \quad . \quad . \quad . \quad (b)$$

Considering first the alternative (b), it is evident from the four equations above that we must also have :

$$k(b_1\mu + c_1) + \mu^2 + a_1\mu = 0,$$

$$k(\mu^2 + b_2\mu + c_2) + a_2\mu = 0.$$

Thus in case (b) we have

$$-k = \frac{\alpha_1}{\beta_1} = \frac{\beta_2}{\alpha_2} = \frac{\mu^2 + a_1\mu}{b_1\mu + c_1} = \frac{a_2\mu}{\mu^2 + b_2\mu + c_2}.$$

This involves relations between the constants of the system, and it is easily seen that these lead to a violation of the fundamental condition of small deformation, irrespective of the time factor. For under these relations the coefficient of  $\lambda^8$  and the absolute term in equation (4) both vanish. This implies that one of  $\lambda_1, \lambda_2$  tends to zero, the other to infinity. Thus the alternative (b) does not contribute a new type of solution.

*The condition of equal roots.*—Returning to the alternative (a),  $\lambda_1 = \lambda_2$ , it is sufficient to remark that our derivation of the determinantal equation becomes invalid if any two values of  $\lambda$  associated with a given  $\mu$  are equal. For if  $\lambda_1 = \lambda_2$ , the expression  $Ae^{\lambda_1 x} + Be^{\lambda_2 x}$  must be replaced by  $e^{\lambda_1 x}(A' + B'x)$  and the expressions (6) for the end conditions become correspondingly modified. Thus the condition  $\lambda_1 = \lambda_2$  must

be rejected, without prejudice, however, to the question as to whether equal roots do in fact arise.

It is evident that equal values of  $\lambda$  can arise only through the satisfaction of certain relations between the constants of the system. For such roots and their associated time factors must satisfy not only equation (5), but also the condition that (5) has equal roots. We thus have sufficient equations to determine  $\mu$  and the repeated  $\lambda$  roots before introducing the end conditions, and the satisfaction of the latter must involve special relations between the constants of the system. It is possible, of course, starting with  $\lambda^4$  and  $(\lambda + d\lambda)^4$ , and proceeding to the limit when  $d\lambda \rightarrow 0$ , to obtain the modified end conditions applicable to repeated roots, and so derive the determinantal equation for this class of solution. This equation is, however, one of great complexity, and the matter, which is of academic interest only, has not been carried further.

#### Cases (4) and (5).

If  $\lambda_1 = 0$  and  $k_1 \neq k_2$ , then reference to equations (6) shows that  $\lambda_2$  must be a root of  $\cosh r\lambda \cos r\lambda + 1 = 0$ . Thus this case is included under Case (2).

*Summary.*—The survey of Cases (3) to (5) has not yielded anything of practical importance. Thus, in general, the system moves in modes of the type :

$$(A_1 \cosh \lambda_1 x + A_2 \sinh \lambda_1 x + A_3 \cos \lambda_1 x + A_4 \sin \lambda_1 x \\ + A_5 \cosh \lambda_2 x + A_6 \sinh \lambda_2 x + A_7 \cos \lambda_2 x + A_8 \sin \lambda_2 x)e^{\mu t},$$

where  $\lambda_1$  satisfies  $\cosh r\lambda \cos r\lambda + 1 = 0$

and  $\lambda_2$  and  $\mu$  are given by equation (4).

### 8. The Stability of the System.

When the motion of an elastic structure takes place in contact with a source of energy such as a fluid medium in motion, the practical problem is to determine under what conditions it becomes unstable. There is a continued interchange of energy between the vibrating structure and the fluid. If on the whole the structure absorbs energy from the fluid its kinetic energy will increase until the elastic limit of the material is passed, and structural failure will follow. Under these conditions the vibration is unstable.

On the other hand, if energy is on the whole dissipated from the structure to the fluid, the structure ultimately comes to rest and the motion is stable. In the intermediate case, when no energy flows on the whole between the structure and the fluid, a condition of permanent oscillation is theoretically attained, and the stability is neutral.

In examining the stability we are only concerned with the values of the time factor  $\mu$ . The condition for stability is that the real part of every value of  $\mu$  shall be negative. The stability analysis is relatively simple because all the values of  $\mu$  are derived from those of  $\lambda_1$  satisfying

$$\cosh r\lambda \cos r\lambda + 1 = 0,$$

and are independent of the complementary series  $\lambda_2$ , the derivation of which makes the construction of the modes a very laborious process. We have to examine the quartic :

$$\mu^4 + C_1\mu^3 + (C_2\lambda^4 + C_3)\mu^2 + C_4\lambda^4\mu + C_5\lambda^8 + C_6\lambda^4 = 0,$$

where, as will be seen from (4),

$$C_1 = a_1 + b_2,$$

$$C_2 = \alpha_1 + \alpha_2.$$

$$C_3 = a_1b_2 - a_2b_1 + c_2,$$

$$C_4 = \alpha_1b_2 - \beta_1a_2 + \alpha_2a_1 - \beta_2b_1,$$

$$C_5 = \alpha_1\alpha_2 - \beta_1\beta_2,$$

$$C_6 = \alpha_1c_2 - \beta_2c_1,$$

and  $r\lambda$  has the infinite series of values, already mentioned, which satisfy

$$\cosh z \cos z + 1 = 0.$$

In this we have put  $a_1c_2 - a_2c_1 = 0$ , a condition which usually holds in the case of fluid reactions.

### 9. The Conditions of Stability.

The conditions of stability of a quartic are that each coefficient, and also Routh's discriminant, must be positive. We must therefore have :

$$C_1 > 0,$$

$$C_2\lambda^4 + C_3 > 0,$$

$$C_4 > 0,$$

$$C_5\lambda^4 + C_6 > 0,$$

$$\text{and } C_1C_4\lambda^4(C_2\lambda^4 + C_3) - C_4^2\lambda^8 - C_1^2(C_5\lambda^8 + C_6\lambda^4) > 0.$$

The last of these reduces to :

$$\begin{aligned} \Delta &= X\lambda^4 + Y > 0, \\ \text{where } X &= C_1 C_2 C_4 - C_4^2 - C_1^2 C_5, \\ Y &= C_1 C_3 C_4 - C_1^2 C_6. \end{aligned}$$

These conditions must be satisfied for each of the infinite series of values of  $\lambda$  given by

$$r\lambda = 1.875, 4.69, 7.85, \dots (n + \frac{1}{2})\pi,$$

when  $n$  is large.

The complete analysis of these conditions would require a detailed consideration of the coefficients  $a_1, b_1, c_1, a_2, b_2, c_2$ , which specify the fluid reaction. These depend in general in magnitude and sign on the angle of presentation of the structure to the fluid in the equilibrium position; analysis on these lines is beyond the scope of this paper. It should be remarked, however, that each of these coefficients is proportional to  $V$ , the equilibrium velocity of the structure through the fluid. A few results of general import in the examination of stability may be mentioned.

(a) *Two types of instability.*—It appears that a distinction of some importance may be drawn between the conditions of stability. Consider a condition of the form  $H\lambda^4 + J > 0$ . If  $H > 0$  the condition is satisfied when  $\lambda$  is large enough, however large and negative  $J$  may be. In this case the condition may be written  $H\lambda_0^4 + J > 0$ , where  $\lambda_0$  is the least value of  $\lambda$ ; and if this is not satisfied a limited number of the gravest modes will be unstable. We may call such a condition one of *limited instability*.

On the other hand, if  $H < 0$ , all the modes involving  $\lambda$  greater than a certain value will be unstable, however large and positive  $J$  may be. This may be called a state of *unlimited instability*.

(b) *A short scheme of stability criteria.*—Of the coefficients  $C$ , it will be seen that  $C_2$  and  $C_5$  are always positive, while the sign of the others, and of  $X$  and  $Y$ , depends on the arrangement of the system.

Thus if, as usually happens,  $C_1$  is positive, we may group the stability conditions thus :

$$\left. \begin{aligned} C_3\lambda_0^4 + C_8 &> 0 \\ C_6\lambda_0^4 + C_8 &> 0 \end{aligned} \right\} \dots \dots \dots (9)$$

$$\left. \begin{aligned} C_4 &> 0 \\ X &> 0 \\ X\lambda_0^4 + Y &> 0 \end{aligned} \right\}, \dots \dots \dots (10)$$

where  $\lambda_0$  is the smallest value of  $\lambda$ .

~ Violation of criteria (9) leads to limited instability. Violation of the first two criteria (10) produces unlimited instability, but if  $X > 0$ , violation of the third of (10) produces limited instability. It is noticeable that if  $C_4 < 0$  then  $X < 0$ , but if  $C_4 > 0$  it does not follow that  $X > 0$ .

The conditions (9) and (10), together with  $C_1 > 0$ , comprise the shortest complete criterion of stability.

(c) *The influence of beam-length, total strength, and speed.*—Assuming that  $C_4$  and  $X$  are both positive, so that only limited instability is in question, the influence of  $r$ ,  $S = B_1 + B_2$ , and the steady speed  $V$  can be at once seen. Under these conditions, stability can be assured :

- (1) by shortening the length of beam  $r$ , for this increases  $\lambda_0$  ;
- (2) by increasing the total strength  $S$ , for  $C_2$ ,  $C_6$ , and  $X$  each involve positive powers of  $S$  ;
- (3) by decreasing the speed  $V$ , which occurs as a factor only of  $C_3$ ,  $C_6$ , and  $Y$ —this statement is only true if one of  $C_3$ ,  $C_6$ , and  $Y$  is negative, and amounts to saying that if instability of the limited type is latent in the system it will be developed by increasing the steady speed of the structure through the fluid.

(d) *The first appearance of instability.*—It is often necessary to trace the changes which, when applied to a system which is known to be stable, will lead to instability. In this connexion it is only necessary to notice that :

- (1) instability arises through the change from negative to positive of the real part of a complex value of  $\mu$  when Routh's discriminant vanishes ;
- (2) instability arises through the change from negative to positive of a real value of  $\mu$  when the coefficient of the absolute term of the quartic vanishes.

Hence the equations which determine the first appearance of instability in a stable system of the form considered here are :

$$X\lambda_0^4 + Y = 0$$

and

$$C_6\lambda_0^4 + C_6 = 0.$$

#### 10. *The Character of the Higher Modes.*

When  $\lambda$  is large the equation for  $\mu$  becomes :

$$\mu^4 + C_1\mu^3 + C_2\lambda^4\mu^2 + C_4\lambda^4\mu + C_6\lambda^8 = 0.$$

This is of the form

$$(\mu^2 + \epsilon_1\mu + \delta_1\lambda^4)(\mu^2 + \epsilon_2\mu + \delta_2\lambda^4) = 0,$$

and in the limit we have

$$\left. \begin{aligned} \epsilon_1 &= \frac{1}{2} \left( C_1 - \frac{N}{K} \right) \\ \epsilon_2 &= \frac{1}{2} \left( C_1 + \frac{N}{K} \right) \\ \delta_1 &= \frac{C_2 + K}{2} \\ \delta_2 &= \frac{C_2 - K}{2} \end{aligned} \right\},$$

where

$$K^2 = C_2^2 - 4C_5$$

$$N = 2C_4 - C_1C_2.$$

$$\text{Thus } \mu = -\frac{\epsilon_1}{2} \pm \sqrt{\delta_1\lambda^2}i, \quad -\frac{\epsilon_2}{2} \pm \sqrt{\delta_2\lambda^2}i.$$

The conditions for stability in these modes are :

$$C_4 > 0$$

and

$$X = \frac{1}{4}(C_1^2K^2 - N^2) > 0.$$

Violation of either of these conditions leads to a positive value of either  $\epsilon_1$  or  $\epsilon_2$ .

Hence the higher modes have constant positive or negative damping of amount  $-\frac{1}{2}(C_1 \pm K)$ .

$$\text{Their frequencies are } \frac{\sqrt{C_2 \mp K}}{2\sqrt{2\pi}}\lambda^2,$$

where  $\lambda = (n + \frac{1}{2})\pi$ , and  $n$  is large.

### 11. The Motion in vacuo.

When the structure vibrates in *vacuo* its energy is constant and the modes are undamped oscillations. The analysis in this case admits of a concise summary.

The coefficients  $C_1, C_3, C_4, C_6$  vanish. Thus the frequency equation is

$$\left(\frac{\mu^2}{\lambda^4}\right)^2 + C_2\left(\frac{\mu^2}{\lambda^4}\right) + C_5 = 0.$$

This, together with

$$\cosh r\lambda \cos r\lambda + 1 = 0,$$

determines the modes.

## 112 *Torsion Flexure Oscillations of Two Connected Beams.*

The two solutions associated with any value  $\lambda_1$  satisfying the transcendental equation are:

$$\lambda_1, \quad \mu^2 = -e^2 \lambda_1^4, \quad \lambda_2^4 = p^4 \lambda_1^4$$

and  $\lambda_1, \quad \mu^2 = -f^2 \lambda_1^4, \quad \lambda_2^4 = q^4 \lambda_1^4,$

where  $e^2 = \frac{1}{2}(C_2 - K), \quad p^4 = \frac{C_2(C_2 - K)}{2C_5} - 1$

$$f^2 = \frac{1}{2}(C_2 + K), \quad q^4 = \frac{C_2(C_2 + K)}{2C_5} - 1,$$

and  $K$  has been defined in § 10.

Thus the frequencies are proportional to  $e\lambda_1^2$  and  $f\lambda_1^2$ , and the modes deriving from a single value of  $\lambda_1$  are:

$$\begin{aligned} & A_1 \cosh \lambda_1 x \cos (e\lambda_1^2 t + \epsilon_1) + A_2 \sinh \lambda_1 x \cos (e\lambda_1^2 t + \epsilon_2) \\ & + A_3 \cos \lambda_1 x \cos (e\lambda_1^2 t + \epsilon_3) + A_4 \sin \lambda_1 x \cos (e\lambda_1^2 t + \epsilon_4) \\ & + A_5 \cosh p\lambda_1 x \cos (e\lambda_1^2 t + \epsilon_5) + A_6 \sinh p\lambda_1 x \cos (e\lambda_1^2 t + \epsilon_6) \\ & + A_7 \cos p\lambda_1 x \cos (e\lambda_1^2 t + \epsilon_7) + A_8 \sin p\lambda_1 x \cos (e\lambda_1^2 t + \epsilon_8), \end{aligned}$$

and a second series in which  $f$  is substituted for  $e$  and  $q$  for  $p$ .

If the mass of the system is wholly concentrated in the spars, the frequencies can be simply expressed in terms of characteristic points of a cross-section.  $P_1$  and  $P_2$  being the spar centres, let  $G$  be the centre of mass of the section, and  $F$  the centroid of  $B_1$  and  $B_2$  the flexural rigidities of the spars, so that  $F$  may be called the "centre of flexure" of the two spars. Then if  $S = B_1 + B_2$  and  $M$  is the mass of the section, the frequencies are proportional to

$$\lambda_1^2 \sqrt{\frac{FP_1}{GP_1} \cdot \frac{S}{M}} \quad \text{and} \quad \lambda_1^2 \sqrt{\frac{FP_2}{GP_2} \cdot \frac{S}{M}}.$$

If, in addition, the spars are of the same shape and material, the frequencies are proportional to

$$\lambda_1^2 \sqrt{\frac{B_1}{M_1}} \quad \text{and} \quad \lambda_1^2 \sqrt{\frac{GP_1}{GP_2} \cdot \frac{B_1}{M_1}},$$

where  $B_1$ ,  $M_1$  refer to the spar  $P_1$ .

12. I have to thank the Air Ministry for permission to publish this work, which in its original form was a contribution to the theory of wing flutter. It should be emphasized that all statements and conclusions which it contains are advanced on my sole responsibility, and carry no official sanction.

Royal Aircraft Establishment,  
Farnborough.

IX. *On the Relations between the Fourier Constants of a Periodic Function and the Coefficients determined by Harmonic Analysis.* By ALBERT EAGLE, B.Sc., Lecturer in Mathematics in the Victoria University of Manchester\*.

IF  $f(t)$  is a periodic function, of period  $2\pi$ , the coefficients of the  $n$ th cosine and sine harmonics are given by

$$a_n = \frac{1}{\pi} \int_{-\pi}^{\pi} f(t) \cos nt \, dt \quad . \quad . \quad . \quad (1a)$$

and

$$b_n = \frac{1}{\pi} \int_{-\pi}^{\pi} f(t) \sin nt \, dt \quad . \quad . \quad . \quad (1b)$$

respectively. These coefficients are termed the "Fourier constants" of the function.

If  $f(t)$  is a function for which these integrals cannot be evaluated, or if it is a function which is only known empirically, these integrals—in the absence of some mechanical harmonic analyser—can only be evaluated approximately by summing the value of the integrand at equidistant ordinates. This constitutes the ordinary method of harmonic analysis; and it can be shown that if we take  $2p$  ordinates per period at intervals of  $\pi/p$ ; and if  $A_q$  denote the value of  $f(t)$  at  $t = q\pi/p$ , the curve given by

$$y = \frac{a_0}{2} + a_1 \cos t + \dots + a_{p-1} \cos \overline{p-1}t + \frac{a_p}{2} \cos pt \\ + b_1 \sin t + \dots + b_{p-1} \sin \overline{p-1}t, \quad . \quad . \quad . \quad (2)$$

where

$$a_n = \frac{2}{p} \sum A_q \cos qu\pi/p \quad . \quad . \quad . \quad (2a)$$

and

$$b_n = \frac{2}{p} \sum A_q \sin qn\pi/p \quad \dagger, \quad . \quad . \quad . \quad (2b)$$

will pass through tops of the given ordinates.

Now, the value of these coefficients, as thus determined, can be expressed in terms of the Fourier constants by the equations

$$a_n = a_n + (a_{2p-n} + a_{2p+n}) + (a_{4p-n} - a_{4p+n}) + \dots \quad (3)$$

and

$$b_n = b_n - (b_{2p-n} - b_{2p+n}) - (b_{4p-n} - b_{4p+n}) - \dagger \dots \quad (4)$$

\* Communicated by the Author.

† A. Eagle, 'A Practical Treatise on Fourier's Theorem and Harmonic Analysis,' p. 77 (Longmans, 1925).

‡ Loc. cit. p. 97.



Further, if the periodic function is an artificial one built up of arcs of parabolas of different degrees, the Fourier constants may be expressed in terms of the discontinuities of the function, and of its several differential coefficients, at the points where the different parabolic arcs join one another. It will be convenient to call a discontinuity that is a sudden jump in magnitude of the  $r$ th differential coefficient, a discontinuity of the  $r$ th order, and to denote it by  $I^r$ , so that  $I^r \equiv f^r(t+0) - f^r(t-0)$  at the point of discontinuity. That being so, it can be shown that if, in one period, the function has discontinuities  $I_1, I_2, \dots$  of zero order;  $I'_1, I'_2, \dots$  of the first order;  $I''_1, I''_2, \dots$  of the second order, and so on, and if  $t=\alpha$  is the location of any of these points of discontinuity, then

$$\begin{aligned} \pi a_n = & -\frac{1}{n} \sum I \sin n\alpha - \frac{1}{n^2} \sum I' \cos n\alpha \\ & + \frac{1}{n^3} \sum I'' \sin n\alpha + \frac{1}{n^4} \sum I''' \cos n\alpha \dots \quad (5) \end{aligned}$$

and

$$\begin{aligned} \pi b_n = & \frac{1}{n} \sum I \cos n\alpha - \frac{1}{n^2} \sum I' \sin n\alpha \\ & - \frac{1}{n^3} \sum I'' \cos n\alpha + \frac{1}{n^4} \sum I''' \sin n\alpha + \dots, \quad (6) \end{aligned}$$

where in each series two positive terms and two negative terms alternate\*. The series terminate if the parabolic arcs are all of finite degree, but they may often be used when the arcs are parabolic arcs of an infinite degree such as arcs of sine or exponential curves etc.

The formulæ in (5) and (6) show clearly that the higher harmonics ultimately depend only upon the discontinuities of lowest order that are present, while if the function only possesses discontinuities of a single order, the formulæ reduce to a single term.

Let us examine this important case in further detail, and suppose that the function is also analysed by the ordinary method of harmonic analysis, and also that the number of ordinates per half period,  $p$ , is chosen so that all the discontinuities lie on the measured ordinates; that is  $\alpha$ , in (5) and (6), is of the form  $N\pi/p$ , where  $N$  is an integer. Let us now substitute these expressions for the  $\alpha$ 's and  $\beta$ 's in (3) and (4). Since  $(2p \pm n)\alpha = (2p \pm n)N\pi/p = 2\pi N \pm n\alpha$  and

\* *Loc. cit.* p. 59.

so on, we get, in the case where all the discontinuities are of zero order, so that

$$\pi a_n = -\frac{1}{n} \sum I \sin n\alpha \quad \text{and} \quad \pi b_n = \frac{1}{n} \sum I \cos n\alpha,$$

$$\begin{aligned} \pi a_n = & -\frac{1}{n} \sum I \sin n\alpha + \frac{1}{2p-n} \sum I \sin n\alpha \\ & + \frac{1}{2p+n} \sum I \sin n\alpha + \dots \end{aligned}$$

and

$$\begin{aligned} \pi b_n = & \frac{1}{n} \sum I \cos n\alpha - \frac{1}{2p-n} \sum I \cos n\alpha \\ & + \frac{1}{2p+n} \sum I \cos n\alpha + \dots \quad (7) \end{aligned}$$

If we divide these expressions, respectively, by  $\pi a_n$  and  $\pi b_n$ , they both give

$$\begin{aligned} \frac{a_n}{a_n} = \frac{b_n}{b_n} = n \left\{ \frac{1}{n} - \frac{1}{2p-n} + \frac{1}{2p+n} \right. \\ \left. - \frac{1}{4p-n} + \frac{1}{4p+n} + \dots \right\}. \quad (8') \end{aligned}$$

Now, the series in brackets is the function  $\frac{\pi}{2p} \cot \frac{\pi n}{2p}$ , whence we have

$$\frac{a_n}{a_n} = \frac{b_n}{b_n} = \frac{\tan \frac{\pi n}{2p}}{\frac{\pi n}{2p}}. \quad (8)$$

Hence for a periodic function which only possesses discontinuities of a zero order, and which is necessarily a step-like function consisting of portions of straight lines parallel to the axis of  $t$  together with portions of the measured ordinates joining them, we see that *we can determine the true Fourier constants by merely calculating the a's and b's by (2a) and (2b)\* and multiplying the result by the function in (8).* Moreover, this result, which is exact under the conditions specified, tends to become true for large values of  $n$  for *all functions* which possess discontinuities of zero order situated on the measured ordinates.

If next we suppose the function only to possess discontinuities of the first order, so that it necessarily consists of

\*  $\frac{1}{2}f(t+0) + \frac{1}{2}f(t-0)$  is to be taken as the value of the ordinates in calculating these formulae.

joined portions of straight lines, all of finite slope, and if all the junctions are on the measured ordinates, we have

$$\pi a_n = -\frac{1}{n^2} \Sigma I' \cos n\alpha \quad \text{and} \quad \pi b_n = -\frac{1}{n^2} \Sigma I' \sin n\alpha.$$

Substituting these results in (3) and (4) as before, and dividing by  $a_n$  and  $b_n$  respectively, it will be found that both give

$$\frac{a_n}{a_n} = \frac{b_n}{b_n} = n^2 \left\{ \frac{1}{n^2} + \frac{1}{(2p-n)^2} + \frac{1}{(2p+n)^2} + \dots \right\}. \quad (9')$$

Now, this series in brackets is the function  $\frac{\pi^2}{4p^2} \operatorname{cosec}^2 \frac{\pi n}{2p}$ , whence

$$\frac{a_n}{a_n} = \frac{b_n}{b_n} = \frac{\sin^2 \frac{\pi n}{2p}}{\left(\frac{\pi n}{2p}\right)^2} \dots \dots \dots (9)$$

Exactly similarly, if  $f(t)$  only possesses discontinuities of the second order, all situated on the measured ordinates, so that it necessarily consists of parabolic arcs joined without any discontinuity of slope, we find

$$\frac{a_n}{a_n} = \frac{b_n}{b_n} = n^3 \left\{ \frac{1}{n^3} - \frac{1}{(2p-n)^3} + \frac{1}{(2p+n)^3} - \dots \right\}, \quad (10')$$

which is readily identified as being

$$\frac{a_n}{a_n} = \frac{b_n}{b_n} = \frac{\sin^3 \frac{\pi n}{2p}}{\left(\frac{\pi n}{2p}\right)^3 \cos \frac{\pi n}{2p}} \dots \dots \dots (10)$$

Lastly, for our present examples, if the discontinuities (all situated on the measured ordinates) are all of the third order, so that  $f(t)$  consists of parabolic arcs of the third degree joined together without any sudden breaks either of slope or curvature, it will be found that

$$\frac{a_n}{a_n} = \frac{b_n}{b_n} = n^4 \left\{ \frac{1}{n^4} + \frac{1}{(2p-n)^4} + \frac{1}{(2p+n)^4} + \dots \right\}, \quad (11')$$

giving

$$\frac{a_n}{a_n} = \frac{b_n}{b_n} = \frac{3 \sin^4 \frac{\pi n}{2p}}{\left(\frac{\pi n}{2p}\right)^4 \left\{ 1 + 2 \cos^2 \frac{\pi n}{2p} \right\}} \dots \dots \dots (11)$$

\* This result is easily obtained by observing that the series (11') is the derivative with respect to  $n$ , of (10'), and that in turn is the derivative of (9').

For readiness in use these four functions in (8)–(11), which we will denote by  $F_0$ ,  $F_1$ ,  $F_2$ , and  $F_3$  respectively, are tabulated below, from which table graphs of the functions, sufficiently accurate for all ordinary use, may readily be constructed. In the case of the functions  $F_0$  and  $F_3$  it will obviously be best to graph the reciprocals, which are readily obtainable by a slide-rule.

TABLE I.

$12n/p$ .	$F_0(n/p)$ .	$F_1(n/p)$ .	$F_2(n/p)$ .	$F_3(n/p)$ .
0.....	1.000	1.000	1.000	1.000
1.....	1.006	.995	1.000	1.000
2.....	1.024	.978	1.000	1.000
3.....	1.055	.949	1.002	.999
4.....	1.103	.912	1.006	.998
5.....	1.172	.865	1.014	.994
6.....	1.273	.810	1.032	.985
7.....	1.422	.750	1.067	.969
8.....	1.654	.684	1.131	.935
9.....	2.049	.615	1.260	.877
10.....	2.852	.545	1.553	.785
11.....	5.275	.474	2.500	.652
12.....	$\infty$	.405	$\infty$	.493

If the discontinuities, while all of a single order, are all of them *situated midway between the measured ordinates*, it is easily seen that the effect will be to change the sign of alternate terms in the series in (8'), (9'), (10'), and (11') so that in place of the four F-functions we shall now have series representing the reciprocals of

$$\frac{\sin \frac{n\pi}{2p}}{\frac{n\pi}{2p}}, \quad \left( \frac{\sin^2 \frac{n\pi}{2p}}{\frac{n\pi}{2p}} \right)^2 \sec \frac{n\pi}{2p},$$

$$\left( \frac{\sin \frac{n\pi}{2p}}{\frac{n\pi}{2p}} \right)^3 \cdot \frac{2}{1 + \cos^2 \frac{n\pi}{2p}} \quad \text{and} \quad \left( \frac{\sin \frac{n\pi}{2p}}{\frac{n\pi}{2p}} \right)^4 \cdot \frac{6 \sec \frac{n\pi}{2p}}{5 + \cos^2 \frac{n\pi}{2p}}$$

respectively.

These four functions, denoted respectively by  $M_0$ ,  $M_1$ ,  $M_2$ , and  $M_3$ , are tabulated in Table II.

TABLE II.

$12n/p$ .	$M_0(n/p)$ .	$M_1(n/p)$ .	$M_2(n/p)$ .	$M_3(n/p)$ .
0.....	1.000	1.000	1.000	1.000
1.....	.997	1.003	1.000	1.000
2.....	.987	1.012	1.000	1.000
3.....	.974	1.028	.998	1.001
4.....	.955	1.053	.995	1.002
5.....	.930	1.090	.987	1.005
6.....	.900	1.146	.973	1.014
7.....	.866	1.232	.947	1.032
8.....	.827	1.368	.905	1.069
9.....	.784	1.607	.841	1.152
10.....	.738	2.110	.754	1.355
11.....	.688	3.632	.643	2.059
12.....	.637	$\infty$	.516	$\infty$

The  $F_0$ ,  $M_1$ ,  $F_2$ , and  $M_3$  functions are infinite when  $n=p$  because, in the cases of even-order discontinuities at the ordinates or odd-order ones *midway between*, it is possible to have a non-zero periodic function, of half period equal to the distance between the ordinates, and of arbitrary amplitude, when all the ordinates are zero. With first-order discontinuities this function is saw-edge-like and the other cases are also easily seen. Hence the  $a$ 's and  $b$ 's will be finite when  $n=p$ , while the  $a$ 's and  $b$ 's are zero.

The fact that these  $F$  and  $M$  functions enable the integrals

$$\frac{1}{\pi} \int_0^{2\pi} f(t) \cos nt \, dt \quad \text{and} \quad \frac{1}{\pi} \int_0^{2\pi} f(t) \sin nt \, dt$$

to be evaluated exactly, in the special conditions assumed, by multiplying the summation results given by (2a) and (2b) by these functions, is truly remarkable and deserves reflecting upon.

As an illustration of the utility of these correction factors we will take an example worked out in my book \* of an odd periodic function of period  $2\pi$  obtained by joining the point  $(\frac{3}{2}\pi, 24)$  to the origin and to the point  $(\pi, 0)$  by straight lines. The exact harmonic analysis of this function, to two decimal places, is

$$\begin{aligned} f(t) = & 19.27 \sin t + 2.98 \sin 2t - 1.32 \sin 3t \\ & - 1.20 \sin 4t + .53 \sin 6t + .24 \sin 7t \\ & - .18 \sin 8t - .24 \sin 9t + \dots \end{aligned}$$

\* *Loc. cit.* pp. 90-91.

When analysed with 10 ordinates per half-period, the result was

$$\begin{aligned} f(t) = & 19.43 \sin t + 3.08 \sin 2t - 1.43 \sin 3t \\ & - 1.38 \sin 4t + .73 \sin 6t + .37 \sin 7t \\ & - .33 \sin 8t - .49 \sin 9t. \end{aligned}$$

Multiplying these coefficients by the appropriate values of the function  $F_1(n/p)$  brings these two results into agreement.

Even when a periodic function possesses discontinuities of different orders, it will generally be better to correct all the  $a$ 's and  $b$ 's by the function appropriate to the lowest-order discontinuities than to leave them uncorrected. As an illustration we will take the practical case of a rectified sine-waved voltage in which a constant voltage is kept back by the polarizing effect of the rectifying device. Taking, for the purpose of illustration, the polarization voltage as half the maximum voltage, and making the period  $2\pi$ , we have  $f(t)$  an even function given by  $f(t) = 2 \cos \frac{t}{2} - 1$  from  $t=0$  to  $t = \frac{2\pi}{3}$ , and  $f(t) = 0$  from  $t = \frac{2\pi}{3}$  to  $t = \pi$ .

The exact harmonic analysis of this function is readily found to be

$$\begin{aligned} f(t) = & 0.4363 + .5515 \cos t + .0551 \cos 2t \\ & - .0630 \cos 3t + .0197 \cos 4t + .0100 \cos 5t \\ & - .0154 \cos 6t + \dots; \end{aligned}$$

while the ordinary harmonic analysis, with six ordinates per half period, is found to give

$$\begin{aligned} f(t) = & 0.4297 + .5577 \cos t + .0619 \cos 2t \\ & - .0773 \cos 3t + .0275 \cos 4t + .0197 \cos 5t \\ & - .0185 \cos 6t. \end{aligned}$$

If these coefficients be multiplied by the values of the function  $F_1(n/p)$  for values of  $12n/p$  of 0, 2, 4, 6, 8, 10, and 12 respectively, and if the last coefficient is then doubled to make up for the fact that this coefficient is, in accordance with equation (2),  $\frac{1}{2}a_6$  and not  $a_6$ , we get

$$\begin{aligned} f(t) = & 0.4297 + .5454 \cos t + .0564 \cos 2t \\ & - .0626 \cos 3t + .0188 \cos 4t + .0107 \cos 5t \\ & - .0147 \cos 6t + \dots, \end{aligned}$$

which is almost indistinguishable from the exact harmonic analysis if allowance is made for the somewhat large errors in the first two terms—which is a *special effect* due to the

120 Mr. Eagle on *Fourier Constants of a Periodic Function*  
*very few ordinates per half period* combined with the fact  
 that the convexity is always of the same sign—although the  
 function possesses discontinuities of all orders save zero.

### *Application to Empirical Functions.*

The ordinary method of harmonic analysis, when applied to ordinary experimental curves, such as oscillograms of voltage wave forms, has very similar disadvantages of lack of accuracy as it has in the case of artificial functions, which we have seen how to correct above. In order to overcome this I have, in my book \*, given a more accurate method. Two varieties of this method consist, respectively, in drawing parabolic arcs from the tops of one even-numbered ordinate to the next, passing through the top of the intervening ordinate, then drawing a similar succession of arcs starting and terminating at the odd numbered ordinates, and passing through the even ones, and taking the mean of these two results for the first case; and in the second case, in drawing third-degree parabolic arcs from the top of one ordinate to the top of the next, and making them parallel, at their extremities, to the lines joining the tops of the two ordinates adjacent to the end ordinates, and taking this as the given function. In either case the exact analysis of these functions is obtained; and in both cases it appears that both the second and fourth differences of the ordinates are required, when the analysis can be effected by using these differences instead of the ordinates in the ordinary Schedules for harmonic analysis constructed for the convenient carrying out of the formulæ in (2a) and (2b).

I wish now to point out the fact that the result of this method can be obtained much more readily by merely multiplying the result obtained by the ordinary method of harmonic analysis by functions similar to the F and M functions tabulated above.

Since in *all* methods of harmonic analysis the results are linear functions of the  $2p$  ordinates, the comparison of different methods resolves itself into a comparison of the different functions which we take to represent the case in which all the ordinates are zero, except one, which is unity, and which we will imagine is situated at  $t = 0$ . The ordinary method represents this function by

$$f(t) = \frac{1}{p} \left\{ \frac{1}{2} + \cos t + \cos 2t + \dots + \cos \overline{p-1} t + \frac{1}{2} \cos pt \right\};$$

\* *Loc. cit.* pp. 102-111.

that is, by

$$\frac{\sin pt}{p \sin t} \cdot \cdot \cdot \cdot \cdot \cdot \cdot \quad (12 a)$$

To compare different functions we will take the ordinates at unit distances of  $x$  apart and the non-zero ordinate as situated at  $x=0$ . If the function passing through these points becomes negligible before  $x=p$ , we may extend the zero ordinates to  $\pm \infty$ . This set of points, viz.  $(0, 1)$  and the points  $y=0$  for all other positive and negative integral values of  $x$ , we will call the "Fundamental Set of Points," and the spaces between adjacent ordinates "intervals"—the two between  $-1$  and  $+1$  being called "central intervals" and all the others "ordinary intervals."

From (12a) we see, on replacing  $t$  by  $\pi x/p$ , that the ordinary method of harmonic analysis adopts

$$\frac{\sin \pi x}{p \sin \pi x/p}, \approx \frac{\sin \pi x}{\pi x} \cdot \cdot \cdot \cdot \cdot \quad (12 b)$$

if  $p$  is large, as the function through the fundamental set of points. This function suffers from the disadvantage of giving far too much disturbance for moderately large values of  $x$ . Little can be said in defence of the function making the displacement at the centre of the second ordinary interval only  $3/5$  of that at the centre of the first one, while it makes the displacement at the centre of the tenth ordinary interval  $19/21$  of that in the ninth.

We will now give some artificial functions passing through this fundamental set of points. In giving the equations of the different arcs of which these functions are built up, we shall in all cases suppose each arc is referred to an origin at its left-hand extremity so that  $x$  will always go from 0 to 1 for each arc.

It will easily be found that the first variety of my method adopts the function :  $y=1-\frac{3}{4}x-\frac{1}{4}x^2$  for the central interval ;  $y=-\frac{1}{4}x(1-x)$  for the first ordinary interval, and zero beyond ; while the second variety takes,  $y=1-\frac{3}{2}x^2+\frac{3}{2}x^3$  for the central interval ;  $y=-\frac{1}{2}x(1-x)^2$  for the first ordinary interval, and zero beyond.

The harmonic analysis of the first of these functions, when the ordinates are reduced to  $\pi/p$  apart, is found to give, instead of the result in (12),

$$f(t) = \frac{1}{p} \left\{ \frac{1}{2} + c_1 \cos t + c_2 \cos 2t + \dots \right\}, \quad (13)$$



where

$$c_n = \left( \frac{\sin \frac{n\pi}{2p}}{\frac{n\pi}{2p}} \right)^3 \left\{ \frac{n\pi}{2p} \sin \frac{n\pi}{2p} + \cos \frac{n\pi}{2p} \right\}; \quad \dots \quad (13a)$$

while the harmonic analysis of the second function is likewise found to give the same series, but with

$$c_n = \left( \frac{\sin \frac{n\pi}{2p}}{\frac{n\pi}{2p}} \right)^3 \left\{ \frac{6p}{n\pi} \sin \frac{n\pi}{2p} - 2 \cos \frac{n\pi}{2p} \right\} \quad \dots \quad (13b)$$

These results are easily deducible from (5), using the discontinuities between the different arcs.

If we had taken the non-zero ordinate at any other position than  $t=0$ , (12) would have involved both sine and cosine harmonics, and so in that case would (13) likewise; but it is obvious that the ratio of both the  $n$ th sine and the  $n$ th cosine harmonic in (13) to the corresponding terms in (12) would still be  $c_n$  in both cases. Since any function to be analysed consists of a sum of these single non-zero-ordinate functions, we see that in all cases the new method will give both the  $n$ th harmonic terms,  $c_n$  times the magnitude given by the ordinary method.

Indeed, it is obvious that *every possible method of harmonic analysis can only give the same result as the ordinary method with both the  $n$ th sine and  $n$ th cosine harmonics multiplied by some function of  $n/p$ .*

Very much better functions through the fundamental set of points may be obtained than any of the three already given; for it is possible to join arcs of third-degree parabolas without any discontinuities either of slope or curvature. In fact, we know from the theory of beams, that a uniform straight flexible lath made to pass through the points automatically gives us this function, provided that the horizontal scale of the function is sufficiently large so that the inclination of the lath to the  $t$  axis is everywhere small.

To obtain the equation of this interesting function, which we will call the "lath function," we note that the equation of the arc, in the (right hand) central interval, must be of the form

$$y = 1 - cx^2 + (c-1)x^3; \quad \dots \quad (14)$$

also, that if  $p_n$  and  $2q_n$  denote the values at the end of the first and second differential coefficients at the beginning of

any ordinary interval, and  $-p_{n+1}$  and  $-2q_{n+1}$  the values at the end of that interval (and the beginning of the next), we have

$$y = p_n x + q_n x^2 - (p_n + q_n) x^3$$

for the equation in the interval concerned ; whence

$$p_{n+1} = 2p_n + q_n \quad . \quad . \quad . \quad . \quad . \quad (15)$$

and

$$q_{n+1} = 3p_n + 2q_n ;$$

whence both the  $p$ 's and  $q$ 's satisfy the equation

$$u_{n+2} - 4u_{n+1} + u_n = 0 ;$$

and hence

$$p_n = A Q^n + A' Q^{-n}$$

and

$$q_n = B Q^n + B' Q^{-n},$$

where  $Q = 2 - \sqrt{3}$  and  $Q^{-1} = 2 + \sqrt{3}$ . If the  $p$ 's and  $q$ 's  $\rightarrow 0$  as  $n \rightarrow \infty$ , we must have  $A' = B' = 0$ , when substitution in (15) shows that  $B = -A\sqrt{3}$  ; so that the equation of the arc in any ordinary interval is given by

$$y = A \{ x - \sqrt{3} x^2 + (\sqrt{3} - 1) x^3 \}.$$

Determining  $A$  and  $c$  so that this shall fit on to (14) without any discontinuities of slope or curvature, we find

$$c = 3\sqrt{3} - 3 \quad \text{and} \quad A = 3\sqrt{3} - 6 ;$$

so that

$$y = 1 - (3\sqrt{3} - 3)x^2 + (3\sqrt{3} - 4)x^3$$

in the (right hand) central interval and

$$y = (3\sqrt{3} - 6)x + (6\sqrt{3} - 9)x^2 + (15 - 9\sqrt{3})x^3$$

in the first ordinary interval ; and in successive ordinary intervals we have merely to multiply this equation by successive powers of  $-(2 - \sqrt{3})$ .

This function, at the middle of the fifth ordinary interval, has a value of only  $1/1500$ , whereas the function  $(\sin \pi x)/\pi x$  has then a value of  $2/11\pi$ —nearly 90 times as great : we may note that it decays exponentially at the same rate as  $e^{x \log (2 - \sqrt{3})} = e^{-1.31x}$  approx.

We must now obtain the harmonic analysis of this lath-function, which is easily done by considering the discontinuities. These are all of the third order and are merely  $1/6$  of the difference of the coefficients of  $x^3$  in successive intervals. Hence we have a discontinuity of  $(6\sqrt{3} - 8)/6$  at  $x = 0$  ; one of  $(19 - 12\sqrt{3})/6$  at  $x = 1$  ; one of  $-12 + 7\sqrt{3}$  at  $x = 2$  ; and thence after discontinuities

equal to this last multiplied by successive powers of  $-(2-\sqrt{3})$ . Using (5) to determine the Fourier constants, and making use of the formula

$$1 + 2c \cos \theta + 2c^2 \cos 2\theta + 2c^3 \cos 3\theta + \dots \\ = \frac{1-c^2}{1-2c \cos \theta + c^2},$$

we easily find—remembering that when the ordinates are reduced from unit distance apart to  $\pi/p$  all the discontinuities, being of the third order, will be increased in the ratio  $(p/\pi)^2$ —that the harmonic analysis is given by (13), where

$$c_n = \left( \frac{\sin \frac{n\pi}{2p}}{\frac{n\pi}{2p}} \right)^4 \left\{ \frac{3}{2 + \cos n\pi/p} \right\} \dots \quad (16)$$

It will be noticed that this expression is the same as that in (11), which it should be, since both refer to periodic functions which only have third-order discontinuities and have them on the measured ordinates.

We leave it as an interesting rider to the reader to prove that this lath function, from  $x=1$  to  $x=\infty$ , is proportional to

$$(2 - \sqrt{3})^x \{ a_1 \cos \pi x + a_3 \cos 3\pi x + a_5 \cos 5\pi x + \dots \\ + b_1 \sin \pi x + b_3 \sin 3\pi x + b_5 \sin 5\pi x + \dots \},$$

where

$$a_n = \frac{n^4 - 6n^2c^2 + c^4}{(n^2 + c^2)^4} \quad \text{and} \quad b_n = \frac{4(cn^3 - c^3n)}{(n^2 + c^2)^4},$$

and where

$$\pi c = \log_e (2 + \sqrt{3}),$$

$$i. e. \quad c = 0.41920 \dots \quad \text{and} \quad c^2 = 0.17573 \dots$$

A simpler artificial function than the lath-function can be constructed through the fundamental set of points out of ordinary parabolic arcs by joining them, without any discontinuity of slope, *midway between the measured ordinates*.

The equation of the central arc must be of the form

$$y = 1 - cx^2 \quad \text{for} \quad -\frac{1}{2} < x < \frac{1}{2}; \quad \dots \quad (17)$$

while if  $r_n$  and  $s_n$  are the values of the ordinate and slope respectively at the beginning of any other arc, and  $-r_{n+1} - s_{n+1}$  the values of these quantities at the end of the same arc, so that the equation of the arc—remembering that it must make  $y=0$  at its mid point—is

$$y = r_n + s_n x - (4r_n + 2s_n)x^2,$$

we easily find

$$r_{n+1} = 3r_n + s_n \quad . \quad . \quad . \quad . \quad . \quad (18)$$

and

$$s_{n+1} = 8r_n + 3s_n ;$$

whence the  $r$ 's and  $s$ 's satisfy the equation

$$u_{n+2} - 6u_{n+1} + u_n = 0 ;$$

and so

$$r_n = A Q^n + A' Q^{-n} \quad \text{and} \quad s_n = B Q^n + B' Q^{-n}$$

where

$$Q = 3 - \sqrt{8} \quad \text{and} \quad Q^{-1} = 3 + \sqrt{8}.$$

If the  $r$ 's and  $s$ 's  $\rightarrow 0$  as  $n \rightarrow \infty$ , we must have  $A' = B' = 0$ , and then substitution in (18) shows that  $B = -\sqrt{8}A$ , so that the equation of the first ordinary arc is of the form

$$y = A \{ 1 - \sqrt{8}x + (2\sqrt{8} - 4)x^2 \}.$$

Making this, at  $x=0$ , join without discontinuity of slope to  $y = 1 - cx^2$  at  $x = \frac{1}{2}$ , we get

$$A = 1 - c/4 \quad \text{and} \quad -A\sqrt{8} = -c,$$

whence

$$y = 1 - 4(\sqrt{2} - 1)x^2$$

is the equation of the central arc, and

$$y = 2 - \sqrt{2} - (4\sqrt{2} - 4)x + (12\sqrt{2} - 16)x^2$$

is the equation of the first ordinary arc, and successive ordinary arcs are given by multiplying this equation by successive powers of  $-(3 - \sqrt{8})$ . This function decays very rapidly; approximately as  $e^{-1.76x}$ , and at the middle of the fourth ordinary interval has a value of only about 1/2000.

The harmonic analysis of this function, which we will call the "parabola-function," is similarly found to be the series (13) with

$$c_n = \left( \frac{\sin \frac{n\pi}{2p}}{\frac{n\pi}{2p}} \right)^3 \left\{ \frac{4}{3 + \cos n\pi/p} \right\} \quad . \quad . \quad . \quad (19)$$

This expression, it will be noted, is the same as the  $M_2$  function of Table II., which again is as it should be.

Various analytic functions may be found to pass through the fundamental set of points. Three, which immediately suggest themselves, are

$$g \frac{\sin \pi x}{\sinh g\pi x}, \quad \frac{\sin \pi x}{\pi x \cosh h\pi x} \quad \text{and} \quad e^{-k^2 \pi x^2} \frac{\sin \pi x}{\pi x},$$

which we will denote by  $\phi(x)$ ,  $\phi_h(x)$ , and  $\phi_k(x)$  respectively. For these to give at all reasonably "smooth" curves

through the points,  $g$ ,  $h$ , and  $k$  must be small. A good way of comparing the suitability of the different functions is to tabulate the curvature they give at  $x=0$  and the numerical slope they give at  $x=1$ ; the results are:—

Function.	Curvature at $x=0$ .	Slope at $x=1$ .
$\frac{\sin \pi x}{\pi x}$	$\pi^2/3$	1
$\phi_g(x)$	$\pi^2(1+g^2)/3$	$1-g^2\pi^2/6$
$\phi_h(x)$	$\pi^2(1+3h^2)/3$	$1-h^2\pi^2/2$
$\phi_k(x)$	$\pi^2(1+6k^2)/3$	$1-k^2\pi^2$
Lath-fn.	4.392	0.804
Parabola-fn.	3.314	0.686

Looking at the graphs, my eyes prefer a slope of between 0.8 and 0.9. The numerical values adopted in Table III. B are  $g^2=0.12$ ,  $h^2=0.04$ , and  $k^2=0.02$ , giving a slope of practically 0.8 in all three cases.

There is, however, another vital condition which must be satisfied before any of these functions can be entertained, and which the lath and parabola functions automatically obey; that is, that if all the ordinates of the periodic function to be analysed are unity, we must have  $y=1$  as the curve through the tops of the ordinates. This requires that

$$\dots + \phi(x-1) + \phi(x) + \phi(x+1) + \phi(x+2) + \dots \quad (20)$$

should be unity for all values of  $x$ . But this expression is a periodic function,  $P(x)$  say, of period unity given by

$$P(x) = \frac{1}{2}\alpha_0 + \alpha_1 \cos 2\pi x + \alpha_2 \cos 4\pi x + \dots, \quad (21)$$

where  $\alpha_m$  is given by

$$\alpha_m = 4 \int_0^{\infty} \phi(x) \cos 2m\pi x \, dx^*, \quad (21a)$$

$\phi(x)$  being an even function. Hence we may take for  $\phi(x)$  any function which passes through the fundamental set of points, provided we divide it by the expression in (21).

Applying this test to the three chosen functions in succession, we have

$$\begin{aligned} \alpha_m &= 4g \int_0^{\infty} \frac{\sin \pi x}{\sinh g\pi x} \cos 2m\pi x \, dx \\ &= \frac{2g}{\pi} \int_0^{\infty} \frac{\sin (2m+1)x - \sin (2m-1)x}{\sinh gx} \, dx \quad (22') \end{aligned}$$

$$= \tanh \frac{(2m+1)\pi}{2g} - \tanh \frac{(2m-1)\pi}{2g} \quad (22)$$

in the first case;

\* *Loc. cit.* p. 155.

$$\begin{aligned}
 a_m &= \frac{4}{\pi} \int_0^{\infty} \frac{\sin \pi x}{x \cosh h x} \cos 2m\pi x \, dx \\
 &= \frac{2}{\pi} \int_0^{\infty} \frac{\sin (2m+1)x - \sin (2m-1)x}{x \cosh h x} \, dx \quad \dots (23') \\
 &= \frac{2}{\pi} \left\{ \tan^{-1} \sinh \frac{(2m+1)\pi}{2h} - \tan^{-1} \sinh \frac{(2m-1)\pi}{2h} \right\} \\
 &\quad \dots \dots \dots (23)
 \end{aligned}$$

in the second case ; and

$$\begin{aligned}
 a_m &= \frac{4}{\pi} \int_0^{\infty} \frac{\sin \pi x}{x} e^{-k^2 \pi^2 x^2} \cos 2m\pi x \, dx \\
 &= \frac{2}{\pi} \int_0^{\infty} \frac{\sin (2m+1)x - \sin (2m-1)x}{x} e^{-k^2 x^2} \, dx \quad (24') \\
 &= \text{Erf} \left( \frac{2m+1}{2k} \right) - \text{Erf} \left( \frac{2m-1}{2k} \right), \quad \dots \dots (24)
 \end{aligned}$$

where Erf( $x$ ) is the tabulated Error-function

$$\frac{2}{\sqrt{\pi}} \int_0^x e^{-x^2} \, dx,$$

(so that Erf( $\infty$ )=1) in the third case.

With the above values for  $g$ ,  $h$ , and  $k$  it is easily seen that these values make  $\frac{1}{2}\alpha_0$  unity to within about  $10^{-3.64}$ ,  $10^{-3.30}$ , and  $10^{-6.23}$  respectively ; make  $\alpha_1$  zero to within the same amounts, and make the higher  $\alpha$ 's differ from unity by incomparably smaller amounts. Hence for ordinary purposes any of these three functions may safely be adopted. We must now find the factors which these functions give for multiplying the ordinarily obtained harmonic coefficients. If we compress the  $\phi_p$  function so that the zero ordinates are reduced to  $\pi/p$  apart, instead of unity, and suppose that  $p$  is not less than about 10 since the function is everywhere negligible past the ninth zero, we have its harmonic analysis given by (2), where

$$\begin{aligned}
 a_n &= \frac{2}{\pi} \int_0^{\pi} \frac{g \sin pt}{\sinh gpt} \cos nt \, dt \\
 &= \frac{2g}{\pi p} \int_0^{\pi} \frac{\sin t}{\sinh gt} \cos \frac{nt}{p} \, dt,
 \end{aligned}$$

where the upper limit may now be replaced by infinity. But this expression is the same as that in (22') multiplied by  $1/2p$  with  $n/p$  replacing  $2m$ . Hence, by (13), the factor to be applied to the coefficients of the  $n$ th harmonic is

$$c_n = \frac{1}{2} \left\{ \tanh \frac{(p+n)\pi}{2pg} + \tanh \frac{(p-n)\pi}{2pg} \right\} \quad \dots (26)$$

In an exactly similar manner  $\phi_h$  and  $\phi_k$  give

$$c_n = \frac{1}{\pi} \left\{ \tan^{-1} \sinh \frac{(\rho + n)\pi}{2ph} + \tan^{-1} \sinh \frac{(p-n)\pi}{2ph} \right\} \quad (26)$$

and

$$c_n = \frac{1}{2} \left\{ \operatorname{Erf} \left( \frac{\rho + n}{2k\rho} \right) + \operatorname{Erf} \left( \frac{\rho - n}{2k\rho} \right) \right\} \quad (27)$$

respectively.

The first term in each of (25), (26), and (27) is sensibly one-half, so that the expressions are odd functions of the ratio of  $(1-n/p)$  to  $g, h$ , or  $k$ , plus one-half. That is, if  $g, h$ , or  $k$  is increased in a given ratio, we shall get the same value for  $c_n$ , provided we increase  $1-n/p$  in the same ratio. We may note that  $g, h$ , and  $k$  can never be large enough to render the first term appreciably different to  $1/2$ ; for if they were given  $\sqrt{2}$ , the values we have taken for them, the slope of the curves at  $x=1$  would be reduced from  $0.8$  to  $0.6$ , which anyone's eye would reject for a smoothly-flowing curve through the fundamental set of points. These three functions for  $c_n$  are tabulated in Table III. B under the columns  $A_g(n/p)$ ,  $A_h(n/p)$ , and  $A_k(n/p)$  respectively.

An entirely different set of  $\phi$  functions may be found in the following manner:—Denote  $\alpha_m$  in (21a) by  $\psi(m)$ , then \*

$$\phi(x) = \int_0^\infty \psi(m) \cos 2\pi x m \, dm.$$

If now, for simplicity, we take  $P(x)=1$ ,  $\psi(m)$  must satisfy the following conditions:— $\psi(N)=0$  if  $N$  is an integer,  $\psi(0)=2$ , and

$$\int_0^1 \psi(m) \cos 2\pi N m \, dm = 0$$

if  $N$  is an integer and equals unity if  $N=0$ . That

$$\left. \begin{aligned} \psi(m) &= 1 + \frac{H(\frac{1}{2}-m)}{H(\frac{1}{2})} \quad \text{for } 0 < m < 1 \\ \text{and} \quad \psi(m) &= 0 \quad \text{for } m > 1, \end{aligned} \right\} \quad (28)$$

where  $H$  is any odd function, satisfies these condition will be evident on reflexion. Three interesting particular cases are:— $\psi(m)=2$  for  $0 < m < \frac{1}{2}$  and  $\psi(m)=0$  for  $m > \frac{1}{2}$ ;  $\psi(m)=1+\cos \pi m$  for  $0 < m < 1$  and  $\psi(m)=0$  for  $m > 1$ , which gives a second-order discontinuity at  $m=1$ ; and

\* *Loc. cit.* p 147.

$\psi(m) = 1 + \frac{2}{3} \cos \pi m - \frac{1}{3} \cos 3\pi m$  for  $0 < m < 1$  and  $\psi(m) = 0$  for  $m > 1$ , which give a fourth-order discontinuity at  $m = 1$ .

The first case gives

$$\phi(x) = \int_0^{\frac{1}{2}} 2 \cos 2\pi x t \, dt = \frac{\sin \pi x}{\pi x},$$

the function that ordinary harmonic analysis works on, while the second and third give

$$\phi(x) = \frac{\sin 2\pi x}{2\pi x} \cdot \frac{1}{1-4x^2}$$

and

$$\phi(x) = \frac{\sin 2\pi x}{2\pi x} \cdot \frac{1}{1-4x^2} \cdot \frac{9}{9-4x^2}$$

respectively.

There are, of course, other solutions for  $\psi$  besides those comprised in (28); in particular for the lath and parabola functions, the  $\psi_{(m)}$  functions are given by  $F_2(m)$  and  $M_2(m)$  respectively.

In the language of physics,  $\phi(x)$  represents a pulse and  $\psi(m)$  represents the distribution of the square root of the energy in the (normal frequency) spectrum of the pulse. The  $(\sin \pi x)/\pi x$  function throws all the energy into frequencies,  $n$ , less than  $p$  and distributes it uniformly over that region. The solutions comprised in (28) take some of this (energy) from frequencies  $n < p$  and distribute it symmetrically over the region  $p < n < 2p$ , but give none to any higher frequencies; while the lath, parabola  $\phi_p$ ,  $\phi_k$ , and  $\phi_k$  functions put some—though extremely little—of the energy into frequencies extending to infinity. However unnatural it may seem to use pulses containing harmonics of infinite frequency, it remains a fact that it is the only way of getting pulses without unnecessarily large oscillations at a large distance from the centre of the pulse, as will be seen by comparing any of these five functions with any pulse which can be obtained from (28) whatever function is taken for  $H$ .

Since ordinary harmonic analysis gives no higher harmonics than the  $p$ th, correction factors cannot be directly applied to any higher-order harmonics. It can be shown, however, that the higher-order coefficients are given by

$$a_{p+n} = a_{p-n}; \quad a_{2p+n} = a_n; \quad \text{and} \quad b_{p+n} = -b_{p-n}; \quad b_{2p+n} = b_n^*.$$

The ordinary harmonic analysis may be regarded as making use of these extended coefficients, but multiplying them by unity for  $n < p$ , by  $\frac{1}{2}$  for  $n = p$ , and by zero for  $n > p$ .

\* *Loc. cit.* p. 104.



The following table summarises the correction factors to be applied to harmonics below the 2pth order according to the different functions which we have investigated. When 12 ordinates per half period are used for the harmonic analysis, the figures in the table may be used directly, but, for any other number of ordinates a graph of the selected function must be drawn and ordinates erected at the appropriate values of  $n/p$ . In Table III. A are given the correction factors from (13 a), denoted by  $E_2(n/p)$ , from (13 b), denoted by  $E_3(n/p)$ , together with those for the lath and parabola functions extended from Tables I. and II. Table III. B gives similar results for the functions  $\phi_p$ ,  $\phi_h$ , and  $\phi_k$  for the previously-selected numerical values of  $g$ ,  $h$ , and  $k$ . The last column, which gives practical agreement with the lath-function,  $F_3(n/p)$ , is obtained by taking  $k^2=0.0225$ , which adopts as the  $\phi_k$  function

$$e^{-x^2} \frac{\sin 20x/3}{20x/3}$$

on reducing the ordinate interval to  $3\pi/20$ . This last column may be recommended for adoption in practical work.

Table III. A.

$12n/p$ .	$E_2(n/p)$ .	$E_3(n/p)$ .	$F_3(n/p)$ .	$M_2(n/p)$ .
0.....	1.000	1.000	1.000	1.000
1.....	1.000	1.000	1.000	1.000
2.....	.999	.999	1.000	1.000
3.....	.994	.995	.999	.998
4.....	.982	.987	.998	.995
5.....	.959	.969	.994	.987
6.....	.921	.939	.985	.973
7.....	.867	.897	.969	.947
8.....	.796	.836	.935	.905
9.....	.709	.765	.877	.841
10.....	.612	.682	.785	.754
11.....	.509	.589	.652	.643
12.....	.405	.493	.493	.516
13.....	.308	.397	.334	.390
14.....	.221	.308	.204	.275
15.....	.149	.227	.116	.182
16.....	.092	.158	.058	.113
17.....	.053	.104	.028	.066
18.....	.026	.063	.012	.036
19.....	.010	.034	.005	.018
20.....	.003	.016	.001	.008
21.....	.000	.008	.000	.003
22.....	.000	.001	.000	.001
23.....	.000	.000	.000	.000
24.....	.000	.000	.000	.000

Table III. B.

$12n/p$ .	$Ag(n/p)$ .	$Ah(n/p)$ .	$Ak(n/p)$ .	Suggest adopt.
0.....	1·000	1·000	1·000	1·000
1.....	1·000	1·000	1·000	1·000
2.....	1·000	·999	1·000	1·000
3.....	·999	·998	1·000	1·000
4.....	·998	·997	1·000	·999
5.....	·995	·994	·998	·997
6.....	·990	·987	·994	·991
7.....	·978	·976	·981	·975
8.....	·954	·954	·952	·942
9.....	·906	·911	·894	·881
10.....	·820	·832	·798	·784
11.....	·681	·695	·662	·653
12.....	·500	·500	·500	·500
13.....	·319	·305	·338	·347
14.....	·180	·168	·202	·216
15.....	·094	·089	·108	·119
16.....	·046	·046	·048	·058
17.....	·022	·024	·019	·025
18.....	·010	·013	·006	·009
19.....	·005	·006	·002	·003
20.....	·002	·003	·000	·001
21.....	·001	·002	·000	·000
22.....	·000	·001	·000	·000
23.....	·000	·000	·000	·000
24.....	·000	·000	·000	·000

*Some New Interpolation Formula.*

The lath-function, or any of the  $\phi$  functions, may be used for interpolation purposes when we know the values of equally-spaced ordinates of a function and have at least six ordinates on each side of the point for which we require to calculate the function. Let  $(0, y_0), (1, y_1) \dots (n, y_n)$  be the tops of the given ordinates, and suppose  $x$ , the value for which we require to calculate the function, lies between the integers  $q$  and  $q+1$ ; then it is easily seen that

$$\begin{aligned}
 y_x = & y_q \phi(q-x) + y_{q+1} \phi(q+1-x) \\
 & + y_{q-1} \phi(q-1-x) + y_{q+2} \phi(q+2-x) \\
 & + \dots
 \end{aligned}$$

may be taken as the value of the function, provided that the terms become small before we have exhausted all the ordinates. The convergence and the accuracy will be increased if the first and last points be joined by a straight line to which the other points are then referred.

This interpolation formula requires only a table or graph of the selected  $\phi$  function and a slide-rule to perform the multiplications.

### *Summary.*

This paper deals with the subject of its title for the cases of both artificial and empirical functions. It is shown that in the case of artificial functions which only possess discontinuities of a single order, the exact harmonic analysis can be found without evaluating the integrals for the Fourier constants, by using the ordinary method of harmonic analysis by selected ordinates, and multiplying the results by certain definite functions.

In the case of empirical functions, the result is shown to depend upon what function we *choose* to represent the case in which all the selected ordinates are zero save one. The ordinary analysis works on the  $(\sin x)/x$  function; other and better functions, both artificial and analytic, are suggested, including the function given by a flexible lath made to pass through the points and hence called the lath-function. All these different functions give a remarkable measure of agreement in the factors which they indicate the coefficients of ordinary harmonic analysis should be multiplied by.

## X. *The Action of Heat on Pleochroic Halos.*

By J. H. J. POOLE, *Sc.D.\**

[Plates I. & II.]

IT has been known for many years that pleochroic halos in biotite disappear if the mica is heated for a short time to a dull red heat. When it was established that these halos are due to radioactive staining of the mica produced by the small amount of uranium present in the nucleus of the halo, it was naturally assumed that their disappearance, when heated, was analogous to similar effects observed in glass and various minerals. If glass is exposed for any length of time to either  $\alpha$ -,  $\beta$ -, or  $\gamma$ -rays it becomes coloured, and it is found that on heating, in some cases, to quite moderate temperatures the colour is completely destroyed. During this process the glass becomes thermo-luminescent, but this property is only of a very short duration. Some observations of J. R. Clarke's (*Phil. Mag.* April 1923) may be quoted

\* Communicated by Prof. J. Joly, F.R.S.

in this connexion. He found that glass became thermo-luminescent at  $110^{\circ}\text{C.}$ , and that the luminescence lasted for about 13 minutes at this temperature. The glass was also completely decolorized at the end of this period. At higher temperatures the thermo-luminescence was more brilliant but of shorter duration, and the glass also lost its colour more rapidly. Some observations I have made myself completely agree with these results. We would accordingly expect that as the halo is also a radioactive staining of the mica, it would also be decolorized by heat, and probably become thermo-luminescent in the process. The microphotographs shown in this paper prove, I think, fairly conclusively that the halo does not lose its colour when heated, and that its apparent disappearance is due to another cause. I may say also that I have totally failed to detect any thermo-luminescence in the halos. As, however, it apparently takes a dull red heat to have any effect on the visibility of the halo, it may be argued that the halo is thermo-luminescent at this temperature, but that the effect of the thermo-luminescence is swamped by the natural temperature radiation of the mica. It would be quite impossible to disprove this view, as the amount of energy liberated in thermo-luminescence is so excessively small; but, at any rate, at temperatures below this the halo is certainly not thermo-luminescent.

My attention was first directed to the action of heat on halos by the large number of reversed halo effects so often found in Ytterby mica. This mica is itself intensely dark, and in it, as well as the usual dark halos, there occur occasionally halos which are lighter in colour than the surrounding mica. More usually the reversed coloration of the mica occurs in streaks down the middle of which a line of small particles can often be seen. There seems to be little doubt that this bleaching of the mica is also due to the presence of uranium in the centre particles, but it is not very easy to explain why sometimes lightening of the mica should be produced by the same agent. One explanation that occurred to us was that possibly a halo if subjected to a high temperature after formation might become reversed. The Ytterby mica is of great geological age and comes from a highly-metamorphosed region, so that it was quite likely that the mica might have been raised to a high temperature at some period long subsequent to its original formation.

To test this theory a series of experiments on the effect of heating various specimens of mica to high temperatures in an electric furnace was tried. To measure the temperature

of the furnace a Calendar self-recording platinum thermometer was employed, and it was also arranged that this thermometer automatically controlled the temperature of the furnace, so that the mica could be kept at any desired temperature. The mica was usually wrapped in platinum foil and fastened on to the end of the platinum thermometer. Temperatures ranging from about  $500^{\circ}\text{C.}$  to  $1000^{\circ}\text{C.}$  were tried. It was found that an hour's heating at  $550^{\circ}\text{C.}$  did not affect the halos, but that after 15 minutes' heating at  $610^{\circ}\text{C.}$  they had completely disappeared. Higher temperatures always completely destroyed the halos, but in no case could any sign of the halos becoming reversed in tone be detected. It was observed that in all cases in which the halos disappeared the mica itself became very much shattered; in fact, when fairly large pieces of mica were employed, the expansion of the mica was sometimes sufficient to actually tear the platinum foil in which it was wrapped. This suggested that the mica actually becomes dehydrated at these temperatures, and that its break up is due to the explosive liberation of steam. Further experiments have confirmed this view, and have also thrown light on the probable mechanism of the formation of the halos.

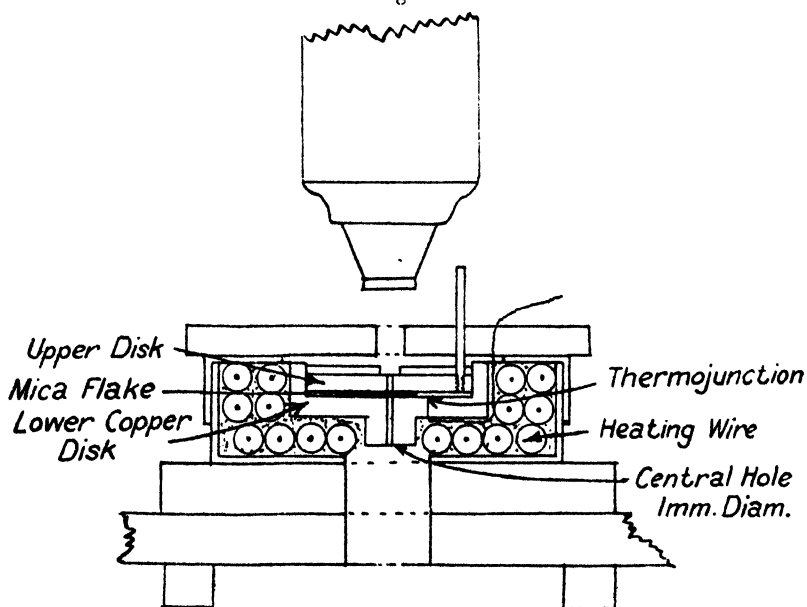
It was now felt that it would be highly desirable to be able to actually see what happened to the mica during the process of heating. A small vertical tube electric furnace was accordingly constructed. The lower end of the furnace tube was closed with a disk of fused silica, and the furnace was so small that it could be placed on the stage of an ordinary petrological microscopic, a long-focus object-glass (2 in.) being employed. The flake of mica under inspection was supported by a platinum framework half-way up the tube, and the halo viewed by light transmitted from below through the fused silica disk. As the latter was not in the same plane as the mica, flaws in it did not confuse the image in the microscope. No method of measuring temperatures was fitted, since the furnace was not very suitable for this purpose.

Not very many experiments were made with this arrangement, as it was not very convenient to use, but sufficient work was done to show that the idea that halos disappear by reverting like glass to the original colour of the mica was entirely incorrect. What actually occurs is that at about a dull red heat the whole surrounding mica begins to decompose and darken in tone, and if the heating is persisted in, the mica assumes the same colour as the halo, and hence, of course, the latter becomes invisible. Both Ballvellen and

Arendal micas behaved in this fashion. In no case could any sign of the halo itself becoming lighter in tone be detected.

These experiments were carried out in the spring of 1922, but no detailed account of them was published at that time. However, as the suggestion by Prof. Evans that possibly a large amount of the energy liberated in the earth's crust was used up in forming these halos lent renewed interest to the question, it was decided to construct a new form of furnace in which the temperature could be fairly accurately measured, and also microphotographs of the halo at various

Fig. 1.



temperatures taken. A sketch of the final form of furnace used is shown (fig. 1). The mica flake is held between the lower metal disk and the upper metal lid, and the halos are viewed by means of the small concentric holes in both disk and lid. As a source of light a pointillite lamp was employed. A platinum platinum-iridium thermocouple inserted into a small hole in the lower disk was used to measure the temperature. This thermocouple had been previously standardized by Johnson Matthey & Co., but it was thought advisable to check its readings by means of standard melting-points. The values obtained were practically identical with the

makers' values. The chief uncertainty in the temperature measurements arises from the fact that, owing to the necessity for having small holes in the upper and lower walls of the furnace to view the mica through, it is possible that the latter might be at a considerably lower temperature than that read by the couple. In most cases, however, the mica flake was large compared with the size of the aperture and completely covered it, so that no actual draught could pass through the furnace. When it was necessary to work with smaller mica flakes, or with halos near the edge of the flake, a thin sheet of muscovite or glass was used to support the mica. On this account the temperatures given must always be considered as the maximum temperatures which the mica could have attained. I do not think that the error introduced can be very large, as an examination of the furnace by its own light when heated under the microscope showed no sign of the central hole containing the mica flake, the whole field of the microscope being apparently equally bright. It may be noted that the temperatures taken to completely destroy the halo are slightly higher than those obtained with the first furnace, as we would expect.

The results obtained agree with those already quoted. Plate I. shows the effect of heat on two specimens of Ballyellen mica, the upper six microphotographs showing one piece of mica, and the lower three the second piece. The temperatures which the mica had attained when the exposure was made are given under the illustrations. In every case the same length of exposure was given so that the photos represent fairly accurately the gradual darkening of the mica. The time of heating for both specimens was about one hour; at a temperature of  $700^{\circ}\text{C}$ . they both became entirely opaque. The first sign of darkening of the Ballyellen mica usually sets in at about  $420^{\circ}\text{C}$ ., but there is in no case much effect below  $500^{\circ}\text{C}$ . The effect is, of course, more apparent in the thicker flakes, and this leads to some pieces of mica darkening at lower temperatures than others. The final darkening of the mica is usually very rapid when once it commences. The photo taken of the second specimen at  $640^{\circ}\text{C}$ . is of some interest, as it shows how the radium C ring of one of the halos has actually been intensified by the heating. Many other photos and visual observations on the Ballyellen mica were made, but the two given may be taken as typical. The temperature at which the mica became finally practically opaque varied somewhat from specimen to specimen, the extremes being about  $610^{\circ}\text{C}$ . and

700° C. There is no reason to doubt, however, that prolonged heating at 600° C. would render the Ballyellen mica opaque.

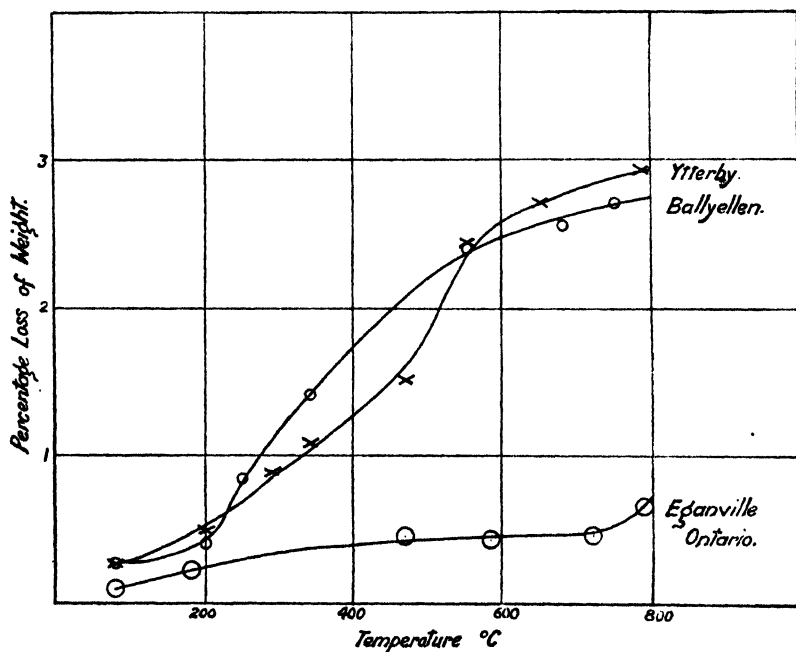
The first four photos in Plate II. illustrate the effect on reversed halos in Ytterby mica. The chain of reversed halos shown are near the edge of a flake. This mica even at air temperature is very opaque, and, as it has a rather poor cleavage, it is much harder to deal with than the Ballyellen mica; but I think the photos show quite clearly that reversed halos also disappear on heating, due to a progressive blackening of the mica. That the mica itself is actually darkening in colour can be seen from a comparison of the appearance of the small prominence on the mica flake at 15° C. and 505° C. It may be noted that the temperature required to destroy the reversed halo effects in Ytterby mica is considerably lower than that necessary for the Ballyellen positive halos. Other observations have confirmed this result. The last four photos in the plate show that prolonged heating at lower temperatures will blacken the mica slowly. The mica used had been originally heated to a temperature of 450° C. in the first furnace employed in 1922. The first photo at air temperature shows that this had not affected it much. The second was taken after 20 minutes' gradual heating when the temperature in the new furnace had reached 485° C. After a further half hour's heating no further change could be observed by visual observation. The third photo, taken an hour later at a slightly higher temperature, shows further darkening going on. The last exposure was made 10 minutes afterwards, when the temperature had been raised to 590° C., and demonstrates how rapidly the mica darkens with increased temperature. All traces of the halos finally disappeared at a temperature of 625° C. a few minutes later.

There is very little doubt, I think, that the darkening of the mica, when heated, is due to the loss of water. Micas always contain a certain percentage of water, amounting in some cases to as much as 4 per cent. by weight. The shattering of the mica observed in the earlier experiments had already led me to adopt this view, and later trials on the loss of weight of various types of mica when heated have confirmed it. Furthermore, that this loss is actually due to the evolution of water has been checked by heating the mica in a slow current of dry air and then absorbing the resulting water in a weighed calcium chloride tube. The following graph (fig. 2) shows the percentage loss in weight of various



micas plotted against the temperature to which they have been raised. It is of some interest, as in the Ytterby and Ballyellen micas, which lose water more easily than the Canadian, the halos also disappear at lower temperatures; in fact, in the latter mica, darkening only commenced at  $690^{\circ}\text{C}.$ , and there was very little difference produced in its appearance by heating up to  $790^{\circ}\text{C}.$  In this respect it differs completely from the other two micas, which become entirely opaque and otherwise much altered when subjected to the same treatment. The chief change produced in the Canadian

Fig. 2.



mica is that it loses its elasticity, becoming very brittle; its opacity is only very slightly increased. The curves also show a general parallelism between the gradual loss of water by heating and the gradual darkening of the mica.

If this theory of the cause of the changes produced in the biotite by heating is correct, it naturally suggests that the original formation of the halo by  $\alpha$ -rays from the nucleus is brought about in a very similar fashion. When  $\alpha$ -rays enter either water or ice, they decompose it to a certain extent into hydrogen and oxygen. It seems highly

probable that they would also decompose the water present in the biotite, which is apparently only very weakly held, and thus indirectly produce dehydration and its resultant darkening of the mica. We can, moreover, calculate on certain assumptions how many  $\alpha$ -rays per gram. would be required to completely dehydrate the mica, and compare this figure with the result obtained experimentally. Since the range of an  $\alpha$ -ray of given velocity in any material is approximately inversely proportional to the density, it is justifiable to assume that, if there is  $x$  per cent. of water present in the mica,  $x$  per cent. of the ions produced by the  $\alpha$ -rays will be produced in the water molecules. Accordingly, the number of  $\alpha$ -rays required to completely dehydrate the mica is independent of the percentage by weight of water present, and is the same as the number required to decompose an equal mass of water. Now, the number of water molecules per gram. is about  $3.3 \times 10^{22}$ , and the average number of ions produced by the  $\alpha$ -rays due to the decay of radium emanation is  $5 \times 10^5$ . Unfortunately, the value we should adopt for the ratio between the number of pairs of ions produced and the number of water molecules decomposed is rather uncertain: thus Duane and Scheuer\* found that in the liquid state the value was approximately unity, but in the solid it fell as low as  $\frac{1}{20}$ . We do not know which of these limits would be most likely to be approached by the water contained in the mica, but, at any rate, the minimum number of  $\alpha$ -rays required to dehydrate 1 gram. of the mica is  $3.3 \times 10^{22} / 2.5 \times 10^5 = 1.3 \times 10^{17}$ , and the maximum  $2.6 \times 10^{18}$ . These figures can be compared with some quantitative measurements on the darkening of Ballyellen mica by exposure to  $\alpha$ -rays from radium emanation published by Professors Joly and Rutherford in the *Philosophical Magazine* for April 1913. They found that  $3.7 \times 10^{13}$   $\alpha$ -rays per sq. cm. produced an amount of darkening comparable with that of the less-developed halos—say about 10 per cent. that of the fully-darkened mica. The penetration of the  $\alpha$ -rays into the mica was on the average about 0.16 mm.; and hence the number of  $\alpha$ -rays required to produce an equal amount of staining in one gram. of mica (density of mica = 2.93 gram. per c.c.) would be  $3.7 \times 10^{13} / 2.93 \times 1.6 \times 10^{-8} = 8 \times 10^{16}$ , or about  $10^{17}$   $\alpha$ -rays to produce fully-darkened mica. This figure is, of course, only a very rough estimate, as the exact percentage darkening produced by the radium emanation can only be very crudely judged;

\* *Le Radium*, x. p. 83.

but it agrees sufficiently well with the minimum number of  $\alpha$ -rays required to decompose the water in the mica to show that there is no impossibility in the theory of halo formation proposed. A further point in its favour is that no halos are found either in the quartz or felspar constituents of the granite, which contain no water, nor in the muscovite, which, although it does contain water, does not darken when dehydrated by heating. It might possibly be contended that the darkening of the mica was really due to the oxidation of the ferrous iron, which is pre-ent in all biotites in large quantities, to the ferric state in the presence of atmospheric oxygen. It may be remarked that the  $\alpha$ -ray, by its decomposition of the water in the mica, would also be capable of producing such an oxidation. Experiments however on the effect of heating biotite in a reducing atmosphere of either coal-gas or hydrogen have shown that the darkening of the mica proceeds just as readily in these cases, which proves that the action cannot be one of simple oxidation.

It is of some interest to calculate on these assumptions how much of the energy of the  $\alpha$ -rays from the nucleus would be used in chemical work. Duane and Scheuer have shown (*loc. cit.*) that the amount of available energy of the  $\alpha$ -rays in liquid water actually accounted for by the chemical work done in decomposing the water is about 6 per cent. In ice, of course, it will be only one-twentieth of this amount. Taking, however, the larger figure for the energy used, and remembering that at the outside only 4 per cent. of the mica is water, we find that the maximum amount of energy which could be used in chemical work will be about  $\frac{1}{4}$  per cent. We thus see that even if all the radioactive elements in the rocks were contained in the biotites, a ridiculous assumption, still only  $\frac{1}{4}$  per cent. of the radioactive energy could be used up in the formation of the halos. This small loss of heat energy would have no detectable effect on earth history. It might, however, be possible, though highly unlikely, that chemical work was done to the same extent in an average rock as in an equal mass of water; but even then only 6 per cent. of the total radioactive energy would disappear as chemical energy, and we would expect that a large part of this chemical energy would soon revert again to the thermal form by recombination of the products of decomposition. As a matter of fact, Duane and Scheuer are inclined to attribute the small amount of decomposition observed in ice to this effect. There is perhaps, however, no object in labouring

this point, as Lawson \* has already pointed out the impossibility on many grounds of believing that any appreciable quantity of energy could be used in producing chemical changes in the rocks.

Iveagh Geological Laboratory,  
October 1927.

*Note.*—This theory of the mechanism of halo genesis does not lend itself to a direct explanation of the formation of reversed halos. The simplest explanation of their origin that can be offered is that they are due to some secondary effect produced in the mica molecule by the  $\alpha$ -ray. If we assume that this secondary change is only brought about in a few collisions between the  $\alpha$ -rays and the molecule, the fact that reversed halos are very rare except in very old micas receives a rational explanation. It would seem justifiable to imagine that it might be necessary for the  $\alpha$ -ray either to collide with an atomic nucleus or to pass comparatively close to one to effect this change; and this would only occur very rarely. It may be remarked that reversed staining has never, as far as I am aware, been produced in the laboratory. It is hoped to conduct some further experiments on this point.

---

XI. *The Reversal of Helium Lines.* By Dr. TOSHIO  
TAKAMINE, *F.Inst.P.*, and Mr. TARO SUGA †.

[Plate III.]

§ I. *Introduction.*

THE phenomenon of the reversal of spectrum lines seen when a Geissler tube is viewed end-on is familiar to spectroscopists. Beside the numerous experiments of previous workers, the recent investigations by McCurdy ‡, Wood §, and Merton || have revealed many interesting features, bringing at the same time a few problems for our closer study.

\* 'Nature,' cxix. pp. 277 & 703 (1927).

† Communicated by Frank Twyman, *F.Inst.P.*, *F.R.S.*

‡ *Phil. Mag.* ii. p. 529 (1926) and *Proc. Nat. Acad.* xii, *Sci.* p. 231 (1926).

§ *Phil. Mag.* ii. p. 876 (1926).

|| *Phil. Mag.* ii. p. 975 (1926).

Thus, for instance, it is often stated that the reversal is seen when we take an end-on view of a narrow capillary tube which opens suddenly into a wide tube. Thereby it is believed that the light from the capillary is absorbed in the wider portion, which is filled with less luminous vapour.

Doubts are, however, expressed about this view—that it is necessary to have less luminous vapour in order to see the line reversed. In the case of the  $H_\alpha$  line of hydrogen, Wood showed that even if we use a tube in which the capillary comes very close to the front end so that the effect of the less luminous layer is precluded, still the reversal of  $H_\alpha$  line is clearly seen. Again, in the case of the  $D_3$  line of helium ( $\lambda$  5876 Å.), Merton mentions that the reversal may not be due to the less-luminous layer at all. He showed that for this line, not only the end-on view, but also the side-on view of the capillary showed the reversal, provided that the current density is large enough.

The aim of the present work was to examine these points in detail.

## § 2. Experiments.

The present experiment deals with the uncondensed discharge in helium at pressures below 10 mm. of mercury.

For analysing the spectrum we used a Hilger 33 plate echelon of 9.3 mm. thickness, the steps of echelon being placed horizontally. After passing through the echelon, the light was dispersed by two large prisms of flint glass of 10 cm. height and 14 cm. base. The objective lens had a focal length of 1 metre. In this way we could obtain an echelon photograph covering the region from  $\lambda$  7065 to  $\lambda$  3889 within a length of about 15 cm.

The discharge-tubes were made either of quartz or of pyrex glass with tungsten electrodes, the helium being purified by charcoal and liquid air.

We examined firstly the case of exciting both the emission and absorption tubes which were placed in a line (Part I.), and later the case of exciting the emission tube alone (Part II.).

### Part I.—EMISSION AND ABSORPTION TUBES BOTH EXCITED.

After repeating McCurdy's experiments using a tube as described by him\*, we have modified the arrangement in a few points.

Firstly, in the case of McCurdy's experiment the capillary portion and the wider tube were directly connected so that

\* See fig. 1 in McCurdy's paper (*loc. cit.*).

we had always the same pressure of helium filling the two parts. In the present experiment we entirely disconnected these two; viz., a discharge-tube having a capillary of 1 mm. bore and 30 cm. length was placed behind another discharge-tube with 10 mm. bore and 80 cm. length. Those two tubes were placed in a line, and the image of the front end of the narrower capillary was projected on to the slit of the echelon spectroscope with a lens of fairly long focal length. Lenses used had focal lengths ranging from 30 to 50 cm.

Secondly, we employed direct-current excitation for these two tubes, besides various kinds of transformers and induction coils. A 1-kilowatt direct-current dynamo of 10,000 volts was used to excite the capillary portion and another 2-kilowatt dynamo of 1200 volts for exciting the wide tube. In this way we could avoid the complexity arising from the difference in phase which is inevitable when we use two independent transformers for exciting the emission and absorption tube. This point was discussed by Ladenburg\* in a recent paper.

The results of the experiments were in general confirmative of McCurdy's work. The parhelium lines were strongly absorbed in low-pressure helium, while at high pressure, orthohelium lines were more strongly absorbed. In the present experiment the pressure of helium in the capillary tube was 7 or 8 mm. of mercury in most cases, and that in the wide tube 1 or 2 mm.

One remarkable feature that came to our notice was the great difference in the appearance of the green line  $\lambda 5016 (\nu=2S-3P)$ † compared with the yellow line  $\lambda 5876 (\nu=2p-3d)$ , when, firstly, the capillary tube alone and, secondly, both the capillary and wide tube were excited.

When the capillary tube alone was excited, the reversal of  $\lambda 5016$  occurred only under favourable conditions, but  $\lambda 5876$  readily appeared reversed. On the other hand, when the wide tube was also excited,  $\lambda 5016$  showed strong absorption so that the line appeared as a very clear doublet, while for  $\lambda 5876$  there was no perceptible difference whether the wide tube was excited or not.

Further, on examining the spectrogram, it was found that  $\lambda 3889 (\nu=2s-3p)$  behaved exactly like  $\lambda 5016$ , while  $\lambda 6678 (\nu=2p-3D)$  was similar to  $\lambda 5876$ .

Summarising, we may state as follows:—

The lines belonging to the principal series which are related with the metastable states  $2s$  and  $2S$  were very

\* Phil. Mag. iii. p. 512 (1927).

† Notation after Paschen and Götzs, 'Seriengesetze der Linien-spektren.' (J. Springer, 1922.)

distinctly absorbed in passing through the wide tube, while the lines belonging to the diffuse series showed no perceptible absorption. The latter, on the other hand, were readily seen reversed, even when the capillary tube alone was excited.

It is to be remarked that this is in conformity with the observations of previous investigators. The fact that metastable state is closely connected with the amount of absorption was shown already by the work of Meissner\* and Dorgelot† in the case of neon, and by McCurdy‡ in the case of helium.

In fig. 1 (Pl. III.) is reproduced an echelon photograph showing the reversal of  $D_3$  line (a) compared with the unreversed one from a side-on view (b). It will be seen that not only the strong principal line  $\lambda 5875.6$  ( $\nu = 2p_1 - 3d$ ), but also its companion  $\lambda 5876.0$  ( $\nu = 2p_2 - 3d$ ) shows reversal, with the difference that for the latter the reversal is much less clear.

According to Houston§, the main line  $2p_1 - 3d$  is a close doublet having  $\delta\nu = 0.120 \text{ cm.}^{-1}$

As stated by McCurdy, the sharp series lines were hardly seen reversed. We saw only one exception in the reversal of  $\lambda 7066$  ( $\nu = 2p - 3s$ ).

The resemblance of the manner of reversal for the lines belonging to one and the same series is striking. As an example, we may mention the case of  $\lambda\lambda 6678, 4922, 4388$ , and  $4144$ , or that of  $5876, 4472$ , and  $4026$ .

Figs. 2 and 3 (Pl. III.) show the reversal of  $\lambda 6678$  and  $\lambda 5016$  respectively.

When we compare the lines belonging to one and the same series, we notice that the lower members show reversal more distinctly, and as we go up to higher members it becomes less and less clear.

In the course of our experiment, we noticed a very good illustration of the effect already described by McCurdy—namely, that of current density in the wide tube on the width of reversal of  $\lambda 5016$ .

The capillary tube being excited at a certain brightness, the excitation of the wide tube made the line  $\lambda 5016$  appear double, as stated before. Now, by varying the current density of the wide tube periodically, we could see the pulsatory variation in the width of this doublet very clearly.

Wood states in his paper that the dark lines we see in the

\* *Ann. d. Phys.* lxxvi. p. 124 (1925).

† *Zeits. f. Physik*, xxxiv. p. 766 (1925).

‡ *Loc. cit.*

§ *Proc. Nat. Acad. Sci.* xlii. p. 91 (1927).

case of the reversal of  $H_\alpha$  are not truly dark, but they appear black only by contrast to the very bright background. This was well illustrated in the case of  $\lambda 5016$  with the arrangement here described—namely, when the wide tube is alone excited, the line  $\lambda 5016$  appears as a fairly bright emission line, but as soon as the capillary is excited, we see at once that the bright line changes into a dark line.

As stated by Paschen\* and McCurdy†, the effect of impurity was very detrimental to clear reversal; thus when the capillary tube was not quite clean,  $D_3$  showed less distinct reversal, and when the helium in the wide tube became impure, the line 5016 was not at all absorbed in passing through it.

## Part II.—EMISSION TUBE ALONE EXCITED.

Reversal of the principal series lines as described in Part I., namely when we pass the light of the emission tube through the absorption tube, is clearly due to absorption, and, in fact, previous work by Meissner‡, Dorgelo§, and others has already emphasized the close bearing of the metastable states on this phenomenon.

Whether the case of the diffuse series lines, namely the reversal seen with the capillary tube having no dead space, should also be due to the simple process of absorption may perhaps be questioned. At least it may be stated that the physical process causing the reversal in this case does not manifest itself so clearly as in the former case.

In Part II. we shall confine our study to the case in which the emission tube alone is excited.

In comparing the degree of reversal, it is convenient to take as a measure the amount of separation between the double lines caused by reversal. It is to be noted, however, that this amount, which we shall denote by  $\delta\lambda$ , depends to a certain degree on the amount of exposure in taking the photograph, and, further, the clearness of the reversal is very sensitive to the difference in the manner of electrical excitation, so that no great accuracy can be expected in this measurement. The yellow line  $D_3$  was found to be most suited for the measurement, the amount of  $\delta\lambda$  varying from 30 m. Å. to 190 m. Å. in this experiment.

Now, on measuring  $\delta\lambda$  for  $D_3$  line with different tubes

\* *Ann. d. Phys.* xlv. p. 625 (1914).

† *Loc. cit.*

‡ *Loc. cit.*

§ *Loc. cit.*

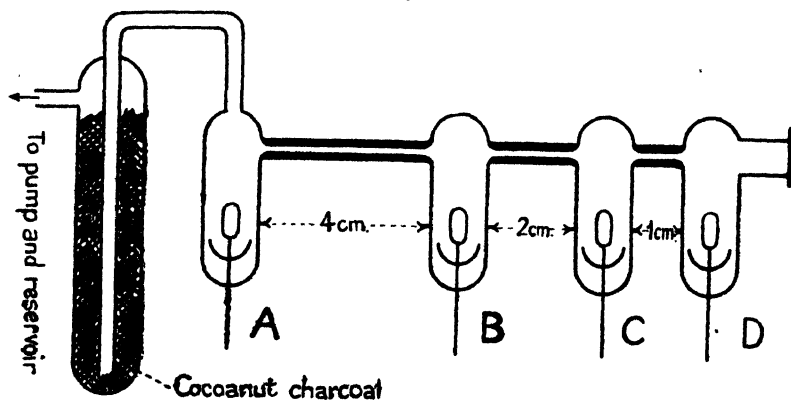


under various conditions, we noticed that apparently the amount depended on the following factors :—

- (i.) Length of the capillary.
- (ii.) Pressure in the discharge-tube.
- (iii.) Current density in the capillary.

As regards (i.), Buisson and Jausseran\* verified this difference in an ingenious way by turning a tube obliquely to the line of sight. We prepared a tube as shown in fig. 4. One end of the transformer or generator was kept connected to A, while the other end was passed from B to C and D to change the length of the capillary. The result showed a steady increase in  $\delta\lambda$  as the length of the capillary was increased.

Fig. 4.



As regards (ii.), we measured  $\delta\lambda$  for the same discharge-tube at different pressures. With pressure less than 1 mm. the line was always sharp. It then began to show reversal at a few mm. pressure, and  $\delta\lambda$  was usually largest at several mm. pressure. Above this point the line became too broad, making the reversal indistinct.

As regards (iii.), we prepared a tube such that the current flows through three capillary tubes, each 10 cm. long, having different diameters (1 mm., 2 mm., and 5 mm.) in succession. Those capillaries were placed parallel and close together so that the images of their ends could be projected on to the slit

\* C. R. clxxx. p. 505 (1925).

of the spectrograph simultaneously. At a very small current density the line appeared sharp, and as we kept increasing it, the narrowest capillary first showed the reversal, and gradually the wider ones began to show the same effect. But here again, as in the case of (ii.), there was a practical upper limit of  $\delta\lambda$ , beyond which the line became too diffuse.

In short, we may state that the effect of the length of the capillary was the most important of the three factors.

During the examination of the above points, we noticed one interesting phenomenon which may be of importance in elucidating the process of reversal of this kind.

We took the end-on view of an ordinary Geissler tube of H form made by Götze in Germany which was filled with helium at about 10 mm. pressure. The capillary had a bore of 2 mm. and was 8 cm. long. The tube was excited by a Siemens induction coil of 15-cm. spark length, provided with an ordinary hammer interrupter. With a spark-gap of a few millimetres in series in the secondary circuit the discharge was found to be quite well rectified, and the line  $D_3$  readily appeared reversed.

Now, the phenomenon which appeared worthy of note is that the reversal was seen decidedly more distinctly in the case when the electrode further away from the slit was made the cathode than when it was the anode. In the latter case there remained a certain amount of luminosity between the components of the doublet caused by reversal of  $D_3$  which made the appearance rather indistinct.

Closer examination of the mode of discharge by means of a rotating mirror showed that there were a few wide striations near the cathode end of the capillary which became indistinct near the anode end.

The same difference due to polarity was observed when we excited the tube with direct current. The striations in the capillary were found also present in this case. We made two different tubes having the forms shown in figs. 5 and 6.

With the tube shown in fig. 5 the middle branch showed more distinct reversal when the back electrode A was anode compared with the other two branches, and *vice versa*.

With the tube shown in fig. 6 all the three branches showed more distinct reversal with the cathode at A than at B. These differences are illustrated in figs. 7, 8, and 9 (Pl. III.), where the length-effect described in (i.) is also seen in that the amount of reversal differs according to the length of the capillary.

Fig. 5.

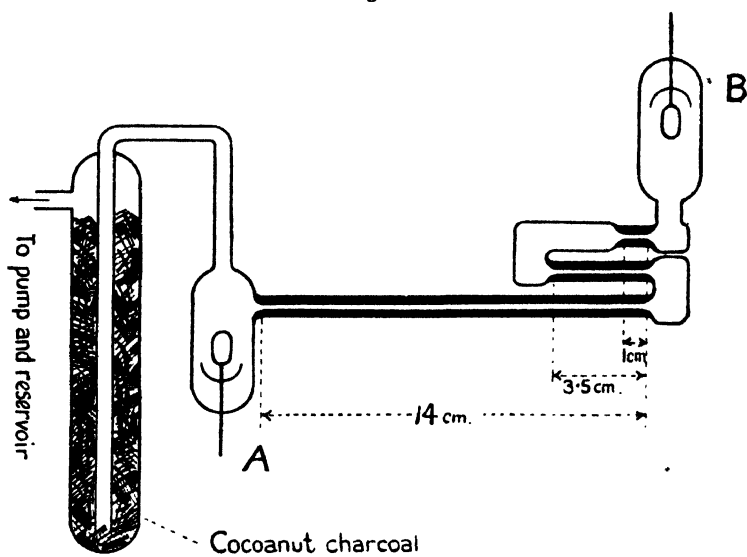
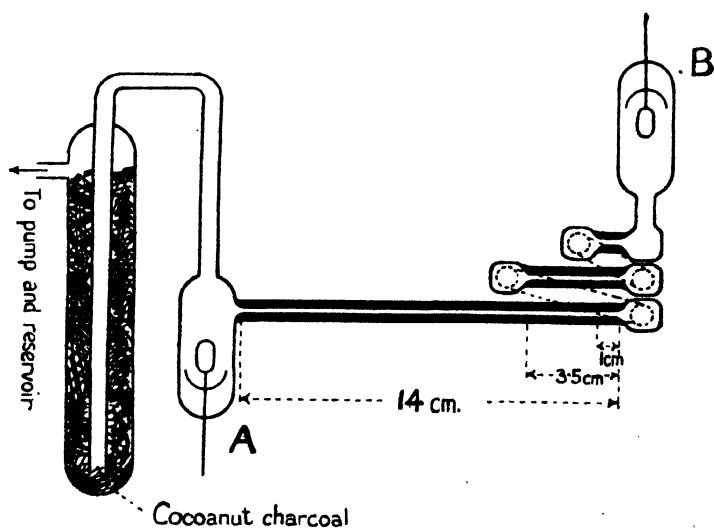


Fig. 6.



In fig. 7 the image "b" due to the middle branch is more distinctly reversed, while in fig. 8 the opposite is the case. In fig. 9 all these branches show reversal. In all the figs, 7, 8, and 9 "a" corresponds to the shortest and "c" to the longest branch.

Altogether, this difference due to polarity seems to indicate the effect of heterogeneous distribution of the excited atoms along the length of the capillary. It may be remarked here that not only the heterogeneity along the tube, but that in the radial direction in the section of a tube, mainly due to the wall of the capillary, may also contribute to the phenomenon of reversal.

### § 3. Summary.

1. Reversal of helium lines was examined by an echelon grating, firstly when a long capillary tube was viewed end-on, and secondly when another long tube of wider bore was placed between the capillary tube and the spectrograph.

2. The lines belonging to the principal series and the diffuse series show reversal, but there is much difference in the manner of reversal for these two series.

The lines belonging to the principal series which are connected with the metastable states ( $2s$  and  $2S$ ) are distinctly absorbed in passing through the wider tube. In other words, the effect of a less-luminous layer is clearly seen for such lines as  $\lambda 5016$  ( $\nu = 2S - 3P$ ) and  $\lambda 3889$  ( $\nu = 2s - 3p$ ).

The lines belonging to the diffuse series, such as  $\lambda 6678$  ( $\nu = 2P - 3P$ ) and  $\lambda 5876$  ( $\nu = 2p - 3d$ ) are seen reversed with the capillary tube alone excited, while the effect of the wider tube is hardly noticeable in this case.

3. A distinct difference in the clearness of the reversal is noticed as regards polarity, or, in other words, according as to whether we pass the current from the front or the back end of the capillary.

XII. *The Spectrum of Ionized Sodium.* By F. H. NEWMAN, D.Sc., A.R.C.S., Professor of Physics, University College of the South West of England, Exeter\*.

1. *Introduction.*

THE spark spectra of potassium, rubidium, and caesium in the visible and near ultra-violet regions have been investigated by many experimenters, but little work has been done on the first spark spectra of sodium, although Schillinger† and Foote, Meggers and Mohler‡ have measured the wave-lengths of the more important lines. Among those listed by Schillinger are several belonging to the arc spectrum of the element. Foote and his collaborators used a three-electrode discharge-tube, and studied the different sets of lines emitted as the accelerating potential gradient was increased. The first ionization potential of sodium vapour is 5.1 volts approximately, and this is sufficient to excite the whole arc spectrum. At higher voltages the spark lines begin to appear. These experimenters noted that the spark lines appeared above 30 volts, and even at 5000 volts very few spark lines were ever observed which were not excited at 50 volts, although their intensity was increased considerably. More recently Mohler§ found that with currents of 0.02 amp. the spark lines were entirely absent at 40 volts, three were barely visible at 42 and 43 volts, while many lines appeared at 45 volts. With 35 volts and 0.35 amp. the lines were bright, so he concluded that the spark lines were excited near 44 volts with small currents and about 10 volts lower with large currents.

From the theory of atomic structure, what might be termed the "spectral centre of gravity" of the sodium spark spectrum should be at a shorter wave-length than that of potassium. The latter is very rich in lines, and their wave-lengths have been carefully measured and classified by different workers||. Shaver¶ extended the study of the alkali spectra in the extreme ultra-violet region by means of

\* Communicated by the Author.

† *Akad. Wiss. Wien Sitz.-Ber.* cxviii. 11 (a) (1909).

‡ *Astrophys. Journ.* lv. p. 145 (1922).

§ Bureau of Standards Scientific Papers, No. 505 (1925).

|| See de Bruin, *Proc. Konin. Akad. Van Wetén te Amsterdam*, vol. xxix. No. 5 (1926).

¶ *Roy. Soc. Canada, Trans.* xviii. Sect. 3, p. 23 (1924).

the electrodeless discharge, using a fluorite vacuum spectrograph, in order to make additions to the lists of wave-lengths available for series analysis, but no sodium lines were found in the fluorite region. Millikan and Bowen\*, using the explosive spark method, found only one definite line in the whole region studied (300 Å. to 2000 Å.), namely that at  $\lambda 372.3$  Å. They also found a line at  $\lambda 376.6$  Å. when pure sodium electrodes were employed, but this line was absent with sodium fluoride electrodes. The line  $\lambda 372.3$  Å. they attributed to the L spectrum of sodium, as a line is definitely predicted by theory at this wave-length and represents the orbital change of an electron from the M to the L shell when an electron is removed from the latter.

Comparing the values of  $\sqrt{\frac{\nu_L}{R}}$  for the  $L_{II}$  and  $L_{III}$  levels of aluminium, magnesium, sodium, and neon,  $\lambda 372.3$  Å. corresponds to the energy difference  $M_I - L_I$ ; and so the value of the  $L_I$  energy level in the sodium atom is fixed at  $\nu = 310,090$  or  $38.3$  volts. This agrees fairly well with the critical potential  $38.9$  volts found by Foote and Mohler†, and represents the work required to eject one electron from the rare gas shell of the ion, the M electron having been removed previously. The  $L_{III}$  limit computed from X-ray frequencies of the K series is  $31.5$  volts.

Accurate measurements of the wave-lengths of lines in the Na II spectrum are necessary and important, because, in accordance with the displacement law, this spectrum should resemble closely the arc spectrum of neon. The latter has been analysed by Paschen‡ into four series of S terms, ten *p* sequences and twelve *d* sequences. The possible number of combinations is very large, but the selection principle prohibits several. In addition to these series, which followed the Ritz formula, he found other series with the limits displaced when calculated by means of the Ritz formula, as indicated by the combinations which gave the first lines of the series. The explanation of this spectrum requires the extraction of an electron from more than one sub-group of the L group, and the simultaneous movement of the two electrons. The series which are represented by the Ritz formula directly are triplets and quintets, while those series which require the addition of a

\* Phys. Rev. vol. xxiii. p. 1 (1924).

† Bureau of Standards Scientific Papers, No. 425 (1921).

‡ Ann. d. Phys. lx. p. 405 (1919), and lxiii. p. 201 (1920).

constant before they can be represented by such a formula are singlets and triplets.

The sodium atom contains in its L group two  $L_{11}$  electrons, two  $L_{21}$  electrons, and four  $L_{22}$  electrons, the suffixes denoting the azimuthal and inner quantum numbers respectively. The single M electron being removed, one of the  $L_{11}$  electrons may be displaced to various higher levels and give rise to a singlet and triplet system. If, on the other hand, one of the  $L_{22}$  electrons in the closed sub-group is removed to different levels, a system of triplets and quintets should be produced. The  $L_{22}$  electron being less firmly bound than the  $L_{21}$  electron, the removal of the latter should leave the residue of the atom with a greater energy than is the case when the  $L_{22}$  electron is removed, so that the sequences arising from the removal of the  $L_{21}$  electron are those requiring the addition of a constant so that they may be expressed by a Ritz formula. In other words, one would expect the first spark spectrum of sodium to resemble the arc spectrum of neon as regards the multiples present, but with the series constant taking the value  $4N$ .

Before any complete analysis of the Na II spectrum is attempted, accurate measurements of the wave-lengths are necessary.

## 2. *Experimental.*

The electrodeless discharge is the most convenient method of exciting the spark spectrum of sodium. A quartz tube, about 30 cm. long and 1 cm. in diameter, with a transparent quartz window sealed at one end was used as the discharge-tube. The metallic sodium, placed in a small side tube, was distilled into the main tube under a vacuum, the latter obtained by means of an ordinary Gaede mercury pump. After enough metal had been distilled, the side tube was sealed off, and afterwards the discharge-tube was sealed off from the pumps. By this means, and after preliminary baking of the main tube, all residual gases were eliminated. The tube, with about fifty turns of fine copper wire wound round it, was enclosed in a glass tube open at both ends, and then placed inside an electric heater. The glass enclosing the tube assists in maintaining a good insulation between the high-tension wire and the wire of the heater. In obtaining the electrodeless discharge, a 16-inch induction coil was used with its secondary joined in parallel with two large parallel plate condensers. The coil was operated by means of a Wehnelt interrupter joined to the 110 A.C. mains. The Wehnelt interrupter is very effective in the production of

this type of discharge. The lowest temperature possible, consistent with fair luminosity, was employed to keep the vapour-pressure low ; otherwise the arc lines predominated. The radiation was yellow in colour, the D lines always appearing bright, but at low vapour-pressures the spark lines were intense. The radiation was focussed by means of a quartz lens on to the slit of a quartz spectrograph. Various types of plates were tested for sensitiveness, including Schumann plates, but no lines of greater refrangibility were obtained with these than on the ordinary type of plate. Although Schillinger recorded a line at  $\lambda$  2138·4, and Foote, Meggers, and Mohler at  $\lambda$  2318·0, no line below  $\lambda$  2386·41 was photographed in the present work. Potassium spark lines below these limits have been measured, and in the spark spectrum of this metal many more lines are present than are recorded with sodium. In addition, many of the lines listed in Table I. are faint, and prolonged exposure did not materially increase their intensity. They were measured against a comparison iron-arc spectrum.

TABLE I.—Wave-lengths in the Na II Spectrum.

Intensity.	$\lambda$ I.A. (Author).	$\lambda$ (Foote, Meggers, Mohler).	$\lambda$ (Schillinger).	$\nu$ (vacuum).
—	—	—	2138·4	—
—	—	2318·0	—	43127·2
1	2386·41	—	—	41891·1
1	2394·14	—	—	41755·9
1	2459·62	—	—	40644·5
0	2469·10	—	—	40488·5
0	2474·92	—	—	40393·1
6	2493·38	2493·36	2493·45	40094·1
1	2497·31	2497·3	—	40031·1
1	2506·27	2506·40	—	39888·1
0	2510·77	—	—	39816·4
1	2515·57	2515·50	—	39740·5
4	2531·64	2531·54	—	39488·2
0	2563·47	—	—	38998·1
0	2578·24	—	—	38774·6
1	2586·87	2586·37	—	38652·7
7	2612·10	2612·18	2612·27	38271·9
6	2661·65	2661·72	2661·82	37559·5
6	2671·90	2671·94	2672·04	37415·5
5	2678·25	2678·2	—	37326·8
6	2809·73	2809·76	2809·87	35580·2
1	2818·58	2818·5	—	35468·4



TABLE I. (*continued*).

Intensity.	$\lambda$ I.A. (Author).	$\lambda$ (Foote, Meggers, Mohler).	$\lambda$ (Schillinger).	$\nu$ (vacuum).
1	2830.01	2830.0	—	35325.2
2	2839.40	2839.36	2839.47	35207.7
7	2841.99	2841.99	2842.10	35176.3
—	—	—	2856.27	—
3	2859.64	2859.56	2859.07	34959.2
0	2861.34	2861.2	—	34938.4
3	2871.04	2870.89	2871.00	34820.9
3	2871.53	2871.39	2871.50	34814.5
0	2873.13	2873.0	—	34795.1
5	2881.38	2881.33	—	34695.5
3	2886.42	2886.46	2886.57	34634.9
4	2894.19	2894.15	—	34541.9
3	2901.36	2901.39	2901.50	34456.5
6	2905.11	2905.16	2905.27	34412.0
6	2917.78	2917.76	2917.87	34262.6
5	2919.34	2919.46	2919.57	34244.3
4	2921.14	2921.14	2921.25	34222.9
2	2923.67	2923.65	2923.76	34193.6
—	—	—	2926.67	—
0	2931.62	2931.44	2931.55	34101.0
1	2934.38	2934.42	2934.53	34068.8
3	2938.06	2938.11	2938.22	34026.1
1	2945.92	2945.83	2945.94	33935.2
3	2947.56	2947.51	2947.62	33916.5
7	2951.50	2951.53	2951.64	33871.2
1	2952.83	—	—	33855.9
1	2960.11	2960.10	2960.22	33772.7
C	2971.17	2971.1	—	33647.0
5	2975.24	2975.20	2975.32	33600.9
0	2977.31	2977.52	2977.64	33577.6
5	2979.96	2979.92	2980.04	33547.7
0	2981.03	—	—	33535.1
5	2984.45	2984.44	2984.56	33497.2
2	3007.65	3007.71	—	33238.9
2	3009.60	—	—	33217.4
4	3015.80	3015.81	3015.93	33149.1
4	3029.56	3029.70	3029.82	32999.5
4	3037.32	3037.29	3037.41	32914.2
3	3045.97	—	—	32820.8
0	3050.43	3050.48	3050.60	32772.8
3	3053.93	3053.97	3054.09	32735.8
5	3056.30	3056.34	3056.46	32709.9
0	3061.72	3061.75	3061.87	32651.9

TABLE I. (continued).

Intensity.	$\lambda$ I.A. (Author).	$\lambda$ (Foote, Meggers, Möhler).	$\lambda$ (Schillinger).	$\nu$ (vacuum).
1	3064.86	3064.8	—	32618.4
1	3066.73	3066.74	—	32598.6
4	3074.56	3074.63	3074.75	32515.6
5	3078.55	3078.51	3078.63	32473.4
1	3080.30	3080.58	3080.70	32455.0
8	3092.98	3092.91	3093.03	32321.8
3	3104.52	3104.6	—	32201.8
0	3107.69	3107.6	—	32168.9
3	3124.64	3124.63	3124.76	31994.5
7	3129.55	3129.57	3129.70	31944.3
4	3135.69	3135.65	3135.78	31881.8
0	3137.80	3138.11	3138.24	31860.8
0	3146.05	3146.07	3146.20	31766.7
4	3149.51	3149.48	3149.61	31741.3
5	3164.16	3164.11	3164.24	31594.9
1	3175.41	3175.38	3175.51	31482.9
2	3179.29	3179.19	3179.32	31444.5
5	3190.05	3189.94	3190.07	31338.4
5	3212.44	3212.42	3212.55	31120.1
0	3216.60	3216.5	—	31079.8
2	3226.16	3226.1	—	30987.7
3	3235.07	3235.1	—	30902.4
1	3251.22	3251.3	—	30748.9
5	3258.38	3258.36	3258.50	30681.4
0	3260.45	3260.4	—	30661.8
3	3274.36	3274.27	3274.41	30531.6
7	3285.86	3285.76	3285.90	30424.7
0	3305.28	3305.2	—	30245.9
3	3318.14	3318.2	—	30128.7
0	3320.70	3320.7	—	30105.5
3	3327.81	3327.9	—	30041.3
0	3345.47	—	—	29882.6
1	3363.29	—	3360.50 ?	29724.3
0	3373.26	—	3371.29 ?	29636.4
0	3381.22	—	—	29566.6
0	3385.61	—	—	29528.3
—	—	3400.2	—	29401.4
1	3405.00	—	—	29380.2
1	3462.68	3462.58	3462.73	28871.1
10	3533.03	3533.08	3533.23	28296.2
0	3608.90	—	—	27701.4
0	3619.20	—	—	27622.6
8	3631.37	3631.31	3631.46	27530.0

TABLE I. (*continued*).

Intensity.	$\lambda$ I. A. (Author).	$\lambda$ (Foote, Meggers, Mohler).	$\lambda$ (Schillinger).	$\nu$ (vacuum).
0	3634.30	3634.3	—	27508.0
0	3651.5	—	—	27379
0	3662.4	—	—	27297
0	3676.1	—	—	27195
3	3711.2	3711.15	3711.30	26938
0	3730.1	—	—	26801
0	3745.6	3745.6	—	26690
0	3798.6	—	—	26318
0	3802.2	—	—	26293
2	3816.8	—	—	26192
0	3849.0	—	—	25973
2	3870.7	—	—	25828
0	3881.1	3881.0	—	25759
0	3889.3	—	—	25704
0	3914.2	—	—	25541
0	3921.0	—	—	25497
0	3928.2	—	—	25450
0	3934.9	—	—	25407
0	3943.8	—	—	25349
0	3983.8	—	—	25095
0	4012.6	—	—	24915
0	4061.8	—	—	24613
0	4094.0	—	—	24419
0	4123.9	4124.0	—	24242
0	4157.3	—	—	24047
0	4178.3	—	—	23926
1	4347.5	—	—	22995
0	4447.0	—	—	22481
0	4455.0	—	4500.0	22441
0	4465.5	—	—	22387
0	4480.3	—	—	22314
—	—	—	—	—
—	—	—	4538.9	—
—	—	—	4542.7	—
—	—	—	4546.5	—
—	—	—	4551.5	—
—	—	—	4564.4	—
—	—	—	4569.4	—
—	—	—	4572.7	—
1	4581.0	—	4581.7	21823
0	4807.0	—	—	20797
2	4830.9 (K II)	—	—	20695

TABLE II.—Constant differences in the Na II Spectrum.

Frequency ( $\nu$ ).	Difference ( $\Delta\nu$ ).	Frequency ( $\nu$ ).	Difference ( $\Delta\nu$ ).
37559.5		34959.2	
37415.5	144.0	34634.9	324.3
35468.4		33871.2	
35325.2	143.2	33547.7	323.5
34959.2		33238.9	
34814.5	144.7	32914.2	324.7
33916.5		30987.7	
33772.7	143.8	30661.8	325.9
32598.6		30748.9	
32455.0	143.6	30424.7	324.2
31482.9			
31338.4	144.5	34938.4	
		34101.0	837.4
34244.3		33547.7	
34026.1	218.2	32709.9	837.8
34412.0		32321.8	
34193.6	218.4	31482.9	838.9
32735.3		31741.8	
32515.6	219.7	30902.4	839.4
31994.5		27530.0	
31776.7	217.8	26690.2	839.8
31338.4			
31120.1	218.3	39888.1	
31120.1		37559.5	2328.6
30902.4	217.7	39740.5	
30748.9		37415.5	2325.0
30531.6	217.3		
		35325.2	
35580.2		32999.5	2325.7
35325.2	255.0	34068.8	
34193.6		31741.8	2327.0
33935.3	258.3	33772.7	
33855.9		31444.5	2328.2
33600.9	255.0		
33497.2		35176.3	
33238.9	258.3	32709.9	2466.4
32772.8		34634.9	
32515.6	257.2	32168.9	2466.0
32709.9		34412.0	
32455.0	254.9	31944.3	2467.7
32201.8		32999.5	
31944.3	257.5	30531.6	2467.9
31594.9		31338.4	
31338.4	256.5	28871.1	2467.3
30681.4			
30424.7	256.7		

TABLE II. (*continued*).

Frequency ( $\nu$ ).	Difference ( $\Delta\nu$ ).	Frequency ( $\nu$ ).	Difference ( $\Delta\nu$ ).
38652.8		39740.5	
35580.2	3072.5	32455.0	7285.5
34814.5		39488.2	
31741.8	3072.7	32201.8	7286.4
34193.6		38271.9	
31120.1	3073.5	30987.7	7284.2
31944.3		37326.8	
28871.1	3073.2	30041.3	7285.5
34412.0		35580.2	
31338.4	3073.6	28296.2	7284.0
33497.2		34814.5	
30424.7	3072.5	27530.0	7284.5
32473.4		34222.9	
29401.4	3072.0	26938.2	7284.7

TABLE III.—Frequency differences in the Na II Spectrum.

No.	Intensity.	$\lambda$ (I.A.) in air.	Frequency in vacuum ( $\nu$ ).	Difference ( $\Delta\nu$ ).
1 .....	—	—	—	—
2 .....	—	—	—	—
3 .....	—	—	—	—
4 .....	7	2841.99	35176.3	
5 .....	3	2859.64	34959.2	217.1
6 .....	6	2917.78	34262.6	696.6
7 .....	1	2945.92	33935.3	327.3
8 .....	1	3064.86	32618.4	1316.9
9 .....	4	3135.69	31881.8	736.6
1 .....	1	2497.31	40031.1	
2 .....	6	2661.65	37559.5	2471.6
3 .....	1	2818.58	35468.4	2091.1
4 .....	—	—	—	530.0
5 .....	0	2861.34	34938.4	
6 .....	5	2819.34	34244.3	694.1
7 .....	3	2947.56	33916.5	327.8
8 .....	1	3066.73	32598.6	1317.9
9 .....	0	3137.80	31860.8	737.8
1 .....	1	2506.27	39888.1	
2 .....	6	2671.90	37415.5	2472.6
3 .....	1	2830.01	35325.2	2090.3
4 .....	—	—	—	530.1
5 .....	0	2873.13	34795.1	
7 .....	1	2931.62	34101.0	694.1
7 .....	—	—	—	1646.0
8 .....	1	3080.30	32455.0	
9 .....	—	—	—	—
4 .....	6	2905.11	34412.0	
5 .....	2	2923.67	34193.6	218.4
6 .....	5	2984.45	33497.2	696.4

TABLE III. (continued).

No.	Intensity.	$\lambda$ (I.A.) in air.	Frequency in vacuum ( $\nu$ ).	Difference ( $\Delta\nu$ ).
4 .....	3	3124.64	31994.5	217.8
5 .....	0	3146.05	31776.7	696.9
6 .....	0	3216.60	31079.8	330.9
7 .....	1	3251.22	30748.9	
4 .....	5	3190.05	31338.4	218.3
5 .....	5	3212.44	31120.1	695.4
6 .....	7	3235.86	30424.7	
6 .....	2	3007.65	33238.9	324.7
7 .....	4	3037.32	32914.2	1319.3
8 .....	5	3164.16	31594.9	
5 .....	5	3078.55	32473.4	2344.7
8 .....	3	3318.14	30128.7	727.3
9 .....	0	3400.2	29401.4	
4 .....	2	3009.60	33217.4	217.9
5 .....	4	3029.56	32999.5	2337.7
8 .....	0	3260.45	30661.8	

A preliminary analysis of the results shows no lines or sequences obeying the Ritz formula, but there are many pairs of lines in the spectrum having constant differences. These have been collected and tabulated in Table II. In addition many of the strong lines can be arranged in groups of nine lines having constant wave-number separation, although all of these groups are incomplete. They are given in Table III. Owing to the incompleteness of the groups and the fact that many of the observed lines are not represented by any of the terms of these groups, no term scheme has been arranged.

Hertz \* found two strong resonance lines in the neon spectrum at  $\lambda 735.7 \pm 0.5$  and  $\lambda 743.5 \pm 0.5$ . Their frequency difference is  $1428 \pm 3$ , and agrees with the difference between the Paschen terms  $1_{\frac{1}{2}}$  and  $1_{\frac{3}{2}}$ , so that they are to be regarded as combinations of the fundamental term with two new terms. The fundamental term must be the optically undiscovered one at approximately  $174,000 \text{ cm}^{-1}$ . It has been noted previously that Millikan and Bowen found the two lines  $\lambda 372.3$  and  $\lambda 376.6$  in the spark spectrum of sodium. Their frequency difference is 3075. If these two lines are analogous to the two neon resonance lines, then 3075 should be an important frequency difference among the Na II lines. Seven pairs of lines with a difference  $3073 \pm 1$  have been discovered, and are shown in Table II. Further investigation in the extreme ultra-violet of the Na II spectrum seems very necessary.

\* *Zeits. f. Physik*, xxxii. 11-12, p. 933 (1925).

**XIII. Notes on the Resonances of a Violin.** By FLORENCE M. CHAMBERS, M.Sc., *Junior Lecturer in Physics, Queen's University, Belfast* \*.

*Introduction.*

THE following investigation was undertaken with the object of finding resonance pitches of a violin, in the hope of throwing light on the "Wolf-note" phenomenon.

As described in an earlier paper †, when a steel wire is mounted on a light metal bar and made to vibrate, two kinds of resonance are found: one associated with the coincidence of an odd mode of the string (or bar) with an even mode of the bar (or string) respectively, and the other with the coincidence of an even (or odd) mode of the string with an even (or odd) mode of the bar respectively.

It is rather a jump from the case of a uniform bar and string to that of a violin, but it was thought that in the case of the violin something corresponding to one or other of the string-bar resonances might lie at the root of the "wolf-note" phenomenon.

As will be seen, resonance pitches were found for the violin; but the behaviour of string and violin bears little resemblance to that of the string and bar.

The method used was to measure at different pitches the resonance amplitude of a steel wire stretched on the violin and maintained in vibration by an applied alternating force of constant amplitude, as described in an earlier paper ‡. On a rigid support the amplitude of vibration of the wire would change more or less gradually with changing pitch (as the damping is usually greater at higher pitches). On a violin the amplitude rose and fell in an apparently arbitrary manner, and graphs of amplitude and pitch showed a large number of definite minima. These minima occurred at the same pitches for different modes

\* Communicated by Prof. W. B. Morton, M.A.

† W. B. Morton and F. M. Chambers, "On the Combined Vibration of a Bar and String, and the Wolf-Note of a Stringed Instrument," *Phil. Mag.* vol. 1. p. 570 (1925).

‡ F. M. Chambers, "Application of a Thermionic Valve to the Measurement of the Damping of Vibrations of a Steel Wire," *Phil. Mag.* xlviii. p. 636 (1924).

of getting the string to give the note, indicating that they are functions of the violin itself.

When the note given by the wire approaches a natural frequency of part of the violin, (1) the part is set into vigorous vibration and the energy to maintain this vibration comes from the string; (2) there is an increase of frictional damping in the motion of the wood; so that, on the whole, there should be a fall in amplitude of vibration of the wire.

Hence the minima seem to indicate the pitches of natural frequencies of the violin.

### *Experiments.*

The gut strings were removed, and a fine steel wire stretched in the place usually occupied by the A string. The oscillating current from a valve circuit, which could be tuned to any desired frequency, was passed through the wire, and this was maintained in vibration by the reaction between the current and the field of a strong electromagnet between whose poles it was placed. Care was taken that the amplitude of the oscillating current, and therefore the alternating force applied to the wire, remained constant throughout a set of observations.

An auxiliary wire, stretched by a weight on a wooden sonometer and through which the oscillating current also passed, was used as a standard of pitch. This wire was placed between the poles of another electromagnet. It was bridged to a suitable length, and then the frequency of the current adjusted so that there was maximum response. The electromagnet of the standard was turned off, that belonging to the violin wire was turned on, and the latter screwed up until it resonated. To ensure that the pitch of the standard was exactly the same as the pitch of the violin wire, slight further adjustments of current and length of standard were usually necessary. The amplitude of vibration of the violin wire was read off on the eyepiece scale of a microscope.

The pitch is inversely proportional to the standard length. In order that a given length of abscissa should represent a given interval, the amplitude of vibration was plotted against the log. reciprocal of the corresponding standard length.

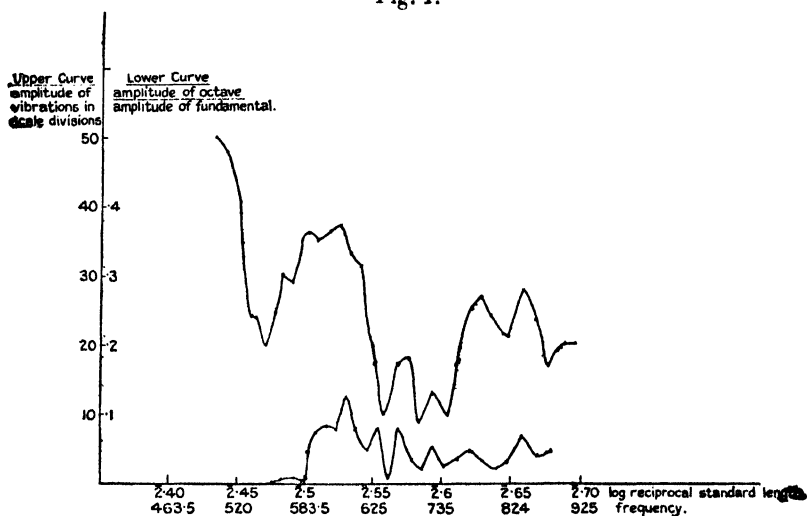
To get higher pitches than could be obtained by tension of the open string alone, a small wooden bridge was put under the wire on the fingerboard, and the tuning for subsequent observations carried out by tension as before.



*Results.*

The results found are outlined above. The upper curve of fig. 1 shows part of a typical amplitude-pitch graph, the observations for which were made with the string giving its fundamental note. A large number of these graphs were plotted for each of the two violins used, each graph corresponding to a definite mode of the string. It was found that in whatever mode the string was vibrating, and whether it was bridged or not, the minima for the same violin always occurred at about the same pitches.

Fig. 1.



The fact that the minima are not always exactly in the same place may be accounted for partly by the nature of the standard used—a sonometer wire. It probably also depends on changes of the atmosphere etc., which would have the effect of making slight alterations in the elasticity of the different parts of the violin.

*Further Experiments.*

In order to approach the matter from another angle, a series of 27 vibration photographs of the same point on the wire were taken, after the manner of Krigar-Menzel and Raps, for different pitches ranging over  $\frac{1}{2}$  of an octave. The string was vibrating in its fundamental mode. Each photo was enlarged, and the enlarged curves analysed by a Mader harmonic analyser.

It was found :

- (1) The preponderating tone in all the curves is the fundamental.
- (2) The highest amplitude of the first overtone is about 12 per cent. of that of the fundamental. The lowest is zero.
- (3) The highest amplitude of the second overtone is 4 per cent. of the corresponding fundamental.
- (4) The highest amplitude of any other overtone is less than 2 per cent. of the fundamental.

The results of the harmonic analysis are not reliable within 1 per cent.

An additional test of the conclusion that the pitches of the minima are functions of the violin itself is provided by examining the amount of first overtone in the vibration curve of the string. Assuming that the first harmonic is present in a constant proportion in the alternating applied force, we should expect its presence in the forced vibration of the string to be determined in the same way as for the fundamental ; the minima of the amplitude of the octave in the complex note should occur at the same pitches. This was found to be the case for the range examined, as is shown in fig. 1. In order to reduce all the amplitudes of the first overtone to the same scale, each was expressed as a fraction of the corresponding fundamental amplitude (*i.e.* approximately, as a fraction of the whole amplitude).

It now remains to trace to which parts of the violin the resonances belong. It is easiest to tackle first the enclosed air.

Helmholtz \* found, on a violin which he examined, resonances at two pitches between  $c'$  and  $c'\sharp$ ; the other between  $a'$  and  $a'\sharp$ . He got them by listening at the back of a violin while a piano was being played, and by noticing that some notes were more strongly reinforced than others.

In these experiments a vibrating telephone diaphragm was used as a faint source of sound. The violin was disconnected, and the telephone connected across the oscillating circuit.

The receiver was held with its diaphragm opposite one of the F holes of the violin, and as the pitch of the oscillating circuit was varied, it was noticed that at certain pitches, corresponding to natural frequencies of the enclosed air, the faint sound from the diaphragm was considerably reinforced.

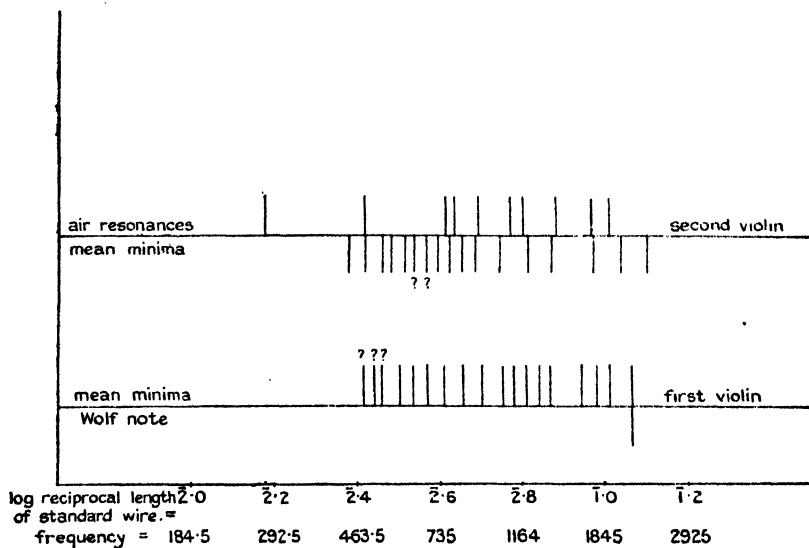
\* 'Sensations of Tone,' English translation by Ellis (1875), ch. v. p. 137.

There were several marked resonances at which the note sang out fairly loudly, and the two lowest of these were at about the pitches recorded by Helmholtz.

On fig. 2 are set out the mean data obtained for the two violins examined. No wolf-note was found on the second violin, and the air resonances were not taken for the first.

It will be seen that for the second violin, two of the minima coincide with air resonances, and most of the other air resonances lie fairly close to the nearest minima. There is a very powerful air resonance about  $\bar{2}\cdot6$ , but the minimum occurs only sometimes, not always, on the graphs. The resonance about  $\bar{2}\cdot7$  is not very marked, but the corresponding minimum appears on all the graphs.

Fig. 2.



It would seem from these results that the natural pitch of the enclosed air does affect the amplitude of the string's vibration.

The majority of the minima are probably due to natural frequencies of different parts of the violin.

It may be noted that there is coincidence between the wolf-note pitch and one of the minima on the first violin.

In order to try to trace the origin of the other minima, the bridge was loaded by small amounts. This had the

effect of shifting some minima and leaving others undisturbed ; but the results found were inconsistent, and no conclusions could be drawn.

*Additional Observations.*

For both violins it was found that at frequencies below about 480 vibrations per sec. (1) the ordinary form of octave vibration became unstable. When started, the string vibrated in the ordinary way with a node in the middle ; then the node disappeared, the string vibrated in one piece, and the fundamental was prominent in the note heard—an example of a note produced by an applied force of double its frequency. (2) When the second overtone was sounding, it was found that the wire had two pitches of maximum response close to one another instead of one, when the frequency of the impressed force was gradually altered in the neighbourhood of the wire's natural frequency, keeping the tension the same.

These two effects were in general noted only on a very slack wire—much slacker than would be the case when playing the violin.

When the third overtone was sounding at frequency 982 and a little on either side of it on the first violin, it was found that the ordinary form of vibration became unstable, and the nodes at  $\frac{1}{4}l$ ,  $\frac{1}{2}l$ ,  $\frac{3}{4}l$  disappeared. There is a minimum on some of the curves at about this pitch.

On the first violin, places of double maximum response were found between frequencies 755–835, usually when the fundamental was sounding ; sometimes this effect appeared slightly in the first and second overtones. The mean pitch corresponds to a good minimum on most of the graphs. Places of double maximum response also occurred sometimes at some pitches on the other violin.

These last observations recall the behaviour of the bar and string in cases where there was coincidence between like modes of vibration. There it was found that in each pair the pitches of maximum response kept one above and one below the natural note of the bar. In the violin case the pitch midway between the pair rose along with them, as if the proper pitch of the violin regarded as a bar were rising as the tension of the string increased. On the violins the places of double maximum response only occurred occasionally, and could not always be found again at will.

*Summary.*

A method of finding resonance pitches of a violin is described. Some of these correspond to natural frequencies of the air enclosed in the violin. The others are taken to correspond to natural frequencies of the body. The results of the harmonic analysis of a number of vibration photos taken at different pitches for the same point of the wire support the view that the resonances found are functions of the violin itself.

It is evident that there are a large number of resonance pitches on a violin which do not correspond to a wolf-note.

The wolf-note on the "wolfy" violin agrees in pitch with one of the resonances found.

I wish to express my grateful thanks to Professor Morton for his interest and his helpful suggestions in connexion with the above piece of work.

XIV. *The Intensities of Forbidden Multiplets.* By JAMES TAYLOR, D.Sc. (Utrecht), Ph.D., *The Physical Institute of the University of Utrecht* \*.

INTRODUCTION.

THE problem of the intensity relations of forbidden multiplets and the relative intensity of forbidden to non-forbidden lines has been studied recently at this Institute. Certain results have been put forward by Ornstein and Burger in a recent preliminary note †.

It is well known that the rule according to which the azimuthal quantum number only changes by +1 is frequently broken. This raises two questions. Does the Sum rule and intensity formula apply in such cases just as in normal multiplets? Secondly, how do the intensity relations of the forbidden to the non-forbidden lines depend upon conditions?

These questions were examined for the case of Cd multiplets, and yielded interesting results which we shall refer to later.

The present work contains some measurements of the intensities of two of the forbidden lines in the S-D series

\* Communicated by Prof. L. S. Ornstein.

† Ornstein and Burger, *Die Naturwissenschaften* J. xv. p. 32.

of potassium,  $1^2S-3^2D_{5/2}$ ,  $1^2S-3^2D_{3/2}$  ( $\lambda=4643\cdot172$  and  $4641\cdot585$ ). They are separated by about one-half of one ångström.

### EXPERIMENTAL METHOD.

#### *Light-source and Apparatus.*

A mixture of dried potassium carbonate and carbon powder, in the required proportion, was ground down so as to be as homogeneous as possible, and packed into a boring (4 mm. diameter) in an arc carbon (9 mm. diameter). The carbon was used as positive pole of an arc, the image of the middle part of which was projected upon the slit of a Rowland grating apparatus (30,000 lines per inch; radius 1 metre) which clearly resolved the lines when they were not unduly broadened.

The spectra were photographed, an iron arc spectrum being used for comparison purposes.

In other experiments a mercury-vapour lamp containing potassium was used, whilst in others electrodeless discharges in potassium vapour were employed.

#### *Method of Intensity Measurements.*

The line-intensities were measured by the photographic method of comparison\*.

In the case of the forbidden lines under consideration the method is comparatively simple, for the sensitivity of the photographic plate is precisely the same for both lines, and the problem is simply to transfer blacknesses or densities of the plate into intensities. The photographic densities are measured by means of the registering microphotometer of Moll, which, in principle, is extremely simple. The image of the filament of a 10-volt lamp run on constant voltage (or of a slit placed before the lamp) is focussed upon the gelatine layer of the photographic plate, which is held in a mechanically-travelling holder in such a way that the lines of the spectrum to be measured pass successively into the correct position. The transmitted light is focussed by a lens system upon the slit of a Moll thermopile which is connected to a galvanometer. The system must, of course, be focussed for the infra-red radiation.

The deflexion of the galvanometer is registered photographically on a rotating drum, by means of which an exact record of the densities of the spectral lines is obtained.

We further require to know the density values in terms

\* Ornstein, Proc. Phys. Soc. Lond. xxxvii. v. p. 334 (1925).

of light-intensity equivalents. This is done in the following manner. The image of a standard lamp run on constant voltage is focussed, so as to give a homogeneous not quite sharp image upon the slit of a spectrograph, and a series of exposures at constant current and time of exposure but with different slit-widths (*e. g.* 100, 60, 40, 26, 16, 6) is made. This plate is measured with the photometer at the wave-length which is being investigated, and gives the blackenings corresponding to 100, 60, 40, 26, 16, etc. if the slit-widths are as given above. (The intensity is proportional to the slit-width.)

If a sufficient density range is not obtained by such a series, then the current of the standard lamp is adjusted to another value and a further set is taken. The logarithms of the transmissions  $\left[ \log \left( \frac{\text{deflexion for clear plate}}{\text{deflexion for line}} \right) \right]$ , or alternatively of the densities, is plotted against the logarithm of the slit-width. The curves for different standard-lamp currents are parallel and can be brought upon one graph by lateral displacement. When such a curve is constructed, the densities can be immediately transferred into intensity units and the relative intensities compared.

In the experiments to be described, it was more convenient to obtain the density marks (curves for intensity) with a spectrograph, for there were difficulties in utilizing the grating with different slit-widths (diffraction etc.) for such a purpose.

Initially, the procedure of cutting a plate into two sections and using one for the density curves, the other for the spectral lines, was adopted. This precaution, however, proved to be unnecessary, for it was found that plates from the same box or even plates with the same emulsion number gave almost identical results.

In comparing the intensity of the forbidden with the non-forbidden lines, the above procedure must be somewhat modified because the wave-length separation is considerable (6000 Å.) and the sensitivity of the plate is not the same. The density-mark curves are constructed for the wave-lengths which are being compared, and the relative intensity relation for the two curves is derived from a knowledge of the energy distribution in the spectrum of the standard lamp. It is found as a rule that the density curves for even widely-separated spectral regions are parallel. This is extremely convenient.

# RESULTS.

## Relative Intensities of the Forbidden Lines.

Table I. gives the results obtained for the relative intensities of the forbidden lines for different concentrations of the potassium-carbonate mixture, and arc currents of about 3 amperes (240 volts).

TABLE I.

Pot. Carbonate Ratio Carbon for filling mixture.	Ratio of Intensities $1^2S-3^2D_{5/2}$ $1^4S-3^2P_{3/2}$	
1	9/4	} First determination.
1/2	9/5.3	
1/5	9/6	
1/2	9/6	} Second determination; spectral background not so large as in first determination.

We should expect to obtain the ratio 3:2; but since the lower levels of the lines are normal ones, this actual ratio will be altered by self-absorption, and we should then only obtain the 3:2 ratio at infinitely dilute K-concentration. Unfortunately, however, the spectral background on the plates was considerable, and increased relatively with the smaller concentrations. This introduces a large experimental error, for, in the procedure whereby the line-intensity is measured, the integrated intensity corresponding to the blackening produced by the line and the background must be found, and from this must be subtracted the corresponding intensity of the background.

At higher concentrations of the potassium carbonate it was also found that the lines were broadened. Nevertheless, the results obtained are good and show the correct limit, so that we may conclude that the ratio of the intensities is certainly for dilute concentrations that given by the Sum rule; and, if the results of Ornstein and Burger\* upon other cases are taken into consideration, we conclude with a fair degree of probability that the ratio is normal for forbidden multiplets.

Further experiments were carried out with a view to reduce

\* *Id.*, *ibid.*; also v. Alphen, Dissertation, Utrecht, 1927.



the relative intensity of the continuous background. In a mercury arc containing about 1 per cent. of potassium the lines were considerably broadened, and were not resolved into the two components.

On the other hand, with electrodeless discharges in potassium vapour at various pressures (different temperatures) it was not found possible to obtain the forbidden lines at all. This is also in accord with the results of Ornstein and Burger \* for cadmium.

*Relative Intensities of the Forbidden to the Non-forbidden Lines.*

A series of experiments were carried out to investigate the relative change of the ratio of the maximum intensity of the compounded 4642 lines to the non-forbidden lines 4044 and 4047, which have the same lower level as the forbidden lines ( $1^2S - 3^2P_{3,2}$ ,  $1^2S - 3^2P_{1/2}$ ).

The ratio is much too small to measure in the normal way, but the difficulty was overcome by comparing the lines 4642 with one of the ghosts of the non-forbidden lines given by the grating. The ghosts were four in number, two from each line, and the intensities were about 1 per cent. of the line-intensities. As a rule the first ghost on the short wave-length side was used; but it was determined initially by experiment that the ratio of the lines and ghosts was constant, so that any of the ghosts could be used for measurements.

For our purpose, only the relative change of the intensities under different conditions is required, so that it is unnecessary to bring the ratios expressing the intensities to real values.

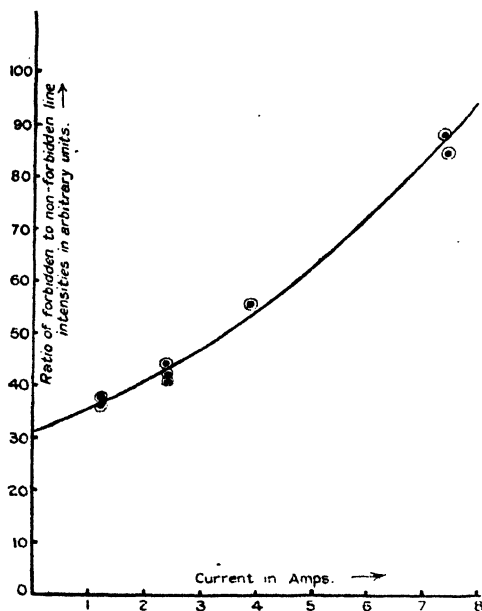
The results of measurements at different current densities are shown in graph I. It is to be seen that the ratio depends upon the intensity of the arc current, the intenser currents giving a greater relative intensity, as is to be expected. The trend of the graphs is similar to that found for the cadmium arc; but it must be remembered that the present case is much more complicated because of the dilution by carbon.

Graph II. shows the variation of the ratio with concentration of potassium carbonate in the filling mixture. The ratio increases as the potassium content of the mixture increases, whilst at the same time the lines become broadened. This result is also in a general way to be expected from the fact of the increased potassium-ion concentration in the arc.

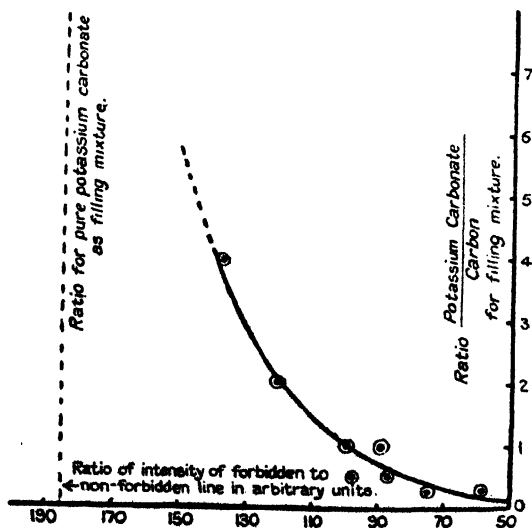
Experiments with an arc in air at different pressures gave inconclusive results. The air lines came up very strongly at pressures lower than about 8 cm., and in a general way the ratio of the forbidden to the non-forbidden lines was found to become smaller at the lower pressures.

\* Ornstein and Burger, *Die Naturwissenschaften J.* xv. p. 82.

GRAPH I.



GRAPH II.



It cannot, however, be claimed that the results were definite, for divergent results were frequently found under the same conditions. This arises probably from "spurts" of potassium-salt vapour and local increases of the ionic concentration.

*Intensity of Forbidden Multiplets etc.*

The experiments of Ornstein and Burger\* upon cadmium were carried out on some of the  $p-f$  lines, employing an arc between cadmium electrodes.

The relation of the lines  $p_0-f$ ,  $p_1-f$ ,  $p_2-f$  ( $\lambda=2961$ , 2862, 2891) was within the limits of experimental error, 1:3:5, which is to be expected from the Sum rule, as the  $f$ -term is not resolved. The second multiplet yielded similar results.

The intensities of a  $p-f$  multiplet can also be represented by a number given by the ratio of a  $pf$  line to the adjacent corresponding  $p-d$  line with the same total and the inner quantum number (cp. above). To investigate the problem from this point of view, an electrodeless discharge in pure cadmium vapour was first investigated, but though the  $p-d$  lines were intense, no trace of the  $pf$  lines was observed.

The cadmium arc in air at different pressures was then examined, and it was found that the ratio  $pf:pd$  was a function of the pressure approximately proportional to  $p^{0.4}$ .

It was also found, at constant pressure, that the ratio  $pf:pd$  increased with increasing current. A corresponding increase in the width of the  $pf$  lines was also observed.

### CONCLUSIONS.

1. The Sum rule is valid for forbidden multiplets.

2. The relative intensity of the forbidden to the non-forbidden lines increases with increasing current and vapour density. This is in accord with the hypothesis that the forbidden lines are brought up by the action of ionic electric fields and that they increase in intensity with increase of the fields. This explanation is in accordance with the results of Takamine and Werner†.

It is a great pleasure to me to express my gratitude to Prof. Ornstein, who suggested the problem, and to Dr. v. Cittert and Dr. Burger for their continued help and advice. I am also indebted to the International Education Board for the Fellowship which enabled the work to be carried out, and to Mr. v. Hasselt, who helped with many of the measurements.

September 29th, 1927.

\* Ornstein and Burger, *Die Naturwissenschaften J.* xv. p. 82.

† Takamine and Werner, *Die Naturwissenschaften J.* 1925.

## XV. *The Classification of Metallic Substances.*

*By W. HUME-ROTHERY, M.A., Ph.D.\**

**I**N recent years considerable discussion has taken place as to whether the different constituents to be found in metallic alloys are to be classified as mixtures or as compounds. From some points of view it may be said that the matter is of little importance, for it may be argued that the properties of a substance do not depend on the particular label which it is given. But as a position has arisen in which different writers are using the term "compound" with entirely different meanings, it may be well to examine the matter a little more closely, and to see if a satisfactory scheme of classification can be devised. The problem is one which does not concern metallurgy alone, but which may arise in many branches of science when the structures of solid substances have been examined in more detail.

The usual text-book definitions for distinguishing between compounds and mixtures give the following three tests for a definite chemical compound:—(1) Fixity of composition; (2) decomposition into its constituents by chemical means only, and not by physical or mechanical means; (3) the possession of properties which, unlike those of a mixture, cannot be calculated from the properties and proportions of the constituents.

The last two of these criteria are admittedly unsatisfactory, and the generally-accepted test for a compound is that it should contain the elements in proportions corresponding to a possible formula—assuming that the atomic weights are known—and that these proportions should be independent (within limits) of the conditions of formation, as for example the composition of the liquid from which the solid phase separates.

In the majority of cases the differences are so clear that little difficulty arises, but the above criteria are really by no means infallible. It has, for example, been pointed out by U. R. Evans (*Trans. Faraday Society*, October 1923) that some of the metallic oxides, such as those of iron, tungsten, and molybdenum, which are generally admitted to be compounds, are, in fact, of distinctly variable compositions, so that the law of constant proportions appears to break down. Even such a well-defined compound as ferric oxide can form solid solutions of limited extent

\* Communicated by Dr. N. V. Sidgwick, F.R.S.

with its component elements, so that perfectly homogeneous samples of different compositions can be obtained; but few chemists would refuse to admit it as a compound on this ground.

It must, I think, be admitted frankly that the ordinary means described for distinguishing between compounds and mixtures have failed to consider the possibility of a compound forming a solid solution with its component elements, and the way in which such solid solutions are to be distinguished from those in which no compounds are formed.

From the point of view of the older atomic theory, however, the distinction was quite plain. The physical mixture of the two elements was considered as a mixture of the individual atoms or molecules, whilst in the compound the different atoms were bound together into compound molecules, and these behaved as distinct entities. For many years this conception was purely hypothetical, but the comparatively recent work on positive-ray analysis and mass spectra has led to the conclusive experimental detection of the individual molecule, the existence of which is now a fact and no longer merely a supposition. The formation of these molecules is regarded as due to the sharing or exchange of electrons between two atoms. At first sight, therefore, it might seem justifiable to define a metallic compound as one in which the constituent atoms had united to form a compound molecule, but unfortunately almost all the methods for detecting the existence of individual molecules depend upon the examination of the substance in the gaseous or liquid state, which is in general very difficult at the temperatures of molten metals. A start in this direction has been made by the Japanese scientists, notably H. Honda and his collaborators, by the study of the magnetic properties of molten alloys, and in this way it has been shown that some of the phases of intermediate composition found in solid alloys correspond to entities in the liquid, whilst others do not. In another connexion the work of Barratt and others on the spectra of metallic vapours has led to the observation of band spectra, which are usually ascribed to compound molecules and not to free atoms. But even in cases such as these, there is always the possibility that a true compound may be formed in the solid, but may decompose on melting or volatilisation. In general, therefore, we have to examine the solid alloys alone, and here the connexion between the molecule and the crystal structure is not always clear. In many compounds, notably those met with in organic chemistry, the molecules retain their

individuality in the solid crystal, but in others, such as sodium chloride, there is no sign of the individual molecule in the crystal lattice, although the high-temperature work of Nernst and others shows that, in the gaseous state, sodium chloride consists entirely of compound molecules. We are not, however, driven to believe that sodium chloride is a compound in the gaseous state and a mixture when solid, because the work of Rubens on Reststrahlen indicates conclusively that the units in the solid crystal are not neutral atoms of sodium and chlorine, but are charged ions, each sodium atom having lost and each chlorine atom gained an electron. This is in agreement with the more refined methods of X-ray analysis. It must again be emphasized that this is now a definite experimental fact, and not merely a supposition.

The above considerations would therefore seem to indicate how we may best classify the various intermediate phases which are so often met with in alloys, and it is suggested that the following scheme of classification might well be adopted :—

At the head of our classification of solid metallic phases we may place the **METALLIC ELEMENTS**, and we may note that these may be isotopically simple or isotopically complex.

We may next define as **PRIMARY METALLIC SOLID SOLUTIONS** those solid solutions in which the crystal structure of the parent metal is retained. These primary solid solutions form the “end phases” when the equilibrium diagrams are drawn in their usual form. The X-ray spectrometer shows that these are of two types—the substitutional type, in which the solute atoms replace the atoms of the solvent metal upon its lattice, and the interstitial type, in which the solute atoms fit into the spaces in the lattice of the parent metal. In the case of ternary alloys the primary solid solution may be of both types : thus in an austenitic manganese steel we have a primary substitutional solid solution of iron and manganese forming an interstitial solid solution of carbon.

We may further define as **SECONDARY SOLID SOLUTIONS** those solid solutions of intermediate composition in which the crystal structure is different from that of the parent metal, but in which there is no indication of the formation of compound molecules or that any exchange or transference of electrons is taking place.

And, finally, we may define as **INTERMETALLIC COMPOUNDS OF FIXED OR VARIABLE COMPOSITION** those intermediate

phases where there is evidence, direct or indirect, that electron exchange or transference is taking place or that a compound molecule is being formed.

The above scheme would appear to give a satisfactory fundamental distinction, although it must be admitted frankly that in some cases our experimental methods may not yet be sufficiently developed to distinguish between the secondary solid solutions and the intermetallic compounds. In such cases we must just select the more probable alternative. Where, for example, we have a phase of fixed or practically fixed composition, or one which shows markedly different properties from those of its components, we may reasonably classify it as an intermetallic compound, even though we cannot definitely prove that electron transference or sharing has taken place or that a compound molecule has been formed. On the other hand, where we have a phase of variable composition whose properties resemble those of its constituents we may reasonably call it a secondary solid solution. It has, for example, been suggested by W. Rosenhain (*J. Inst. Metals*, xxxv. p. 353, 1926) that in cases such as those of the  $\beta$  brasses we have to do with what is essentially a solid solution of zinc in an allotropic form of copper. In many ways this illustration is very apt, for it indicates just what it is desired to express above, namely that although the lattice type of the  $\beta$  brasses is different from that of copper, the atoms have not shared or exchanged electrons, but are bound together by forces of the same nature as those in the primary solid solutions. In order to avoid confusion, it is thought better to use the term secondary solid solution. For where a metal, such as iron, exists in different allotropic forms, each allotropic form may give rise to its own primary solid solution, and the term allotrope is better confined to this phenomenon.

In conclusion, it may be well to refer very briefly to two previous suggestions that have been made in connexion with the subject of this paper.

It was long ago suggested by C. A. Edwards that in complex alloy systems every phase except the two end phases, which we have called primary solid solutions, should be regarded as based on a definite compound. It would seem that this is using the term compound in a sense very different from that of the chemist. For it ignores the possibility that the atoms of two elements may build themselves into different lattice patterns without any electron transference or sharing taking place.

A quite different suggestion has recently been made by

Westgren and Phragmén (*Phil. Mag.* vol. 1. p. 311, 1925), according to whom in an ideal chemical compound structurally equivalent atoms are chemically identical, whilst in an ideal solid solution all atoms are structurally equivalent. Thus, in the case of the  $\beta$  brass solid solution, which ranges round the equi-atomic composition, the above authors would call it a solid solution in a compound if the equi-atomic alloy had the zinc and the copper atoms arranged in a definite pattern relatively to each other, and they would call it a simple solid solution if the two kinds of atoms were arranged at random on a common lattice. It would again seem that this is using the term chemical compound in a new sense. For whilst it is quite true that in all definite compounds structurally equivalent atoms are chemically identical, the reverse argument does not necessarily follow. If, for example, we imagine two sets of spheres of different sizes to exert attractive forces, we can well understand how some whole-number ratios may give a particularly close packing when those of one size occupy definite positions relatively to those of the other. But this may occur without the exertion of any forces other than those which exist when one set of spheres alone is packed together, and it is only in some cases, the so-called "Riesenmolekül" substances, that these crystal forces are regarded as forces of chemical combination. In the same way, the fact that a solid solution of wide range shows a maximum hardness, melting-point, or electrical conductivity at some simple whole-number ratio of atoms does not necessarily imply that a compound is formed. It may mean that a definite compound exists, or it may simply mean a symmetrical packing of the atoms, and the term chemical combination, in the chemist's sense of the word, implies more than the mere arrangement of atoms in symmetrical patterns. A term such as a SYMMETRICALLY-PACKED SOLID SOLUTION can readily be devised for this phenomenon. But it is desired to emphasize that a phenomenon of this sort may be quite distinct from chemical combination in the usual sense of the word, and as the term "chemical compound" has already a clear and definite meaning to the chemist, it would seem most undesirable that the physicist should use the same term with an entirely different meaning.

From some points of view it may be said that any scheme of classification is arbitrary, and is to some extent a mere matter of definition, but it is suggested that the system described above is one in which the fundamental distinctions



are clear, and in which no term has been given a meaning different from that with which it is usually associated. It can only lead to confusion if terms such as "chemical compound" are used loosely, and are given different meanings in different branches of science, and if the present paper helps to remove some of the existing confusion, it will have served its purpose.

The author must express his thanks to Dr. N. V. Sidgwick, F.R.S., for his kind interest and criticism.

Magdalen College, Oxford.

---

XVI. *Electrodeless Discharges.* By J. S. TOWNSEND, M.A., Wykeham Professor of Physics, Oxford, and R. H. DONALDSON, M.A., University College, Oxford\*.

1. **T**HE improvements in the methods of maintaining continuous electric oscillations by means of valves may be used in experiments on electrodeless discharges in gases, and the properties of the discharges may thus be determined to a degree of accuracy which cannot be attained with damped oscillations obtained by means of disruptive discharges.

Several methods of using valves in short-wave generators are given by Mesny in his book, '*Les Ondes Électriques Courtes*,' where an account is also given of the first experiments made by Gutton with gases at low pressures rendered conducting by the action of continuous oscillations.

Continuous wave generators have been found very useful for many ordinary experiments, also in connexion with researches when it is desirable to have a simple means of testing samples of gases. Since the high-frequency currents may be produced in electrodeless tubes, the effect of impurities from metal electrodes in a gas may be avoided, and in many cases a discharge is more easily obtained with external electrodes than with electrodes in contact with the gas.

With ordinary cylindrical tubes the discharge is most easily obtained when the direction of the electric force is along the axis of the tube, and tubes without electrodes may

\* Communicated by the Authors.

be used to show the direction and the intensity of electric forces in the field of an oscillating circuit.

The tubes may also be used with external electrodes in the form of sleeves, and the potentials required to produce a discharge with the sleeves at various distances apart may be found. Thus a long tube with a sliding sleeve may be calibrated and used as a voltmeter to determine the amplitude of a high-frequency potential.

In this paper we propose to describe some of the properties of electrodeless discharges which we have determined, using tubes that had been made up at various times in the laboratory to examine the spectrum of samples of gases. These tubes were of various shapes, the simplest forms being cylindrical or spherical. It is generally of advantage to use cylindrical tubes not less than 3 or 4 cm. in diameter and large spheres 10 or 12 cm. in diameter.

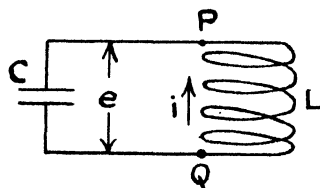
In another paper we propose to describe experiments with tubes of different shapes specially designed to investigate properties of high-frequency discharges.

2. In considering the forces in the field inside or outside a solenoid, it is necessary to distinguish between the electric forces due to electric charges on the solenoid and those due to the variation of the magnetic force. The latter will be indicated by the suffix  $m$ ; thus  $E_m$  and  $F_m$  will be used to denote the electromotive force round a circle, and the electric force along the tangent to the circle due to electromagnetic induction, and  $E$  and  $F$  the potentials and force due to electric charges. In the field either inside or outside a solenoid the forces  $F$  are generally very large compared with the forces  $F_m$ . At points of the central plane—the plane through the centre of the solenoid with the axis normal to the plane—the forces  $F$  are parallel to the axis, and the forces  $F_m$  in directions perpendicular to the axis.

3. In order to determine the relative values of these forces the simple case of a circuit consisting of a solenoid of self-induction  $L$  and a condenser of capacity  $C$  may be considered, and for the purpose of an elementary calculation it may be assumed that the capacity of the condenser is large compared with the capacity of the coil. In the principal mode of oscillation the current at any instant is approximately the same in all the turns of the solenoid. Let  $i = I \sin pt$  be the current, and  $e = E \cos pt$  the potential difference between the points  $P$  and  $Q$  (fig. 1) at the ends of the

solenoid when continuous oscillations are maintained. If  $n$  be the number of turns per unit length of the solenoid,  $l$  the distance between P and Q, the magnetic force  $H$  inside the

Fig. 1.



solenoid is  $4\pi ni$ , so that  $e$ , which is equal to  $L di/dt$ , may be expressed in terms of  $H$ . Thus

$$e = L \frac{di}{dt} = \pi n a^2 l \frac{dH}{dt},$$

and the electric force  $F$  on the line from P to Q is

$$F = \frac{e}{l} = \pi n a^2 \frac{dH}{dt},$$

$2a$  being the diameter of the solenoid.

The force  $F_m$  inside the solenoid is obtained from the electromotive force  $E_m$  round a circle of radius  $b$  in the principal plane. Thus

$$F_m = \frac{E_m}{2\pi b} = \frac{b}{2} \frac{dH}{dt},$$

and the ratio of the two forces is

$$F/F_m = 2\pi n a^2/b.$$

Hence in a solenoid, when the distance between the turns is not greater than 1 cm. ( $n > 1$ ) and the radius of the solenoid not less than 5 cm., the electric force  $F$  is more than thirty times as great as the electromagnetic force  $F_m$ .

It is remarkable that in the explanation usually given of the currents in electrodeless tubes or bulbs placed inside solenoids the large forces  $F$  are not taken into consideration. It is generally supposed that the currents in the gas flow in circles round the axis under the action of the forces  $F_m$  as in the theory recently given by Sir J. J. Thomson\*.

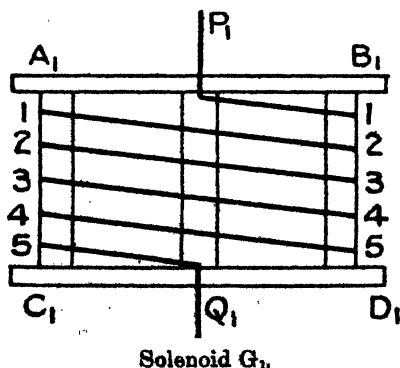
\* Sir J. J. Thomson, *Phil. Mag.* Nov. 1927.

4. In general the capacity of the coils cannot be neglected when the capacity of the condenser is reduced in order to obtain short-waved oscillations; and with short solenoids the ordinary formulæ for  $H$  and  $L$  are inaccurate. With a small condenser the current flowing through the turns of the wire near the centre of the solenoid may be much greater than the current flowing into the condenser.

In these cases it is necessary to determine the forces in the field experimentally and to find the wave-lengths of the oscillations by means of a short-wave wave-meter. The wave-meters used in these experiments were calibrated by adjusting the wave-length of a generator to an exact multiple of a 5-metre or 10-metre wave which can be measured by means of Lecher wires\*.

5. In order to find the relative values of the forces  $F$  and  $F_m$ , and to show how the effects of the forces  $F$  may be exhibited by means of a large bulb placed inside a solenoid, two solenoids  $G_1$  and  $G_2$  were used. The solenoids were wound differently so that when currents giving the same values of the force  $F_m$  in the central plane flow in each coil, there is a large difference in the intensity and in the distribution of the forces  $F$ . The solenoids had the same number of turns and were of the same section and same length. They were wound in hexagonal form on frames consisting of six ebonite rods 10 cm. long fixed at equal distances apart to two wooden rings, as shown in figs. 2 and 3.

Fig. 2.



The outer diameter of the rings was 19 cm. and the inner diameter 15.5 cm. In the diagram (fig. 2)  $A_1B_1$  and  $C_1D_1$

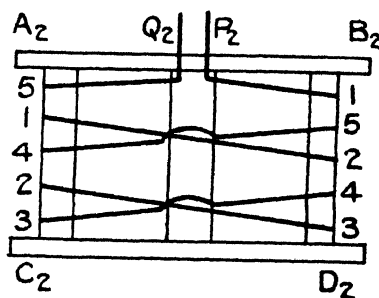
\* J. S. Townsend and J. H. Morrell, *Phil. Mag.* xlii. p. 265 (1912).

are the rings of the frame of the coil  $G_1$ , and  $A_2, B_2$  and  $C_2, D_2$ , those of the coil  $G_2$  in fig. 3.

The coil  $G_1$  was wound in the ordinary manner in a single layer of 13 turns, 7 mm. apart, from the upper to the lower part of the frame.

The coil  $G_2$  was wound with  $6\frac{1}{2}$  turns, 14 mm. apart from the upper to the lower part of the frame, and  $6\frac{1}{2}$  turns from the lower to the upper part, also at 14 mm. apart. Thus the two coils were each 8.4 cm. in length.

Fig. 3.

Solenoid  $G_2$ .

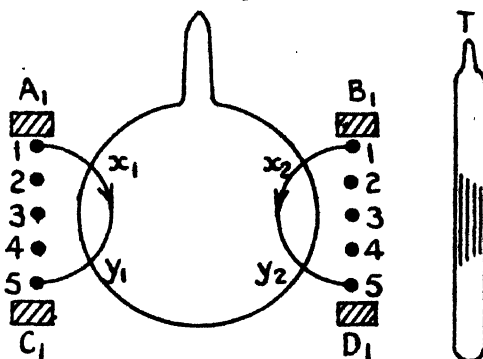
In the diagrams the coils are represented as having five turns each instead of thirteen in order to simplify the figures. The centre of the third turn (assuming there were five turns in the solenoid) may be taken as being at zero potential for the high-frequency oscillations; and as the potential difference between the ends is  $C = E \cos pt$ , one end oscillates in potential from  $+E/2$  to  $-E/2$ , while the other end oscillates from  $-E/2$  to  $+E/2$ . The average rate of change of potential along the wire is  $e/2\pi Na$ , and the potential difference between adjacent points (1 and 2, 2 and 3, etc.) of consecutive turns is  $e/N$ . Thus the potential difference between the points 1 and 5 (marked at the sides of the coils in figures) is  $4e/N$ , and between the points 2 and 5,  $3e/N$ , etc.

6. In the coil  $G_1$  the turns which differ in potential by the largest amount are far apart, 8.4 cm., so that there is a large electric force in the field at a considerable distance from the coil, both inside and outside. The lines of force inside the coil are indicated by the arrows in fig. 4, which represents a section of the coil through its axis, the vertical rows of points on each side being the sections of the wire.

When a spherical bulb containing gas at a low pressure is

placed inside the solenoid  $G_1$ , there are large forces along the lines from  $x_1$  to  $y_1$  and from  $x_2$  to  $y_2$  which cause a discharge in the gas when the current in the solenoid is increased up

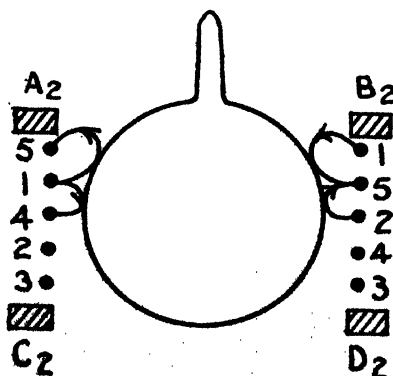
Fig. 4.

Solenoid  $G_1$ .

to a certain point. The glow which accompanies the discharge is equally distributed above and below the central plane.

7. In the coil  $G_2$ , which is shown in section in fig. 5, the turns of the wire which differ most in potential are near together (7 mm. apart) in the upper part of the solenoid.

Fig. 5.

Solenoid  $G_1$ .

The electric force is therefore much greater in the upper part of the field above the central plane than in the lower part of the field. The lines marked with arrows in fig. 5 indicate the distribution of the force  $F$  in the coil  $G_2$ .

In this case, when the bulb containing the gas at low pressure is placed inside the solenoid as in fig. 5 with the centre of the bulb at the centre of the solenoid, there is no current in the gas when the current in the solenoid is the same as that required to produce a discharge with the bulb in a similar position inside the solenoid  $G_1$ . In order to obtain a discharge, the current which is required with the bulb inside  $G_2$  is more than four times the current required with the bulb inside  $G_1$ .

When the discharge is obtained with the bulb inside the solenoid  $G_2$ , the glow is concentrated in the upper part of the bulb where the electric force is large. Also, by raising the bulb so as to bring more of the gas into the space where the force is large, the discharge is obtained with a smaller current in the solenoid.

8. When a cylindrical tube T containing a gas at low pressures is placed outside the solenoid  $G_1$  in the position shown in fig. 4, a discharge is produced in that part of the tube where the lines of force are parallel to the axis of the tube.

The discharge may be started by holding the tube close to the solenoid, and if the tube is withdrawn keeping it parallel to the axis of the solenoid, the length that is illuminated contracts.

The shading of the centre of the tube T in fig. 4 indicates the extent of the glow when the tube is moved away from the solenoid.

If the tube is rotated and its axis brought into the central plane of the solenoid, the discharge ceases even when the tube is quite close to the coil.

9. In most of the experiments which we describe the wave-lengths of the oscillations were from 100 to 40 metres, and the capacities of the coils were comparable with the capacities of the condensers, so that it was necessary to measure the electric potentials and the electromotive forces due to induction by direct experiment.

The potential difference  $E$  between the ends of the solenoid (fig. 1) may be obtained accurately by the following method. A system of three adjustable condensers is substituted for the capacity of C, two in series each of capacity  $2S$  and one in parallel of capacity  $C'$  as shown in fig. 6.

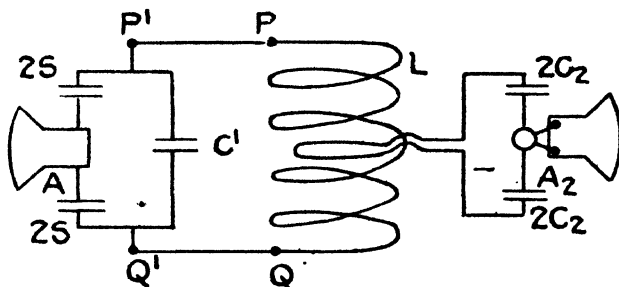
The condensers  $2S$  are connected through a low-resistance milliammeter A. The capacity C between the terminals  $P'$  and  $Q'$  is  $C' + S$ , and it may be adjusted to any required value by adjusting  $C'$ .

The ammeter current depends on the capacities  $2S$ , and a value of  $S$  may be selected to obtain an ammeter deflexion in the sensitive part of the scale.

The condensers  $2S$  were carefully constructed, and a range of small capacities was determined very accurately. They were calibrated by comparison with a small standard condenser at intervals of the scales over a range from  $2S = 15$  cm. to  $2S = 120$  cm.

In the arrangement shown in fig. 6 the milliammeter is connected in the circuit at a point of zero potential, and the readings are not affected by the capacity of the milliammeter.

Fig. 6.



If  $I$  be the current in the milliammeter, the potential difference  $E$  between  $P'$  and  $Q'$  is  $I/S\rho$ .

The electromotive force  $E_m$  was measured in a similar manner. A loop of copper wire 12.5 cm. in diameter was fixed in the central plane of the solenoid, and the ends brought out to a pair of adjustable condensers which were connected in series through a thermojunction. The current  $I_2$  in the condensers was obtained from the deflexion of the microammeter  $A_2$ .

If  $2C_2$  be the capacity of each condenser,  $l_2$  the self-induction, and  $R_2$  the resistance of the loop circuit, the quantities  $l_2\rho$  and  $R_2$  were small compared with  $I/C_2\rho$ . Hence the electromotive force  $E_m$  is equal to  $I_2/C_2\rho$ .

Since the current  $I_2$  is proportional to  $C_2$ , the deflexion of the microammeter may in this case also be brought to any convenient position on the scale by adjusting the value of  $C_2$ .

With oscillations of 83 metres in wave-length the ratio  $E : E_m$  was 30 : 1, the same for each of the coils  $G_1$  and  $G_2$ .

10. The experiments on the discharges in bulbs were made with two spherical bulbs of 12.5 cm. in diameter, one



containing neon at 1.06 mm. pressure and the other neon at .1 mm. pressure.

In one set of experiments the coils  $G_1$  and  $G_2$  were connected to valves with the two condensers 2S connected in series through an ammeter as shown in fig. 6.

The oscillatory current  $I$  in the condensers was gradually increased by increasing the heating current in the filament. At a definite point  $I_1$  a discharge is obtained in the bulb, and the potential difference  $E_1 = I_1/S_p$  between the ends of the solenoid required to start the discharge is thus obtained.

If the current in the solenoid be reduced after the discharge is started, the current in the gas diminishes at first uniformly with the current in the solenoid, but at a certain point  $I = I_2$  the current in the gas ceases abruptly. The minimum potential  $E_2 = I_2/S_p$  under which the current continues to flow in the gas is less than one-third of the minimum potential  $E_1$  required to start the discharge.

The amplitudes of the oscillatory potentials are obtained from the observed mean potentials by multiplying the latter by the factor  $\sqrt{2}$ .

The critical potentials  $E_1$  and  $E_2$  for the two solenoids, for discharges in the bulb containing neon at 1.06 mm. pressure in the position shown in figs. 4 and 5, are given in Table I., the wave-length of the oscillations being 83 metres in all cases.

The numbers in the table are the amplitudes of the potentials in volts.

The corresponding values of the electromotive forces  $Em_1$  and  $Em_2$  round a circle of 12.5 cm. diameter are also given.

TABLE I.

	$E_1$ .	$E_2$ .	$Em_1$ .	$Em_2$ .
Solenoid $G_1$ .....	280	88	9.4	2.9
Solenoid $G_2$ .....	1344	372	44	12.3

The amplitude of the force  $F_m$  in the central plane is  $Em/40$ , the highest value being that obtained in the solenoid  $G_2$ . The mean value in this force,  $2F_m/\pi$ , is .7 volt per centimetre, which is too small a force to impart sufficient energy to electrons in neon at 1.06 mm. pressure to obtain any appreciable effect of ionization by collision.

The discharges in the gas must therefore be attributed to the potentials  $E$ ; but it is difficult to obtain the electric force  $F$  from these experiments where the conductors are so far from the bulb containing the gas. A closer estimate of the critical electric forces in the gas is obtained from the experiments in which the oscillation potential is applied to external electrodes resting on the surface of the bulb.

The experiments with the tube containing neon at .1 mm. pressure gave results which were nearly the same as those obtained with the gas at 1.06 mm. pressure.

11. Experiments were also made with the same bulbs under the action of forces in a secondary circuit loosely coupled to a high-frequency generator maintained in oscillation by a valve, the wave-length of the oscillations being the same as in the experiments described above. Any effects of the harmonic oscillations which occur when a solenoid is directly coupled to a valve are greatly reduced in the secondary circuit.

The secondary circuit which was used consisted of the solenoid  $G_1$  connected to the condenser system ( $SC'$ ) shown in fig. 6. The capacity  $C$  of the system was adjusted to a point just above the value corresponding to resonance, in order to avoid abrupt changes in potential which occur when a discharge is started with the capacity below the point of resonance. These changes are due to a small additional capacity introduced by the discharge in the gas, which causes the total capacity of the secondary circuit to approach or pass through the exact value corresponding to resonance.

The potentials  $E$  at the terminals of the solenoid  $G_1$  are obtained from the current in the milliammeter which is between the condensers  $2S$ . Continuous variations in the potential  $E$  of the secondary circuit were obtained by varying the filament current of the valve in the generator.

Determinations of the critical potentials were made with the bulb containing neon at 1.06 mm. pressure placed inside the solenoid in the secondary circuit, as in fig. 4, to test the results obtained with the same solenoid  $G_1$  when it was connected to a valve.

With the bulb in the secondary circuit the values obtained for the critical potentials were  $E_1 = 288$  volts and  $E_2 = 85$  volts, which are practically the same as the potentials 280 and 88 obtained with the solenoid connected to the valve.

12. In order to apply the total potential  $1/Sp$  more directly to the gas, two rings of lead-foil were fixed to the bulb, at 10 cm. apart, which acted as external electrodes.

The lead rings were connected by short wires to the terminals P and Q of the solenoid, and were used with the bulb either inside or outside the solenoid. The rings were split, to prevent induced current flowing round them when the bulb was inside the solenoid.

The critical potentials obtained with the bulb inside the solenoid were almost the same as those obtained with the bulb outside. In the former case the values of  $E_1$  and  $E_2$  were found to be 125 volts and 34 volts; and in the latter case 130 volts and 35 volts respectively. This shows that the magnetic force inside the solenoid has no marked effect on the discharge. As the electrodes were 10 cm. apart, the mean force between them corresponding to the potential  $E_2$  is 3.5 volts per cm. This is not the mean force at points in the gas, as the potentials at the external electrodes are not the potentials at neighbouring points in the gas. The electric force in the gas is easily found from the values of  $E_2$  obtained for cylindrical tubes with external electrodes at different distances apart.

13. The minimum potentials  $E_1$  and  $E_2$ , required to start and to maintain discharges, were determined for gases contained in cylindrical tubes about 30 cm. long. External electrodes of lead-foil in the form of sleeves which fitted the tubes were connected to the terminals of the inductance of a secondary circuit, and gradual variations of potential were obtained by small changes in the filament current of the valve in the primary circuit. The potentials  $E_1$  and  $E_2$  were determined for different distances between the electrodes.

When the discharge starts a glow extends in a uniform column in the part of the tube between the electrodes and the current continues to flow as the potential is reduced. There is a minimum value  $E_2$  of the potential under which a uniform glow is maintained in the tube.

14. In a quartz tube 4.2 cm. in diameter, containing pure neon at one millimetre pressure, the minimum potential  $E_2$  is about one-sixth of the starting potential  $E_1$ . In this tube the glow retains its characteristic red colour as the potential is reduced to  $E_2$ .

In neon and helium small traces of impurities have an effect on the colour of the discharge, which becomes very marked as the potential is reduced. Small amounts of impurity in neon are thus easily detected even when the amount is so small that it is difficult to detect it spectroscopically. This method of testing gases has been in use for

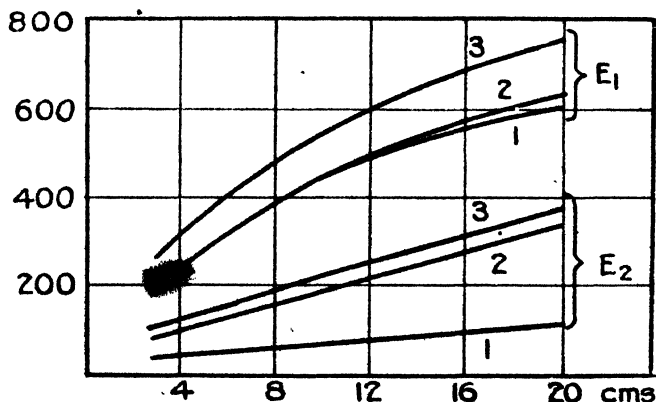
some time in the laboratory in connexion with researches for which pure gases were required.

15. In order to determine the effect of the diameter of the tube on a discharge, the critical potentials were measured for three tubes containing nitrogen at  $\cdot 25$  mm. pressure. The diameters of the nitrogen tubes were  $2a_1=2\cdot 9$  cm.,  $2a_2=3\cdot 5$  cm., and  $2a_3=3\cdot 9$  cm.

The critical potentials for the tube 3.5 cm. in diameter were almost the same as those of the tube 3.9 cm. in diameter. With the small tube, 2.9 cm. in diameter, the critical potentials were larger than with the tube 3.9 cm. in diameter.

The minimum potential  $E_1$  required to start a discharge, and the minimum  $E_2$  required to maintain the current with the distances  $D$  between the sleeves, from  $D=2\cdot 5$  cm. to  $D=20$  cm., are given by the curves, fig. 7. The ordinates

Fig. 7.



represent the amplitudes of the potentials in volts and the abscissae the distances  $D$  in centimetres. The upper set of curves give the potentials  $E_1$  and the lower set the potentials  $E_2$ .

Curves 1 give the potentials for the tube 4.2 cm. in diameter, containing neon at one millimetre pressure.

Curves 2, the potentials for the tube 3.9 cm. in diameter, containing nitrogen at  $\cdot 25$  mm. pressure.

Curves 3, the potentials for the tube 2.9 cm. in diameter, containing nitrogen at the same pressure.

16. For distances between the external electrodes exceeding 5 cm. the increase in the potential  $E_2$  is proportional to the increase in  $D$ , as shown by the straight parts of the curves. The distribution of electric force in the gas near the electrodes is independent of the distance  $D$ , and the force  $F$  in the uniform column of the glow in the central part of the tube is constant. Hence the increase in the potential  $E_2$  corresponding to the increase  $D_1 - D_2$  between the electrodes  $F \times (D_1 - D_2)$ .

In the neon tube  $E_2$  increases from 66 volts to 106 volts when  $D$  is increased from 10 to 20 centimetres, hence the amplitude of the force in the gas is 4 volts per centimetre, and the average force  $2F/\pi$  is 2.55 volts per centimetre.

In the nitrogen tube 3.9 cm., in diameter the minimum force  $F$  required to maintain a current is 14 volts per centimetre, and the average force  $2F/\pi$  9 volts per centimetre.

The principle of this method of finding the force in a long column of gas is the same as that used by Kirkby\*, where he finds the force in the uniform positive column of a current maintained by a battery of cells by changing the distance between the electrodes in the gas.

17. The motion of the electrons in gases at pressures of the order of one millimetre in high frequency currents may be deduced from the velocities acquired in fields of uniform constant force †. Under the continued action of the force  $E \sin pt$ , the electrons acquire energy of agitation at the same rate as under the action of a constant force  $Z$ , equal in intensity to the mean value  $2F/\pi$  of the high-frequency force.

The mean energy of agitation of electrons in the high-frequency discharge is the same as that attained in the uniform field  $Z$ , and the distance traversed by a group of electrons in each half-cycle is obtained from the velocity  $W$  in the direction of the force  $Z$ . The mean velocity of agitation  $U$  and the velocity  $W$  for neon have been determined by Bailey ‡, and the values corresponding to the force of 2.5 volts per cm. in the gas at one millimetre pressure are  $U = 1.98 \times 10^8$  and  $W = 3.3 \times 10^8$  cm. per second. Thus the mean energy of agitation is the energy acquired under a potential of about 10 volts.

The distance traversed by a group of electrons in the

\* Rev. P. J. Kirkby, *Phil. Mag.*, April 1908.

† 'Motion of the Electrons in Gases,' Clarendon Press, Oxford.

‡ V. A. Bailey, *Phil. Mag.* xlvii. p. 379 (1924).

direction of the force  $F$  in the half-period  $T/2 = 1.4 \times 10^{-7}$  sec. is 4.6 mm. Thus in each half-period of the oscillations the electrons acquire a small amount of energy. When they lose a large proportion of their energy in collisions with atoms of the gas they move backwards and forwards several times in the direction of the force  $F$  before they regain sufficient energy to ionize the atoms or to excite radiation.

---

XVII. *Waves associated with Moving Electrons.*

By SIR J. J. THOMSON, O.M., F.R.S.\*

THE experiments recently made by Professor G. P. Thomson and Mr. Reid on the scattering of cathode rays by very thin sheets of metal or celluloid supply very direct evidence in favour of the view that a moving electron—even a uniformly moving one—is accompanied by waves whose wave-length depends on the velocity of the electron, the product of the wave-length and the velocity being approximately at any rate, constant.

The existence of these waves is required by the very interesting theory of wave dynamics put forward by L. de Broglie. I hope to show in this paper that the waves are also a consequence of classical dynamics if that be combined with the view that an electric charge is not to be regarded as a point without structure, but as an assemblage of lines of force starting from the charge and stretching out into space. These constitute a system of a much more detailed and elaborate character than a point charge. When the charge is at rest and at a large distance from other charges the lines of force are uniformly distributed round the centre; the lines can, however, be displaced relatively to each other, and they are so displaced when the particle is acted upon by an electric force, such for example as that produced by the passage through the region occupied by the lines of force of a rapidly-moving electron. The displacement of one line of force relatively to another sends out a wave of electric force, even though the electron itself, or rather its core, be at rest. Again, when the uniformity of distribution is destroyed by the passage of a cathode ray, after the ray has passed out the non-uniform distribution will not be in equilibrium, but will vibrate about the uniform one or else pass off as a wave into space. Thus an electron, and also a proton, when regarded as an assemblage of lines of force, has definite periods of

\* Communicated by the Author.

vibration associated with it ; these periods are natural constants, and, as we shall see, influence the wave-lengths of the waves associated with an electron. Thus, behind the electron and the proton there is a structure which can transmit and absorb electrical waves, even though the centre of it is, at rest, and which has definite periods of vibration. Lines of force will thus modify the properties, the optical properties for example, of the medium through which they pass, so that electrons and protons are the centres of regions of exceptional optical properties.

In two papers, one on "The Scattering of Light by Electrons," *Phil. Mag.* xl. p. 713 (1920), and the other on "Mass, Energy, and Radiation," *Phil. Mag.* xxxix. p. 679, I investigated the effect produced by free electrons on electrical waves by calculating directly the secondary waves emitted by the electrons when set in motion by the electric force in the primary wave, and then combining these with the primary wave. It was shown that, when the primary wave first enters the medium, the front advances with the velocity  $c$ , that of light through a vacuum. Soon, however, the secondary waves coming from the electrons unite with the primary waves and produce a new distribution of electric force in the wave. In a short time things settle down into a new regime ; and when the free periods of the electrons are long compared with the period of the light, the distance between two places in the wave which are in the same phase is greater than that in the incident wave before it struck the electrons. Thus the phase-velocity, which is defined to be the quotient of the distance between two places in the same phase by the time of vibration of light, is greater than  $c$ , though the wave system is the resultant of waves, all of which are propagated with the velocity  $c$ . The phase-velocity is a mathematical rather than a physical conception ; the fact that it is greater than  $c$  does not involve that a sudden disturbance would be propagated through the medium at a speed greater than that of light.

It is shown in the papers referred to that this method leads to the same results as those deduced from Lorentz's theory of dispersion, so that the components of the electric and magnetic forces in the wave will satisfy equations of the form

$$c^2 \left( \frac{d^2 \psi}{dx^2} + \frac{d^2 \psi}{dy^2} + \frac{d^2 \psi}{dz^2} \right) = \frac{d^2 \psi}{dt^2} + \Sigma \left\{ \frac{p_r e^2 / m \cdot \frac{d^2}{dt^2}}{\frac{d^2}{dt^2} + n_r^2} \right\} \psi,$$

where  $p_r$  is the number of electrons which have a frequency  $n_r$ .

When the frequencies of the waves are large compared with the free periods of the electrons,  $n_r^2$  is small compared with  $d^2/dt^2$ , and the equation becomes

$$c^2 \left( \frac{d^2\psi}{dx^2} + \frac{d^2\psi}{dy^2} + \frac{d^2\psi}{dz^2} \right) = \frac{d^2\psi}{dt^2} + (\Sigma(p_r e^2/m))\psi.$$

When the density of the electrons is uniform,  $\Sigma(p_r e^2/m)$  is constant. Let it be denoted by B, then

$$c^2 \left( \frac{d^2\psi}{dx^2} + \frac{d^2\psi}{dy^2} + \frac{d^2\psi}{dz^2} \right) = \frac{d^2\psi}{dt^2} + B\psi. \quad . \quad . \quad (1)$$

If  $\psi = \cos \frac{2\pi}{\lambda} (vt - x)$  is a solution,

$$v^2 = c^2 + \frac{B}{4\pi^2} \lambda^2, \quad . \quad . \quad . \quad . \quad . \quad . \quad . \quad (2)$$

where  $v$  is the phase-velocity of a wave of length  $\lambda$ .

We see from this equation that the radiation from free electrons endows a medium through which light is travelling with remarkable optical properties. These are :—

1. The phase-velocity is always greater than the velocity of light through a vacuum.
2. The phase-velocity increases with the wave-length and, when the waves are very long, is proportional to it.
3. A small change in the frequency corresponds to a large change in the wave-length.

When a medium possesses these properties we shall say that it is in a super-dispersive state.

We have supposed that the scattered secondary radiation which gives rise to this state was due to electrons, but it is evident that similar effects will be produced by anything which

- (1) radiates electric force when moved ;
- (2) is moved by the electric forces which exist in a wave of light.

The lines of electric forces which stretch from charged bodies possess these properties, and the regions round electrons and protons are crowded with such lines. Indeed, we regard an electron or a proton as an assemblage of lines of electric force, and as having a definite physical structure determined by the disposition of these lines, and not as a mere point charge without structure. Since the region round an electron or a proton is full of systems (the lines of



electric force) which can scatter the light, these regions are "super-dispersive" regions through which light is propagated according to very special laws. The disposition of these lines of force round the electron or proton will depend upon the law of force. If, as I have suggested, the law is more complicated than that of the inverse square, the structure of the field will be more favourable for the production of radiation than the simpler field.

We now proceed to consider the optical properties of these super-dispersive regions arising from the lines of force. The equations in the field are of the type of equation (1), where  $B$  is now a quantity depending on the density of the lines of force.

Since 
$$v^2 = c^2 + \frac{B}{4\pi^2} \lambda^2,$$

$u$  the group-velocity,  $v - \lambda \frac{dv}{d\lambda}$ , is given by the equation

$$u = \frac{c^2}{\sqrt{c^2 + \frac{B}{4\pi^2} \lambda^2}} = \frac{c^2}{v}; \quad \dots \dots (3)$$

hence

$$uv = c^2.$$

The wave-length corresponding to group-velocity  $u$  is by (3):

$$\sqrt{B} \cdot \frac{\lambda}{2\pi} = c \sqrt{\frac{c^2}{u^2} - 1}. \quad \dots \dots (4)$$

The frequency  $n$  of waves of this length is given by

$$n = \frac{2\pi}{\lambda} v = \frac{\sqrt{B} \cdot c}{\sqrt{c^2 - u^2}}, \quad \dots \dots (5)$$

and is thus nearly constant and equal to  $\sqrt{B}$  unless  $u$  approaches  $c$ .  $\sqrt{B}$  is the reciprocal of a time which is determined by the structure formed by the lines of force round the electron.

If  $\mu$  is the refractive index of the medium,

$$\mu = \frac{c}{v} = \sqrt{1 - \frac{B}{n^2}}. \quad \dots \dots (6)$$

We can prove easily that no waves of smaller frequency than  $\sqrt{B}$  can travel through the super-dispersive medium.

For from equation (1) we have for plane waves

$$c^2 \frac{d^2 \psi}{dx^2} = \frac{d^2 \psi}{dt^2} + B \psi;$$

if  $\psi$  varies as  $e^{ipt}$ ,

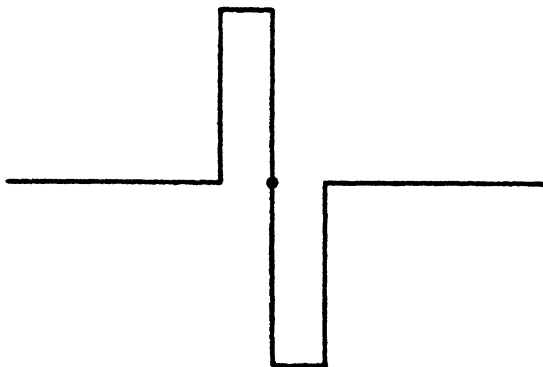
$$c^2 \frac{d^2 \psi}{dx^2} = (B - p^2) \psi;$$

hence, unless  $p^2$  is greater than  $B$ ,  $\psi$  will not be a harmonic function, and a wave will not pass through the medium.

*The Electron in motion and the Waves which accompany it.*

Let us consider from this standpoint the state of things round a moving electron. What is it that happens on this view when an electron is set in motion? We have to interpret the physical effects in terms of lines of electric force. The primary effect of an impulse is to alter the disposition of the lines of force. Before the impulse these were uniformly distributed round the electron; after it they are compressed in some places, dilated in others. Suppose, to fix our ideas, that the lines of force which before the impulse were uniformly distributed across a strip  $AB$  get transferred by the impulse from the right to the left of the strip, so that the curve

Fig. 1.



representing the disturbance in density would be represented by a graph like that in fig. 1. This non-uniform distribution is not a configuration of equilibrium, and, like a local strain in an elastic solid, travels out as a system of waves through the medium. To find the wave-lengths we must express by Fourier's series the initial disturbance as a system of harmonic terms, and these harmonics will travel out each with its appropriate velocity. If the wave-lengths involved are within narrow limits, there will be a series of waves of

phase of this wave-length starting from the electron, and thus the moving electron will be associated with a system of waves. These waves will show the same interference effects as Röntgen rays, and when they pass through a crystalline lattice will have their energy concentrated in definite directions, the energy associated with the electron following them in these directions. The wave-length of these will depend upon the distribution of the original disturbance; for example, in the case just considered it would be a quantity of the order of the breadth of the slit. When the Fourier waves are within small limits of wave-length, any disturbance such as that represented in the diagram will travel with the group-velocity corresponding to this wave-length. The disturbance consists of a special arrangement of the lines of electric force, and these lines travel along with it; and since the electron is just the termination of these lines, it travels along with them. Thus we conclude that the velocity of the electron is the group-velocity of a system of waves.

I may remark in passing that on the view expressed in my paper on "Mass Energy and Radiation" the kinetic energy of the electron is not due to any particular mass moving with the velocity of the electron, but because the lines of force, when arranged so as to produce a disturbance which travels with this velocity, grip more of the energy in the surrounding field than when they are uniformly distributed: the excess of energy is the kinetic energy of the electron.

To put the reasoning into a more analytical form, the disturbance at the time  $x$  and  $t$  can by Fourier's theorem be expressed in the form

$$\int_0^{\infty} \phi(k) \cos k(x-vt-\alpha) dk, \quad . \quad . \quad . \quad (7)$$

where 
$$\phi(k) = \int_{-\infty}^{+\infty} f(\omega) \cos(k\omega + \beta) d\omega,$$

where  $f(x)$  represents the disturbance at  $x$  when  $t=0$ .

When, as in our case,  $v$  the phase-velocity depends upon the wave-length ( $2\pi/k$ ),  $v$  in equation (1) must be regarded as a function of  $k$ . When the initial disturbance is confined to a small distance,  $\phi(k)$  will have a decided maximum for a value of  $k$  of the order of  $2\pi/a$ , where  $a$  is the length over which the initial disturbance is spread. Thus the wave-length of the electronic waves will be  $2\pi/k_1$ , where  $k_1$  is the value which makes  $\phi(k)$  a maximum, and the velocity of the

electron will be the group-velocity corresponding to this wave-length.

We see from equation (4) that

$$\lambda u = \frac{2\pi}{\sqrt{B}} c^2 \sqrt{1 - u^2/c^2}, \dots \dots \dots (8)$$

or if  $m$  is the mass of the electron when its velocity is  $u$ ,  $m_0$  the mass when it is at rest.

$$m\lambda u = \frac{2\pi}{\sqrt{B}} m_0 c^2. \dots \dots \dots (9)$$

Thus  $m\lambda u$  should be constant. This relation is accurately satisfied in Professor G. P. Thomson's experiments, from which we can deduce the value of  $B$ . He finds that when  $u = 10^{10}$ ,  $\lambda = 7.8 \times 10^{-10}$ . Substituting these values in equation (8), we find

$$\frac{2\pi}{\sqrt{B}} = 9 \times 10^{-21}.$$

$2\pi/\sqrt{B}$  is a time depending on the structure of the lines of force.

We see from equation (5) that  $\sqrt{B}$  is the frequency of the waves accompanying electrons whose velocity is small compared with  $c$ . Since  $\sqrt{B} = 7 \times 10^{20}$ , this frequency is comparable with that of the hardest  $\gamma$ -rays.

Equation (8) would be identical with the one given by de Broglie's theory if

$$\frac{2\pi}{\sqrt{B}} m_0 c^2 = h,$$

where  $h$  is Planck's constant.

If the lines of force in the electric field round an electron are discrete entities, so that the field possesses a finite structure both in time and space, we can see that the velocity of an electron under an electric field might increase by finite increments and not continuously. Thus, for example, if the electron had a finite structure in space, the breadth of such a disturbance as that represented in the figure might not be able to take all values, but only those of which an integral number were in a length fixed by the structure. In this case  $1/\lambda$  would change discontinuously; and it follows from equation (9) that  $u$ , the velocity of the electron, would do the same. Thus, if the electric field associated

with an electron had a structure in time and space, we should expect to find results analogous to those attributed to quanta.

*Waves near Moving Protons.*

Since the proton is also the origin of a system of lines of force, we should expect that the motion of protons as well as of electrons should be accompanied by a train of waves, though, owing to the differences between the masses and dimensions of the proton and electron, the lengths of the waves and the frequencies for the same velocity would be different in the two cases. We should expect that  $B$  would be greater for the proton than for the electron, so that the frequency of the waves accompanying the proton would be greater than that of the electronic waves. On the assumption that  $m\mu\lambda$  is constant,  $\sqrt{B}$  is proportional to the mass of the moving charge, so that the frequency of the waves accompanying a moving proton would be about  $1.2 \times 10^{24}$ .

Since  $B$  will depend on the density of the lines of force, it will be a function of the distance from the charged body. Thus the equations in the field round the charged body will be of the form

$$c^2 \left( \frac{d^2\psi}{dx^2} + \frac{d^2\psi}{dy^2} + \frac{d^2\psi}{dz^2} \right) = \frac{d^2\psi}{dt^2} + f(r)\psi,$$

where  $r$  is the distance of the point  $xyz$  from the charged body. As the distance from the charged body increases, the value of  $B$  diminishes, so that by equation (5) the refractive index of the region round the charge will increase with  $r$ .

Thus a ray of light, if it is able to pass through this region, will be passing from an optically dense to an optically rare medium, and so will appear to be repelled by the charge.

In this paper the electron has been supposed to be moving uniformly. I hope on another occasion to discuss from the same point of view the motion of an electron under electric force.

XVIII. *The Calculation of the Equivalent Conductivity of Strong Electrolytes at Infinite Dilution.*—Part II. (i.) *Methyl Alcoholic Solutions.* (ii.) *The Effect of Temperature on the Constants in the Equation  $\Lambda_0 = \Lambda + BC^n$ .* By ISRAEL VOGEL, M.Sc., D.I.C., Beit Scientific Research Fellow\*.

IN previous communications (Ferguson and Vogel, this Journal, 1925, i. p. 971; 1927, iv. pp. 1, 233, 300; compare also Trans. Far. Soc. 1927, xxiii. p. 404) the formula

$$\Lambda_0 = \Lambda + BC^n \quad . \quad . \quad . \quad . \quad . \quad . \quad (1)$$

was applied to the calculation of the equivalent conductivity at infinite dilution,  $\Lambda_0$ , of aqueous solutions of strong electrolytes of very varied types. The results obtained may be summarised as follows:—

- (a) The constants B and  $n$  vary from electrolyte to electrolyte and in a regular manner for related electrolytes.
- (b) The extreme variations  $n$  lie between 0.3742 for potassium chloride at 25° and 0.9687 for iodic acid at 25°.
- (c) The constants B and  $n$  vary with temperature, although owing to the scarcity of reliable data no definite conclusions could be drawn as to the exact mode of variation.
- (d) The formula is applicable to uni-uni, uni-bi, and bi-bivalent electrolytes, and also to such strong acids as hydrochloric and iodic acids.

These results, which can be taken as an expression of the facts of observation, are not in agreement with the requirements of the complete ionization theory of Debye and Hückel (*Phys. Zeit.* 1923, xxiv. p. 305; compare also Debye, Trans. Far. Soc. 1927, xxiii. p. 334; Onsager, *ibid.* 1927, xxiii. p. 341), which leads to an equation of the form

$$\Lambda_0 = \Lambda + PC^{\frac{1}{2}} \quad . \quad . \quad . \quad . \quad . \quad . \quad (2)$$

i. e. the exponent of C, which is equal to  $\frac{1}{2}$ , is independent of the nature of the electrolyte, of temperature, and of the solvent. This equation has been extensively employed for the extrapolation of  $\Lambda_0$  in non-aqueous solutions (compare

Walden, *Z. anorg. Chem.* 1920, cxv. p. 49). Formulæ in which the exponent of C is other than  $\frac{1}{2}$  have also been employed, such as  $\frac{1}{3}$  (Philip and Courtman, *J. Chem. Soc.* 1910, xcvii. p. 126 ; King and Partington, *Trans. Far. Soc.* 1927, xxiii. pp. 522, 531), 0.45 (Lorenz, *Z. anorg. Chem.* 1919, cviii. p. 191 ; Walden, *ibid.* 1920, cxv. p. 49) and unity—Ostwald dilution law—(Kraus and Bishop, *J. Amer. Chem. Soc.* 1922, xlv. p. 2206 ; Morgan and Lammert, *ibid.* 1924, xlv. p. 1117). These are all, however, special cases of the general formula (1), and all involve an *a priori* assumption as to the value and constancy of the exponent  $n$ . It appeared of interest, therefore, to extend the calculations to non-aqueous solutions, and the present paper is concerned with (i.) solutions in methyl alcohol (a solvent closely related to water), and (ii.) the effect of temperature.

### Methyl Alcoholic Solutions.

The data employed were those of Frazer and Hartley at 25° (*Proc. Roy. Soc. A*, 1925, cix. p. 351), and  $\Lambda_0$  was calculated by the method previously described (this Journal, 1925, l. p. 971), the values of  $\Lambda$  at the requisite concentrations being *interpolated* from a large-scale  $\Lambda$ -C graph. In view of the small range of concentration available for the calculation of  $\Lambda_0$ —it was usually between 0.0002 to 0.002 normal,—the value of  $r$  used was 1.5, and in this way values for B and  $n$  were obtained more reliable than those given in preliminary computations (*Trans. Far. Soc.* 1927, xxiii. p. 414), in which  $r$  was taken as 2. The actual results are given in full in Table I. below ; those for lithium nitrate are somewhat doubtful, owing to a slight ambiguity in the exact position of the conductivity-concentration curve. Potassium nitrate has been omitted, since the results for both runs do not lie on one  $\Lambda$ -C curve.

TABLE I.

Concentration, $\times 10^{-4}$ .	LiCl.		NaCl.		KCl.	
	$\Lambda$ .	$\Lambda_0$ .	$\Lambda$ .	$\Lambda_0$ .	$\Lambda$ .	$\Lambda_0$ .
2.000 .....	87.66	89.91	93.64	97.24	101.35	104.95
3.000 .....	87.02	89.92	92.94	97.29	100.55	104.97
4.500 .....	86.19	89.92	92.03	97.29	99.54	104.97
6.750 .....	85.11	89.91	90.94	97.30	98.27	104.94
10.18 .....	83.75	89.92	89.63	97.31	96.75	104.95
15.20 .....	82.15	90.09	88.02	97.31	94.89	104.96

TABLE I. (continued).

Concentration, $\times 10^{-4}$ .	RbCl.		CsCl.		LiNO <sub>3</sub> .	
	$\Lambda$ .	$\Lambda_0$ .	$\Lambda$ .	$\Lambda_0$ .	$\Lambda$ .	$\Lambda_0$ .
2.000 .....	104.69	109.42	109.43	113.73	96.59	100.23
3.000 .....	103.76	109.42	108.54	113.79	95.79	100.22
4.500 .....	102.65	109.43	107.89	113.78	94.82	100.23
6.750 .....	101.26	109.39	105.99	113.78	93.63	100.23
10.13 .....	99.65	109.38	104.30	113.80	92.16	100.22
15.20 .....	97.74	109.39	102.20	113.78	90.53	100.37

Concentration, $\times 10^{-4}$ .	NaNO <sub>3</sub> .		RbNO <sub>3</sub> .		CsNO <sub>3</sub> .	
	$\Lambda$ .	$\Lambda_0$ .	$\Lambda$ .	$\Lambda_0$ .	$\Lambda$ .	$\Lambda_0$ .
2.000 .....	102.36	105.99	113.00	117.19	117.65	123.25
3.000 .....	101.47	105.99	111.93	117.19	116.39	123.23
4.500 .....	100.36	105.99	110.59	117.19	114.88	123.24
6.750 .....	99.00	106.01	108.90	117.19		
10.13 .....	97.24	105.96	106.82	117.22		
15.20 .....	95.20	106.06				

Concentration, $\times 10^{-4}$ .	AgNO <sub>3</sub> .		KBr.		KI.	
	$\Lambda$ .	$\Lambda_0$ .	$\Lambda$ .	$\Lambda_0$ .	$\Lambda$ .	$\Lambda_0$ .
2.000 .....	106.08	109.97	105.69	109.17	111.11	114.38
3.000 .....	104.89	109.97	104.86	109.19	110.31	114.39
4.500 .....	103.33	109.97	103.82	109.19	109.29	114.37
6.750 .....	101.30	109.97	102.57	109.17	108.04	114.37
10.13 .....	98.65	109.97	101.01	109.19	106.50	114.38
15.20 .....	95.40	(110.20)	99.18	109.29		

It will be seen that the consistency of  $\Lambda_0$  leaves little to be desired. A summary of the results is shown in Table II.;

TABLE II.

Salt.	$\Lambda_0$ (Author).	B.	n.	$\Lambda_0$ (Frazer & Hartley).
LiCl .....	89.92	447.6	0.6213	90.90
NaCl .....	97.29	192.3	0.4670	90.95
KCl .....	104.96	271.2	0.5074	106.05
RbCl .....	109.41	209.0	0.4448	108.65
CsCl .....	113.78	275.2	0.4882	113.60
LiNO <sub>3</sub> .....	100.22	240.7	0.4926	100.25
NaNO <sub>3</sub> .....	106.00	363.5	0.5409	106.45
RbNO <sub>3</sub> .....	117.20	495.8	0.5604	118.15
CsNO <sub>3</sub> .....	123.24	373.3	0.4930	122.95
AgNO <sub>3</sub> .....	109.97	1068.1	0.6591	112.95
KBr .....	109.20	300.3	0.5226	109.35
KI .....	114.38	331.4	0.5422	114.85



for purposes of comparison the values of  $\Lambda_0$  calculated by Frazer and Hartley (*loc. cit.*) by means of the square-root formula are included.

The superiority of the general equation (1) over the widely-used square-root formula (2) is evident from Table III. below, in which are tabulated the values of  $\Lambda_0$  for silver nitrate over a range of concentration.

TABLE III.— $\text{AgNO}_3$  25° C.

Concentration, $\times 10^{-4}$ .	$\Lambda_0 = \Lambda + 1066 \cdot 1 C^{0.6591}$ .	$\Lambda = \Lambda + 451 C^{0.5000}$ .
2.000.....	109.97	112.46
3.000.....	109.97	112.70
4.500.....	109.97	112.90
6.750.....	109.97	113.02
10.13 .....	109.97	113.00
15.20 .....	110.20	112.98

The results of a test of Kohlrausch's law of independent migration of ions are given in Table IV. No explanation is at present offered of the irregularities, although it should be stated that Frazer and Hartley obtained good agreement by using values of  $\Lambda_0$  computed from the formula (2)\*.

TABLE IV.

Cation.	Li.	Na.	Rb.	Cs.
$\Lambda_0$ nitrate — $\Lambda_0$ chloride .....	10.30	8.71	7.79	9.46

*The Effect of Temperature on the Constants B and n in the Equation  $\Lambda_0 = \Lambda + BC^n$ .*

Practically the only reliable data for the conductivities of salts in non-aqueous solutions over a wide range of temperature appear to be those of Philip and Oakley (*J. Chem. Soc.* 1924, cxxv. p. 1189; compare, however, McBain and Coleman, *Trans. Far. Soc.* 1919, xv. p. 27; Robertson and Acree, *J. Phys. Chem.* 1915, xix. p. 413) for potassium iodide in nitromethane. Their results are expressed in the form of a table in which are tabulated the values of the dilution in litres V, the specific conductivity  $\kappa$ , and the equivalent conductivity  $\Lambda$  (Philip and Oakley, *loc. cit.*

\* Compare, however, Part I. (*Phil. Mag.* 1925, l. p. 971) for aqueous solutions, in which by application of formula (1) better agreement for Kohlrausch's law was obtained than that deduced by Kohlrausch and Maltby from equation (2).

table 1). The values of  $\Lambda$  employed by the author were those obtained by multiplying the dilution in litres V by the specific conductivity  $\kappa$ , except for the figures at 25°, where the tabulated values of  $\Lambda$  were used, since the product  $V\kappa = \Lambda$  leads to obviously untenable values of the equivalent conductivity. The complete results are presented in Table V., while a conspectus is given in Table VI. below.

TABLE V.—KI in Nitromethane.

Concentration, $\times 10^{-4}$ .	0°.		25°.		40°.	
	$\Lambda$ .	$\Lambda_0$ .	$\Lambda$ .	$\Lambda_0$ .	$\Lambda$ .	$\Lambda_0$ .
2·000 .....	88·10	90·80	119·30	123·01	139·5	144·1
3·000 .....	87·41	90·81	118·27	123·02	138·3	144·1
4·500 .....	86·52	90·81	116·94	123·01	136·7	144·1
6·750 .....	85·35	90·76	115·27	123·04	134·7	144·1
10·13 .....	83·94	90·77	113·10	123·05	132·1	144·1
15·20 .....	82·15	90·76	110·27	123·00	128·8	144·1

Concentration, $\times 10^{-4}$ .	55°.		70°.	
	$\Lambda$ .	$\Lambda_0$ .	$\Lambda$ .	$\Lambda_0$ .
2·000 .....	160·53	165·30	184·8	193·0
3·000 .....	159·17	165·33	182·7	193·0
4·500 .....	157·36	165·31	180·1	193·0
6·750 .....	154·99	165·27	176·8	192·9
10·13 .....	151·98	165·26	172·8	193·0
15·20 .....	148·01	165·16	167·8	193·1

TABLE VI.—KI in Nitromethane.

Temperature.	$\Lambda_0$ .	B.	$n$ .
0° .....	90·79	353·8	0·5726
25° .....	123·02	659·6	0·6083
40° .....	144·1	717·6	0·5939
55° .....	165·27	1034·5	0·6317
70° .....	193·0	928·6	0·5552

Both the constants B and  $n$  increase steadily with temperature up to 55°\*, and then pass through a maximum between this temperature and 70°. Whether this manner of variation is general in non-aqueous solutions or is peculiar to nitromethane is a question which can only be answered when more experimental data for the conductivities of salts in non-aqueous solutions over a wide range of temperature are available.

\* Except for the value of  $n$  at 25°.

On plotting the values of  $\Lambda_0$  here calculated against the reciprocals of the viscosities or fluidities determined by Philip and Oakley (*loc. cit.*), a straight line is obtained, indicating that the relationship between the conductivity at infinite dilution and the fluidity  $f$  over the range of temperature 0–70° is of the form

$$\Lambda_0 = a + bf,$$

where  $a$  and  $b$  are constants.

In conclusion, the author wishes to thank the Trustees of the Beit Scientific Research Fellowships for a Fellowship, Dr. A. Ferguson for his kind interest, and the Dixon Fund of the University of London for a grant which has defrayed most of the expenses of the research.

Imperial College of Science  
and Technology,  
South Kensington, London, S.W. 7.

### XIX. *Interference between Grating-Ghosts.*

By SVEN FAGERBERG, *Upsala* \*.

[Plate IV.]

IT is well known that the illuminated field behind the focus of a grating spectrograph generally presents a characteristic appearance as to the distribution of intensity. Surveying the illuminated field behind the focus with an eyepiece at a sufficient distance from the focus, one finds the field traversed by several closely-lying sharp luminous lines separated by dark intervals parallel to the spectral lines. The arrangement of the lines is rather irregular.

In order to investigate this fact more closely, the wave-front of a single spectral line ( $\text{Fe } \lambda = 4384 \text{ T. A.}$ , third order) was photographed. The line was separated from the remaining part of the spectrum by a slit in the focal plane, and a photographic plate was placed in the way of the diverging beam.

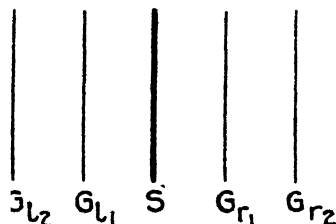
The spectrograph used consists of a Rowland plane grating ( $\text{AE}'''$ , 14,438 lines to the inch, ruled in the year 1889), rotating about an axis perpendicular to the collimator and camera. These are fixed at an angle of about 35° to each other. The focal distance of the lenses is 165 cm., and the plate was placed about 95 cm. behind the focal plane.

\* Communicated by Prof. Manne Siegbahn, D.Sc.

If only one spectral line passes the slit in the focal plane, the wave-front has the appearance shown in A (Pl. IV.). From this it will be seen that the variations of intensity along the wave-front are quite irregular and not very definitely marked.

The grating in question shows, however, in the third order, in addition to the principal line of high intensity, fainter lines, the so-called ghosts, which are of the same wave-length as the principal line and are symmetrically located about it. The arrangement of the lines appears from fig. 1.  $S$  is the principal spectral line,  $G_{r1}$ ,  $G_{r2}$  and  $G_{l1}$ ,  $G_{l2}$  the ghosts of the first and second orders to the right and left. The ghosts and the principal line are all equidistant.

Fig. 1.



Now widening the slit in the focal plane in order to transmit also the ghost of the first order on one side, the wave-front shows a totally different appearance (C, Pl. IV.). One obtains a number of equidistant luminous lines separated by dark intervals. On the other hand, the ghost alone gives a wave-front, in its general character agreeing with that of the principal line (B, Pl. IV.).

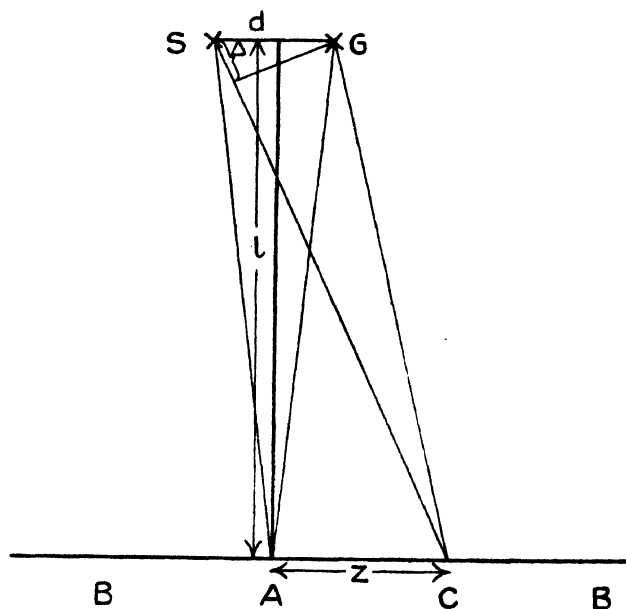
It is reasonable to suppose that the appearance of the luminous and dark lines in the case when the principal line and the ghost both pass the slit is due to interference behind the two diverging beams when they are superposed between the focus. Thus we may regard the spectral line and its ghost as two linear coherent sources of light.

The elementary treatment of the phenomenon (see fig. 2) is entirely analogous to the treatment of, for example, the Fresnel mirrors. In the diagram the points  $S$  and  $G$  are the projections of the spectral line and the ghost on a plane perpendicular to them, and  $AB$  indicates the photographic plate. In A the rays have travelled the equal path, and therefore reinforce each other, provided that

they are in the same phase in S and G. In C the beams have the path-difference  $\Delta = \frac{dz}{l}$  (see fig. 2), supposing that  $d$  and  $z$  are small in comparison with  $l$ , this also in reality being the case.

Thus the beams will reinforce each other when  $\Delta = \frac{dz}{l} = n\lambda$ ,  $\lambda$  being the wave-length and  $n=1, 2, 3, \dots$ . Consequently, the position of a luminous line is  $z = n \frac{\lambda l}{d}$ . On the plate we get equidistant lines at the distance of  $a = \frac{\lambda l}{d}$  from each other.

Fig. 2.



In order to test the correctness of the above assumption, the distances  $a$ ,  $l$ , and  $d$  were measured. The position of the focal plane was determined, successively photographing the spectrum with different adjustments of the camera slide, and in each case noting the reading on the camera scale. Examining these photographs, the one which showed the spectral lines with the greatest sharpness was chosen. The corresponding reading on the camera scale gave the position

of the focal plane. On this plate the distance between the principal line and ghost was measured.

In order to obtain a good value of  $a$ , the distance between every tenth interference fringe was measured. It appears, however, that the distance between two adjacent fringes is subject to small accidental variations with their position on the plate. The mean distance determined in the way described above is, on the contrary, constant within a wide region in the middle of the plate.

The following values were obtained :—

$$a = 0.554 \text{ mm.}$$

$$d = 0.750 \text{ ,,}$$

$$l = 943.7 \text{ ,,}$$

$$\text{Hence } \lambda = 440 \pm 4 \mu\mu.$$

$$\text{Standard value } \lambda_s = 438.4 \mu\mu.$$

The agreement is undoubtedly good.

In order to get another control, the slit in the focal plane was widened to transmit also the ghost of the second order on the same side of the principal line. As the distances between the principal line and the ghosts are equal, the appearance of the interference phenomenon (provided the three rays are in the same phase when passing the focus) must be the same as in the preceding case, with the distinction that fainter maxima of intensity are to occur between those already observed. This is also the case, as seen from D (Pl. IV.).

Making the principal line and *all* the ghosts to interfere, more complicated circumstances take place (E, Pl. IV.). As already stated, the grating in question gives (in the third order) ghosts of the first and second order on both sides of the principal line. Thus, if the whole complex passes the slit, five beams are brought to interference. On account of the rather irregular structure of this plate, it seems as if all waves do not pass the focus in the same phase, and the wave-fronts from the grating are not completely plane, they being subject to some small divergencies due to errors in the spacing of the grating. These plates, where more than two rays have been brought to interference, have much in common with photographs carried out by Dowling and Teegan (Phil. Mag. l. p. 241, 1925). In order to obtain several coherent sources, they used a complex of bi-prisms, which thus gave birth to interference fringes of the same kind as those described above.

At first it seems surprising that the plates can show the interference so markedly, using beams of intensities so different as a spectral line and its ghosts. A rough estimate of the ratio between the intensity of the spectral line and that of the ghost of the first order gives, however, 25 : 1. The ratio between the amplitudes is thus 5 : 1, and the ratio between maximum and minimum intensity in the case of interference  $(6 : 4)^2 = 9 : 4$ .

A phenomenon analogous to that above described has been observed by Wood (Phil. Mag. xlviii. p. 497, 1924), who worked with a small concave grating. He illuminated the collimator slit by monochromatic light, and placed the plate *between* the grating and the focus. Assuming that the circumstances are symmetrical with respect to focus, the lines observed by him would correspond to the interference fringes treated above, evidently with the difference that Wood was not able with his arrangement to shut out the ghosts, but observed the resulting effect of the spectral line and all its ghosts. Thus he did not photograph the wave-front of the spectral line alone (see A, Pl. IV.). He however, is of the opinion that the observed luminous lines belong to this wave-front. According to this conception, the periodical errors of the grating have influenced the wave front of the principal line in such a way as if it had passed a system of parallel slits in an opaque screen, and the ghosts are regarded as spectra of different orders of this assumed system of slits.

Upsala, Physical Laboratory  
of the University,  
Oct. 1927.

## XX. *Prof. Joly and the Earth's Thermal History.*

By HAROLD JEFFREYS, F.R.S.\*

PROF. JOLY uses an extract from a paper of mine in the 'Geological Magazine' for November 1926 as the basis for a further discussion†. He would have done better to choose a different passage, as follows (p. 521) :—

"In any case the onus of proof that the theory of magnetic cycles explains anything at all rests with its supporters, at least if the word 'explain' is understood in the sense given to it by physicists. A theory explains a fact if it starts from

\* Communicated by the Author.

† Phil. Mag. August 1927.

a set of stated hypotheses and shows how the fact in question follows from them. But the theory of magnetic cycles considers itself at liberty to use the observed facts to enable it to infer its own consequences; and any fact can be explained on any theory if that is permitted. If resolidification under excess of internal heat is possible, it should be well within the experimental powers of both Professor Joly and Professor Holmes to demonstrate it; without this no case for the theory has been made out."

From Prof. Joly's omission to mention this passage many readers may be inclined to draw their own conclusions. But I think that further remarks on elaborate attempts such as his to solve difficult problems in theoretical physics with no mathematics beyond simple proportion are relevant at this stage, especially since he accuses me of misrepresenting his views. My answer to this charge is that I have devoted a great deal of time to trying to understand his theory, that I am as well qualified to understand it as most people, and that if I have misinterpreted it in any respect the reason is that it is unintelligible, and that the reason for its unintelligibility is his omission to state in proper form the laws he assumes.

A specimen of the difficulty of seeing what Prof. Joly really means is provided by his assertion (p. 338) that "the heat is latent, and there is but little variation of temperature," maintaining at the same time that his object was not what I said, namely to explain a periodic variation of temperature. Yet he quotes, apparently with approval, on p. 340, a passage from Mr. J. R. Cotter, as follows: "Prof. Joly thinks that the  $\theta_0$  isotherm (that where the temperature is equal to the melting-point) would rise to within a very few miles of the surface. It would, however, finally become stationary, and then descend. . . . The whole series of changes would form a cycle which would be repeated." If this is not a periodic variation of temperature I do not know what is. Again, in 'The Surface History of the Earth,' p. 105, we have: "In periods of liquefaction and tidal movements the floor must be at first rapidly reduced in thickness. For, in fact, much of it is near the melting-point. . . . It seems certain that the ocean floor cannot be indefinitely reduced in thickness. There will be a certain limiting thickness which will be attained when the rate of escape of heat into the ocean becomes equal to the rate of supply from beneath." When the abnormally large supply of heat is being conducted through the abnormally thin ocean floor an abnormally high temperature gradient



must exist. This is one of the things I meant in referring to variation of underground temperature.

Anyhow, my objection to periodicity in the flux of heat is equally strong whether or not it is associated with periodicity in temperature.

I gave in a previous paper \* two diagrams indicating the course of events to be expected if there is an excess of heating underground. Two were necessary on account of ambiguities as to the initial state assumed by Prof. Joly. He has not pointed out where, if anywhere, he disagrees with these diagrams, nor has he offered any alternative. He does try to dismiss my analogy with the motion of a stretched string subject to damping as misleading, but does not say explicitly what alterations are to be made in the inferences.

He remarks about this analogy † that there is nothing in it analogous to the accumulation of energy in the form of latent heat or to the transfer of this energy by convection. Both phenomena are fully allowed for in the analogy. In the thermal problem the fluid region is represented by the portion of the string in contact with the rigid barrier. The rate of extension of this region is given by the condition that the amount of fluid melting, multiplied by the latent heat of fusion, is equal to the excess of the heat generated within the fluid over that conducted out at the top and bottom. Since convection transfers heat upwards, the growth downwards will not extend below the bottom of the radioactive region ; the partition between growth at the bottom and the top before that stage is reached could be stated in a given case. The string allows for these phenomena automatically if, as I explicitly stated, the transverse force originally applied to the constrained region is transferred to its upper margin. Convection again is allowed for by the supposition that the distribution of temperature in the fused region is the adiabatic for a mixture of solid and liquid ; this is expressed by the slope of the barrier.

Specimens of Prof. Joly's way of dealing with opposition are to be found on pp. 934-5 of his paper of May 1926. He says that the differential equation of heat conduction used by me is the same as that used by Mr. Cotter in 1924, save that I assume the rate of supply of heat constant. "Of course the time should enter through a negative exponential factor." Is it seriously suggested that this equation was not published till 1924, or that the decay of uranium and thorium during

\* Phil. Mag. i. pp. 923-931 (1926).

† Phil. Mag. i. p. 934 (1926).

geological time is of any importance in the present problem? Mr. Cotter himself takes the rate constant.

My doubts as to the reason why Prof. Joly assumes fusion to occur under the oceans, as expressed in the first two paragraphs on p. 927 of my paper, are treated by him on p. 935. Direct comparison of the two passages is the only way of judging how far he has answered. I would add only that a flat contradiction on a question of fact, without a reference, is not in accordance with the best scientific practice. The views I expressed agree with those of J. H. L. Vogt\*.

Prof. Joly's next paragraph contains the elegant remark: "We have here the mathematical point of view with a vengeance." It does not, however, answer my statement that "radioactivity within the granitic layer . . . only ensures that the temperatures below that layer become higher than they would in its absence." Incidentally, this will produce the further effect of diminishing viscosity and enabling convection to bring up the heat generated below with greater ease and at an earlier stage, so that its escape is made easier, not obstructed.

His paper opens with a reply to my arguments that the thickness of the granitic layer does not exceed about 15 km.; but as all his arguments are now out of date and mine have received additional support †, I do not propose to deal with them further.

Prof. Joly's new paper (Aug. 1927) offers a series of periodic phenomena due to a steady supply of heat, and considers that they provide an answer to my statement that periodic phenomena cannot be produced in this way. Perhaps I ought to have added a list of exceptional cases where the proposition might not be expected to hold, as is done at great length in works on pure mathematics. But in physics the discovery of these is usually left to the reader. After all, the whole science of engineering is devoted to constructing systems that will, if suitably treated, behave in an extraordinary way. But in the present problem we are entitled to suppose that the system has not been so designed. Prof. Joly has indeed done a service in mentioning the four examples he does, because they are admirable examples of the kind of exception that proves the rule. But as the conditions of convection in a layer of fluid of great horizontal extent are by this time fairly well understood, and as

\* *Econ. Geol.* 1926, pp. 207-233. Cf. also 'Natura,' March 5, 1927, p. 343.

† M. N. R. A. S. *Geoph. Suppl.* i. pp. 385-402, 483-494. *Gerlands Beiträge z. Geophysik.* xviii. pp. 1-29 (1927).

the basaltic layer, if fused, would be such a layer, we may as well consider the actual case first. It is, of course, well known that if a fluid is incompressible, but the density increases with height on account of variation of temperature or composition, the potential energy can be decreased by interchanging upper and lower layers. This is not, however, a sufficient condition for instability, though it was long believed to be one. Direct interchange of the layers is impossible because they obstruct each other; it can occur only by upward currents in some places combined with downward ones in others, and these are hindered by conduction and viscosity. Consequently instability does not actually arise until the vertical gradient of temperature exceeds a certain finite value. When compressibility is taken into account, instability arises when the gradient exceeds the adiabatic by a certain amount. When the system first becomes unstable, the motion takes the form of a set of polygonal cells, fluid rising in the centres and sinking around the edges. The motion is continuous and steady. This was found experimentally by Bénard, and contributions to the theory have been made by Lord Rayleigh and others\*. With increasing gradient of temperature other types of instability arise and other modes of motion become superposed, till we get the complete turbulence known in the ordinary heating of a liquid from below.

Now the horizontal extent of the cells is comparable with the depth. Also the tendency of the currents is to restore the adiabatic gradient of temperature; and the departure from it needed to start them is proportional to the inverse fourth power of the depth, and is negligible when the depth is of the order of a few kilometres. Consequently we must infer that when a fluid is heated at the bottom or internally, the convection currents generated will prevent the gradient of temperature from ever departing far from the adiabatic. Their effect is to carry the heat to the top as fast as it is supplied; increasing the rate of supply increases the intensity of the convective circulation, but not the gradient of temperature. But here we come to the essential point: the heat, on account of the limited size of the cells, always reaches the top within a horizontal distance of the place where it was originally supplied comparable with the depth of the liquid. At the top the liquid is in contact, in the geophysical problem, with the solid upper layer, the bottom surface of which must be at the same temperature as the top of the liquid. In the

\* *Cf. Phil. Mag. ii. pp. 833-844 (1926).*

upper layer the heat is transmitted to the outer surface by conduction. The whole thickness of the two layers being of the order of 30 km., a region whose horizontal extent is over, say, 100 km. will be thermally practically self-contained. Mutual influence of continental and oceanic conditions will be negligible.

In the terrestrial case the transference of heat will be partly by way of latent heat ; some liquid will solidify when it rises to the top, and the descending currents will contain suspended solid particles, which will gradually melt as they descend. But this does not affect the argument ; the only difference is that in the region where solid is present the gradient is the adiabatic for a mixture of solid and liquid, and not that for a liquid alone. There is no possibility of what Prof. Joly calls superheating—that is, rise of temperature far above the melting-point\*. These inferences are at all points in agreement with those I made previously and illustrated by diagrams. Convection simply straightens out part of the graph of temperature against depth, and in no respect facilitates periodicity.

Of the four self-acting periodic systems considered by Professor Joly, three differ from the geophysical problem through the working fluid being enclosed in a tube. I refer to the geyser, the Air Tester, and E. H. Griffiths's heat engine. The essence of the geophysical problem is the possibility of interchange between layers of the liquid by ascending currents in some places and descending ones elsewhere. In a tube this is obstructed, and far greater gradients of temperature are needed to start convection. On account of the constricted character of the systems, the liquid in two of them acts as a movable valve capable of opening and closing communication between two masses of gas ; but in the geophysical one communication is open all the time. Griffiths's engine, with a trifling change in the constants, is converted into the ordinary apparatus for finding the coefficient of increase of pressure at constant volume. In Professor Joly's experiment with the rotating sphere containing camphor and heated below, we have again a system with only a single infinity of possible positions of equilibrium, of which only two are realized in practice, so that the system can only pass from one to the other discontinuously. The greater freedom of an extended horizontal

\* In Preston's 'Heat,' 1919, pp. 344-348, this term is used for a rise in temperature above the normal boiling-point. What Professor Joly calls a superheated liquid is, in fact, an ordinary liquid.

layer makes continuous interchange possible ; and this is what actually occurs. A better analogy with the conditions within the earth's crust would indeed have been the boiling of the domestic kettle or, still better, the melting of a tray of paraffin wax by heating below.

At the close of my former paper in this Magazine I stated four objections to Professor Joly's theory, any one of which would by itself be decisive. He has entirely refused to face three of them, and partly the other (c). But I would point out that my main objection to the theory is not merely the existence of serious arguments against it ; it is that there are no serious arguments for it. The question is essentially one of theoretical physics : given a certain set of assumptions, to investigate their consequences in the light of physical laws and to compare the results with observation. This investigation will necessarily involve a considerable amount of mathematics ; at the least the equations of fluid motion and of heat conduction must appear in it and be solved. But until it is carried out, there is no reason to believe that the consequences would be anything like those asserted by Professor Joly. The onus of proof in a question of theoretical physics is on the advocate of a theory, not on its opponents ; and it ought in this case to have been carried out before Professor Joly proceeded to publication in an important physical journal and followed it up with an ambitious book. If the problems to be solved are in any way more complex than I have considered, so much the more complex must the problem be that Professor Joly has to solve before his theory will command the respect of physicists. The reason for this situation is simple : inadequately tested theories can be constructed more rapidly than people in the habit of taking reasonable care can point out the mistakes. I am sorry to have to point this out, but the number of suggestions that have been made in public and in private by non-physicists, to the effect that it is the duty of a mathematical physicist to drop any work he may consider more important in order to examine some theory of the type under consideration—with the certainty that the results will be accepted only if they are favourable—have made it necessary. I add that, since I have already devoted more attention to Professor Joly's theory than I consider it worth, I do not propose to take any part in further discussion of it unless he produces more satisfactory arguments than he has done hitherto.

XXI. *The Earth's Thermal History.**By J. JOLY, F.R.S.\**

MY paper entitled "Dr. Jeffreys and the Earth's Thermal History" (*Phil. Mag.* August 1927) has stirred Dr. Jeffreys into a rejoinder revealing so much irritation that I feel a real difficulty in pursuing the matter any further lest quite unintentionally I should say anything which might prove to be a source of further annoyance. At the same time he has raised issues which, not only for the advance of the subject under discussion, but as matter of courtesy, seem to render a further statement from me imperative.

My paper was based upon one appearing from the pen of Dr. Jeffreys in the '*Geological Magazine*' of November 1926, in which he enunciates his "main conclusion." I cite this statement in my paper and proceed to comment upon it, pointing out that it appeared tacitly to assume that no relative motion of the parts of the medium takes place. Mr. Cotter's clear statement of what is involved in the theory of thermal cycles follows; and then certain phenomena are cited as showing that cyclic thermal phenomena might take place without involving any departure from the "main conclusion" arrived at by Dr. Jeffreys.

To this procedure Dr. Jeffreys takes exception in his paper appearing in this issue of the *Philosophical Magazine*. His first complaint is that I make the formal statement of his main conclusion the subject of my remarks, instead of some general observations of his, which appear later, as to the nature of "a theory" and how its supporters should defend it.

I think most scientific readers would regard it as more incumbent upon me—and probably more fruitful—to deal with the "main conclusion" than to embark upon the very wide topic favoured by Dr. Jeffreys.

Dr. Jeffreys objects to the analogy of the geyser. He says in effect—"Without boundary constraints there would be no cyclic effects in the case of the geyser, and therefore it 'proves the rule'—i. e. that such effects cannot arise."

It is true that there will be no cyclic effects without constraints. But the statement overlooks the fact that the cyclic nature of the phenomena turns on constraints, not only in the case of the geyser, but also in the case of the substratum; and of necessity must do so in all similar cases where storage of heat followed by change of state occurs.

\* Communicated by the Author.

In the case of the geyser the medium is fluid; and constraints hindering free circulation are required while the energy necessary to attain the boiling-point at all levels is accumulating. In the case of the substratum the medium is solid to start with, and the corresponding constraint is in the rigidity of the working substance which determines quiescence while the energy necessary to attain the melting-point at all levels is accumulating. The difference in the character of the constraints, which arises necessarily out of the differing mobility of the media, possesses no fundamental significance. As thermal energy accumulates, similar conditions of instability arise in both cases—*i. e.*, a medium charged with energy proper to the pressure at all levels and necessarily changing state if any movement occurs to bring any part of it to a higher level.

The use of the word "rigidity" in connexion with the substratum should be qualified. For, in fact, every stage of viscosity must, in the substratum, successively prevail during long periods of time. Siliceous rocks have no definite melting-point. As thermal storage progresses, their viscous resistance to movement diminishes, the heat becoming latent in the gradual change of state. These conditions exist at all levels, but in the depths the thermal storage is greatest as higher melting-points have to be attained before movement can occur. Equilibrium finally breaks down, either spontaneously or due to tidal forces. The ensuing circulation involves the superheating and perfect fluidity of rising magma brought into regions of lower pressure. The possibility of storage turns, throughout, upon the resistance to translatory movement during a certain time-interval. The same may be said of the geyser, where the necessary constraints are not involved in the properties of the substance, but are, as it were, "external."

In short, the geyser, or its experimental realization, is a fair and direct demonstration of the inapplicability of Dr. Jeffreys's "main conclusion" to the conditions to which he would apply it, and in which, as I have said, he tacitly assumes that no relative motion of the parts of the medium takes place. In other cases, also, the inadequacy of his statement may be demonstrated.

There exists a source of thermal instability which does not call for the external constraints of the geyser, and which might be supposed to actuate a geyser of any dimensions whatsoever and which, indeed, in some cases probably takes a part in geyser activity. I refer to the phenomena attending ebullition in liquids which contain no undissolved gases; *i. e.*, no bubbles

It is well known that this condition permits of a rise in temperature of the liquid greatly over the boiling-point. Boiler explosions have been traced to this source as well as unpleasant experiences with wash-bottles which have been left for long standing on the hot-plate. The fact that a sod, or a handful of gravel, cast into the geyser will precipitate eruption supports the view that its explosive character may be—at least in part—traceable to this phenomenon.

Obviously an ideally tranquil ocean, continually receiving a supply of heat from any source, might be brought into a state of instability in this way. The temporary constraint in this case resides in the tensile strength or molecular adhesion of the medium. A tidal movement or some other periodic source of disturbance may then initiate the catastrophic break-down. And we may fancy the rising vapour, condensing into clouds, as being seasonally or periodically restored as rain. Heat is here carried from source to refrigerator intermittently so long as the thermal supply continues. In other words, “successive revolutions” dominate the history of the region.

In the case of the “Air Tester” the conditions are more complex. A net physical analogy arises which I sum in the statement—“There is a steady supply of heat entering the system accompanied by cyclical movements of a working substance with and against gravity.”

Interesting possibilities arise out of the “Sublimation Engine,” which, although differing from the preceding systems in many respects, leads to the same end—*i. e.*, the cyclic transfer of thermal energy from source to refrigerator. I can—as I write—see no reasons why the principle involved might not be applied to a system of unlimited extent and dimensions. A steady thermal supply from beneath, or originating radioactively in the working substance, causes this to sublime and diffusing upwards to finally condense upon a horizontal ceiling kept cool by a refrigerator. When a considerable deposit has collected, its adhesion gives way and the instability rapidly spreading causes the whole deposit to sink back to its original position. A homely example is the periodic fall of soot from an unswept flue. A source of vibration might be supposed to time the period of break-down. The analogy is obvious and need not be further pursued.

Towards the end of Dr. Jeffreys's comments upon periodic phenomena, we reach what I regard as the most important passage in his paper in so far that for the first time it places a clear and definite issue before us. He writes:—“In the terrestrial case the transference of heat



will be partly by way of latent heat ; some liquid will solidify when it rises to the top, and the descending currents will contain suspended solid particles, which will gradually melt as they descend. But this does not affect the argument ; the only difference is that in the region where solid is present the gradient is the adiabatic for a mixture of solid and liquid, and not that for a liquid alone. There is no possibility of what Professor Joly calls superheating—that is, rise of temperature far above the melting-point.

The importance of this passage is in the assumption that descending solid particles will gradually melt away as they descend.

Now the accumulation of solid or crystallized magma in the depths is, I believe, as essential to the theory of thermal cycles as it is to Lord Kelvin's contention that a crust forming at the surface of the cooling Earth and breaking up must collect beneath till all is solidified. In fact, the conditions are very much alike, save that in Kelvin's theory the loss of heat is at the very surface. Kelvin was very clear that the gradient of temperature downwards in the cooling Earth must be sufficiently slow as not to annul the effects of pressure in raising the melting-point. Dr. Jeffreys discusses this matter in 'The Earth,' and gives an expression defining the limiting gradient according to Kelvin's "thermo-dynamic law of freezing."

In the theory of thermal cycles this condition is equally essential. The crystals rise in melting-point as they descend. The thermal gradient must not rise steeply enough to counteract this rise of melting-point and cause the remelting of the crystals. This is quite clear, and it directs our attention to extraneous sources of a downward-rising temperature gradient.

Are there deeper-lying sources of heat ? Here we must recall the fact that thermal supplies to the surface of the continents, as determined by temperature gradients and conductivity of the rocks, can, mainly or entirely, be ascribed to heat of radioactive origin in the continents themselves ; while in what appear to be the deeper-lying basal rocks, we find a diminishing supply of radioactive substances as we go downwards.

We seem, therefore, led to the conclusion that there can be only a very small supply of heat from regions deeper than those with which we are concerned.

Again, we can hardly invoke the contemporaneous output of radioactive heat. For this is too slow : about 3·4 calories per gram in the case of basalt, and 1·7 calories per gram in the case of eclogite, in one million years.

The gradient prevailing in a molten substratum must arise almost entirely from its own previous radioactivity and convective movements. The latter will tend to make the temperature uniform or diminish the temperature gradient. Tidal shearing movements, while operative, will tend towards uniformity of temperature. We cannot evaluate these effects, but it seems plain that the assumption of a sustained rise of temperature downwards adequate to counteract the effects of pressure in raising the melting-point is not allowable unless some sufficient reason can be adduced. Dr. Jeffreys advances no reasons for such a downward rise of temperature—so far as I know.

But if this high gradient does not exist, then Dr. Jeffreys's "steady state" must fail. For the congealed basalt must build up from beneath concurrently with the escape of heat from the higher regions of the magma into the overlying solid ocean-floor; and the original solid state must in this way be restored.

I am reprimanded by Dr. Jeffreys for not citing chapter and verse in support of my denial of his statement (Phil. Mag. May 1926) "that the melting-points of rocks increase with the basicity; so oceanic rocks must on the whole have higher melting-points than continental rocks." My defence is that I thought the experimental data were sufficiently well known to require no citation. I shall now endeavour to make good the omission.

Dr. Jeffreys upholds his statement and gives two references: "Vogt's *Econ. Geol.* 1926, pp. 207-233; cf. also 'Nature,' March 5, 1927, p. 343." The last is a review of Gutenberg's 'Lehrbuch der Geophysik' by Dr. Jeffreys himself, and apparently contains his reference to Vogt. A quotation from the review, although the wording is rather obscure, appears to show that there has been confusion between "melting-point" and "crystallization-point." It is well known that these differ widely. I quote from Dr. Jeffreys's review:—

"There is a remark on p. 52 that the melting point of basaltic rocks at atmospheric pressure is about 200-300° C. lower than that of granite ones, which is given as 1100°. F. W. Clarke gives 1240° for granite, and values from 1060° to 1250° for basalt ('Data of Geochemistry,' 1924, pp. 298-301). J. H. L. Vogt gives 1250° for the crystallization-point of gabbro, which is chemically similar to basalt, and 1000° for granite ('Economic Geology,' 1926, pp. 207-233). The latter estimates refer explicitly to dry material, but it

seems to be generally believed by geologists that in natural conditions the melting-point of granite is more affected by water than that of basic rocks. A reconsideration of the data on this question is overdue ; such a conflict of opinion on some of the most important experimental data of geophysics should not be allowed to persist."

There is nothing in this, nor in the originals referred to, so far as I can find, to sustain Dr. Jeffreys's contention that the melting-point of rocks increases with the basicity ; but quite the contrary. In confusing the melting-point with crystallizing-point serious error is involved.

In the case of "crystallization-point" we deal with solutions : "The relation of the several compounds in a magma is one of mutual solution" (Harker, 'The Natural History of Igneous Rocks,' p. 169). It results "that the order in which the minerals crystallize is not determined by their relative fusibility as separately tested. This *lowering of freezing-point* is the most characteristic property of solutions" (p. 170). The italics are Dr. Harker's.

Again, volatile substances play an important part in determining the temperature of crystallization of the constituents ; and as these substances escape more freely from extruded than from intruded magmas, the former may crystallize at higher temperatures than the latter. Also, volatile substances (such as water) are more abundant in acid than in basic magmas, and hence play a more important part in the crystallization of the former. "It follows that *under like conditions acid magmas crystallize at lower temperatures than basic magmas.*"

But there is no doubt as to the fact that the *melting-point* rises with the percentage of silica. Thus Barus and Iddings find as follows :—

	Melting-point.	Silica percentage.
Basalt . . . . .	1250°	48.49
Hornblende-mica-porphry	1400°	61.50
Rhyolite . . . . .	1500°	75.50

These figures bring out strikingly the difference, already referred to, between the melting-point and the crystallization-point. Rhyolite is generally regarded as the volcanic equivalent of a granite. Clarke, who cites these results ('Data of Geochemistry,' 1924, p. 301), continues : "At 1300° the basalt was quite fluid, but at 1700° the rhyolite was still viscid."

Doelter found that basic rocks softened between 1000°

and 1150°, and acidic rocks softened at 1200°–1300° (Phys. Chem. Min. 1905, p. 124).

Clarke (*loc. cit.* p. 297) states the issue clearly. "In the geological interpretation of the melting-points there is one particularly dangerous source of error. We must not assume that the temperature at which a given oxide or silicate melts is the temperature at which a mineral can recrystallize from a "magma."

The experiment of floating a piece of granite in molten basalt may easily be made. The conditions are stable, because the crystallization temperature of basalt (1050°) is beneath the melting-point, or rather the decomposition-point, of orthoclase (1170°) and the melting-point of albite (1100°), and, of course, much below the rather indefinite melting-point of quartz. (See J. H. L. Vogt, 'Physical Chemistry of the Magmatic Differentiation of Igneous Rocks,' ii. 1926.)

There remains one more point. Dr. Jeffreys refers to his deduction, on seismic evidence, of a low continental thickness, assuming that this has been verified. A recent paper by Mohorovičić in Gerlands 'Beiträge zur Geophysik' (Bd. xvii. Heft 2) disputes his low estimate, and contends that the thickness of the continental sial is about 40 km. (*loc. cit.* p. 198). The discussion is still proceeding. Meanwhile the following statement by Dr. Jeffreys ('Nature,' Sept. 25, 1926) referring to certain seismic determinations is of interest. He refers to the Kulpa Valley earthquake of 1909, the Wurttemberg earthquake of 1911, the Tauern earthquake of 1923, and the Oppau explosion.

"The observations permit of a rough determination of the depths of the granite and basaltic layers. The former may be about 12 km., the latter about 20 km. Both are subject to an accidental error of about 4 km. In addition there is a possibility of systematic error. Uncertainty as to the depth of focus may allow the thickness of the granite layer to be doubled. . . . *I think, therefore, that determinations of the depths of the layers by means of near earthquakes are not more reliable than those based on the Earth's thermal state, isostatic balance between continents and oceans, and the group velocities of surface-waves,*" etc. The italics are mine.

Isostatic considerations appear to favour 37 km. or thereabouts as the continental thickness ('Nature,' Oct. 29, 1927). Thermal estimates based on surface gradients and the radio-activity of the rocks are not very trustworthy.

The point is not very important, and does not directly affect the theory of thermal cycles.

XXII. *Double Excitation of Upper Levels in the Mercury Atoms by Collisions of the Second Kind.*

*To the Editors of the Philosophical Magazine.*

GENTLEMEN,—

**M**AY we make some remarks concerning the very interesting paper of Professor R. W. Wood in the September issue of your Magazine on "Optical Excitation of Mercury, with Controlled Radiating States and Forbidden Lines" (Phil. Mag. [7] iv. p. 466, 1927).

Professor Wood describes the radiation of the mercury resonance lamp which contains some nitrogen. He finds "effects of obscure origin, which can be explained only with difficulty." Very strange is the development of the line 2856 caused by the addition of the nitrogen, whereas the resonance is only excited by light of shorter wave-length than 2750. The line 4916 from the same upper level 3S is also enormously strengthened.

In observations made on the mercury resonance-tube with addition of sodium (*Naturwiss.* xv. p. 540, 1927) we have shown that upper levels of an atom are excited in high selectivity by collisions of the second kind if the energy of the colliding atom can be accepted very completely by the atom struck. At the collision of two metastable (in Wood's terminology  $2p_3$ ) Hg atoms this effect of resonance can have the result that one accepts the whole energy,  $2 \times 4.68$  volts, while the other returns to the normal state. This process has a certain probability, because nearly under the theoretical level of resonance ( $2 \times 4.68 = 9.36$  volts) an actual level of the mercury is located with 9.25 volts, that is, only 0.11 volt is to be transformed into energy of translation; this equals the thermal energy of the two atoms at  $300^\circ \text{K}$ . The level from which the mentioned lines 2856 ( $2p_2-3S$ ) and 4916 ( $1P-3S$ ) originate is the level under the point of resonance 3S.

Investigations are under way aiming to substantiate this hypothesis of the accumulation of energy.

Yours faithfully,

H. BEUTLER and B. JOSEPHY.

Kaiser Wilhelm-Institut für physikalisch  
Chemie und Elektrochemie, Berlin-Dahlem.  
December 6, 1927.

XXIII. *Notices respecting New Books.*

*The Nature of the World of Man.* By Sixteen Members of the Faculty of the University of Chicago. Edited by H. H. NEWMAN. 8vo. Pp. xxiv+566, 132 figs. and 4 charts. (University of Chicago Press; Cambridge University Press, London, 1926. Price 20s. net.)

THE purpose of this book is to present an outline of our knowledge of the physical and the biological world, and to show the position of man in the universe in which he lives. It contains the subject-matter of a "survey course" given each year by its authors at the University of Chicago to a group of selected first-year students of superior intelligence. The course was designed to give such students a preliminary view of the rich intellectual fields that lie before them, so that, on the one hand, all of their work shall have a large measure of unity and coherence, and on the other hand, they will be able to decide early what particular subjects they may wish more thoroughly to explore. There has been full co-operation between the various experts engaged in this educational experiment, and its success has seemed to make advisable the production of this volume.

The arrangement adopted is from the general to the specific. Beginning with: I. Astronomy (by Forest Ray Moulton), II. The Origin and Early Stages of the Earth (by Rollin T. Chamberlin) leads naturally to III. Geological Processes and the Earth's History (by J. Harlan Bretz). Physics and Chemistry follow, represented by IV. Energy: Radiation and Atomic Structure (by Harvey Brace Lemon), and V. The Nature of Chemical Processes (by Julius Stieglitz). Biology commences with VI. The Nature and Origin of Life (by Horatio Hackett Newton), followed by VII. a chapter on The Bacteria (by Edwin O. Jordan), after which Merle C. Coulter and Henry Chandler Cowles deal respectively with VIII. Evolution of the Plant Kingdom, and IX. Interaction between Plants and their Environment. General Zoology finds expression in X. The Evolution of the Invertebrates (by W. C. Allee) and XI. The Evolution of the Vertebrates (by Alfred S. Romer), after which XII. The Coming of Man is described by Fay-Cooper Cole. H. H. Newman (the Editor of the series) then discusses XIII. The Factors of Organic Evolution, and Elliot B. Downing XIV. Human Inheritance. XV. Man from the point of view of his Development and Structure (by George W. Bartelmez), XVI. The Dynamics of Living Processes (by Anton J. Carlson), and XVII. Mind in Evolution (by Charles H. Judd), conclude the series. A few selected references are given at the end of each chapter, and a somewhat limited glossary precedes the index.

The volume is well printed and the illustrations, which in part are photographic reproduction in the form of plates and in part simple line text-figures, are clear and helpful.

The book should have a wide appeal to readers who seek a general knowledge of the world about them, and take an interest in the history and future of their own species.

---

## XXIV. *Proceedings of Learned Societies*

### GEOLOGICAL SOCIETY.

[Continued from vol. iv. p. 256].

November 2nd, 1927.—Dr. F. A. Bather, M.A., F.R.S.,  
President, in the Chair.

THE following communication was read:—

‘The Stratigraphical Distribution of the Cornbrash: I.—The South-Western Area.’ By James Archibald Douglas, M.A., D.Sc., Sec.G.S., and William Joscelyn Arkell, B.A., B.Sc., F.G.S.

This paper gives an account of the stratigraphical distribution of the Cornbrash in South-Western England, from Oxford to the south coast near Weymouth. The evidence obtained by the Authors is used in a critical discussion of the eleven brachiopod zones proposed by Mr. S. S. Buckman in a recent communication to the Society, and as a result a number of amendments in the list are suggested.

A general description is given of the faunal sequence, and the distribution of the zones throughout the area is indicated by a detailed account of many type-exposures.

The new records obtained are added to Mr. Buckman’s faunal range-diagram, and in this way it is shown that many of his conclusions regarding penecontemporaneous erosion and non-sequences in the Cornbrash, as expressed in his clinal diagram, have been based on insufficient data, and that lack of geological information, in many instances due merely to exposure-failure or faulty collection, has been used as evidence of stratal failure.

The introduction of new stratigraphical terms is criticized, and a twofold rather than a threefold subdivision of the Cornbrash is advocated. The more important brachiopods and lamellibranchs are discussed in palæontological notes, and several new species are described and figured.

---

[*The Editors do not hold themselves responsible for the views expressed by their correspondents.*]

THE  
LONDON, EDINBURGH, AND DUBLIN  
PHILOSOPHICAL MAGAZINE  
AND  
JOURNAL OF SCIENCE.

[SEVENTH SERIES.]

FEBRUARY 1928.

XXV. *New Evidence of the Existence of Charges smaller than the Electron.*—(a) *The Micromagnet*; (b) *The Law of Resistance*; (c) *The Computation of Errors of the Method.* By FELIX EHRENHAFT, *Dr.Phil., Acting Professor of Physics and Head of Physics Institute III. of the University of Vienna*, and EMANUEL WASSER, *Dr.Phil., of Vienna* \*.

§ 1. *Introduction.*

IN a former paper, published in this Magazine †, we have referred to a new method of observations which enables us to demonstrate the nature of single colloidal test bodies moving in gases. This method, which depends upon velocity measurements of a single test body in an inhomogeneous magnetic field, is not only suitable for the determination of the magnetic constants of the observed particles, but can also be applied to the measurement of strong magnetic fields of small dimensions.

If we set, according to Faraday (1848), the susceptibility of vacuum  $k=0$ , and denote a weak magnetic body as paramagnetic when  $k>0$ , as diamagnetic when  $k<0$ , then the energy of a small particle of the volume  $V$  in the magnetic field  $H$  is  $\frac{1}{2}kVH^2$ . From this results that the force acting on a single particle in the direction of the  $x$  axis is  $kVH \frac{dH}{dx}$ .

While in a homogeneous field this force disappears, in an

\* Communicated by the Authors.

† F. Ehrenhaft and E. Wasser, *Phil. Mag.* vol. ii. (July 1926).  
*Phil. Mag.* S. 7. Vol. 5. No. 28. Feb. 1928.

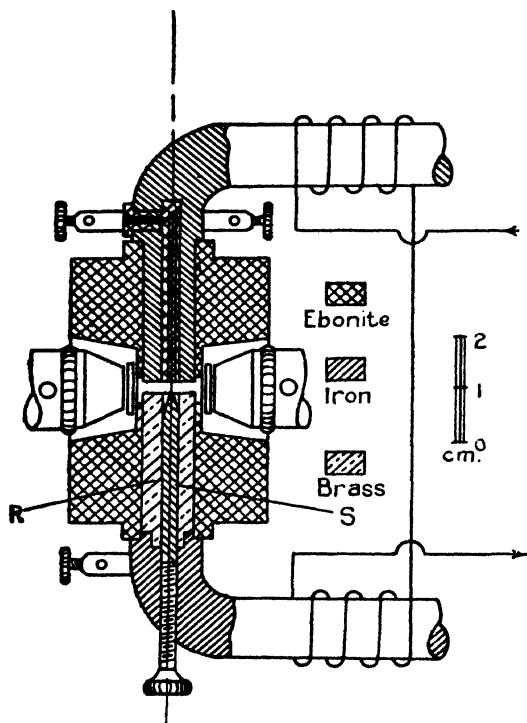


inhomogeneous field a paramagnetic test body would be driven to the region of the greater force, a diamagnetic body in the opposite direction. We now wish to examine in this way as small test bodies as possible, and construct for this purpose the suitable magnetic field.

### § 2. *The Micromagnet.*

For the following measurements the circular poles of an Ehrenhaft condenser of the diameter 9 mm. were rebuilt

Fig. 1.



into poles of a strong electromagnet. The upper plate consists of a hollow cylinder of soft iron with an external diameter of 9 mm. and an internal diameter of 2 mm. Into this is introduced an electric insulated solid cylinder of the same iron with a diameter of 1 mm. These cylinders can be brought to various electric potentials. The lower plate ends in a conical iron pin, 2 mm. thick, which has a circular base with a diameter of 1 mm. The pin is surrounded by a mantle of brass with a diameter of 9 mm., so that its base

lies in the same plane as that of the pin. The described condenser plates go over into two iron cores (12 mm. thick, 190 mm. long), each of which is wound with 14 layers of 2-mm. copper wire. An accumulator battery of 120 volts cross-potential and very great capacity furnishes a quite constant current. The number of the ampere turns per 1 cm. is 1080. The two cores are closed by an iron yoke which is insulated from them by leaves of mica. In this way the plates can also be used as an electrical condenser. Four coolers fed with flowing water, two for each core, provide for a sufficient removal of the heat and hold the temperature constant. When the windings are connected with the electrical circuit, there are produced two opposite magnetic poles in the vertical  $x$  axis. In this way we get a symmetrical inhomogeneous magnetic field between the plates of an Ehrenhaft condenser, which are at a distance 1.8 mm. apart.

### § 3. *The Measurement of the Micromagnetic Field.*

It is well known that under the influence of a constant force  $P$  the velocity  $v$  of the test body in a frictional medium is proportional to the force acting. If  $B$  denotes the mobility of the test body, then we may write  $v = B \cdot P$ . If  $P$  is a function of position, the velocity of the test body will change proportionally to the change in the force. In the following the measurements of the velocities are made over such small regions that the force  $\bar{P}$  in these regions may be regarded as constant, and hence proportional to the velocity  $\bar{v}$ . If the direction of the magnetic field is the same as that of gravity, and if the test body acquires, under the action of gravity and of the magnetic force, a velocity  $\bar{v}_m$  in the frictional medium, then

$$mg \pm kVH \frac{dH}{dx} = \bar{v}_m \cdot B \quad . \quad . \quad . \quad . \quad . \quad (1)$$

Here  $\bar{v}_m$  is the velocity,  $H$  the magnetic intensity, and  $\frac{dH}{dx}$  the gradient of the intensity in a practically very small region in which the force may still be regarded as uniform. The positive sign holds for paramagnetic, the negative sign for diamagnetic bodies. In our case the gradient of the field in the central  $x$  axis is in the same direction as gravity. Hence the action of the magnetic field on paramagnetic bodies will be in the direction of gravity, and on diamagnetic bodies in the opposite direction.

In order to undertake the measurement of the inhomogeneous magnetic field, we must first define its geometrical configuration. The observations were made with a microscope objective of the numerical aperture 0.34 and with a Huygens ocular 4. According to this the magnification was 95. This combination of ocular and objective gave a field of vision of a diameter about 2 mm., so that both the plates (distance 1.8 mm.) were still visible. By a scale introduced in the ocular the space between the poles was divided into equal intervals of  $9 \cdot 10^{-3}$  cm. Of this, only the central part of the scale, 1.08 mm. long, was used for the observations. This central part of the field of vision was divided into 12 intervals. The measurements, however, were made over two intervals at once, as it was found that the velocity under the influence of the magnetic force was sufficiently uniform in this stretch. The magnetic field could therefore be examined over six double intervals of the length of  $18 \cdot 10^{-3}$  cm., *i.e.* about two-thirds of the space between the poles.

For the purpose of calibration an aqueous solution of 3.01 per cent.  $\text{FeCl}_3$  was used. It was necessary to hold the concentration as low as possible in order that the susceptibility might not be too high. In this case the velocities in the magnetic field would be very large and difficult to measure, and, furthermore, small susceptibility makes possible a comparison with diamagnetic bodies, most of which have very small susceptibilities. The susceptibility of ferric chloride solution was determined relative to water by repeated measurements, using a large magnet and the buoyancy method. Assuming the value  $k = -0.77 \cdot 10^{-6}$  for water, the value  $k = 1.14 \cdot 10^{-6}$  was found for the 3.01 per cent.  $\text{FeCl}_3$  solution.

The solution was mechanically sprayed, and upon the test bodies the following measurements were made. Each test body is allowed to fall under the influence of gravity alone, and is repeatedly drawn up again by the electrical field. After ten measurements of the times of fall and rise had been made, the same measurements were repeated in the magnetic field. For the motion in the magnetic field we have the relationship

$$mg + kVH \frac{dH}{dx} = \frac{v_m}{B}; \quad . . . . . (2)$$

for the motion under the action of gravity alone the relationship

$$mg = V\sigma g = \frac{v_f}{R}, \quad . . . . . (3)$$

where  $V$  denotes the volume of the test body. From this follows

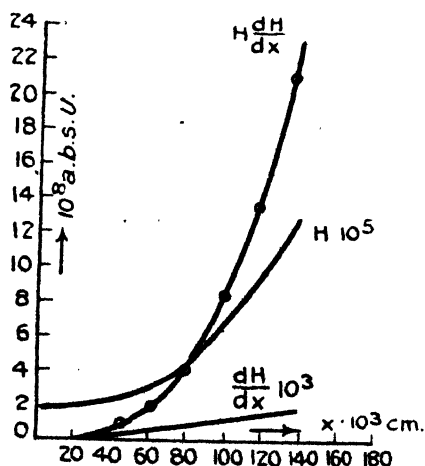
$$1 + \frac{k}{\sigma g} \cdot \overline{H} \frac{dH}{dx} = \frac{v_m}{v_f} \quad (4)$$

From this results that for each interval the mean product of the magnetic intensity into the gradient is

$$\overline{H} \frac{dH}{dx} = \left( \frac{v_m}{v_f} - 1 \right) \cdot \frac{\sigma g}{k} \quad (5)$$

If, now, in (5) we give the density the value 1.03 and the susceptibility  $k$  the value as above determined, we can compute the value of  $\overline{H} \frac{dH}{dx}$  for each interval, and can plot this as a function of position. In the diagram of fig. 2 the

Fig. 2.



lengths of the intervals measured in  $10^{-8}$  cm. are plotted as abscissæ, the values of  $\overline{H} \frac{dH}{dx}$  measured in  $10^8$  abs. units as ordinates. In the other two curves the ordinates are measured in  $10^3$  gauss, and  $\frac{dH}{dx}$  measured in  $10^5$  abs. units. The marked points show the measured values of  $\overline{H} \frac{dH}{dx}$  in the six intervals. In order to determine the values of  $\overline{H}$ , a cubical parabola was drawn to the points by the method

230 Prof. Ehrenhaft and Dr. Wasser on *New Evidence of the* of least squares. This parabola fits the observed values extremely well. The deviations are all within the region of the errors of observation and are, in mean value, about 1.5 per cent.

Hence the product  $H \frac{dH}{dx}$  can be written in a form

$$H \frac{dH}{dx} = f(x),$$

where  $f(x) = ax^3$ . For the constant  $a$  the value  $0.856 \cdot 10^{12}$  was obtained.

The equation

$$H \frac{dH}{dx} = 0.856 \cdot 10^{12} \cdot x^3$$

can easily be integrated. From this results that the magnetic intensity as a function of the position is

$$H = (0.428 \cdot 10^{12} x^4 + c)^{1/2}.$$

From the number of ampere turns and from the dimensions of the magnet we have as the initial condition for  $c = H_0^2$  the value  $\sim 4 \cdot 10^6$  abs. units. Hence

$$H = (0.428 \cdot 10^{12} x^4 + 4 \cdot 10^6)^{1/2}.$$

This curve is also shown in fig. 2. The quotient of the two ordinates  $H \frac{dH}{dx}$  and  $H$  at every point gives the third curve of the diagram  $\frac{dH}{dx}$ . In this way it is possible to examine the nature of the magnetic field in all its details. Here we have a new method of measuring inhomogeneous strong magnetic fields of small dimensions. As can be seen from fig. 2, the intensities run from about 2000 to 13,000 gauss. Of course very close to the point the intensity is still essentially greater, and may even exceed 20,000 gauss.

#### § 4. *The Determination of the Magnetic Constants of Small Particles by means of the Micromagnetic Field.*

As the structure of the magnetic field is already known, we can undertake the measurements on other paramagnetic and diamagnetic substances in order to determine their susceptibilities. In the following the results of these researches on several test bodies of selenium and silver are given.

The procedure is here the same<sup>\*</sup> as described for  $\text{FeCl}_3$ . If  $\overline{v_{m_0}}$  denotes the velocity of a drop of ferric chloride in the magnetic field, and  $v_f$  the velocity under the influence of gravity alone in a certain interval, and if, furthermore,  $\overline{v_{m_1}}$  and  $v_{f_1}$  have the same meaning for a particle of selenium, we get, according to (5), the two equations

$$\left. \begin{aligned} \frac{k_0}{\sigma_0 g} \cdot H \frac{dH}{dx} &= \left( \frac{\overline{v_{m_0}}}{v_{f_0}} - 1 \right), \\ \frac{k_1}{\sigma_1 g} \cdot H \frac{dH}{dx} &= \left( \frac{\overline{v_{m_1}}}{v_{f_1}} - 1 \right). \end{aligned} \right\} \dots \dots (6)$$

As  $H \frac{dH}{dx}$ , under the assumption made above, has the same value in both cases, there results

$$\frac{k_0}{\sigma_0} : \frac{k_1}{\sigma_1} = \left( \frac{\overline{v_{m_0}}}{v_{f_0}} - 1 \right) : \left( \frac{\overline{v_{m_1}}}{v_{f_1}} - 1 \right)$$

or

$$\frac{k_1}{\sigma_1} = \frac{k_0}{\sigma_0} \frac{\left( \frac{\overline{v_{m_0}}}{v_{f_0}} - 1 \right)}{\left( \frac{\overline{v_{m_1}}}{v_{f_1}} - 1 \right)} \dots \dots \dots (7)$$

In this way, assuming the susceptibility of a calibrating substance as known, the mass susceptibilities of various substances can be determined from velocity measurements alone. Moreover, the advantage of the method is that the magnetic field can be controlled after each measurement; and this we have done in every case. During these measurements we have not only taken care that the electrical current for the exciting of the electromagnet should be as constant as possible, and that the measurement should be carried out on the same spot in the direction of the  $x$  axis, but, furthermore, that the particle should not leave the central line of the field of vision. The deviations from the centre, *e.g.* on account of the Brownian movement, could not have been greater than 0.2 mm. In this way we could be assured that the product  $H \frac{dH}{dx}$  was measured on one and the same spot during the time of observation.

The results of the measurements are given in the following table. In the first and second columns the quotients  $\frac{\overline{v_m}}{v_f}$  for the substance in question and that for ferric chloride are shown, measured always in the corresponding interval.

In the third column stand the mass susceptibilities for Ag and Se. The mass susceptibilities agree perfectly well with those for the material in bulk. In particular, the mean values of  $\frac{k}{\sigma}$  show quite clearly that the particles actually consist of selenium and silver.

It may further be mentioned that we are here working with red selenium, the mass susceptibility of which has in bulk the value  $0.117 \cdot 10^{-6}$ , which agrees exactly with our value. The value for silver,  $\frac{k}{\sigma} = -0.20 \cdot 10^{-6}$ , comes also within the limits  $-0.19 \cdot 10^{-6}$  to  $-0.22 \cdot 10^{-6}$ , which have been given by several authors for the susceptibility of silver between  $18^\circ$  and  $1100^\circ$ .

TABLE I.

	T. b.	$(\overline{v_m/v_f})_{\text{Ag}}$	$(\overline{v_m/v_f})_{\text{FeCl}_3}$	$\left(\frac{k}{\sigma}\right) \cdot 10^6$
Silver.	15. vii. 1926 .....	0.723	2.519	-0.20
	16. „ „ (a) .....	0.907	1.966	-0.22
	16. „ „ (b) .....	0.910	1.966	-0.21
	17. „ „ .....	0.697	2.519	-0.22
	20. „ „ (a) .....	0.615	3.392	-0.18
	20. „ „ (b) .....	0.566	3.392	-0.20
	Mean value .....			-0.20
Selenium.	T. b.	$(\overline{v_m/v_f})_{\text{Se}}$	$(\overline{v_m/v_f})_{\text{FeCl}_3}$	$\left(\frac{k}{\sigma}\right) \cdot 10^6$
	31. v. 1926 .....	0.807	2.752	-0.12
	5. vi. „ .....	0.913	1.669	-0.14
	18. „ „ .....	0.835	2.752	-0.10
	24. „ „ .....	0.579	4.980	-0.12
	Mean value .....			-0.12

### § 5. *Results of the Researches on Single Colloidal Test Bodies at different Gas Pressures.*

Since the nature of the particles in question has been examined by means of the micromagnetic field, we can now complete the proof of the validity of some other assumptions as to normal density and spherical form of the test bodies. These assumptions, it is well known, must be made if we wish to determine the magnitude of the particles according to the law of resistance. With regard to this problem, we may also refer to the above-cited publication. The method

described in this paper enables us to determine, in a purely mechanical way, the constants of the law of resistance by means of velocity measurements on the same test body at different gas-pressures.

This series of researches, which up to the present time has been made on fluid drops and on solid particles of average density, has now been extended to heavy metallic test bodies. Papers prepared in our Institute \*, which will shortly be published, show that when suitably produced in the electrical arc, silver and gold particles of constants within the limits of the theoretical derived law of resistance can also be obtained. The observed limits between which the single constants vary are much closer than those theoretically determined. The values of the constants of the law of resistance experimentally found closely agree with the values of the constants found for the substances already tested.

TABLE II.

Substance.	$\sigma$ .	$A^2\sigma$ .	A.	Interval of the radii in $10^5$ cm.	$e \cdot 10^{10}$ .	$n$ .
Oil .....	0.93	0.82	0.93	3.59-11.52	4.67	21
$K_2Hg_2I_4$ .. ...	3.01	3.04	1.00	1.96- 4.21	3.75	7
$BaHgI_4$ .....	3.50	3.90	1.05	1.13- 3.25	3.26	17
$Se_I$ .....	4.26	4.35	1.01	1.30- 3.72	2.80	26
$Se_{II}$ .....	"	3.89	0.95	3.19- 5.55	2.56	5
$Se_{III}$ .....	"	4.02	0.97	1.08- 3.34	1.49	17
Ag .....	10.50	12.15	1.07	1.12- 4.08	1.13	21
Au .....	19.18	19.19	1.00	0.83- 1.80	1.04	24

The above table shows the complete results of all the experiments concerning the validity of the law of resistance for single particles of magnitudes down to  $1 \cdot 10^{-5}$  cm. This table is illustrated by fig. 3, which gives the results of measurements of several particles of selenium. The corresponding values of the mean free path of the molecules  $l$  and of the velocities  $u$  define a straight line the intercepts  $\alpha$  and slopes  $\beta$  of which were found by means of the method of least squares. Since for the mobility we have the relation

$$B = \frac{1}{6\pi\mu a} \left( 1 + A \frac{l}{a} \right), \quad . \quad . \quad . \quad . \quad . \quad (8)$$

\* O. Trauner, *ZS. f. Ph.*; M. Slopkovitzer, *ZS. f. Ph.*



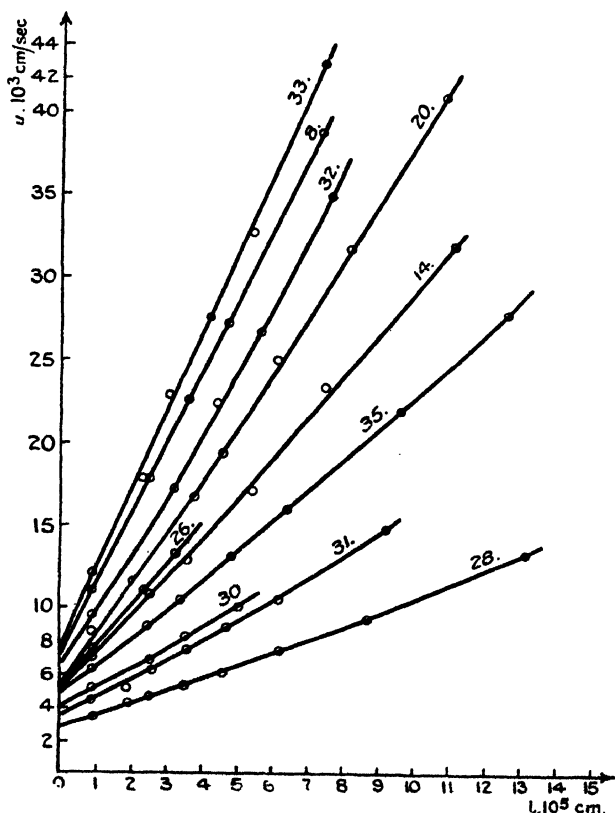
234 Prof. Ehrenhaft and Dr. Wasser on *New Evidence of the*  
the resulting expressions for the above coefficients, taking  
the acting forces † into consideration, are

$$\alpha = \frac{2}{9} \frac{g\sigma}{\mu E^*} a^2; \quad \beta = \frac{2}{9} \frac{g\sigma}{\mu E^*} Aa. \quad . \quad . \quad . \quad (9)$$

From these result the values for  $A^2\sigma$  and  $e/A$  :

$$A^2\sigma = \frac{9}{2} \frac{\mu E^*}{g\sigma} \cdot \frac{\beta^2}{\alpha}; \quad e/A = 6\pi\mu \cdot \frac{\alpha^2}{\beta}. \quad . \quad . \quad . \quad (10)$$

Fig. 3.



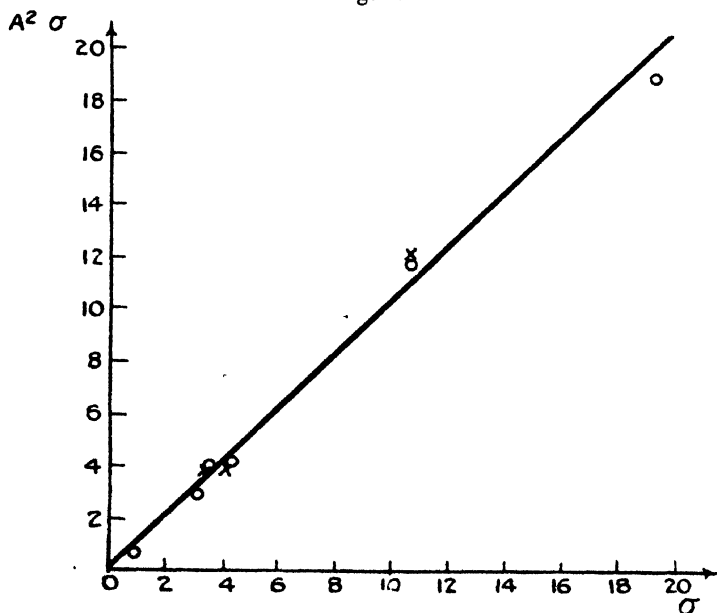
The mean values of  $A^2\sigma$  for all materials tested up to the present time are given in Table II. The number of particles used for the computation of the mean values is marked in the table by "n." If we now compare the densities of the materials in bulk, which run from 0.93 (oil) to 19.2 (gold),

† Cf. F. Ehrenhaft and E. Wasser, *Phil. Mag.* *l. c.*

with the products  $A^2\sigma$ , we notice the proportionality between these two magnitudes. We can illustrate this relationship if we plot in a diagram the densities as abscissæ and  $A^2\sigma$  as ordinates. Fig. 4 shows this diagram. The circles mark the values obtained by computation of the arithmetical mean, while the crosses denote the average values of  $A^2\sigma$  computed by taking the errors of the measurements into consideration.

The results given below were got by measurements on 140 particles of various densities. The number of single observations used for this purpose was about 32,000. As

Fig. 4.



a result of this great number of observations, we may regard the relationship mentioned above as being better established than many well-known laws of physics.

From the proportionality between the densities and the products  $A^2\sigma$ , as well as from the fact that the products  $A^2\sigma$  for one and the same substance show very small deviations from their mean value, the conclusion can be drawn that the single particles produced in various ways have their normal densities and structures. Under this assumption we get the constants  $A$  of the law of resistance, which are also shown in Table II. They all lie in the interval 0.93–1.07, and thus show still smaller deviations from each other than is permitted by the limits theoretically computed. The mean

value of all constants  $A$  is 1.02, whereof the error is certainly no greater than 0.5 per cent., as very many observations have been used for its calculation.

As the constants  $A$ , experimentally determined, prove the validity of all assumptions made for the purpose of the determination of the magnitudes of single test bodies, the charges on these particles can be computed. In each case the smallest charge for each substance is given in Table II. The charges shown there are much smaller than the electron. In particular the value  $1 \cdot 10^{-19}$  E.S.U. was often found for the gold particles; and these values can be repeated. These small charges can neither be explained by deviations from the normal structure of the test bodies, nor by errors in the observations, as will be shown in the next paragraph.

#### § 6. *The Determination of the Errors of the Experimental Results.*

In a paper which is shortly to appear in the *Zeitschrift für Physik*, E. Wasser gives a computation of the errors of observations according to the evacuation method. For this purpose new measurements were made on selenium particles the magnitudes of which were  $1 \cdot 10^{-5}$  cm. to  $3 \cdot 10^{-5}$  cm. Since this critical order of magnitude is characteristic for the determination of small charges, the errors calculated there may be regarded as typical for all other substances.

The averaging of the observations can only be made in accordance with a law which is theoretically well founded. It is well known, theoretically, that for large particles,  $\frac{l}{a} \ll 1$ , the Stokes-Cunningham formula holds in the form as shown by equation (8). For very small particles, however,  $\frac{l}{a} \gg 1$ , the theory gives the relation

$$B = \frac{(A + D)l}{6\pi\mu a^2} \quad \dots \quad (11)$$

An exact theoretical law of resistance should therefore contain both these cases as limits. The empirical formula of Knudsen and Weber\* fulfils these conditions, and also closely agrees with the experiment. If, therefore, we wish to take into consideration the curvatures of the lines experimentally found, we are obliged to make use of the formula

$$B = \frac{1}{6\pi\mu a} \left[ 1 + \frac{l}{a} (A + D e^{-0.5}) \right] \quad \dots \quad (12)$$

\* M. Knudsen and S. Weber, *Ann. d. Phys.* xxxvi. p. 981 (1911).

According to this, the results of measurements on the selenium particles are first approximated to the linear form of the law of resistance, and the errors resulting from this are calculated in the paper cited. The exponential law is then used for the determination of the sizes and charges of the particles, and the errors in these magnitudes are also computed.

If, on the one hand, we assume the relation between the directly measured values of the mean free path,  $l$ , and velocities,  $u$ , to be linear, then we can set

$$u_i = \alpha + \beta l_i, \quad \dots \dots \dots (13)$$

where  $\alpha$  and  $\beta$  have the meaning given above. Taking the expressions for  $\alpha$  and  $\beta$  into consideration, we get

$$A^2\sigma = F(\alpha, \beta, E^*)$$

and

$$e/A = F'(\alpha, \beta). \quad \dots \dots \dots (14)$$

The errors in the products  $A^2\sigma$  and quotients  $e/A$  are therefore composed of the errors in the values for  $\alpha$ ,  $\beta$ , and  $E^*$ . The errors in the last magnitudes were computed according to the method of least squares †, and give the compound errors for  $A^2\sigma$  and  $e/A$  shown in Table III.

TABLE III.

T. b. no.	$A^2\sigma$ .	$\pm m_{A^2\sigma} \%$ .	$e/A$ .	$\pm m_{e/A} \%$ .	$n$ .
1 .....	4.338	9.66	1.479	13.94	3
3 .....	4.710	12.64	1.773	24.80	5
8 .....	3.903	2.10	3.669	3.01	6
9 .....	3.390	7.95	1.920	12.27	4
14 .....	3.645	10.23	2.629	17.30	6
15 .....	3.980	8.23	2.531	13.02	7
20 .....	4.518	11.54	2.202	20.14	6
22 .....	4.655	6.95	2.703	11.64	8
24 .....	5.849	7.68	2.874	12.16	6
28 .....	3.498	4.50	2.740	6.43	8
29 .....	4.686	6.46	2.621	9.83	6
30 .....	4.570	5.07	4.130	5.11	4
31 .....	4.168	7.79	2.338	11.40	6
32 .....	4.614	6.25	3.254	9.16	6
33 .....	5.550	7.08	3.550	10.71	6
35 .....	4.229	5.08	3.364	7.62	8
36 .....	3.625	5.00	3.820	4.52	3
Average mean errors.....		7.30		11.35	

† For the extended formulas used in this case we may refer to the paper by E. Wasser.

As may be seen from the above table, the errors run from 2.1 per cent. to 12.6 per cent. for  $A^2\sigma$ , and from 3.0 per cent. to 24.8 per cent. for  $e/A$ . The average errors for these two magnitudes are 7.3 per cent. and 11.3 per cent. The mean value of the products  $A^2\sigma$ , as well as of the quotients  $e/A$ , cannot be calculated according to the formula for an arithmetical mean, for the reason that each observation carries its own error. For the purpose of calculating the mean value, we must therefore regard the value of exactitude of each single observation. Taking this into consideration, we get

$$\overline{A^2\sigma} = 4.015; \quad \overline{e/A} = 3.066 \cdot 10^{-10}.$$

The average errors for these two mean values are 1.3 per cent. and 1.8 per cent. respectively\*. As the result of measurements on 17 selenium particles, we obtain

$$\overline{A^2\sigma} = 4.015 \pm 0.053; \quad \overline{e/A} = (3.066 \pm 0.056) \cdot 10^{-10}.$$

In order to determine the absolute values of  $A$ ,  $a$ , and  $e$  from the results of observations  $A^2\sigma$  and  $e/A$ , a further assumption must be made about one of the three magnitudes  $A$ ,  $\sigma$ , and  $e$ . Considering the proportionality between the densities  $\sigma$  and the products  $A^2\sigma$  measured on various sub-stances, we may assume for the density its value for selenium in bulk. This assumption enables us to calculate the constants  $A$ , the radii of the test bodies  $a$ , and their charges  $e$ . The corresponding values for these magnitudes are given in Table IV.

By assuming the density  $\sigma$  as an exact figure, the total error in the product  $A^2\sigma$  is reduced to the error in  $A^2$ . In this way we get the average error of each separate value of the constant  $A$  at 3.65 per cent. and the error in the mean value  $\bar{A} = 0.974$  at 0.66 per cent. Table IV. shows these errors in the constants  $A$  as well as the charges  $e$  and the radii  $a$ . Since the average errors in the charges run from 3.2 per cent. to 23.6 per cent., the majority of the charges is much smaller than the elementary unit  $4.77 \cdot 10^{-10}$  E.S.U.

\* There remains the question, how great is the actual variation for the separate values of  $A^2\sigma$  and  $e/A$ . Above all it is to be considered if this average variation is within the probable error. Should this not be the case, it would be an argument in favour of the presence of real deviations; in fact the  $e/A$  vary so much that it is questionable if a mean value is justified. This can, of course, be decided by means of the computation of errors. It is shown in the paper by E. Wasser that these actual variations of the values for  $e/A$  are as great as 39.3 per cent., and thus exceed the limits of the average errors in these magnitudes. Accordingly the charges  $e$  cannot be regarded as constant.

TABLE IV.

T. b. no.	A.	$\pm m_A \%$	$a \cdot 10^5$ cm.	$\pm m_a \%$	$e \cdot 10^{10}$	$\pm m_e \%$
9.....	0.892	3.97	1.08	7.52	1.71	12.90
3.....	1.051	6.32	1.16	13.20	1.86	23.63
15.....	0.966	4.11	1.21	7.90	2.44	13.65
1.....	1.009	4.83	1.25	8.60	1.49	14.75
20.....	1.030	5.77	1.44	11.76	2.27	20.95
8.....	0.957	1.05	1.53	1.91	3.51	3.20
14.....	0.925	5.11	1.66	10.27	2.43	18.03
32.....	1.040	3.12	1.69	5.72	3.38	9.68
33.....	1.141	3.54	1.70	6.60	4.05	11.30
24.....	1.171	3.84	1.91	7.47	3.36	12.76
22.....	1.045	3.47	2.02	6.91	2.82	12.15
36.....	0.922	2.50	2.03	3.74	3.52	5.17
29.....	1.048	3.23	2.06	6.16	2.75	10.34
35.....	0.996	2.54	2.34	4.73	3.35	8.03
31.....	0.989	3.89	2.35	7.23	2.31	12.04
28.....	0.906	2.25	2.92	4.15	2.48	6.81
30.....	1.035	2.53	3.34	4.07	4.27	5.71
Average mean errors ...		3.65		6.93		11.83

Now, the deviations in the charges from the above value cannot be explained by the assumption of the non-validity of the law of resistance, provided this be linear, as has been shown in the above paragraphs.

#### § 7. *The Averaging of the Observational Data according to the Exponential Law of Resistance.*

Should the law of resistance be continuous in the interval between the extreme limits mentioned above, then we are obliged to assume a curvature of the  $(u, l)$ -lines if the mean free path of the molecules,  $l$ , is comparable with the radius  $a$ ; i. e. if  $\frac{l}{a} \sim 1$ . This dependence of the constants  $A$  upon the ratios  $\frac{l}{a}$  is given by the empirical formula of Knudsen and Weber, to which we also made reference in our publication cited above.

Considering the acting forces and the formula (12) for the mobility, we get

$$u = \frac{2 a^3 \sigma g}{9 \mu E^*} \left[ 1 + \frac{l}{a} (A + D e^{-\frac{a}{l}}) \right]. \quad . \quad . \quad . \quad (15)$$

# 240 *Existence of Charges smaller than the Electron.*

We set  $\frac{2}{9} \frac{\sigma g}{\mu E^*} = k$ , and make the averaging according to the constants A, D, C and the radius  $a$ . For this purpose the above expression for  $u$  must be made linear. This can be done by differentiating the equation (15) with regard to the constants A, D, C and the radius  $a$ , and by introducing approximate values for these magnitudes. We therefore set

$$A = A_0 + \beta; \quad D = D_0 + \gamma; \quad C = C_0 + \delta; \quad a = a_0 + \alpha.$$

In this way we obtain linear equations of the form

$$\alpha m_i + \beta n_i + \gamma s_i + \delta t_i = r_i. \quad . \quad . \quad . \quad (16)$$

The minimum condition

$$\Sigma (\alpha m_i + \beta n_i + \gamma s_i + \delta t_i - r_i)^2 = \min. \quad . \quad . \quad (17)$$

gives the normal equations, from which we can calculate the corrections  $\beta$ ,  $\gamma$ ,  $\delta$ ,  $\alpha$ , and from these the averaged values of A, D, C, and  $a$ .

This method of computation enables us to determine the radii of the particles, taking the curvatures of the  $(u, l)$ -lines into consideration. The measurements made up to the present time allow us only in single cases to make use of the averaging above. In the majority of cases, only six points were measured for each  $(u, l)$ -line, which give two surplus equations for the determination of the corrections. This number of equations, however, does not appear to be sufficient for the exact evaluation of the curvature, as the application of the above method of computation to the selenium particles measured in our case has shown. Only in the case of two particles which furnished eight points for the  $(u, l)$ -line did we succeed in averaging the observations according to the exponential law of resistance. In all other cases the errors were so great that a curvature of an opposite sign was also probable.

TABLE V.

T. b. no.	A.	D.	C.	$a, 10^5 \text{ cm.}$	$e, 10^{10} \text{ E.S.U.}$
28 .....	0.860	0.127	3.58	3.02	2.72
35 .....	0.776	0.220	2.38	2.49	4.04
T. b. no.	$\pm m_A$	$\pm m_D$	$\pm m_C$	$\pm m_a$	$\pm m_e$
28 .....	0.140	0.085	1.15	0.08	0.21
35 .....	0.133	0.073	0.89	0.07	0.35

The data for these two particles are shown in Table V.

The calculated error for each magnitude stands under the value in question, and is marked by  $m_A$ ,  $m_D$ ,  $m_C$ ,  $m_a$ ,  $m_e$  respectively. If we now compare the values for  $A$ ,  $a$ , and  $e$  of the above table with the corresponding values for these two particles as calculated according to the linear form of the law of resistance, we may draw the following conclusions :—

If we take the curvatures of the  $(u, l)$ -lines into account, the constants  $A$  become smaller ; but also in this case they remain within the theoretical limits. The radii of the test bodies increase by so much as the constants decrease. Accordingly the charges, too, grow ; they do not, however, reach the value of the electron. If we consider the above two examples, we may assert that, on account of the exponential law of resistance, the charges increase by about 10 per cent. to 15 per cent., as against the charges calculated according to the linear formula. This circumstance, however, cannot explain the large deviations of the charges measured in our case from the value of the elementary unit of electricity.

Vienna,  
Aug. 6, 1927.

XXVI. *Riemannian Null-Geometry.* By J. L. SYNGE, *Sc.D.*, *F.T.C.D.*, University Professor of Natural Philosophy, and A. J. McCONNELL, *B.A.*, Lecturer in Mathematics, Trinity College, Dublin\*.

#### SYNOPSIS.

PART I.—§ 1. Introduction. § 2. Contact of surfaces. § 3. Conjugate cones. § 4. Null-surfaces ; characteristic lines ; geodesic null-lines. § 5. The finite null-cone. § 6. Conditions that a family of geodesic null-lines may constitute a null-surface. § 7. The two null-surfaces passing through an  $(N-2)$ -space. § 8. Geometrical solution of  $\phi=0$ , when  $\phi$  is given over a surface.

PART II.—§ 9. Optical significance of geometrical results. § 10. Reflexion at a moving surface. § 11. Refraction at a moving surface.

#### § 1. Introduction.

WHEN a non-definite line-element is used in Riemannian geometry, there is introduced an important geometrical entity, the null-cone, which does not exist when the line-element is definite. The present paper is concerned with some aspects of the geometry of the null-cone.

\* Communicated by the Authors.

*Phil. Mag.* S. 7. Vol. 5. No. 28. Feb. 1928.

R



In Part I., which treats of pure geometry, the contact of surfaces at ordinary and double points is discussed. A null-surface is defined as an envelope of null-cones, and its partial differential equation is shown to be

$$\Delta_1\phi \equiv g^{mn}\phi_m\phi_n = 0, \quad (\phi_r = \partial\phi/\partial x^r), \quad . \quad (1.1)$$

while the characteristic lines on a null-surface prove to be geodesic null-lines\*. The finite null-cone, formed from all the geodesic null-lines issuing from a point, is shown to be a null-surface. It is proved that through an arbitrary subspace of  $(N-2)$  dimensions there pass two null-surfaces, formed from geodesic null-lines issuing from the points of the subspace, two directions being defined at each point. The duality of the solution of (1.1), when the value of  $\phi$  is given arbitrarily over a surface, is then evident.

Part II. deals with the application of the geometrical results to optics. The propagation of light in space-time being defined by a generalized Huyghens's construction, the history of a light wave in space-time is a null-surface. The history of a light-ray, defined as a characteristic on the history of a wave, is therefore a geodesic null-line. By regarding the wave, instead of the ray, as fundamental, we are able to discuss reflexion and refraction at a moving surface. The results are applicable to the general theory of relativity, but it is hoped that the generality of method may also be of some value in the discussion of other problems.

## PART I.

### § 2. *Contact of surfaces.*

Let there be a manifold  $V_N$  with a coordinate system  $(x^1, x^2, \dots, x^N)$ . Let  $S_{N-1}$  be a surface immersed in  $V_N$ , and let  $P$  and  $Q$  be two points on this surface. Let  $Q$  approach  $P$  along any curve on the surface, and let  $\eta^r$  be quantities proportional to  $(x^r)_Q - (x^r)_P$  in the limit as  $Q$  tends to  $P$ . Any such vector  $\eta^r$  is said to be a *tangent* to the surface at  $P$ , and the totality of tangent vectors constitute the *tangent element* at  $P$ . If the equation of the tangent element is of the form

$$a_m\eta^m = 0, \quad . \quad . \quad . \quad . \quad . \quad . \quad (2.1)$$

\* Equation (1.1) will be found in von Laue's 'Relativitätstheorie,' ii. p. 149 (1921), where he develops the theory of the propagation of electromagnetic waves of evanescent wave-length. He also derives the equations of the light-rays from this equation. Here, however, we are concerned with the geometrical aspect.

we say that P is an *ordinary point*. If the equation of the tangent element is of the form

$$a_{mn}\eta^m\eta^n = 0, \quad . \quad . \quad . \quad . \quad . \quad . \quad (2.2)$$

then P is a *double point*; and so on. Equation (2.1) defines the *elementary tangent plane* at an ordinary point; (2.2) defines the *elementary tangent cone* at a double point.

The contact of surfaces will be defined in terms of the contact of their tangent elements.

Let us consider the intersection of an elementary cone  $C_{N-1}$ , given by (2.2), in which without loss of generality we assume  $a_{mn}$  symmetrical, with an elementary two-space  $V_2$  given by the equation

$$\eta^r = \alpha\lambda^r + \beta\mu^r, \quad . \quad . \quad . \quad . \quad . \quad (2.3)$$

where  $\alpha$  and  $\beta$  are parameters, and  $\lambda^r$  and  $\mu^r$  are fixed vectors.  $V_2$ , in general, cuts  $C_{N-1}$  in two vectors. If these two vectors coincide, we say that  $V_2$  touches  $C_{N-1}$ , and the common vector is the *vector of contact*. The condition for contact is

$$(a_{mn}\lambda^m\mu^n)^2 = a_{mn}\lambda^m\lambda^n \cdot a_{pq}\mu^p\mu^q, \quad . \quad . \quad (2.31)$$

and the vector of contact may be written in the form

$$\eta^r = \lambda^r \cdot a_{mn}\mu^m\mu^n - \mu^r \cdot a_{mn}\lambda^m\mu^n. \quad . \quad . \quad (2.32)$$

In order that  $\lambda^r$  may be the vector of contact, it is necessary and sufficient that

$$a_{mn}\lambda^m\lambda^n = 0 \quad . \quad . \quad . \quad . \quad . \quad (2.33)$$

and

$$a_{mn}\lambda^m\mu^n = 0. \quad . \quad . \quad . \quad . \quad . \quad (2.34)$$

If  $\lambda^r$  be any vector in  $C_{N-1}$  and  $\mu^r$  any vector satisfying (2.34), then the elementary two-space given by (2.3) touches  $C_{N-1}$ ,  $\lambda^r$  being the vector of contact. Thus all the elementary two-spaces touching  $C_{N-1}$  along  $\lambda^r$  constitute an element of  $(N-1)$  dimensions, whose equation is

$$a_{mn}\lambda^m\eta^n = 0, \quad . \quad . \quad . \quad . \quad . \quad (2.4)$$

and which we shall call the *elementary tangent plane* to  $C_{N-1}$  along the vector  $\lambda^r$ .

In order that the elementary plane

$$b_m\eta^m = 0 \quad . \quad . \quad . \quad . \quad . \quad (2.41)$$

may touch the elementary cone

$$a_{mn}\eta^m\eta^n = 0, \quad (a_{ma} = a_{an}), \quad (2.42)$$

it is necessary and sufficient that  $\lambda^r$  exist such that (2.33) is satisfied and the elementary planes (2.4) and (2.41) coincide. This is the case if, and only if,

$$a_{mn}\lambda^m = \theta b_n, \quad . \quad . \quad . \quad . \quad . \quad (2.43)$$

where  $\theta$  is a factor of proportionality. Hence

$$\lambda^m = \theta A^{mn}b_n, \quad . \quad . \quad . \quad . \quad . \quad (2.44)$$

where  $A^{mn}$  is the cofactor of  $a_{mn}$  in the determinant  $|a_{mn}|$ , divided by the determinant. Substitution in (2.33) gives the condition for contact

$$A^{mn}b_m b_n = 0, \quad . \quad . \quad . \quad . \quad . \quad (2.45)$$

while the vector of contact is given by (2.44), from which the factor of proportionality may be omitted.

We can now define the contact of surfaces. If a point common to two surfaces is an ordinary point on each, the surfaces are said to touch when their elementary tangent planes coincide. If the common point is a double point on one surface, the surfaces touch when the elementary tangent cone to one surface is touched by the elementary tangent plane to the other. If the common point is a double point on each surface, the surfaces touch when their elementary tangent cones have a common vector, and the elementary tangent planes to the elementary tangent cones along this common vector coincide.

Let a surface be given by

$$\phi(x^1, x^2, \dots, x^N) = 0. \quad . \quad . \quad . \quad . \quad . \quad (2.5)$$

If  $\partial\phi/\partial x^r$  do not all vanish at P, then P is an ordinary point, and the elementary tangent plane is

$$\phi_m \eta^m = 0. \quad . \quad . \quad . \quad . \quad . \quad (2.51)$$

If  $\partial\phi/\partial x^r$  are all zero, but  $\partial^2\phi/\partial x^r \partial x^s$  do not all vanish, then P is a double point, and the elementary tangent cone is

$$\phi_{mn} \eta^m \eta^n = 0, \quad . \quad . \quad . \quad . \quad . \quad (2.52)$$

where  $\phi_{mn}$  is the second covariant derivative of  $\phi$ .

If P is an ordinary point common to  $\phi=0$  and  $\psi=0$ , the condition for contact is

$$\phi_r = \theta \psi_r, \quad . \quad . \quad . \quad . \quad . \quad (2.6)$$

where  $\theta$  is a factor of proportionality.

If P is a double point on  $\phi=0$  and an ordinary point on

$\psi=0$ , the condition for contact is

$$\Phi^{mn}\psi_m\psi_n = 0, \quad . \quad . \quad . \quad . \quad . \quad (2.61)$$

where  $\Phi^{mn}$  is the cofactor of  $\phi_{mn}$  in  $|\phi_{mn}|$ , divided by this determinant\*.

If P is a double point on  $\phi=0$  and  $\psi=0$ , the condition for contact is that  $\lambda^r$  exist, satisfying

$$\phi_{mn}\lambda^m\lambda^n = 0, \quad \psi_{mn}\lambda^m\lambda^n = 0, \quad . \quad . \quad (2.7)$$

and making the elementary planes

$$\phi_{mn}\lambda^m\eta^n = 0, \quad \psi_{mn}\lambda^m\eta^n = 0. \quad . \quad . \quad (2.71)$$

coincide. Thus we must have

$$\phi_{mn}\lambda^m = \theta\psi_{mn}\lambda^m, \quad . \quad . \quad . \quad . \quad (2.72)$$

where  $\theta$  is a root of the determinantal equation

$$|\phi_{mn} - \theta\psi_{mn}| = 0. \quad . \quad . \quad . \quad . \quad (2.73)$$

Equation (2.72) shows that the satisfaction of the first of (2.7) implies the satisfaction of the second. Thus, to determine whether the surfaces touch, it will be necessary to solve (2.73) and substitute in the first of (2.7) the values of  $\lambda^r$  obtained from (2.72).

### § 3. Conjugate cones.

Let us now introduce a fundamental symmetrical tensor  $g_{mn}$ , which is such that the quadratic form  $g_{mn}dx^mdx^n$  is not definite. The raising or lowering of indices is effected by means of the fundamental tensor. At every point of the manifold there exists an *elementary null-cone*,

$$g_{mn}\eta^m\eta^n = 0. \quad . \quad . \quad . \quad . \quad . \quad (3.1)$$

Two vectors  $\lambda^r, \mu^r$  are said to be *conjugate* (or *perpendicular*) when they satisfy

$$g_{mn}\lambda^m\mu^n = 0. \quad . \quad . \quad . \quad . \quad (3.2)$$

If we are given a plane element  $b_m\eta^m=0$  at a point, there is one, and only one, vector conjugate to every vector in this element, viz.  $b^r$ . If we are given an elementary cone  $C_{N-1}$  with the equation

$$a_{mn}\eta^m\eta^n = 0, \quad (a_{mn} = a_{nm}), \quad . \quad . \quad . \quad (3.21)$$

the *conjugate cone* is defined as the elementary surface formed

\* The notation  $|\phi_{mn}|$ , used indifferently for determinant and modulus, is not satisfactory. We suggest the notation  $|\phi_{mn}|$  for determinant, retaining the customary  $|\phi_{mn}|$  for modulus.

of all the vectors conjugate to the tangent planes of  $C_{N-1}$ . The vector conjugate to the tangent plane  $a_{mn}\lambda^m\eta^n=0$  is

$$\xi^r = g^{rm}a_{mn}\lambda^n. \quad (3.3)$$

Hence

$$\xi_r = a_{rn}\lambda^n \quad (3.31)$$

and

$$\lambda^r = A^{rn}\xi_n, \quad (3.32)$$

where  $A^{mn}$  is defined as in § 2. Substitution in the equation of the cone gives for the conjugate cone the equation,  $\eta^r$  being written instead of  $\xi^r$  for the variable vector,

$$A^{mn}\eta_m\eta_n = 0 \quad (3.33)$$

or

$$A_{mn}\eta^m\eta^n = 0. \quad (3.34)$$

It is easily seen that the relation between conjugate cones is reciprocal. For the vector conjugate to the tangent plane to (3.34) along  $\lambda^r$  is

$$\xi^r = g^{rm}A_{mn}\lambda^n, \quad (3.35)$$

and when this value of  $\xi^r$  is substituted for  $\eta^r$  in (3.21), that equation is satisfied. Thus every vector conjugate to a tangent plane of the conjugate cone belongs to the original cone.

The condition for contact of an elementary plane with a cone may be stated as follows:—*An elementary plane touches a cone if, and only if, the vector conjugate to the plane lies in the conjugate cone.*

If we put  $a_{mn}=g_{mn}$ , we have  $A^{mn}=g^{mn}$  and  $A_{mn}=g_{mn}$ . Thus the null-cone is self-conjugate. The elementary tangent plane to the null-cone along the vector  $\lambda^r$  is

$$g_{mn}\lambda^m\eta^n = 0. \quad (3.4)$$

We may state the following result:—*An elementary plane touches the null-cone if, and only if, the plane contains its own conjugate vector; that vector is then the vector of contact.*

#### § 4. Null-surfaces; characteristic lines; geodesic null-lines.

A null-surface is defined as a surface which touches the elementary null-cone at every point. Equivalently, we may say that it is the envelope of an  $\infty^{N-1}$  family of elementary null-cones. Hence, putting  $A^{mn}=g^{mn}$  and  $b_r=\phi_r$  in (2.45), we see that, in order that the family of surfaces

$$\phi(x^1, x^2, \dots, x^N) = \text{constant} \quad (4.1)$$

may be null-surfaces, it is necessary and sufficient that

$$\Delta_1\phi \equiv g^{mn}\phi_m\phi_n = 0 \quad (4.2)$$

at every point of the manifold. A surface whose normal at every point is a null-vector is a null-surface\*. A surface whose normal at every point lies in the tangent plane is a null-surface.

At every point of a null-surface there exists a vector of contact with the elementary null-cone, given by

$$\lambda^r = \phi^r. \quad . \quad . \quad . \quad . \quad . \quad (4.3)$$

Thus every null-surface contains a congruence of lines defined by these vectors. These are *characteristic lines*. Their differential equations will now be found†. By suitable choice of the parameter  $u$  along any one of these lines we can make

$$\frac{dx^r}{du} = \phi^r \quad . \quad . \quad . \quad . \quad . \quad (4.31)$$

Hence, taking the contravariant derivative with respect to  $u$  along the line, we obtain

$$\frac{d^2 x^r}{du^2} + \left\{ \begin{matrix} r \\ mn \end{matrix} \right\} \frac{dx^m}{du} \frac{dx^n}{du} = \phi^r_{,s} \frac{dx^s}{du} = \phi^r_{,s} \phi^s. \quad (4.32)$$

Covariant derivation of (4.2) with respect to  $x^r$  gives

$$g^{mn} \phi_{mr} \phi_n = 0, \quad . \quad . \quad . \quad . \quad . \quad (4.33)$$

which, since  $\phi_{mr}$  is symmetrical, may be written

$$\phi_{rm} \phi^m = 0. \quad . \quad . \quad . \quad . \quad . \quad (4.34)$$

Thus the last expression in (4.32) vanishes, and the characteristic lines satisfy the equations

$$\frac{d^2 x^r}{du^2} + \left\{ \begin{matrix} r \\ mn \end{matrix} \right\} \frac{dx^m}{du} \frac{dx^n}{du} = 0. \quad . \quad . \quad . \quad (4.4)$$

These equations, together with the particular first integral

$$g_{mn} \frac{dx^m}{du} \frac{dx^n}{du} = 0, \quad . \quad . \quad . \quad . \quad (4.41)$$

determine the characteristic lines. We shall follow the usual custom in referring to any solution of (4.4) and (4.41) as a *geodesic null-line*, reserving the name *characteristic* for those cases where the line is considered in relation to the null-surface on which it lies.

\* Cf. Eisenhart, 'Riemannian Geometry,' p. 41 (1926).

† The work is similar to that of von Laue, *loc. cit.*, but we preserve tensorial form throughout.

If we transform from the parameter  $u$  to a general parameter  $v$ , (4.4) and (4.41) become

$$\left. \begin{aligned} \frac{d^2 x^r}{dv^2} + \left\{ \begin{matrix} r \\ mn \end{matrix} \right\} \frac{dx^m}{dv} \frac{dx^n}{dv} &= \theta \frac{dx^r}{dv}, \\ g_{mn} \frac{dx^m}{dv} \frac{dx^n}{dv} &= 0, \end{aligned} \right\} \quad \dots \quad (4.5)$$

where  $\theta$  is a factor of proportionality. Furthermore, a set of equations in the form (4.5) can always be transformed to (4.4) by transformation of the parameter †. If we put  $v = x^N$ , and eliminate  $\theta$  from (4.5), we obtain  $(N-1)$  differential equations of the second order for the determination of  $x^1, x^2, \dots, x^{N-1}$  as functions of  $x^N$ . Thus a geodesic null-line is uniquely determined when its direction (or the ratios  $dx^1 : dx^2 : \dots : dx^N$ ) is given at a point.

It may be remarked that, although there is no "distance" along a geodesic null-line, there does exist a privileged group of parameters for which the equations take the form (4.4). If  $u$  is any privileged parameter, then all the other privileged parameters are given by

$$w = au + b, \quad \dots \quad (4.6)$$

where  $a$  and  $b$  are constants. Thus any four points  $P_1, P_2, P_3, P_4$  on a geodesic null-line determine a number,

$$\frac{u_2 - u_1}{u_4 - u_3}, \quad \dots \quad (4.61)$$

independent of the particular privileged parameter employed, since this fraction is invariant under the transformation (4.6). Ordinary geodesics also possess a privileged group of parameters,

$$w = as + b, \quad \dots \quad (4.62)$$

and for them the ratio (4.61) reduces to  $P_1 P_2 : P_3 P_4$ .

If we change the fundamental tensor to  $g^{*mn} = \lambda g_{mn}$ , where  $\lambda$  is a function of the coordinates, the elementary null-cones are not changed. Thus null-surfaces and the characteristic lines on them remain unchanged. Hence we expect that geodesic null-lines also remain unchanged. We shall show that this is in fact the case, although the privileged parameters are changed. Since  $g^{*mn} = g^{mn}/\lambda$ , we have

$$\left\{ \begin{matrix} r \\ mn \end{matrix} \right\}^* = \left\{ \begin{matrix} r \\ mn \end{matrix} \right\} + \frac{1}{2\lambda} \left( \delta_n^r \frac{\partial \lambda}{\partial x^m} + \delta_m^r \frac{\partial \lambda}{\partial x^n} - g^{rs} g_{mn} \frac{\partial \lambda}{\partial x^s} \right) \quad \dots \quad (4.7)$$

† Cf. Veblen & Thomas, "The Geometry of Paths," Trans. Amer. Math. Soc. xxv. p. 556 (1923).

and hence

$$\begin{aligned} \frac{d^2 x^r}{du^2} + \left\{ \begin{matrix} r \\ mn \end{matrix} \right\}^* \frac{dx^m}{du} \frac{dx^n}{du} \\ = \frac{d^2 x^r}{du^2} + \left\{ \begin{matrix} r \\ mn \end{matrix} \right\} \frac{dx^m}{du} \frac{dx^n}{du} + \frac{1}{\lambda} \frac{d\lambda}{du} \frac{dx^r}{du} - \frac{1}{2} g^{*rs} \frac{\partial \lambda}{\partial x^s} g_{mn} \frac{dx^m}{du} \frac{dx^n}{du}. \end{aligned} \quad (4.71)$$

Thus, if a curve satisfies (4.4) and (4.41), it also satisfies

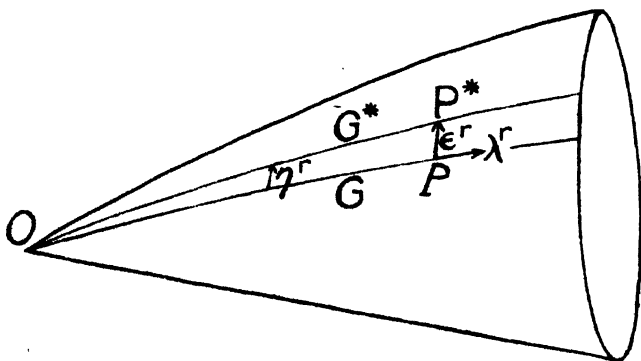
$$\left. \begin{aligned} \frac{d^2 x^r}{du^2} + \left\{ \begin{matrix} r \\ mn \end{matrix} \right\}^* \frac{dx^m}{du} \frac{dx^n}{du} &= \theta \frac{dx^r}{du}, \quad \theta = \frac{1}{\lambda} \frac{d\lambda}{du}, \\ g^{*mn} \frac{dx^m}{du} \frac{dx^n}{du} &= 0, \end{aligned} \right\} \quad (4.72)$$

which are the equations of a geodesic null-line in the form (4.5).

### § 5. The finite null-cone.

The totality of geodesic null-lines issuing from a point  $O$  form a surface which we shall call *the finite null-cone with vertex  $O$* . It is not evident that a finite null-cone is a null-surface in the sense of our definition. We shall now prove that this is in fact the case.

Fig. 1.



It is required to prove that the finite null-cone touches the elementary null-cone at every point on it, other than the vertex  $O$ . Thus, if  $P$  be any point on the finite null-cone and  $G$  the geodesic null-line passing through  $O$  and  $P$ , it is required to prove that the vector  $\epsilon^r$ , drawn from  $P$  to any neighbouring point  $P^*$  of the finite null-cone, is conjugate to the tangent to  $G$  at  $P$ .



Let  $G^*$  be the geodesic null-line through  $O$  and  $P^*$  (fig. 1). Having selected a privileged parameter  $u$  for  $G$ , so that its equations take the form (4.4), it will be possible to choose a privileged parameter  $u$  for  $G^*$  in such a way that the parameters for  $G$  and  $G^*$  have the same value at  $O$  and the same value at  $P$  and  $P^*$ . Now, if  $\eta^r$  denote the infinitesimal vector joining any point of  $G$  to the point of  $G^*$  having the same value of the parameter, we have

$$(\eta^r)_P = \epsilon^r, \quad . \quad . \quad . \quad . \quad . \quad (5.1)$$

and, since  $G^*$  has a null direction at every point,

$$\left(g_{mn} + \frac{\partial g_{mn}}{\partial x^r} \eta^r\right) \frac{d}{du} (x^m + \eta^m) \frac{d}{du} (x^n + \eta^n) = 0, \quad . \quad (5.2)$$

where  $x^r$  denote the coordinates of any point on  $G$ . Subtracting the equation

$$g_{mn} \frac{dx^m}{du} \frac{dx^n}{du} = 0, \quad . \quad . \quad . \quad . \quad (5.21)$$

and retaining only terms of the first order, we obtain

$$g_{mn} \bar{\eta}^m \frac{dx^n}{du} = 0, \quad . \quad . \quad . \quad . \quad (5.3)$$

where

$$\bar{\eta}^m = \frac{d\eta^m}{du} + \left\{ \begin{matrix} m \\ pq \end{matrix} \right\} \eta^p \frac{dx^q}{du}. \quad . \quad . \quad . \quad (5.31)$$

But from (4.4) we have

$$\frac{d}{du} \left( g_{mn} \eta^m \frac{dx^n}{du} \right) = g^{mn} \bar{\eta}^m \frac{dx^n}{du}, \quad . \quad . \quad . \quad (5.4)$$

and this vanishes by virtue of (5.3). Thus along  $G$  we have

$$g_{mn} \eta^m \frac{dx^n}{du} = \text{constant}. \quad . \quad . \quad . \quad (5.5)$$

But  $\eta^r$  vanishes at  $O$ ; therefore the constant is zero. Hence at  $P$

$$g_{mn} \epsilon^m \lambda^n = 0, \quad . \quad . \quad . \quad . \quad (5.6)$$

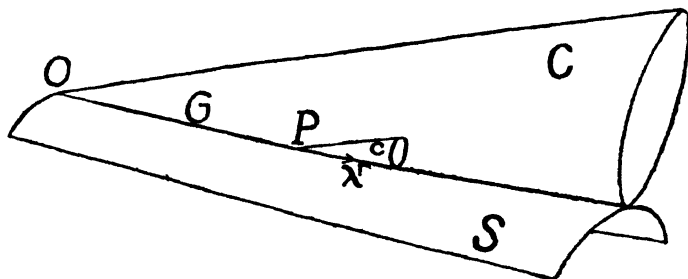
where  $\lambda^r$  is the tangent vector to  $G$ . Thus  $\epsilon^r$  is the conjugate to  $\lambda^r$ , and we have proved that *a finite null-cone is a null-surface*.

Let  $S$  be a null-surface and  $O$  a point on it. Let  $C$  be the finite null-cone with vertex  $O$ . Since  $S$  touches  $C$  at  $O$  they have a common tangent vector at  $O$ , and this vector defines a geodesic null-line  $G$  contained in  $C$  and also in  $S$ ,

as a characteristic line (fig. 2). We shall now prove that  $S$  touches  $C$  at every point of  $G$ .

Let  $P$  be any point on  $G$ , and let  $c$  be the elementary null-cone at  $P$ . Then, by the result established above,  $C$  touches  $c$  at  $P$ , the vector of contact being  $\lambda^r$ , the tangent vector

Fig. 2.



to  $G$ . But  $S$  also touches  $c$ , and has the same vector of contact. Thus the tangent planes to  $S$  and  $C$  at  $P$  coincide, being the tangent plane to  $c$  along  $\lambda^r$ ; thus the result is established.

#### § 6. Conditions that a family of geodesic null-lines may constitute a null-surface.

In the case of the finite null-cone we dealt with an  $\infty^{N-2}$  family of geodesic null-lines constituting a null-surface. An  $\infty^{N-2}$  family of geodesic null-lines picked at random, subject only to a condition of continuity, will not in general form a null-surface. We proceed to investigate the conditions which the family must satisfy.

Let  $S_{N-1}$  be a surface cut by the family. Each geodesic null-line cuts a surface in a point, and thus all the points of section form an  $(N-2)$ -space,  $\Sigma_{N-2}$ . Let the parametric equations of  $\Sigma_{N-2}$  be

$$x^r = x^r(\alpha_1, \alpha_2, \dots, \alpha_{N-2}) \dots \dots \dots (6.1)$$

There will be associated with every point of  $\Sigma_{N-2}$  a direction, viz. that of the geodesic null-line passing through it, which we shall denote by  $\xi^r$ . Thus

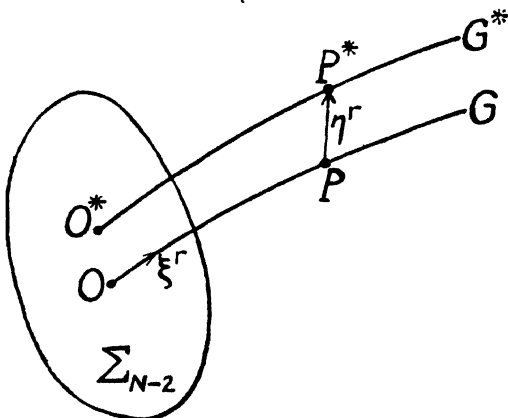
$$\xi^r = \xi^r(\alpha_1, \alpha_2, \dots, \alpha_{N-2}), \quad g_{mn} \xi^m \xi^n = 0. \dots (6.2)$$

The problem before us is the investigation of the conditions controlling the functions in (6.2). The method adopted is similar to that used in § 5.  $G$  and  $G^*$  are two neighbouring

geodesic null-lines, cutting  $\Sigma_{N-2}$  at  $O$  and  $O^*$  (fig. 3). Privileged parameters are chosen, having the same value at  $O$  and  $O^*$ .  $P$  and  $P^*$  are points with equal values of the parameter, and  $\eta^r$  the vector from  $P$  and  $P^*$ . We derive exactly as before

$$g_{mn}\eta^m \frac{dx^n}{du} = \text{constant.} \quad (6.3)$$

Fig. 3.



In order that the geodesic null-lines may form a null-surface, it is necessary and sufficient that this constant should vanish all over  $\Sigma_{N-2}$ . Thus all over  $\Sigma_{N-2}$  we must have

$$g_{mn}\eta^m \xi^n = 0. \quad (6.4)$$

for all values of  $\eta^r$  given by

$$\eta^r = \sum_{A=1}^{N-2} \frac{\partial x^r}{\partial \alpha_A} \delta \alpha_A. \quad (6.41)$$

Hence at all points of  $\Sigma_{N-2}$  we must have

$$g_{mn} \frac{\partial x^m}{\partial \alpha_A} \xi^n = 0, \quad (A = 1, 2, \dots, N-2), \quad (6.5)$$

$$g_{mn} \xi^m \xi^n = 0. \quad (6.51)$$

From (6.5) we derive  $(N-2)$  of the ratios  $\xi^1 : \xi^2 : \dots : \xi^N$  as linear functions of the remaining ratio. Substitution in (6.51) gives a quadratic equation for this remaining ratio. Thus at every point of  $\Sigma_{N-2}$  the direction of the geodesic null-line must be one of two directions, which are given when  $\Sigma_{N-2}$  is known. These two directions may be called the *characteristic directions associated with any point of  $\Sigma_{N-2}$* .

They are, in fact, the characteristic directions on the elementary envelope of the  $N-2$  family of elementary null-cones having their vertices in  $\Sigma_{N-2}$ .

§ 7. *The two null-surfaces passing through an  $(N-2)$ -space.*

Let  $\Sigma_{N-2}$  be an arbitrary subspace immersed in  $V_N$ . From § 6 we see that there are two families of geodesic null-lines passing through  $\Sigma_{N-2}$  and forming null-surfaces. From (6.5) we see that the characteristic directions on these null-surfaces are conjugate to every direction tangent to  $\Sigma_{N-2}$ . Now, the normal at a point on a surface is unique, but the normals at a point on a subspace of  $(N-2)$  dimensions form a linear two-space. Thus the characteristic directions at any point lie in the linear two-space normal to  $\Sigma_{N-2}$ . Let  $\lambda^r$  and  $\mu^r$  be two vectors assigned at every point of  $\Sigma_{N-2}$  and lying in the normal two-space. Then for either of the characteristic directions at any point we may write

$$\xi^r = \alpha\lambda^r + \beta\mu^r, \quad . \quad . \quad . \quad (7.1)$$

where  $\alpha$  and  $\beta$  are as yet undetermined. Since  $\xi^r$  is a null-vector, we have

$$\alpha^2 g_{mn} \lambda^m \lambda^n + 2\alpha\beta g_{mn} \lambda^m \mu^n + \beta^2 g_{mn} \mu^m \mu^n = 0, \quad . \quad (7.2)$$

a quadratic equation for the determination of the ratio  $\alpha : \beta$ ; hence the directions of the characteristic vectors  $\xi_{(1)}^r, \xi_{(2)}^r$  are determined. The totality of geodesic null-lines drawn in the directions  $\xi_{(1)}^r, \xi_{(2)}^r$  at all points of  $\Sigma_{N-2}$  constitute the two null-surfaces passing through  $\Sigma_{N-2}$ .

Let it be required to determine the second null-surface passing through the intersection of a surface  $S_{N-1}$ , given by  $f = \text{constant}$ , and a null-surface, given by  $\phi = \text{constant}$ . The characteristic directions at a point in  $\Sigma_{N-2}$ , the subspace of intersection, are given by (7.1), with  $\lambda^r = f^r$  and  $\mu^r = \phi^r$ . But

$$g_{mn} \phi^m \phi^n = 0, \quad . \quad . \quad . \quad (7.3)$$

and therefore (7.2) reduces to

$$\alpha^2 g_{mn} f^m f^n + 2\alpha\beta g_{mn} f^m \phi^n = 0. \quad . \quad . \quad (7.4)$$

This gives as one solution  $\alpha = 0$ , leading by (7.1) to the characteristic direction  $\xi_{(1)}^r = \phi^r$ , belonging to the given null-surface. The other solution is

$$\frac{\alpha}{\beta} = -2 \frac{g_{mn} f^m \phi^n}{g_{mn} f^m f^n}. \quad . \quad . \quad . \quad (7.5)$$

Hence the second characteristic direction, belonging to the required null-surface, may be written

$$\xi_{(2)}^r = 2f^r \cdot g_{mn} f^m \phi - \phi^r \cdot g_{mn} f^m f^n, \quad \dots \quad (7.6)$$

the sense of  $\xi_{(2)}^r$  and the magnitudes of its components being at present of no significance. We note that the two characteristic directions and the normal to the given surface lie in a linear two-space, as is, indeed, also obvious from (7.1), since the normal to  $S_{N-1}$  at a point in  $\Sigma_{N-2}$  must lie in the linear two-space normal to  $\Sigma_{N-2}$ .

The second characteristic direction is the second intersection of the null-cone at the point with the linear two-space containing the first characteristic direction and the normal to  $S_{N-1}$ .

§ 8. *Geometrical solution of  $\Delta_1 \phi = 0$ , when  $\phi$  is given over a surface.*

The integrals  $\phi = \text{constant}$  of the partial differential equation

$$\Delta_1 \phi \equiv g^{mn} \phi_m \phi_n = 0 \quad \dots \quad (8.1)$$

are null-surfaces in the language of this paper. Let it be required to find a function  $\phi(x^1, x^2, \dots, x^N)$  to satisfy (8.1) and to have arbitrarily-assigned values at all points of a surface  $S_{N-1}$ . The given subspaces  $\phi = \text{constant}$  in  $S_{N-1}$  are each of  $(N-2)$  dimensions; we have seen how to construct the two null-surfaces passing through each such subspace. In this way we obtain two singly-infinite families of null-surfaces. Thus at any point P outside  $S_{N-1}$  there are two values of  $\phi$ , which are the two values of  $\phi$  on  $S_{N-1}$  at the intersections of  $S_{N-1}$  with the two null-surfaces (one belonging to each family) passing through P.

If the finite null-cone with vertex P be drawn, the two null-surfaces passing through P touch this cone along two geodesic null-lines. Thus there pass through P two geodesic null-lines such that the two values of  $\phi$  at P are equal respectively to the two values of  $\phi$  at the points where  $S_{N-1}$  is cut by these two geodesic null-lines. These two geodesic null-lines may be selected from those forming the finite null-cone by the condition that their directions at the points where they meet  $S_{N-1}$  must coincide with one or other of the two characteristic directions associated with each point of the subspace of  $(N-2)$  dimensions formed by the intersection of  $S_{N-1}$  with the finite null-cone.

If  $\phi$  is constant over  $S_{N-1}$ , the method requires modification.

PART II.

§ 9. *Optical significance of geometrical results.*

The subject of geometrical optics deals with rays and phase-waves. It is the limit to which physical optics approximates as the wave-length tends to zero. We wish here briefly to develop a theory of geometrical optics, applicable to the gravitational field of Einstein, and based on a generalization of Huyghens's construction.

We define the mode of propagation of light by the condition that *the history of a light-wave in space-time is an envelope of elementary null-cones*. The history of a light-wave is therefore a null-surface. We define the history of a light-ray as a characteristic line on the history of a light-wave. Our method therefore enables us to deduce from our generalization of Huyghens's construction the well-known equations—(1.1) for the history of a light-wave and (4.4), (4.41) for the history of a light-ray. The optical disturbance from a point-event is the finite null-cone having its vertex at the event, and the histories of the rays are the geodesic null-lines which form the finite null-cone.

It is to be observed that, while this theory is formulated so as to be applicable to the general theory of relativity, all the results of ordinary geometrical optics can be deduced from it by putting

$$g_{mn}dx^m dx^n = d\sigma^2 - V^2 dt^2, \quad . \quad . \quad . \quad (9.1)$$

where  $d\sigma$  is the spatial line-element and  $V$  the velocity of light.

§ 10. *Reflexion at a moving surface.*

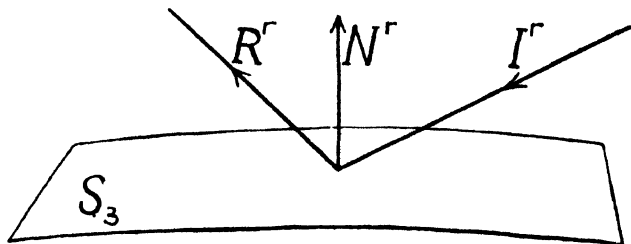
The history of a moving body fills up a portion of space-time. That portion is bounded by a surface  $S_2$ , which is the history of the surface (in the ordinary sense) of the material body. Let us suppose that a light-wave impinges on the surface. The intersection of the history of the light-wave with  $S_2$  forms a subspace  $\Sigma_2$  in space-time. Through  $\Sigma_2$ , according to § 7, there pass two null-surfaces, of which one is the history of the incident wave and the other is the history of the reflected wave. The two characteristic directions at any point of  $\Sigma_2$  belong to the histories of the incident and reflected rays. From the remark at the end of § 7, we see how the history of the reflected ray can be constructed when the history of the incident ray and the normal to the history of the reflecting surface are known.

We may state the law of reflexion in space-time: *The*

histories of the incident and reflected rays and the normal to the history of the reflecting surface lie in an elementary linear two-space. It is impossible to state anything concerning the "angles of incidence and reflexion" in space-time, since the angle between a null-vector and another vector is not defined.

The ratios of the components of a tangent vector to a geodesic null-line indicate the curve in space-time along which light is propagated. The sense in which the propagation actually takes place will be indicated by the signs of the components of the tangent vector.

Fig. 4.



Let us denote by  $I^r$  and  $R^r$  respectively vectors tangent to the histories of the incident and reflected rays and indicating the senses of propagation of those histories; let  $N^r$  be a vector normal to the history of the reflecting surface (fig. 4). Then, instead of (7.6), in which no attention was paid to the sense of  $\xi_{(2)}^r$ , we write

$$kR^r = 2N^r \cdot g_{mn} I^m N^n - I^r \cdot g_{mn} N^m N^n, \quad (10.1)$$

where the sign of  $k$  is physically determinate.

Now it is evident that, whether  $N^r$  be drawn as in the figure or in the reverse direction, we must have

$$N^r = \alpha I^r + \beta R^r, \quad (10.2)$$

where  $\alpha$  and  $\beta$  have opposite signs. Thus  $k$  and  $g_{mn} N^m N^n$  must have opposite signs. Remembering that the actual values of the components of  $R^r$  have no physical significance, we may write

$$k = -g_{mn} N^m N^n, \quad (10.21)$$

and hence

$$R^r = I^r - 2N^r \frac{g_{mn} I^m N^n}{g_{mn} N^m N^n}. \quad (10.3)$$

This is the formula for reflexion at a moving surface.

Let us now apply our result to the case of a stationary gravitational field in which  $x^1, x^2, x^3$  are spatial coordinates and  $x^4$  the time. If we understand a range or summation from 1 to 3 when Greek indices are used, such a field is characterized by the equations

$$g_{\mu 4} = 0, \quad \partial g_{mn} / \partial x^4 = 0. \quad . \quad . \quad . \quad (10.4)$$

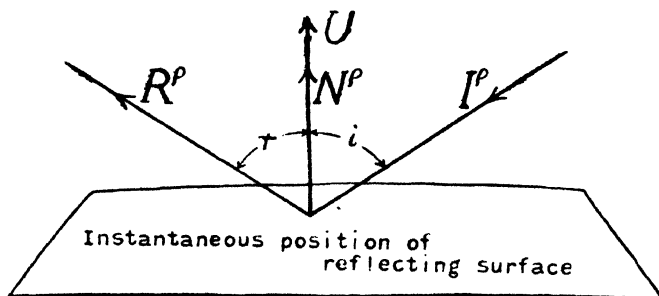
The spatial line-element is given by

$$d\sigma^2 = g_{\mu\nu} dx^\mu dx^\nu, \quad . \quad . \quad . \quad (10.41)$$

and the velocity of light by

$$V^2 = -g_{44}. \quad . \quad . \quad . \quad (10.42)$$

Fig. 5.



The vectors  $I^\rho$  and  $R^\rho$  represent the directions of the incident and reflected rays in space. The vector  $N^\rho$  is the normal in space to the instantaneous position of the reflecting surface. We shall assume it drawn into the region of incidence (fig. 5). If  $i$  and  $r$  denote the angles of incidence and reflexion in the ordinary sense, we have

$$\left. \begin{aligned} \cos i &= -g_{\mu\nu} I^\mu N^\nu / [(g_{\rho\sigma} I^\rho I^\sigma)^\dagger (g_{\theta\phi} N^\theta N^\phi)^\dagger], \\ \cos r &= g_{\mu\nu} R^\mu N^\nu / [(g_{\rho\sigma} R^\rho R^\sigma)^\dagger (g_{\theta\phi} N^\theta N^\phi)^\dagger]. \end{aligned} \right\} \quad (10.5)$$

Since  $I^\rho$  and  $R^\rho$  are null-vectors, we have

$$g_{\rho\sigma} I^\rho I^\sigma = -g_{44} (I^4)^2, \quad g_{\rho\sigma} R^\rho R^\sigma = -g_{44} (R^4)^2. \quad (10.6)$$

Moreover, since  $x^4$  increases along these vectors,  $I^4$  and  $R^4$  are positive. Thus

$$(g_{\rho\sigma} I^\rho I^\sigma)^\dagger = V I^4, \quad (g_{\rho\sigma} R^\rho R^\sigma)^\dagger = V R^4. \quad . \quad (10.61)$$

Now, in (10.3) the magnitudes of the components of  
*Phil. Mag.* 8. 7. Vol. 5. No. 28. Feb. 1928. S



$I^r$  and  $N_r$  are arbitrary. We may therefore choose them so that  $I^p$  and  $N^p$  are unit vectors in space. Then

$$g_{\rho\sigma}I^pI^\sigma = 1, \quad g_{\rho\sigma}N^pN^\sigma = 1, \quad . \quad . \quad . \quad (10.62)$$

and hence

$$I^4 = 1/V. \quad . \quad . \quad . \quad (10.63)$$

Thus (10.5) give

$$\cos i = -g_{\mu\nu}I^\mu N^\nu, \quad \cos r = g_{\mu\nu}R^\mu N^\nu / VR^4. \quad (10.7)$$

If  $dx^1, dx^2, dx^3$  denote the infinitesimal displacement in time  $dx^4$  of a hypothetical particle confined to the reflecting surface, we have

$$g_{\mu\nu}dx^\mu N^\nu + g_{44}dx^4N^4 = 0, \quad . \quad . \quad . \quad (10.71)$$

and, if the displacement of the particle is along the instantaneous normal to the reflecting surface, we have

$$dx^\rho/dx^4 = \theta N^\rho. \quad . \quad . \quad . \quad (10.72)$$

Thus, from (10.71),

$$\theta = -g_{44}N^4; \quad . \quad . \quad . \quad (10.73)$$

and hence, if  $U$  denotes the normal velocity of the reflecting surface in the sense of  $N_p$ ,

$$U = -g_{44}N^4, \quad N_4 = U/V^2. \quad . \quad . \quad . \quad (10.74)$$

We deduce

$$\frac{g_{mn}I^mN^n}{g_{mn}N^mN^n} = -\frac{V(V\cos i + U)}{V^2 - U^2}. \quad . \quad . \quad (10.8)$$

Using the first three equations of (10.3), we obtain

$$g_{\mu\nu}R^\mu N^\nu = \frac{V^2\cos i + 2VU + U^2\cos i}{V^2 - U^2}, \quad . \quad (10.81)$$

while the last of (10.3) gives

$$R^4 = \frac{V^2 + 2VU\cos i + U^2}{V(V^2 - U^2)}. \quad . \quad . \quad (10.82)$$

Thus, substituting in (10.7), we find for the angle of reflexion

$$\begin{aligned} \cos r &= \frac{V^2\cos i + 2VU + U^2\cos i}{V^2 + 2VU\cos i + U^2} \\ &= \cos i + \frac{2VU\sin^2 i}{V^2 + 2VU\cos i + U^2}. \end{aligned} \quad (10.9)$$

Here  $V$  is the velocity of light, and  $U$  is the normal velocity of the reflecting surface along the normal drawn into the region of incidence.

It must be pointed out that, while (10.3) is believed to be

new and important, (10.9) can be deduced by a direct constructional method by means of the classical Huyghens's construction; the method presents no difficulties as soon as one is satisfied as to the legitimacy of reducing the problem to that of the incidence of a plane wave on a plane mirror which has a motion of translation in Euclidean space\*. The deduction is given here as an example of the general method, which has the advantage of being obviously invariant in character. The result is also valid for a Galileian frame.

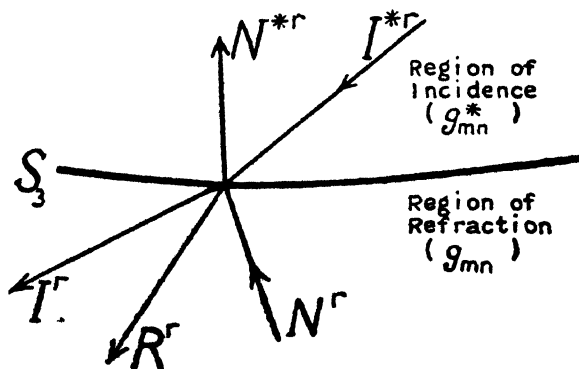
### § 11. Refraction at a moving surface.

The history of the surface of separation of two media constitutes a surface  $S_3$  in space-time.  $S_3$  divides space-time into two regions, the region of incidence and the region of refraction. Let the null-cones in these regions be respectively

$$g_{mn}^* \eta^m \eta^n = 0, \quad g_{mn} \eta^m \eta^n = 0. \quad . \quad . \quad (11.1)$$

The fundamental tensor is, in general, discontinuous across  $S_3$ .

Fig. 6.



Let a light-wave be incident on the surface of separation. Then the intersection of the history of this wave with  $S_3$  forms a two-space,  $\Sigma_2$ . From each point of  $\Sigma_2$  there issue four characteristic directions, two in the region of incidence (corresponding to the incident and reflected rays), and two in the region of refraction.

Let  $f=0$  be the equation of  $S_3$ , and  $\phi=0$  the equation of

\* A formula equivalent to (10.9), developed in this way for this special case, will be found in Silberstein's 'Theory of Relativity,' p. 89 (1924).

the history of the incident wave. There are two contra-variant vectors normal to  $S_3$ , viz.:

$$N^{*r} = g^{*rm} f_m, \text{ for the region of incidence ; } . \quad (11.2)$$

$$N^r = g^{rm} f_m, \text{ for the region of refraction } . \quad (11.21)$$

Similarly the history of the incident wave has two normals at every point where it meets  $S_3$ , viz.:

$$I^{*r} = g^{*rm} \phi_m, \text{ in the region of incidence ; } . \quad (11.22)$$

$$I^r = g^{rm} \phi_m, \text{ in the region of refraction. } . \quad (11.23)$$

We shall suppose the sign of  $\phi$  so chosen that  $I^{*r}$  indicates the sense of propagation of the incident ray, *i. e.* is directed towards  $S_3$  (fig. 6).

The vectors  $N^r$  and  $I^r$  are normal to  $\Sigma_2$  in the region of refraction. Hence (*cf.* (7.1)) the vector  $R^r$ , tangent to the history of the refracted ray and indicating its sense of propagation, will be given by

$$kR^r = \alpha N^r + \beta I^r, \quad . \quad . \quad . \quad (11.3)$$

where  $k$  is a number whose sign is physically determinate when values have been assigned to  $\alpha$  and  $\beta$ , and where the ratio  $\alpha : \beta$  is determined by

$$\alpha^2 g_{mn} N^m N^n + 2\alpha\beta g_{mn} I^m N^n + \beta^2 g_{mn} I^m I^n = 0. \quad (11.31)$$

If the roots of this equation are imaginary, there is *total reflexion*. If the roots are real, we have

$$\frac{\alpha}{\beta} = -\frac{g_{mn} I^m N^n}{g_{mn} N^m N^n} \left[ 1 \pm \left( 1 - \frac{g_{pq} I^p I^q \cdot g_{uv} N^u N^v}{(g_{pq} I^p N^q)^2} \right)^{\frac{1}{2}} \right]. \quad (11.4)$$

Now, in the particular case where  $g_{mn} = g^{*mn}$  on  $S_3$ ,  $I^r$  is a null-vector in the region of refraction. Thus (11.4) reduces to

$$\frac{\alpha}{\beta} = -\frac{g_{mn} I^m N^n}{g_{mn} N^m N^n} [1 \pm 1], \quad . \quad . \quad (11.41)$$

But in this case there will be no refraction; therefore we require  $\alpha = 0$ . Thus the minus sign must be taken in (11.41). From continuity this sign must be taken in general in (11.4). Furthermore, in the particular case considered,  $R^r$  and  $I^r$  must indicate the same sense. Hence we see that the general formula may be written

$$R = I^r - N^r \frac{g_{mn} I^m N^n}{g_{mn} N^m N^n} \left[ 1 - \left( 1 - \frac{g_{pq} I^p I^q \cdot g_{uv} N^u N^v}{(g_{pq} I^p N^q)^2} \right)^{\frac{1}{2}} \right]. \quad (11.5)$$

This is the formula for refraction at a moving surface.

We may state the following law of refraction: *The history of the refracted ray and the normals (in the region of refraction) to the histories of the incident wave and the surface of separation lie in an elementary linear two-space. An analogous theorem holds in the region of incidence.*

Let us apply our result to the case of refraction at a moving surface in a stationary gravitational field. We assume

$$g_{\mu 4}^* = g_{\mu 4} = 0, \quad \frac{\partial g_{mn}^*}{\partial x^4} = \frac{\partial g_{mn}}{\partial x^4} = 0, \quad . \quad (11.6)$$

and, on  $S_3$ , the history of the moving surface,

$$g_{\mu\nu}^* = g_{\mu\nu} \quad . \quad . \quad . \quad (11.61)$$

Hence we have

$$I^{*\rho} = I^\rho, \quad N^{*\rho} = N^\rho. \quad . \quad . \quad . \quad (11.62)$$

Let the magnitudes of  $I^\rho$  and  $N^\rho$  be chosen so that

$$g_{\mu\nu} I^\mu I^\nu = 1, \quad g_{\mu\nu} N^\mu N^\nu = 1. \quad . \quad . \quad (11.63)$$

Let  $V^*$ ,  $V$  be the velocities of light in the regions of incidence and refraction respectively. Then

$$V^{*2} = -g_{44}^*, \quad V^2 = -g_{44}. \quad . \quad . \quad (11.64)$$

Let  $U$  be the normal velocity of the moving surface, measured from the region of refraction into the region of incidence, and let us define  $\mu$  and  $\nu$  by the equations

$$V^* = \mu V, \quad U = \nu V. \quad . \quad . \quad . \quad (11.65)$$

Then, as in (10.63) and (10.74) respectively,

$$I^{*4} = 1/V^*, \quad N^4 = U/V^2 = \nu/V. \quad . \quad . \quad (11.66)$$

Now

$$I^4 = g^{44} g_{44}^* I^{*4} = g_{44}^* I^{*4} / g_{44} = \mu / V, \quad . \quad . \quad (11.67)$$

and therefore

$$g_{mn} I^m I^n = 1 - \mu^2, \quad g_{mn} N^m N^n = 1 - \nu^2. \quad . \quad (11.68)$$

Also, since

$$\cos i = -g_{\mu\nu} I^\mu N^\nu, \quad . \quad . \quad . \quad (11.69)$$

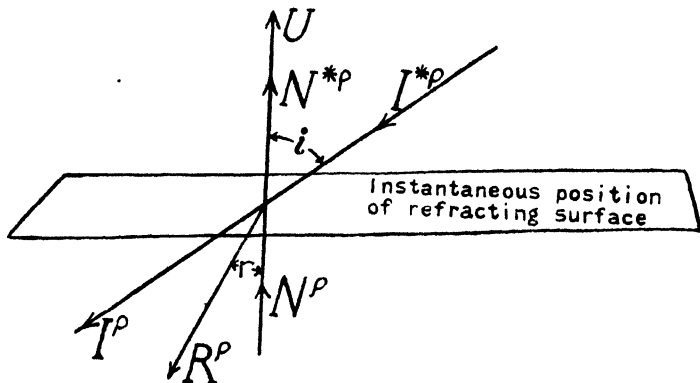
where  $i$  denotes the angle of incidence in the ordinary sense (fig. 7), we have

$$g_{mn} I^m N^n = -\cos i = -\mu\nu. \quad . \quad . \quad (11.7)$$

Thus we have, as the evaluation of the expression in (11.5),

$$\left\{ 1 - \frac{g_{pq} I^p I^q \cdot g_{uv} N^u N^v}{(g_{pq} I^p N^q)^2} \right\}^{\frac{1}{2}} = \left\{ 1 - \frac{(1-\mu^2)(1-\nu^2)}{(\cos i + \mu\nu)^2} \right\}^{\frac{1}{2}}, \quad (11.71)$$

Fig. 7.



and if we denote this quantity by K, we have, by (11.5),

$$R^{\rho} = I^{\rho} + N^{\rho} \frac{\cos i + \mu\nu}{1-\nu^2} (1-K), \quad \dots \dots \dots (11.72)$$

$$\begin{aligned} R^4 &= \frac{\mu}{V} + \frac{\nu \cos i + \mu\nu}{V(1-\nu^2)} (1-K) \\ &= \frac{(\mu + \nu \cos i) - \nu K (\cos i + \mu\nu)}{V(1-\nu^2)} \dots \dots \dots (11.73) \end{aligned}$$

But, if  $r$  denotes the angle of refraction in the ordinary sense, we have

$$\cos r = -g_{\mu\nu} R^{\mu} N^{\nu} / VR^4, \quad \dots \dots (11.74)$$

and therefore, by the above equations,

$$\cos r = \frac{-\nu(\mu + \nu \cos i) + K(\cos i + \mu\nu)}{(\mu + \nu \cos i) - \nu K(\cos i + \mu\nu)}. \quad \dots (11.75)$$

This is the formula for refraction at a moving surface in a stationary gravitational field, the quantities  $\mu$  and  $\nu$  being defined by (11.65) and K by (11.71).

If  $U=0$ , we have  $\nu=0$  and

$$K^2 = 1 - \frac{1-\mu^2}{\cos^2 i} = \frac{\mu^2 - \sin^2 i}{\cos^2 i}. \quad \dots (11.8)$$

Equation (11.75) then gives

$$\cos r = \frac{K \cos i}{\mu} \quad . \quad . \quad . \quad . \quad . \quad (11.81)$$

Hence

$$\sin^2 r = 1 - \frac{K^2 \cos^2 i}{\mu^2} = \frac{\sin^2 i}{\mu^2} \quad . \quad . \quad . \quad (11.82)$$

or

$$\frac{\sin i}{\sin r} = \mu, \quad . \quad . \quad . \quad . \quad . \quad (11.83)$$

the ordinary formula for refraction at a stationary surface.

## XXVII. On the Constant of Mass Action.

By R. D. KLEEMAN, B.A., D.Sc.\*

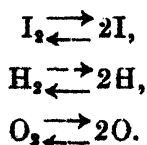
**T**HE molecules taking part in a gaseous reaction according to a given reaction equation may be divided into two kinds, depending on their behaviour when isolated. One kind does not dissociate, while the other kind dissociates into molecules which themselves do not dissociate. Thus, for example, according to the gaseous reaction expressed by the equation



the iodine and hydrogen molecules when isolated do not dissociate; while the hydrogen iodide molecules when isolated dissociate in part into molecules of hydrogen and iodine. Again, in the case of the reaction expressed by the equation



the carbon dioxide molecules when isolated dissociate in part into molecules of carbon monoxide and oxygen, while molecules of the latter kind on isolation remain unchanged. If the molecules  $\text{H}_2$ ,  $\text{I}_2$ , and  $\text{O}_2$  also dissociate when isolated, this would be expressed by the additional reaction equations



The molecules which now dissociate on isolation are  $\text{HI}$ ,  $\text{I}_2$ ,

\* Communicated by the Author.

$H_2$ ,  $O_2$ , and the molecules and atoms that do not dissociate are  $CO$ ,  $I$ , and  $H$ .

It is very important to make a distinction between these two kinds of molecules. Every gaseous reaction would evidently involve both kinds. It will be convenient to distinguish them by names; in this paper the molecules that do not dissociate on isolation will be called *sepro-stable*, and those that dissociate *sepro-unstable* molecules.

The *sepro-stable* molecules when isolated will evidently obey the gas equation, which for our present purpose will be written for one mol in the form

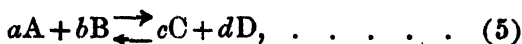
$$v = \frac{RT}{p}, \quad . \quad . \quad . \quad . \quad . \quad . \quad (3)$$

where  $v$  denotes the volume at the pressure  $p$  and absolute temperature  $T$ . The *sepro-unstable* molecules will also obey this equation if there be no change in the number of molecules on dissociation. Hydrogen iodide is a case in point: two molecules on dissociation form a molecule of hydrogen and a molecule of iodine, and thus the pressure would not be altered. On the other hand, if molecules of  $CO_2$  are isolated from a reacting mixture, some of them will dissociate till equilibrium exists between the remaining  $CO_2$  molecules and the dissociation products  $CO$  and  $O_2$ . The total number of molecules in the end will, however, not be the same as the number of  $CO_2$  molecules isolated in the beginning. Besides, the total number of molecules when equilibrium has been reached will evidently depend on the volume. The resultant mixture will therefore not obey the gas equation, but an equation which for one mol of the original molecules we will write in the form

$$v = \frac{RT}{p} + \sum \frac{A_n}{p^n}, \quad . \quad . \quad . \quad . \quad . \quad . \quad (4)$$

where  $A_n$  is a function of  $T$ . In general it may be said that *sepro-stable* molecules on being isolated from a reacting mixture obey the gas equation (3), while *sepro-unstable* molecules obey the equation (4), but that in certain types of *sepro-unstable* molecules the function  $A_n$  is zero.

Let us next consider the constant of mass-action of a reaction between the substances  $A$ ,  $B$ ,  $C$ ,  $D$  in equilibrium, proceeding according to the reaction equation



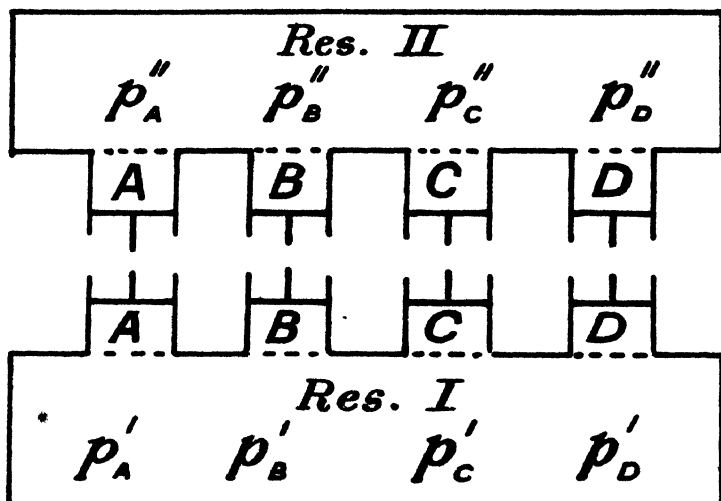
where  $a$  molecules \* of the substance  $A$  and  $b$  molecules of the

\* Meaning gram molecules or mols.

substance B combine to form  $c$  molecules of the substance C and  $d$  molecules of the substance D, and *vice versâ*. The substances A and B will be supposed sepro-stable and the substances C and D sepro-unstable.

Let us consider two different equilibrium systems of these molecules at the same temperature, obtained by allowing two different mixtures of the reacting substances to come to equilibrium in reservoirs, shown diagrammatically in fig. 1,

Fig. 1.



and let these two systems be so large that removal of small quantities of the reacting molecules does not appreciably alter the composition. Furthermore, let us suppose that the vessels are provided with membranes permeable only to molecules A, B, C, and D respectively, in communication with cylinders provided with pistons, by means of which any given component of the mixture may be withdrawn, or added to either system. Now let us :

(a) withdraw from reservoir I.  $a$  molecules A and  $b$  molecules B at the partial pressures  $p_A'$  and  $p_B'$ , at which they are present in the reservoir. The free energy change for this step is evidently zero, since the partial pressures of the substances are not measurably altered.

(b) change reversibly the pressure of the two gases to the pressures  $p_A''$  and  $p_B''$ , at which they exist in the reservoir II.



The free energy increase of this step is

$$\Delta F_1 = a \int_{p_A'}^{p_A''} v \cdot \partial p + b \int_{p_B'}^{p_B''} v \cdot \partial p = aRT \ln \frac{p_A''}{p_A'} + bRT \ln \frac{p_B''}{p_B'}$$

since these are sepro-stable substances and the gas law (3) is obeyed.

(c) introduce the gases into the reservoir II., and since this does not measurably affect the partial pressures, the free energy increase is again zero.

(d, e, f) by a similar series of steps remove  $c$  molecules of the substance C and  $d$  molecules of the substance D from the reservoir II. and introduce into the reservoir I. The pressures in the cylinders during the process of removing the molecules from the reservoir II. will not be the same as the partial pressures  $p_C''$  and  $p_D''$  in the reservoir, on account of the molecules being sepro-unstable. As soon as a number of molecules C have passed through a permeable membrane into the associated cylinder they dissociate till equilibrium is reached between the undissociated molecules C and the dissociation products, and a similar change takes place with the molecules D. The pressures in the cylinders will therefore be *greater* than the partial pressures in the reservoir, and we will therefore write them  $C''p_C''$  and  $D''p_D''$ , where  $C''$  and  $D''$  are quantities greater than unity. Similarly, when the molecules are transferred into the reservoir I. their pressures in the cylinders will not be equal to the partial pressures  $p_C'$  and  $p_D'$  in the reservoir but greater, and will be written  $C'p_C'$  and  $D'p_D'$ , where  $C'$  and  $D'$  are quantities greater than unity.

The total free energy increase during the foregoing operation is

$$\begin{aligned} \Delta F_2 = & c \int_{C''p_C''}^{C'p_C'} v \cdot \partial p' + d \int_{D''p_D''}^{D'p_D'} v \cdot \partial p' = cRT \ln \frac{p_C'}{p_C''} + dRT \ln \frac{p_D'}{p_D''} \\ & + cRT \ln \frac{C'}{C''} + dRT \ln \frac{D'}{D''} + c \left[ \sum \frac{-C_n}{(n-1)p^{n-1}} \right]_{C''p_C''}^{C'p_C'} \\ & + d \left[ \sum \frac{-D_n}{(n-1)p^{n-1}} \right]_{D''p_D''}^{D'p_D'}. \end{aligned}$$

where, since the substances are sepro-unstable, the equations

$$\begin{aligned} v &= \frac{RT}{p} + \sum \frac{C_n}{p^n} \\ v &= \frac{RT}{p} + \sum \frac{D_n}{p^n} \end{aligned}$$

are used instead of the gas equation, where  $C_n$  is a function of  $T$  referring to the substance  $C$ , and  $D_n$  a function of  $T$  referring to the substance  $D$ .

The foregoing steps are supposed to be carried out at corresponding times and so slowly that the removed substances are in chemical equilibrium while in the cylinders, and the substances  $A$  and  $B$  removed from the reservoir I. react in the reservoir II. to replace the substances  $C$  and  $D$  which have been removed therefrom, which in turn react in the reservoir I. to form the substances  $A$  and  $B$ . Each step has then been carried out isothermally and reversibly, and the composition of each system is just what it was at the beginning of the process. The total free energy increase is therefore zero, or

$$\Delta F_1 + \Delta F_2 = 0,$$

which becomes, after substituting for  $\Delta F_1$  and  $\Delta F_2$  and rearranging

$$\begin{aligned} RT \ln \frac{(p_C'')^c (p_D'')^d}{(p_A'')^a (p_B'')^b} &= RT \ln \frac{(p_C')^c (p_D')^d}{(p_A')^a (p_B')^b} \\ &+ \left[ cRT \ln C + c \Sigma \frac{-C_n}{(n-1)(C'p_C')^{n-1}} \right. \\ &- cRT \ln C'' - c \Sigma \frac{-C_n}{(n-1)(C''p_C'')^{n-1}} \\ &+ dRT \ln D' + d \Sigma \frac{-D_n}{(n-1)(D'p_D')^{n-1}} \\ &\left. - dRT \ln D'' - d \Sigma \frac{-D_n}{(n-1)(D''p_D'')^{n-1}} \right]. \quad (6) \end{aligned}$$

If we write  $X$  for the expression within the square brackets in this equation and assume that

$$X = 0, \quad . \quad . \quad . \quad . \quad . \quad . \quad (7)$$

the equation becomes

$$RT \ln \frac{(p_C'')^c (p_D'')^d}{(p_A'')^a (p_B'')^b} = RT \ln \frac{(p_C')^c (p_D')^d}{(p_A')^a (p_B')^b},$$

whence

$$\frac{(p_C'')^c (p_D'')^d}{(p_A'')^a (p_B'')^b} = \frac{(p_C')^c (p_D')^d}{(p_A')^a (p_B')^b}.$$

This equation expresses that if the temperature is kept constant the value of each side is independent of the values

of the partial pressures, and we may accordingly write

$$K = \frac{(p_C)^c (p_D)^d}{(p_A)^a (p_B)^b}, \quad \dots \quad (8)$$

where  $K$  is a constant at constant temperature which has been called the constant of mass action. If, however, equation (7) does not hold, equation (6) may be written in the form

$$K = \frac{(p_C'')(p_D'')^d}{(p_A'')^a (p_B'')^b} = \frac{(p_C')^c (p_D')^d}{(p_A')^a (p_B')^b} e^{X/RT} \quad \dots \quad (9)$$

It is evident that  $K$  is now not independent of the values of the partial pressures of the interacting molecules. Since these pressures are fundamentally functions of the independent variables, the volume of the mixture, its temperature, and the masses of the elemental constituents,  $K$  is in general also a function of these variables.

It appears, therefore, that in order that in general  $K$  be a constant at constant temperature, equation (7) must hold besides equation (6). But there is *a priori* no thermodynamical reason why equation (7) should hold exactly, though it may of course hold approximately in the case of most reactions. In previous investigations of the constant of mass action it has been tacitly assumed, following van't Hoff, that the substances  $C$  and  $D$  when taken out of the reservoir II. do not dissociate. In that case  $C'$ ,  $C''$ ,  $D'$ , and  $D''$  would each be unity, and  $C_n$  and  $D_n$  each zero, giving to  $X$  a zero value. But this would assume that on one side of the permeable membranes the molecules  $C$  and  $D$  may dissociate, while on the other side they do not, which is manifestly an untenable assumption.

It may be suggested that possibly the variables  $C'$ ,  $p_C'$ ,  $C''$ ,  $p_C''$ ,  $D'$ ,  $p_D'$ ,  $D''$ ,  $p_D''$  in the expression  $X$  identically vanish, and that therefore equation (7) holds. In that case

$$cRT \ln C' + c \sum \frac{-C_n}{(n-1)(C'p_C')^{n-1}} = 0$$

separately, and the other similar expressions of  $X$  also vanish separately, since each expression contains a different set of variables. On adding  $cRT \ln p_C'$  to each side of the equation, it may be written

$$\int v. \partial(C'p_C') = RT \ln p_C' \quad \dots \quad (10)$$

by means of equation (4). The equation is manifestly absurd, since  $C'$  cannot vanish from the left-hand side independently of  $p_C'$ . The expression  $X$  cannot therefore

identically vanish, and equation (7) does not hold. It may happen, however, that the value of the integral is not sensitive to variations of  $C'$  from unity upwards over a considerable range, in which case the equation holds approximately. If the same is true for the integral in a similar equation referring to the substance D, equation (7) would hold approximately.

It may also be suggested that possibly equation (7) identically vanishes if  $C'$ ,  $C''$ ,  $D'$ ,  $D''$ ,  $C_n$ , and  $D_n$  are expressed in terms of the partial pressures by the help of the mass-action equation (8), and that therefore the latter equation holds. Let us suppose that this is true, though actually it can be shown not to be true in most cases. The constancy of  $K$  will then still rest on the assumption expressed by equation (7), which is an assumption, since in general, without introducing assumptions, the equation  $V + Z = 0$  may be decomposed into the two equations  $V + W = 0$  and  $Z - W = 0$  only, where  $W$  is an arbitrary function.

But it is likely that in most cases  $K$  is approximately a function of the temperature only, as shown by experiment. The reason for this can be given. If the dissociation is small the substances C and D approximately obey the gas laws, and in that case,  $C'$ ,  $C''$ ,  $D'$ ,  $D''$  do not differ appreciably from unity and the quantities  $C_n$  and  $D_n$  are small, and hence  $X$  is small. In that case  $K$  is approximately a function of the temperature only. If the dissociation is large the substances C and D will again approximately obey the gas laws, and  $C_n$  and  $D_n$  will be small as before. The quantities  $C'$ ,  $C''$ ,  $D'$ ,  $D''$  will, however, now be large. The expression involving them may be written

$$cRT \ln \frac{C'}{C''} + dRT \ln \frac{D'}{D''}.$$

Since the number of undissociated molecules available is small the pressure of the mixture may be varied considerably without much further dissociation taking place, and hence we may write  $C' = C'' + x$  and  $D' = D'' + y$ , where  $x$  and  $y$  are quantities which are very small in comparison with  $C''$  and  $D''$  respectively. The foregoing expression therefore becomes

$$cRT \ln \left( 1 + \frac{x}{C''} \right) + dRT \ln \left( 1 + \frac{y}{D''} \right),$$

which is approximately equal to zero. Thus, under these conditions also the constant of mass action is approximately a function of the temperature only. This may therefore also hold for intermediate degrees of dissociation, which is

rendered highly likely from the following considerations:

The series  $\sum \frac{C_n}{p^n}$  in the equation of the substance C is as a whole positive, and its integral  $\sum \frac{-C_n}{(n-1)p^{n-1}}$  therefore as a whole negative. The quantities  $cRT \ln C'$  and

$$c \sum \frac{-C_n}{(n-1)(C'p_C')^{n-1}}$$

will therefore have different signs and may therefore approximately cancel each other. This corresponds to the integral in equation (10) not being sensitive to variations of  $C'$ . Similar remarks apply to the terms involving  $D'$ ,  $C''$ , and  $D''$ .

It must happen, however, in certain cases and under certain conditions, that the constant of mass action varies appreciably with the volume of the mixture and the masses of the elemental constituents. Taking this possibility into account will help to explain many things that have been puzzling the chemist up to the present.

This possibility can also be predicted from purely kinetic considerations. Let us consider, for example, the reaction expressed by equation (2). The chance of two molecules of  $\text{CO}_2$  forming two molecules of CO and one of  $\text{O}_2$  depends on their chance of encounter. The number of molecules of  $\text{CO}_2$  dissociating per sec. per c.c. is therefore given by

$$k_1 C_{\text{CO}_2}^2,$$

where  $C_{\text{CO}_2}$  denotes the concentration of the  $\text{CO}_2$  molecules and  $k_1$  the velocity constant of dissociation. But the chance of a molecule of  $\text{CO}_2$  getting dissociated may not only depend on its chance of encountering another  $\text{CO}_2$  molecule but on its previous encounters with other molecules, or two  $\text{CO}_2$  molecules on encountering each other will dissociate only if they have been activated, so to speak, by previous encounters with other molecules. This activation will be expressed by the factor, or activation constant,  $\kappa_1$  in the foregoing expression, so that the number of molecules dissociating per second is

$$\kappa_1 k_1 C_{\text{CO}_2}^2.$$

Similarly, the number of molecules of  $\text{O}_2$  and CO forming molecules of  $\text{CO}_2$  per second per c.c. is not expressed by

$$k_2 C_{\text{CO}} C_{\text{O}_2},$$

but by

$$\kappa_2 k_2 C_{\text{CO}} C_{\text{O}_2},$$

where  $C_{CO}$  and  $C_{O_2}$  denote the concentrations of the CO and  $O_2$  molecules respectively, and  $\kappa_2$  the activation constant of a pair of molecules due to encounters with other molecules. When there is equilibrium

$$\kappa_1 k_1 C_{CO_2} = \kappa_2 k_2 C_{CO} C_{O_2}, \quad . . . . (11)$$

whence 
$$K = \frac{\kappa_1 k_1}{\kappa_2 k_2}, \quad . . . . (12)$$

where  $K$  is the constant of mass action. From the kinetic theory of gases it follows that  $k_1$  and  $k_2$ , expressing chances of encounter per unit concentration, are functions of the temperature only. But the quantities  $\kappa_1$  and  $\kappa_2$  evidently depend on the frequencies of the encounters and their nature, and are therefore functions of the fundamental independent variables the volume of the mixture, its temperature, and the masses of the elemental constituents. Therefore, unless  $\kappa_1 = \kappa_2$ ,  $K$  will also be a function of these variables. It may be pointed out that  $\kappa_1$  and  $\kappa_2$  contain the whole theory of catalytic action, a subject that will be discussed in detail at some future period.

It may finally be pointed out that if  $K$  in general is not a constant but a function of the above-mentioned independent variables, differential equations should exist connecting  $K$  with these variables. These differential equations will be given in a subsequent paper.

Schenectady, N.Y., U.S.A.

XXVIII. *The Conductivities of some Dilute Amalgams at various Temperatures.* By A. I. JOHNS, M.Sc., and E. J. EVANS, D.Sc., *Physics Department, University College of Swansea* \*.

#### INTRODUCTION.

THE work described in this paper is a continuation of that carried out by E. J. Williams † and T. I. Edwards ‡, who determined accurately the conductivities of dilute amalgams of cadmium, indium, magnesium, thallium, germanium, antimony, yttrium, cerium, aluminium, and beryllium.

Many investigations have been made on the conductivity of liquid amalgams, notably by Matthiessen and Vogt §,

\* Communicated by Prof. E. J. Evans.

† Phil. Mag. Sept. 1925, p. 589.

‡ Phil. Mag. July 1926, p. 1.

§ Phil. Mag. (4) xxiii. p. 171 (1862).

Weber\*, and Batelli†, but these observations, in the majority of cases, have been made at comparatively low temperatures, and furthermore the results are not altogether in agreement.

In this research the dilute amalgams investigated were those of germanium, gallium, silver, and copper, and observations were carried out between room temperature and about 300° C. When the metal employed is only soluble to a small extent in mercury, observations could only be made at comparatively high temperatures, but in other cases it was possible to make observations at both high and low temperatures.

One of the main difficulties encountered in these experiments, especially when the solubility of the metal is small, is uncertainty concerning the purity of the specimen. This uncertainty is more pronounced in the case of rare metals, which are difficult to prepare in a state of purity. For this reason, the experiments carried out by Edwards‡ on germanium amalgams were repeated for two concentrations of the metal. The germanium used in these experiments was supplied by Adam Hilger, and had been analysed spectroscopically. The specimen of the rare metal gallium was also obtained from the same source, and, in each case, the metals used in preparing the amalgams were in a high state of purity. The results of the spectroscopic analysis will be given later.

In the case of copper and silver there was no difficulty in obtaining material of a high state of purity.

The results obtained in this investigation will be examined in relation to a theory put forward by Skaupy§.

Let  $L$  and  $\eta$  be the conductivity and viscosity respectively of the pure solvent (mercury), and  $c$  the concentration of metal dissolved in mercury expressed in gram atoms per 100 gram atoms of mercury.

If  $\Delta L$  and  $\Delta\eta$  be the changes in conductivity and viscosity corresponding to the small concentration  $c$ , and putting

$$\frac{1}{L} \frac{\Delta L}{c} = l \quad \text{and} \quad \frac{1}{\eta} \frac{\Delta \eta}{c} = r,$$

Skaupy showed that  $l_{\infty} + r_{\infty}$  is of the same order of magnitude for different metals dissolved in mercury. Except in the case of some alkali amalgams, the values of  $l_{\infty}$  are

\* *Wied. Ann.* xxiii. p. 470 (1884).

† *Atti Accad. Lincei*, (4) iv. p. 206 (1887).

‡ *Loc. cit.*

§ Skaupy, *Zeit. für Physik. Chemie*, lxviii. p. 560 (1907); *Verh. Deut. Phys. Ges.* xvi. p. 156 (1914); *ibid.* xviii. p. 252 (1916); *Phys. Zeit.* xxi. p. 597 (1920).

||  $l_{\infty}$  and  $r_{\infty}$  express the values of  $l$  and  $r$  for infinite dilution.

approximately the same when different metals are dissolved in mercury, and as the variation of viscosity with concentration is not sufficiently known, especially in the neighbourhood of 300° C., the values of  $l_{\infty}$  for the different amalgams will be discussed in the present paper. Skaupy\* also showed, in the case of amalgams in which the change of viscosity is not as great as in the alkali amalgams, that

$$\frac{l_{\infty} - l}{c}$$

is constant.

Before the work on the amalgams was commenced, preliminary experiments on the electrical conductivity of pure mercury contained in a quartz tube were carried out at various temperatures ranging from 0° C. to about 300° C. The results agreed within experimental error with those already obtained by Williams† and Edwards‡.

The amalgams employed in this investigation were very dilute, the percentage weight of the metals dissolved in mercury varying from about .01 to .1.

In most cases the tube containing the amalgams was open to the atmosphere, but the results for one or two concentrations in the case of silver, gallium, and copper were confirmed by preparing the amalgams and measuring their conductivities in a sealed apparatus containing hydrogen.

#### EXPERIMENTAL ARRANGEMENT.

It is not proposed here to enter into a detailed account of the apparatus and method of using it, as that has already been given by Williams§ and Edwards||.

The conductivity of an amalgam was determined by measuring the electrical resistance of a fine cylindrical column of it by means of a Callendar and Griffiths bridge in conjunction with a moving-coil galvanometer of high sensitivity. The resistances measured were about 0.6 ohm, and could be determined with an accuracy of .00005 ohm. This latter quantity was equivalent to a change of temperature of the amalgam column of about .09° C. at 300° C. The various resistances of the Callendar and Griffiths bridge were all calibrated in terms of the largest resistance by the usual method, and thus the relative values of the bridge resistances were accurately known. These relative values

\* *Loc. cit.*

† *Loc. cit.*

‡ *Loc. cit.*

§ *Loc. cit.*

|| *Loc. cit.*



are sufficient for an accurate determination of the temperature coefficient of resistivity of mercury or of an amalgam. Even for a determination of the absolute value of the resistivity of mercury or of an amalgam at a given temperature, a knowledge of the correct absolute values of the various bridge resistances is not necessary if the standard value ( $94074 \times 10^{-9}$ ) of the resistivity of mercury at  $0^{\circ}\text{C}$ . be used. This value of the resistivity corresponds to a known value of the resistance of a column of mercury at  $0^{\circ}\text{C}$ ., as determined by the bridge. The values of the resistivities of pure mercury at various temperatures previously obtained by Williams and Edwards were again confirmed in preliminary experiments; and, as the resistances of the various amalgams were measured in the same tube and under the same conditions as employed for mercury the absolute values of the resistivities and conductivities of the amalgams could be determined at the same temperature.

The mercury or amalgam was placed in a quartz capillary tube, which opened out at each end into wide limbs at right angles to the capillary. Glass tubes containing mercury and having short pieces of platinum wires sealed into their closed ends fitted into the limbs, and served as leads for the current. This tube and also the special glass apparatus used for determinations in an atmosphere of hydrogen were described in detail by Edwards\*.

When the latter apparatus was employed, the resistances of both mercury and amalgam were determined at the same temperature. The resistance of the glass leads was measured separately, and in this way the resistance of a column of mercury or amalgam of constant dimensions was obtained after the application of a small correction for the expansion of the quartz envelope. The resistance measurements at various temperatures were obtained by immersing the tube in a liquid of an appropriate boiling-point. The substances employed were water, aniline, engenol, and diphenylamine. The temperature of each boiling liquid, which was contained in an iron bath, did not remain absolutely constant with continual use, but slowly increased in value with time.

In this way the resistance could be measured at a practically steady temperature, which was determined by a calibrated platinum thermometer placed alongside the capillary. The temperature of the amalgam column corresponding to a given resistance could be determined accurately to within  $1/10^{\circ}\text{C}$ . even at  $300^{\circ}\text{C}$ ., and the temperature measurements

\* *Loc. cit.* pp. 4-6.

have the necessary accuracy in comparison with those of the resistance.

The main experimental difficulties encountered in the research were caused by thermoelectric currents and the formation of air-bubbles in the capillary, especially at high temperatures. The former difficulty was overcome by keeping the galvanometer arm of the Wheatstone bridge closed, and adjusting the resistances so that there was no change in deflexion on completing the battery circuit. The latter difficulty was overcome by heating the column in an electric furnace to a higher temperature ( $320^{\circ}\text{C}.$ ) than that at which a determination was made. The tube was then carefully examined by a lens, and if a bubble was observed, the warm amalgam was run through the tube until the bubble was removed. When an amalgam of the desired concentration could be prepared at room temperature, the quartz tube was allowed to cool from the temperature of the electric furnace, and the resistance of the column determined at room temperature. The column was then placed in the liquid heating bath, and the resistance again determined at the high temperature. The tube was then removed from the bath and carefully examined for air-bubbles. The presence of air-bubbles was again tested by redetermining the resistance of the column at room temperature. In general it was found that the resistance of the column returned to its previously determined value. It is, however, of interest to point out that the solution in mercury of the metals employed in this investigation produced a diminution of resistance, whilst the presence of a small air-bubble increased the resistance. The diminution of resistance in the case of very dilute amalgams is small, and great care was exercised in getting rid of all air-bubbles.

Furthermore, in the case of metals like germanium only sparingly soluble in mercury even at  $300^{\circ}\text{C}.$ , the column was kept at the boiling-point of diphenylamine for several hours to ensure that the small quantity of metal put into the limbs had completely diffused through the mercury. When this had occurred the resistance of the column became constant.

#### *Calculation of the Conductivities of the Amalgams.*

The resistivities of pure mercury at various temperatures, as determined by Williams and Edwards, can be represented by the equation

$$\rho_t = \rho_0(1 + 0.8877 t + 0.977 t^2 + 0.19 t^3) *.$$

\* Edwards in deducing this equation from his experimental results had corrected for the expansion of quartz.

The above equation also represents the results of the present experiments on mercury within experimental error.

If  ${}_aR_t$  be the resistance of the amalgam column of length  $l$  and cross-section  $A$  at temperature  $t$ , and  ${}_mR_t$  the corresponding quantity for mercury, then

$${}_aR_t = {}_a\rho_t \cdot \frac{l}{A}$$

$${}_mR_t = {}_m\rho_t \cdot \frac{l}{A}$$

$$\text{and } {}_aP_t = \frac{{}_aR_t}{{}_mR_t} \cdot {}_m\rho_t.$$

Thus the resistivity and conductivity of an amalgam at temperature " $t$ " can be calculated from the resistivity of mercury at the same temperature, and the corresponding values of the resistances of the amalgam and mercury at temperature " $t$ ."

The percentage probable error in the values of the resistivity and conductivity of mercury and amalgams is estimated to be on the average about .01.

Since the amalgams of germanium, gallium, and copper employed in these experiments were so very dilute, the values of  $\frac{1}{c} \frac{\Delta I}{L}$  and  $l_\infty$  given in Table V. cannot claim great accuracy, and errors ranging from about 4 to 8 per cent. depending on concentration are possible on the average. The same is also true for the extremely dilute silver amalgams, but the results for the more concentrated amalgams were determined with greater accuracy.

## EXPERIMENTAL RESULTS.

### *The Electrical Conductivities of dilute Germanium Amalgams.*

Edwards\* determined the conductivities of four dilute germanium amalgams having concentrations varying from .0339 to .0753 at 301.8° C., and also the conductivity of an amalgam having concentration of .0182 at 250.1° C. He obtained the value 4.7 for  $l_\infty \times 10^3$ . The solubility of the metal in mercury is comparatively small, and the resistance measurements were consequently carried out at about 300° C. The change of resistance as compared with mercury is small, and the purity of the germanium is therefore a question of

\* *Loc. cit.*

primary importance. It was considered advisable to repeat Edwards's observations for two concentrations, employing a specimen of germanium obtained from Messrs. Adam Hilger, Ltd., London. The sample from which the specimen was supplied was subjected by them to spectroscopic analysis. The only foreign line found in the spectrum was a very faint one at 2516 Å.U., indicating the presence of a minute trace of silicon. Chemically a trace of sulphur and a minute quantity of arsenic were recognized, but these substances did not give any lines in the spectrum. These results show that the specimen of germanium employed in the present experiments was in a high state of purity. Some difficulty was experienced in bringing about solution of small pieces of the metal in mercury, even at 300° C. The small pieces of germanium, although lighter than mercury, were found sticking to the sides and bottom of the quartz bulbs at the ends of the capillary, and only a small proportion of the metal had passed into solution. This difficulty was not, however, encountered when the germanium was powdered, and the measured resistance showed a diminution as compared with mercury. The specimen of the metal employed by Edwards was already in the powdered form, and was obtained from Dr. Schuchardt Görlitz.

TABLE I.

Nature of Amalgam.	Temp. in degrees centigrade.	Percentage weight of substance in Mercury.	Concentration "c."	Resistivity of Mercury, $\times 10^8$ .	Conductivity of Mercury.	Resistivity of Amalgam, $\times 10^8$ .	Conductivity of Amalgam.
Germanium.	299.28	.01226	.0339	12778	7827	12757	7839
	"	.02503	.0692	"	"	12733	7853
Gallium.	301.0	.00764	.0219	12803	7811	12787	7820
	"	.01427	.0408	"	"	12772	7829
	"	.03299	.0944	"	"	12740	7849
	"	.04497	.1287	"	"	12709	7868
	* 300.33	.01427	.0408	12793	7817	12764	7835
Copper.	301.76	.01003	.0316	12813	7804	12786	7821
	"	.02006	.0633	"	"	12763	7835
	* "	.0150	.0473	"	"	12776	7827

\* These determinations were made in a sealed apparatus containing an atmosphere of hydrogen.

The experimental results are given in Tables I. and V. In Table I. the concentration "*c*" is expressed in gram atoms per 100 gram atoms of mercury, *i.e.* in atom atoms per cent. approximately. In the fourth column of Table V. are calculated the values of  $\frac{\Delta L}{L} \times 10^3$ , *i.e.* the increase of conductivity relative to that of mercury at the same temperature multiplied by 100; and in the fifth column the values of  $\frac{\Delta L}{L} \times 10^3$  divided by the concentration.

The difference between 4.52 and 4.79 can be accounted for by experimental error, and as the amalgams experimented upon were very dilute, the mean value 4.7 is taken to be equal to  $l_{\infty} \times 10^3$ , which is the value of  $\frac{1}{c} \frac{\Delta L}{L} \times 10^3$  for infinite dilution.

*The Electrical Conductivities of dilute Gallium Amalgams.*

As found by Ramsay\*, gallium readily amalgamates with mercury, and as the amalgam does not readily oxidise, even at 300°C., measurements of the resistance were carried out in the quartz tube in air.

The metal used in these experiments was supplied by Messrs. Adam Hilger, who also made a qualitative and quantitative spectroscopic analysis of the sample from which the specimen was taken. The foreign elements found were, indium (the chief impurity), lead, and possibly silver. The two chief lines of silver were evident in strong spectra only. The quantitative determinations were:—

Indium.....	0.8 per cent.
Lead.....	0.013 per cent.

The conductivities of indium amalgams had previously been determined by Williams†, and it is evident from his values that the small quantity of impurities present in the gallium could not possibly affect the experimental results to any material extent.

The conductivity of gallium amalgam of concentration 0.0408 prepared in a sealed apparatus containing hydrogen gas was measured at a temperature of 300.33°C., and the results agreed with those determined in the quartz tube.

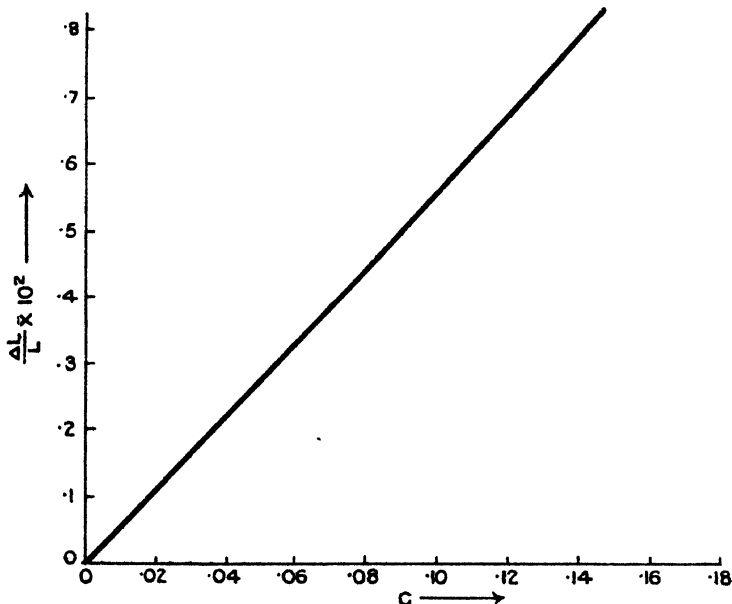
\* Journ. Chem. Soc. lv. p. 521 (1889).

† *Loc. cit.*

Possible oxidation did not, therefore, affect the experimental results obtained with the quartz tube to any measurable extent.

The results \* obtained for four amalgams of concentrations varying from .0219 to .129, and also for the amalgam of concentration .0408 prepared in an atmosphere of hydrogen,

GRAPH I.—Gallium.



are given in Tables I. and V. The value of  $l_{\infty} \times 10^2$  is taken to be the mean of the values of  $\frac{1}{c} \frac{\Delta L}{L} \times 10^2$ , which are constant within experimental error. The values of  $\frac{\Delta L}{L} \times 10^2$  are plotted against  $c$  in Graph I., and the relation between them is a linear one.

*The Electrical Conductivities of dilute Copper Amalgams.*

The electrical conductivities of copper amalgams have been investigated by Batelli † and Schleicher ‡. Batelli employed

\* The authors have not found any reference to work carried out by other investigators on the conductivities of gallium amalgams.

† *Loc. cit.*

‡ *Zeit. Electrochem.* xviii. p. 998 (1912).

amalgams whose atomic composition varied from  $\text{Cu}_1\text{Hg}_{127}$  to  $\text{Cu}_4\text{Hg}_{127}$ , and determined the relative resistance of these amalgams (*i.e.* resistance of amalgam relative to that of mercury at  $0^\circ\text{C}.$ ) at  $13^\circ\text{C}.$  and  $100^\circ\text{C}.$  Schleicher measured the electrical resistance of amalgams whose concentrations were much greater than those employed in this investigation, and the results are therefore not comparable with those obtained in the present experiments. The solubility of copper in mercury is very small at room temperature, but increases with rise of temperature. Two dilute amalgams of concentration  $\cdot 0316$  and  $\cdot 0633$  were prepared, and their resistivities determined at about  $300^\circ\text{C}.$  The finest electrolytic copper was employed in the preparation of the amalgams, and the measurements were carried out in the quartz tube. Later, a copper amalgam of concentration  $\cdot 0473$  was prepared in an atmosphere of hydrogen, and its conductivity measured at about  $300^\circ\text{C}.$  The results are in agreement with those previously obtained with the quartz tube, and are given in Tables I. and V.

#### *The Electrical Conductivity of dilute Silver Amalgams.*

The electrical conductivities of silver amalgams have been determined by Matthiessen and Vogt\*, Weber†, Batelli‡, Calvo§, and Parravano and Jovanovich||.

Matthiessen and Vogt measured the conductivities of silver amalgams containing from  $\cdot 01$  per cent. to  $1\cdot 0$  per cent. of silver at a temperature of about  $13^\circ\text{C}.$  The conductivities were compared with that of a gold-silver alloy, whose conductivity at  $0^\circ\text{C}.$  was taken to be 100. The ratio of the conductivities at  $15^\circ\text{C}.$  of silver amalgams containing  $\cdot 1$  per cent. and  $\cdot 01$  per cent. of silver, as determined in the present experiments, is  $1\cdot 0068$ , whilst the value of the ratio as calculated from Matthiessen and Vogt's measurements is  $1\cdot 0059$ . Weber in his investigations deals with more concentrated amalgams than those studied in the present experiments. A. Batelli also employed amalgams of greater concentrations. He measured the relative resistances of silver amalgams (*i.e.* relative resistance with respect to mercury at  $0^\circ\text{C}.$ ) at  $13^\circ\text{C}.$  and  $100^\circ\text{C}.$ , using amalgams whose atomic composition ranged from  $\text{Ag}_1\text{Hg}_{400}$  to  $\text{Ag}_1\text{Hg}_{50}$ .

\* *Loc. cit.*

† *Loc. cit.*

‡ *Loc. cit.*

§ A. R. Calvo, 'Ion,' ii. p. 409 (1910).

|| N. Parravano and G. Jovanovich, *Gazz. Chim. Ital.* xlix. p. 16 (1919).

A. R. Calvo \* found for very dilute amalgams containing from .0015 per cent. to .06 per cent. of silver, that between 0° C. and 20° C. the electrical resistance is a linear function of the concentration. For higher temperatures the resistance-concentration graph is a curve concave to the concentration axis. Parravano and Jovanovich† measured the conductivities of amalgams very rich in silver, the percentage of mercury varying from 0 to 14. In the present experiments the electrical resistances of silver amalgams of concentrations ranging from .018 to .186 have been determined. The resistance of each amalgam contained in the quartz tube was measured at three temperatures, viz. at room temperature, 100° C., and about 300° C., and for one amalgam of concentration  $c = .186$  the resistance was measured at two temperatures between 100° C. and 300° C. Finally, a silver amalgam of concentration .0743 was prepared in an atmosphere of hydrogen, and its conductivity measured at room temperature and at 300° C. The results are in agreement with those previously obtained, when the measurements were carried out in the quartz tube. The amalgams of various concentrations were prepared from the purest silver obtainable, and the experimental results are given in Tables II., III., IV., and V.

Table III. shows the variation of the average temperature coefficient of resistivity of silver amalgam of concentration  $c = .186$  as the temperature difference is increased. The average temperature coefficient of resistivity increases as the temperature difference increases, but the values are less than the corresponding ones in the case of pure mercury.

The values of  $\frac{\Delta L}{L}$ , the increase of conductivity relative to that of mercury at the same temperature, have also been calculated. For the same concentration the value of  $\frac{\Delta L}{L}$  increases with temperature.

The values of the average temperature coefficient of resistivity of amalgams of various concentrations between 15° and 100° C. are given in Table IV., and the results show that this average temperature coefficient diminishes as the concentration increases.

\* *Loc. cit.*

† *Loc. cit.*



TABLE II.

Nature of Amalgams.	Temp. in degrees centigrade.	Percentage weight of Silver in Mercury.	Concentration "c."	Resistivity of Mercury, $\times 10^9$ .	Conductivity of Mercury.	Resistivity of Amalgam, $\times 10^9$ .	Conductivity of Amalgam.
Silver.	15	00995	0185	9535	10488	9527,	10496
	"	02017	0375	"	"	9519	10505
	"	03012	0560	"	"	9513	10512
	"	03978	0739	"	"	9505,	10520
	"	05499	1022	"	"	9498	10528
	"	06500	1208	"	"	9489	10538
	"	08503	1580	"	"	9480	10548,
	"	10001	1859	"	"	9463	10568
*	18.05	03997	0743	9561	10459	9531	10492
Silver.	100	00995	0185	10336	9675	10325	9685
	"	02017	0375		"	10315	9695
	"	03012	0560		"	10306	9703
	"	03978	0739		"	10296	9712
	"	05499	1022		"	10283	9725
	"	06500	1208		"	10268	9739
	"	08503	1580		"	10252	9754
Silver.	303	00995	0185	12831	7793,	12810,	7806
	"	03012	0560	"	"	12775	7828
Silver.	300.5	03978	0739	12795	7816	12721	7861
	"	05499	1022	"	"	12707	7870
	"	06500	1208	"	"	12697	7876
	"	08503	1580	"	"	12678	7888
	"	10001	1859	"	"	12664	7897
	300.9	01966	0366	12801	7812	12762,	7835,
*	300.33	03997	0743	12793	7817	12720	7862
Silver	15	10001	1859	9535	10488	9463	10568
	100	"	"	10336	9675	10231	9774
	188.47	"	"	11320	8834	11204	8925
	266.89	"	"	12325	8114	12199	8198
	300.5	"	"	12795	7816	12664	7897

\* These determinations were made in a sealed apparatus containing an atmosphere of hydrogen.

TABLE III.  
Silver Amalgams of Concentration ·1859.

Temperature, $t^{\circ}\text{C.}$	Resistivity of Mercury, $\times 10^3.$	Resistivity of Amalgam, $\times 10^3.$	Average temperature coefficient of resistivity of Mercury from $15^{\circ}\text{C.}$ to $t^{\circ}\text{C.},$ $\times 10^4.$	Average temperature coefficient of resistivity of Amalgam from $15^{\circ}\text{C.}$ to $t^{\circ}\text{C.},$ $\times 10^4.$	$\frac{\Delta L}{L} \times 10^3.$
15·0	9535	9463	—	—	·763
100·0	10336	10231	9·883	9·548	1·023
188·47	11320	11204	10·792	10·606	1·030
266·89	12325	12199	11·617	11·478	1·034
300·5	12795	12654	11·976	11·848	1·036

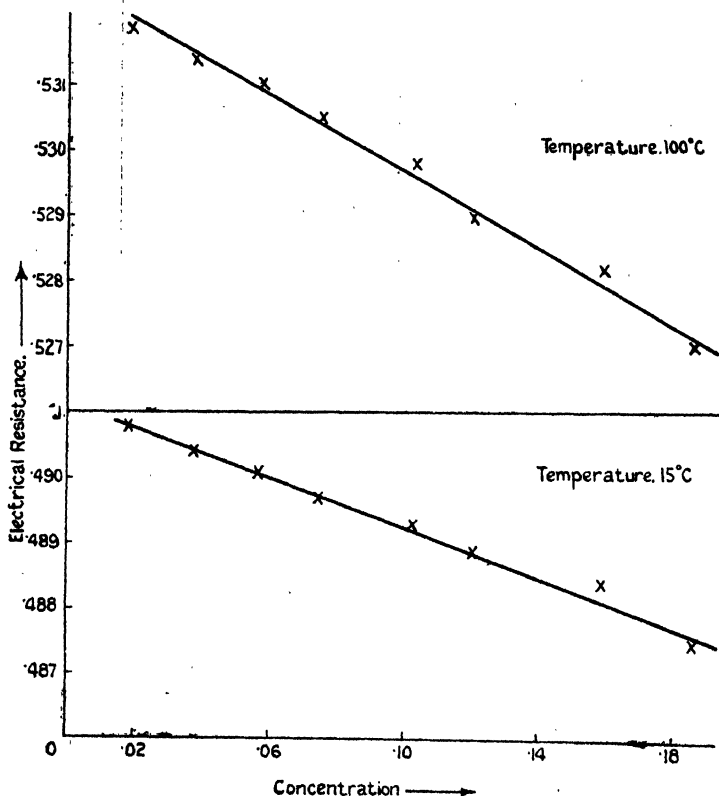
TABLE IV.  
Silver Amalgams.

Concentration "c."	Average tem- perature coefficient of resistivity of Amalgams from $15^{\circ}$ to $100^{\circ}\text{C.},$ $\times 10^4.$	Concentration "c."	Average tem- perature coefficient of resistivity of Amalgams from $15^{\circ}$ to $100^{\circ}\text{C.},$ $\times 10^4.$
·0185	9·841	·1022	9·723
·0375	9·838	·1208	9·658
·0560	9·807	·1580	9·581
·0739	9·784	·1859	9·548

The relation between the electrical resistance (which is proportional to the resistivity) and the concentration "c" at  $15^{\circ}\text{C.}$  and  $100^{\circ}\text{C.}$  is shown in Graph II. At these temperatures the relation is almost linear. The same result is also obtained if the electrical resistance is plotted against concentration at  $300\cdot5^{\circ}\text{C.}$

Graph III. gives the relation between  $\frac{\Delta L}{L} \times 10^3$  and "c" at 15° C., 100° C., and 300° C. The graphs for 15° C. and 100° C. are straight lines, showing that for the comparatively dilute silver amalgams examined the increase of conductivity relative to mercury at the same temperature is proportional to the concentration. This result is, however, not obtained at 300° C.

GRAPH II.—Silver.

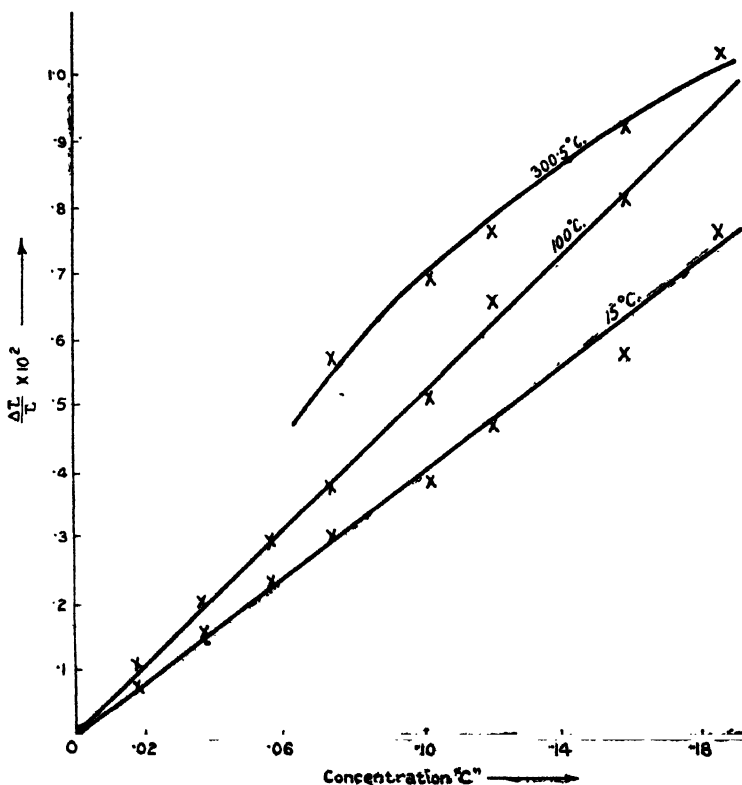


## DISCUSSION OF RESULTS.

For purposes of discussion, the results obtained for all the amalgams examined have been collected in Table V. The meanings of the various quantities tabulated have, in most cases, been previously explained. The sixth column gives the value of "l" for infinite dilution: i. e., the value of the

increase of conductivity relative to the conductivity of mercury at the same temperature divided by the concentration when the latter is very small. According to Skaupy's theory, which has been referred to previously, the value of  $H_{\infty} = l_{\infty} + r_{\infty}$  should be of the same order of magnitude for different metals dissolved in mercury. The values of  $r_{\infty}$  at  $15^{\circ}\text{C}$ .,  $100^{\circ}\text{C}$ ., and  $300.5^{\circ}\text{C}$ . are not known for amalgams of

GRAPH III.—Silver.



the concentrations employed in the present experiments, and consequently the values of  $l_{\infty}$  for the different amalgams are considered. It is seen that for germanium, gallium, and copper the values of  $l_{\infty}$  vary from  $4.7 \times 10^{-2}$  to  $6.5 \times 10^{-2}$ , and the mean value of  $l_{\infty}$  obtained for germanium in the present experiments is in good agreement with the value ( $4.7 \times 10^{-2}$ ) previously determined by Edwards\*.

\* *Loc. cit.*

TABLE V.

Nature of Amalgam.	Temperature in degrees centigrade.	Concentration "c."	$\frac{\Delta L}{L} \times 10^3$ .	$\frac{1}{c} \frac{\Delta L}{L} \times 10^3 = l \times 10^3$ .	$l_{\infty} \times 10^3$ .
Germanium.	299.23	.0339	.153	4.52	4.7
	"	.0692	.332	4.79	
Gallium.	301.0	.0219	.115	5.25	5.5
	"	.0408	.230	5.64	
	"	.0944	.487	5.20	
	"	.1287	.730	5.67	
	300.33	.0408	.230	5.64	
Copper.	301.76	.0316	.218	6.90	6.5
	"	.0633	.397	6.27	
	"	.0473	.295	6.24	
Silver.	15	.0185	.0763	4.12	4.0
	"	.0375	.162	4.32	
	"	.0560	.229	4.09	
	"	.0739	.305	4.13	
	"	.1022	.381	3.73	
	"	.1208	.477	3.95	
	"	.1580	.577	3.65	
	"	.1859	.763	4.05	
	18.05	.0743	.316	4.25	
Silver.	100.0	.0185	.103	5.57	5.3
	"	.0375	.207	5.52	
	"	.0560	.289	5.16	
	"	.0739	.382	5.17	
	"	.1022	.517	5.06	
	"	.1208	.661	5.47	
	"	.1580	.816	5.17	
	"	.1859	1.023	5.50	
Silver.	303.0	.0185	.162	8.74	
	"	.0560	.443	7.91	
Silver.	300.5	.0739	.577	7.81	9.0
	"	.1022	.691	6.76	
	"	.1208	.768	6.36	
	"	.1580	.921	5.83	
	.1859	1.036	5.57		
	300.9	.0366	.301	8.23	
Silver.	300.33	.0743	.577	7.77	
	15.0	.1859	.763	4.05	
	100.0	"	1.023	5.50	
	188.47	"	1.030	5.54	
	266.89	"	1.034	5.56	
	300.5	"	1.036	5.57	

The values of  $\frac{1}{c} \frac{\Delta L}{L} \times 10^2$  were determined at about 303°C., and were found to be constant within experimental error at different concentrations. The mean value of  $\frac{1}{c} \frac{\Delta L}{L} \times 10^2$  for each amalgam was therefore taken to be the value of  $l_\infty$  for that amalgam. In the case of silver, the values of  $\frac{1}{c} \frac{\Delta L}{L} \times 10^2$  were determined at 15°C., 100°C., and at about 300°C. At 15°C. and 100°C. the values of this quantity were practically constant, and  $l_\infty$  was taken to be the mean value. In this way it was found that  $l_\infty$  is  $4.0 \times 10^{-2}$  at 15°C., and  $5.30 \times 10^{-2}$  at 100°C. At about 300°C., however, the value of  $\frac{1}{c} \frac{\Delta L}{L} \times 10^2$  decreases with increasing concentration, and varies from 8.74 at the concentration .0185 to 5.57 at the highest concentration .1859. The value of  $l_\infty \times 10^2$  at 300.5°C. as deduced from a graph in which  $\frac{1}{c} \frac{\Delta L}{L} \times 10^2$  is plotted against concentration is 9.0.

According to Skaupy's theory, the value of  $\frac{H_\infty - H}{c}$  should be constant, and if the variation of viscosity with concentration be neglected, the expression  $\frac{l_\infty - l}{c}$  should be constant.

According to this relation, the greater the value of the concentration the smaller the value of  $l$ ; and this is in agreement with the results obtained at the high temperature.

The values of  $(l_\infty - l) \times 10^2$  are plotted against concentration in graph IV., and the relation between the two quantities as approximately a linear one. It is, however, important to

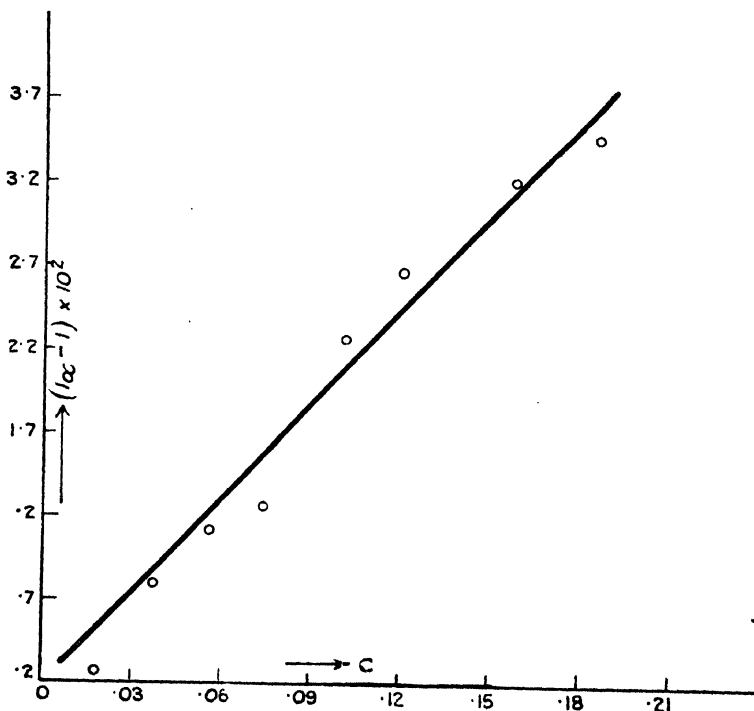
point out that the values of  $l = \frac{1}{c} \frac{\Delta L}{L}$  are difficult to determine with the necessary accuracy, for a perfectly satisfactory verification of the relation  $\frac{l_\infty - l}{c} = \text{constant}$ . The values of  $l$

obtained for silver amalgams of concentrations examined in this investigation increase with rise of temperature, and in this respect agree with results previously obtained by Edwards\* for thallium amalgams. This increase in the

\* *Lec. cit.*

value of  $l$  at high temperature may possibly be due both to an increase of electron concentration with rise of temperature, and also a diminution in viscosity under the same conditions. It is hoped that accurate measurements of the conductivities

GRAPH IV.



and viscosities of dilute amalgams at various temperatures will throw further light on the nature of conduction in amalgams. The results obtained for the amalgams examined in the present work show that the values of  $l_\infty$  are of the same order of magnitude in all cases.

#### SUMMARY.

1. The conductivities of dilute amalgams of germanium, gallium, silver, and copper have been determined. The conductivities of germanium, gallium, and copper amalgams of different concentrations were measured only at about  $300^\circ\text{C}.$ , but the conductivities of silver amalgams of various concentrations were determined at  $15^\circ$ ,  $100^\circ\text{C}.$ , and at about

300° C. In the case of silver amalgam of concentration  $c = \cdot 186$  the conductivity was also measured at 184·4° C. and 266·8° C.

2. The average temperature coefficient of resistivity between 15° C. and various higher temperatures of silver amalgam of concentration  $\cdot 186$  was found to increase as the temperature difference increased. The values were less than the corresponding ones in the case of pure mercury.

3. The values of the average temperature coefficient of resistivity of silver amalgams of various concentrations between 15° and 100° C. showed a diminution as the concentration increased.

4. In the case of dilute germanium, gallium, copper, and silver amalgams (at 0° and 100° C.) examined it was found that the increase of conductivity relative to the conductivity of mercury at the same temperature was practically proportional to the concentration. This, however, was not found to be the case for silver amalgams at about 300° C.

5. It was found that the increase of conductivity relative to the conductivity of mercury divided by the concentration (when the latter was extremely small) was of the same order of magnitude for all the amalgams examined.

The authors wish to thank Mr. Frank Homeyard for his valuable assistance in the construction of the apparatus.

---

XXIX. *The Angular Velocity of a Rigid Body.* By E. A. MILNE, F.R.S., Beyer Professor of Applied Mathematics in the University of Manchester\*.

### 1. *The Usual Treatment.*

CONSIDER a rigid body in motion about some fixed point. The fundamental property of the motion is that it can be described by a certain vector, which is called the angular velocity of the body.

It is customary in treatises on dynamics † to deduce this property by considering first the finite displacement of a rigid body, secondly the infinitesimal displacement of a rigid

\* Communicated by the Author.

† E. g. Whittaker, 'Analytical Dynamics,' Chap. I. Routh, 'Elementary Rigid Dynamics,' Chap. V. Lamb, 'Higher Mechanics,' Chap. V. Appel ('Mécanique Rationnelle,' Chap. II.) gives, however, an analytical method which deals with the body in motion.



body. It is proved that if a body suffers two rotations about given axes passing through a fixed point, then the final position of the body is independent of the order in which the rotations occur, provided these are "infinitesimal." It is proved further that the resultant rotation may be described by a vector which is the vector sum of the vectors representing the separate rotations. From the fact that the result of *successive* small rotations is equivalent to a rotation represented by the vector sum of the small rotations, it is inferred by proceeding to a limit that a rigid body in continuous motion can be regarded as possessing *simultaneously* angular velocities whose vector sum gives the instantaneous angular velocity of the body. This is also expressed by saying that angular velocities may be compounded according to the vectorial law.

## 2. Criticism.

There seem to the writer to be certain difficulties about this procedure. The essence of the theory of small displacements is that they are *successive*. It is not clear how it is ever possible from this theory to derive a result concerning *simultaneous* motions. Moreover, if we use the ordinary theory of infinitesimal displacements, we do not, in fact, know where the body is after two such displacements unless the order is specified. The difficulty is scarcely overcome by the process of letting an interval  $\delta t$  tend to zero: the displacements remain successive, and are never simultaneous. It could probably be overcome by introducing the notion of simultaneous displacements, by displacing the rigid body in a frame of reference which is itself being displaced as a rigid body. The final position of the rigid body would then be unique, even for finite displacements. The necessary theory would, however, be somewhat different from the usual theory of displacements.

The following treatment avoids these difficulties. It begins with the rigid body actually in motion, and avoids any reference to the theory of displacements or any passage to the limit. After a few years' experience of teaching it to students, the author feels that it may be of interest to other teachers. Even if the above-mentioned objections are not considered weighty, the theory may be held to have the æsthetic advantage of not deducing properties of bodies in motion from the properties of bodies at rest. It involves only elementary vector analysis.

We use the notations  $\mathbf{A} \cdot \mathbf{B}$  and  $\mathbf{A} \wedge \mathbf{B}$  to denote respectively the scalar and vector products of two vectors  $\mathbf{A}$  and  $\mathbf{B}$ .

We need the results

$$(\mathbf{A} \wedge \mathbf{B}) \cdot \mathbf{C} = (\mathbf{B} \wedge \mathbf{C}) \cdot \mathbf{A} = (\mathbf{C} \wedge \mathbf{A}) \cdot \mathbf{B}, \quad \text{I.}$$

$$(\mathbf{A} \wedge \mathbf{B}) \wedge \mathbf{C} = -\mathbf{A}(\mathbf{B} \cdot \mathbf{C}) + \mathbf{B}(\mathbf{C} \cdot \mathbf{A}), \quad \text{II.}$$

together with the elementary distributive theorems etc. of vector analysis.

### 3. The Existence Theorem for the Angular Velocity of a Rigid Body.

Consider a rigid body in motion about a fixed point O. Let P denote any point of the body, and let  $\mathbf{r}$  denote the vector distance OP. We use the symbol  $\dot{\mathbf{r}}$  to denote the velocity of P. The theorem in question is :

*There exists a unique vector  $\Omega$  which is such that the velocity of any point of the body is given by the relation*

$$\dot{\mathbf{r}} = \Omega \wedge \mathbf{r}. \quad (1)$$

*Proof.*—Let  $P_1$  be any definite point of the rigid body. Let  $P_2$  be a second point, such that  $OP_2$  is not perpendicular to the velocity of  $P_1$ . Let  $\mathbf{r}_1$  and  $\mathbf{r}_2$  be the vectors representing  $OP_1$  and  $OP_2$ . ( $\mathbf{r}_2 \cdot \dot{\mathbf{r}}_1 \neq 0$ .) The necessary and sufficient conditions of rigidity are

$$\mathbf{r}_1^2 = \text{constant},$$

$$\mathbf{r}_2^2 = \text{constant},$$

$$(\mathbf{r}_1 - \mathbf{r}_2)^2 = \text{constant}.$$

Differentiating these with respect to the time, we have

$$\mathbf{r}_1 \cdot \dot{\mathbf{r}}_1 = 0, \quad (2)$$

$$\mathbf{r}_2 \cdot \dot{\mathbf{r}}_2 = 0, \quad (3)$$

$$(\mathbf{r}_1 - \mathbf{r}_2) \cdot (\dot{\mathbf{r}}_1 - \dot{\mathbf{r}}_2) = 0. \quad (4)$$

Expanding (4) and using (2) and (3), we have

$$\mathbf{r}_1 \cdot \dot{\mathbf{r}}_2 + \mathbf{r}_2 \cdot \dot{\mathbf{r}}_1 = 0. \quad (5)$$

The relation  $\mathbf{r}_2 \cdot \dot{\mathbf{r}}_1 \neq 0$  accordingly implies  $\mathbf{r}_1 \cdot \dot{\mathbf{r}}_2 \neq 0$ . Moreover, since  $\dot{\mathbf{r}}_1$  is perpendicular to  $\mathbf{r}_1$  and not perpendicular to  $\mathbf{r}_2$ , it follows that  $\mathbf{r}_1$  and  $\mathbf{r}_2$  are not parallel.

Now consider the pair of equations

$$\Omega \wedge \mathbf{r}_1 = \dot{\mathbf{r}}_1, \quad (6)$$

$$\Omega \wedge \mathbf{r}_2 = \dot{\mathbf{r}}_2. \quad (7)$$

We propose to show that these have one and only one solution in  $\Omega$ , i. e. that they define a unique vector  $\Omega$ .

We first show that they have at most one solution. For, if possible, let them have two solutions  $\Omega, \Omega'$ . Then

$$(\Omega - \Omega') \wedge \mathbf{r}_1 = 0,$$

$$(\Omega - \Omega') \wedge \mathbf{r}_2 = 0.$$

Hence either  $\Omega - \Omega' = 0$ , or  $\Omega - \Omega'$  is parallel both to  $\mathbf{r}_1$  and  $\mathbf{r}_2$ . But  $\mathbf{r}_1$  and  $\mathbf{r}_2$  are not parallel. Hence  $\Omega = \Omega'$ .

We now show that they have a solution. Multiply (6) and (7) vectorially by  $\dot{\mathbf{r}}_2$  and  $\dot{\mathbf{r}}_1$  respectively, and expand the continued vector products by II. We find

$$-\Omega(\mathbf{r}_1 \cdot \dot{\mathbf{r}}_2) + \mathbf{r}_1(\Omega \cdot \dot{\mathbf{r}}_2) = \dot{\mathbf{r}}_1 \wedge \dot{\mathbf{r}}_2. \quad (8)$$

$$-\Omega(\mathbf{r}_2 \cdot \dot{\mathbf{r}}_1) + \mathbf{r}_2(\Omega \cdot \dot{\mathbf{r}}_1) = \dot{\mathbf{r}}_2 \wedge \dot{\mathbf{r}}_1. \quad (9)$$

Add (8) and (9), and use (5). We find

$$\mathbf{r}_1(\Omega \cdot \dot{\mathbf{r}}_2) + \mathbf{r}_2(\Omega \cdot \dot{\mathbf{r}}_1) = 0. \quad (10)$$

But  $\mathbf{r}_1$  and  $\mathbf{r}_2$  are not parallel. Hence if a solution  $\Omega$  exists, (10) requires that

$$\Omega \cdot \dot{\mathbf{r}}_1 = 0. \quad (11)$$

and

$$\Omega \cdot \dot{\mathbf{r}}_2 = 0. \quad (12)$$

Equation (8) now gives

$$\Omega = -\frac{\dot{\mathbf{r}}_1 \wedge \dot{\mathbf{r}}_2}{\dot{\mathbf{r}}_1 \cdot \dot{\mathbf{r}}_2}, \quad (13)$$

since  $\mathbf{r}_1 \cdot \dot{\mathbf{r}}_2 \neq 0$ , and similarly equation (9) gives

$$\Omega = -\frac{\dot{\mathbf{r}}_2 \wedge \dot{\mathbf{r}}_1}{\dot{\mathbf{r}}_1 \cdot \dot{\mathbf{r}}_2}. \quad (13')$$

These are equal by (5). It is immediately verified that this value satisfies the original equations (6) and (7) on using the conditions of rigidity. Relations (11) and (12) are also satisfied. We have accordingly found the unique solution of (6) and (7). It may be written also in the form

$$\Omega = \frac{\dot{\mathbf{r}}_1 \wedge \dot{\mathbf{r}}_2}{\dot{\mathbf{r}}_1 \cdot \dot{\mathbf{r}}_2} = \frac{\dot{\mathbf{r}}_2 \wedge \dot{\mathbf{r}}_1}{\dot{\mathbf{r}}_2 \cdot \dot{\mathbf{r}}_1}. \quad (13'')$$

We now consider any third point P, whose vector distance from O is  $\mathbf{r}$ . We suppose in the first instance that OP does not lie in the plane  $OP_1P_2$ . Put

$$\Omega \wedge \mathbf{r} = \mathbf{X}.$$

We propose to show that

$$\mathbf{X} = \dot{\mathbf{r}}.$$

To do this we shall show that

$$\left. \begin{aligned} \mathbf{X} \cdot \mathbf{r} &= \dot{\mathbf{r}} \cdot \mathbf{r}, \\ \mathbf{X} \cdot \mathbf{r}_1 &= \dot{\mathbf{r}} \cdot \mathbf{r}_1, \\ \mathbf{X} \cdot \mathbf{r}_2 &= \dot{\mathbf{r}} \cdot \mathbf{r}_2. \end{aligned} \right\} \dots \dots \dots (14)$$

It will then follow that  $\mathbf{X} = \dot{\mathbf{r}}$ . For otherwise  $\mathbf{X} - \dot{\mathbf{r}}$  would be perpendicular to each of  $\mathbf{r}$ ,  $\mathbf{r}_1$ , and  $\mathbf{r}_2$ , which is impossible by hypothesis.

The conditions that  $\mathbf{r}$  is rigidly connected to  $O$ ,  $P_1$ , and  $P_2$  are

$$\begin{aligned} r^2 &= \text{constant}, \\ (\mathbf{r} - \mathbf{r}_1)^2 &= \text{constant}, \\ (\mathbf{r} - \mathbf{r}_2)^2 &= \text{constant}, \end{aligned}$$

which give, on differentiation with respect to the time,

$$\mathbf{r} \cdot \dot{\mathbf{r}} = 0, \dots \dots \dots (15)$$

$$\mathbf{r} \cdot \dot{\mathbf{r}}_1 + \mathbf{r}_1 \cdot \dot{\mathbf{r}} = 0, \dots \dots \dots (16)$$

$$\mathbf{r} \cdot \dot{\mathbf{r}}_2 + \mathbf{r}_2 \cdot \dot{\mathbf{r}} = 0. \dots \dots \dots (17)$$

We have now, on using (15), (16), and (17), and theorem,

$$\begin{aligned} \mathbf{X} \cdot \mathbf{r} &= \Omega \wedge \mathbf{r} \cdot \mathbf{r} = 0 = \dot{\mathbf{r}} \cdot \mathbf{r}, \\ \mathbf{X} \cdot \mathbf{r}_1 &= \Omega \wedge \mathbf{r} \cdot \mathbf{r}_1 = -\Omega \wedge \mathbf{r}_1 \cdot \mathbf{r} = -\dot{\mathbf{r}}_1 \cdot \mathbf{r} = \dot{\mathbf{r}} \cdot \mathbf{r}_1, \\ \mathbf{X} \cdot \mathbf{r}_2 &= \Omega \wedge \mathbf{r} \cdot \mathbf{r}_2 = -\Omega \wedge \mathbf{r}_2 \cdot \mathbf{r} = -\dot{\mathbf{r}}_2 \cdot \mathbf{r} = \dot{\mathbf{r}} \cdot \mathbf{r}_2, \end{aligned}$$

which establish (14). Hence we have result (1), provided  $\mathbf{r}$  does not lie in the plane of  $\mathbf{r}_1$  and  $\mathbf{r}_2$ .

Now let  $P$  lie in the plane of  $P_1$  and  $P_2$ . Take a neighbouring point  $P'$ , vector distance  $\mathbf{r}'$ , not lying in the plane  $OP_1P_2$ . Then

$$\Omega \wedge \mathbf{r}' = \dot{\mathbf{r}}'.$$

As  $\mathbf{r}' \rightarrow \mathbf{r}$ ,  $\Omega \wedge \mathbf{r}' \rightarrow \Omega \wedge \mathbf{r}$ , and  $\dot{\mathbf{r}}' \rightarrow \dot{\mathbf{r}}$ . Hence

$$\Omega \wedge \mathbf{r} = \dot{\mathbf{r}}.$$

We have thus established (1) generally. Further,  $\Omega \cdot \dot{\mathbf{r}} = 0$ . We have thus found a vector  $\Omega$  satisfying any number of equations of the type  $\Omega \wedge \mathbf{r}_n = \dot{\mathbf{r}}_n$ ; and since each pair of such equations has only one solution by the above, the vector  $\Omega$  is unique.

When the motion is such that  $\Omega$  is constant, we have

$$\frac{d}{dt}(\Omega \cdot \mathbf{r}) = \Omega \cdot \dot{\mathbf{r}} = \Omega \cdot \Omega \wedge \mathbf{r} = 0,$$

and hence

$$\Omega \cdot \dot{\mathbf{r}} = \text{constant}.$$

In this case the vector  $\mathbf{r}$ , of constant length, is inclined at a constant angle to the fixed direction of  $\Omega$ . Moreover,

$$\dot{\mathbf{r}}^2 = (\Omega \wedge \mathbf{r})^2 = \Omega^2 \mathbf{r}^2 - (\Omega \cdot \mathbf{r})^2 = \text{constant}.$$

Hence the speed of P is constant. In other words, OP rotates round  $\Omega$  at a constant speed. The time of a complete revolution is the length of the path of P, which is

$$2\pi \frac{|\mathbf{r} \wedge \Omega|}{|\Omega|},$$

divided by  $|\dot{\mathbf{r}}|$ , namely  $|\Omega \wedge \mathbf{r}|$ , *i.e.* the time of a complete revolution is  $2\pi/|\Omega|$ . For this reason the vector  $\Omega$  is called the angular velocity of the body round the point O.

#### 4. Notes on the Proof.

The idea of the proof \*, it will be seen, is that we use the motion of two given points to fix  $\Omega$ , and then show that the motion of any third point is determined in terms of  $\Omega$ . We naturally need the complete set of conditions of rigidity, namely those expressing that  $P_1$  and  $P_2$  are rigidly connected with O and with one another, and that P is rigidly connected with O,  $P_1$ , and  $P_2$ .

For the velocity  $\dot{\mathbf{r}}$  of any point we have now the explicit formula

$$\begin{aligned} \dot{\mathbf{r}} &= \Omega \wedge \mathbf{r} = \frac{(\dot{\mathbf{r}}_1 \wedge \dot{\mathbf{r}}_2) \wedge \mathbf{r}}{\dot{\mathbf{r}}_1 \cdot \dot{\mathbf{r}}_2} \\ &= \dot{\mathbf{r}}_1 \left( \frac{\mathbf{r} \cdot \dot{\mathbf{r}}_2}{\dot{\mathbf{r}}_1 \cdot \dot{\mathbf{r}}_2} \right) + \dot{\mathbf{r}}_2 \left( \frac{\mathbf{r} \cdot \dot{\mathbf{r}}_1}{\dot{\mathbf{r}}_2 \cdot \dot{\mathbf{r}}_1} \right). \end{aligned}$$

This shows that the velocity of any point P of a rigid body in motion round a fixed point is a linear function of the velocities of any two given points  $P_1$  and  $P_2$  (provided  $\dot{\mathbf{r}}_1 \cdot \dot{\mathbf{r}}_2 \neq 0$ ), *i.e.* that the velocities of all points are parallel to the plane. It is an interesting exercise in vector analysis to prove this result without the intervention of  $\Omega$ , using only the conditions of rigidity.

The following additional remarks may be of interest.

#### 5. The Theorem of Relative Angular Velocities.

Let a rigid body or frame of reference (2) have an angular velocity  $\Omega_2$  relative to a frame of reference (1), and let (1) have an angular velocity  $\Omega_1$  relative to a frame of reference (0). Then (2) has an angular velocity  $\Omega = \Omega_1 + \Omega_2$ .

\* A similar proof, using quaternions, is given by Tait, 'Quaternions' (3rd edition, 1890), p. 288.

relative to (0). For if  $\mathbf{r}$  denotes any point,  $\mathbf{v}$  its velocity in (0),  $\mathbf{v}_2$  its velocity in (2), and  $\mathbf{v}_1$  the velocity in (0) of the same point considered as belonging to (1), then we have

$$\mathbf{v} = \mathbf{v}_1 + \mathbf{v}_2,$$

$$\mathbf{v}_1 = \Omega_1 \wedge \mathbf{r},$$

$$\mathbf{v}_2 = \Omega_2 \wedge \mathbf{r},$$

whence

$$\mathbf{v} = (\Omega_1 + \Omega_2) \wedge \mathbf{r},$$

and so

$$\Omega = \Omega_1 + \Omega_2.$$

### 6. Angular Velocity independent of Origin of Reference.

Let a rigid body have an angular velocity  $\Omega$  round a point O, which is moving with velocity  $\mathbf{v}_0$ . Let  $O_1$  be any other point, and let the angular velocity round  $O_1$  be  $\Omega_1$ . Then  $\Omega = \Omega_1$ . For if  $OO_1 = \mathbf{r}_1$ , and  $\mathbf{v}_1$  is the velocity of O, then

$$\mathbf{v}_1 = \mathbf{v}_0 + \Omega \wedge \mathbf{r}_1.$$

But if  $\mathbf{r}$  denote any point of the body,  $\mathbf{v}$  its velocity,

$$\mathbf{v} = \mathbf{v}_0 + \Omega \wedge \mathbf{r}.$$

Put

$$\mathbf{r} = \mathbf{r}_1 + \mathbf{r}'.$$

Then

$$\begin{aligned} \mathbf{v} &= \mathbf{v}_0 + \Omega \wedge (\mathbf{r}_1 + \mathbf{r}') \\ &= \mathbf{v}_1 + \Omega \wedge \mathbf{r}'. \end{aligned}$$

But

$$\mathbf{v} = \mathbf{v}_1 + \Omega_1 \wedge \mathbf{r}'.$$

This is true for all points  $\mathbf{r}'$ . Hence  $\Omega_1 = \Omega$ .

7. The last two results complete the minimum necessary to describe the most general motion of a rigid body in terms of an angular velocity.

The theorem of relative angular velocities allows us to dispense with the somewhat difficult notion of a body possessing *simultaneously* two or more angular velocities. Such cases can always be reduced to the case of a definite velocity in one frame of reference, together with the angular velocity of that frame of reference in a second frame of reference, and so on. The advantage of this is that each angular velocity can then always be measured in principle by a revolution-counter.

XXX. *On the Capillary Rise of Liquids in Wide Tubes.*  
 By CLAUDE H. BOSANQUET, M.A., *Dr. Lee's Reader in Physics, Christ Church, Oxford* \*.

THE form of the surface of a liquid at rest in a circular tube under the influence of capillary forces is given by the equation :

$$\frac{h}{\alpha} - \frac{\alpha}{r} \sin \phi - \alpha \frac{d}{dr} \sin \phi = 0, \quad . \quad . \quad . \quad (1)$$

where  $h$  is the height above the free surface,  $\phi$  is the angle between the radial tangent and the horizontal, and  $\alpha^2 = \frac{T}{\rho g}$ . For a plain circular tube and a liquid which wets it,  $\phi = 0$  at the axis and  $\frac{\pi}{2}$  at the walls.

Lord Rayleigh † gives an approximate relation between  $h$  at the axis of the tube and  $r$  : —

$$\log_e \frac{h}{\alpha} = -\frac{r}{\alpha} + 0.8381 + 0.2798 \frac{\alpha}{r} + \frac{1}{2} \log_e \frac{r}{\alpha}. \quad . \quad (2)$$

This formula is only applicable to very wide tubes ( $\frac{r}{\alpha} > 6$ ); he also gives a formula for narrow tubes.

Bashforth and Adams ‡ have attacked the problem of a numerical solution of equation (1). They tabulate corresponding values of  $\phi$  and  $\frac{x}{b}$  for various values of a parameter  $\beta$ , where  $\frac{x}{b} = \frac{r h}{2 \alpha^2}$  and  $\beta = \frac{4 x^2}{h^2}$  in the notation of this paper. This table extends as far as  $\beta = 100$ , and in this case where  $\phi = 90^\circ$ ,  $\frac{x}{b} = 0.31646$ , so that  $\frac{h}{\alpha} = 0.2$  when  $\frac{r}{\alpha} = 3.1646$ .

Sugden § gives a table of values of  $\frac{r}{\alpha}$  and  $\frac{r}{b}$  for  $\phi = 90^\circ$ , using the results of Bashforth and Adams. In his notation

\* Communicated by the Author.

† Rayleigh, 'Collected Papers,' vi. p. 356.

‡ Bashforth & Adams, 'Capillary Action' (Camb. Univ. Press. 1863).

§ Sugden, Tr. Chem. Soc. 1921, p. 1483.

$a^2 = 2\alpha^2$ . He bridges the gap between the end of the tables and the point where Rayleigh's formula begins to apply by graphical interpolation.

It is the object of the present paper to give the results of some direct computations covering this region.

### Method of Calculation.

The method employed, though on the same lines as that of Bashforth and Adams, differed in that the central difference notation was used. This method involves working by successive approximations, but it is so much less laborious than their method that the total time for a computation is considerably reduced, besides which the successive approximations provide useful checks on the accuracy of the arithmetic.

In this notation, if a table of values of  $y$  for equal increments of  $x$  and their differences be formed as below:—

$y_{-2}$				
	$\Delta_{-1\frac{1}{2}}^I$			
$y_{-1}$		$\Delta_{-1}^{II}$		
	$\Delta_{-\frac{1}{2}}^I$		$\Delta_{-\frac{1}{2}}^{III}$	
$y_0$		$\Delta_0^{II}$		$\Delta_0^{IV}$
	$\Delta_{\frac{1}{2}}^I$		$\Delta_{\frac{1}{2}}^{III}$	
$y_1$		$\Delta_1^{II}$		
	$\Delta_{1\frac{1}{2}}^I$			
$y_2$				

Then

$$\begin{aligned} & \frac{1}{x_1 - x_0} \int_{x_0}^{x_1} y \, dx \\ &= \frac{y_0 + y_1}{2} - \frac{1}{24} \left\{ (\Delta_0^{II} + \Delta_1^{II}) - \frac{11}{60} (\Delta_0^{IV} + \Delta_1^{IV}) \right. \\ & \quad \left. + \frac{191}{5040} (\Delta_0^{VI} + \Delta_1^{VI}) - \frac{2497}{302400} (\Delta_0^{VIII} + \Delta_1^{VIII}) + \dots \right\}. \quad (3) \end{aligned}$$

This series is much more convergent than that used by Bashforth and Adams; in addition it only uses the even terms in the difference series.

A still more convergent series can be obtained if  $\frac{dy}{dx}$  is



known in addition to  $y$ . Calling this  $y'$  and forming the table as below :—

$y'_{-1}$	$\delta_{-\frac{1}{2}}^I$		
$y'_0$	$\delta_0^{II}$		
	$\delta_{\frac{1}{2}}^I$	$\delta_{\frac{1}{2}}^{III}$	
$y'_1$	$\delta_1^{II}$		
	$\delta_{1\frac{1}{2}}^I$		
$y'_2$			

Then

$$\begin{aligned} \frac{1}{x_1 - x_0} \int_{x_0}^{x_1} y \, dx \\ = \frac{y_0 + y_1}{2} - \frac{x_1 - x_0}{12} \left( \delta_{\frac{1}{2}}^I - \frac{1}{60} \delta_{\frac{1}{2}}^{III} + \frac{1}{560} \delta_{\frac{1}{2}}^V - \frac{79}{302400} \delta_{\frac{1}{2}}^{VII} \right. \\ \left. + \frac{1759}{39916800} \delta_{\frac{1}{2}}^{IX} - \dots \right). \quad (4) \end{aligned}$$

A table was constructed showing the values of  $\frac{h}{\alpha}$ ,  $\sin \phi$ ,  $\tan \phi$ , and  $\alpha \frac{d}{dr} \sin \phi$ , and the differences of  $\tan \phi$  and  $\alpha \frac{d}{dr} \sin \phi$  for values of  $\frac{r}{\alpha}$  differing by 0.1, using various initial values of  $\frac{h}{\alpha}$ . Up to the point where the difference between  $\sin \phi$  and  $\tan \phi$  becomes appreciable, the equation can be written :

$$y - \frac{1}{x} \cdot \frac{dy}{dx} - \frac{d^2 y}{dx^2} = 0, \quad (5)$$

and values of  $\frac{y}{y_0}$  and  $\frac{1}{y_0} \cdot \frac{dy}{dx}$  can be obtained from tables of Bessel functions.

After the table had been started in this way, inspection of the general run of the differences gave approximations for the next value of  $\alpha \frac{d}{dr} \sin \phi$  and for the required differences. Using only the first term of the correction series, new values

were obtained for  $\phi$  and  $\frac{h}{\alpha}$ ; substitution of these values in equation (1) gave a new value for  $\alpha \frac{d}{dr} \sin \phi$ . If this value differed from the original extrapolation, the new values of  $\phi$  and  $\frac{h}{\alpha}$  were corrected, but with a little practice it was possible to guess the run of the curve with considerable accuracy.

After extending the table by twenty or so steps in this way, a second approximation was made, using the first to provide the correction terms and the approximations for  $\alpha \frac{d}{dr} \sin \phi$ . This table was then extended to form a first approximation over a new range of  $\frac{r}{\alpha}$ , and in this way the accumulation of large errors was avoided. Two approximations over any one range of  $\frac{r}{\alpha}$  were always sufficient, the full correction series being, of course, used in the second approximation, though terms beyond the second were never required.

When  $\phi$  approaches  $\frac{\pi}{2}$ , the differences begin increasing rapidly, and it is more convenient to use  $\frac{h}{\alpha}$  as the independent variable, the equation becoming

$$\frac{h}{\alpha} - \frac{\alpha}{r} \sin \phi + \alpha \frac{d}{dh} \cos \phi = 0. \quad . \quad . \quad (6)$$

The change of variable was made approximately at the point where  $\phi = \frac{\pi}{4}$ , and the curve was continued up to the point where  $\phi = \frac{\pi}{2}$ .

$\frac{r}{\alpha}$  was worked out for several values of  $\frac{h}{\alpha}$ , and for purposes of interpolation use was made of equation (5). If the difference between  $\sin \phi$  and  $\tan \phi$  be neglected, then, if in equation (5)  $\frac{dy}{dx} = 1$  where  $x = \frac{r}{\alpha}$ ,  $\frac{h}{\alpha} = y_0$ . It can easily be shown that in the limit where  $r = \infty$ ,

$$\log_e \frac{h}{\alpha} = \log_e y_0 - 0.08087.$$

### 300 *On the Capillary Rise of Liquids in Wide Tubes.*

A curve was drawn showing the relation between

$$\log_{10} \frac{\alpha y_0}{h} - 0.03512 \quad \text{and} \quad \frac{\alpha}{r};$$

and since the curve must pass through the origin, it can be used for extrapolation of the correction to larger values of  $r$ .

#### *Results.*

Five values of  $\frac{r}{\alpha}$  were worked out, corresponding to values of  $\log_{10} \frac{h}{\alpha}$  differing by 0.5; in addition, two points were taken from Bashforth and Adams's tables. The results are given in Table I.

TABLE I.

$\frac{r}{\alpha}$	$\text{Log}_{10} \frac{h}{\alpha} \times 10^{10}$	$\text{Log}_{10} \frac{\alpha y_0}{h} - 0.03512$
3.0	9.36603	0.00188
3.1	9.32651	0.00227
3.9278	9.0	0.00395
5.1866	8.5	0.00406
6.4294	8.0	0.00346
7.6584	7.5	0.00289
8.8764	7.0	0.00262

The first two values were obtained by interpolation from the tables of Bashforth and Adams, the remainder are new points; the values of  $\frac{r}{\alpha}$  are somewhat uncertain in the fourth place, but when the figures in the third column are plotted against  $\frac{\alpha}{r}$ , the smoothness of the curve shows that the values of  $\log_{10} \frac{h}{\alpha}$  are unlikely to be in error by as much as three in the fourth place.

The final results are given in Table II., which extends the table given by Sugden up to a point where the capillary rise is infinitesimal.

TABLE II.  
 $\text{Log}_{10} \frac{h}{\alpha} \times 10^{10}.$

$\frac{r}{a}$	0.0.	0.2.	0.4.	0.6.	0.8.	1.0.
3.0 .....	9.3660	9.2870	9.2082	9.1294	9.0505	8.9715
4.0 .....	8.9715	8.8924	8.8132	8.7338	8.6542	8.5746
5.0 .....	8.5746	8.4947	8.4147	8.3345	8.2540	8.1734
6.0 .....	8.1734	8.0927	8.0119	7.9309	7.8497	7.7685
7.0 .....	7.7685	7.6870	7.6054	7.5238	7.4420	7.3601
8.0 .....	7.3601	7.2781	7.1960	7.1138	7.0315	6.9491
9.0 .....	6.9491	6.8666	6.7840	6.7014	6.6187	6.5359
10.0 .....	6.5359	6.4530	6.3700	6.2871	6.2040	6.1208
11.0 .....	6.1208	6.0376	5.9543	5.8711	5.7877	5.7042

XXXI. *A Method of Measuring the Radiant Heat emitted during Gaseous Explosions.* By C. H. JOHNSON, Ph.D.  
 (Chemical Department, University College, London) \*.

THE radiation from flames has long been known to represent a considerable fraction of the total heat of combustion. This radiation lies mainly in the infra-red, with very small amounts in the visible and ultra-violet regions of the spectrum. The percentage of the heat of combustion appearing as radiation is governed by a large number of independent factors, so that its magnitude is very largely determined by the experimental conditions. Thus Callendar (Brit. Assoc. Rep. 1910) found that 16 per cent. of the gross heat of combustion was radiated from a large coal-gas flame burning under the most favourable conditions, whilst small flames radiated much less—2 to 3 per cent. only. The latter figures agree with the earlier results of R. Helmholtz (*Verhandlungen des Vereins zur Beförderung des gewerbliesses in Preussen*, lxxviii. 1889).

Hopkinson (Proc. Roy. Soc. A, lxxxiv. p. 155, 1910) was responsible for the pioneer work upon measurements of radiant energy emitted during gaseous explosions, and using coal-gas and air in such proportions as to ensure complete combustion, found that the energy radiated during explosion

\* Communicated by Prof. W. E. Garner, D.Sc.

and cooling amounted to 22 per cent. of the gross heat of combustion; only 3 per cent. appeared up to the time of attainment of maximum pressure, which must represent roughly that emitted during the period of inflammation. David (Proc. Roy. Soc. A, xcvi. p. 183, 1920) has obtained further data which may be summarized briefly. Hydrogen-air mixtures sustained losses by radiation of 8 to 16 per cent. of the total heat of combustion, depending on the strengths of the mixtures employed; the losses from explosions of coal-gas and air varied between 23 and 26 per cent. It is necessary to emphasize the fact that these figures refer to the radiation emitted both during explosion and during the process of cooling. The percentages emitted up to the time of attainment of maximum pressure were from 0.5 to 1.4 per cent. in the case of hydrogen-air mixtures, and from 3.3 to 7.0 per cent. with coal-gas.

This practically represents the whole of the present-day knowledge of this subject. From the standpoint of the engineering sciences, such data are of great value; but from the point of view of physical chemistry in its endeavour to unravel the problems of mechanism of chemical reaction, and in particular of the part played by radiation from the flame front in "activating" the unburnt gases ahead of the wave, all the above measurements suffer from two vital defects. In the first place the gas mixtures which have been studied are very complex, and in the second place it is impossible to distinguish between the radiation received from the burning gases in the wave-front and the purely thermal emission by the hot products of combustion.

Another important aspect is the recognized dual character of radiant heat: first there is thermal emission, which is emitted from any hot material in thermal equilibrium whatever its state of aggregation; and secondly chemiluminescence or luminous heat, which may be emitted by flames. It is possible that an appreciable part of the available chemical energy of flames is liberated directly as radiation from the freshly-formed molecules, the latter originally containing more energy associated with the so-called internal degrees of freedom than corresponds to their mean kinetic energy. It is unnecessary to enter into a lengthy consideration of this question; practically every contribution connected with the subject contains an elaborate discussion of the meagre experimental data available.

It is nowadays taken for granted that a gas can radiate by virtue of its temperature, and it is fairly certain that the

greater part of the radiation produced during combustion in engine cylinders is of this type. There are, however, two isolated observations—one due to David and the other to R. Helmholtz—which are frequently quoted in support of the view that a portion of the radiation from flames is of the second type, which it is convenient to call “chemiluminescence.” David found that the maximum rate of emission of energy from an exploded mixture of coal-gas and air occurred 0.025 sec. before the attainment of maximum temperature, which may indicate occurrence of chemiluminescence in this explosion.

The second experiment is that by Helmholtz, in which he showed that preheating the gases (coal-gas and air) diminished the intensity of radiation from the flame in spite of the fact that the mean temperature of the flame is raised by the preheating. Helmholtz explained the decreased emission as caused by an increase in the rate of attainment of thermal equilibrium at the higher temperature of the flame. In other words, the supposed chemiluminescence was decreased on preheating the gases on account of the more rapid degradation of the chemical energy into thermal energy by molecular collisions. Reference to the original publication and examination of the diagram of the burner used in the experiments shows that the gases (preheated separately to about  $1800^{\circ}$  K.) mixed before appearing at the jet. Thus there is no doubt that some chemical combination appeared here, and that consequently there was less reaction in the flame and therefore less energy radiated. Haslam, Lovell, and Hunneman (*J. Ind. and Eng. Chem.* 1925, p. 272), who successfully verified the result, admit that their experiments were inconclusive for the same reason. While, therefore, it would be untrue to say that there have been no indications of luminescent heat, yet up to the present time no certain demonstration of the phenomenon has been given.

It is in this connexion that the augmentation of the infra-red energy which accompanies the drying of mixtures of carbon monoxide and oxygen is particularly interesting (see Garner and Johnson, *Phil. Mag.* iii. p. 97, 1927). There can be no doubt that the mean flame temperature in the case of an explosion of dried carbon monoxide and oxygen is lower than when a trace of water is present, since the explosion time is relatively long and the combustion less complete. Yet more than three times as much energy is liberated as radiation from the wave-front in the case of the dried gases. Even supposing there were differences in the modes

of propagation in the two cases, it seems impossible to avoid the conclusion that the extra radiation is luminescent in character. This is probably the first reliable evidence of the existence of "luminescent heat."

It may be well to emphasize here the importance attaching to the design of bomb for use in such investigations. It was anticipated that with a narrow cylindrical bomb the very rapid cooling of the gases would reduce to negligible proportions the amount of radiation emitted by the products of combustion. The analyses of total-radiation curves (see later) confirm this expectation, and prove that to all practical purposes the effective radiation is from the wave-front. This is in very sharp contrast with David's experimental conditions, where at least 90 per cent. of the radiation originates in the hot products of combustion. The bomb used by David has a capacity of about 21 litres, which was 150 times that used in these investigations. In explosions of coal-gas and air, only about 3 per cent. of the gross heat of combustion was received upon the bolometer up to the time of attainment of maximum pressure; of this, only part originated in the flame. Chemiluminescence, if it occurred, would thus be very largely masked by thermal emission in David's experiments.

Having observed the remarkable sensitiveness of the infra-red spectrum of burning carbon monoxide to traces of water and other catalysts (Garner and Johnson, *loc. cit.*), and having established a relationship between the emission of radiant energy and the speed of propagation of flame, it was necessary to determine the absolute amounts of energy emitted, in order to ascertain whether they were of sufficient magnitude to account for the large variations in explosion velocity. The experiments about to be described were carried out with this end in view.

The problem of calculating the percentage of the heat of combustion appearing as radiation is by no means simple with a bomb such as that used in this work in conjunction with a linear thermopile placed at some distance in front of it.

#### EXPERIMENTAL.

The explosions were carried out in a cylindrical bomb of phosphor bronze, 36 cm. long and internal diameter 2.4 cm., with a standard mixture of pure carbon monoxide and oxygen in the proportions 2 : 1, ignited by the fusion of 1.5 mm. of thin iron wire. The radiation penetrating a fluorite window

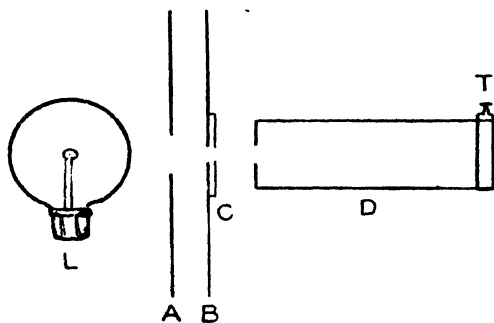
was recorded upon a sensitive quick-acting linear thermopile placed some 30 cm. in front of the window, the thermopile working in conjunction with a Downing galvanometer, critically damped. The movements of the latter instrument were recorded photographically upon a revolving drum, and thus was obtained a series of deflexion-time curves the areas of which were proportional to the amount of heat received by the thermopile. For a full account of the experimental procedure, reference should be made to the published work already referred to.

In order to determine the calorific equivalents of these total radiation records, their areas were compared with that of a "Control Curve" obtained by placing suddenly upon the thermopile a known small quantity of radiation and registering the galvanometer deflexion thus obtained, all other experimental conditions being maintained precisely as when recording radiation from the explosions.

*To obtain a Control Curve.*

Fig. 1 shows the disposition of the apparatus. The pointolite lamp L is held in position in front of the

Fig. 1.



thermopile T, and between them is placed an iron shield A with a circular orifice of 3 cm. diameter, an asbestos board B with an orifice of 1 cm. diameter, and a camera shutter C, mounted with its diaphragm open to about 0.8 cm. The orifices are centrally placed in regard to one another, and of such dimensions that the whole thermopile slit can "see" the glowing point of the pointolite. The thermopile has the same slit-width, and the galvanometer the same sensitivity as in the explosion experiments. It was found that opening and closing the camera shutter caused no deflexion of the galvanometer, provided the lamp was not in circuit. With the camera shutter closed the lamp is turned on (run at a



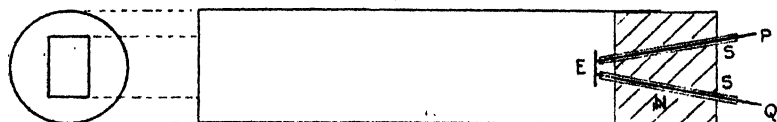
constant current of 1.25 amps.) and allowed to remain for five minutes before starting the experiment ; several records are then taken with the shutter adjusted to give an exposure of " $\frac{1}{250}$ " second. These are the control curves. They were found to be exceedingly reproducible, but the control curve used in the analysis of the explosion record was an average curve obtained by taking means of the ordinates of the individual control curves at corresponding times.

*Measurement of the Energy Equivalent of the Control Curve.*

There being no standard source of radiant heat available, the problem resolved itself into the measurement of the rate of emission of energy (in absolute units) from a pointolite lamp. The calibration was based upon an experiment by Denning (Phil. Mag. x. p. 270, 1905)), but many modifications were necessary to suit the particular problem in hand. The method is a calorimetric one, the lamp being allowed to illuminate a metal disk of known mass, and the initial rate of rise of temperature determined. It can be shown that the quantity of radiation received by unit area of the disk per second  $(R) = \frac{ms}{A} \frac{dT}{dt}$ , where  $m$  is the mass of the disk,  $A$  its area,  $s$  the specific heat, and  $\frac{dT}{dt}$  ( $^{\circ}\text{C./sec.}$ ) the initial rate of rise of temperature. The main part of the experiment centres round the measurement of  $\frac{dT}{dt}$ .

A copper disk, 1 cm. in diameter and 2 mm. thick, is made one junction of a copper-eureka couple, and mounted in an iron tube as shown in fig. 2 ; before mounting, the disk and tube are carefully blacked over a smoky turpentine flame.

Fig. 2.



In explanation of fig. 2, R is the iron tube, N a tight-fitting cork, S, S thin silica tubes, and P and Q are, respectively, fine copper and eureka wires affixed to the copper disk E with a minute amount of solder. The dimensions of the iron tube are very nearly the same as those of the brass tube in front of the thermopile slit (D, fig. 1), and a cardboard disk with an orifice ( $1.2 \times 2$  cm.) affixed to the end of the iron tube is exactly similar to the corresponding orifice

in the thermopile tube. The thermopile is removed and the iron tube put in its place, so that the copper disk is in the same vertical plane as previously occupied by the thermopile. Before finally inserting the cork carrying the copper disk it is important to make sure that the tube is aligned in such a way that all parts of the disk can "see" the pointolite, and thus ensure uniform illumination. The other junction of the couple is maintained at constant temperature by immersing in water contained in a Dewar vessel, and the wires are connected to the Downing galvanometer (critically damped). The work consists essentially of two experiments: first, the determination of the rate of change of galvanometer deflexion ( $\frac{d\theta}{dt}$  cm./sec.) upon opening the camera shutter with the lamp running at 1.25 ampz. (as before); second, the recording of deflexions produced by maintaining the two junctions of the thermocouple at different temperatures; both junctions, in this case, are kept immersed in water in Dewar vessels, the water being stirred by bubbling air through it, and the temperatures measured by means of standardized Beckmann thermometers. The galvanometer deflexions are recorded photographically in both experiments. The  $\frac{d\theta}{dt}$  curves are time-marked, and can thus be measured up accurately. In the second case the temperature differences are plotted against deflexions, and  $\frac{d\theta}{dT}$  (cm./° C.) obtained from the slope of the straight-line graph.

Now  $\frac{d\theta}{dt} \div \frac{d\theta}{dT} = \frac{dT}{dt}$ , the initial rate of rise of temperature in ° C. per sec. The mass of the disk is determined, and its mean diameter when blackened measured with the aid of a travelling microscope. Thus all the data necessary for the calculation of  $R$ , the quantity of radiation falling on the disk per sq. cm. per sec., has been obtained. The galvanometer sensitivity has to be considerably reduced for this work and the instrument shunted; the only necessary precaution is to ensure that the sensitivity and shunt are the same in both  $\frac{d\theta}{dt}$  and  $\frac{d\theta'}{dT}$  experiments. In order to check the accuracy of the method, the whole experiment was repeated with a silver disk in place of the copper. The result with the silver disk was almost precisely the mean of two obtained with the copper disk.

*Calibration of the Camera Shutter.*

The pointolite lamp is enclosed in a light-tight box with a small opening, in front of which is placed the camera shutter. A condensing lens (mounted in a tube) focusses the image of the camera diaphragm upon the drum. The method is to take two or three " $\frac{1}{250}$  sec." exposures upon a film with the drum at rest, and then to give " $\frac{1}{250}$  sec." exposures with the drum rotating at a high speed; the film is independently time-marked so that the speed of rotation is readily calculated. From the images thus recorded several things become apparent: first, that even with this short exposure the shutter opens completely and closes instantaneously; a very slight (and not always appreciable) tailing-off in the front of the image indicates that there is sometimes a small lag in the opening process. The maximum error introduced on this account is, however, negligibly small. From the elongation of the image and the speed of rotation of the drum the true time of exposure is easily calculated.

The thermopile line was examined under a low-power travelling microscope, and the discontinuities were found to amount to less than 0.5 per cent. of the total length.

**RESULTS.**

1. Amount of heat radiated from the pointolite lamp to thermopile per sq. cm. of thermopile surface per second.

Experiment.	Calories/sq. cm./sec.	Mean.
Cu disk .....	0.0023	0.0027
Ag „ .....	0.0024	
Cu „ .....	0.0026	

2. Exposure time (" $\frac{1}{250}$ " second).

Experiment.	Exposure time.	Mean.
1 .....	0.0028	0.0028
2 .....	0.0027	
3 .....	0.0029	
4 .....	0.0027	

3. Effective area of thermopile surface = 0.0574 sq. cm.  
Length of thermopile line = 1.13 cm.  
Width „ „ „ = 0.504 mm.

CALCULATION.

$$\begin{aligned} &\text{Energy corresponding to area of control curve} \\ &= \text{Energy/cm}^2/\text{sec.} \times \text{Area of thermopile surface} \\ &\hspace{15em} \times \text{Exposure time} \\ &= 0.0024 \times 0.0574 \times 0.0028. \\ &= \underline{3.86 \times 10^{-7} \text{ calorie.}} \end{aligned}$$

The energy equivalents of all the total radiation records have been estimated from this basic result.

The calorific values of the total-radiation records can be calculated from the product of the energy equivalent of the control curve and the ratio of the areas of the explosion and control curves. The radiation received on the thermopile represents only a minute portion of the total energy radiated during an explosion. The ratio of the energy received on the thermopile to the total radiation is  $3.519 \times 10^{-7}$ . The evaluation of this fraction is a long and complicated process, and is dealt with fully in the appendix to this paper.

There are also several factors that reduce the radiation falling on the thermopile, for which allowance must be made in calculating the true value for the amount of energy radiated during explosion. These are as follows: absorption by the cold carbon monoxide ahead of the wave; absorption and reflexion from the fluorite window; reflexion from the thermopile surface; penetration of the thermopile line due to discontinuities; and absorption by atmospheric moisture and carbon dioxide.

Since the thermopile line cannot "see" the walls of the bomb, reflexion effects do not enter into the problem; the very slight focussing action of the fluorite window is probably negligible. It is not possible to make allowance for absorption of thermal radiation by hot carbon dioxide; the analysis of the radiation curves indicates, however, that practically all the radiation is from the wave-front. The corrections to be applied for the various losses are now considered in detail.

1. *Absorption by Carbon Monoxide.*

The calculation is lengthy, but the steps can be stated briefly:—From data given by Coblentz (Pubns. of Carnegie Inst. No. 35, 1905) the average absorption by carbon monoxide in each of the two regions covered by the emission

bands from the explosion is calculated (Garner and Johnson, *loc. cit.*). From this is computed the average extinction coefficient in both bands, separately, and the emission spectra corrected; the true ratio of emission intensity in the  $2.8\mu$  and  $4.4\mu$  bands of the explosion becomes  $1.34:1$ . From this result and the values for the two extinction coefficients is calculated the average extinction coefficient of the cold carbon monoxide in the explosion; the value obtained was  $0.000171$ . From the relation  $\frac{E_0}{E} = e^{kpl}$ , where  $l$  is the length of the column of carbon monoxide,  $p$  the partial pressure of the gas, and  $k$  the average extinction coefficient, the mean value of  $\frac{E_0}{E}$ , the ratio of the true to the apparent emission intensity (averaged over the entire length of the bomb), is readily obtained.

The final result showed that 14 per cent. of the total infra-red emission is absorbed by the cold carbon monoxide.

## 2. Absorption and Reflexion by the Fluorite Window.

Coblentz (Pubns. of Carnegie Inst. No. 97, 1908) has found that the extinction coefficient of colourless fluorite is practically constant over the range of wave-lengths between  $2\mu$  and  $7\mu$ .

By experiment it was found that the losses due to these causes for the window used ( $1.0$  cm. thickness) amounted to 14 per cent. of the energy radiated.

## 3. Reflexion from the Blackened Thermopile Surface.

Correction ..... 2 per cent. (Glazebrook's Dict. of Applied Physics.)

## 4. Penetration of Thermopile Line and Atmospheric Absorption.

The losses are negligible.

The total losses therefore represent approximately 30 per cent. of the energy radiated. Thus the radiation curves only register about 70 per cent. of the total energy emitted in the direction of the thermopile. The multiplying factor is therefore  $1.43$ .

*Calculation of the percentage of the gross heat of combustion liberated as radiation in an explosion of wet gas mixture, i. e., of standard mixture containing 1.9 per cent. of water-vapour.*

Area of curve for wet gas =  $4.19 \times$  area of control curve.

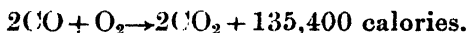
$\therefore$  Calorific value of wet gas curve =  $4.19 \times 3.86 \times 10^{-7}$  calorie.

Corrected calorific value of wet gas curve\* =  $4.19 \times 3.86 \times 10^{-7} \times 1.43$  calorie.

Ratio of energy received by thermopile to total energy radiated =  $3.519 \times 10^{-7}$ .

$\therefore$  Total energy radiated during wet gas explosion = 6.57 calorie.

*Gross Heat of Combustion.*



The volume of gas mixture held by the bomb = 164 c.c. (see Appendix). This volume of standard mixture corresponds to a calorific value of 308 calories.

Analyses made upon the gas mixture and upon the products of combustion show that this value needs to be corrected, since in no case is the combustion complete.

TABLE I.—Gas Analysis.

Description.	Percentage of Mixture unburnt after explosion.	Corrected Gross Heat.
Wet gas .....	9.0	280 calories.
Dried gas .....	9.8	278 „
Dried gas + $\text{CCl}_4$ ...	10.0	277 „

The large amount of gas remaining unburnt even in the presence of water-vapour is surprisingly large. Less than 1 per cent. of impurity (probably nitrogen) was detected in the standard mixture. No great accuracy is claimed for the analyses, but a large number were carried out and the results were quite consistent. In any case, the above correction makes little difference to the order of the final result.

Thus percentage of total heat radiated during explosion of wet gas mixture =  $\frac{6.57 \times 100}{280} = 2.3$  per cent.

\* Water-vapour of this concentration does not appreciably absorb the energy emitted from the explosion.

Similar calculations have been made in the other cases, and the results are tabulated below.

TABLE II.—Herein are summarized the main results of the research.

Description.	Per cent. of Gross Heat of Combustion radiated during explosion.
Wet gas .. .. .	2.3
Dried gas .. .. .	8.6
Dried gas + $\text{CCl}_4$ * ...	9.5

It is obvious from the involved nature of the calculations that these percentages can only indicate the order of magnitude of the emission intensities. It is satisfactory that they are in agreement with the results of other similar investigations. Probably a large part of the radiation emitted from an explosion of wet gas mixture is thermal in character; the 6–7 per cent. increase represents the extent of chemiluminescence.

*Note.* The last two figures should be increased by about 10 per cent. of their values in order to allow for losses by conduction to the parts of the thermopile during the period over which radiation is received upon it. This correction has not been made.

It is at present impossible to take into account the relation of speed of chemical combination to the velocity of propagation of flame, since there appears to be no data relevant to temperature coefficients and velocity constants of the homogeneous reaction between carbon monoxide and oxygen. Assuming a temperature in the neighbourhood of  $2500^\circ \text{K}$ . for the explosion wave in wet gas, the loss of an extra 6 or 7 per cent. of the gross heat of combustion from the dried gas mixture may reduce this temperature by  $100\text{--}150^\circ$ , and quite apart from other factors which also enter in, such a temperature difference is capable of producing large changes in the velocity of combustion, and hence in the rate of propagation of flame.

\* About 1 per cent. by volume of  $\text{CCl}_4$ . See other publications, *loc cit*.

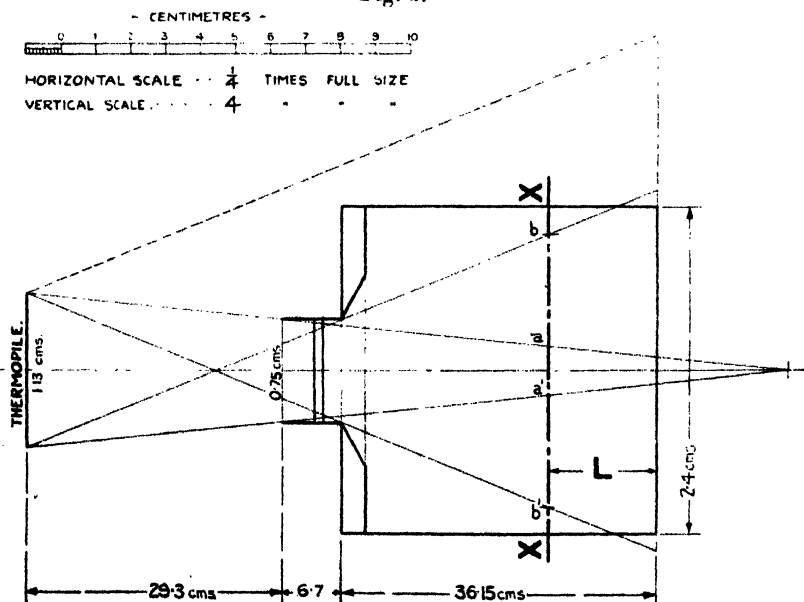
APPENDIX.

*Calculation of the Fraction of Energy received by the Thermopile of the total amount radiated during an Explosion.*

The method is long and somewhat involved, but may summarily be divided into three stages :—

- I. By graphical construction, and a drawing to scale, to determine the boundaries of the space within the bomb from which the thermopile, either the whole or part, receives radiation.
- II. To determine the average length of thermopile visible from any section of the bomb. Obviously at any section (taken through a plane at right angles to the axis of the bomb) part only will radiate to the whole of the thermopile, and part will illuminate portions of the thermopile.
- III. Making use of the general equation obtained in II. to calculate an expression for the fraction of the total radiant energy received upon the thermopile from any section of the bomb, whence the total energy radiated is readily obtained.

Fig. 3.



For this work it was necessary to construct accurate drawings to scale, and in II. to obtain a solution by mean



of graphical projections. In this connexion the author is greatly indebted to his friend, E. T. Hutt of the Great Western Railway Co., both for inspiration and for the time spent in making the drawings.

I. The bomb and its relation to the thermopile are drawn to scale in fig. 3. Lines have been drawn from the thermopile to indicate the limits of the effective radiating beam. It is at once apparent from consideration of any length  $XX$  at right angles to the length of the bomb and parallel to the thermopile, that only a fraction of it ( $a, a'$ ) "sees" the whole of the thermopile; the parts ( $ab, a'b'$ ) "see" portions only, whilst beyond  $bb'$  none of the radiation emitted can be received on the thermopile. From the known dimensions of the diagram and from the properties of similar triangles, it is a fairly simple matter to derive expressions for the lengths  $aa'$  and  $bb'$  merely involving  $L$ , the distance of any section from the end of the bomb, viz. :—

$$aa' = 0.012968 L - 0.19428, \quad . \quad . \quad . \quad (1)$$

$$bb' = 2.6379 - 0.0522 L. \quad . \quad . \quad . \quad (2)$$

II. On account of the fact that the thermopile is rectangular and the orifice of the bomb a cylindrical tube of small bore, the shape of the beam responsible for the radiation falling upon it can only be determined by making orthographic projections at various sections along the bomb. These projections can be contoured in such a way as to show the proportion of the length of thermopile line visible from the different parts of the given sections. Such a contoured projection is reproduced in fig. 4 (6). Details of the construction are now given.

### *The Method of Projections.*

It was convenient to make projections upon a scale eight times the actual dimensions of the bomb. In order to visualize the method, it is helpful to imagine the reverse process of what actually occurs; namely, the illumination of the interior of the bomb by the thermopile line. Then the shadow cast by the outer circular orifice of the small cylindrical tube determines  $aa'$  (fig. 3), and that cast by the inner circular orifice  $bb'$ . The radii of the shadows cast from the outer and inner orifices can be obtained readily, for any section, from the known dimensions of the small cylindrical

tube, the distances of the thermopile and of the line XX from the window. In this way the following formulæ were obtained :—

Radius of shadow cast by inner orifice,

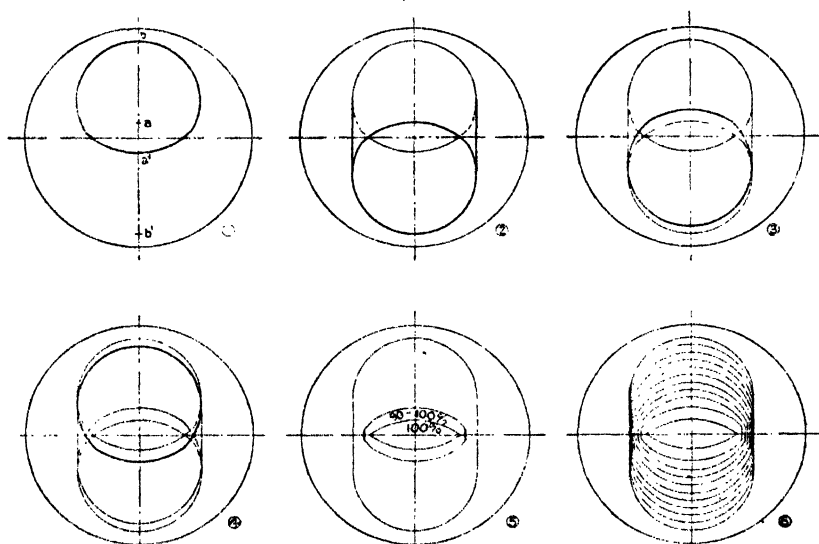
$$r_i = 0.7516 - 0.0104 L.$$

“ “ “ outer orifice,

$$r_o = 0.92342 - 0.12798 L.$$

Thus  $r_i$  and  $r_o$  can be calculated for any given section.

Fig. 4.



In order to make a contoured projection, the cross-section of the bomb is drawn and rectangular coordinates added; on the vertical axis the lengths  $bb'$ ,  $aa'$  for the given section are set off symmetrically about the centre. Through  $b$  the arc of a circle is drawn of radius  $r_i$ . Through  $a'$  another arc of radius  $r_o$  is drawn to intersect the first. Clearly, the area enclosed by these arcs represents the portion of the given cross-section of the bomb from which the lowest point of the thermopile is visible (fig. 4 (1)). See also fig. 3. This is repeated for  $b'$  and  $a$ , and thus is obtained the corresponding area for the topmost point of the thermopile. The area included by the overlap of these two outlines gives the portion of the given cross-section of the bomb from which the whole of the thermopile is visible. By drawing the common tangents, an outline (2) is obtained which circumscribes the area from which any fraction whatever of the

thermopile is visible. Any part of the section outside this boundary is invisible from the thermopile and non-effective for the purpose of radiation measurement. In the successive stages of the projection process illustrated in fig. 4, the new construction lines are shown broader than those drawn in preceding stages.

Now consider the similar but slightly more complicated problem of finding the outline of the area within which the thermopile is visible to the extent of 90-100 per cent. In this case a continuous length equivalent to 90 per cent. of the thermopile may be considered to occupy any position along the full length of the thermopile line. First, consider that the 90 per cent. length is measured from the bottom upwards; as previously, for the full length of the thermopile, the lowest point will again produce the outline (1) in fig. 4, but the topmost point will produce a new outline formed by the intersection of an arc of radius  $r_0$  drawn at a distance  $p$  above  $a$ , and an arc of radius  $r_i$  at a distance  $q$  above  $b'$ . The distances  $p$  and  $q$  may be calculated from the diagram in fig. 3 by the method of similar triangles. The area covered by the overlap of these two outlines represents the area of a given cross-section from which the thermopile is at least 90 per cent. visible, in the lower position (3). This process is repeated for the case of the 90-per-cent. length measured from the top downwards, when a similar but inverted outline is obtained as shown in (4). Joining these outlines by vertical straight lines an area is obtained within which 90 per cent. or more of the thermopile line is visible (5).

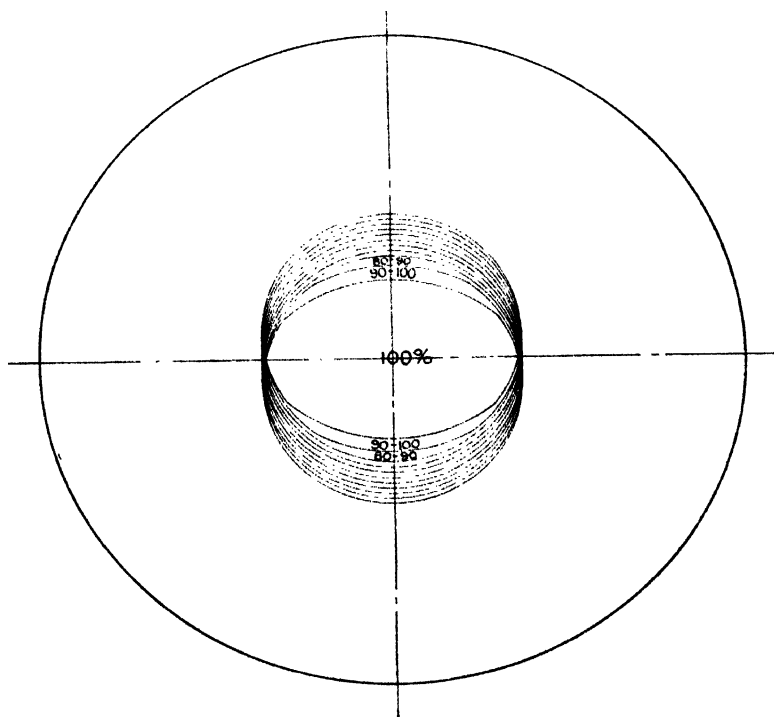
The quantities  $p$  and  $q$  are constant for constant decrements of the thermopile length, and thus for 10 per cent. decrements a series of outlines may be obtained, subject, however, to the fact (incidental to the nature of the orifice of the bomb) that  $r_0$  ceases to modify the outlines beyond a certain point. This is easily verified by reference to fig. 3. By repetition of the process the whole of the outline (2) may be contoured. The final result is shown in (6).

The diagram (6) is to be regarded as a contoured map; it is, in fact, an orthographic projection of a three-dimensional figure with base representing the given cross-section of the bomb and with perpendicular ordinates proportional to the length of thermopile visible from each point in it. Fig. 5 is the projection of another section taken nearer the fluoride window than (6).

In order to obtain the average length of thermopile visible from the given section across the bomb, which from now onwards will be denoted by  $T$ , it is necessary to measure

the volume of the three-dimensional figure. This was done by the accurate but laborious method of finding the areas of the separate contours, determining the volume enclosed by each adjacent pair, and summing them. The formula used for calculating the volume enclosed by any two irregular areas  $A$  and  $a$  separated by a distance  $d$  was  $v = \frac{d}{3}(A - \sqrt{Aa} + a)$ . Since the contours were taken

Fig. 5.



at intervals of 10 per cent.,  $d$  in the formula is equal to one-tenth of the length of the thermopile line, *i. e.* 0.113 cm.  $\Sigma v$  represents the volume of the solid figure  $V$ . Then  $V \div \frac{\pi D^2}{4}$ , where  $D$  is the diameter of the bomb, gives the average height to the solid figure, which is the mean value of  $T$  for the section considered. Care must be taken when estimating  $v$  that due allowance is made for the enlarged scale of the section.

In this way a value of  $T$  was obtained at three different sections distant 10, 20, and 30 cm. from the end of the bomb.

From the relation  $T = AL^2 + BL + C$  the constants A, B, C were evaluated, with the result:

$$T = 0.0000685 L^2 - 0.011505 L + 0.43370. \quad (3)$$

From equation (3) it is obvious that when  $L=0$ ,  $T=0.4337$ .  $T$  was therefore determined by graphical construction for the section through the extreme end of the bomb, and a value 0.432 obtained. This gives some idea of the accuracy with which the method can be applied, and at the same time proves the general correctness of equation (3).

The justification for assuming an equation of the type  $AL^2 + BL + C = T$  is that it had previously been found to apply for the imaginary case of a surface thermopile with a circular receiving surface. In this simpler case the contoured projections are made up of a series of concentric circles, the effective beam of radiation within the bomb being conical. If  $H$  represents the full diameter of the thermopile surface,  $D$  the internal diameter of the bomb, and  $A$  and  $B$  respectively the values of  $aa'$  and  $bb'$ , then it is readily proved that

$$T = \frac{H}{3D^2}(B^2 + AB + A^2),$$

or, substituting the values of  $A$  and  $B$ ,

$$T = 0.0001447 L^2 - 0.01609 L + 0.49098. \quad (4)$$

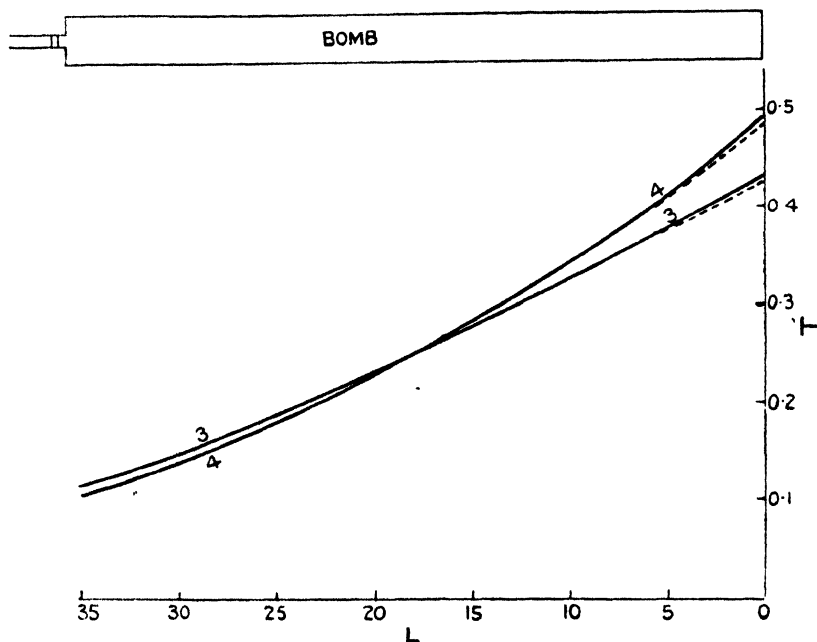
In this particular case of a surface thermopile,  $T$  is a mean diameter. Comparison of the  $T$  curves obtained from equations (3) and (4) is shown in fig 6. Since with the experimental arrangement the last 4.56 cm. of bomb wall truncate the extreme portions of the  $bb'$  region, slight corrections are necessary, and are indicated by dotted lines on the curves. The corrections were determined graphically by re-drawing the extreme limits of the  $bb'$  region on a large scale and, by taking 2 per cent. visibility increments instead of 10 per cent., finding the area cut off by intersection of the bomb walls.

The close resemblance of the curves derived from equations (3) and (4) is rather surprising; the areas enclosed differ only by about 2 or 3 per cent.

III. The next steps in the calculation can be stated summarily as follows:—If the flame-front is considered instantaneously to occupy any particular section of the bomb distant  $K$  cm. from the thermopile, it will radiate in a practically uniform manner in all directions, and concentric

spheres proceeding outwards from the flame-front will form surfaces of uniform radiation density. The thermopile can therefore be considered to occupy part of the surface of one of these spheres (radius  $K$  cm.), and the fraction of the total energy radiated received by the thermopile is given by the ratio of the area of the thermopile (average length visible  $\times$  slit-width) to the area of the sphere,  $4\pi K^2$ . Thus at any

Fig. 6.



section of the bomb distant  $K$  from the thermopile the fraction of the energy received by the thermopile of the total amount radiated  $= 4 \frac{bT}{4\pi K^2}$ , where  $b$  is the slit-width.

*Note.*—Obviously, only the central portion of the thermopile lies in the surface of the sphere of radius  $K$ , and moreover, all parts of the wave-front will be distant  $K$  cm. from the thermopile, but with the experimental arrangement used, errors introduced on this account are absolutely inappreciable, and neglecting them greatly simplifies the subsequent procedure.

$T$  has already been expressed as a function of  $L$  in

equation (3). This can readily be transformed into a function of  $K$ , since the thermopile and bomb are fixed in definite relationship to one another. Thus  $T=f(K)$ , and the above expression becomes

$$\frac{b[f(K)]}{4\pi K^2}.$$

Integration of this expression between the limits imposed by the length of the bomb gives the area enclosed by the curve obtained by plotting values of the above fraction against  $K$ . Dividing this area by the length of the bomb, the mean value of the fraction averaged over the length of the bomb is obtained. Thus is calculated the average fraction of the total energy radiated received upon the thermopile.

#### CALCULATION.

For the purposes of integration, as has already been pointed out, it is necessary to transform equation (3) from a function of  $L$  into a function of  $K$ .

When this is done ( $L=72.15-K$ ), equation (3) becomes

$$T=0.0000685 K^2+0.0016205 K-0.0398. \quad (5)$$

$$\begin{aligned} \frac{\text{Average area of thermopile visible}}{\text{Area of corresponding sphere}} &= \frac{bT}{4\pi K^2} \\ &= \frac{b(0.0000685 K^2+0.0016205 K-0.0398)}{4\pi K^2} \\ &= \frac{b}{4\pi} (0.0000685 + 0.0016205 K^{-1} - 0.0398 K^{-2}). \quad (6) \end{aligned}$$

From equation (6) can be calculated the fraction of the total energy radiated reaching the thermopile from any section of the bomb.

Integration of (6) gives

$$\frac{b}{4\pi} (0.0000685 K + 0.0016205 \log_e K + 0.0398 K^{-1} + C). \quad (7)$$

The limits of the long cylindrical portion of the bomb between which the integration is to be made are  $K=36.0$  cm. and  $K=72.15$  cm. This length also includes a small conical part of the bomb leading from the main portion into the narrow cylindrical tube carrying the fluorite window (see fig. 3). Since no part of the conical neck is visible to the thermopile, it is permissible to treat it as though the transition from the large to the small cylindrical tube was abrupt, provided that allowance is made when estimating the capacity of the bomb for the small extra space assumed to

exist. This method is much less laborious than dealing separately with the small conical space, and perfectly accurate.

Evaluation of equation (7) gives the area enclosed by the  $\frac{Tb}{4\pi K^2}$ , K curve. Dividing this area by the effective length of the bomb (36.15 cm.), the average fraction of the total radiation received on the thermopile is obtained. The value of this fraction is  $3.406 \times 10^{-7}$ .

The average value of this fraction for the very small cylindrical section between the main bomb tube and the fluorite window is very easily calculated. T is practically constant at 1.10 cm., and the limits of K are 36 and 34.7 cm. The fraction is  $3.558 \times 10^{-6}$ .

The volume of the main cylindrical part of the bomb is 163.5 cc.

The volume of the small cylindrical part of the bomb is 0.57 cc.

By simple proportion, therefore, the fraction of the total radiated energy received by the thermopile, averaged over the entire bomb,

$$= 3.519 \times 10^{-7}.$$

The following table is of interest in showing that under the experimental conditions the energy received on the thermopile from any part of the bomb is practically constant.

K.	$\frac{bT}{4\pi K^2}$ .
36	$3.348 \times 10^{-7}$
40	3.403 „
45	3.431 „
50	3.437 „
55	3.430 „
60	3.414 „
72.15	3.368 „

The above method of calculation has been given at some length, since it may be of use, at any rate in principle, to others engaged upon similar work. A very great simplification is possible if, instead of a linear thermopile, a thermopile with a circular receiving surface or, secondly, a "point" thermopile is used. In these cases no accurate drawings are necessary, since the effective radiating beam within the



bomb is conical in section, and thus the projections (if made) would merely be concentric circles, and the volume of the three-dimensional figure (see text) readily estimated by means of the ordinary formula for the frustum of a cone. In this connexion reference should be made to equation (4). Unfortunately, a surface thermopile is not suitable for this kind of work, having large thermal capacity, being slow-acting and very susceptible to losses by conduction. A sensitive, single-element, vacuum thermopile (approximating to a "point" thermopile) constructed by Moll is now on the market, and might possibly be adapted for work in the infra-red.

#### SUMMARY.

When conducting a physico-chemical examination of the radiation from a gaseous explosion, it is very important to discriminate between the emission of radiant energy from the wave-front and that from the hot products of combustion, a point to which little consideration seems to have been given by other investigators. In order to attain the desired result, a long narrow explosion vessel was used in which the rapid cooling of the burnt gases behind the wave reduced to almost negligible proportions the amount of radiation received from that source. A simple method for the calibration of a linear thermopile, necessarily placed at some distance from the bomb, has been described which enabled a quantitative extension of work detailed in other publications to be made.

The effect of water, and incidentally of other catalysts, upon the emission of infra-red radiation from the wave-front in explosions of carbon monoxide and oxygen has proved to be of considerable magnitude. In particular, an additional 7 per cent. of the gross heat of combustion was radiated from a dried gas mixture, in excess of that emitted in the presence of 1.9 per cent. of water-vapour. In future, therefore, no theory designed to explain the action of water in promoting spread of flame through carbon monoxide-oxygen mixtures can be considered complete that does not include the hitherto unrecognized radiation factor.

The author wishes to express his indebtedness to Professor W. E. Garner for helpful criticism and advice during the course of the investigation, to Mr. Allis who constructed the explosion vessel, and to the Department of Scientific and Industrial Research for a maintenance grant.

The Ramsay Laboratories of  
Inorganic and Physical Chemistry,  
University College, London.

XXXII. *A Study of the Rectification Efficiency of Thermionic Valves at Moderately High Frequencies.* By W. E. BENHAM, B.Sc.\*

*Introduction.*

THE principle involved in the valve voltmeter due to Moullin † is well known. If a small oscillatory e.m.f. is suitably applied to a thermionic valve, a certain change  $\Delta I$  in mean anode current takes place. This change in mean anode current is proportional to the square of the amplitude of the input e.m.f., provided this amplitude does not exceed a certain value generally of the order of 1 volt. Calibration of the voltmeter, which may be either of the diode or triode type, is effected by means of measured low-frequency voltages. Suppose, however, that it is suspected that high-frequency voltages will not produce the same value of  $\Delta I$  as low-frequency voltages of the same amplitude. The calibration would then be subject to correction for frequency. Moullin himself states in his book ‡ that a frequency error of the voltmeter is less than 1.5 per cent. at  $\lambda 300$  metres, this result being based on measurements with a sensitive electrostatic voltmeter or radio-frequency electrometer. The object of the present paper is to show that for wave-lengths much shorter than  $\lambda 300$  metres a frequency error is apparent, and to indicate the nature of the frequency variation of  $\Delta I$  at constant input voltage amplitude. The experiments about to be described consist essentially of measurements on a Moullin diode type voltmeter with a view to investigating the frequency error referred to, the input voltage being measured by means of an electrometer of the suspended needle type. Owing to the large number of variables, the experiments are necessarily very incomplete, and must be regarded as of a preliminary nature only, relative rather than absolute accuracy being aimed at.

*Experimental Details.*

Various types of valve were tested. In the first experiments the valve was used as a diode.

Referring to the diagram (fig. 1), it will be seen that the grid  $g$  is connected externally to the anode  $a$ . The filament  $f$  was heated by a current supplied by an accumulator  $e$  through

\* Communicated by Prof. Alfred W. Porter, F.R.S.

+ J. I. E. E. lxi. p. 295 (1923).

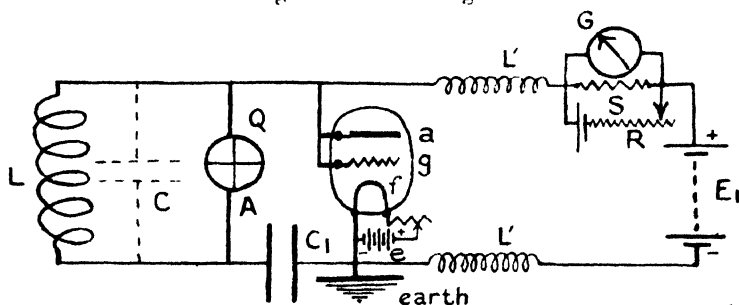
‡ 'Radio-frequency Measurements' (Griffin), 1926, p. 38.

a variable rheostat  $r$ . The source of steady potential  $E_1$  was a high-tension accumulator.

The source of high-frequency oscillations was a valve oscillator covering the range of frequencies from 4.1 to 16.8 megacycles. (N.B. The term megacycle is used throughout this paper to denote  $10^6$  cycles per second.) The oscillator was calibrated against a standard by a method of harmonics. The coil  $L$  had four or five turns only, and was loosely coupled to the oscillator (not shown in the diagram).

The quadrant electrometer  $Q$  was a Dolezalek, and served to measure the root mean square value of the high-frequency e.m.f. induced in the coil  $L$ ; the needle of the instrument was connected to the point  $A$ . The condenser  $C_1$  was a blocking condenser of  $2\mu$  F. capacity, and is needed to isolate the high-tension accumulator, which would otherwise

Fig. 1.—Circuit diagram.



short-circuit. With the frequencies in use, its impedance is always less than 0.04 ohm, so that the voltage drop across it is negligible as far as the high-frequency current through the valve is concerned. The quadrant electrometer can, therefore, be regarded as connected directly across the valve. The electrometer was found to have a capacity of about  $0.0005\mu$  F. This was the only capacity connected across the coil  $L$  save that in the valve itself, so its capacity is represented by the dotted condenser  $C$  in the diagram.

The rectified component of the current passes through the system  $G, S, E_1, R$ , which is adjusted so that there is no current through the galvanometer until the oscillator is brought into play. The shunt  $S$  controls the sensitivity of the galvanometer, and makes it sufficiently damped for readings to be taken as quickly as the electrometer itself will allow. The oscillating component is prevented from passing through the galvanometer etc. by air-core chokes  $L'$ .

This arrangement confines the high frequency to the left, and the direct currents to the right, in the diagram.

On the high-frequency side of the apparatus all leads were kept short and thick. In view of the importance of ensuring that the valve is subject to the same high-frequency potential as the electrometer, which would not be the case if the leads had an inductance comparable with  $L$  or a capacity comparable with  $C$ , the valve was mounted near the terminals of the electrometer, and the condenser  $C_1$  was also held very near by means of a wooden stand. The electrometer was at first screened; but this was afterwards found to make no difference, the reason being that stray static potentials have no effect, since the coil  $L$  permanently short-circuits the instrument so far as static potentials are concerned.

#### *Sensitivity of Electrometer.*

The idiostatically-connected electrometer was connected to sources of steady potential which could be applied in either direction, and the deflexions  $\phi$  on a millimetre scale placed 100 cm. from the instrument were read. The results are recorded in the following table, the last column giving  $K$  in the formula  $K\phi = V^2$ , where  $K$  is constant and  $V$  is the applied potential in volts,  $\phi$  being in millimetres.

V.	$V^2$ .	Mean $\phi$ .	K.
26.0	676	97.0	6.97
17.3	299	42.1	6.89
4.0	16	2.2	7.2
2.1	4.4	0.7	6.3

This table shows how insensitive the instrument becomes for low voltages, and it is just the low voltages for which we require to use it. Taking  $K=6.9$ , we note that for  $\phi=5$  mm.  $V=5.9$  volts; for  $\phi=10$  mm.  $V=8.3$  volts. In order to get the peak voltage of the corresponding alternating voltages, the above voltages must be multiplied by  $\sqrt{2}$ , giving 8.3 volts at  $\phi=5$  mm. and 11.7 volts at  $\phi=10$  mm.

#### *Method of Experiment—Outline.*

The filaments of the valves were turned on for such time as was necessary for the steady currents to attain constant values. The resistance  $R$  was then adjusted to balance out the steady current. The oscillator was then brought into play by completing the plate circuit of the oscillator. The coil  $L$  was then coupled sufficiently to the oscillator to deflect the electrometer by a certain amount  $\phi$  read on a millimetre scale. The corresponding deflexion  $\theta$  of the galvanometer  $G$

was then taken. The oscillator was then cut out and its frequency altered to another value, and the above readings repeated. The zeros of both the electrometer and galvanometer were inclined to change; but while the change of the former was gradual, and therefore not serious, the changes in the latter were often sudden. This is due to irregularities in the emission from the filament—the well-known Schottky effect\*,—and is troublesome when the deflexions are very small, as is the case when measuring small changes in steady current. The trouble caused by these irregularities was to some extent overcome by taking several readings of  $\theta$ .

In the following series of measurements the input voltage was given several different values at a given frequency. Each of the tables (I. *a-d*) is devoted to a definite frequency. The deflexion  $\phi$  was first adjusted to 1 mm., and the deflexion  $\theta$  noted as accurately as possible, and then given successively increasing values up to  $\phi$  1·3 mm., which corresponds to a range of peak voltages from about 3·7 to 13·5 volts. The voltage was then given successively decreasing values. The mean value of  $\theta$  only is shown.

## DATA—Marconi R-type Valve.

Filament voltage .....	$e_f = 4\cdot0$
Grid } voltage (steady) .....	$E_1 = 26\cdot0$
Anode }	
Peak value of input voltage.....	$e = 3\cdot7 \rightarrow 13\cdot5$
Mean anode current .....	$I = 4\cdot18$ m. A. $\frac{1}{2}$
Change in anode current .....	$\Delta I = 0\cdot017 \theta$ ,,
(where $\theta$ is in cm. deflexion)	

TABLE I. (a).—N = 15·00.

Electrometer deflexion. $\phi$ (cm.).	Galvanometer deflexion. Mean $\theta$ (cm.).	$\frac{\Delta I}{I}$	$\frac{1}{\phi} \frac{\Delta I}{I}$
0·2	0·325	$1\cdot24 \times 10^{-2}$	$6\cdot2 \times 10^{-2}$
0·3	0·5	1·01	6·37
0·4	0·6	2·29	5·73
0·5	0·8	3·05	6·1
0·6	1·025	3·90	6·5
0·7	1·2	4·57	6·53
0·8	1·525	5·8	7·25
0·94	2·05	7·81	8·30
1·0	2·25	8·57	8·57
1·1	2·625	10·0	9·09
1·2	3·075	11·7	9·75
1·3	4·05	15·4	11·85

\* *Ann. der Phys.* lvii, p. 541 (1918).

TABLE I. (b).— $N=10.89$ .

Electrometer deflexion. $\phi$ (cm.).	Galvanometer deflexion. Mean $\theta$ (cm.).	$\frac{\Delta I}{I}$ .	$\frac{1}{\phi} \frac{\Delta I}{I}$ .
0.2 } 0.2 }	0.3375	$1.35 \times 10^{-2}$	$6.75 \times 10^{-2}$
0.3	0.475	1.90	6.33
0.4	0.65	2.60	6.50
0.5	0.825	3.30	6.60
0.6	0.975	3.90	6.50
0.7	1.15	4.60	6.57
0.8	1.425	5.70	7.12
0.9	—	—	—
1.0	1.825	7.30	7.30
1.1	2.15	8.60	7.82
1.2	2.425	9.70	8.08
1.3	2.775	11.10	8.54

TABLE I. (c).— $N=8.02$ .

Electrometer deflexion. $\phi$ (cm.).	Galvanometer deflexion. Mean $\theta$ (cm.).	$\frac{\Delta I}{I}$ .	$\frac{1}{\phi} \frac{\Delta I}{I}$ .
0.2	0.4	$1.57 \times 10^{-2}$	$7.85 \times 10^{-2}$
0.3	0.55	2.135	7.12
0.4	0.725	2.86	7.15
0.5	0.875	3.45	6.90
0.6	1.05	4.14	6.90
0.7	1.25	4.93	7.04
0.8	1.4	5.62	6.90
0.94	1.85	(7.29)	7.75
1.0	1.85	7.29	7.29
1.1	2.175	8.56	7.78
1.2	2.425	9.56	7.97
1.3	2.7	10.63	8.18

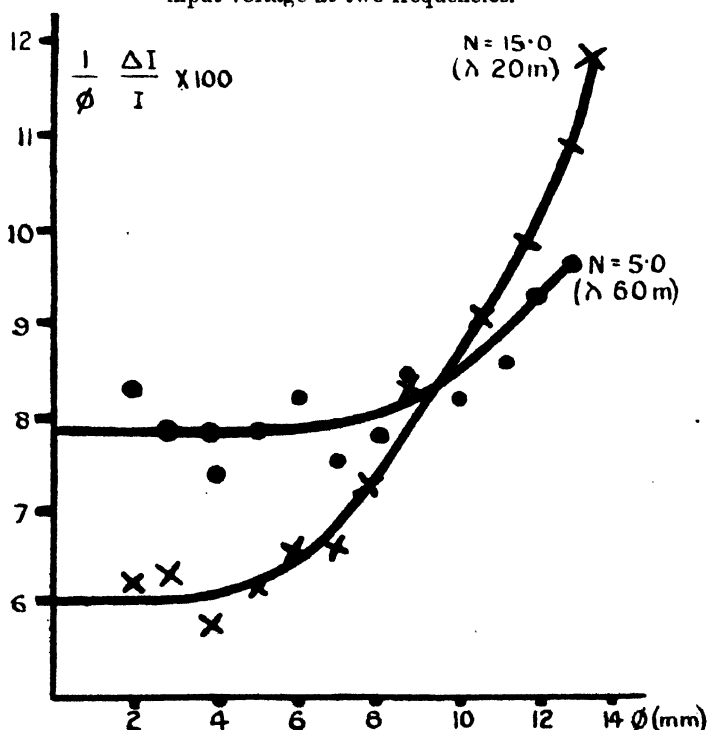
TABLE I. (d).— $N=5.02$ .

Electrometer deflexion. $\phi$ (cm.).	Galvanometer deflexion. Mean $\theta$ (cm.).	$\frac{\Delta I}{I}$ .	$\frac{1}{\phi} \frac{\Delta I}{I}$ .
0.2	0.425	$1.65 \times 10^{-2}$	$8.25 \times 10^{-2}$
0.3	0.60	2.33	7.77
0.4	0.75	2.91	7.28
0.5	1.0	3.68	7.76
0.6	1.25	4.85	8.08
0.7	1.325	5.14	7.34
0.8	1.575	6.11	7.64
0.94	2.025	7.85	8.35
1.0	2.075	8.05	8.05
1.1	2.4	9.31	8.46
1.2	2.85	11.05	8.21
1.3	3.175	12.32	9.48

On fig. 2  $\frac{1}{\phi} \frac{\Delta I}{I}$  is plotted against  $\phi$  for two frequencies. The result would be horizontal straight lines if rectification took place according to a square law. It will be seen from the curves—

- (a) That departure from square-law rectification takes place at some value of input voltage amplitude *which is different at different frequencies.*
- (b) That the rectified current is in general *different at different frequencies* for a given voltage amplitude.

Fig. 2.—Showing relation between rectified current and square of input voltage at two frequencies.

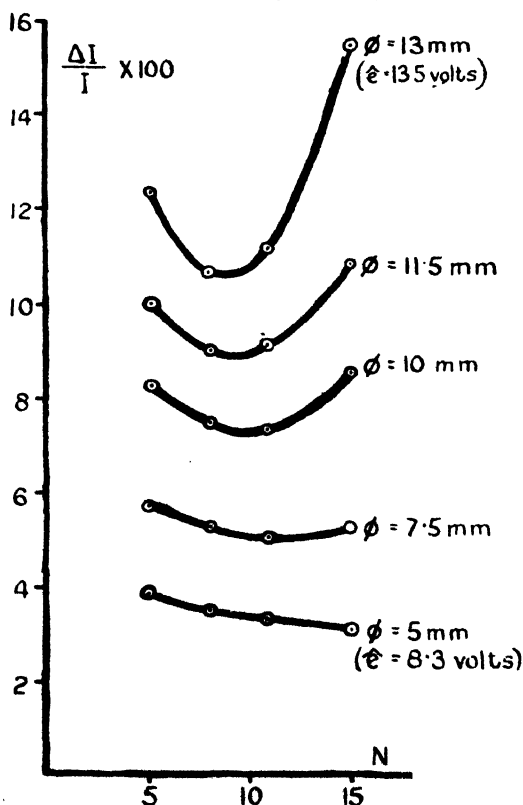


With regard to (b), it is to be noted that the frequency variation referred to is independent of the external impedances, and must not be confused with the case in which an oscillatory e.m.f. of given value is supplied to the valve *in series with an external impedance*. In this case (*cf.* Chaffee and Browning, Proc. I. R. E. Am. xv. p. 2, Feb. 1927) a frequency variation arises from the fact that the voltage

across the valve is different at different frequencies. If the voltage across the valve is kept constant, the external impedances have no influence on the rectified current, and any observed frequency variation must be due to the valve itself.

The variation of rectified current with frequency is indicated by fig. 3. The values of  $\frac{\Delta I}{I}$  for a given value of

Fig. 3.—Showing the variation of rectified current with frequency at different input voltages.



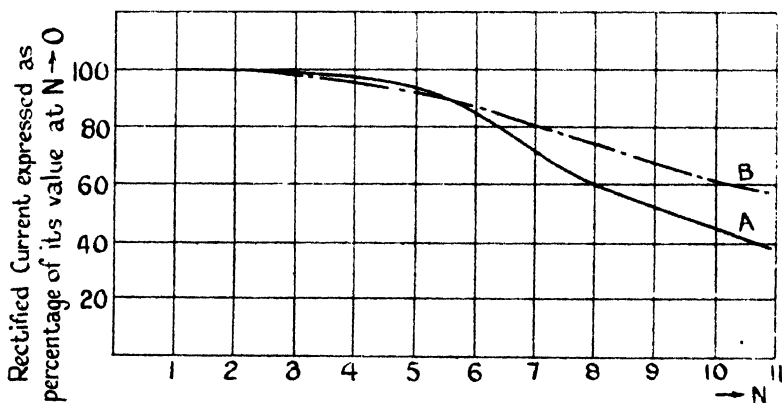
$\phi$  are smoothed values obtained by plotting a curve having  $\frac{\Delta I}{I}$  as ordinates and  $\phi$  as abscissæ. Fig. 3 gives some idea of the increase of input voltage amplitude on frequency variation, but must not be taken as an accurate representation of the variation of rectified current with frequency, as the curves are based on four frequencies only.



*Variation of Rectified Current with Frequency for Small Values of Input Voltage Amplitude.*

The lowest curve of fig. 3 is of most immediate interest, since the value of  $\phi$  to which it corresponds is low enough to ensure square-law rectification over the greater part of the range  $N=4.1 \rightarrow 16.9$  mega-cycles. The departure from square-law rectification at  $\phi=5$  mm. is seen from fig. 2 to be in the neighbourhood of 2 per cent. at 15.00 mega-cycles. In order to establish the form of this curve accurately, it is necessary to take measurements at a large number of frequencies. The resulting curves for two valves are shown in figs. 4 and 5. In the case of the Marconi R-type valve,

Fig. 4.—Showing variation of rectified current with frequency at constant (input) voltage amplitude.



Marconi R-type Valve.

Conditions:—

A. Filament voltage = 4.2.

B. „ „ = 5.0.

For both curves  $\epsilon = 8.3$  volts ( $\phi = 5$  mm.).

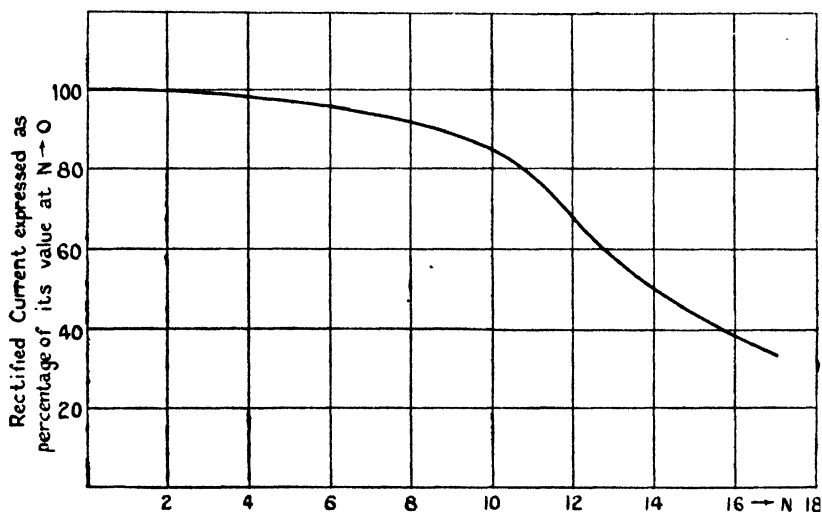
$E = 24$  „

measurements were made at two filament temperatures. The broken curve B corresponds to a filament voltage of  $E_f 5.0$ , the full-line curve to  $E_f 4.2$ . Now temperature saturation is approached at a filament voltage of 5 in the case of the valve quoted, so that for this case Langmuir's  $3/2$  power law is most nearly satisfied. Fig. 5 indicates that the variation is less in the case of a Dutch valve (bright valve, now obsolete), possibly due to the smaller electrode dimensions.

With regard to the upper curves of fig. 3, it appears that the magnitude of the frequency variation is greatly enhanced by increase of input voltage amplitude. For large amplitudes the rectified current arises from a whole series of terms in  $\sin n\pi t$ , where  $n$  is even. The frequency variation of such terms is likely to increase rapidly with  $n$ .

It was expected that the anode voltage  $E$  would have, for given values of  $\phi$  and  $E_f$ , an appreciable effect on the magnitude of the variation. This was not found to be the

Fig. 5.—Showing variation of rectified current with frequency for a Dutch valve.



Conditions :—

Filament voltage = 4.0 volts.

$\phi = 8.3$  „

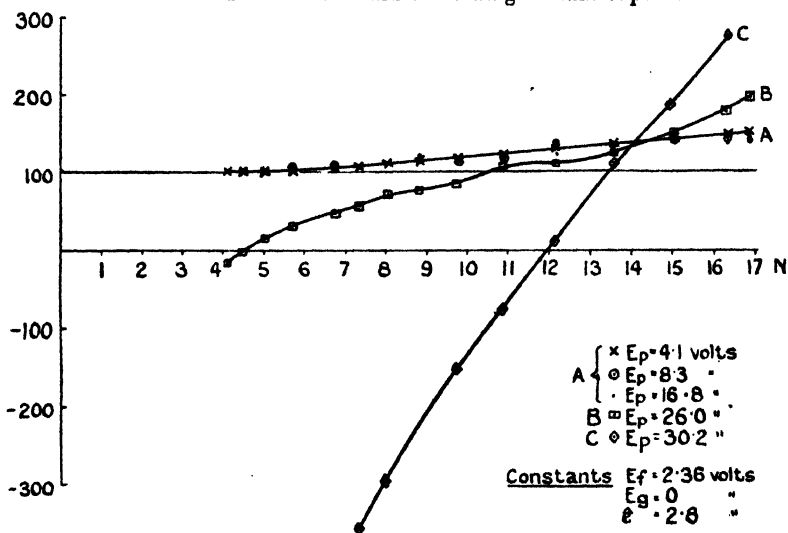
$E = 24$  „

case for values of  $E$  below that required for voltage saturation, the variation for  $E=0$  being sensibly of the same form and magnitude as the variation for  $E=24$ . If the voltage  $E$  is increased above voltage saturation value, it becomes necessary to increase  $E_f$  in order to obtain a reading at all. The variation is then appreciably diminished, and none could be detected at  $E 60$ ,  $E_f 5$ . The variation must depend on  $E_f$  in a very complex manner in view of the crossing of the two curves of fig. 4.

*Effect of Gases.*

With a view to obtaining information as to the effect of gases a helium-filled valve (Type A.R. 1) was used. Substantially the results were similar to those obtained with gas-free valves, below the critical potential. Above the critical potential enormous frequency variations took place, the change in mean anode current being positive at some frequencies and negative at others; the curves are very unreliable, due to the large amount of ionization. The plate voltage has a very marked effect above the critical potential, inasmuch as increase of plate voltage increases

Fig. 6.--Showing rectified current as function of frequency in case of valve used as a triode and containing helium vapour.



The curve A corresponds to plate potentials  $E_p$  below the critical potential of helium ( $=21.4$  volts), and represents the rectified current as a percentage of its value at  $N \rightarrow 0$ . The curves B and C correspond to potentials above the critical potential of helium. The input voltage amplitude ( $\hat{e} = 2.8$ ) was the maximum consistent with square-law rectification.

the degree of ionization and therefore the number of slowly-moving ions. The fact that the rectified current changes sign is doubtless due to the fact that two kinds of thermions are present— $\text{He}^+$  and electrons. At low frequencies the observed rectified current is mainly due to  $\text{He}^+$  ions. At high frequencies these ions become exceedingly sluggish, and the rectified current is again carried mainly by electrons. The curves for this helium valve are shown on fig. 6. The

valve was used as a *triode* in order to diminish the chance of overrunning. The grid was connected through a coupling coil to the filament. It will be seen that the rectified *anode* current *increases* with frequency for a given voltage amplitude between filament and *grid*. The irregularities in the curves obtained for voltages below the critical potential may be due to small traces of ionization. These irregularities did not repeat regularly or in the same place, so that, while the points are shown, the curve drawn corresponds to the average form, which repeated itself. The points  $x$  corresponding to  $E = 4$  volts lie very nearly on this curve. The curves corresponding to values of  $E$  above the critical potential are plotted on the same diagram. The most interesting result to be obtained from fig. 6 is that the curves A, B, and C cross one another at a frequency of 14 megacycles, approximately. The obvious interpretation of this result is that the contribution of the positive ions towards the rectified current is zero at this point.

The presence of gases clearly complicated matters. It would seem as if the observed frequency variation in the absence of gas is in some way due to the inertia of the electrons. The theoretic aspect of this question will be relegated to a subsequent paper.

#### *Summary.*

1. Experiments with a diode are described which show that—

- (a) For a given input voltage amplitude the rectified current is in general different at different frequencies, the frequencies employed in the experiments lying between 4.1 and 16.8 megacycles ( $\lambda$  73– $\lambda$  17.8 metres).
- (b) The value of input voltage amplitude at which departure from square-law rectification takes place decreases as the frequency is increased.

2. The form of the frequency variation is investigated in detail in the case where the input voltage amplitude is small enough for rectification to take place according to a square law. In this case the rectified current falls off as the frequency is increased, the rate of variation being markedly affected by the filament temperature.

3. Experiments with a helium-filled valve used as a triode show a variation of similar form and magnitude for plate voltages below the critical potential, the variation corresponding, however, to an increase with frequency as

distinct from the decrease with a two-electrode valve. For plate voltages above the critical potential the variation with frequency is much more rapid, doubtless due to the presence of slowly-moving ions; at a certain frequency, depending on the potential, the rectified current is zero, the rectified current due to the space-charge being neutralized by a similar current due to the helium ions. At a higher frequency (about  $N=14$  megacycles) the rectified current is the same as it would be in the absence of helium ions; in other words, there is no rectification due to helium ions in the neighbourhood of this frequency.

In conclusion, the author wishes to thank Prof. E. V. Appleton for the loan of a Helium valve, and the Department of Scientific and Industrial Research for a maintenance grant, with the aid of which this research has been made possible.

XXXIII. *The Problem of a Hidden Polarized Sphere.* By Prof. A. PETROWSKY, Hon. Member of Rori (*The Russian Society of Radio Engineers*)\*.

CONTENTS.

Introduction.

Part I.

- § 1. Differential equations and boundary conditions in the case of a limitless medium.
- § 2. Expression of the electric potential and of the electric force for such case.
- § 3. A polarized sphere in a medium bordered on one side by a plane.
- § 4. Final expression of the electric potential and force.
- § 5. Transformation of the formulæ.
- § 6. A general characteristic of longitudinal electropfiles.
- § 7. A general characteristic of transversal electropfiles.
- § 8. Generalization of solving the problem of a hidden sphere.
- § 9. A general characteristic of oblique electropfiles.

*Introduction.*

A WIDE application of physics in various regions of knowledge evokes new questions which insistentlly demand their solution. In this respect geology and mining are in advance, where the spreading of physical methods of investigating the structure of the earth's crust and the quest

\* Communicated by the Author.

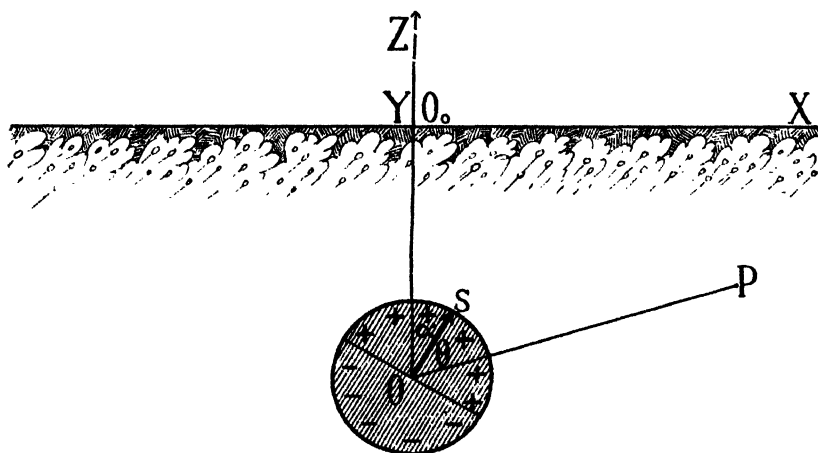
of useful minerals is daily increasing. It follows, as a matter of course, that the circumstances in which one is obliged to solve physical problems are often so complicated that a mathematical analysis of the question meets with unsurmountable difficulties; in such a case the engineer is assisted by the laboratory and by experimental investigation on models, taking into account the definite demand of similarity. Thus the greater value attaches to the analytical investigation of the simplest cases, especially of those where the question is solved to the end and expressions are obtained in the form of algebraic-trigonometrical formulæ, which give from the first glance a clear conception of the phenomenon.

The examination of one of such simple cases is the subject of the present paper. We shall call it "The Problem of a Hidden Polarized Sphere."

The problem consists in the following :—

All infinite space is divided into two parts by a plane  $XO_0Y$  (fig. 1), and the medium filling the upper part represents a dielectric, whereas the medium filling the lower part possesses conductivity.

Fig. 1.—The sphere hidden in a homogeneous isotropic half-space.



In some region of the lower part an ideally conducting sphere is hid, of a radius  $r_0$ , the centre of which  $O$  is at the depth  $h$  under the plane of division, and is projected on the latter in the point  $O_0$ .

By any causes whatever the above-mentioned sphere is polarized—i. e., it develops an electromotive force of its own

which has the greatest value along a certain diameter (axis of polarization), inclined at an angle  $\alpha$  to the vertical, and diminishes by cosine law in dependence on the angle  $\theta$ , which is formed by the given direction and the axis of polarization

$$e = E \cos \theta. \quad . \quad . \quad . \quad . \quad . \quad (1)$$

At the same time, in the conducting medium surrounding the sphere a current is formed which spreads over the whole lower part of the space, evoking electric and magnetic effects. It is required to determine whether it is possible, and in what manner, by observing the above-mentioned effects on the plane of division (or near it), to find all elements characterizing the hidden sphere—i. e., the exact situation of  $O_0$ , the projection of the centre, the depth of its bed  $h$ , and the radius of the sphere  $r_0$ .

In solving the question we shall make the following assumptions:—

(a) Each of the mediums filling the two parts of the space is homogeneous and isotropic.

(b) The bed's depth to the centre of the sphere,  $h$ , is considerably greater in comparison with the radius of this sphere  $r_0$ .

## PART I.

### *Electric Field of a Hidden Sphere.*

§ 1. Let us suppose that the plane of division is absent, and that the whole space is filled with a homogeneous isotropic medium.

Let the right-hand system of coordinates (fig. 2) be disposed so as to place its beginning in the centre of the sphere; the axis  $O\xi$  to correspond in direction with the axis of polarization, viz. of the greatest development of the electromotive force; the axis  $O\xi$  to be perpendicular to  $O\xi$  in the plane of the drawing, and the axis  $O\eta$  perpendicular to the latter. In such a case, the system being symmetrical in respect of the axis  $O\xi$ , we may assume that the electric potential  $U$  and all other values are functions of two derivatives only; for example, of the radius  $r$  and the polar angle  $\theta$ ,

$$U = U(r, \theta).$$

The value  $U$  must satisfy the differential equation of Laplace, which for the considered case will take the form

$$\frac{\partial^2 U}{\partial r^2} + \frac{2}{r} \frac{\partial U}{\partial r} + \frac{1}{r^2} \frac{\partial^2 U}{\partial \theta^2} + \frac{\cot \theta}{r^2} \frac{\partial U}{\partial \theta} \quad . \quad . \quad . \quad . \quad . \quad (2)$$

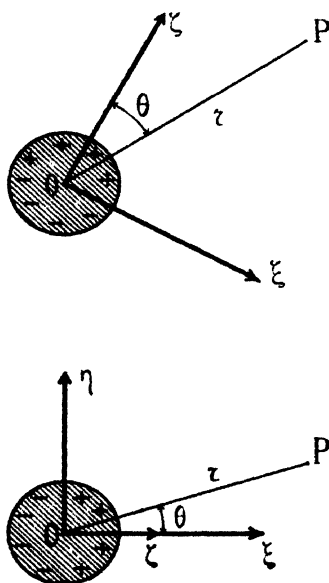
Moreover, this function must be finite, single-valued, and continuous, and must satisfy the following conditions:—

(a) For the surface of a sphere it must take the form expressed by the formula (1), namely for

$$r=r_0, \quad U = \frac{E}{2} \cos \theta. \quad . \quad . \quad . \quad (3)$$

In fact, the distribution of the electricity over the surface will then be symmetrical, and the difference of potentials in each point will be balanced by the electromotive force.

Fig. 2.—Distribution of the axis of coordinates (vertical and horizontal projections).



(b) For any very distant point of the space it must be reduced to zero. Consequently

$$r=\infty, \quad U=0 \quad . \quad . \quad . \quad (4)$$

§ 2. The solution of these differential equations will be sought in the form

$$U = U'(r) \cos \theta + U''(r), \quad . \quad . \quad . \quad (5)$$

where  $U'(r)$  and  $U''(r)$  are unknown functions of the variable  $r$  only. Following the method used in my paper "On the Theory of Earth-Currents' Measurement\*," we

\* Phil. Mag. vol. iii. pp. 60-62 (January 1927).



shall easily find that the function  $U$  must have the form

$$U = \left( Ar + \frac{B}{r^2} \right) \cos \theta + \frac{C}{r} + D. \quad (6)$$

According as we are dealing with the outer ( $r > r_0$ ) or the inner space ( $r < r_0$ ), we can write two functions of the type (6), though with different arbitrary constants  $A_{ex}$ ,  $B_{ex}$ ,  $C_{ex}$ ,  $D_{ex}$  and  $A_{in}$ ,  $B_{in}$ ,  $C_{in}$ ,  $D_{in}$ , viz.

$$U_{ex} = \left( A_{ex}r + \frac{B_{ex}}{r^2} \right) \cos \theta + \frac{C_{ex}}{r} + D_{ex}, \quad (6')$$

$$U_{in} = \left( A_{in}r + \frac{B_{in}}{r^2} \right) \cos \theta + \frac{C_{in}}{r} + D_{in}. \quad (6'')$$

Let us consider the former.

To make it satisfy the condition (a), the following equations must hold :—

$$C_{ex} = D_{ex} = 0, \quad (7)$$

$$A_{ex}r_0 + \frac{B_{ex}}{r_0^2} = \frac{E}{2}. \quad (8)$$

Whereas, to make it satisfy the condition (b), it is necessary that

$$A_{ex} = 0, \quad (9)$$

which, on comparison with (8), gives

$$B_{ex} = \frac{Er_0^2}{2}. \quad (10)$$

Let us consider the second function (6'').

To make it satisfy the condition (a), it is also necessary that the following equations hold :—

$$C_{in} - D_{in} = 0, \quad (11)$$

$$A_{in}r_0 + \frac{B_{in}}{r_0^2} = \frac{E}{2}. \quad (12)$$

Whereas, to make it remain finite in the centre of the sphere, it is necessary to have

$$B_{in} = 0, \quad (13)$$

which, compared with (12), gives

$$A_{in} = \frac{E}{2r_0}. \quad (14)$$

Thus we finally have expressions for the electric potential in any outer and in any inner point of the sphere :—

$$U_{ex} = \frac{E_0 r^2}{2r_0^2} \cos \theta, \quad . \quad . \quad . \quad (15)$$

$$U_{in} = \frac{Er}{2r_0} \cos \theta. \quad . \quad . \quad . \quad (15'')$$

On translation into Descartes's coordinates, the following expressions have to be substituted for  $r$  and  $\theta$  :—

$$r = \sqrt{\xi^2 + \eta^2 + \zeta^2}, \quad . \quad . \quad . \quad (16)$$

$$\cos \theta = \frac{\zeta}{\sqrt{\xi^2 + \eta^2 + \zeta^2}}. \quad . \quad . \quad . \quad (17)$$

Because of symmetry the electric force in any point of the outer field will lie in the plane passing through the given point and through the axis of polarization ; in particular, if the point lies in the plane of the paper, the electric force will lie in the same plane, and can be transformed into two components : that of the axis directed parallel to  $O\xi$  and the normal one directed perpendicular to  $O\xi$ , viz. towards P. They are obtained from functions (15') and (15'') by means of differentiating according to  $-\xi$  and  $-\rho$ , and are expressed by

$$(F_\xi)_{ex} = \frac{Er_0^2}{2} \cdot \frac{3 \cos^2 \theta - 1}{r^3}, \quad . \quad . \quad . \quad (18')$$

$$(F_\rho)_{ex} = \frac{3Er_0^2}{2} \cdot \frac{\sin \theta \cos \theta}{r^3}. \quad . \quad . \quad . \quad (19')$$

The electric force in a point of the inner field is obtained by the same procedure. It is easy to make certain that it is in all points directed parallel to the direction  $-O\xi$ , and is consequently expressed by :

$$(F_\xi)_{in} = -\frac{E}{2r_0}, \quad . \quad . \quad . \quad (18'')$$

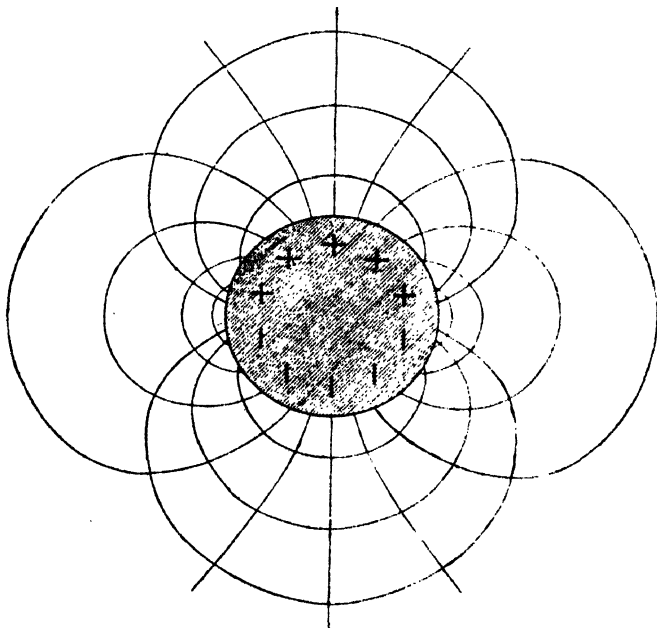
$$(F_\rho)_{in} = 0. \quad . \quad . \quad . \quad (19'')$$

In fig. 3 is graphically shown the distribution of isopotential lines of force in the plane passing through the axis of polarization.

§ 3. It has been supposed so far that the sphere is situated in a limitless medium. In reality its centre is placed at some depth under the earth. In such a case the ascending current lines, when reaching the surface, are forced to curve

and continue their way horizontally. It follows, therefore, that the new function  $W$ , which expresses the electric potential, must, in addition to all the above conditions, enumerated under 3, satisfy another condition more, namely :

Fig. 3.—Electric field produced by a polarized sphere in a limitless medium.



*On the parting surface of the two media the electric force must have a tangent component only.*

Let us trace a new right-hand system of coordinates (fig. 4) in such manner that its beginning shall be point  $O_0$ ; in which point the centre of the sphere  $O$  is projected on the parting surface. The axis  $OX$  shall be directed horizontally either in the plane  $O_0O\xi$  or  $O_0O\zeta$ , passing through the axis of polarization of the sphere; the axis  $O_0Y$  horizontally too and perpendicularly to  $O_0X$ , whereas the axis  $O_0Z$  will be vertically upwards. In such a case the new boundary condition can be expressed by the equation

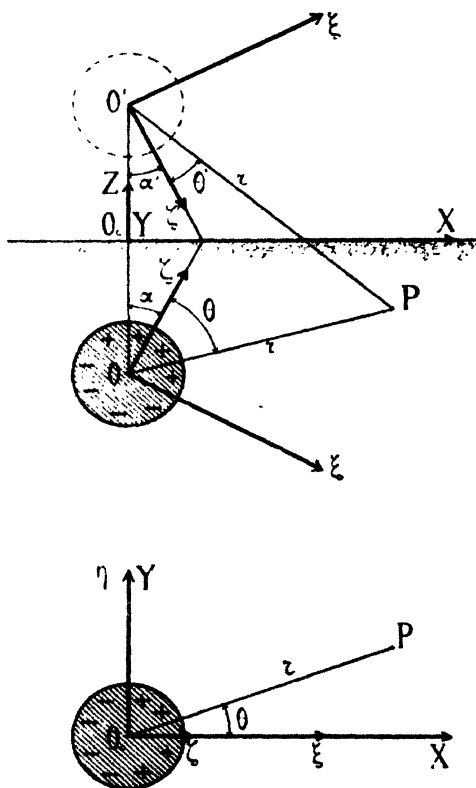
$$z=0, \quad \frac{\partial W}{\partial z}=0 \dots \dots \dots (20^b)$$

The function  $W$  expressing the electric potential for the

considered case can be found approximately by means of the following consideration.

¶ Let us figure the real electric image of the given sphere  $O$  in the plane of parting. It shall be the sphere  $O'$  with radius  $r_0$ , situated above the parting surface on the same vertical and at the height  $h$  equal to the depth of the centre of the

Fig. 4.—Polarized sphere and its electrical image (vertical and horizontal sections).



sphere  $O$ , polarized in addition according to the cosine law (1) along the line  $O'\zeta'$ ; the latter lies in the plane  $OO'Z$  or  $OO'\zeta$ , and is bent towards  $O'O_0$  at the angle  $\alpha' = \alpha$ .

Should we imagine a third system of coordinates with the axes  $O'\xi'$ ,  $O'\eta'$ ,  $O'\zeta'$  which also presents the real image of the system  $O\xi$ ,  $O\eta$ ,  $O\zeta$  in the plane of parting, the electric potential produced by the imaginary sphere  $O'$  in any point

P of a uniform, isotropic, limitless medium will obviously be expressed through the formula

$$U'_{ex} = \frac{Er_0^2}{2r'^2} \cos \theta', \quad . \quad . \quad . \quad (21')$$

$$U'_{in} = \frac{Er'_0}{2r_0} \cos \theta', \quad . \quad . \quad . \quad (21'')$$

where  $r'$  is the distance of the point P to the centre of the sphere  $O'$ , and  $\theta'$  is the angle between the direction  $O'P'$  and the axis  $O'\zeta'$ .

The functions (21') and (21'') evidently satisfy all the conditions enumerated under 3.

§ 4. Let us accept the formulæ below for expression of the final potential W in a medium which is limitless on one side and is bordered on the other by the plane  $z=0$ .

$$W_{ex} = U_{ex} + U'_{ex} = \frac{Er_0^2}{2} \left[ \frac{\cos \theta}{r^2} + \frac{\cos \theta'}{r'^2} \right], \quad . \quad (22')$$

$$W_{in} = U_{in} + U'_{in} = \frac{E}{2r_0} \left[ r \cos \theta + r_0^3 \frac{\cos \theta'}{r'^2} \right]. \quad (22'')$$

It is easy to be convinced that the former satisfies all requirements, including the condition (20), whereas the latter meets them but approximately\*. The distribution of the potential within the sphere presenting no practical interest, we may, ignoring the latter circumstance, take the formula (22') for the sought expression of the electric potential created by the polarized sphere situated at some depth under the surface of the plane  $XO_0Y$ .

Translating this formula into the coordinates of Descartes, corresponding to the axes X, Y, Z we obtain

$$W = \frac{Er_0^2}{2} \left[ \frac{x \sin \alpha + (h+z) \cos \alpha}{[x^2 + y^2 + (h+z)^2]^{3/2}} + \frac{x \sin \alpha + (h-z) \cos \alpha}{[x^2 + y^2 + (h-z)^2]^{3/2}} \right], \quad (23)$$

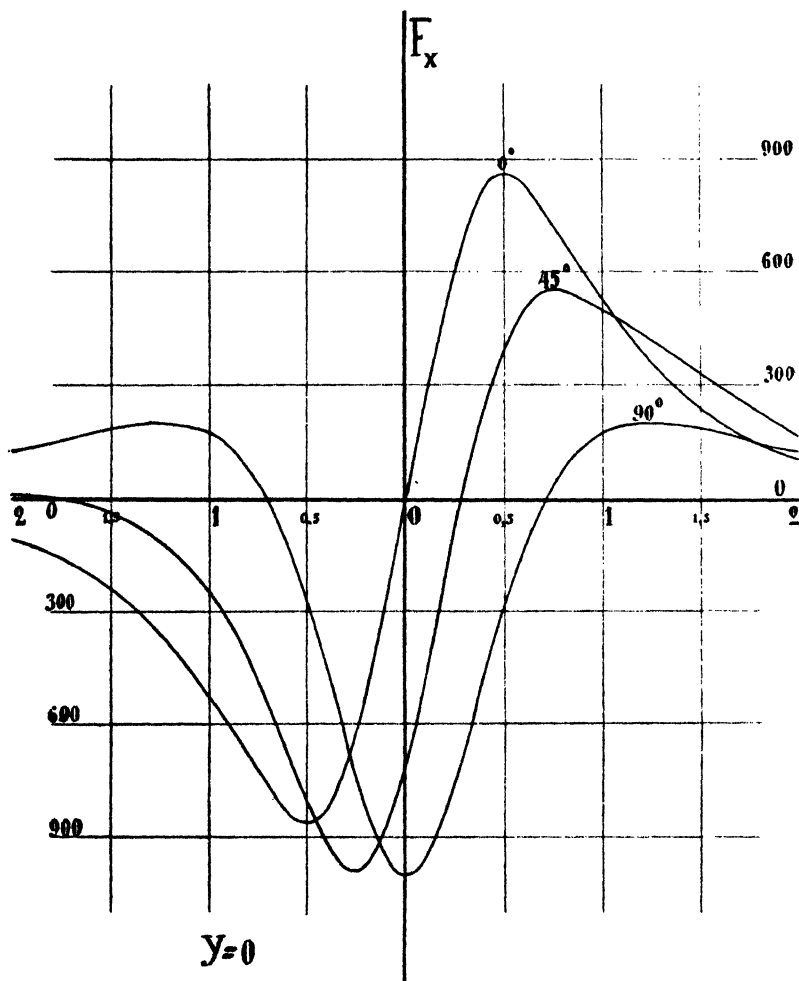
\* In the first approximation the coefficient E, standing in the formula (23) and following, is the value of the electric force developed by the sphere; therefore the same expression E is being conserved. In the second approximation it proves to be somewhat lower, namely, instead of E we must put the value A, which is expressed by the formula

$$A = \frac{E}{1 + \frac{r_0^2}{8A^2} \left[ \frac{\left(1 - \frac{r_0}{h} \cos \alpha\right) \cos \alpha + \frac{r_0}{2h}}{\left(1 - \frac{r_0}{h} \cos \alpha + \frac{r_0^2}{4h^2}\right)^{3/2}} - \frac{\left(1 + \frac{r_0}{h} \cos \alpha\right) \cos \alpha - \frac{r_0}{2h}}{\left(1 + \frac{r_0}{h} \cos \alpha + \frac{r_0^2}{4h^2}\right)^{3/2}} \right]}. \quad (24)$$

and on the plane  $XO_0Y$ , viz. for  $z=0$ ,

$$W = Er_0^3 \frac{x \sin \alpha + h \cos \alpha}{[x^2 + y^2 + h^2]^{3/2}}. \quad . \quad . \quad . \quad (25)$$

Fig. 5.—The electrophile obtained in the plane of polarization.



Taking the derivatives of  $W$  according to coordinates, we shall find the expressions for respective projections of the electric force too, which on the plane  $XO_0Y$ , viz. for

$z=0$ , take the form

$$F_x = Er_0^2 \frac{3hx \cos \alpha - (h^2 + y^2 - 2x^2) \sin \alpha}{[h^2 + x^2 + y^2]^{5/2}}, \quad (26)$$

$$F_y = Er_0^2 \frac{3(h \cos \alpha + x \sin \alpha)y}{[h^2 + x^2 + y^2]^{5/2}}, \quad (27)$$

$$F_z = 0. \quad (28)$$

§ 5. To get an exact idea of the character of the electro-profile, let us give the graphical representation of the discovered formulæ. For that purpose we introduce the denotations

$$u = \frac{x}{h}, \quad (29)$$

$$v = \frac{y}{h}. \quad (30)$$

We have then

(a) The electric potential in any point of the plane  $XO_0Y$ , possessing the coordinates  $x$  and  $y$ :

$$W = \frac{Er_0^2}{h^2} \cos \alpha + u \sin \alpha \quad (31)$$

(b) The projection of the electric force on the horizontal direction parallel to the plane of polarization of the sphere:

$$F_x = \frac{Er_0^2}{h^3} \frac{3u \cos \alpha - (1 + v^2 - 2u^2) \sin \alpha}{[1 + u^2 + v^2]^{5/2}}. \quad (32)$$

(c) The projection of the electric force on a horizontal direction perpendicular to that plane:

$$F_y = \frac{Er_0^2}{h^3} \frac{3(\cos \alpha + u \sin \alpha)v}{[1 + u^2 + v^2]^{5/2}}. \quad (33)$$

§ 6. In fig. 5 are shown the values of the horizontal projection of the electric force  $F_x$  for  $y=0$ , viz. those obtained when the observer is moving along the axis  $O_0X$  (in other words, along the line passing through the horizontal projection of the centre of the sphere and lying in the plane of polarization of that sphere). On the axis of the abscissæ are reckoned the values of  $u$ , on the axis of ordinates those of  $F_x$ , the coefficient being taken as equal to 1000 (viz.  $\frac{Er_0^2}{h^3} = 1000$ ). The first curve corresponds to the value  $\alpha=0^\circ$  (the axis of polarization of the sphere is running

vertically); the second to the value  $\alpha=45^\circ$  (the axis of polarization is inclined); and the third to the value  $\alpha=90^\circ$  (the axis of polarization is horizontal).

Inspection of fig. 5 leads to the following conclusions:—

1. An electrophile in a plane of polarization presents in a general case a curve with three numerical maxima, of which two are positive and one negative; besides this the curve has two zero-points, and falls to zero asymptotically when moved from the point where the centre of the hidden sphere is projected.

2. The distribution of the curve of the electrophile relatively to the projection of the centre of the hidden sphere is not symmetrical:

(a) The front zero-point is nearer to the projection of the centre of the sphere than the rear one.

(b) The front positive maximum is also nearer than the rear one, and it is greater than the latter.

(c) The negative maximum is behind the projection of the centre of the hidden sphere, being nearer to this projection than the front maximum; in absolute value it is greater than either of the positive maxima.

(d) In a particular case, when  $\alpha=0^\circ$ , *i.e.* in a vertical direction of the axis of polarization, the front zero-point is just above the centre of the hidden sphere, whereas the rear point passes into infinity; at the same time the front positive maximum becomes numerically equal to the negative maximum, and both are placed at a distance from the projection of the centre of the sphere equal to the half of the depth of the sphere's centre; *i.e.*, we have

$$u_m = \pm 0.5. \quad . \quad . \quad . \quad . \quad . \quad (34)$$

The value of each of these two maxima is expressed by the formula

$$F_m = \frac{Er_0^3}{h^3} \cdot \frac{3}{2(1.25)^{5/2}} = 0.859 \frac{Er_0^3}{h^3}. \quad . \quad . \quad (35)$$

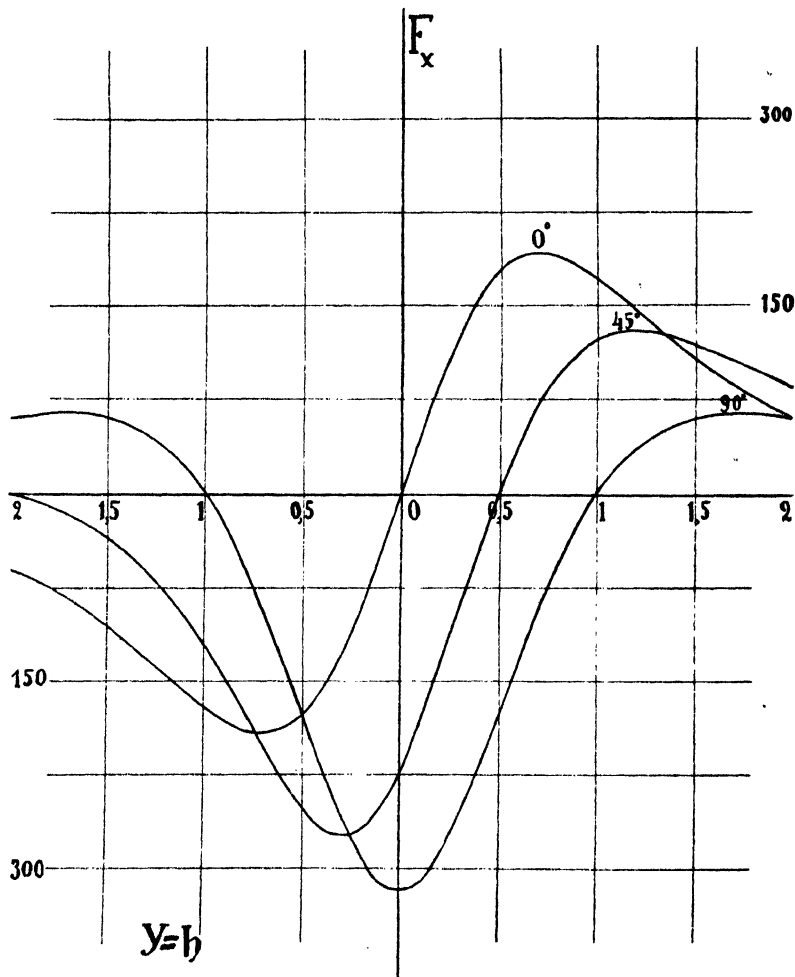
The rear positive maximum in the case under discussion is entirely absent.

(e) In a particular case, when  $\alpha=90^\circ$ , *i.e.* in a horizontal position of the axis of polarization, the front and rear zero-points are placed at distances from the projection of the centre of the hidden sphere equal to

$$u_0 = \pm \frac{1}{\sqrt{2}} = \pm 0.707. \quad . \quad . \quad . \quad . \quad (36)$$



Fig. 6.—The electroprofile obtained along a line parallel to the plane of polarization.



The value of each of them equals

$$F_m = \frac{Er_0^2}{h^3} \cdot \frac{4}{(2.5)^2 \sqrt{10}} = 0.202 \frac{Er_0^2}{h^3} \dots (37)$$

The negative maximum is situated below the very centre of the sphere, and is expressed by the formula

$$E'_m = \frac{Er_0^2}{h^3} \dots \dots \dots (38)$$

On fig. 6 an electrophile is given, obtained in a survey along the line parallel to the plane of polarization (but not lying in this plane).

From that it is seen :

3. Curves expressing a longitudinal electrophile in a side dislocation retain the same shape as in a plane of polarization, but zero-points (where there are two) retreat further from the projection of the centre of the sphere ; likewise also do the maxima separate, losing gradually at the same time their sharpness (*i. e.* diminishing numerically).

§ 7. On fig. 7 an electrophile is represented, obtained along the line perpendicular to the plane of polarization and passing over the centre of the hidden sphere.

From it is seen the following :—

1. The curve expressing the electrophile has only one zero-point, one positive and one negative maximum ; the curve asymptotically tends to zero the further it moves from the projection of the centre of the sphere.

2. The distribution of a curve of the transversal electrophile relatively to the projection of the centre of the hidden sphere has a mirror symmetry.

(a) The zero-point is always over the centre of the hidden sphere.

(b) The maxima are placed at distances from the projection of the centre of the sphere equal to the half of its depth.

$$r_m = \pm \frac{h}{2} \dots \dots \dots (39)$$

(c) The values of the maxima are numerically alike and are expressed as follows :

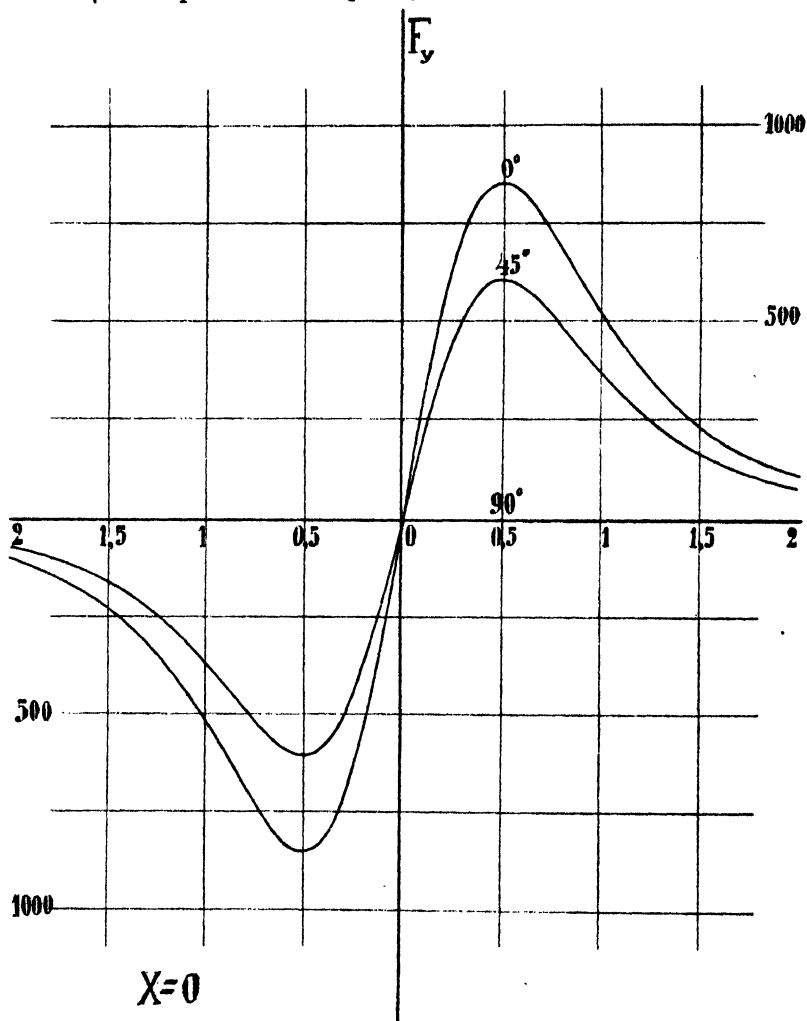
$$F_m = \pm \frac{48Q}{25\sqrt{5}} \cos \alpha \dots \dots \dots (40)$$

(d) In a particular case, when  $\alpha = 0^\circ$ , *i. e.* in a vertical direction of the axis of polarization, the transversal electrophile does not differ from the longitudinal one.

(e) In a particular case, when  $\alpha = 90^\circ$ , *i. e.* in a horizontal

direction of the axis of polarization, the transversal electroprofile is entirely absent ; *i.e.*, the electric force is everywhere equal to zero.

Fig. 7.—The electroprofile obtained along the line perpendicular to the plane of polarization and passing over the centre of the sphere.

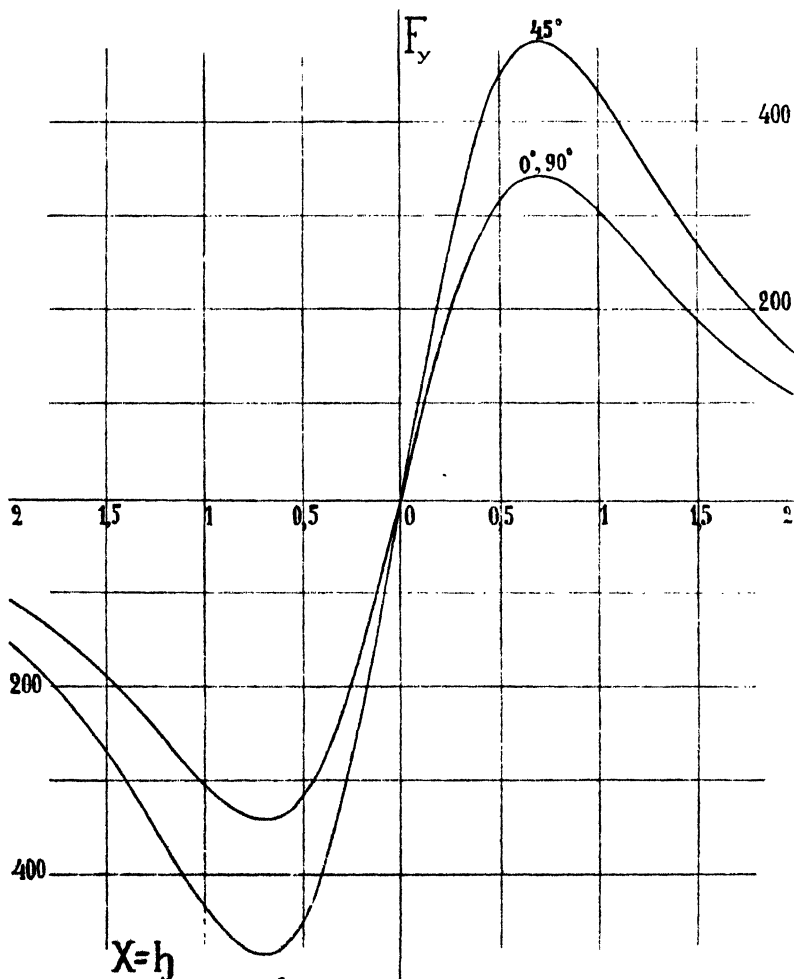


On fig. 8 is given a transversal electroprofile which does not pass over the centre of the hidden sphere.

From this is to be seen :

3. Curves expressing a transversal electrophile in side displacement do not change their shape, their zero-points

Fig. 8.—The electrophile obtained along a line perpendicular to the plane of polarization and not passing over the centre of the sphere.



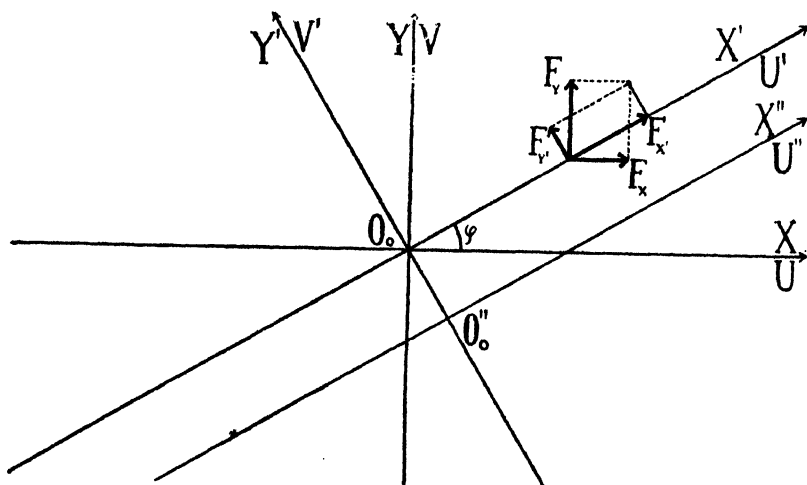
remain in their places, but the maxima gradually separate in different directions and diminish in value the further they are removed from the projection of the centre of the sphere.

§ 8. Let us now suppose that the observer is tracing an electrophile along the line  $O_0X'$ , inclined to the line  $O_0X$  (and at the same time also to the plane of polarization at the angle  $\phi$  (fig. 9)); and he observes the projection of electric force to the direction  $O_0X'$ , i.e. the value  $F_{x'}$ , expressing it in the function of coordinates  $x', y'$  or in the function of values  $u', v'$ , connected with  $x', y'$  by the following relations:—

$$u' = \frac{x'}{h}, \dots \dots \dots (41)$$

$$v' = \frac{y'}{h} \dots \dots \dots (42)$$

Fig. 9.—Distribution of the axis of coordinates in a general case.



Let us find the expression of the potential and of the electric force in the function of these values. For that purpose we substitute in formula (31) the values  $u, v$  by the expressions

$$u = u' \cos \phi - v' \sin \phi, \dots \dots \dots (43)$$

$$v = u' \sin \phi + v' \cos \phi, \dots \dots \dots (44)$$

and obtain a formula for the potential  $W$  as follows:

$$W = P \frac{\cos \alpha + u' \cos \phi \sin \alpha - v' \sin \phi \sin \alpha}{[1 + u'^2 + v'^2]^{3/2}}. \dots (45)$$

By differentiating this formula by  $x'$  or  $y'$ , and taking into consideration the relations (41), (42), we obtain the expressions for projections of electric force sought for at the point  $u'$ ,  $v'$  along the directions  $O_0 X'$ ,  $O_0 Y'$ .

$$F_{x'} = -\frac{\partial W}{\partial x'} = -\frac{\partial W}{h \partial u'} \\ = Q \frac{3u' \cos \alpha - (1 + v'^2 - 2u'^2) \cos \phi \sin \alpha - 3u'v' \sin \phi \sin \alpha}{[1 + u'^2 + v'^2]^{5/2}} \quad (46)$$

$$F_{y'} = -\frac{\partial W}{\partial y'} = -\frac{\partial W}{h \partial v'} \\ = Q \frac{3v' \cos \alpha + (1 + u'^2 - 2v'^2) \sin \phi \sin \alpha + 3u'v' \cos \phi \sin \alpha}{[1 + u'^2 + v'^2]^{5/2}}, \quad (47)$$

where

$$Q = \frac{Er_0^2}{h^3} \quad (48)$$

§ 9. On fig. 10 an electrophile is given obtained along the line inclined to the plane of polarization at an angle  $\phi = 45^\circ$  and passing through the point  $O_0$  lying over the centre of the hidden sphere.

Examining it, we see the following :—

1. Curves expressing an electrophile in general have the same shape as in the case of an electrophile obtained along the line lying in the plane of polarization.

2. Points (2a), (2b), (2c), (2d), and (2e) enumerated in § 6, corresponding to the above-mentioned curves, retain their meaning also in the given case, but with the following differences:

(a) The zero-points are nearer to the point  $O_0$  than in the electrophile taken along the line lying in the plane of polarization.

(b) The maxima are numerically less than in the case of the above-mentioned electrophile.

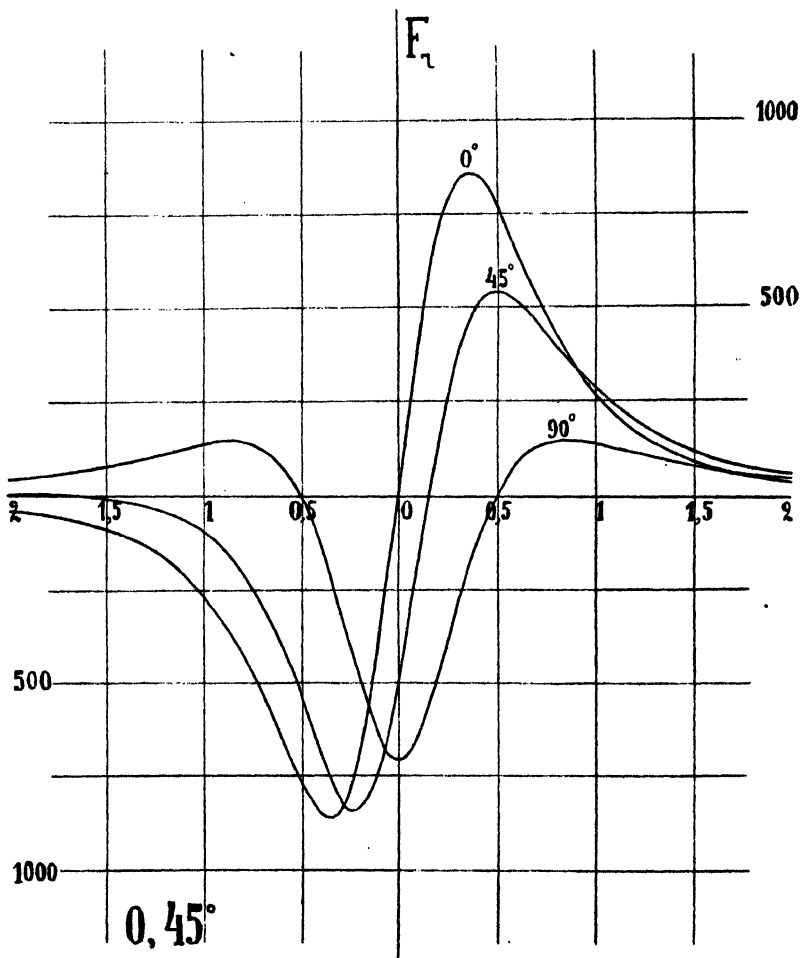
(c) When  $\alpha = 0^\circ$  this diminution is entirely absent; it is the more considerable the nearer  $\alpha$  is to  $90^\circ$ .

3. The electrophile also does not undergo any essential changes in the case when the line of surveying  $O_0''X''$ , remaining inclined at the same angle  $\phi$  to the plane of polarization, does not pass through the point  $O_0$  lying over the centre of the sphere; such an electrophile is given on fig. 11.

In this case the following particulars are to be noticed :

(a) The zero-points recede from the point  $O_0$ —the front one somewhat, the rear one considerably.

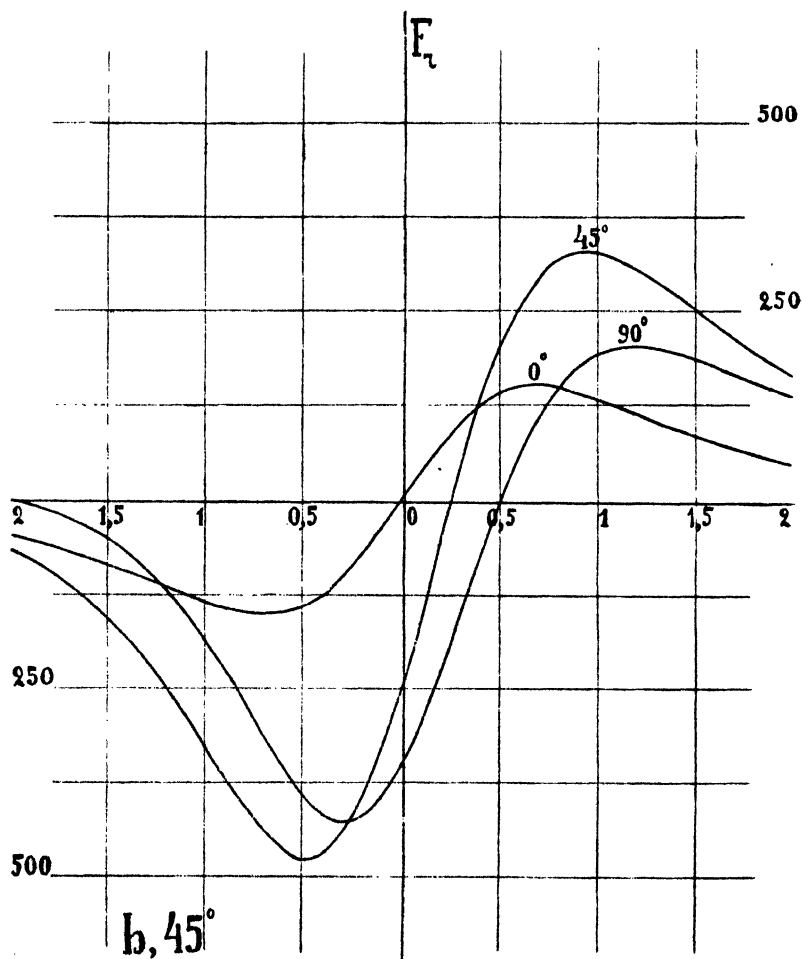
Fig. 10.—An electrophile along the line, inclined to the plane of polarization, but passing through the projection of the sphere's centre.



(b) The maxima also recede from the point  $O_0$ —the front positive maximum and the rear negative one not so quickly as the rear positive maximum ; the numerical values of the

rear maxima diminish; the numerical values of the front maxima diminish at small angles  $\alpha$  and increase at large angles  $\alpha$ .

Fig. 11.—An electrophile along the line, inclined to the plane of polarization, and not passing through the projection of the sphere's centre.



(c) At  $\alpha=90^\circ$  the electrophile loses its symmetry with respect to points  $O_0$  lying above the centre of the bed 0, because the front zero-point remains in its place, whereas the negative maximum shifts back.



**XXXIV. The Crystal Structure of the Isomorphous Sulphates of Potassium, Ammonium, Rubidium, and Cæsium.** By A. OGG, M.A., Ph.D., F.Inst.P., Professor of Physics, University of Cape Town\*.

[Plates V. & VI.]

1. **T**HE sulphates of potassium, ammonium, rubidium and cæsium form isomorphous crystals, which belong to the holosymmetric class of the orthorhombic system. The crystallographic characters of this isomorphous series have been very carefully investigated by Tutton†.

The dimensions of the unit cells of potassium, ammonium, rubidium, and cæsium sulphates and the number of molecules per unit cell were determined by Ogg and Hopwood‡. Each cell contains four molecules. Table I. gives the lengths of the sides of the unit cells in Å.U. ( $10^{-8}$  cm.).

TABLE I.

Crystal.	a.	b.	c.	Axial ratios $a : b : c.$
K <sub>2</sub> SO <sub>4</sub> .....	5·731	10·008	7·424	0·573 : 1 : 0·742
(NH <sub>4</sub> ) <sub>2</sub> SO <sub>4</sub> ...	5·951	10·560	7·729	0·563 : 1 : 0·732
Rb <sub>2</sub> SO <sub>4</sub> .....	5·949	10·391	7·780	0·572 : 1 : 0·748
Cs <sub>2</sub> SO <sub>4</sub> .....	6·218	10·884	8·198	0·571 : 1 : 0·753

The ratio of  $b : a$  is very nearly  $\sqrt{3} : 1$  or  $1 : 0·577$ . The “c” axis is an axis of pseudohexagonal symmetry. Potassium sulphate shows a marked prevalence of repeated twinning in the form of three individuals interpenetrating to form what appears to be simple hexagonal prisms. Tutton has shown that the other salts of the series frequently twin in the same way. Ogg and Hopwood observed the spectral intensities for the  $K_{\alpha}$  radiation of palladium. I am indebted to Mr. E. N. Grindley, Lecturer, Physics Department of the University of Cape Town, for repeating and extending the observations on potassium and ammonium sulphates for the  $K_{\alpha}$  radiation of molybdenum.

2. Since the intensity of the reflexion of X-rays from any plane depends on the distribution of the scattering power in

\* Communicated by the Author.

† ‘Crystalline Structure and Chemical Constitution,’ by A. E. H. Tutton.

‡ Phil. Mag. xxxii. p. 518 (1916).

a direction perpendicular to that plane, and corrections have to be made for absorption and extinction which are difficult to evaluate, the structure of such crystals has to be determined by a process of trial and error. Atomic arrangements have to be assumed, and then tested by comparing the calculated intensities of the X-ray spectra with the observed intensities. In these crystals, which are orthorhombic, the atoms have, as far as symmetry is concerned, considerable degrees of freedom. The difficulty in such a case is to fix on possible atomic arrangement. The most certain aid to such a selection is that of symmetry. There are 28 space-groups to which these crystals may belong. They are  $V_h1$  to  $V_h28$  in the notation of Schoenflies, or  $Q_h1$  to  $Q_h28$  in the notation of Hilton. Each space-group is characterized by certain internal regularities which cause reflexions from certain planes to have zero intensities\*. A comparison of these predicted from the regularities of the space-group with the observed intensities is sufficient to fix the space-group.

The observed spacings of the important planes referred to the spacings of the unit cell given in Table I. were:—

TABLE II.

(100) halved	(021) normal
(010) halved	(110) normal
(001) halved	(011) normal
(111) normal	(130) normal

These spectral observations suggest that this isomorphous series of crystals belongs to the symmetry group  $V_h16$ , a conclusion which can be tested when the symmetry elements have been placed within the unit cell. This symmetry group contains two reflexion planes, four glide planes, twelve dyad screw axes, and two sets of four centres of symmetry.

### 3. ELEMENTS OF SYMMETRY.

Bradley†, James and Wood‡, Dickson and Binks§, and Wasastjerna|| have shown that in crystals the sulphate  $SO_4$  group forms a tetrahedron with the sulphur atom or ion at the centre of the tetrahedron, and the oxygen atoms or ions at the corners. If we assume this tetrahedral form for the  $SO_4$  group, symmetry and spectral intensities give us at once

\* Astbury and Yurdley, *Phil. Trans. A*, cciv. p. 221.

† *Phil. Mag.* xlix. p. 1225 (1925).

‡ *Proc. Roy. Soc.* cix. p. 598 (1925).

§ *Phil. Mag.* ii. p. 114 (1926).

|| *Soc. Scient. Fenn. Comm. Phys. Maths.* ii. p. 26.

certain information about the distribution of the symmetry elements and of the  $\text{SO}_4$  groups. The two sets of symmetry centres of the  $\text{V}_{16}$  group form two sets of four-fold points without freedom. The four sulphur atoms cannot, however, be placed at any one of these sets of symmetry centres, because the centre of a tetrahedron with oxygen atoms at the corners cannot be a centre of symmetry. There is, however, another alternative. A point on a reflexion plane with two degrees of freedom is multiplied into four by the action of the symmetry elements. All other points with three degrees of freedom are multiplied into eight by the elements of symmetry. We may say, then, that the sulphur atoms must lie on reflexion planes. It follows that a reflexion plane is a plane of symmetry of the  $\text{SO}_4$  group. If the S atom lies on a reflexion plane, two oxygen atoms of the group must also lie on the plane, and two be equidistant from the plane, one being the mirror image of the other in the plane. To fix the position of the  $\text{SO}_4$  group three parameters have to be determined, if we assume the dimensions of the tetrahedron constant. The S atom has two degrees of freedom on the plane, and the group may be rotated round an axis perpendicular to the plane.

The spacing of the (100) planes is  $a/2$ , and the intensities fall off normally for all members of the series, showing that the structure must consist of layers of atoms parallel to (100) with spacings  $a/2$ . The sulphur atoms will lie in these layers, and since they also lie on reflexion planes, we conclude that the reflexion planes are  $(100)_{1/4}$  and  $(100)_{-1/4}$ , if we take the centre of the unit as the origin of coordinates. Also, since the " $c$ " axis is an axis of pseudohexagonal symmetry, we can settle the positions of the glide planes.

The proposed elements of symmetry, referred to the symmetry centre at the centre of the unit as origin, are:—

#### Reflexion Planes :

$$(100)_{1/4}, (100)_{-1/4}.$$

#### Glide Planes :

$$(010)_{1/4}, (010)_{-1/4}, \text{ Translation } c/2.$$

$$(001)_{1/4}, (001)_{-1/4}, \text{ Translation } a/2, b/2.$$

#### Centres of Symmetry :

$$\text{I. } (0, 0, 0), (\frac{1}{2}, 0, 0), (0, \frac{1}{2}, \frac{1}{2}), (\frac{1}{2}, \frac{1}{2}, \frac{1}{2}).$$

$$\text{II. } (0, 0, \frac{1}{2}), (\frac{1}{2}, 0, \frac{1}{2}), (0, \frac{1}{2}, 0), (\frac{1}{2}, \frac{1}{2}, 0).$$

Dyad Screw Axes :

$(100)_{00}$ ,  $(100)_{1/2\ 1/2}$ ,  $(100)_{1/2\ 0}$ ,  $(100)_{0\ 1/2}$ , Translation  $a/2$ .  
 $(010)_{0\ 1/4}$ ,  $(010)_{0\ -1/4}$ ,  $(010)_{1/2\ 1/4}$ ,  $(010)_{1/2\ -1/4}$ , Translation  $b/2$ .  
 $(001)_{1/4\ 1/4}$ ,  $(001)_{-1/4\ -1/4}$ ,  $(001)_{-1/4\ -1/4}$ ,  $(001)_{1/4\ 1/4}$ ,  
 Translation  $c/2$ .

#### 4. THE ARRANGEMENT OF THE ATOMS.

It has been shown by Bradley\* that the distance between S and O centres of the  $\text{SO}_4$  group in potassium lithium sulphate crystals lies between 1.5 and 1.6 Å.U. James and Wood† have found that the distance 1.5 gives good agreement with observation for barytes, celestine, and anglesite. The tetrahedral form of  $\text{SO}_4$  was assumed as well as the distance S—O 1.5 Å.U., and it has been found that such an  $\text{SO}_4$  group fits well with observation.

Since the structure must consist of layers of atoms on reflexion planes parallel to (100), the metallic atoms must lie on reflexion planes. They must consist of two sets of four, and not of one set of eight‡. The environment of the metal atoms may therefore be of two kinds.

A very strong (130) spectrum, a strong (330) spectrum, and the "c" axis being an axis of pseudohexagonal symmetry indicate hexagonal packing or two interpenetrating base-centred structures. Models of  $\text{SO}_4$  groups were constructed and built together to satisfy the elements of symmetry, and it soon became clear how the metal atoms would fit into the structure. The atoms were finally adjusted to give as good agreement as possible between the calculated and observed intensities.

If we take the symmetry centre at the centre of the unit as origin, an atom whose coordinates are  $x, y, z$  is converted by the elements of symmetry into eight atoms within the unit cell, whose coordinates are :—

$$\begin{aligned} &\pm(x, y, z), \quad \pm(a/2 - x, y, z), \\ &\pm(x, b/2 - y, -c/2 + z), \quad \pm(-a/2 + x, -b/2 + y, c/2 - z). \end{aligned}$$

If the amplitude of the reflected wave due to a given atom is A, when reflexion is taking place in the ( $hkl$ ) plane, then

\* *Loc. cit.*

† *Loc. cit.*

‡ W. L. Bragg and G. B. Brown have found a similar condition for aluminium atoms in chrysoberyl ( $\text{BeAl}_2\text{O}_4$ ), Proc. Roy. Soc. cx. p. 46 (1926).

the eight corresponding atoms contribute a wave whose amplitude is

$$A \Sigma \cos 2\pi m \left( \frac{hx}{a} + \frac{ky}{b} + \frac{lz}{c} \right),$$

where  $m$  is the order of the spectrum.

The summation taken over the eight atoms gives the expression

$$8A \cos 2\pi m \left( \frac{hx}{a} + \frac{h}{4} \right) \cos 2\pi m \left( \frac{ky}{4} + \frac{l+k}{4} \right) \cos 2\pi m \left( \frac{lz}{c} + \frac{h+k+l}{4} \right) \cos (h+k+l)\pi.$$

The factor  $\cos(h+k+l)\pi$  affects only the sign of the expression. This expression for the amplitude shows that planes of the type  $(okl)$ , when  $k$  and  $l$  are not zero, give normal spacings.

Planes of the type  $(hol)$  have their spacings halved, when  $l$  is odd.

Planes of the type  $(hko)$  have their spacings halved, when  $(h+k)$  is odd.

Planes of the type  $(hkl)$  have normal spacings.

As special cases of the above rules, all pinakoid spacings are halved.

The deductions from the chosen elements of symmetry are in agreement with the observed spacings enumerated in Table II.

In calculating the spectral intensities, Hartree's\* values for the scattering functions of potassium and sulphur were used, while for oxygen those of James and Wood† were used. Only general agreement was to be expected.

It was of considerable help in solving the structure to compare the spectral intensities of different members of the series for the same plane, and to observe the effect of the change of the metal atoms. Take, for example, the spectra from the (001) planes. The odd orders are absent. The (002) spectrum of ammonium sulphate is much stronger than the (004) spectrum. The (002) spectrum of potassium sulphate is slightly weaker than the (004) spectrum. The (004) spectrum of rubidium sulphate is the stronger. The (002) spectrum of caesium sulphate vanishes and the (004) spectrum is very strong. These observations are explained by the proposed structure.

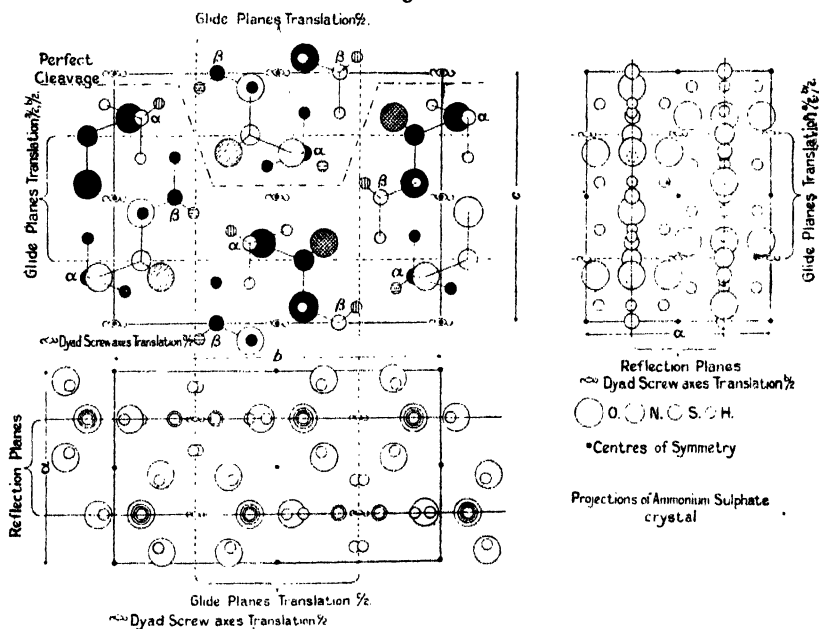
\* Phil. Mag. 1. p. 289 (1925).

† Loc. cit.



positions of the hydrogen atoms cannot, however, be determined from intensity measurements. Two possible ways of forming the group can be proposed. The nitrogen atom could take up three electrons from the hydrogen atoms to its 2<sub>s</sub> system and become a nitrogen ion with a charge -3, while the fourth hydrogen atom would give up an electron to one of the oxygens of the SO<sub>4</sub> group. The NH<sub>4</sub> group would then consist of a central nitrogen ion with charge -3 surrounded by four ions, each of charge +1. The NH<sub>4</sub> group

Fig. 2.



would be equivalent to a polar ion of charge +1. The nitrogen atom could, however, in accordance with the suggestion made by Niven \* for ammonia, give up four electrons to the four hydrogen atoms to complete their 1<sub>s</sub> systems, and also one electron to one of the oxygen atoms giving a nitrogen ion of charge +5, surrounded by four hydrogen ions, each with a charge -1. The orientation of the (NH<sub>4</sub>) groups would, however, be different in the two cases. The first alternative in which the positive hydrogen ions would form the connecting-link between the nitrogen and oxygen ions has been adopted.

\* Phil. Mag. iii. p. 1315 (1927).





In this case the orientation of the  $\alpha$  ( $\text{NH}_4$ ) groups would appear to be fairly certain; but there are two possible orientations of the  $\beta$  groups consistent with the symmetry and the linkage of hydrogen to oxygen. The one which gives the hydrogen linked to those oxygen which have the closest approach to the metal ions of the other crystals has been taken.

The coordinates of the atoms with the centre of the unit as origin are summarized in Table III. In each case the coordinates of one atom is given, the others being derived from it by the operation of the symmetry elements.

The oxygen environment of the metal atoms is different for the two sets of metal atoms in the structure. In the diagrams one set is marked  $\alpha$  and the other  $\beta$ .

The distances between the atomic centres of the metal atoms and oxygen atoms and the number of times any particular measurement occurs are summarized in Table IV.

TABLE IV.  
Atomic distance  $\text{M}_\alpha - \text{O}$  in Å.U.

No.	$\text{K}_\alpha - \text{O}$ .	$\text{Rb}_\alpha - \text{O}$ .	$\text{Cs}_\alpha - \text{O}$ .	$(\text{NH}_4)_\alpha - \text{O}$ .
1.....	2.71	2.89	3.10	2.86
4.....	2.89	2.95	3.20	2.91
3.....	3.00	3.12	3.20	3.15
2.....	3.15	3.17	3.28	3.25
1.....	3.50	3.50	3.70	3.60

Atomic distance  $\text{M}_\beta - \text{O}$ .

No.	$\text{K}_\beta - \text{O}$ .	$\text{Rb}_\beta - \text{O}$ .	$\text{Cs}_\beta - \text{O}$ .	$(\text{NH}_4)_\beta - \text{O}$ .
4.....	2.71	2.89	3.10	2.86
2.....	2.91	3.01	3.17	3.10
1.....	2.95	3.15	3.30	3.15
2.....	3.10	3.20	3.37	3.20

The distance of closest approach is the same for both kinds, and is

$\text{K}-\text{O}$ .....	2.71 Å.U.
$\text{Rb}-\text{O}$ .....	2.89 "
$\text{Cs}-\text{O}$ .....	3.10 "
$(\text{NH}_4)-\text{O}...$	2.86 "

These atomic distances are in close agreement with the distances suggested by Wasastjerna \* for atomic radii with a clear recognition of the fictitious nature of atomic radii. The values were

$$K-O = 1.30 + 1.35 = 2.65,$$

$$Rb-O = 1.50 + 1.35 = 2.85,$$

$$Cs-O = 1.75 + 1.35 = 3.05.$$

Bradley † mentions in his paper on the structure of lithium potassium sulphate that Prof. W. L. Bragg ‡ modified the values originally proposed by him in the manner suggested by Wasastjerna, and proposed the value for

$$K-O = 1.34 + 1.36 = 2.70,$$

which is in very close agreement with the value given above.

The  $M_\beta$  atoms appear to be more closely linked to oxygen than the  $M_\alpha$  atoms.

Bradley's structure for  $KLiSO_4$  crystals indicates that it is  $K_\alpha$  that is replaced by Li.

The closest approach of the metals is

$$K_\alpha - K_\beta \dots\dots\dots 3.55 \text{ \AA.U.}$$

$$Rb_\alpha - Rb_\beta \dots\dots\dots 3.75 \text{ ,,}$$

$$Cs_\alpha - Cs_\beta \dots\dots\dots 3.95 \text{ ,,}$$

$$(NH_4)_\alpha - (NH_4)_\beta \dots\dots 3.75 \text{ ,,}$$

The structure of these sulphates is one in which each positive metallic ion is surrounded as closely and as uniformly as possible by negative oxygen ions, perfect freedom of adjustment being prevented by the attachment of the oxygen ions in fours to sulphur to form the sulphate group. The  $SO_4$  groups are in turn surrounded by metallic ions. In potassium sulphate the distances of the potassium atoms, surrounding an  $SO_4$  group, from the nearest oxygen of that group are two at 2.71, five at distances from 2.900 to 3.00, and three at 3.15  $\text{\AA.U.}$

5. In potassium sulphate the cleavage (001) is distinct, and the cleavages (010) and (110) are imperfect. In ammonium sulphate the cleavage (001) is perfect. These cleavage planes are indicated in figs. 1 and 2.

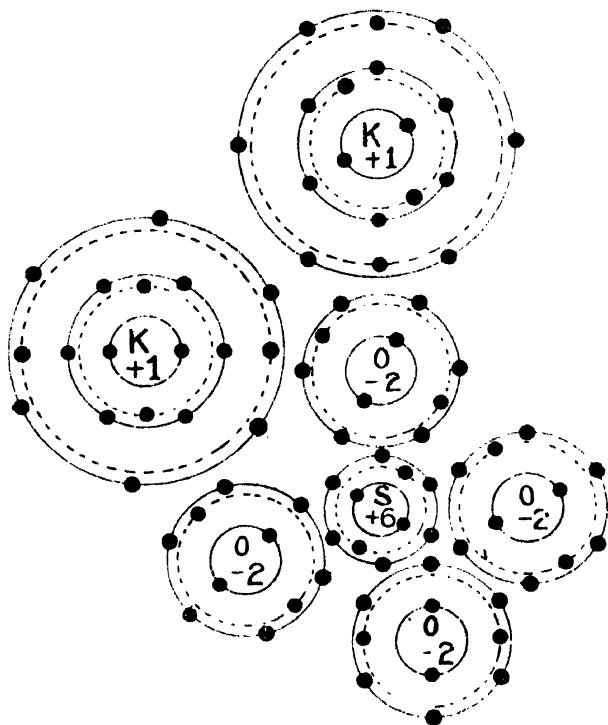
\* J. A. Wasastjerna, "On the Radii of Ions," Soc. Scient. Fenn. Comm. Phy. Maths. i. p. 38 (1923).

† *Loc. cit.*

‡ "Interatomic Distances in Crystals," Phil. Mag. ii. p. 258 (1927).

Although the ions of such a structure are in equilibrium in electric fields produced by the surrounding ions, it seems probable from the position of the cleavage planes and from the distances of closest approach of the metallic ions to the oxygen ions that one metal ion of each kind belongs to each  $\text{SO}_4$  group to form the molecule. Fig. 3 represents the molecule of potassium sulphate as it occurs in these crystals. The potassium, sulphur, and two oxygen atoms

Fig. 3.

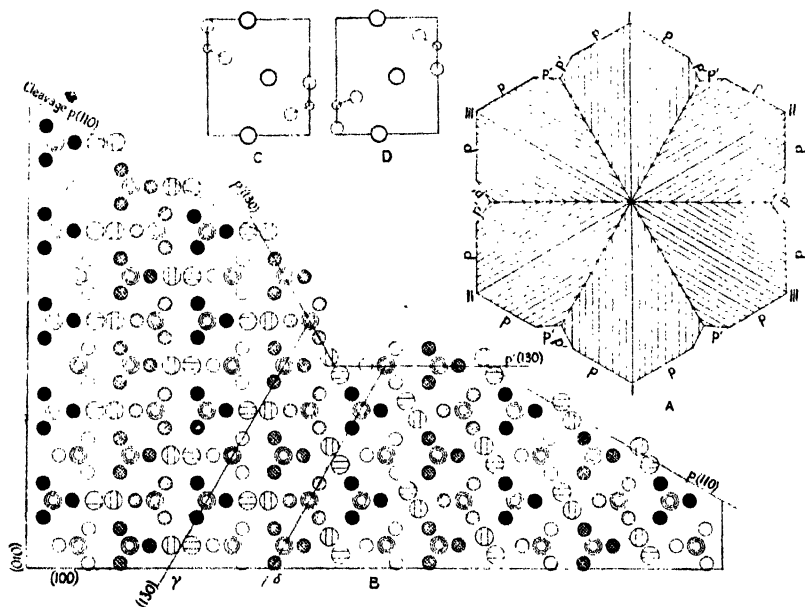


lie in a plane. The other two oxygen atoms, which are equidistant from that plane, are also represented as lying in that plane, and have been displaced to prevent the electron systems from intersecting in the diagram.

6. The crystals of this series show repeated twinning, which results in interpenetrating groups which are almost indistinguishable from simple hexagonal crystals. Fig 4 A

shows a section of such a crystal built from three crystals, I., II., and III.\* Figures of characteristic triplets of potassium selenate are given by Tutton†. The external faces of the crystal are the planes  $p$  (110) and  $p'$  (130). The twinning plane (130) is nearly at right angles to the plane (110). If the re-entrant angles formed by the planes (130) vanish by the growth of the crystal, there results an almost true hexagonal prism terminated by a hexagonal pyramid. Each face is however composed of two halves, which are inclined at a small angle to one another. This inclination can be detected by reflecting light from the face of the crystal.

Fig. 4.



Section of Potassium Sulphate perpendicular to "C" axis twinned on (130)

A twinning plane must have special characteristics. The cases hitherto observed show twinning planes to be planes of closely-packed atoms. It must also be such that, if the crystal is built up to this plane, its continuance on the other side of the plane may follow one or more alternatives. One of these is correct and continues the plan of the crystal.

\* 'Physikalische Krystallographie,' Groth, p. 406.

† 'Crystalline Structure and Chemical Constitution,' A. E. H. Tutton, p. 93.

The others are not so easy to follow. The plane (130) satisfies these conditions.

Fig. 4 B, which is a section of potassium sulphate perpendicular to the "c" axis, explains the process of twinning in these crystals. The figure shows the  $\beta$ -potassium atoms in the projection lying inside a nearly true hexagon of oxygen atoms, which in turn lie inside a larger hexagon of S atoms. These potassium atoms lie in the reflexion planes parallel to (100). Their positions relative to the oxygen atoms are shown in fig. 4 C. If these potassium atoms are rotated through nearly  $60^\circ$  into the plane (130), they would occupy positions relative to oxygen atoms illustrated in fig. 4 D. The crystal would now grow in that direction as the (100) plane of the twin. The potassium atoms might equally well be rotated through nearly  $60^\circ$  in the opposite direction into the plane (130). Arcanite ( $K_2SO_4$ ) is described in Dana's 'System of Mineralogy' as giving repeated twins on the planes (110) and also on (130) resembling aragonite.

The diagonal of the "hexagon" of S atoms parallel to the plane (100) is slightly longer than that parallel to (130) or (130). The lengths are 6.67 and 6.63 Å.U. The longer direction is the correct direction for the potassium atoms. The section between the lines  $\gamma$  and  $\delta$  would serve as origin for the growth of either system on each side of it.

7. Models of  $SO_4$  groups were made with spheres of 1.5 cm. diameter to represent both S and O. The distance  $S-O=1.5$  cm. The  $K_2SO_4$  unit was then constructed with  $SO_4$  models and with spheres of 2.7 cm. diameter to represent K atoms. The radii of these spheres were not intended to represent "atomic radii." A similar model of the  $(NH_4)_2SO_4$  unit was made, taking a sphere of 1.5 cm. diameter to represent N and a sphere of 1.0 cm. diameter to represent H. The whole  $NH_4$  group would then lie within a sphere of 1.75 cm. radius.

Two views of the (100) planes of each of these models are given in Pl. V. (figs. 5 A & B) and in Pl. VI. (figs. 6 A & B).

It can be seen from the model that, if ammonium sulphate were to twin like potassium sulphate, not only would the  $NH_4$  group have to be rotated through nearly  $60^\circ$  about an axis parallel to "c," but the groups would also have to be inverted; i. e., rotated through  $180^\circ$  about an axis through its centre parallel to "b."

SUMMARY.

The structures of the isomorphous sulphates of potassium, ammonium, rubidium, and caesium have been investigated. The structure is based on a simple orthorhombic lattice having four molecules to the unit cell, and the space-group is  $V_h 16$ . The positions of the atoms in the structures have been determined. An explanation of the characteristic twinning of these crystals has been given.

In conclusion, I wish to express my thanks to Dr. A. E. H. Tutton, F.R.S., for supplying me with certain crystals for this investigation, to the South African Research Grant Board for some financial assistance, and to Mr. J. A. Linton for skilful assistance in making models and diagrams.

---

XXXV. *Energy Distribution among Secondary Electrons from Nickel, Aluminium, and Copper.* By D. A. WELLS, Assistant Professor of Physics, University of Cincinnati\*.

A REVIEW of experimental work indicates that results do not always agree as to the energy distribution of secondary electrons. The highest velocities found by Barber† working with copper correspond to from 2 to 5 volts. The results of McAllister‡, using practically the same apparatus and continuing the work of Barber, indicate that there are a few electrons reflected or emitted with velocities approaching the velocity of the primary stream. Davisson and Kunsman§, investigating the maximum velocity of secondary electrons from aluminium, platinum, and magnesium, found that secondary electrons with velocities "not appreciably less than that of the primaries proceed from the platinum and magnesium for all bombarding potentials up to the highest investigated in each case, 1000 volts and 1500 volts respectively."

\* Communicated by the Author.

† I. G. Barber, "Secondary Electron Emission from Copper and Copper Oxide," *Phys. Rev.* vol. xvii. pp. 322-338 (1921).

‡ L. E. McAllister, "The Effect of Ageing on the Secondary Electron Emission from Copper Surfaces," *Phys. Rev.* vol. xix. p. 246 (1922).

§ C. Davisson and C. H. Kunsman, *Phys. Rev.* vol. xxii. p. 242 (1923).

*Description of Apparatus.*

Fig. 1 gives a diagram of apparatus and connexions. F, a flat spiral tungsten filament (Coolidge X-ray cathode) heated by means of lead storage-cells, was used as the source of primary electrons. A nickel shield S served as an anode and allowed a narrow beam of primary electrons to fall on  $d$ , the metal from which secondaries were to be studied. The large disk D, carrying the small disks  $d$ , could be rotated from the outside by the action of an electromagnet on a short iron bar attached to the extreme end of the axle. The

Fig. 1.

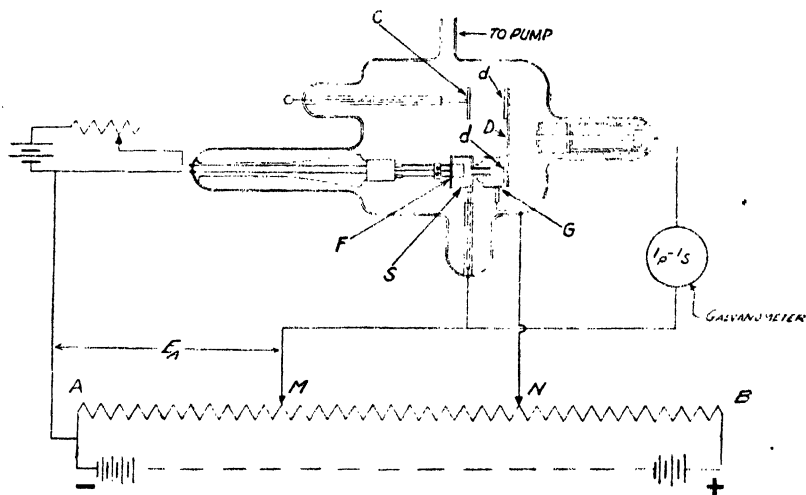


FIGURE 1

*APPARATUS AND DIAGRAM OF CONNECTIONS*

Faraday cylinder G could be put at any potential with respect to  $d$  by moving the point N. The primary electrons could be given any desired energy by moving the contact M. From the diagram it may be seen that the galvanometer reads  $I_p - I_s$ , the difference between the primary current striking and the secondary current leaving  $d$ . Therefore the complete energy distribution among secondary electrons for a given value of primary accelerating potential  $E_a$  may be obtained by moving N from A to B.

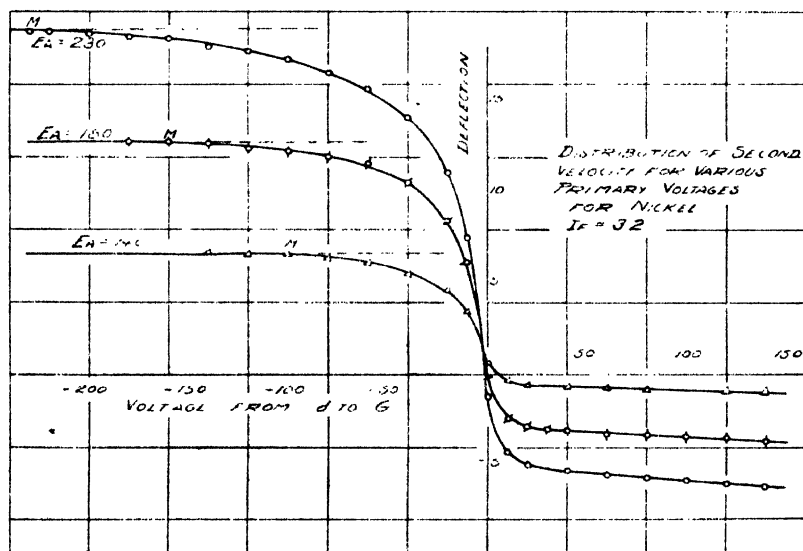
The aluminium cathode C was used for bombarding the metals to remove adsorbed gases. The negative terminal of a 7-inch induction coil was connected to this cathode, and

the other terminal to D. When a vacuum just high enough to give a yellow glow had been obtained, the high potential from the coil was applied, and the metal to be investigated was bombarded until the vacuum was of such a degree as to allow no discharge to pass. An iron Langmuir condensation pump, backed by a two-stage rotary oil-pump, was used to maintain the vacuum. Two traps were interposed between the pump and the tube. The one nearest the tube was kept continuously in a freezing-mixture, while the other was filled with coconut charcoal, which, during the first part of the exhaustion, was heated for an hour or more at a temperature of approximately  $400^{\circ}\text{C}$ . and then surrounded by a freezing-mixture.

### Experimental Results.

Typical secondary energy-distribution curves for nickel at various primary voltages are shown in fig. 2. The first break

Fig. 2.

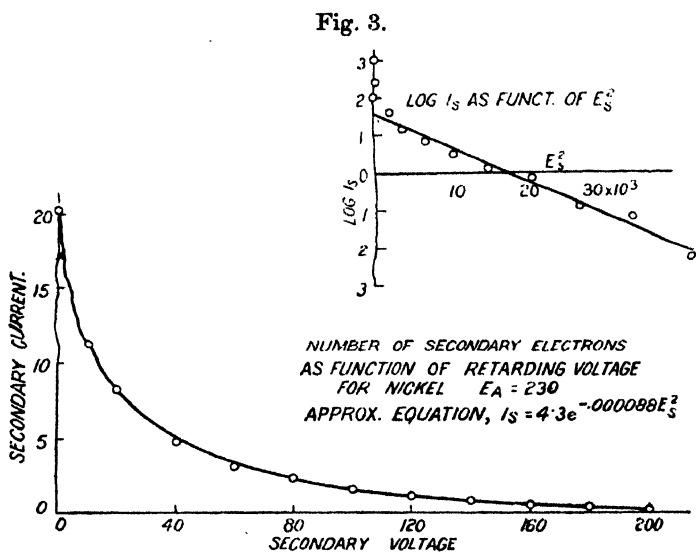


in a curve, shown by the point M where the dotted line becomes tangent to the curve, indicates the maximum energy, expressed in volts, of a perceptible number of secondary electrons emitted for that particular primary voltage. For further decrease in the negative potential of G with respect



to  $d$ , more electrons with less energy reach  $G$ . When the potential of  $G$  with respect to  $d$  is zero, practically all secondary electrons have energy enough to reach  $G$ . The curve then soon begins to approach saturation as  $G$  is made positive with respect to  $d$ .

If from the value  $M$ , where a curve just begins to break, any other following value is subtracted, it will give the number of secondary electrons having corresponding energies or greater. Repeating this for a number of points to where the voltage of  $G$  becomes zero with respect to  $d$ , the curve shown in fig. 3 is obtained. This secondary



energy-distribution curve has an advantage over the original curve in that it gives directly, for a fixed value of  $E_a$ , the number of electrons having a given energy or greater up to the maximum. Values of  $\log I_s$  plotted as a function of  $E_s^2$  gave (except for the first few points) a straight line, which shows that the curve is closely approximated by the general equation  $y = ae^{bx^2}$ . The actual equation for the curve for nickel where  $E_a = 230$  volts is  $I_s = 4.3e^{-0.00088E_s^2}$ .

A series of curves similar to those of fig. 2 were taken for aluminium and copper, and in each case were found to have the same general form. With this apparatus it is true that secondaries may be emitted from the collector  $G$ . However,

in taking the curves of fig. 2 the first electrons from *d* to reach *G* do so with a velocity equal to zero, and the energy with which the electrons from *d* reach *G* is never greater than the difference between their energy of emission and the retarding field. Therefore secondary emission from *G* cannot appreciably affect the energy-distribution curves except for low values of retarding potential.

As mentioned before, the points *M* (fig. 2), where the curves just begin to break, give the maximum secondary energy for a fixed primary voltage. When values of maximum secondary energy were plotted as a function of primary voltage, for nickel, a straight line was obtained. If the secondary electrons are a result of the atoms absorbing the radiation produced when the primary electrons strike the plate—in other words, if secondary electrons are due to photo-electric effect,—the above graph should be a straight line having a slope of unity. However, the actual slope obtained was 1.34. Data are insufficient to make definite conclusions regarding this.

#### *Conclusions.*

In every case the curves indicate that there are a few secondary electrons with energies approaching that of the primary beam. This is shown by the fact that in every case the curves begin to bend while *G* is still at a high negative potential with respect to *d*. The number having high values of energy is relatively small; indicated by the slight change in slope which first occurs.

The empirical equation found for the curve of fig. 3 is the regular probability equation; and although it does not hold for low values of secondary energy, it indicates that within a certain range the number of electrons having a given energy or greater up to the maximum energy of any being emitted is determined by a law related to the law of probability.

XXXVI. *Metallic Spectra excited by Active Nitrogen.* By  
J. OKUBO and H. HAMADA. (*From the Laboratory of  
Physics, Sendai, Japan* \*.)

[Plate VII.]

INTRODUCTION.

SINCE the discovery of the active modification of nitrogen by E. P. Lewis†, a large number of investigations with a view to find out its real nature have been carried out. Though as the results of the continued experimental work by Lord Rayleigh‡, A. Fowler§, E. P. Lewis, R. T. Birge||, and others many important properties of the gas have come to light, the real nature of its activity still remains obscure. In recent years two different theories to explain this activity have been put forward. The first, advanced by M. N. Saha and N. K. Sur¶, maintains that active nitrogen is simply nitrogen molecules in the state of excitation, and the contents of its energy are 8·9 volts. If such a molecule collides with other molecules or atoms, parts of its energy can be transferred to those others by the collision of the second kind, as put forward by O. Klein and S. Rosseland\*\* and confirmed experimentally by J. Franck†† and his students. From the excitation potential of the mercury lines which are excited when active nitrogen is made to act upon this vapour, the energy contents of the nitrogen molecule can be deduced.

The second theory has been put forward by H. Sponer‡‡, and she is of opinion that the active nitrogen is simply a neutral nitrogen atom. If two nitrogen atoms encounter a neutral metallic atom or molecule, the energy corresponding to the heat of dissociation of a nitrogen molecule can be utilized to excite the neutral atom or molecule, and the spectra of the gas are emitted. From the facts of the peculiar enhancement of the first positive group and the complete lack of the second positive group in the after-glow spectra, H. Sponer concluded that the energy of dissociation is greater than 11·4 volts and smaller than 13 volts, and the

\* Communicated by the Authors.

† E. P. Lewis, *Astrophys. Journ.* xii. p. 8 (1900).

‡ R. J. Strutt, *Proc. Roy. Soc. lxxxv.* p. 219 (1911); xciii. p. 254 (1917).

§ R. J. Strutt and A. Fowler, *Proc. Roy. Soc. lxxxv.* p. 377 (1911); lxxxvi. p. 105 (1912).

|| R. T. Birge, 'Nature,' cxiv. p. 642 (1924).

¶ M. N. Saha and N. K. Sur, *Phil. Mag.* xlviii. p. 421 (1924).

\*\* O. Klein and S. Rosseland, *Zeit. f. Phys.* iv. p. 46 (1921).

†† J. Franck, *Zeit. f. Phys.* ix. p. 259 (1922).

‡‡ H. Sponer, *Zeit. f. Phys.* xxxiv. p. 622 (1925)

spectral lines of the other gas excited in the after-glow must be lower than 11.4 volts.

Observations on the rate of decay of the after-glow by Angerer \* and Rudy † are closely in agreement with the consequences following from Sponer's triple-collision hypothesis, and the experimental results recently published by Ruark, Foote, Rudnick, and Chenault ‡ have also confirmed the same assumption.

As above stated, an exact knowledge of the spectra of various metallic vapours excited by the stream of active nitrogen is very important in throwing light on the real nature of the activity and in other views of chemiluminescences. We have been investigating, for the last two years, the properties of ionized and excited nitrogen molecules and atoms, and spectroscopic observations of the after-glow and of light-emissions from various metallic vapours under bombardment by active nitrogen have been carefully carried out. The results obtained, as shown in the following paragraph, differ in the case of mercury from that observed by Ruark and others, and other metallic spectra are more fully extended than has been hitherto reported.

#### EXPERIMENTAL ARRANGEMENTS.

Various types of discharge-tube were used in this investigation. The one which was mainly used is one similar to that of Strutt and Fowler, also used by R. S. Mulliken § in his researches on the copper iodide spectra. Nitrogen was prepared chemically in the usual manner, from ammonium chloride and sodium nitrite. After passing through a row of purifying and drying tubes the continued stream of nitrogen enters the activating tube, then the activated gas flows into the light-trap of a cranked glass tube, and then into an after-glow tube made of Pyrex glass or fused silica. A small cylindrical side bulb containing the metals under examination connects with the main one, 1 or 2 cm. distant from the connecting part of a light trap, and the bulb is gently heated with a Bunsen burner. The light emitted was always observed end-on through a quartz window at the end of the tube.

The discharge was carried from the secondary coil of an induction coil with a spark-gap and a suitable condenser, and the electrode near the after-glow tube was always

\* E. v. Angerer, *Phys. Zeit.* xxii. p. 97 (1921).

† R. Rudy, *Phys. Rev.* xxvii. p. 110 (1926).

‡ A. E. Ruark, P. D. Foote, P. Rudnick, and R. L. Chenault, *J. O. S. A.* xiv. p. 17 (1927).

§ R. S. Mulliken, *Phys. Rev.* xxvi. p. 1 (1925).

earthed. A Hilger quartz monochromator was adapted to serve as a spectrograph by substituting a camera for the telescope.

#### THE SPECTRA OF THE AFTER-GLOW.

In the first place it is necessary to study exactly the light-emissions due to the after-glow itself. Our results were exactly the same as those recorded by Strutt and Fowler, and recently observed by R. C. Johnson and H. G. Jenkins\*. The  $\alpha$ ,  $\beta$ , and  $\gamma$  groups are emitted but the  $\alpha$  group are especially enhanced, while traces of the second group of positive bands due to the nitrogen molecules could not be observed, though we endeavoured to expose the photographic plates for more than 60 hours. No one has ever reported the appearance of this group, which contradicts the results obtained by Ruark and his co-operators, and it may be questioned whether their sector-disk operated satisfactorily and perfectly cut out the direct discharge or not. (Pl. VII., a.)

Next we went on to the study of the light-emissions from metallic vapours under the bombardment of active nitrogen. All the metallic vapours tried cause deposits as coating of mixtures on the colder parts of the wall of the after-glow tube. The products consist of mixtures of metallic nitrides and of the excess of metal condensed there from vapours.

At the beginning of the experiments the characteristic glow of the metallic vapours appeared very brightly at the places where the metallic vapours met the stream of active nitrogen. It gradually faded out as the coating increased in thickness, and can be explained by the metallic nitrides acting as a poison on the activity of the gas. Other experimental difficulties are that the bulb containing the metals occasionally bursts after the burner has been removed.

We took very great care to prevent the stray discharge from entering the after-glow tube. When the earthing of the electrode near the tube is very good and no metallic clamps are used, no traces of any stray discharge diffuses in the tube. By observing the second positive band, it can be ascertained whether the stray discharge enters or not; but to obtain absolute security a sector-disk of the same kind as that described by R. C. Johnson was used, and confirmed the fact that our tube was quite free from the stray discharge even when the sector-disk was not placed in the proper position.

\* R. C. Johnson and H. G. Jenkins, *Phil. Mag.* ii. p. 621 (1926).

We have observed metallic spectra under a great variety of conditions. Some plates were exposed for a long time to obtain lines having higher levels of energy, and the results are described in the following paragraph with special remarks.

#### THE AFTER-GLOW SPECTRA OF METALS.

1. *Mercury*.—As shown in the following table, all the lines excited are arc lines, and the resonance line at  $\lambda$ , 2537 Å., specially enhanced. The highest level of energy appearing in our records was 4d, corresponding to the excitation potential 9.51 volts. To obtain lines up to this level only four hours were needed, but we could not find any traces of lines higher than those levels of energy even after 100 more hours. On these points there is quite a difference from observations made by Ruark and his co-operators, and we shall discuss this later. Mercury nitrides are black powders and very explosive, as small cracking sounds are heard in the tube and occasionally the explosion was great enough to break the tube. Accompanying these explosions, light of a bluish colour flashed out instantaneously. (Pl. VII., g.)

The lines recorded on our plates are :

Obs. Lines.	Class.	Remarks.	Obs. Lines.	Class.	Remarks.
5461	$2p_1-2s$		3026-22	$2p_1-4d$	
4358	$2p_2-2s$		2654-52	$2p_2-4d$	
4047	$2p_3-2s$				
3341	$2p_1-3s$		5791-70 ?	$\left\{ \begin{array}{l} 2P-3D \\ 2P-3d \end{array} \right.$	Masked by $\alpha$ group.
2894	$2p_2-3s$				
2753	$2p_3-3s$		4078	$2p_2-2S$	
3663-50	$2p_1-3d$		2537	$1S-2p_2$	Very strong.
3132-26	$2p_2-3d$				
2967	$2p_3-3d$				

2. *Cadmium*.—Cadmium nitrides are dark-grey powders. Ruark failed to photograph lines of this metal and remarked that it destroys the after-glow. We think that in these experimental arrangements the active nitrogen does not collide with the vapour in the concentrated proportions, and the light excited is very feeble. (Pl. VII., f.)

Our records are :

Obs. Lines.	Class.	Remarks.	Obs. Lines.	Class.	Remarks.
5086	$2p_1-2s$		2982-81	$2p_1-4d$	
4800	$2p_2-2s$		2881	$2p_2-4d$	
4678	$2p_3-2s$	[Cd 1S- $2p_2$ .	2837	$2p_3-4d$	
3253 ?	$2p_1-3s$	Masked by	2764	$2p_1-5d$	
3133 ?	$2p_2-3s$	Masked by	2678 ?	$2p_2-5d$	Masked by $\beta$ group 2679.
3061	$2p_3-3s$	Hg 3132-26.	2640	$2p_3-5d$	
3614-11	$2p_1-3d$		3261	$1S-2p_2$	Very strong.
3468-66	$2p_2-3d$				
3404	$2p_3-3d$		2288	$1S-2P$	

3. *Zinc*.—Nitrides of this metal are also dark grey powders. In addition to the lines described by Lewis, we observed many other lines. (Pl. VII., *e*.)

Obs. Lines.	Class.	Remarks.	Obs. Lines.	Class.	Remarks.
4811	$2p_1-2s$		2516	$2p_1-6d$	
4722	$2p_2-2s$		2491	$2p_2-6d$	
4680	$2p_3-2s$		2480	$2p_3-6d$	
3072 ?	$2p_1-3s$	Masked by Zn $1S-2p_2$ .	2463	$2p_1-7d$	
3036	$2p_2-3s$		2440	$2p_2-7d$	
3018	$2p_3-3s$		2431	$2p_1-8d$	
2712	$2p_1-4s$		2408	$2p_2-8d$	
2684	$2p_2-4s$		2397	$2p_3-8d$	[Zn $2p_2-8d$ .
2670	$2p_3-4s$		2409 ?	$2p_1-9d$	Masked by
			2387 ?	$2p_2-9d$	Masked by $\beta_2$ group 2387.
3346-45	$2p_1-3d$		2139	$1S-2P$	
3303	$2p_2-3d$				
3282	$2p_3-3d$		4630	$2P-4D$	
2801	$2p_1-4d$				
2771	$2p_2-4d$		3076	$1S-2p_2$	Very strong.
2756	$2p_3-4d$		4293	$2p_2-2S$	
2609	$2p_1-5d$				
2582	$2p_2-5d$				
2570	$2p_3-5d$				

4. *Magnesium*.—The intensity distributions of the lines are exactly similar to those observed previously by Lord Rayleigh and Fowler. In addition to these lines we have observed  $2p-2s$ ,  $2p-4s$ , and  $2p-6d$ . Nitrides of this metal need special notice, as some black coatings were produced at the neck of the bulb, while on the wall near the bulb the product was red in colour. After the experiment a cotton-like white compound remains in the bulb, among which crystals of bright golden colour were found; but it is questionable whether these are varieties of magnesium nitrides or not, for the insides of the bulb, made of pyrex glass, are attacked severely by the vapour. The product is very hygroscopic, as it smells as strongly as ammonia gas, in consequence of its absorbing atmospheric moisture. (Pl. VII., *d*.)

Lines observed are listed in the following :

Obs. Lines.	Class.	Remarks.	Obs. Lines.	Class.	Remarks.
5184-67	$2p-2s$		4571	$1S-2p_2$	Very strong.
3337-30	$2p-3s$		2852 ?	$1S-2P$	Masked by Na 2853.
2942-37	$2p-4s$				
3838-29	$2p-3d$		2783-76	$2p-2p'$	Strong.
3097-91	$2p-4d$				
2852-47 ?	$2p-5d$	Masked by Na			
2737-32	$2p-6d$	2853.			

5. *Sodium*.—Nitrides of this metal are dark grey, and it burns in air. When the metal is heated in the bulb a bright green light column is seen at the neck where the dense vapour meets the stream of active nitrogen, and surrounding this

column broad yellow aureoles diffuse in large volumes. Spectroscopic observation shows the green lines  $\lambda$  5688–83 Å. strongly at the centre of the column, and at the outside the D line strongly appears, as Lord Rayleigh and Fowler remarked. After several trials it seems that the difference in these colours depends absolutely on the density difference of the vapour, and we shall publish some quantitative investigations of this point in the near future. The glow of this metal is very intense, and nitrides are not so harmful to the activity of gas as that of other metals, and we could not understand why Ruark and his co-operators could not observe any lines in their tube (Pl. VII., *b*). The lines observed are:

Obs. Lines.	Class.	Remarks.	Obs. Lines.	Class.	Remarks.
5890–96	1s–2p		5688–83	2p–4d	
3302–03	1s–3p		4983–79	2p–5d	
2853	1s–4p		4669–65	2p–6d	
2680	1s–5p		4498–94	2p–7d	
2594	1s–6p		4393–90	2p–8d	
2544	1s–7p		4324–21	2p–9d	
2512	1s–8p		4277–73	2p–10d	
			4242–39	2p–11d	
5154–49	2p–4s		4216–13 ?	2p–12d	
4752–48	2p–5s				
4545–42	2p–6s				
4423–20	2p–7s				

6. *Potassium*.—Nitrides of this metal resemble those of sodium, but it acts as a powerful poison of activity, so it was difficult to obtain sufficient exposure of the plates. Our observations (Pl. VII., *c*.) are :

Obs. Lines.	Class.	Remarks.	Obs. Lines.	Class.	Remarks.
4044–47	1s–3p		5832–13	2p–5d	
3447–48	1s–4p		5360–43	2p–6d	
3217–18	1s–5p		5112–97	2p–7d	
3102	1s–6p	[group 3035.	4965–51	2p–8d	
3035 ?	1s–7p	Masked by $\beta$	4870–56	2p–9d	
			4805–91	2p–10d	
			4759–46	2p–11d	

7. *Thallium*.—Reddish-yellow nitrides are formed. Besides the lines Ruark has reported, 2p–5s, 2p–7d, 2p–8d, and 2p–9d were clearly seen. (Pl. VII., *h*.)

Obs. Lines.	Class.	Remarks.	Obs. Lines.	Class.	Remarks.
5350	2p <sub>1</sub> –2s		3529–19	2p <sub>1</sub> –3 d	
3776	2p <sub>2</sub> –2s		2768	2p <sub>2</sub> –3 d	
3230	2p <sub>1</sub> –3s		2921–18	2p <sub>1</sub> –4 d	
2580	2p <sub>2</sub> –3s		2380	2p <sub>2</sub> –4 d	
2826	2p <sub>1</sub> –4s		2711–09	2p <sub>1</sub> –5 d	
2316	2p <sub>2</sub> –4s		2238	2p <sub>2</sub> –5 d	
2666	2p <sub>1</sub> –5s		2610–09	2p <sub>1</sub> –6 d	
2207	2p <sub>2</sub> –5s		2169	2p <sub>2</sub> –6 d	
2586 ?	2p <sub>1</sub> –6s	Masked by $\gamma$ group 2596.	2553	2p <sub>1</sub> –7 d	
			2517	2p <sub>1</sub> –8 d	
			2494	2p <sub>1</sub> –9 d	
			2211	Unclassified.	



8. *Calcium*.—The excitation potential of the spark resonance lines of this metal is 9.2 volts, and it is very interesting to ascertain whether these lines appear or not in the after-glow spectra. We have made several attempts to obtain the spectra of this metal, but unfortunately none of the trials was successful, because as soon as the stream of active nitrogen passes through, even in the solid state, it forms nitrides.

9. *Surface Fluorescence of Metals*.—Surface fluorescence was observed when metallic sodium, potassium, magnesium, calcium, and barium were put in the after-glow tube. But it cannot be observed when the surface of pure magnesium is freshly cut with a knife, and it is revealed again after being thrown in the air. Perhaps this phenomenon of the surface fluorescence is intimately connected with the surface conditions of the metal.

#### INTERPRETATION AND DISCUSSION OF THE RESULTS.

As described in the preceding tables, the metallic spectra excited by active nitrogen are arc lines of the vapours, and no spark lines are observed. It must be remarked that the relative intensities differ from those in the common arcs, and especially that the resonance line  $1S-2p_2$  of alkali earth metals is more strongly excited than in other cases. Ruark and others reported that the distribution of intensities did not obey the usual rules of arc, but said nothing about the resonance lines, for they observed accurately only the cases of mercury and thallium.

It will be very worth while to compare our results with the metallic spectra excited by atomic hydrogen in the report recently published by F. L. Mohler\*. From his report we can see that the resonance line of sodium and cadmium appeared strongly, very weak and only just observable lines in potassium and mercury, and no lines at all in magnesium and zinc. As the work of dissociation of hydrogen molecule is 4.38 volts, and is so small that it is insufficient to excite the resonance line of mercury, we cannot expect the excitation of lines corresponding to higher levels of energy, but it can be conceived that his results fairly coincide with our cases of nitrogen, and the resonance lines were excited in a comparatively high degree. In other words, it seems that the probability of exciting resonance lines, as triple collisions occur, is comparatively greater than in other cases of excitation.

\* F. L. Mohler, *Phys. Rev.* xxix. p. 419 (1927).

The highest level of energy obtained in our experiments was that of  $4d$  of mercury corresponding to the excitation potential 9.51 volts. As above remarked, lines up to this level develop satisfactorily with four hours' exposure, but we could not detect any traces of lines having higher level than this. For example, in mercury the triplets 3026-22, 2654-52 appeared clearly with four hours' exposure, but triplets 2925, 2576, 2464, and 2805-03, 2483-82, 2378 do not appear even with runs of a week's exposure, though the differences in the excitation potentials of the latter are only about 0.14 and 0.32 volt greater than that of the former.

In conflict with our results, Ruark has reported the appearance of series members up to 10.0 volts energy. Of course, the dissociation energy being higher than the excitation potentials of these lines, there are no theoretical objections to this result, but it is very questionable whether these lines can be excited only by the active nitrogen itself or not. We believe that if they had been observed under the conditions as above mentioned, these triplets would not have appeared. It can be stated with certainty that the mercury atom can receive from active nitrogen the energy corresponding to 9.51 volts, but not attain that corresponding to 9.65 volts, and it is smaller than the value expected from Sponer's hypothesis. This discrepancy can be explained after the mechanism of the triple collision has been fully studied.

As the ionization potentials of cadmium, zinc, magnesium, sodium, potassium, and thallium are lower than 9.51 volts, the ionizations of these metallic atoms are theoretically possible. Saha and Sur also pointed out this in connexion with their theory.

Magnesium lines  $\lambda$  2796 Å. and  $\lambda$  2803 Å. are intense spark resonance lines corresponding to 12.0 volts, and it is very interesting to see whether these are observable or not; but we could not find them at all. Using titanium tetrachlorides, Jevon\* found a few singly ionized titanium lines in the after-glow tube, but his experimental conditions are very complicated and nothing can be deduced as to whether these are due to the atomic nitrogen or not. Thus observations do not tell us that the metallic atoms are ionized in the triple collision. It is very remarkable that from the fact that lines  $2p-2p'$  of magnesium appear strongly, two electrons may be displaced simultaneously to higher levels of energy.

\* W. Jevon, Proc. Roy. Soc. lxxxix. p. 187 (1913).

Lastly, we have carefully examined the band spectra due to formations or decompositions of metallic nitrides, but contrary to the cases of atomic hydrogen, no traces were found, at least in the observed ranges of wave-lengths. As Ruark remarked, from the thermochemical point of view, it is very questionable whether metallic atoms can be excited, as the result of the decomposition of metallic nitrides in the after-glow tube.

All the experimental results recently obtained favour Spomer's hypothesis, but no exact explanation of the mechanisms of triple collisions have been hitherto proposed. It is very desirable to attempt some experiments in this direction.

In conclusion, the present writers express their best thanks to the Saito Gratitude Foundation for the expenses of this experiment, which were paid by the Research Fund from the Foundation.

Sendai, Japan.  
May 1927.

---

XXXVII. *On the Diamagnetic Susceptibilities of Gases at Low Pressures.* By V. I. VAIDYANATHAN\*.

ABSTRACT.

*The Instrument.*—The apparatus employed is a modified form of Curie balance of high sensitivity and specially adapted for investigations on weakly magnetic gases. It consists of a thin closed bulb, suspended from the balance-beam in a suitable non-homogeneous field. The gases under investigation surround this bulb. The glass of the bulb is diamagnetic, but it is almost compensated for diamagnetism by enclosing the requisite quantity of air; so that in a vacuum there is very little magnetic force acting on it at atmospheric temperature. When a diamagnetic gas surrounds the bulb, it is attracted towards the stronger part of the field, causing a twist in the suspension fibre of the balance-beam and *vice versa*. The deflexions give a relative measure of the volume susceptibilities. The balance is enclosed in an air-tight chamber of required shape, into which gases are let in.

*Results.*—A complete investigation at low pressures showed strict proportionality between pressure and volume susceptibility. The relative values obtained were  $-0.00092 \times 10^{-6}$ ,  $-0.00113 \times 10^{-6}$  and  $-0.00058 \times 10^{-6}$  for the

\* Communicated by Prof. C. V. Raman, F.R.S.

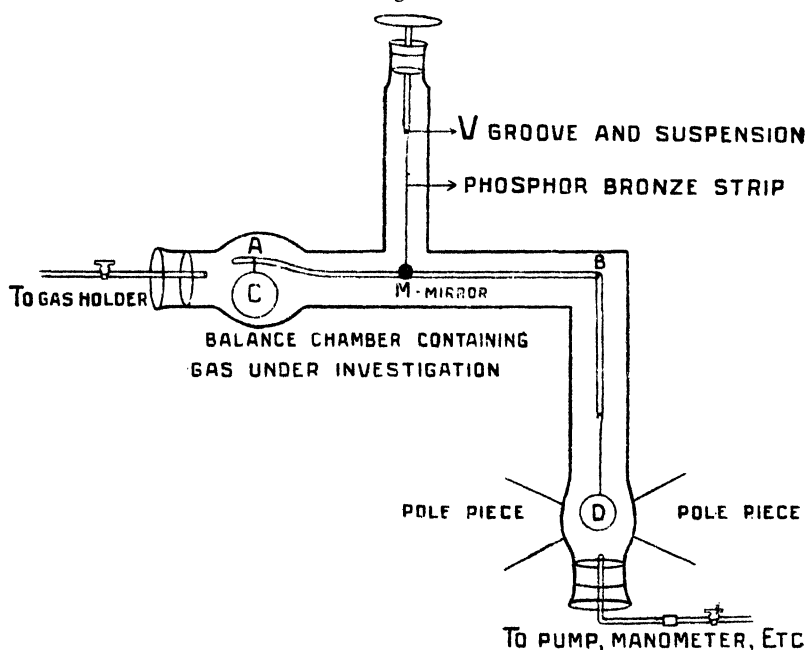
volume susceptibilities of carbon dioxide, argon, and nitrogen respectively at 0° C. and 760 mm. (Air: 0.0308  $\times 10^{-6}$  at 0° C. and 760 mm.)

*Sensitiveness.*—A change of volume susceptibility of  $0.000006 \times 10^{-6}$  in a field of 1400 Gauss corresponds to a deflexion of 1 mm. on a scale at a distance of a metre, and this is much higher than those attained in any previous investigation. The relative values obtained are accurate to within about 5 per cent.

### *The Susceptibility Balance.*

THE instrument\* was developed in an investigation by the author on the magnetic susceptibilities of carbon dioxide at low pressures, and is illustrated in fig. 1. It consists essentially of a hollow glass bulb D, which is

Fig. 1.



sealed and suspended from one end of a light aluminium bar AB, the latter being suspended by a torsion fibre. The bulb D is blown out of feebly-diamagnetic glass selected by preliminary investigation on various specimens, and this

\* Vadiyanathan, Ind. Journ. Phys. vol. i. p. 183 (1926).

diamagnetism is compensated as nearly as possible by enclosing within it the requisite quantity of air. The bulb hangs in a suitable non-homogeneous field between the pole-pieces of an electro-magnet. The bulb C, attached to the other end of the balance, counterpoises the weight of D, and in addition its volume is so adjusted that the hydrostatic buoyancy due to introducing gases into the balance-chamber is completely neutralized. The shape of the balance-chamber is suitably adjusted for the free movement of the balance within it. The chamber is connected to an elaborate arrangement for the introduction of gas and for altering of pressure. M is a galvanometer mirror by which the deflexions of the beam are read by the usual lamp-and-scale arrangement.

When the magnet is excited, the bulb is slightly attracted or repelled in vacuum owing to the imperfection in compensation and temperature fluctuations changing the susceptibility of the contained air. By rotating the torsion head, the balance is so adjusted that the beam lies along the axis of the chamber. Now, if we introduce a diamagnetic gas around the bulb, it apparently becomes more paramagnetic and is drawn towards the stronger part of the field, and on introducing a paramagnetic gas, it becomes diamagnetic to that medium and is repelled. The movement of the bulb D is adjusted to be in a perfectly horizontal plane and at right-angles to the non-homogeneous field, causing a couple in the torsion-fibre of the balance-beam. From the relative deflexions, the volume susceptibility of one gas can be determined if the other is known. The chief difficulty was due to the heating of the coils of the magnet and the consequent rise of temperature. This causes a decrease of the susceptibility of the air used for the compensation of the bulb. To avoid this, only single intervals of pressure were investigated at a time, the next observation for a different pressure being made after a considerable interval. The temperature fluctuations of the atmosphere cause a shift in the zero reading of the spot of light, but do not influence the actual change of deflexion, which alone need be taken account of in the measurements.

#### *Purification of Argon and Nitrogen.*

The compressed gas argon, supplied in a cylinder, was purified by passing it in succession through freshly cut phosphorus\*, concentrated solution of ferrous sulphate kept

\* Hon. R. J. Strutt, Proc. Roy. Soc. A, lxxxv. p. 219 (1911).

cooled in ice, concentrated sulphuric acid, calcium chloride, hard glass tubes containing magnesium, freshly reduced copper heated over a furnace, and a cooling spiral. The stream of gas was maintained for about 15 hours, and 5 litres were collected for subsequent investigations. Nitrogen was prepared by warming a concentrated solution of equi-molar quantities of pure sodium nitrite and ammonium chloride. The purification was effected as in the case of argon, the magnesium tube being substituted by a U-tube containing caustic potash.

### Results for Argon.

In the following tables, column I. indicates the pressure  $p$  in mm. of mercury between which the measurements are made; II. the corresponding readings of the spot of light; III. the change of pressure; IV. the relative change of deflexion; V. the ratio of the change of deflexion to the pressure; the last column is also a relative measure of susceptibility. The constancy of the ratios in column V. shows that the volume susceptibility is proportional to pressure, and the anomalous behaviour observed by Glaser\* is also not found.

TABLE I.

I.	II.	III.	IV.	V.
$p$ .	$\theta$ .	$dp$ .	$d\theta$ .	$\frac{d\theta}{dp}$ .
0-50	180-188.5	50	8.5	.170
0-86	190-205	86	15	.176
0-176	190-224	176	34	.192
100-196	202-220	96	18	.184
200-300	206-224	100	18	.180
250-540	193-247	290	54	.182
400-500	230-248	100	18	.180
2-500	200-293	500	93	.168
0-250	218-264	250	46	.180

Mean = .179

A similar experiment was conducted with pure  $\text{CO}_2$  to obtain the value of argon relative to it. The mean value of  $d\theta/dp$  for  $\text{CO}_2$  was 0.145. Taking the volume susceptibility of  $\text{CO}_2$  as  $-0.00092 \times 10^{-6}$  at  $0^\circ \text{C}$ . and 760 mm.†, this reduces to  $-0.00113 \times 10^{-6}$  at  $0^\circ \text{C}$ . and 760 mm. for the volume susceptibility of argon.

\* Glaser, *Ann d. Phys.* lxxiv. p. 459 (1924).

† Vaidyanathan, *loc. cit.*

*Results for Nitrogen.*

TABLE II.

I.	II.	III.	IV.	V.
<i>p.</i>	<i>θ.</i>	<i>dp.</i>	<i>dθ.</i>	$\frac{d\theta}{dp}$
0-90	273-284	90	11	·122
90-182	283-294	92	11	·120
100-197	271-283	97	12·5	·128
187-273	283-292·5	86	9·5	·109
189-304	270-282	105	12	·113
300-400	282-294	100	12	·120
480-562	277-287	82	10	·121
0-230	260-287	230	27	·118
0-302	255-292	302	37	·120

Mean = ·119

Over the same regions the change of deflexion corresponding to the change of susceptibility of 1 mm. of air was 5·44 divisions at 30° C. The pressure-changes required in the case of air being of the order of a few mm., these were read with a cathetometer. Taking the volume susceptibility of air as  $0\cdot0308 \times 10^{-6}$  at 0° C. and 760 mm.\*, and performing the necessary calculations, the volume susceptibility of nitrogen is  $-0\cdot000525 \times 10^{-6}$  at a mean temperature of 29° C. and 760 mm. pressure.

TABLE III.—Susceptibilities.

Gas.	$K_0 \times 10^6$ .	$\chi_s \times 10^6$ .	$\chi_m \times 10^6$ .
N <sub>2</sub> .....	-0·00058	·46	12·9
A .....	-0·00113	·635	25·3
CO† .....	-0·0009	·465	20·5

In the above table  $K_0$  is the volume susceptibility observed and reduced to 0° C. and 760 mm.,  $\chi_s$  the specific and  $\chi_m$  the atomic or molecular susceptibilities.

*Sensitiveness and Source of Error.*

The relation between the change of deflexion of the balance-beam and of volume susceptibility is

$$c \cdot d\theta = lvH \cdot \frac{dH}{dx} \cdot Kg$$

where  $c$  denotes the couple per unit twist of the torsion fibre,  $d\theta$  the change in the angle of deflexion corresponding to the change  $Kg$  of the volume susceptibility of the surrounding medium,  $l$  the distance between the point of suspension of

\* Také Soné, Phil. Mag. xxxix. p. 305 (1920).

† Vaidyanathan, loc. cit.

the beam and the bulb D,  $v$  its volume and  $H \cdot \frac{dH}{dx}$  a vector.

(In the experiment,  $x$  is the horizontal axis at right-angles to the field.) From the expression, it is easily seen that the sensitiveness mainly depends on  $c$ ,  $l$ , and  $v$ . The advantage secured in the experiment was the possibility of the variation of  $c$ . Since the bulb D has practically very little susceptibility at atmospheric temperature and the suspended system is very light, a very sensitive fibre could be employed.  $v$  was about 3 c.c., and this was the convenient maximum for the volume, since it had to be suspended within the balance-chamber and oscillate within it without jamming.  $l$  was about 11 cm. Since it was the aim to make measurements in small fields,  $H$  was not increased beyond 3000 gaussess. The retorsion method was found impossible, owing to the mechanical disturbances resulting from the process, but the torsion method was found to be sufficiently accurate. The constancy of the

factor  $H \cdot \frac{dH}{dx}$  was tested experimentally, and the assumption was found justifiable within experimental errors. The adjustment for hydrostatic buoyancy was tested with a microscope. A series of preliminary experiments were found necessary to select the proper diamagnetic glass, to obtain a thin uniform bulb, to secure the compensation, and to adjust the volume and weight of the counterpoise, making the experimental investigation somewhat difficult and tedious.

Taking the experiment on nitrogen, a change of  $0.0000066 \times 10^{-6}$  of volume susceptibility corresponds to one division on the scale in a field of 1400 gaussess, and this could be easily detected. When a continuous current was running in the magnet for about 6 minutes, a drift of about one division of the spot of light could be observed on the scale, due to various disturbing influences. The current was kept fairly constant with necessary arrangements. Allowing for the maximum effect of the various sources of error, the relative values are accurate to within about 5 per cent.

#### *Comparison of Experimental Data on Diamagnetic Gases.*

TABLE IV.—Specific susceptibilities  $\times 10^6$ .

Gas.	Také Soné *.	Hector †.	Glaser ‡.	Lehrer §.	Author.
CO <sub>2</sub> .....	-0.423	—	-0.43	-0.47 -0.52	-0.48
N <sub>2</sub> .....	-0.265	-0.42	-0.26	—	-0.46
A .....	—	-0.45	—	-0.48 -0.50	-0.64

\* Také Soné, *loc. cit.*

† Hector, *Phys. Rev.* xxiv. p. 418 (1926).

‡ Glaser, *loc. cit.*

§ Lehrer, *Ann. der Phys.* lxxxi. p. 229 (1926).



In the case of argon the value of the susceptibility is 40 per cent. higher than Hector's and 28 per cent. higher than Lehrer's. The values for nitrogen and carbon dioxide are in fair agreement with those of Hector and Lehrer. In investigating argon it was found that the cylinder argon generally supplied contains a large quantity of air, and the purification requires a number of tubes to remove the oxygen and nitrogen. Special attention has been paid to this point. If we substitute the present value in Langevin's formula, after necessary calculations, the mean atomic radius comes out as 1.06 A.U. (approximately), in very close agreement with 1.02 A.U. and 1.43 A.U. obtained from Bragg's determinations and Rankine's viscosity measurements. According to L. Pauling \* the calculated value for the gram atomic susceptibility of argon is  $21.5 \times 10^{-6}$ , and according to Dr. Stoner †  $30 \times 10^{-6}$  (the latter is a rough calculation from the ionization potential), while the value obtained in the present investigation is  $25.3 \times 10^{-6}$ .

After the work of the present investigation had been completed, a preliminary note by Hammar ‡ and a paper by Lehrer § appeared in the *Proc. N. A. S.* and *Ann. der Phys.* respectively, in which they have also found a linear relation between pressure and susceptibility.

In conclusion, I have the greatest pleasure in acknowledging my indebtedness to Prof. C. V. Raman, F.R.S., for suggesting the problem and for taking a deep interest in the work. The work has been carried out in the Physical Laboratory of the Indian Association for the Cultivation of Science.

210 Bowbazar Street, Calcutta (India).

5th May, 1927.

### XXXVIII. *The Fine Structure of Mercury Lines.*

By W. H. McCURDY, Ph.D.‖

[Plate VIII.]

**N**AGAOKA, Sugiura and Mishima ¶ have made an extensive examination of the fine structure of the strong lines of the mercury arc spectrum. They used quartz

\* L. Pauling, *Proc. Roy. Soc. A*, cxiv. p. 181 (1927).

† Stoner, *Phil. Mag.* iii. p. 336 (Feb. 1927).

‡ Hammar, *Proc. N. A. S.* xii. p. 594 (1926).

§ Lehrer, *loc. cit.*

‖ Communicated by the Author.

¶ Nagaoka, Sugiura and Mishima, *Jap. Journ. of Phys.* ii. p. 121 (1928).

Lummer-Gehrcke plates which enabled them to examine the lines in the ultra-violet, which region has, until recently, been little investigated. As a source of radiation they used an Aron's quartz mercury arc, water-cooled to prevent excessive broadening of the lines.

Wood\* has repeated their work on the strong line  $2537 \text{ \AA}$ ., and has found the earlier results to be incorrect. He has found that the apparent structure of the line may be varied at will by varying the temperature of the arc. Using a carefully cooled Cooper-Hewitt quartz arc and forcing the discharge against the wall of the tube by means of a weak magnetic field, he has found the structure of the line to be entirely different from that given by Nagaoka and his co-workers. He explained the results of the earlier work as due to broadening and self-reversal of the components of the line, the overlapping of the unabsorbed wings accounting for the fact that the number of components found by Nagaoka was not double the number of true components.

In the course of his experiments on Optical Excitation of Mercury Vapour, Wood has observed that one of the components of the line  $3650 \text{ \AA}$ . and also of the line  $2967 \text{ \AA}$ . appears self-reversed under certain conditions. It was therefore considered advisable to repeat Nagaoka's work on these lines, in order to determine whether or not the earlier results were sufficiently reliable to justify attempts to construct the fine structure energy diagrams for mercury.

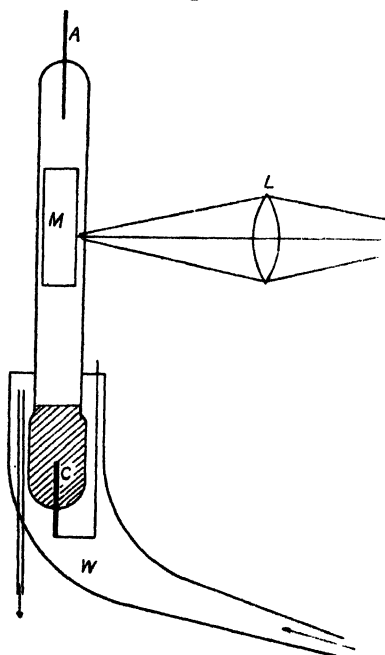
#### APPARATUS.

A quartz Cooper-Hewitt mercury arc was used as source throughout the work, with the mercury cathode cooled in running water, as shown in fig. 1. The pressure of mercury vapour is controlled by the temperature of the cathode, provided there are no drops of mercury on the sides of the arc; consequently the lines were made sharp by keeping the cathode at a low temperature. This type of arc has the additional advantage of making possible the observation of the arc from the side. It is well known that the width of a spectral line increases as the length of the radiating column is increased, also that the shape of the line is different when the tube is observed end on from the shape when the same tube is observed side on. The long source gives a line with a flat top, and in some cases a reversed or partially reversed line, while the intensity distribution in the case of the tube viewed side on is that given by the probability law. The

\* Wood, *Phil. Mag.* 1. p. 761 (1925).

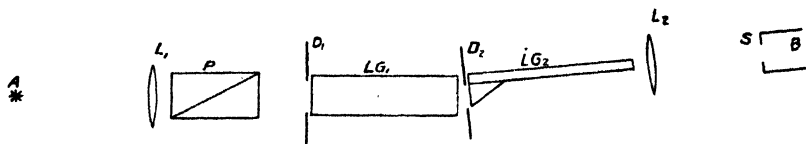
arc was so arranged that the discharge could be thrown against the wall of the tube by means of a magnetic field.

Fig. 1.



The optical arrangement is shown in fig. 2. The light was polarized before entering the first Lummer-Gehrcke plate by means of the double-image prism  $P$ . The two quartz Lummer-Gehrcke plates  $LG_1$  and  $LG_2$  were placed

Fig. 2.

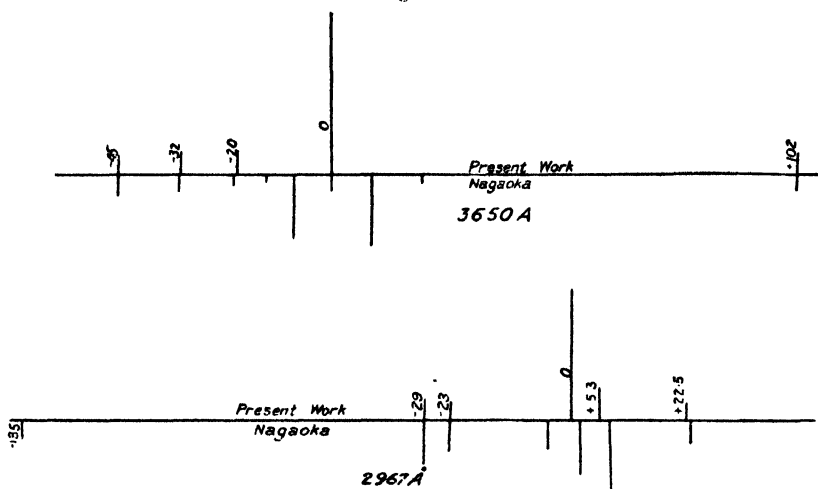


perpendicular to each other as shown, and the light was focussed on the prism of the first plate by the quartz lens  $L_1$ . The interference fringes were photographed by means of the large quartz spectrograph  $B$ , which served to separate the lines. The slit  $S$  was placed at the principal focus of the quartz fluorite lens  $L_2$  as the light is necessarily parallel on

emerging from the interferometer. The photographic plates were placed as nearly as possible perpendicular to the direction of the light from the prism of the spectrograph, which made it possible to obtain approximately square patterns and at the same time circular interference points.

Hammer Special plates were used throughout the work, as they were found to be both fast and clear. Exposure times ranged from  $\frac{1}{2}$  to 8 hours.

Fig. 3.



The structures found for the two lines are shown diagrammatically in fig. 3. They are so arranged that comparison with the results of Nagaoka's work is very easy. The components found in the present work are placed above the line, while those found by Nagaoka are placed below.

#### DISCUSSION OF RESULTS.

In the case of the line 3650 Å. the three weak components to the short wave-length side of the main component coincide, within the limits of error of the work, with the corresponding ones measured by Nagaoka, as does also the single one to the long wave-length side. As may be seen in fig. 3, the strong central component is found to coincide with a weak one found by Nagaoka. The two stronger components reported by Nagaoka are not found, however. Exposures taken without the water-cooling on the arc show a slightly

different result. Reproductions of photographs taken with and without water-cooling on the arc are shown in Pl. VIII. (figs. 1 and 2). It may be observed that in the case of a hot arc the central component of the line has become very broad and appears self-reversed. In the case of the cold arc, however, the strong central component appears as an almost circular dot, indicating that within the limits of the apparatus the central component is single, and not multiple as given by the earlier work.

From the above observations it appears probable that the explanation of the results reported by Nagaoka and his co-workers is that they have mistaken a broadened and partially self-reversed line for a group of at least three and probably five components. The two unabsorbed wings of the line and the incompletely absorbed central portion of the line are mistakenly termed three separate components. The two weak components on either side of the central group have not been found in the present work, as may be seen by the plates given in Pl. VIII. (figs. 1 and 2). The only apparent explanation of this is that the excessive broadening of the central component has produced such a broad interference point that it has been mistakenly interpreted as including a weak unresolved component on either side. It is barely possible that these are so weak that they have not appeared in the present work, but this explanation appears improbable considering the relative intensities reported by Nagaoka. It may also be pointed out that the intensity of the main component in the present work is much greater relative to that of the others than is the case in the earlier work. This is apparently further confirmation of the supposed absorption.

As the line  $2967 \text{ \AA}$ . has a place in the energy level diagrams of mercury similar to that occupied by the line  $3650 \text{ \AA}$ ., it may be expected to show similar peculiarities. Photographs of the fine structure of this line were also taken with both hot and cold arc. The broadening in the hot arc, however, was so great that it was found impossible to analyse the structure of the line from the plates obtained. Further, the line was so weak that exposures of over eight hours were necessary, using crossed Lummer-Gehrke plates. For this reason the plates were used crossed only to determine the position of the components, and they were used separately for examining the structure in the vicinity of the central component.

The structure of this line in the cold arc, using crossed plates, is shown in Pl. VIII. (fig. 3). This shows the two

components to the short wave-length side of the central group and the single one on the long wave-length side. The weak component reported by Nagaoka at  $-185 \text{ m.}\text{\AA}.$  does not appear, as it would be expected to almost coincide with one of the stronger components with the particular plates used. Pl. VIII. (fig. 4) shows the structure around the central group. This group is seen to consist of the strong central component, with a weak component on the long wave-length side. The reproduction also shows the other components found with the crossed plates. A diagrammatic representation of the structure of this line is given in fig. 3, contrasted with the structure reported earlier by Nagaoka.

The structure found in the hot arc, using a smaller plate, is shown in Pl. VIII. (fig. 5). This shows the unsymmetrically reversed main component. The asymmetry here is due to the fact that the weak component is not resolved but included in the unabsorbed long wave-wing.

Fig. 3 shows that the two short wave-length components and the single long wave-length one may be made to coincide, within the limits of the work, with the corresponding one reported earlier. The central group, however, is entirely different in the two cases. The explanation appears to be that in the earlier work Nagaoka observed a broadened and partially reversed main component and an incompletely resolved weaker component. The group was mistakenly considered to consist of three separate components of almost equal intensity.

Thus we find that instead of nine components originally reported for the line  $3650 \text{ \AA}.$  there are actually five components, and instead of seven for the line  $2967 \text{ \AA}.$  there are actually six. The separation of these from the main component is given in fig. 3.

#### CONCLUSION.

Ruark \* has recently attempted to work out the fine structure energy levels of mercury with but limited success. The results of Wood's experiments on the line  $2537 \text{ \AA}.$  and of the present experiments on the lines  $3650$  and  $2967 \text{ \AA}.$  show the necessity for a complete review of the fine structure of the mercury arc spectrum, although the lines cited are the most liable to be incorrect owing to the difficulties involved in the observations, the first being a principal series line and the others ending on metastable levels. Since the study of fine structure is proving of

\* Ruark, *Phil. Mag.* vol. i. p. 977 (1926).

importance as a tool in the study of atomic structure, it is well that the importance of the source of radiation as well as the reliability of the optical apparatus be realized. The present work shows how unreliable results may prove when care is not taken in selecting a proper source for work with optical apparatus of such high resolving power.

In conclusion, the author wishes to express his most sincere thanks to Prof. R. W. Wood, who first suggested the problem and placed the necessary apparatus at his disposal; also to the National Research Council for the grant of a Fellowship, which made the work possible.

Johns Hopkins University,  
Baltimore, Md.

XXXIX. *Some Approximate Formulæ for the Numerical Integration of Differential Equations.* (Analysis and generalization of a method given by H. T. H. Piaggio.)  
By E. REMES, Aspirant of the Cathédre Mathématique, Kieff, Russia\*.

WE shall examine here the case of a single equation,

$$\frac{dy}{dx} = F(x, y). \quad . \quad . \quad . \quad . \quad . \quad (1)$$

The approximate determination of an integral curve which passes through the initial point  $x=a$ ,  $y=b$ , comes, as is well known, to the successive determination of the increments  $\Delta y$  corresponding to the small successive increments  $\Delta x$ . H. T. H. Piaggio has given † a practical method for finding two limits between which  $\Delta y$  must lie.

Considering first the simple case where  $F(x, y) = f(x)$ , depending only on  $x$ , and assuming that  $f''(x)$  keeps the same sign in the interval  $(a, a+h)$ , we can take as limits of the increment

$$\Delta y = \int_a^{a+h} f(x) dx,$$

corresponding to  $\Delta x = h$ , either of the two pairs of numbers  $p, q$  or  $p, r$ , where  $p, q, r$  measure respectively the following

\* Communicated and translated by Prof. H. T. H. Piaggio, M.A., D.Sc., University College, Nottingham.

† Phil. Mag. xxxvii. (1919).

rectilineal areas (see figure) :—

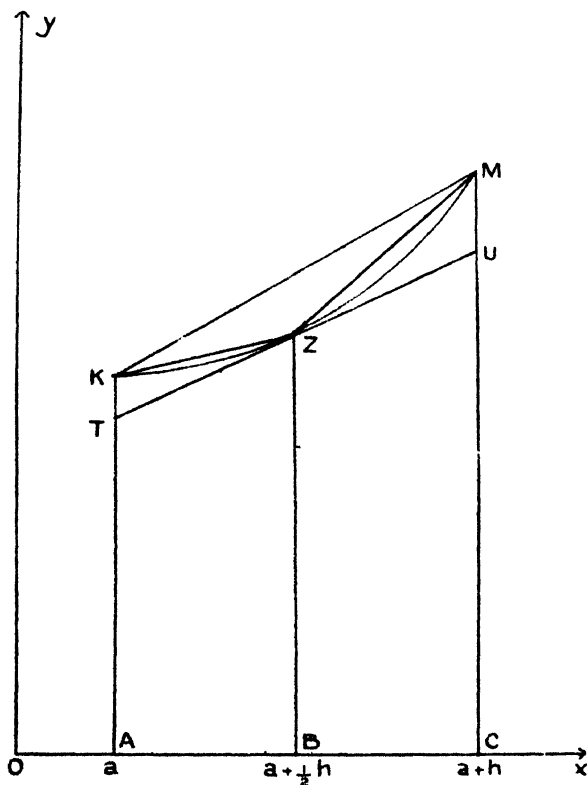
$$p = \text{trapezium ATUC} = hf(a + \tfrac{1}{2}h)$$

(TU is the tangent at Z) ;

$$q = \text{trapezium AKZB} + \text{trapezium BZMC}$$

$$= \tfrac{1}{2}h[f(a) + 2f(a + \tfrac{1}{2}h) + f(a + h)] ;$$

$$r = \text{trapezium AKMC} = \tfrac{1}{2}h[f(a) + f(a + h)] .$$



The linear combinations

$$\sigma = \tfrac{1}{3}[3\lambda p + (4 - 6\lambda)q + (3\lambda - 1)r] . . . (2)$$

gives for every value of  $\lambda$ , as is easily verified, the well-known Simpson's Rule, which gives the increment  $\Delta y$  with an error of the 5th order of the small number  $h$ . Two particularly remarkable combinations are obtained by putting  $\lambda = \tfrac{1}{3}$  and  $\lambda = \tfrac{2}{3}$ , namely

$$\sigma' = \tfrac{1}{3}(p + 2q), . . . . . (3)$$

$$\sigma'' = \tfrac{1}{3}(2p + r), . . . . . (4)$$



The extension of formulæ (4) and (3) to the general case, where  $F(x, y)$  involves  $y$  as well as  $x$ , leads respectively to the approximate formulæ of Runge\* and Piaggio†. But, as there occur in the general case supplementary errors which depend on the approximate evaluation of  $p, q, r$ , the total error of these approximate formulæ is generally greater than before, say of the 3rd or 4th order instead of the 5th. To Piaggio is due the idea of using the numbers  $p$  and  $q$ , each calculated with a suitable upper and lower value so chosen that the signs of the differences  $p - \Delta y$  and  $q - \Delta y$  are known, as exact limits for  $\Delta y$ . With these he then forms the approximate combination  $\sigma'$ . Generalizing this idea of Piaggio's, we can obviously use in the same manner, as limits for  $\Delta y$ , the two numbers  $p, r$ , each calculated with a suitable upper and lower value, and use these to form the approximate combination  $\sigma''$ . We propose now to examine the last two methods of calculation in respect of their precision in order to arrive by combining them to a generalization of Piaggio's method, giving in every case the order of approximation‡.

We shall assume that the function  $F(x, y)$  has, in the neighbourhood of the initial point  $(a, b)$ , certain continuous partial derivatives of some of the lowest orders, which appear in the discussion. We can trace beforehand the curves on which the functions

$$\frac{\partial F}{\partial y}, \quad \frac{dF}{dx} = \frac{\partial F}{\partial x} + F \frac{\partial F}{\partial y},$$

$$\frac{d^2 F}{dx^2} = \frac{\partial^2 F}{\partial x^2} + 2F \frac{\partial^2 F}{\partial x \partial y} + F^2 \frac{\partial^2 F}{\partial y^2} + \frac{\partial F}{\partial x} \frac{\partial F}{\partial y} + F \left( \frac{\partial F}{\partial y} \right)^2$$

are zero or cease to be continuous, and likewise the curves on which  $F$  is equal to  $\pm 1$  or becomes discontinuous. Disregarding the case when the integral curve cuts one of these loci of exceptional points, we can obviously assume§ that the integral curve is contained in the rectangular

\* *Math. Ann.* xlv. (189 ).

† *Loc. cit.*

‡ The second form of calculation that we wish to examine depends on the same linear combination  $\sigma''$  as Runge's method, and these two methods coincide for the trivial case  $F(x, y) = f(x)$ ; but there is certainly an important distinction between them in the general case, for in Runge's method there is no attempt to find exact limits for  $\Delta y$ .

§ Taking  $y$  instead of  $x$  as independent variable, if  $\left| \frac{dy}{dx} \right| > 1$ .

domain \*

$$a \leq x \leq a+h, \quad b-h < y \leq b+h,$$

and that the functions  $\partial F/\partial y$ ,  $dF/dx$ ,  $d^2F/dx^2$  do not change sign in this domain.

Taking the equation of the integral curve to be  $y = \phi(x)$ , we shall use the following notation:—

$$x_\alpha = a + \alpha h; \quad y_\alpha = \phi(x_\alpha); \quad F_\alpha = F(x_\alpha, y_\alpha); \quad \dots (\alpha = 0, \frac{1}{2}, 1)$$

$$P = hF_{\frac{1}{2}}; \quad Q = \frac{1}{4}h(F_0 + 2F_{\frac{1}{2}} + F_1); \quad R = \frac{1}{2}h(F_0 + F_1);$$

$$\Sigma' = \frac{1}{3}(P + 2Q); \quad \Sigma'' = \frac{1}{3}(2P + R).$$

The maximum and minimum values of the function  $F$  on the part of the integral curve between the ordinates  $x=a$  and  $x=a+h$  will be denoted by  $\bar{M}$  and  $\underline{M}$  respectively, while the approximation used instead of these, respectively greater and less than them, by  $\bar{M}$  and  $\underline{M}$ .

Finally

$$\left. \begin{aligned} \bar{F}_\alpha &= F(a + \alpha h, b + \bar{M}\alpha h); \\ \underline{F}_\alpha &= F(a + \alpha h, b + \underline{M}\alpha h); \\ \bar{F}_\alpha &= F(a + \alpha h, b + \bar{M}\alpha h); \\ \underline{F}_\alpha &= F(a + \alpha h, b + \underline{M}\alpha h); \end{aligned} \right\} (\alpha = 0, \frac{1}{2}, 1)$$

$$\bar{P} = h\bar{F}_{\frac{1}{2}}; \quad \underline{P} = h\underline{F}_{\frac{1}{2}}; \quad \bar{Q} = h\bar{F}_{\frac{1}{2}}; \quad \underline{Q} = h\underline{F}_{\frac{1}{2}};$$

with a similar meaning for  $\bar{Q}$ ,  $\underline{Q}$ ,  $\bar{R}$ ,  $\underline{R}$ ,  $\bar{R}$ ,  $\underline{R}$ .

It is clear that

$$\bar{F}_0 = \underline{F}_0 = F_0 = \bar{F}^0 = F_0,$$

and that the numbers  $\bar{M}$  and  $\underline{M}$  coincide respectively either with  $F_1$  and  $F_0$ , or with  $F_0$  and  $F_1$ , according to the sign of  $dF/dx$ . It follows that one of the numbers  $\bar{M}$ ,  $\underline{M}$  may be taken equal to  $F_0$ , and so found immediately. As for the other, we could take for it one of the numbers  $F(a+h, b \pm h)$ , according to the signs of  $dF/dx$  and  $\partial F/\partial y$ , but to obtain the desired order of accuracy we shall take the value  $F(a+h, b+\mu h)$ ,  $\mu$  being as follows:

$$F_0, \quad \text{if } \partial F/\partial y < 0;$$

$$F(a+h, b+h), \quad \text{if } \partial F/\partial y > 0 \text{ and } dF/dx > 0;$$

$$F(a+h, b-h), \quad \text{if } \partial F/\partial y > 0 \text{ and } dF/dx < 0.$$

\* To fix ideas, we assume  $h > 0$ .

Hence

$$\bar{P} \geq \dot{P} > P > \underline{P} \geq \underline{P}, \quad \text{if } \partial F / \partial y > 0,$$

but

$$\bar{P} \leq \dot{P} < P < \underline{P} \leq \underline{P}, \quad \text{if } \partial F / \partial y < 0.$$

There are analogous inequalities for  $Q$  and for  $R$ .

By considering the signs of  $d^2F/dx^2$  and  $\partial F/\partial y$  we get four possible cases, in each of which we can indicate limits for  $\Delta y$ , and indeed do so in two different ways. In the first place, using the numbers  $P$  and  $Q$ , we get:

$$\bar{Q} > \Delta y > P, \quad \text{if } d^2F/dx^2 > 0 \text{ and } \partial F/\partial y > 0;$$

$$\underline{Q} < \Delta y < \bar{P}, \quad \text{if } d^2F/dx^2 < 0 \text{ and } \partial F/\partial y > 0;$$

$$\bar{Q} > \Delta y > \bar{P}, \quad \text{if } d^2F/dx^2 > 0 \text{ and } \partial F/\partial y < 0;$$

$$\underline{Q} < \Delta y < \underline{P}, \quad \text{if } d^2F/dx^2 < 0 \text{ and } \partial F/\partial y < 0.$$

The combination  $\Sigma'$  formed with a pair of corresponding numbers  $\bar{Q}$ ,  $P$ , or  $Q$ ,  $\bar{P}$ , will be denoted by  $\Sigma'(\bar{M}, \underline{M})$ .

Secondly, we can use a pair of corresponding numbers  $\bar{R}$ ,  $\underline{P}$ , or  $\bar{R}$ ,  $\bar{P}$  (according to the signs of  $d^2F/dx^2$  and  $\partial F/\partial y$ ) as limits for  $\Delta y$ . The combination  $\Sigma''$  formed with such a pair will be denoted by  $\Sigma''(\bar{M}, \underline{M})$ .

We shall now find the order of smallness of the differences  $\Delta y - \Sigma'(\bar{M}, \underline{M})$  and  $\Delta y - \Sigma''(\bar{M}, \underline{M})$ . As the differences  $\Delta y - \Sigma'$ ,  $\Delta y - \Sigma''$  are of the 5th order (taking  $h$  as small of the 1st order), we must examine the order of the differences  $\Sigma' - \Sigma'(\bar{M}, \underline{M})$ ,  $\Sigma'' - \Sigma''(\bar{M}, \underline{M})$ .

Now

$$\Sigma' - \Sigma'(\bar{M}, \underline{M}) = \{\Sigma' - \Sigma'(\bar{M}, \underline{M})\} + \{\Sigma'(\bar{M}, \underline{M}) - \Sigma'(\bar{M}, \underline{M})\},$$

where  $\Sigma'(\bar{M}, \underline{M})$  is what  $\Sigma'(\bar{M}, \underline{M})$  becomes when  $\bar{M}, \underline{M}$  are replaced by  $\bar{M}, \underline{M}$  respectively; and similarly  $\Sigma'' - \Sigma''(\bar{M}, \underline{M})$  may be written as the sum of parts. But if we choose  $\bar{M}$  and  $\underline{M}$  as above, the differences  $\bar{M} - \bar{M}$ ,  $\underline{M} - \underline{M}$  will be of the 2nd order\*. Hence the differences  $\bar{F}_a - \bar{F}_a$ ,  $\underline{F}_a - \underline{F}_a$  will be of the 3rd order, and consequently  $\dot{P} - \bar{P}$ ,  $\underline{P} - \underline{P}$ ,  $\dot{Q} - \bar{Q}$ , ... etc. of the 4th order. Thus  $\Sigma'(\bar{M}, \underline{M}) - \Sigma'(\bar{M}, \underline{M})$  and  $\Sigma''(\bar{M}, \underline{M}) - \Sigma''(\bar{M}, \underline{M})$  are also of the 4th order.

\* Other ways of choosing  $\bar{M}$  and  $\underline{M}$  are available, but these may lower the order of smallness of the differences.

It remains to examine the order of the differences  $\Sigma' - \Sigma'(\dot{M}, M)$  and  $\Sigma'' - \Sigma''(\dot{M}, M)$ . We shall show that it depends on the sign of the product

$$\frac{\partial F}{\partial y} \frac{dF}{dx} \frac{d^2 F}{dx^2} = \Omega(x, y), \quad \text{say.} \quad (5)$$

If  $\Omega < 0$ ,  $\Sigma' - \Sigma'(\dot{M}, M)$  is of the 4th order,

$\Sigma'' - \Sigma''(\dot{M}, M)$  of the 3rd.

If  $\Omega > 0$ , the orders are the 3rd and 4th respectively.

Hence the orders of the differences  $\Sigma' - \Sigma'(\bar{M}, \underline{M})$  and  $\Sigma'' - \Sigma''(\bar{M}, \underline{M})$  are also the 4th and 3rd respectively if  $\Omega < 0$ , or the 3rd and 4th if  $\Omega > 0$ .

The proof is a direct application of Taylor's series. Take first the case  $\Omega < 0$ , and to fix ideas take  $\partial F / \partial y > 0$ ,  $d^2 F / dx^2 > 0$ ,  $dF / dx < 0$ . Using the suffix 0 to denote values at the initial point  $(a, b)$ , we have \*

$$\dot{M} = F_0; \quad M = F_1;$$

$$\begin{aligned} \Sigma' - \Sigma'(\dot{M}, M) &= \frac{1}{3}(P + 2Q) - \frac{1}{3}(P + 2\dot{Q}) \\ &= \frac{1}{6}h(F_1 - \dot{F}_1) + \frac{1}{6}h(F_{\frac{1}{2}} - \dot{F}_{\frac{1}{2}}) + \frac{1}{6}h(F_{\frac{1}{4}} - \dot{F}_{\frac{1}{4}}); \end{aligned}$$

$$\begin{aligned} \Sigma'' - \Sigma''(\dot{M}, M) &= \frac{1}{3}(2P + R) - \frac{1}{3}(2\dot{P} + \dot{R}) \\ &= \frac{1}{6}h(F_1 - \dot{F}_1) + \frac{2}{3}h(F_{\frac{1}{2}} - \dot{F}_{\frac{1}{2}}). \end{aligned}$$

But

$$\begin{aligned} &\frac{1}{6}h(F_1 - \dot{F}_1) \\ &= \frac{1}{6}\{F(x_1, y_1) - F(x_1, b + hF_0)\} \\ &= \frac{1}{6}h\{y_1 - (b + hF_0)\} \cdot \partial F(a + h, b + \theta h) / \partial y \\ &= \frac{1}{6}h \left\{ \left[ b + hF_0 + \frac{h^2}{2} \left( \frac{dF}{dx} \right)_0 + \frac{h^2}{6} \left( \frac{d^2 F}{dx^2} \right)_0 + \dots \right] - (b + hF_0) \right\} \\ &\quad \left\{ \left( \frac{\partial F}{\partial y} \right)_0 + h \left( \frac{\partial^2 F}{\partial x \partial y} \right)_0 + \theta h \left( \frac{\partial^2 F}{\partial y^2} \right)_0 + \dots \right\} \\ &= \frac{h^3}{12} \left( \frac{dF}{dx} \right)_0 \left( \frac{\partial F}{\partial y} \right)_0 + Ah^4 + \dots, \end{aligned}$$

\* For simplicity we use infinite series, but it is really sufficient to use finite series with a remainder term, involving only the assumption of the existence and continuity of a few partial derivatives of  $F(x, y)$ .

where  $0 < \theta < 1$ , and

$$A = \frac{1}{36} \left( \frac{d^2 F}{dx^2} \right)_0 \left( \frac{\partial F}{\partial y} \right)_0 + \frac{1}{12} \left( \frac{dF}{dx} \right)_0 \left\{ \left( \frac{\partial^2 F}{\partial x \partial y} \right)_0 + \theta \left( \frac{\partial^2 F}{\partial y^2} \right)_0 \right\},$$

so  $A$  is a bounded number depending on  $h$ .

Similarly

$$\frac{h}{3} (F_{\frac{1}{2}} - \dot{F}_{\frac{1}{2}}) = \frac{h^3}{24} \left( \frac{dF}{dx} \right)_0 \left( \frac{\partial F}{\partial y} \right)_0 + Bh^4 + \dots;$$

$$\begin{aligned} \frac{h}{3} (F_{\frac{1}{2}} - F_{\frac{1}{2}}) &= \frac{h}{3} \{ y_{\frac{1}{2}} - (b + \frac{1}{2}hF_1) \} \cdot \partial F(a + \frac{1}{2}h, b + \frac{1}{2}h) / \partial y \\ &= \frac{h}{3} \left\{ \left[ b + \frac{1}{2}hF_0 + \frac{h^2}{8} \left( \frac{dF}{dx} \right)_0 + \dots \right] \right. \\ &\quad \left. - \left[ b + \frac{1}{2}hF_0 + \frac{h^2}{2} \left( \frac{dF}{dx} \right)_0 + \dots \right] \right\} \left\{ \left( \frac{\partial F}{\partial y} \right)_0 + \dots \right\} \\ &= -\frac{h^3}{8} \left( \frac{dF}{dx} \right)_0 \left( \frac{\partial F}{\partial y} \right)_0 + Ch + \dots, \end{aligned}$$

where  $0 < \vartheta < 1$ , and  $B, C$  are bounded numbers.

Hence

$$\Sigma' - \Sigma'(\dot{M}, \dot{M}) = (A + B + C)h^4 + \dots, \quad \text{of the 4th order;}$$

$$\Sigma'' - \Sigma''(\dot{M}, \dot{M}) = -\frac{h^3}{6} \left( \frac{dF}{dx} \right)_0 \left( \frac{\partial F}{\partial y} \right)_0 + (A + 2C)h^4 + \dots, \\ \text{of the 3rd order.}$$

Now take the second case,  $\Omega > 0$ , and to fix ideas take  $\partial F / \partial y > 0$ ,  $dF/dx > 0$ ,  $d^2 F/dx^2 \geq 0$ . We get

$$\dot{M} = F_1; \quad \dot{M} = F_0;$$

$$\Sigma' - \Sigma'(\dot{M}, \dot{M}) = -\frac{h^3}{6} \left( \frac{dF}{dx} \right)_0 \left( \frac{\partial F}{\partial y} \right)_0 + \dots, \quad \text{of the 3rd order;}$$

$$\Sigma'' - \Sigma''(\dot{M}, \dot{M}) = Dh^4 + \dots, \quad \text{of the 4th order.}$$

( $D$  is a bounded number.)

Thus we obtain the following result:—

*The error of the approximate formula which uses limits between which  $\Delta y$  must lie is of at least the 4th order of smallness, provided that we choose the special values for  $\dot{M}$ ,  $\underline{M}$  specified above, and use the combination  $\Sigma'(\dot{M}, \underline{M})$ , i. e., Piaggio's method, in the case  $\Omega < 0$ , but the combination  $\Sigma''(\dot{M}, \underline{M})$ , i. e. the generalization of Piaggio's method, in the case  $\Omega > 0$ .*

The often-discussed example of Runge's

$$[dy/dx = (y-x)/(y+x); \quad a = 0, b = 1]$$

provides an example of the case  $\Omega < 0$ . The high degree of precision which the combination  $\Sigma'(\bar{M}, \underline{M})$  may give is well shown in Piaggio's paper\*.

For the other case,  $R > 0$ , let us examine the example:

$$dy/dx = 4y/x = F(x, y); \quad a = 1, b = 0.1,$$

taking the increment  $\Delta x = h$  first as 0.1, secondly as 0.01, and thirdly as 0.001. Here

$$\partial F / \partial y = 4/x > 0; \quad dF/dx = 12y/x^2 > 0;$$

$$d^2F/dx^2 = 24y/x^3 > 0.$$

The exact integral is

$$y = 0.1 x^4 = \phi(x) \quad \text{say,}$$

so that

$$\phi(1.1) = 0.14641; \quad \phi(1.01) = 0.104060401;$$

$$\phi(1.001) = 0.1004006004001.$$

These exact results enable us to find the degree of precision in the approximate work.

(i.)

$$h = 0.1; \quad \underline{M} = F_0 = 0.4;$$

$$\mu = F(a+h, b+h) = 4 \times 0.2/1.1 < 0.8;$$

$$\bar{M} = F(a+h, b+\mu h) = 4 \times 0.18/1.1 < 0.7.$$

$$F_0 = 0.4; \quad F_{\frac{1}{2}} = 4 \times 0.12/1.05 > 0.457.$$

$$\bar{F}_{\frac{1}{2}} = 4 \times 0.135/1.05 < 0.515; \quad \bar{F}_1 = 4 \times 0.17/1.1 < 0.619.$$

$$\underline{P} = 0.0457; \quad \bar{R} = 0.0510; \quad \bar{Q} = 0.0513.$$

$$\Sigma''(\bar{M}, \underline{M}) = \frac{1}{2}(2\underline{P} + \bar{R}) = 0.0475,$$

with an error  $-1.1 \times 10^{-3}$ .

$$[\Sigma'(\bar{M}, \underline{M}) = \frac{1}{2}(\underline{P} + 2\bar{Q}) = 0.0494,$$

with an error  $-3.0 \times 10^{-3}$ .

\* Phil. Mag. xxxvii. (1919). [Translator's note. I am afraid that this high degree of precision was a lucky accident, due to the values I took for  $\bar{M}$ ,  $\underline{M}$ . These values were not chosen in the way specified by Mr. Remes.—H. T. H. P.]

(ii.)

$$h = 0.01; \quad \underline{M} = 0.4; \quad \mu = 0.436; \quad \overline{M} = 0.414.$$

$$F_0 = 0.4; \quad \underline{F}_{\frac{1}{2}} = 0.405970; \quad \overline{F}_{\frac{1}{2}} = 0.406249;$$

$$\overline{F}_1 = 0.412436.$$

$$P = 0.00405970; \quad \overline{R} = 0.00406218; \quad (\overline{Q} = 0.00406234).$$

$$\Sigma''(\overline{M}, \underline{M}) = 0.00406053, \text{ with an error } -1.3 \times 10^{-7}.$$

$$[\Sigma'(\overline{M}, \underline{M}) = 0.00406146, \text{ with an error } -1.06 \times 10^{-6}.]$$

(iii.)

$$h = 0.001; \quad \underline{M} = 0.4; \quad \mu = 0.40360; \quad \overline{M} = 0.40122.$$

$$F_0 = 0.4; \quad \underline{F}_{\frac{1}{2}} = 0.400599700; \quad \overline{F}_{\frac{1}{2}} = 0.400602139;$$

$$\overline{F}_1 = 0.401203677.$$

$$P = 0.000400599700; \quad \overline{R} = 0.000400601839;$$

$$(\overline{Q} = 0.000400601989).$$

$$\Sigma''(\overline{M}, \underline{M}) = 0.000400600413, \text{ with an error } -1.3 \times 10^{-11}.$$

$$[\Sigma'(\overline{M}, \underline{M}) = 0.000400601226, \text{ with an error } -8.26 \times 10^{-10}.]$$

# XL. The Lowest Natural Frequency of Circular Arcs.

By J. P. DEN HARTOG \*.

## ABSTRACT.

FORMULÆ are derived for the first and second natural frequencies of a part of a circular ring, hinged or clamped at its ends. It is shown that the type of vibration, in which extension of the fibres occurs, under certain conditions may have a lower natural frequency than any non-extensional type of vibration. The results are given in the form of curves and tables.

THE problem of finding the natural frequencies of vibration of a part of a circular ring has been attacked by Lamb †, who derived the differential equation and solved it for the case

\* Communicated by Mr. R. V. Southwell, F.R.S.

† Proc. London Math. Soc. xix. p. 865 (1888).

of small curvatures. The exact integration for the general case of a central angle  $\alpha$  having any value between  $0^\circ$  and  $360^\circ$  becomes extremely complicated. In this note the approximate method of Rayleigh-Ritz has been applied for calculating the lowest natural frequency of circular arcs subtending any angle, for hinged as well as for clamped ends.

The following notations are used :—

$w, v$  = radial and tangential displacements (fig. 1).

$\alpha$  = the central angle.

$R$  = mean radius.

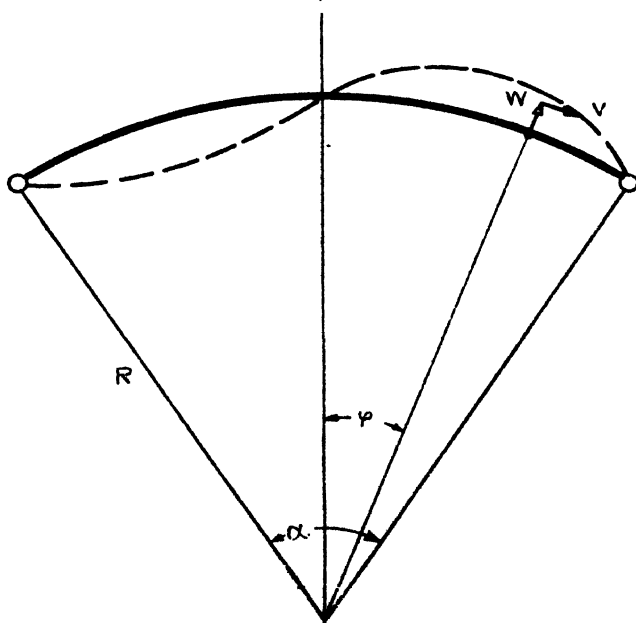
$\gamma$  = mass per unit length of the centre line.

$EI$  = rigidity against bending.

$k$  = radius of gyration of the cross-section.

$S$  = cross-sectional area.

Fig. 1



#### A. HINGED ENDS.

The boundary conditions are :—

$$\phi = \pm \frac{\alpha}{2}, \quad w = v = \frac{d^2 w}{d\phi^2} = 0. \quad . \quad . \quad . \quad (1)$$



We will first consider the non-extensional vibrations, in which case  $w$  and  $v$  have to satisfy the condition

$$w + \frac{dv}{d\phi} = 0. \quad (2)$$

As a suitable analytical expression for the displacements satisfying (1) and (2) we may take

$$\left. \begin{aligned} w &= A \sin \frac{2\pi\phi}{\alpha} \sin \omega t, \\ v &= \frac{A\alpha}{2\pi} \left( \cos \frac{2\pi\phi}{\alpha} + 1 \right) \sin \omega t. \end{aligned} \right\} \quad (3)$$

Substituting this in the expressions for the elastic and kinetic energies of the arc,

$$V = \frac{EI}{2R^3} \int_0^\alpha \left\{ w + \frac{\partial^2 w}{\partial \phi^2} \right\}^2 d\phi, \quad (4)$$

$$T = \frac{\gamma R}{2} \int_0^\alpha \left\{ \left( \frac{\partial v}{\partial t} \right)^2 + \left( \frac{\partial w}{\partial t} \right)^2 \right\} d\phi, \quad (4a)$$

and equating their maximum values, the circular frequency  $\omega$  is found:

$$\omega^2 = \frac{EI}{\gamma R^4 \alpha^4} \cdot \frac{\alpha^4 - 8\pi^2 \alpha^2 + 16\pi^4}{1 + 0.75\alpha^2/\pi^2}. \quad (5)$$

For the angle  $\alpha=0$  this result coincides with the exact solution for a straight bar, having a node in the middle. For  $\alpha=2\pi$  we have a complete ring turning about one hinge, and consequently have zero frequency.

As another assumption satisfying (1) and (2) we take

$$\left. \begin{aligned} w &= A \left[ \frac{\phi}{\alpha} - \frac{40}{7} \left( \frac{\phi}{\alpha} \right)^3 + \frac{48}{7} \left( \frac{\phi}{\alpha} \right)^5 \right] \sin \omega t, \\ v &= \alpha A \left[ \frac{3}{28} - \left( \frac{\phi}{\alpha} \right)^2 + \frac{20}{7} \left( \frac{\phi}{\alpha} \right)^4 - \frac{16}{7} \left( \frac{\phi}{\alpha} \right)^6 \right] \sin \omega t, \end{aligned} \right\} \quad (6)$$

from which in the same manner

$$\omega^2 = \frac{EI}{\gamma R^4 \alpha^4} \cdot \frac{\alpha^4 - 78.5\alpha^2 + 1585}{1 + 0.094\alpha^2}. \quad (7)$$

For angles  $60^\circ < \alpha < 270^\circ$  this will give smaller and therefore better results for  $\omega$  than (5). From (5) and (7) is deduced

$$\omega = \frac{C_1}{R^2} \sqrt{\frac{EI}{\gamma}}, \quad (8)$$

in which  $C_1$  is to be taken from the following table :—

TABLE I.

$\alpha \dots$	0°	20	40	60	80	100	120	140	160	
$C_1 \dots$	$\infty$	321	78.5	33.6	17.8	10.65	6.80	4.55	3.14	
$\alpha \dots$	180°	200	220	240	260	280	300	320	340	360
$C_1 \dots$	2.20	1.56	1.11	.796	.562	.386	.255	.145	.063	0

These values have been calculated from (5) for angles smaller than 60° and larger than 270°; from (6) for angles between 60° and 270°. For small angles  $\alpha$  it is more convenient to have the result in the form

$$\omega = \frac{C_2}{l_2} \sqrt{\frac{EI}{\gamma}}, \dots \dots \dots (9)$$

where  $l$  is the length of the chord subtending the arc and  $C_2$  has the following values :—

TABLE II.

$\alpha \dots$	0°	20	40	60	80	100	120	140	160	180
$C_2 \dots$	39.4	38.6	36.7	33.6	29.4	25.1	20.4	16.1	12.15	8.80

This non-extensional type of vibration, in the limit  $\alpha=0$ , reduces to the second natural mode of the straight bar (with a node in the middle). The deformation, corresponding to the lowest natural mode of the *straight* bar, which does not have nodes except at the ends, becomes extensional as soon as the bar becomes curved. For small angles  $\alpha$ , therefore, the question arises, whether a shape of vibration not fulfilling the condition of non-extensibility (2) may not have a lower period than the one expressed by (8). We take as an analytical expression for the shape of deformation

$$\left. \begin{aligned} w &= A \cos \frac{\pi \phi}{\alpha} \sin \omega t, \\ v &= \left[ a_1 \sin \frac{2\pi \phi}{\alpha} + a_2 \sin \frac{6\pi \phi}{\alpha} \right] \sin \omega t, \end{aligned} \right\} \dots \dots (10)$$

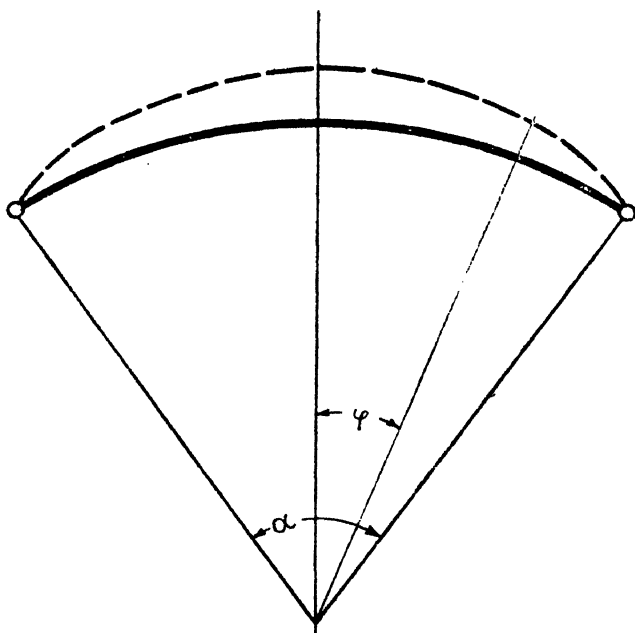
fulfilling the boundary and symmetry conditions, but not the non-extensibility condition (2).

Here  $a_1$  and  $a_2$  are arbitrary constants, which will be determined so as to make the elastic energy,

$$V = \frac{ES}{R} \int_0^{\alpha/2} \left( w + \frac{\partial v}{\partial \phi} \right)^2 d\phi + \frac{EI}{R^3} \int_0^{\alpha/2} \left( w + \frac{\partial^2 w}{\partial \phi^2} \right)^2 d\phi, \quad (11)$$

a minimum\*.

Fig. 2.



Substituting (10) in (11),  $a_1$  and  $a_2$  have been calculated from  $\frac{\partial V}{\partial a_1} = 0$ ;  $\frac{\partial V}{\partial a_2} = 0$  leading to the results :

$$a_1 = -\frac{2}{3} \cdot \frac{c}{\pi^2} \cdot A,$$

$$a_2 = -\frac{2}{105} \cdot \frac{\alpha}{\pi^2} \cdot A.$$

With these values the elastic energy becomes

$$V = \frac{EIA^2\alpha}{4R^3} \left[ 820 \left( \frac{R}{k} \right)^2 + \left( 1 - \frac{\pi^2}{\alpha^2} \right)^2 \right] \sin^2 \omega t.$$

This involves less calculation than determining  $a_1$  and  $a_2$  from the condition that  $\omega$  be minimum, the result being about as accurate.

The kinetic energy from (10) and (4) is

$$T = \frac{\gamma R \omega^2 A^2 \alpha}{4} [1 + .004 \alpha^2] \cos^2 \omega t.$$

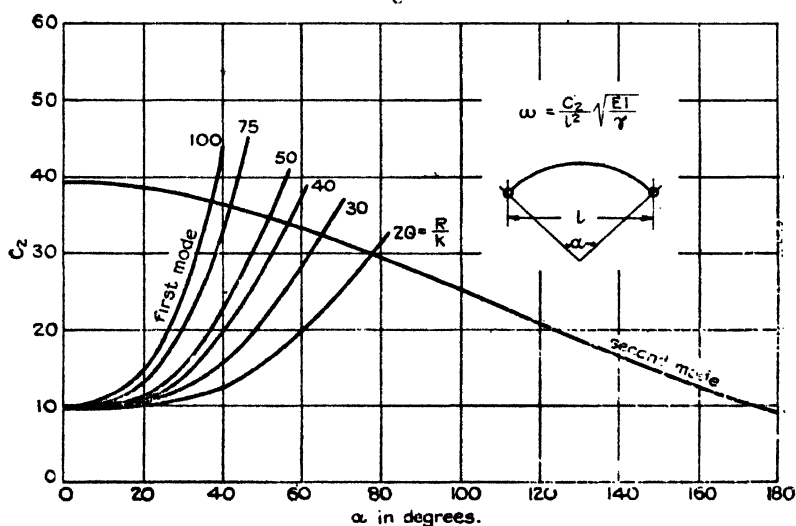
For angles  $\alpha$  not over  $80^\circ$  an error of less than .3 per cent. in the frequency is made by neglecting  $.004 \alpha^2$  with respect to 1 in the expression for T. Then it is found

$$\omega^2 = \frac{EI}{\gamma R^4} \left[ .820 \left( \frac{R}{k} \right)^2 + \left( 1 - \frac{\pi^2}{\alpha^2} \right)^2 \right]. \quad (12)$$

This can be brought to the form (9) with the constant

$$C'_2 = 4 \sin^2 \frac{\alpha}{2} \sqrt{.820 \left( \frac{R}{k} \right)^2 + \left( \frac{\pi^2}{\alpha^2} - 1 \right)^2}. \quad (13)$$

Fig. 3.



The numerical values of this constant and of the one in Table II. are shown in fig. 3.

It is seen that for angles  $\alpha$  smaller than about  $60^\circ$  the *extensional mode of vibration* has a lower period than the *non-extensional*.

### B. CLAMPED ENDS.

The boundary conditions for clamped ends are

$$\phi = \pm \frac{\alpha}{2}, \quad v = w = \frac{dw}{d\phi} = 0. \quad (14)$$

The simplest non-extensional shape for W, fulfilling (14) and (2), has a node in the middle. Due to the tangency at the ends, however, this shape is more complicated than with hinged ends, so that an assumption, like (3), with *one* parameter does not give accurate enough results. We have to take recourse to two parameters A and B for instance :

$$\left. \begin{aligned} w &= \left( \frac{A}{8} - \frac{B}{32} \right) \frac{\phi}{\alpha} - \left( A - \frac{3B}{8} \right) \left( \frac{\phi}{\alpha} \right)^3 + \left( 2A - \frac{2B}{2} \right) \left( \frac{\phi}{\alpha} \right)^5 \\ &\quad + 2B \left( \frac{\phi}{\alpha} \right)^7, \\ v &= \alpha \left[ \left( \frac{A}{192} - \frac{B}{1024} \right) - \left( \frac{A}{16} - \frac{B}{64} \right) \left( \frac{\phi}{\alpha} \right)^2 + \left( \frac{A}{4} - \frac{3B}{32} \right) \left( \frac{\phi}{\alpha} \right)^4 \right. \\ &\quad \left. - \left( \frac{A}{3} - \frac{B}{4} \right) \left( \frac{\phi}{\alpha} \right)^6 + \frac{B}{4} \left( \frac{\phi}{\alpha} \right)^8 \right]. \end{aligned} \right\} \quad \dots \dots (15)$$

Substituting this in (4) and equating the maximum values of V and T, we arrive at an expression for  $\omega$  in terms of A and B.

Determining these two parameters in such manner as to make  $\omega$  a minimum, the following result is obtained :

$$\omega = \frac{C_3}{R^2} \sqrt{\frac{EI}{\gamma}}, \quad \dots \dots (16)$$

where  $C_3$  is to be taken from

TABLE III.

$\alpha \dots$	0°	20	40	60	80	100	120	140	160	180
$C_3 \dots$	$\infty$	504	124	53.8	29.2	17.9	11.85	8.22	5.93	4.38
$\alpha \dots$	200	220	240	260	280	300	320	340	360	
$C_3 \dots$	3.31	2.54	1.98	1.57	1.25	1.01	.821	.677	.567	

Again, for small angles  $\alpha$  it is more convenient to use the chord  $l$  rather than the radius R :

$$\omega = \frac{C_4}{l^2} \sqrt{\frac{EI}{\gamma}} \quad \dots \dots (17)$$

with

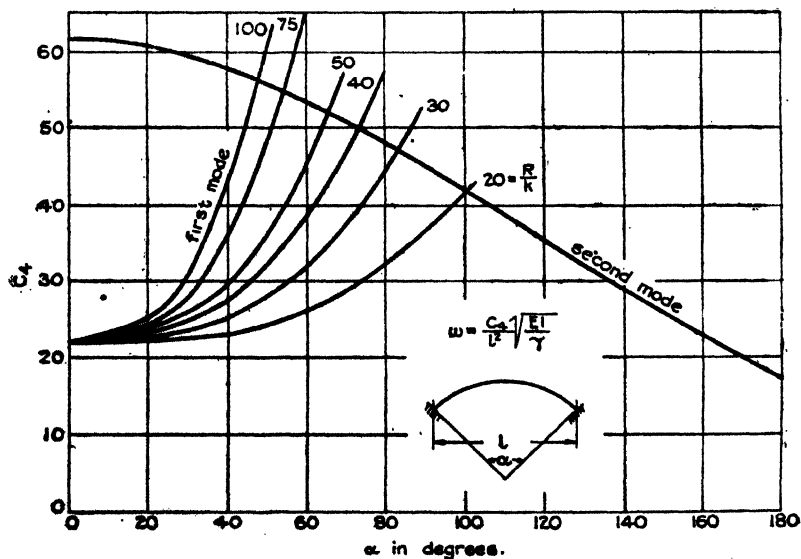
TABLE IV.

$\alpha \dots$	$0^\circ$	20	40	60	80	100	120	140	160	180
$C_1 \dots$	61.7	60.7	58.0	53.8	48.3	42.1	35.6	29.0	23.0	17.55

For the extensional vibrations of the arc with clamped ends corresponding to the fundamental mode of the straight bar, we follow the same course as before for hinged ends, assuming

$$\left. \begin{aligned} w &= A \left( 1 + \cos \frac{2\pi\phi}{\alpha} \right), \\ v &= a_1 \sin \frac{2\pi\phi}{\alpha} + a_2 \sin \frac{6\pi\phi}{\alpha}. \end{aligned} \right\} \dots (18)$$

Fig. 4.



With the aid of (11) we find

$$a_1 = -\frac{\alpha}{2\pi} A, \quad a_2 = 0.$$

The elastic energy becomes

$$\frac{EIA^2\alpha}{2R^3} \left[ \frac{R^2}{k^2} + 1 + \frac{1}{2} \left( 1 - \frac{4\pi^2}{\alpha^2} \right)^2 \right] \quad . \quad . \quad . \quad (19)$$

and the kinetic energy

$$\gamma RA^2\omega^2\alpha \left[ \frac{3}{4} + \frac{1}{16} \frac{\alpha^2}{\pi^2} \right] \quad . \quad . \quad . \quad (20)$$

Equating (19) and (20), making some simplifications and bringing  $\omega$  in the form (17), we find for the constant:

$$C_4 = 4 \sin^2 \frac{\alpha}{2} \sqrt{\frac{2}{3} \left( \frac{R}{k} \right)^2 + \frac{1}{3} \left( \frac{4\pi^2}{\alpha^2} - 1 \right)^2} \quad . \quad . \quad (21)$$

The value of this constant for various ratios  $R/k$  and various angles  $\alpha$  can be taken from figure 4.

Research Laboratory,  
Westinghouse Elec. & Mfg. Co.,  
East Pittsburgh, Penna.

XLI. *The Results of Classical Wave Mechanics obtained by using the Methods of Relativity Mechanics.* By T. LEWIS, M.Sc., University College of Wales, Aberystwyth\*.

### Introduction.

THE close similarity between the Principle of Least Action in the Maupertuis form and Fermat's Principle of Least Time led de Broglie† to associate a wave of phase with every type of energy quantum in motion. Schrödinger's‡ "Wave Mechanics" is a development of this idea along lines slightly different from de Broglie's. He pays more attention to the amplitude of the associated wave, and practically ignores the phase. O. Klein§ has interpreted Wave Mechanics from the standpoint of a five-dimensional "universe," and has shown that the path of the material particle emitting the wave is the projection in space-time of a null-geodesic in this five-fold "universe." In this paper we will show that the spatial path of a particle

\* Communicated by Prof. G. A. Schott, F.R.S.

† J. Phys. t. vii. pp. 1-6 (1926): "Ondes et Mouvements," par L. de Broglie.

‡ Ann. der Phys. Bd. lxxix. (1926)

§ Zeit. für Phys. Bd. xxxvii. (1926).

moving in a conservative field according to classical laws is the projection of a null-geodesic in a certain space-time, and that this geodesic is the "track" of a ray of its associated wave. It will be seen that the equations of motion of the particle and those of a ray of its associated wave follow from the same principle of variation, thus demonstrating the close connexion between the above-named principles. These equations will then be expressed in canonic form—the same set represents the motion of the particle and the ray it follows, provided the parameters are suitably interpreted in each case. We next derive the Hamilton-Jacobi equation, and show that the phase, regarded as a function of time and position, is a solution. Finally, we derive Schrödinger's equation from a principle of variation. No new results are given. We merely apply the methods of Relativity Mechanics in order to derive the known results of Classical Mechanics, including Wave Mechanics. But, first of all, for the sake of continuity, we deduce the equations of motion of a particle from the Principle of Least Action, and those of the ray which it follows from Fermat's Principle.

§ 1. *The Principle of Least Action.*—Let a particle of mass  $m$  move in a conservative field according to classical laws. If  $V$  is its potential energy and  $E$  its total energy, its velocity  $u$  is given by

$$u = \sqrt{2(E - V)/m}. \quad . \quad . \quad . \quad (1.1)$$

The path joining two points  $A$  and  $B$  of the field corresponds to a stationary value of the action, the total energy being kept constant for all variations considered. This is expressed mathematically by the equation

$$\delta A = \delta \int_A^B u^2 dt = \delta \int_A^B u d\sigma = 0, \quad . \quad . \quad . \quad (1.2)$$

where  $d\sigma$  is an element of the path.

Let  $\tau$  be any parameter, and let differentiation with respect to it be denoted by dots. Then

$$\delta A = \delta \int_A^B u \dot{\sigma} d\tau = 0, \text{ with } \dot{\sigma}^2 = \dot{x}^2 + \dot{y}^2 + \dot{z}^2.$$

The parameter  $\tau$  can be chosen so that the values corresponding to  $A$  and  $B$  in the varied path are the same as for the actual path. Bearing this in mind, the above equation



410 Mr. T. Lewis on the Results of Classical Wave Mechanics  
is equivalent to three of the following type :

$$\frac{d}{d\tau}\left(\frac{u\dot{x}}{\sigma}\right) - \dot{\sigma}\frac{\partial u}{\partial x} = 0. \quad . \quad . \quad . \quad (1.3)$$

The form of this equation is invariant with respect to change of parameter ; so if  $\tau$  denote the time, (1.3) becomes

$$\ddot{x} - \frac{1}{2} \frac{\partial u^2}{\partial x} = 0. \quad . \quad . \quad . \quad (1.3)'$$

§ 2. *Fermat's Principle of Least Time.*—Let us regard the conservative field as an isotropic medium of refractive index  $\beta (=u/c$ , where  $c$  is a constant having the dimensions of a velocity). The velocity of light in this medium will be

$$v = \beta^{-1}c = c^2/u, \quad . \quad . \quad . \quad (2.1)$$

and the path of a ray joining two points A and B is given by

$$\delta(t_A - t_B) = \delta \int_A^B \frac{d\sigma}{v} = c^{-2} \delta \int_A^B u d\sigma. \quad . \quad . \quad (2.2)$$

We see that (2.2) is identical with (1.2). However, the law of description of the path is different. Proceeding as before, and this time denoting the actual time by  $t$  and differentiation with respect to it by accents, we find the equations of motion to be of the type

$$\frac{d}{dt}\left(\frac{x'}{v^3}\right) + \frac{\partial v}{\partial x}/v = 0. \quad . \quad . \quad . \quad (2.3)$$

§ 3. *The Geodesic Principle.*—Let us now consider the space-time characterized by the quadratic form

$$ds^2 = v^2 dt^2 - (dx^2 + dy^2 + dz^2) = v^2 dt^2 - d\sigma^2. \quad . \quad (3.1)$$

The critical velocity in this space-time is that of the wave associated with a particle moving in the conservative field already described. The determinant of the coefficients is  $-v^2$ . Hence the four-dimensional element of volume is

$$d\Omega = v dt dx dy dz. \quad . \quad . \quad . \quad (3.2)$$

As before,  $\tau$  is any parameter, and we write

$$2L = v^2 \dot{t}^2 - (\dot{x}^2 + \dot{y}^2 + \dot{z}^2) = v^2 \dot{t}^2 - \dot{\sigma}^2 = \dot{S}^2. \quad . \quad (3.3)$$

A geodesic in this space-time is defined by

$$\delta \int_P^Q ds = 0,$$

where P and Q are two fixed points in space-time. But

this is not the only integral which is stationary along a geodesic. If the parameter  $\tau$  is chosen so that the values corresponding to P and Q in the varied curves are the same as for the geodesic joining P and Q, the integral

$$S = \int_P^Q L d\tau \dots \dots \dots (3.4)$$

is stationary along the geodesic. In view of the fact that we shall be dealing with geodesics of zero length, it is more convenient to define them by the equation

$$\delta S = \delta \int_P^Q L d\tau = 0. \dots \dots \dots (3.5)$$

Performing the variation and bearing in mind the condition imposed on  $\tau$ , we arrive at the equations

$$\frac{d}{d\tau}(v^2 \dot{t}) = 0, \quad \ddot{x} + v \frac{\partial v}{\partial x} \dot{t}^2 = 0, \dots \dots \dots (3.6)$$

with two more of the latter type. From the first of these equations we get

$$v^2 \dot{t} = \text{constant} = c^2. \dots \dots \dots (3.7)$$

Let  $c^2$  have the same meaning as in (2.1), and substitute for  $v$  in terms of  $u$ . The second of equations (3.6) now becomes

$$\ddot{x} - \frac{1}{2} \frac{\partial u^2}{\partial x} = 0. \dots \dots \dots (3.8)$$

This equation is identical with (1.3)'. So the parameter  $\tau$  is the time of the material particle describing the path which is the spatial projection of the geodesic. However, it must not be thought that the track of a material particle in space-time is a geodesic. For the equations (3.6) have an integral

$$L = \text{constant}. \dots \dots \dots (3.9)$$

This equation, together with (3.7), is inconsistent with  $\dot{\sigma} = u$ .

If we eliminate  $\tau$  from (3.6) and denote differentiation with respect to  $t$  by accents as before, we get three equations of the type

$$\frac{d}{dt} \left( \frac{x'}{v^2} \right) + \frac{\partial v}{\partial x} / v = 0, \dots \dots \dots (3.10)$$

which is identical with (2.3), provided

$$x'^2 + y'^2 + z'^2 = v^2;$$

i. e., provided the constant on the right-hand side of (3.9)

is zero. In other words, the track of a ray of the wave associated with the particle is a geodesic of zero length.

§ 4. *The Canonic form of the Equations of Motion.*—The covariant components of the four-vector  $(\dot{t}, \dot{x}, \dot{y}, \dot{z})$  are defined in the following manner :

$$p_t = \frac{\partial L}{\partial \dot{t}} = v^2 \dot{t}, \quad p_x = \frac{\partial L}{\partial \dot{x}} = -\dot{x}, \quad . \quad . \quad (4.1)$$

with two more equations of the second type.

If we express  $L$  in terms of these covariant components and the coordinates, it becomes

$$L = H(p, x) = \frac{1}{2} \{ v^{-2} p_t^2 - (p_x^2 + p_y^2 + p_z^2) \}, \quad . \quad (4.2)$$

and the system of equations (3.6) is equivalent to the double system

$$\frac{dt}{d\tau} = \frac{\partial H}{\partial p_t}, \quad \frac{dx}{d\tau} = \frac{\partial H}{\partial p_x}; \quad . \quad . \quad . \quad (4.3)$$

$$\frac{dp_t}{d\tau} = 0, \quad \frac{dp_x}{d\tau} = -\frac{\partial H}{\partial x} \quad . \quad . \quad . \quad (4.4)$$

The equations of motion of the particle, as well as of the rays of its associated wave, are contained in (4.3) and (4.4). As before,  $\tau$  is the time of the particle and  $t$  the time of a ray. The double system has an integral  $H = \text{constant}$ . This constant is zero in the present case. Another integral is  $p_t = \text{constant}$ . If, as before, we put this constant equal to  $c^2$  and substitute in  $H$ , the latter differs from the ordinary Hamiltonian function by a constant—the total energy.

§ 5. *The Hamilton-Jacobi Equation.*—This equation is obtained by assuming that the covariant components  $(p_t, p_x)$  are derivable from a scalar potential. We write

$$p_t = \frac{\partial \psi}{\partial t}, \quad p_x = \frac{\partial \psi}{\partial x} \quad . \quad . \quad . \quad (5.1)$$

Substituting these values in (4.2), we get the desired equation

$$\begin{aligned} H &= \frac{1}{2} \left\{ v^{-2} \left( \frac{\partial \psi}{\partial t} \right)^2 - \left( \frac{\partial \psi}{\partial x} \right)^2 - \left( \frac{\partial \psi}{\partial y} \right)^2 - \left( \frac{\partial \psi}{\partial z} \right)^2 \right\} \\ &\equiv H(\psi, \psi) \quad . \quad . \quad (5.2) \end{aligned}$$

If we put  $H = 0$  and  $\frac{\partial \psi}{\partial t} = C^2$ , we arrive at the usual

Hamilton-Jacobi equation for a particle in a conservative field. However, this particular form does not correspond to de Broglie's point of view. He assumes the particle to move along a natural path (in our case, a Fermat path described according to the laws of classical mechanics) and to emit at every point of its path a disturbance  $\psi$ , which is propagated in all directions with velocity  $v$ . If the disturbance is a periodic one, the surface of constant phase ( $\phi$ , say) is the locus of the extremities of Fermat paths (corresponding to the same time of description) which issue from the point where the particle was situated when in that phase. We will now show that  $\phi$ , considered as a function of position and time, satisfies the Hamilton-Jacobi equation (5.2).

Write

$$\phi = 2\pi\nu(t - \chi + \text{const.}), \quad \chi(A, B) = \int_A^B \frac{d\sigma}{v}, \quad (5.3)$$

where A is the position of the particle at the time  $t_0$  when it emitted the phase which reaches B at time  $t$ . The coordinates of A will be denoted by  $(x_0, y_0, z_0)$  and those of B by  $(x, y, z)$ .

Let us consider once again the function S defined by (3.3) and (3.4). If we vary it in the most general manner possible, we get

$$\begin{aligned} \delta S = [L\delta t]_P^Q + [v^2\dot{t}\delta t - \dot{x}\delta x \dots]_P^Q - \int_P^Q \left\{ \frac{d}{d\tau} (v^2\dot{t})\delta t \right. \\ \left. - \left( \ddot{x} + v \frac{\partial^2}{\partial x^2} \dot{t}^2 \right) \delta x \dots \right\} d\tau. \quad (5.4) \end{aligned}$$

We now impose the condition that the varied tracks are also geodesics of zero length. (5.4) then reduces to

$$\delta S = [v^2\dot{t}\delta t - \dot{x}\delta x \dots]_P^Q = 0.$$

Or, writing  $c^2$  for  $v^2\dot{t}$ ,

$$c^2\delta t_0 - \dot{x}\delta x_0 \dots = c^2\delta t - \dot{x}\delta x \dots \quad (5.5)$$

The accompanying diagrams will help us to interpret (5.5). P (fig. 1) is the position of the particle in space-time when it emits a wave, a ray of which reaches the point Q in space-time. PQ is therefore a null-geodesic. PP' is the natural track of the particle, and P'Q' is another null-geodesic.

A (fig. 2) is the spatial position of the particle at time  $t_0$  when it emits the disturbance which reaches the space-point B at time  $t$ . AB is therefore a Fermat path, the spatial projection of PQ. AA' is the path of the particle and therefore the spatial projection of PP'. A'B', the projection of P'Q', is another Fermat path.

Fig. 1.

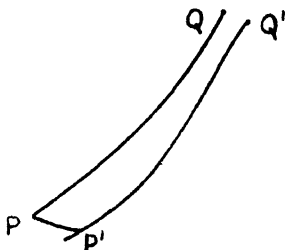
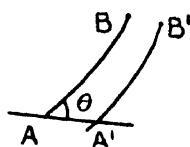


Fig. 2.



From what we have said, it follows that

$$\delta x_0 = u_x \delta t_0, \quad \delta y_0 = u_y \delta t_0, \quad \delta z_0 = u_z \delta t_0, \quad \dots \quad (5.6)$$

where  $(u_x, u_y, u_z)$  are the velocity components of the particle, and  $u_0$  its resultant velocity. These components must not be confused with  $(\dot{x}_0, \dot{y}_0, \dot{z}_0)$ , for, although the resultant of the latter is  $u_0$ , they refer to a different direction—that of the path AB.

If we substitute the expressions (5.6) in (5.5), we get

$$\begin{aligned} c^2 \left( 1 - \frac{u_0^2}{c^2} \cos \theta \right) \delta t_0 &\equiv c^2 \left( 1 - \frac{c^2}{v_0^2} \cos \theta \right) \delta t_0 \\ &\equiv c^2 \left( 1 - \frac{u_0}{v_0} \cos \theta \right) \delta t_0 = c^2 \delta t - \dot{x} \delta x - \dots, \end{aligned} \quad (5.7)$$

where  $\theta$  is the angle between the path of the particle and AB. If we regard  $t_0$  as a dependent variable and write

$$K = (1 - (u_0/v_0) \cos \theta), \quad \dots \quad (5.8)$$

we get

$$\frac{\partial t_0}{\partial t} = 1/K, \quad \frac{\partial t_0}{\partial x} = -\dot{x}/Kc^2 \equiv -x'/Kv^2, \quad \dots \quad (5.9)$$

and we can easily verify that  $t_0$  satisfies (5.2) with  $H=0$ . Again from (5.3)

$$\phi = 2\pi\nu(t - \chi + \text{const.}) = 2\pi\nu(t_0 + \text{const.}).$$

It follows that  $\phi$  satisfies the Hamilton-Jacobi equation (5.2).

On account of the motion of the particle the frequency of

the disturbance at B is not the frequency of the particle, but that multiplied by the Doppler factor  $1/K$ .

§ 6. *Stationary States of the Atom*.—Let an electron describe a closed orbit about the nucleus, as in the case of the hydrogen atom. De Broglie imagines the electron to emit a periodic disturbance which is propagated in the manner explained. A ray of the wave of phase will describe the orbit of the electron in the same sense as the electron itself, while another will describe it in the opposite sense. A stationary state is possible only when the length of the orbit consists of an integral number of wave-length, *i. e.*

$$\oint \frac{v d\sigma}{v} = n.$$

But  $v = E/h = mc^2/h$ . Hence the above condition becomes

$$\oint m u d\sigma = nh.$$

We will now assume that the electron is a pulsating sphere—the periodic expansion and contraction being due to the pressure of the æther and some internal pressure. On account of this pulsation the surrounding æther will be subject to a periodic disturbance; and if we assume that the phase is propagated with velocity  $v$ , the velocity of transfer of energy at any point will be the group-velocity

$$u \left( = \frac{dv}{d\left(\frac{v}{v}\right)} \right).$$

In the vicinity of the surface of zero-velocity (in this case, the sphere  $E - V = 0$ ) the phase-velocity becomes very great and ultimately infinite. The group-velocity, on the other hand, becomes small and ultimately zero—the æther becomes rigid in this neighbourhood. Outside this surface both  $u$  and  $v$  become imaginary. It follows that the atom is a closed system in a very real sense. The electron radiates energy even when the atom is in a stationary state, but none of this energy can escape—most of it will be reabsorbed by the electron, while an infinitesimal amount may accumulate on the surface of zero-velocity. When for some reason or other the atom passes from one stationary state to another, it will radiate the quantum of energy demanded by Bohr's theory. Hence it appears that, in some respects, the Quantum Theory and the Wave Theory are not irreconcilable.

§ 7. *Schrödinger's Equation.*—If we multiply  $(H(\psi, \psi))$  by a scalar quantity  $\rho/v$  and integrate throughout a portion of space-time, we get an invariant integral

$$I = \frac{1}{2} \iiint \left\{ v^{-2} \left( \frac{\partial \psi}{\partial t} \right)^2 - \left( \frac{\partial \psi}{\partial x} \right)^2 - \left( \frac{\partial \psi}{\partial y} \right)^2 - \left( \frac{\partial \psi}{\partial z} \right)^2 \right\} \rho dt dx dy dz. \quad (7.1)$$

The conditions that this integral should be stationary for small variations in  $\psi$  which vanish on the boundary is

$$\frac{1}{v^2} \frac{\partial}{\partial t} \left( \rho \frac{\partial \psi}{\partial t} \right) - \frac{\partial}{\partial x} \left( \rho \frac{\partial \psi}{\partial x} \right) - \frac{\partial}{\partial y} \left( \rho \frac{\partial \psi}{\partial y} \right) - \frac{\partial}{\partial z} \left( \rho \frac{\partial \psi}{\partial z} \right) = 0. \quad (7.2)$$

This equation is identical with Schrödinger's when  $\rho$  is constant. In any case, it gives the ordinary Hamilton-Jacobi equation for  $S (=h \log \psi / 2\pi i)$ , when  $h^{-1}$  is neglected in comparison with  $h^{-2}$ .

Schrödinger seeks solutions of (7.2) which are finite, continuous, and one-valued throughout the whole of physical space-time, and thereby obtains the accepted energy-levels—at least for the standard cases already worked out.

De Broglie, on the other hand, seeks a solution which has a moving singularity—the electron. His solutions are of the nature of retarded and advanced potentials for which he assumes the form

$$\psi = f e^{i\phi}. \quad (7.3)$$

If we substitute this value for  $\psi$  in (7.2) and denote by  $\square$  the operator on  $\psi$  in that equation, we get the two following:

$$\square(f) - \rho f H(\phi, \phi) = 0, \quad 2\rho H(f, \phi) + f \square(\phi) = 0. \quad (7.4)$$

De Broglie does not assume  $H(\phi, \phi) = 0$ , but it is natural to do so; and since we have an extra function  $\rho$  to dispose of, we can do so here. The consequence of this is that  $f$  satisfies the same equation as the complete wave-function  $\psi$ . We can also verify the following equation:

$$\square(f\phi) = 0. \quad (7.5)$$

A solution can therefore be got by assuming  $f$  to be a function of  $\phi$ , and regarding (7.5) as a linear equation of the first order to determine the function  $\rho$ .

In conclusion, I wish to express my gratitude to Prof. Schott for his encouragement and valuable advice.

Applied Mathematics Department,  
Aberystwyth.

XLII. *The Structure of Vortex Sheets.* By A. FAGE, A.R.C.Sc., and F. C. JOHANSEN, B.Sc., of the Aerodynamics Department, The National Physical Laboratory\*.

### I. INTRODUCTION.

(1) **T**HE outstanding features of the two-dimensional flow behind an infinitely long obstacle of bluff cross-section immersed in a moving fluid are now well known. Two thin bands of vorticity are shed at the after end of the obstacle, or edges in the case of an inclined flat plate, and these as they flow downstream separate the freely-moving stream from a low-pressure region of nearly motionless fluid at the back of the obstacle. At some distance behind, these sheets break up with a uniform frequency into two trails of discrete cylindrical vortices of opposite direction of rotation, to form a vortex street. The vortices are arranged alternately in the street so that each vortex in one trail is midway between two successive vortices in the other trail.

(2) In an earlier paper † the writers describe an investigation undertaken to furnish information on the flow of air behind an inclined flat plate. Experiments were then made to determine, for several angles of inclination of the plate, the frequency and speed with which the individual vortices pass downstream, the dimensions of the vortex system, the average strength of the vortices, and the rate at which vorticity was leaving the edges of the plate. The present investigation ‡ can be regarded as a continuation of this earlier work, in that it includes a more detailed examination of the structure of the vortex sheet shed from the edge of a plate set normal to an air stream. To obtain more generality, an examination has also been made of the sheets shed from other bodies of widely different forms—such as an aerofoil, a cylinder, and wedges,—and it has been possible to show how some of the characteristics of these sheets, such as the velocity distribution across a section and the rate of opening-out, depend on the form of the body. Some of the experimental results are compared with those predicted by the theory § of the rate of spread of turbulence in

\* Communicated by Ernest F. Relf, A.R.C.Sc.

† Proc. Roy. Soc. A, vol. cxvi. (1927).

‡ Permission to communicate the results was kindly granted by the Aeronautical Research Committee.

§ *Zeitschrift für Angewandte Mathematik und Mechanik*, December 1926 (Tollmien) and April 1925 (Prandtl).



a vortex sheet, which has been developed by W. Tollmien on the basis of earlier work by L. Prandtl.

In addition, measurements have been made to determine the longitudinal spacing between consecutive vortices in the vortex street at some distance behind each body, and also the frequency and speed at which these vortices pass downstream. Finally, an analysis has been made to determine to what extent these characteristics of the vortex sheet are influenced by the structure of the sheets leaving the body.

(3) All the experimental work has been carried out in a wind tunnel, with each model extending between the floor and roof, and the observations have been in the median plane of the tunnel, where the flow is two-dimensional. A summary of some of the principal results obtained is given at the end of the paper.

## II. LIST OF SYMBOLS.

$V$  = velocity at any point in the field.

$V_0$  = velocity of the undisturbed air relative to model.

$V_1$  &  $V_2$  = velocities at points in the outer and inner boundaries respectively.

$V_s$  = downstream velocity of the individual vortices.

$p_0$  = pressure in the undisturbed air.

$p$  = pressure at any point in the field.

$p_m$  = mean pressure at the back of a model.

$H_0$  = total head in the undisturbed wind.

$H$  = total head at any point in the field.

$\alpha$  = angle of incidence of the plate or aerofoil (degrees).

$\theta$  = wind direction at any point in the field relative to undisturbed wind direction (degrees).

$b$  = a representative dimension of a model (see figs. 7 and 8).

$x$  &  $y$  = the longitudinal and lateral coordinates of a point in the field. They are measured along and at right angles to the undisturbed wind direction (see figs. 7 and 8).

$a$  = longitudinal spacing between two consecutive vortices in the same row.

$f$  = frequency per second with which the individual vortices in each row leave the model.

$T$  = time-interval between the shedding of successive vortices in the same row.

$K$  = total strength of vorticity leaving each side of the body in one second.

$\rho$  = density of the air.

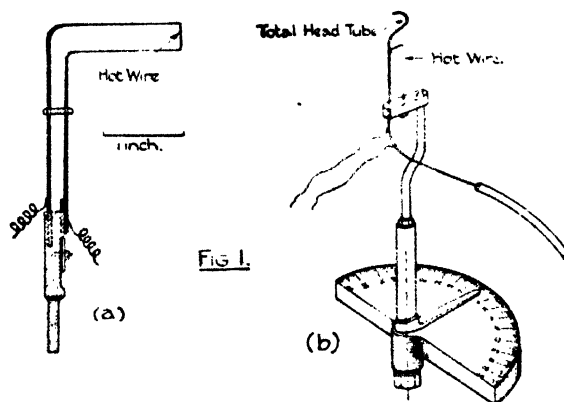
$\Delta$  = breadth of a vortex sheet.

$s$  = longitudinal distance behind a body of a section of a sheet.

### III. THE SHEET SHED FROM A NORMAL FLAT PLATE.

(4) *Observations of Velocity and Total Head.*—The vortex sheet selected for a detailed examination was that shed from the sharp edge of a flat plate 6 in. broad, mounted normal to the air stream and extending between the floor and roof of a 7-ft. wind-tunnel. To obtain some idea of the structure of

Fig. 1.



this sheet, observations of velocity and total head were taken along transverse lines parallel to the plate,  $r/b = 0.034, 0.084, 0.168, 0.252, 0.336$ , and  $0.504$  respectively, and situated in the median plane of the tunnel, where the flow is two-dimensional. The observations of velocity were taken with a small hot-wire velocity meter (fig. 1 (a)) mounted so that the wire was parallel to the edge of the plate—that is, normal to the plane of the two-dimensional flow. The wire was of platinum 0.3 in. long and 0.001 in. diameter. A complete description of this instrument and

also of its method of use is given in the paper referred to in § (2).

The direction and total-head observations were taken with the instrument shown in fig. 1 (*b*). The principle of direction measurement is the same as that described by A. Bailey \*, and depends on the fact that the shielding effect of a cylindrical rod mounted in a wind stream in front of a heated wire is a maximum when the plane passing through the axes of the rod and wire is along the local wind direction. In use the hot wire was maintained at a constant resistance (and therefore temperature) on a Wheatstone bridge. The instrument, mounted so that the hot wire was parallel to the edge of the plate, was rotated about an axis midway between those of the shield and hot wire through an angular range including the position for which the current was a minimum, and the direction of the local wind obtained from a curve showing the variation of current with angular position. To obtain compactness, the shielding cylinder was made of steel tube of outside diameter 0.032 in., and used for the measurement of total head. Fig. 1 (*b*) shows that the upper part of the tube was shaped so that its mouth, situated in the axis of rotation, pointed into the local wind when the hot wire was completely shielded by the stem. Although the direction and total head are measured at different points in the axis of rotation, no appreciable error is introduced thereby because the flow is two-dimensional. The total head ( $H$ ) was measured against the total head ( $H_0$ ) in the undisturbed wind. It should perhaps be mentioned that the advantage of the hot-wire direction meter over the standard pressure-direction meter † commonly used at the laboratory is that it is more suitable for use in a region of steep velocity gradient, such as that which occurs in a vortex sheet. In other regions, where the velocity changes slowly from point to point, the standard instrument is to be preferred because of its greater accuracy.

(5) The actual observations of velocity and total head taken across the several transverse lines of exploration, expressed as non-dimensional coefficients by dividing by  $V_0$  and  $\rho V_0^2$  respectively, are plotted in figs. 2 and 3. These curves show that immediately behind the plate the total head is a minimum and the velocity is small, and

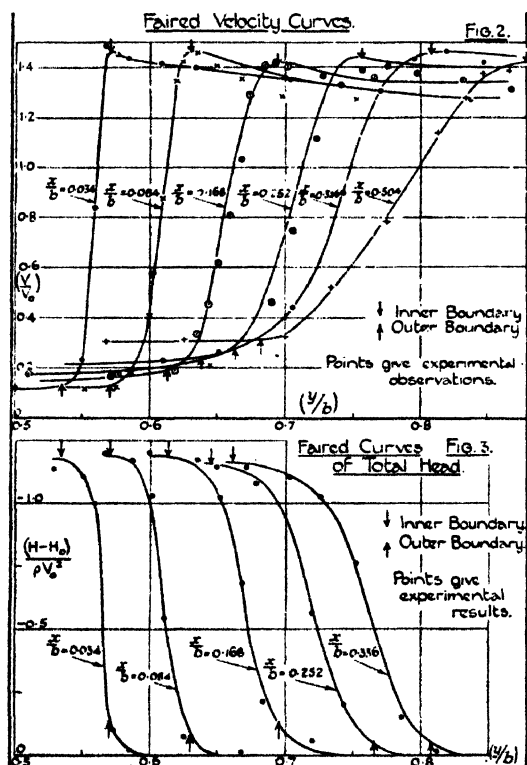
\* Aeronautical Research Committee, Reports and Memoranda, No. 777.

† T. Lavender, Aeronautical Research Committee, Reports and Memoranda, No. 844.

that outward beyond this region rapid increases in both velocity and total head occur.

There is, then, a vortex sheet or band separating the freely-moving stream from the stationary air at the back of the plate. The increase in the breadth of the sheet and its lateral displacement with increasing distance behind the plate are shown in fig. 7 (a), where dotted lines have been drawn to represent the boundaries of the vorticity region.

Figs. 2 and 3.



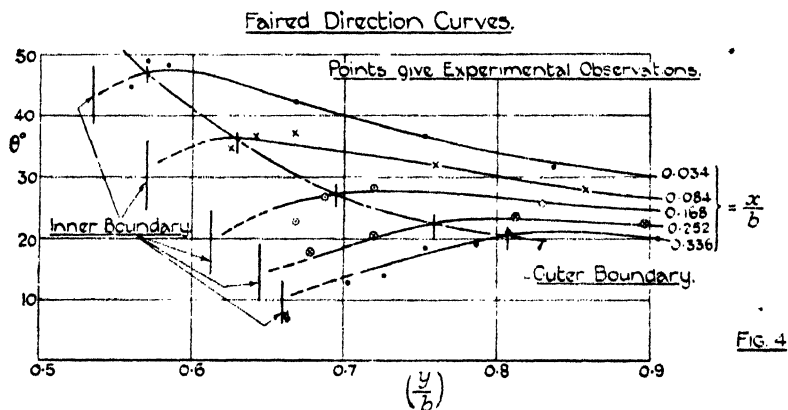
It is of course obvious that these dotted lines are not stream-lines; since, as will be shown in § (14), there is a flow across them.

6. The instruments just described give average values over comparatively long intervals of time; and so the observations obtained with them can only be accepted with confidence when the flow is steady. Records of the velocity

fluctuations were accordingly taken in the region immediately behind the plate, where the explorations were made, in order to examine the steadiness of the flow. These records are analysed later in the paper (§ 12), but it is necessary to mention now that most of the observations which are about to be analysed were taken in a region where the flow was comparatively steady. Some uncertainty undoubtedly exists in a restricted region near the inner boundary of the sheet, but this does not appreciably affect the conclusions arrived at from the calculations made throughout the paper because the velocity in this region is so small.

(7) To eliminate, as far as possible, small experimental errors of observation, and also to obtain greater accuracy in

Fig. 4.



the subsequent calculations, the observed values of  $\left(\frac{V}{V_0}\right)$ ,  $\left(\frac{H-H_0}{\rho V_0}\right)$ , and  $\theta$  have been faired by the usual system of

cross-plotting. Figs. 2-4 show that, in general, the faired curves pass closely through the actual observations. It should be noticed in fig. 4 that no direct observations of  $\theta$  were taken near the inner boundary. The direction of the flow in this region of the sheet was obtained from extrapolations of the curves drawn through observations taken in the steadier region near the outer boundary.

(8) *Boundaries of the Sheet.*—Fig. 2 shows that at each

section of the sheet the velocity rises from a small to a well-marked maximum value, which is a constant  $\left[\frac{V_1}{V_0} = 1.45\right]$  within the accuracy of measurement. We shall first assume, as was done in the paper referred to in § (2), that the outer boundary of the sheet is the line passing through the points of maximum velocity ( $V_1$ ), and the inner boundary is the line passing through the points of minimum velocity ( $V_2$ ). If this assumption is justifiable, these boundaries should be in close agreement with those obtained from direct calculations of vorticity. It will now be shown that this is so. The time-average value of the vorticity,

$\frac{b}{V_0} \left( \frac{\partial v}{\partial x} - \frac{\partial u}{\partial y} \right)$ , at any point was determined from the

paired observations of  $\left(\frac{V_1}{V_0}\right)$  and  $\theta$  given in figs. 2 and 4.

The values of  $\left(\frac{\partial v}{\partial x}\right)$  and  $\left(\frac{\partial u}{\partial y}\right)$  were estimated graphically

from the slopes of tangents drawn to the curves of  $v$  and  $u$  on  $x$  and  $y$  bases respectively, where  $u = V \cos \theta$ ,  $v = V \sin \theta$ , and  $x$  and  $y$  are measured from the centre of the plate respectively, parallel to and normal to the direction of the

undisturbed wind. The estimated values of  $\frac{b}{V_0} \left( \frac{\partial v}{\partial x} - \frac{\partial u}{\partial y} \right)$

plotted against  $\left(\frac{y}{b}\right)$  for several constant values of  $\left(\frac{x}{b}\right)$  are

given in fig. 5 *a*. It will be noticed that there is a progressive opening-out of the sheet, and also a progressive diminution in the value of the maximum vorticity at each section. There is therefore a lateral spreading of vorticity due to an inflow of fluid from outside.

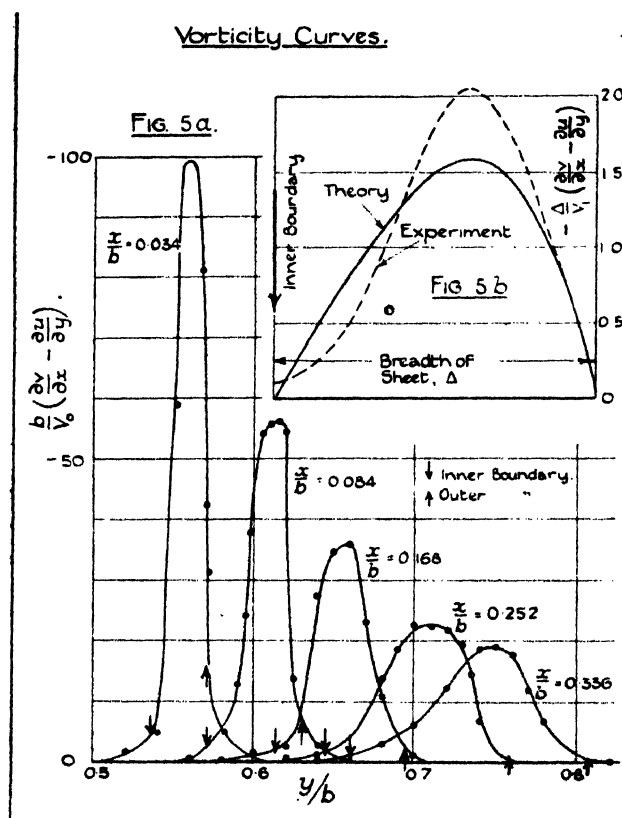
Arrows are placed on each of the curves of fig. 5 *a* to indicate the position of the boundaries of the vortex sheet as estimated from the velocity curves of fig. 2. These arrows are seen to be in close proximity to the points of zero vorticity on the curves; so that almost all the vorticity leaving the edge is contained within the boundaries estimated from the velocity curves.

(9) The average experimental distribution of vorticity across the sheet estimated from the five curves of fig. 5 *a* is shown by a dotted line in fig. 5 *b*, where values of

$\frac{\Delta}{V_1} \left( \frac{\partial v}{\partial x} - \frac{\partial u}{\partial y} \right)$ —where  $\Delta$  represents the breadth of the

sheet and  $V_1$  the velocity at points in the outer boundary—are plotted on a base representing the breadth of the sheet. Included in this figure is a curve giving the theoretical distribution of vorticity which, according to the Prandtl-Tollmien\* theory, is identical at all sections across the sheet. The agreement between the theoretical and experimental curves is not very close; but some discrepancy is to be

Figs. 5a and 5b.



expected because, owing to the steep velocity gradient across the sheet, it is difficult to determine with good accuracy the experimental values of  $\frac{\Delta}{V_1} \left( \frac{\partial v}{\partial x} - \frac{\partial u}{\partial y} \right)$ . Both curves exhibit the interesting feature that the vorticity has

\* See § (2).

its maximum value not at the centre of the sheet, but along a line situated about 60 per cent. of the breadth from the inner boundary.

(10) Since the values of  $\left(\frac{\partial v}{\partial x} - \frac{\partial u}{\partial y}\right)$  were obtained graphically from the slopes of tangents to velocity curves, they are liable to be in error. To check the accuracy of these estimations, the cross-section of the sheet was included by several rectangular contours (see fig 7 (a)), and the total strength of the vorticity within each rectangle determined from the integral over the surface of the estimated values of  $\left(\frac{\partial v}{\partial x} - \frac{\partial u}{\partial y}\right)$ . These results are given in Table I., where they are compared with those obtained by the more simple and accurate method of finding the circulation  $\int (u dx + v dy)$  around the contour of each rectangle. The agreement between the two series of results is reasonably close, from which it is inferred that the accuracy of the values of  $\left(\frac{\partial v}{\partial x} - \frac{\partial u}{\partial y}\right)$  is satisfactory. It should be noted that the comparison undertaken in this section has been made on the assumption that the motion in the sheet is steady. It will be shown in § (12) that the motion is steady except near the inner boundary; but the unsteadiness in this region should not appreciably lessen the value of the work because the velocity there is very small.

TABLE I.

Rectangle (see fig. 7 (a)).	$\frac{1}{V_0 b} \iint \left(\frac{\partial v}{\partial x} - \frac{\partial u}{\partial y}\right) dx \cdot dy$ over the area.	$\frac{1}{V_0 b} \int (u dx + v dy)$ around the contour.
I. ....	-0.097	-0.107
II. ....	-0.136	-0.139
III. ....	-0.125	-0.128
IV. ....	-0.118	-0.116

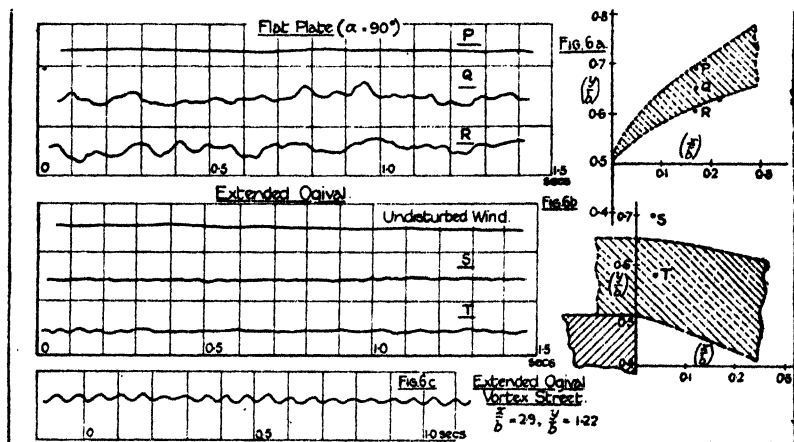
(11) The boundaries of the vortex sheet have also been marked on the curves of total head given in fig. 3. As would be expected, the total head beyond the outer boundary is approximately uniform and equal to the total head in the



undisturbed wind,  $H_0$ ; and the total head in the dead-air region contained within the inner boundaries is also approximately constant. These conditions of flow provide further evidence to support the method of estimating the boundaries of the vortex sheet. This method has therefore, because of its simplicity, been used to determine the boundaries of the vortex sheets considered later in the paper.

(12) *Steadiness of Sheet.*—To examine the steadiness of the sheet, photographic records of the velocity fluctuations were taken with an Einthoven galvanometer used in conjunction with a hot wire. The method of observation was the same as that described in the paper to which reference has been made in § (2). To illustrate the general character

Figs. 6a and 6b.



of the velocity fluctuations, three records taken in the section  $\frac{x}{b} = 0.168$ , at points situated in the outer boundary, the centre of the sheet, and the inner boundary respectively, are given in fig. 6a. The mean values of  $(\frac{V}{V_0})$  at these points are 1.42, 0.68, and 0.18 respectively. These records show that the velocity fluctuations near the outer boundary—where the mean velocity is a maximum—are very small, but that they become appreciable near the inner boundary, where the mean velocity is low; and also that the fluctuations at any point do not appear to be regular either in amplitude or frequency, although there is an occasional indication of a frequency

( $T=0.202$  sec.,  $V_0=16.8$  ft./sec.) equal to that with which the individual vortices, arising from the rolling-up of the sheets, are shed. Other records (not included in the paper) showed that the amplitude of the velocity fluctuations tended to increase with the distance behind the plate. In all cases, therefore, velocity observations have been taken at sections as close to the body as possible, and away from the region where the sheet was rolling-up. Some evidence of a "flutter" or "whip" of the sheet, of a slow indefinite frequency, was also obtained. It was suspected from the magnitude of the angular amplitude that this disturbance was associated with the ordinary disturbances in the tunnel wind; the evidence was not, however, conclusive.

(13) *Rate at which Vorticity is shed from Edge.*—In steady motion the vorticity at any point  $(x, y)$  is given by  $\left(\frac{\partial v}{\partial x} - \frac{\partial u}{\partial y}\right)$ , so that the total amount of vorticity,  $K$ , passing a section of a sheet in unit time is, in non-dimensional units,

$$\frac{1}{V_0^2} \int_{y_2}^{y_1} \left(\frac{\partial v}{\partial x} - \frac{\partial u}{\partial y}\right) u dy,$$

where  $y_1$  and  $y_2$  are the limits of the sheet. For a theoretical sheet of infinitesimal breadth the above expression reduces to

$\left(\frac{V_1^2 - V_2^2}{2V_0^2}\right)$ , where  $V_1$  and  $V_2$  are the velocities at points in the boundaries of the sheet. In the earlier paper [see § (2)] it was shown that the breadth of the sheet, although increasing with the distance downstream, is small compared with its radius of curvature, and it was assumed that the latter expression,  $K=(V_1^2 - V_2^2)/2V_0^2$ , gave a reasonably accurate value for the amount of vorticity leaving the edge in unit time. The additional observations since taken allow an estimate to be made of the accuracy of this approximate expression for  $K$ .

Values of

$$\frac{1}{V_0^2} \int_{y_2}^{y_1} \left(\frac{\partial v}{\partial x} - \frac{\partial u}{\partial y}\right) u \cdot dy$$

estimated for several sections of the sheet are given in Table II. The values of  $u$ , that is  $V \cos \theta$ , used in these calculations were determined from values of  $V$  and  $\theta$  taken from the faired curves of figs. 2 and 4. The values of

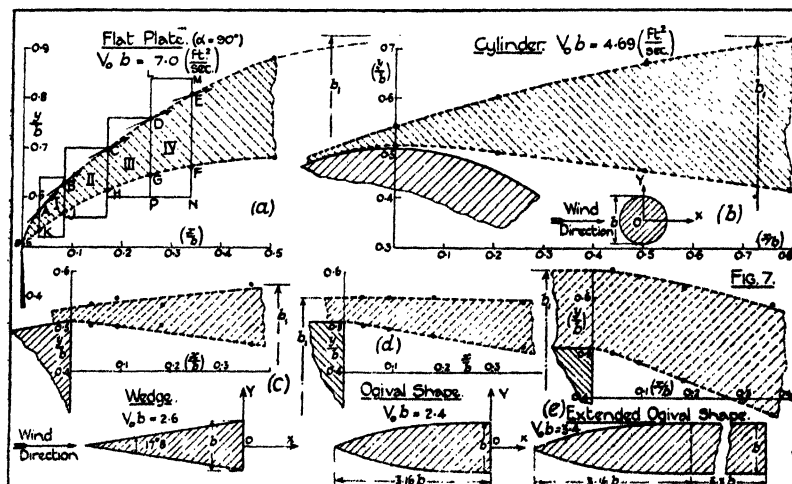
$\left(\frac{\partial v}{\partial x} - \frac{\partial u}{\partial y}\right)$  were taken from the curves of fig. 5a. Included in the table are the corresponding values of  $\left(\frac{V_1^2 - V_2^2}{2V_0^2}\right)$ .

A comparison of the two series of values given in this table shows that the approximate expression  $K = \left( \frac{V_1^2 - V_2^2}{2V_0^2} \right)$  underestimates the amount of vorticity leaving the edge in unit time by about 9 per cent. Closer agreement between the two expressions for  $K$  is to be expected for other types of sheet, such as those considered later in the paper, for which the curvature is smaller than that for the flat plate.

TABLE II.

$\frac{x}{b}$	$-\frac{1}{V_0^2} \int_{y_2}^{y_1} \left( \frac{\partial v}{\partial x} - \frac{\partial u}{\partial y} \right) u \cdot dy.$	$\left( \frac{V_1^2 - V_2^2}{2V_0^2} \right).$
0.034	1.18	1.07
0.084	1.20	1.07
0.168	1.15	0.99
0.252	1.11	1.02
0.336	1.10	1.05

Fig. 7 (a), (b), (c), (d), (e).



(14) *Flow across each Boundary.*—To determine these flows, the field containing the sheet was divided into rectangles by lines parallel to and normal to the section of the plate, as shown in fig. 7(a). The flow through an arc of a boundary was then obtained by the evaluation of  $\int (u dy - v dx)$  around the contour of that part of the rectangle cut off by the arc. For example, for the arc DE of the outer boundary,

the integration was taken around the contour DLME. and for the arc GF of the inner boundary around the contour GLMF. The results are given in Table III., and indicate that air is flowing into the sheet across both boundaries. The values in the last column of this table give the flow per sec. per unit length of each arc. The agreement between the values for the arcs of each boundary is not very close; there is, however, no indication of any systematic variation along the boundary. Average values of the flow per sec. per unit length of arc have therefore been taken for the outer boundary from A to E, and for the inner boundary from K to F. They are  $0.189 V_0$  and  $0.083 V_0$  respectively, the ratio being 2.3 \*. This ratio on the Prandtl-Tollmien theory is 2.6. The close agreement between these two values must be regarded as partly fortuitous in view of the following discussion in § (15).

TABLE III.

Arc of boundary (see fig. 7 (a)).		Flow per sec. $bV_0$ .	$\frac{1}{V_0}$ (flow per sec. per unit length).
Outer boundary.	AB	0.0111	0.140
	BC	0.0220	0.204
	CD	0.0231	0.222
	DE	0.0175	0.180
		0.0737	
Inner boundary.	KJ	-0.0050	-0.081
	JH	-0.0059	-0.062
	HG	-0.0058	-0.064
	GF	-0.0109	-0.128
		-0.0276	

(15) The reason why estimates of the flow across arcs of the inner boundary are included in the paper, when no measurements of the direction of flow in this region could be taken—see § (7),—is that the method of estimation is such that no exact knowledge of the direction of the flow near the inner boundary is needed. Thus the magnitude of the flow across an arc such as FG (fig. 7 (a)) has been determined from the fact that it must be equal and opposite to that of the flow through the contour FMLG. If, therefore, any uncertainty in the direction of flow at points situated in the sections MF and LG, and also near the inner boundary—where, it must be noted, the velocity is very small compared with that at points near the outer boundary—does not greatly modify the flow across these sections, a reasonable estimate of the flow

\* Lengths of arcs AE and KF are  $0.388 b$  and  $0.333 b$  respectively.

across the arc FG can be obtained. To show that this is the case, the flow across the inner boundary from K to F has been determined on two assumptions: (a) that the unknown directions at K and F are taken from the dotted lines in fig. 4, that is, more or less tangential to the boundary; and (b) that the directions are normal to the boundary. The results are given below, and indicate that, although the assumptions are so different, the reduction in the flow through the inner boundary does not exceed 17 per cent. of the value given in Table III.

	(a). See Table III.	(b).
See fig. 7 (a). Flow across EF .....	-0.1156	-0.1094
"    "    AE (outer boundary) .	0.0737	0.0737
"    "    AK .....	0.0143	0.0127
Flow across KF (inner boundary).	-0.0276	-0.0230

This percentage corresponds to an increase in the ratio of the flows across the outer and inner boundaries AE, KF from 2.3 to 2.8. It would be possible, of course, so to adjust the values of  $\theta$  at points in the inner boundary that the flow calculated by an integration along its length would be exactly equal to that obtained by an integration around the contour formed by the two end sections and the outer boundary. This, however, has not been attempted, because the velocity at points in the inner boundary is too small and unsteady to be measured with reliable accuracy. In short, it follows that a reasonable estimate of the flow across the inner boundary can be made because the method adopted takes advantage of the fact that the air which is passing across this boundary at a low velocity and in an unmeasurable direction is gradually absorbed into the sheet (together, of course, with the air flowing across the outer boundary), and eventually acquires a higher velocity and a measurable direction. The direction of the flow across the outer boundary is indicated by arrows in fig. 7 (a).

#### IV. SHEETS SHED FROM OTHER BODIES.

(16) Attention has been centred, so far, on the sheet shed from a sharp edge of a flat plate mounted normally to the wind. To obtain more generality, the research has been extended to include an analysis of the vortex sheets shed from bodies of widely different forms. This work shows how the rate of spread of turbulence and the velocity distribution in a sheet depends on the form of the body.

(17) The sectional shapes of the models selected are shown in figs. 7 and 8. The models were:—

No. 1.—A flat plate normal to wind (fig. 7 (a)). Breadth,  $b=0.5$  ft. (This model is included here for the purpose of a general comparison with the other models.)

No. 2.—Cylinder (fig. 7 (b)). Diameter,  $b=0.281$  ft.

No. 3.—Flat-sided wedge with the apex pointing into the wind. Width of base,  $b=0.232$  ft.; apex-angle,  $17^{\circ}.8$ . (fig. 7 (c).)

No. 4.—An "ogival" wedge with the apex pointing into the wind (fig. 7 (d)). This shape is formed by the arcs of a cubic parabola,  $y = \pm \frac{b}{2} \left[ 1 + \frac{x^3}{h^3} \right]$ , from  $x = -h$  to  $x = 0$ .

Width of base,  $b=0.232$  ft.; height,  $h=3.16 b$ .

No. 5.—Ogival model, with parallel-sided extension at the back (fig. 7 (e)). Width of base,  $b=0.232$  ft.; overall length  $=9.46 b$ .

No. 6.—An aerofoil inclined at  $10^{\circ}$ ,  $20^{\circ}$ , and  $45^{\circ}$  to the undisturbed wind (fig. 8 (a), (b), (c)). Length of chord  $=0.5$  ft. At the speeds of the experiment there was a pronounced dead-air region behind the aerofoil at each angle of incidence. The air-flow at  $10^{\circ}$  incidence was, however, sensitive to the wind-speed, and it was found that at this incidence the dead-air region disappeared at speeds greater than 40 ft./sec.

No. 7.—Flat plate inclined at  $40^{\circ}$  to the undisturbed wind (fig. 8 (d)). Breadth,  $b=0.5$  ft.

(18) Each model had a length of 7 ft., and was mounted between the floor and the roof of a 7-ft. wind-tunnel. Observations were confined to the median section of the tunnel where the flow is two-dimensional. The product ( $V_0 b$ ), where  $V_0$  is in ft./sec. and  $b$  is in feet, together with the position of the axes OX and OY in relation to each model, are given in figs. 7 and 8. The models fall into two groups: first, symmetrical models with the axes of symmetry in the direction of the wind (fig. 7), and second, asymmetric models (aerofoil and inclined flat plate, fig. 8). The sheets shed from each model of the first group are arranged symmetrically, whereas those for the second group are asymmetric both in shape and position.

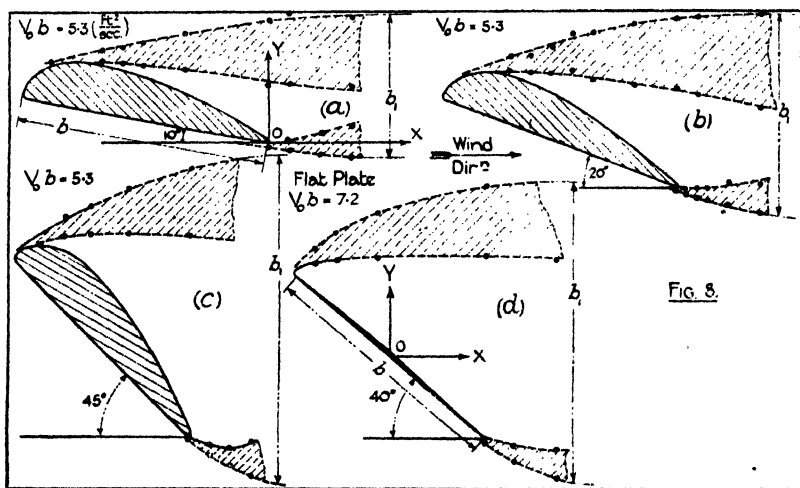
(19) The boundaries of the sheets shed from each model were determined, as before, from velocity observations along several lines, taken at right angles to the undisturbed wind-direction. The lines selected were taken close to the model,

and in a region where the motion was comparatively steady. The estimated coordinates of points in the boundaries of each sheet, and also the velocity at these points, are given in Tables IV. and V. Included in these tables are the values of  $K$  estimated from the approximate expression

$$K = \left( \frac{V_1^2 - V_2^2}{2V_0^2} \right).$$

The boundaries of the various sheets are shown by the dotted lines in figs. 7 and 8. The values given in Tables IV. and V. show that the velocity at a point on

Fig. 8 (a), (b), (c), (d).



each outer boundary is uniform, within the accuracy of measurement—except for the aerofoil at  $\alpha = 20^\circ$ , for which two types of flow appear possible,—and that the velocity at a point on each inner boundary, taken close behind the model, is small. For any one sheet the values of  $K$  are also in fairly close agreement if the sections are taken near the model ( $V_2$  small). Table V. also brings out the important fact that vorticity is shed from the upper and lower surfaces of an asymmetric model at the same rate.

(20) *Velocity Distribution in Sheets.*—The observations of Tables IV. and V. show that, although at points on the outer boundary the velocity is uniform, it slowly increases on the inner boundary with the distance of a point downstream. The velocity distribution across a section depends therefore

on its distance behind a model. To make a genuine comparison between the velocity distributions for the various sheets it is necessary, therefore, to take observations in a section close behind a model for which the value of  $V_2$  is small. The breadth of the sheet immediately behind a model is in most cases small, and it is difficult to take observations with good accuracy. An approximation to the velocity distribution across a section of the sheet close behind each model has, however, been obtained by drawing a fair curve through observations taken in several sections near the model, the closeness of these sections being such that the velocity at the inner boundary did not exceed  $0.1 V_1$  approximately ( $V_1$ =velocity at a point in the outer

TABLE IV.—Symmetrical Models.

Model.	$\left(\frac{x}{b}\right)$	Ordinates of boundaries.		Velocity in boundaries.		K.
		$\left(\frac{y_1}{b}\right)$	$\left(\frac{y_2}{b}\right)$	$\left(\frac{V_1}{V_0}\right)$	$\left(\frac{V_2}{V_0}\right)$	
Flat plate ( $\alpha = 90^\circ$ ).	0.034	0.570	0.535	1.47	0.13	1.07
	0.084	0.630	0.570	1.47	0.13	1.07
	0.168	0.695	0.613	1.42	0.18	0.99
	0.252	0.759	0.645	1.44	0.22	1.02
	0.336	0.807	0.660	1.47	0.26	1.05
	0.504	0.880	0.680	1.43	0.51	—
	—	—	—	—	—	1.05
Cylinder.	0	0.540	0.505	1.42	0	1.01
	0.204	0.600	0.490	1.37	0.07	0.94
	0.500	0.670	0.456	1.38	0.23	0.93
	0.796	0.720	0.415	1.25	0.35	—
Wedge.	-0.180	0.504	—	1.20	—	—
	0.036	0.535	0.490	1.40	0.07	0.97
	0.090	0.545	0.490	1.38	0.07	0.95
	0.180	0.530	0.490	1.27	0.08	0.81
	0.360	0.575	0.455	1.23	0.22	0.73
Ogival model.	0.036	0.550	0.400	1.13	0.05	0.64
	0.090	0.550	0.485	1.14	0.07	0.65
	0.180	0.550	0.470	1.18	0.09	0.69
	0.360	0.540	0.450	1.23	0.19	—
Extended ogival model.	-4.35	0.612	—	1.04	—	—
	0.036	0.656	0.490	1.19	0.04	0.71
	0.090	0.641	0.471	1.18	0.05	0.69
	0.180	0.620	0.433	1.16	0.12	0.67
	0.360	0.597	0.366	1.15	0.16	—

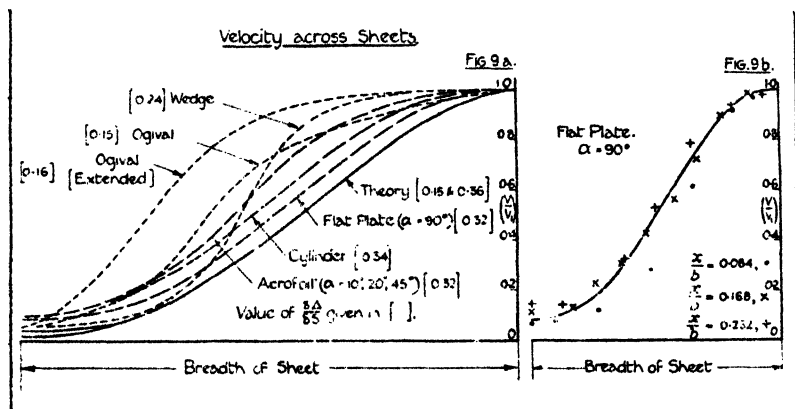


TABLE V.—Asymmetric Models.

Model.	UPPER SURFACE.				K.	LOWER SURFACE.				K.	
	$\left(\frac{z}{b}\right)$ .	Ordinates of boundaries.		Velocity in boundaries. $\left(\frac{V_1}{V_0}\right)$ .		$\left(\frac{z}{b}\right)$ .	Ordinates of boundaries.		Velocity in boundaries. $\left(\frac{V_1}{V_0}\right)$ .		
		$\left(\frac{y_1}{b}\right)$ .	$\left(\frac{y_2}{b}\right)$ .				$\left(\frac{y_1}{b}\right)$ .	$\left(\frac{y_2}{b}\right)$ .			
Aerofoil ( $\alpha=10^\circ$ )	-0.870	0.323	—	1.27	—	0	-0.020	—	1.18	0	0.70
	-0.667	0.370	0.330	1.16	0.67	0.083	-0.030	0.003	1.19	0.14	0.70
	-0.583	0.383	0.323	1.23	0.75	0.208	-0.030	0.010	1.20	0.28	0.68
	-0.500	0.400	0.310	1.24	0.74	0.333	-0.060	0.065	1.19	0.36	—
	0	0.433	0.295	1.20	0.69	—	—	—	—	—	—
Aerofoil ( $\alpha=20^\circ$ )	+0.083	0.494	0.230	1.15	0.64	—	—	—	—	—	—
	0	0.525	0.235	1.19	0.61	—	—	—	—	—	—
	0.333	0.500	0.225	1.20	0.63	—	—	—	—	—	—
	-0.467	0.525	0.407	1.32	0.87	0	-0.017	—	1.20	0	0.72
	-0.583	0.527	0.458	1.24	0.76	0.042	-0.032	-0.007	1.21	0.09	0.75
Aerofoil ( $\alpha=30^\circ$ )	-0.580	0.560	0.453	1.33	0.87	0.083	-0.047	-0.005	1.22	0.12	0.74
	-0.417	0.617	0.467	1.24	0.76 or	0.125	-0.052	-0.007	1.23	0.14	0.75
	-0.333	0.620	0.435	1.26	0.77	0.208	-0.075	+0.017	1.26	0.19	0.71
	-0.167	0.650	0.410	1.25	0.78	0.333	-0.107	0.010	1.19	0.29	0.67
	0	0.675	0.392	1.32	0.86	—	—	—	—	—	—
Aerofoil ( $\alpha=40^\circ$ )	+0.083	0.675	0.367	1.30	—	—	—	—	—	—	—
	0.333	0.690	0.320	1.19	—	—	—	—	—	—	—
	0.876	0.797	0.797	1.40	0.98	0	-0.013	—	1.37	0	0.94
	-0.500	0.911	0.803	1.37	0.93	0.083	-0.077	-0.027	1.39	0.16	0.96
	-0.400	1.065	0.800	1.36	0.91	0.167	-0.115	-0.050	1.37	0.22	0.92
Flat plate ( $\alpha=40^\circ$ )	-0.250	0.900	0.810	1.37	0.93	0.250	-0.155	-0.020	1.36	0.19	0.91
	-0.303	0.434	0.372	1.36	0.92	0.383	-0.339	-0.321	1.35	0	0.91
	-0.218	0.493	0.383	1.38	0.91	0.503	-0.412	-0.348	1.37	0.17	0.93
	-0.051	0.575	0.390	1.38	0.94	0.672	-0.490	-0.367	1.35	0.35	—
	+0.383	0.682	0.403	1.36	0.90	—	—	—	—	—	—
0.672	0.700	0.333	1.37	—	—	—	—	—	—	—	

boundary). The curves obtained are shown in fig. 9a, where values of  $\left(\frac{V}{V_1}\right)$  are plotted on a base representing the breadth of the sheet. The actual observations from which these faired curves have been obtained are too numerous to be shown conveniently in the paper. An exception has, however, been made in the case of the flat plate ( $\alpha=90^\circ$ ), in order to convey some idea of the accuracy of this method of estimation. These results are given in fig. 9b. The agreement between the separate sets of observations for this sheet can be regarded as representative of that obtained for the other sheets, and is considered to be sufficiently close to justify the taking of a mean curve.

Figs. 9a and 9b.



The velocity distribution in the sheets shed from the aerofoil at  $10^\circ$ ,  $20^\circ$ , and  $45^\circ$  incidence has been represented by one curve, because although the curves for the lower surface were somewhat higher than those from the upper surface, the differences were of the same order as those obtaining between the observations in any one sheet.

(21) The rate at which the breadth of each sheet increases with the distance downstream has been determined, and was found to have a constant value throughout the length.

These values, denoted by  $\frac{\partial \Delta}{\partial s}$ , where  $\Delta$  is the breadth of a section and  $s$  is its distance downstream from the body measured along the sheet, are given on the curves of fig. 9a.

They are seen to lie between the limits 0.15 and 0.36. The distributions of velocity predicted by the Prandtl-Tollmien theory for these two values of  $\frac{\partial \Delta}{\partial s}$  have been determined, and they are also shown in fig. 9 *a*. They were found to be identical except near the inner boundary.

(22) The velocity curves of fig. 9 *a* show a progressive departure from the theoretical curve in the order: flat plate, cylinder, aerofoil, wedge, ogival, extended ogival. Also they appear to fall into two more or less distinct groups: (flat plate, cylinder, aerofoil) and (wedge, ogival, extended ogival). The curves of the first group resemble more closely the theoretical curve, and the values of  $\frac{\partial \Delta}{\partial s}$  are in close agreement; whereas those of the second group show more marked departures from theory, and the values of  $\frac{\partial \Delta}{\partial s}$  are, by comparison, distinctly lower. Another difference—exhibited in figs. 7 and 8—is that each sheet of the second group has a relatively larger breadth where it leaves the model, due to the appreciably larger surface exposed to the wind-stream, for the same area of obstruction. In this connexion it is of interest to note that the addition of the extension piece to the ogival model increases the overall length in the ratio 3:1, and also increases the breadth of the sheet, leaving the model in about the same proportion (2.8:1). The experiments demonstrate, then, how the shape of the body influences both the rate of opening-out and the velocity distribution across the vortex sheets trailing behind.

(23) One of the assumptions of the Prandtl-Tollmien theory is that the breadth of a sheet is initially zero. Of the sheets considered above, that shed from the flat plate most closely realises this condition, and it is of interest to note that it is for this case that the velocity distribution is in closest agreement with that predicted by theory.

(24) To determine whether the flow around the surface of the extended ogival model had become unsteady, records of the velocity fluctuations both within and without the vortex sheet were taken immediately behind the body. The positions at which these records were taken, and also tracings of the records, are shown in fig. 6 *b*. A comparison of these records with that taken in the undisturbed wind shows that, although there are occasional indications of a slight periodic

disturbance, the motion both within and without the sheet is comparatively steady. There does not appear in this case to have been any tendency for the creation of vortices of appreciable size, due to the coalescence of neighbouring vortices as they pass along the surface from nose to tail, as has been tentatively suggested by H. Levy \* in his paper on the growth of eddies in a viscous fluid. In fact, throughout the present experiment, there appeared to be fairly definite evidence that the large vortices, which pass downstream at some distance behind a body, are created by the rolling-up of the sheets after they have left the body. A record of the velocity fluctuations due to the vortices in the *vortex street*, taken at a point  $\left(\frac{x}{b} = 2.9, \frac{y}{b} = 1.22\right)$  situated some distance behind the extended ogival model, is given in fig. 6c. A comparison of this record with those given in fig. 6b shows that the velocity fluctuations within the sheet are small compared with those which occur outside the street at some distance behind the body.

(25) *Relation between  $p_m$  and  $p_1$ .*—Table VI. gives the

TABLE VI.

Model.	Coordinates of point in boundary.		$\left(\frac{p_1-p_0}{\rho V_0^2}\right)$ .	$\left(\frac{p_m-p_0}{\rho V_0^2}\right)$ .	
	$\left(\frac{x}{b}\right)$ .	$\left(\frac{y}{b}\right)$ .			
Flat plate ( $\alpha=90^\circ$ ).	0.034	0.570	-0.71	-0.65	-0.69
	0.084	0.630	-0.66		
	0.168	0.695	-0.63		
	0.252	0.765	-0.59		
	0.336	0.807	-0.63		
Flat plate ( $\alpha=40^\circ$ ).	0.672	0.700	-0.49	-0.47	-0.55
	0.672	-0.490	-0.45		
	-0.218	0.493	-0.47		
Aerofoil ( $\alpha=45^\circ$ ).	-0.400	0.911	-0.45	-0.47	-0.51
	0.167	-0.115	-0.48		
Cylinder.	0.204	0.600	-0.45	-0.49	-0.51
	0.500	0.670	-0.52		
Ogival.	0.090	0.550	-0.170	-0.183	-0.252
	0.180	0.550	-0.196		
Extended ogival.	0.36	0.656	-0.208	-0.207	-0.225
	0.090	0.641	-0.206		

\* Phil. Mag. October 1926.

relation between the pressure  $p_m$  at the back of each model (except the wedge, which has been excluded because the position of the outer boundary was not determined very exactly) and the pressure  $p_1$  in the outer boundary of the sheet. The values of  $p_m$  were measured directly, while those of  $p_1$  were deduced from observations of velocity and total head. A comparison of the results shows that, in general, the pressure in the outer boundary is slightly greater than that measured in the dead-air region behind a model. It should here be mentioned that it was also found for the flat plate,  $\alpha=90^\circ$ , that the average pressure  $p_2$  at points in the inner boundary was equal to  $(p_0-0.69\rho V_0^2)$ , that is, the pressure,  $p_m$ , measured directly behind the plate.

### V. VORTEX STREETS BEHIND MODELS.

(26) It is well known that the vortex sheets behind a body are unstable, and that at some distance behind the body they break up into two rows of discrete vortices, to form a vortex street. To determine some general characteristics of vortex streets, measurements have been made for each model of the frequency,  $f$ , with which the vortices pass downstream, and also of the longitudinal spacing,  $a$ , between consecutive vortices in the same row. The method of

TABLE VII.

Model.	Col. 1. $\left(\frac{V_1}{V_0}\right)$	Col. 2 K.	Col. 3. $\left(\frac{fb}{V_0}\right)$	Col. 4. $\left(\frac{a}{b}\right)$	Col. 5. $\left(\frac{V_2}{V_0}\right)$	Col. 6. $\left(\frac{b'}{b}\right)$	Col. 7. $\left(\frac{fb'}{V_0}\right)$	Col. 8. $\left(\frac{a}{b'}\right)$
Flat plate ( $\alpha=90^\circ$ ).	1.45	1.06	0.146	5.25	0.77	1.85	0.270	2.84
Flat plate ( $\alpha=40^\circ$ ).	1.37	0.93	0.231	3.55	0.82	1.20	0.277	2.16
Cylinder.	1.39	0.96	0.187	4.27	0.80	1.45	0.271	2.95
Aerofoil ( $\alpha=45^\circ$ ).	1.37	0.94	0.210	3.67	0.77	1.31	0.275	2.80
Aerofoil ( $\alpha=10^\circ$ ).	1.19	0.70	0.735	1.25	0.92	0.57	0.418	2.19
Wedge...	1.32	0.86	0.238	3.45	0.82	1.15	0.273	3.00
Ogival ...	1.15	0.66	0.271	3.16	0.86	1.10	0.298	2.87
Extended ogival.	1.18	0.69	0.254	3.33*	0.81	1.31	0.332	2.54

\* Value steadily increases with distance behind model.

measurement was precisely the same as that described in the paper previously mentioned (§2). The speed,  $V_3$ , with which the vortices in each row pass downstream has also been calculated from the product  $(fa)$ . The results are given in Table VII., together with values of  $V_1$  and  $K$  (taken from Tables IV. and V). The values in columns 1, 2, and 5 (Table VII.) show that, in general, the speed ( $V_3$ ) with which the individual vortices pass downstream decreases with an increase in ( $V_1$ ) and consequently in  $K$ . The values of both  $\left(\frac{f \cdot b}{V_0}\right)$  and  $\left(\frac{a}{b}\right)$  for the different models—columns 3 and 4—are seen to vary considerably. This variation is, of course, not surprising, since the values of  $b$  taken refer to a particular dimension of each model, and so are unrelated.

(27) If the sheets shed from the models were parallel bands of small breadth, and if they had the same velocity  $V_1$  in the outer boundary, the frequency ( $f$ ) would vary inversely, and the longitudinal spacing ( $a$ ) directly, as the distance between the bands, at the velocity  $V_0$ . If, then,  $b'$  represented the distance between the outer boundaries of the sheets, both  $\left(\frac{fb'}{V_0}\right)$  and  $\left(\frac{a}{b'}\right)$  would have constant values, even although the values of  $\left(\frac{fb}{V_0}\right)$  and  $\left(\frac{a}{b}\right)$  varied from model to model. Calculations of  $\left(\frac{fb'}{V_0}\right)$  and  $\left(\frac{a}{b'}\right)$ —where  $b'$  represents the maximum distance between the outer boundaries, as shown in figs. 7 and 8—have accordingly been made, and the results are given in columns 7 and 8. Except for the extreme cases of the aerofoil at  $10^\circ$  incidence and the extended ogival, the values of  $\left(\frac{fb'}{V_0}\right)$  and also  $\left(\frac{a}{b'}\right)$  are in close agreement. It appears, then, at a constant speed  $V_0$ , both the frequency ( $f$ ) and the longitudinal spacing ( $a$ ) of the individual vortices behind a body depend largely on the lateral spacing between the vortex sheets, and that these characteristics are influenced to a much smaller extent (except possibly in extreme cases) by the shape and structure of the sheets.

(28) The values of  $\left(\frac{fb}{V_0}\right)$  measured in the vortex streets, behind the flat plate and aerofoil at several angles of incidence, are given in Table VIII. It is of interest to note that the two series of values are in close agreement, except below  $30^\circ$ , where the values for the plate are greater than

those for the aerofoil. The agreement at a large incidence is not unexpected, because only the flat lower surface of the aerofoil, which resembles a flat plate except for the curvature at the edges, is then exposed to the wind; at a small incidence this is not the case, as a part of the upper surface is also exposed.

TABLE VIII.  
Values of  $\left(\frac{fb}{V_0}\right)$ .

$\alpha^\circ$ .	Flat plate ( $b$ =breadth).	Aerofoil ( $b$ =chord).
90 .....	0.146	0.150
60 .....	0.173	0.179
50 .....	0.196	0.197
45 .. ...	0.205	0.210
40 .....	0.231	0.247
30 .....	0.307	0.313
20 .....	$\left\{ \begin{array}{l} 0.478 \\ 0.503 \end{array} \right.$	0.448
10 .....	$\left\{ \begin{array}{l} 0.548 \\ 0.677 \end{array} \right.$	0.544
14 .....	$\left\{ \begin{array}{l} 0.746 \\ 0.900 \end{array} \right.$	0.608

## VI. SUMMARY.

The structure of the sheets shed from infinitely long bodies of widely different cross-section has been examined. Measurements have also been made to determine the principal characteristics of the vortex streets formed at some distance behind each body.

It is established from estimations of vorticity and also from observations of total head, that the outer boundary of a sheet can be taken as a line drawn through the points in the field of maximum velocity ( $V_1$ ), and the inner boundary as the line passing through the points of minimum velocity ( $V_2$ ).

The motion in a sheet is steady near the body, except possibly near the inner boundary.

The pressure at points in an outer boundary is slightly greater than that in the dead-air region behind the body.

Air flows into a sheet through both boundaries, but at a greater rate through the outer boundary.

The simple expression  $\left(\frac{V_1^2 - V_2^2}{2V_0^2}\right)$  gives a close estimate

of the total amount of vorticity passing a section of a sheet in unit time.

Vorticity is shed from the two sides of an asymmetric body at the same rate.

The variation of velocity across a section of a sheet, and also the rate of increase of the breadth with the distance downstream, depend on the form of the body. The velocity distribution in the sheet shed from a flat plate normal to the stream is in close agreement with that predicted by the Prandtl-Tollmien theory.

At a constant forward speed, both the frequency and the longitudinal spacing of the individual vortices in the vortex street depend largely on the lateral spacing between the sheets, and to a smaller extent on the form of the body.

In conclusion, the writers wish to acknowledge their indebtedness to Dr. H. Lamb, F.R.S., for valuable suggestions made during the preparation of the paper, and also to Mr. J. H. Warsap for assistance in carrying out the experimental work.

### XLIII. *On the Geyser Theory.*

*To the Editors of the Philosophical Magazine*

GENTLEMEN,—

IN the August number last year of the *Philosophical Magazine*, p. 341, Professor J. Joly has based arguments on the geyser theory of Bunsen. I desire, therefore, to call attention to the fact that I and other students of the geyser phenomena have come to the conclusion that this theory is inadequate to explain the geyser phenomena. Some of my arguments against Bunsen's theory are brought forward in my paper, "The Hot Springs of Iceland," pp. 54-56 (*D. Kgl. Danske Vidensk. Selsk. Skrifter*, 7. Række. *Naturvidensk. og Mathem. Afd.* viii. København, 1910, pp. 232-244).

The Bunsen theory is partly based upon incorrect measurements of the temperature in the geyser channel, and does not explain the intensity and periodicity of the eruptions. The well-known fact that soap is an efficient agent in producing eruptions cannot be brought into accordance with the theory. The heat from the surrounding strata does not enter the geyser channel, where the source of the periodicity is located. The heat conveyed by hot gases and steam from the origin of heat deeper down in



the earth is, on the contrary, liable to dissipate from the geyser channel to its surroundings.

The explanation of the geyser phenomena is to be sought in the interaction of the hot-spring gases, steam, and water in suitable channels and concavities belonging to the geyser (*loc. cit.* and my paper, "Undersøgelse af nogle varme Kilder paa Nordisland," pp. 10-19, *Det Kgl. Danske Vidensk. Selsk. Mathematisk-fysiske Meddelelser*, iii. 1, København, 1920). The evolution of gases is a common feature of the hot springs, and is of utmost importance for the geyser eruptions. Although there is a great variety in the manifestations of the geyser phenomena, I have in every case been able to explain them on these lines.

I take the opportunity of communicating my last experience regarding the Icelandic geysers. Two months ago I visited Reykjanes, the extreme south-western point of Iceland. There is a geyser there situated in a fissure of the rock. In the interval between the eruptions no water is to be seen in the fissure. The first sign of the approaching eruption is the low rumbling produced by the spring water as it advances up through the channel. Apparently the water is strongly agitated by penetrating gas-bubbles. As soon as the spring water reaches the surface the eruption commences. Great bubbles filled with gases and water-vapour forcing their way out of the channel throw the water columns 3-4 metres into the air. When the eruption has lasted for a time the eruptive force is apparently exhausted, and the spring water disappears, receding down into the channel.

The eruptions of this geyser occurred with great regularity, as evidenced by the following observations on August 24, 1927 :—

No.	Eruption commenced.			Eruption ended.			Period.
	h.	m.	sec.	h.	m.	sec.	m. sec.
1 .....	10	16	10	10	18	40	— —
2 .....	10	31	10	10	33	15	15 00
3 .....	10	45	50	10	48	05	14 40
4 .....	11	00	45	11	03	10	14 55
5 .....	11	15	30	11	18	05	14 45
(12) .....	13	00	30	13	03	25	7 × (15 00)
(25) .....	16	15	00	16	17	45	13 × (14 54)
Mean .....							14 57

The temperature of the spouting spring was 99° C., the atmospheric pressure being 750 mm. The colour of the spring water during the eruption was whitish, owing to diminutive gas-bubbles dispersed throughout the fluid. The spring water turned out to be real sea-water. In connexion with this interesting fact, it is worth mentioning

that the shortest distance to the sea-shore is 1350 metres and the elevation of the geyser orifice above sea-level is 20 metres. There are hot springs in abundance in the neighbourhood. I tested the water of several springs in different places, but failed to detect sea-water anywhere.

In my opinion it is impossible to bring the above-described geyser phenomena in accordance with the theory of Bunsen. In conformity with the views set forth in my papers quoted above, I have therefore assumed a principal channel connecting the orifice of the geyser with the interior, where the steam and the hot-spring gases are produced. Through a narrow side channel the sea-water oozes into the principal channel and for a moment bars the flux of gases through the main channel. Owing both to the accumulation of the gaseous exhalations locked up in the channel and its eventual adjacent concavities, and probably also to the increasing temperature, the pressure increases, and the gases will soon be able to force their way up through the channel and expel the sea-water: the eruption takes place. When the accumulated energy in the principal channel and its concavities has spent itself, the steady flux of gaseous exhalations from the interior is unable to prohibit the channel being blocked up, either by the water in the orifice or by the sea-water from the side-channel. In both cases the result will be the same. The current of steam and hot gases through the channel is checked, and consequently the water at the orifice recedes into the channel. Evidently the well is intermittent.

Among the hot springs in the neighbourhood of the geyser I observed in Reykjanes, there are two vents with powerful outflow of steam and gaseous exhalations, which fact renders still more probable my assumption of a main channel with originally steady current of gases and steam.

Yours faithfully,

THORKELL THORKELSSON,

Veurstofan, Reykjavik,  
Iceland.

Director of the Icelandic  
Meteorological Office.

*Editorial Note.*—It appears to be generally admitted that Bunsen's theory, which was based upon a study of the Great Geyser of Iceland, may not be applicable to all cases of geyser activity. Tyndall, Arrhenius, and many other authorities accept Bunsen's views as regards the Great Geyser. Bunsen's thermometric observations were confirmed by Coles in 1881. In Supan's 'Grundzuge der Physichen Erdkunde' extensive references to geyser literature will be found.

There is nothing in M. Thorkelsson's interesting letter which affects the matters discussed by Dr. Jeffreys and myself in this Journal. Our opposing deductions might be based upon the model geyser constructed by Tyndall. The teaching would be the same.—J. JOLY.

*XLIV. Note on the Formation of Pleochroic Halos in Biotite.*  
*By J. H. J. POOLE, Sc.D.\**

**I**N my paper on the Action of Heat on Pleochroic Halos, appearing in the January issue of this Journal, I refer to an alternative view of the mode of formation of the halo; *i.e.*, the direct oxidation of the ferrous iron in the biotite by the oxygen liberated by the  $\alpha$ -ray from the water present. On the strength of an experiment showing that the darkening of the mica by heating took place even in a reducing atmosphere, I left the genesis of the halo as referable simply to the loss of water by the mica brought about by the radioactive decomposition of the former.

On reconsideration, however, the view that the actual oxidation of the ferrous iron is responsible for the halo would appear to be deserving of direct acceptance. It is plain that the presence of a reducing atmosphere would have little if any effect on changes proceeding within the mica. Now, biotite is distinguished from muscovite (which neither darkens on heating nor contains halos) by its much greater content of ferrous iron. The water present is probably loosely combined with the silica, and when oxygen is radioactively liberated by the decomposition of the water, it would be at once taken up by the ferrous iron and the highly-coloured ferric salt formed.

Coming now to the experiment showing that when biotite is heated water is given up and the mica darkens, we have to remember that here the water is liberated at a high temperature and is present in the form of a gas since it is well above its critical temperature. It seems certain that under these conditions it would oxidize some of the ferrous iron to the ferric state, thus producing the observed darkening of the mica.

Thus we seem to have a simple and consistent explanation of the mode of formation of the halo in biotite based on quite definite and well-known chemical changes attending the ionizing activity of the  $\alpha$ -ray.

Iveagh Geological Laboratory,  
January 9th, 1928.

\* Communicated by Professor Joly, F.R.S.

XIV. *A Reply to the Paper "Ionization by Collision."\**  
*To the Editors of the Philosophical Magazine.*

GENTLEMEN,—

**I**N the Nov. issue of the Phil. Mag., Mr. Huxley discusses the points raised in my reply to his previous criticism of the Photoelectric Theory of Sparking Potentials which I put forward for discharges in rare gases. In the first criticism he raised objections gathered from results on active gases, and applied them to the consideration of rare gas discharges. Notwithstanding this I accepted the application, and showed that the objections raised did not invalidate the theory. Mr. Huxley apparently agrees with this.

At the same time, it was pointed out that the writer looked to a definite experimental testing of the theory to give a conclusive answer. This has been carried out for the case of helium (see 'Nature,' Oct. 1, p. 477, and *Zts. f. Phys.* xlv. 1927, "Ueber eine neue photoelektrische Theorie der Funkenspannung," Proc. Roy. Soc. A, cxvii. p. 508, 1928), and the agreement between theory and experiments was quantitatively correct. It is probable that the other rare gases—if the investigations could be carried out—would yield similar results.

With "impure" rare gases or mixtures of gases, collisions of the second order and other complications may occur to alter the conditions so that no *a priori* judgement in the matter may be pronounced, and there is, up to the present time, no quantitative experimental evidence on the matter. Nevertheless, for such cases the photoelectric hypothesis appears to be as probable as any other.

My general ideas are given in my Utrecht Dissertation (1927), chaps. 5 and 6. Quoting from page 60:—"The initiation of the self-sustained electrical discharge will be brought about by that particular action of the positive ions that is most easily accomplished under the conditions of experiment."

Mr. Huxley is wrong in imagining that I bring up the objections against Townsend's theory of ionization by collision by electrons, to disprove the Classical Theory of Sparking Potentials—this will be evident from a consideration of the previous papers and the references given above. That the Townsend theory is not universally adopted is proved by the existence of other theories (cp. *Handbuch der Phys.* xiv. 1927, pp. 39–42, 380) and the recent controversies.

\* Phil. Mag. Nov. 1927.

With regard to ionization by collision by positive ions, in addition to the objections of Sir J. J. Thomson and Horton and Davies, there are the difficulties described in Franck and Jordan's book, 'Anregung von Quantenspruengen durch Stoesse,' p. 188. The points brought forward in support of ionization by collision of positive ions in gases are all controversial ones, and it is wrong to assume that the conditions under which a positive ion can give rise to ionization by collision will be the same as those for a neutral atom or molecule (cp. Franck and Jordan, *loc. cit.* p. 190, also Bloch, 'Ionisation et Resonance des Gas et des Vapeurs,' p. 183).

That Prof. Townsend had considered alternative theories I was well aware (Taylor, *Phil. Mag.* iii. p. 765, 1927), but the question of cathode falls of potential does not come into considerations for sparking potential theories (though there may be a parallel variation).

So far as I can see, Mr. Huxley brings no new evidence to bear upon the problem, nor any experimental results for rare gases or discharge-tubes with electrodes of variable surface. The subject of the collisions between ions and atoms etc. is in great need of interpretation, but is one that requires experimental investigation.

Believe me,

The Cavendish Laboratory,  
Cambridge, November 9th, 1927.

Yours truly,  
JAMES TAYLOR.

#### XLVI. Cathode Rays in the Electrodeless Ring-Discharge.

*To the Editors of the Philosophical Magazine.*

GENTLEMEN,—

**I**N a recent publication in the *Philosophical Magazine* (ser. 7, ii. p. 674, 1926) which I have just received, Sir J. J. Thomson notes that the electrodeless discharge is a copious source of that radiation of very short wavelength which he has detected in discharge tubes. At very low pressure, when an ordinary discharge was no longer visible, he found a green phosphorescence of the glass walls which he believed to be caused by that radiation because it was not affected by a magnet brought near.

While investigating the electrodeless ring-discharge in hydrogen in a cylindrical quartz tube\*, I also found, without being aware of Sir J. J. Thomson's experiments, a very

\* A full report of these experiments will be published later on in another place. Note added in proof: Meanwhile published *Ann. d. Phys.* lxxxiv. p. 553 (1927).

brilliant phosphorescence, in this case a blue one, which here was present under various conditions of the discharge, also at relatively high pressure. Usually the walls continued phosphorescing for some time (about 15 minutes) after the discharge was stopped, a fact which seems to have not yet been recorded. With decreasing pressure the duration of this after-luminosity became remarkably less. Still, at the lowest obtainable pressures (0.0001 mm.), when a visible luminosity of the gas had already completely disappeared, the phosphorescence remained observable while the after-luminosity had nearly vanished. The same results were obtained in oxygen and air; merely the colour of the phosphorescence seemed to be a little different.

When in hydrogen the pressure was above about 0.001 mm. Hg, but below that point at which the visible discharge disappears, the phosphorescence was very much strengthened in the middle of the plates which covered the quartz cylinder. A magnet brought near deflected these luminous spots to the border of the plates in a sense which proved them to be caused by cathode rays coming from the middle of the tube, where under ordinary conditions the discharge took place. At the same time they became more diffuse, indicating that the velocity of these cathode rays is not homogeneous. They seem to be caused in the following way:—The potential difference at the ends of the coil overlapping the high-frequency electromagnetic field, which causes the ordinary discharge, accelerates the electrons produced in the invisible ring-discharge parallel to the axis of the tube. By the magnetic field in the coil this electron current is concentrated into the axis of the tube. The spectrum of the phosphorescence caused by the cathode rays was a continuous band between  $\lambda 4800$  and  $\lambda 4300$ . In air and oxygen the cathode rays could not be detected because the pressure which was necessary to cause the ordinary discharge to vanish was less than the pressure at which the cathode rays would appear in hydrogen. But I do not doubt that they have been present, the increased phosphorescence in the middle of the plates being hidden by the brilliant luminosity of the discharge.

Sir J. J. Thomson's failure to detect the presence of cathode rays may be caused by the special design of his apparatus. The most essential point seems to be that I used very high potentials, the spark-gap consisting of spheres of 5 cm. in diameter which were 2 cm. apart.

On account of my experiments, it is clear that at least part of the observed phosphorescence is caused by cathode rays. Whether the phosphorescence observed when a

definite cathode ray is absent is produced by diffuse electrons or by the short wave-length radiation as suggested by Sir J. J. Thomson will further be investigated; likewise the cause of the long-lasting after-luminosity. At any rate, the production of a well-defined cathode ray in the axis of an electrodeless ring-discharge tube is proved by my experiments—a fact which presumably has not yet been recorded.

Physikalisches Institut der  
Technischen Hochschule,  
Darmstadt, Germany.  
April 8th, 1927.

Yours faithfully,  
GERHARD HERZBERG.

*Note added in proof (January 23rd, 1928).*—In a more recent publication Sir J. J. Thomson (Phil. Mag. iv. p. 1128, 1927) has given an extensive theory of the electrodeless ring-discharge and a description of further experiments on this subject. Among others he observed, in the "sensitive state of the ring-discharge" in cyanogen, a bright line which was bent by a magnet in a sense opposite to that of the deflexion of the above-mentioned spots. Already at the time when I wrote the above I had observed such a bright line in hydrogen and nitrogen, as well as in oxygen, in a relatively wide range of pressure. I believed (*l. c.*) it to be caused by the cathode rays described above, but did not succeed in deflecting it by a magnet, because it was only as long (6 cm.) as the coil (12 turns of 1 mm. copper wire) which produced the discharge. An enumeration of the different phosphorescences in the electrodeless ring-discharge is to be found in the Appendix of a paper by the author in the *Zeitschr. f. Phys.* in print.

#### XLVII. *Notices respecting New Books.*

*Abstracts of Theses, Science Series, Vol. III.* (University of Chicago Press, Chicago, Illinois, U.S.A., and Cambridge University Press. Price 15s.)

**BY** recent regulations of the University of Chicago, candidates for the degree of Doctor of Philosophy are required to publish abstracts of their theses, between 3,000 and 1,200 words in length. This volume includes nearly sixty abstracts in the departments of the Ogden School of Science. Practically all the branches of Natural Science are represented—mathematics, physics, geology, geography, botany, and zoology, with six abstracts in the departments of anatomy, physiology, and hygiene. A number of the theses are of special interest to students in the States of America, but a considerable proportion, especially mathematical, physical, and chemical, have a wider appeal.

[*The Editors do not hold themselves responsible for the views expressed by their correspondents.*]

THE  
LONDON, EDINBURGH, AND DUBLIN  
PHILOSOPHICAL MAGAZINE  
AND  
JOURNAL OF SCIENCE.

[SEVENTH SERIES.]

MARCH 1928.

XLVIII. *Vortices behind Aerofoil Sections and Rotating Cylinders.* By E. TYLER, M.Sc., A.Inst.P. (Lecturer in Physics, College of Technology, Leicester) \*.

*Introduction* †.

THIS paper is supplementary to that of Richardson ‡ on "The Critical Velocity of Flow past Objects of Aerofoil Section." In his paper he confined his attention to: (1) the measurement of critical velocities of flow at which eddying motion was first produced in the wake of an aerofoil for varying angles of incidence  $\theta$  with the air-stream, and his results showed a gradual drop in the Reynolds number  $\frac{VD}{\nu}$  from 60 to 45 as the angle  $\theta$  increased from 0 to 20°, followed by a sharper drop for increasing angles up to 30°; and (2) the relation between the non-dimensional quantities  $\frac{V}{ND}$  and  $\frac{VD}{\nu}$  for different values of  $\theta$  ranging from 0 to 30°, where

$V$  = velocity of the air-stream.

$N$  = frequency of formation of the eddies.

$D$  = maximum thickness of aerofoil.

$\nu$  = kinematical viscosity of the Fluid.

\* Communicated by the Author.

† This work was carried out in the Carey Foster Laboratory, University College, London, in 1926.

‡ Proc. Phys. Soc. Lond. vol. xxxvii. April 1925.

*Phil. Mag.* S. 7. Vol. 5. No. 29. March 1928.

2 G



The results cited by the author indicated that  $\frac{V}{ND}$  was unaltered for increasing values of  $\theta$ , and no definite empirical relation existed between the quantities  $\frac{V}{ND}$  and  $\frac{VD}{\nu}$ , and it was from this point of view that I investigated further into the behaviour of such eddying flow behind aerofoils.

Many theoretical and experimental\* results have been given with respect to fluid motion past objects of finite dimensions, and recently much attention has been given to the study of air-flow past aerofoil sections; and in all such work, provided the velocity of flow exceeds a critical value (*cf.* Reynolds's value), a turbulent region of vorticity is indicated in the wake; but at the time of investigation I was not aware of any method having been given for the determination of the actual paths of the centres of the vortex system therein, neither any results obtained except those given by Richardson for values of  $\frac{V}{ND}$  for varying values of  $\frac{VD}{\nu}$  and  $\theta$ .

The work contained in the present paper divides itself into two sections:—

(1) The application of Relf and Simmons's † Hot-wire method for the determination of the frequency of formation of the Benard-Kármán ‡ system of vortices behind obstacles of different sections, primarily aerofoil sections inclined at different angles of incidence to the wind-stream; and (2) the tracing-out of the paths of the centres of the vortices formed behind stationary and rotating obstacles (*e. g.*, rotating cylinder and stationary aerofoils).

### *Frequency Determination of Vortices behind Aerofoils in Air.*

In order to determine the frequency  $N$  of the vortices formed behind the aerofoil, the method employed was

\* Piercy, *Aeronautical Soc. Journ.* Oct. 1923. Levy, *ibid.* June 1919 and *Phil. Mag.* vol. x. Oct. 1926. Howland, *Aeronautical Soc. Journ.* April 1925. Bairstow and Lanchester, 'Aerodynamics and Aeronautics,' Judge, 'Theory of Aerofoils.' Glauert, 'Aerofoil and Airscrew Theory.'

† *Phil. Mag.* vol. xlii. (1925); vol. xlix. (1925). Relf, *Aeronautical Soc. Journ.* April 1925.

‡ *Comptes Rendus*, cxlvii. p. 839 (1908). *Phys. Zeit.* xiii. p. 433 (1912).

essentially that first used by Relf and Simmons, and described by me in the 'Journal of Scientific Instruments' \*.

An electrically-heated platinum wire (1 inch long and .001 inch diameter) was mounted horizontally behind the obstacle in a wind-channel  $1\frac{1}{2} \times 1\frac{1}{2} \times 12$  feet, and was connected up in series with the primary of a step-up transformer (ratio 1 : 2), the secondary of which formed part of a shunted vibration galvanometer circuit. The wind-speed measured by a Chattock gauge was adjusted until resonance occurred between the frequency of formation of the vortices and the galvanometer set at known frequency, the latter being previously calibrated by means of a previously-calibrated vibrating reed.

The galvanometer frequency was also checked by stroboscoping a reflected spot of light from a mirror attached to the instrument. An Einthoven string galvanometer was substituted later for the vibration galvanometer, but this arrangement proved too insensitive. Precautions were however taken to ensure that the velocity of the air-stream  $V$ , and the frequency  $N$  of the vortices, were not too high, in order to give an appreciable drop in the resistance of the hot wire between successive periodic heatings and cooling, thereby increasing the sensitivity of the method employed, for results obtained by Richards† on the resistance of a hot wire in an alternating air-current clearly emphasized the importance of this condition being satisfied.

These conditions were met with partly in the design of the aerofoils, but care was taken that the ratio of maximum width to chord was of the same order as met with in actual practice. Different lengths of aerofoil consisting of brass and wood were used, and in most cases their length extended completely across the wind-channel and at right angles to the direction of the stream. Dimensions of sections of

TABLE I.

Section No.	Type.	Length.	D.	O.
1.....	Wooden.	37.5 cm.	.775 cm.	5.00 cm.
2.....	"	38.0 "	.337 "	2.50 "
3.....	Brass.	16.0 "	.330 "	2.60 "
4.....	"	20.8 "	.182 "	1.30 "

\* Journal of Scientific Instruments, vol. iii. Sept. 1926.

† Phil. Mag. vol. xlv. May 1928.

models are shown in Table I. and fig. 1, and results for aerofoils in air are included in Tables II. and III.

Fig. 1.

No. 4

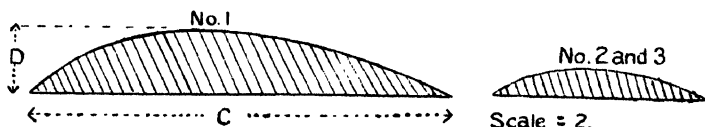


TABLE II.

Type of Aerofoil.	Angle of Incidence. $\theta^\circ$ .	D. cm.	N. per sec.	V cm./sec.	$\frac{V}{ND}$ .	$\frac{VD}{N}$ .
Wooden. No. 1. (Blunt Trailing Edge.)	-5.0	.791	15.0	80.0	6.74	$4.28 \times 10^3$
	-3.0	"	15.0	92.0	7.74	4.92 "
	-3.0	"	22.5	125.0	7.00	6.66 "
	0	"	22.5	137.0	7.68	7.30 "
	5.0	"	22.5	133.0	7.46	7.12 "
	6.5	"	22.5	138.0	7.74	7.37 "
	8.0	"	22.5	173.0	9.74	9.25 "
	8.0	"	26.5	205.0	9.76	10.85 "
	10.0	"	15.0	120.0	10.20	6.42 "
	*10.0	"	22.5	175.0	9.68	9.32 "
Wooden. No. 1. (Sharp Trailing Edge.)	0	.775	22.5	108.0	6.22	$5.67 \times 10^3$
	2.5	"	22.5	125.0	7.20	6.55 "
	2.5	"	30.0	170.0	7.30	8.92 "
	5.0	"	22.5	142.5	8.16	7.45 "
	7.5	"	30.0	215.0	9.48	11.21 "
	7.5	"	22.5	180.0	10.38	9.45 "
	*10.0	"	30.0	226.0	9.94	11.84 "
Wooden. No. 2.	0	.337	22.5	70.0	9.20	$1.60 \times 10^3$
	0	"	30.0	87.0	8.60	1.98 "
	0	"	37.5	113.0	8.96	2.57 "
	5.0	"	22.5	83.0	10.92	1.92 "
	5.0	"	30.0	105.0	10.38	2.39 "
	5.0	"	37.5	126.0	10.00	2.87 "
	10.0	"	22.5	87.3	11.50	1.99 "
	10.0	"	30.0	114.0	11.30	2.60 "
	10.0	"	37.5	147.0	11.70	3.34 "
	15.0	"	22.5	106.0	13.94	2.41 "
	15.0	"	30.0	140.0	13.88	3.19 "
	20.0	"	30.0	185.0	18.20	4.22 "
	25.0	"	22.5	150.0	19.96	3.42 "

\* Limit of observations.

Table IV. also shows a few results for cylinders and square section obstacles which are in good agreement with results

of previous experimenters using different methods, and a summary of the results contained in Tables II., III., and IV. is represented graphically in figs. 2 and 3.

TABLE III.

Type of Aerofoil.	Angle of Incidence. $\theta$ .	D. cm.	N. per sec.	V. cm./sec.	$\frac{V}{ND}$	$\frac{VD}{\nu}$
Brass. No. 1.	2.5	182	30.0	75.0	13.74	$.92 \times 10^3$
	2.5	"	30.0	85.0	15.60	1.04 "
	7.5	"	30.0	87.0	16.00	1.07 "
	5.0	"	30.0	75.0	13.74	.92 "
	7.5	"	30.0	78.0	14.30	.96 "
	7.5	"	37.5	98.0	14.38	1.20 "
	9.5	"	30.0	90.0	16.50	1.11 "
	12.0	"	30.0	100.0	18.30	1.23 "
	15.5	"	30.0	106.0	19.50	1.30 "
Brass. No. 2.	0.0	330	31.7	102.0	9.70	$2.28 \times 10^3$
	0.0	"	27.5	95.0	10.40	2.11 "
	6.0	"	29.5	105.0	10.78	2.34 "
	7.0	"	25.0	106.0	12.84	2.36 "
	10.0	"	29.5	125.0	12.88	2.78 "
	10.0	"	36.5	211.0	14.26	4.71 "
	11.0	"	27.5	143.0	15.70	3.19 "
	15.0	"	25.0	156.0	18.92	3.48 "
	15.0	"	15.0	135.0	18.20	3.01 "
	30.0	"	29.5	150.0	(15.40)	3.35 "

TABLE IV.

Obstacle.	D. cm.	N. per sec.	V. cm./sec.	$\frac{V}{ND}$	$\frac{VD}{\nu}$
Cylinder.	2.0	34.0	360.0	5.29	$4.87 \times 10^3$
	—	30.0	322.0	5.36	4.37 "
	—	28.5	302.0	5.26	4.10 "
	—	14.25	146.0	5.12	1.98 "
	*2.0	1.0	10.50	5.20	$1.42 \times 10^2$
Square Cords.	1.30	15.0	213.0	10.94	$1.87 \times 10^3$
	1.30	14.75	246.5	13.30	2.17 "
	.65	14.75	100.0	11.46	$4.40 \times 10^2$
	.615	15.0	103.0	11.20	4.28 "
	.615	22.5	155.0	11.20	6.49 "
Wooden.	.615	30.0	201.0	10.94	8.35 "
	.265	30.0	85.0	10.70	$1.52 \times 10^3$
	.250	30.0	85.0	11.30	1.43 "
	.250	37.5	115.0	12.30	1.94 "
	*.340	146.0	580.0	11.70	$1.33 \times 10^3$

\* Richardson's results.

Fig. 2.

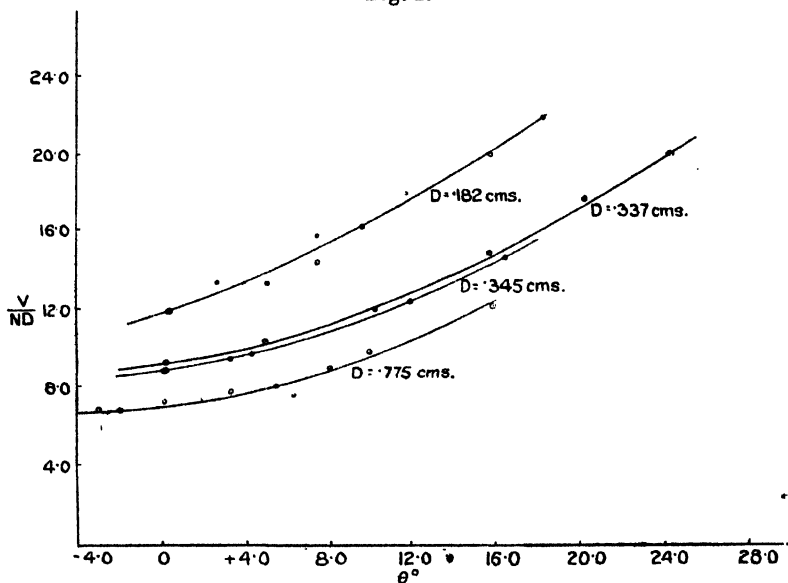
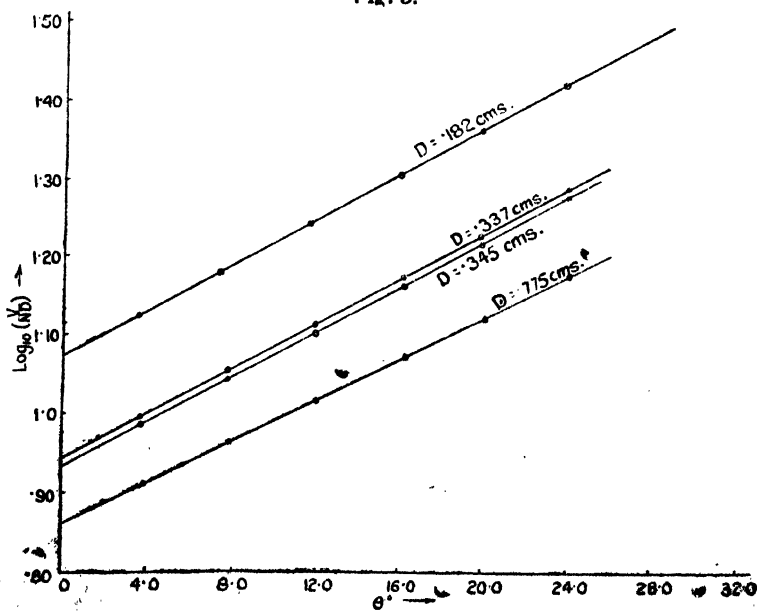


Fig. 3.

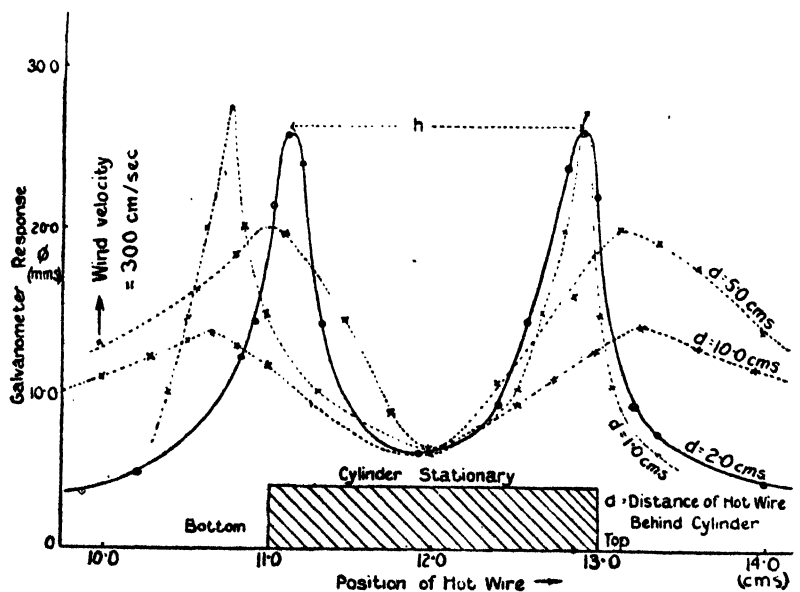


*Determination of the Paths of Vortices.*

The wind-speed having been adjusted until resonance occurred between the frequency of formation of the vortices and the galvanometer set at a known frequency, the deflexion  $\phi$  of the galvanometer was assumed proportional to the amount of periodic cooling of the hot wire.

The wire was then traversed in a vertical plane and at distances  $d$  behind the obstacle and corresponding deflexions  $\phi$  observed. Typical results for a stationary cylinder are shown in fig. 4, the curves each showing two maxima, and

Fig. 4.



the distance between such was taken as a measure of the separation distance  $h$  between the two rows of alternate vortices, since the maximum amount of periodic cooling occurs along the paths of the centres of the vortices.

The variations of  $h$  with  $d$ , both for a cylinder and inclined aerofoil (wooden) at  $0^\circ$ ,  $5^\circ$ , and  $8^\circ$  to the stream, are shown in fig. 5, and the results are shown in Table V.

A limit to the observations for this aerofoil was reached at an angle between  $8^\circ \sim 10^\circ$ , for on increasing the angle of incidence beyond this value the motion of the air in the wake

of the aerofoil exhibited a general turbulent motion; and no definite resonance frequency was found.

Fig. 5.

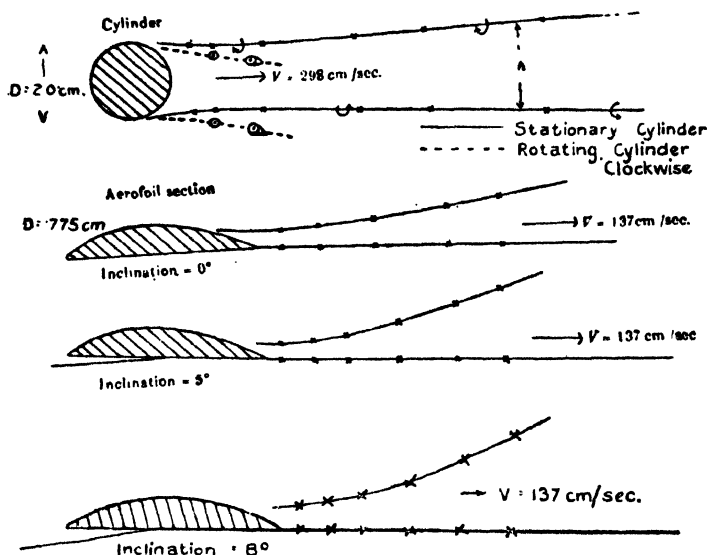


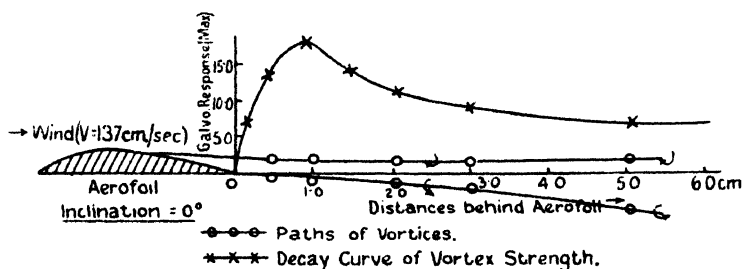
TABLE V.

Aerofoils. Wind-speed = 137 cm./sec.				Stationary. Cylinder D = 2.0 cm. Wind-speed = 298 cm./sec.	
<i>d.</i> cm.	$\theta = 0^\circ$ . <i>h</i> (cm.).	$\theta = 5^\circ$ . <i>h</i> (cm.).	$\theta = 8^\circ$ . <i>h</i> (cm.).	<i>d.</i> cm.	<i>h.</i> cm.
.10	.60	.67	.70	.50	2.30
.50	.50	.56	.86	1.00	2.10
1.0	.45	.52	.90	2.0	1.80
1.50	.70	.80	1.0	5.0	2.15
3.00	1.00	1.10	1.15	7.0	2.41
5.00	1.20	1.30	1.55	10.0	2.60

This condition was no doubt due to the sudden change in the ratio of lift to drag at this inclination, which is characteristic of aerofoils in general. With other aerofoils used, it was found, however, possible to extend the results to higher values of  $\theta$  (*vide* Tables II., III., and IV.).

The maximum response of the vibration galvanometer (previously tuned to resonance frequency with the vortices) is shown clearly in fig. 6, for different positions of hot wire behind the aerofoil. The curve shows the growth and decay of a vortex as it leaves the aerofoil, and the merit of such a result is entirely dependent on keeping the heating current constant. Notice that it takes some time before the vortex reaches its maximum strength, and then it seems to

Fig. 6.



decay exponentially. It must be remembered that in working with such small-scale models there is a limit to such investigations, for the vortex strengths are small and, owing to the widening-out effect, soon decay after travelling a few cms. along their paths, and the hot-wire detector becomes insensitive to these small fluctuations of velocity, which is masked by general turbulence.

### Results for a Rotating Cylinder in Air.

The above method was used to investigate the Magnus Effect \* for a cylinder ( $D=2.0$  cm.) rotating in air, which, according to Prandtl †, results in vortices of unequal strengths being detached from the opposite sides of the cylinder when rotating. The effect is clearly shown in figs. 7, 8, and 9, which give results for different speeds of rotation of the cylinder, the curves clearly showing a lateral displacement and unequal maxima. The time at my disposal did not enable me to investigate this effect to any considerable extent, but the graphs do show the position of the vortex centres for different distances behind the rotating cylinder,

\* Poggen, *Ann. d. Phys.* 1853.

† *Die Naturwissenschaften*, Feb. 6, 1925. *Low, Aero. Soc. Journ.* Feb. and March 1925.



Fig. 7.

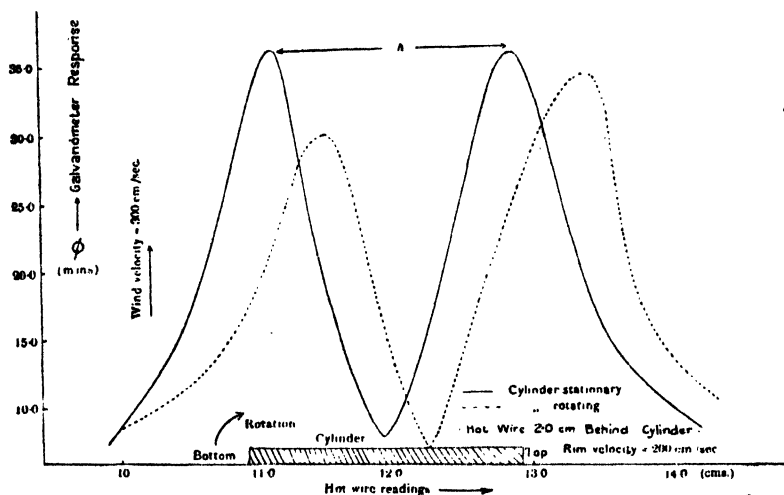
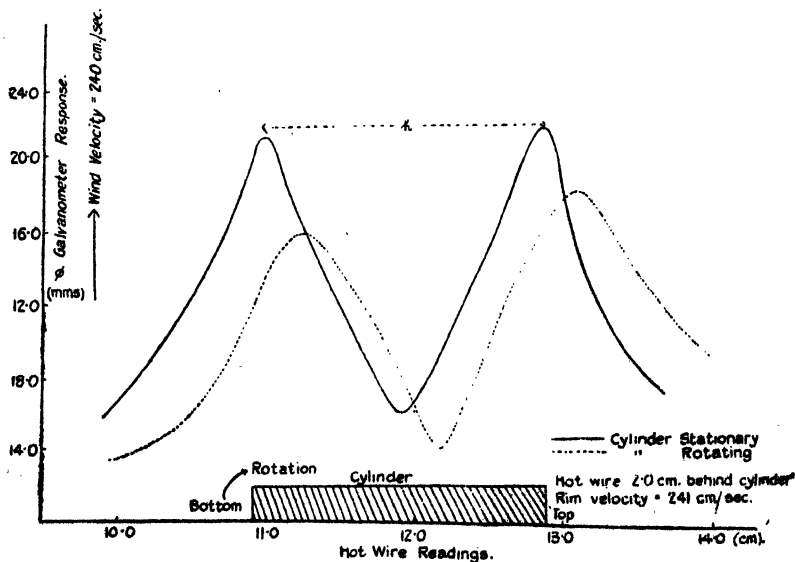


Fig. 8.



and the work could no doubt be extended to trace out the paths more completely for rotating bodies such as a cylinder, as used in this case.

Fig. 9.

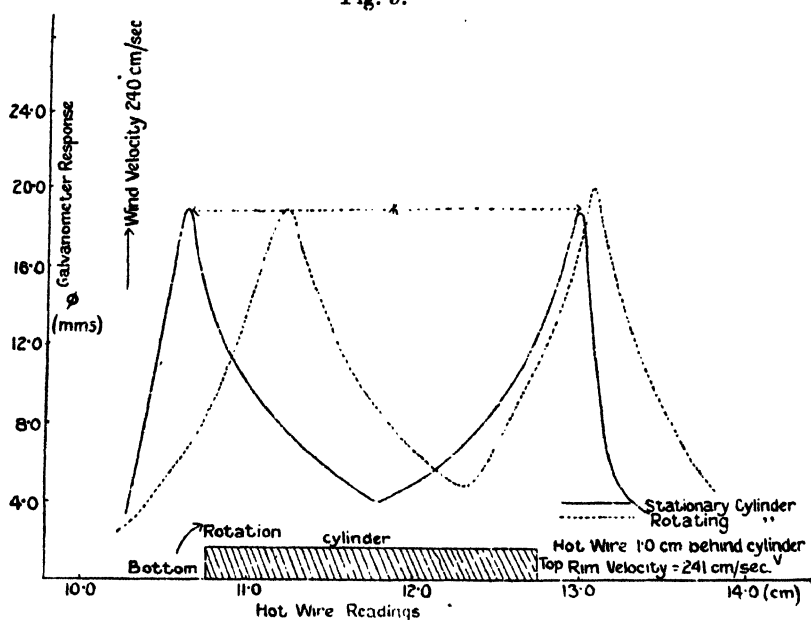


TABLE VI.\*

D. cm.	$\theta^\circ$	$\frac{V}{ND}$	$\frac{V}{ND} \cdot e^{-0.0323\theta} = A.$
182	0	12.0	12.0
	4	13.7	12.3
	8	15.7	12.3
	12	17.8	12.2
	16	20.2	12.2
	20	23.0	12.2
337	0	8.8	8.8
	4	10.0	8.9
	8	11.7	9.1
	12	13.2	9.0
	16	15.1	9.1
	20	17.2	9.3
	24	19.5	(10.0)
	28	22.0	8.9
775	0	7.50	7.5
	4	8.0	7.1
	8	9.00	7.0
	12	10.30	7.0
	16	12.00	7.2

\* Values of  $\theta$  and  $\frac{V}{ND}$  were interpolated from graph (fig. 2).

(1) *Relation between  $\frac{V}{ND}$ ,  $\frac{VD}{\nu}$ , and  $\theta$ .*—The variation of these non-dimensional quantities with variation of  $\theta$  shows that  $\frac{V}{ND}$  increased with  $\theta$ . There does not seem to be any dynamical similarity existing between the quantities  $\frac{V}{ND}$  and  $\frac{VD}{\nu}$  following Rayleigh's treatment, but the following empirical formula was found to fit the results approximately for  $\frac{V}{ND}$  and  $\theta$ , viz. :—

$$\frac{V}{ND} = Ae^{.0323\theta},$$

where A is a constant for any given aerofoil and is numerically equal to the value of  $\frac{V}{ND}$  when  $\theta=0$ . It should, however, be observed that A varies for different aerofoils (*vide* Table VI.).

The results of Richardson indicated no definite empirical relation existing, but his results were of the same order as mine, although obtained by a different method.

Results for square-section chords and rods (*vide* Table IV.) do compare favourably.

Benard \*, working with square plates, has obtained the following relation for his results :—

$$N = \frac{.430(V - 166\nu)}{D + .307} \text{ in C.G.S. units,}$$

where N=frequency of the vortices,

V=velocity of plate relative to the liquid,

D=thickness of plate normal to stream direction,

$\nu$ =kinematic viscosity of the liquid.

His results again show no strict dynamical similarity, even with square-section obstacles, and it may be doubted whether in actual experience any simple relation is applicable to the results. The method employed is not, however, delicate enough to investigate the point at which the vortex layer leaves the surface, where such a layer on leaving the surface of the body provides the mechanism which gives rise to the Benard-Kármán system of vortices. The position of this

point no doubt determines in the main the drag upon the body which controls the value of  $\frac{V}{ND}$ .

For large values of  $\frac{VD}{v}$  the position of this point (*vide* Lock \*) is unaffected, while for small values this point may vary appreciably, and hence corresponding changes in  $\frac{V}{ND}$ . The upper limit of  $\frac{VD}{v}$  where the sudden shifting back of this point causes a change in  $\frac{V}{ND}$  was not reached in the experiments with the aerofoils.

## (2) Path of Vortices behind Obstacles.

The paths traced out by the vortex centres behind a stationary cylinder show that in actual practice Kármán's theoretical results for the condition of maximum stability of vortices in two parallel rows behind an obstacle is not strictly applicable, but must be modified to meet the case of the widening-out of the rows as indicated in the results.

He has shown that if  $h$  = distance between the rows and  $l$  = distance between successive vortices in the same row, the condition for maximum stability is given by

$$\cosh \frac{2\pi h}{l} = 2$$

$$\text{and} \quad u = \frac{K}{2l} \tanh \frac{\pi h}{l},$$

where  $u$  = the translational velocity of the vortices relative to the stream and  $K$  the vortex strength, these relations giving  $\frac{h}{l} = 2.83$ .

Levy † has subsequently shown that no such system is completely stable.

This widening-out effect may be due to interference by the walls of the chamber, or may be due in the main to viscosity. Similar results have been obtained photographically by Föppl ‡, whose results were confirmed mathematically by Levy. Moreover, Kármán and Rubach § have also obtained, photographically, results of vortices in liquids, and

\* Phil. Mag. Nov. 1925.

† Proc. Roy. Soc. Edin. xxxv. p. 95 (1914).

‡ Münchener Sitzungsberichte, 1923.

§ Loc. cit. ref. p. 450, and 'Aerodynamics,' by Fuch and Hopf, p. 170.

they also show this slight divergence of the rows. An analogous behaviour was observed by Richardson and myself in a recent paper \* on eddy flow from annular nozzles, and Benton † has also shown that in tracing out the boundaries of the eddy tracks in the case of a straight slit and wedge over a considerable range, we get a widening of the eddy paths. Fage and Johansen ‡ have also shown that there is a widening-out of the paths for vortices behind an inclined plate as the vortices recede from the plate.

Referring to fig. 5, it will be seen that the paths behind the given aerofoil also indicate a gradual widening as the vortices recede from the aerofoil ; but as the inclination is increased, the vortices tend to widen out more rapidly, and there is a limit to the observations that can be made, owing to the insensitiveness of the method used.

Piercy §, using a Pitot-tube method, has obtained a few similar results, but the work of Bryant and Williams, Fage, Simmons and Taylor ||, who show regions of vorticity in the wake of an aerofoil, is well supported by my results. Bjerknes's ¶ idea of only one vortex being detached from the tip of the aerofoil, which leaves it with the stream while the next alternate one circulates round the aerofoil, thereby contributing to the circulation, is evidently not supported by my results, for they point to two vortices being detached, say, alternately one from the tip of the aerofoil and one from the upper surface, both practically of equal strength (in so far as the apparatus is able to detect), for the maxima of the resonance curves on either side of the section were equal, though relatively closer than for a cylinder.

According to Prandtl's theory, he supports Bjerknes's idea, but this condition I have failed to detect if it exist. The results suggest the vortices are in the main due to ordinary "æolian tone" phenomena, the effective thickness  $D$  of an aerofoil being modified as its angle of inclination to wind-stream is varied ; and since the stagnation points are symmetrically placed with respect to the trailing edge, yet at different distances along the boundary from the leading edge, these conditions tend to maintain equal vorticity on both sides.

In the case of the rotating cylinder, whereas there is no

\* Phil. Mag. vol. ii. Aug. 1926.

† Proc. Phys. Soc. vol. xxxviii. p. 114 (1926).

‡ Proc. Roy. Soc. vol. A, p. 116 (1927).

§ Loc. cit. ref. p. 450.

|| Phil. Trans. A, p. 630, Nov. 1925 ; p. 632, Dec. 1925.

¶ Journal de Physique, 1924.

change in the frequency of the vortex formation for a rotating as compared with a stationary cylinder, there are vortices of unequal strengths formed, each displaced laterally from its original path.

Relf and Lavender \*, photographing the flow round a rotating cylinder, conclude from their results that the total vorticity is less for a rotating cylinder than for a stationary cylinder, thus accounting for a reduction in the drag. I

have failed to detect any change in the value of  $\frac{V}{ND}$  which may occur owing to this reduction, but it may be noted that the peaks of the curves (figs. 8 and 9) for a rotating cylinder—cases in which the vortex has had time to reach its maximum strength—do indicate smaller values than when the cylinder is stationary.

A similar phenomena has been observed by Befort †, using spinning disks in an air-stream, and also by MM. Turpain and Bouy de Lavergne ‡. Photographs by Bairstow § also confirm this, but recently Tietjens || claims to have detected the formation of vortices on one side only of a rotating cylinder, and he supports his results by photographs, a result which would favour Bjerknes's theory for the aerofoil; but it is to be doubted whether such evidence will lead to any simple theory.

It is hoped, however, that the results given herewith, although entirely experimental, will provide data for further suggestions in aeronautical research.

In conclusion, I wish to express my best thanks to my colleague, Dr. E. G. Richardson, who suggested to me this line of research as an extension of his earlier investigations, and also to Professor A. W. Porter, F.R.S., for his kindly interest taken and also for putting the facilities at my disposal during the course of this research.

\* Adv. Committee of Aeronautics, No. 1010 (1925).

† *Zeits. f. Phys.* vol. xxxvi. 5, p. 374 (1926).

‡ *Comptes Rendus*, vol. clxxxii. April 1926.

§ 'Nature,' March 28, 1925.

|| *J. de Wiss. Geo. f. Luftfahrt*, vol. xviii. p. 56 (1925).



make  $k$  grow at first proportionally to  $n$ , i.e., to the exposure itself, and then still slower, while experimentally  $k$  was found to increase (after the very first short stage of slow linear growth) as rapidly as and even more rapidly than the square of the exposure. This state of things is not much changed when formula (b) is replaced by the somewhat more refined equation

$$\frac{k}{N} = 1 - e^{\bar{\kappa}(e^{-n\omega} - 1)}, \quad . \quad . \quad . \quad (c)$$

obtained (III. paper, *loc. cit.* p. 1066) by splitting the sensitive fraction  $\epsilon a$  of the area of each grain into a number of separate sensitive "spots," each of area  $\omega$ , distributed haphazardly among the grains,  $\bar{\kappa}$  being the average number of such spots per grain. In fact, this modification not only does not increase the rate of growth of  $k$ , but rather reduces it somewhat. Similarly as for (b), the gradient  $dk/dn$  corresponding to formula (c) decreases always with increasing  $n$  from its initial value  $N\omega\bar{\kappa}$  down to zero for  $n = \infty$ . In fact, the second derivative is, by (c),

$$\frac{d^2k}{dn^2} = -\frac{\bar{\kappa}\omega}{N} e^{-n\omega} [1 + \omega(N - k)], \quad . \quad . \quad (c'')$$

and thus throughout negative. In fine, the corresponding  $k, n$  curve has no inflexion point, while there is a distinct indication of such a point in the experimental curves.

To meet this difficulty, two more modifications of the light-dart theory were tried.

The first of these consisted in assuming that a silver halide grain is made developable when it is hit (within its sensitive part  $\epsilon a$ ) not by a single light-dart, but by at least *two*, or at least *three*, generally by at least  $r$  darts. The formula corresponding to this assumption is easily found to be \*, for  $r = 2$ ,

$$\frac{k}{N} = 1 - e^{-\epsilon an} (1 + \epsilon an), \quad . \quad . \quad (d_2)$$

and generally, for any  $r$ ,

$$\frac{k}{N} = 1 - e^{-\epsilon an} \left[ 1 + \frac{\epsilon an}{1!} + \frac{(\epsilon an)^2}{2!} + \dots + \frac{(\epsilon an)^{r-1}}{(r-1)!} \right]. \quad (d_r)$$

Now, each of these  $k, n$  curves has an inflexion point, namely at  $\epsilon an = r - 1$ . Thus, for example, the curve ( $d_2$ )

\* It is enough to remember that, if  $\bar{\kappa}$  be the average number of darts per grain (within the sensitive part of its area), the probability that the sensitive area of a grain shall be hit by  $s$  darts is  $e^{-\bar{\kappa}} \bar{\kappa}^s / s!$ , and that in the present case  $\bar{\kappa} = \epsilon an$ .



has its inflexion point at

$$\epsilon a n = 1, \quad \frac{k}{N} = 0.264$$

(i. e., where 26 per cent. of the grains are made developable), and it actually approaches the experimental curves belonging to the Slow Process emulsion\* within a certain interval somewhat more closely than did the original curve ( $r=1$ ), yet without representing any of these curves accurately enough. The ordinate of the inflexion point of ( $d^2$ ) being already somewhat too great, the curves ( $d_r$ ) corresponding to  $r=3, 4$ , etc., have their inflexion points placed still higher,

at  $\frac{k}{N} = 0.32, 0.35$ , etc., and thus much above the more or less distinct indications of the experimental inflexion points. Accordingly, none of these theoretical curves can be expected to give a satisfactory representation of the experimental results, and they may be left on one side.

In the second modification it was assumed that, even for equal grains, the sensitive fraction  $\epsilon$  of their area differs from grain to grain, the form of the frequency distribution law of the  $\epsilon$ -values among the grains being left entirely free. Thus, let the number of grains, whose sensitivity factor lies between  $\epsilon$  and  $\epsilon + d\epsilon$ , be given by

$$Nf(\epsilon)d\epsilon,$$

where  $f$  is an arbitrary (but of course positive) function of  $\epsilon$  and  $N$  the total number of grains. Then, by the original, single-hit assumption of the quantum theory of exposure, and noticing that the whole range of  $\epsilon$  extends from 0 to 1, the number of grains affected by an exposure  $n$  will be

$$k = N \int_0^1 f(\epsilon) [1 - e^{-n\epsilon}] d\epsilon,$$

and remembering that

$$\int_0^1 f(\epsilon) d\epsilon = 1,$$

$$\frac{k}{N} = 1 - \int_0^1 f(\epsilon) e^{-n\epsilon} d\epsilon. \quad . . . . (e)$$

Now, developing the exponential function into a power series, this formula can be written

$$\frac{k}{N} = na \int_0^1 \epsilon f(\epsilon) d\epsilon - \frac{n^2 a^2}{2!} \int_0^1 \epsilon^2 f(\epsilon) d\epsilon + \frac{n^3 a^3}{3!} \int_0^1 \epsilon^3 f(\epsilon) d\epsilon - \dots$$

$$. . . . (e')$$

\* These data will be quoted below.

This series is convergent for every value of  $na$ . For so is the series

$$na - \frac{n^2 n^2}{2!} + \frac{n^3 a^3}{3!} - \dots,$$

and, since

$$\int_0^1 f(\epsilon) d\epsilon = 1,$$

all the coefficients

$$\int_0^1 \epsilon^k f(\epsilon) d\epsilon$$

are smaller than unity. For small values of  $na$  (which is a pure number) the number  $k$  of grains affected will be proportional to  $n$  or to the exposure, regardless of the form of the function  $f$ . If this initial proportionality of  $k$  to  $n$  is to pass into a more rapid increase of  $k$ , to be necessarily followed again by a slower one (since ultimately the rate of increase tends to zero), the corresponding curve must have an inflexion point, or  $d^2k/dn^2$  must be zero for a certain value of  $n$ . Now, by (e),

$$\frac{d^2k}{dn^2} = -Na^2 \int_0^1 \epsilon^2 f(\epsilon) e^{-\epsilon an} d\epsilon,$$

and since the integrand is always positive,  $d^2k/dn^2$  cannot vanish for any finite value of  $n$ . In other words, the gradient  $dk/dn$  of the curve always decreases, from  $n=0$  to  $n=\infty$ . There is thus no possible form of the distribution function  $f(\epsilon)$  which would give a faithful representation of the experimental findings.

### *Nuclear Theories.*

The possibilities of the quantum theory of photographic exposure being thus completely exhausted, it has seemed worth while to investigate the implications of theories which are based upon essentially different assumptions and concepts, and which may summarily be referred to as *nuclear theories* of exposure. In these theories the chance factor which we have thrown upon the impinging light, making the developability of a grain of silver halide depend upon the chance of its being hit by one or more light-darts, is transferred upon the grains themselves, which are assumed to contain, before the exposure, certain heterogeneities, specks of a foreign substance\* accompanied by some free silver atoms, or incipient nuclei haphazardly distributed among them with

\* Notably silver sulphide (Sheppard).

respect to number as well as to size. The part played by the incident light (whose possibly discrete structure becomes irrelevant) consists, then, in maturing or completing these nuclei by depositing upon and around them further free silver atoms, and thus increasing them until they become "active" (*i.e.* developable), while every grain containing at least one active nucleus is assumed to be developable as a whole. The latter property can actually be considered as an experimentally established fact.

The concept of nuclei, which could be traced back a long way, has been utilized in a theory proposed in 1922 by F. C. Toy\* and more recently (1925), and in a modified form in a theory outlined by Sheppard, Trivelli, and Loveland (*loc. cit.*), who refer to it as the "concentration speck" theory. The former is of a semi-quantitative nature, Dr. Toy's assumptions not being given by him a definite mathematical form, while the latter is mainly qualitative, and leaves therefore its quantitative development free within wide limits.

In what follows, our purpose is, first, to put Toy's theory into a definite mathematical form, and, second, to substantiate some of the possible interpretations of the concentration speck theory or, rather, to develop the consequences of assumptions which were suggested by this theory.

### *Mathematical Formulation of Toy's Theory.*

According to Toy's assumption, there are, previous to exposure, a certain number of nuclei distributed haphazardly among the grains. These nuclei are supposed to differ in "sensitivity," *i.e.* to require different light-intensities  $I$  (at constant exposure time), or ultimately † different (energy-) exposures  $E$  in order to become active nuclei or development centres. Of the curve which is to represent the distribution of the nuclei over the  $E$ -range (or, in his own case, the  $I$ -range), Toy assumes only in a qualitative way that it will be "similar in general form to that obtained by Maxwell for the distribution of the velocities between the molecules of a gas," without committing himself to any definite mathematical formula. The curve drawn in Toy's fig. 1 (*loc. cit.*) resembles Maxwell's frequency-distribution curve for *resultant* velocities (regardless of direction), which would be expressed by

$$f(v)dv = \text{const. } e^{-\lambda v^2} v^2 dv,$$

and thus passes through the origin,  $v=0$ . But there is

\* Phil. Mag. vol. xliv. p. 352.

† Apart from the failure of the reciprocity law.

manifestly no reason for supposing the (reciprocal) "sensitivities," *i.e.* the  $E$ -values, to be thus distributed among the nuclei. The case in hand can rather be expected to be ruled by Maxwell's distribution law for each of the three rectangular *components* of velocity, which is simply the normal frequency-distribution law. A factor  $E^2$  corresponding to  $v^2$ , which in the case of the molecules is due to replacing the volume-element of the velocity-space  $dv_x dv_y dv_z$  by  $v^2 \sin \theta d\theta d\phi dv$  and which remains in the formula after an integration over all directions  $(\theta, \phi)$  in that space, has no justification whatever in the case of the nuclei, whereas it is reasonable to assume for these the normal distribution law.

Let us therefore definitely assume that the number of nuclei requiring an exposure  $E$  to  $E + dE$  in order to become active nuclei is

$$f(E)dE = A e^{-h^2(E-E_0)^2} dE, \quad . \quad . \quad . \quad (1)$$

where  $A$ ,  $h$ , and  $E_0$  are constants. Then the number of *active nuclei*,  $N\kappa_a$  say, produced by an exposure  $E$  will be

$$N\kappa_a = A \int_0^E e^{-h^2(E-E_0)^2} dE,$$

or, in terms of the error-function

$$\Phi(x) = \frac{2}{\sqrt{\pi}} \int_0^x e^{-u^2} du,$$

$$N\kappa_a = C \{ \Phi[h(E-E_0)] + \Phi(hE_0) \}, \quad . \quad . \quad . \quad (2)$$

where  $C$  is a constant proportional to  $A/h$ . Let  $N\kappa$  be the total number of nuclei. This will be given by (2) for  $E = \infty$ .

Thus, and since  $\Phi(\infty) = 1$ ,

$$N\kappa = C \{ 1 + \Phi(hE_0) \}, \quad . \quad . \quad . \quad (2')$$

which determines the constant  $C$ . Since  $N$  is the number of grains,  $\kappa$  is the average number of all nuclei, and  $\kappa_a$  the average number of active nuclei per grain.

Thus, by (2) and (2'), the average number of active nuclei per grain produced by an exposure  $E$  will be

$$\kappa_a = \kappa \frac{\Phi[h(E-E_0)] + \Phi(hE_0)}{1 + \Phi(hE_0)}. \quad . \quad . \quad . \quad (3)$$

Let us now assume, after Toy, that every grain which happens to have one or more active nuclei will be developable. This, at any rate, is a safe assumption; for, as already mentioned, it is only a re-statement of the well-established fact that a grain which once starts developing will be developable entirely.

Now, since the  $N\kappa_a$  active nuclei can be supposed to be haphazardly distributed among the grains, the probability of a grain having none of these nuclei is  $e^{-\kappa_a}$ . The number of grains, out of the large total  $N$ , having no active nucleus will be  $Ne^{-\kappa_a}$ , and the number of grains having at least one active nucleus, and therefore, by the last assumption, the number of grains made developable,

$$k = N(1 - e^{-\kappa_a}). \quad (4)$$

If we put for brevity

$$v \equiv \log \frac{N}{N-k},$$

this result can be written

$$v = \kappa_a. \quad (4a)$$

Thus, ultimately, by (3),

$$v = \kappa \frac{\Phi[h(E - E_0)] + \Phi(hE_0)}{1 + \Phi(hE_0)}. \quad (5)$$

Such, then, would be the relation between  $v$  and the exposure  $E$  as a consequence of assuming (1) as the distribution law of sensitivity. The equation (4a) itself, is, of course, independent of any such law, its validity being based only on the assumption that the active nuclei are distributed haphazardly among the grains.

Now, while the equality  $v = \kappa_a$  seems to hold accurately enough, in Toy's two sets of data\*, at least, the curve (5) does not resemble very much that sketched in his fig. 2, and certainly does not represent well enough either his own observed  $v$ -values or those found by Trivelli for the Slow Process emulsion. The curve (5) has an inflexion point, namely at  $E = E_0$ , but it differs considerably in shape from the experimental curves. To see this, it is enough to take a few numerical examples of equation (5), which, with  $y = v/\kappa$  and  $x = hE$ , can be written

$$y = \frac{\Phi(x - x_0) + \Phi(x_0)}{1 + \Phi(x_0)}, \quad (5')$$

\* These two sets are contained in Toy's Table II. (*loc. cit.* p. 361). Assuming that the grains which show no nuclei would not develop at all, we find from the first set

$$N - k = 91, v = \log \frac{150}{91} = 0.50, \text{ as against } \kappa_a = 0.48 \text{ (Toy's } N_0),$$

and from the second set

$$v = \log \frac{150}{45} = 1.25, \text{ while } \kappa_a = 1.19.$$

$x_0$ , the abscissa of the inflexion point, being its only parameter.

Thus for  $x_0=0.20$  we have

$x$	0.05	0.10	0.20	.30	.40	.60	.80	1.20	1.60	2.50
$y \dots$	0.045	0.090	0.182	.274	.364	.533	.676	.872	.961	.999.

This curve is up to about  $y=0.50$  scarcely distinguishable from a straight line through the origin,  $y$  being almost proportional to  $x$ . The behaviour of the curve (5) is very much the same for other values of  $x_0$ . Since the experimental inflexion point lies, at any rate, in the lower part of the  $v$ -scale (and the extreme, asymptotic value of  $y$  is 1), it is enough to consider such values of  $x_0$  for which  $2y_0$  does not approach unity. Thus, on the one hand, for  $x_0=0$ ,  $y$  becomes equal to  $\Phi(x)$  itself, which from zero up to about  $y=0.40$  is very nearly proportional to  $x$ , as may be seen from a table of the error-function. On the other hand, for  $x_0=0.75$ , which places  $y_0$  already too high, pairs of corresponding values are

$x$ .....	$\frac{1}{2}x_0$	$\frac{1}{2}x_0$	$\frac{1}{2}x_0$	$x_0$	$2x_0$	$4x_0$
$y$ .....	0.038	.080	.179	.416	.831	.999 <sub>3</sub>

Even here  $y$  increases, but slightly more rapidly than  $x$ .

Now, the relation between  $v$  and exposure as found experimentally is of a distinctly different type, especially for the smaller grains. Thus, in Toy's experiments (*loc. cit.* Table IV.), when for the smallest grains, class (a), the exposure is nearly doubled (61:128), the value of  $v$  increases from .05 to .62, more than tenfold, and in the next size class, on doubling the exposure, the value of  $v$  is more than trebled, and so on. The disagreement with (5) is still more pronounced in the case of Trivelli's results for the Slow Process emulsion. In fact, for the smallest grains ( $a=0.115\mu^2$ ) the observed  $v$ -values, for exposures  $E$  increasing in the ratio 1 :  $\sqrt{2}$ , are

0.026	0.11	0.36	0.74	1.29, etc.,
-------	------	------	------	-------------

i. e. increasing much more rapidly than  $E$ , and for the next size class ( $0.3\mu^2$ )

0.14	0.21	0.37	0.72	1.44	2.13, etc.,
------	------	------	------	------	-------------

still increasing more rapidly than  $E$ .

Notice that while by (5)  $v$  should tend with indefinitely increasing exposure to a finite limit  $v_\infty = \kappa$  = average number of all nuclei per grain, it is difficult to tell whether the experimental results, either Toy's or Trivelli's, give an indication of the existence of such a limit at all. It is, at any rate, impossible to derive from these data anything but a very

rough value of this limit. (In Trivelli's case, in which  $v$ -values as high as 6 are quoted, one would as well be justified in taking  $v=\infty$ , since experimentally  $k/N=0.99$  to which corresponds  $v=4.6$  is just distinguishable, and  $k/N=0.999$  is scarcely discernible at all from unity to which corresponds  $v=\infty$ ). We may only, in the case of Toy's size class (a), take provisionally for  $v_\infty=\kappa$  a value just above 2.45, the highest  $v$  observed, and for the inflexion point, from Toy's smoothed curve (a) in his fig. 10, the value  $v_0=0.50$ , corresponding to I or E=0.12, and in this way determine  $x_0=hE_0$  and compare the  $v$ -values given by (5) with the observed ones. Thus, assuming

$$v_\infty=\kappa=2.55, \quad v_0=0.50, \quad E_0=0.12,$$

we have, from

$$\frac{\Phi(x_0)}{1+\Phi(x_0)} = \frac{v_0}{\kappa},$$

$$\Phi(x_0) = \frac{v_0}{\kappa - v_0} = 0.244, \text{ whence } x_0 = 0.220, h = 1.83; .$$

so that formula (5) becomes

$$v = 2.05\{\Phi(1.83E - 0.22) + 0.24\},$$

and this gives, with E written for Toy's I in his arbitrary units,

E .....	1	0.689	.490	.270	.128	.061	.033	.016	.008
$v_{\text{calc.}}$ .....	2.50	2.26	1.86	1.12	0.58	.25	.14	.06	.03

against

$v_{\text{obs.}}$ .....	2.45	2.30	2.04	1.39	0.62	.05	.00	.00	.00
-------------------------	------	------	------	------	------	-----	-----	-----	-----

There is a marked disagreement between the calculated and the observed  $v$ -values; the deviations increase with decreasing exposure down to the fourth and reappear in the sixth step, to become henceforth systematic. This result cannot be improved by changing the value of  $\kappa$ , which would only change all  $v$ -values in the same ratio. Nor can  $v_0$ ,  $E_0$  be changed appreciably without clashing with the position of the inflexion point in Toy's smoothed curve (a). Thus, Toy's set (a) of data cannot be satisfactorily represented by formula (5). The deviations in the case of Trivelli's data for the Slow Process emulsion (quoted below), especially for the first two size-classes of grains, have turned out to be even more pronounced, while Toy's remaining sets, (b), (c), (d), and the corresponding smoothed curves, for which the values

of  $v_0$ ,  $E_0$ , and especially  $\kappa$  cannot be estimated at all, would lead to no relevant results.

In fine, the available experimental data cannot be adequately represented by the formula (5), which was arrived at by giving a definite mathematical form to Toy's assumptions. A weak point of this type of formula is, moreover, the presence of the factor  $\kappa$ , whose numerical determination, through  $v$ , is essentially elusive.

Such being the case, some alternative forms of nuclear theory of exposure were next considered in which the growth of the nuclei was explicitly taken into account. These forms were suggested by the "concentration speck" theory (Sheppard, Trivelli, and Loveland, *loc. cit.* p. 72) inasmuch as, in this theory, the process of growth of the nuclei is explicitly mentioned.

Two such modifications were considered and worked out in some detail; one, based upon the assumption that the rate of growth of the size (area) of the nuclei by accretion of silver atoms under the action of light is proportional to their instantaneous *perimeter*; and another in which this rate of growth was assumed to be proportional to their instantaneous *size* itself.

The former has led to a type of characteristic curves ( $k$ ,  $E$  curves) clashing markedly with the experimental ones, and need not therefore be described here, and the latter, which thus far seems promising, is treated in the following part of the paper.

#### *Rate of Growth of Nucleus Proportional to its Size.*

Let  $s$  be the size, that is to say, the area\* of a nucleus of silver before exposure, and  $\sigma'$  its size at any stage of its growth during the exposure by accretion of further silver atoms.

Without entering into the mechanism of this process, let us assume that, in the presence of light of sufficiently high frequency and intensity, each nucleus grows in size at a rate proportional to its instantaneous size and to the incident light-intensity  $I$ ,

$$\frac{d\sigma'}{\sigma'} = cI dt = c dE, \quad . . . . . (6)$$

where  $c$  is a coefficient which, for grains of a given size in a given emulsion, will be considered as a constant, but which may vary with the grain size and the kind of emulsion.

\* If, indeed, it be the area of the nucleus which is relevant for its developability.



Notice that by the very assumption of proportionality of growth to  $I$ , the cases in which the reciprocity failure is pronounced are excluded. These may be taken into account by substituting for  $I$  itself some more complicated function of the intensity; also by requiring that if  $I$  falls below a certain value, there shall be no increase of the nuclei. For the present, however, we will assume that  $I$  lies within the limits of (approximate) validity of the reciprocity law. Since  $\sigma' = s$  for  $E=0$ , we have from (6)

$$\sigma' = se^{cE}.$$

In particular, let  $\sigma$  be the size of the nucleus at which it just becomes an "active" nucleus and thus makes the grain containing it developable\*, and let  $E$  be the corresponding exposure. Then

$$se^{cE} = \sigma; \quad E = \frac{1}{c} \log \frac{\sigma}{s}, \quad . \quad . \quad . \quad . \quad (7)$$

a relation between the original size of a nucleus and the exposure required for maturing it.

The law (6), of course, is not supposed to hold indefinitely, but only up to a certain nucleus size exceeding  $\sigma$ , beyond which the growth must be imagined to be slowed down and eventually come to an end. A correspondingly modified differential equation, to replace (6), could easily be written down. Such a modification, however, which would introduce purely formal complications into our results, would be superfluous. For our only object is to find the number  $k$  of grains made developable by a given exposure  $E$ ; and since every grain whose nucleus has once attained the size  $\sigma$  becomes developable, the number  $k$  as a function of  $E$  will be entirely independent of the form of the law of growth beyond  $\sigma$ .

A grain of the emulsion will, in general, contain several nuclei of different sizes. Of these the largest, if all grow according to (6), will be the first to become an active nucleus and, therefore, to make the grain developable.

Now, let the number of grains whose *largest* nuclei are, before exposure, of size  $s$  to  $s+ds$  be given by

$$Ae^{-h^2(s-s_0)^2}ds, \quad . \quad . \quad . \quad . \quad (8)$$

where  $A$ ,  $h$ , and  $s_0$  are constants. (Notice that this assumption differs essentially from that made in connexion with Toy's theory, where the "sensitivity" was taken to be normally distributed over the nuclei.) In the distribution

\* The value of  $\sigma$ , which plays here the part of a constant, will, of course, vary with the development conditions.

law (8) the variable  $s$  will be expressed in terms of exposure according to (7), i. e., by

$$s = \sigma e^{-cE}. \quad (9)$$

In accordance with this let us still introduce a constant  $E_0$  defined by

$$s_0 = \sigma e^{-cE_0}. \quad (9_0)$$

The formula for the proportionate number of grains made developable by a given exposure can now be deduced without difficulty.

In fact, the number of grains with their largest nuclei ranging in original size from the limit value  $\sigma$  down to  $s$ , and therefore made developable by an exposure  $E = \frac{1}{c} \log \frac{\sigma}{s}$ , will be

$$k = A \int_s^\sigma e^{-h^2(s-s_0^2)} ds.$$

The upper limit of the integral corresponds to  $E = \theta$  and the lower to the given exposure  $E$ . If  $\Phi$  be again the error-function and  $C$  a constant proportional to  $A/h$ , the last formula can be written

$$k = C \{ \Phi[h(\sigma - s_0)] - \Phi[h(s - s_0)] \}.$$

Let  $N$  be the total number of grains with nuclei ranging originally in size from  $s=0$  up to  $s=\sigma$ , that is to say, not counting the fog grains for which  $s \geq \sigma$ . Then we shall have  $k=N$  for  $s=0$ , and by the last equation,

$$N = C \{ \Phi[h(\sigma - s_0)] + \Phi[hs_0] \}.$$

Thus, eliminating the constant  $C$ ,

$$k = N \frac{\Phi[h(\sigma - s_0)] - \Phi[h(s - s_0)]}{\Phi[h(\sigma - s_0)] + \Phi[hs_0]}.$$

Ultimately, substituting  $s, s_0$  from (9), (9<sub>0</sub>), and putting for brevity

$$g = h\sigma, \quad \alpha = hs_0 = ge^{-cE_0}, \quad (10)$$

we have for the number  $k$  of grains made developable by an exposure  $E$

$$\frac{k}{N} = \frac{\Phi(g - \alpha) - \Phi(ge^{-cE} - \alpha)}{\Phi(g - \alpha) + \Phi(\alpha)}. \quad (11)$$

This is the required formula. We may notice that if the law of growth (6) were retained, but the sizes  $s$  were assumed

to have a normal frequency distribution over the nuclei themselves (instead of the grains), as in the section on Toy's theory, then the same formula (11) would hold with  $k/N$  replaced by  $v/\kappa$ , where  $\kappa$  is the average number of nuclei per grain and  $v = \log N/(N - k)$ . But formula (11), as it stands, turned out to cover the observed facts much better. It has, moreover, the advantage of being free from the elusive factor  $\kappa$  or  $v_\infty$ .

The original parameters  $h$ ,  $\sigma$ ,  $s_0$  appear only through the two products  $g$  and  $\alpha$ . These may be expected to retain the same values even for grains of different sizes within a given emulsion, while the coefficient  $c$ , appearing originally in the law of growth (6), is likely to vary with the size of the grain, and may even vary from grain to grain in the case of equal grains. For the growth of the relevant (*i. e.*, largest) nucleus will be influenced by the presence of other nuclei upon the same grain. Under these circumstances the constant coefficient  $c$  in (11) has to be considered as the result of averaging over a number of grains of equal size. In all, formula (11) contains three independent constants— $g$ ,  $\alpha$ , and  $c$ . The parameter  $E_0$  is defined by  $cE_0 = \log \frac{\sigma}{s_0}$ , and here  $s_0$  is the mode of the frequency distribution (8).

The  $k$ ,  $E$  curve (11) has, in general, an inflexion point, which makes it adaptable to the experimental characteristic curves. Its position,  $x_i = cE_i$ , is given by the vanishing of the second derivative of the variable part of  $k/N$ , say of

$$f(x) = \frac{\sqrt{\pi}}{2} \Phi[g(e^{-x} - e^{-x_0})], \text{ where } x = cE.$$

Write  $u = g(e^{-x} - e^{-x_0})$ . Then  $f'(x) = -ge^{-u^2-x}$ , and the equation  $f''(x) = 0$  becomes

$$2u \frac{du}{dx} + 1 = 0$$

or

$$2g^2(e^{-x_i} - e^{-x_0}) = e^{x_i},$$

a quadratic for  $e^{x_i}$ , which gives

$$e^{x_i} = g^2 e^{-x_0} \left\{ \sqrt{1 + \frac{2e^{2x_0}}{g^2}} - 1 \right\} \dots \dots (12)$$

Since  $x$  or  $cE$  is positive, an inflexion point will exist only

if the right-hand member of (12) is greater than 1, or

$$\sqrt{1 + \frac{2e^{2x_0}}{g^2}} > 1 + \frac{e^{x_0}}{g^2}$$

i. e.,

$$e^{x_0} \left( 1 + \frac{1}{2g^2} \right) > 1,$$

which can also be written

$$g \left( 1 - \frac{1}{2g^2} \right) > \alpha. \quad . \quad . \quad . \quad . \quad (12a).$$

In the numerical cases to be considered in the sequel, in which  $g$  amounts to some units while  $\alpha$  does not much exceed unity, this inequality will be amply satisfied.

If, on the other hand,  $g$  is a small fraction (when there is no inflexion point), the functions  $\Phi$  in (11) can all be identified with the first powers of their arguments, and formula (11) degenerates into

$$k/N = 1 - e^{-\alpha E},$$

which is of the same type as that following from the quantum theory of exposure. As has already been mentioned, the observed curves deviate considerably from this simple form, and call accordingly for large values of the coefficient  $g$ , amounting to some units.

One more theoretical point, relating to fog grains, may be mentioned here. Suppose that the assumed frequency distribution (8) of nuclear sizes holds also for  $s > \sigma$ , the largest nucleus size occurring at all. Then the number  $N_f$  of fog-grains will be given by

$$N_f = A \int_0^\tau e^{-k^2(s-s_0)^2} ds = C \{ \Phi[h(\tau-s_0)] - \Phi[h(\sigma-s_0)] \},$$

where  $C$  is the same constant as above, i. e., given by

$$C \{ \Phi[h(\sigma-s_0)] + \Phi(hs_0) \} = N.$$

Here  $h(\tau-s_0)$ , a pure number, can be assumed to be large enough (say of the order of two or three units) \* to make  $\Phi[h(\tau-s_0)] \div 1$ . Thus

$$\frac{N_f}{N} = \frac{1 - \Phi(g - \alpha)}{\Phi(\alpha) + \Phi(g - \alpha)}. \quad . \quad . \quad . \quad . \quad (13)$$

Notice that  $N$  comprises the non-fogged grains only, so that the total number of grains is  $N + N_f$ . From (13) we see

$$* \quad \Phi(2) = 0.985, \quad \Phi(2.5) = 0.9998, \quad \Phi(3) = 0.99998.$$

that if an emulsion contains but a small fraction of fog-grains, only large values of  $g$ , amounting to two or three units, will be admissible in representing the data obtained with such an emulsion; the more so if  $\alpha$  is not negligible.

Turning now to the experimental verification of the formula (11), let us first consider the complete set of data obtained in this laboratory on four size-classes of grains of the Slow Process emulsion, mentioned above.

In the following table (I.) the observed values of  $100 k/N$ , the percentage of grains made developable, are those given in Sheppard, Trivelli, and Loveland's paper (*l. c.* p. 66),  $E$  being the "exposure" in arbitrary units, in this case proportional to the exposure time at constant light-intensity.

TABLE I.

Values of  $100 k/N$  for Slow Process Emulsion.

E ...	4	4 $\sqrt{2}$	8	8 $\sqrt{2}$	16	16 $\sqrt{2}$	32	32 $\sqrt{2}$	64	64 $\sqrt{2}$	128	$\alpha$	$c$
Calc. ...	—	—	3.7	10.1	25.3	49.5	74.2	89.8	96.8	99.2	99.9	0.115	0.050
Obs. ...	—	—	2.6	10.5	30.4	52.0	72.4	82.8	89.3	93.0	96.1		
Calc. ...	5.4	14.7	33.7	59.5	81.4	93.3	98.1	99.6	100	100	100	0.3	0.115
Obs. ...	13.1	19.0	30.9	51.3	76.3	88.1	93.3	95.7	98.0	99.4	99.8		
Calc. ...	20.2	42.7	68.4	86.7	95.5	98.8	99.8	100	100	100	—	0.5	0.184
Obs. ..	25.3	45.9	69.1	85.1	93.4	96.7	98.9	99.5	99.9	100			
Calc. ...	49.6	74.3	89.9	96.8	99.2	99.9	100	—	—	—	—	0.7	0.285
Obs. ...	52.0	73.8	85.0	94.7	98.0	98.8	100	—	—	—	—		

The average grain sizes for the four classes were, in square microns,

$$\alpha = 0.115, \quad 0.3, \quad 0.5, \quad 0.7,$$

with a common class breadth of 0.2. There was no perceptible fog. The theoretical values of  $k/N$  were calculated by means of formula (11) with constants determined after a good many trials. The values of the constants  $g$  and  $\alpha$  finally chosen for the first class turned out to suit also the remaining three classes of grains, which called only for different values of the coefficient  $c$  or a contraction of the original curve along the exposure axis. Ultimately, the constants chosen for the whole set are

$$g = 3.50, \quad \alpha = 1.05,$$

so that, for all classes,

$$\frac{k}{N} = \frac{1}{1.862} [1 - \Phi(3.50e^{-cE} - 1.05)] \quad (11 a)$$

(where 1 has been written for  $\Phi(2.45) = 0.9995$ ), and

$$c = 0.050, \quad 0.115, \quad 0.184, \quad 0.285$$

for the classes 1 to 4 respectively. The condition of absence of perceptible fog is amply satisfied by these values of  $g$ ,  $\alpha$ .

In fact, substituting them into (13) one finds  $100 \frac{N_f}{N} = 0.016$ .

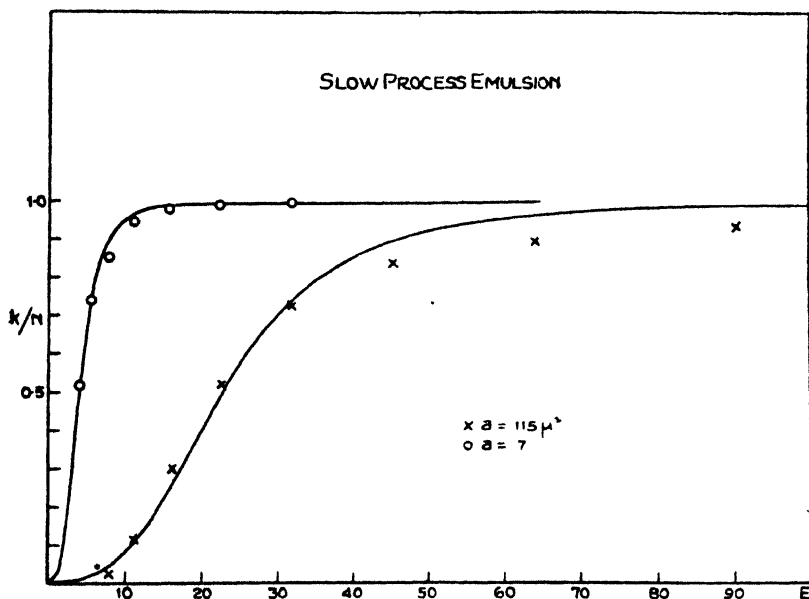


FIG. 1.

A graphic representation of these results is given in fig. 1 for the first and the fourth, and in fig. 2 for the second and the third classes of grains. The theoretical curves, especially those for class 3 and class 4, seem to follow the observed points closely enough, the deviations being on the whole irregular and scarcely exceeding the limits of the experimental error in determining the numbers  $k$ . Only the upper part of the first and, to a lesser extent, that of the second-class curve are systematically a few per cent. above

the points representing the observations. This, however, does not much disturb the characteristic similarity of the theoretical and the experimental curves.

The following is an interesting property of this set. The ratios of the values of the coefficient  $c$  for the four classes are

$$c_1 : c_2 : c_3 : c_4 = 10 : 23 : 37 : 57,$$

while

$$a_1 : a_2 : a_3 : a_4 = 10 : 26 : 43 : 61.$$

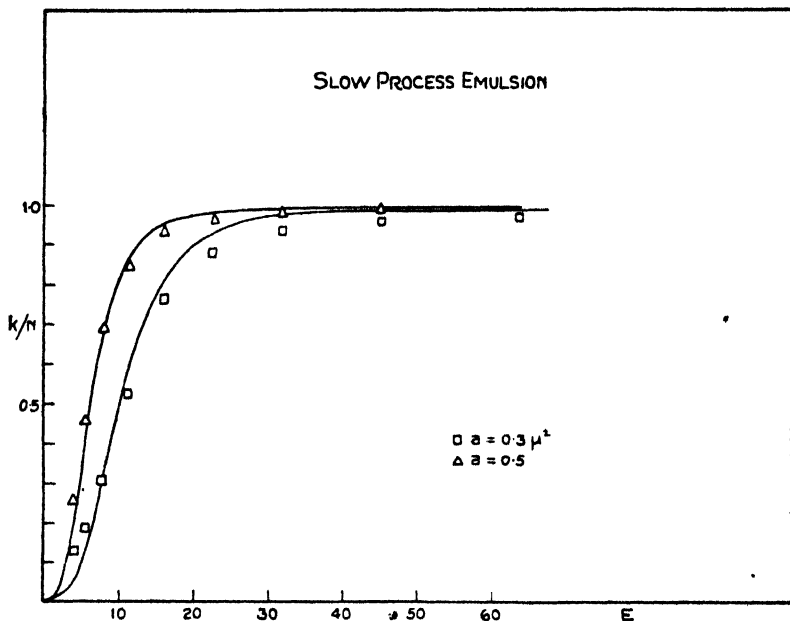


FIG. 2.

Thus the coefficient  $c$  increases but a little more slowly than the size (area) of the grains. In fact, the four values of  $c/a$  being

$$0.43, 0.38, 0.37, 0.41,$$

$c$  may, within the limits of experimental error, be taken to be proportional to the size  $a$ . If the mean of these four values is adopted,  $c=0.40 a$ . Approximately, therefore,  $k$  depends in this case on the product  $Ea$  only (incident light flux per grain), the data for all four classes being represented by the single formula (11a) with the exponent  $cE$  replaced by  $0.40 Ea$ . The dependence of the photographic effect upon  $Ea$  alone, which on the quantum theory appeared as an essential property, may of course be only a peculiarity of this

emulsion without, for the present, deserving to be considered as a general rule.

At any rate the totality of the data is fairly well represented by the formula (11a). The corresponding curve is redrawn in fig. 3 with  $x=cE$  as abscissa, the observed values of  $k/N$  for all four classes of grains being now plotted against  $x$ , with the original  $c$ -values. (The observed "points" are marked by crosses, squares, triangles, and circlets for the 1st to 4th classes respectively.)

Thus far the Slow Process emulsion.

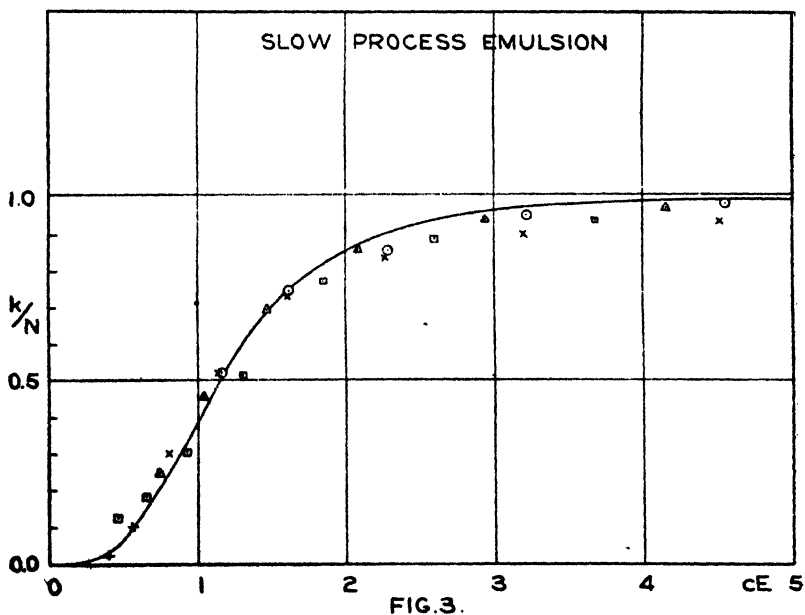


FIG. 3.

In the next place we will consider the experimental results obtained by Toy with the Ilford Process emulsion. Dr. Toy \* gives two sets of his "smooth-curve" values of the percentage of grains ( $100 k/N$ ) made developable by light of different intensities at constant exposure time, one set for grains of diameter  $0.75 \mu$  and another for grains of diameter  $0.60 \mu$ . The former, a rather short set (starting from the high percentage 35.5), cannot be adequately represented by our formula (11), but the latter set agrees with this formula well enough. This set of observed values is arrayed in the third row of Table II. The numbers of the second row are

\* Phil. Mag. vol. xlv. p. 720 (1923).



calculated according to formula (11), with the constants

$$g=2.50, \quad \alpha=0.25, \quad \text{and} \quad c=7.37.$$

The relative exposures  $E$  are identified with Toy's relative intensities (at constant exposure time).

TABLE II.

$E \dots$	0.050	0.075	0.100	0.150	0.200	0.250	0.300	0.350	0.400	0.450	0.500
$100 \ k/N$											
calc. ...	2.8	7.2	14.1	32.4	50.8	65.5	76.3	83.7	88.8	92.3	94.6
obs. ...	2.0	7.0	16.0	35.5	52.0	63.5	73.0	79.0	84.5	89.8	93.5

A graphic representation of these results is given in fig. 4.

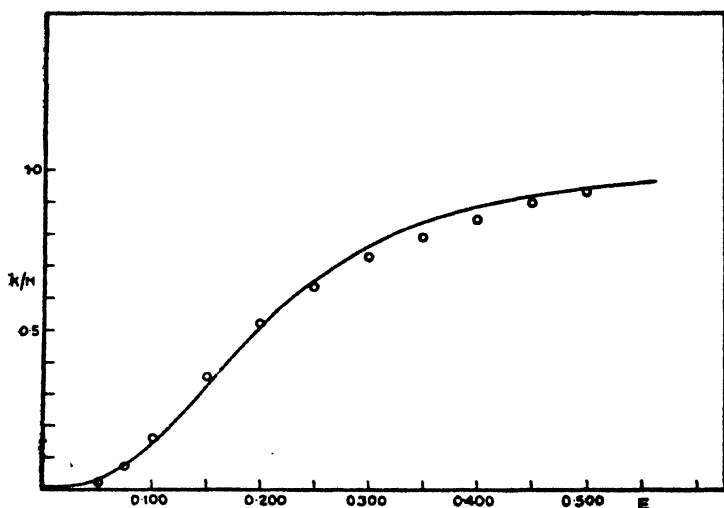


FIG. 4.

The agreement between the calculated and the observed values is fairly close, the largest difference being 4.7. The small residues could still be reduced somewhat by slightly modifying the constants, but this is hardly worth the trouble, especially as, the original observations not being quoted, the amounts carried away by Toy's smoothing process are unknown. The percentage of fog-grains corresponding to the adopted values of  $g, \alpha$  would, by (13), be as low as 0.12 per cent., and thus again imperceptible. As Toy's computation method is independent of the number of fogged grains present, no such number is quoted in his paper, so

that in this respect no definite objection can be raised against these values of the constants.

Further, we may apply the formula (11) to some unpublished experimental results obtained in this laboratory by Trivelli and Loveland (July 1926) on the Eastman 40 emulsion. These data consist of three sets, relating to grains of size 0.4, 0.8, 1.2  $\mu^2$ . The first class of grains, for which the results are

E .....	1	$\sqrt{2}$	2	$2\sqrt{2}$	4	$4\sqrt{2}$	8	$8\sqrt{2}$	16	$16\sqrt{2}$	32	$32\sqrt{2}$
100 $k/N$ ...	1.1	3.2	7.4	10.6	15.5	22.2	27.6	38.9	46.3	54.6	58.2	62.3,

shows the peculiar behaviour that its  $k/N$ -values tend with increasing exposure \* apparently to 0.62 or 0.65 instead of unity, as if about 35 per cent. of these, the smallest grains, were completely insensitive to the applied intensity of light (i. e.,  $s \ll \sigma$ , and not growing at that light-intensity). This state of things cannot be represented by the theory under discussion without modifying essentially our assumption about the law of growth or the size-distribution law of the nuclei, unless one decided to consider as  $N$  only the fraction 0.65 of all grains originally present. The data for the second-, and especially the third-size class of grains ( $a=1.2$ ), do not show this peculiar tendency, and can be covered by our formula (11) rather closely, as will be seen from Table III. and the corresponding graph (fig. 5). As a number of trials have shown, about the best agreement is obtained when the constants in formula (11) are given the values

$$g=1.00, \quad \alpha=0.50, \quad c=0.311;$$

with these the numbers of the second row of the tables were calculated.

TABLE III.

E .....	1	$\sqrt{2}$	2	$2\sqrt{2}$	4	$4\sqrt{2}$	8	$8\sqrt{2}$	16	$16\sqrt{2}$	32	$32\sqrt{2}$
100 $k/N$												
calc. ...	25.2	34.6	46.0	62.4	73.0	84.2	92.7	97.4	99.3	99.9	100	100
obs. ....	21.5	35.2	43.0	62.7	72.7	85.8	93.5	95.3	(95.3)	99.4	99.4	99.4

The values of  $g$ ,  $\alpha$ , however, would imply, by (13), the presence of a very high percentage of fog-grains, namely little less than 32 per cent., which of course is out of the question. (The constants  $g=1.40$ ,  $\alpha=0.25$ , and  $c=0.43$ , giving a somewhat less close but still tolerable agreement

\* Increasing exposure time, that is, at constant intensity.

with the observed  $k/N$ , would reduce the theoretical fog to 8 per cent., but even this may be too high; the actual fog, if any, scarcely exceeded 2 or 3 per cent.) Thus, if, in view of the close agreement exhibited by the last table, we wished to retain these values of  $g, \alpha$ , we would have to assume that, in this emulsion at least, pre-exposure nuclei larger than  $\sigma$  are comparatively rare; *i.e.*, that for  $s > \sigma$  the number of grains having such nuclei diminishes more rapidly than would correspond to the normal frequency distribution (8). This would evidently make the number of

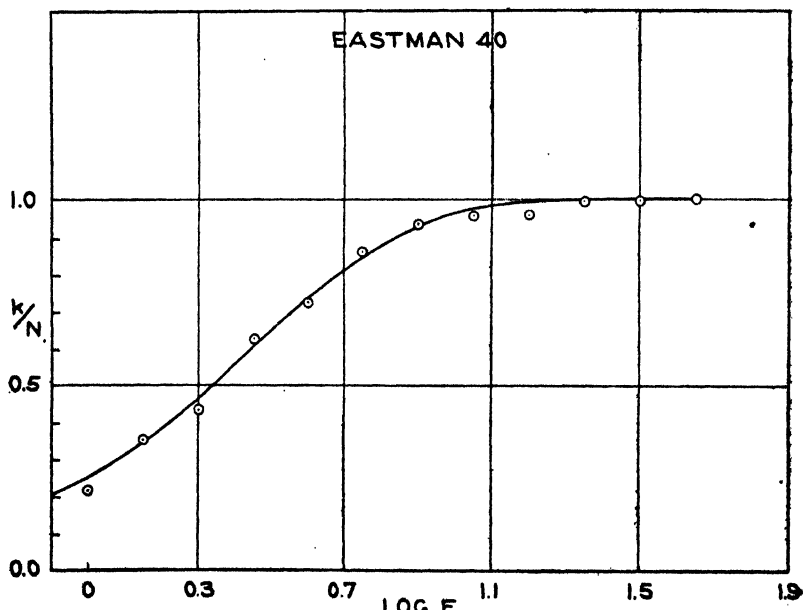


FIG. 5.

fog-grains smaller than that required by (13). Yet it must be admitted that, although not unlikely, such a hypothesis, introduced *ad hoc*, is not very satisfactory.

For the present but one more set of experimental data is available, and will be considered here. These, not yet published, were recently obtained in this laboratory by Trivelli and Loveland with a pure bromide emulsion. The grains were divided into four size-classes, ranging from 0.02 to 1.5, 1.5 to 3.0, etc., up to  $6\mu^2$ , and a "remainder" extending from  $6\mu^2$  upwards. The results,  $k/N$  as function of exposure time at constant intensity, were for the first

four classes utterly irregular, and only the last class could at all be utilized for the purpose in hand. The observed (not smoothed) values of  $100 k/N$  are given in the last row of Table IV., the numbers of the second row being calculated by formula (11), with the constants

$$g=1.25, \alpha=0.40, \text{ and } c=0.133.$$

TABLE IV.

E .....	1	$\sqrt{2}$	2	$2\sqrt{2}$	4	$4\sqrt{2}$	8	$8\sqrt{2}$	16	$16\sqrt{2}$
100 $k/N$										
calc. ....	8.1	11.6	16.8	24.0	34.0	46.7	61.4	75.8	87.4	95.0
obs. ....	7.6	—	20.5	(32.2)	33.3	45.6	57.9	74.6	88.6	98.3

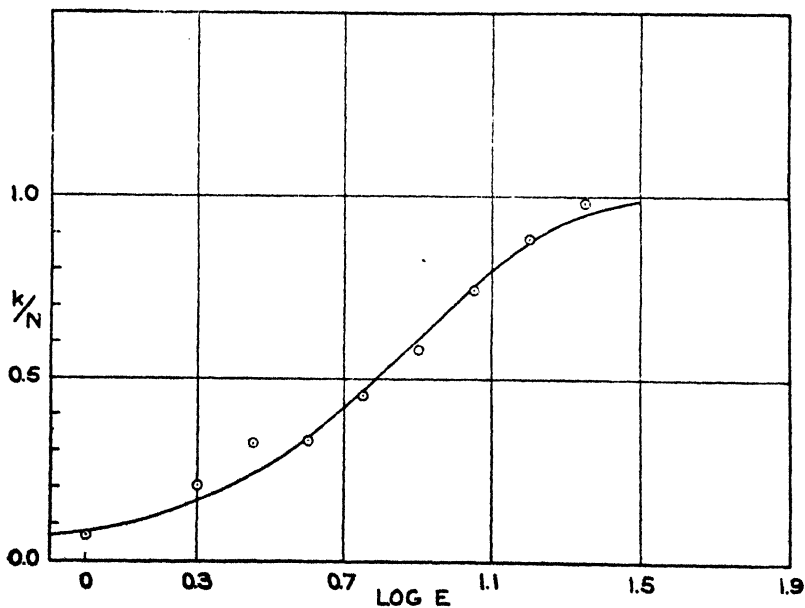


FIG. 6.

The agreement, as shown also in fig. 6, seems in itself quite satisfactory. But these values of  $g$ ,  $\alpha$  would again imply through (13) the presence of too many fog-grains, though not so many as in the preceding case, viz., 16 per cent. The above-said limitation of the distribution law (8) would then again have to be applied.

To sum up, the formula (11) for the number of grains made developable by a given exposure, based upon the size-frequency distribution (8) and the law of growth (6) of the nuclei, can be said to represent the greater part of the

available experimental data with fair accuracy, the deviations being mostly within the limits of experimental error. The number of fog-grains ( $s > \sigma$ ), however, implied by the best values of  $g, \alpha$  is, according to the subsidiary formula (13), in two cases much too large; and since the latter formula is a direct consequence of the distribution law (8), this would have to be replaced by a frequency which beyond  $\sigma$  falls off more rapidly. Whenever  $g - \alpha$  is large enough (say only 1.5), as in most cases considered above, this difficulty does not arise, and it remains to be seen whether such will not be also the case of the majority of future experimental findings.

*A Refinement of the Main Formula. Effect of Finite Size of and Competition between the Nuclei.*

Formula (11) for the number of grains affected by a given exposure is capable of a certain refinement which, though verifiable only on much more accurate data than those hitherto available, has even at this stage seemed to offer some interest.

In deriving that formula, account was taken only of a single nucleus for each grain, namely the largest of those present upon the grain; and its logarithmic rate of growth was assumed to be proportional to the incident light-intensity, the coefficient  $c$  being supposed constant. This assumption, expressed by (6), gave the simple relation  $s/\sigma = e^{-cE}$ .

Now, since the nuclei grow, simultaneously, by accretion of silver atoms derived more or less directly from the whole grain, it is reasonable to assume that the (logarithmic) rate of growth of each nucleus is, *ceteris paribus*, some function of that part of the area of the grain which is not occupied by nuclei formed up to the given instant. The nuclei being very small compared with the grain, such a modification of our original assumption will affect the final result only to a small degree. Yet the effect may turn out to be perceptible, and it has therefore seemed worth while to derive the consequence of the proposed modification.

Let us then consider a grain having  $\kappa + 1$  nuclei of initial sizes  $s, s_1, s_2, \dots s_\kappa$ , of which  $s$  is the largest. Let  $\sigma', \sigma'_1, \sigma'_2, \dots \sigma'_\kappa$  be their sizes at any stage  $t$  of growth, and  $a$  the size of the grain. Then the modified assumption may be written

$$\left. \begin{aligned} \frac{d\sigma'}{\sigma'} &= f(a - \sigma' - \sigma'_1 - \sigma'_2 - \dots - \sigma'_\kappa) I dt, \\ \frac{d\sigma'_1}{\sigma'_1} &= f(a - \sigma' - \sigma'_1 - \sigma'_2 - \dots - \sigma'_\kappa) I dt, \text{ etc.,} \end{aligned} \right\} \quad (14)$$

where the form of the function  $f$ , which will be left unspecified, may vary from emulsion to emulsion. Thus, for instance, in the case of the four classes of the Slow Process emulsion  $f$  would be nearly proportional to its argument.  $\Sigma\sigma''$  being small compared with  $a$ , and also (as we will assume) compared with  $f(a)/f'(a)$ , we can write

$$f(a - \sigma' - \sigma_1' - \dots - \sigma_{\kappa}') = c[1 - \beta(\sigma' + \sigma_1' + \dots + \sigma_{\kappa}')],$$

where  $c = f(a)$ ,  $\beta = f'(a)/f(a)$ .

The right-hand members of the  $\kappa + 1$  equations (14) being all equal, we have, for  $i = 1, 2, \dots, \kappa$ ,

$$\frac{d\sigma_i'}{\sigma_i'} = \frac{d\sigma'}{\sigma'},$$

whence  $\log \frac{\sigma_i'}{\sigma'} = \text{const.}$ ,  $\sigma_i'/\sigma' = \text{const.}$ , i. e.,

$$\sigma_i'/\sigma' = s_i/s. \quad \dots \quad (15)$$

In fine, all the nuclei upon the same grain grow proportionally to each other. It is thus enough to consider only one of the equations (14). We will take that for the largest nucleus, since this decides the final developability of the grain. Thus, introducing (15) into the first of (14), and writing  $\text{Idt} = dE$ ,

$$\frac{d\sigma'}{\sigma'} = c \left[ 1 - \beta\sigma' \left( 1 + \frac{s_1}{s} + \frac{s_2}{s} + \dots + \frac{s_{\kappa}}{s} \right) \right] dE,$$

or, putting

$$\zeta = 1 + \frac{s_1}{s} + \frac{s_2}{s} + \dots + \frac{s_{\kappa}}{s},$$

which for a given strain is a constant,

$$\frac{d\sigma'}{\sigma'(1 - \beta\zeta\sigma')} = \left[ \frac{1}{\sigma'} - \frac{1}{\sigma' - \frac{1}{\beta\zeta}} \right] d\sigma' = c dE.$$

Thus  $\sigma' / \left( \sigma' - \frac{1}{\beta\zeta} \right) = A e^{cE}$ ,  $A = \text{const.}$ ,

and since  $\sigma' = s$  for  $E = 0$ ,

$$\frac{\sigma'(1 - \beta\zeta s)}{s(1 - \beta\zeta\sigma')} = e^{cE}.$$

In particular, if  $\sigma' = \sigma$  be the size at which the nucleus

becomes developable, and  $E$  the exposure which makes it grow from  $s$  to  $\sigma$ ,

$$\frac{\sigma}{1 - \beta \zeta \sigma} = \frac{s}{1 - \beta \zeta s} e^{cE}.$$

Since  $\beta \sigma$ , and even  $\zeta \beta \sigma$ , will be a small fraction of unity, and the more so  $\zeta \beta s$ , we have, up to second-order terms,

$$\frac{\sigma}{s} [1 + \beta \zeta (\sigma - s)] = e^{cE},$$

and here we may put, in the small correction term,  $s = \sigma e^{-cE}$ .

Thus, ultimately,

$$\left. \begin{aligned} s/\sigma &= e^{-cE} [1 + \beta \zeta \sigma (1 - e^{-cE})], \\ \zeta &= 1 + \frac{1}{s} (s_1 + s_2 + \dots + s_\kappa), \end{aligned} \right\} \quad (16)$$

$c$  being some function of  $a$ , and  $\beta = c'(a)/c(a)$ . This value of  $s/\sigma$ , replacing the original expression  $e^{-cE}$ , is now to be substituted into the previous equation :

$$\frac{k}{N} = \frac{\Phi(g - \alpha) - \Phi\left(g \frac{s}{\sigma} - \alpha\right)}{\Phi(g - \alpha) + \Phi(\alpha)}, \quad (17)$$

giving the number of grains  $k$  made developable by an exposure  $E$ . The departure from the original formula (11) will depend on  $\beta \zeta \sigma$ . (Notice that  $\beta$  is a reciprocal area. If  $c$  is proportional to  $a$ , then  $\beta = 1/a$ .)

The value of the coefficient  $\zeta$  of the correction term may vary from grain to grain, the number of nuclei  $(\kappa + 1)$  as well as their relative sizes,  $\frac{s_1}{s}$ ,  $\frac{s_2}{s}$ , etc., being different for different grains, even if the latter be all of the same size  $a$ . But in applying formula (16), we may as well take for  $\zeta$  a unique number, to be considered as an average value of this grain-coefficient. Thus  $\kappa + 1$  can be replaced by the average number of nuclei per grain, and for every ratio  $s_i/s$  the mean of these ratios can be taken, for which some reasonable value, such as  $\frac{1}{2}$ , may be provisionally adopted. This would give

$$\zeta = 1 + \kappa \left( \frac{s_i}{s} \right) = 1 + \frac{1}{2} \kappa,$$

where, of course,  $\kappa + 1$ , the average number of all nuclei per grain, would still remain unknown and to be determined

experimentally. Thus far, data of this kind, apart from a few probably incomplete results (disclosing perhaps only some of the nuclei), due to Svedberg and Toy, do not seem to be available. Still less known is  $\sigma$ , the minimum size of an "active" or developable nucleus. This, moreover, will depend on the development. Under such circumstances the whole coefficient  $\beta\zeta\sigma$  of the correction term in formula (16) would have, for the present, to be considered as one more empirical parameter, in addition to the main parameters  $g$ ,  $\alpha$ ,  $c$ , to be adapted to the observed  $k$ ,  $E$  curves.

Rochester, N.Y.

October 3, 1927.

---

*L. On the Coefficient of Sound-absorption Measured by the Reverberation Method. By E. T. PARIS, D.Sc.\**

**T**HERE are several methods of measuring the coefficients of sound-absorption for different materials†. In the reverberation method of W. C. Sabine a specimen of the material to be tested is mounted inside a reverberation-chamber, and the coefficient of absorption (defined as the ratio of the difference between the incident and reflected energy-fluxes to the incident energy-flux) is deduced from the observed effect of the presence of the specimen on the rate of decay of sound in the chamber. According to the theory of reverberation, the specimen receives sound at all angles of incidence from  $0^\circ$  to  $90^\circ$ .

There are, however, other methods of measuring sound-absorption in which plane-waves of sound are made to impinge on a specimen at some definite angle of incidence. For example, in Watson's experiments a beam of sound (produced by means of a source at the focus of a paraboloidal reflector) was directed on to the specimen to be tested. In this method the angle of incidence is determined at will by suitably arranging the relative positions of the specimen and the reflector. Again, in the stationary-wave method sound-waves fall normally on the specimen, the coefficient of absorption being deduced from observations on the interference pattern in front of the specimen.

In general the coefficient of absorption of a given substance is a function of the wave-length of the sound and of

\* Communicated by the Author.

† A description of the methods at present in use is given by Davis and Kaye, 'Acoustics of Buildings,' chap. v. (Bell, 1927).



the angle of incidence, so that the value of the coefficient obtained by the reverberation method cannot be expected to agree with that obtained by one of the other methods mentioned above.

In the present paper an attempt is made to correlate the coefficient of absorption of a substance, measured at some particular wave-length and expressed as a function of the angle of incidence, with the coefficient of absorption determined by Sabine's reverberation method for the same wave-length.

The coefficient measured by Sabine's method will be called the "reverberation coefficient of absorption" and denoted by  $\alpha_r$ . The coefficient of absorption for waves incident at an angle  $\theta$  will be denoted by  $\alpha(\theta)$ .

The theory of reverberation as developed by Sabine, Jäger, and others is a departure from classical methods in theoretical acoustics, and involves certain assumptions regarding the distribution and behaviour of sound-energy in an enclosed space in which reverberation is occurring. Accounts of the theory and of the assumptions made have been given in recent years by E. A. Eckhardt\* and E. Buckingham†. The question of the validity of the assumptions involved will not be discussed here, but attention will be confined to examining the result of introducing the coefficient  $\alpha(\theta)$  into the theory of reverberation with the object of finding a relation between  $\alpha(\theta)$  and  $\alpha_r$ .

The rate at which sound-energy strikes the walls of a room in which reverberation is occurring is found as follows‡. Let  $dS$  be an element of area of the wall of a room in which the acoustical energy-density  $\rho$  is uniform, and let  $dV$  be an element of volume at a distance  $r$  from  $dS$  in a direction making an angle  $\theta$  with the normal  $n$  to  $dS$  (fig. 1). Of the energy  $\rho dV$  contained within  $dV$  at any instant, that portion will ultimately strike  $dS$  which is moving within directions included within the solid angle

$$d\omega = dS \cos \theta / r^2$$

subtended by  $dS$  at  $dV$ . This fraction is  $d\omega/4\pi$ , so that the amount of energy inside  $dV$  which will ultimately strike  $dS$  is

$$(\rho dV dS \cos \theta) / (4\pi r^2).$$

The total amount of sound-energy that falls on  $dS$  in one

\* Journ. Franklin Inst. cixv. p. 799 (1923).

† Sci. Paper of the Bureau of Standards, No. 506 (1925).

‡ Cf. Buckingham, *loc. cit.* p. 201.

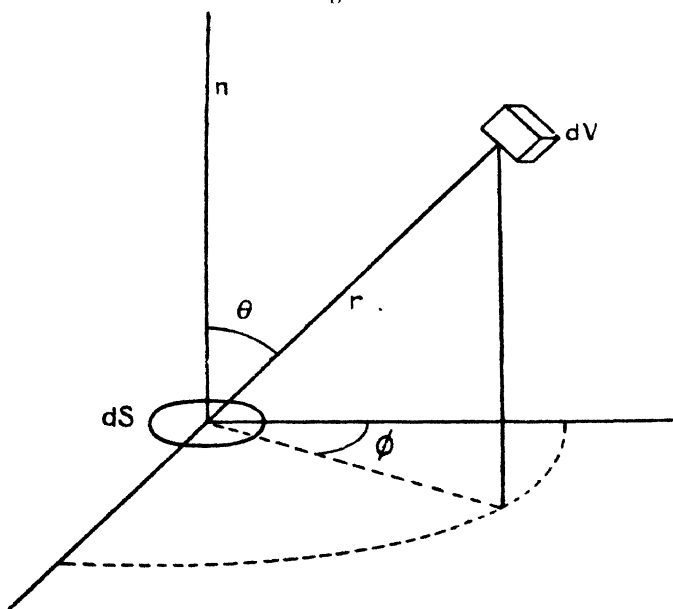
second is obtained by integrating this expression throughout a hemisphere of radius  $a$  described about  $dS$  as centre,  $a$  being the distance traversed by sound in one second. Thus, using polar coordinates  $r, \theta, \phi$  (fig. 1) so that

$$dV = r^2 \sin \theta \, dr \, d\theta \, d\phi,$$

we have for the rate at which sound-energy falls on  $dS$  :

$$\frac{\rho \, dS}{4\pi} \int_0^a dr \int_0^{2\pi} d\phi \int_0^{\pi/2} \sin \theta \cos \theta \, d\theta = \frac{\rho a \, dS}{4} \quad (1)$$

Fig. 1.



The rate at which sound is absorbed at  $dS$  is

$$\alpha_r \left( \frac{\rho a \, dS}{4} \right), \quad (2)$$

where  $\alpha_r$  is the reverberation absorption-coefficient appropriate to the surface of which  $dS$  forms a part.

Another expression for the rate at which sound is absorbed at  $dS$  can be formed by making use of the coefficient  $\alpha(\theta)$ . Thus the rate at which energy coming from  $dV$  is absorbed at  $dS$  is

$$\alpha(\theta) \cdot (\rho \, dV \, dS \cos \theta) / (4\pi r^2),$$

and hence the total rate of sound-absorption at  $dS$  is

$$\begin{aligned} \frac{\rho dS}{4\pi} \int_0^a dr \int_0^{2\pi} d\phi \int_0^{\pi/2} \alpha(\theta) \sin \theta \cos \theta d\theta \\ = \frac{\rho a dS}{2} \int_0^{\pi/2} \alpha(\theta) \sin \theta \cos \theta d\theta. \quad (3) \end{aligned}$$

By equating the expressions (2) and (3) for the rate at which sound is absorbed at  $dS$ , we find

$$\alpha_r = 2 \int_0^{\pi/2} \alpha(\theta) \sin \theta \cos \theta d\theta. \quad (4)$$

This equation provides a means for finding  $\alpha_r$  when  $\alpha(\theta)$  is known. It is clear, however, that in general the determination of  $\alpha_r$  in this way would be very laborious, for it would be necessary to find  $\alpha(\theta)$  for all values of  $\theta$  between 0 and  $\pi/2$  (probably with apparatus of the type used by Watson) before the integration in (4) could be effected. Incidentally, equation (4) shows that a simple determination of the coefficient of absorption at normal incidence, that is  $\alpha(0)$ , by stationary-wave or other small-scale testing apparatus, supplies insufficient data for calculating the reverberation coefficient  $\alpha_r$ .

There is, however, a class of substances for which the difficulty of finding  $\alpha(\theta)$ , and thence  $\alpha_r$  by means of equation (4), is not great. The substances referred to are the porous acoustic tiles and plasters used in architectural acoustics. For such materials it is possible to determine a quantity called the "acoustical admittance per unit area of reflecting surface" from which the coefficient of absorption at any angle of incidence,  $\alpha(\theta)$ , can readily be calculated\*.

Substances of this type absorb sound by virtue of the fact that during reflexion there is a movement of air into and out of the pores of the material. If the pores are small this in-and-out movement of air is accompanied (owing to viscosity) by the degradation of sound-energy into heat. If  $\Phi$  is the velocity-potential due to incident and reflected sound-waves at the surface of a porous medium of the kind indicated, and  $q$  is the volume of air per unit area of surface moving periodically in and out of the pores, then  $q = \Omega \Phi$ , where  $\Omega$  is the "acoustical admittance per unit area of reflecting surface."

An ideal substance of the type contemplated would consist of a flat solid wall perforated by a great number of pores,

\* Proc. Roy. Soc. A, cxv. p. 407 (1927).

bounded by surfaces everywhere perpendicular to the flat face of the wall. The characteristic feature of such a reflecting surface is that sound-waves are produced only in the pores and not in the solid material itself. Also the wave-motion in the pores is not transmitted internally from one part of the reflecting surface to another, so that  $\Omega$  is independent of the angle of incidence. Acoustic tiles and plasters, while not conforming precisely to this specification, appear to do so to an extent which justifies the employment of an "acoustical admittance" (assumed independent of the angle of incidence) in connexion with the investigation of their acoustical properties.

It can be shown\* that the coefficient of absorption of a porous substance of the kind under consideration can be expressed in terms of acoustical admittance per unit area as follows:—

$$\alpha(\theta) = 1 - \left| \frac{\cos \theta - a\Omega}{\cos \theta + a\Omega} \right|^2, \quad \dots \dots (5)$$

where  $a$  is the velocity of sound, and  $\theta$ , as before, is the angle of incidence. If  $\Omega$  is separated into its real and imaginary parts, say  $\Omega = \Omega_1 + i\Omega_2$ , then

$$\alpha(\theta) = \frac{4a\Omega_1 \cos \theta}{\cos^2 \theta + 2a\Omega_1 \cos \theta + a^2(\Omega_1^2 + \Omega_2^2)}. \quad (6)$$

By substituting this value for  $\alpha(\theta)$  in (4), we obtain

$$\alpha_r = 8a\Omega_1 \int_0^{\pi/2} \frac{\cos^2 \theta \sin \theta d\theta}{\cos^2 \theta + 2a\Omega_1 \cos \theta + a^2(\Omega_1^2 + \Omega_2^2)}. \quad (7)$$

Let

$$x = \cos \theta, \quad A = a^2(\Omega_1^2 + \Omega_2^2), \quad \text{and} \quad B = 2a\Omega_1.$$

Then, since  $4A - B^2 > 0$ ,

$$\begin{aligned} \alpha_r &= 4B \int_0^1 \frac{x^2 dx}{x^2 + Bx + A} \\ &= 4B \left[ x - \frac{1}{2}B \log_e (x^2 + Bx + A) \right. \\ &\quad \left. + \frac{B^2 - 2A}{\sqrt{4A - B^2}} \tan^{-1} \left( \frac{2x + B}{\sqrt{4A - B^2}} \right) \right]_0^1. \quad (8) \dagger \end{aligned}$$

\* Proc. Roy. Soc. A, cxv. p. 418 (1927).

† Peirce, 'Short Table of Integrals,' p. 9 (Ginn & Co.).

Or, putting in the values of A and B,

$$\alpha_r = 8a\Omega_1 \left[ 1 - a\Omega_1 \log_e \frac{(1 + a\Omega_1)^2 + (a\Omega_2)^2}{a^2(\Omega_1^2 + \Omega_2^2)} + \frac{a^2(\Omega_1^2 - \Omega_2^2)}{a\Omega_2} \left\{ \tan^{-1} \left( \frac{1 + a\Omega_1}{a\Omega_2} \right) - \tan^{-1} \left( \frac{a\Omega_1}{a\Omega_2} \right) \right\} \right]. \quad (9)$$

By means of (2) the reverberation coefficient can be calculated for any porous reflecting surface for which the acoustical admittance per unit area is known.

For example, a determination was made, by means of stationary-wave apparatus, of the acoustical admittance of "Akoustolith" tile (supplied through the Building Research Board of the Department of Scientific and Industrial Research) at 512 vibrations per second. Details of the apparatus employed and the method of finding "acoustical admittance" have been given elsewhere\*. The value obtained for  $\Omega$  was  $0.0641 - i \times 0.0643$ , and inserting this value in (5) and (9), we find that  $\alpha(0) = 0.23$  and  $\alpha_r = 0.35$ . Thus, according to this calculation, the reverberation coefficient is considerably greater than the coefficient at normal incidence†.

The calculated value of  $\alpha_r$  agrees well with that quoted by Watson‡ for Akoustolith tile at 512 vibrations per second, viz. 0.36. Davis§, however, quoting results obtained at the Building Research Station of the Department of Scientific and Industrial Research by a reverberation method, give the surprisingly low value of 0.19 for the coefficient at the same frequency, this being less than the coefficient at normal incidence. There appears, therefore, to be some uncertainty as to the true value of the reverberation absorption-coefficient of this substance, and no conclusion can safely be drawn as to whether the calculated value of  $\alpha_r$  is or is not confirmed by experiment.

The absorption of sound by an ideal porous substance,

\* The apparatus is described in Proc. Phys. Soc. xxxix. p. 274 (1927); the method of finding  $\Omega$  is given in Proc. Roy. Soc. A, cxv. p. 418 (1927).

† The value of 0.23 for  $\alpha(0)$  is less than that given in an earlier paper, viz. 0.26 (Proc. Phys. Soc. xxxix. p. 281, 1927); this may be due to the fact that the specimen used in the present test was an old one and had suffered some damage which had been repaired with plaster of Paris.

‡ 'Acoustics of Buildings,' p. 25.

§ 'Acoustics of Buildings,' p. 116.

presenting a flat surface to the incident sound, and perforated by a large number of similar channels bounded by surfaces perpendicular to the face, was the subject of a theoretical investigation by Rayleigh \*. It has been pointed out in a previous paper † that, in the special case when the pores are so long that the vibrations within them are sensibly extinguished before the stopped ends are reached, the acoustical admittance per unit area (derived from equations given by Rayleigh) has a specially simple form, being proportional to the fraction of the area of the reflecting face which is occupied by the pore-openings. If  $\sigma$  is the perforated and  $\sigma'$  the corresponding unperforated area,

$$a\Omega = \sigma/(\sigma + \sigma'). \quad . \quad . \quad . \quad . \quad (10)$$

The coefficient of absorption at an angle  $\theta$  is, by (5),

$$\alpha(\theta) = \frac{4a\Omega \cos \theta}{(a\Omega + \cos \theta)^2}, \quad . \quad . \quad . \quad (11)$$

which becomes unity when  $\cos \theta = a\Omega$ , so that there is always some angle of incidence, given by  $\cos \theta = \sigma/(\sigma + \sigma')$ , at which total absorption occurs. With  $B = 2a\Omega$  we have, instead of (8),

$$\begin{aligned} \alpha_r &= 4B \int_0^1 \frac{x^2 dx}{(x + \frac{1}{2}B)^2} \\ &= 8a\Omega \left\{ \frac{1 + 2a\Omega}{1 + a\Omega} - 2a\Omega \log_e \frac{1 + a\Omega}{a\Omega} \right\}. \end{aligned} \quad (12) \dagger$$

Some numerical results obtained by means of (11) and (12) are given in the following table and serve (in the absence of

$\sigma/(\sigma + \sigma')$ .	$\theta_m$ .	$\alpha(0)$ .	$\alpha_r$ .
0.05	87 08	0.18	0.30
.1	84 15	.33	.49
.2	78 28	.56	.72
.3	72 32	.71	.84
.5	60 00	.89	.94
.7	45 34	.97	.95
.9	25 50	.997	.93
1.0	00 00	1.000	.91

\* Phil. Mag. xxxix. p. 225 (1920); Sci. Papers, vi. p. 662.

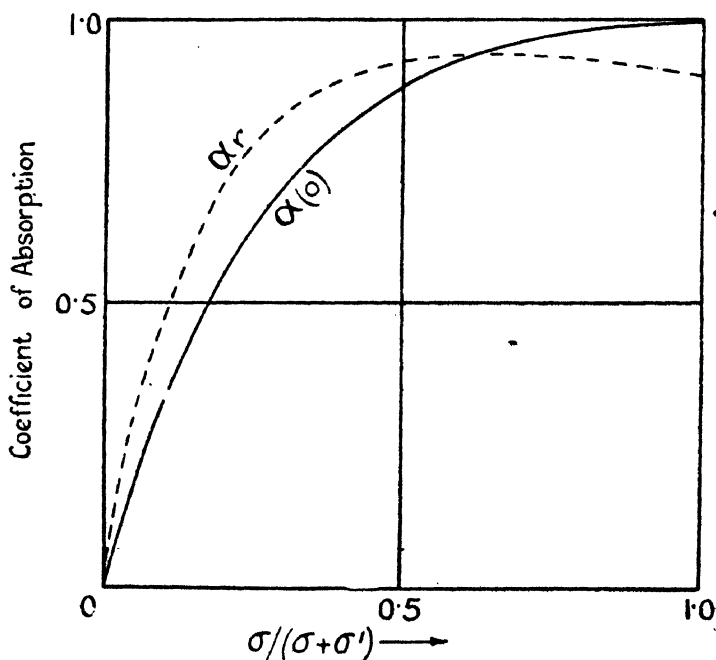
† Proc. Roy. Soc. A, cxv. p. 413 (1927).

‡ Peirce, 'Short Table of Integrals,' p. 6 (Ginn & Co.).

data concerning substances actually employed for absorbing sound) to indicate how a reverberation coefficient may differ from the coefficient at normal incidence. The first column gives the value of  $a\Omega$ , or  $\sigma/(\sigma + \sigma')$ ; the second column gives the value ( $\theta_m$ ) of the angle of incidence at which total absorption occurs; the third and fourth columns give the values of  $\alpha(0)$  and  $\alpha_r$  calculated from (11) and (12) respectively.

If the figures in the last two columns are plotted against

Fig. 2.



$\sigma/(\sigma + \sigma')$  as in fig. 2, it is seen that  $\alpha_r = \alpha(0)$  when  $\sigma/(\sigma + \sigma') = 0.65$  approximately,  $\alpha_r$  being greater than  $\alpha(0)$  when  $\sigma/(\sigma + \sigma')$  is smaller than this value and less than  $\alpha(0)$  when it is greater. The rise in  $\alpha_r$  as  $\sigma/(\sigma + \sigma')$  is increased from 0 to 0.3 is very rapid, but little can be gained by making the proportion of perforated area greater than 0.3.

The reverberation coefficient passes through a maximum value of about 0.95 when  $\sigma/(\sigma + \sigma')$  is between 0.6 and 0.7,

that is when  $\theta_m$  is between  $45^\circ.5$  and  $53^\circ.1$ . This result is in accordance with the fact that the amount of energy incident at an angle  $\theta$  on an element of surface is proportional to  $\sin 2\theta$ , and is a maximum when  $\theta = 45^\circ$ . It is therefore reasonable that  $\alpha_r$  should be a maximum when  $\theta_m$ , the angle at which total absorption occurs, is in the neighbourhood of  $45^\circ$ .

In conclusion, it should perhaps be emphasized that the results obtained in this paper are dependent on the assumption made in the theory of reverberation as to the behaviour of aoustical energy in an enclosed space. Interference is entirely ignored. The justification for this assumption is that it provides a theoretical basis for the reverberation formulæ which have been used with such striking success in auditorium acoustics. It remains to be seen whether its employment for establishing a relation between reverberation coefficients of absorption and those obtained by other methods will be justified by experimental results.

The investigation described in this paper was undertaken in connexion with experiments on sound-absorption carried out in the Aoustical Section of the Air Defence Experimental Establishment with the aid of funds provided by the Department of Scientific and Industrial Research on the recommendation of their Physics Research Board.

### *Summary.*

A formula is deduced from reverberation theory by means of which the reverberation coefficient of absorption of a material can be calculated if the coefficient for plane waves is known for all angles of incidence between 0 and  $\pi/2$ . In the case of certain porous substances the reverberation coefficient can be found if the aoustical admittance per unit area is known. It is shown that in general the reverberation coefficient differs from the coefficient at normal incidence. Some numerical values for an ideal porous substance are given by way of illustrating the results obtained.

Biggin Hill, Kent,  
November 1927.



LI. *A Theory of Light-Scattering in Liquids.*  
 By Prof. C. V. RAMAN, F.R.S., and K. S. KRISHNAN \*.

1. *Introduction.*

THE theory of light-scattering in gases with optically anisotropic molecules was discussed by the late Lord Rayleigh † and by Born ‡, whose investigations showed that the anisotropy results in the transversely scattered light becoming imperfectly polarized and also in making its intensity greater than for a gas of equal refractivity with isotropic molecules. In a monograph § by one of us, published in February 1922, and in further papers communicated shortly afterwards to the *Philosophical Magazine* ||, the case of dense fluids was dealt with, and it was shown that by considering the scattering due to the thermal fluctuations of density in the fluid and also the additional scattering due to the anisotropy and varying orientations of the molecules, the observed phenomena could be satisfactorily explained. A general theory of light-scattering in fluids from the molecular standpoint was worked out shortly afterwards in two papers by Dr. K. R. Ramanathan ¶. His treatment is very wide in its scope and is applicable equally to the case of polar and non-polar molecules. Dr. Ramanathan has returned again to the subject, and in a recent paper \*\* has examined critically the relation of his general theory to the special treatment worked out by R. Gans †† for the restricted class of liquids with non-polar molecules.

An examination of the data for depolarization of the light scattered by fluids with the aid of Ramanathan's formulæ indicates an apparent change (usually a large diminution) in the optical anisotropy of the molecules of a given substance as it passes from the condition of vapour to that of liquid ‡‡. A similar discrepancy becomes apparent when the optical anisotropy of the molecule is determined from the

\* Communicated by the Authors.

† Lord Rayleigh, *Phil. Mag.* vol. xxxv. p. 373 (1918).

‡ M. Born, *Deutsch. Phys. Gesell. Ver.* vol. xix. p. 243 (1917).

§ C. V. Raman, 'Molecular Diffraction of Light,' *Calcutta Univ. Press* (1922).

|| C. V. Raman and K. R. Ramanathan, *Phil. Mag.* vol. xlv. p. 113 (1923); C. V. Raman and K. S. Rao, vol. xlv. p. 625 (1922).

¶ K. R. Ramanathan, *Proc. Ind. Assoc. Cult. Sc.* vol. viii. pp. 1 & 181 (1923).

\*\* K. R. Ramanathan, *Indian Journal of Physics*, i. p. 413 (1927).

†† R. Gans, *Zeits. für Physik*, xvii. p. 363 (1923).

‡‡ K. S. Krishnan, *Proc. Ind. Assoc. Cult. Sc.* ix. p. 251 (1926).

electric double refraction in the liquid \*, using the well-known formula due to Langevin, and is compared with the value derived from observations on light-scattering in the vapour. As an explanation of this phenomenon it may of course be suggested that some kind of temporary grouping or association of neighbouring molecules occurs in the liquid in such a manner as to diminish their effective optical anisotropy. Such an assumption however, besides being artificial and qualitative, would appear difficult to sustain, particularly when it is noticed that the apparent diminution of optical anisotropy is quite as marked in liquids usually considered as "non-associated," *e. g.* the paraffins, as in others which are typically "associated" like the alcohols. The facts stated above necessitate a revision of the theory of light-scattering in liquids. It is proposed in this paper to put forward a theory which does not involve any artificial hypotheses and which offers a natural explanation of the observed facts.

## 2. The Fundamental Postulates.

Any satisfactory theory of our subject must consider the optical properties of the molecules composing the fluid, their distribution and orientations in space, and the field actually acting on them. We assume that the molecules are polarizable differently along three mutually perpendicular directions fixed to them, which might be called the principal optic axes of the molecules. As to their distribution and orientations in space, we have not at present full knowledge. The molecular aggregation in liquids is presumably intermediate in character between the two extreme cases of an ideal crystalline solid and a perfect gas. If we follow an individual molecule in a liquid over a sufficiently long time, it can take up all possible positions and orientations, and thus the conditions approximate to those of a gas. If, however, we consider a molecule in relation to its immediate neighbours, the analogy between the solid and liquid states is closer. We are not justified in treating the space-distribution as random, because the molecules have a finite size, and in the dense assemblage forming a liquid they would naturally restrain each other's freedom of movement to a considerable extent. On the other hand, we shall not be seriously in error if we assume the freedom of orientation of the molecules to be comparatively unrestricted in most liquids. It is true that in many actual cases the molecules

\* C. V. Raman and K. S. Krishnan, *Phil. Mag.* iii. p. 727 (1927).

are highly unsymmetrical in shape, and hence in finding the probability of any particular configuration of neighbouring molecules, both spacing and orientation have to be considered together. Nevertheless, we may regard the effect of molecular collisions as equivalent approximately to a restriction of the possible arrangements of the molecules in space, while their freedom of orientation is retained.

To make our ideas more precise, we may fix our attention on a volume element in the liquid whose linear dimensions are large in comparison with the size of a molecule, and consider the spontaneous fluctuations in the number and orientations of the molecules contained in it. We shall make the following assumptions:—

(1) That the fluctuations in density of the fluid present in an element of volume  $\delta v$  are given by the usual Smoluchowski-Einstein expression

$$\overline{\delta n^2} = \frac{RT\beta n_0^2}{N\delta v}, \quad . \quad . \quad . \quad . \quad . \quad (1)$$

where  $\overline{\delta n^2}$  is the mean square of the deviation of the number of molecules per unit volume from its mean value  $n_0$ ,  $R$  and  $N$  are the gas constant and Avogadro number respectively per gram molecule,  $\beta$  is the isothermal compressibility, and  $T$  is the absolute temperature.

(2) That the number of molecules in the volume element having at any instant any given orientation, will be the same as though all the molecules in the volume element were oriented entirely at random, and that fluctuations in orientations are entirely uncorrelated with the fluctuations in density.

### 3. *The Polarization Field in Liquids.*

We have next to consider the question of the field actually acting on any molecule in the liquid. In a gas this will evidently be the same as the field of the incident light-wave. In a liquid, however, we have also to take into account the field due to the doublets induced in the surrounding molecules. This "polarization field" is usually taken to be

$\frac{4\pi}{3}\chi E$ , where  $\chi$  is the susceptibility of the medium per unit volume and  $E$  is the incident field, it being thus tacitly assumed that the polarization field acting on any given molecule is independent of its orientation in the field. This assumption would be valid, only if the molecules surrounding

it were distributed in such a manner as to be equivalent to a spherically symmetrical arrangement of polarizable matter. While this assumption may be justified for molecules at a sufficient distance from the one under consideration, it is not necessarily true in respect of its immediate neighbours. If the shape of a molecule departs greatly from spherical symmetry, it would be incorrect to regard the distribution of polarizable matter immediately surrounding it as completely symmetrical. The polarization field acting on a molecule must thus, in general, vary with its orientation in the external field. To express this "anisotropy" of the polarization field in mathematical language, we choose three mutually perpendicular axes fixed in the molecule such that when the incident field lies along any one of them, the polarization field is also in the same direction, and is given by  $p_1\chi E$ ,  $p_2\chi E$ , or  $p_3\chi E$ , where  $p_1$ ,  $p_2$ ,  $p_3$  are constants characteristic of the molecule for the given density and temperature of the liquid. It is quite possible to discuss the general case where these axes of the molecule are different from its optic axes. However, for simplicity we may assume that the two sets of axes are coincident in direction.

An important question which arises here is whether the local field acting on a molecule is influenced appreciably by the fluctuations of density and molecular orientation in its immediate neighbourhood. This question has been discussed by Ramanathan in his recent paper, and he has given reasons for assuming that the local field should be regarded as constant. His argument may be modified and expressed in the following way:—The local field arises in part from the external field, and in part from the polarization of the entire medium surrounding the molecule under consideration. If the distribution at any instant, of polarizable matter surrounding the molecule, can be regarded as spherically symmetrical, it can be shown by dividing up the medium into concentric spherical shells that the polarization field acting on the molecule at the centre is unaffected by either a diminution or an increase of density in its immediate neighbourhood. This conclusion remains valid even if there be fluctuations from spherical symmetry in the distribution of polarizable matter round the molecule, for it may be shown that this would give rise to a fluctuation of the polarization field which would be uncorrelated in sign with the local variation of density and may therefore be left out of account. The argument of Ramanathan appears to be correct, and, as we shall show later in the course of the paper, its validity remains substantially unaffected even when, as

in our present treatment, the polarization field acting on a molecule is assumed to vary with its orientation in the external field. We now proceed to modify the treatment of light-scattering given by Ramanathan so as to take the 'anisotropy' of the polarization field into account.

#### 4. Radiation from a given Molecule.

Let a beam of plane-polarized light be incident in the medium along the  $x$ -axis of a system of coordinates  $xyz$  fixed in space, the electric vector of the light-wave, equal to  $E$ , say, lying along the  $z$ -axis. Let us consider a molecule at  $O$  radiating under the influence of the light-wave. We choose the optic axes of the molecule as the axes of another coordinate system  $\xi\eta\zeta$ , of course rigidly fixed to the molecule, their orientation in space being defined with reference to the  $xyz$  axes by the usual Eulerian angles  $\theta, \phi, \psi$ . Then the cosines of the angles between the different axes are given by the following table

TABLE I.

	$x.$	$y.$	$z.$
$\xi \dots$	$\alpha_{11} = \cos \theta \cos \phi \cos \psi$ $\quad - \sin \phi \sin \psi.$	$\alpha_{12} = \cos \theta \sin \phi \cos \psi$ $\quad + \cos \phi \sin \psi.$	$\alpha_{13} = - \sin \theta \cos \psi.$
$\eta \dots$	$\alpha_{21} = - \cos \theta \cos \phi \sin \psi$ $\quad - \sin \phi \cos \psi$	$\alpha_{22} = - \cos \theta \sin \phi \sin \psi$ $\quad + \cos \phi \cos \psi.$	$\alpha_{23} = \sin \theta \sin \psi.$
$\zeta \dots$	$\alpha_{31} = \sin \theta \cos \phi.$	$\alpha_{32} = \sin \theta \sin \phi.$	$\alpha_{33} = \cos \theta.$

Now, if  $A, B, C$  be the moments induced in a molecule per unit field acting respectively along its three axes, then the actual moments induced in the molecule at  $O$  along its axes by the electric vector of the light-wave are

$$\left. \begin{aligned} &AE(1+p_1\chi)\alpha_{13}, \\ &BE(1+p_2\chi)\alpha_{23}, \\ &CE(1+p_3\chi)\alpha_{33} \end{aligned} \right\} \dots \dots \dots (2)$$

and

respectively. We may denote these expressions shortly by  $A'E\alpha_{13}$ ,  $A'E\alpha_{23}$ , and  $C'E\alpha_{33}$ , where

$$\left. \begin{aligned} &A' = A(1+p_1\chi), \\ &B' = B(1+p_2\chi), \\ &C' = C(1+p_3\chi). \end{aligned} \right\} \dots \dots \dots (3)$$

When these moments are resolved along the  $x$ -axis, their sum is equal to

$$M_x = E(A'\alpha_{13}\alpha_{11} + B'\alpha_{23}\alpha_{21} + C'\alpha_{33}\alpha_{31}). \quad (4)$$

At a large distance  $d$  from the molecule measured along the  $y$ -axis, *i. e.* transversely to both the direction of vibration and the direction of propagation of the incident light, the amplitude of the  $x$ -component in the radiation from the given molecule is obviously equal to

$$\frac{k^2}{d} M_x, \quad (5)$$

where

$$k = \frac{2\pi}{\lambda}.$$

Similarly, the amplitude of the  $z$ -component of the radiation from the given molecule will be equal to

$$\frac{k^2}{d} M_z, \quad (6)$$

where  $M_z$  is the sum of the resolved components along the  $z$ -axis, of the moments induced in the molecule, and is given by

$$M_z = E(A'\alpha_{13}^2 + B'\alpha_{23}^2 + C'\alpha_{33}^2). \quad (7)$$

### 5. Orientation Scattering.

We now imagine the space occupied by the fluid to be divided into a large number of equal volume elements forming the cells of a regular cubic space-lattice. The linear dimensions of the volume element are assumed to be small in comparison with a wave-length, and at the same time large enough to include a great many molecules. The fluctuations in the number and orientations of the molecules in any one element may, in the circumstances, be considered to be independent of the fluctuations in the adjoining ones. At any given instant the radiations from the different molecules in a volume element may be taken to be in the same phase; and in order to get their instantaneous aggregate effect at the point of observation, we have merely to add up the amplitudes due to the individual molecules. Thus, for instance, the amplitude, at any given instant, of the  $x$ -component of the radiation from a volume element  $\delta v$  will be given by

$$X = \frac{k^2}{d} \Sigma M_x, \quad (8)$$

where  $\Sigma$  denotes summation over all the molecules in  $\delta v$ .

We have next to compound the effects due to the different

volume elements. Since each of these contains a large number of molecules, which, as mentioned in section 2, are oriented at random, the average value of  $\Sigma M_x$  (given by (4)) taken over the different volume elements will be nothing. However, for any single element,  $\Sigma M_x$  will, in general, be finite, being as often positive as negative, its actual value being determined by the chance orientations at the given instant of the molecules present in it. The values of  $\Sigma M_x$  for different volume elements will thus be entirely uncorrelated, and the resultant effect is accordingly obtained by addition of the intensities (represented by the squares of the amplitudes), and not by addition of the amplitudes. Thus the problem reduces to one of finding the average value of the intensity taken over all the volume elements, and will evidently be the same as finding what is called in the theory of probabilities the "expectation" of intensity from a single volume element; *i. e.*, the mean value of the intensity to be expected after a very large number of trials in each of which the number and the orientations of the molecules present in it are rearranged arbitrarily according to the principles of statistical mechanics.

Since, as is evident from (1), the fluctuation of density is very small in comparison with the mean density, we may reasonably assume in the calculation that in the different trials the total number of molecules in the element of volume does not vary, only their orientations varying arbitrarily. The expectation of  $X^2$  from  $\delta v$  will then be given by

$$\overline{X^2} = \frac{k^4}{d^2} \times \text{expectation of } (\Sigma M_x)^2 \text{ from } \delta v,$$

which can easily be shown to be equal to

$$\frac{k^4}{d^2} n_0 \delta v \overline{M_x^2}, \quad . . . . . (9)$$

where  $\overline{M_x^2}$  denotes the average value of  $M_x^2$  taken over all the molecules in the element, *i. e.* over all orientations, and is therefore given by

$$\overline{M_x^2} = \frac{\int_{\theta=0}^{\theta=\pi} \int_{\phi=0}^{\phi=2\pi} \int_{\psi=0}^{\psi=2\pi} E^2 (A' \alpha_{13} \alpha_{11} + B' \alpha_{23} \alpha_{21} + C' \alpha_{33} \alpha_{31})^2 \sin \theta \, d\theta \, d\phi \, d\psi}{\int_{\theta=0}^{\theta=\pi} \int_{\phi=0}^{\phi=2\pi} \int_{\psi=0}^{\psi=2\pi} \sin \theta \, d\theta \, d\phi \, d\psi} \quad . . . . . (10)$$

$$= E^2 F, \quad . . . . . (11)$$

where

$$F = \frac{1}{3} [(A' - B')^2 + (B' - C')^2 + (C' - A')^2]. \quad . . . (12)$$

Then from (9) we get for the intensity of the  $x$ -component of the scattering per unit volume

$$I_x = \frac{k^4}{d^2} E^2 n_0 F. \quad (13)$$

Coming now to the  $z$ -component, we may write expression (7) for  $M_z$  shortly as

$$M_z = EL, \quad (14)$$

where

$$L = A' \alpha_{13}^2 + B' \alpha_{23}^2 + C' \alpha_{33}^2. \quad (15)$$

As before, by summing up the amplitudes of the radiations from the individual molecules in  $\delta v$  at any instant, we get for the resultant amplitude

$$Z = \frac{k^2}{d} E \Sigma L, \quad (16)$$

$\Sigma$ , as before, denoting summation over all the molecules in  $\delta v$ . For convenience in discussion we can rewrite the expression in the form

$$Z = \frac{k^2}{d} E \left[ \Sigma \frac{A' + B' + C'}{3} + \Sigma \left( L - \frac{A' + B' + C'}{3} \right) \right]. \quad (17)$$

$$= \frac{k^2}{d} E \frac{A' + B' + C'}{3} n \delta v + \frac{k^2}{d} E \Sigma \left( L - \frac{A' + B' + C'}{3} \right). \quad (18)$$

The two terms in (18) may be denoted by  $Z_1$  and  $Z_2$  respectively. We shall in the first place consider the second term  $Z_2$ , reserving a discussion of the other term to the next section.

At any instant the average value of  $\Sigma \left( L - \frac{A' + B' + C'}{3} \right)$

for the different volume elements can easily be shown to be zero. But as in the previous case its actual value for any single element will be finite, in general, and will be determined wholly by the chance orientations of the molecules in it. Hence, so far as the second term of (18), viz.  $Z_2$ , is concerned, we have as before to add up the intensities due to the different volume elements in order to get the total intensity.

Following the same reasoning as in the case of the  $x$ -component, we get for the expectation of intensity on account of the second term of expression (18) from a volume element  $\delta v$

$$\bar{Z_2^2} = \frac{k^4}{d^2} E^2 n_0 \delta v \left( L - \frac{A' + B' + C'}{3} \right)^2, \quad (19)$$

where the bar over the last factor denotes averaging over



all orientations,

$$= \frac{k^4}{d^2} E^2 n_0 \delta v \times \frac{2}{45} [(A' - B')^2 + (B' - C')^2 + (C' - A')^2]. \quad (20)$$

$$= \frac{k^4}{d^2} E^2 n_0 \delta v \times \frac{1}{3} F. \quad \dots \dots \dots (21)$$

Thus we get for the intensity of this part of the  $z$ -component, scattered per unit volume

$$I_{z2} = \frac{4}{3} \frac{k^4}{d^2} E^2 n_0 F. \quad \dots \dots \dots (22)$$

The expression

$$I_x + I_{z2} = \frac{7}{3} \frac{k^4}{d^2} E^2 n_0 F \quad \dots \dots \dots (23)$$

gives the "orientation" scattering per unit volume. In the special case when  $A' = B' = C'$ , *i. e.* when the moments induced in a molecule are isotropic,  $F = 0$  and the orientation scattering naturally disappears.

### 6. Density Scattering.

We have still to consider the first term in (18), *viz.*

$$Z_1 = \frac{k^2}{d} E \frac{A' + B' + C'}{3} n \delta v. \quad \dots \dots \dots (24)$$

$\frac{A' + B' + C'}{3}$  is the average moment induced in a molecule per unit external field, the average being taken over all directions of incidence of the field with respect to the molecule. The actual field on the molecule which produces this moment can be divided into three parts :—

- (a) The external field.
- (b) The field arising from the doublets outside a spherical volume element containing the molecule at its centre.
- (c) The field arising from the molecules within the volume element.

For the reasons given in section 3, the fields (a) and (b) will be unaffected by the fluctuations of density in the volume element, and hence the corresponding contribution from these fields to the mean moment of the molecule, *viz.*

$$\frac{A + B + C}{3} \left( 1 + \frac{4\pi}{3} \chi \right),$$

can be regarded as constant.

The rest of the contribution to the mean moment, viz.

$$\frac{1}{3}(A\sigma_1 + B\sigma_2 + C\sigma_3)\chi, \quad . \quad . \quad . \quad (25)$$

$$\left. \begin{aligned} \sigma_1 &= p_1 - \frac{4\pi}{3}, \\ \sigma_2 &= p_2 - \frac{4\pi}{3}, \\ \sigma_3 &= p_3 - \frac{4\pi}{3}, \end{aligned} \right\} . \quad . \quad . \quad . \quad (26)$$

comes from field (c) due to the immediate neighbours, and hence will vary directly with the fluctuation of  $n$  in the volume element. However, in any actual case  $A\sigma_1 + B\sigma_2 + C\sigma_3$  is negligible in comparison with  $A + B + C$  (generally 1 or 2 per cent.), and hence we may reasonably assume that the whole of the mean moment, i. e.  $\frac{A' + B' + C'}{3}$ , is independent of the fluctuations of  $n$ .

Expression (24) can then be written in the form

$$Z_1 = \frac{k^2}{d} E \frac{A' + B' + C'}{3} n_0 \delta v + \frac{k^2}{d} E \frac{A' + B' + C'}{3} \delta n \delta v. \quad (27)$$

The first term represents that part of the amplitude which will be constant for the different volume elements, and on compounding will cancel each other out by mutual interference, owing to the regularity in the arrangement of the volume elements in the medium. The amplitude represented by the second term, however, being determined by the chance fluctuation  $\delta n$ , will be uncorrelated for the different volume elements, and we shall have to add their squares to get the resultant intensity. Thus

$$\overline{Z_1^2} = \frac{k^4}{d^2} E^2 \left( \frac{A' + B' + C'}{3} \right)^2 \overline{\delta n^2} \delta v^2, \quad . \quad . \quad (28)$$

which, using (1) and the relation

$$n_0 \frac{A' + B' + C'}{3} = \frac{\mu^2 - 1}{4\pi}, \quad . \quad . \quad . \quad (29)$$

where  $\mu$  is the refractive index of the medium, reduces to

$$\overline{Z_1^2} = \frac{k^4}{d^2} E^2 \frac{RT\beta}{N} \left( \frac{\mu^2 - 1}{4\pi} \right)^2 \delta v. \quad . \quad . \quad (30)$$

Thus we have for the "density scattering" per unit volume

$$I_{s1} = \frac{k^4}{d^2} E^2 \frac{RT\beta}{N} \left( \frac{\mu^2 - 1}{4\pi} \right)^2 . \quad . \quad . \quad (31)$$

The total intensity of the  $z$ -component

$$I_z = I_{z1} + I_{z2}, \dots \dots \dots (32)$$

where  $I_{z1}$  and  $I_{z2}$  are given by (31) and (22) respectively.

### 7. *Depolarization and Intensity of the Scattered Light.*

If the incident light travelling along  $Ox$  is unpolarized, we shall have to take into consideration also the  $y$ -component of the primary vibrations, which, being along the direction of observation, will contribute equally to the intensities of the  $x$ - and  $z$ -components of the transversely scattered light, an amount given by (13).

Thus in this case the intensity of the  $x$ -component will be equal to  $2I_x$  and that of the  $z$ -component to  $I_x + I_z$ , and the ratio of the components is given by

$$\begin{aligned} r &= \frac{2I_x}{I_x + I_z} \\ &= \frac{2n_0 F}{\frac{RT\beta}{N} \left( \frac{\mu^2 - 1}{4\pi} \right)^2 + \frac{2}{3} n_0 F} \dots \dots \dots (33) \end{aligned}$$

Also the total intensity of the transversely scattered light expressed in terms of the incident intensity  $I_0 = 2E^2$ , becomes

$$I = I_0 \frac{\pi^2}{2d^2} \frac{RT\beta}{N\lambda^4} (\mu^2 - 1)^2 \frac{6 + 6r}{6 - 7r} \dots \dots \dots (34)$$

In the special case when the polarization field is isotropic,

$$p_1 = p_2 = p_3 = \frac{4\pi}{3}$$

and

$$\begin{aligned} F &= \frac{1}{30} [(A - B)^2 + (B - C)^2 + (C - A)^2] \left( 1 + \frac{4\pi}{3} \chi \right)^2 \\ &= \frac{1}{30} [(A - B)^2 + (B - C)^2 + (C - A)^2] \left( \frac{\mu^2 + 2}{3} \right)^2, \quad (35) \end{aligned}$$

and the expressions  $r$  and  $I$  reduce naturally to those obtained recently by Ramanathan.

### 8. *Comparison with Experiment : (a) Intensity.*

We now proceed to consider how far the above expressions are in conformity with actual experimental results. First we take up the intensity of the transversely-scattered light. From a critical examination of the available data, it has

been shown by one of us \* that relative measurements of intensity in a large number of organic liquids entirely support expression (34). We reproduce here the calculations for some typical cases for which we have accurate values for the compressibility from the measurements of Tyrer †.

TABLE II.

Liquid.	$r$ (observed).	I (relative to ether=1) at 30° C.	
		Calculated according to (34).	Observed.
Water .....	0.085	0.19	0.13
Methyl alcohol .....	0.060	0.51	0.56
Ethyl alcohol .....	0.053	0.58	0.57
Ethyl acetate .....	0.230	0.95	0.98
Carbon tetrachloride .....	0.053	0.96	1.02
Chloroform .....	0.240	1.31	1.26
Acetic acid .....	0.455	1.39	1.42
Ethylene chloride.....	0.36	1.40	1.44
Ethyl bromide .....	0.250	1.55	1.58
Benzene.....	0.47	3.13	3.2
Toluene.....	0.51	3.29	3.4
Aniline .....	0.60	3.59	3.42
Meta xylene .....	0.57	3.90	3.87
Chlorobenzene .....	0.58	4.09	4.10
Nitrobenzene.....	0.74	7.6	10.5
Carbon bisulphide .....	{ 0.64 0.685	{ 10.9 14.1 }	12.9

Thus over the whole range of intensities from 0.2 to 13, relative to ether, the agreement between the observed and calculated values is very satisfactory. Nitrobenzene is the only exception, the discrepancy being too large to be attributable to error of measurement. However, since it shows a very high depolarization (the highest in the list), any impurity present in the liquid is likely to lower the observed value of  $r$  and consequently the calculated value of  $I$  considerably; whereas the actual intensity will be

\* K. S. Krishnan, Proc. Ind. Assoc. Cult. Sc. ix. p. 251 (1926).

† D. Tyrer, Journ. Chem. Soc. cv. p. 2534 (1914).

increased. Further it is a coloured liquid. It would be of interest to repeat the measurement with a specially purified specimen.

Recently in the authors' laboratory, Mr. Ramachandra Rao \* has studied the scattering by six typical organic liquids over a wide range of temperature up to the critical point. The relative values of the intensity at different temperatures again confirm the validity of the above expression for I.

Absolute measurements of intensity available also support expression (34), as will be evident from Table III.  $\frac{I}{I_0} d^2$  gives, according to our notation, the fraction of the incident unpolarized light scattered transversely per unit volume of the liquid, per unit solid angle.

TABLE III.

Liquid.	$\lambda$ in A.U.	Temperature ° C.	$r$ .	$\frac{I}{I_0} d^2 \times 10^6$ .		Observer.
				Calculated according to (34).	Observed.	
Ethyl ether..	4358	20	0.080	8.85	9.2	Martin & Lehrman †.
Benzene .....	5440	15 {	0.41	8.85	$10.7 \pm 0.55$	Cabannes & Daure ‡.
		0.47	10.7			

### 9. Comparison with Experiment: (b) Depolarization.

Expression (33) enables us to determine the depolarization of the light scattered by a fluid in terms of A, B, C, the optical constants of the molecule and  $p_1, p_2, p_3$ , the constants of anisotropy of the polarization field. In the case of a rarefied fluid, the polarization field is very small and may be neglected. For a dense fluid, if we disregard the "anisotropy" of the field and assume that

$$p_1 = p_2 = p_3 = \frac{4\pi}{3},$$

\* S. Ramachandra Rao, Indian Journal of Physics, ii. p. 7 (1927).

† W. H. Martin and S. Lehrman, Journ. Phys. Chem. xxiv. p. 478 (1920).

‡ J. Cabannes and P. Daure, Comptes Rendus, clxxxiv. p. 520 (1927).

then the depolarizations in the liquid and gaseous states are connected by the simple relation

$$\frac{RT\beta}{N} n_0 \cdot \frac{r_{\text{liq.}}}{6-7r_{\text{liq.}}} = \frac{r_{\text{gas}}}{6-7r_{\text{gas}}} \quad (36)$$

The value of  $r_{\text{liq.}}$  calculated from expression (36) usually, however, differs widely from the observed value. In the case of the carbon compounds, the differences are very marked in the case of the paraffins and the monohydric alcohols, the observed depolarization being much smaller than the calculated value; the differences are less conspicuous in the aromatic series of compounds.

A natural explanation of these facts is furnished by taking into account the anisotropy of the polarization field. It is sufficient as an illustration to consider the cases of the paraffin series of hydrocarbons. As is well-known from chemical considerations and from X-ray data, the molecules of these compounds form elongated chains of carbon atoms, to which the hydrogens are linked. The length of the chain is much greater than its cross-section. X-ray study of the liquid shows, as might be expected *a priori*, that the molecules lie much more frequently touching one another side to side and much less frequently end to end. In these circumstances it would obviously be incorrect to assume the polarization field acting on a molecule to be independent of its orientation in the field. A much closer approximation to the truth is to consider the molecule as equivalent to a doublet placed at the centre of a prolate ellipsoidal cavity scooped out of a continuous isotropic medium, the dimensions of the cavity being determined by those of the molecule. The values of  $p_1$ ,  $p_2$ ,  $p_3$  are readily calculated from the expressions

$$p_1 = 4\pi \left( \frac{1}{e^3} - 1 \right) \left( \frac{1}{2e} \log \frac{1+e}{1-e} - 1 \right), \quad (37)$$

$$p_2 = p_3 = 2\pi \left( \frac{1}{e^3} - \frac{1-e^2}{2e^3} \log \frac{1+e}{1-e} \right), \quad (38)$$

where  $e$  is given by

$$b = c = \sqrt{1-e^2} \cdot a, \quad (39)$$

$a$ ,  $b$ ,  $c$  being the axes of the cavity.

In Table IV. are given the values of the depolarization factor computed in this way, and those observed are tabulated for comparison. A satisfactory agreement is indicated.

TABLE IV.

All the quantities refer to 30° C.

Substance.	Dimensions of the molecule in A.U.		$r_{\text{gas.}}$	$r_{\text{liq.}}$ calculated from		$r_{\text{liq.}}$ observed.
	$a.$	$b=c.$		(36). (Isotropic polarization field).	(33). (Anisotropic polarization field).	
Pentane ...	8.7	4.9	0.0136	0.21	0.074	0.075
Hexane ...	10.0	„	0.015	0.31	0.087	0.100
Heptane...	11.3	„	0.0158	0.38	0.083	0.127
Octane ..	12.6	„	0.0186	0.46	0.105	0.100 0.129

## 10. Summary.

An examination of the data for the depolarization of the light scattered by fluids, with the aid of the molecular theory due to Ramanathan, indicates an apparent change, usually a large diminution, in the optical anisotropy of the molecules of a given substance, as it passes from the condition of vapour to that of liquid. In the present paper a new theory is put forward which offers a natural explanation of the foregoing fact without any artificial hypotheses. In the treatment of the optical properties of liquids usually given, the polarization field acting on a molecule is assumed to be independent of its orientation in the field. This assumption is not justifiable when the shape of the molecule departs greatly from spherical symmetry, and consequently the distribution of polarizable matter surrounding it ceases to be symmetrical. The strength of the polarization field will in these circumstances be dependent on the orientation of the molecule in the field, and may be expressed in terms of three constants characteristic of the molecule for the given density and temperature of the fluid. The theory of light-scattering is developed on this basis, and gives an expression for the intensity of scattering which is in close accord with facts. It also enables the depolarization of the scattered light in the liquid to be successfully calculated from that of the corresponding vapour, at least in those cases where the constants of anisotropy of the polarization field can be determined from the shape of the molecule.

210 Bowbazar Street,

Calcutta, India.

18th August, 1927.

LII. *The Influence of Charged Metallic Points on the Spark Discharge.* By JOHN THOMSON, M.A., B.Sc., Houldsworth Research Student in the University of Glasgow\*.

THE well-known action of a sharp metallic point in facilitating the passage of a spark across a gap near which it is placed has recently been the subject of two papers, the main object of which was the elucidation and explanation of the effect. In the first of these, by C. E. Wynn-Williams†, a number of experiments are described which led the author to the conclusion that the effect is mainly due to the ionization of the air in the gap by a radiation proceeding from the metallic point, and that the properties of the radiation are identical with those of the *Entladungstrahlen* discovered by E. Wiedemann in 1895. The second paper is by J. D. Morgan‡, whose experiments support the conclusions arrived at by Wynn-Williams, but are claimed to indicate also that the radiation emanating from the metallic point is effective only when the potential of the point is transitory, and that when the point is subjected to a steady potential (as by a Wimshurst machine) the effect on the spark is due, not to electromagnetic radiation, but to a streaming of ions from the point to the gap.

The experiments to be described in the present communication were initiated for the purpose of further investigating the source and properties of the radiation referred to; they have, however, also led the present writer to a rather different explanation of the action of the charged metallic point.

*Experimental Arrangements.*

It will be well here to refer briefly to the principal arrangements of the spark-gap and metallic point which were used in the experiments to which reference has just been made. Fig. 1a shows the arrangement known as the "three-point gap," in which A, B are the main spark-gap electrodes, and C an insulated metal rod the point of which is placed very near one of the main electrodes. The effect is produced only when small sparks pass between C and the main electrode adjacent to it. In this arrangement the rod C need not be very sharply pointed; a blunt point is almost equally effective.

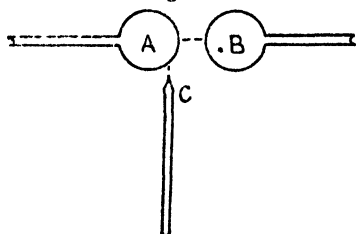
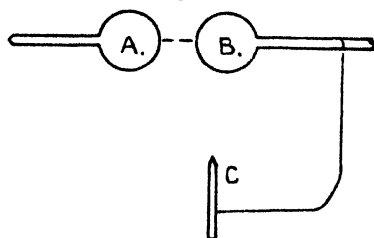
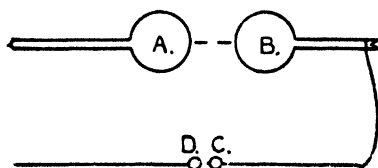
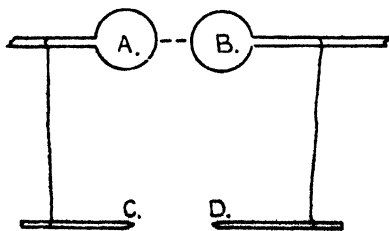
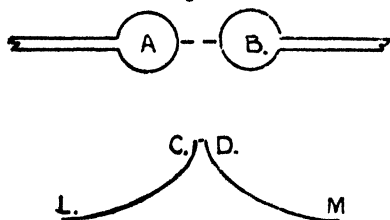
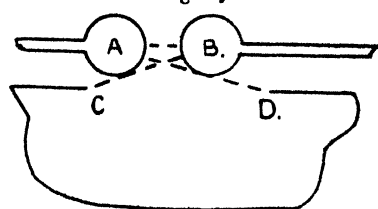
\* Communicated by Prof. E. Taylor Jones, D.Sc.

† C. E. Wynn-Williams, *Phil. Mag.* vol. i. p. 353 (1926).

‡ J. D. Morgan, *Phil. Mag.* vol. iv. p. 91 (1927).



In fig. 1 *b* is shown an arrangement in which the rod C is connected to one of the main electrodes. This is the arrangement used by Wynn-Williams in most of his experiments. The end of C need not be very near one of the main electrodes, but it must be very sharply pointed to produce the effect on the main gap. In this case the radiation is believed to originate in the silent discharge at the sharp point of C.

Fig. 1 *a*.Fig. 1 *b*.Fig. 1 *c*.Fig. 1 *d*.Fig. 1 *e*.Fig. 1 *f*.

Another arrangement used by Wynn-Williams is shown in fig. 1 *c*. The pointed third electrode is replaced by a small metal sphere connected to one of the main electrodes and held near another small sphere D attached to the end of an insulated wire. The small spark passing between C and D was found by Wynn-Williams to give rise to ionizing radiations similar in their properties to those proceeding from the silent discharge from C in fig. 1 *b*.

*The Spark-gaps employed in the Present Experiments.*

The present writer has found that, in addition to the arrangements of gap and auxiliary conductors described in the previous section, there are a number of other systems in which similar effects are produced. Some of these are shown in fig. 1. Fig. 1 *d* shows a symmetrical arrangement in which two sharp needles, C, D, are connected to the main electrodes. If the distance between the points C and D is just great enough to prevent a spark from passing between them, the effect on the main gap is very marked if the distance between AB and CD is not more than 10 cm. (AB was 1 cm.). Another symmetrical arrangement is shown in fig. 1 *e*, in which a very small spark passing between C and D, the adjacent ends of insulated wires, takes the place of the silent discharge. This arrangement is also very effective up to the distance of 4 cm. between AB and CD. If the ends L, M are joined by a copper wire, the effect is still found if the small auxiliary gap CD is within 1 cm. of A or B. In fig. 1 *f* C and D are the points of two needles the outer ends of which are connected by a copper wire, but which are otherwise insulated. In this arrangement the effect on the main gap is very marked, even though no sparks pass between A and C or between B and D.

*The Source of the Radiations.*

With the arrangement of fig. 1 *d* a series of experiments was made with the object of determining the exact source of the radiations. The potential applied to the main gap (generated by an induction coil with motor mercury jet interrupter) being adjusted so that sparks just failed to appear, a thin plate of paraffin wax having a narrow aperture was placed between AB and CD, and moved about until the effect on the passage of the spark was greatest. In this way it was found that practically the whole of the effect originated in the immediate neighbourhood of one or other of the points C, D. The effect was most marked when the aperture allowed a straight path in air from the positive point to the point A of the negative electrode (fig. 2). This result was confirmed by attaching a narrow tube of the same material to the wax plate, as shown in fig. 2, in order to limit the radiation to a still narrower pencil. The most favourable position of the shield is shown in the figure. With this arrangement the greatest distance, AC, at which the effect could be produced was 8 cm., the width of the main gap,

AB, being as usual 10 mm. If the shield was so placed that the pencil failed to strike either of the main electrodes, but passed directly between them, the effect on the main gap was much weaker, being only observable when the distance AC was not more than 4 cm. In another experiment one of the main electrodes, A, was covered with a thin layer of paraffin wax except at the point nearest the other electrode.

Fig. 2.

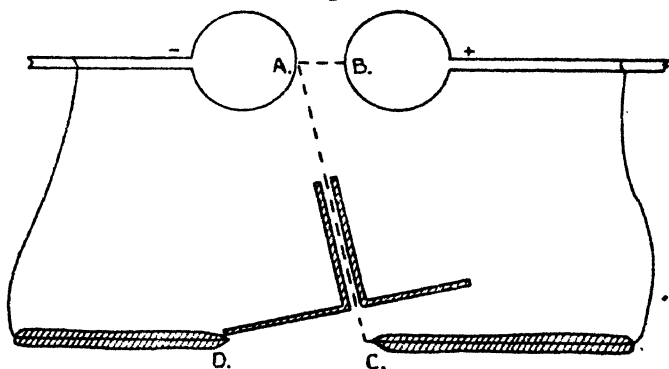
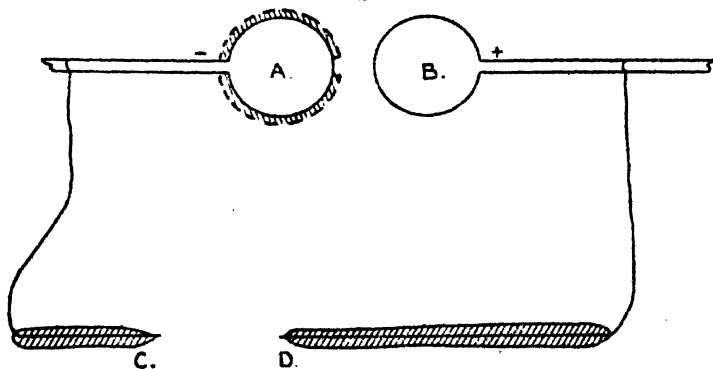


Fig. 3.



The auxiliary gap, CD, was then moved to one side as shown in fig. 3, so that no radiation could pass directly from C or D on to the uncovered part of A. With this system the effect on the main gap was much more marked when B and D were negative than when they were positive.

Practically identical results were obtained when the aperture in the wax shield was covered with a thin film of celluloid. This indicates that the effect on the main gap is caused by electromagnetic radiation, since it is highly

improbable that positive or negative ions can penetrate such a film in the conditions of the present experiments. Such penetration would be likely to occur only if the charged particles were *projected* with high velocity from the points, but in other experiments strong evidence was found (as will be seen later) against this supposition.

On the whole this series of experiments strongly suggests that, while a small effect arises from a radiation which ionizes the air in the main gap, a much greater part of the effect is photo-electric in character, arising probably from ultra-violet radiation proceeding from the neighbourhood of the positive point. This conclusion seems to be borne out by the fact that the effect of the metallic point in facilitating the discharge at the main gap is very much less marked if the electrodes of the latter are dirty or oxidized. It may be remarked that results practically identical with those just described were found when either of the main spark electrodes was earthed.

With the arrangement of fig. 2, in which a very narrow directing tube was attached to the wax shield, a series of observations was made with the object of determining more exactly the source or sources of the radiation. First the tube was placed so as to be in line with the point A and various points in the line CD, thus examining the relative intensities of the photo-electric radiation from different parts of the discharge. The radiation was found to be much more intense at the positive than at the negative point, while an important conclusion was that, in order to obtain the effect to a marked degree, it is not necessary that C or D should be in line with the point A. The air near C or D is almost equally effective, and an appreciable effect is produced by points in the air at 2 mm. from C or D. Similar experiments in which the main electrodes were shielded allowed the source of the ionizing radiation to be investigated. The effect due to ionization appears to be of almost equal intensity whether it proceeds from the neighbourhood of the positive or the negative point. Again, the air near the point seems to be the source of the radiation.

For comparison with these results a series of measurements was made of the potential at various points in the auxiliary gap CD. For this purpose a water-dropping collector, consisting of a fine glass capillary tube, was placed just above the line CD, so that water fed into it broke into drops in this line. The water was connected to one terminal of a Kelvin vertical voltmeter, the other terminal of the instrument being connected to D. The reading on the voltmeter indicated the R.M.S. voltage between D and the collector.

The results of these experiments are shown in fig. 4, the ordinate representing the R.M.S. potential difference between D and various points of the gap CD. The derivative curve, Fig. 4.

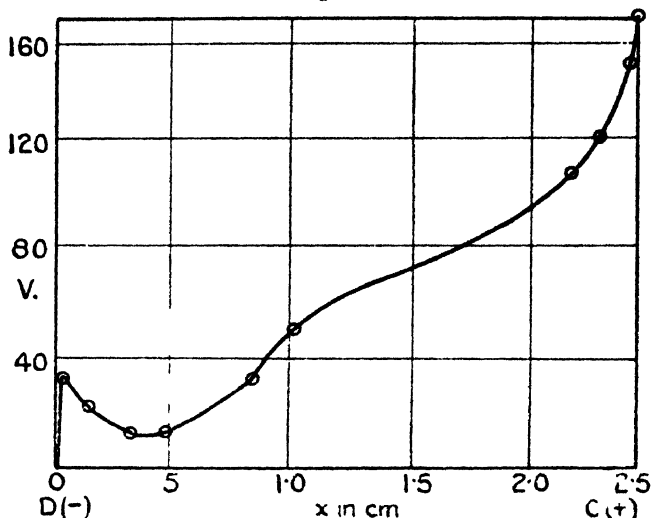
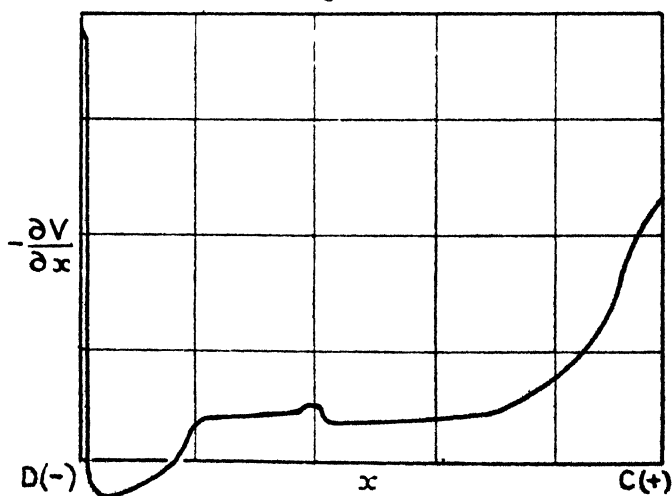


Fig. 5.



representing the potential gradient along CD, is shown in fig. 5. A comparison of these curves with the results obtained for the intensity of the radiations across the source CD shows that the most effective part of the source is not

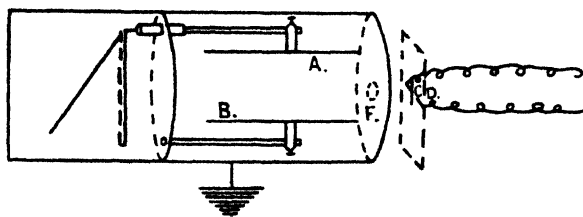
that part where the electric force is greatest, but the part where the positive potential is greatest.

The electric force is greatest near the negative point D (cathode fall), and, on the assumption that the radiations are generated by the impact of ions on air molecules, it is to be expected, according to the quantum theory, that the radiation of greatest frequency will be generated near D. If  $V$  is the fall of potential in a very short distance (comparable with the mean free path of the electron in air at atmospheric pressure), the frequency is given by the quantum relation  $h\nu = Ve$ . It seems probable therefore that the radiation which produces the effect on the main gap is not the radiation of greatest frequency. The most effective portion is that which originates in the region of highest positive potential near C.

#### *Experiments with an Ionization Chamber.*

In order to obtain further information as to the properties of the radiations, the main gap AB was removed and replaced

Fig. 6.



by an ionization chamber containing two parallel metal plates, A, B, one of which, A, was insulated and connected to an ordinary gold-leaf electroscope. The other plate, B, was at first connected to the wall of the chamber. The arrangement is shown in fig. 6. The point gap, CD, connected to the induction coil, was placed horizontally in front of the chamber and 2 cm. from it, and by means of the slotted shield the radiation from C or D could be allowed to enter the chamber through the aperture F. C was the positive and D the negative point. The upper plate A, and consequently the electroscope, was charged to about +600 or -600 volts, and the rate of discharge was observed with C or D opposite the slot. The numbers given in the table below indicate the angular movement of the gold-leaf in a fixed time (about 10 seconds), and are assumed

to be proportional to the currents flowing to or from A. The normal leakage of the electroscope in 10 seconds was quite negligible. The rate of discharge of the electroscope was comparable with the normal leak when points between C and D were opposite the slot.

Potential of A.	Point Source.	Current to A.
+600	C	7
-600	C	120
+600	D	550
-600	D	9

These results clearly indicate that the current to the plate A is not due to ionization of the air between A and B alone, since in that case the first two results in the table would be equal and also the last two. To investigate this further, a Wilson tilted electroscope was substituted for the ordinary electroscope and the following series of experiments was carried out:—The earthed plate B of the ionization chamber was replaced by a similar insulated plate which could be charged to any desired potential, while the plate A was connected to the leaf of the tilted electroscope. The aperture F was covered with gauze connected to the earthed walls of the chamber in order to eliminate inductive effects on A due to the charges at the point gap. The electroscope was found to be sufficiently sensitive with the attracting plate charged to a potential (with respect to the earth) of  $\pm 210$  volts, the leaf system and plate A to  $\pm 25$  volts, and the instrument tilted to about  $30^\circ$ . The case of the electroscope was of course earthed, and the point gap with shield was arranged as in the former experiment.

(a) The plate A was charged to  $+25$  volts, the electrode D (negative) being placed opposite the aperture. Plate B was charged to various potentials,  $V_B$ . The rate of discharge of the electroscope was found to vary as  $V_B$  was varied; the graph of the results is shown in fig. 7, curve *a*. The ordinate represents the rate of discharge of A, the abscissa the potential  $V_B$ .

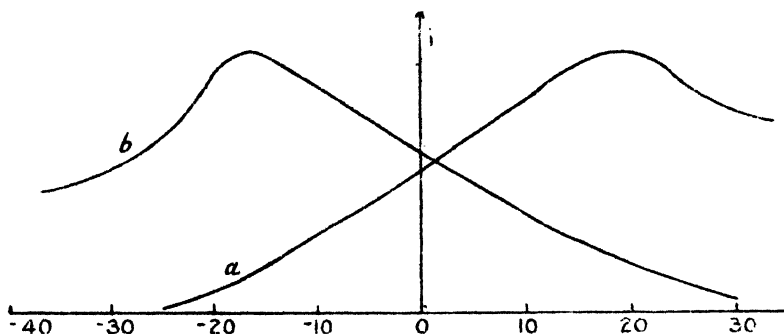
(b) In the next experiment the plate A was charged to  $-25$  volts, and electrode C (positive) was placed opposite the aperture. The relation between the rate of discharge of A and  $V_B$  is shown in fig. 7, curve *b*.

In order to interpret these results it may be supposed that

there are three conceivable ways in which the point C or D might cause discharge of the electrode A, viz. :—

- (i.) By the emission of an electromagnetic radiation which ionizes the air between A and B.
- (ii.) By the emission of ions of the same sign as the point, projected with a comparatively large velocity through the air between A and B.
- (iii.) By the production of ions in the vicinity of the aperture F, but not in the space between the plates A and B.

Fig. 7.



(i.) According to the first hypothesis, the current from A to B should clearly be zero when A and B are at the same potential, and as the difference between  $V_A$  and  $V_B$  increases, the current should steadily increase, *i.e.* the current varies with  $\pm(V_A - V_B)$ .

(ii.) In this case also the current would be due to the electric field between A and B. If the projected ions did not ionize the air through which they passed, then the current would increase as the negative potential of B increased. If the projected ions ionized the air, then this case would reduce to (i.), and the current would vary as in that case.

(iii.) On the third hypothesis the current to A would depend entirely on the electric field between the edge of the electrode A and the earthed gauze over the aperture. A consideration of the distribution of electric charge in the system within the ionization chamber leads to the conclusion that the gauze will have a very small charge when the potentials of the plates A and B are equal but opposite. On the other hand, when A and B are charged to the same potential, the induced charge on the gauze is very much greater. Since tubes of electric force originate in charges



on conductors, and since the electric force in the vicinity of a conductor is measured by the number of tubes of force per unit area originating on it, it is concluded that the force between the plate A and the gauze F is very much greater when A and B are at the same potential than when they are at equal but opposite potentials. Consequently it is to be expected that a much greater current of ions will move from the gauze to either plate when they are at the same potential than when they are at opposite potentials.

Another way of looking at the same problem is to consider extreme cases of the potential  $V_B$ . If  $V_B$  is very large and of the opposite sign to  $V_A$ , then the potential near the gauze F will be of the same sign as potential  $V_B$ . Consequently ions of this sign will be repelled to the gauze, and none will reach the plate A. Now the current measured was the current to A, and this was due to ions of the opposite sign to  $V_A$ . Therefore, if  $V_B$  is large and of the opposite sign from  $V_A$ , no current will be obtained. As the potential of the plate B approaches that of the plate A, there will come a time when a fairly large current of ions will move towards A. Then if  $V_B$  is very large and of the same sign as  $V_A$ , although ions will be attracted in large numbers from the gauze into the chamber, they will almost all find their way to the plate B, since the field of force between A and B will tend to drive them towards B. Thus, again, when  $V_B$  is very large, a very small current will be obtained. This indicates that a maximum current will occur when  $V_B$  is somewhere near to  $V_A$ .

The curves of fig. 7 obtained experimentally agree very well with this hypothesis, and accordingly it is concluded that the ions produced by the discharge do not reach the air between A and B, unless they are assisted by the action of an electric field. It is thus possible to put a limit to the distance from the discharge at which ions are produced. This limit as shown by these experiments is about 3 cm.

Similar experiments with A negatively electrified and D opposite the aperture, or with A positively electrified and C opposite, led again to the curves of fig. 7. Now, since in this case the ions causing the current were of opposite sign to the point source, this experiment shows that both kinds of ions are produced by the influence of each point.

In order to test the matter further, the following experiment was tried. The earthed wire gauze across the aperture F was replaced by an insulated piece of gauze which could be charged to various potentials. With A at

+ 25 volts, and B at + 20 volts, it was found that the current to A varied almost directly as the field from the gauze to A, the current increasing as the negative potential of the gauze increased. Similarly, with A charged to - 25 volts and B to - 16 volts, the current from A increased as the positive potential of the gauze increased. No current could be observed in either case if the gauze and A were at the same potential, or if the distance of C or D from the gauze was more than 3 cm. These experiments also support the hypothesis that the ions are produced near the gauze, but not in the space well between the plates A and B.

Another experiment was arranged to determine roughly the relative number of ions present at various distances from the source of the radiation. For this purpose a strong electric field was required, and therefore the tilted electroscope was replaced by the upright type, which could be used at potentials of about 600 volts relative to the case, which was earthed. The gauze was removed from the aperture F (fig. 6), and the point gap was arranged so that it could be moved in a direction perpendicular to itself and the face of the ionization chamber. This allowed the distance  $x$  from F to CD to be varied and to be accurately measured. The experiment consisted in observing the rate of discharge of the electroscope for different values of  $x$ , which was varied from 4 cm. to 6 cm. In all cases the relation between the rate of discharge and  $x$  was found to be represented by an exponential expression of the form  $i = i_0 e^{-kx}$ , where  $i$  is the rate of discharge of the electroscope and  $i_0$  is some constant.

The exponential decrease in the current must now be explained on the assumption that no ions are *produced* at distances greater than 3 cm. from the discharge. Since ions *did* reach the chamber, there must be a field of force between the place where the ions are formed and the aperture F. This is not surprising when the high potential of the plate A is considered. This plate (positive) will attract negative and repel positive ions, so that the current flowing from the vicinity of the discharge to the aperture will consist entirely of negative ions. Let this current at any point be  $i$  across unit cross-section, and let the current at the point beyond which no ions are formed (3 cm. from the discharge) be  $i_0$ . The decrease in the current must be due to some form of diffusion of the ions. No recombination occurs, since there are assumed to be no positive ions present. This diffusion is principally due to the mutual repulsion of the ions, causing them to move away from one another.

Consequently the decrease in the current,  $i$ , will be proportional to the number of ions present, or, if the flow of ions is being considered, will be proportional to the current itself. Thus, if  $k$  is the fraction of the current lost along 1 cm. of the distance  $x$ , the increase in the current across an element  $dx$  will be represented by the quantity  $-kidx$ . That is,

$$di = -kidx,$$

giving  $i = i_0 e^{-kx}.$

It is to be noted that this diffusion is not the same as that occurring when ions of one sign are present in a closed chamber. There the diffusion current is due to the absorption of ions near the surface of the chamber; the expression representing such diffusion is entirely different.

There now remains to be investigated the question of how these ions are produced by the action of the point discharge. The experiments made with the spark gap indicate that ionizing radiations emanate from the vicinity of the point. None of the experiments described above have given any evidence to contradict this view. On the other hand, they have established that the production of the ions is brought about either by fast-moving ions, projected from the points and capable by reason of their velocity of ionizing air, or by an electromagnetic radiation. They have also shown that in either case the ionization ceases at a distance of about 3 cm. from the gap.

Again the tilted electroscope was employed, and the aperture F was screened by an earthed wire gauze. In this experiment, however, the aperture was also covered by a thin film of celluloid similar to that used in the spark-discharge investigations. The electrode B was earthed, and the point gap was about 1 cm. from the aperture F. Observations were taken of the rate of discharge of A. In this case the normal leakage of the electroscope had to be measured and deducted. The readings varied considerably with the intensity of the field across the gap CD, a typical result being given in the following table:—

Potential of A in volts.	Source.	Rate of discharge of A.
+25	Positive point.	6
+25	Negative point.	4
-25	Positive point.	6
-25	Negative point.	4

In each experiment the ratio of the rates of discharge of plate A due to C and D did not vary when the potential

of A was changed from  $-25$  to  $+25$  volts. This means that whatever emanates from the point and penetrates the celluloid produces equal numbers of positive and negative ions. That is, in this case true ionization of the air in the chamber is taking place, either by the action of a radiation or by the impact of high-velocity ions on air molecules. It is highly improbable that anything of the nature of cathode or positive rays is given off by a point discharge in air at atmospheric pressure, and ions of smaller velocities than these would be stopped (or at least lose their ionizing speed) by the impact with the celluloid film. Moreover, the previous experiments have shown that ionization does not take place at distances greater than 3 cm. from the discharge; material particles brought to rest by 3 cm. of air would certainly be unable to penetrate the film. The conclusion is therefore that the ionization is caused by an electromagnetic radiation.

Another point to be noted is that the experiment did not allow any photo-electric radiation which might be present to be detected, since the electrodes A and B were not in a direct line from C or D. The numbers given are therefore measures of the relative intensities of the ionizing radiations from the two points, as detected at 3 cm. distance from their sources. It cannot be stated, however, that the relative intensities at the sources are in the same ratio, as that assumes that the radiations from the two points are of the same average wave-length or "hardness."

The next experiment was intended to detect and measure the photo-electric radiations which were suspected to be present. The plate B was removed and A was replaced by a clean zinc plate Z, facing the aperture F and about 1 mm. from the wire gauze. Thus radiations from the point acting as source actually fell on the zinc plate, whereas in the previous experiments they did not fall on *any* metal surface inside the chamber. The aperture was again covered by a celluloid film. The usual measurements of the rate of discharge of the plate Z were taken with the positive point C and then with the negative point D as source. The results are shown below.

Potential of Z in volts.	Source.	Rate of discharge of Z.
+25	Positive point.	6
+25	Negative point.	4
-25	Positive point.	24
-25	Negative point.	4

The results with Z positive are a repetition of the results in the previous experiment. Since there is no photo-electric

effect with Z charged to +25 volts, the numbers represent the relative intensities of the ionizing radiations at 3 cm. from their sources, thus confirming the results already obtained. With Z negative, however, the results are different. The rate of discharge with the negative point as source is as before, showing that little or no photo-electric radiation emanates from it; but the rate of discharge with the positive point as source is about four times as great as before. This indicates a strong photo-electric effect due to radiations from the neighbourhood of the positive point. It also shows that the ionizing effect of the radiations is much less powerful than the photo-electric effect, confirming the results obtained with the spark discharge. It is possible and in fact probable that some photo-electric radiation emanates from the vicinity of the negative point. Our experiment merely indicates that its intensity must be less than one-twentieth of the intensity of the similar radiation from the positive point. So far, direct experiment has given no indication as to whether the photo-electric effect is produced by the radiation responsible for the ionization effect or by one of different wave-length. The spark-discharge experiments, however, showed that a photo-electric effect could be produced at the gap when the source of the radiation was (under favourable circumstances) 15 cm distant. The ionizing radiation under no circumstances will penetrate more than 3 cm. of air. Consequently it may be said that whether the ionizing radiation can or cannot produce the photo-electric effect, other radiations are present whose absorption by air is smaller and which are photo-electric.

It is well known that the photo-electric emissivity of a metal is a function of the wave-length of the incident radiation. The maximum emission is due to radiation of a certain fixed wave-length. It is also known that the wave-length corresponding to the maximum emissivity varies from metal to metal; in general the more electro-positive metals respond to longer wave-lengths, and the more electro-negative to shorter wave-lengths. Consequently the experiment just described cannot be said to give any general information with regard to the intensity of the radiations. The results must be taken to refer only to zinc or allied metals.

The experiments just described show that both ionizing and photo-electric radiations are emitted by a point charged to a high positive potential. Photo-electricity is in general associated with radiations of longer wave-lengths than those

which ionize air, and therefore it is reasonable to suppose that the radiations from the point are very heterogeneous in character. A rough spectral analysis might be performed by a series of experiments on the velocities of photo-electrons. With the positive point at a fixed distance from the zinc plate a determination might be made of the minimum wave-length of the incident radiations, by the usual method of measuring the positive potential to which the plate rises. By making similar determinations with different distances between the source and the plate, a curve might be obtained giving the minimum wave-length as a function of this distance. Such a curve would indicate the type of spectrum emanating from the point. It would of course be necessary to see that the ionizing radiations were not allowed to interfere, by using suitable distances (greater than 3 cm.) between the source and the plate, and by using the celluloid screen. The difficulty in the way of such experiments is the small intensity of the radiations.

#### *Theory of the Action of Charged Points.*

The results enumerated above can now be applied to the explanation of the action of a third point or system of points on the spark discharge; but before proceeding to the explanation, it may be well to clear away a preliminary difficulty. Throughout the present paper the action of the third point has been described as a "lowering of the sparking potential." In practice, when an induction coil is the source of energy, this is undoubtedly what occurs. But the term "sparking potential" has a technical meaning which is not implied here. The "sparking potential" across a gap is the potential difference at which a spark will pass, when this potential difference is applied gradually, and is continued for an indefinite time. The effect of "time lag" is thus eliminated, and it is questionable if any external mechanism can cause any lowering of this potential. In the case of an induction coil the peak potential difference is applied for a very short time only, and consequently the "lag" causes an apparent rise in the "sparking potential." The true action of the third point must be described as eliminating this "lag." The preliminary ionization of the gas in the gap takes place more rapidly, and the current rises more quickly to that necessary to produce a spark. "Lowering of the sparking potential" is therefore a vague description of the action of the point. It is merely a convenient expression,

and wherever it occurs in the present paper the above reservations must be kept in mind.

The results described above have led the writer to put forward the following hypothesis :—

1. The lowering of the sparking potential is caused in different ways by different arrangements of points, and the effects of different causes may vary considerably in relative importance as the type of discharge is varied.

2. The two main causes are :—

- (a) Photo-electric effects due to ultra-violet radiations from small sparks or the air near positive points.
- (b) Ions produced by the ionization of the gas by radiations which emanate from the air near positively or negatively charged points.

(a) The photo-electric radiations are more powerful than the ionizing radiations in any arrangement where there is a positive point at a distance greater than three centimetres from the main gap. At distances greater than three centimetres the ionizing radiations are completely absorbed by the air before they get to the gap, while the photo-electric radiation can, if the main electrodes are of clean zinc, affect the sparking potential when its source is as much as fifteen centimetres away. If the electrodes are dirty or oxidized, however, it is difficult with the same length of gap to obtain an effect at more than three centimetres distance. Similarly the substitution of copper for zinc reduces the range of the effect considerably. These results, along with those described earlier in the paper, show that the photo-electric radiation is of prime importance.

(b) The ionizing radiation also affects the sparking potential, but the range of its effect is smaller. Also its action appears to be somewhat complicated. When the distance of a charged point from the spark gap is less than three centimetres, the air in the gap is directly ionized. That this must be the case is shown by the ionization chamber experiments, and it is well known that a spark appears more readily in any gap after previous ionization of the gas in it. But experiments have shown that the radiation can affect the air in the gap when its source is at greater distances. Using the auxiliary gap of fig. 1 *d* and shielding both electrodes from photo-electric radiations, under certain conditions a lowering of the sparking potential is found with the distance

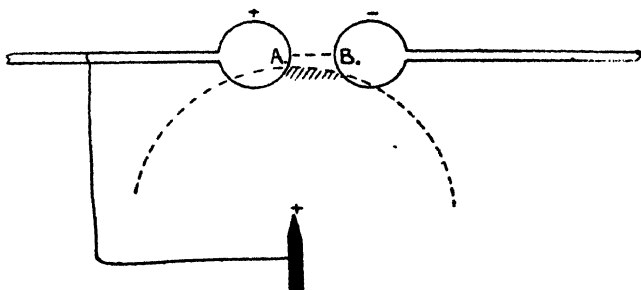
AB to CD equal to four centimetres. The following two experimental facts must therefore be reconciled :

- (a) The radiation can affect the spark when its source is 4 cm. distant.
- (b) The range of the radiation is 3 cm. as determined by the tilted electroscope.

The writer has come to the conclusion that the ions produced by the radiation can affect the sparking potential even when they are not in the line of the spark, and suggests the following explanation :—

The ions are produced within the sphere whose central section is indicated by the dotted circle (fig. 8). Ions in the shaded portion of the sphere move under the field of electric force to one or other of the electrodes, the diffusion

Fig. 8.



being negligible, owing to the strength of the field. The energy acquired under the field of force is liberated when the ions strike an electrode and this energy takes the form of pulses of electromagnetic radiation which are probably photo-electric in character. This secondary radiation ultimately penetrates to the line AB and increases the conductivity of the gas there, thus facilitating the passage of the spark. The explanation was suggested by the recent work of Sir J. J. Thomson \* on the action of low-velocity ions.

If this hypothesis is correct, it should be possible to effect a lowering of the sparking potential even when the radiating point is "invisible" from the path of the spark, so long as some part of a sphere of radius 3 cm. about the point as centre is "visible" and within about 1 cm. from the spark

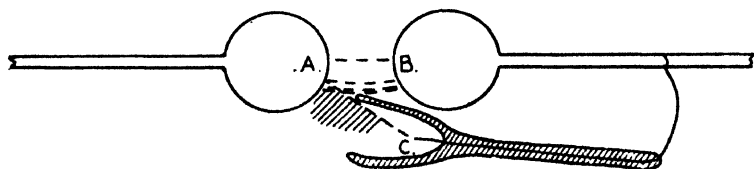
\* Phil. Mag. vol. ii. p. 675 (1926).



line. To investigate this the following experiment was tried :—

The point C (fig. 9) was sheathed in an open cylinder of clean paraffin-wax and brought up to the gap in the position shown in the diagram. C was “invisible” from any part of the spark, AB, yet a distinct effect was observed. It follows, therefore, that the ionized air in the shaded portion of the diagram was able to cause a lowering of the sparking potential. It is to be noted, however, that a straight line is necessary from C to within less than 1 cm. from AB. Other forms of the experiment just described can be arranged, where, without the use of a shield, C is placed very close to the electrode B. Here, again, an effect can be obtained when no straight line in air exists from C to AB. A striking example of this type of action is observed when the point gap of fig. 1*f* is used. Here the effect will *only* occur if C and D are so close to A and B that no straight line can

Fig. 9.



be drawn to the path of the spark, the radiation emanating from the silent discharges between C and A and between D and B.

*Experiments with the Metallic Point connected to a Source of constant potential.*

When the metallic point C (fig. 1*b*) was connected to one pole of a Wimshurst machine instead of to one electrode of the main gap, the point was found to have only a slight effect in facilitating the passage of the spark across the main gap AB. The effect was much smaller than the usual three-point effect. It was also noticed that no violet glow could be detected round the point in the dark, and if two such points were connected to the opposite poles of the Wimshurst, no spark could be produced between them. No evidence was found of radiation proceeding from the point under these conditions, although careful tests were made with the ionization chamber. The reason probably is that the point never reached a sufficiently high potential,

the charge leaking from the point very rapidly in the form of an electric wind.

Somewhat similar results were found by Morgan \* in the paper already mentioned. That writer also concluded that no radiation was given off by a metallic point connected to the pole of a Wimshurst machine, and that any effect in the main gap in these conditions is due to an ionized stream, proceeding from the point. The experimental results of Morgan are therefore confirmed by the present experiments, but a somewhat different explanation of them is now offered. It was suggested by Morgan that in order that a point should emit an ionizing radiation, its potential should be of an impulsive or transient character. The present writer agrees with this view, but is of the opinion that the transient nature of the potential is only necessary in order that the point should be raised to a sufficiently *high* potential. With a continuous source the potential of the point never reaches a value high enough for the emission of radiation. It does not seem probable that the emission of radiation can depend, as Morgan suggests, on the *time* rate of change of potential of the point, but it does depend, as the present experiments have shown, on the *space* rate of variation of potential near the point.

*The Influence of the State of the Cathode Surface on the Effect of the Ionizing Radiation.*

A series of experiments was carried out with the object of determining whether the action of the ionizing radiation in lowering the sparking potential of the main gap was affected in any way by the state of the cathode surface. In these experiments the two main electrodes were, of course, entirely shielded from any direct (photo-electric) radiation from the metallic points, the air gap between these being alone in a direct line with the discharge. Otherwise the arrangement of fig. 1 *d* was used. In these circumstances it was found that the state of the surface of the cathode was an important factor in the action. If the cathode surface was dirty or oxidized, the point produced no effect if further than 2.6 cm. from the main gap ( $AB=1$  cm.). When the cathode surface was cleaned by rubbing with emery paper, the limiting distance of the point was slightly over 3 cm. When the cathode surface was brightly polished, the limiting distance was over 4 cm. Experiments in which different metals were used as main electrodes also led to the same conclusion.

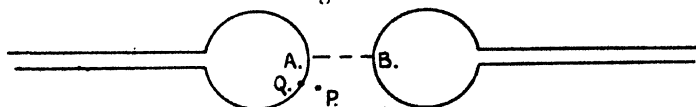
\* J. D. Morgan, *loc. cit.*

With a brass cathode the effect was slightly less than with zinc, while with a cathode of copper (whether polished or not) the limiting distance of the point never exceeded 2 cm. These experiments show that, even when no radiation from the metallic point reaches the surface of the cathode directly, the effect of the radiations in lowering the sparking potential depends on the nature of the cathode surface. It was difficult to determine whether the anode surface had any such effect, but, if so, it was certainly very much smaller than the effect of the cathode surface.

### *Mechanism of the Spark Discharge.*

One of the chief facts which emerge as a result of the experiments described in the present paper is that ions produced at some distance from the line in which the main spark passes can in some way facilitate the passage of this spark, and that the intensity of this effect depends upon the nature and state of the cathode surface. These results seem to be in entire agreement with the theory of the spark discharge recently proposed by J. Taylor \* and based upon

Fig. 10.



Sir J. J. Thomson's researches on the action of low-velocity positive ions †. An essential feature of this theory is that the positive ions in a low-pressure discharge, when neutralized at the cathode surface, give rise to ultra-violet (Schumann) radiations, and that these radiations, acting as an intermediate cause, produce the liberation of photo-electrons.

In the present experiments a positive ion formed at P (fig. 10), at some distance from the line of spark, AB, is moved under the influence of the intense field to near the point Q of the cathode surface. There it excites ultra-violet radiation which liberates electrons from the metal in the neighbourhood. These electrons travel towards the anode surface, causing ionization by collision with neutral molecules in their paths. The process may repeat itself many times before the disruptive discharge takes place.

\* J. Taylor, *Phil. Mag.* iii. p. 753 (1927); *Proc. Roy. Soc. A*, 114, p. 78 (1927).

† *Phil. Mag.* vol. xlviii. p. 1 (1924), and *loc. cit.*

Further evidence in favour of this theory is given by the point discharge itself. As the experiments have shown, electromagnetic radiations of fair intensity emanate from the parts of the discharge path near the points. These radiations are undoubtedly due to the liberation of the kinetic energy of the ions. The differences between the discharge between points and the discharge between spheres are of degree rather than of kind. The field of force in the former case is much more irregular, and the surface density of the electricity is greater in the case of a point than in the case of a sphere, but the discharge mechanism is similar in nature. Consequently, if radiations emanate from the point discharge, it is to be expected that radiations of the same type but of less intensity will be present near the spherical electrodes. That the *visible* radiations from a point discharge can also be obtained from spheres just before sparking takes place was shown many years ago by Walter\*. The latter took photographs of sparks on rapidly-moving plates, and found that each spark was preceded by a faintly luminous brush discharge. It is highly probable, therefore, that ultra-violet radiations are present near the spherical electrodes when the potential approximates to that required for a spark to pass.

From these considerations, then, the conclusion may be drawn that the action of the metallic points on sparking potentials is similar to the action of the discharge itself. The behaviour of ions in the line along which the spark passes must be similar to the behaviour of ions outside of this line but within the field of electric force. If this is so, then the current through the gas must depend on the nature of the cathode surface, and some sort of photo-electric action must be assumed to take place. This is the conclusion to which the experiments of Taylor have led: it is not accounted for in Townsend's theory of the spark discharge, in which the positive ions are assumed to produce ions by collision with neutral molecules, but not as a result of their impact on the negative electrode.

That Taylor's hypothesis leads to a formula which gives accurately the current through a gas, when recombination of the ions can be neglected, was shown by Townsend himself†, while in 1923 Dubois‡ derived a formula which allowed both for ionization by the collision of positive ions and for photo-electric action of the latter at the negative electrode.

\* *Wied. Ann.* lxvi. p. 636; lxviii. p. 776.

† 'Electricity in Gases,' pp. 330, 331.

‡ *Ann. de Phys.* t. xx. p. 222 (1923).

Dubois's formula reduces to those given by Townsend when  $\beta$  or  $\gamma$  is made zero. It is

$$N = n_0 \frac{(\alpha - \beta) e^{(\alpha - \beta)D}}{\alpha(1 + \gamma) - (\alpha\gamma + \beta) e^{(\alpha - \beta)D}},$$

where  $D$  is the distance between the parallel plate electrodes.

It appears to the writer that the problem of deciding between the "ionization by collision of positive ions" theory and a "photo-electric" theory of sparking potentials resolves itself theoretically into the question whether radiation, or ionization by collision occurs first in a discharge. It is known that a collision between an ion and a gas molecule can give rise to a pulse of electromagnetic radiation. It is also known that a collision between an ion and a molecule can cause ionization of the molecule—that is, can cause the molecule to lose an electron. Which of these two phenomena will occur first if the speed of a positive ion is gradually increased? It would appear reasonable to suppose that less energy is required to move an electron from one orbit to another (as when radiation is emitted) than to remove an electron from the molecule entirely (as when ionization occurs); consequently it appears reasonable to conclude that radiation occurs before ionization.

If this view is correct, there can be little doubt that the "photo-electric" theory is true, since sufficient ions can be generated by this means to satisfy the requirements of the sparking current. If, on the other hand, ionization occurs first, then the photo-electric effects will be very subsidiary and of little importance.

It is again urged that the point discharge and the usual spark discharge between spheres or planes differ only in degree. What is found in the one may be expected to be found in the other with the appropriate modifications. But the point discharge gives evidence of radiations from the vicinity of the cathode long before a spark passes. We may therefore expect that the same occurs in a modified way in the spark discharge between spheres.

It may be remarked in passing that one of Townsend's objections to a theory of the discharge in which the positive ions only form others at the cathode, is that the current from a positive point to a negative plane cannot be explained on this hypothesis. In view, however, of the fact that a positive point is the source of electromagnetic ionizing and photo-electric radiations, quite sufficient to account for the current

in these conditions, it would scarcely seem necessary to assume any ionizing action of the positive ions in the point and plane system.

*Summary.*

1. Experiments are described showing :

i. That electromagnetic radiations emanate from the air in the immediate neighbourhood of charged metallic points from which electric discharges are taking place in air at atmospheric pressure. The intensity of the radiations increases with the intensity of the discharge.

ii. That the radiations produce photo-electric effects and ionization.

iii. That the radiations producing the photo-electric effects emanate only from the neighbourhood of positively charged points.

iv. That the ionizing radiations emanate from the neighbourhood of both positive and negative points.

v. That the photo-electric radiations can penetrate 15 cm. of air at atmospheric pressure.

vi. That the ionizing radiations are absorbed by 3 cm. of air at atmospheric pressure.

2. These results differ from those of Wynn-Williams in regard to the precise locality of the source of the radiations, and in regard to their penetrating powers.

3. A theory is suggested of the action of a charged metallic point in facilitating the passage of a spark between spherical electrodes.

4. This theory differs from that offered by Wynn-Williams in ascribing the greater part of the action to the photo-electric effect.

5. The action of the ionizing radiations in facilitating the passage of the spark is found to depend on the nature and state of the surface of the cathode.

6. The ionizing radiations are found to be capable of facilitating the passage of the spark, even when no straight line can be drawn in air from the metallic point to the line of the spark discharge.

7. It is suggested that the action of the ionizing radiations in such cases is an indirect effect due to the impact of positive ions on the metal of the cathode.

8. The experimental results of Morgan are examined and confirmed, but a somewhat different explanation of them is given.

9. The results of the present experiments are considered

in relation to the theory of the spark discharge recently put forward by J. Taylor, and are found generally to support this hypothesis.

10. Some of Townsend's conclusions with reference to his theory of the spark discharge are considered in the light of the results of the present experiments, and modifications of these conclusions are suggested.

In conclusion, the writer wishes to express his thanks to Professor Taylor Jones for his continued advice and encouragement and for many helpful suggestions. The experimental part of the work was performed in the Research Laboratories of the Natural Philosophy Department of the University of Glasgow.

November 1927.

---

LIII. *An Extension of Langevin's Theory of Atomic Magnetism to Molecules constituting Electronic Isomers.* By Professor S. S. BHATNAGAR, D.Sc. (London), University Professor of Physical Chemistry, Punjab University, Lahore, and Mr. CHAMAN LAL DHAWAN, B.Sc. (Hons.) \*.

ON modern views regarding the structure of matter it is natural to expect that two molecules containing the same number of electrons and having those electrons grouped in the same way will show a certain similarity of physical properties. This resemblance is closely brought out in the case of nitrogen and carbon monoxide. Caven† has brought out the close likeness in the physical properties of nitrous oxide and carbon dioxide, and has shown that the value of the magnetic susceptibilities of the gases at 40 atmos. at  $16^{\circ}$  is  $0.12 \times 10^{-6}$  in both cases.

Both on the Valency Theory of Langmuir and the Atomic Theory of Bohr such should be the case, as these gases constitute identical electronic configuration.

The verification of this view from the standpoint of magnetic data presents special interest. A theory of atomic structure which explains the magnetic properties of atoms and molecules has a lasting future. The periodic curve connecting atomic numbers of elements and their magnetic susceptibilities does not indicate any immediate and strikingly

\* Communicated by the Authors.

† 'Structure of Matter,' p. 156 (1924 edition).

simple relations, although a few regularities show up when attention is confined to members of a single family. For example, there seems to be a tendency for the atomic diamagnetic susceptibilities to increase with atomic number. This is clear from the table shown below :—

TABLE I.

Atomic number.		Atomic magnetic susceptibility.
Cl .....	17	$19.5 \times 10^{-6}$
Br .....	35	$32.0 \times 10^{-6}$
I .....	53	$45.7 \times 10^{-6}$
S .....	16	$16.0 \times 10^{-6}$
Se .....	34	$25.4 \times 10^{-6}$
Te .....	52	$40.5 \times 10^{-6}$
Zn .....	30	$10.2 \times 10^{-6}$
Cd .....	48	$20.2 \times 10^{-6}$
Hg .....	80	$38.1 \times 10^{-6}$

The question of the susceptibilities of the inert-gas configuration has been elegantly treated by Joos\*. If we consider the argon atom with 18 electrons, it has the same electronic configuration as the  $K^+$  and  $Cl^-$  ions. The magnetic susceptibilities of these substances ought to be identical on the viewpoint of Langmuir. But in passing through the series  $Cl^-$ , A,  $K^+$ , the ionic (or atomic) susceptibility should decrease as a result of the decrease in size of the electronic orbits owing to the increasing nuclear charge. If  $Z$  represents the effective nuclear charge, then for orbits characterized by the same quantum numbers

$$r_1^2 \propto \frac{1}{Z^3}.$$

According to Langevin's theory the diamagnetic susceptibility is given by

$$\chi_{\text{at.}} = -\frac{e^2}{4mc^2} \sum n \bar{r}^2, \quad \dots \dots (1)$$

the summation being extended over the  $n$  electrons in the

\* *Zeit. f. Phys.* xix. p. 347 (1923); *ibid.* xxxii. p. 835 (1925).



atom, and  $\bar{r}^2$  being the mean square of the radius of the projected orbit in a plane perpendicular to the field.

For  $K^+$  and  $Cl^-$  therefore as a sufficiently close approximation from (1) one gets the relation

$$\chi_{K^+} : \chi_{Cl^-} = \frac{1}{(19)^2} : \frac{1}{(17)^2}.$$

Joos has thus got the values of  $K$ ,  $Cl$ , and  $A$  as follows :—

$K$ .....	15.5
$A$ .....	17.5
$Cl$ .....	19.5

The value of argon is in excellent agreement with the experimental values of Hector and Wills\*. The values of  $K$  and  $Cl$  are also in good agreement with recognized experimental values.

Following the lead of Joos, we have tried to explore the possibility of finding a simple relationship between the values of molecular magnetic susceptibilities of electronic isomers and the isomorphous substances belonging to the same family and the radii of these molecules.

The radii of these molecules may be calculated from the values of the diameters of the atoms constituting a molecule. The question, however, arises as to what is meant by the diameter of an atom. From the point of view of the Kinetic Theory the diameter, or rather the sum of the radii of the two atoms would be the minimum distance between the centres of two colliding atoms. The closeness with which two atoms subject to electrical repulsions would approach would obviously depend upon their relative speeds, so that the dimensions of atoms calculated from the mean velocity of the molecules of a gas would apparently give the mean of varying diameters. The second view of regarding the diameter of the atom is to identify it with the diameter of the orbit of the outermost electron.

A third method of regarding the atomic diameter is used by W. L. Bragg†. In our calculations for the radii of the molecules use has been made of the values of the atomic diameters of elements as obtained by W. L. Bragg. For example, in the case of the isomorphous series  $BaCO_3$ ,  $SrCO_3$ ,  $MgCO_3$ ,  $CaCO_3$  the radii of the constituent atoms are as follows :—

\* Phys. Rev. xxiii. p. 209 (1924).

† Phil. Mag. xl. p. 169 (1920).

TABLE II.

Names.	Atomic radii of metallic particles.	Atomic radius from C.	Atomic radii for 3 atoms of oxygen.
BaCO <sub>3</sub> .....	2.10	0.77	3×0.65
SrCO <sub>3</sub> .....	1.95	0.77	3×0.65
CaCO <sub>3</sub> .....	1.7	0.77	3×0.65
MgCO <sub>3</sub> .....	1.425	0.77	3×0.65

The radii of the molecules have not been obtained by adding up, as this would hardly represent the exact state of affairs in molecule-building. A more correct way will be to calculate the radius from the volume of the new sphere formed by the closest packing of the atoms constituting the molecules by employing the following equation :

$$\frac{4}{3}\pi r_n^3 = \left\{ \frac{4}{3}\pi r_1^3 + \frac{4}{3}\pi r_2^3 + \dots \right\},$$

from which

$$r_n = \{r_1^3 + r_2^3 + \dots\}^{\frac{1}{3}}.$$

The radii of the molecules discussed in this communication calculated on the above view are shown in the table below :—

TABLE III.

Substance.	$r_n$ calculated.
BaCO <sub>3</sub> .....	2.193
SrCO <sub>3</sub> .....	2.056
CaCO <sub>3</sub> .....	1.836
MgCO <sub>3</sub> .....	1.620
KNO <sub>3</sub> .....	2.156
NaNO <sub>3</sub> .....	1.884
NaClO <sub>3</sub> .....	2.41
KHSO <sub>3</sub> .....	2.58
SrSO <sub>4</sub> .....	2.086
KClO <sub>4</sub> .....	2.254
*NaCl .....	2.825
*CaO .....	2.35
*AgCl .....	2.825
*BaO .....	2.750
CaSO <sub>4</sub> .....	1.922
K <sub>2</sub> CO <sub>3</sub> .....	2.675
*NaF .....	2.45
*MgO .....	2.075

\* In the case of compounds containing only two atoms, the radii have been calculated by simple addition. This is as it should be.

TABLE III. (*continued*).

Substance.	$r_n$ calculated.
Isobutylaldehyde.....	1.305
Methylethylketone .....	1.305
Phenyl acetate .....	1.620
Methyl benzoate .....	1.620
Ethylaniline .....	1.601
Dimethylaniline .....	1.601
$\text{TeH}_2\text{O}_4$ .....	1.471
$\text{ZnSO}_4$ .....	1.051
Glycerine .....	1.323
Aniline .....	1.461

In Table IV. we have assembled the values of magnetic susceptibilities of some substances which are isomorphous and whose elements constituting the molecules have also close family resemblances with each other. These values are shown against their radii, calculated on the equation of closest packing :—

TABLE IV.

Names.	$\chi_m \times 10^{-6}$ . Experimental.	Radius of the molecules calculated on the equation of closest packing.
$\text{BaCO}_3$ .....	43.42	2.193
$\text{SrCO}_3$ .....	25.25	2.056
$\text{CaCO}_3$ .....	14.01	1.836
$\text{MgCO}_3$ .....	6.999	1.620

An examination of this table shows at once that there is a decrease in the magnetic susceptibility of the compound as the radius of the molecule is decreased, a conclusion which is in line with the views of Joos regarding the variation of the value of magnetic susceptibility with the change in the value of  $\bar{r}^2$  in the case of atoms constituting electronic isomers (*loc. cit.*).

Now, according to Langevin's theory

$$\chi_{\text{At.}} = -\frac{e^2}{4mc^2} \sum_n \bar{r}^2.$$

Multiplying this by the Avogadro number, we get

$$\chi_{\text{At.}} = -2.85 \times 10^{10} \Sigma \bar{r}^2, \dots \dots \dots (2)$$

and for a molecule constituting an electronic isomer or an isomorphous body equation (2) may be written as

$$\chi_m = -2.85 \times 10^{10} \Sigma (K r_1)^2, \dots \dots \dots (3)$$

where  $r_1$  represents the value of the radius of the molecule calculated as described before and  $K$  is an arbitrary constant, but which in a series of isomers is found to exhibit variations depending upon the summation of the atomic numbers extending over all the atoms constituting the molecule. Its significance has been discussed later on in this paper.

We shall try to verify the equation adopted, *i. e.*  $K_m = -2.85 \times 10^{10} \Sigma (K r_1)^2$ , by calculating the value of  $K_m$  for electronic isomers and isomorphous series (both organic and inorganic).

The results obtained by calculation from equation (3) are tabulated against the experimental values (most of which are taken from the Physico-Chemical Tables of Landolt and Börnstein). Some values which were not known have been determined experimentally in our laboratory by Mr. S. L. Bhatia, M. Sc., and are communicated for publication in a paper by him.

TABLE V.

Case of Isomorphous substances belonging to the same family.

Names.	$\chi_m \times 10^{-6}$ . Experimental.	$\chi_m \times 10^{-6}$ . Calculated from equation (3).
BaCO <sub>3</sub> , .....	-43.42	-52.46
SrCO <sub>3</sub> , .....	-25.25	-29.18
CaCO <sub>3</sub> , .....	-14.01	-13.28
MgCO <sub>3</sub> , .....	- 6.999	- 7.17
KNO <sub>3</sub> , .....	-33.66	-33.66
NaNO <sub>3</sub> , .....	-26.35	-20.91

TABLE VI.  
Case of Electronic Isomers (Inorganic).

Atomic number.	Names.	$\chi_m \times 10^{-6}$ , Experimental.	$\chi_m \times 10^{-6}$ , Calculated on equation (3).
28	NaCl.....	-23.98	-22.94
28	CaO .. .. .	-15.12	-15.74
64	BaO .....	-18.40	-21.55
64	AgCl.....	-40.13	-31.99
20	NaF .....	-11.76	-10.95
20	MgO .....	-6.73	-7.83
68	K <sub>2</sub> CO <sub>3</sub> .....	-76.02	-81.57
68	CaSO <sub>4</sub> .....	-51.73	-43.0
78	TeH <sub>2</sub> O <sub>3</sub> .....	-33.72	-33.68
78	ZnSO <sub>4</sub> .....	-43.58	-42.44

TABLE VII.  
Case of Electronic Isomers (Organic).

Atomic number.	Names.	$\chi_m \times 10^{-6}$ , Experimental.	$\chi_m \times 10^{-6}$ , Calculated on equation (3).
40	$\left\{ \text{CH}_3 \cdot \text{CH}_2 \cdot \text{CH}_2\text{CHO} \right\}$ ..... Isobutylaldehyde	-47.45	-47.56
40	$\left\{ \begin{array}{l} \text{CH}_3 \\ \text{C}_2\text{H}_5 \end{array} \right\} \text{CO}$ ..... Methylethylketone	-47.74	-47.56
72	$\left\{ \text{CH}_3\text{COOC}_6\text{H}_5 \right\}$ ..... Methyl benzoate	-83.23	-82.90
72	$\left\{ \text{C}_6\text{H}_5\text{COOCH}_3 \right\}$ ..... Phenyl acetate	-82.69	-82.90
66	$\left\{ \text{C}_6\text{H}_5\text{NHC}_6\text{H}_5 \right\}$ ..... Ethylaniline	-89.30	-89.4
66	$\left\{ \text{C}_6\text{H}_5\text{N}(\text{CH}_3)_2 \right\}$ ..... Dimethylaniline	-89.66	-89.4
50	$\left\{ \text{OH} \cdot \text{CH}_2 \cdot \text{CHOH} \cdot \text{CH}_2\text{OH} \right\}$ ..... Glycerine	-56.12	-53.31
50	$\left\{ \text{C}_6\text{H}_5\text{NH}_2 \right\}$ ..... Aniline	-65.1	-65.1

It is to be noted that the agreement between the experimental and the calculated values of  $\chi_m$  in the case of electronic isomers is excellent. In the case of isomorphous series (Table V.) the agreement is fair.

*Significance of K employed in Equation (3).*

K is an arbitrary constant characteristic of a particular group of electronic isomers. The values of  $\chi$  have been assembled in Table VIII. In this table the ratios of K for a set of substances have been compared with the ratios of the summation of atomic numbers constituting these molecules. A very characteristic relationship is at once noticeable.

TABLE VIII.

Substance.	Summation of atomic numbers of elements constituting the compound.	Value of K.	Ratio of the summation of atomic numbers.	Ratio of K.
<b>I.</b>				
BaCO <sub>3</sub> .....	86	1.96	86/42=2.0	1.96 /0.98 =2.0
SrCO <sub>3</sub> .....	68	1.56	68/42=1.6	1.56 /0.98 =1.6
CaCO <sub>3</sub> .....	50	1.176	50/42=1.19	1.176/0.98 =1.19
MgCO <sub>3</sub> .....	42	0.98	42/42=1.0	0.98 /0.98 =1.0
<b>II.</b>				
KNO <sub>3</sub> .....	50	1.7	50/42=1.19	1.7 /1.43 =1.19
NaNO <sub>3</sub> .....	42	1.43	42/42=1.0	1.43/1.43 =1.0
<b>III.</b>				
NaClO <sub>3</sub> .....	52	1.55	52/52=1.0	1.55 /1.55 =1.0
KHSO <sub>3</sub> .....	60	1.788	60/52=1.15	1.788/1.55 =1.15
<b>IV.</b>				
NaCl.....	28	1.0	28/28=1.0	1.0/1.0 =1.0
CaO.....	28	1.0	28/28=1.0	1.0/1.0 =1.0
<b>V.</b>				
AgCl.....	64	1.184	64/64=1.0	1.184/1.184=1.0
BaO.....	64	1.184	64/64=1.0	1.184/1.184=1.0
<b>VI.</b>				
CaSO <sub>4</sub> .....	68	2.0	68/68=1.0	2/2 =1.0
K <sub>2</sub> CO <sub>3</sub> .....	68	2.0	68/68=1.0	2/2 =1.0

TABLE VIII. (continued).

Substance.	Summation of atomic numbers of elements constituting the compound.	Value of K.	Ratio of the summation of atomic numbers.	Ratio of K.
VII.				
NaF.....	20	0.8	20/20=1.0	0.8/0.8 =1.0
MgO .....	20	0.8	20/20=1.0	0.8/0.8 =1.0
VIII.				
Isobutaldehyde ...	40	3.131	40/40=1.0	3.131/3.131=1.0
Methylethylketone	40	3.131	40/40=1.0	3.131/3.131=1.0
IX.				
Phenyl acetate ..	72	3.311	72/72=1.0	3.311/3.311=1.0
Methyl benzoate...	72	3.311	72/72=1.0	3.311/3.311=1.0
X.				
Ethylaniline .....	66	3.497	66/66=1.0	3.497/3.497=1.0
Dimethylaniline .	66	3.497	66/66=1.0	3.497/3.497=1.0
XI.				
TeH <sub>2</sub> O, ... ..	78	2.337	78/78=1.0	2.337/2.337=1.0
ZnSO <sub>4</sub> .....	78	2.337	78/78=1.0	2.337/2.337=1.0
XII.				
Aniline .. ..	50	3.271	50/50=1.0	3.271/3.271=1.0
Glycerine .....	50	3.271	50/50=1.0	3.271/3.271=1.0

It is seen that the values of the constant K in a series are proportional to the atomic numbers. In the case of isomorphous series (Nos. I. and II in the table) the value of K decreases as the summation of atomic number decreases. In the case of electronic isomers the values of K are identical. A very characteristic feature of K is that it is roughly proportional to the number of atoms contained in the molecules. For example, in the case of molecules containing two atoms K has an approximate value of 1 (0.8 to 1.184). For molecules containing four to five the mean value of K is about 1.5 to 1.6 (ranging between 1.43 to 1.96). For molecules containing six atoms it is approximately 2, and rises continuously as the atoms in the molecules are increased. Thus, in the case of iso-butaldehyde and methylethylketone, where the number of atoms is 13,

the value of  $K$  is 3.131. In the case of phenyl acetate and methyl benzoate, with 18 atoms, the value of  $K$  is 3.311, and for ethylaniline and dimethylaniline, with 20 atoms, the value of  $K$  is 3.497. These regularities about the constant suggest that equation (3) may be of fundamental physical significance.

Further work on the magnetic susceptibilities of electronic isomers is in progress.

The authors take this opportunity of thanking Messrs. K. N. Mathur and S. L. Bhatia.

University Chemical Laboratories,  
University of the Punjab,  
Lahore (India).

---

*IIIV. Supplementary Note on the Parallel-plate Condenser in Two Dimensions.* By DORIS MONA HIRST, M.A., and W. B. MORTON, M.A., *Queen's University, Belfast* \*.

IN a note which appeared in this Magazine for October 1926† there was given, along with other results, a graph connecting the "capacity-factor" and the "shape-constant" of a condenser formed by long parallel strips (*loc. cit.* fig. 8). By capacity-factor is meant the ratio of the capacity, per unit length, to the value which would be derived from the elementary formula, on the supposition that the lines of force between the plates are everywhere straight. The shape-constant is the ratio of the distance between the plates to the breadth of either plate. These magnitudes are functions of the modulus of the elliptic functions used to express the solution, and the plates come close together as the modulus approaches unity. Unfortunately, the logarithmic manner in which  $K$  becomes infinite at the limit has the consequence that the shape-factor is comparatively large even when the modular angle is quite near to  $90^\circ$ ; its value is .459 for  $89^\circ$ , so that the capacity, when the planes are closer than this, cannot be calculated by use of Legendre's tables without interpolation. Thus the most interesting part of the graph, corresponding to planes which are close together, was only obtained on a small scale as a prolongation of the curve towards the origin.

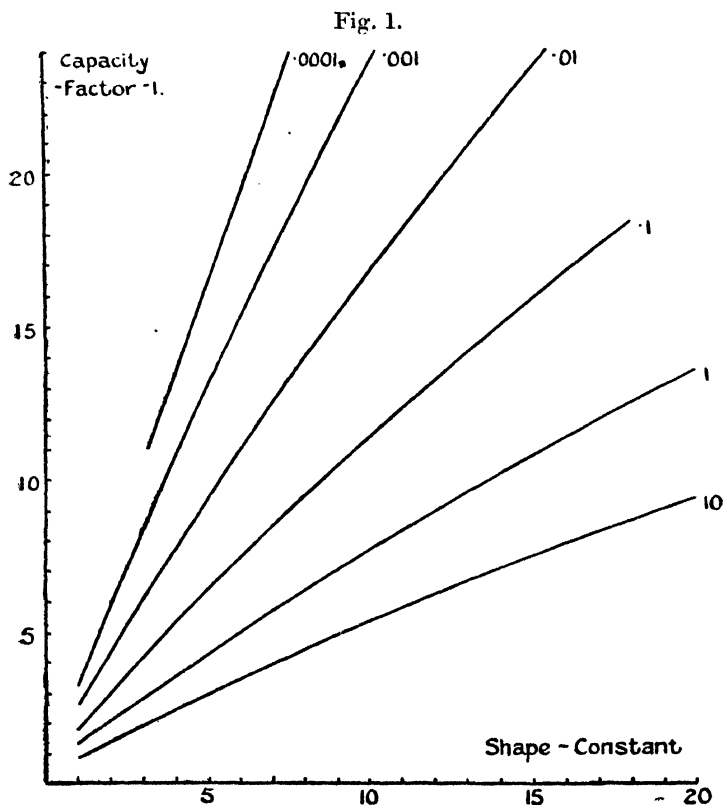
\* Communicated by the Authors.

† W. B. Morton, "On the Parallel-plate Condenser and other Two-dimensional Fields Specified by Elliptic Functions," *Phil. Mag.* ii. p. 827 (1926).



# 546 *Supplementary Note on the Parallel-plate Condenser.*

The object of the present note is to extend the calculated range in this direction. The numerical values were computed by expanding the functions in powers of  $1/K$ . The results are shown on the accompanying diagram. In order to give adequate representation of the entire range of values the graph has been broken into a number of pieces on different



scales. The magnitude marked on each curve is the value to be assigned to the unit of the scales marked along the axes. It will be noticed that even at the smallest values the curve still makes a considerable angle with the vertical axis, although it ultimately touches this axis at the origin.

The following values of the capacity-factor, for selected shapes of condenser, were calculated by interpolation, and are quoted to give an idea of the magnitude of the correction.

Shape-constant 1,	Capacity-factor	2·118
„ „1,	„	1·168
„ „01,	„	1·024

The smallest values calculated were ·000315 and 1·00109, shape-constant and capacity-factor corresponding to  $K=5000$ .

This work was done without knowledge of any previous investigation, except that of Sir Joseph Thomson, mentioned in 'Recent Researches' and quoted in the former note. We owe to Dr. Bromwich a reference to two papers on the same subject—one by J. H. Michell \*, published in 1893, the year in which 'Recent Researches' appeared, and the other by Dr. Bromwich himself † in 1902. In the former paper expansions are given equivalent to those which we have used, but in terms of  $\log 4/k'$  and  $k'$  instead of  $1/K$ . In Dr. Bromwich's work the problem is solved directly by Schwarz's method, and Weierstrass's functions are used.

LV. *On the Acoustics of Strings struck by a Hard Hammer.*

By K. C. KAR, D.Sc., R. GANGULI, M.Sc., and S. C. Laha, M.Sc.‡

INTRODUCTION.

THE theoretical treatment of the problem of struck strings has proceeded on two different lines. To the first class of theories belong those put forward by Helmholtz §, Delemer ||, and Lamb ¶, each of which is based on some assumed law of pressure between the hammer and the string during the time of contact. The second method of attacking the problem is due to Kaufmann \*\*, who gives a rigorous functional solution—provided the duration of contact ( $t$ ) is less than but comparable with the free period ( $\theta$ ) of the string (i. e.  $\frac{t}{\theta} < \frac{l-a}{l}$ )—of the case of a massive particle striking (1) a string of infinite length, (2) a string of finite length at its centre or very near the end. In the case when the

\* J. H. Michell, *Quarterly Journal of Mathematics*, xxiii. p. 72 (1893).

† T. J. Ya. Bromwich, *Messenger of Mathematics*, xxxi. p. 184 (1902).

‡ Communicated by the Authors.

§ Helmholtz, 'Sensations of Tone.'

|| Delemer, *Ann. Soc. sci. de Bruxelles*, xxx. pts. 3-4, pp. 299-310 (1905-6).

¶ Lamb, 'Dynamical Theory of Sound,' p. 74.

\*\* Kaufmann, *Wied. Ann.* liv. pp. 675-712 (1895).

hammer strikes the string near its end, Kaufmann has, however, assumed that the portion of the string between the hammer and the nearer end vibrates as a rigid rod. This assumption of Kaufmann has been done away with by P. Das\*, who, however, makes the further assumption that the hammer gives discontinuous impulses to the string during the time of contact, the time between two successive impulses being the time taken by a wave to start from the hammer and to come back to it after reflexion from the nearer end. With the above assumption Das has extended Kaufmann's theory by proceeding on a line similar to that of Love† for the longitudinal vibration of a string struck at the end.

The experimental work in this direction has been done by Kaufmann‡ himself and also by Hipkins§, who find no agreement with the Helmholtz-Delemer-Lamb theories. The recent experiments of George|| and R. N. Ghose¶ generally support Kaufmann's theory. Recently Datta\*\* has also got results which go to support Das's theory. Systematic data on struck strings appear to be still wanting. In conclusion, we may make a note of Hayashi's†† experiment, where vain attempts have been made to reach the conditions demanded by Helmholtz's theory.

The above is a summary, made up to date, of George's introduction to his paper appearing in *Phil. Mag.* xlvii. p. 591 (1924).

In the present paper, attempts have been made (1) to study the amplitudes of the different harmonics for different striking-points when  $\frac{t}{\theta} >$  or  $< \frac{l-a}{l}$ ,  $t$  being the duration of contact,  $\theta$  the free period of vibration; (2) to subject Das's theory to an experimental test; (3) to determine the impulses given by the hammer to the string at different

\* P. Das, *Proc. Ind. Assoc.* vii. pts. 1 & 2, pp. 13-20 (1921).

† Love, 'Theory of Elasticity,' pp. 411, art. 281 (2nd ed.).

‡ Kaufmann, *l. c.*

§ Hipkins, *Proc. Roy. Soc.* xxxvii. pp. 37-39, and xxxviii. pp. 83 (1884).

|| George, *Phil. Mag.* xlviii. pp. 34 & 48 (1924), I. pp. 91-99 (1924); *Proc. Roy. Soc.* cviii. pp. 284-295 (1925). George & Beckett, *Proc. Roy. Soc. A*, cxiv. (1927).

¶ R. N. Ghose, *Phil. Mag.* xlvii. p. 1125 (1924); *Proc. Ind. Assoc.* ix. pp. 111, 194 (1925); *Phys. Rev.* xxiv. p. 456 (1924), xxviii. p. 1315 (1926).

\*\* S. K. Datta, *Proc. Ind. Assoc.* viii. pt. ii. (1923).

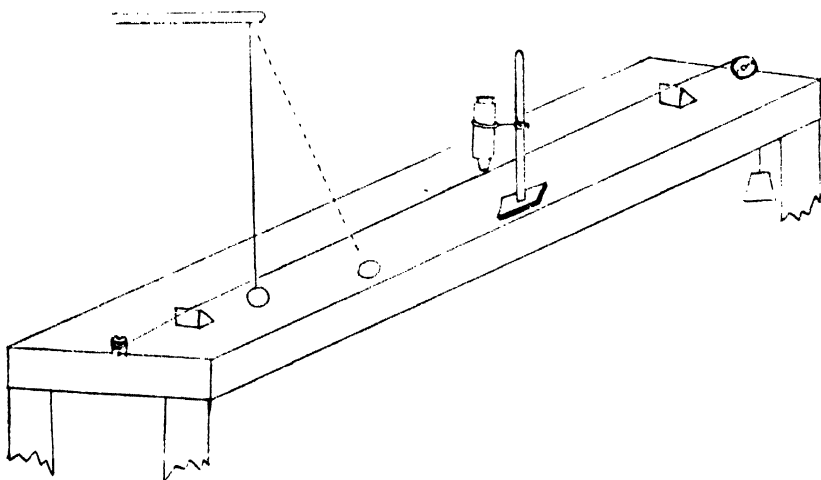
†† Hayashi, *Kyoto Coll. Sci. Mem.* vi. pp. 165-169 (1923).

points ; and (4) to study the effects of the material and the area of contact of the hammer on the changes of amplitudes of different harmonics.

#### EXPERIMENT.

The experimental wire was horizontally stretched over two bridges fixed on the table. The wire was fixed at one end, and the other end, passing over a rigidly-fixed pulley, carried a heavy weight. The striking-hammer consisted of a metal ball suspended freely by means of a fine thread, thus constituting a simple pendulum. When at rest the bob just touched the wire, and the centre of the bob and the wire lay in the same horizontal plane. Thus struck by the bob-

Fig. 1.



hammer the stretched wire began to vibrate in a horizontal plane. A reading microscope of Becker & Co. of magnifying power 40 was focussed on the wire from above (*vide* fig. 1). We may note, in conclusion, that by the above arrangement we can vary the velocity of impact at will.

In order to measure the amplitude of the fundamental, the microscope was focussed on the middle of the wire, which was illuminated by sunlight from below. The bob being taken aside was released and allowed to strike the wire only once, and the amplitude of vibration was determined by the micrometer scale with the eyepiece, one smallest micro

division being equal to  $\cdot 027$  mm. Again, to get the amplitude of the octave, observations were taken with the microscope at  $1/4$ , while the wire was damped at the middle immediately after the impact so as to stop the fundamental. Similarly, for the other harmonics, readings were taken with the microscope at an antinode, the corresponding node being damped immediately after impact. The different amplitudes as observed by the microscope were then corrected for the amplitudes of other harmonics for which the point of observation is an antinode. For instance, from the observed amplitude of the fundamental was subtracted the amplitudes of the 3rd, 5th, and so on, and similarly for others.

The results of our investigations are given in three sections.

In section A, Tables I. and III. give the corrected amplitudes of the first six harmonics for different striking-points along wires of steel and eureka. In Tables II. and IV. are given the amplitudes of the fundamental, and the displacements of the centre of the string at the instant of impact when the hammer strikes the wire at different points with different velocities. In section B, Das's equation has been put to an experimental test. The theoretical and the experimental values of different harmonics are compared in Table V. In section C, Table VI. gives the impulses imparted to the string by the hammer striking with different velocities at different points on the string. And in Table VII. are given the changes of amplitudes of the first three harmonics with changes of the area of contact and the material of the hammer.

The values given in different tables are generally means of about ten observations.

## RESULTS.

### *Section A.*

#### Steel wire :—

Mean diameter of the wire .....	$\cdot 38$ mm.
Mass per unit length .....	$\cdot 00892$ gm.
Length of the vibrating wire ...	290 cm.
Tension in the wire .....	3.5 kg.

#### Striking-bob of iron :—

Mean diameter .....	3.2 cm.
Mass of the bob .....	140.7 gm.

TABLE I.

Initial velocity of impact—60·11 cm./sec.,  $\frac{t}{\theta} > \frac{l-a}{l}$ .

$a$ —distance of striking-point from nearer end.

$a$ (cm.)	Amplitude of Harmonics (in mm.)*.					
	1st.	2nd.	3rd.	4th.	5th.	6th.
20 .....	2·8047	·3370	·0940	·0405	·0573	·0270
29 .....	2·1602	·2835	·1458	·0810	·0240	·0405
32 .....	2·6935	·4320	·1620	·1215	·0945	·0112
40 .....	1·1131	·4590	·1215	·1080	·0054	·0270
50 .....	2·4191	·1080	·1485	·0810	·0324	·0540
60 .....	2·0312	·3100	·1134	·0675	·0054	·0124
70 .....	1·4056	·5940	·1485	·0405	·0459	·0270
80 .....	2·8447	·8050	·0810	·1134	·0243	·0405
90 .....	1·2299	·5030	·0945	·0540	·0756	·0200
100 .....	2·0218	·2160	·1215	·0540	·0567	·0540
110 .....	1·7992	·4750	·0945	·0648	·0513	·0540
120 .....	1·6448	·4620	·1512	·0810	·0540	·0130
130 .....	1·7380	·5070	·1215	·0567	·0405	·0540
140 .....	1·6353	·4050	·1512	·1080	·0134	—

\* Amplitudes of harmonics beyond the 6th were too small to be measured by the microscope at our disposal.

Now, for a string struck at mid-point the maximum value of the displacement, according to Kaufmann's theory †, is given by the equation :

$$y = \frac{v_0 \theta m}{4M} \left\{ 2e^{-\frac{2M}{m}} \right\}, \quad . . . . (1)$$

where  $y$ =the max. displ.,  $v_0$ =vel. of the hammer before impact,  $\theta$ =the free period of the string,  $m$ =the mass of the hammer, and  $M$ =the mass of the string. Substituting the experimental values of  $v_0$ ,  $\theta$ ,  $m$ , and  $M$  for the eureka wire and brass hammer, we find  $y=1·11$  cm., whereas from Table IV.  $y=1·01$  cm. Such a close agreement between

† Kaufmann, *l. c.* See also George, *Phil. Mag.* xlvii. p. 591 (1924).

TABLE II.

 $v$ —velocity of the hammer before impact. $y$ —displacement at mid-point. $F$ —amplitude of the fundamental.

$a$ (cm.).	$v$ cm./sec.	$y$ (cm.).	$F$ (cm.).	$y/v$ $\times 10^{-3}$ .	$F/v$ $\times 10^{-3}$ .
10 .....	44.86	.65	...	14.4	
	89.72	1.24	...	13.8	
	112.10	1.51	...	13.4	
20 .....	44.86	.88	.280	19.0	6.24
	89.72	1.59	.600	17.7	6.68
	112.10	1.91	.784	17.0	7.00
40 ....	44.86	1.12	.111	24.9	2.48
	89.72	2.10	.184	23.4	2.06
	112.10	2.53	.304	22.6	2.71
70 .....	44.86	1.49	...	33.2	
	89.72	2.82	...	31.4	
	112.10	3.48	...	31.0	
90 .....	44.86	1.68	...	37.4	
	89.72	3.15	...	35.1	
	112.10	4.00	...	35.5	
110 .....	44.86	1.95	...	43.4	
	89.72	3.50	...	39.0	
	112.10	4.40	...	39.2	
130 ..	44.86	2.10	...	46.8	
	89.72	4.10	...	45.7	
	112.10	5.10	...	45.5	

the experimental and the theoretical values is a good confirmation of Kaufmann's theory. For the steel wire the experimental value of  $y$  ( $=2.5$  cm. from Table II. for  $v=44.86$  cm./sec.) is much less than the theoretical value 22.3 cm., as it should be due to the fact that in this case \*  $\frac{t}{\theta} > 1$ . It appears from Table II. that the displacement of

the centre of the wire at the instant of impact, as also the amplitude of the fundamental, are approximately proportional to the velocity of impact of the hammer, the constant of proportionality depending on the striking-point.

\*  $t$  is roughly found to be of the order .1 sec.

Eureka wire:—

Mass per unit length of the wire ... 0.569 gm.  
 Length of the wire ..... 290 cm.  
 Tension in the wire ..... 11 kg.

Striking-bob of brass:—

Mass of the bob ..... 26.5 gm.  
 Mean diameter of the bob ..... 2.38 cm.  
 Velocity of the bob before impact . 89.72 cm./sec.

TABLE III.

$a$ (cm.).	Amplitude of Harmonics (mm.).					
	1st.	2nd.	3rd.	4th.	5th.	6th.
10 .....	3.2035	.4050	.6210	.0972	.1755	.0540
20 .....	4.9030	.2700	.2160	.2700	.0810	.0810
29 .....	5.4250	.3510	.4860	.0810	.1890	.0540
40 .....	5.9438	.0675	.4320	.2160	.1242	.0101
50 .....	5.8380	.0540	.1620	.0756	.0110	.0270
60 .....	4.4600	.2025	.4320	.1485	.1080	.0945
70 .....	3.4060	.2700	.5130	.2025	.0810	.1620
80 .....	2.3992	.2800	.4050	.3780	.1458	.0972
90 .....	1.8520	.2970	.4050	.1080	.2430	.0810
100 .....	3.5545	.4860	.3240	.2700	.1215	.0810
110 .....	3.3115	.3240	.4860	.0945	.2025	.0270
120 ... ..	3.9680	.3240	.2700	.3510	.1620	.0120
130 .....	2.8925	.2970	.5400	.0945	.0675	.0540
140 .....	2.4600	.2430	.4050	.2700	.1350	.0810

TABLE IV.

$a$ (cm.).	$y$ (mm.).	Uncorrected Amplitude of the Fundamental (mm.).
10 .....	4.00	4.00
20 .....	5.20	5.20
29 .....	6.10	6.10
40 .....	6.50	6.50
50 .....	7.00	6.01
60 .....	7.50	5.00
70 .....	8.10	4.00
80 .....	8.52	2.94
90 .....	9.00	2.50
100-140 .....	10.10	—



On comparing the displacements and the uncorrected amplitudes of the fundamental\*, *i. e.* the amplitude of vibration of the string as given in Table IV., we find that the two are equal up to about  $L/7$ , when the amplitude of the fundamental is maximum for the first time. After  $L/7$  the displacement goes on increasing while the fundamental decreases. Again, with steel wire and iron hammer we find from Table I. that the amplitude of vibration of the wire never exceeds 3 mm. By extrapolation we find that the displacement of mid-point is 3 mm. when the hammer strikes at about  $L/77$ . Thus the fundamental should be maximum when the striking-point is at about  $L/77$ .

Again, according to George †, for  $m/M = 1$  the fundamental is maximum at  $L/7$ , while for  $m/M = 9.625$  the maximum is at  $L/30$ . In our case, for  $m/M = 1.606$  the maximum is at  $L/7.2$ . Thus on extrapolating we find that for  $m/M = 54.39$  the maximum is at about  $L/80$ . And this agrees fairly well with the value found otherwise. Thus one is led to think that the displacement of the centre and the amplitude of vibration of the wire first begin to differ from the point where the fundamental is maximum for the first time. It may also be noted, in conclusion, that the maxima and the minima of the fundamental and other harmonics become fewer and less pronounced as the relative mass of the hammer ( $m/M$ ) is reduced.

### Section B.

We have already pointed out in our introduction that P. Das ‡ has started with the assumption that the hammer gives discontinuous impulses at  $t = 0, \frac{2a}{c}, \frac{4a}{c}, \dots$ ; *i. e.*, the times at which the waves starting from the hammer come back to it after successive reflexions from the nearer end. Now, according to Das, the pressures in the successive epochs are given by the equations :

$$F_1 = 2\rho v_0 c e^{-kat}, \quad \dots \dots \dots (2a)$$

$$F_2 = 2\rho v_0 c [e^{-kat} + e^{-k(ct-2a)} \{1 - k(ct-2a)\}], \quad \dots \dots (2b)$$

$$F_3 = 2\rho v_0 c \left[ e^{-kat} + e^{-k(ct-2a)} \{1 - k(ct-2a)\} + e^{-k(ct-4a)} \{1 - 2k(ct-4a) + \frac{k^2}{2!}(ct-4a)^2\} \right], \quad (2c)$$

and so on,

\* Obtained by adding ampls. of 1st, 3rd, 5th harmonics.

† George, Phil. Mag. l. p. 495 (1924).

‡ P. Das, *l. c.*

where  $\rho$ =mass per unit length of the string,  $m$ =mass of the hammer,  $k=\frac{2\rho}{m}$ ,  $c$ =velocity of propagation of transverse waves on the string,  $v_0$ =initial velocity of the hammer,  $a$ =distance of the striking-point from the nearer end, and  $t$ =the variable time.

Thus at time  $t=0$  the pressure suddenly increases to  $2\rho v_0 c$ , and then continuously decreases till the reflected pulse arrives at the hammer at time  $t=\frac{2a}{c}$ . During this time, which is the first epoch, the pressure is given by eq. (2a). At  $t=\frac{2a}{c}$  the pressure suddenly increases by  $2\rho v_0 c$ , and again goes on falling according to equation (2b). Thus at the beginning of every epoch the pressure increases by an equal jump,  $2\rho v_0 c$ , and then falls off continuously till after a number of epochs the impact ceases. Having got the pressure-time curve between  $t=0$  and  $t=T$ , where  $T$  is the duration of contact, we proceed to calculate the values of the amplitudes of different harmonics with the help of the well-known equation (notations being same as in eq. 2) :

$$\phi_s = \frac{2}{s\pi c\rho} \sin \frac{s\pi a}{l} \int_0^T F \sin n_s(t-t') dt', \quad (3)$$

where  $T$ =the duration of contact,  $l$ =the length of the string, and  $n_s = \frac{s\pi c}{l}$ . The above equation can also be written as

$$\phi_s = \frac{2}{s\pi c\rho} \sin \frac{s\pi a}{l} \left[ \sin n_s t \int_0^T F \cos n_s t' dt' - \cos n_s t \int_0^T F \sin n_s t' dt' \right]. \quad (4)$$

Thus for the numerical computation of eq. (4) we multiply each ordinate of the pressure-time curve by  $\cos n_s t'$  and  $\sin n_s t'$  respectively, and obtain two new curves for each harmonic. The areas of these curves between  $t=0$  and  $t=T$  give the values of the two integrals in eq. (4). The areas were measured with a planimeter, and the amplitudes of different harmonics were obtained by putting  $s=1, 2, 3$ , etc. The calculated and the experimental values of the amplitudes of the first six harmonics for the eureka

wire and brass hammer under the experimental conditions prevailing are given as follows :—

TABLE V.

Harmonics.	Striking-point $L/10$ .		Striking-point $L/7.2$ .	
	Observed.	Calculated.	Observed.	Calculated.
	mm.	mm.	mm.	mm.
First .....	5.4250	6.8130	5.9438	5.4710
Second .....	.3510	1.5750	.0675	.6304
Third .....	.4860	2.6140	.4320	.1808
Fourth .....	.0810	2.3900	.2160	.1709
Fifth .....	.1890	.4461	.1240	.5500
Sixth .....	.0540	.0909	.0101	.5676

Thus there is no agreement between the theoretical and the observed values, even if some allowance be made for the dissipation of energy in the system and for the fact that some time must elapse, however small, between the striking of the hammer and the measurement by the microscope. It may also be noted that from Das's theory the total impulses given by a brass hammer to the eureka wire (used in our exp.) at  $L/10$  and  $L/7.2$  are equal to 3026 and 3841 gm. wt., whereas the corresponding observed values are 4425 and 4376 gm. wt. Thus Das's theory goes against experimental evidence.

Before concluding this section we should like to make a few remarks on Mr. Datta's work under Prof. Raman's guidance, already referred to in the introduction. Mr. Datta

seems to have made a serious error in taking  $\int_0^T \frac{\cos n_s t'}{\sin} dt'$

"between the limits  $t=0$  and the time where the curve cuts the axis of time." It is quite obvious\*, however, that the other limit will be  $T$ , the time of contact between the hammer and the string. Further, he seems to have ignored the fact that  $n_s$  within the above integral is different for different harmonics. These have, we think, vitiated his calculations

\* Rayleigh, 'Theory of Sound,' vol. i. *L. c.*

throughout. Moreover, he has refrained from giving sufficient data (*e.g.* tension or frequency of the wire), thus making it impossible to repeat his experiment or to check his calculations. At any rate, we fail to see how he could get such a close agreement (sometimes up to 4th place of decimal) between his experimental and theoretical values.

*Section C.*

TABLE VI.

With steel wire and iron ball described in Sec. A.

<i>a</i> (cm.).	Velocity of hammer before impact, $v_i$ .	Velocity of hammer after impact, $v_a$ .	$m(v_i - v_a)$ .	Velocity of hammer before impact, $v_i'$ .	Velocity of hammer after impact, $v_a'$ .	$m(v_i' - v_a')$ .
	cm./sec.	cm./sec.		cm./sec.	cm./sec.	
20	44.86	42.83	12340	60.11	55.04	16200
29	„	44.18	12530	„	57.19	16500
40	„	43.86	12480	„	56.25	16370
50	„	43.77	12470	„	55.84	16310
60	„	43.41	12420	„	55.11	16350
70	„	43.37	12410	„	55.66	16290
80	„	44.22	12540	„	56.20	16360
90	„	43.95	12510	„	56.87	16450
100	„	44.40	12560	„	56.79	16440
110	„	43.60	12450	„	55.89	16300
120	„	42.97	12360	„	56.34	16390
130	„	43.46	12430	„	54.95	16190

Table VI. shows that the impulses imparted to the string pass through a number of maxima and minima as the striking-point is shifted towards the centre from one end. It is of interest to note that in the case of steel wire and iron hammer under consideration the impulse is maximum at about  $L/10$  and  $L/4$ . It appears from Table VII. that the nature of the metal of the hammer plays an important part in determining the amplitudes of the harmonics. Further, as the area of contact is increased by increasing the size of the brass hammer, the fundamental is considerably weakened.

Table VII.

Steel wire under experimental conditions given in Sec. A.

$$a = L/10.$$

Hammer.	Velocity of hammer before impact $v$ cm./sec.	Initial Impulse $mv$ .	Amplitude of Harmonics (mm.).			
			1st.	2nd.	3rd.	
Hollow lead ball	$\left. \begin{array}{l} \text{diameter} = 3.2 \text{ cm.} \\ \text{wt.} = 48.5 \text{ gm.} \end{array} \right\}$	43.45	...	1.157	.3770	.1690
„ iron „		43.45	...	1.066	.3445	.1560
„ copper „		43.45	...	.988	.3055	.1560
Brass ball	$\left\{ \begin{array}{l} \text{diameter} = 2.38 \text{ cm.} \\ \text{wt.} = 26.5 \text{ gm.} \end{array} \right.$	88.40	2342.6	3.5570	.0702	.0243
Brass ball	$\left\{ \begin{array}{l} \text{diameter} = 5.2 \text{ cm.} \\ \text{wt.} = 629 \text{ gm.} \end{array} \right.$	4.00	2516.0	.0189	.0027	...
		88.40	55623.6	.883	.0918	.0297

## CONCLUSION.

(1) Observations taken support Kaufmann's theory. P. Das's extension of Kaufmann's theory is found to have no agreement with experimental evidence. Calculations made by Mr. S. K. Datta to confirm Das's theory are shown to be wrong.

(2) The striking-point for which the fundamental is maximum has been shown to depend on the ratio of the mass of the hammer and the string. For this striking-point the amplitude of vibration of the string is found to be equal to the displacement at the centre.

(3) The displacement at the centre and the amplitude of the fundamental are found to be proportional to the velocity of the hammer before impact.

(4) The velocity of the hammer before impact remaining the same, the velocity after impact is found to change discontinuously with the striking-point, in agreement with George and Beckett's recent observations.

(5) The area of contact and the nature of the metal of the hammer has a great influence on the strengths of the different harmonics.

(6) When struck at  $L/n$  the  $n$ th harmonic is not absent, in agreement with the experiments of Hipkins and Kaufmann.

Further investigations regarding the effect of elasticity of the hammer and the string and direct determination of the duration of contact are in progress and will appear in a later communication.

In conclusion, we express our thanks to Mr. Bhupendra nath Bannerji, M.Sc., for helping us in some of our calculations.

Physics Laboratory,  
Serampore College,  
Bengal, India.  
July, 1927.

---

LVI. *On making very Sensitive Helical Springs from Quartz Fibre.* By H. D. H. DRANE, M.Sc., Ph.D., Research Laboratory, The Thermal Syndicate Limited, Wallsend-on-Tyne \*.

**D**IRECT weighing by loading helical springs made of fused quartz is a simple and convenient method, which has been of service notably in studying adsorption phenomena. Most springs used in this way have been made up by bending rod  $\frac{1}{2}$ –1 mm. or so in diameter approximately to the desired helical shape in an oxygen-fed blowpipe flame, and have had a maximum sensitivity of the order  $10^2$  cm. per gram, but very much more sensitive springs can be produced. The convenience of this method of weighing, or otherwise of applying a small but accurately measurable force, suggests the use of these springs in many types of physical investigation. The present note describes how springs of perfectly uniform curvature may be produced from quartz fibre with a sensitivity of the order  $10^5$  cm. per gram. The sensitivity may easily be made greater than this, but for reasons of difficulty in manipulation probably  $10^5$  cm. per gram represents the practical limit of utility.

The whole process of making a spring need not occupy more than five minutes and is simple to carry out. Four things are required: a supply of quartz fibre, an oxy-coal gas blowpipe, a piece of fused quartz tube of uniform diameter, and a tubular wire-wound furnace in which the quartz tube may be heated to about  $1000^\circ\text{C}$ . A length of the quartz fibre is selected (diameters 0.005 cm. and below are suitable) and weighted at one end by a small pellet of wax. The silica tube, which may conveniently be 1–2 cm. in

\* Communicated by Lord Rayleigh, F.R.S.

diameter, is softened near one end over an area about 3 mm. square by heating in a small oxy-gas flame. Then, holding the fibre an inch or so from its free end so that this portion projects horizontally, the heated zone of the tube is lowered on to the fibre, keeping the fibre at a right angle to the axis of the tube. Lowering the tube on to the fibre avoids trouble from convection-currents of air which rise from the heated tube. In this manner the fibre becomes attached to the tube by fusion and may later be wound up in the form of a helix. The weighted fibre should not, however, be allowed to hang directly from its point of attachment to the tube where it may easily be broken. The first half turn of the helix should be made very loosely by looping the fibre over the tube with the weight of the wax pellet supported, and only then allowing the pull of the weighted fibre to make this half turn taut. The fibre is then wound up at will, and secured by fusion to the tube near the weighted end in a similar manner to that already described. A small area of the tube 1 cm. or so from the last made turn of the helix is softened, and over this the remaining portion of the fibre, is wound. In this process the surplus piece of fibre is usually drawn off automatically by the weight of the wax pellet.

The coiled fibre on its supporting tube is now placed axially into the uniformly heated zone of the tubular furnace and brought to  $1000^{\circ}\text{C.}$ , for a few (one or two) minutes. It saves time and is otherwise advantageous to keep the furnace ready at about  $1000^{\circ}\text{C.}$  After heating, the tube and fibre are removed and allowed to cool immediately. The attachments at the end of the fibre are then broken by the finger-nail or otherwise, and the fibre, now in the form of a helix of slightly larger diameter than the tube, may be easily removed. If required, the ends of the spring may be bent about by heating in a very fine jet of coal-gas or hydrogen burning in air.

As an example of the method, coiling fibre  $4.0 \times 10^{-3}$  cm. diameter on to a tube 0.69 cm. diameter and heating for two minutes at  $970^{\circ}\text{C.}$ , gave a fibre spring 1.02 cm. diameter. The sensitivity of this spring was not determined, but a similar spring with twenty turns, 0.88 cm. diameter, extended at the rate of  $0.33 \times 10^5$  cm. per gram, the diameter of the fibre being  $1.65 \times 10^{-3}$  cm. By altering the conditions of heating, springs of varying diameters may be produced, and it is proposed later to communicate a study of the elastico-viscous behaviour of fused quartz based upon this method.

LVII. *Oscillatory Ionization Currents from Clouds of Cadmium-Oxide Particles.* By H. P. WALMSLEY, M.Sc.\*

[Plate IX.]

THE ionization currents which are obtained from clouds of cadmium-oxide particles dispersed in air by an arc discharge between cadmium electrodes have been described previously<sup>(1)</sup>. The currents obtained seem to be the sum of two effects<sup>(2)</sup>. The ionization present on formation of the cloud diminishes with time by recombination, and, as the cloud ages, new ions are produced whose number increases from zero to a maximum and then diminishes. The problem of the present paper is to determine whether the new ions are produced by a continuous process, such as one usually associates, say, with a chemical reaction, giving rise to a smooth ionization curve, or whether the ions are produced by several continuous processes each of which passes through a maximum at a time distinct from the others, thus producing the apparently oscillatory curves which have been described.

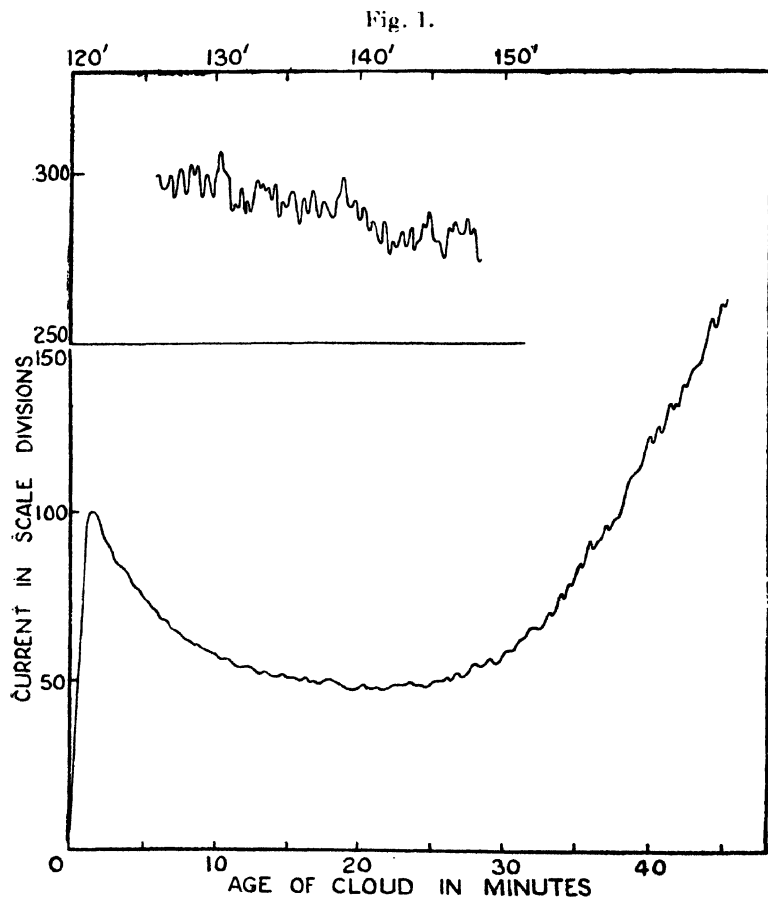
The apparatus employed was similar to the one used before, but instead of measuring the ionization currents by the rate of change of potential of the system, the insulated quadrant of the electrometer was connected to earth through a xylol-alcohol high resistance, and the steady deflexion method was employed. The high resistance increased the electrical capacity of the system and reduced the sensitivity of the apparatus, so that only the currents from the more strongly-ionized clouds could be measured easily. These always gave a curve showing a rise in current strength at some time after the initial sparking in the arc had ceased.

A number of clouds were examined which had been dispersed in dry air free from dust and carbon dioxide. The currents from both positive and negative ions were found to behave similarly. Fig. 1 is an ionization current from the negative charges of a cloud which was dispersed by arcing for 15 seconds. The subsequent variation with time of the deflexions of the electrometer needle are shown in scale divisions. For steady currents 11 scale divisions represent a current of  $10^{-18}$  ampere approximately. In all cases it was found that the ionization curves apparently consisted of a series of kicks following each other rapidly. Their magnitudes varied considerably and the time-intervals between the kicks seemed irregular. Compared with the

\* Communicated by the Author.



fluctuations on the weaker clouds, which were measured by the time-rate of the deflexions, those from the denser clouds measured by the steady deflexion method are more numerous, though their mean excursion expressed as a fraction of the total current flowing is considerably less. The diminution in number with the weaker clouds is at least



partially accounted for by the method of measurement which averages the effects over the time occupied in obtaining each reading. This not only reduces the number of fluctuations observed, but smoothes them out and tends to eliminate them. Thus, had the currents from the *same* cloud been measured by the two methods, the record by the steady deflexion method should show more numerous and relatively

greater fluctuations in current strength. Provided the fluctuations are not fortuitous, but result from real physical processes such as have been postulated, the decrease in the relative magnitude found for the more strongly-ionized clouds suggests that the number of such processes increases with increasingly denser clouds, and that an ultimate state might be attained in which they were so numerous that the resulting currents would simulate those from a smooth continuous process.

Experimentally, the view that the current is built up of component parts and that each fluctuation indicates the presence of one of them depends upon the extent to which the fluctuations are greater than the experimental errors. Those obtained by the "rate of change" method certainly appeared to be greater than the possible errors. However, as the fluctuations obtained by the more reliable "steady deflexion" method were both more numerous and relatively smaller, the results of a detailed examination of the question are given in what follows.

#### *Photographic Registration of the Currents.*

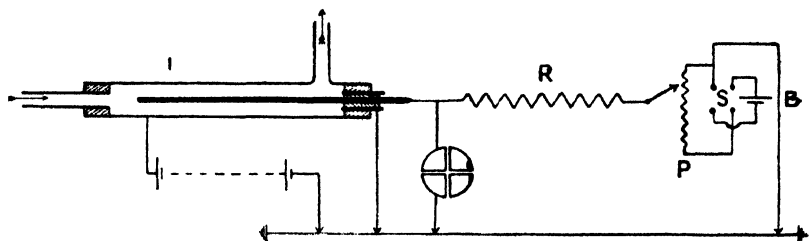
To obtain a more accurate record of the currents, the motion of the electrometer needle was photographed by means of an Edelmann apparatus, where the lateral movements could be registered as an oscillatory line on sensitized paper. A second stationary image of the lamp filament was placed on the paper to provide a fiducial line and to check any movement of the apparatus during an experiment. This image was cut out during an exposure for the first five seconds of every minute. Hence on the record the fiducial line appears broken and forms a convenient time-scale. To avoid errors in numbering the minutes, the half hours were usually distinguished by a break of 15 seconds instead of 5.

Since the width of the sensitive paper is only 6 cm., it is necessary to confine the deflexion of the image to that range; i. e., the potential of the electrometer must be maintained near zero—a favourable circumstance, for the readings thereby reap some of the advantages enjoyed by null methods of working with the electrometer. This was done by applying a suitable potential from a potentiometer to the end of the high resistance whenever the spot of light tended to leave the camera lens. The arrangement of the electrometer circuit is shown in fig. 2. The central electrode of a cylindrical ionization chamber I is connected to the insulated quadrant of the electrometer and to one end of

the xylol-alcohol resistance  $R$ . The other end of  $R$  is in contact with a potentiometer  $P$  to which a Weston cell  $B$  is connected in circuit with a reversing switch  $S$ . By means of  $S$  the potential of  $P$  can be made either positive or negative according to whether the currents from negative or positive charges are being measured, without changing connexions. It is also useful when testing the sensitivity of the electrometer.

A Dolezalek electrometer was used at a sensitivity of from 400 to 2000 scale divs. per volt at the camera, according to the purpose of the particular experiment. The sensitivity could be measured on a scale fixed near the camera lens, but usually a record of the deflexion of the needle charged to a known potential was taken on the sensitive paper just before

Fig. 2.



dispersing the cloud. After running the paper a few centimetres, the needle was earthed and the reel stopped when the deflexion again became steady. The speed of the paper was between 100 cm. and 120 cm. per hour. It was cut into metre lengths after exposure for ease in development.

The carrying-out of an experiment with the apparatus is quite straightforward, but, as most of the work has to be done in a darkened room, it is advantageous to make a list of the rather numerous initial operations to be performed, and follow the same routine with each experiment.

### *Experimental Results.*

In fig. 3 (Pl. IX.) are reproduced parts of a record obtained by this method. This cloud was produced by arcing between cadmium electrodes in dry air free from dust and carbon dioxide for 15 seconds. The current rises sharply almost immediately after the dispersal commences and the trace tends to leave the paper. The drop at 0' 45'', and the subsequent falls which occur at 5' 15'', 8' 15'', and

at 13' 15'', are caused by the alteration of the potential at the end of the high resistance, which was necessary to keep the deflexions on the record. To obtain the ionization curve showing the variation of current with the age of the cloud, it is necessary to cut the film at the time corresponding to the change of potential and raise the fiducial line by an amount equivalent to the change in voltage. If this be the same at each alteration and equal to that employed in determining the sensitivity, the true deflexion, *i. e.* the ionization curve with an arbitrary ordinary scale, is obtained by taking the difference between the curve on the raised section and the trace representing the dead-beat swing of the electrometer needle. This gives a graph corresponding to that of fig. 1.

The photographic records (Pl. IX. figs. 3 & 4) bring out clearly the fluctuating nature of the ionization current. The deflexions in fig. 3 (Pl. IX.) are sharp, and show considerable variations in magnitude over any short interval of time, as well as a general increase as the cloud ages. The latter, however, is not proportional to the deflexion. At 6½ minutes the deflexion is 18.7 cm., at 11 minutes it is 12.3 cm., at 73 minutes it is 37.0 cm., and at 150 minutes it is 38.5 cm. Taking the magnitude of the fluctuations to be the average width between two smooth lines enclosing them, the ratios of the magnitude to the deflexion at these times are 2.30, 2.03, 1.08, and 1.30 per cent. respectively. The ratio thus falls to a minimum and subsequently rises.

Fluctuating currents have been obtained from every cloud examined. They are not wholly due to irregularities in the rate of flow of cloud through the ionization chamber, for they are perceptible when no flow of cloud is taking place and the current is derived from cloud left in the chamber when the flow ceased. The fluctuations are not destroyed when the cloud in the dispersal chamber is continually stirred by a fan, and they are not due to unsteadiness of the electrometer needle. Although this is not perfectly steady as a rule, before the cloud is dispersed, the resulting movements are quite distinct from the fluctuations, as may be seen in fig. 3 (Pl. IX.). The fluctuations, therefore, are due to some property of the cloud.

#### *The Source of the Oscillations.*

On the assumption that the ions enter the electric field with the gas stream, there are two possible sources of origin. If at every given instant the ionization throughout the cloud

is homogeneous, the oscillations recorded must represent changes in the density of ionization with time. If, however, there are fortuitous fluctuations in the density of the ions throughout the medium, the oscillations may be due to ions entering the field in clusters or groups. In the latter case the oscillations are occasioned by the flow of cloud past the collecting electrode, whilst in the former case they are not dependent upon the flow.

Density fluctuations may arise in two ways. Even in a homogeneous cloud or a gas, the Brownian motion of the particles causes the number of particles  $\nu$  in a given volume to fluctuate about the average  $\nu_0$  appropriate to the cloud or gas. Writing  $\nu/\nu_0 = 1 + \delta$  the mean value of the deviation  $\delta$  is obviously zero, but the mean of its absolute value  $|\delta|$  is equal to  $\sqrt{2/\nu\pi}$  provided  $\nu$  is a large number<sup>(3)</sup>. The fluctuations in density increase relatively as the number of particles per unit volume decreases. Thus, if the number of ions discharging per unit time at the inner electrode of the ionization chamber is sufficiently small, we may expect fluctuations in current strength due to this cause.

Density fluctuations may also arise in the cloud if, during the dispersal process, the matter removed from the neighbourhood of the arc by the air stream from the fan is not subsequently thoroughly mixed with the gas in the cloud chamber. The distribution of density in this case will be somewhat analogous to that which accounts for the appearance of the quivering air over a heated surface. It would cause ions to enter the electric field in clusters or groups.

(a) To determine whether the magnitude of the observed fluctuations at any time is of the order to be expected from probability considerations, requires a knowledge of the average number of ions per unit volume of the cloud at that time. Assuming that the ions carry the electronic charge, this number can be calculated from the mean current which will now be proportional to the deflexion of the electrometer needle. Taking the case of the cloud of fig. 3 (Pl. IX.) when 73 minutes old, the current corresponding to a steady deflexion of 37 cm. is  $4.25 \times 10^{-12}$  ampere. This current is given by negative charges in the cloud; so the number of electrons passing through the collecting electrode per second is  $4.25 \times 10^{-12} / 1.6 \times 10^{-19} = 2.66 \times 10^7$ , which we assume to be the number of ions involved. Inserting this value in Smoluchowski's formula, we find  $|\delta| = 1.55 \times 10^{-4}$ . The calculated fluctuation from second to second is therefore  $2 \times 1.55 \times 10^{-4}$ , i.e. 3.1 parts per

10,000 of the normal current strength. The observed fluctuation is about 1.08 per cent.\*, so is approximately 35 times greater than that to be expected with the above assumptions from density fluctuations due to the Brownian motion of the ions. If we take into consideration that the time-interval between the successive fluctuations on the trace is more nearly 4 seconds than 1 second, a more appropriate value for the theoretical fluctuation would be  $1.55 \times 10^{-4}$ , making the ratio 70 instead of 35. In any case, the theoretical value  $3.1 \times 10^{-4}$  could hardly have been detected at all in the experiment, as it would be represented by an oscillation about one-tenth of the thickness of the photographic trace itself—much less than the motion due to unsteadiness of the electrometer needle.

Brownian motion might account for the observed fluctuations if the ions carried multiple charges. Reversing the calculation and inserting the value  $\frac{1}{2} \times 1.08 \times 10^{-2}$  for  $|\delta|$  we obtain  $\nu = 2.18 \times 10^4$ . The rate of flow of cloud through the ionization chamber was 4 c.c. per second. With a time-interval of 4 seconds the value of  $\nu$  corresponds to a cloud containing  $1.36 \times 10^3$  ions per c.c. The average charge per ion  $= 4 \times 2.66 \times 10^7 / 2.18 \times 10^4 = 4.88 \times 10^3$  electrons. Brownian motion could therefore account for the observed fluctuations if the cloud contained 1360 ions per c.c., each carrying

\* If the deflexions recorded were proportional to the current. Since the current is fluctuating, the potential at the electrometer side of the high resistance will be less than that due to a steady current of equal strength. The fluctuations recorded are forced oscillations produced by changes in this potential, and as the free motion of the needle was aperiodic, these will in general be again much less than those due to steady changes in potential of equal magnitude. For example, if the ionization current were given by  $i \sin pt$ , the fluctuating potential acting on the electrometer would be ultimately given by

$$V = \frac{Ri}{\sqrt{1 + C^2 R^2 p^2}} \sin(pt - \epsilon),$$

where C is the capacity of the system, R the high resistance, and  $\tan \epsilon = CRp$ . The motion of the electrometer needle is given by

$$\ddot{\theta} + k\dot{\theta} + \mu\theta \propto V;$$

so if the instrument is calibrated as a voltmeter, the readings in volts are given by

$$v = \frac{\mu}{\sqrt{\frac{1}{4}(\mu - p^2)^2 + k^2 p^2}} \times \frac{Ri}{\sqrt{1 + C^2 R^2 p^2}} \sin(pt - \epsilon - \epsilon'),$$

where  $\tan \epsilon' = kp/(\mu - p^2)$ .

The steady deflexions ( $p=0$ ) are of course given by  $v=Ri$ . Thus the actual fluctuations are in all probability considerably greater than the fluctuations recorded. Hence the calculations which follow are of necessity only accurate as regards the order of magnitude of the quantities involved.

an average charge of nearly 5000 electrons. The number of ions, 1360 per c.c., is much smaller than the number of ultra-microscopic particles in the cloud. The latter was probably of the order of  $10^7$  per c.c. at least. Hence, if the clouds are homogeneous in the sense that the ions in a given volume not taken too small, say 1 c.c., are similar in number, size, etc., to those in any other c.c. on the average, and the fluctuations in current strength are due to density variations in the cloud, some of the ions must be very heavily charged. This seems to be a very improbable state of affairs if the ions enter the electric field with the gas stream.

Some of the particles might, however, acquire large charges if they acted as conductors and acquired a charge from the charged electrode by contact. To account for the effect the charge per ion is  $(4.88 \times 10^3) \times (4.8 \times 10^{-10})$  E.S.U.  $= 2.34 \times 10^{-6}$  E.S.U. The outer cylinder of the ionization chamber was charged to 400 volts  $= 1.33$  E.S.U.; hence the average capacity of the carriers involved is  $1.75 \times 10^{-6}$  cm. Assuming the carriers to be spherical, this is their radius. They are therefore almost amicrons. On this hypothesis it is difficult to see why so few particles and those amicrons should possess the property of transferring charge. It would be more difficult to explain why their numbers should increase with time to a maximum, and still more to explain why the property should be more marked in dense clouds than in sparse ones, particularly as in the former their chances of disappearance by coalescence would appear to be more favourable.

We can hardly escape these difficulties by postulating larger carriers. We have still to explain the increase in efficiency with time, and, in addition, some explanation would be required of why the fluctuations did not obey Smoluchowski's formula, for we can only increase the size of the carriers by diminishing their number.

(b) The view that the oscillations are caused by the ions entering the electric field in clusters or groups owing to imperfect mixing of dispersoid and the medium seems equally untenable. The fluctuations persist whether the fan in the cloud chamber is rotating slowly or rapidly, or not rotating at all, during the whole life of the cloud after dispersal. Apparently they cannot be destroyed by mechanically mixing the cloud. Even if the mixing were imperfect initially and the cloud not disturbed by the fan, the Brownian motion of the particles would tend to produce a

uniform distribution as the cloud aged<sup>(4)</sup>. We should therefore expect the magnitude of the fluctuation to diminish with time. Actually the oscillations grow in magnitude as the cloud ages, and although the fluctuation diminishes for a time, it passes through a minimum and afterwards increases.

The frequency of the oscillations lends no support to the theory of imperfect mixing. For simplicity, suppose we had employed a parallel plate type of ionization chamber and consider only the flow of ions. Ions of mobility  $\kappa$  in a plane perpendicular to the direction of the flow are driven by the field to the collecting electrode, and are spread out over a distance  $y = Q/\kappa V$  in the direction of flow, where  $Q$  is the rate of flow into the ionization chamber and  $V$  the potential gradient in the field. Hence, if all the ions have the same mobility, the groups crossing this plane will strike the collecting electrode as groups in which the distribution of ions is unaltered<sup>(5)</sup> and the resulting ionization current will be oscillatory. If, however, the groups contain ions of different mobilities, the field will sort each group containing  $n$  different mobilities into  $n$  groups, each of which takes a different time to cross the field. Thus, if  $g$  such groups enter the field in unit time and are distributed at random in the gas stream, we may expect  $ng$  groups of ions to strike the collecting electrode per unit time, provided we neglect the possibility of a slowly-moving group of ions from one cluster striking the electrode simultaneously with a more mobile group from a later cluster. Thus the  $g$  groups would give rise to  $ng$  fluctuations per unit time. I have seldom found more than 7 or 8 fluctuations per minute in any cloud, using a flow  $Q$  of 250 c.c. per minute. The maximum value of  $ng$ , therefore, is 32 per litre. As the work in a previous paper<sup>(1)</sup> has shown that  $n$  is probably large, it follows that the number of groups or clusters, if any, must be very small\*.

From their mobility, the ions have been shown to be

\* This argument fails, of course, if the mobilities of the particles are so close that the dispersive action of the field is insufficient to separate the groups. In this case the effect of the field would be to increase the volume occupied by each cluster before it entered the ionization chamber. The fluctuations would now indicate a sparse distribution (32 per litre) of locations where the volume density of electrification was relatively great. It is difficult to see how such a state could develop in the cloud and then be maintained for long periods against the self-repulsion of the charges. A system of doublets might overcome the question of electrostatic stability, but would lead to consequences for which there is no experimental justification at present.



charged particles in the cloud <sup>(1)</sup>; so an irregular distribution of ions such as would exist on the theory of imperfect mixing suggests an irregular distribution of particles. This distribution of density will become more marked as the volume of the cloud examined diminishes. Observations of the particles in clouds produced from an arc have been made by Whytlaw Gray, using an ultra-microscope, upon a volume of  $1.27 \times 10^{-6}$  c.c.<sup>(6)</sup> This should be eminently suitable for the purpose. The individual counts of the number of particles in successive volumes of cloud of this size give no indication whatever of clustering. As these counts presumably are typical of arc clouds, it is evident that successions of numbers much higher and much lower than the average were not found. The fluctuation of the individual counts about the mean seems no greater than is to be expected from the probability variations in a homogeneous cloud.

Collecting the evidence for imperfect mixing, the frequency of the oscillations shows that the resulting clusters are few in number. They have not been observed in the ultra-microscope, and they are not destroyed by diffusion or mechanical agitation. The conclusion that imperfect mixing does not account for the oscillations seems inevitable. The clouds are homogeneous, therefore, in the sense that the contents of one c.c., say, are similar to the contents of any other c.c. within the limits imposed by statistical fluctuations. It is equally certain that the current is not wholly carried by ions possessing a large average charge.

(c) It is possible that the oscillatory current is the resultant of two effects. The main current may be carried by ions with small charges whose density varies relatively slowly with time, giving rise to a smooth curve, and the fluctuations fig. 3 (Pl. IX.) are superposed upon this by ultramicros acting as carriers of large charges. There is an upper limit to the charge which can be acquired by an ultra-micron by contact with the charged boundary of the electric field. This is determined by the dimensions of the tube carrying the gas stream from the cloud chamber to the field. With a steady flow the particles in motion in the stream slowly settle under gravity. Assuming them spherical, Stokes's law gives the relation between the velocity of fall and their radius  $a$ . The tube is horizontal. Hence, if the time taken by a particle to fall through a distance equal to the diameter of the tube is less than the time

required for it to pass through the tube, it will settle on the wall of the tube, and no particles of that size will enter the field—provided we neglect the growth by coalescence during the passage of the particles through the tube. Taking the axis of  $y$  vertically downwards and that of  $x$  horizontal, with sufficient accuracy

$$\dot{y} = v = 2/9 \cdot a^2 g \rho / \eta. \quad (\text{Stokes's Law.})$$

Assuming the particle moves with the stream, the velocity

$$\dot{x} = 2Q(\alpha^2 - r^2)/\pi\alpha^4,$$

where  $Q$  is the flux and  $\alpha$  the radius of the tube.

$$\text{Substituting} \quad r = \alpha - vt,$$

$$\dot{x} = 2Qvt(2\alpha - vt)/\pi\alpha^4,$$

$$\text{and} \quad x = 2Qvt^2(\alpha - \frac{1}{2}vt)/\pi\alpha^4,$$

the particle hits the bottom of the tube when  $\dot{x} = 0$ ; *i. e.*,  $vt = 2\alpha$  at a distance

$$x = 8Q/3\pi\alpha r.$$

If  $L$  be the length of the tube, the particle will not leave it unless

$$v < 8Q/3\pi\alpha L;$$

$$\text{i. e.,} \quad \alpha < (12\eta Q/\pi\rho g\alpha L)^{\frac{1}{2}}.$$

Inserting the experimental values for the case of the lighter trace of fig. 4 (Pl. IX.),

$$Q = 3.12 \text{ c.c./sec.}, \quad L = 120 \text{ cm.}, \quad \text{and} \quad \alpha = 0.25 \text{ cm.},$$

no particles will enter the field if  $\alpha \geq 2.95 \times 10^{-4} \text{ cm.}$  To obtain an appreciable proportion of the number of particles entering the tube,  $\alpha$  must be considerably less. With a value  $\alpha = 2 \times 10^{-4}$ , little more than one-third of the particles reach the field\*.

The upper limit to the charge carried across the field by a particle is  $2.95 \times 10^{-4} \times 500/300 = 4.9 \times 10^{-4} \text{ E.S.U.}$  For steady currents the charge ( $\int idt$ ) collected by the electrode

\* The order of magnitude of these quantities agrees with the experimental values found on the previous paper. When the cloud of fig. 3 of that paper was  $2\frac{1}{2}$  hours old, the radius of the slowest-moving ions, estimated from their mobilities on the assumption that they carried the electronic charge, was  $1.76 \times 10^{-4} \text{ cm.}$  The values of  $Q$ ,  $\alpha$ , and  $L$  were substantially the same as those above, and the ions must have been present in appreciable numbers to have been detected.

is proportional to the area enclosed by the trace. The sensitivity was 2040 mm./volt, the high resistance  $1.05 \times 10^{11} \omega$ , and the paper was run at a rate of 20 mm./min. Hence 1 sq. mm. on the paper (which is 6 cm. wide) represents a charge of  $3/2040 \times 1.05 \times 10^{11}$  coulombs  $= 1.5 \times 10^{-5}$  E.S.U. The charge carried by the particles is represented, therefore, by an area of 12 sq. mm. on the paper. It is evident from the record that, even on these assumptions which overestimate the effect of a solitary particle, it would be necessary for numbers of them to act together to account for the oscillations. Thus, whether the current is wholly due to the ions carrying small charges, or to heavily-charged ions alone, or to a mixture of both, each fluctuation results from the joint contributions of many ions to the current.

Since the current as a whole is due to ions which have appeared in the cloud as it ages, the magnitude of the fluctuations conforms with the theory that the disruptive process to which they are due is not continuous, but consists of a series of component continuous processes, each of which gives rise to an ionization current which passes through a maximum occurring perhaps at a characteristic time in the life of the cloud. On this hypothesis the superposition of these components would produce the fluctuating current observed, and the number of components would equal the number of fluctuations observed.

Evidence has been given previously that the current as a whole is due to charged particles which have arisen from the disruption of unstable aggregates produced in the cloud during the process of coalescence of primary particles formed by the arc<sup>(2)</sup>. From the present results it seems a legitimate deduction, that each component of the current is due to the disruption of a specific group of unstable aggregates, and that, as the cloud ages, the disruptions in individual groups become successively dominant. That the number of these groups is so large, being equal, when the field does not separate the resulting ions into distinct groups, to the number of the fluctuations, need occasion no surprise. If the particles of a cloud in which the primary particles are coalescing to form aggregates are analysed into groups according to the number of primaries contained in each particle, we expect, *a priori*, to obtain a complex distribution, for both the number of groups and the number of particles in each group would be expected to change as the cloud aged. If, further, certain of the unions between primaries in the aggregates are unstable and possess something of the nature of an average life, we could hardly expect an analysis

into groups of the unstable particles to be less complex. The results of the experiments therefore lead to the conclusion that, from a study of the fluctuating ionization currents, we may hope to obtain ultimately an analysis and a life-history of at least the unstable aggregates in clouds. As this would be of some importance in the study of disperse systems in gases, further experiments are being undertaken to check the accuracy of these deductions.

### *Summary.*

The ionization currents from cadmium-oxide clouds dispersed from an arc have been registered photographically, using the steady-deflexion method of measuring currents. They are found to fluctuate rapidly. On experimental grounds, and by comparison of the magnitude of the effect with what would be expected from the theory of chance fluctuations it is concluded that the observed fluctuations represent time-changes in the density of ionization throughout the cloud. As the currents investigated arise from the disruption of unstable complex particles which have been produced in the cloud during the process of coagulation, it is suggested that each fluctuation is due to a group of unstable complexes which apparently possess the same average life. The current due to a group is conceived to be zero initially, increase with time to a sharp maximum (corresponding to the fluctuation) at the mean time of disruption of the group, and afterwards to steadily diminish. The superposition of currents corresponding to successive groups of unstable particles gives the fluctuating current which is observed.

### *References.*

- (1) Walmsley, *Phil. Mag.* (7) i. p. 1266 (1926).
- (2) Walmsley, *Phil. Mag.* (7) iii. p. 587 (1927).
- (3) Smoluchowski, Boltzmann *Festschrift*, p. 626 (1904);  
*Ann. d. Phys.* xxv. p. 205 (1908).
- (4) Smoluchowski, *Phys. Zeit.* xvii. p. 557 (1916).
- (5) Townsend, 'Electricity in Gases,' p. 134 (Oxford, 1915).
- (6) Whytlaw Gray, *Proc. Roy. Soc. A*, cii. p. 600 (1923).

*Erratum.*—Fig. 3 (Pl. IX.) for 45' read 145'.

LVIII. *Some Experiments on the Auto-Electronic Discharge.*

By N. A. DE BRUYNE. (Communication by the Staff of the General Electric Company, Limited, Wembley.)

[Plate X.]

## SUMMARY.

A CLEAN tungsten cathode of small diameter was produced by burning out a tungsten filament. The auto-electronic currents from this cathode in a high vacuum were reproducible. The currents were decreased by hydrogen and still more by air; they were increased by coating the cathode with barium. It is concluded that auto-electronic currents are not due to gas, but that they depend on the nature of the cathode in somewhat the same way as the thermionic emission.

LILIENTFELD discovered that if a cold cathode is subjected to a sufficiently high electric field, currents of the order of microamperes flow from it; such currents he terms auto-electronic. Recent workers on the subject include, besides Lilientfeld himself \*, Millikan and Eyring †, the staff of these laboratories ‡, Rother §, and del Rosario ||. Of these, Lilientfeld and ourselves connect the magnitude of the currents with the nature of the cathode, and produce evidence that the currents are the greater from the more electro-positive cathode. Del Rosario considers that the whole effect is due to residual gas. The experiments here described were directed to decide between these alternatives.

*Experimental Details.*

In order to investigate the effect of gases on the discharge, it is obvious that the cathode must be as clean and gas free as possible. For this reason the cathode was formed in a high vacuum by burning out a tungsten filament at a high current density. This produced two smooth fused ends,

\* J. E. Lilientfeld, *Zeit. f. Phys.* xv. p. 46 (1923); *Phys. Zeit.* xxiii. p. 507 (1922).

† R. A. Millikan and C. F. Eyring, *Phys. Rev.* xxvii. p. 51 (1926). A preliminary note appears in *Phys. Rev.* xxii. p. 525 (1923).

‡ Research staff of the G. E. C., Ltd. (B. S. Gossling), *Phil. Mag.* 1. p. 609 (1926).

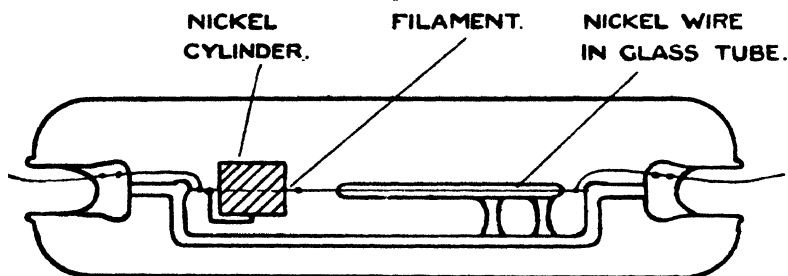
§ F. Rother, *Ann. d. Phys.* lxxxi. p. 317 (1926). This paper contains a bibliography of previous work.

|| C. del Rosario, *J. Franklin Soc.* cciii. p. 243 (1927).

one of which was used as a cathode. The form of discharge-tube used is shown in fig. 1. One end of a straight tungsten filament was spot welded to the bottom of the closed end of a concentric nickel cylinder. The other end of the filament was spot welded to a long nickel electrode encased in a glass tube to increase its rigidity. The electrodes were assembled on a framework consisting of two lamp pinches joined by a glass rod; the completed assembly was then slid into a glass tube and sealed in.

The tubes made in this way were baked at  $400^{\circ}\text{C}$ . for an hour; the nickel cylinder was heated to bright red heat by an eddy-current heater for twenty minutes. The filament, which before sealing-in had been thinned down locally by a tiny flame, was lit at bright white heat for half an hour. It was then burnt out by suddenly raising the current; a

fig. 1.



slow increase of current always resulted in a tangled filament. Fig. 2 (Pl. X.) shows a silhouette of a cathode formed in this way, and fig. 3 (Pl. X.) shows the brilliant lustre produced.

The high-tension supply (up to 20,000 volts) was supplied by a full-wave thermionic rectifier, with smoothing condenser and electrostatic voltmeter. The voltage control was carried out by a tapped auto-transformer, and was only variable in rather large steps.

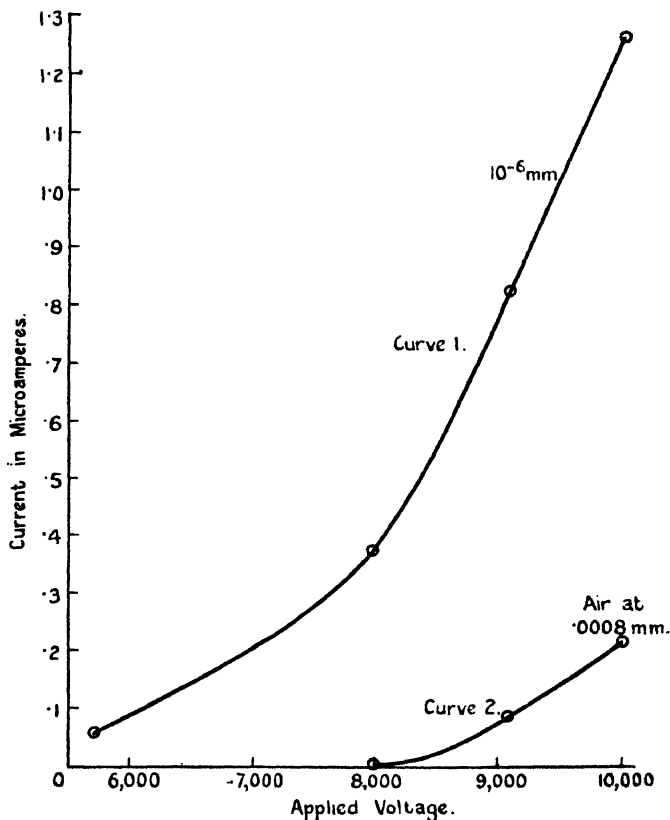
To guard against electrical leaks an earthed guard-ring was clamped round the discharge-tube. The fact that no current was ever observed to pass, even at 20,000 volts, when the nickel cylinder was made the cathode showed that there was no measurable leakage.

The current was measured with a Tinsley portable reflecting galvanometer of sensitivity 35 mm./microamp.

The pumping equipment consisted of a three-stage glass diffusion-pump connected through a reservoir to the central

backing system. Next to the diffusion-pump was a mercury cut-off, then a MacLeod gauge, liquid-air trap, ionization-gauge, and the discharge-tube.

GRAPH 1.



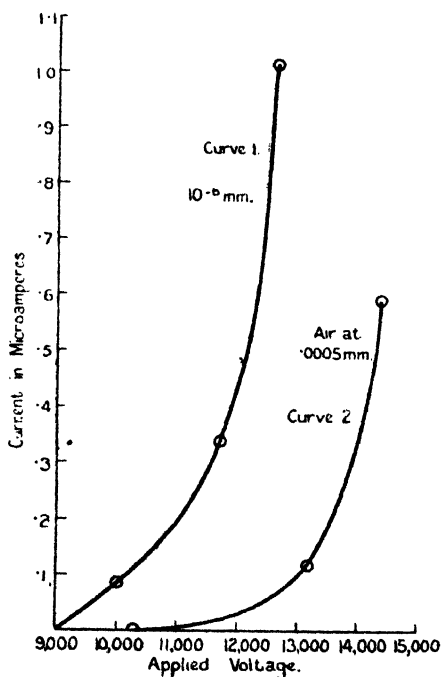
### *Results obtained.*

It was found possible to obtain reproducible characteristics provided that the voltage was not carried too high, in which case a bright star could be seen momentarily on the cathode and a new characteristic was obtained. This star evidently signifies the tearing-off of a particle from the cathode surface. Curves 1 of graphs 1 and 2 show the characteristics of two different tubes when the pressure was less than  $10^{-6}$  mm. Each point is the mean of a number of observations with ascending and descending voltages. The curves 2 are those

obtained when air was admitted; they were also reproducible; pumping the air out did not restore the original characteristic.

A similar but less marked effect was found when hydrogen was admitted. The hydrogen was purified by passing electrolytic hydrogen over two KOH towers, red-hot copper, two KOH towers, six  $P_2O_5$  towers, and red-hot chromium, in that order. Graphs 3 and 4 show the results with hydrogen.

GRAPH 2.

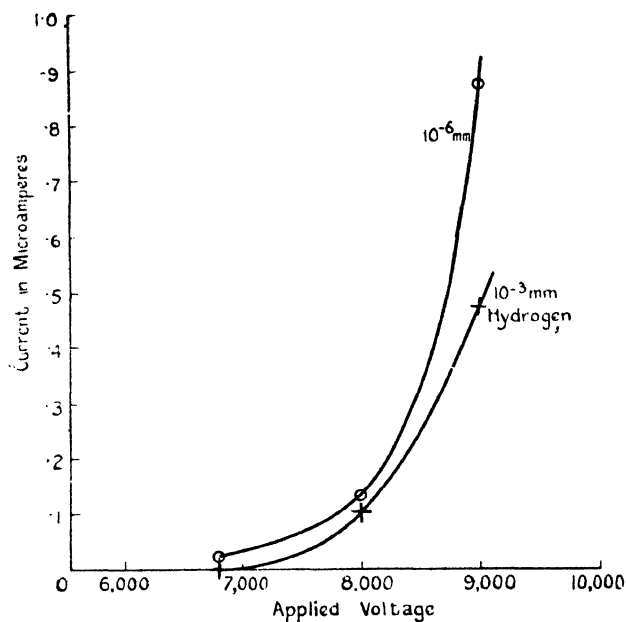


N.B.—The voltages for this characteristic were extrapolated from the primary voltage, which had been calibrated below 10,000 v. against the electrostatic voltmeter.

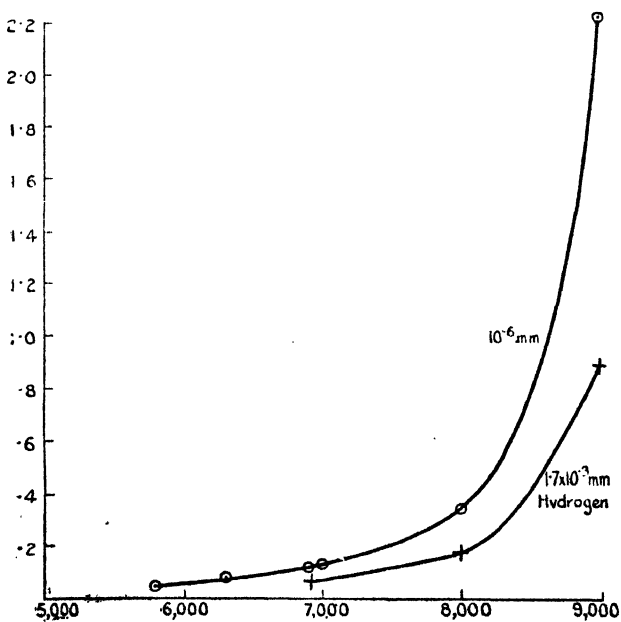
The inside of the nickel cylinder of a discharge-tube was coated with barium azide and baked *in vacuo* at 400° C., leaving a deposit of barium on the inside of the cylinder. The filament was then burnt out and the characteristic 1 in graph 5 was obtained. The nickel cylinder was heated up by the eddy-current heater and a positive potential of 100 volts was applied to the burnt-out filament; the barium



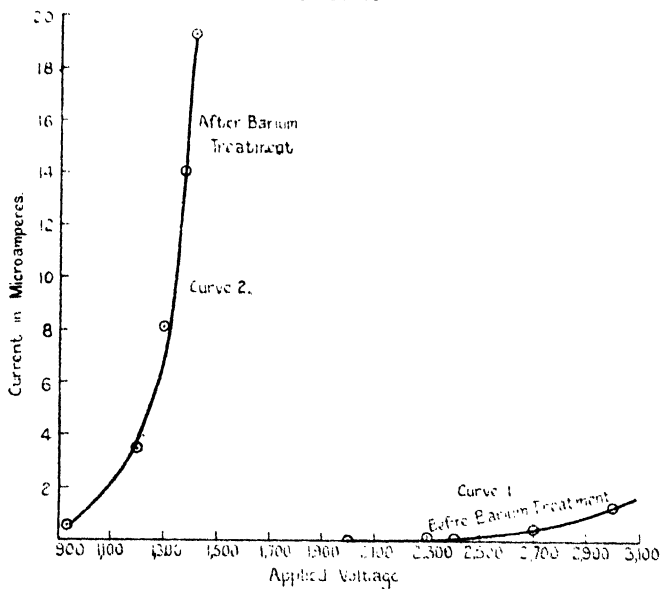
GRAPH 3.



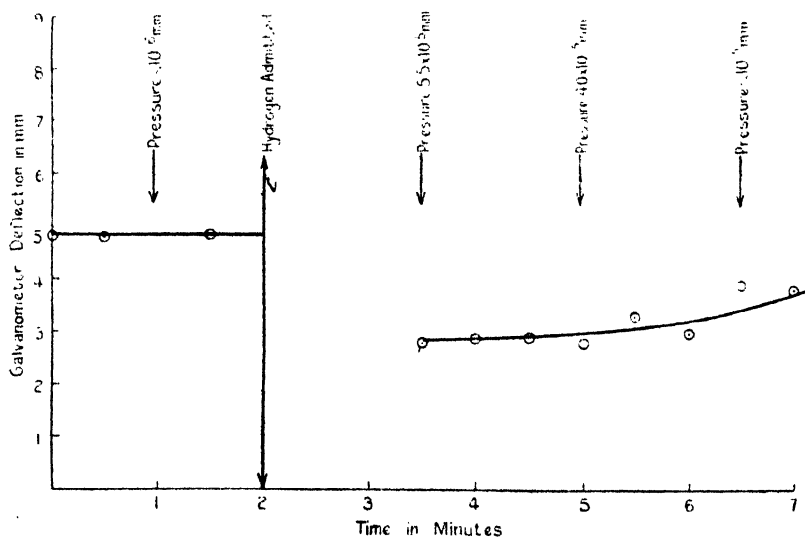
GRAPH 4.



GRAPH 5.



GRAPH 6.



was vaporized and a glow-discharge set in, the positive barium ions being attracted to the filament. The characteristic 2 was obtained after this treatment; it was not reproducible. The barium coating increases the emission, but is evidently torn off by the discharge.

The gas-pressures marked in the graphs were taken immediately after the characteristic had been obtained. Actually the pressure decreased continuously, as graph 6 shows, due to the disappearance of the gas in the discharge.

### *Discussion of Results.*

It appears, then, that the effect of the agencies studied upon the auto-electronic currents is of the same kind as their effects upon thermionic emission at a given temperature.

This conclusion is consistent with the theory of Schottky \*, which, however, seems not to explain why the auto-electronic current should be almost independent of the temperature while the thermionic current varies so rapidly with it. It is not consistent with del Rosario's theory that auto-electronic currents are due to traces of residual gas.

The author wishes to thank the Director of the Research Laboratories of the General Electric Company for granting permission to carry out this work at the laboratories, and to Miss M. Crowe for her assistance. He also wishes to express his great indebtedness to Mr. B. S. Gossling, whose interest and helpful advice made this work possible, and in particular for suggesting the process of burning out a filament to obtain a clean surface.

LIX. *On the Effect of Constrictions in Kundt's Apparatus and the End Corrections of a Partially-stopped Tube*  
By ERIC J. IRONS, B.Sc., East London College †.

[Plate XI.]

### 1. *Introduction.*

**A**T the suggestion of Professor C. H. Lees ‡ experiments have been made to determine the effect on the distribution of nodes and loops of introducing diaphragm constrictions in Kundt's sound apparatus.

\* W. Schottky, *Zeit. f. Phys.* xiv. p. 63 (1923).

† Communicated by Prof. C. H. Lees, D.Sc., F.R.S.

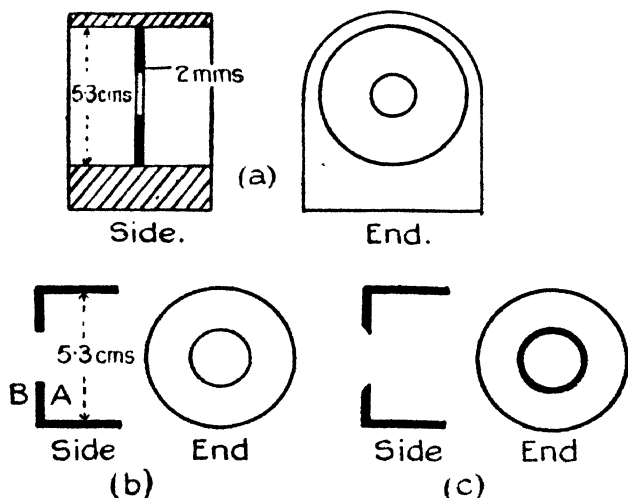
‡ To whom I am indebted both for facilities for carrying out this work and for counsel during its progress.

The method of investigation has been further applied to the problem of the end corrections of a tube fitted with caps containing holes of different radii, and the results are herein described.

## 2. Apparatus and Preliminary Results.

As a source of vibration a hollow cylindrical bar of brass 110 cm. long and 1 cm. external diameter was used. It was so clamped at its centre between two triangular prisms of wood that a definite node was formed at that point. A firmly fitting circular cork disk was attached to that end of the bar which protruded into the sound-tube, and the other end of the bar was weighted so that it balanced about its centre.

Fig. 1.



Because of the facility with which it formed into figures without special precautions as to dryness, cork dust (obtained by sifting through a fine copper mesh) was chosen as a powder to indicate the positions of the antinodes.

Preliminary experiments showed that it was possible to obtain dust figures in an open tube, in a tube fitted with a stop covered by a considerable thickness of felt, and also on a lath placed along the axis of the tube. The figures in the last instance did not admit of such easy measurement so that the device was not subsequently used.

The constrictions and caps were of aluminium and of the shapes shown in fig. 1. The former were designed to carry a sound-tube on either side, thus forming a "single tube with a constriction." The tube further from the vibrating rod was furnished with a solid movable stop, and will be referred to as the "stop tube" in contradistinction to the "vibrator tube" into which the end of the rod protruded.

With the constrictions two types of experiments were carried out.

For the first type the *modus operandi* was to adjust the distance from the constriction to the end of the rod (by moving both the tubes with the constriction), and to the stop (by moving the stop itself) until *good figures* were obtained in both tubes. The tubes were then cleaned, relaid with dust, and placed in their former positions. If good figures were obtained by stroking the rod once, or at most twice, with a resined duster, then the positions of the antinodes were recorded.

The second type of experiment was designed to determine the positions of the loops for a given position of the stop; in some instances a considerable amount of stroking was required to produce any semblance of figures in the tubes.

With the caps the adjustment followed the lines of the first type of constriction experiment, except that it was much simpler, there being but one length (viz. the distance between the cap and the end of the vibrating rod) to alter. This was effected by sliding the tube in or out relatively to the rod. Care was taken that the cap projected well over the end of the bench supporting the apparatus and was removed from any near object likely to give rise to a reflected wave.

### 3. Results.

The results (the means of a large number of observations) are best described by reference to the figures.

#### I. CONSTRICTIONS.

##### *First Type of Experiment.* (See fig. 2.)

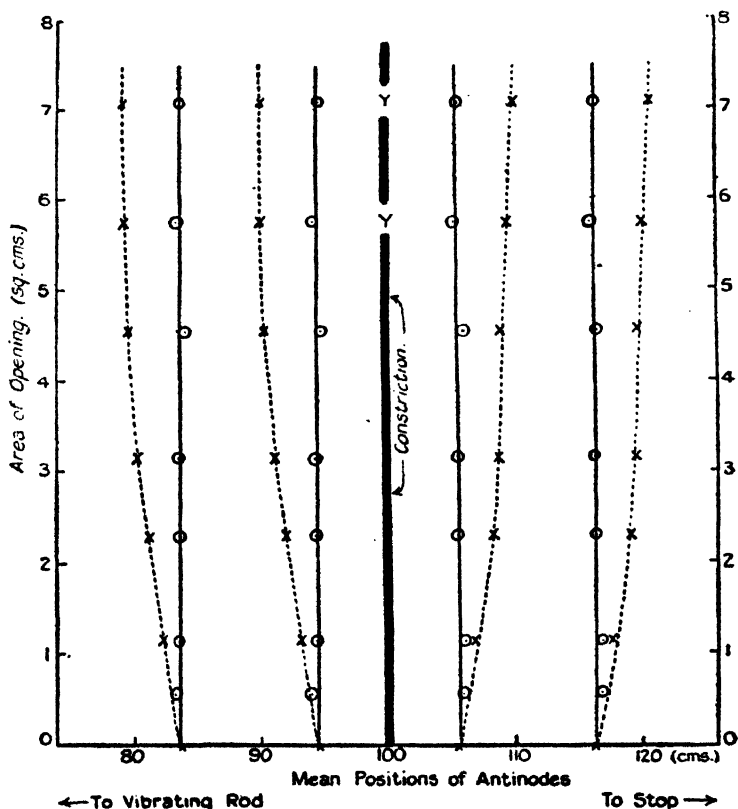
In the figure the area of the opening is plotted as ordinate against the positions of the antinodes as abscissa—the constriction being at 100,—and the results correspond to a half wave-length of 10·8 cm.

The results occur in two groups, viz. :—

*Group A* (marked  $\odot$ ) in which there is no displacement of the antinodes, the constriction appearing to form a node whatever the area of the opening.

For results of this type the distance of the stop from the constriction approximated to an integral number of half

Fig. 2.—Internal Area of Cross-section of Tubes = 17.3 sq. cm.



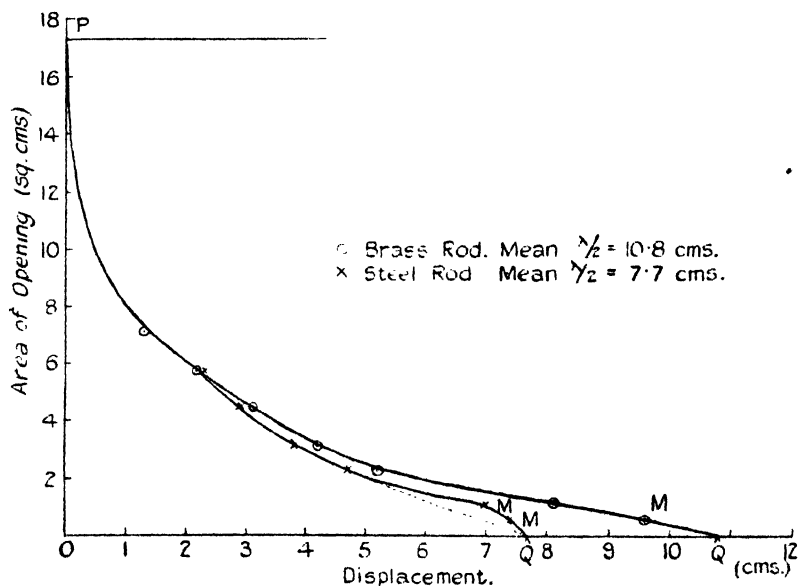
wave-lengths, while the distance of the end of the vibrating rod from the constriction (*i. e.* a node) exceeded in general an integral number of half wave-lengths by about a centimetre.

*Group B* (marked  $\times$ ). The antinodes are symmetrical about the constriction but are moved out from it in both tubes.

Here the difference between the distance of the stop from the constriction and a whole number of half wave-lengths was comparatively large, and tended to increase with the aperture as it (the stop) was always at a distance of  $\lambda/4$  ( $\lambda$  is the wave-length of the disturbance in the tube) from the nearest antinode in the tube. No general rule could be found for the position of the end of the rod.

Fig. 3 indicates the extent of the displacement for the various openings for Group B. If it be assumed that an antinode would occupy the position of the constriction were it removed, then the point P is fixed as a point of no displacement. As the area of the opening decreases the

Fig. 3.—Internal Area of Cross-section of Tubes = 17.3 sq. cm.



nodes on either side of the partition approach it, and when the partition is solid the nodes coincide with it. It follows that the point Q is also fixed, since the distance between the two antinodes which are adjacent to the constriction in the two tubes is half a wave-length.

The points marked M represent the mean displacement for results of both groups (see note (i.) below); in consequence the variation is probably better represented by the dotted line for the steel rod (see below). With this rod results corresponding to Group B were not noted with an aperture of 7.1 sq. cm.

The following afford further explanation of fig. 2 :—

(i.) For the constriction having an opening 0.55 sq. cm. in area the accuracy of the experiments does not justify the division of the results into groups.

(ii.) Figures for the opening of area 0.55 sq. cm. indicate that results of Group B are probably present, but indistinguishable from those of Group A.

(iii.) In the places marked "Y" in experiments of Group B it was noted that the dust near the constriction was disturbed.

(iv.) With a constriction of aperture 9.08 sq. cm. the results were not sufficiently consistent to justify their classification at all—due, probably, to the fact that the apparatus acted as a single resonator.

By substituting for the brass rod one of steel having the same dimensions, figures were obtained in the tube with an antinodal distance of c. 7.7 cm. In general the results were similar to those already described for the brass rod. The relation between the area of the opening and the displacement in results of Group B for this rod is also shown in fig. 3.

An experiment with a diaphragm having an opening of diameter 0.3 cm. was tried with this rod. With prolonged stroking, faint figures, which were capable of fairly accurate measurement, were obtained in the stop tube. In the vibrator tube the antinodes were destroyed, and the dust was first carried along and deposited in heaps at the nodes in the manner described by Barton\*, while finally a transverse ring of fine dust was formed there. This effect appears to be illustrated diagrammatically in Tyndall's 'Sound'†, to which the reader is referred for an interesting account of Kundt's experiments.

#### *Second Type of Experiment.* (See fig. 4.)

The first type of experiment having demonstrated the positions of *good* and easily obtained figures, it was thought desirable to investigate the positions and modes of production of any other figures that could be obtained. To this end experiments with any one constriction were made in which the position of the stop was fixed and that of the end of the vibrating rod varied, and *vice versa*. It became

\* 'Text-book of Sound,' p. 369. (Macmillan & Co.)

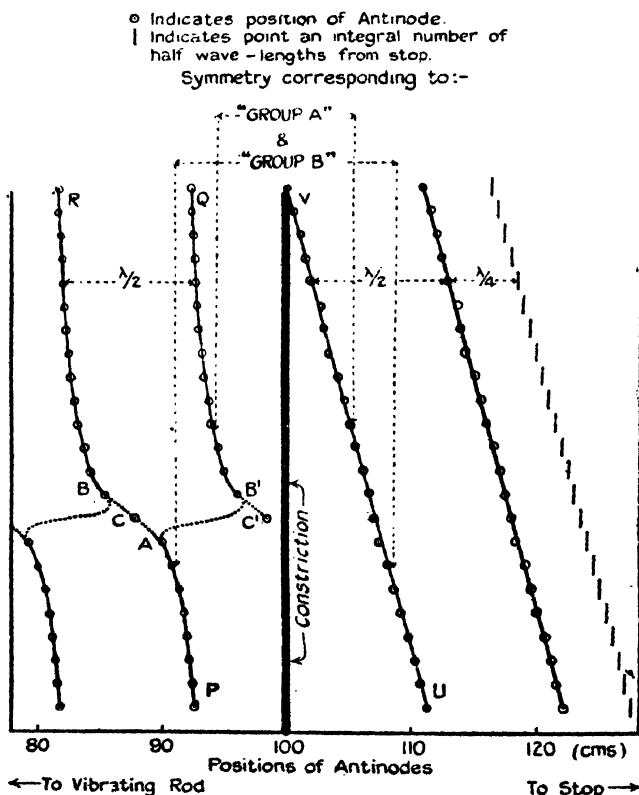
† Fourth Edition, 1883, p. 213. (Longmans Green & Co.)



apparent that whether the stop was fixed at a distance of an integral number of half wave-lengths from the constriction or not, the position of the end of the vibrating rod played such a very minor part in the production and position of figures that its influence could well be neglected compared with that of the stop.

The curves obtained with the brass rod for a constriction.

Fig. 4.



having an opening of 3.1 sq. cm. are shown in fig. 4, and illustrate the characteristics of similar results obtained with larger and smaller openings. In this instance the position of the end of the vibrating rod was fixed at 110.2 cm. from the constriction, and that of the stop was altered progressively by steps of half a centimetre.

It should be noted that where the dust figures were too

near the constriction for complete formation or convenient measurement, the positions of the antinodes they represent were determined by adding or subtracting half a wave-length from the neighbouring antinode in the same tube.

The positions of the antinodes (marked  $\odot$ ) in the stop tube are seen to depend on the position of the stop, which was at an integral number of half wave-lengths from the points marked J.

In the vibrator tube the results varied considerably with the area of the aperture in the constriction. For the example illustrated by fig. 4 it is seen that a movement of the stop through a centimetre was sufficient to cause the antinodes to move from A to B or B'. By moving the stop through half a centimetre from the position corresponding to A, indifferent figures were obtained indicating antinodes at C and C'.

With constrictions having *small* openings the curve was of the same form, but the shift A to B' was much less and no intermediate positions such as C could be detected—the sequence of events being represented by PAB'Q (for a considerable portion of its length an almost straight line parallel to the constriction and at a distance approaching to a quarter of a wave-length from it), rather than PABR (see fig. 4). In these instances the dust figures in the vibrator tube were good, while those in the stop tube were unsatisfactory over the straight portion of PAB'Q.

With constrictions having *large* openings the line PABR appeared to be continuous, and became straighter, each point in it tending to be at a distance of a wave-length from the corresponding point in UV—a condition that would be completely realised in the absence of any constriction.

The shapes of PAB'Q and UV are such that there are two positions for which the figures in the two sound-tubes are symmetrically placed with respect to the constriction. During experiments of the second type it was noted that the figures in these cases were both easier to obtain and more clearly defined than usual, and, in fact, corresponded to those already measured in the first type of experiment.

## II. CAPS.

The fact, already noted, that it is possible to obtain dust figures using an open tube led to experiments being performed to determine the effect of placing on the end of the tube caps having openings of different apertures.

This method of investigation affords a convenient means of estimating "end corrections." The value of the half wave-length of the disturbance in the tube ( $\lambda/2$ ) being known from the antinodal distance, and the distance of the antinode nearest the end from that end ( $c$ ) being measurable, it follows that the end correction is  $(\lambda/2 - c)$ . In practice the positions of some six antinodes were measured, and a mean position of the end antinode was calculated.

Experiments of a more general nature on end corrections and allied problems are in progress, and it is hoped that the results of these will be published in due course; it is thought well, however, to introduce here the results obtained by the Kundt's tube method.

The caps were 2 mm. thick, and the first experiments have been carried out with those of the type shown in fig. 1 (b). The question arose as to the position of the "end of the tube," *i.e.* whether measurements should be made from inside the cap at A or outside the cap at B (see fig. 1 (b)). To obviate this difficulty caps of the type shown in fig. 1 (c), having the edge of the aperture bevelled at  $45^\circ$ , are now employed and measurements are made from the inside edge. The effect of this alteration on the vibration at the end of the tube is described later.

In addition, experiments have been performed using a flange\* 120 cm. in diameter fitted over and flush with the caps.

In order to increase the range of wave-lengths a two metre vibrating rod of brass was employed. This rod when clamped at its centre was capable of emitting both its fundamental and first overtone giving rise to antinodal distances in the tube of approximately 19.6 and 6.5 cm. respectively. In general the overtone was generated when the rod was stroked near its centre and the fundamental

\* By the electrical analogy of Rayleigh a very rough measure of the deviation of this flange from an "infinite" flange may be obtained.

Remembering that the resistance between spherical equipotential surfaces of radii  $r_1$  and  $r_2$  is  $(1/4\pi) \cdot (1/r_1 - 1/r_2)$ , it follows that, assuming the waves diverge in hemispherical form, the resistance between a hemisphere at the end of the tube of radius  $r_1$  and the edge of the flange of radius  $r_2$  is  $(2/4\pi) \cdot (1/r_1 - 1/r_2)$ . Further, between the edge of the flange and infinity the resistance may be written as  $(1/4\pi) \cdot (1/r_2 - 1/\infty)$ , making a total of  $(2/4\pi) \cdot (1/r_1 - 1/2r_2)$  for a small flange and  $(2/4\pi) \cdot (1/r_1)$  for an infinite flange ( $r_2 = \infty$ ). In round numbers for the case in question,  $r_1 = 2.5$  and  $r_2 = 60$  cm., so that the actual resistance is measured by  $196/\pi$  and the resistance of an infinite flange by  $200/\pi$ .

when it was stroked towards its end. In many cases the effect of the overtone in the tube was somewhat difficult to eliminate, because its striæ joined those due to the fundamental on one side or the other to form a composite figure. Satisfactory results with the fundamental were obtained using caps of the first type and are described below.

Fig. 6.—Internal Area of Cross-section of Tube=18.9 sq. cm.

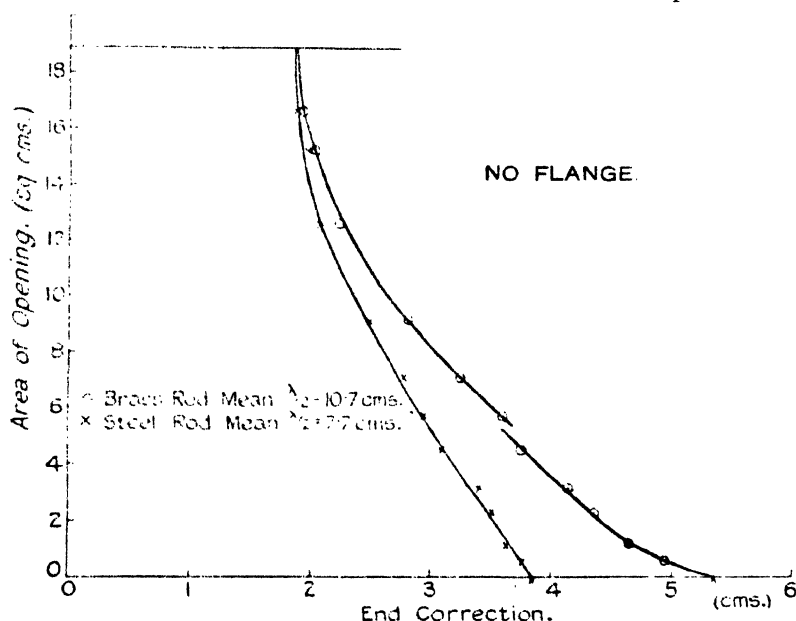


Fig. 5 (a) (Pl. XI.) shows the effect obtained in a particular instance in which antinodes due to the two notes are seen to alternate down the tube.

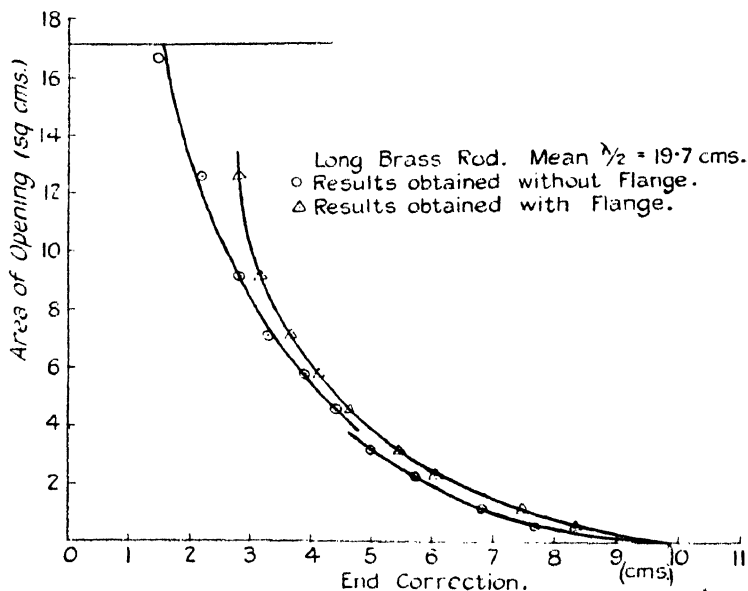
The other photographs of fig. 5 (Pl. XI.) show the tube after an experiment with, and the removal of, a cap having an aperture of 0.55 sq. cm., and demonstrate the difference in the appearance of the dust—noted especially with small aperture caps—according as the cap is bevelled (b) or plane (c). In the former instance the dust is violently agitated near the end while in the latter the antinode is well formed.

There follow graphs setting forth the means of a number of results in good agreement obtained for various combinations of cap and vibrating rod. Distances are measured

from the end of the glass sound-tube in each case (*i. e.* from A in fig. 1 (b)), and by "end correction" is denoted the distance from the end of the tube of an external point which is half a wave-length from the last antinode inside the tube.

The curves for the brass rods and unflanged caps (figs. 6 and 7) appear to consist of two parts according as the area of the opening of the cap is relatively small or great. In

Fig. 7.—Internal Area of Cross-section of Tube = 17.1 sq. cm.



what follows attention will be confined to the results shown in fig. 7 which correspond to the largest wave-length used.

Considering the *unflanged* caps: when the holes are *small* the space between the cap and the nearest node in the tube may be considered as a resonator whose frequency  $N$  is proportional to  $\omega^{\frac{1}{2}}/Q^{\frac{1}{2}}$ \*, where  $\omega$  and  $Q$  are the area of the opening and the volume of the resonator respectively. In these experiments,  $N$  being constant and the resonator

\* See, *e. g.*, Lamb, 'Dynamical Theory of Sound,' pp. 267-68 (Arnold & Co., 1925.)

cylindrical, it follows that  $(r/d)^{\frac{1}{2}}$  should be constant, where  $r$  is the radius of the opening and  $d = \lambda/4$  — (end correction) } is the distance of the nearest node from the cap.

The following table shows the variation of  $(r/d)^{\frac{1}{2}}$  for the small-holed caps :—

$r$ (cm.).....	0.42, 0.60, 0.85, 1.00,	1.20
$(r/d)^{\frac{1}{2}}$ .....	.443, .447, .455, .455,	
		.471

From this it would appear that for holes in the caps up to a radius of 1 cm. the system may be regarded as a resonator of the type indicated, although theory supposes the wave-length to be large compared with the linear dimensions concerned.

The *flanged* caps for *small* openings do not follow this rule so well but it may be noted that there is a variation of about 12 per cent. in the value of  $(r/d)^{\frac{1}{2}}$  over the whole range. With *flanged* caps and *large* openings, however, the product end correction times radius of hole in cap is a constant, as appears from the following table :—

Radius (cm.) .....	2.0, 1.7, 1.5, 1.35, 1.2, 1.0
End correction $\times$ Radius...	5.56, 5.36, 5.46, 5.55, 5.57, 5.43

It remains to discuss some results for the end correction of an open tube as ordinarily understood. For notes corresponding to half wave-lengths of 6.6, 7.7, 10.7 and 19.7 cm., values of the end correction corresponding to 0.57, .62, .58 and .64 times the internal radius of the glass tube were obtained. The mean value, .60, is higher than .583 which has been obtained by Stucker\* from a series of experiments. It must be remembered, however, that the thickness of the walls of the glass tube used in the present work was of the order of 2 mm.

Experiments to determine the end correction of an open tube fitted with a flange were made corresponding to a half wave-length of 19.7 cm. The cap with the largest aperture was opened until its diameter was exactly equal to the internal diameter of the tube, the flange was fitted over it and measurements were taken to the outside of the cap. In this instance a value of .79 times the radius was obtained. Substituting the value of the internal radius of the tube in the formula for flanged caps (viz. end

\* N. Stucker, *Akad. Wiss. Wien. Ber.* cxvi. pp. 1, 231 (1907).

correction  $\times$  radius = 5.5), and correcting for the fact that the end corrections were measured from *inside* the cap, a higher value of .92 is obtained. Rayleigh's \* estimate (assuming a long wave-length) was .82 for an infinite flange.

A point of interest in connexion with the position of the end of the vibrating rod may be noted here. In different experiments for the same cap the readings of the antinodes were constant although the position of the end of the vibrating rod varied considerably—its most frequent positions being between points distant  $n \cdot \lambda/2$  and  $(n + 1/4) \cdot \lambda/2$  from a node (where  $n$  is an integer and  $\lambda$  is the wave-length).

The method described is limited by the accuracy with which the positions of the antinodes can be read, but it has the advantage over the ordinary resonance method of Blaikley † in that the aperture is unobstructed by a tuning-fork. Moreover, having varied the position of the fork with respect to the open end of the tube, W. M. Boehm ‡ (who used Blaikley's method in conjunction with a vibration-galvanometer to measure intensity) has concluded that "A maximum of intensity outside the tube may not indicate that the resonator is nearest to unison with the pitch produced." This is noteworthy as revealing a source of error to which experiments made by this method are liable. Curves are given by Boehm showing the relation between end correction and width of flange, and from them he deduces a mean result equal to .656 times the internal radius for tubes having a thickness of wall of 3.1 mm.; for tubes having an "infinite" flange the results lie between .849 and .909 times this quantity.

Efforts are now being made to increase the accuracy and range of measurements by the use of a hot wire detector in conjunction with a valve oscillator.

\* Rayleigh, "On the Theory of Resonance," *Scientific Papers*, vol. i. p. 33.

† D. J. Blaikley, *Phil. Mag. ser. 5*, vol. vii. p. 339 (1879).

‡ *Phys. Review*, xxxi. p. 341 (1910).

LX. *The Magnetic Rotary Dispersion of Methyl and Propyl Alcohols.* By D. O. JONES, M.Sc., and Prof. E. J. EVANS, D.Sc., *Physics Department, University College of Swansea* \*.

### INTRODUCTION.

THE magnetic rotations of a large number of substances for sodium light have been examined by Perkin and others, and the magnetic rotary dispersion of several substances has been investigated by several observers, notably by Borel, Siertsema, Landau, Meyer, Lowry, Richardson, and Roberts. Our knowledge of the magnetic rotary dispersion of a large number of substances, especially in the ultra-violet region of the spectrum, is still very incomplete, and the present investigation, which is a continuation of the work carried out by Stephens and Evans †, was undertaken with the intention of measuring accurately the magnetic rotation of methyl and propyl alcohol in the region  $\cdot 4300 \mu$  to about  $\cdot 2500 \mu$ . The results could then be examined in relation to Larmor's ‡ theory of magneto-optical rotation and the position of the absorption bands determined. Richardson §, in two very interesting papers, discusses fully the magneto-optical properties of several substances in relation to theory, and the nomenclature used in this paper is the same as the one adopted by him.

An expression for the magnetic rotation of a medium may be obtained from the equation expressing the natural dispersion by making use of a formula deduced by Larmor ||, namely,

$$\delta = \frac{e}{2mC^2} \lambda \frac{dn}{d\lambda}, \quad . \quad . \quad . \quad . \quad . \quad (1)$$

where  $\delta$  is the magnetic rotation,  $C$  the velocity of light,  $n$  the refractive index, and  $e/m$  is the ratio of charge to mass for all the resonators.

If the natural dispersion be given by an equation of the Ketteler-Helmholtz type, viz.,

$$n^2 - 1 = b_0 + \frac{b_1}{\lambda^2 - \lambda_1^2} + \frac{b_2}{\lambda^2 - \lambda_2^2} + \dots, \quad . \quad . \quad (2)$$

\* Communicated by the Authors.

† *Phil. Mag.*, March 1927, p. 546.

‡ 'Æther and Matter,' Appendix F, p. 352.

§ *Phil. Mag.* xxxi. pp. 232, 454.

|| Larmor, *loc. cit.*



it can be shown \* that

$$\phi = n\delta\lambda^2 = K_1 \left( \frac{\lambda^2}{\lambda^2 - \lambda_1^2} \right)^2 + K_2 \left( \frac{\lambda^2}{\lambda^2 - \lambda_2^2} \right)^2 + \dots, \quad (3)$$

where  $k_1, k_2$ , etc., are constants and  $\lambda_1, \lambda_2$ , etc., are wave-lengths corresponding to the free periods of the vibrators. \*

For substances which are transparent in the visible and infra-red,  $\lambda_1$  and  $\lambda_2$  will represent wave-lengths corresponding to ultra-violet free periods, and when a substance possesses only one free period in the ultra-violet, the equation reduces to the form

$$\phi = K_1 \left( \frac{\lambda^2}{\lambda^2 - \lambda_1^2} \right)^2 \dots \dots \dots (4)$$

From the two values of  $\phi$  corresponding to two values of  $\lambda$  it is therefore possible to determine  $k_1$  and  $\lambda_1$  for that region of the spectrum. If it be found that the experimental results lead to different values of  $\lambda_1$ , depending on the wave-lengths chosen, and if the values change progressively when the chosen wave-lengths are taken in regions of shorter and shorter wave-lengths, it is presumed that the substance has more than one free period. If, however, the values of  $\lambda_1$  were constant within experimental error, the values of  $\phi$  are given by equation (4).

#### EXPERIMENTAL ARRANGEMENT.

A full account of the experimental arrangement has been previously given †, and consequently it is not essential here to describe the apparatus in detail. The source of light, a nickel-steel spark or a tungsten arc, was placed at the focus of a quartz lens, which formed a part of the polarizing unit. The parallel beam of light thus obtained was passed through a Jellet prism, which formed the other part of the polarizing unit, and produced a beam the two semi-circular halves of which were polarized at a small angle with each other. The emergent beam traversed the liquid contained in a polarimeter tube, which is made of clear fused quartz, and is supported by two cork disks inside the core of a solenoid through which a current of 2 amperes was passed. A water-jacket separated the tube from the coil carrying the current, and the temperature of the liquid in the polarimeter tube was kept constant, during an experiment, by

\* Richardson, *loc. cit.*

† Stephens & Evans, *loc. cit.*

passing a stream of water through the jacket. On emerging from the polarimeter tube, the beam of light passed through the analyser, and was brought to a focus on the slit of a quartz spectrograph by means of a quartz-fluorite lens.

The polarimeter used in these experiments was supplied by Bellingham and Stanley, and had been designed for work in the ultra-violet region of the spectrum. The two components of the polarizer were assembled without any intervening film, which may cause absorption in the ultra-violet.

The quartz polarimeter tube was 30.5 cm. long and about 1 cm. in diameter, and was closed by fusing on to the ends two disks of polished fused quartz. These disks were fused along the outside circumference of the tube, and in this way the distortion of the beam of light, especially by the central portions of the disks, was avoided. The liquid was introduced through a small neck which had been fused to the middle of the tube, and which was closed by a tight-fitting quartz cap. Owing to the rotation produced by the quartz ends, due to the magnetic field, a correction was necessary in determining the rotation produced by the liquid under investigation. The corrections at definite wave-lengths were determined by special experiments, and the order of the correction can be seen from the result that the measured rotation was 13.4 minutes of arc for the wave-length  $2753 \mu$ .

The solenoid, which was wound on a brass tube 47.3 cm. long and 4.27 cm. diameter, was connected in series with a battery of accumulators, a Weston ammeter, and two variable resistances. One of these resistances was fitted with a fine adjustment, and by means of the Weston ammeter the current of 2 amperes passing through the solenoid could be kept constant to within 1 part in 600. By passing a stream of water through the jacket, and continuously adjusting its rate of flow, the variation in the temperature of the liquid during an exposure could be kept very small. During long exposures of over one hour, the temperature could be kept constant to within  $0^{\circ}.3$  C., and in a large number of cases the temperature was constant to within  $0^{\circ}.1$  C.

The value of the magnetic field at various points inside the solenoid had been previously determined by Stephens and Evans\* by means of a delicate ballistic galvanometer and an accurately constructed search-coil. The value of  $\Sigma Hl$ , where  $H$  is the magnetic field at a given point of the polarimeter

\* *Loc. cit.*

tube and  $l$  the length of tube over which  $H$  is very approximately constant, was found to be 12445 gauss cm, for the quartz tube employed in the present experiments. The observed and calculated values of the field agreed to within 1 part in 300. An error in the determination of the magnetic field will not affect the relative values of Verdet's constant for different wave-lengths, and it is important to note that the position of the absorption bands can be determined from these relative values.

The spectrograph was constructed in the laboratory, and its optical parts consisted of two quartz lenses and a Cornu quartz prism. Photographs were taken with Imperial and Wellington rapid plates, and exposures with the nickel-steel spark varied from about 45 minutes to 2 hours. The exposures required with the tungsten arc were of smaller duration, but even with the arc, when investigating the region below  $3000\ \mu$  for propyl alcohol, exposures of about one hour's duration were necessary. In the case of methyl alcohol, rotations were measured for wave-lengths ranging from  $4400\ \mu$  to  $2600\ \mu$ , and in the case of propyl alcohol for wave-lengths ranging from  $4400\ \mu$  to  $2850\ \mu$ .

#### MODE OF EXPERIMENT.

The two semi-circular half-fields, consisting of two beams of plane polarized light vibrating in directions making a small angle with each other, after passing through the Cornu prism, gave rise to two spectra, one above the other. These spectra are, in general, of different intensity, but if there is no liquid in the tube, and the magnetic field is absent, it is possible, by rotating the analyser, to make the two contiguous spectra have the same intensity throughout their length. There are four positions of the analyser separated by  $90^\circ$ , which will give equality of fields, and two of these positions, separated by  $180^\circ$ , give a minimum intensity. The position of minimum intensity gives the maximum sensitivity, and the reading on the scale corresponding to this position is called the zero reading of the instrument. When making observations the following procedure was adopted. The polarimeter tube was filled with the liquid and placed inside the solenoid through which a constant current of 2 amperes was passed. The analyser was then rotated through a known angle and the photographic plate exposed. On examining the plate it was seen that the intensities of corresponding lines in the upper and lower spectra were, in general, unequal, but it was possible to determine the wave-length of a definite

line which was of the same intensity in both spectra. It sometimes occurred that this point of equality fell into the small gap between two lines, and in such a case the reading of the analyser was slightly altered, so that the point of equality fell on one of the lines situated on either side of the gap.

Let  $\lambda$  be the wave-length of the line which gave equality of intensity in both spectra, and  $\theta_1$  be the corresponding reading of the analyser when the liquid was in the polarimeter tube.

Let  $\theta_2$  be the reading of the analyser, which gave equality at the same wave-length with no liquid in the tube, for the same value of the magnetic field.

Then  $\theta_1 - \theta_2$  gives the rotation corresponding to the wave-length  $\lambda$  produced by the liquid due to a value of  $\Sigma Hl$  equal to 12,445 gauss cm. Verdet's constant  $\delta$  for a given wave-length  $\lambda$  is given by the relation

$$(\theta_1 - \theta_2)_\lambda = \delta_\lambda \Sigma Hl,$$

and can therefore be determined for the various wave-lengths. The same values of  $\delta_\lambda$  were obtained when the magnetic field was reversed and the analyser was rotated through the same angles in the opposite direction.

The rotation corresponding to a particular wave-length was repeated several times, and it is considered that the absolute values of Verdet's constant are correct to about  $\frac{1}{2}$  per cent. on the average.

## EXPERIMENTAL RESULTS.

### *Methyl Alcohol.*

The magnetic rotation of methyl alcohol for sodium light has been determined by Quincke\*, who obtained the value .00989 for Verdet's constant. The molecular magnetic rotation relative to water was determined for the same wave-length by Perkin†, who obtained the value 1.640 at 18°·7 C. The value of Verdet's constant for methyl alcohol calculated from Perkin's result is .00956 at 18°·7 C. The rotation of methyl alcohol for .4359  $\mu$  relative to the rotation for .5461  $\mu$  was determined by Lowry‡, who found the value 1.629. In the present experiments the magnetic rotations of pure methyl alcohol were determined for about fifteen wave-lengths ranging from .4380  $\mu$  to about .2600  $\mu$ ,

\* *Wied. Ann.* xxiv. p. 614 (1885); Luntolt & Börnstein, ii. p. 1013.

† *Journ. Chem. Soc.* xlv. p. 466 (1884).

‡ *Journ. Chem. Soc.* i. p. 91 (1914).

and the values of Verdet's constant were determined for those wave-lengths. Two series of experiments were carried out with the alcohol, and the results are given in Tables I. (a) and I. (b). The density of the methyl alcohol at 15° C. and its boiling point were determined and found to be .797 and 64°·7 C. respectively.

TABLE I. (a).

Temperature in degrees centigrade.	Wave-length in microns (10 <sup>-4</sup> cm.).	Verdet's Constant in min. per cm. gauss.	Refractive Index, n.
7·8	·4380	·0181 <sub>9</sub>	1·3365
7·6	·4360	·0184 <sub>2</sub>	1·3366
8·5	·4260	·0193 <sub>6</sub>	1·3371
8·5	·4045	·0217 <sub>3</sub>	1·3387
8·4	·3828	·0246 <sub>8</sub>	1·3405
8·3	·3600	·0286	1·3435
8·3	·3404	·0326 <sub>2</sub>	1·3462
8·1	·3175	·0386 <sub>3</sub>	1·3504
8·0	·3155	·0395	1·3508
8·2	·2980	·0455 <sub>4</sub>	1·3547
8·3	·2967	·0464	1·3550
8·2	·2925	·0473	1·3562
8·1	·2850	·0508 <sub>4</sub>	1·3583
8·2	·2756	·0560 <sub>4</sub>	1·3617

TABLE I. (b).

Temperature in degrees centigrade.	Wave-length in microns (10 <sup>-4</sup> cm.).	Verdet's Constant in min. per cm. gauss.	Refractive Index, n.
8·7	·4378	·0181 <sub>9</sub>	1·3365
9·2	·4256	·0193 <sub>6</sub>	1·3371
8·7	·4055	·0217 <sub>3</sub>	1·3386
9·3	·3958	·0229	1·3394
8·5	·3826	·0246 <sub>6</sub>	1·3406
9·7	·3595	·0286 <sub>6</sub>	1·3435
9·3	·3413	·0326	1·3460
9·0	·3200	·0381 <sub>4</sub>	1·3498
8·7	·2855	·0508 <sub>4</sub>	1·3582
8·9	·2757	·0560 <sub>4</sub>	1·3618

The methyl alcohol was then introduced into a flask fitted with fractionating column and distilled. The middle fraction was retained, and employed in the determination of Verdet's

constant for several wave-lengths. The results obtained with the distilled liquid were practically the same as those previously obtained with the unfractionated liquid, and are given in Table II. There was evidence, however, that the original material contained a very small trace of a substance absorbing light between  $\cdot 2700 \mu$  and  $\cdot 2600 \mu$ . Experiments on the rotation have been carried out with the liquid subjected to further fractional distillation, but the results were exactly the same as before.

TABLE II.

Temperature in degrees centigrade.	Wave-length in microns ( $10^{-4}$ cm.).	Verdet's Constant in min. per cm. gauss.	Refractive Index, $n$ .
8.7	$\cdot 4380$	$\cdot 0181_3$	1.3365
9.2	$\cdot 4050$	$\cdot 0217_3$	1.3386
9.0	$\cdot 3602$	$\cdot 0286$	1.3435
9.3	$\cdot 3196$	$\cdot 0381_4$	1.3498
8.5	$\cdot 3108$	$\cdot 0404_5$	1.3517
8.8	$\cdot 2980$	$\cdot 0455_5$	1.3547
8.8	$\cdot 2856$	$\cdot 0508_5$	1.3583
9.6	$\cdot 2754$	$\cdot 0560_1$	1.3618
9.5	$\cdot 2627$	$\cdot 0637_2$	1.3672

In the last column of Table III. are calculated the values of the function  $\phi$  (which is equal to  $n\delta\lambda^2$ ) for different wave-lengths. The values of the refractive indices of methyl alcohol have been obtained from a graph, which has been constructed from values given by Victor Henri \*.

TABLE III.

Wave-lengths in microns.	Refractive Index, $n$ .	Verdet's Constant in min. per cm. gauss.	Verdet's Constant in circular measure, $\times 10^6$ , i. e., $\delta \times 10^6$ .	$\phi \times 10^{14}$ ( $\phi = n\delta\lambda^2$ ).
(a) $\cdot 4379$	1.3365	$\cdot 0181_3$	5.291	1.356
(b) $\cdot 4050$	1.3387	$\cdot 0217_3$	6.321	1.388
(c) $\cdot 3600$	1.3435	$\cdot 0286$	8.319	1.449
(d) $\cdot 3198$	1.3498	$\cdot 0381_4$	11.094	1.532
(e) $\cdot 2980$	1.3547	$\cdot 0455_5$	13.259	1.595
(f) $\cdot 2754$	1.3618	$\cdot 0560_1$	16.301	1.684
(g) $\cdot 2628$	1.3667	$\cdot 0637_2$	18.535	1.750

\* 'Etudes de Photochemie,' p. 61.

We have not been able to find a reference to the temperature at which the determinations of refractive indices have been carried out, but by comparison with values given in Landolt and Börnstein\*, it is presumed that the temperature was in the neighbourhood of 17° C. Also the values given in Landolt and Börnstein† for the refractive indices of methyl alcohol at 15°·5 C. in the ultra-violet agree for wave-lengths above ·2900  $\mu$  to about 1 in a 1000 with the values given in Tables I. and II., but the values for wave-lengths in the neighbourhood of ·2700  $\mu$  differ by about 1 in 400 from those given in the Tables. The experiments on magnetic rotation were carried out at temperatures in the neighbourhood of 8° C., and, owing to a small negative temperature coefficient, the refractive indices corresponding to 8° C. will probably be slightly higher than the values given in Tables I. and II. The values of  $\lambda_1$  (the wave-length of the absorption band) will not, however, be seriously affected by the small corrections to be applied to the refractive indices, as  $\lambda_1$  is calculated from the ratio of two values of  $\phi(n\delta\lambda^2)$  corresponding to two wave-lengths.

The values of  $\lambda_1$ , the wave-length of the absorption band determined from the above observations on the assumption that

$$\phi = K_1 \left( \frac{\lambda^2}{\lambda^2 - \lambda_1^2} \right)^2,$$

are as follows :—

From (a) and (b) = ·1108 $\mu$ .	From (a) and (d) = ·1101 $\mu$ .
„ (b) and (c) = ·1100 $\mu$ .	„ (a) and (g) = ·1100 $\mu$ .
„ (c) and (d) = ·1099 $\mu$ .	„ (d) and (g) = ·1099 $\mu$ .
„ (d) and (e) = ·1094 $\mu$ .	„ (b) and (e) = ·1098 $\mu$ .
„ (e) and (f) = ·1096 $\mu$ .	„ (e) and (g) = ·1101 $\mu$ .
„ (f) and (g) = ·1108 $\mu$ .	„ (c) and (f) = ·1095 $\mu$ .

The mean value of  $\lambda_1$  is approximately ·1100  $\mu$ , and the magnitude of  $K_1$  in the above formula can be calculated from the value of  $\phi$  corresponding to a known value of  $\lambda$ . The calculated value of  $K_1$  is 1·190, and the variation of  $\phi$  with wave-length in the visible and ultra-violet regions of the spectrum is given by the equation

$$\phi = 1\cdot190 \left( \frac{\lambda^2}{\lambda^2 - (\cdot1100)^2} \right)^2,$$

\* Vol. ii. p. 968.

† *Loc. cit.*

A further test of the accuracy of the above equation is obtained by calculating the values of  $\phi$  and hence  $\delta$  corresponding to different wave-lengths in the visible and ultra-violet regions of the spectrum, and comparing the calculated values of Verdet's constant with those obtained experimentally. The results of the calculations are given in Table IV.

TABLE IV.

Wave-length in microns.	Verdet's Constant calculated.	Verdet's Constant observed.
5893	00951	00956 *
4258	0193 <sub>c</sub>	0193 <sub>c</sub>
3958	0228 <sub>s</sub>	0229 <sub>d</sub>
3826	0247 <sub>c</sub>	0246 <sub>s</sub>
3413	0326	0324 <sub>7</sub>
3108	0408	0405
2855	0509 <sub>2</sub>	0508 <sub>s</sub>

\* Calculated from Perkin's result.

*The Magnetic Rotary Dispersion of Normal  
Propyl Alcohol.*

The magnetic rotation of propyl alcohol relative to water for sodium light was determined by Perkin \*, who found the value  $\cdot 9139$  at  $15^{\circ} \cdot 6$  C. The value of Verdet's Constant calculated from the above result is  $\cdot 01197$ . The value of the rotation at  $\cdot 4359 \mu$  relative to its value at  $\cdot 5461 \mu$  has been determined by Lowry †, who found  $1\cdot 635$  for  $\frac{\delta_{\cdot 4359 \mu}}{\delta_{\cdot 5461 \mu}}$ .

In the present experiments the rotation of propyl alcohol for several wave-lengths ranging from  $\cdot 4400 \mu$  to  $\cdot 2850 \mu$  has been measured, and the results have been collected in Tables V. to IX. Several samples of normal propyl alcohol were employed, but in all cases it was found that they contained a small quantity of an active impurity producing a natural rotation, which was superimposed on the rotation produced by the magnetic field. In the present experiments, for the direction of the magnetic field mainly employed, the natural rotation was in the opposite direction to that produced by the field.

Normal propyl alcohol is generally prepared by the

\* Journ. Chem. Soc. xlv. p. 467 (1884).

† *Ibid.* l. p. 91 (1914).



fractional distillation of fusel oil, which contains normal amyl alcohol and other homologues of the alcohol series. It is therefore suggested that the optically active impurity is lævotary amyl alcohol, which boils at  $128^{\circ}\text{C}$ . In one of the earlier samples experimented upon, this natural rotation amounted to 49.3 minutes at  $0.3420\ \mu$ . Under these circumstances the total rotation produced by the propyl alcohol when placed in a magnetic field is equal to the magnetic rotation due to the normal propyl alcohol plus the sum of the natural and magnetic rotations due to the impurity. It has been assumed in constructing Tables V., VI. and VII. that the magnetic rotation of pure normal propyl alcohol for a given  $\lambda$  is equal to the sum of the measured rotation in the magnetic field and the natural rotation for that wave-length. It is considered that, as the quantity of impurity is comparatively small, and as it is probably active amyl alcohol whose strong absorption band is near that of propyl alcohol, the error introduced by the above mode of calculation is very small. The magnetic rotation of the propyl alcohol was also measured for two wave-lengths when the magnetic field was reversed, and the magnetic rotation was in the same direction as the natural rotation due to the impurity. The values of the magnetic rotation were found to be the same as before.

The results given in Tables V. to IX. refer to the purest normal propyl alcohol prepared by Dr. Schuchardt of Görlitz. The liquid was placed in a flask provided with a fractionating column, and practically all of it distilled over at a constant temperature of  $97^{\circ}\text{C}$ . The alcohol was also satisfactory from the point of view of absorption in the ultra-violet. With the tungsten arc as the source of light, magnetic rotations could be measured for wave-lengths in the ultra-violet as far as  $0.2800\ \mu$ . The alcohol, however, showed the presence of a small quantity of impurity which was optically active. The results of experiments on what is called the first sample of normal propyl alcohol are given in Table V. In this sample the natural rotation, which was measured for several wave-lengths, varied from 12 min. at  $0.4500\ \mu$  to 33.1 min. at  $0.2850\ \mu$ . The propyl alcohol was then purified by repeated fractional distillation, and the results for the second sample are given in Table VI.

The natural rotations for this sample were also measured at different wave-lengths, and were found to vary from 4.7 min. at  $0.4500\ \mu$  to 13.9 min. at  $0.2850\ \mu$ .

The alcohol was again purified by fractional distillation over a long period, and the results for the third sample are given in Table VII. The natural rotation for this sample varied from 2.7 min. at 4500  $\mu$  to 7.7 min. at 2850  $\mu$ .

In this case the natural rotation for sodium light would be about 1.46 min. The rotation for sodium light found by Pedler \* for the purest lævo-rotary amyl alcohol he could obtain was  $-6^{\circ}.8$  for 200 mm., and consequently, if the tube used in the present experiments contained pure optically active amyl alcohol, the rotation could not be less than 622 min. The percentage of optically active substance contained in the third sample, if it be assumed that the impurity is active amyl alcohol, is, therefore, not greater than .23 per cent., and the correction to be applied for the natural rotation is only about 1 per cent. of the magnetic rotation. The results obtained, as explained above, for the samples containing various percentages of the active impurity are in good agreement. In these experiments the presence of the active impurity is easily detected, especially in the ultra-violet, owing to the length of tube employed, but the results obtained seem to indicate that

TABLE V.  
First Sample of Propyl Alcohol.

Temperature in degrees centigrade.	Wave-length in microns ( $10^{-4}$ cm.),	Verdet's Constant in min. per cm. gauss.	Refractive Index. n.
17.0	.4390	.0227 <sub>7</sub>	1.3935
16.5	.4300	.0240	1.3942
16.8	.4055	.0273 <sub>5</sub>	1.3973
17.0	.3975	.0287	1.3983
15.5	.3894	.0301 <sub>5</sub>	1.3993
15.0	.3670	.0346 <sub>5</sub>	1.4025
17.0	.3600	.0362 <sub>5</sub>	1.4034
15.5	.3406	.0417	1.4069
16.5	.3306	.0445 <sub>5</sub>	1.4094
16.0	.3180	.0492 <sub>5</sub>	1.4119
16.7	.3115	.0520	1.4140
16.9	.3055	.0541 <sub>5</sub>	1.4152
17.0	.2980	.0594	1.4182
16.9	.2940	.0602 <sub>0</sub>	1.4188
16.4	.2856	.0647	1.4216

\* Perkin, *loc. cit.*

TABLE VI.  
Second Sample of Propyl Alcohol.

Temperature in degrees centigrade.	Wave-length in microns ( $10^{-4}$ cm.).	Verdet's Constant in min. per cm. gauss.	Refractive Index. $n$ .
16.7	.4310	.0239	1.3941
16.0	.3975	.0286 <sub>0</sub>	1.3983
16.6	.3895	.0301	1.3992
16.5	.3675	.0346	1.4023
15.1	.3400	.0415 <sub>0</sub>	1.4070
15.6	.3203	.0482 <sub>5</sub>	1.4114
16.2	.3065	.0540 <sub>3</sub>	1.4150
16.8	.2945	.0603	1.4187
17.1	.2850	.0650	1.4219

TABLE VII.  
Third Sample of Propyl Alcohol.

Temperature in degrees centigrade.	Wave-length in microns ( $10^{-4}$ cm.).	Verdet's Constant in min. per cm. gauss.	Refractive Index, $n$ .
17.2	.4295	.0240	1.3943
17.8	.3985	.0285	1.3982
17.7	.3910	.0290	1.3991
17.6	.3670	.0346	1.4025
17.5	.3399	.0416	1.4070
17.5	.3205	.0482	1.4114
17.2	.3060	.0542	1.4150
17.5	.2936	.0604	1.4189

TABLE VIII.

Wave-length in microns ( $10^{-4}$ cm.).	Refractive index, $n$ .	Verdet's Constant in min. per cm. gauss.	Verdet's Constant in circular measure, $\times 10^6$ , $i. e.,$ $\delta \times 10^6$ .	$\phi \times 10^{14}$ ( $\phi = n\delta\lambda^2$ ).
(a) .4295	1.3943	.0240	6.981	1.796
(b) .3985	1.3982	.0285	8.290	1.841
(c) .3670	1.4025	.0346	10.065	1.901
(d) .3205	1.4114	.0482	14.021	2.033
(e) .2936	1.4189	.0604	17.570	2.149

practically no improvement would be obtained by further fractional distillation. The values of the refractive indices given in Tables V., VI., VII., and VIII. have been obtained from a graph, which has been constructed from values given by Victor Henri\*. In this case again we have been unable to find a reference to the temperature at which the measurements were made, but values of the refractive indices of normal propyl alcohol at 18° C. in the ultra-violet † differ by about 1 in 400 from the values given in the Tables VI. to VIII. for wave-lengths between .2800 and .3080  $\mu$ , and by about 1 in 1000 for wave-lengths between .3080 and .3940  $\mu$ .

The values of the function from which the wave-length  $\lambda_1$  of the absorption band is calculated are given in Table VIII.

The values of  $\lambda_1$ , the wave-length of the absorption band determined from the above observations on the assumption that

$$\phi = K_1 \left( \frac{\lambda^2}{\lambda^2 - \lambda_1^2} \right)^2,$$

are as follows :—

From (a) and (b) = .1143 $\mu$ .	From (a) and (c) = .1143 $\mu$ .
„ (b) and (c) = .1142 $\mu$ .	„ (c) and (e) = .1134 $\mu$ .
„ (c) and (d) = .1134 $\mu$ .	„ (a) and (e) = .1137 $\mu$ .
„ (d) and (e) = .1134 $\mu$ .	

The mean value of  $\lambda_1$  is .1138  $\mu$ , and the value of  $K_1$  calculated from the value of  $\phi$  corresponding to a known value of  $\lambda$  was found to be 1.553. The variation of  $\phi$  with wave-length in the visible and ultra-violet regions of the spectrum is therefore given by the equation

$$\phi = 1.553 \left( \frac{\lambda^2}{\lambda^2 - (.1138)^2} \right)^2.$$

A further test of the accuracy of the above formula is obtained by making use of it to calculate the values of Verdet's constant for different wave-lengths in the visible and ultra-violet regions of the spectrum, and comparing the results obtained with those determined experimentally. Table IX. gives the results of such calculations.

\* V. Henri, *loc. cit.*

† Landolt & Börnstein, ii. p. 969.

TABLE IX.

Wave-length in microns ( $10^{-4}$ cm.).	Verdet's Constant observed.	Verdet's Constant calculated.
·4390	·0227 <sub>7</sub>	·0228
·4055	·0273 <sub>3</sub>	·0273 <sub>7</sub>
·3910	·0299	·0298
·3895	·0301	·0300 <sub>7</sub>
·3600	·0362 <sub>2</sub>	·0362 <sub>4</sub>
·3399	·0416	·0416 <sub>3</sub>
·3306	·0445 <sub>5</sub>	·0446
·3180	·0492 <sub>2</sub>	·0492
·3115	·0520	·0518
·3060	·0542	·0542 <sub>6</sub>
·2960	·0594	·0592
·2856	·0647	·0650

If the equation be employed to determine the value of Verdet's constant for sodium light, the result obtained is ·0119<sub>6</sub>. This calculated value is in good agreement with that determined experimentally by Perkin \*, viz., ·01197.

#### DISCUSSION OF RESULTS.

The experimental results obtained for methyl alcohol over the range ·4379  $\mu$  to about ·2600  $\mu$  can be represented by the equation

$$n\delta\lambda^2 = \phi = 1.190 \left( \frac{\lambda^2}{\lambda^2 - (.1100)^2} \right)^2,$$

where  $\delta$  = Verdet's constant,  $n$  the refractive index of the liquid for wave-length  $\lambda$ , and ·1100  $\mu$  is the wave-length corresponding to the free period of the resonators.

The corresponding expressions for ethyl alcohol over the range ·4390  $\mu$  to ·2600  $\mu$ , and for propyl alcohol over the range ·4390  $\mu$  to ·2856  $\mu$ , are

$$n\delta\lambda^2 = \phi = 1.444 \left( \frac{\lambda^2}{\lambda^2 - (.1114)^2} \right)^2,$$

\* *Loc. cit.*

† Stephens & Evans, *loc. cit.*

and

$$n\delta\lambda^2 = \phi = 1.553 \left( \frac{\lambda^2}{\lambda^2 - (\cdot 1138)^2} \right) \dots$$

respectively.

The magnetic rotations over the ranges of spectrum investigated can therefore in each case be represented by a formula involving only one free period, and also the values of Verdet's constant for sodium light deduced from the three equations agree, within the limits of experimental error, with those determined by Perkin\* for the three alcohols. It is also evident from the three equations that the absorption band shifts towards the region of longer wave-length as the molecular weight of the alcohol increases but the change in the frequency of the absorption band in passing from one alcohol to the next in the series does not appear to be constant.

The dispersion and absorption of the alcohols in the ultra-violet and infra-red regions of the spectrum have been measured by Victor Henri†. From these data he concluded that the alcohols have absorption bands of frequencies related to one another, as follows:—

$$\underbrace{\nu_0, \frac{\nu_0}{2}, \nu_0, 2\nu_0}_{\text{infra-red;}} \quad 15\nu_0, \quad \text{ultra-violet;} \quad 30\nu_0, \quad \text{extreme ultra-violet.}$$

From his experimental results on the absorption of light by methyl, ethyl, and propyl alcohols he obtained for the wave-lengths of the absorption bands in the central region of the ultra-violet (corresponding to  $15\nu_0$ ) the values  $\cdot 2207 \mu$ ,  $\cdot 2231 \mu$ , and  $\cdot 2273 \mu$  respectively.

It is interesting to point out that the wave-lengths of the absorption bands deduced in the present investigation from measurements of the magnetic rotation of methyl, ethyl, and propyl alcohols are  $\cdot 1100 \mu$ ,  $\cdot 1114 \mu$ , and  $\cdot 1138 \mu$  respectively.

The frequencies of these bands are very approximately double the frequencies determined by Victor Henri‡ in the central region of the ultra-violet, and correspond to  $30\nu_0$  in the above scheme. The bands at  $\cdot 2207 \mu$ ,  $\cdot 2231 \mu$ , and  $\cdot 2273 \mu$  do not contribute materially to the magnetic rotation of methyl, ethyl, and propyl alcohols respectively.

\* *Loc. cit.*

† 'Etudes de Photochemie,' pp. 41-64.

‡ *Loc. cit.*

From the equations for  $\phi$  in the case of methyl and propyl alcohols the values of  $\frac{\delta_{\cdot 4359 \mu}}{\delta_{\cdot 5461 \mu}}$  were calculated, and found to be 1.640 and 1.645<sub>6</sub> respectively.

These values are about .6 per cent. higher than those determined experimentally by Lowry\*.

#### SUMMARY OF RESULTS.

1. The magnetic rotation of methyl alcohol has been examined for wave-lengths ranging from .4379  $\mu$  to .2600  $\mu$ , and the values of  $\delta$  (Verdet's constant) can be represented by the equation

$$\phi = n\delta\lambda^2 = 1.189 \left( \frac{\lambda^2}{\lambda^2 - (\cdot 1100)^2} \right)^2,$$

where  $n$  is the refractive index of methyl alcohol for wave-length  $\lambda$  and .1100  $\mu$  is the wave-length of absorption band in the extreme ultra-violet.

The weak absorption band in the central region of the ultra-violet at .2207  $\mu$  does not contribute materially to the magnetic rotation, but the wave-length of the strong absorption band (.1100  $\mu$ ) deduced from the magnetic rotation experiments is very nearly one half that of the weak absorption band.

2. The magnetic rotation of propyl alcohol has been examined over the range .4390  $\mu$  to .2856  $\mu$ , and the value of  $\delta$  can be represented by the equation

$$\phi = n\delta\lambda^2 = 1.553 \left( \frac{\lambda^2}{\lambda^2 - (\cdot 1138)^2} \right)^2.$$

The wave-length of the absorption band (.1138  $\mu$ ) is almost exactly one half that of the weak absorption band at .2273  $\mu$ , but the latter does not contribute materially to the magnetic rotation.

The authors wish to thank Mr. C. C. Evans, B.Sc., for his help during the later stages of the investigation, and also Mr. Frank Homeyard, who was responsible for making most of the apparatus employed in the research.

\* *Loc. cit.*

LXI. *On the Properties of Dry Liquids.*

By Prof. S. B. MALL, D.Sc., A.E.S.\*

PROF. BAKER has recently shown that the boiling-points of many liquids which are ordinarily supposed to be pure are markedly changed when these liquids are subjected to intensive desiccation for a long time (J. C. S. vol. ci. p. 2329, 1912). He proved experimentally that the change in the boiling-points of the liquids had really been brought about by the removal of water, for the introduction of the slightest amount of moisture restored the boiling-points to their former values. He also satisfied himself that the effect was not due to the superheating of the liquids.

As an explanation of this phenomenon, Baker suggested that in the liquid state there is ordinarily a balance between associated and dissociated molecules, and that the absence of water-vapour tends to prevent the dissociation, so that the boiling-points of dried liquids consisting mostly of associated molecules is much higher than for normal liquids.

In 1922, Dr. A. Smits explained Baker's results by supposing that "by intensive drying the inner transformations in a unary phase are stopped, the inner equilibrium is fixed, and a mixture is obtained which on distillation generally gives a distillate with a lower boiling-point and a residue with a higher boiling-point than the original liquid" (*Zeits. Phys. Chem.* c. p. 477, 1922).

In 1923, Prof. G. N. Lewis contradicted, on thermodynamic grounds, the explanations put forward by Smits (J. A. C. S. xlv. p. 2836, 1923). According to him, the mere removal of the last traces of water from a liquid cannot appreciably change the existing equilibrium between several molecular species which may be supposed to exist; but if water acts as a catalyst for the process of interchange between one molecular species and another, its removal can only serve to freeze the already existing state of equilibrium by inhibiting further interchange among the various forms.

In response to these objections, Smits modified his views later. He assumed that in ordinary liquids there are at least two modifications with different properties between which reversible reactions of the type  $\alpha \rightleftharpoons \beta$  are always taking place. By the process of drying, the velocity of one or both of these reactions is attenuated or even reduced to zero.

\* Communicated by the Author.



If the velocity of only one of these reactions (say  $\alpha \rightarrow \beta$ ) is attenuated, we shall have in the dried liquid a mixture of  $\alpha$  and  $\beta$ , the quantity of  $\alpha$  predominating over that of  $\beta$ . The effect of drying in this case will be a shift of the inner equilibrium followed by freezing or fixation of the inner equilibrium. If, on the other hand, the velocities of both these reactions ( $\alpha \rightarrow \beta$  and  $\beta \rightarrow \alpha$ ) are attenuated, we shall have in the dried liquid a mixture of the two compounds  $\alpha$  and  $\beta$ , in the same proportions in which they exist in moist liquids and between which there may be further mutual transformations. The effect of drying in this case will be simply the fixation of the inner equilibrium. If water acts as a catalyst for one reaction, the vapour-pressure (and hence the boiling-point) of the dried liquid will change, independent of whether or not the distillate is allowed to escape. On the other hand, if water acts as a catalyst for the direct as well as the reverse reactions between the components  $\alpha$  and  $\beta$ , the boiling-point of the dried liquid will change only when the distillate is allowed to escape, and not otherwise. Hence, Smits suggests that, if the vapour-pressure (and hence the boiling-point) of the dried liquid changes without any portion of the liquid boiling off, it must be due to shift of the inner equilibrium followed by fixation; if not, the effect must be simply due to a fixation of the inner equilibrium.

The present writer tested the suggestions of Smits experimentally, and he found that in the case of dried liquids the inner equilibrium is first shifted and then fixed (*Zeitschr. f. Anorg. u. Allg. Chemie*, cxlix. p. 150, 1925).

It appears that the physical properties of ordinary liquids (*e. g.* density, refractive index, viscosity, surface-tension, and conductivity) are but the properties of mixtures. The properties of the components of ordinary liquids which are supposed to be binary mixtures may be studied by drying the liquids intensively so that in the dried product only one component prevails. Since by intensive drying the nature and the relative amount of the molecules in a liquid are changed, it is expected that the absorption spectra of dried liquids and their vapours will differ from the absorption spectra of moist liquids and their vapours; and on account of the predominance in the dried liquids of one kind of molecule over the other, the absorption bands and lines will differ in intensity in the case of moist and dry liquids and their vapours.

No attempts seem to have as yet been made to calculate the relative amounts of the two components in moist and dried liquids which are supposed to be binary mixtures.

The following is an attempt in this direction in the case of those liquids whose rise of boiling-point by drying was measured by Baker. A binary moist liquid will contain the two components  $\alpha$  and  $\beta$  in a certain fixed proportion. By drying, this proportion will change, the relative amount of the less volatile component increasing. We may suppose that the dried liquid is for all practical purposes a solution of a portion of the less volatile component in a mixture of the two components existing in the same proportion in which they exist in a moist liquid. Of course in the dried liquid we have actually a solution of the less volatile component in the more volatile component, but, for want of data, we make the above simplifying assumptions in order to render the calculation possible. Suppose in the moist liquid we have the two components  $\alpha$  and  $\beta$  in the percentage proportion  $x : 100 - x$ , and suppose that in the dried liquid the percentage is changed to  $x' : 100 - x'$ . If  $x' < x$ , we may suppose that the dried liquid is a solution of  $\beta$  in a mixture of  $\alpha$  and  $\beta$ , and that an amount

$$\left\{ (100 - x') - \frac{(100 - x)x'}{x} \right\}$$

of the solute  $\beta$  is contained in an amount

$$\left\{ x + \frac{(100 - x)x'}{x} \right\}$$

of the solution.

We know from thermodynamics that there is a relation between the rise of the boiling-point of the solution and the amount of solute present in the solution. For a dilute solution the relation is given by the formula

$$M = \frac{RT_0^2 x}{VL\rho\Delta T}$$

$$\text{or} \quad \frac{x}{M} = \frac{VL\rho\Delta T}{RT_0^2},$$

where

$M$  = molecular weight of the solute,

$x$  = grams of solute dissolved in  $V$  c.c. of the solution,

$T_0$  = absolute boiling-point of the solvent,

$L$  = latent heat of evaporation of one gram of the solvent,

$\rho$  = density of the solvent in grams per c.c.

$\Delta T$  = rise of boiling-point of the solution, and

$R$  = gas constant for a gram mol.

If we consider the molar amount of the solute dissolved in 1 c.c. of the solution, the formula may be simplified to the form

$$\frac{x}{M} = \frac{L\rho\Delta T}{RT_0^2}.$$

In the case of a concentrated solution a correction to this formula has to be applied on account of the volume of the solute molecules. If the volume correction for a gram mol. of the solute be "*b*," the molar concentration of the solute will be given by the formula

$$\frac{\frac{x}{M}}{1-b\frac{x}{M}} = \frac{L\rho\Delta T}{RT_0^2}.$$

The value of "*b*" being unknown, the calculated values of

$$\frac{\frac{x}{M}}{1-b\frac{x}{M}}$$

corresponding to the liquids intensively dried by Prof. Baker are given in the following table (p. 613). The values of  $\Delta T$  are taken from Baker's paper (Trans. Chem. Soc. cxxi. p. 568, 1922). The values of the other quantities are taken from Kaye and Laby's 'Tables of Physical Constants.' It may be remarked here that Baker found that the densities of dry liquids do not appreciably differ from the densities of moist liquids.

The values in the last column are calculated on the assumption that the molecules are normal and not associated. If association be supposed to exist, these values will be lowered. The true concentrations of the solutes will be lower than those given in column 6 in the ratio  $\left(1-b\frac{x}{M}\right):1$ .

A glance at columns 6 and 7 will show that in the case of benzene,  $CS_2$ ,  $CCl_4$ , and bromine the amount of the less volatile component in the dried liquid is very large compared with the amount of the more volatile component. In the case of ethyl alcohol, methyl alcohol, propyl alcohol, and ethyl ether the total number of mols of solute in 1 c.c. of the solution (dried liquid) is much greater than the total number of mols of the solvent in 1 c.c. of the moist liquid, unless

the values of "b" be supposed to be excessively large. If we suppose that the value of "b" is of the same order in the case of all the solutions, we cannot explain the anomalies in the case of the alcohols and ether without supposing that in the dried liquid the molecules are dissociated—a fact which will be in direct contradiction to the explanation put forward by Prof. Baker himself. It thus appears that in the case of alcohols and ether the molecular volumes of the less volatile components are excessively large compared with the molecular volumes of the more volatile components.

Name of liquid.	Density in grams per c.c.	Boiling-point in ° C.	Latent heat of evaporation for 1 gram.	ΔT.	$\frac{x}{M} \cdot 1 - b \frac{x}{M} = \frac{L_0 \Delta T}{RT_0}$	Gram mol. of moist liquid in 1 c.c. (molecules supposed to be normal.)
Benzene.	0.879 20° C.	80.2	95.49	26	0.009	0.011
CS <sub>2</sub> .	1.292 0° C.	46.2	85	30	0.016	0.017
CCl <sub>4</sub> .	1.582 21° C.	76.7	46	34	0.010	0.010
Ethyl alcohol.	0.7937 15° C.	78.3	207	60	0.04	0.017
Methyl alcohol.	0.796 15° C.	64.7	267	54	0.050	0.025
Bromine.	3.102 25° C.	63	46	55	0.0348	0.0388
Mercury.	1.56 15° C.	356.7	68	62	0.072	0.067
Ethyl ether.	0.718 17° C.	34.6	84	48	0.0152	0.097
Propyl alcohol.	0.804 20° C.	97.2	163	39	0.019	0.0133

The catalytic behaviour of water in the transformations of the components of binary mixtures of moist liquids may be explained on Baly's theory of residual affinity (Baly's 'Spectroscopy,' 1918 ed., p. 487). Under residual affinity Baly includes every type of unsaturation whether as regards the primary or the secondary valencies. Since the possession of residual affinity tends to endow a compound with the

power of forming additional compounds with other substances, the existence of residual affinity is accompanied by the existence of force lines in the surrounding æther. Every group of atoms must have round it a field of force whose magnitude must depend on the amount of residual affinity present. As a consequence, there must be a certain amount of condensation of the lines of force of the various atom groups, and the system will be more or less closed. If these closed systems receive suitable energies they may open again. The presence of a third substance may serve to open these compounds so that they will be capable of free existence and also will be free to take part in chemical reactions. This third substance can open the compounds by itself absorbing radiations selectively (probably in an excited state) and emitting them again in the space occupied by the compounds. It thus plays the role of a catalytic agent.

Coming now to the problem in hand, we may suppose that the simple unassociated molecules of a dry liquid do ordinarily form compounds among themselves on account of their residual affinities. But in the presence of moisture these molecules are energized by radiations selectively absorbed and radiated by water molecules, and are capable of independent existence as individual molecules. The amount of radiation from the water molecules which energizes the closed molecular systems of the moist liquid must be a function of temperature, and it is expected to increase with temperature. On this theory we expect that at very low temperatures most of the molecules of a moist liquid will behave as closed systems. In other words, there will be little or no difference between a moist and a dry liquid at very low temperatures according to the present theory.

Cotton College,  
Gauhati, India.

*Note added in proof.*—In the case of nitrogen tetroxide Smits (J. C. S., Oct. 1926) proved that the vapour-pressure rises with drying, and this result has recently been corroborated by Smith. It therefore appears that moisture not only retards association in liquids, but sometimes also promotes it. The catalytic behaviour of water in moist liquids therefore appears to be a complex thing. Besides, there is reason to believe that most of the water molecules in moist liquids are in an ionized state, and it is the ions that are responsible for the catalytic behaviour of water.

LXII. *A Modification of the Rayleigh Disk Method for measuring Sound-Intensities.* By L. J. SIVIAN\*.

THE usual procedure is to measure the steady deflexion of the disk under the influence of a steady sound-field. Following is an outline of a procedure which has been found useful when the sound amplitude can be made a suitable function of time. The scheme depends on the fact that the torque which the sound-wave exerts on the disk is a non-linear function of the sound amplitude. The amplitude of the sound-wave to be measured is modulated with a frequency equal to that of the free vibration of the suspended disk. The measurement consists in reading the amplitude of oscillations corresponding to the modulating frequency, rather than a steady deflexion of the disk. The disturbances caused by spurious air-currents are largely reduced. In addition, for many practical cases at least, there is a gain in absolute sensitivity.

For a thin circular disk whose normal makes an angle  $\theta$  with the direction of the undisturbed fluid stream, the torque  $M$  tending to diminish  $\theta$  is † :

$$M = \frac{4}{3} \rho a^3 \cdot U^2 \cdot \sin 2\theta, \dots \dots \dots (1)$$

where  $\rho$  = fluid intensity,  $a$  = radius of disk, and  $U$  = stream-velocity. If, as in a sinusoidal sound-wave,  $U = U_0 \cdot \sin nt$ ,

$$\begin{aligned} M &= \frac{4}{3} \rho a^3 \cdot \sin 2\theta \cdot \left( \frac{1}{2} - \frac{1}{2} \cos 2nt \right) U_0^2 \\ &= B \cdot \frac{1}{2} U_0^2 - B \cdot \frac{1}{2} U_0^2 \cdot \cos 2nt. \end{aligned}$$

The torque contains a rectified and a double-frequency component. The former accounts for the deflexion observed in the static method. The alternating component usually is unobservably small, owing to the high motional impedance of the disk at the sound-frequencies.

Suppose, now, that a completely modulated wave

$$U = U_0 \cdot (1 + \sin \omega t) \cdot \sin nt \dots \dots (2)$$

is incident upon the disk. The torque acting is

$$M(t) = B \cdot \frac{1}{2} U_0^2 \left[ \frac{3}{2} + 2 \sin \omega t - \frac{1}{2} \cos 2\omega t \right] (1 - \cos 2nt).$$

\* Communicated by Rollo Appleyard, M.Inst.C.E.

† W. König, Wied. *Ann.* xliii. p. 43 (1891).

If the motion of the disk is given by

$$I\ddot{\phi} + R\dot{\phi} + S\phi = M(t),$$

the modulating frequency is chosen so that

$$I\omega^2 - S = 0.$$

If  $n \gg \omega$ , as is the case in practice, the steady state deflexions produced by the modulated torque, which need be considered, are:

$$\left. \begin{aligned} D_0 &= \frac{3}{4} B U_0^2 \cdot \frac{1}{S}, \\ D_1 &= B U_0^2 \cdot \frac{1}{R\omega}, \\ D_2 &= \frac{1}{4} B U_0^2 \cdot \frac{1}{2R\omega \sqrt{1 + \frac{9S^2}{4R^2\omega^2}}}, \end{aligned} \right\} \dots (3)$$

where  $D_0$  is a steady deflexion,  $D_1$  corresponds to the frequency  $\frac{\omega}{2\pi}$ , and  $D_2$  to  $\frac{2\omega}{2\pi}$ .  $D_1$  is the amplitude observed in the dynamic method. In the static method,

$D_s = \frac{3}{4} B U_0^2 \cdot \frac{1}{S}$  for an unmodulated wave of the same r.m.s. amplitude as in the modulated wave assumed above.

The ratio  $\frac{D_1}{D_s} = \frac{4}{3} \cdot \frac{S}{R\omega}$  gives the relative sensitivity of the two methods. Suppose, further, that the spurious air-drifts produce essentially a steady torque. Then, as a rough

approximation, the "sound-drift ratio" is  $\frac{4}{3} \cdot \frac{S}{R\omega}$  times greater for the dynamic than for the static method. A

numerical example will indicate the orders of magnitudes involved. For a certain disk designed to measure  $D_s$ ,  $T = \text{period} = 2.59 \text{ sec.}$ ,  $R = 3.53 \times 10^{-5}$ , and  $I = 8.04 \times 10^{-5}$ .

The value of  $\frac{4}{3} \cdot \frac{S}{R\omega}$  is 7.3. By choosing a heavier disk, say  $I = 40.2 \times 10^{-5}$ , and a correspondingly thicker or shorter suspension so that  $S$  is also five times greater than before, the dynamic "sound-drift ratio" is improved five-fold. The absolute value of the dynamic sensitivity is unchanged, since  $\frac{1}{R\omega}$  is the same as before.

From (1), (3), and (4) it is seen that for thin disks the dynamic sensitivity is independent of the disk radius, provided the disk period remains constant. The static sensitivity is proportional to the cube of the radius. The distinction is particularly important in high-frequency measurements, since the disk diameter must always be small in comparison with the sound wave-length.

On the other hand, it might be supposed that for low frequencies the static sensitivity can be greatly increased by choosing  $a$  as large as possible, subject only to  $a \ll \lambda$ . Actually, however, two circumstances tend to offset (and sometimes more than offset) the advantage to be expected. Firstly, the time required for the static deflexion to settle down within a prescribed fraction of its final value. This time is proportional to  $\frac{I}{R}$ . Since  $I$  is proportional to  $a^4$ , and  $R$  is approximately proportional to  $a^3$ , the time required is proportional to  $a$ . Secondly, the sound-drift ratio may decrease quite rapidly as  $a$  increases. This would not be the case if the drift-torque were perfectly sustained, as in the sound-torque. Actually, the drift-torques observed in an enclosed box appear to be of two kinds:—

1. Slowly-fluctuating drifts, in effect containing alternating components of the order of 5 to 10 seconds per cycle. Such components are favoured, since their periods more nearly coincide with the free periods of the larger disks.
2. Short, sudden puffs of air, of the order of one second or less, which roughly may be regarded as torque impulses. The number of impulses received is proportional to the time required by the disk to settle down. And this time, as already pointed out, is approximately proportional to  $a$ .

*Disturbance due to Double-frequency Amplitude.*—Superposed on  $D_1$ , there is the amplitude  $D_2$  of an oscillation with double the modulating frequency. For the particular disk described,  $\frac{D_1}{D_2} = 66$ . The effect of the  $2\omega$  term on the measurement of  $D_1$  is seen to be rather small. If the disk and suspension were altered as stated above,  $\frac{D_1}{D_2}$  would be increased nearly fivefold, and the effect of  $D_2$  rendered quite negligible.



*Modulation of the Sound-wave.* When the sound-source is electro-acoustic, it is only necessary to modulate the alternating current. Two methods have been used :—

(A) A resistance potentiometer to carry the sound-frequency current is wound on the periphery of a disk. A brush driven from a geared-down adjustable speed motor makes contact with the resistance units. The latter are so wound that the amplitude of the a.c. voltage tapped off by the brush varies in accordance with (1). The modulated voltage is impressed on an amplifier which feeds the sound-source.

(B) The sound-source is fed from two a.c. generators of equal amplitudes and nearly equal frequencies. The difference between the two frequencies is adjusted to equality with the natural frequency of the disk.

An error in the adjustment of  $\omega$  will cause the observed  $D_1$  to differ from its value in (3). It is easy to show that, for a given small percentage error in  $\omega$ , the error in  $D_1$  will be much less if  $\omega$  is too low rather than too high.

*Motional Resistance of Disk.*—The value of  $R$  in (3) must be determined independently. The rate of decay of the free vibrations,  $e^{-\frac{R}{2I}t}$ , is observed. This gives  $R$ , provided  $I$  is known. The latter can be computed from the mass and dimensions of the disk,  $I = m\left(\frac{a^2}{4} + \frac{l^2}{12}\right)$ . In the case of a small, fairly heavy disk (such as would normally be best fitted for the dynamic method) the moment of inertia which the air adds to the above value of  $I$  is quite negligible. But even in the case of a large light disk, the correct value of  $I$  is readily determined by observing the change in the free period caused by adding to the disk a known moment of inertia.

The above experimental determination of  $R$  is a simple matter. However, in selecting disk and suspension for any particular type of measurement, it is helpful to know  $R$  as a function of the disk dimensions, approximately at least. This function can be arrived at by regarding the disk as the limiting case of an ellipsoid. Suppose the ellipsoid  $\frac{x^2}{a^2} + \frac{y^2}{b^2} + \frac{z^2}{c^2} = 1$  to rotate about the axis of  $X$  in an infinite viscous fluid. The motion is assumed to be so slow that the product of the velocities may be neglected. Then the couple

K, acting on the ellipsoid, is \* :

$$K = \frac{32\mu\pi\omega(b^2 + c^2)}{5(b^2B + c^2C)},$$

where

$$B = \int_0^\infty \frac{d\psi}{(b^2 + \psi)^{1/2} P} \quad \text{and} \quad C = \int_0^\infty \frac{d\psi}{(c^2 + \psi)^{1/2} P},$$

and

$$P = [(a^2 + \psi)(b^2 + \psi)(c^2 + \psi)]^{1/2}.$$

For a thin circular disk we take  $a=b$  and  $c=0$ . Evaluating the above integrals gives

$$K = \frac{64}{5}\mu a^2\omega \quad \text{and} \quad R = \frac{64}{5}\mu a^3.$$

The assumed smallness of  $\omega$  is equivalent to the condition  $\frac{\omega a^2 \rho}{\mu} \ll 1$ .

If the area of the disk-edge is not negligible, a first-order correction is obtained by regarding the surface of the edge as part of a sphere of radius  $a$ . The total resistance of a slowly-rotating sphere being  $8\pi\mu a^3$ , the resistance corresponding to the edge surface ( $2\pi a l$ ) is  $4\pi\mu a^2 l$ . The following table gives a comparison of disk resistance computed from

$$R = \frac{64}{5}\mu a^3 + 4\pi\mu a^2 l$$

with those obtained from measurements on the rate of decay. The moments of inertia used in deducing the "observed" values of  $R$  were computed from the disk- and air-constants

$$I = m\left(\frac{a^2}{4} + \frac{l^2}{12}\right) + \frac{16}{45}\rho a^5$$

rather than directly measured.

$a$ .	$l$ .	R obs.	R calc.
0.15 cm.	0.026 cm.	$9.64 \times 10^{-5}$	$9.15 \times 10^{-6}$
0.254 "	0.11 "	$3.55 \times 10^{-5}$	$3.96 \times 10^{-6}$
0.316 "	0.052 "	$7.96 \times 10^{-6}$	$8.50 \times 10^{-6}$
0.476 "	0.03 "	$2.62 \times 10^{-4}$	$2.66 \times 10^{-4}$
0.479 "	0.0046 "	$2.32 \times 10^{-4}$	$2.57 \times 10^{-4}$
0.502 "	0.017 "	$2.84 \times 10^{-4}$	$2.96 \times 10^{-4}$

\* D. Edwards, *Quart. Journ. Pure and Appl. Math.* xxvi. p. 70 (1893).

The added moment of inertia,  $\frac{16}{45}\rho a^5$ , is that for a disk rotating in an incompressible inviscid fluid \*. Clearly, even for the slow vibrations of disks used in sound-measurements, both the resistance and moment of inertia due to the air are greater for the case of rotatory oscillations than the "steady rotation" values used above. A quantitative discussion of the air corrections for slow rotatory oscillations will be given elsewhere. For the purpose stated—to guide in selecting suitable disk-constants—the above expression for  $R$  is seen to be sufficiently accurate.

I am indebted to Mr. W. R. Goehner, of this laboratory, for his aid in connexion with the experimental part of this work.

Bell Telephone Laboratories, Inc., New York.

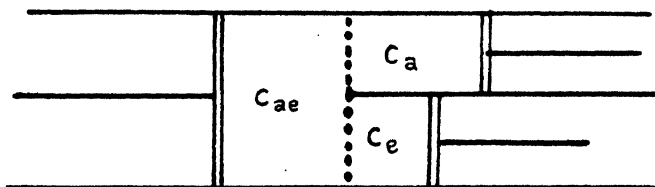
August 1927.

### LXIII. *The Differential Equations of a Reacting Mixture.* By R. D. KLEEMAN, B.A., D.Sc.†

**W**HEN a number of substances are mixed and they react chemically, the final state of equilibrium we would expect should be governed by a number of differential equations. These equations will be deduced in this paper.

Let us first consider a mixture consisting of  $M_a$  gram atoms of the substance  $a$ , and  $M_e$  gram atoms of the sub-

Fig. 1.



stance  $e$ , which combine to form various molecules. This mixture we will suppose is passed through an isothermal cycle by means of an apparatus shown diagrammatically in fig. 1. It consists of three adjacent chambers whose

\* Lamb's 'Hydrodynamics,' 4th ed. p. 141.

† Communicated by the Author.

volumes may be varied by means of pistons—the chamber  $C$  is separated from the chamber  $C_{ae}$  by a membrane permeable to the molecules composed of the constituent  $a$ , and the chamber  $C_e$  is separated from the chamber  $C_{ae}$  by a membrane permeable to the molecules composed of the constituent  $e$ . The mixture is initially contained in the chamber  $C_{ae}$ . Now let us at constant temperature:—

(a) Transfer the mixture from the chamber  $C_{ae}$  into the chambers  $C_a$  and  $C_e$ , keeping the pressure  $p$  of the mixture and the pressures  $p_a$  and  $p_e$  of the substances  $a$  and  $e$  in the chambers  $C_a$  and  $C_e$  constant during the process. The external work done is equal to

$$M_a v_a p_a + M_e v_e p_e - v p,$$

where  $v$  denotes the initial volume of the mixture, and  $v_a$  and  $v_e$  the volumes of gram atoms of the substances  $a$  and  $e$  in the chambers  $C_a$  and  $C_e$ .

(b) Increase the volume of each of the chambers  $C_a$  and  $C_e$  by a small amount. The external work done is equal to

$$p_a M_a \cdot \partial v_a + p_e M_e \cdot \partial v_e.$$

(c) Return the substances to the chamber  $C_{ae}$  in the reverse way that they were separated, keeping the pressures in the chambers  $C_{ae}$ ,  $C_a$ , and  $C_e$  constant during the process. This gives rise to the external work

$$-(M_a v_a p_a + M_e v_e p_e - v p) - \partial(M_a v_a p_a + M_e v_e p_e - v p).$$

(d) Compress the mixture until it has assumed its original volume. The external work done is

$$-p \cdot \partial v,$$

which completes the cycle.

On equating to zero the external work done, the equation

$$v \left( \frac{\partial p}{\partial v} \right)_{T, M_a, M_e} - M_a v_a \left( \frac{\partial p_a}{\partial v} \right)_{T, M_a, M_e} - M_e v_e \left( \frac{\partial p_e}{\partial v} \right)_{T, M_a, M_e} = 0 \quad (1)$$

is obtained.

If the mixture contains the additional constituent  $c$ , the apparatus will involve an additional chamber separated from the chamber  $C_{ae}$  by a membrane permeable to the molecules composed of atoms  $c$ . The equation then contains the additional term

$$-M_c v_c \left( \frac{\partial p_c}{\partial v} \right)_{T, M_a, M_e, M_c},$$

and so on. It will also be recognized that similar equations may be obtained corresponding to each membrane being permeable to any given kind of molecule. These various equations evidently hold independently of the state of the mixture.

A set of equations similar to equation (1) may be obtained in each of which the mass of one of the constituents is the independent variable instead of the volume, by means of an isothermal cycle differing somewhat from the one just given. Thus let us:—

(a) Permit the transfer of a mass  $\partial M_a$  of the constituent  $a$  from the mixture into the chamber  $C_a$ , keeping the volume  $v$  of the mixture constant during the process. The external work done is

$$-p_a v_a \cdot \partial M_a.$$

(b) Transfer the mixture from the chamber  $C_{ae}$  into the chambers  $C_a$  and  $C_e$ , keeping the pressures in the chambers constant during the process. The external work done is

$$M_a v_a p_a + M_e v_e p_e - v p + \partial(M_a v_a p_a + M_e v_e p_e - v p).$$

(c) Change the volumes of the chambers  $C_a$  and  $C_e$  till the pressures of the substances they contain correspond to equilibrium with the mixture when it was completely contained in the chamber  $C_{ae}$ . The external work

$$-(M_a p_a \cdot \partial v_a + M_e p_e \cdot \partial v_e)$$

is obtained. The sign of this is negative because we are on the return path of the cycle.

(d) Return the substances in the chambers  $C_a$  and  $C_e$  to the chamber  $C_{ae}$ , keeping the pressures constant during the process. The external work done is

$$-(M_a v_a p_a + M_e v_e p_e - v p),$$

which completes the cycle. On equating the external work done to zero, we obtain \*

$$v \left( \frac{\partial p_e}{\partial M_a} \right)_{v, T, M_e} - M_a v_a \left( \frac{\partial p_a}{\partial M_a} \right)_{v, T, M_e} - M_e v_e \left( \frac{\partial p_e}{\partial M_a} \right)_{v, T, M_e} = 0. \quad (2)$$

\* It will be helpful if it is pointed out that we may first carry out the processes (a) and (b) of the cycle, then begin again with the mixture in the chamber  $C_{ae}$  and carry out the processes (d) and (e) in the reverse manner, beginning with (d) and equating the external work done in the two cases. Similar remarks apply to the previous cycle.

A similar equation holds referring to the constituent  $e$ , which may be obtained from equation (2) on substituting  $M_e$  for  $M_a$ . If the mixture contains the additional constituent  $c$ , equation (2) contains the additional term

$$-\left(\frac{\partial p_c}{\partial M_a}\right)_{v, T, M_e, M_c},$$

and an additional equation will hold in which the independent variable is  $M_c$ , and so on. These various equations apply to a mixture in any state.

One of the most important applications of the foregoing equations is in connexion with the equilibrium of a reacting gaseous mixture. Additional equations hold under these conditions. The pressure  $p$  of the mixture is given by

$$p = RT \Sigma C, \quad . . . . . (3)$$

where  $\Sigma C$  denotes the sum of the concentrations of the various molecules. Similarly, if  $p_1, p_2, \dots$  denote the partial pressures of the various molecules which will be denoted by 1, 2, ..., and  $C_1, C_2, \dots$  denote their concentrations, we have

$$\left. \begin{aligned} p_1 &= RT C_1, \\ p_2 &= RT C_2, \\ . & . . . . \end{aligned} \right\} . . . . . (4)$$

The masses in gram atoms of the constituents  $a, e, \dots$  are given by

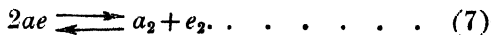
$$\left. \begin{aligned} v \Sigma n_a C_a &= M_a, \\ v \Sigma n_e C_e &= M_e, \\ . & . . . . \end{aligned} \right\} . . . . . (5)$$

where  $C_a$  denotes the concentration in gram molecules of the molecules which contain  $n_a$  gram atoms  $a$ ,  $C_e$ , the concentration of the molecules containing  $n_e$  gram atoms  $e$  etc. Lastly, we have the mass-action equation, which may be written in the generalized form

$$KC_1 C_2 \dots = C_4 C_5 \dots, \quad . . . . . (6)$$

where  $K$  denotes the constant of mass action. The foregoing equations are the complete differential equations determining the equilibrium of a reacting gaseous mixture.

Let us apply them, for example, to a mixture reacting according to the equation



Equation (3) then gives

$$p = RT(C_{ae} + C_{a_2} + C_{e_2}), \quad . \quad . \quad . \quad . \quad . \quad (8)$$

where  $C_{ae}$ ,  $C_{a_2}$ , and  $C_{e_2}$  denote the concentrations of the molecules  $ae$ ,  $a_2$ , and  $e_2$  respectively. Equations (4) and (5) give

$$\left. \begin{aligned} p_{ae} &= RT C_{ae}, \\ p_{a_2} &= RT C_{a_2}, \\ p_{e_2} &= RT C_{e_2}, \end{aligned} \right\} \quad . \quad . \quad . \quad . \quad . \quad (9)$$

$$\left. \begin{aligned} v(C_{ae} + 2C_{a_2}) &= M_a, \\ v(C_{ae} + 2C_{e_2}) &= M_e, \end{aligned} \right\} \quad . \quad . \quad . \quad . \quad . \quad (10)$$

and equation (6)

$$K C_{ae}^2 = C_{a_2} C_{e_2}. \quad . \quad . \quad . \quad . \quad . \quad (11)$$

Equation (1) may now be written

$$v \frac{\partial p}{\partial v} - M_{a_2} v_{a_2} \frac{\partial p_{a_2}}{\partial v} - M_{e_2} v_{e_2} \frac{\partial p_{e_2}}{\partial v} = 0, \quad . \quad . \quad (12)$$

where  $M_{a_2}$  and  $M_{e_2}$  denote the number of gram molecules of molecules  $a_2$  and  $e_2$ , and  $v_{a_2}$  and  $v_{e_2}$  the volumes per gram molecule, respectively, into which the mixture can be separated. Since the molecules  $a_2$  and  $e_2$  do not dissociate when by themselves, we shall also have the gas equations

$$\left. \begin{aligned} v_{a_2} p_{a_2} &= RT, \\ v_{e_2} p_{e_2} &= RT. \end{aligned} \right\} \quad . \quad . \quad . \quad . \quad . \quad (13)$$

Now, from equations (8), (9), (10), (12), and (13) expressions can be obtained for the concentrations  $C_{ae}$ ,  $C_{a_2}$ , and  $C_{e_2}$  in terms of  $T$ ,  $v$ ,  $M_a$ , and  $M_e$ , and an arbitrary function of  $T$ ,  $M_a$ , and  $M_e$ , where  $2M_{a_2} = M_a$  and  $2M_{e_2} = M_e$ . If these are substituted in equation (11), it expresses the functional nature of  $K$  with respect to  $v$ .

It should be mentioned here that in a previous paper \* the writer showed that  $K$  is in general a function of  $T$ ,  $v$ , and the masses of the constituents instead of a function of  $T$

\* Phil. Mag. v. p. 263 (1928).

only, as has usually been accepted, but that in special cases, as we shall see presently, this may be the case. The equations obtained in this paper enable us to determine completely the functional nature of  $K$  \*.

If equation (2) is applied to the reaction (7), it becomes

$$v \frac{\partial p}{\partial M_{a_2}} - M_{a_2} v_{a_2} \frac{\partial p_{a_2}}{\partial M_{a_2}} - M_{e_2} v_{e_2} \frac{\partial p_{e_2}}{\partial M_{a_2}} = 0. \quad (14)$$

Expressions for the molecular concentrations may now be obtained from equations (8), (9), (10), (13), and (14) in terms of  $T$ ,  $v$ ,  $M_a$ , and  $M_e$ , and an arbitrary function of  $T$ ,  $v$ , and  $M_e$ , remembering that  $2M_{a_2} = M_a$  and  $2M_{e_2} = M_e$ . If these expressions are substituted in equation (11), it expresses the functional nature of  $K$  with respect to  $M_a$ . Similarly, the functional nature of  $K$  with respect to  $M_e$  may be obtained.

Let us solve equations (13), (12), (11), (10), (9), and (8) for the special case corresponding to  $M_a = M_e$ , or  $M_{a_2} = M_{e_2}$ , in which also  $p_{a_2} = p_{e_2}$  and  $C_{a_2} = C_{e_2}$ . Equation (8) may then be written  $p = RT M_a / v$  by means of equations (10). From this equation and equations (13), (12), and (9) we then have

$$\frac{1}{v} + \frac{1}{C_{a_2}} \frac{\partial C_{a_2}}{\partial v} = 0.$$

The solution of this equation is

$$C_{a_2} = \frac{\phi(T, M_a, M_e)}{v}, \quad \dots \quad (15)$$

where  $\phi$  is an arbitrary function of  $T$ ,  $M_a$ , and  $M_e$ . From this equation and equations (11) and (10) we then have

$$K = \frac{\phi^2}{(M_a - 2\phi)^2} \cdot \dots \quad (16)$$

Thus in this particular case  $K$  is not a function of  $v$ , which agrees with the experiments that have been carried out on the dissociation of hydriodic acid. The case corresponding to  $M_a$  not being equal to  $M_e$  is more complicated.

\* Provided the perfect gas equation has the form  $pv = MRT$ . Thermodynamics has something to state in this connexion, which will be pointed out in a subsequent paper. It need not concern us for the present.



From equations (8) and (10) we have

$$p = RT \frac{(M_a + M_e)}{2v}, \quad . \quad . \quad . \quad (17)$$

$$C_{a_2} - C_{e_2} = \frac{M_a - M_e}{2v} \quad . \quad . \quad . \quad (18)$$

By means of equations (17), (13), and (9) we may write equation (12)

$$\frac{M_a + M_e}{2v} + \frac{M_{a_2}}{C_{a_2}} \frac{\partial C_{a_2}}{\partial v} + \frac{M_{e_2}}{C_{e_2}} \frac{\partial C_{e_2}}{\partial v} = 0. \quad . \quad . \quad (19)$$

Let us write  $C_{a_2} = y/v$  and  $C_{e_2} = z/v$  in this equation and equation (18), and they become

$$2(y + z) = M_a - M_e, \quad . \quad . \quad . \quad (20)$$

$$\frac{M_{a_2}}{y} \frac{\partial y}{\partial v} + \frac{M_{e_2}}{z} \frac{\partial z}{\partial v} = 0. \quad . \quad . \quad . \quad (21)$$

It is evident from these equations that  $y$  and  $z$  are functions of  $T$ ,  $M_a$ , and  $M_e$  only. It can now easily be shown that

$$K(M_a - 2y)^2 = yz, \quad . \quad . \quad . \quad (22)$$

and thus  $K$  is not a function of  $v$ . This agrees with the experiments on the equilibrium of reacting mixtures of  $H_2$  and  $I_2$  in various proportions.

Let us next consider a gaseous reaction proceeding according to the equation



According to equations (3), (4), (5), and (6) we then have

$$p = RT(C_{ae} + C_a + C_e), \quad . \quad . \quad . \quad (24)$$

$$\left. \begin{aligned} p_{ae} &= RT C_{ae}, \\ p_a &= RT C_a, \\ p_e &= RT C_e, \end{aligned} \right\} \quad . \quad . \quad . \quad (25)$$

$$\left. \begin{aligned} v(C_{ae} + C_a) &= M_a, \\ v(C_{ae} + C_e) &= M_e, \end{aligned} \right\} \quad . \quad . \quad . \quad (26)$$

$$K C_{ae} = C_a C_e. \quad . \quad . \quad . \quad (27)$$

Since the molecules  $a$  and  $e$  when by themselves do not dissociate, we also have the gas equations

$$\left. \begin{aligned} r_a p_a &= RT, \\ v_e p_e &= RT. \end{aligned} \right\} \cdot \cdot \cdot \cdot \cdot \cdot (28)$$

Let us consider the special case corresponding to  $M_e = M_a$ , in which case also  $p_a = p_e$  and  $C_a = C_e$ . Equation (24) may then be written

$$p = RT \left( \frac{M_a}{v} + C_a \right).$$

From this equation and equations (1), (28), and (25) it can then be deduced that

$$- \frac{RT M_a}{v} + RT v \frac{\partial C_a}{\partial v} - \frac{2RT M_a}{C_a} \frac{\partial C_a}{\partial v} = 0,$$

or

$$\frac{\partial C_a}{\partial v} = \frac{M_a}{v} \left( \frac{C_a}{C_a v - 2M_a} \right) \cdot \cdot \cdot \cdot \cdot (29)$$

Instead of solving this equation we may proceed in a somewhat different way, which is shorter. Let us write equation (27) in the form

$$K \left( \frac{M_a}{v} - C_a \right) = C_a^2 \cdot \cdot \cdot \cdot \cdot (30)$$

by means of equation (26), and differentiate it with respect to  $v$ , supposing  $K$  not a function of  $v$ , which gives

$$-K \left( \frac{M_a}{v^2} + \frac{\partial C_a}{\partial v} \right) = 2C_a \frac{\partial C_a}{\partial v}.$$

On eliminating  $\frac{\partial C_a}{\partial v}$  and  $K$  from this equation by means of equations (29) and (30) the equation identically vanishes. Thus the supposition made is true, or  $K$  is not a function of  $v$ . This is borne out by experiments on the dissociation of nitrogen tetroxide ( $N_2O_4$ ).

Further cases may be found for which  $K$  is not a function of  $v$ . Let us consider a reaction proceeding according to the equation



The equations corresponding to equations (3) and (4) are

$$p = RT(C_{ae_2} + C_{ae} + C_{e_2}), \quad . \quad . \quad . \quad (32)$$

$$\left. \begin{aligned} p_{ae_2} &= RT C_{ae_2}, \\ p_{ae} &= RT C_{ae}, \\ p_{e_2} &= RT C_{e_2}, \end{aligned} \right\} \quad . \quad . \quad . \quad . \quad . \quad (33)$$

and the equations corresponding to equations (5), (6), and (1) are

$$\left. \begin{aligned} C_{ae_2} + C_{ae} &= M_a/v, \\ 2C_{ae_2} + C_{ae} + 2C_{e_2} &= M_e/v, \end{aligned} \right\} \quad . \quad . \quad . \quad (34)$$

$$K C_{ae_2}^2 = C_{ae} C_{e_2}, \quad . \quad . \quad . \quad . \quad (35)$$

$$v \frac{\partial p}{\partial v} - M_{ae} v_{ae} \frac{\partial p_a}{\partial v} - M_{e_2} v_{e_2} \frac{\partial p_{e_2}}{\partial v} = 0. \quad . \quad . \quad (36)$$

Since the molecules  $ae$  and  $e_2$  are supposed to remain unchanged when by themselves, we also have

$$\left. \begin{aligned} p_{ae} v_{ae} &= RT, \\ p_{e_2} v_{e_2} &= RT. \end{aligned} \right\} \quad . \quad . \quad . \quad . \quad (37)$$

Let us consider the special case corresponding to  $2M_a = M_e$ . From equations (34) we then have

$$C_{ae} = 2C_{e_2}, \quad . \quad . \quad . \quad . \quad (38)$$

and from this equation and equations (34), (32), (33), and (35) we have

$$p = RT \left( \frac{M_e}{2v} + C_{e_2} \right), \quad . \quad . \quad . \quad (39)$$

$$\left. \begin{aligned} p_{ae} &= RT 2C_{e_2}, \\ p_{e_2} &= RT C_{e_2}, \end{aligned} \right\} \quad . \quad . \quad . \quad . \quad (40)$$

$$K C_{ae_2}^2 = 4C_{e_2}^3, \quad . \quad . \quad . \quad . \quad (41)$$

taking into account that

$$\left. \begin{aligned} M_{ae} &= M_a = M_e/2, \\ 2M_{e_2} + M_{ae} &= M_e. \end{aligned} \right\} \quad . \quad . \quad . \quad (42)$$

Equation (36) may now be written

$$RT \left\{ -\frac{M_e}{2v} + v \frac{\partial C_{e_2}}{\partial v} \right\} - \frac{3}{4} \frac{RT M_e}{C_{e_2}} \frac{\partial C_{e_2}}{\partial v} = 0,$$

or

$$\frac{\partial C_{e_2}}{\partial v} = \frac{M_e}{v} \frac{2C_{e_2}}{4C_{e_2}v - 3M_e}, \quad \dots \quad (43)$$

by means of equations (39), (40), (41), and (42).

From equations (34), (38), and (42) we have

$$C_{ae_2} = \frac{M_e}{2v} - 2C_{e_2}. \quad \dots \quad (44)$$

On differentiating equation (41) with respect to  $v$ , supposing  $K$  not a function of  $v$ , it may be written

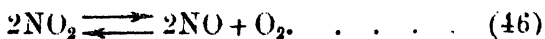
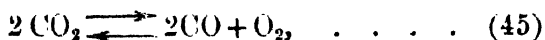
$$-2KC_{ae_2} \left\{ \frac{M_e}{2v^2} + \frac{2\partial C_{e_2}}{\partial v} \right\} = 12C_{e_2}^2 \frac{\partial C_{e_2}}{\partial v}$$

by means of equation (44). It reduces to

$$-\frac{KC_{ae_2}M_e}{v^2} \left\{ \frac{12C_{e_2}v - 3M_e}{4C_{e_2}v - 3M_e} \right\} = \frac{24M_e}{v} \frac{C_{e_2}}{4C_{e_2}v - 3M_e}$$

by means of equation (43). Eliminating  $C_{e_2}$  by means of equation (41), and then  $C_{ae_2}$  by means of equation (44), the equation reduces to zero.

Hence the supposition made is true, or  $K$  is not a function of  $v$ . This result will apply to the well-known reactions



The various results obtained fall into line with the general result obtained in a previous paper, that the constant of mass action is in general a function of  $T$ ,  $v$ , and the masses of the constituents, but that in special cases it may be a function of the temperature only. It is also evident that the functional nature of the constant of mass action is in all cases determined by equations of the type given. The subject admits of considerable further development, which will be carried out in subsequent papers.

LXIV. *On Approximate Theories of Diffusion Phenomena.*  
*By S. CHAPMAN, M.A., D.Sc., F.R.S.\**

1. **T**HE object of this note is to draw attention to the erroneous character of an argument often used in approximate theories of diffusion phenomena. It is the basis of Meyer's theory of diffusion<sup>(1)</sup>, which is now about fifty years old, and is generally reproduced, with modifications not affecting the error here described, in modern text-books on the kinetic theory of gases. The argument has recently been used in an attempt to explain the Soret phenomenon in liquids<sup>(2)</sup>.

2. In some cases it leads to results which are qualitatively correct in certain respects, but other no less valid applications of it can be found in which it predicts phenomena that either do not occur (§ 7), or are inconsistent with the initial hypotheses (§ 8), or which, though of an observed kind, are deduced with the wrong sign (§ 9). It is therefore unsafe to use it in searching for new phenomena, and scarcely satisfactory to make it the basis of a theory, even in cases where it gives approximately correct results—better no simple theory than one based on unsafe or erroneous arguments.

3. Diffusion phenomena can be most simply considered with reference either to steady diffusive flow, in which all the properties of the system at every point remain constant: or to the maintenance of a steady state in which no diffusion occurs because two separate causes each tending to produce it are balanced against one another. An instance of the latter is the equilibrium of a mixed fluid subject to gravity; the heavier component is in excess in the lower strata, but its preponderance is limited by the tendency of diffusion towards a uniform mixture. Likewise, if there is a gradient of temperature along a tube containing a mixed gas, one set of molecules (usually the lighter) will diffuse towards the hotter regions, until a steady state is attained in which there is a gradient of concentration sufficient to neutralize further thermal diffusion<sup>(3)</sup>. A similar process occurs in mixed liquids, and is known as the Soret effect.

4. The argument will first be considered in relation to steady states of the second kind. Let there be two sorts of

\* Communicated by the Author.

molecules (1, 2), of masses  $m_1$ ,  $m_2$ , numbers per unit volume  $n_1$ ,  $n_2$ , mean speeds  $C_1$ ,  $C_2$ . We write

$$n = n_1 + n_2, \quad c_1 = n_1/n, \quad c_2 = n_2/n, \quad . \quad . \quad . \quad (1)$$

so that

$$c_1 + c_2 = 1. \quad . \quad . \quad . \quad . \quad . \quad (2)$$

Pressure and absolute temperature will be denoted by  $p$  and  $T$ ; then

$$m_1 C_1^2 = m_2 C_2^2 = aT, \quad . \quad . \quad . \quad . \quad (3)$$

where  $a$  is a universal constant.

5. Suppose there is a temperature gradient along the direction of  $z$ , the pressure being uniform. The argument states that the number of molecules (1) which cross any plane of constant  $z$ , per unit area per unit time, in the positive direction, is  $k(n_1 C_1)_{z-\lambda_1}$ , where  $k$  is a numerical constant, while the suffix implies that the value of  $n_1 C_1$  is that at the plane  $z - \lambda_1$ , at a distance  $\lambda_1$  on the negative side of the plane  $z$ ;  $\lambda_1$  is a multiple of the mean free path of the molecules (1), by a factor which, like  $k$ , is independent of the nature of the gas and of the variables of state. Similarly, the rate of flow in the opposite direction is  $k(n_1 C_1)_{z+\lambda_1}$ . The gas being in a steady state of equilibrium, there being no resultant diffusion, these two quantities must be equal, and therefore  $n_1 C_1$  is independent of  $z$ . Hence, by (3),  $n_1 T^{\frac{1}{2}}$  is constant along the tube <sup>(2)</sup>.

This simple and general argument applies to either a liquid or a gas, and to each kind of molecule in a mixture. Hence it indicates that for the molecules (2) likewise,  $n_2 T^{\frac{1}{2}}$  is constant. Consequently  $n_1 T^{\frac{1}{2}} : n_2 T^{\frac{1}{2}}$  or  $n_1 : n_2$  is independent of  $z$ , so that there can be no gradient of concentration. This is contrary to the facts.

6. The argument must therefore be wrong in regard to one or both of the constituents; the experiments of C. C. Tanner <sup>(4)</sup> on the Soret effect have shown <sup>(2)</sup> that in the case of an aqueous solution of KCl (taken as substance 1)  $n_1 T^{\frac{1}{2}}$  is nearly constant over the temperature range of the observations; but the existence of a concentration gradient shows that  $n_2 T^{\frac{1}{2}}$  cannot also be constant. The agreement in the case of KCl can only be regarded as accidental, and indeed other substances fail to show it.

Since this method of attempting to explain the Soret effect is unsound as well as unsuccessful, it is to no purpose to attribute the failure of constancy of  $n_1 T^{\frac{1}{2}}$  in other cases

to ionization; particularly since in gases a concentration gradient is set up by temperature differences in cases where there is certainly no appreciable ionization (*cf.* the experiments of T. L. Ibbs<sup>(b)</sup> on thermal diffusion in mixtures of argon and helium, and other gases).

7. The argument of § 5 is equally applicable to a *simple* gas at rest, in which a temperature gradient is maintained. The result is the same, that  $nT^{\frac{1}{2}}$  is constant, whereas in fact, since the pressure is uniform,  $nT$  is constant, *i. e.*  $nT^{\frac{1}{2}} \propto T^{-\frac{1}{2}}$ .

8. Analogous discrepancies with fact occur when the argument is used in relation to states of steady diffusion. The ordinary case (I.) is that in which  $p$  and  $T$  are uniform, while  $c_1, c_2$  vary. Other important cases are those in which  $c_1$  and  $c_2$  are uniform, while (II.)  $T$  varies and  $p$  is uniform or (III.)  $p$  varies and  $T$  is uniform; case II. is that of thermal diffusion, case III. that of pressure diffusion.

In all three cases we will suppose that there is no resultant flow of molecules across any stationary plane. Let  $\nu_1, \nu_1'$  be the numbers of molecules (1) flowing per unit area per unit time across such a plane, in the positive and negative directions respectively; and let  $\nu_2, \nu_2'$  have similar significance for the molecules (2). Then the stated condition implies

$$\nu_1 + \nu_2 = \nu_1' + \nu_2' \quad \text{or} \quad \nu_1 - \nu_1' = -(\nu_2 - \nu_2'); \quad . \quad (4)$$

*i. e.*, the net rates of flow for the two kinds are equal and opposite. The velocity of diffusion,  $w_{12}$ , and the coefficient of diffusion  $D_{12}$ , are defined by

$$\begin{aligned} nw_{12} = \nu_1 - \nu_1' &= -nD_{12} \frac{dc_1}{dz}, & nw_{12} &= -(\nu_2 - \nu_2') \\ &= -nD_{12} \frac{dc_2}{dz}, & . \quad . \quad . \quad (5) \end{aligned}$$

which are consistent since, by (2),

$$\frac{dc_1}{dz} = -\frac{dc_2}{dz} \quad . \quad . \quad . \quad . \quad . \quad (6)$$

It may be noted that, if the molecular masses are unequal, there is a resultant flow of *mass* across the plane  $z$ . This is given by

$$m_1(\nu_1 - \nu_1') + m_2(\nu_2 - \nu_2') = (m_1 - m_2)(\nu_1 - \nu_1'),$$

by (4).

The "mean mass-velocity"  $w$  is defined by

$$w = (m_1 - m_2)(\nu_1 - \nu_1')/n \quad . \quad . \quad . \quad (7)$$

9. In Meyer's theory of diffusion due to a concentration gradient (case I.) it is assumed in effect that for each constituent the molecular velocities are distributed about this mean velocity  $w$  approximately in the Maxwellian manner; this is true, but the small deviation, which is neglected, is the essence of the phenomenon, and vital to any satisfactory theory of it. Further, Meyer assumed that the rate of flow of molecules (1) across a plane moving with the velocity  $w$  was

$$k(n_1C_1)_{z-\lambda_1} - k(n_1C_1)_{z+\lambda_1}, \quad \text{or} \quad -2k\lambda_1 \frac{d(n_1C_1)}{dz} \quad (8)$$

much as in § 5. To get  $v_1 - v_1'$ , the rate of net flow of molecules (1) across a stationary plane, we must add  $n_1w$ , so that

$$v_1 - v_1' = n_1w - 2k\lambda_1C_1 \frac{dn_1}{dz}, \quad \dots \quad (9)$$

since  $T$  and therefore  $C_1, C_2$  (cf. 3) are constant in case I. Likewise

$$v_2 - v_2' = n_2w - 2k\lambda_2C_2 \frac{dn_2}{dz} = n_2w + 2k\lambda_2C_2 \frac{dn_1}{dz} \quad (10)$$

if, as in a perfect gas at uniform pressure,  $n_1 + n_2$  is constant.

The usual procedure is to eliminate  $w$  from (9), (10) by means of (4). This gives

$$v_1 - v_1' = -(v_2 - v_2') = -(2k/n)(n_2\lambda_1C_1 + n_1\lambda_2C_2) \frac{dn_1}{dz}, \quad \dots \quad (11)$$

or, comparing with (5), and remembering that  $n$  is constant, so that  $ndc_1/dz = dn_1/dz$ ,

$$D_{12} = (2k/n)(n_2\lambda_1C_1 + n_1\lambda_2C_2). \quad \dots \quad (12)$$

Different authors have given different estimates of the constant  $k$  and of the appropriate mean free paths  $\lambda_1, \lambda_2$ , in some cases taking into account the persistence of velocities after collision<sup>(6)</sup>; this step undoubtedly produces a better value of  $D_{12}$ , but it should be noted that the formula (12) is deduced from a set of equations that are inconsistent with one another, so that however refined the methods of calculation of  $\lambda_1$  and  $\lambda_2$  may be, the result must be unsatisfactory. The inconsistency appears on deducing  $w$  from (4), (9), (10), giving

$$w = \frac{2k}{n_1 - n_2} (\lambda_1C_1 - \lambda_2C_2) \frac{dn_1}{dz}, \quad \dots \quad (13)$$

which is incompatible with (7). The disagreement is



particularly obvious when  $m_1 = m_2$ , for then  $w = 0$  (cf. 7), and  $C_1 = C_2$  (cf. 3); (9) and (10) are compatible with (4) only if  $\lambda_1 = \lambda_2$ , which is untrue, on any reasonable definitions of the  $\lambda$ 's, if the molecular diameters are unequal.

Gross<sup>(7)</sup> criticized Meyer's deduction of (12) on different grounds, and proposed the alternative formula  $D_{12} = k(\lambda_1 C_1 + \lambda_2 C_2)$ , but without any proper justification; this formula, like (12), is known to be incorrect.

10. Similar contradictions with the initial hypotheses, and with fact, arise when the same method of argument is applied, as one is tempted to do, to explain the steady diffusive flow in cases II. and III. (§ 8), which can be treated together. In (8)  $C_1$  is no longer independent of  $z$ ; writing  $n_1 = c_1 n$ , where  $c_1$  but not  $n$  is independent of  $z$ , we get, analogous to (9), (10),

$$\nu_1 - \nu_1' = n_1 w - 2k\lambda_1 C_1 \frac{dnC_1}{dz}, \quad . \quad . \quad . \quad (14)$$

$$\nu_2 - \nu_2' = n_2 w - 2k\lambda_2 C_2 \frac{dnC_2}{dz} \quad . \quad . \quad . \quad (15)$$

In a perfect gas  $n \propto p/T$ , so that, also using (3), we have

$$\nu_1 - \nu_1' = n_1 w - k'(\lambda_1 c_1 / m_1^{\frac{1}{2}}) \frac{d(pT^{-\frac{1}{2}})}{dz}, \quad . \quad . \quad (16)$$

$$\nu_2 - \nu_2' = n_2 w - k'(\lambda_2 c_2 / m_2^{\frac{1}{2}}) \frac{d(pT^{-\frac{1}{2}})}{dz}, \quad . \quad . \quad (17)$$

where  $k'$  is another numerical constant independent of the nature and state of the constituents. Case II. corresponds to  $p$  constant,  $T$  variable, and *vice versa* for case III.

As in § 9, (16) and (17) are incompatible with (4) and (7). Their erroneous character is specially obvious when  $m_1 = m_2$ , with its corollary  $w = 0$ ; for then  $\nu_1 - \nu_1'$ ,  $\nu_2 - \nu_2'$  are both of the same sign, and proportional to  $\lambda_1 c_2$  and  $\lambda_2 c_2$  respectively, so that for both reasons they cannot satisfy (4). As applied to case II. they imply that both sets of molecules should diffuse in the same direction; either (16) or (17) must be wrong in sign, and therefore in error by more than its whole amount. As regards case III., it is known that when  $m_1 = m_2$ ,  $\nu_1 - \nu_1'$  and  $\nu_2 - \nu_2'$  vanish; this again is not in accordance with (16) and (17). Hence this method of argument cannot be applied to explain either thermal diffusion or the simpler process of diffusion due to a pressure gradient.

11. The correct theory of these various diffusion phenomena depends on the determination of the velocity distribution function, which in non-uniform states deviates slightly from the Maxwellian form. In case II., for example, the function, for the velocity  $u_1, v_1, w_1$ , of a typical molecule (1), relative to the mean numerical velocity of all the molecules (without regard to mass) at any point, is easily shown to be

$$f_1 \left\{ 1 + \left( u_1 \frac{\partial T}{\partial x} + v_1 \frac{\partial T}{\partial y} + w_1 \frac{\partial T}{\partial z} \right) \phi_1 (u_1^2 + v_1^2 + w_1^2) \right\} \quad . . . . . (18)$$

to a first approximation, where  $f_1$  is the Maxwellian function for the constituent (1), while  $\phi_1$  is a function depending on the nature and proportions of the two gases; (18) reduces to  $f_1$  when  $T$  is uniform. The velocity of diffusion in the  $z$  direction is the mean value of  $w_1$ , i. e.,

$$w_{12} = \frac{dT}{dz} \int \int \int w_1^2 f_1 \phi_1 du_1 dv_1 dw_1; \quad . . . (19)$$

there is a similar expression for the mean value of  $w_2$ , which must equal  $-w_{12}$ . This is one of the conditions which  $\phi_1$  and  $\phi_2$  have to satisfy. These considerations establish the expectation that a thermal gradient in an otherwise uniform gas will set up a diffusive flow, though the actual determination of  $\phi_1, \phi_2$  and  $w_{12}$  is a very difficult matter. In spite of many attempts I have failed to find any simple arguments on which to base an easy approximate theory of thermal diffusion.

12. In conclusion, it may be noted that steady diffusive flow in a cylindrical tube requires that  $w_{12}$  shall be constant along the tube. In cases I., II., III. respectively this implies the constancy of

$$D_{12} \frac{dc_1}{dz}, \quad D_T \frac{dT}{dz}, \quad D_p \frac{dp}{dz},$$

where  $D_T, D_p$  are the coefficients of thermal diffusion and pressure diffusion. In general, in the given circumstances, the coefficients will vary along the tube in a definite manner,  $D_{12}$  depending on  $c_1$  and  $c_2$ ,  $D_T$  on  $T$ , and  $D_p$  on  $p$ . Hence the gradients of  $c_1, p$ , and  $T$  cannot be arbitrary. In case I. the concentration gradient will vary along the tube so as to render  $D_{12} dc_1/dz$  constant; cases II. and III. are possible

only if  $p$  and  $T$  are imposed so as to satisfy the condition of continuity—otherwise this condition will be secured, in a state of steady flow, by an accompanying variation of  $c_1$  and  $c_2$  along the tube.

### References.

- (1) Meyer's 'Kinetic Theory of Gases' (English translation), p. 255.
- (2) Trans. Faraday Soc. xxiii. p. 314 (1927).
- (3) D. Enskog, *Phys. Zeit.* xii. p. 538 (1911); *Ann. d. Phys.* xxxviii. p. 742 (1912); Dissertation, Uppsala, 1917; *Arkiv f. Nat. Astro. o. Fysik*, xvi. (1921). S. Chapman, Proc. Roy. Soc. A, xciii. p. 1 (1916); Phil. Trans. A, ccxvii. p. 157 (1917). S. Chapman and F. W. Dootson, Phil. Mag. xxxiii. p. 268 (1917).
- (4) C. C. Tauner, Trans. Faraday Soc. xxiii. p. 91 (1927).
- (5) T. L. Ibbs, Proc. Roy. Soc. xcix. p. 385 (1921); *ib.* cvii. p. 470 (1925); Proc. Phys. Soc. xxxix. p. 227 (1927). Cf. also Elliott and Masson, Proc. Roy. Soc. A. cviii. p. 378 (1925).
- (6) J. P. Kuenen, *Comm. Phys. Lab. Leiden*, Jan. 1913, Suppls. 28 & 33. Also J. H. Jeans, 'Dynamical Theory of Gases,' ch. xiii.
- (7) Gross, *Annalen der Physik*, xl. p. 424 (1890).

### LXV. A Note on the Problem of the "Mass" of a Moving Electron. By T. J. P.A. BROMWICH\*.

AS far as I am aware, the only *direct* evidence of the Lorentz formula for the "mass" of an electron (moving with velocity  $v$ ), namely

$$m = m_0 / \sqrt{1 - \beta^2} \quad \text{if } \beta = v/c,$$

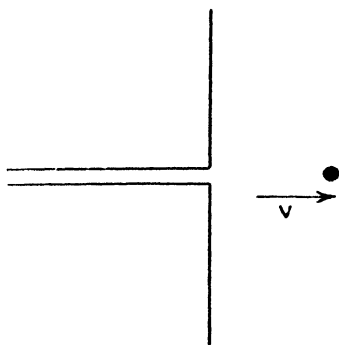
where  $c$  is the velocity of radiation, is derived from Bucherer's experiments (and similar experiments conducted later). The mathematical treatment of Lorentz consists in replacing the *moving* particle by a *fixed* particle; this led Lorentz to the familiar Larmor-Lorentz transformation, afterwards used by Einstein as the basis of his theory of Relativity.

Now, in the actual experiment the particles of radium pass through a narrow slit between the two faces of a condenser. We can make the problem a little more manageable by treating the condenser as composed of two large conducting blocks with plane faces, at different potentials—as in fig. 1.

\* Communicated by the Author.

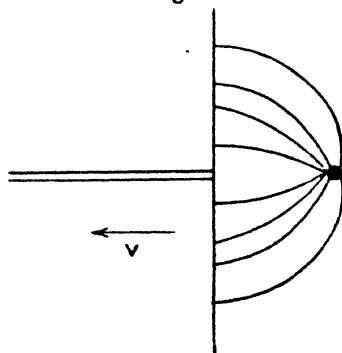
If we apply the Lorentz transformation to this diagram (ignoring the slit), we obtain a similar figure (fig. 2) in which the condenser moves and the particle is at rest.

Fig. 1.



Here the lines of force (although complicated in actual fact) cannot differ very greatly from those in the corresponding *electrostatic* problem. On account of the potential difference of

Fig. 2.



the two plates of the condenser, it is evident that the lines *cannot* be symmetrical about the horizontal plane (although the principal deviation from symmetry is due to the fact that the condenser is on the *left* of the particle).

Now, Lorentz assumes that the particle is so far from the condenser that all deviations from symmetry can be ignored: otherwise the formulæ become hopelessly complicated.

It would therefore seem that the Lorentz formula for  $m/m_0$  can be applied safely only when the distance of the electron from the condenser is large compared with the radius of the electron. A consideration of the approximate dimensions shows that the deviations in Bucherer's experiments can be

calculated by Lorentz's method with sufficient accuracy : but that does not justify the argument that  $\beta$  can never be equal to 1.

In the case  $v=c$  ( $\beta=1$ ), two simple problems can be worked out by Heaviside's methods ; these seem sufficiently near to the experimental results to be worth noticing here.

First suppose that  $v=c$  ( $\beta=1$ ) and that the particle is moving parallel to a conducting plate at zero potential—this corresponds to the assumption that the electron is between the two plates, while the upper plate is far enough away to be ignored.

The problem is then the same as the electrostatic problem of a circular cylinder above a plane at zero potential ; thus the lines of electric force are arcs of coaxial circles, and these are cut orthogonally by the lines of magnetic force.

Secondly, suppose that the particle is moving with speed  $v=c$  at right angles to a plane at zero potential. This corresponds to the assumption that the whole condenser can be replaced by one plane ; this problem (for a point-charge) is actually worked out in vol. i. of Heaviside's 'Electromagnetic Theory' (p. 62). It is then easy to verify that all the conditions of the problem are satisfied by assuming the lines of force to be circular—with a centre at the point representing the slit in the condenser.

The transverse electric force is found to be equal to \*

$$Q/(ar \sin \theta),$$

using spherical polar coordinates (so that  $r=0$  gives the slit and  $\theta=\pi/2$  gives the plane conductor). The resultant force on the electron is equal to

$$Q^2/avt$$

(where  $t$  is the time since the centre of the electron left the slit).

Also the energy is equal to †

$$\frac{Q^2}{a} \left\{ \log \left( \frac{vt}{a} \right) + 1 \right\}.$$

[Since the above note was written out for the press, news of the death of H. A. Lorentz has reached me ; I had hoped to submit these ideas for his comments, but it is now too late to do more than record a personal feeling of regret.—T. J. I'a. B.]

13th Feb., 1928.

\* A slight modification is necessary at points *inside* the electron.

† It may be worth while to note that (under ordinary experimental conditions) the value of the bracket varies between 1 and 30, roughly.

LXVI. *The Relativistic Rule for Equipartition of Energy.*  
(Further note.) By F. F. P. BISACRE, M.A., O.B.E.\*

IN my previous note on this subject, I concluded that

$$\bar{\epsilon} \rightarrow \frac{3}{2} RT \quad \text{as} \quad T \rightarrow \infty,$$

or

$$\bar{\epsilon} \rightarrow RT \quad \text{as} \quad T \rightarrow \infty,$$

depending on whether we take  $\tau\beta^4$  or  $\tau\beta^5$  as the volume of the cell of "equal *a priori* probability" †.

The problem can be presented in a way that seems to point decisively to the latter hypothesis as the correct one.

Boltzmann's probability-theory proceeds on the assumption that, if we use Hamiltonian coordinates and measure the element of volume in the generalized  $(p, q)$  diagram by

$$dV = dq_1 dq_2 dq_3 dp_1 dp_2 dp_3,$$

the distribution of representative points in the  $(p, q)$  diagram, over equal elements, can be determined by Boltzmann's lottery. The  $(p, q)$  diagram and not the  $(\dot{q}, q)$  diagram must, in general, be used in order that the results shall be independent of the particular system of coordinates used.

If, for instance, we can define the state of the particle by the coordinates  $q_1, q_2, q_3, \alpha_1, \alpha_2, \alpha_3$ , and  $q_1', q_2', q_3', \alpha_1', \alpha_2', \alpha_3'$ , as alternative coordinate systems at rest with respect to each other, then the element of volume  $dq_1 \dots d\alpha_3$  is equal to the element  $dq_1' \dots d\alpha_3'$  if the Jacobian

$$\frac{D(q_1, q_2, q_3, \alpha_1, \alpha_2, \alpha_3)}{D(q_1', q_2', q_3', \alpha_1', \alpha_2', \alpha_3')} = 1.$$

This Jacobian is unity if  $\alpha_1, \alpha_2, \alpha_3$  are defined by the equations

$$\alpha_1 = \frac{\partial T}{\partial \dot{q}_1}, \quad \dots, \quad \alpha_3 = \frac{\partial T}{\partial \dot{q}_3},$$

where  $T$  is a function of  $q_1, q_2, q_3, \dot{q}_1, \dot{q}_2, \dot{q}_3$ , which is an invariant quantity of the alternative coordinate systems ‡.

Such a function exists in particle dynamics of the special theory of relativity; for, if we identify the  $\alpha$ 's with the momenta,  $p_1, p_2, p_3$ , the equations

$$p_1 = \frac{\partial T}{\partial \dot{q}_1}, \quad \dots, \quad p_3 = \frac{\partial T}{\partial \dot{q}_3}$$

\* Communicated by the Author.

†  $\beta = (1 - v^2/c^2)^{-\frac{1}{2}}$ .

‡ For details of the proof, see Lorentz, 'Lectures on Theoretical Physics,' vol. ii. p. 150. (Macmillan, 1927.)

hold good where

$$T = m_0 c^2 \left\{ 1 - \left( 1 - \frac{v^2}{c^2} \right)^{\frac{1}{2}} \right\},$$

which is obviously invariant, as it depends only on the velocity,  $v$ , and constants. It is not the kinetic energy, however.

The conclusion of all this is that the calculation should be based, fundamentally, on a momentum diagram\* (where all the coordinates can and do go to infinity). If we use a velocity diagram, we must apply a correcting factor to the element of volume of this diagram.

If the momentum coordinates are  $p_1, p_2, p_3$ , and the velocity coordinates  $\dot{q}_1, \dot{q}_2, \dot{q}_3$ , we have

$$dp_1 dp_2 dp_3 = \frac{D(p_1, p_2, p_3)}{D(\dot{q}_1, \dot{q}_2, \dot{q}_3)} d\dot{q}_1 d\dot{q}_2 d\dot{q}_3.$$

The correcting factor is therefore

$$\frac{D(p_1, p_2, p_3)}{D(\dot{q}_1, \dot{q}_2, \dot{q}_3)},$$

where

$$p_1 = m_0 \dot{q}_1 \left\{ 1 - \frac{v^2}{c^2} \right\}^{-\frac{1}{2}} = m_0 \beta \dot{q}_1,$$

$$p_2 = m_0 \beta \dot{q}_2,$$

$$p_3 = m_0 \beta \dot{q}_3,$$

and it turns out that the value of this Jacobian is  $m_0^3 \beta^5$  :

$$i. e., \quad dp_1 dp_2 dp_3 = m_0^3 \beta^5 d\dot{q}_1 d\dot{q}_2 d\dot{q}_3.$$

It will be seen that the factor,  $\beta^5$ , arises quite naturally—it is the price we pay for the use of the velocity diagram. The surfaces of equal energy in both diagrams are spheres, the radii being connected by the equation

$$R^2 = m_0^2 \beta^2 \rho^2.$$

The surface corresponding to an infinite energy in one diagram is the sphere at infinity ; in the other the sphere of radius  $c$ .

Since the correcting factor is  $\beta^5$ , it appears that  $\epsilon \rightarrow RT$  as  $T \rightarrow \infty$ , *i. e.*, the mean energy tends to exactly double the classical value, as the temperature tends to infinity. The exact formula for  $\epsilon$  was given in my previous communication.

\* We can ignore the coordinates  $q_1, q_2, q_3$ , as the energy is assumed not to depend on these coordinates.

LXVII. *Theory of the Internal Action of Thermionic Systems at Moderately High Frequencies.*—Part I. By W. E. BENHAM, B.Sc.\*

ABSTRACT.

EQUATIONS are given applying to a parallel plane thermionic system subject to potentials varying in time. These equations are similar to Child's equations for steady potentials, but contain extra terms. A solution of the alternating case is obtained, taking into account space-charge but neglecting emission velocities, in the special case of a small oscillatory potential superimposed on a large steady potential. The time of transit of the electrons appears in the solution. The theory is used to explain certain experimental results on the frequency variation of rectified current (W. E. Benham, *Phil. Mag.*, Feb. 28.).

The qualitative agreement between theory and experiment is satisfactory, but the observed effect is much the greater. The discrepancies between theory and experiment are discussed at some length. It is pointed out that electrons emitted with certain velocities are liable to execute a to-and-fro motion about the surface of minimum potential. This effect would increase with the frequency, with a corresponding modification of rectified current.

*Introduction.*

IN a recent paper † experiments were quoted indicating a discrepancy between the static and dynamic characteristic of a diode at moderately high frequencies. In particular, a small oscillatory potential of given amplitude was found to give rise to less and less rectified current as the frequency was increased from 4 to 17 megacycles. Part I. of the present paper constitutes an attempt to explain this phenomenon by taking into account the laws governing the motion of the space-charge when subject to rapidly alternating potential differences. While the theory has only been worked out in the case of zero initial velocities and plane electrodes, it forms nevertheless a possible starting-point for more exact theoretical investigation.

\* Communicated by Dr. Norman Campbell.

† W. E. Benham, *Phil. Mag.* v. p. 323.



*Theory.*

The now familiar equations of Child\*, *e. g.*

$$\frac{d^2V}{dx^2} = -4\pi P, \quad . \quad . \quad . \quad . \quad . \quad (1)$$

$$I = PU, \quad . \quad . \quad . \quad . \quad . \quad (2)$$

$$U \frac{dU}{dx} = -\frac{e}{m} \frac{dV}{dx}, \quad . \quad . \quad . \quad . \quad . \quad (3)$$

are intended to apply only in the case of steady potentials. Any solution of these equations in the form  $I=f(V)$  is therefore valid only when  $I$  and  $V$  are invariant in time. The justification for the standard practice of using the static characteristic,  $I=f(V)$ , to predict a periodic change in  $I$  consequent on a periodic change in  $V$  lies in the fact that the response of the electrons can for most practical purposes be taken as instantaneous. When the periodicity of  $V$  is very great, however, this is no longer the case. Under these circumstances Child's equations must be extended so that they apply to the case of potentials varying in time.

We shall reserve the symbols  $V$ ,  $P$ ,  $I$ , and  $U$  for the "steady" values of potential, space-charge per unit volume, current density, and velocity.

Let  $\mathbf{V}$ ,  $\mathbf{P}$ ,  $\mathbf{J}$ , and  $\mathbf{U}$  (in Clarendon type) be the values of potential, space-charge per unit volume, current density, and velocity at any point  $(x, 0, 0)$  and instant  $t$ . For the present,  $\mathbf{V}$ ,  $\mathbf{P}$ ,  $\mathbf{J}$ , and  $\mathbf{U}$  may vary with time in any manner.

For moving fields or fields varying with time at a given place, we have

$$\nabla^2 \mathbf{V} - \frac{1}{c^2} \frac{\partial^2 \mathbf{V}}{\partial t^2} = -4\pi \mathbf{P}.$$

The term  $\frac{1}{c^2} \frac{\partial^2 \mathbf{V}}{\partial t^2}$  reminds us that the potential is propagated with a finite velocity  $c$ . Now, this term can be neglected, provided the (time)<sup>2</sup> taken by e.m. waves to travel a given distance in the region considered is negligible compared not only with the (time)<sup>2</sup> taken by electrons to travel that distance, but also with the (time period of oscillation)<sup>2</sup> of  $\mathbf{V}$ . The first condition is satisfied for fields not exceeding a few thousand volts per cm., while the second is satisfied in the case of periodicities not exceeding some  $10^9$  cycles per second (for plates 0.5 cm. apart). The conditions for the

\* Phys. Rev. xxxii. p. 499 (1911). Used equations for case of positive thermions. For electrons see Langmuir, *loc. cit.* ii. p. 456 (1913).

neglection of the term

$$\frac{1}{c^2} \frac{\partial^2 \mathbf{V}}{\partial t^2}$$

are therefore satisfied experimentally. Since the lines of force are parallel to the axis of  $x$ , as for the steady case, we have therefore

$$\frac{\partial^2 \mathbf{V}}{\partial x^2} = -4\pi \mathbf{P}. \quad . \quad . \quad . \quad . \quad . \quad (1 a)$$

The current density is composed of two parts :

$$\mathbf{J} = \mathbf{P}\mathbf{U} - \frac{\partial^2 \mathbf{V}}{\partial x \partial t} \text{ (e.s. units).} \quad . \quad . \quad . \quad (2 b)$$

The second term represents the displacement, or "capacity" current, while the current  $\mathbf{I}$  actually carried by the thermions is given by

$$\mathbf{I} = \mathbf{P}\mathbf{U}. \quad . \quad . \quad . \quad . \quad . \quad (2 a)$$

Equating the rate of change of momentum of an electron to the instantaneous value of the electric force acting on it,

$$\begin{aligned} m \frac{d\mathbf{U}}{dt} &= -e \frac{\partial \mathbf{V}}{\partial x} \\ \text{or} \quad \frac{\partial \mathbf{U}}{\partial t} + \mathbf{U} \frac{\partial \mathbf{U}}{\partial x} &= -\frac{e}{m} \frac{\partial \mathbf{V}}{\partial x}. \quad . \quad . \quad . \quad . \quad (3 a) \end{aligned}$$

Since the current density must be the same at all values of  $x$ ,

$$\frac{\partial \mathbf{J}}{\partial x} = 0,$$

which leads, with the help of (2  $b$ ) and (1  $a$ ), to

$$\frac{\partial}{\partial x} (\mathbf{P}\mathbf{U}) = -\frac{\partial \mathbf{P}}{\partial t}. \quad . \quad . \quad . \quad . \quad . \quad (3 b)$$

Equations (3  $a$ ) and (3  $b$ ) correspond respectively to the general hydrodynamical equations of motion and continuity. Equation (3  $b$ ) could, of course, have been obtained independently on the basis of analogy with fluids. Writing  $\mathbf{I} = \mathbf{P}\mathbf{U}$ , we have

$$\frac{\partial \mathbf{I}}{\partial x} = -\frac{\partial \mathbf{P}}{\partial t}. \quad . \quad . \quad . \quad . \quad . \quad (4 a)$$

For steady currents it is always true that

$$\frac{dI}{dx} = 0. \quad . \quad . \quad . \quad . \quad . \quad . \quad (4)$$

Equation (4a) involves that the  $x$ -variation of the current carried by the thermions is not in general zero, but is equal and opposite to the  $x$ -variation of displacement current.

The equations (1a), (2a), (3a), and (4a) replace (1), (2), (3), and (4) in the case of potentials varying with time not more rapidly than would justify the omission of the term  $\frac{1}{c^2} \frac{\partial^2 V}{\partial t^2}$  from equation (1a). Before proceeding to the solution of equations (1a) to (4a) we note that equations (1) to (4) can be readily solved by the following method.

Differentiating (3) with respect to  $x$  and using (1),

$$\frac{d}{dx} \left( U \frac{dU}{dx} \right) = 4\pi \frac{e}{m} P.$$

Multiplying throughout by  $U$  and using (2),

$$U \frac{d}{dx} \left( U \frac{dU}{dx} \right) = 4\pi \frac{e}{m} I. \quad . \quad . \quad . \quad . \quad (5)$$

In view of (4),  $I$  is independent of  $x$ .

The solution to (5), subject to  $U=0$  when  $x=0$ , is

$$\left. \begin{array}{ll} \text{(i.) } U = \alpha x^{2/3}, \\ \text{(ii.) } \alpha = \left( 18 \frac{e}{m} \pi I \right)^{1/3}. \end{array} \right\} \quad . \quad . \quad . \quad . \quad (6).$$

where

The well-known 3/2 power law connecting  $I$  and  $V$  is readily obtained from (6), using (3).

No attempt will be made to include the effect of initial velocities in obtaining a solution to equations (1a) to (4a): the complexity of the solution of the steady case, allowing for initial velocities\*, is such as to make an attempt at accurate solution of the alternating case almost out of the question. The undoubtedly important effect of initial velocities is, however, examined qualitatively after a solution for zero emitted velocities has been arrived at. Any solution we obtain will therefore reduce to the form (6), or to expressions obtainable from (6), in the case when the time variation is nil.

\* Cf. Fry, Phys. Rev. xvii. p. 441 (1921).

Rewriting the equations, for convenience,

$$\frac{\partial^2 V}{\partial x^2} = -4\pi P. \quad . \quad . \quad . \quad (1 a)$$

$$I = PU. \quad . \quad . \quad . \quad (2 a)$$

$$\frac{\partial U}{\partial t} + U \frac{\partial U}{\partial x} = -\frac{e}{m} \frac{\partial V}{\partial x} \quad . \quad . \quad . \quad (3 a)$$

$$\frac{\partial I}{\partial x} = -\frac{\partial P}{\partial t} \quad . \quad . \quad . \quad (4 a)$$

Differentiating (3 a) with respect to  $x$ , and using (1 a),

$$\frac{\partial}{\partial x} \left( \frac{\partial U}{\partial t} + U \frac{\partial U}{\partial x} \right) = 4\pi \frac{e}{m} P.$$

$$\therefore \quad U \frac{\partial}{\partial x} \left( \frac{\partial U}{\partial t} + U \frac{\partial U}{\partial x} \right) = 4\pi \frac{e}{m} I. \quad . \quad . \quad . \quad (7)$$

Integrating equation (4 a) at constant  $t$  for the space between the cathode and any place  $x=x$ ,

$$\begin{aligned} I - I_0 &= -\frac{\partial}{\partial t} \int_{x=0}^{x=x} P dx \\ &= \frac{1}{4\pi} \frac{\partial}{\partial t} \left| \frac{\partial V}{\partial x} \right|_0. \end{aligned}$$

Now, from (6) and (3),

$$\frac{dV}{dx} = U \frac{dU}{dx} = \frac{2}{3} \alpha^2 x^{1/3};$$

$$i. e., \quad \left| \frac{dV}{dx} \right|_0 = 0.$$

We shall assume that at all instants  $V$  differs so little from  $V$  that, as in the steady case, the field at the cathode is at all instants vanishingly small compared with its value at the plane  $x=x$ , up to which we have integrated. It should be noted that, even in the steady case, it is necessary

to suppose that  $\left| \frac{dV}{dx} \right|_0$ , while differing from zero by as small a quantity as we please, is always positive, otherwise no electrons starting from rest would be extracted from the cathode. In the present case, also, we must suppose that

$\left| \frac{\partial V}{\partial x} \right|_0$  is never actually negative at any instant. The sequel is thus confined to the case of a very small variable potential

646 Mr. W. E. Benham *on the Internal Action of*  
superimposed on a large steady potential. Omitting the  
term  $\left| \frac{\partial \mathbf{V}}{\partial x} \right|_0$ ,

$$\frac{1}{4\pi} \frac{\partial}{\partial t} \left( \frac{\partial \mathbf{V}}{\partial x} \right) = \mathbf{I} - \mathbf{I}_0$$

$$\text{or} \quad \frac{\partial}{\partial t} \left( \mathbf{U} \frac{\partial \mathbf{U}}{\partial x} + \frac{\partial \mathbf{U}}{\partial t} \right) = 4\pi \frac{e}{m} (\mathbf{I}_0 - \mathbf{I}). \quad (8)$$

Adding equations (7) and (8), thus eliminating  $\mathbf{I}$ ,

$$\left( \frac{\partial}{\partial t} + \mathbf{U} \frac{\partial}{\partial x} \right) \left( \frac{\partial \mathbf{U}}{\partial t} + \mathbf{U} \frac{\partial \mathbf{U}}{\partial x} \right) = 4\pi \frac{e}{m} \mathbf{I}_0. \quad (5a)$$

Equation (5a) is to be compared with equation (5) for the "steady" case. Now we can make  $\mathbf{I}_0$  what we please, as it is a boundary value of current. Let

$$\mathbf{I}_0 = \mathbf{I}_0 + \hat{i}_0 \sin pt + \hat{i}_0' \sin^2 pt + \dots, \quad (9)$$

where  $\mathbf{I}_0$ ,  $\hat{i}_0$ ,  $\hat{i}_0'$  are independent of  $t$ . We are not immediately concerned with the values of  $\hat{i}_0$ ,  $\hat{i}_0'$  beyond asserting that they are respectively of the first and second order of small quantities. Accordingly let

$$\mathbf{U} = \mathbf{U} + u + u' + \dots, \quad (10)$$

where  $\mathbf{U}$  is defined as obeying the relation

$$\mathbf{U} \frac{d}{dx} \left( \mathbf{U} \frac{d\mathbf{U}}{dx} \right) = 4\pi \frac{e}{m} \mathbf{I}_0, \quad (11)$$

while  $u, u' \dots$  must be chosen to satisfy the partial differential equation (5a) with the help of (9), (10), and (11). Since  $\mathbf{I}_0$  is independent of  $t$ , so also must  $\mathbf{U}$  be;

$$\text{i. e.,} \quad \frac{\partial \mathbf{U}}{\partial t} = 0. \quad (12)$$

With the help of (9), (10), (11), and (12), (5a) gives rise to an equation which may be split into three equations, corresponding to the three terms of equation (9).

The first is equation (11) itself; the second is linear in  $u$  and  $\hat{i}_0$  and does not contain  $u'$  and  $\hat{i}_0'$ ; while the third is linear in  $u'$  and  $\hat{i}_0'$ , and of the second degree in  $u$  and  $\hat{i}_0$ . There will, of course, be as many equations as there are terms in equation (9), but since we are taking  $\hat{i}_0'$  and  $u'$  to be of the second order of small quantities, it is sufficient to retain

three only. The second equation reads :

$$U \frac{\partial}{\partial x} \left( u \frac{\partial U}{\partial x} + U \frac{\partial u}{\partial x} \right) + u \frac{\partial}{\partial x} \left( U \frac{\partial U}{\partial x} \right) + \frac{\partial^2 u}{\partial t^2} \\ + \frac{\partial}{\partial t} \left( 2U \frac{\partial u}{\partial x} + u \frac{\partial U}{\partial x} \right) = 4\pi \frac{e}{m} \hat{i}_0 \sin pt. \quad (13)$$

The third reads :

$$U \frac{\partial}{\partial x} \left( u' \frac{\partial U}{\partial x} + U \frac{\partial u'}{\partial x} \right) + u' \frac{\partial}{\partial x} \left( U \frac{\partial U}{\partial x} \right) \\ + \frac{\partial^2 u'}{\partial t^2} + \frac{\partial}{\partial t} \left( 2U \frac{\partial u'}{\partial x} + u' \frac{\partial U}{\partial x} \right) \\ + U \frac{\partial}{\partial x} \left( u \frac{\partial u}{\partial x} \right) + u \frac{\partial}{\partial x} \left( u \frac{\partial U}{\partial x} + U \frac{\partial u}{\partial x} \right) \\ + 2 \frac{\partial}{\partial t} \left( u \frac{\partial u}{\partial x} \right) = 4\pi \frac{e}{m} \hat{i}_0' \sin^2 pt. \quad (14)$$

In order to obtain a solution to equation (13), we must use the solution of (11), which is evidently

$$U = \alpha x^{2/3}. \quad \text{Cf. (6).}$$

It is convenient to effect the transformations

$$\left. \begin{aligned} \frac{3}{\alpha} \cdot p x^{1/3} &= \xi, \\ u &= \frac{\omega}{\xi} \end{aligned} \right\} \dots \dots \dots (15)$$

and the substitutions

$$\left. \begin{aligned} \gamma &\equiv \frac{3}{\alpha}, \\ \beta &\equiv 4\pi \frac{e}{m} \hat{i}_0. \end{aligned} \right\} \dots \dots \dots (16)$$

Then

$$\left. \begin{aligned} U &= \frac{3\xi^2}{\gamma^2 p^2}, \\ \frac{\partial}{\partial x} &= \frac{\gamma^2 p^2}{3\xi^2} \frac{\partial}{\partial \xi}, \\ U \frac{\partial}{\partial x} &= p \frac{\partial}{\partial \xi}, \\ \frac{\partial U}{\partial x} &= 2 \frac{p}{\xi}. \end{aligned} \right\} \dots \dots \dots (17)$$

648 Mr. W. E. Benham on the Internal Action of  
Equation (13) then becomes

$$\frac{\partial^2 \omega}{\partial \xi^2} + \frac{2}{p} \frac{\partial}{\partial t} \frac{\partial \omega}{\partial \xi} + \frac{1}{p^2} \frac{\partial^2 \omega}{\partial t^2} = \frac{\beta}{p^2} \xi \sin pt,$$

or, symbolically,

$$\left( \frac{\partial}{\partial \xi} + \frac{1}{p} \frac{\partial}{\partial t} \right)^2 \omega = \frac{\beta}{p^2} \xi \sin pt. \quad \dots (18)$$

Equation (18) can be solved in two stages, and the result is, putting  $\omega = u\xi$ ,

$$u = -\frac{\beta}{p^2} \left( \sin pt + \frac{2 \cos pt}{\xi} \right) + \frac{1}{\xi} F_1(\xi - pt) + F_2(\xi - pt), \quad (19)$$

where  $F_1, F_2$  are arbitrary functions.

Since  $u=0$  when  $x=0$ , i. e. when  $\xi=0$ , for all values of  $t$  the functions  $F_1, F_2$  must be chosen accordingly. The solution can then be written in any of the following forms:—

$$\left. \begin{aligned} u &= -\frac{\beta}{p^2} \left[ \sin pt + \frac{2}{\xi} \cos pt + \sin(pt - \xi) - \frac{2}{\xi} \cos(pt - \xi) \right], \\ u &= +\frac{\beta}{p^2} \left[ \left( -\cos \xi + \frac{2}{\xi} \sin \xi - 1 \right) \sin pt \right. \\ &\quad \left. + \left( \sin \xi + \frac{2}{\xi} \cos \xi - \frac{2}{\xi} \right) \cos pt \right], \\ \frac{u}{U} &= \frac{\hat{i}_0}{3I} T_u \sin(pt - \Xi_u). \end{aligned} \right\} \quad \dots (20)$$

N.B.—It will be found on substitution that  $\frac{\beta \xi^2}{6p^2} = \frac{\hat{i}_0}{3I} U$ .

The last form serves to demonstrate the effect of frequency on the value of  $u$  at any point. We have

$$\left. \begin{aligned} T_u &= \frac{12}{\xi^2} \left[ \frac{\sin \frac{1}{2}\xi}{\frac{1}{2}\xi} - \cos \frac{1}{2}\xi \right], \\ \Xi_u &= \frac{1}{2}\xi. \end{aligned} \right\} \quad \dots (21)$$

Whence, as  $\xi \rightarrow 0$ ,  $T_u \rightarrow 1$  and  $\Xi_u \rightarrow 0$ .

Before proceeding with the solution, we would draw attention to the physical meaning of  $\xi$ .

In total differential notation

$$U = \frac{dx}{dt}.$$

$$\begin{aligned}\therefore dt &= \frac{dx}{U} \\ &= \frac{d\xi}{p} \text{ by equation (17).} \\ \therefore \xi &= pT, \quad . . . , \quad . . . \quad (22)\end{aligned}$$

where  $T$  = time of transit of electrons from cathode to plane in question in the absence of alternating current. We note in passing one consequence of this result.

For  $pT = 2\pi$ ,

$$T_u = \frac{3}{\pi^2}, \quad \Xi_u = \pi.$$

Hence, when the time period of oscillation is equal to the time of transit, the amplitude of motion at the plane in question is reduced some 70 per cent. as a direct result of the extreme rapidity of alternation, the reduction in amplitude being accompanied by a reversal of phase at this plane.

The above result may be useful in connexion with the oscillations of extremely short wave-length discovered by Barkhausen and Kurz \*, whose experiments were repeated in this country by Gill and Morell †. This point will, however, be deferred to Part II. of this paper.

Having obtained  $U$  and  $u$ , we are now in a position to solve equation (14) for  $u'$ . The mathematics are greatly simplified if we content ourselves with an approximate formula for  $u$  in which  $\frac{\cos}{\sin} \xi$  have been replaced by their appropriate expansions in powers of  $\xi$ ; *e. g.*,

$$\frac{\beta \xi^2}{6\rho^2} \left[ \left( 1 - \frac{3\xi^2}{20} + \frac{\xi^4}{161} - \dots \right) \sin pt - \left( \frac{\xi}{2} - \frac{\xi^3}{30} + \dots \right) \cos pt \right]. \quad . . . \quad (23)$$

The above expression differs by much less than 1 per cent. from the exact formula, for  $0 < \xi < 2$ . The details of analysis need not be entered into. The solution is naturally of the general form

$$u' = X + Y \sin 2pt + Z \cos 2pt. \quad . . . \quad (24)$$

The values of  $Y$  and  $Z$  are not of immediate interest, and need not be written down. The mean value of  $u'$  during the cycle is as follows :

$$\bar{u}' = X = \frac{U}{181} \left[ 3\hat{i}_0' - \frac{\hat{i}_0^2}{1} \left( 1 - \frac{\xi^2}{16} + \frac{11\xi^4}{8400} \right) \right]. \quad . . \quad (25)$$

\* *Phys. Zeit.* xxi. p. 1 (1920).

† *Phil. Mag.* xliv. p. 161 (1922).



We have now completely determined  $\mathbf{U}$  in terms of  $I_0$ ,  $\hat{i}_0$ , and  $\hat{i}_0'$ . We can now substitute for  $\mathbf{U}$  in equation (3a) to obtain  $\mathbf{V}$  in terms  $I_0$ ,  $\hat{i}_0$ , and  $\hat{i}_0'$ . For this purpose let

$$\mathbf{V} = V + v + v'. \quad . \quad . \quad . \quad (26)$$

The values of  $V$ ,  $v/V$  are found to be as follows:

$$\left. \begin{aligned} V &= \left(\frac{I_0}{k}\right)^{2/3} \cdot x^{4/3}, \\ k &= \sqrt{\left(\frac{2e}{m}\right)/9\pi}, \end{aligned} \right\} \quad . \quad . \quad . \quad (27)$$

in which

$$\frac{v}{V} = \left(\frac{2\hat{i}_0}{3I_0}\right) \mathbf{T}_v \sin(pt - \Xi_v), \quad . \quad . \quad . \quad (28)$$

where, for  $0 < \xi < 2$ ,

$$\left. \begin{aligned} \mathbf{T}_v^2 &= 1 - \frac{13\xi^2}{300} + \frac{11\xi^4}{12,600}, \\ \Xi_v &= \frac{3\xi}{10}. \end{aligned} \right\} \quad . \quad . \quad . \quad (29)$$

If  $\bar{v}'$  denote the mean value  $v'$  during the cycle, we find also

$$\frac{\bar{v}'}{V} = \left(\frac{1}{18I_0}\right) \left[6\hat{i}_0' - \frac{\hat{i}_0^2}{I_0} \left(1 - \frac{3\xi^2}{40} + \frac{13\xi^4}{8400}\right)\right] \quad . \quad . \quad (30)$$

Now, at the anode,  $\bar{v}'$  must vanish, since the anode is maintained at a potential  $V$  with respect to the cathode by means of a battery. In actual practice the potential at the anode is to some extent modified by any resistance in the anode circuit, but when such resistance is negligible compared with that of the valve, the mean potential of the anode can be taken as the battery potential. These conditions were actually realized in the experiments, since the battery was of the accumulator type having low internal resistance, the only other resistance being that of the shunted galvanometer arrangement, which was also negligible.

Hence, at the anode, for all frequencies

$$\bar{v}' = 0,$$

whence from (30):

$$\frac{\hat{i}_0'}{2} = \frac{\hat{i}_0^2}{12I_0} \left(1 - \frac{3\xi_d^2}{40} + \frac{13\xi_d^4}{8400}\right) \quad . \quad . \quad . \quad (31)$$

The suffix " $d$ " denotes that the value of  $\xi$  is that corresponding to the anode ( $x=d$ ). Equation (31) gives the

rectified current  $i_0'/2$  in terms of  $\hat{i}_0$  and  $\xi_a$ . It must be emphasized that, while the *rectified* current varies with  $\xi_a$  (i. e. with  $p$ ), it by no means varies with  $\xi$  (i. e. with  $x$ ), as does the alternating component of *thermionic* current ( $q.v.$ ). For the cathode-anode space we have, from (30) and (31),

$$\frac{\bar{v}'}{V} = \frac{i_0^2}{18 I_0} \left[ \frac{3}{40} \cdot (\xi^2 - \xi_a^2) - \frac{13}{8400} \cdot (\xi^4 - \xi_a^4) \right]. \quad (32)$$

Since  $\xi \leq \xi_a$ , we draw the following conclusion for future reference; *e. g.* :—

*“For given boundary values of the potential components, the mean potential at any point intermediate between cathode and anode is less at finite frequencies than at zero frequency.”*

We have yet to express the rectified current in terms of the boundary value of the alternating component of *potential*. Let  $\hat{v}$  denote the amplitude of  $v$ . Then, from equation (28),

$$\frac{\hat{v}}{V} = \left( \frac{2\hat{i}_0}{3I_0} \right) T_v.$$

Hence (31) becomes, substituting for  $\hat{i}_0$ ,

$$\frac{\hat{v}'}{2} = \left( \frac{3I_0}{16} \right) \left( \frac{\hat{v}^2}{V^2} \right) \left( \frac{1}{T_v^2} \right) \left( 1 - \frac{3\xi_a^2}{40} + \dots \right).$$

Substituting for  $T_v^2$  from (29) and putting  $\xi = \xi_a$ ,  $v = v_a$ ,  $V = V_a$ , we have, after rationalising,

$$\frac{\hat{i}_0'}{2} = \left( \frac{3I_0}{16} \right) \left( \frac{\hat{v}_a^2}{V_a^2} \right) \left( 1 - \frac{19\xi_a^2}{600} - \frac{7\xi_a^4}{10,000} \right),$$

in which little accuracy is claimed for the last term, which is, fortunately, exceedingly small.

Thus, for given values of  $\hat{v}_a$  and  $V_a$  the rectified current varies with the frequency according to the expression in round brackets. We shall refer to this expression for convenience as  $T_{\Delta I}$ .

In decimal form we have

$$T_{\Delta I} = (1 - 0.0317 \xi_a^2 - 0.0007 \xi_a^4). \quad \dots \quad (33)$$

### *Application to Experimental Results.*

$T_{\Delta I}$  has been plotted on fig. 1 for values of  $\xi$  between 0 and 3. We note a general agreement in form between theoretical and experimental curves.

For plates 0.5 cm. apart subject to an anode potential of 16 volts we find, after expressing  $\xi_a$  in terms of  $p$ ,  $V$ , and  $d$

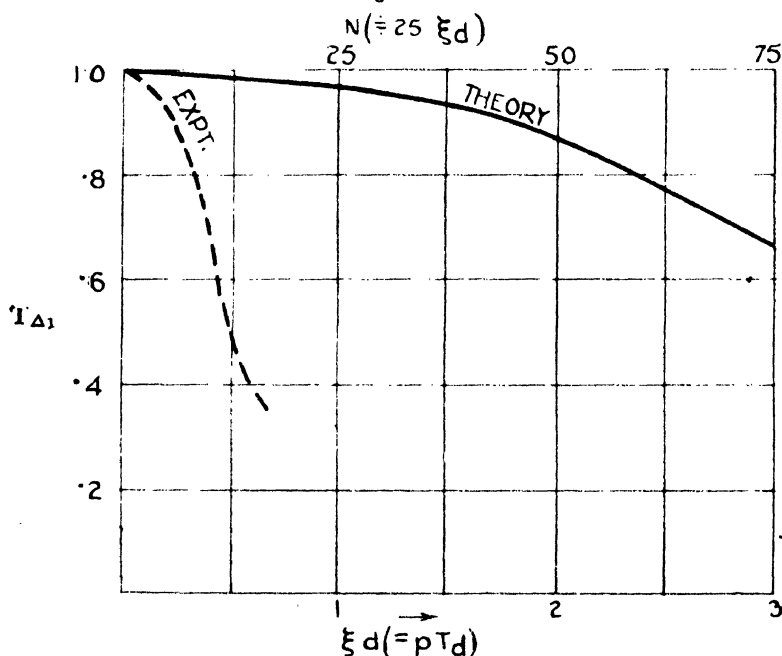
(*q. v.* equation 36), that the frequency in megacycles (1 megacycle =  $10^6$  cycles/sec.) is given very nearly by

$$N = 25\xi.$$

Thus for a frequency of 12.5 megacycles ( $\lambda 24m$ ), which corresponds to a typical frequency in the range of experiments,

$$\xi = 0.5.$$

Fig. 1.



Variation of Rectified Current with Frequency.  
( $N$ =frequency in megacycles.)

So that in this case

$$T_{AI} = 1 - 0.0072 = 0.992. \quad (34)$$

According to the experimental curves, however, we have, at  $N 12.5$ ,

$$T_{AI} \doteq 0.5. \quad (35)$$

The frequency variation obtained in practice is therefore very much more pronounced than that predicted by equation (33). In order to bring the experimental curves into approximate agreement with the formula (33), it would be

necessary to assume that the time of transit of the electrons were about five times the time of transit calculated from the formula

$$T_d = \frac{3d}{\sqrt{\left(2 \frac{e}{m} V\right)}} \quad \dots \quad (36)$$

Moreover (36) refers to parallel planes; for cylinders it can be shown that for the same clearance and potential difference the time of transit approaches  $T_d/2$  as the radius of the cathode approaches zero. The effective anode radius corresponding to the valves used would be intermediate between the radii of grid and anode (these electrodes, being connected external to the valve, are both at the same time potential). The effective anode radius, while somewhat indeterminate, cannot differ much from 0.5 cm.

Thus to obtain any sort of quantitative agreement with equation (33) it would be necessary to assume that, due to some cause, the actual time of transit of the electrons were about ten times the time of transit calculated directly from the dimensions and potentials.

#### *Other Factors influencing the Time of Transit.*

Increase in the average time of transit would result :

- (a) If some of the electrons were to suffer collisions with molecules before completing transit.
- (b) If the result of such collisions were to produce ionization; i. e., to give rise to heavy thermions.
- (c) From consideration of finite emission velocities.

In view of the high vacuum ( $\pi \times 10^{-5}$  mm. Hg), it is safe to conclude that the effects (a) and (b), while inevitably present if only in a minute degree in every thermionic device, are not responsible for more than a small fraction of the increase in time of transit. These remarks are not intended to apply to any of the results quoted for a helium-filled valve. The effect of (c) will be examined when we have inquired into other possible experimental factors tending to increase the frequency variation.

One such possibility is that the e.m.f. measured by the electrometer was not composed exclusively of the fundamental component  $v$ , but partly of harmonic components.

654 Mr. W. E. Benham on the Internal Action of  
*The Effect of Harmonics in the Oscillatory Voltage.*

It is convenient to divide voltage harmonics into two kinds:—

- (1) Those produced from the fundamental by the valve itself in virtue of its peculiar conducting properties.
- (2) Those introduced along with the fundamental from the source of oscillations.

Both types of harmonics are registered by the electrometer in addition to the fundamental. Thus, if harmonics in the voltage, whether of type (1) or (2), are comparable in amplitude to the fundamental, the electrometer reading will be greater than that corresponding to the mean square of  $v$ ; i. e., greater than that corresponding to the rectified current. The harmonics in the current will increase as the harmonics in the potential increase, but the important point to notice is that current harmonics are not registered, while potential harmonics are. The rectified current is clearly due only to the fundamental  $v$  over the range of  $v$  for which square law rectification takes place.

We have therefore to inquire into the effect of potential harmonics of both types on the electrometer reading.

In order to find the magnitude of type (1) harmonics, it is necessary to work out the values of  $Y$  and  $Z$  (equation 24) and then to use equation (3a) to find the corresponding potential harmonics. The mathematics involved is exceedingly clumsy, and it will suffice to give the final approximate result, which is correct to 5 per cent. for  $0 < \xi < 0.5$ ; namely

$$v' = 0.375 \frac{\hat{v}^2}{V} (0.128 \xi \sin 2\pi t - 0.136 \xi^2 \cos 2\pi t). \quad (37)$$

That the value of  $v'$  at finite frequencies is not zero involves that it is impossible to avoid potential harmonics, even though the potential wave-form be pure in the absence of the thermionic device. It turns out, however, that  $v'$  is exceedingly small at practical frequencies (at any rate for a system obeying the  $3/2$  power law). The electrometer reading is proportional to

$$\int_{t=0}^{t=p/2\pi} (v + v')^2 dt,$$

which gives finally

$$\frac{\hat{v}^2}{2} \left( 1 + 0.00015 \frac{\hat{v}^2}{V^2} \xi^2 \right).$$

The effect of harmonics of type (1) is thus exceedingly small and can be neglected.

Harmonics of type (2) must next be considered. These are much easier to deal with. Thus instead of considering the fundamental, which we will call  $v_1$ , as the input oscillatory voltage, one might equally well consider the harmonic  $v_n$  to be the input oscillatory voltage. The rectified current due to  $v_n$  will then be proportional to

$$\hat{v}_n^2 [1 - 0.0317(n\xi)^2 - \dots], \quad . \quad . \quad . \quad (38)$$

in which  $n$  is the order of the harmonic and  $\xi$  still corresponds to the fundamental frequency.

The rectified current due to the fundamental and  $n-1$  harmonics of type (2) is thus proportional to the sum to  $n$  terms of the above expression.

It is therefore necessary to know the relative amplitudes of any harmonics in the input, or preferably to cut them out altogether—if possible. One method of cutting out the harmonics which is fairly effective is to couple a tuned circuit loosely to the oscillator coil, and then couple the valve test circuit to this tuned circuit. This was done, but the frequency variation proved to be the same within experimental error.

It appears, therefore, that both kinds of harmonics in the input voltage were of amplitude negligible compared with that of the fundamental: and we conclude that the observed frequency variation was that corresponding to the fundamental frequency alone.

The large discrepancy between theoretical and observed frequency variation is thus left unexplained by the foregoing considerations. The time is now ripe for noting a further important discrepancy between theory and experiment. It was found that change in the anode voltage had negligible effect on the frequency variation over a range of voltages corresponding to the infra-saturation region: change of anode voltage, of course, alters the absolute value of the rectified current, but the ratio of the rectified current at any two frequencies was found to be sensibly independent of the anode voltage. But in view of the dependence of the calculated time of transit  $T$  on anode voltage, any frequency variation due to the finite value of  $T$  must become less pronounced as the anode voltage is increased. Hence the frequency variation due to the finite time of transit  $T$  must be too small to affect the observations.

In order to account for the observations, it is accordingly necessary to suppose that the actual *effective* time of transit is sensibly independent of  $V$  and considerably greater

than  $T$ . We therefore put forward the following tentative suggestions as working hypotheses :—

- (1) The electrons take a finite average time  $T_f$  to free themselves from the neighbourhood of the filament,  $T_f$  being sensibly independent of  $V$  and considerably greater than  $T$ .
- (2)  $T_f$  is determined by the condition of the filament, especially by the filament temperature.

The second hypothesis seems a reasonable adjunct to the first, and is in qualitative agreement with the observed marked effect of filament voltage on the frequency variation.

We will now examine the effect of initial velocities, with the above hypotheses in mind.

The theory for zero initial velocities is at best only an approximation to the actual facts. The behaviour of the electrons in the neighbourhood of the filament is, in fact, totally different from the case of zero emitted velocities\*.

The theory for zero initial velocities applies, strictly speaking, only in cases in which the accelerating field due to the anode potential everywhere exceeds the retarding field due to the space-charge, the excess vanishing, however, at the filament ( $\frac{dV}{dx} \rightarrow 0$ , when  $x \rightarrow 0$ ). It is noteworthy that, in order to drag the (hypothetically at rest) electrons away from the filament, it must be supposed that  $\left| \frac{dV}{dx} \right|_0$  is slightly positive, but can be made, for the purposes of the theory for zero emitted velocities, to differ from zero by an infinitesimal amount. Thus, in the theory for zero emitted velocities,

$$\left| \frac{dV}{dx} \right|_0 \rightarrow \delta \rightarrow 0.$$

Furthermore, if  $\delta$  is positive, *all* the emitted electrons will reach the anode: if negative, *none*†.

\* Cf. Fry (*loc. cit.*) and Langmuir, Phys. Rev. xxi. p. 419 (1923).

† That the  $3/2$  power law is a sufficiently accurate relation for many practical purposes is at first sight somewhat surprising. The widespread practical application of the  $3/2$  power law, especially in the design of large valves, is justified by the closeness of the cathode to the surface of minimum potential, which surface may be regarded as a "virtual cathode" at which  $\left( \frac{dV}{dx} \right)_0 = 0$ . This does not alter the fact that the

Now, in the practical case of finite emission velocities  $\delta$  is negative in the infra-saturation region, since all the electrons do not reach the anode. For  $\delta$  negative there will be a surface of minimum potential ( $\left|\frac{dV}{dx}\right| = 0$ ) at some value  $x_1$  of  $x$ . If  $U_c$  be the critical value of initial velocity, such that electrons emitted with this velocity come to rest at  $x = x_1$ , the time of transit of these electrons to the anode (assuming the electrons just to *succeed* in passing the plane  $x = x_1$ ) is greater than the time of transit for  $x_1 = 0$ ,  $U_0 = 0$ . This point is illustrated \*, for  $x_1 = 1$  mm.,  $d = 5$  mm., on fig. 2. The ordinates to these curves represent, in arbitrary units, the time of transit to any abscissa  $x$ . The value of  $T$  corresponding to  $U_0 = V_c$  is taken to be proportional to  $[(x - x_1)^{1/3} + x_1^{1/3}]$ , since it follows from equation (5) that, for those electrons which come to rest at  $x = x_1$ ,

$$U = \alpha(x - x_1)^{2/3};$$

$$\text{i. e., } U_c = \alpha(-x_1)^{2/3} = +\alpha x_1^{2/3}.$$

Curves corresponding to  $U_0$  slightly less and slightly greater than  $U_c$  are clearly indicated on fig. 2.

A slight disturbance in potential at the instant when the electron reaches the potential minimum suffices to determine whether it will return to the filament or whether it will pass over to the anode. In the event of the disturbance being of oscillatory character, the electrons which are momentarily at rest, or nearly so, will be made to execute a to-and-fro motion of small amplitude † about the surface of minimum potential. Perhaps it would be more accurate to say that the surface of minimum potential executes a to-and-fro motion about the electrons, placing the latter first in an accelerating and then in a retarding field. It is

field at the actual cathode is, in general, very different from zero, whether or no the  $3/2$  power law gives accurate results. At the surface of minimum potential the mean velocity of the electrons is, of course, very much less than at the cathode. Thus at the "virtual cathode" the condition of zero "emission" velocity is approached, and the condition of zero field is realized.

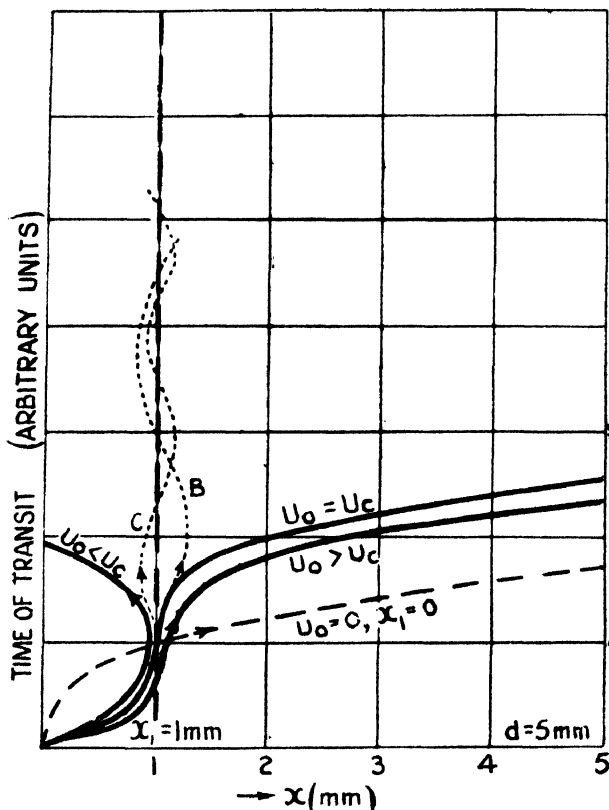
\* For a plane cathode at  $2400^\circ$  K. the anode potential for  $x_1 = 1$  mm.  $d = 5$  mm. is only 2 v. and only 0.1 per cent. of the emitted electrons reach the anode. The example is thus an extreme one.

† Cf. Zilitinkewitsch, *Archiv. f. Electrot.* xv. p. 482 (1925), who assumed electrons to oscillate in a somewhat similar manner in the case of a valve generating oscillations of the type discovered by Barkhausen and Kurz (*loc. cit.*).



legitimate to regard the electrons as executing oscillations about the mean position of the potential minimum. The electrons in question will presumably remain indefinitely in this oscillating condition (B, C, fig. 2). For a given frequency, the number of electrons so oscillating is equal to the number of electrons reaching the potential minimum

Fig. 2.



The time taken by electrons emitted with velocities in the neighbourhood of the critical velocity (see text) to reach any plane  $x = x$  is illustrated above in the special case  $x_1 = 1 \text{ mm}$ ,  $d = 5 \text{ mm}$ .

with velocities less than a certain small value  $U_m$ , where  $U_m$  will depend on the amplitude of the applied potential as well as on the cathode temperature. Since  $U_m$  can be greater for larger values of  $\hat{v}$ , the number of oscillating electrons would increase with the value of  $\hat{v}$ . Clearly, also,  $U_m$  can

be greater the greater the frequency (within certain limits), so that the number of oscillating electrons increases with the frequency. Periodical instability at high frequencies is likely, such as was noticed in the experiments; the observed instabilities were then put down to the Schottky effect.

We can, if we like, regard the effective average time of transit as being lengthened due to certain electrons remaining an indefinite time in the cathode-anode space. But this conception, while exceedingly convenient from the mathematical standpoint, is unsatisfactory from the physical point of view. One physical consequence of electrons oscillating about the potential minimum is an increased space-charge density in that region.

Now, the theory for zero initial velocities gives some indication of accumulated space-charge. The mean potential at any point in the cathode-anode space was found to be less at finite frequencies than at zero frequency (equation 32). This result is closely related in the theory to the frequency variation of the rectified component of current (equation 31). The reason for the reduction in potential is bound up with the peculiar conducting properties of thermionic systems. The interpretation of the reduction follows from the fact that for a given mean anode potential a reduction in mean potential at any point in the cathode-anode space can only be brought about by an increase of space-charge density at that point.

Now, in practice the increase of space-charge density, *i. e.* the reduction in mean potential, especially at points near the potential minimum, is likely to be on a much larger scale than in the theory for initial velocities, in view of accumulated space-charge due to oscillating electrons. If, then, the frequency variation of rectified current is, in fact, as closely related to the increase of space-charge density as it is in theory, the observed frequency variation would, like the reduction in mean potential, be on a much larger scale than that predicted by the theory for zero emitted velocities.

If the true explanation of the observations lies in the direction indicated, the effects of filament and anode voltages on the value of the rectified current are alike somewhat obscure; a purely physical explanation, if not altogether out of the question, would be very involved.

Such questions could be settled by further experiments on a larger scale and with improved apparatus. The sensitivity of the instrument used to measure the oscillatory voltage should be as great as is consistent with rapidity of

reading: no valve keeps absolutely constant characteristics over a period of an hour, especially under the somewhat severe conditions of experiment, and the smallest changes are of vital importance in measurements of this kind. The idiostatically-connected Dolezalek electrometer is definitely not sufficiently sensitive and the needle takes too long to come to rest.

The electrometer might be disposed of when the frequency variation of one valve has been fully determined, as this valve could then be incorporated in a Moullin voltmeter circuit, whose frequency error would be known. The voltmeter thus provided is very much more convenient to work with. Incidentally, the author's experiments on a helium-filled valve were effected in this manner. The valve used as voltmeter was a Marconi D.E.V. type valve which showed a negligible frequency error when used as triode. In choosing a valve for investigation a simple form of electrode design is desirable. Indirectly heated cathode valves are now available. These valves conform very nearly to the theoretical parallel plane system.

This research was begun early in 1926 at University College, London, under the supervision of Professor A. W. Porter, F.R.S., and with much appreciated financial assistance from the Department of Scientific and Industrial Research.

The author wishes to thank Professor Porter for his able advice and opportune criticism on many occasions, and all those who have taken an interest in the work for helpful suggestions. He would also like to thank Dr. Campbell for his great kindness in communicating the paper.

### *Summary.*

1. With the more immediate object of explaining certain experimental results on frequency variation of rectified current, but also as a starting-point for further theoretical investigation, Child's space-charge equations are modified so as to make them apply to the case of potentials varying in time.

2. The equations of motion and continuity represent the electrical counterpart of the corresponding hydrodynamical equations.

3. The equation of continuity in the thermionic case involves that, while the sum of the instantaneous values of

thermionic and displacement (capacity) current is the same at all points, each type of current varies from point to point.

4. The primary equation (5 *a*) obtained from the modified equations (1 *a*) to (4 *a*) lends itself to solution if we assign a permissible value to the current at the cathode. It is supposed that the alternating components of current and potential are of very small amplitude. The corresponding alternating components of velocity are thus obtained at any value of  $x$  and  $t$ .

5. These velocity components come out in functions of  $\xi \left( = \frac{3}{\alpha} p x^{1/3} = pT \right)$ . The interpretation of  $\xi$  follows from the fact that  $T$  represents the time of transit of electrons from the cathode ( $x=0$ ) to any plane ( $x=x$ ).

6. A solution for the potential is obtained by inserting the solution for the velocity in equation (3 *a*).

7. By imposing on this last solution the experimentally-realised condition that the mean potential difference between cathode and anode is constant (being maintained so by the anode battery), a relation between the rectified current and the alternating component of current is obtained, involving functions of  $\xi_a (= pT_a)$ , where  $T_a$  is the time of transit from cathode to anode.

8. A further short analysis gives the rectified currents in terms of  $\xi_a$  and the potential components.

9. The solution obtained agrees qualitatively with the experimental results, but the magnitude of the frequency variation predicted by theory is much smaller than that found by observation.

10. In order to bring theory and observation into line, it is necessary to suppose that the time of transit is for some reason much greater than the value calculated from the dimensions and potentials of the valve. It is not possible to explain the observed variation of (square-law) rectified current on the basis of harmonics in the potential.

11. It is pointed out that collisions with residual molecules are too infrequent to produce the required lengthening of time of transit.

12. A further discrepancy between theory and practice lies in the apparent non-dependence of frequency variation on (steady) anode potential.

13. To account for the discrepancies the working hypothesis is adopted: "That the electrons take a certain time to escape from the proximity of the filament, this time being

determined by the temperature of the filament, but hardly at all by the anode potential."

14. Due to initial velocities a surface of minimum potential is present for voltages below saturation. Electrons emitted with a certain critical velocity execute oscillations about the surface of minimum potential. Mathematically this effect can be interpreted as giving rise to an increased effective average time of transit.

15. The physical consequence of this effect is accumulated space-charge in the neighbourhood of the potential minimum. A certain result obtained in the theory (equation 32) is used to associate the frequency variation of rectified current with the degree of accumulation of space-charge. Further lines for experiment are suggested.

#### LXVIII. *The Thermal Instability of the Earth's Crust.*

*By H. H. POOLE Sc.D., and J. H. J. POOLE, Sc.D.\**

**I**N Dr. Jeffreys's interesting, if rather heated, paper on "Dr. Joly and the Earth's Thermal History" in the January number of the *Philosophical Magazine*, his main contention seems to be that, if the substratum contains more radioactive elements than are sufficient to supply the present loss of heat from the earth's surface, the future state of the earth will be one in which a layer of molten rock of fixed thickness and temperature-gradient will be overlain by a solid crust, also of a fixed thickness. The thickness of this crust will be such that the loss of heat by conduction through it will exactly counterbalance the generation of radioactive heat, both in itself and in the underlying layers, so that a steady state will be attained with no possibility of any orogenic movements due to thermal expansion or contraction. As, according to Dr. Jeffreys, the earth is about 1300 million years old already, it seems peculiar that it has not yet reached this state. Moreover, if, as he assumes, the earth has always been falling in temperature, we should not expect the present temperature gradient to be less than the finally-attained gradient, which must be sufficient to carry off the heat generated.

The only logical conclusion that can be drawn from this assumption is that the substratum cannot contain more radioactive materials than are sufficient to account for the present rate of loss of heat.

\* Communicated by the Authors.

This view is opposed by all the actual measurements of the uranium and thorium contents of the materials which might be reasonably supposed to constitute the substratum ; but, of course, its incorrectness cannot be absolutely proved by experiment, as we are unable to obtain specimens of absolutely unimpeachable derivation from the layer in question.

However, apart entirely from this consideration, his contention is based on the assumption that it would be possible for a layer of molten magma to persist indefinitely beneath a roof of solidified magma of the same composition. A very elementary consideration of the thermodynamical principles involved shows that this assumption cannot be true, unless the magnitude of the subterranean pressures introduces effects which, *a priori*, we would not expect.

It is well known that, as Dr. Jeffreys points out, in a deep layer of liquid, if the vertical temperature gradient becomes steeper than the adiabatic, convection currents will be set up. These currents will transfer heat so readily from the bottom to the top of the layer that we are entitled to assume, with Dr. Jeffreys, that they will effectively prevent any appreciable increase in the temperature gradient above the adiabatic value.

If this adiabatic temperature gradient were steeper than the rate of rise of melting-point with depth, then the liquid at the top of the layer might be at its melting-point, and so in equilibrium with the solid roof : but if the melting-point gradient is the steeper of the two, then, since the deeper parts cannot be below their melting-point, the upper layers must be above their melting-point, and so the roof must melt. This was pointed out many years ago by Lord Kelvin, who, however, had not the necessary data to decide whether the "ice line" for basalt is more or less steep than the adiabatic for liquid basalt. He showed that if, as he expected, the "ice line" were the steeper, then a column of basalt cooled at the top would solidify at the bottom, but the reverse would hold if the adiabatic were the steeper. Our knowledge of the required data is a little more complete, and enables us to form some quantitative idea of the two gradients in question.

The adiabatic gradient is given at once from the well-known formula,

$$\left(\frac{\partial \tau}{\partial p}\right)_\phi = \left(\frac{\partial v}{\partial \phi}\right)_p,$$

where  $\tau$ ,  $\phi$ ,  $p$ , and  $v$  represent the absolute temperature,

entropy, pressure, and volume, respectively, of a given mass of any substance, and the suffixes indicate the constancy of the quantity named. Substituting for the right-hand side, we get

$$\left(\frac{\partial \tau}{\partial p}\right)_\phi = \frac{\tau \alpha}{\sigma \rho},$$

where  $\alpha$  is the coefficient of cubical expansion and  $\sigma$  the specific heat (in work units), both at constant pressure, and  $\rho$  is the density.

If  $x$  is the depth measured from any origin, we have, since  $\frac{d\rho}{dx} = g\rho$ ,

$$\left(\frac{\partial \tau}{\partial x}\right)_\phi = \frac{\tau \alpha g}{\sigma}.$$

$\tau$  may be taken as  $1200^\circ \text{C.}$ , *i. e.*  $1473^\circ$  absolute.

From Day, Sosman, and Hostetter's \* work we find that, at atmospheric pressure,  $\alpha$  for liquid basalt is about  $6.5 \times 10^{-5}$ . Some allowance for the effect of pressure might be made from the relation  $-\left(\frac{\partial \alpha}{\partial p}\right)_\theta = \left(\frac{\partial C}{\partial \theta}\right)_p$ , where  $C$  is the compressibility, if we knew the value of  $\left(\frac{\partial C}{\partial \theta}\right)_p$  for liquid basalt. This is unknown, but is almost certain to be positive, so that  $\alpha$ , and hence the adiabatic gradient, will decrease with increase of depth.  $g$  may be taken as  $981 \text{ cm. (per sec.)}^2$ .

As regards  $\sigma$ , the value that we should expect for solid basalt at sufficiently high temperature, as calculated from its composition, is about 0.28. This accords perfectly with some measurements made by one of us †, which gave values rising at a decreasing rate from 0.20 at  $50^\circ \text{C.}$  to 0.26 at  $600^\circ \text{C.}$  The specific heat of a substance always being greatest in the liquid state, it would seem that the specific heat of liquid basalt must be at least 0.30, or when reduced to work units,  $1.25 \times 10^7$ .

Putting in these values, we find that the adiabatic temperature gradient comes out at  $0.75^\circ$  per kilometre, at the surface, decreasing with increase in depth.

The melting-point gradient is, of course, found from the equation

$$\frac{dT}{dp} = \frac{T(v_2 - v_1)}{L},$$

where  $T$  is the melting-point (absolute),  $L$  the latent heat

\* Amer. J. Sc., January 1914.

† Phil. Mag., January 1914.

of fusion in work units, and  $v_2$  and  $v_1$  the specific volumes of the liquid and solid magma respectively.

Hence, as before, since  $\rho = \frac{1}{v_2}$ ,

$$\frac{dT}{dx} = \frac{gT}{L} \left( 1 - \frac{v_1}{v_2} \right),$$

$T$  may be taken as identical with  $\tau$ , *i. e.*  $1473^\circ$ , and  $L$  as  $90 \times 4.2 \times 10^7 = 3.8 \times 10^9$  work units.

To find  $\frac{v_1}{v_2}$  we have Day, Sosman, and Hostetter's result that solid basalt expands 10 per cent. on melting at air-pressure. On the other hand, allowance must be made for the different compressibilities of the solid and the liquid. Adams and Williamson\* have shown that, up to pressures of about 12,000 megabars (corresponding to a depth of about 40 kilometres),  $C$  for solid gabbro is about  $1.2 \times 10^{-6}$  per megabar, and is very nearly independent of the pressure. These experiments were made at air temperature, but the good agreement between the velocities of earthquake waves calculated from them and those found for moderate depths indicates that the effect of temperature is small.

Very few measurements are available on the effect of liquefaction on the compressibility of substances. Richards, Bartlett, and Hodge† found  $30.5 \times 10^{-6}$  and  $72 \times 10^{-6}$  as the values of  $C$  for solid and liquid benzene, respectively, showing that melting increased the compressibility about 2.4 times. On the other hand, liquids always show a decrease of compressibility with increase of pressure. Thus Adams, Williamson, and Johnston‡ found that the mean compressibility of kerosine oil fell from  $27 \times 10^{-6}$  for a pressure range 2000–3000 megabars to  $15 \times 10^{-6}$  for a range 2000–12,000 megabars, the value for the range 11,000 to 12,000 being only  $8 \times 10^{-6}$ .

Thus it would seem to be very unlikely that, at the pressure involved, the compressibility of liquid basalt would be greater than twice that of the solid, *i. e.*  $2.4 \times 10^{-6}$ .

This would have the effect of reducing  $v_1$  by 1.44 per cent., and  $v_2$  by 2.88 per cent. at 12,000 megabars pressure, so that the expansion on melting would be reduced to 8.56 per cent. Thus, at a depth of 40 kilometres,  $1 - \frac{v_1}{v_2}$  would be 0.079. This would make  $\frac{dT}{dx} = 3.0^\circ$  per kilometre.

\* J. Franklin Inst., April 1923.

† J. Amer. Chem. Society, July 1921.

‡ J. Amer. Chem. Society, January 1919.



Thus the melting-point gradient comes out as 4 times as steep as the adiabatic at a depth of 40 kilometres. It will be noticed that the effect of the compressibilities, assumed above, is to reduce the melting-point gradient by 14.4 per cent., no allowance being made for the effect on the adiabatic. To make the gradients equal at this level, we should have to assume a compressibility for the liquid nearly 6.5 times as great as that of the solid, and disregard the effect of this compressibility on the coefficient of expansion. With the above assumptions as to compressibilities, the gradients would become equal at a depth of about 220 kilometres.

It would therefore appear to be very improbable that, at depths less than 200 kilometres, the adiabatic could be steeper than the melting-point gradient. It is possible that at greater depths the adiabatic might be the steeper. Here, however, other materials would probably occur, and the pressures involved would be so far beyond those for which any data are available that speculation at present appears rather futile.

Let us consider a layer of basaltic magma of such a depth that thermal conduction through the solid cannot carry off the heat generated by radioactivity in the magma, and that rising from below, readily enough to prevent the deeper layers from rising above their melting-point. In course of time melting would occur, and as the lower parts of the melted layer could not be below their melting-point, the top of the layer would necessarily be above its melting-point. Thus it would constantly melt its way upwards through the overlying roof.

The liquid which had been cooled by contact with the roof, and that formed by the fusion of the roof, would be above their melting-point but below the temperature proper to their level, and would sink through the magma. As this liquid sank, it would, in spite of the rise due to adiabatic compression, always be at a lower temperature than its surroundings, until it might reach such a depth that partial solidification occurred. Thus, unless there were a source of heat below, and in, the magma layer sufficient to provide all the latent heat of the melted roof and that lost by conduction through the roof, this heat would be partly provided by the solidification of magma in the deeper layers.

At first the resolidification in the deeper layers might be small or entirely absent, and the liquid layer would increase in thickness at the expense of the overlying crust. As this became thinner the heat-loss through it would increase, and resolidification would set in in the deeper layers of the

magma. This would in time become equal to, and finally greater than, the rate of melting of the roof, so that the liquid layer would attain a maximum thickness, after which it would decrease again, while continuing all the time to eat its way upwards. It would finally disappear when it had risen to such a level that the loss of heat through the reduced crust caused complete solidification. The resolidified magma, underlying the liquid layer, would, as Lord Kelvin pointed out, be everywhere near its melting-point: thus at a depth of 40 kilometres the temperature gradient would be about  $3^{\circ}\text{C.}$  per kilometre, falling slowly with increase of depth. This gradient would only suffice to carry off by solid conduction the radioactive heat generated in a layer of basalt about 4 kilometres thick, or in one of eclogite or dunite 8 kilometres thick. Thus, remelting of the deeper layers would be inevitable, followed by repetition of the entire cycle.

Thus we seem to be driven to the conclusion that a deep layer of magma whose radioactivity is at all comparable with that of surface specimens of basic or ultra-basic rocks would undergo periodic changes of state, which would be accompanied by corresponding changes in the temperature gradient in the overlying crust.

The result would be quite independent of all assumptions as to the effects of tidal displacements, if the infusible continental masses were absent. Where, however, such granitic materials form an infusible crust of sufficient thickness, resolidification of the underlying basaltic magma would be prevented, so that the present solidity of the magma underlying the continents seems to be most readily explained by Dr. Joly's assumption that, during revolutionary periods, tidal effects in the liquid magma produce lateral displacements of the continental masses, and so allow the accumulated heat to escape.

We seem, then, to be faced with two alternatives:—

We may deny that the radioactivity of the deep-seated rocks is at all comparable to that of the specimens which are available to us. We must then either deny the occurrence of the revolutions that geologists have found such strong evidence for, or accept them as unexplained facts.

We may, on the other hand, assume that the radioactive measurements of available specimens are of some value. We then have an explanation of these revolutions forced upon us.

*LXIX. The Absolute Zero of the Externally Controllable Entropy and Internal Energy of a Substance and a Mixture.*

*To the Editors of the Philosophical Magazine.*

GENTLEMEN,—

**I**N a paper that appeared in the April number of the *Phil. Mag.* (1927) I showed that the controllable internal energy and entropy are zero of a substance under its vapour-pressure at the absolute zero of temperature, by means of the theorem, established in a certain way, that the specific heat at constant volume is a positive quantity. I would like to point out that this theorem can be shown to follow simply from our notions of heat as follows :—Suppose that a substance A is completely surrounded by a substance B at the same temperature, and that the former substance has a negative specific heat. Now suppose that the substance B is raised in temperature by  $\partial T$ . An initial flow of heat from B to A will take place; otherwise there would be nothing to indicate to the substance A that the temperature of the substance B has been raised by  $\partial T$ . An evolution of heat in the substance A will now take place, tending to produce a flow of heat in the opposite direction since its specific heat is negative. But suppose that this flow of heat is checked by keeping the substance B at the same temperature as that of the substance A till no further change in its temperature takes place. In this manner the temperature of the substance A may be raised to any value we please by repeating the process the necessary number of times. The substance A will evidently only receive heat under these conditions—in other words, a negative specific heat is impossible. The result will evidently hold whether the substance A is kept at constant volume or at constant pressure.

Yours faithfully,

R. D. KLEEMAN.

*LXX. Notices respecting New Books.*

*Ordinary Differential Equations.* By E. L. INCE, Professor of Pure Mathematics in the Egyptian University. Pp. viii+558, with 18 figures. (London: Longmans, Green & Co. 1927. Price 36s. net.)

**T**HE subject of differential equations is one that has of recent years been seriously neglected in England. The reason for this, in the words of the author, is that "England has but one

school of Pure Mathematics, which implies a high development in certain fields and a comparative neglect of others. To spread the energies of this school over the whole domain of Pure Mathematics would be to scatter and weaken its forces; consequently its interests, which were at no time particularly devoted to the subject of Differential Equations, have now turned more definitely into other channels, and that subject is denied the cultivation which its importance deserves."

The standard English work on the subject, the 'Theory of Differential Equations,' by Professor Forsyth, is too comprehensive for the ordinary student, and now requires to be brought up to date, as there has been much work done in this subject since its publication. There was thus need for a treatise such as the one under review.

The treatise is not intended for the elementary student or for the student of physics or engineering, whose aim is merely to derive solutions of the equations which present themselves in the course of their work. It is written for the advanced student of pure mathematics, and demands of the reader a fairly comprehensive knowledge of modern analysis.

The volume is divided into two parts which deal with differential equations in the real and complex domains respectively. The appendices include a historical note on formal methods of integration and a note on the numerical integration of ordinary differential equations. References to original papers are given throughout.

The treatment is throughout clear and logical, and no serious errors have been noted, though there are a number of misprints—generally obvious—which are accounted for by the fact that, owing to his appointment at the Egyptian University, the author was unable to correct the final proofs.

Professor Ince is to be congratulated on having written a treatise which will undoubtedly be found of very great value by the students of pure mathematics and which, it may be hoped, will do something towards stimulating the study of differential equations in England.

*An Outline of Stellar Astronomy.* By PETER DOIG, F.R.A.S.  
Pp. viii+183, with 24 figures. (London: Draughtsman Publishing Co. 1927. Price 7s. 6d., post free.)

MR. DOIG writes in a very lucid manner of some of the modern developments of stellar astronomy, and the student who from lack of mathematical equipment is unable to appreciate many of the original papers will find this little volume a great help. Even the more advanced student will find it of interest, for the author brings an original mind to bear upon the subject.

The volume is not suitable for a first introduction to stellar astronomy. It is not sufficiently connected or comprehensive. It consists to all intents and purposes of a series of notes which illuminate different aspects of the subject. An extensive field is covered; the observational data are first dealt with—the dimensions, luminosities, and masses of the stars; their numbers, movements, and distribution; binary and variable stars. Modern views as to the nature of a star and the cause of stellar evolution are summarised. Finally, the structure of the galactic system and of external systems—the Magellanic Clouds, spiral nebulae, etc.—is discussed.

There are numerous diagrams and reproductions of astronomical photographs, but the latter are in general of poor quality.

## LXXI. *Proceedings of Learned Societies.*

### GEOLOGICAL SOCIETY.

[Continued from p. 224.]

November 30th, 1927.—Dr. F. A. Bather, M.A., F.R.S.,  
President, in the Chair.

Prof. D. I. MUSHKETOV, Director of the Russian Geological Survey, gave a brief account, illustrated by lantern-slides, of the results of recent work in the Alai and Trans-Alai chains in Southern Turkestan, north of the Pamirs. The first geological survey of this region was made in 1909. The results then obtained have been confirmed and amplified by the surveys of 1925 and the two succeeding years made by the speaker and by A. P. Markovski. In the western part of the Alai chain abundant confirmatory evidence was obtained of a Pamir (Alpine) system of folding, due to pressure from the south acting in Kainozoic times and causing overthrusting of Palaeozoic rocks over Cretaceous and Tertiary. Observations in the western part of the Trans-Alai chain lead to the conclusion that the northern slope of this part of the chain is a large isosyncline, overturned northwards and lying nearly horizontal. Its core consists of much-folded Upper Cretaceous and Eocene marls and clays, raised by the folding to a height of some 18,000 feet. It seems likely that the whole of the Trans-Alai chain was overthrust on to the Alai chain to the north.

East of the meridian of Mount Kaufmann the direction of the whole Alai chain swings from an east-to-west to a north-to-south direction—the ‘Ferghana flexure.’ On the southern limb of this flexure there has occurred another great overthrust, a sheet of massive Devonian limestones having been thrust from south to

north over Kainozoic and Cretaceous beds. The surface of this over-riding sheet dips distinctly south-eastwards at 35°. The observations of the recent Pamir expedition under D. V. Nalivkin confirm the views arrived at in the Alai chains.

The following communication was read :—

‘The Granites of the Scilly Isles, and their Relation to the Dartmoor Granites.’ By Charles William Osman, M.Inst.C.E., F.G.S.

Assuming that the whole of the granites of Devon and Cornwall are due to the same cause, late adjustments of the post-Carboniferous revolution, it is shown, by comparing the two ends of the series, that the isostatic correction-sequence of intrusions is similar in both areas.

The separate successive intrusions are tabulated for both areas in their corresponding stages.

Previous to the intrusion of the granites the South-West of England had been subjected to three separate foldings, and the positions of the granite-laccolites are directly related to the intersection of the ridges of these folds: (*a*) Post-Silurian, Caledonian folding; (*b*) Post-Middle Coal-Measures, Malvernian folding; and (*c*) Post-Carboniferous, Armorican folding.

Although the order of the granitic intrusions is found to be the same throughout the whole district, it would not appear that all these took place simultaneously, and reasons are given to show that the Scilly Isles and Bodmin-Moor Stage 2 A granites were intruded earlier, and had consolidated before the Dartmoor Stage 2 A was intruded.

The Scilly Isles being a typical granite-laccolite that has been dissected by Nature, afford exceptional advantages for the study of the formation of such compound intrusions, having been planed down by the advance and retreat of the seas of the Upper Cretaceous Period, the Eocene uplift, and the Pliocene sea—so that now no part rises higher than 166 feet above mean sea-level. Also numerous cross-sections have been made by the formation of north-south sea-channels, probably due to slight further Malvernian movement.

Stage 1 is a basic microgranite found only as inclusions in Stage 2 A coarse-grained, and Stage 2 B medium-grained granites.

The directions of flow of the granite for Stages 2 A & 2 B are traced back to their inlet. Stage 3 is a fine-grained granite, intruded after the previous stages had consolidated, and it is shown that Stage 3 not only made a new inlet, but, in doing this, formed thrust-planes of low hade in Stage 2 A and Stage 2 B intrusions. The later subsidence of the inlets produced Crow Sound and St. Mary's Sound, and the age of these inlet subsidences are possibly as late as the Pneumatolytic Stage. Stage 4 is a later fairly large marginal intrusion of a microgranite of

aplitic nature, intruded locally between Stage 2 B above and Stage 3 beneath. All these stages in Scilly entered the laccolite from the two inlets mentioned.

The secondary smaller intrusions of aplites have dyke sources principally along Caledonian direction-faults, and form sill-intrusions into shrinkage and other joints.

The Pneumatolytic Stage is represented by greisen lines and schorl-quartz reefs, which generally infill small faults of Caledonian trend.

The principles of the granite-magma crystallization shrinkage-jointing are described in regard to the production of pseudo-anticlines and synclines, as being significant of direct roof-cooling influence, and the effect of roof-subsidence during the consolidation of such structures is dealt with and examples are given. It is also shown that the deeper into the laccolite the jointing is observed the flatter the bed-joints become, as the roof-cooling influence is exhausted, until in the centre of the islands the bedding-joints are horizontal.

The later faulting and bands of slip-shearing in the granites are considered, and the effect on the present features of the Scilly Isles is described.

Petrological details are given to show the distinct differences between the granites of Bodmin Moor and the Scilly Isles and the remainder of the South-Western granites, indicating a different source; and it is suggested that these two granite-laccolites were supplied from a great Caledonian direction-fault or series of faults parallel with, but some miles off, the north-western coast of Cornwall; also that only from such great faults could the allied Lundy-Island granite have been intruded, all the other granite-laccolites being intruded from the Start-Lizard series of faults.

The pre-granitic xenolithic inclusions in the Scilly granites indicate a great difference in age between the floor and the roof of this laccolite. The contorted schist inclusions are similar to the biotite-felspar-andalusite-garnet-schists of the south-west of the Lizard. These may be Archæan, or possibly of Lower Palæozoic (Mylor) age, and the granites probably rest on a platform of similar rocks; while the uncontorted quartz-biotite-cordierite-spinel-schists, though possibly of Devonian age, so closely resemble the Lower Carboniferous inclusions of Dartmoor, that those rocks probably formed the roof of this laccolite.

---

*[The Editors do not hold themselves responsible for the views expressed by their correspondents.]*

THE  
LONDON, EDINBURGH, AND DUBLIN<sup>7</sup>  
PHILOSOPHICAL MAGAZINE  
AND  
JOURNAL OF SCIENCE.

[SEVENTH SERIES.]

APRIL 1928.

LXXII. *The Stream-line Motion of Fluid in a Curved Pipe.*  
(Second Paper.) By W. R. DEAN, M.A., Imperial  
College of Science\*.

**I**N a previous paper † a first approximation has been found to the steady motion of incompressible fluid through a pipe of circular cross-section (radius  $a$ ) coiled in a circle of radius  $R$ . The first approximation gives a motion in qualitative agreement with that found experimentally, but is valid only in a limited field, and fails to show that the relation between pressure gradient and rate of flow through a curved pipe is dependent on the curvature; the present paper is the outcome of an attempt to extend the analysis so as to find this dependence theoretically.

This extension, so far as it has been carried, represents a fourth approximation to the problem; it is given in §§ 2–9. It leads to no important quantitative result; it shows that the rate of flow is slightly reduced by curvature, even in the limited range of velocities to which it applies, and makes possible an estimate of the velocity at which in a given case the reduction is first likely to be measurable. The difficulty of making the successive approximations increases so rapidly that no further extension on the same lines is worth while.

It appears, however, in the course of the work that the reduction in the rate of flow due to curvature depends on a single variable  $K$ , equal to  $2\pi^2 a/R$  when the motion is slow,

\* Communicated by Prof. S. Chapman, F.R.S.

† Phil. Mag. iv. p. 208 (1927).



$n$  being the Reynolds' number, and always of this order of magnitude. The problem of determining the relation between flux and pressure gradient in any curved pipe (the motion being, of course, supposed stream-line) therefore reduces to that of finding a single function  $f(K)$ . This result is not exact: in §3 the assumption that  $a/R$  is small is made, but it is shown in §7 by consideration of an analogous assumption that the error, nominally of order  $a^2/R^2$ , is not likely to be serious.

The function  $f(K)$  can be determined by experiment on a single curved pipe, and it is therefore possible to correlate experimental results for pipes of different curvatures. In §§ 12-18 the theory is applied to observations due to Prof. J. Eustice of the rate of flow of water through pipes of various radii of curvature,  $R$ . In these experiments a single flexible tube was used, and wound on cylinders of different radii in order to vary  $R$ ; there was in consequence distortion, considerable in some cases, of the tube. The tube was found to be sinuous when free, and may have remained in this condition when coiled. It therefore appeared better to correlate several pairs of results than to attempt to determine  $f(K)$  absolutely. The agreement found when the motion is stream-line (by this is meant, when  $n < 2000$ ) is good, except in one case, wherein the distortion of the tube due to coiling was exceptionally large.

All calculations have been extended to velocities above the assumed critical velocity. Though the errors that result are not in certain conditions large, it is clear that the theory applies only to stream-line motion; it can, however, probably be modified so as to apply to all velocities by substituting a coefficient of eddy viscosity for the ordinary coefficient  $\mu$ .

2. Fig. 1 shows the system of coordinates that has been used. The surface of a pipe of circular section, coiled in a circle, is an anchor ring; the figure shows  $OZ$ , the axis of the anchor ring, and a section of it by an axial plane that makes an angle  $\theta$  with a fixed axial plane. The position of any point  $P$  is specified by the orthogonal coordinates  $r, \phi, \theta$ . The components of the velocity of the fluid corresponding to these coordinates are  $U, V, W$ ;  $U$  is therefore in the direction  $CP$ ,  $V$  perpendicular to  $U$  and in the plane of the cross-section, and  $W$  perpendicular to this plane. The radius of any cross-section is  $a$ , while  $R$  is the radius of the circle in which the pipe is coiled.

It is assumed that the motion of the fluid is steady, and,

further, that  $U$ ,  $V$ , and  $W$  (but not  $P$ , the pressure) are independent of  $\theta$ .

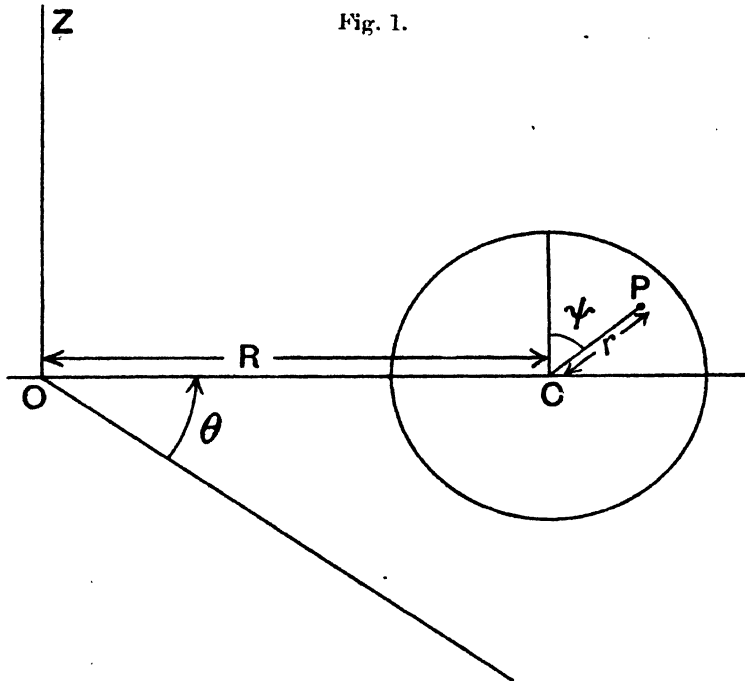


Fig. 1.

The equations of motion are then

$$U \frac{\partial U}{\partial r} + \frac{V}{r} \frac{\partial U}{\partial \psi} - \frac{V^2}{r} - \frac{W^2 \sin \psi}{R + r \sin \psi} = - \frac{\partial}{\partial r} \left( \frac{P}{\rho} \right) - \nu \left( \frac{1}{r} \frac{\partial}{\partial \psi} + \frac{\cos \psi}{R + r \sin \psi} \right) \left( \frac{\partial V}{\partial r} + \frac{V}{r} - \frac{1}{r} \frac{\partial U}{\partial \psi} \right), \quad (1)$$

$$U \frac{\partial V}{\partial r} + \frac{V}{r} \frac{\partial V}{\partial \psi} + \frac{UV}{r} - \frac{W^2 \cos \psi}{R + r \sin \psi} = - \frac{1}{r} \frac{\partial}{\partial \psi} \left( \frac{P}{\rho} \right) + \nu \left( \frac{\partial}{\partial r} + \frac{\sin \psi}{R + r \sin \psi} \right) \left( \frac{\partial V}{\partial r} + \frac{V}{r} - \frac{1}{r} \frac{\partial U}{\partial \psi} \right), \quad (2)$$

and

$$U \frac{\partial W}{\partial r} + \frac{V}{r} \frac{\partial W}{\partial \psi} + \frac{UW \sin \psi}{R + r \sin \psi} + \frac{VW \cos \psi}{R + r \sin \psi} = - \frac{1}{R + r \sin \psi} \frac{\partial}{\partial \theta} \left( \frac{P}{\rho} \right) + \nu \left[ \left( \frac{\partial}{\partial r} + \frac{1}{r} \right) \left( \frac{\partial W}{\partial r} + \frac{W \sin \psi}{R + r \sin \psi} \right) + \frac{1}{r} \frac{\partial}{\partial \psi} \left( \frac{1}{r} \frac{\partial W}{\partial \psi} + \frac{W \cos \psi}{R + r \sin \psi} \right) \right]. \quad (3)$$

The fluid is assumed incompressible; then the equation of continuity is

$$\frac{\partial U}{\partial r} + \frac{U}{r} + \frac{U \sin \psi}{R + r \sin \psi} + \frac{1}{r} \frac{\partial V}{\partial \psi} + \frac{V \cos \psi}{R + r \sin \psi} = 0. \quad (4)$$

3. It is now assumed that the curvature of the pipe is small: that is, that  $a/R$  is small. We can then, for example, replace  $(R + r \sin \psi)$  by  $R$ , and

$$\frac{\partial}{\partial r} + \sin \psi / (R + r \sin \psi)$$

by  $\partial/\partial r$ ; on the other hand, there is clearly no immediate reason for neglecting

$$W^2 \sin \psi / (R + r \sin \psi)$$

in comparison with  $V^2/r$ . This assumption greatly simplifies the four fundamental equations, but there is little doubt that it leaves unaffected the terms which are most important in deciding the effect of curvature on the motion. (See § 7.)

Equations (1) to (4) now become

$$U \frac{\partial U}{\partial r} + \frac{V}{r} \frac{\partial U}{\partial \psi} - \frac{V^2}{r} - \frac{W^2 \sin \psi}{R} = - \frac{\partial}{\partial r} \left( \frac{P}{\rho} \right) - \frac{\nu}{r} \frac{\partial}{\partial \psi} \left( \frac{\partial V}{\partial r} + \frac{V}{r} - \frac{1}{r} \frac{\partial U}{\partial \psi} \right), \quad (5)$$

$$U \frac{\partial V}{\partial r} + \frac{V}{r} \frac{\partial V}{\partial \psi} + \frac{UV}{r} - \frac{W^2 \cos \psi}{R} = - \frac{1}{r} \frac{\partial}{\partial \psi} \left( \frac{P}{\rho} \right) + \nu \frac{\partial}{\partial r} \left( \frac{\partial V}{\partial r} + \frac{V}{r} - \frac{1}{r} \frac{\partial U}{\partial \psi} \right), \quad (6)$$

$$U \frac{\partial W}{\partial r} + \frac{V}{r} \frac{\partial W}{\partial \psi} = - \frac{1}{R} \frac{\partial}{\partial \theta} \left( \frac{P}{\rho} \right) + \nu \left( \frac{\partial^2 W}{\partial r^2} + \frac{1}{r} \frac{\partial W}{\partial r} + \frac{1}{r^2} \frac{\partial^2 W}{\partial \psi^2} \right), \quad (7)$$

and 
$$\frac{\partial U}{\partial r} + \frac{U}{r} + \frac{1}{r} \frac{\partial V}{\partial \psi} = 0. \quad (8)$$

As  $U$ ,  $V$ , and  $W$  are assumed independent of  $\theta$ , it follows from (7) that  $P/\rho$  must be of the form  $\theta f_1(r, \psi) + f_2(r, \psi)$ , and then from (5) and (6) that  $f_1(r, \psi)$  must be a constant. We can therefore write

$$- \frac{1}{R} \frac{\partial}{\partial \theta} \left( \frac{P}{\rho} \right) = \frac{G}{\rho}, \quad (9)$$

where  $G$  is a constant which may be termed the mean

pressure gradient; it is equal to the space-rate of decrease in pressure along the central line\*.

From (8) we can write

$$rU = -\frac{\partial f}{\partial \psi}, \quad V = \frac{\partial f}{\partial r}, \quad \dots \quad (10)$$

where  $f$  is a function of  $r$  and  $\psi$  only. Inserting these expressions for  $U$  and  $V$  in the equations and eliminating  $P$  from (5) and (6), we have the two equations

$$\left(\frac{\partial f}{\partial \psi} \frac{\partial}{\partial r} - \frac{\partial f}{\partial r} \frac{\partial}{\partial \psi}\right) \nabla_1^2 f + \frac{2W}{R} \left(r \cos \psi \frac{\partial W}{\partial r} - \sin \psi \frac{\partial W}{\partial \psi}\right) = -\nu r \nabla_1^4 f, \quad \dots \quad (11)$$

$$\text{and} \quad \frac{1}{r} \left(\frac{\partial f}{\partial r} \frac{\partial W}{\partial \psi} - \frac{\partial f}{\partial \psi} \frac{\partial W}{\partial r}\right) = G/\rho + \nu \nabla_1^2 W, \quad \dots \quad (12)$$

$$\text{where} \quad \nabla_1^2 \equiv \frac{\partial^2}{\partial r^2} + \frac{1}{r} \frac{\partial}{\partial r} + \frac{1}{r^2} \frac{\partial^2}{\partial \psi^2}. \quad \dots \quad (13)$$

4. Equations (11) and (12) can be put in non-dimensional form by the substitutions

$$f = \nu \phi, \quad W = W_0 w, \quad r = ar', \quad \dots \quad (14)$$

where  $W_0$  is assumed to have the dimensions of a velocity; they then become

$$\left(\frac{\partial \phi}{\partial \psi} \frac{\partial}{\partial r'} - \frac{\partial \phi}{\partial r'} \frac{\partial}{\partial \psi}\right) \nabla_1^2 \phi + Kw \left(r' \cos \psi \frac{\partial w}{\partial r'} - \sin \psi \frac{\partial w}{\partial \psi}\right) = -r' \nabla_1^4 \phi, \quad (15)$$

$$\text{and} \quad \frac{1}{r'} \left(\frac{\partial \phi}{\partial r'} \frac{\partial w}{\partial \psi} - \frac{\partial \phi}{\partial \psi} \frac{\partial w}{\partial r'}\right) = C + \nabla_1^2 w. \quad \dots \quad (16)$$

In these equations

$$K = 2W_0^2 a^3 / \nu^2 R, \quad \dots \quad (17)$$

and

$$C = Ga^2 / \mu W_0; \quad \dots \quad (18)$$

$\nabla_1^2$  now stands for the operator derived from expression (13) by replacing  $r$  by  $r'$ : there is no need to alter the notation. As to the constant  $K$ : if the motion is slow,  $W_0$  can be taken to be the " $\theta$ " component of the velocity of the fluid at any point of the central line, and the distribution of this component approximates to that in a straight pipe, and is nearly parabolic. Consequently  $aW_0/\nu$  is roughly

\* The circle traced out by  $C$ , fig. 1.

equal to the Reynolds' number  $n$ , which is  $\bar{v}d/\nu$ , where  $\bar{v}$  is the mean velocity and  $d$  the diameter of the pipe. Thus for slow motion,  $K=2n^2a/R$ .

The problem is now to find solutions of equations (15) and (16) that will satisfy the boundary conditions; these require that the velocity ( $U, V, W$ ) should vanish at the surface of the pipe,  $r=a$ , so that we must have

$$\frac{\partial \phi}{\partial r'} = \frac{\partial \psi}{\partial \psi} = w = 0, \quad . \quad . \quad . \quad (19)$$

when  $r'=1$ .

5. Very little progress has at present been made analytically. No method has so far been found other than that of successive approximation, which is effectively equivalent to expanding  $\phi$  and  $w$  in ascending powers of  $K$ . The difficulty is, that  $K$  is not small in most cases. Suppose that  $a/R=0.01$ ; this must be considered a small value of  $a/R$ , though pipes of smaller curvature have certainly been used in experiment. Suppose, further, that the critical velocity in this pipe is the same as if the pipe were straight: it is then such that  $n=2000$ . Although  $K$  is not always equal to  $2n^2a/R$ , it is always of this order of magnitude, and consequently for a complete discussion of stream-line motion we must have a solution of the equations that holds for values of  $K$  up to perhaps  $10^5$ . It is certain that such solutions cannot be obtained by successive approximation; four approximations have been found, and give a result probably not valid when  $K$  exceeds 400. Some account of the method is given in the following paragraphs.

It follows immediately that there is no theoretical ground for supposing that if  $a/R$  is small the motion in a curved pipe must approximate to that in a straight pipe; the far more stringent condition that  $K$  must be small has to be fulfilled.

6. If the pipe is straight,  $a/R$ , and therefore  $K$ , are zero, and equations (15) and (16) can be satisfied by

$$w=1-r'^2, \quad \phi=0,$$

provided  $C=4$ . No arbitrary constant is required in the expression for  $w$ ;  $W_0$  is the only constant needed.

If  $K$  is not zero, let

$$\left. \begin{aligned} w &= w_0 + Kw_1 + K^2w_2 + \dots, \\ \phi &= K\phi_1 + K^2\phi_2 + \dots, \end{aligned} \right\} \quad . \quad . \quad . \quad (20)$$

where  $w_0, w_1, \phi_1, w_2, \phi_2, \dots$  are functions of  $r'$  and  $\psi$  only.

Substituting these expressions in the equations and equating coefficients of powers of  $K$ , we have a series of relations from which  $w_0, w_1, \phi_1 \dots$  can successively be found:

The first equation from (16) is

$$\nabla_1^2 w_0 + C = 0; \quad . \quad . \quad . \quad (21)$$

this and the boundary condition  $w=0, r'=1$  are satisfied by

$$w_0 = 1 - r'^2, \quad C = 4. \quad . \quad . \quad . \quad (22)$$

The first equation from (15) is

$$\begin{aligned} r' \nabla_1^4 \phi_1 &= -r' \cos \psi w_0 \frac{\partial w_0}{\partial r}, \\ &= 2r'^2(1-r'^2) \cos \psi; \quad . \quad . \quad . \quad (23) \end{aligned}$$

to satisfy this and the boundary conditions  $\frac{\partial \phi}{\partial r'} = \frac{\partial \phi}{\partial \psi} = 0$ ,  $r'=1$ , we must take

$$\phi_1 = \frac{\cos \psi}{144} r'(1-r'^2)^2(1-r'^2/4). \quad . \quad . \quad . \quad (24)$$

The second equation from (16) is

$$\nabla_1^2 w_1 = -\frac{1}{r'} \frac{\partial \phi_1}{\partial \psi} \frac{\partial w_0}{\partial r'}, \quad . \quad . \quad . \quad (25)$$

whence

$$w_1 = \frac{\sin \psi}{576} \left( \frac{19r'}{40} - r'^3 + \frac{3r'^5}{4} - \frac{r'^7}{4} + \frac{r'^9}{40} \right). \quad . \quad (26)$$

7. At this stage it is convenient to consider the probable effect of the assumption made in § 3. In the first paper \* the functions  $\phi_1$  and  $w_1$  were calculated exactly, so that the errors in expressions (24) and (26) can be found. In (24) there is no error, while to get the correct expression for  $w_1$  there must be added to (26)

$$-3ar'(1-r'^2) \sin \psi / 4RK.$$

$K$  can certainly exceed  $10^4$ , and only cases in which  $K$  is large are of interest; it can be concluded that, at least in the early stages, the important parts of the terms are unaffected. The assumption can, however, be examined from a more general point of view. It is purely geometrical; by a sufficient decrease in  $a/R$  the error due to it can be reduced to within any given limit; but if at the same time the mean velocity is sufficiently increased,  $K$  will not be small, and the motion will be quite different from that in a

\* Phil. Mag. iv. p. 214 (1927), equations (23) to (25).

straight pipe. What is of most interest is the effect of curvature on the relation between pressure gradient and rate of flow. The reason why the pressure required to maintain a given rate of flow is greater in a curved pipe than in a straight one is mainly that in a curved pipe part of the fluid is continually oscillating between the central part of the pipe, where the velocity is high, and the neighbourhood of the boundary, where the velocity is low. This movement is due to the centrifugal tendency of the fluid, and implies a loss of energy which has no counterpart in stream-line motion in a straight pipe. It is clear from equations (5) and (6), wherein two terms equivalent to an inward acceleration of  $W^2/R$  appear, that the lateral motion of the fluid is not eliminated by the assumption made; we can say, then, that it ignores in the equations of motion the geometrical terms due to curvature, but leaves the dynamical terms unaffected.

In the similar problem of flow in a curved channel (bounded by two coaxial circular cylinders) there is no lateral motion of the fluid. Hence the effect of curvature is, in the sense defined, purely geometrical, and as its magnitude is known, we can get an idea of the error likely to result from the assumption made in the other problem.

The ratio of the flux due to given pressure gradient\* in a channel whose boundaries are cylinders of radii  $R \pm a$ , to that due to the same gradient in a channel bounded by parallel plane walls a distance  $2a$  apart, is

$$\frac{3}{16a^4} \left[ 4R^2a^2 - (R^2 - a^2)^2 \left\{ \log \frac{R+a}{R-a} \right\}^2 \right].$$

When  $a/R$  is small this expression is approximately

$$1 - 2a^2/15R^2; \quad \dots \dots (27)$$

when  $a/R$  has its maximum value unity (the inner cylinder being then a line) the ratio has its minimum value  $3/4$ . Hence in this case the geometrical effect of curvature cannot in any circumstances reduce the rate of flow by more than  $1/4$ , and from expression (27) we can perhaps infer that the error due to the assumption made in the other problem, nominally of order  $a^2/R^2$ , is not likely to be really greater on account of large coefficients.

8. The rate of flow is proportional to

$$\int_0^1 dr' \int_0^{2\pi} r' w d\psi,$$

\* This is a mean pressure gradient defined as in § 3.

and is therefore determined by the part of  $w$  that is independent of  $\psi$ . Consequently  $w_1$  makes no contribution, so that at the present stage of the approximation the relation between flux and pressure is the same as if the pipe were straight. The next approximation does modify this relation, and can be found without difficulty.

From equation (15)

$$\begin{aligned} -r' \nabla_1^4 \phi_2 = & \left( \frac{\partial \phi_1}{\partial \psi} \frac{\partial}{\partial r'} - \frac{\partial \phi_1}{\partial r'} \frac{\partial}{\partial \psi} \right) \nabla_1^2 \phi_1 \\ & + w_0 \left( r' \cos \psi \frac{\partial w_1}{\partial r'} - \sin \psi \frac{\partial w_1}{\partial \psi} \right) \\ & + w_1 r' \cos \psi \frac{\partial w_0}{\partial r'}, \end{aligned}$$

and  $\phi_2$  is therefore proportional to  $\sin 2\psi$ . Again,

$$r' \nabla_1^2 w_2 = \left( \frac{\partial \phi_1}{\partial r'} \frac{\partial w_1}{\partial \psi} - \frac{\partial \phi_1}{\partial \psi} \frac{\partial w_1}{\partial r'} \right) - \frac{\partial \phi_2}{\partial \psi} \frac{\partial w_0}{\partial r'},$$

and it follows that  $w_2$  is of the form  $f_2(r') + F_2(r') \cos 2\psi$ . The second of these terms need not be calculated, as it does not affect the flux to order  $K^2$  \*. Consequently  $\phi_2$  need not be evaluated. We then have, to determine that part of  $w_2$  which is a function of  $r'$  only,

$$r' f_2''(r') + f_2'(r') = \frac{1}{2} (\chi_1' f_1 + \chi_1 f_1'),$$

where dashes denote differentiations with respect to  $r'$ ,  $\phi_1 = \chi_1 \cos \psi$ , and  $w_1 = f_1 \sin \psi$ . On integrating this equation we have

$$r' f_2'(r') = \frac{1}{2} f_1 \chi_1,$$

the arbitrary constant vanishing; thence by using (24) and (26), and integrating again,

$$\begin{aligned} f_2(r') = \frac{1}{32(144)^2} [ & -0.1839 + 0.95 r'^2 - 2.0687 r'^4 + 2.4750 r'^6 \\ & - 1.7781 r'^8 + 0.7850 r'^{10} - 0.2062 r'^{12} \\ & + 0.0286 r'^{14} - 0.0016 r'^{16} ]. \end{aligned}$$

\* It must be calculated for a closer approximation:  $w_1$  cannot be found until  $F_2(r')$  is known.



The corresponding approximation to the flux is given by

$$\begin{aligned}\int_0^a 2\pi r W dr &= 2\pi W_0 a^2 \int_0^1 r' w dr' \\ &= 2\pi W_0 a^2 \int_0^1 r' [1 - r'^2 + K^2 f_2(r')] dr' \\ &= \frac{\pi W_0 a^2}{2} \left[ 1 - \left( \frac{K}{576} \right)^2 (0.03058) \right].\end{aligned}$$

If the pipe were straight the flux would be  $\pi W_0 a^2/2$ . The factor in square brackets, and similar factors below, will be denoted  $F_c/F_s$ . Then

$$F_c/F_s = 1 - \left( \frac{K}{576} \right)^2 (0.03058) \quad . \quad . \quad (28)$$

represents the decrease in flux due to the curvature; it is the ratio of the rates of flow due to a given pressure gradient in two pipes of the same cross-section which are respectively curved and straight.

9. It is possible to find the limits within which equation (28) is reliable only by carrying the process of approximation to a further stage. The difficulty of successively finding the functions  $\phi$  and  $w$  becomes rapidly greater, and only the third term has been found of the series whose first two terms are given by (28); even this calculation is rather long, and no numerical details will be given. The resulting expression for the ratio is

$$F_c/F_s = 1 - \left( \frac{K}{576} \right)^2 (0.03058) + \left( \frac{K}{576} \right)^4 (0.01195). \quad (29)$$

A rough estimate of the range of validity of equation (29) can be made. It can certainly be assumed that if the curvature of a pipe of given cross-section is increased, the flux due to a given pressure gradient will diminish. Hence  $F_c/F_s$  must decrease as  $a/R$  increases; it must therefore decrease as  $K$  increases. Expression (29) for  $F_c/F_s$  has a minimum value when  $K$  is roughly 650, so that the result cannot in any case be used if  $K$  exceeds this value. The error of (29) when  $K=576$  is not likely to be serious\*. For this value of  $K$ ,  $F_c/F_s$  is 0.981, so that the flux is reduced in consequence of the curvature by about 1.9 per cent. The reduction will be greater if  $K$  is increased, by increasing either the curvature or the mean velocity.

\* This is clear from the expressions for  $\phi_3$ ,  $w_3$ ,  $w_4$ , not given here.

This is the only ~~result~~ <sup>Equation (29)</sup> that can be obtained from the preceding work at its present stage, and any extension of it on the same lines is not likely to lead to anything of much greater value. Suppose, for instance, that  $K$  is 1000, a value which, as we have seen, must be considered relatively small. Equation (29) gives a value of  $F_c/F_s$  greater than unity, so that the fourth term of this series must be calculated, and even if the value of  $F_c/F_s$  is then less than unity, at least one more term must be found to see to what extent the result given by the first four terms is reliable. In the most favourable case eight more of the functions  $\phi$  and  $w$  must be evaluated, and each of these evaluations will be lengthier than the one before.

10. Some information of a more general character can, however, be deduced from the preceding work. In the first place we can roughly estimate the velocity at which the relation between pressure gradient and flux in a given curved pipe begins to differ appreciably from that for a straight pipe of the same cross-section. To take a numerical example, suppose that pressure and flux can be measured to an accuracy of one per cent. We see that  $F_c/F_s = 0.99$  when  $K$  is roughly 350, using equation (29), which is valid for such a small value of  $K$ . For this value of  $K$ , again, the velocity at points of the central line will not differ much from  $W_0$ , and  $K$  will be approximately  $2n^2a/R$ . Consequently  $F_c/F_s = 0.99$  when  $2n^2a/R = 350$ , and the effect of curvature should be first measurable when the values of  $n$  and  $a/R$  are roughly such that the last equation is true.

Some experimental work by J. H. Grindley and A. H. Gibson\* bears upon this. In these experiments air was forced under pressure through a circular pipe of radius 0.16 cm. coiled in a circle of radius † 18 cm.; the value of  $a/R$  was accordingly  $1/112$ . Values of  $\mu$ , the coefficient of viscosity, were calculated from observed pressure and flux on the assumption that these quantities were related as if the pipe were straight. Coefficients of viscosity so calculated were found to increase with the flux, and it was determined that the increase first became sensible when the mean velocity was about 2 feet per second. The value of the corresponding Reynolds' number is given ‡ as 130. Accordingly  $2n^2a/R$  is about 300.

\* Proc. Roy. Soc. A, vol. lxxx. p. 114 (1908).

† This value is taken from one of the articles by Prof. Gibson in 'Mechanical Properties of Fluids,' p. 163.

‡ *Op. cit.* p. 164.

Now, the value of  $a/R$  in relation to the experiments is certainly small enough for the error due to the assumption of § 3 to be negligible, so that it can be stated with confidence that when  $a/R=1/112$  and  $2n^2a/R=350$ , the flux in the curved pipe is one per cent. less than that in a straight one, and hence that the value of  $\mu$  calculated as explained above should exceed by one per cent. its proper value. If, then, the experimental determinations had been accurate to one per cent., the increase in measured values of  $\mu$  would not have been appreciable till  $K$  was 350. The increase in  $\mu$  was, in fact, found sensible when  $K$  had the smaller value 300; this suggests that the measurements were more accurate than has been assumed in the numerical illustration. As it was estimated\* that the results were accurate to  $\frac{1}{2}$  per cent., some confirmation of the theory is provided by this comparison.

The velocity corresponding to the Reynolds' number 130 has been called† the critical velocity. But there is, I think, no conclusive evidence that this velocity is what is usually called a critical velocity; there is no evidence, that is to say, that at this velocity any change in the type of motion takes place. There is no need to assume a change in the motion to account for the increased values of  $\mu$ ; they can be attributed to the fact that the effect of curvature increases with the mean velocity, and the rough numerical agreement just found suggests that this alternative explanation is the correct one. There is, however, more direct evidence. In experiments by Prof. Eustice‡ it has been shown directly (by observation of colour bands) that the motion of water in curved pipes can be stream-line when the Reynolds' number is greater than 1000, and  $a/R$  much greater than  $1/100$ .

11. Another general result which is of some importance can be deduced. The ratio of the rate of flow due to a given pressure gradient in a curved pipe to that caused by the same gradient in a straight pipe of equal area depends only on the value of  $K$ . This can be expressed

$$F_c/F_s = f(K). \quad . \quad . \quad . \quad . \quad . \quad (30)$$

The problem of determining the relation between flux and gradient in any curved pipe (the motion being, of course, supposed stream-line) therefore reduces to that of finding

\* *Loc. cit.* p. 118.

† 'Mechanical Properties of Fluids,' p. 163; also p. 130 of the paper.

‡ *Proc. Roy. Soc. A*, vol. lxxxv. p. 119 (1911).

the single function  $f(K)$ . Equation (30) is not exactly true because of the assumption of § 3, but the error will in most cases be of little consequence.

Very little progress has been made with the analytical determination of  $f(K)$ , but there remains the possibility of deducing it from experiment; it can obviously be found from experiments on a single curved pipe, provided only the range of values of  $K$  is large enough. It is therefore possible to correlate experimental results for pipes of different curvatures.

It is convenient to write (30) in a different form. The analysis is most simply done in terms of  $K$ , but except when the motion is relatively slow, the quantity so denoted is not of much direct significance.

From equation (22) the constant  $C$  of (16) is equal to 4. Hence from equation (18)

$$Ga^2/\mu W_0 = C = 4,$$

where  $G$  is the pressure gradient. From (17)

$$\begin{aligned} K &= 2W_0^2 a^3/\nu^2 R \\ &= G^2 a^7/8\mu^2 \nu^2 R. \end{aligned}$$

We can therefore replace (30) by

$$F_c/F_s = f\left[\frac{G^2 a^7}{\mu^2 \nu^2 R}\right]. \quad \dots \quad (31)$$

This result is used below in the following form. Suppose that fluid flows under gradient  $G$  through a pipe of radius  $a$  coiled in a circle of radius  $R$ , and that the ratio of the flux to  $\pi a^4 G/8\mu$ \* is known; then the ratio of the flux due to gradient  $G'$  in a pipe of radii  $a'$  and  $R'$  to  $\pi a'^4 G'/8\mu'$  is the same, provided that

$$\frac{G^2 a^7}{\mu^2 \nu^2 R} = \frac{G'^2 a'^7}{\mu'^2 \nu'^2 R'}. \quad \dots \quad (32)$$

12. In the rest of this paper an attempt is made to use equation (32) of the preceding paragraph to correlate results obtained by Prof. Eustice† by observation of the flow of water through pipes of various radii of curvature.

\* The flux through a straight pipe of radius  $a$  due to gradient  $G$ . Lamb, 'Hydrodynamics,' § 331.

† Proc. Roy. Soc. A. vol. lxxxiv. p. 107 (1910). In the numerical work that follows observed values were in the first instance got by measurement of the curves in fig. 5 of this paper, and some errors necessarily resulted; the values given below are taken from copies of tables of results not given in full in the paper. I am much indebted to Prof. Eustice for these copies, and also for references to papers which he has written on this subject, among them that now quoted.

There are some difficulties in the way of the application of the theory to these experiments. A single flexible tube of rubber and canvas was used, and the radius of curvature,  $R$ , was varied by winding a given length of the tube on circular cylinders of various diameters. When the tube was free and the motion stream-line, it was found that the pressure gradient was roughly proportional to  $\bar{v}^{1.2}$ , because the tube in this condition was sinuous; in a straight tube the gradient is, of course, proportional to the first power of the mean velocity. It seems possible that some influence due to this unstrained configuration of the tube may have persisted when the tube was coiled, particularly when the number of coils was small.

The second point is that the coiling was accompanied in every case by a decrease (in one instance of more than 30 per cent.) in the area of the cross-section. From (32) it is evidently possible to allow for an alteration in the radius of the section, but it is not possible to allow for the effect of the alteration in the form of the section that the diminution in area implies. It must therefore be assumed that the cross-section of the tube when coiled is circular. (See § 17.)

Consequently the function  $f(K)$  has not been calculated absolutely. It appeared better to use the result stated in equation (32). The method is then to start from the observed  $(F, G)$  relation for one value of  $R$ , deduce the relation for a different value of  $R$ , and compare this with experiment. The first source of error indicated above will then be of less consequence.

13. Three such comparisons are given below. In the first we take the experimental  $(F, G)$  relation when the given length (81.5 cm.) of tube is wound into a single coil, and deduce from it the relation when the length is wound in 5 coils. Table I. shows the method of calculation. In the first two columns,  $F_1^*$  and  $g_1^*$  give the observed relation for the single coil:  $F_1$  is the flux at  $14^\circ \text{C}$ . in c.c. per second; the formula

$$F \propto (1 + 0.03368T + 0.000221T^2),$$

where  $T$  is temperature centigrade †, was used to deduce the flux at temperature  $14^\circ \text{C}$ . from the observed value. In the second column  $g_1$  denotes the decrease in pressure,

\* The suffix denotes here and subsequently the number of coils.

† It follows from (31) that a different temperature correction is required for a curved pipe, but as the temperatures were all near  $14^\circ \text{C}$ . the difference is probably small; no allowance has been made for this.

measured in cm. of water, in the length 81.5 cm. of the coiled tube. The corresponding pressure gradient  $G_1$  in c.g.s. units is very approximately given by

$$G_1 = \frac{981}{81.5} g_1,$$

but as we are concerned only with ratios of pressure gradients it is more convenient to work with  $g_1$ , for instance, than with  $G_1$ .

The area of cross-section, which is assumed a circle of radius  $a_1$ , is given as 0.1065 cm.<sup>2</sup> Then

$$\pi a_1^2 = 0.1065,$$

and for  $(F_s)_1$ , the rate of flow of water at 14° C. through a straight pipe of radius  $a_1$  due to pressure gradient  $G_1$ , we have

$$\begin{aligned} (F_s)_1 &= \pi a_1^4 G_1 / 8 \mu_{14} \\ &= \frac{(\cdot 1065)^2 (981)}{8 \pi (\cdot 01174) (81.5)} g_1 = 0.4627 g_1. \end{aligned}$$

$(F_s)_1$  is given in the third column, and  $(F_s)_1/F_1$  in the fourth.

The ratio  $(F_s)_5/F_5$  is the same as  $(F_s)_1/F_1$  when the pressure difference  $g_5$  is such that

$$g_1^2 a_1^7 / R_1 = g_5^2 a_5^7 / R_5.$$

When the tube was wound in 5 coils the area of the section diminished to 0.0996 cm.<sup>2</sup>, so that  $\pi a_5^2 = 0.0996$  and  $R_1 = 5R_5$ . Hence corresponding values of  $g_1$  and  $g_5$  must be such that

$$g_5 = 0.5028 g_1.$$

In the sixth column  $(F_s)_5$ , the flux in a straight pipe of radius  $a_5$  due to pressure difference  $g_5$ , is tabulated; then dividing each value by the value  $(F_s)_1/F_1$  in the same row, we have finally values of the flux  $F_5$  in the coiled tube due to pressure difference  $g_5$ . Not all the values that have been calculated are given in Table I.; a selection has been made such that consecutive values of  $F_5$  differ by about 0.5.

In the same way the  $(F_{1/2}, g_{1/2})$  relation has been calculated from the observed  $(F_1, g_1)$  relation. The calculated and observed relations in both cases are compared in Tables II. and III., and shown graphically in fig. 2.

TABLE I.

Calculation of  $(F_5, g_5)$  from observed  $(F_1, g_1)$ .

Observed values.		$(F_5)_1$	$(F_5)_1/F_1$	$g_1$	$(F_5)_5$	$F_5$
$g_1$ , cm.	$F_1$ , c.c./sec.					
3.37	1.02	1.56	1.53	1.69	.684	.45
8.64	2.15	4.00	1.86	4.34	1.76	.95
17.6	3.65	8.14	2.23	8.85	3.58	1.61
26.5	4.87	12.3	2.53	13.3	5.38	2.13
35.4	5.94	16.4	2.76	17.8	7.20	2.61
43.8	6.93	20.3	2.93	22.0	8.90	3.04
52.6	7.86	24.3	3.09	26.4	10.7	3.46
63.9	9.22	29.6	3.21	32.1	13.0	4.05
75.8	10.6	35.1	3.32	38.1	15.4	4.64
83.9	11.2	38.8	3.45	42.2	17.1	4.96
125	14.3	57.8	4.05	62.9	25.5	6.30

TABLE II.  $(F_5, g_5)$ 

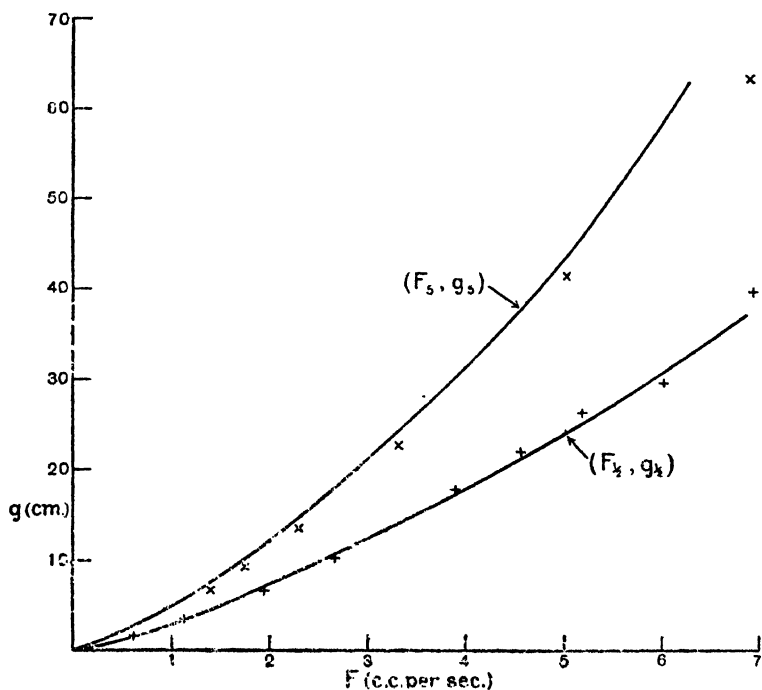
Calc.		Obs.	
$g_5$	$F_5$	$g_5$	$F_5$
1.69	.45	3.99	.94
4.34	.95	6.89	1.41
8.85	1.61	9.13	1.76
13.3	2.13	13.5	2.30
17.8	2.61	22.8	3.32
22.0	3.04	41.3	5.02
26.4	3.46	63.2	6.90
32.1	4.05		
38.1	4.64		
42.2	4.96		
62.9	6.30		

TABLE III.  $(F_{1/2}, g_{1/2})$ 

Calc.		Obs.	
$g_{1/2}$	$F_{1/2}$	$g_{1/2}$	$F_{1/2}$
1.18	.48	1.70	.63
2.46	.86	3.40	1.11
4.76	1.44	6.74	1.94
8.54	2.30	11.2	2.68
11.2	2.79	17.8	3.90
18.4	4.10	21.9	4.58
24.8	5.16	26.1	5.20
31.3	6.22	29.5	6.02

14. It must be noticed that in calculating part of the  $(F_s, g_s)$  relation from the observed  $(F_1, g_1)$  relation, the theory is used outside the limits within which it is necessarily valid, because the result stated in equation (32) is applicable only to the correlation of two steady motions. Let it be assumed that the critical velocity in a slightly curved pipe is the same as if the pipe were straight; it is then such that  $\bar{v}d/\nu=2000$ .

Fig. 2.



$(F_s, g_s)$ ; calculated from  $(F_1, g_1)$ , (—), and observed (x).

$(F_1, g_1)$ ; calculated from  $(F_1, g_1)$ , (—), and observed (+).

At temperature  $14^\circ \text{C}$ . the value of  $\nu$  for water is  $0.01174$ , and if it is assumed that the tubes with which we are concerned have a circular section of area  $0.1 \text{ cm}^2$ ,  $d=0.357 \text{ cm}$ . Consequently the critical velocity is such that

$$\bar{v}=65.8 \text{ cm./sec.},$$

the corresponding flux being  $6.6 \text{ c.c./sec.}$  When the flux is greater than this we may suppose that the motion is turbulent.



In finding part of the  $(F_5, g_5)$  relation given in Table I., the  $(F_1, g_1)$  relation is used at velocities above the critical. Thus the pair of values,  $F_5 = 3.04$ ,  $g_5 = 22.0$ , is calculated from the pressure observed when the flux in the tube in one coil was 6.93, and the motion presumably turbulent. All pairs of values in which  $F_5$  is greater than 3.04 are calculated under the same condition. The reason is simply that the corresponding pressure differences in the two tubes are not equal, so that one pressure may cause stream-line motion in one pipe while the corresponding pressure causes turbulent motion in the other. The difficulty can be avoided by starting from the observed values in the pipe of greater curvature; thus in the calculation of  $(F_{1/2}, g_{1/2})$  from  $(F_1, g_1)$ , corresponding pressures are such that

$$g_1/g_{1/2} = 0.708,$$

so that if  $g_{1/2}$  is small enough to produce steady motion the corresponding value of  $g_1$  will certainly do so.

The agreement between the theoretical and calculated  $(F_5, g_5)$  relations is, however, little worse in a certain range above the flux 3.04 than it is below. This suggested that the theory might be of some value as a rough means of calculation, or might even hold good without modification, above the critical velocity; both the calculations above have therefore been extended so as to include values of the flux greater than 6. The agreement gets steadily, but not rapidly, worse. (See § 18.)

15. As a more severe test of the theory the  $(F_1, g_1)$  relation has been calculated from the observed  $(F_{10}, g_{10})$  for values of the flux up to about 30, and is compared with observation in Table IV. and fig. 3. When the flexible tube was wound into ten coils the area of its section diminished to 0.0735 cm.<sup>2</sup>; it has been assumed, as in the other calculations, that the section is a circle of this area.

This comparison differs from the previous two in that calculated values of the flux are consistently less than the observed at low pressures, but consistently greater at high pressures; in the second case above, with only a few exceptions, the calculated values are greater than the observed, while in the first case they are, without exception, less.

16. If the flux does not exceed 6.6, in which range the motion of the water may be supposed stream-line, only in the calculation of  $(F_1, g_1)$  from  $(F_{10}, g_{10})$  is there a discrepancy of any importance between calculated and observed values.

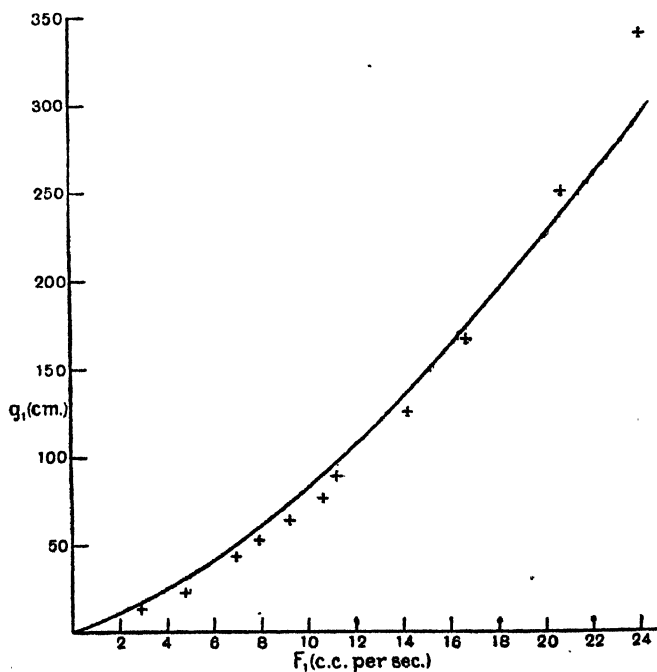
TABLE IV.

$(F_1, g_1)$ ; calculated from  $(F_{10}, g_{10})$ , and observed.

Calc.	$g_1$ .....	2.31	3.80	9.39	12.6	26.4	47.4
	$F_1$ .....	.54	.83	1.81	2.30	4.18	6.58
	$g_1$ .....	76.4	115	150	193	299	379
	$F_1$ .....	9.37	12.7	15.2	18.0	24.6	28.8

Obs.	$g_1$ ...	1.74	3.37	6.05	8.64	13.0	17.6	22.2	31.0
	$F_1$ ...	.61	1.02	1.63	2.15	2.90	3.65	4.42	5.41
	$g_1$ ...	39.8	52.6	63.9	125	166	250	340	420
	$F_1$ ...	6.45	7.86	9.22	14.3	16.8	20.8	24.1	27.0

Fig. 3.



$(F_1, g_1)$ ; calculated from  $(F_{10}, g_{10})$ , (—), and observed (+).

In the calculation of  $(F_5, g_5)$  from  $(F_1, g_1)$  the differences between calculated and observed rates of flow are all of the same sign, and all except one are less than 0.2; in the exceptional case the difference is less than 0.6, and the observed rate of flow 6.90. In the calculation of  $(F_{1/2}, g_{1/2})$  from  $(F_1, g_1)$  the agreement is still better; the differences are not all of the same sign and do not exceed 0.2 until the observed flux is 6.94, in which case the difference is less than 0.3. In a part of the first of these calculations the theory has, as stated, been used when it is not necessarily valid, but it appears that the accuracy is not immediately affected.

In the calculation of  $(F_1, g_1)$  from  $(F_{10}, g_{10})$  the agreement in stream-line motion is poor. The maximum difference between calculated and observed rates of flow lies between 0.7 and 0.8; for the small value 1.02 of the observed rate of flow the fractional error is about 1/4, but it decreases as the flux increases, and is about 1/10 at the critical velocity. But there are several sources of error which together may account for this discrepancy.

17. It has been assumed that the cross-section of the tube when in ten coils was circular, while in fact it was oval. Allowance for this, if it could be made\*, would improve the agreement; this is easily seen from the method of calculation shown in Table I. Assume that the section is circular when the tube is in one coil, but elliptical when it is in ten; then the theory would give the  $(F_1, g_1)$  relation correctly if for the observed values of  $F_{10}$  are substituted the larger values of the flux through a circular pipe of the same sectional area. For given  $g_{10}$ ,  $F_{10}$  must be increased.  $(F_*)_{10}$  depends on  $g_{10}$  and  $a_{10}$ , and will be unaltered; so will  $g_1$  and hence  $(F)_1$ , but the ratio  $(F_*)_{10}/F_{10}$  will be decreased, and thus finally  $F_1$  will be increased. As the calculated values are too small, this correction will improve the agreement. It must, however, be pointed out that a considerable distortion due to coiling would have to be assumed to account for the whole of the difference that has been found above. The ratio of the rates of flow through two straight pipes of the same area, one circular and the other elliptical, is†

$$2ab/(a^2 + b^2),$$

if  $a, b$  are the semi-axes of the ellipse. This ratio is 0.9

\* The dimensions (apart from the area) of the section of the tube when coiled are not given, and would probably be difficult to find with accuracy.

† Lamb, *op. cit.* § 332.

when  $b/a=0.63$ , and if the rate of flow is not more sensitive to form of section in a curved pipe than in a straight one, a distortion of at least this magnitude must be assumed.

A correction for form of section is needed only in this case, as in the other two the alterations in area were much smaller. The area of the section,  $0.1066 \text{ cm.}^2$  when the tube was free, decreased by only  $0.0070 \text{ cm.}^2$  when it was in five coils; the correction for the small change of form that may have accompanied this decrease is certainly negligible.

It may be noted that the theory applies, in certain conditions, to tubes of elliptical cross-section. Suppose that the sections are elliptical when the tube is in 1 and  $1/2$  coils. As the areas are almost the same (the difference is given as  $10^{-4} \text{ cm.}^2$ ), the ellipses can be assumed geometrically similar. In such a case as this no alteration in the calculation above is required. The only reference to the form of the section in the fundamental equations of §4 is contained in the boundary condition in which the boundary is given as  $r'=1$ . If we are to compare two tubes whose sections are similar ellipses, the boundary is  $r'=f(\psi)$ , the function  $f$  being the same for both. The quantity  $a$  may now stand for the mean radius. The standard of comparison is not now a straight pipe of circular section, but a straight pipe whose section is a similar ellipse. Hence in what corresponds to Table I. for this calculation the numbers in the columns  $(F_s)_1$  and  $(F_s)_{1/2}$  have to be multiplied by the same constant, and the final result is unaffected.

There are other corrections that should strictly be made, but none likely to be important. The error due to the assumption of §3 is, of course, greatest when the tube is in ten coils; the external and internal diameters of the coil are then 3.2 cm. and 1.9 cm. respectively, and taking  $a$  to be 0.153 cm., we have  $a/R=0.12$ . The fractional error, nominally of order  $a^2/R^2$ , would be only 0.002 if equation (27) were correct, and in any case can hardly result in a final error of much importance. If a correction were to be made its effect would be to improve agreement.

Another point is that no allowance can be made for the effect of the sudden change in curvature at the ends of the coiled tube. It is likely that the flow will be more disturbed when the tube is in ten coils than when it is in one, so that, although the method of calculation eliminates some of the end effect, a correction may be required which again would improve agreement.

Although the differences between calculated and observed

values are in this case large, they do not therefore necessarily imply that the theory is at fault, especially as any calculated value of  $F_1$  is more than three times the observed value of  $F_{10}$  from which it is derived, so that errors of observation (likely to be greatest when the flux is small) are magnified.

18. In all three cases the calculations have been extended to values of the flux greater than 6.6, the assumed limit of stream-line motion, in order to see what errors resulted from the use of the theory outside its proper scope. Some of the results in the calculation of  $(F_1, g_1)$  from  $(F_{10}, g_{10})$  are shown in fig. 3. For all observed values of  $F_1$  between 6.6 and 24.1, the difference between observed and calculated values of  $F_1$  does not exceed 10 per cent.; in this range the Reynolds' number varies from about 2000 to over 7000. However, in the last paragraph the need has been shown for corrections which will certainly decrease the range in which the theory is correct to within 10 per cent. In the calculation of  $(F_{1/2}, g_{1/2})$  from  $(F_1, g_1)$ , observed and calculated values of  $F_{1/2}$  differ by less than 5 per cent. for all observed values of  $F_{1/2}$  up to 10.7, which corresponds to a Reynolds' number of over 3000.

The agreement in the calculation of  $(F_5, g_5)$  from  $(F_1, g_1)$  is much worse. The difference between the two values of  $F_5$  is 10 per cent. when the observed value of  $F_5$  is 8.6, increases steadily, and is 24 per cent. when the observed value is 17.5.

It can be concluded that if an attempt is to be made to correlate results in which the critical velocity is exceeded, it is better to start from the observed values for the pipe of greater curvature, and that then the errors will not be very serious if the Reynolds' number does not exceed perhaps 4000. The reason why it is better to correlate in one way rather than in the other is partly that it is better to make a crude interpolation than an equally crude extrapolation; but there is also the fact that in finding, for instance, the calculated value  $F_5=16.5$ , the observed value  $F_1=37.6$ , to which, corresponds a Reynolds' number of more than  $10^4$ , is used.

19. The theory can probably be extended so as to apply to all velocities by substituting a coefficient of eddy viscosity for the ordinary coefficient  $\mu$ . For this, however, the absolute determination of the function  $f(K)$ , by experiment or otherwise, is almost a necessity; the method of comparison used in this paper would be unsuitable, as it would be much more difficult to find the corresponding motions in the two

pipes compared. It is clear from some of the results above that at velocities just above the critical the coefficient of eddy viscosity must differ only slightly from the ordinary coefficient if there is to be agreement: this follows immediately from the statement of Prof. Eustice \* that there is no marked critical velocity in the coiled tubes. The reason for this difference between straight and curved pipes appears clear. That the pressure gradient required to maintain a given rate of flow increases more or less suddenly when the critical velocity is exceeded is a consequence of the sudden change in the type of motion: turbulence is accompanied by a lateral movement of the fluid, which implies a loss of energy that has no counterpart in steady motion. In a curved pipe, on the other hand, lateral movement is already taking place before the critical velocity is reached; it is probably increased when turbulence sets in, but there is clearly less reason in this case to expect a rapid increase in the resistance to flow.

---

LXXIII. *Electrical Properties of Monatomic Gases.* By J. S. TOWNSEND, *F.R.S.*, *Wykeham Professor of Physics, Oxford*, and S. P. MACCALLUM, *Fellow of New College, Oxford*†.

1. **I**N the course of an investigation of the electrical properties of monatomic gases we made several experiments to determine the best method of purifying the gases, and we observed that small traces of an impurity are removed in a few seconds by the action of a high-frequency discharge. This effect of the discharge, which may be obtained with external electrodes, was observed in the process of filling a quartz tube with neon.

The tube was heated to a temperature of about 600° C., and washed out with pure neon in order to remove the gas given off from the surface. This operation was repeated until a stage was reached at which no effect of impurities was seen in the colour of the discharge, and there were no lines in the spectrum except those due to neon.

A constriction in a narrow quartz side-tube through which the gas was admitted was then sealed in order to disconnect the electrodeless tube containing neon. Immediately after

\* *Loc. cit.* p. 114; see also fig. 4.

† Communicated by the Authors.

sealing off the tube a high-frequency discharge was produced in the gas, and at first it appeared to be very impure, but after a few seconds the impurity disappeared and the colour of the discharge and the lines in the spectrum became exactly as they were before the constriction was sealed. The impurity was probably hydrogen which got into the gas when the constriction was heated to the very high temperature required for sealing, and the high-frequency discharge, which ionized the gas, caused the hydrogen to be rapidly absorbed by the quartz.

In other experiments we have observed that the effect of an impurity is more noticeable in a wide tube where the force required to maintain the discharge is comparatively small, than in a narrow tube where a larger force is required.

From measurements of the currents in these discharges, and the potentials at the external electrodes, it has been found that the positive ions and the electrons do not recombine to any appreciable extent in the gas\*.

The disappearance of ions from the gas is due primarily to the electrons which diffuse rapidly to the sides of the vessel, leaving a positive charge in the gas. The positive ions are repelled to the sides by this charge, and in the stable distribution which is established almost instantaneously the positive ions reach the sides at the same rate as the electrons. These losses are balanced by the process of ionization by collisions of electrons with molecules, and a constant steady state is maintained. Thus molecules of diatomic gases which are easily ionized are driven by the force on their positive charges into contact with the sides of the quartz, where they remain for a considerable time.

We have found this property of the electrodeless discharge to be very useful in cases where it is necessary to remove small traces of impurities.

2. In order to obtain accurate measurements of sparking potentials and photo-electric currents, an apparatus comprising parallel plates was made up with quartz insulation and fitted into one end of a quartz cylinder 23 cm. long and 5.8 cm. in diameter. The free space at the other end of the cylinder, about 10 cm. long, was used for obtaining a high-frequency discharge with external electrodes. One of the plates of the measuring instrument was mounted on a micrometer screw to which a rod of soft iron was attached. By

\* J. S. Townsend and R. H. Donaldson, *Phil. Mag.* p. 179 (Jan. 1928). J. S. Townsend, *Comptes Rendus*, p. 55 (Jan. 1928).

this means it was possible to adjust the distance between the plates with a magnet.

Each specimen of gas used in the experiments was purified by passing it slowly along a tube containing copper oxide at a high temperature, to remove traces of hydrogen, and thence into a tube containing charcoal which was cooled by liquid air. The gas was kept for sixteen hours in the charcoal tube before it was admitted into the quartz cylinder.

The apparatus was heated to a temperature of about  $300^{\circ}\text{C.}$  to  $400^{\circ}\text{C.}$  for several hours and washed out with pure neon. This operation was repeated until there was no visible change in the colour of the high-frequency discharge when the gas was left in the cylinder for twenty-four hours. A point was thus reached at which the sparking potential, as found by the parallel plate electrodes with a battery of small accumulators, was constant for a given value of the product of the pressure and distance between the plates, and remained at that value for some hours after the gas was admitted to the cylinder. Very small traces of impurities have a comparatively large effect on the sparking potential, and a considerable change was obtained when the gas was left in the quartz cylinder for twenty-four hours; but the impurity accumulated in the gas in that time is immediately removed by the high-frequency discharge, and the sparking potential regains the same value observed in a fresh sample of pure gas.

3. As an example of these experiments the sparking potentials observed in neon at a pressure of 37.2 mm. are given in Table I., the potentials being in volts and the distance  $S$  between the plates in millimetres. The sparking potentials obtained a few hours after the gas had been in the apparatus are given in column  $A_1$ . At this stage there is no change in the potentials of more than one volt, due to the passage of the high-frequency discharge through gas. The potentials obtained after the gas had been in the apparatus for twenty-four hours are given in columns  $B_1$  and  $C_1$ , the latter being the potentials after the high-frequency discharge had been maintained in the gas for one or two minutes.

These methods of purifying the gas are very reliable, and constant results are obtained on repeating the experiments. Thus, after the gas at 37.2 mm. pressure had been in the apparatus for a week, the quartz cylinder was heated and the gas was pumped out. After washing out the apparatus with pure gas, a fresh quantity at 37.4 mm. was admitted and the experiments were repeated. The sparking potentials obtained



shortly after admitting the gas are given in column  $A_2$ , and those obtained after twenty-four hours in columns  $B_2$  and  $C_2$ , the change from  $B_2$  to  $C_2$  being effected by means of the high-frequency discharge, as in the experiments with the gas at 37.2 mm. pressure.

TABLE I.—Sparking Potentials in Neon.

S.	$p=37.2$ mm.			$p=37.4$ mm.		
	$A_1$ .	$B_1$ .	$C_1$ .	$A_2$ .	$B_2$ .	$C_2$ .
4.....	263	251	263	264	254	264
5.....	292	278	292	294	277	294
6.....	317	300	318	319	298	320
7.....	342	320	344	344	312	344

Small traces of impurities which are not easily observed in a direct-vision spectroscope are easily detected by a measurement of the sparking potential.

The agreement between the figures in columns A and C indicates the degree of accuracy which may be obtained.

4. The photo-electric currents obtained with a constant electric force and a constant gas-pressure were also determined with different distances  $x$  between the plates. The current  $n$  in terms of the distance was found to be in accordance with the formula

$$n = n_0 \frac{(\alpha - \beta)e^{(\alpha - \beta)(x - \delta)}}{\alpha - \beta e^{(\alpha - \beta)(x - \delta)}}$$

for a range of distances from a certain small distance  $\delta$  to the sparking distance  $S$ . The sparking distance is the value of  $x$  obtained by equating to zero the denominator of the term on the right of the equation. The effect of small traces of impurities on the constants  $\alpha$  and  $\beta$  is easily observed, but the experimental error involved in the determination of these coefficients is much greater than in the determination of a sparking potential. As an example of the determinations of these coefficients, the results of experiments made with the sample of gas at 37.2 mm. pressure are given in Table II. The figures in column A give the results obtained after the gas was in the quartz cylinder for a few hours,

those in columns B and C after twenty-four hours, the change from B to C being produced by the action of a high-frequency discharge. A slightly different value of the electric force was taken in the three sets of experiments as indicated by the values of X in the first line of figures, which are the forces in volts per centimetre.

TABLE II.—Neon,  $p=37.2$ .

	A.	B.	C.
X .....	183	476	487
$\alpha$ .....	4.2	4.76	4.3
$\beta$ .....	32	24	31

Thus there are two completely different methods of removing small traces of impurities from a monatomic gas—that involving the use of charcoal cooled with liquid air and that of the high-frequency discharge. It may be concluded that the gas taken from the charcoal tube contains no impurities which alter the electrical properties of the gas, as the gas is not affected by the high-frequency discharge until after it has been in the quartz cylinder containing the parallel-plate apparatus for several hours.

These experiments therefore lead to the conclusion that the atoms of monatomic gases are ionized by the collisions of electrons, and that the development of large currents in gases is principally due to this process. This conclusion applies even in cases where ratio  $X/p$  is small, as in the experiments with the gas at 37.2 mm. pressure, where  $X/p=13$ , or in an electrodeless discharge where the ratio  $X/p$  may be as low as 2.5.

5. These conclusions are not in accordance with other theories which have been adopted without taking into consideration the general properties of electric discharges. These theories have appeared in different forms, and there is at present a tendency to attribute predominating effects to impurities which some time ago were attributed to electrons set free from the electrodes by radiation from the gas. They all involve the hypothesis that an electron loses all or most of its energy in a collision with a molecule when the kinetic energy is equal to, or slightly greater than, the energy corresponding to the first resonance potential of the gas. Thus, when electrons move in a gas at a high pressure under

the action of a small electric force, they will never attain sufficient energy to ionize molecules.

It would be interesting to know the order of the electric force as well as the pressure of a monatomic gas in a discharge-tube when the energy of the electrons is thus limited. An example of the application of this hypothesis is suggested by Merton and Pilley\* in the case of a tube containing helium at about 30 mm. pressure and a very small quantity of nitrogen. It is stated that a large excess of helium atoms in the discharge must act as "safety valves" which blow off when they are struck by 20.4-volt electrons, and which, therefore, set a superior limit to the energy which there is any significant probability that an electron will acquire. The intensity of the electric force is not mentioned, and it is not stated whether any helium lines were observed in the visible spectrum of the discharge in the experiments in which the energy of the electron is thus limited.

The "safety-valve" action would presumably be a predominant factor in determining the energy of the electron whether the gas is pure or impure, so that electrons would never acquire sufficient energy to ionize atoms of a monatomic gas under the action of small forces. The electrons under the above circumstances would not acquire even as much energy as that represented by the second or third resonance potential, so that the line corresponding to the first resonance potential, which is in the ultra-violet, would be the only helium line in the spectrum of a discharge.

With regard to impurities, it is quite plain there must be processes by which impurities have been successfully removed to such an extent that they have no predominant effect on the discharge. In the well-known neon lights used for commercial purposes, there is a long column of luminous gas where the current is maintained by a small electric force. In order to maintain the current a continuous rate of supply of ions and electrons must be maintained throughout the luminous column, as positive ions are being continually removed towards the negative electrode. A simple calculation shows that, in order to maintain the current, it would be necessary according to this theory to suppose that no small amount of diatomic material is conveyed along the luminous column, and that this process is maintained indefinitely while the light in the visible spectrum of the gas may be almost completely free from lines corresponding to the material from which the positive ions are derived.

\* T. R. Merton and J. G. Pilley, *Proc. Roy. Soc. A*, vol. cvii. p. 411 (1925).

LXXIV. *Some Problems in the Conduction of Heat.* By  
 GEORGE GREEN, D.Sc., *Lecturer in Physics in the Applied  
 Physics Department of the University of Glasgow* \*.

THE present paper contains a continuation of the work published in a former paper to the Philosophical Magazine under the same title †. In the paper referred to the method of solution of problems in heat-conduction employed is such that each problem in heat-conduction is treated as a problem in wave-motion. For the solution of two-dimensional problems in heat-conduction it is shown that there are two fundamental wave-trains travelling in the positive direction and two corresponding wave-trains travelling in the negative direction, and that the solution of any problem can be expressed in terms of these four wave-trains. Similarly, in the case of cylindrical and spherical waves there are two positive wave-trains and two negative wave-trains, and the solution of any problem can be expressed in terms of these four wave-trains. The former paper dealt with several fundamental problems involving plane and spherical waves, and it is intended in the present paper to deal with some of the fundamental problems involving cylindrical waves by the method employing positive and negative wave-trains, and to investigate the nature of the special solutions usually employed in cylindrical heat problems, and the relation of these solutions to the four fundamental wave-trains. An interesting feature of the investigations is the comparison which they enable us to make between different methods of arriving at equivalent solutions of the same problem.

We proceed first to obtain the four fundamental wave-trains referred to above. The equation of conduction of heat in a uniform medium, in its simplest form for cylindrical conduction, is

$$\frac{\partial v}{\partial t} = \kappa \left( \frac{\partial^2 v}{\partial \rho^2} + \frac{1}{\rho} \frac{\partial v}{\partial \rho} \right), \quad . . . . . (1)$$

and the solutions which we require are those for which the temperature  $v$  at radius  $\rho$  from the axis of coordinates varies with the time  $t$  according to the factor  $e^{ikt}$ , where  $k$  represents the frequency of a periodic vibration. The equation to determine  $v$  as a function of  $\rho$  then becomes

$$\frac{\partial^2 v}{\partial \rho^2} + \frac{1}{\rho} \frac{\partial v}{\partial \rho} - \frac{ik}{\kappa} v = 0, \quad . . . . . (2)$$

\* Communicated by the Author.

† Phil. Mag. vol. iii. Suppl. April 1927, pp. 784-800.

of which the general solution is

$$v = AI_0\left(\sqrt{\frac{ik}{\kappa}} \cdot \rho\right) + BK_0\left(\sqrt{\frac{ik}{\kappa}} \rho\right),$$

where A and B are arbitrary constants, and  $I_0\left(\sqrt{\frac{ik}{\kappa}} \rho\right)$  and  $K_0\left(\sqrt{\frac{ik}{\kappa}} \rho\right)$  are functions of  $\rho$  defined by

$$I_0(z) = 1 + \frac{z^2}{2^2} + \frac{z^4}{2^2 \cdot 4^2} + \frac{z^6}{2^2 \cdot 4^2 \cdot 6^2} + \text{etc.}, \quad (3)$$

$$K_0(z) = \alpha I_0(z) - \log z I_0(z) + \frac{z^2}{2^2} + \left(1 + \frac{1}{2}\right) \frac{z^4}{2^2 \cdot 4^2} + \text{etc.}, \quad (4)$$

where  $\alpha = \log -\gamma$ ,  $\gamma$  being Euler's constant.

By employing Stokes's method to obtain the solutions of equation (1), we find asymptotic expansions for these functions when  $\rho$  is large. These expansions are given by

$$I_0(z) = \frac{e^z}{\sqrt{2\pi z}} \left\{ 1 + \frac{1^2}{(8z)} + \frac{1^2 \cdot 3^2}{2! (8z)^2} + \text{etc.} \right\}, \quad (5)$$

$$K_0(z) = \pi \frac{e^{-z}}{\sqrt{2\pi z}} \left\{ 1 - \frac{1^2}{(8z)} + \frac{1^2 \cdot 3^2}{2! (8z)^2} - \text{etc.} \right\}. \quad (6)$$

The function  $K_0(z)$  becomes infinite as  $\log z$  as  $z$  tends to zero, and as  $z$  tends to infinity its value tends to zero. The  $I_0(z)$  function is finite at the origin and becomes infinite in value as  $z$  increases indefinitely. The two fundamental positive or diverging wave-trains are accordingly represented

by the real and imaginary parts of  $e^{ikt} K_0\left(\sqrt{\frac{ik}{\kappa}} \rho\right)$  respectively: the two fundamental negative wave-trains are represented by the real and imaginary parts of  $e^{ikt} I_0\left(\sqrt{\frac{ik}{\kappa}} \rho\right)$  respectively.

We can now find the solution representing a line source at which there is a periodic heat supply of amount  $q \cos kt$  or  $q \sin kt$  per unit length. It involves only the diverging waves; hence we may take

$$v = Ae^{ikt} K_0\left(\sqrt{\frac{ik}{\kappa}} \rho\right),$$

and determine the constant A from the condition

$$\lim_{\rho \rightarrow 0} \left( -2\pi K \rho \frac{\partial v}{\partial \rho} \right) = q e^{ikt}. \quad (7)$$

In this way we find that the periodic line source is represented by

$$v = \frac{q}{2\pi K} e^{ikt} K_0 \left( \sqrt{\frac{ik}{\kappa}} \rho \right). \quad (8)$$

This result may also be obtained as follows. Take the solution given in equation (39) of the former paper, representing a periodic heat supply  $q \cos kt$  or  $q \sin kt$  at a point which is origin of the coordinate  $r$ ,

$$v = \frac{q}{4\pi K r} e^{-r\sqrt{\frac{k}{2\kappa}}} \left\{ \cos \left( kt - r\sqrt{\frac{k}{2\kappa}} \right) + i \sin \left( kt - r\sqrt{\frac{k}{2\kappa}} \right) \right\}. \quad (9)$$

In this replace  $q$  by  $q dz$  and integrate along the axis of  $z$  from  $-\infty$  to  $+\infty$ . The periodic line source solution is thus obtained in the form

$$v = \frac{q}{4\pi K} \int_{-\infty}^{+\infty} \frac{dz}{r} e^{ikt - \sqrt{\frac{ik}{\kappa}} r}; \quad r^2 = \rho^2 + z^2, \quad (10)$$

and by substituting  $\rho \sinh \theta$  for  $z$  in this, it becomes

$$\begin{aligned} v &= \frac{q e^{ikt}}{2\pi K} \int_0^\infty d\theta e^{-\rho \cosh \theta} \sqrt{\frac{ik}{\kappa}} \\ &= \frac{q}{2\pi K} \int_0^\infty d\theta e^{-\rho \cosh \theta} \sqrt{\frac{k}{2\kappa}} \left\{ \cos \left( kt - \rho \cosh \theta \sqrt{\frac{k}{2\kappa}} \right) + i \sin \left( kt - \rho \cosh \theta \sqrt{\frac{k}{2\kappa}} \right) \right\}, \quad (11) \end{aligned}$$

which is an equivalent form of equation (8) above.

To verify that the periodic line source solution given above leads by integration to the well-known plane source solution, replace  $q$  in the above expression by  $q dz$ , and  $\rho$  by  $\sqrt{z^2 + x^2}$ , and integrate with respect to  $z$  from  $-\infty$  to  $+\infty$ . Thus we find that

$$v = \frac{q e^{ikt}}{2\pi K} \int_{-\infty}^{+\infty} dz K_0 \left( \sqrt{\frac{ik}{\kappa}} \sqrt{z^2 + x^2} \right), \quad (12)$$

and by using the evaluation of this integral given in

Watson's 'Theory of Bessel Functions,' p. 417, we obtain the solution

$$v = \frac{qe^{ikt}}{2\pi K} \cdot \frac{\pi}{\sqrt{\frac{ik}{\kappa}}} e^{-2\sqrt{\frac{ik}{\kappa}}}, \dots \quad (13)$$

which represents a periodic plane source supplying  $qe^{kt}$  per unit area.

Proceed now to determine the solution representing a surface source at which there is a periodic heat supply of amount  $q \cos kt$  or  $q \sin kt$  per unit area. Let  $\rho = a$  be the surface at which the heat is supplied; then outside this surface the solution involves only the diverging wave, and inside this surface it involves only the inward travelling wave. Hence we take

$$v_i = A e^{ikt} I_0\left(\sqrt{\frac{ik}{\kappa}} \rho\right) \dots \rho < a, \quad (14)$$

$$v_o = B e^{ikt} K_0\left(\sqrt{\frac{ik}{\kappa}} \rho\right) \dots \rho > a, \quad (14')$$

and determine the two constants A and B from the conditions which hold at the surface  $\rho = a$ ; namely,

$$v_i = v_o, \quad \text{and} \quad -K\left(\frac{\partial v_o}{\partial \rho} - \frac{\partial v_i}{\partial \rho}\right) = qe^{ikt}. \quad (15)$$

In this way we find that a periodic surface source of strength  $qe^{ikt}$  at  $\rho = a$  is represented by

$$v_i = \frac{qa}{K} e^{ikt} K_0\left(\sqrt{\frac{ik}{\kappa}} a\right) I_0\left(\sqrt{\frac{ik}{\kappa}} \rho\right) \dots \rho < a, \quad (16)$$

$$v_o = \frac{qa}{K} e^{ikt} I_0\left(\sqrt{\frac{ik}{\kappa}} a\right) K_0\left(\sqrt{\frac{ik}{\kappa}} \rho\right) \dots \rho > a. \quad (16')$$

Verify that

$$\begin{aligned} & -K\left(\frac{\partial v_o}{\partial \rho} - \frac{\partial v_i}{\partial \rho}\right)_{\rho=a} \\ &= qe^{ikt} \sqrt{\frac{ik}{\kappa}} a \left\{ K_0\left(\sqrt{\frac{ik}{\kappa}} a\right) I_1\left(\sqrt{\frac{ik}{\kappa}} a\right) \right. \\ & \quad \left. + K_1\left(\sqrt{\frac{ik}{\kappa}} a\right) I_0\left(\sqrt{\frac{ik}{\kappa}} a\right) \right\} \\ &= qe^{ikt} \dots \dots \dots (17) \end{aligned}$$

as required.

An alternative method by which this result may be arrived at is to take the periodic line solution given in equation (8), replace the  $q$  in it by  $qa d\theta'$  and  $\rho$  by  $r$ , and integrate with respect to  $\theta'$  from  $-\pi$  to  $+\pi$ . The solution obtained for a periodic cylindrical surface source of strength  $qe^{ikt}$  per unit area of the surface,  $\rho=a$ , is accordingly

$$v = \frac{qa}{2\pi K} \int_{-\pi}^{+\pi} d\theta' e^{ikt} K_0\left(\sqrt{\frac{ik}{\kappa}} r\right), \quad \dots (18)$$

where  $r^2 = a^2 + \rho^2 - 2a\rho \cos \theta'$ .

But by the addition theorem we have

$$K_0\left(\sqrt{\frac{ik}{\kappa}} r\right) = \sum_{m=-\infty}^{+\infty} K_m\left(\sqrt{\frac{ik}{\kappa}} a\right) I_m\left(\sqrt{\frac{ik}{\kappa}} \rho\right) \cos m\theta' \quad \dots a > \rho \quad \dots (19)$$

$$= \sum_{m=-\infty}^{+\infty} K_m\left(\sqrt{\frac{ik}{\kappa}} \rho\right) I_m\left(\sqrt{\frac{ik}{\kappa}} a\right) \cos m\theta' \quad \dots \rho > a; \quad \dots (19')$$

hence, when these values are inserted in (18), and when the integration with respect to  $\theta'$  is carried out, we reach again the result already given in equation (16) above.

From the above periodic solutions we can obtain others by integration. Thus, by taking the real part only of equation (8) which represents a periodic line source emitting  $q \cos kt$  per unit length, and integrating with respect to  $k$ , we obtain the solution representing an instantaneous line source of strength  $q$  per unit length; that is,

$$\begin{aligned} v &= \frac{q}{2\pi^2 K} \int_0^\infty dk e^{ikt} K_0\left(\sqrt{\frac{ik}{\kappa}} r\right) \\ &= \frac{q}{2\pi^2 K} \int_0^\infty d\theta \int_0^\infty dk e^{-\rho \cosh \theta} \sqrt{\frac{k}{2\kappa}} \\ &\quad \cos \left\{ kt - \rho \cosh \theta \sqrt{\frac{k}{2\kappa}} \right\}. \quad (20) \end{aligned}$$

The integration with respect to  $k$  has already been given in equation (13) of the former paper, and when the value there given is inserted in the above, we obtain the result in the form

$$v = \frac{q}{2\pi K} \int_0^\infty d\theta \frac{\rho \cosh \theta}{2 \sqrt{\pi \kappa t^3}} e^{-\frac{\rho^2 \cosh^2 \theta}{4\kappa t}}; \quad \dots (21)$$



and as the integral that remains is easily transformed into a well-known integral, we obtain, finally, the evaluation indicated by

$$v = \frac{q}{2\pi^2 K} \int_0^\infty dk e^{ikt} K_0\left(\sqrt{\frac{ik}{\kappa}} \rho\right) = \frac{q}{4\pi K t} e^{-\frac{\rho^2}{4\kappa t}}. \quad (22)$$

In this equation the real part of the integral only is equated to the well-known instantaneous line source solution corresponding to a generation of  $q$  heat units per unit of length of the line. When in the above process we take the imaginary part of equation (8), the evaluation given in equation (15) of the former paper becomes available, and we find as the equation corresponding to (22) for the imaginary part of the integral

$$\begin{aligned} v = \frac{q}{2\pi^2 K} \int_0^\infty dk e^{ikt} K_0\left(\sqrt{\frac{ik}{\kappa}} \rho\right) \\ = -\frac{q}{\pi^2 K t} \left( \frac{(8\kappa t)}{(2\rho)^2} + \frac{2 \cdot 1 \cdot 3 \cdot (8\kappa t)^2}{3 \cdot (2\rho)^4} \right. \\ \left. + \frac{2 \cdot 4 \cdot 1 \cdot 3 \cdot 5 \cdot (8\kappa t)^3}{3 \cdot 5 \cdot (2\rho)^6} + \text{etc.} \right). \quad (23) \end{aligned}$$

Similarly we may obtain by integration of (16) the solution representing an instantaneous cylindrical surface source at  $\rho = a$ ,  $q$  being the amount instantaneously generated per unit area. The solution is given by

$$v_i = \frac{qa}{\pi K} \int_0^\infty dk e^{ikt} K_0\left(\sqrt{\frac{ik}{\kappa}} a\right) I_0\left(\sqrt{\frac{ik}{\kappa}} \rho\right) \dots a > \rho, \quad (24)$$

$$v_0 = \frac{qa}{\pi K} \int_0^\infty dk e^{ikt} K_0\left(\sqrt{\frac{ik}{\kappa}} \rho\right) I_0\left(\sqrt{\frac{ik}{\kappa}} a\right) \dots \rho > a. \quad (24')$$

Both these integrals can be evaluated by the same method; hence this need be indicated for the upper only. When we make use of the equation

$$\begin{aligned} e^{ikt} K_0\left(\sqrt{\frac{ik}{\kappa}} a\right) \\ = \int_0^\infty d\theta e^{-\rho \cosh \theta} \sqrt{\frac{k}{2\kappa}} \left\{ \cos\left(kt - \rho \cosh \theta \sqrt{\frac{k}{2\kappa}}\right) \right. \\ \left. + i \sin\left(kt - \rho \cosh \theta \sqrt{\frac{k}{2\kappa}}\right) \right\}, \quad (25) \end{aligned}$$

along with the expansion for  $I_0\left(\sqrt{\frac{ik}{\kappa}}\rho\right)$  given in (3)

above, we obtain under the integral sign a series which can be integrated term by term. For the real terms in the integration with respect to  $k$ , the evaluation given in equation (13) of the former paper is again available, and the integration with respect to  $\theta$  then follows easily, exactly as in the case of the instantaneous line source solution obtained immediately above. These two integrations lead to the result:

$$v_i = \frac{q}{2K} \left\{ 1 + \frac{1}{2^2} \cdot \frac{\rho^2}{\kappa} \frac{\partial}{\partial t} + \frac{1}{2^2 \cdot 4^2} \cdot \frac{\rho^4}{\kappa^2} \frac{\partial^2}{\partial t^2} + \text{etc.} \right\} \left( e^{-\frac{a^2}{4\kappa t}} / t \right), \quad \dots (26)$$

$$v_0 = \frac{q}{2K} \left\{ 1 + \frac{1}{2^2} \cdot \frac{a^2}{\kappa} \frac{\partial}{\partial t} + \frac{1}{2^2 \cdot 4^2} \cdot \frac{a^4}{\kappa^2} \frac{\partial^2}{\partial t^2} + \text{etc.} \right\} \left( e^{-\frac{\rho^2}{4\kappa t}} / t \right), \quad \dots (26')$$

each of which is converted into the other by the interchange of  $a$  and  $\rho$ . The reciprocal nature of these results is made clear by taking out the factor  $e^{-\frac{\rho^2 + a^2}{4\kappa t}}$  in both; in this way we find that

$$v_i = \frac{qa}{2Kt} e^{-\frac{a^2 + \rho^2}{4\kappa t}} I_0\left(\frac{a\rho}{2\kappa t}\right), \quad \dots (27)$$

$$v_0 = \frac{qa}{2Kt} e^{-\frac{a^2 + \rho^2}{4\kappa t}} I_0\left(\frac{a\rho}{2\kappa t}\right), \quad \dots (27')$$

represents an instantaneous cylindrical surface source of strength  $q$  per unit area of the cylinder  $\rho = a$ .

To obtain a solution representing a periodic cylindrical surface source of the type supplying  $qe^{ikt} \cos n\theta$  per unit area, we have merely to follow the process adopted above. But in this case the differential equation to be solved is

$$\frac{\partial^2 v}{\partial \rho^2} + \frac{1}{\rho} \frac{\partial v}{\partial \rho} - \frac{ik}{\kappa} v - \frac{n^2}{\rho^2} v = 0, \quad \dots (28)$$

and the general solution is

$$AI_n\left(\sqrt{\frac{ik}{\kappa}}\rho\right) + BK_n\left(\sqrt{\frac{ik}{\kappa}}\rho\right),$$

where  $A$  and  $B$  are arbitrary constants and  $I_n(z)$  and  $K_n(z)$  are functions of  $z$  derivable from the functions  $I_0(z)$  and

$K_0(z)$  already defined. The required solution is given by

$$v_i = A \cos n\theta e^{ikt} I_n\left(\sqrt{\frac{ik}{\kappa}} \rho\right) \dots a > \rho, \quad (29)$$

$$v_0 = B \cos n\theta e^{ikt} K_n\left(\sqrt{\frac{ik}{\kappa}} \rho\right) \dots \rho > a, \quad (29')$$

where the constants A and B are to be determined by the conditions to be fulfilled at the surface  $\rho = a$ ; namely,

$$v_i = v_0; \quad \text{and} \quad -K\left(\frac{\partial v_0}{\partial \rho} - \frac{\partial v_i}{\partial \rho}\right) = q e^{ikt} \cos n\theta. \quad (30)$$

These conditions lead to the result

$$v_i = \frac{qa}{K} \cos n\theta e^{ikt} K_n\left(\sqrt{\frac{ik}{\kappa}} a\right) I_n\left(\sqrt{\frac{ik}{\kappa}} \rho\right), \dots \quad (31)$$

$$v_0 = \frac{qa}{K} \cos n\theta e^{ikt} K_n\left(\sqrt{\frac{ik}{\kappa}} \rho\right) I_n\left(\sqrt{\frac{ik}{\kappa}} a\right) \dots \quad (31')$$

Verify that

$$\begin{aligned} -K\left(\frac{\partial v_0}{\partial \rho} - \frac{\partial v_i}{\partial \rho}\right)_{\rho=a} &= q e^{ikt} \cos n\theta \sqrt{\frac{ik}{\kappa}} a \\ &\quad \left[ -K'_n\left(\sqrt{\frac{ik}{\kappa}} a\right) I_n\left(\sqrt{\frac{ik}{\kappa}} a\right) \right. \\ &\quad \left. + K_n\left(\sqrt{\frac{ik}{\kappa}} a\right) I'_n\left(\sqrt{\frac{ik}{\kappa}} a\right) \right] \\ &= q e^{ikt} \cos n\theta. \dots \dots \dots (32) \end{aligned}$$

An alternative method of deriving this result is to take the periodic line source solution (8), replace  $q$  by  $qa d\theta' \cos n\theta'$ , and integrate round the cylindrical surface  $\rho = a$ . In this way we find

$$v = \frac{qa e^{ikt}}{2\pi K} \int_0^{2\pi} d\theta' \cos n\theta' K_0\left(\sqrt{\frac{ik}{\kappa}} r\right) \dots \quad (33)$$

for all values of  $\rho$ ,

where  $r^2 = a^2 + \rho^2 - 2a\rho \cos(\theta' - \theta)$ . The integration can be performed after using the addition theorem (19), when it is found that only those terms in the series for which  $m$  has the values  $+n$  and  $-n$  contribute to the final result. Thus for

$a > \rho$  the above integral reduces to

$$v_i = \frac{qa e^{ikt}}{2\pi K} \int_0^{2\pi} d\theta' \cos n\theta' \\ \cdot 2K_n \left( \sqrt{\frac{ik}{\kappa}} a \right) I_n \left( \sqrt{\frac{ik}{\kappa}} \rho \right) \cos n(\theta' - \theta), \quad (34)$$

which is readily seen to be in agreement with the results given above.

Alternative methods are again available to determine the solution representing a cylindrical surface source at which there is an instantaneous heat supply of amount  $q \cos n\theta$  per unit area at  $\rho = a$ . We may start from the solution for an instantaneous line source  $q$  per unit of length, given in equation (22) above. Replace the  $q$  by  $qa d\theta' \cos n\theta'$  and  $\rho$  by  $r$ , and integrate with respect to  $\theta'$  round the cylindrical surface,  $\rho = a$ . The temperature at point  $(\rho, \theta)$ , due to the whole surface distribution, is represented by

$$v = \frac{qa}{4\pi Kt} \int_0^{2\pi} d\theta' \cos n\theta' e^{-\frac{r^2}{4\kappa t}}, \quad \dots (35)$$

$$\text{where} \quad r^2 = \rho^2 + a^2 - 2a\rho \cos(\theta' - \theta).$$

If we alter the variable in this integration from  $\theta'$  to  $\phi$ , where  $\theta' - \theta = \phi$ , we can rewrite the above solution in the form:

$$v = \frac{qa e^{-\frac{\rho^2 + a^2}{4\kappa t}}}{4\pi Kt} \int_{-\theta}^{2\pi - \theta} d\theta \cos n(\theta + \phi) e^{\frac{a\rho}{2\kappa t} \cos \phi}, \quad (36)*$$

which leads us finally to the solution represented by

$$v = \frac{qa \cos n\theta}{2Kt} e^{-\frac{\rho^2 + a^2}{4\kappa t}} I_n \left( \frac{a\rho}{2\kappa t} \right), \text{ for } \rho > a \text{ and } \rho < a. \quad (37)$$

The alternative method open to us is to integrate with respect to  $k$  the solution representing a periodic cylindrical surface source of the type  $q \cos n\theta e^{ikt}$  per unit area, which has been derived immediately above. This method gives

$$v_i = \frac{qa \cos n\theta}{\pi K} \int_0^\infty dk e^{ikt} K_n \left( \sqrt{\frac{ik}{\kappa}} a \right) I_n \left( \sqrt{\frac{ik}{\kappa}} \rho \right) \dots \rho < a, \\ \dots \dots \dots (38)$$

$$v_0 = \frac{qa \cos n\theta}{\pi K} \int_0^\infty dk e^{ikt} K_n \left( \sqrt{\frac{ik}{\kappa}} \rho \right) I_n \left( \sqrt{\frac{ik}{\kappa}} a \right) \dots \rho > a. \\ \dots \dots \dots (38')$$

\* See Rayleigh, 'Scientific Papers,' vol. vi. p. 55.

A demonstration of the equivalence of the two solutions (37) and (38) could doubtless be obtained by applying the method already used to prove the equivalence of the two solutions in the case where  $n=0$  given in (24) and (27) above.

In the cases which we have dealt with above, the initial conditions refer to heat supply. It is of interest to take up here some of the fundamental problems in which the initial conditions refer to temperature. Before we proceed to build up solutions from the two fundamental wave-trains, as we have done in the cases considered above, we shall find it worth while to examine the solution obtained from that representing an instantaneous supply of heat  $q$  per unit area at  $\rho=a$ .

If we differentiate with respect to  $a$  the solution given by equation (27) above, under the condition that the total heat supply of unit length of the cylinder is kept constant ( $qa=\text{const.}$ ), we obtain the solution

$$v = -\frac{q}{2K} \cdot \frac{a}{2\kappa t^2} e^{-\frac{a^2+\rho^2}{4\kappa t}} \left\{ a I_0\left(\frac{a\rho}{2\kappa t}\right) - \rho I_1\left(\frac{a\rho}{2\kappa t}\right) \right\}, \quad (39).$$

which is equivalent to the doublet-solution for the surface  $\rho=a$ . When  $t$  tends to zero,  $\frac{a\rho}{2\kappa t}$  tends to become infinite,

and the two functions  $I_0\left(\frac{a\rho}{2\kappa t}\right)$  and  $I_1\left(\frac{a\rho}{2\kappa t}\right)$  may be represented with sufficient accuracy each by the first term only of its asymptotic expansion. Thus when  $t \rightarrow 0$  (or  $\rho \rightarrow \infty$ ) the above equation may be replaced by

$$v = -\frac{q}{2K} \cdot \frac{a}{2\kappa t^2} e^{-\frac{a^2+\rho^2}{4\kappa t}} \left\{ e^{\frac{a\rho}{2\kappa t}} \sqrt{\frac{\kappa t}{\pi a\rho}} (a-\rho) \right\} \quad (40)$$

$$= \frac{q}{2K} \cdot \sqrt{\frac{a}{\rho}} \cdot \frac{(\rho-a)}{2\sqrt{\pi\kappa t^3}} e^{-\frac{(\rho-a)^2}{4\kappa t}} \dots \dots \dots (40')$$

Now compare this result with equation (13) of the former paper, and it becomes evident that, in the limit  $t \rightarrow 0$ , the value of  $v$  is  $(q/2K)$  for  $\rho > a$ , and it is  $-(q/2K)$ , for  $\rho < a$ . Thus the solution

$$v = -\frac{\theta a}{2\kappa t^2} e^{-\frac{a^2+\rho^2}{4\kappa t}} \left\{ a I_0\left(\frac{a\rho}{2\kappa t}\right) - \rho I_1\left(\frac{a\rho}{2\kappa t}\right) \right\} \quad (41)$$

gives initially  $v=\theta$  on the outer side, and  $v=-\theta$  on the inner side of the surface,  $\rho=a$ . At the same time the

gradient of temperature on the two sides of the surface is continuous; that is,  $\left(\frac{\partial v_i}{\partial \rho} = \frac{\partial v_0}{\partial \rho}\right)_{\rho=a}$ . If we differentiate with respect to  $a$ , the solution given in equation (24) above, keeping ( $qa = \text{constant}$ ) as before, we ought to obtain a solution equivalent exactly to that given in (39) above; namely,

$$v_i = -\frac{qa}{\pi K} \int_0^\infty dk e^{ikt} \sqrt{\frac{ik}{\kappa}} \cdot K_1\left(\sqrt{\frac{ik}{\kappa}} a\right) I_0\left(\sqrt{\frac{ik}{\kappa}} \rho\right) \dots a > \rho, \quad (42)$$

$$v_0 = \frac{qa}{\pi K} \int_0^\infty dk e^{ikt} \sqrt{\frac{ik}{\kappa}} \cdot K_0\left(\sqrt{\frac{ik}{\kappa}} \rho\right) I_1\left(\sqrt{\frac{ik}{\kappa}} a\right) \dots \rho > a. \quad (42')$$

Replace ( $q/K$ ) by  $2\theta$  in this, and we obtain a solution satisfying all the conditions fulfilled by the solution (41); that is,

$$\text{at } t = 0, \quad (v_0 = +\theta, \quad v_i = -\theta)_{\rho=a}; \quad \text{and} \quad \left(\frac{\partial v_i}{\partial \rho} = \frac{\partial v_0}{\partial \rho}\right)_{\rho=a}. \dots (43)$$

Verify that

$$\begin{aligned} (v_0 - v_i)_{\rho=a} &= \frac{2\theta}{\pi} \int_0^\infty dk e^{ikt} \sqrt{\frac{ik}{\kappa}} a \left\{ K_0\left(\sqrt{\frac{ik}{\kappa}} a\right) I_1\left(\sqrt{\frac{ik}{\kappa}} a\right) \right. \\ &\quad \left. + K_1\left(\sqrt{\frac{ik}{\kappa}} a\right) I_0\left(\sqrt{\frac{ik}{\kappa}} a\right) \right\} \quad (44) \\ &= \frac{2\theta}{\pi} \int_0^\infty dk e^{ikt} = 2\theta \text{ at } t = 0 \text{ (real part) and} \\ &= 0 \text{ for } t > 0 \end{aligned}$$

by Fourier's fundamental integral. Note also that when  $\rho$  and  $a$  both become infinite, while the difference between them ( $\rho - a$ ) remains finite, the solution becomes identical with (13) of the former paper. The peculiar nature of these solutions, especially with reference to the initial space distributions of temperature which they represent, is a matter requiring further careful examination; but we shall leave it to another occasion.

We may treat the problem dealt with above from a different standpoint, by starting out from the solutions of

equation (28), represented by

$$v_i = -\Theta \cos n\theta \cdot e^{ikt} I_n\left(\sqrt{\frac{ik}{\kappa}} \rho\right) / I_n\left(\sqrt{\frac{ik}{\kappa}} a\right), \quad (45)$$

$$v_0 = \Theta \cos n\theta \cdot e^{ikt} K_n\left(\sqrt{\frac{ik}{\kappa}} \rho\right) / K_n\left(\sqrt{\frac{ik}{\kappa}} a\right). \quad (45')$$

These obviously fulfil the condition that at the surface  $\rho=a$  the temperature is given by  $\mp \Theta \cos n\theta \cdot e^{ikt}$ , but they also require that the heat-flow from the surface  $\rho=a$  on the outward side is not equal to the heat-flow to the surface on the inward side, since

$$\left. \begin{aligned} \frac{\partial v_0}{\partial \rho_{\rho=a}} &= \Theta \cos n\theta e^{ikt} \sqrt{\frac{ik}{\kappa}} \cdot K'_n\left(\sqrt{\frac{ik}{\kappa}} a\right) / K_n\left(\sqrt{\frac{ik}{\kappa}} a\right) \\ - \frac{\partial v_i}{\partial \rho_{\rho=a}} &= \Theta \cos n\theta e^{ikt} \sqrt{\frac{ik}{\kappa}} I'_n\left(\sqrt{\frac{ik}{\kappa}} a\right) / I_n\left(\sqrt{\frac{ik}{\kappa}} a\right). \end{aligned} \right\} \quad (46)$$

If we take the periodic heat supply from the surface  $\rho=a$ , represented by these terms respectively, and deduct the corresponding solutions as given by (31) from the solution (45), we obtain a new solution :

$$v_i = -\Theta \cos n\theta e^{ikt} \frac{I_n\left(\sqrt{\frac{ik}{\kappa}} \rho\right)}{I_n\left(\sqrt{\frac{ik}{\kappa}} a\right)} \left\{ 1 - \sqrt{\frac{ik}{\kappa}} a K_n\left(\sqrt{\frac{ik}{\kappa}} a\right) I'_n\left(\sqrt{\frac{ik}{\kappa}} a\right) \right\}, \quad (47)$$

$$v_0 = \Theta \cos n\theta e^{ikt} \frac{K_n\left(\sqrt{\frac{ik}{\kappa}} \rho\right)}{K_n\left(\sqrt{\frac{ik}{\kappa}} a\right)} \left\{ 1 + \sqrt{\frac{ik}{\kappa}} a K'_n\left(\sqrt{\frac{ik}{\kappa}} a\right) I_n\left(\sqrt{\frac{ik}{\kappa}} a\right) \right\}, \quad (47')$$

which satisfies the condition of equality in the flow of heat

outwards and inwards from the surface  $\rho=a$ ; that is,

$$\left(\frac{\partial v_0}{\partial \rho} - \frac{\partial v_i}{\partial \rho}\right)_{\rho=a} = \Theta \cos n\theta e^{ikt} \sqrt{\frac{ik}{\kappa}} \left[ \frac{K'_n}{K_n} + \frac{I'_n}{I_n} + \sqrt{\frac{ik}{\kappa}} a \left\{ \frac{K_n'^2 I_n'^2 - K_n^2 I_n'^2}{K_n I_n} \right\} \right] = 0. \quad (48)$$

Now proceed to the solution derived from this by an integration with respect to  $k$ , representing a temperature instantaneously generated at the surface  $\rho=a$  :—

$$v_i = \frac{\Theta a}{\pi} \cos n\theta \int_0^\infty dk e^{ikt} \sqrt{\frac{ik}{\kappa}} K'_n \left( \sqrt{\frac{ik}{\kappa}} a \right) I_n \left( \sqrt{\frac{ik}{\kappa}} \rho \right), \quad \dots \quad (49)$$

$$v_0 = \frac{\Theta a}{\pi} \cos n\theta \int_0^\infty dk e^{ikt} \sqrt{\frac{ik}{\kappa}} K_n \left( \sqrt{\frac{ik}{\kappa}} a \right) I'_n \left( \sqrt{\frac{ik}{\kappa}} a \right), \quad \dots \quad (49')$$

and it will be seen that a solution exactly similar to (42) is obtained. The first terms of (47) and (47') in this form of the solution, taken by themselves, evidently give after integration

$$-v = v_0 = \Theta \cos n\theta$$

at the surface  $\rho=a$ , and it follows that ( $t>0$ )

$$\begin{aligned} \int_0^\infty dk e^{ikt} \sqrt{\frac{ik}{\kappa}} K'_n \left( \sqrt{\frac{ik}{\kappa}} a \right) I_n \left( \sqrt{\frac{ik}{\kappa}} a \right) \\ = \int_0^\infty dk e^{ikt} \sqrt{\frac{ik}{\kappa}} K_n \left( \sqrt{\frac{ik}{\kappa}} a \right) I'_n \left( \sqrt{\frac{ik}{\kappa}} a \right). \end{aligned} \quad (50)$$

A confirmation of this result by another method is desirable. The two equivalent solutions of the problem of finding the temperature due to the instantaneous generation of temperature  $\Theta \cos n\theta$  at the surface  $\rho=a$ , derived by the methods indicated above, are given by

$$v = - \frac{\Theta a \cos n\theta}{2\kappa t^{\frac{3}{2}}} e^{-\frac{a^2+\rho^2}{4\kappa t}} \left\{ a I_n \left( \frac{a\rho}{2\kappa t} \right) - \rho I'_n \left( \frac{a\rho}{2\kappa t} \right) \right\}, \quad \dots \quad (51)$$

$$v_i = \frac{2\Theta a \cos n\theta}{\pi} \int_0^\infty dk e^{ikt} \sqrt{\frac{ik}{\kappa}} K'_n \left( \sqrt{\frac{ik}{\kappa}} a \right) I_n \left( \sqrt{\frac{ik}{\kappa}} \rho \right), \quad \dots \quad (52)$$

$$v_0 = \frac{2\Theta a \cos n\theta}{\pi} \int_0^\infty dk e^{ikt} \sqrt{\frac{ik}{\kappa}} K_n \left( \sqrt{\frac{ik}{\kappa}} \rho \right) I'_n \left( \sqrt{\frac{ik}{\kappa}} a \right), \quad \dots \quad (52')$$

respectively.



The solutions which we have obtained above may be regarded as fundamental solutions, in the sense that they form the basis from which we derive the solution of any problem for which the initial conditions include a given heat distribution throughout space, or a given temperature condition at particular surfaces. For example, starting from equation (27) we may obtain by integration the effect of a uniform instantaneous supply of heat  $q$  per unit volume of a cylinder of radius  $\rho = a$ . By replacing  $q$  by  $qda'$  and integrating with respect to  $a'$ , we obtain

$$v = \frac{q}{2Kt} \int_0^a da' a' e^{-\frac{\rho^2 + a'^2}{4\kappa t}} I_0\left(\frac{a'\rho}{2\kappa t}\right). \quad (53)$$

In this connexion it is very important to investigate the special solutions usually employed in building up solutions for cylindrical heat conduction problems, and, in the first instance, to establish these special solutions from the fundamental wave-trains employed in the present paper. Consider the case of a heat distribution  $q \cos n\theta J_n(k'a)$  per unit volume, instantaneously generated throughout space. We have, again, alternative methods of proceeding. In the first method we start from the solution representing the effect of an instantaneous surface distribution  $q \cos n\theta$  per unit area at the surface  $\rho = a$ , given in equation (37) above. Replace  $q$  by  $qJ_n(k'a)$ , and integrate with respect to  $a$  from 0 to  $\infty$ . This gives the solution which we require in the form:

$$v = \frac{q \cos n\theta}{2Kt} e^{-\frac{\rho^2}{4\kappa t}} \int_0^\infty da a e^{-\frac{a^2}{4\kappa t}} J_n(k'a) I_n\left(\frac{a\rho}{2\kappa t}\right). \quad (54)$$

By means of an evaluation given in Watson's 'Theory of Bessel Functions,' p. 395, this solution takes the form:

$$v = \frac{q \cos n\theta}{2Kt} e^{-\frac{\rho^2}{4\kappa t}} \cdot 2\kappa t e^{-k'^2 \kappa t + \frac{\rho^2}{4\kappa t}} I_n\left(\frac{ik'\rho}{2\kappa t} \cdot 2\kappa t\right). \quad (55)$$

$$= q \cos n\theta \cdot \frac{\kappa}{K} e^{-k'^2 \kappa t} J_n(k'\rho), \quad (56)$$

which is the well-known form of the solution of this problem. Now take, instead of (37), the equivalent solution in terms of  $K_n$  and  $I_n$ ; namely,

$$v_i = \frac{qa \cos n\theta}{\pi K} \int_0^\infty dk e^{ikt} K_n\left(\sqrt{\frac{ik}{\kappa}} a\right) I_n\left(\sqrt{\frac{ik}{\kappa}} \rho\right). \quad \rho < a, \quad (57)$$

$$v_0 = \frac{qa \cos n\theta}{\pi K} \int_0^\infty dk e^{ikt} K_n\left(\sqrt{\frac{ik}{\kappa}} \rho\right) I_n\left(\sqrt{\frac{ik}{\kappa}} a\right) \dots \rho > a. \quad (57')$$

To find the effect at  $(\rho, \theta)$  of the heat distribution specified above, we repeat the process just employed. Replace  $q$  by  $q da J_n(k'a)$  and integrate from 0 to  $\infty$ . For values of  $a$  less than  $\rho$  we must use  $v_0$  in this integration, and for values of  $a$  greater than  $\rho$  we must use  $v_i$  in the integration. Hence the solution equivalent to (54) is

$$v = \frac{q \cos n\theta}{\pi K} \int_0^\infty dk e^{ikt} F(k, a),$$

where

$$F(k, a) = K_n\left(\sqrt{\frac{ik}{\kappa}} \rho\right) \int_0^\rho da a I_n\left(\sqrt{\frac{ik}{\kappa}} a\right) J_n(k'a) \\ + I_n\left(\sqrt{\frac{ik}{\kappa}} \rho\right) \int_\rho^\infty da a K_n\left(\sqrt{\frac{ik}{\kappa}} a\right) J_n(k'a). \quad (58)$$

Each of the above integrations with respect to  $a$  can be performed by means of Lommel's method of integration (Gray, Mathews and MacRobert, 'Bessel Functions,' p. 69). By this method we find that

$$\left(k'^2 + \frac{ik}{\kappa}\right) \int_\rho^\infty da a J_n(k'a) K_n\left(\sqrt{\frac{ik}{\kappa}} a\right) \\ = -\rho \left\{ \sqrt{\frac{ik}{\kappa}} J_n(k'\rho) K'_n\left(\sqrt{\frac{ik}{\kappa}} \rho\right) \right. \\ \left. - k' J'_n(k'\rho) K_n\left(\sqrt{\frac{ik}{\kappa}} \rho\right) \right\}, \quad (59)$$

$$\left(k'^2 + \frac{ik}{\kappa}\right) \int_0^\rho da a J_n(k'a) I_n\left(\sqrt{\frac{ik}{\kappa}} a\right) \\ = \rho \left\{ \sqrt{\frac{ik}{\kappa}} J_n(k'\rho) I'_n\left(\sqrt{\frac{ik}{\kappa}} \rho\right) \right. \\ \left. - k' J'_n(k'\rho) I_n\left(\sqrt{\frac{ik}{\kappa}} \rho\right) \right\}, \quad (60)$$

and when we insert these results in the right-hand side of equation (58) we obtain

$$v = \frac{q \cos n\theta}{\pi K} J_n(k'\rho) \int_0^\infty dk \frac{e^{ikt}}{k'^2 + \frac{ik}{\kappa}} f\left(\sqrt{\frac{ik}{\kappa}} \rho\right), \quad (61)$$

where

$$f(z) = +z \{K_n(z) I'_n(z) - I_n^2(z) K'_n(z)\} = 1. \quad (62)$$

Hence

$$v = \frac{q \cos n\theta}{\pi K} J_n(k'\rho) \int_0^\infty dk \frac{e^{ikt}}{k'^2 + \frac{ik}{\kappa}}, \quad (63)$$

in which form the solution depends upon a well-known integral. If we retain the real part only of the expression on the right-hand side, the result arrived at by integration is

$$v = q \cos n\theta \cdot \frac{\kappa}{K} J_n(k'\rho) e^{-k'^2 \kappa t}, \quad (64)$$

as before. It is worthy of note, in connexion with this group of special solutions, that the initial heat distributions which they represent are distributions for which the total quantity of heat is zero. It is evident also from the above that we can deal with any arbitrary initial heat distribution by two distinct methods, and that the investigation of this general case should lead to the establishment of certain mathematical theorems.

Having obtained the above important confirmation of the method of solution by means of wave-trains, we can now employ this method to determine solutions in more general problems. One of the most important fundamental problems is that of determining the Green's Function in various special cases. As an example, we may consider the effect of an instantaneous line source emitting  $q$  units of heat per unit of length at  $(a', \theta')$ , the cylindrical surface  $\rho = a$  being kept at zero temperature, ( $a > a'$ ). We may start from the solution representing a periodic line source  $q e^{ikt}$  situated at  $(a', \theta')$ ,

$$v = \frac{q}{2\pi K} e^{ikt} K_0\left(\sqrt{\frac{ik}{\kappa}} r\right); \quad r^2 = \rho^2 + a'^2 - 2\rho a \cos(\theta - \theta') \quad (65)$$

$$= \frac{q}{2\pi K} e^{ikt} \sum_{-\infty}^{+\infty} K_m\left(\sqrt{\frac{ik}{\kappa}} \rho\right) I_m\left(\sqrt{\frac{ik}{\kappa}} a'\right) \cos m(\theta - \theta'); \quad \rho > a'. \quad (66)$$

Each term of this expression indicates a periodic temperature at the surface  $\rho = a$ ; and to reduce the temperature at  $a$  to zero, we have, therefore, to add a negative wave-train corresponding to each positive component in the above solution.

From equation (45) it appears that the solution determined by the above temperature condition at  $\rho=a$  is

$$v = \frac{q}{2\pi K} e^{ikt} \sum_{-\infty}^{+\infty} K_m \left( \sqrt{\frac{ik}{\kappa}} a \right) I_m \left( \sqrt{\frac{ik}{\kappa}} a' \right) \cos m(\theta - \theta') \cdot \frac{I_m \left( \sqrt{\frac{ik}{\kappa}} \rho \right)}{I_m \left( \sqrt{\frac{ik}{\kappa}} a \right)}. \quad (67)$$

To fulfil the condition stated at the surface  $\rho=a$ , this has to be deducted from the solution representing a line source at  $(a', \theta')$ . Thus the periodic solution which represents a line source at  $(a', \theta')$ , the boundary  $\rho=a$  being kept at zero temperature, is

$$v = \frac{q}{2\pi K} e^{ikt} \sum_{-\infty}^{+\infty} \cos m(\theta - \theta') F_m(\rho, a, a'), \quad (68)$$

where

$$F_m = \frac{I_m \left( \sqrt{\frac{ik}{\kappa}} a' \right)}{I_m \left( \sqrt{\frac{ik}{\kappa}} a \right)} \left\{ K_m \left( \sqrt{\frac{ik}{\kappa}} \rho \right) I_m \left( \sqrt{\frac{ik}{\kappa}} a \right) - I_m \left( \sqrt{\frac{ik}{\kappa}} \rho \right) K_m \left( \sqrt{\frac{ik}{\kappa}} a \right) \right\}, \quad (69)$$

and the corresponding solution, which represents an instantaneous line source  $q$  at  $(a', \theta')$ , the boundary  $\rho=a$  being kept at zero temperature, is

$$v = \frac{q}{2\pi^2 K} \sum_{-\infty}^{+\infty} \cos m(\theta - \theta') \int_0^\infty dk e^{ikt} F_m. \quad (70)$$

By means of the substitutions

$$\sqrt{\frac{ik}{\kappa}} = i\lambda, \quad ik = -\kappa\lambda^2,$$

this transforms into

$$v = \frac{q\kappa}{\pi^2 K i} \sum_{-\infty}^{+\infty} \cos m(\theta - \theta') \int d\lambda \lambda e^{-\lambda^2 \kappa t} \frac{J_m(\lambda a')}{J_m(\lambda a)} \{ G_m(\lambda \rho) J_m(\lambda a) - J_m(\lambda \rho) G_m(\lambda a) \}. \quad (71)$$

If the expression under the integral sign be integrated round a contour consisting of the two lines inclined to the

real axis of  $\lambda$  at angle  $\frac{\pi}{4}$  on each side and the circular arcs of infinite radius connecting them, we find by the theory of residues that

$$v = \frac{q\kappa}{\pi K a} \sum_{-\infty}^{+\infty} \cos m(\theta - \theta') \sum_{s=1}^{s=\infty} \lambda_s e^{-\lambda_s^2 \kappa t} \frac{J_m(\lambda a') G_m(\lambda a) J_m(\lambda \rho)}{J'_m(\lambda a')}, \quad (72)$$

the summation with respect to  $s$  extending over the roots of  $J_m(\lambda a) = 0$ . Further, since

$$G_m(\lambda \rho) J'_m(\lambda \rho) - J_m(\lambda \rho) G'_m(\lambda \rho) = \frac{1}{\lambda \rho}, \quad (73)$$

at each root of  $J_m(\lambda \rho) = 0$  we have

$$G'_m(\lambda_s a) = \frac{1}{\lambda_s a J'_m(\lambda_s a)} \quad (74)$$

and

$$v = \frac{q\kappa}{\pi K a^2} \sum_{m=-\infty}^{m=+\infty} \cos m(\theta - \theta') \sum_{s=1}^{s=\infty} e^{-\kappa \lambda_s^2 t} \frac{J_m(\lambda_s a') J_m(\lambda_s \rho)}{[J'_m(\lambda_s a)]^2}, \quad (75)$$

which is identical with the result given in Carslaw, 'Fourier Series and Integrals,' p. 394.

The problem of determining the Green's Function in the corresponding case, where radiation takes place at the outer boundary  $\rho = a$ , can be dealt with in an exactly similar manner. We start again from (66). Each wave-train represented in this expression suffers reflexion at the surface  $\rho = a$ , under the condition

$$-K \frac{\partial v}{\partial \rho} = hv,$$

and the reflected waves are all of the type

$$A_m \cos m(\theta - \theta') e^{ikt} I_m\left(\sqrt{\frac{ik}{\kappa}} \rho\right).$$

Hence the required solution, obtained by adding the reflected waves, may be written in the form :

$$v = \frac{q}{2\pi^2 K} \sum_{-\infty}^{+\infty} \cos m(\theta - \theta') \int_0^{\infty} dk e^{ikt} \left[ K_m\left(\sqrt{\frac{ik}{\kappa}} \rho\right) I_m\left(\sqrt{\frac{ik}{\kappa}} a'\right) + A_m I_m\left(\sqrt{\frac{ik}{\kappa}} \rho\right) \right], \quad (76)$$

where  $A_m$  is a complex constant (to include both types of

inward travelling wave-trains) determined by the condition stated above. The value for  $A_m$  is

$$A_m = - \frac{K \sqrt{\frac{ik}{\kappa}} K'_m \left( \sqrt{\frac{ik}{\kappa}} a \right) I_m \left( \sqrt{\frac{ik}{\kappa}} a' \right) + h K_m \left( \sqrt{\frac{ik}{\kappa}} a \right) I_m \left( \sqrt{\frac{ik}{\kappa}} a' \right)}{K \sqrt{\frac{ik}{\kappa}} I'_m \left( \sqrt{\frac{ik}{\kappa}} a \right) + h I_m \left( \sqrt{\frac{ik}{\kappa}} a \right)}, \quad (77)$$

and the solution corresponding to an instantaneous line source at  $(a', \theta')$ , the boundary condition being

$$-K \frac{\partial v}{\partial \rho} = hv \quad \text{at} \quad \rho = a,$$

is accordingly

$$v = \frac{q}{2\pi^2 K} \sum_{-\infty}^{+\infty} \cos m(\theta - \theta') \int_0^{\infty} dk e^{ikt} f(k, \rho), \quad (78)$$

where  $f(k, \rho)$

$$\begin{aligned} &= \frac{I_m \left( \sqrt{\frac{ik}{\kappa}} a' \right)}{I_m \sqrt{\frac{ik}{\kappa}} I'_m \left( \sqrt{\frac{ik}{\kappa}} a \right) + h I_m \left( \sqrt{\frac{ik}{\kappa}} a \right)} \\ &\quad \left[ K_m \left( \sqrt{\frac{ik}{\kappa}} \rho \right) \left\{ K \sqrt{\frac{ik}{\kappa}} I'_m \left( \sqrt{\frac{ik}{\kappa}} a \right) + h I_m \left( \sqrt{\frac{ik}{\kappa}} a \right) \right\} \right. \\ &\quad \left. - I_m \left( \sqrt{\frac{ik}{\kappa}} \rho \right) \left\{ K \sqrt{\frac{ik}{\kappa}} K'_m \left( \sqrt{\frac{ik}{\kappa}} a \right) + h K_m \left( \sqrt{\frac{ik}{\kappa}} a \right) \right\} \right]. \end{aligned} \quad (79)$$

By the substitution  $\sqrt{\frac{ik}{\kappa}} = i\lambda$ , employed in the former problem, the evaluations required can be obtained by means of the integrand

$$\lambda e^{-\kappa \lambda^2 t} \frac{J_m(\lambda a') [G_m(\lambda \rho) \{K\lambda J'_m(\lambda a) + h J_m(\lambda a)\} - J_m(\lambda \rho) \{K\lambda G'_m(\lambda a) + h G_m(\lambda a)\}]}{K\lambda J'_m(\lambda a) + h J_m(\lambda a)}. \quad (80)$$

When this expression is integrated round the contour employed in the preceding problem, a result similar to (72)

is obtained; namely,

$$v = \frac{q\kappa}{\pi K} \sum_{-\infty}^{+\infty} \cos m(\theta - \theta') \sum_{s=1}^{s=\infty} \lambda_s^2 e^{-\lambda_s^2 \kappa t} \\ \frac{J_m(\lambda_s a') J_m(\lambda_s \rho) \{ K \lambda_s G'_m(\lambda_s a) + h G_m(\lambda_s a) \}}{\frac{d}{d\lambda} \{ K \lambda_s J'_m(\lambda a) + h J_m(\lambda a) \}}, \quad (81).$$

where the summation with respect to  $s$  extends over the roots of

$$K \lambda J'_m(\lambda a) + h J_m(\lambda a) = 0. \quad . \quad . \quad (82)$$

Since equation (73) holds in addition to (82), it follows that at each root of (82) we have

$$K \lambda G'_m(\lambda a) + h G_m(\lambda a) = - \frac{K \lambda}{\lambda a J_m(\lambda a)}, \quad . \quad . \quad (83)$$

also

$$\begin{aligned} \frac{d}{d\lambda} \{ K \lambda J'_m(\lambda a) + h J_m(\lambda a) \} \\ &= a K \lambda J''_m(\lambda a) + K J'_m(\lambda a) + h a J'_m(\lambda a) \\ &= a K \lambda \left\{ -J_m(\lambda a) + \frac{m^2}{\lambda^2 a^2} J_m(\lambda a) \right\} + h a J'_m(\lambda a) \\ &= -J_m(\lambda a) \left\{ K \lambda \left( 1 - \frac{m^2}{\lambda^2 a^2} \right) + \frac{h^2}{K \lambda} \right\} a. \quad (84) \end{aligned}$$

By means of (82) and (84), our solution given by (81) becomes

$$v = \frac{q\kappa}{\pi K a^2} \sum_{-\infty}^{+\infty} \cos m(\theta - \theta') \sum_{s=1}^{s=\infty} \lambda_s^2 e^{-\lambda_s^2 \kappa t} \\ \frac{J_m(\lambda a') J_m(\lambda_s \rho)}{\left( \frac{h^2}{K^2} - \frac{m^2}{a^2} + \lambda_s^2 \right) [J_m(\lambda_s a)]^2}, \quad (85)$$

which is also in agreement with Carslaw, 'Fourier Series and Integrals,' p. 396.

The application of the methods illustrated above to problems involving continuous heat supply, and to problems involving change of medium, would lead to further useful results.

My thanks are due to James F. Shearer, M.A., B.Sc., of this University for his friendly interest and assistance in the work.

LXXV. *The Corona Discharge in Helium and Neon.*  
 By L. G. H. HUXLEY, B.A., *New College, Oxford* \*.

1. **T**HE theory of corona discharges in gases is of particular interest, as some of the properties of positive ions and of electrons may be deduced from measurements of the potentials required to start or maintain a current between a wire and a cylinder.

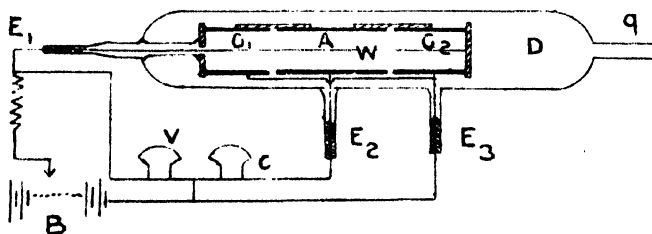
It was considered desirable to investigate this type of discharge in helium and neon, especially with a view to determining the velocities of the positive ions, and their effects in ionizing the gas.

In order to determine the dimensions of an apparatus to be enclosed in a quartz cylinder, I first made a preliminary investigation with an apparatus in a brass cylinder and found that a quartz cylinder of about 6 centimetres in diameter would be sufficiently large to enable me to make accurate measurements of the velocities of positive ions, and to determine the general properties of these discharges.

It is of great advantage to have the electrodes in a transparent envelope to see whether the corona is evenly distributed along the wire, and when a quartz tube is used the whole apparatus may easily be heated to a high temperature in order to expel occluded gases from the electrodes.

2. The apparatus finally adopted is shown in fig. 1. It

Fig. 1.



consisted of a long nickel cylinder 4.6 cm. in diameter, in three sections, the middle section A, which was 12 cm. long, being insulated by gaps of 2 mm. from the two end sections G<sub>1</sub> and G<sub>2</sub>, which were each 9 cm. long.

\* Communicated by Prof. J. S. Townsend, F.R.S.



The end sections acted as guard-rings, so that in the space between the wire and the central section A the electric force was along the radius.

The two sections  $G_1$  and  $G_2$  were fixed rigidly to the central section A by means of six quartz rods clamped by nickel cleets to the outer surface of the sections, so that the axes of the three sections coincided. Two of these rods are shown in the figure.

The two ends  $G_1$  and  $G_2$  were connected by a wire running through a thin quartz tube. A straight length of nickel wire 1.65 mm. in diameter was fixed along the axis of the nickel cylinder by pieces of quartz clamped to the ends of the sections  $G_1$  and  $G_2$ . The free end of the wire at  $G_2$  was screened from the discharge by the quartz support.

The quartz envelope was a cylinder of transparent silica 6.7 cm. diameter and 42 cm. long, thus leaving a space D about 12 cm. long near the open end of the tube in which to form an electrodeless discharge.

The nickel electrodes were placed in the quartz cylinder with the section  $G_1$  near the closed end, and the three connectors ( $E_1$ ,  $E_2$ , and  $E_3$ ) to the wire  $W_1$  the central section  $A_1$  and the two ends  $G_1$  and  $G_2$  were brought through quartz tubes and made air-tight with lead seals. The apparatus was connected to the pump and the charcoal tubes used for purifying the gas through the quartz tube  $q$ , which was ground to fit a glass tube with a tap,  $T_1$  (fig. 2). Another apparatus was also made of exactly the same dimensions with the exception of the central wire  $W$ , which was 2 mm. in diameter instead of 1.65.

The quartz work involving the sealing of the connectors E into the side tubes was carefully performed by the Mullard Radio Valve Co., and there was no trace of a leak in any of the quartz joints.

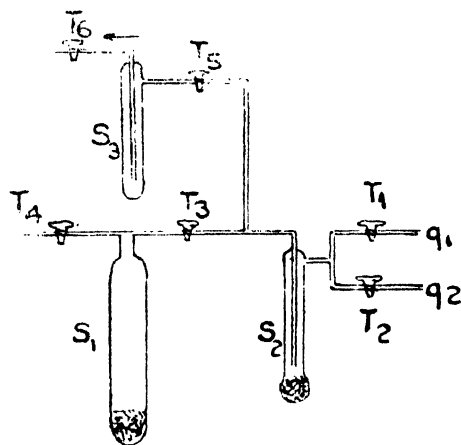
3. The current between the wire  $W$  and the central section A of the nickel tube was measured by a sensitive low resistance galvanometer C (fig. 1). The potential of the wire was adjusted by means of a battery of small accumulators, and the potential difference between the wire and the cylinder was given by the voltmeter V. The end sections  $G_1$  and  $G_2$  were connected through  $E_3$  to the wire joining C and V.

4. The gas was admitted to the cylinders through the tubes  $G_1$  and  $G_2$  (fig 2). The ground-glass joint was made air-tight with an elastic cement, and the taps were lubricated with grease. The contamination of the gas due to the

cement and the grease was so small that in the course of twenty-four hours there was no appreciable effect due to this cause, either in the spectrum of an electrodeless discharge in D or in the conductivity of the gas between the wire and the cylinder.

When the gas had remained in the apparatus for two or three days a small effect of impurity was noticeable, which became more marked when the quartz was heated. To remove these impurities the quartz was heated to a high temperature while a discharge was passed between the electrodes, and as the gas was pumped out the impurity

Fig. 2.



was carried with it\*. This method of treating the electrodes was used by Dubois in his researches on sparking potentials, and enabled him to obtain very consistent results with diatomic gases†. When the apparatus had cooled and a fresh supply of pure gas was admitted, no impurity was observable in the spectrum of the electrodeless high frequency discharge in D, and the potentials required to maintain currents between the wire W and the cylinder A were at the same definite values, always obtained when the

\* It is assumed by some experimenters that impurities may be completely removed from a gas in a vessel with electrodes, by diffusion into a side tube containing charcoal cooled with liquid air. This method is very slow, and it has been found that impurities are not removed for many hours, and in some cases for days.

† E. Dubois, *Ann. de Phys.* (9) vol. xx. Sept. & Oct. (1923).

gas was perfectly pure. Several precautions were taken to avoid impurities from other sources.

Before sealing the electrodes into the quartz tubes, the nickel apparatus was washed with carbon tetrachloride in order to remove grease due to handling. Also after the apparatus was connected to the pumps it was heated in an atmosphere of hydrogen to remove any oxide which may have formed on the nickel while the quartz was heated, during the sealing of the connectors E into the side tubes.

Two mercury vapour traps  $S_3$  and  $S_2$  cooled with liquid air were used between the taps  $T_1$  and  $T_2$  and the mercury pump, as in the preliminary experiments with the brass cylinder it was found very difficult to remove all traces of mercury. From time to time during the course of the experiments the mercury trap  $S_2$  was heated while  $S_3$  was cooled, in order to get rid of mercury and other impurities from the tubing near the apparatus.

In the quartz apparatus there was never any trace of mercury in the spectrum of the electrodeless discharge.

This method of avoiding any effects of impurities was found in this and other researches to be very effective, and constant results were obtained which could be easily repeated.

The gas from the apparatus was restored to the containing flask through the tube  $S_3$  and it was also admitted to the pressure gauge through  $S_3$ . In all cases the pressure in the gauge and the pump was reduced below the pressure in the apparatus and in the tube  $S_2$ , before the taps  $T_5$  and  $T_6$  were opened. Thus the gas always flowed in the direction of the arrow through the tube  $S_3$  (which was cooled with liquid air), so that no mercury vapour was carried from the pump or the gauge into the apparatus.

The gas was kept in the large tube  $S_1$  containing charcoal which was cooled by liquid air, for about sixteen hours, before being admitted into the apparatus. All impurities except hydrogen were thus completely removed. In order to get rid of any hydrogen the gas was brought from the containing flask into the charcoal tube  $S_1$  through a quartz tube containing copper oxide, which was heated by a coil of wire to the temperature required to convert hydrogen into water vapour. The gas was kept in the copper oxide tube for about ten minutes, and then admitted to the charcoal tube  $S_1$  through the tap  $T_4$ . As the copper oxide tube was of comparatively small volume the operation was repeated several times in order to collect a sufficient quantity of gas in the charcoal tube.

The tube  $S_2$ , through which the pure gas was passed from  $S_1$  to the apparatus, also contained charcoal cooled with liquid air. By these means perfectly constant results were obtained. The experiments on the currents between wires and cylinders were frequently repeated, using a fresh supply of gas each time, and the different observations at each pressure agreed within one or two per cent.

5. Experiments on corona discharges give results that determine two of the properties of positive ions in gases. They give a means of deciding as to whether electrons set free by positive ions arriving at the negative electrode are of importance compared with electrons derived from other processes. They also give a means of finding the velocities of the positive ions in the direction of the electric force for those cases in which the ratio of the electric force,  $X$ , to the pressure,  $p$ , is large.

The conclusions which may be drawn from the determinations of the potentials required to start the discharges may be considered first.

The generally accepted (S. Whitehead, 'Dielectric Phenomena, Electrical Discharge in Gases,' and W. O. Shumann 'Electrische Durchbruchfeldstärke von Gasen') theory is that given by Townsend. In this theory it is assumed that both electrons and positive ions generate others by collision with molecules of the gas, and that these two processes are predominant when the pressure of the gas is greater than that corresponding to the minimum sparking potential.

This theory gives a satisfactory explanation of the discharges between parallel plate electrodes and the corona discharges and shows that they are produced by the same processes of ionization. The results of experiments on discharges between concentric cylinders in diatomic gases were used to show that the effect of positive ions in setting free electrons from the negative electrode is negligible at the larger pressures. This conclusion may be extended to the properties of monatomic gases by considering the curves for the positive and negative discharges obtained for helium and neon.

The potentials required to start the discharges in pure helium for the wire of 1.65 mm. diameter are given by the curves of fig. 3\*, where the ordinates represent the

\* It was necessary at one stage in the experiments to open the cylinder with the wire 1.65 mm. diameter and to replace the wire by another of the same diameter. Points given by both wires are shown in the curves of fig. 3, those marked with arrows corresponding to the first wire. It is evident that both wires give points in good agreement.

Fig. 3.

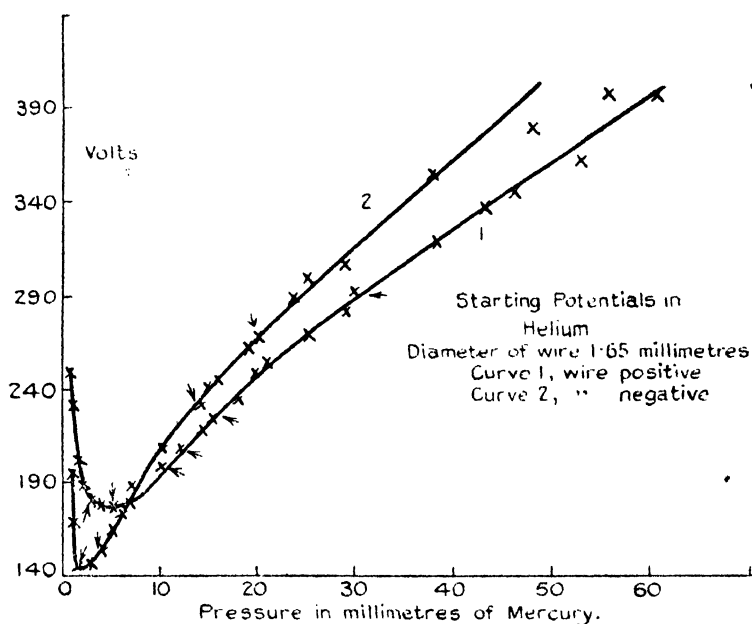
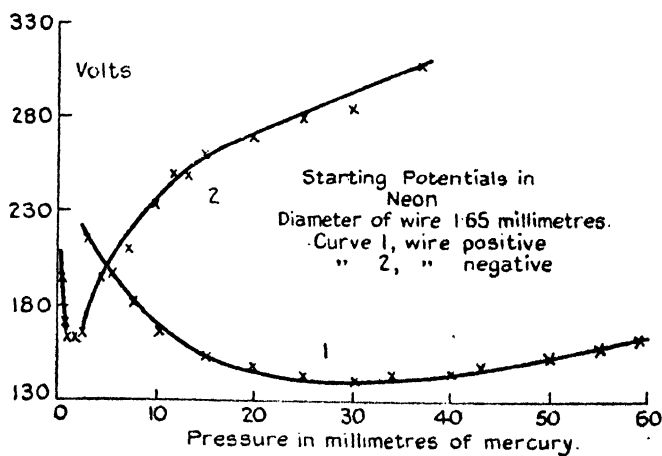


Fig. 4.



potential difference between the wire and cylinder in volts, and the abscissæ the pressure in millimetres of mercury.

Curve 1 gives the potentials with the wire positive and curve 2 with the wire negative. In fig. 4 the corresponding curves are given for pure neon. It can be seen that the curves for the discharges with the wire positive and those for the wire negative cross; at the higher pressures the positive discharge is obtained with a smaller potential than the negative.

This is of theoretical importance in determining the method by which positive ions produce new ions. By an extension of Townsend's continuity theorem (Townsend, 'Electricity in Gases,' p. 428), it may be shown that if the discharge were maintained by the action of electrons in ionizing the molecules of the gas by collision, and of the positive ions in liberating electrons from the negative electrode, the following condition must be satisfied:—

$$\int_0^S \alpha dx - \frac{1}{\gamma} = 1, \dots \dots \dots (1)$$

where  $\alpha$  is the average number of molecules ionized by an electron in moving 1 cm. in the direction of the electric force  $\gamma n$  the number of electrons set free from the cathode by a number  $n$  of positive ions impinging on it ( $\gamma$  may be supposed to depend on the velocity of impact),  $S$  the distance in centimetres between the electrodes, and  $x$  the distance along the path of the discharge measured in centimetres from the negative electrode.

This expression may be applied to the case in which the electrodes are concentric cylinders of the type under consideration. The value of the integral  $\int_0^S \alpha dx$  is approximately the same when the integration is taken from the wire to the cylinder as when taken from the cylinder to the wire, but may be slightly greater in the former case. Thus when the field is reversed this term is practically unchanged.

If  $\gamma$  were independent of the velocity of impact of the positive ions on the negative electrode, the positive and negative discharges should start with the same electromotive force between the wire and cylinder. If  $\gamma$  depended on the velocity of impact of the positive ions, it would be greater in the negative discharge than in the positive owing to the large value of the force near the wire compared with that

near the cylinder. The negative discharge would then be started with a smaller force than the positive.

These conclusions are contrary to the results obtained experimentally. The curves in figs. 3 and 4 show that at the larger pressures the positive discharge is obtained with smaller potentials than the negative. This occurs both in helium and in neon, but is more pronounced in the latter. In helium at a pressure of 30 mm. the positive discharge starts with a potential of 290 volts between the wire and the cylinder, and the negative with 320 volts. In neon at the same pressure the positive discharge is obtained with a potential of 140 volts, and the negative with 290 volts. In view of these results it is clear that the discharges cannot be explained on the hypothesis that the current is maintained by the ionization of the molecules of the gas by electrons combined with the liberation of electrons from the negative electrode by the action of positive ions.

6. It was found by leaving gas in the apparatus that the presence of an impurity produced considerable variations in its conductivity. The effect of impurity in helium is shown in fig. 5, where curves for the potentials required to start positive discharges with the wire 2 mm. in diameter for pure and impure helium are compared. Curve 1 is for pure and curve 2 is for impure helium.

At the higher pressures the potentials required to start the discharge are greater in the pure than in the impure gas, while at the lower pressures an impurity has the opposite effect. A similar effect was obtained for the negative discharges.

For positive discharges in neon the starting potentials were greater for the impure than the pure gas at all pressures, but in negative discharges the potentials were affected in a manner similar to those in helium.

When the potentials were the same as those given in curve 1 (fig. 5) the spectrum as shown by the electrodeless discharge was that of the pure gas, but when those corresponding to curve 2 (fig. 5) the spectrum indicated the presence of impurities.

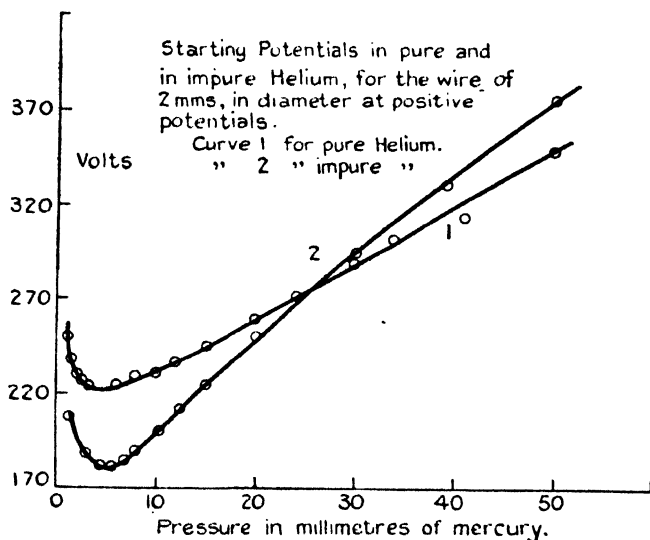
The spectrum of the impurities formed a continuous background to the characteristic lines of the pure gas, both in helium and in neon.

7. It is a well-known property of the discharges between coaxial cylinders, that the force  $X_1$  at the surface of the inner cylinder necessary to start the discharge is independent

of the diameter of the outer cylinder, provided the latter exceeds a certain value, depending on the pressure of the gas.

This indicates that the space in which the ions are generated does not extend beyond a certain distance  $c$  from the wire, and that ions are not generated by collision when the force is less than  $\frac{V}{c \log A/a}$ , where  $V$  is the potential difference between the electrodes and  $A$  and  $a$  the diameters of

Fig. 5.



the outer and inner cylinders. In these circumstances it may be shown theoretically (Townsend, *loc. cit.* p. 367) that the quantity  $aX_1$  depends only on the product  $a \times p$ , where  $a$  and  $X_1$  have the meanings given them above and  $p$  is the pressure of the gas. This is confirmed experimentally by comparing the values of  $a \times X_1$  for a given value of  $a \times p$  for discharges obtained with wires of different diameters.

When  $aX_1$  is expressed graphically as a function of  $ap$ , the points obtained from the experiments with the two wires lie on the same curve.

The curves 1 and 2 in fig. 6 are for helium, curve 1 for the positive and curve 2 for the negative discharge, the ordinates being the values of  $aX_1$  and the abscissæ those of  $ap$ . The points given by the wire of 1 mm. diameter are

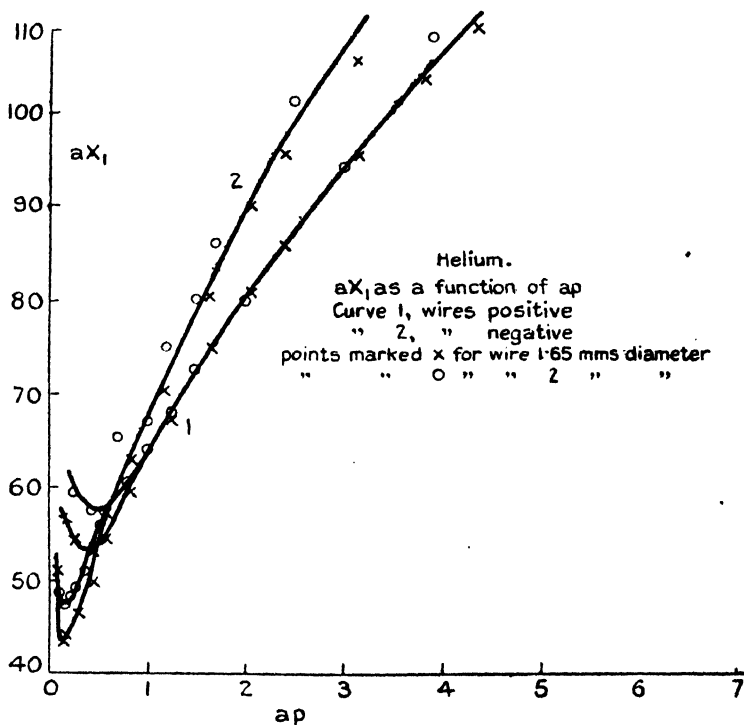


indicated by crosses, and those by the wire of 2 mm. diameter by circles.

The corresponding curves for neon are shown in fig. 7.

For the larger pressures, the value of  $aX_1$  obtained with wire of 1.65 mm. diameter are the same as those obtained with the 2 mm. wire, and the points lie on the same curve. As the pressure is reduced the ionization extends further into the space between the electrodes and eventually touches the

Fig. 6.



outer cylinder. For a given value of  $X/p$  the quantity  $c$  is proportional to  $a$ , and it follows that the ionization will have extended to the outer cylinder in the apparatus with the 2 mm. wire, at a higher pressure than in the apparatus with the wire 1.65 mm. diameter.

This is shown by the curves where the values of  $aX_1$  are greater at the lower pressures for the larger wire than for the smaller, with the exception of curve 1 for the positive discharge in neon.

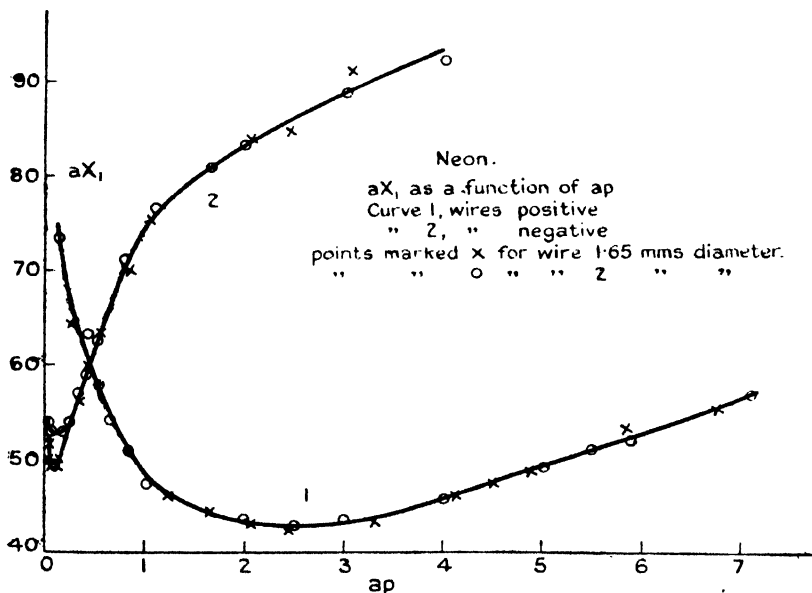
8. The velocities of the positive ions in the direction of the electric force were found from measurements of the currents which are maintained between a wire and a cylinder by potentials greater than those required to start the discharge.

The following equations given by Townsend (Phil. Mag., July 1914, p. 83) connect the currents with the potentials required to maintain them :—

$$\frac{(v-V)}{V} \log A/a = (1+\theta)^{\frac{1}{2}} - 1 + \log \frac{2}{(1+\theta)^{\frac{1}{2}} + 1} \quad (2)$$

$$\text{and} \quad \theta = \frac{2IA^2}{wa^2Z_1^2}, \dots \dots \dots (3)$$

Fig. 7.

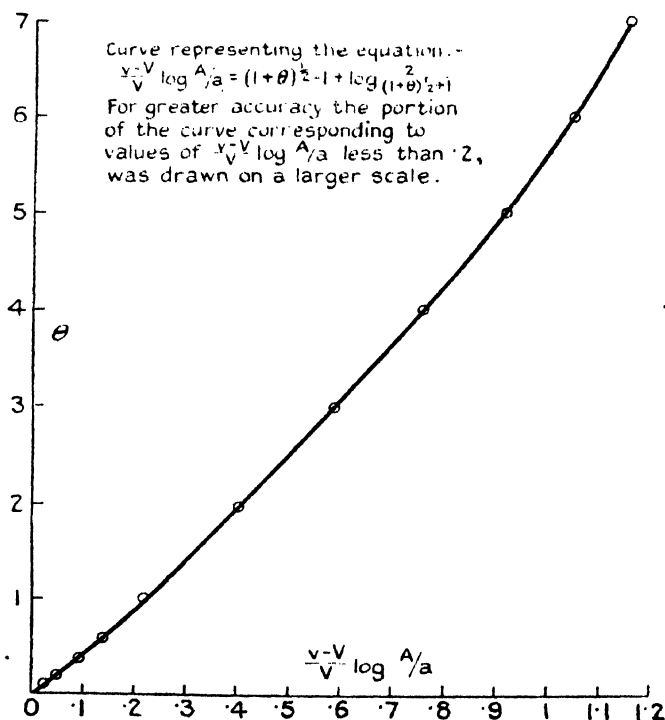


where  $I$  is the current per unit length of the wire,  $v$  the potential required to maintain the current,  $V$  the potential required to start the discharge,  $A$  and  $a$  the radii of the cylinder and the wire,  $wZ$  the velocity in centimetres per second of the ions in the direction of the electric force  $Z$ ,  $Z_1$  the force at the surface of the wire, the currents, potentials, and forces being expressed in electrostatic units.

The equations (2) and (3) serve to determine  $w$  from measurements  $v$ ,  $V$ , and  $I$ .

Equation (2) is represented by the curve in fig. 8, where the ordinates are the values of  $\theta$  and the abscissæ the values  $(v-V) \log A/a$ . Having determined the quantities  $v$ ,  $V$ , and  $I$ ,  $\theta$  is obtained from the curve, and  $w$  from equation (2):

Fig. 8.



It was found impossible to measure the velocities of the negative ions in helium and neon by this method, owing to the formation of a cathode fall of potential at the wire, making the discharge disruptive.

[In Table I. a series of potentials and currents with the corresponding values of  $w$  is given for helium at 57 mm. pressure, the diameter of the wire being 2 mm.

There is good agreement between the numbers found for  $w$  for different currents.

The mean values of  $w$  for pressures above 30 mm., obtained from experiments made with the two wires, are

given in Table II. The values of the product  $wv$  are also given.

TABLE I.

$v$ .	$I \times 10^{-4}$ .	$w \times 10^{-5}$ .
1.33	0	—
1.37	5.3	1.04
1.39	10.1	1.09
1.41	13.9	1.06
1.43	19.3	1.14
1.47	25.4	1.03
1.49	29.2	1.04

TABLE II.

Wire 1.65 mm. diameter.			Wire 2 mm. diameter.		
Pressure $p$ in mm. of mercury.	$w \times 10^{-5}$ .	$wv \times 10^{-6}$ .	Pressure $p$ .	$w \times 10^{-5}$ .	$wv \times 10^{-6}$ .
93 .....	1.74	6.9	67 .....	.95	6.4
80 .....	.85	6.8	57 .....	1.1	6.3
77 .....	.87	6.7	50 .....	1.2	6.0
53 .....	1.3	6.9	39 .....	1.9	7.4
43 .....	1.6	6.9	30 .....	2.5	7.5
29 .....	2.6	7.5			

Since  $wv$  is constant, for the larger pressures the velocity  $W$  of a positive ion in the direction of the electric force is given by the formula  $W = bX/p$ , where  $b$  is a constant equal to  $2.27 \times 10^{-4}$  when  $X$  is in volts per centimetre, and  $p$  in millimetres of mercury. This formula is applicable when  $X/p$  is less than 2.5. According to this formula the velocity of the positive ions in helium at 760 mm. pressure under a force of one volt per centimetre would be 30 centimetres per second, if the mass of the ion were the same at 760 mm. pressure as at 50 mm. pressure.

The velocities for larger values of  $X/p$  are obtained from the experiments with pressures less than about 30 mm.

At these pressures the values of  $w$  for a given pressure increase with the current and therefore also with the force.

The results obtained at pressures of 20 and 15 mm. are given in Table III. The diameter of the wire was 2 mm.

TABLE III.

Pressure 20 mm.				Pressure 15 mm.			
$v$ .	$I \times 10^{-2}$ .	$w \times 10^{-5}$ .	$wp \times 10^{-6}$ .	$v$ .	$I \times 10^{-2}$ .	$w \times 10^{-5}$ .	$wp \times 10^{-6}$ .
·833	0	...	...	·757	0	...	...
·853	8·35	3·3	6·6	·777	9·75	6·2	9·3
·880	28·6	3·9	7·8	·790	41·2	11·3	16·7
·897	36	5·1	10·2				

In these cases  $w$  increases with the electric force.

At pressures less than 12 mm. the current increases so rapidly with increase of voltage that the discharge becomes disruptive and  $w$  cannot be found.

Thus with the large values of  $X/p$ ,  $W$  may be represented by the formula

$$W = bX/p, \text{ where } b \text{ increases with } X/p.$$

In neon there was no range of values of  $X/p$  for which  $b$  was constant, as in helium. Over the whole range of pressures  $b$  increased with  $X/p$ . This is illustrated in Table IV., where  $v$ ,  $I$ ,  $w$  are given for neon at 82 mm. pressure, with the wire of 1·65 mm. diameter.

Table IV.

$v$ .	$I \times 10^{-2}$ .	$w \times 10^{-6}$ .
·615	0	...
·617	2·6	·45
·743	6·4	·56
·773	10·5	1·03
·807	10	1·4
·827	31·6	

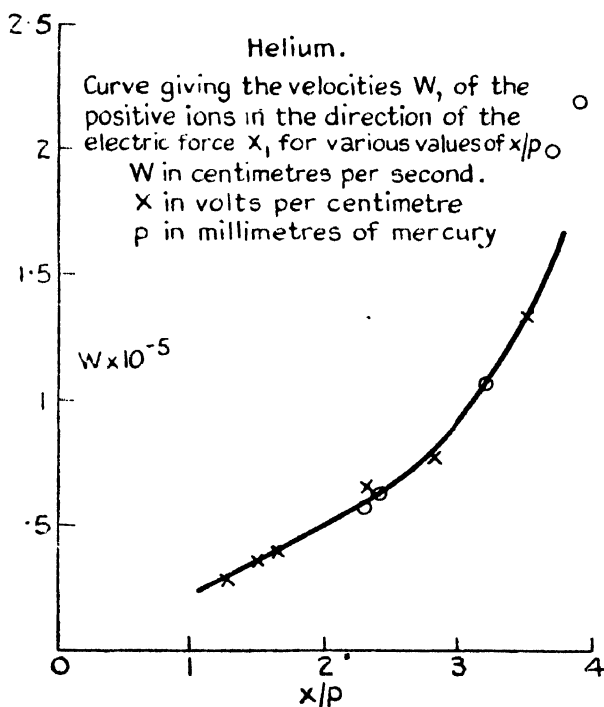
The experimental results are most conveniently expressed by a curve giving the velocity  $W$  as a function of  $X/p$ .

In order to evaluate  $X/p$  it is necessary to consider the distribution of the field between the electrodes while a current is passing. It may be shown that the radial force  $Z$  at the distance  $r$  centimetres from the axis is given by the equation

$$Z^2 = \frac{a^2 Z_1^2}{r^2} + \frac{2I}{w}.$$

With the larger currents the value of  $Z$  is nearly constant for the larger values of  $r$ , and since the most effective part

Fig. 9.



of the space charge is that near the surface of the outer cylinder, the mean value of  $Z$  over this space may be taken as the force at  $r=1.5$  cm.

The curve in fig. 9 gives  $W$  as a function of  $X/p$  for helium, while that in fig. 10 is the corresponding curve for neon.

The ordinates have the values  $W \times 10^{-5}$ , and the abscissæ the values of  $X/p$ ,  $X$  being in volts per centimetre,  $p$  in

millimetres of mercury, and  $W$  the velocity of the positive ions in centimetres per second. The points marked with a cross were given by the wire of 1.65 mm. diameter and those marked with a circle by the 2 mm. wire.

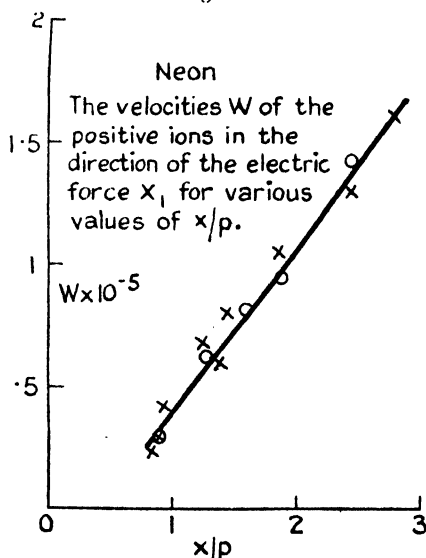
In both gases  $Wp/X$  increases with  $X/p$ .

The simplest theoretical formula for the velocity  $W$  of an ion in the direction of electric force is of the form

$$W = g \frac{e}{m} \frac{X}{p} \frac{l}{u},$$

where  $g$  is a constant,  $e$  and  $m$  the charge and mass of the ion,  $l$  its mean free path, and  $u$  its velocity of agitation.

Fig. 10.



Since  $u$  does not decrease, the large increase of  $W$  with  $X/p$  must be due to an increase in the mean free path  $l$ .

The molecules of helium and neon show, then, towards positive ions of certain velocities large reductions in the effective diameter, analogous to those obtained in the study of the velocities of electrons. For the value  $X/p=2$ , the velocity of the positive ions is  $1.05 \times 10^6$  in neon, and  $.5 \times 10^6$  in helium. Thus the mean free paths in neon are about five times the mean free paths in helium. The corresponding result for electrons is shown by the tables for

the values of the mean free paths obtained with small velocities by Townsend and Bailey ('Motion of Electrons in Gases,' University Press, Oxford). The mean free path of electrons moving with a velocity  $6 \times 10^8$  cm. per second in neon at 1 mm. pressure is .21 cm. and in helium .048 cm.

9. It cannot be assumed as an objection to the hypothesis of the ionization of molecules of a gas by collision with positive ions, that positive ions cannot acquire sufficient energy to ionize molecules. In view of the fact that both in helium and neon the positive ions can have long free paths and can acquire comparatively large energies, it is necessary when proposing a theory of electrical discharges in gases to consider ionization of molecules by impact with positive ions, as a possible process by which new ions may be generated.

I wish to conclude by expressing my gratitude to Professor Townsend for his constant assistance and inspiration throughout the course of the investigation.

*Note.*—A variation in the mean free paths of positive ions in Helium has been found by Dempster \*. The ions were liberated from a hot electrode and possessed greater energies than those occurring in the above experiments.

## LXXVI. *Chemical Dynamics in a Rigidly Coherent Phase.*

By D. H. BANGHAM, M.A., D.Sc. †

**T**HIS paper is an attempt to interpret the observation of Bangham and Burt ‡ that the rate at which sorption of gases takes place at a surface of glass is given in the early stages of process by an equation of the form

$$s = \text{constant} \times t^{1/m},$$

$$\frac{ds}{dt} \propto t^{-(1-1/m)} \propto s^{-m+1}. \quad \dots \quad (1)$$

Here  $s$  is the amount of gas accepted by the solid at time  $t$ , and  $m$  a constant greater than unity.

In the sequel it was found that this behaviour is not peculiar to glass (as an absorbent), or even to vitreous bodies in general, but that it is also met with in cases of sorption

\* A. J. Dempster, Ph.D., "The Passage of Positively-charged Particles through Helium," *Phil. Mag.*, Jan. 1927, p. 115.

† Communicated by the Author

‡ *Proc. Roy. Soc. A*, cv. p. 481 (1924).



by a whole variety of crystalline and semi-crystalline solids. A similar form of equation applies equally well to the taking up of iodine by charcoal \*, of ammonia gas by carborundum powder and sapphire †, and of oxygen by "activated" graphite ‡.

The failure to approach anything like an equilibrium is not in all cases surprising, since it is well known that the superficial coating of a solid with a layer of adsorbed molecules—a process requiring only a short time for its completion—is often accompanied by the slow diffusion of the molecules into the interior. There is ample evidence that molecules of water can be gained or lost by the layers of glass that are beneath the surface, and there is little difficulty in crediting ammonia with the same power of penetrating a glass surface and participating in the chemical equilibrium in the interior. The other cases—those in which the sorbent is crystalline—are less readily explained. Yet the rejection of the diffusion hypothesis for the latter class rests less on the qualitative behaviour of the individual members than on the impossibility of reconciling equation (1)—established by measurements of some accuracy—with the ordinary theory of diffusion §.

After several attempts to formulate a theory that would lead to a dynamical equation in harmony with the experimental results, the author was led to examine the literature for data bearing on the rate of progress of other, and completely different, physical and chemical changes taking place in solid substances. Here he was more successful, for it soon became apparent that the "power" time-law is the rule rather than the exception where changes taking place in the solid phase are concerned—a fact not generally recognized ||. In coming to this conclusion the author has been aided, not only by the data of those workers who have definitely set out to measure the time-changes, but also of many others who, having noticed a steady drift in the properties of the substances they were using, have observed and recorded its rate. It has frequently been assumed that this drift was following an exponential course, so that equilibrium or steady values could be calculated on the basis

\* McBain and Davis, *Trans. Faraday Soc.* xiv. p. 202 (1919).

† Private communication from Mr. J. B. M. Herbert.

‡ Bangham and Stafford, *J. C. S.* cxxvii. p. 1085 (1925).

§ Bangham and Sever, *Phil. Mag.* xlix. p. 935 (1925).

|| The term "solid" where used in this paper is intended to include non-crystalline bodies in which the thermal motions of the atoms are vibratory, not translational.

that the rate of progress was proportional to the distance from completion; but a wide survey of the subject leaves a strong impression that the number of exponential terms required to fit the experimental observations is often limited only by the range and accuracy of the latter. While the discussion below is confined to simple types of change which have been examined in sufficient detail to establish definitely the "power" type of time-law in their case, there are in fact countless others which, though less unequivocal, are quite consistent with a time-law of this type\*. This generality is important since, together with the fact that typical liquids do not show a parallel behaviour (except perhaps in one or two cases of surface effects), it indicates the direction in which we are to seek an explanation of the law in question. As the surface layers of liquids are known to contain molecules in a definite condition of orientation, we may suppose the same causes to be operative here as in the case of solids.

*The Non-validity of the Law of Viscous Flow  
in the Case of Solids.*

The rate of deformation under steady loads of a large number of solid substances have been examined by Trouton and Rankine †, Larard ‡, Phillips §, and others. The general results of the authors named may be summed up in the statement that the strain ( $x$ ) and the time ( $t$ ) (reckoned from the moment of application of the steady stress) were found to be related by an equation of the form

$$x = a + b \log t, \\ \frac{dx}{dt} = bt^{-1} = be^{\frac{-x}{b}}, \quad . \quad . \quad . \quad . \quad . \quad (2)$$

where  $a$  and  $b$  are constants. This law which, as Trouton points out, is at complete variance with all established theories, holds with considerable accuracy for such widely different substances as copper, silver, lead, steel, glass, and indiarubber.

\* For example: The phenomenon of photo-electric fatigue investigated by Hallwachs, H. S. Allen (Proc. Roy. Soc. A, lxxviii. p. 483, 1907; A, cxxxii. p. 161, 1909), Pochettino (*Atti dei Lincei*, xv. p. 171, 1906), and many others; the variation of capacities of lead accumulators during charging (see, for example, Hazelett, Trans. Amer. Electrochem. Soc. xxxiii. p. 95, 1909); the time-variation of the resistance of selenium on exposure to light (Brown, Phys. Rev. xxxiii. p. 410, 1911, and later papers).

† Trouton and Rankine, Phil. Mag. viii. p. 538 (1904).

‡ Larard, Proc. Phys. Soc. London, xxv. p. 83 (1912).

§ Phillips. Proc. Phys. Soc. London, xix. p. 491 (1903).

Nutting\*, on the other hand, suggests as the form of empirical equation most widely applicable

$$x = \text{constant} \times t^{1/n},$$

$$\frac{dx}{dt} \propto t^{-(1-1/n)} \propto t^{-n+1}, \quad \dots \dots \dots (3)$$

where  $n$  is a constant greater than unity.

For reasons which will appear, it is the differential forms of these equations which are all-important. It is seen at once that differential equation (2) is but a special case of Nutting's differential equation (3), in which  $n$  is infinite. It follows that while any series of observations which shows agreement with equation (2) must also be consistent with Nutting's differential equation (3), the converse holds only when  $n$  is very great. For example, equation (3) in its integrated form represents with great accuracy the data of Trouton and Andrews† for the twist suffered by rods of pitch (at room temperature) at different times after the application of a constant torque. It is worthy of note that Trouton's own equation gives very poor agreement in this instance, even if a constant term is added to the expression for the rate, to take into account the possibility of ordinary viscous flow (that is, flow taking place without elastic storage of energy).

### *The Behaviour of Dielectrics.*

When a potential difference is set up and maintained constant between a pair of electrodes in contact with the two sides of a plate of dielectric or poorly-conducting material, the observed current (initially relatively great) gradually decays until, at least in certain cases, it ultimately approaches zero. If the external E. M. F. is removed and the electrodes short-circuited, a current in the opposite sense makes its appearance and falls off to zero as time goes on. These effects are more noticeable in more obviously heterogeneous bodies; and in order to reconcile with them the accepted theory of dielectrics (according to which an *immediate* electric displacement depending on the material should be followed by a steady current proportional to its conductivity), Maxwell supposed the presence in the dielectric of the phases characterized by different specific inductive

\* P. G. Nutting, Journ. Franklin Inst. cxcii. p. 679 (1921).

† Trouton and Andrews, Proc. Phys. Soc. London, xix. p. 47 (1904); Phil. Mag. vii. p. 347 (1904).

capacities. He considered that the energy used in forcing the current through the dielectric was not wholly degraded into heat, but was used in doing work against the elastic forces of the solid by causing a relative motion of the two phases. The anomalous discharge current he attributed to gradual return to the original state brought about by the agency of these elastic forces.

Maxwell's theory led him to an exponential expression for the decay with time of the discharge current. If  $i_0$  be the discharge current immediately the electrodes are short-circuited, and  $i_t$  its value  $t$  minutes afterwards, then according to Maxwell,

$$i_t = i_0 e^{-ht}, \quad . \quad . \quad . \quad . \quad . \quad . \quad (4)$$

where  $h$  is a constant.

It has been abundantly proved that neither the discharge nor the charging current decays in accordance with this equation. Trouton and Russ\* and also H. A. Wilson† have found that the discharge-current was practically proportional to  $t^{-1}$  (*cf.* equation (2)), while, according to Schweidler‡, the decay of the charging current can in general be represented by the equation (*cf.* (3)) above for plastic deformation.

$$i_t = \text{constant} \times t^{-r}, \quad . \quad . \quad . \quad . \quad . \quad . \quad (5)$$

where  $r$  is a positive constant often closely approaching unity.

### *The Chemical Character of the Changes Considered.*

An explanation of the power time-law must clearly be sought in the chemical forces which are the primary cause of rigid cohesion. The response of any rigid body to external mechanical forces—for instance, the stretching or bending of a wire or piece of indiarubber—must, in so far as it involves changed mutual relationships between the constituent atoms, be termed a chemical reaction. The same applies when a plate of insulating material is placed between charged electrodes, and when a photo-active substance such as selenium is exposed to light. In all these cases there is a well-marked drift in the properties of the solid, the extent of which depends on the time for which the disturbing influence is maintained.

To sum up, there is abundant evidence that solids, even of

\* Trouton and Russ, *Proc. Phys. Soc. London*, xx. p. 551 (1905).

† H. A. Wilson, *Proc. Roy. Soc. A*, lxxxii. p. 409 (1909).

‡ Schweidler, *Ann. Physik*, xxiv. p. 711 (1907).

the simplest chemical types, have an inner complexity of structure, rendering the attainment of a reproducible minimum potential energy a matter of extreme practical difficulty in their case\*. For solids and liquids alike, the well-known theory of Smits† accounts for this complexity in terms of the different energy states in which the simplest chemical unit can exist, such states being often only slowly mutually convertible. In Smits's nomenclature an ideal solid—in the sense of the ordinary theory of elasticity—should be classed as an "unary" system, since it attains a new equilibrium immediately on application of a steady load. A body showing "creep," on the other hand, must be at least "pseudo-binary," the drift of properties measuring the rate of a slow change of the fundamental chemical unit from one energy state to another, while the "elastic after-working" effect which often manifests itself on removal of the load finds a ready explanation in the setting-in of the reverse reaction.

Whatever may be the nature and size of the chemical units in terms of which the macroscopic change is ultimately expressible, the certainty that in coherent solids the rate of reaction does not depend on their chance encounters is sufficient to justify its formulation as a unimolecular reaction  $A_1 \rightarrow A_2$ . The only assumption made here is that similar changes of configuration are undergone by a large number of leptonic units‡, each of which is sufficiently small (as compared with the parent body) to permit application of the usual statistical principles.

The empirical expressions (2) and (3) above are alike in taking no cognisance of any limit to the extent of the change as  $t$  approaches infinity; and it follows that the rate can be governed neither by the nearness of approach to equilibrium

\* Cf., for instance, Lewis and Randall, 'Thermodynamics' (McGraw-Hill Book Co., 1923).

† Smits, 'Theory of Allotropy' (English translation, Longmans, 1924).

‡ This assumption is at least justified in the special case of india-rubber, a substance which, as already mentioned, undergoes slow deformation in accordance with a time-law of the "power" type. Katz (*Kolloid-Z.* xxxvi. p. 300, 1925) has shown by the X-ray method that, when rubber is stretched, a strongly-marked crystalline structure is developed which disappears gradually on releasing the tension. An investigation of this phenomenon by Hauser and Mark has revealed that the amount of crystalline material is increased, not by the growth of old crystallites, but by the continuous formation of new ones (Hauser and Mark, *Koll. Chem. Beih.* xxiii. p. 64, 1926; *Ambrohn Festschrift.* lxiii. 1926 (cf. W. L. Bragg, Chemical Society Annual Reports, xxiii. p. 277, 1926)).

(setting-in of the reverse reaction), nor by the falling-off in the concentration of the reactant species. The explanation of its decay may well lie, however, in the circumstance that the chemical units are not independent molecules, but are structurally bound to their neighbours. Since each unit is subject to forces which balance its own external field, it follows that the occurrence of catastrophic change of configuration on the part of any one group of atoms must have the effect of placing the others in its vicinity under a mechanical stress, which is only balanced when the elastic properties of the body as a whole are called into play. The forces knitting the groups of atoms together must therefore vary as the reaction proceeds; and since this force determines the chance that any given group will undergo change of configuration, the decay in the reaction rate becomes explicable on these lines\*.

Making use of the fact that the forces binding the atomic groups, though chemical in origin, are expressible (in so far as their generalized effects are concerned) in terms of mechanical stresses, the above theory is capable of quantitative expression in cases where the solid body is originally isotropic, and the disturbing influence is such as to permit it to remain so.

It is assumed that the initial and final states  $A_1$ ,  $A_2$  of the chemical unit  $A$  are characterized by volumes  $V_1$ ,  $V_2$ , which are independent of the stress within the solid, and of the external pressure. To take into account the fact that transition from state  $A_1$  to  $A_2$  is possible only to groups which possess sufficient thermal energy of vibration to render them partially detached from their neighbours, we shall postulate also the transitory existence of an "activated" state  $A_A$ , the characteristic volume  $V_A$  of which far exceeds the average volume of the reactant species  $A_1$ . From this activated condition the group may relapse into either of the configurations  $A_1$ ,  $A_2$ , the relative probabilities of these events depending only on the inner structure of the group. During the progress of the unidirectional change the relations between the three states  $A_1$ ,  $A_A$ ,  $A_2$  may then be summarized thus :



\* It is possible that the increased hardness characteristic of strained solids is connected with this increase in the force restraining the thermal movements of constituent units. Since it appears in vitreous as well as in crystalline solids, it cannot be due entirely to distortion of glide-planes.

If  $\Pi$  be the pressure with which the rigid framework as a whole opposes the expansion of any individual group of atoms, the work which must be done in the process of activation is  $\Pi(V_A - V_1)$ , and the rate of change, being determined by the probability of activation, should be proportional to  $e^{-\frac{\Pi}{RT}(V_A - V_1)}$  if the number of  $A_1$  groups remains sensibly constant. A comparison of this result with the two alternative empirical expressions for the rate (2 and 3 above) now tells us how the internal stress  $\Pi$  varies with the "strain" or extent of the reaction.

It is seen at once that Trouton's equation (2) is satisfied if

$$\frac{d\Pi}{dx} = \text{constant}, \quad . . . . . (6)$$

implying a sort of extension of Hooke's law to the conditions within the solid.

Nutting's equation (3), on the other hand, requires that the relation between  $\Pi$  and  $x$  should take the form

$$\frac{d\Pi}{d \log x} = \text{constant}. \quad . . . . . (7)$$

From the theoretical standpoint the form of this last equation is not altogether surprising, as the following discussion may serve to demonstrate. Suppose a solid body composed of the fundamental unit  $A$  to be undergoing compression under a constant hydrostatic pressure, which is causing reaction  $A_1 \rightarrow A_2$  to take place. Let the change be still in progress when the fraction  $y$  of the groups of atoms are in the more compact configuration  $A_2$ . The further increase of  $y$  to  $(y + dy)$  is accompanied by an increase  $dP$  in the external pressure which the body as a whole can withstand without further change; and the same applies to a block of atom-groups chosen in the interior of the solid, in regard to the pressure exerted by the rigid envelope surrounding it. The relation of  $dP$  to  $dy$  is given by the thermodynamic equation expressing the effect of pressure on the reaction constant  $K$ , which is here equal to  $\frac{y}{1-y}$ :

$$dP = \frac{RT}{V_1 - V_2} d \log \frac{y}{1-y}. \quad . . . . . (8)$$

During the slower stages of the reaction the solid may be conceived as passing through a continuous series of false equilibria, in each of which the external pressure is opposed

partly by an active restoring force, and partly by a passive resistance due to internal stress, which opposes change in either direction. The permanence of each equilibrium state is destroyed, however, by the fortuitous internal property of the atom-groups which enables them, under certain conditions, to change their configuration. As the reaction proceeds, the active restoring force gradually decays, and the body loses to an increasing extent its power of immediate recovery, though its power of ultimate recovery remains unimpaired.

On this basis, as  $y$  increases to  $(y + dy)$ , some estimate of the change in the stress due to rigid cohesion should be gained by considering it equal to the accompanying change in an imaginary force-system capable of holding the existing chemical systems, before and after the change  $dy$ , in equilibrium with the constant external pressure. But this has been shown above to be equivalent simply to a negative decrease, that is, a positive increase, of pressure  $dP$ .

In the range where  $y$  is small compared with unity, the variation of  $(1 - y)$  is negligibly small compared with that of  $y$ , and substituting  $d\Pi$  for  $dP$ , we have, as an approximation valid within this range,

$$d\Pi = \frac{RT}{V_1 - V_2} d \log y. \quad . \quad . \quad . \quad (9)$$

The strain  $x$  is proportional, not to  $y$  itself, but to the increment  $(y - y_0)$ , reckoned from an original value  $y_0$ , which characterizes the unstressed solid. The relation (9) therefore reproduces the form of (7) above, provided  $y$  is always great compared with  $y_0$ ; that is, provided the amount of the resultant species  $A_2$  produced by the disturbing influence far exceeds that present in the original solid.

While not providing a derivation of the "power" time-law in any instance in which it has been found actually to hold, the above offers at least a partial explanation of the law, if it be supposed that  $\Pi$  is independent of the nature of the disturbing influence, and dependent only on the degree of the disturbance.

The rate of change being proportional to  $e^{-\frac{\Pi}{RT}(V_A - V_1)}$  and  $dy$  to  $dx$ , the suggested significance of the index constant  $n$  is arrived at by using equations (3) and (9). We get

$$n = \frac{V_A - V_2}{V_1 - V_2}. \quad . \quad . \quad . \quad (10)$$

It should therefore be nearly independent of the temperature.



Such experimental evidence as is available appears to support this conclusion \*.

*A New Aspect of the Sorption Problem.*

The difficulty commonly experienced in realizing complete equilibrium in sorption experiments is not necessarily due to the occurrence of diffusion; if the sorption follows the "power" time-law, it is to be inferred that the atomic groups forming the rigid framework of the sorbent are unable in their "average" condition to combine with gas molecules, but they require first to be activated at the expense of work done against the forces binding them. Those atomic groups which have entered into combination with gas molecules are in a configuration different from the remainder, and the change they have undergone imposes a stress on the rigid framework which surrounds them. That a porous sorbent like charcoal is actually distended in the process has recently been confirmed by the interesting experiments carried out by Meehan† at the Building Research Station, Garston. A very similar effect, the change of volume accompanying ionic exchange and variation of water-content of the zeolites, has been somewhat more fully investigated‡.

The extension of Langmuir's well-known "chemical" theory of sorption to such generally active sorbents as charcoal requires that the ultimate chemical units of these substances should be characterized by extreme reactivity. This activity may be almost completely masked, however, when the units are rigidly bound together; a parallel behaviour is shown by those metallic oxides which, by high-temperature ignition, are made to lose their power of rehydration. These oxides are strong *sorbents* of water, but

\* It will perhaps bear emphasis that the above considerations apply only to the slow "creep" following the disturbance of a solid, and not to the initial disturbance itself. The wide application of the "power" time-equation in its integrated form is partly connected with the fact that as long as  $n$  is fairly great, the linearity of the graph on which the logarithms of the variables are plotted is but little affected by adding constants (within limits) to the variable representing the extent of the change. Since the instantaneous effects earlier referred to would give rise to such constants, which may alter considerably the slope of the logarithmic graph, it follows that conclusions based on this method of determining the index may be widely in error.

† Proc. Roy. Soc. A, cxv. p. 199 (1927).

‡ G. Schultze, *Zeitschr. f. Phys. Chem.* lxxxix. p. 168 (1915) and subsequent papers.

the reaction is retarded to such an extent by the forces of rigid cohesion as to be practically arrested.

A sorbent is normally prepared by driving out the volatile matter from a substance originally mechanically rigid. This being carried out well below the sintering-point of the residue, the latter, though somewhat shrunken, may be freely permeable to gas molecules. A rough calculation from X-ray data indicates that even the lattices of certain crystalline solids, without having part of their structure removed by heat, contain lacunæ large enough to permit small molecules to enter. Imperfections in the crystal would render its interior even more accessible, and, to go to the extreme, it is clearly illogical to attempt to estimate the internal surface of substances like charcoal.

Calling the gas molecule  $G$  and the initial, active, and final states of the sorbent atom-group  $A_1$ ,  $A_A$ ,  $A_2$  respectively, our conception of the reaction may be formulated :



Its rate decays with the building-up of a stress which makes it more and more difficult for the  $A_1$  groups to attain the activated state as the reaction proceeds. It is not, of course, contended that the influence of this stress, rather than the accessibility of the gas molecules to a free surface, will invariably set a limit to the rate ; with certain types of solids, however, the conditions for accessibility and activation would be tantamount, since both require the partial detachment of the atom-group from its neighbours\*.

The mechanism described goes far to explain the hysteretic effects so common in sorption and occlusion phenomena. The behaviour of a particular sorbent will depend largely on whether or not its atom-groups are capable of losing their gas without reverting to the unreactive configuration. If this is the case, the sorption-value at a particular pressure will depend largely on the past history of the sorbent. Owing to the larger number of reactive groups present, the sorption will be greater if the "equilibrium" is approached from a higher than if from a lower pressure. Moreover, if the gas is removed by exhausting at a sufficiently low temperature, the sorbent, for the same reason, will appear more active on a second exposure to the gas. Removal of gas at high temperature, on the other hand, especially if followed

\* A very similar postulate forms the basis of a theory of contact catalysis recently advanced by H. S. Taylor. Taylor (Proc. Roy. Soc. A, cviii. p. 105, 1925) does not, however, require that the necessary degree of detachment should be attainable by thermal oscillation.

by slow cooling, would permit the groups to revert to the unreactive form, with consequent loss of activity. All these effects are common phenomena in sorption work.

#### SUMMARY AND CONCLUSIONS.

The equations of the form

$$s = \text{constant} \times t^{1/m}$$

found empirically to govern in many cases the rate of the sorption process are not peculiar to this phenomena alone, but are somewhat widely applicable to the time-course of processes involving the disturbance of the "inner equilibrium" of solid substances (either by mechanical deformation or by other physical or chemical means), provided the solid after disturbance remains rigidly coherent. It is shown that the rate of such a change may be limited by conditions which do not apply in a liquid reaction medium, and which are not concerned in any way with the distance of the reaction from completion. Owing to the incongruity of the initial and final stages of the groups of atoms undergoing transition, the partial occurrence of the reaction disturbs the balance of elastic forces, and therefore influences the internal work that must be done before further groups of atoms can rearrange themselves.

On the hypothesis that the condition for rearrangement is the momentary occupation by the groups of a volume considerably greater than the average, calculations are made of the mode of variation during the progress of the reaction of the force restraining their thermal movements. A tentative explanation of the form of this variation is offered as an alternative to the linear variation required by an extension of Hooke's law to the conditions in the interior of the solid. According to this the intensity of the internal stress set up by the partial occurrence of the reaction is given by the difference between the hydrostatic pressures with which the initial and actual states of the solid would be in complete equilibrium. On this basis it is shown that the index-constant of the "power" time-equation is given by the ratio

$$\frac{V_A - V_2}{V_1 - V_2},$$

where  $(V_A - V_2)$  is the difference of volume between the activated and final states of the atomic groups, and  $(V_1 - V_2)$  the difference between their initial and final volumes.

Application of these ideas to the sorption problem provides

an immediate explanation of the dependence of the activity of the sorbent on its past history, and leads to a revised conception of the mutual relations of sorbent and sorbate in cases where the "power" time-equation holds. The sorbed molecules are regarded as distending the rigidly coherent structure of the sorbent, which consequently becomes stressed. This distension may occur even if the structure is a sufficiently open one to permit easy penetration by the gas molecules in their free state.

University of Manchester and  
the Egyptian University.

LXXVII. *Sign Conventions applied to Flexing Problems.*

*By W. H. BROOKS, B.Sc.(Eng.).\**

THE widespread lack of agreement respecting the sign conventions to be applied to flexing problems in general, results in unfortunate confusion and recurring discussion, especially amongst students.

Any convention may, of course, be arbitrarily chosen for any particular problem, and, if consistently applied throughout, will lead to correct results. When, however, certain fundamental equations are established by the adoption of different sign conventions for bending-moments, experience shows that confusion results from comparisons being made, and erroneous solutions may at first accrue.

For example, the Clapéyron equation for a girder continuous over spans  $l_1$  and  $l_2$  under distributed loading  $w_1$  and  $w_2$  per unit run respectively, and supported level at A, B, and C, may be written

$$M_A l_1 + 2M_B(l_1 + l_2) + M_C l_2 \pm \frac{1}{4}(w_1 l_1^3 + w_2 l_2^3) = 0,$$

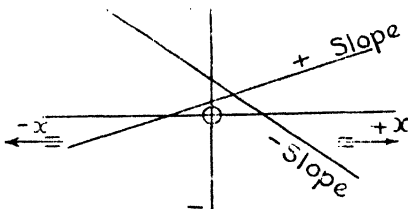
according to the signs assumed for the moments at A, B, and C.

The writer of the present article ventures to suggest that, when applying rectangular coordinates to the solution of practical engineering problems, the well-established mathematical sign conventions shown in fig. 1 should be consistently used throughout, so that when considering any of the successive integrals: load, shearing-force, bending-moment, slope, and deflexion, an agreed criterion shall be available, to determine what sign to affix to the function considered.

\* Communicated by the Author.

Consider the case of a simply-supported horizontal beam under a distributed load as shown in fig. 2 (a), in which at any point X the ordinate represents a load =  $w$  per unit length.

Fig. 1.



Clearly this loading will produce negative deflexion ( $y$ ), as shown in fig. 2 (e), the form of which may be sketched, and from it the forms of the graphs (d), (c), and (b) may be successively derived by applying the well-known relations:

$$\text{Load } (w) = E_I \frac{d^4 y}{dx^4}.$$

$$\text{Shearing-force } (F) = \int w dx = E_I \frac{d^3 y}{dx^3}.$$

$$\text{Bending-moment } (M) = \int F \cdot dx = E_I \frac{d^2 y}{dx^2};$$

$$\text{i. e.,} \quad \frac{d^2 y}{dx^2} = \frac{M}{E_I}.$$

$$\text{Slope } (\theta) = \int \frac{M}{E_I} dx.$$

$$\text{Deflexion } (y) = \int \theta \cdot dx = \int \left( \int \frac{M}{E_I} dx \cdot dx \right).$$

As a mnemonic, these relations may be written in the form :

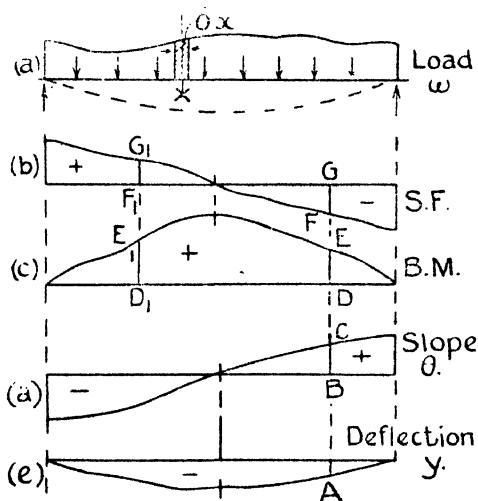
$$\int f(x) dx \quad \downarrow \quad \begin{array}{c} w \\ F \\ M \\ E_I \cdot \theta \\ E_I y \end{array} \quad \uparrow \quad \frac{d}{dx} f(x).$$

Having inferred the form of the deflexion graph—which

represents the form taken by the neutral axis for the given loading—any ordinate in fig. 2(d) may be readily derived from this curve. Thus the ordinate BC in fig. 2(d) represents the positive slope  $\frac{dy}{dx}$  of the deflexion curve at A in fig. 2(e).

In like manner, any ordinate in fig. 2(c) may be derived from consideration of the slope of the curve (d). Thus the ordinate DE represents  $\frac{d\theta}{dx}$  at C in fig. 2(d).

Fig. 2.



The slope of this latter curve, being positive at all points (except at the extremities, where it is zero for this case), shows that, when sagging occurs as shown in fig. 2(e), the bending-moment has a positive sign. In other words, when the centre of curvature is *above* the neutral axis of the beam, the bending-moment is *positive*. Conversely, when the centre of curvature is *below* the neutral axis, the bending moment is *negative*, as may readily be deduced by inverting the curves of fig. 2.

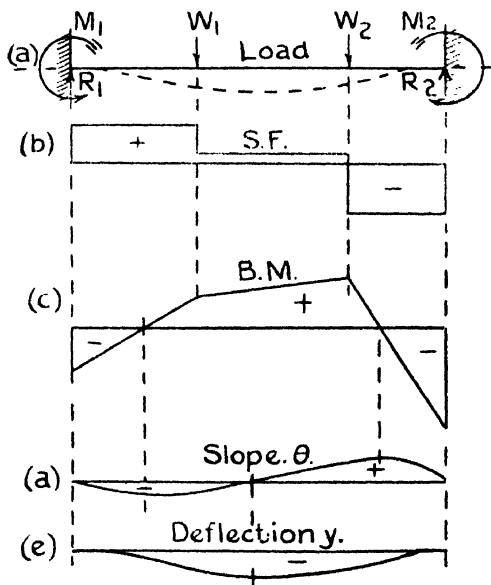
Again, the slope at E ( $\frac{dM}{dx}$ ) in fig. 2(c) is negative; hence the shearing-force represented by the ordinate FG in

fig. 2 (b) is negative. At E, in fig. 2 (c)  $\frac{dM}{dx}$  is positive ; hence the ordinate  $F_1G_1$  in fig. 2 (b) is positive.

Further, since the slope at all points of the S.F. diagram is negative, and  $\frac{dF}{dx} = w$ , downward loading as shown should be considered negative, which sign is also consistent with that of the deflexion it produces.

If it be agreed, therefore, that the mathematical convention of signs should be consistently applied, the signs to be given to any of the functions shown in fig. 2 should not be

Fig. 3.

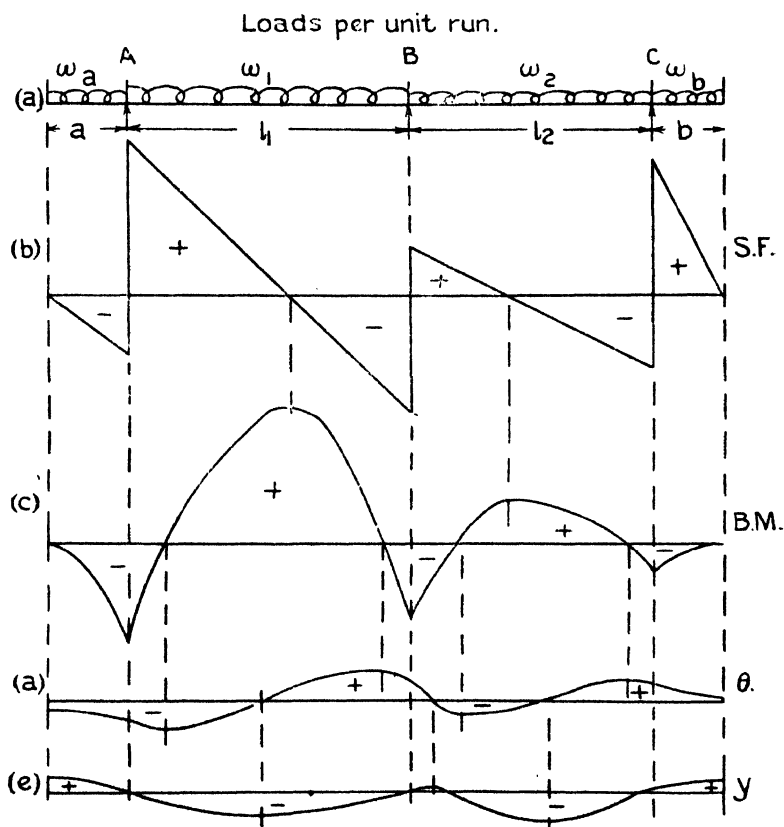


arbitrarily chosen. It will be seen that the criterion, "sagging is produced by positive BM," does not depend upon a fixed origin ; the slope of any of the curves (e), (d), (c) of fig. 2 is not determined by the position of the origin from which  $x$  is taken, provided  $x$  is considered *positive* when taken to the *right* of a chosen origin, and *negative* when taken to the *left*, in accordance with the rule of signs, as shown in fig. 1.

In fig 3 the convention is again applied to the case of an encastré beam, loaded as shown in fig. 3 (a). Proceeding

as in the foregoing example, figs. 3(d), (c), and (b) are successively derived from fig. 3(e), which is first inferred from the load diagram. In this case the fixing couples  $M_1$  and  $M_2$  send the centre of curvature below the beam, and consequently are considered as negative. The test should also be applied—when working from fig. 3(e) to fig. 3(b)—

Fig. 4.



that the slope of any curve is represented in sign and magnitude by the ordinate of the curve immediately above.

Again, consider the case of a beam continuous over three supports A, B, and C at the same level, and loaded as shown in fig. 4(a). Applying the mathematical sign convention



the equation giving  $M_B$  is

$$M_A l_1 + 2M_B(l_1 + l_2) + M_C l_2 + \frac{1}{4}(w_1 l_1^3 + w_2 l_2^3) = 0,$$

assuming  $M_B$  is *positive*.

The overhanging load to the left of A, results in a *negative* position for the centre of curvature of the beam at A. Similarly at C. Hence the bending-moment at A should be written

$$M_A = -\frac{1}{2}w_a a^2 \quad \text{and} \quad M_C = -\frac{1}{2}w_b b^2.$$

Thus

$$-\frac{1}{2}w_a a^2 l_1 + 2M_B(l_1 + l_2) - \frac{1}{2}w_b b^2 l_2 + \frac{1}{4}(w_1 l_1^3 + w_2 l_2^3) = 0,$$

giving

$$M_B = \frac{1}{4(l_1 + l_2)} \{w_a a^2 l_1 + w_b b^2 l_2 - \frac{1}{2}(w_1 l_1^3 + w_2 l_2^3)\}.$$

When  $w_a a^2 l_1 + w_b b^2 l_2 = \frac{1}{2}(w_1 l_1^3 + w_2 l_2^3)$ ,  $M_B = 0$ ; *i. e.*, the centre of curvature for the point B is at infinity.

When  $w_a a^2 l_1 + w_b b^2 l_2 < \frac{1}{2}(w_1 l_1^3 + w_2 l_2^3)$ ,  $M_B$  is *negative*, showing that the centre of curvature is *below* the beam.

When  $w_a a^2 l_1 + w_b b^2 l_2 > \frac{1}{2}(w_1 l_1^3 + w_2 l_2^3)$ ,  $M_B$  is *positive*, showing that the centre of curvature is *above* the beam.

In the special case  $a = b = c$  say,  $l_1 = l_2 = l$  say, and  $w_a = w_1 = w_2 = w_b = w$  say,

$M_B = 0$ , negative or positive, according as

$$2c^2 = l^2, < l^2 \text{ or } > l^2 \text{ respectively.}$$

In sketching the graphs of fig. 4, it has been assumed that

$$w_a a^2 l_1 + w_b b^2 l_2 < \frac{1}{2}(w_1 l_1^3 + w_2 l_2^3).$$

In cases such as this, where the bending-moment over a support may be either positive or negative, it is important that an agreed criterion should be applied so as to determine whether the beam is sagging or hogging over the supports, otherwise erroneous values are likely to be obtained for the reactions of the piers at these points.

Thus, applying the sign conventions used in the foregoing, when  $M_B = 0$ , taking moments about B, clearly

$$R_A l_1 = w_a a \left( l_1 + \frac{a}{2} \right) + w_1 \frac{l_1^2}{2};$$

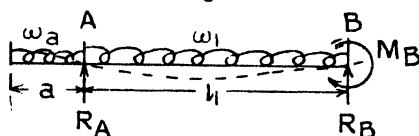
$$\therefore R_A = w_a a \left( 1 + \frac{a}{2l_1} \right) + w_1 \frac{l_1}{2}.$$

Similarly

$$R_C = w_b b \left(1 + \frac{b}{2l_2}\right) + w_2 \frac{l_2}{2}.$$

When  $M_B$  is negative, it is causing hogging at B, and therefore operating, as shown in fig. 5, on the left-hand portion of the beam.

Fig. 5.



For equilibrium, therefore,

$$M_B + R_A l_1 = w_a a \left(l_1 + \frac{a}{2}\right) + w_1 \frac{l_1^2}{2};$$

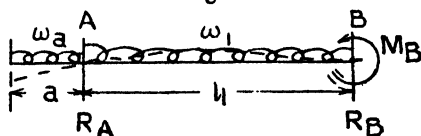
$$\therefore R_A = w_a a \left(1 + \frac{a}{2l_1}\right) + w_1 \frac{l_1}{2} - \frac{M_B}{l_1}.$$

Similarly

$$R_C = w_b b \left(1 + \frac{b}{2l_2}\right) + w_2 \frac{l_2}{2} - \frac{M_B}{l_2}.$$

When  $M_B$  is positive, it is causing sagging at B, and

Fig. 6.



therefore operating as shown in fig. 6. Here, for equilibrium,

$$R_A l_1 = w_a a \left(l + \frac{a}{2}\right) + w_1 \frac{l_1^2}{2} + M_B;$$

$$\therefore R_A = w_a a \left(1 + \frac{a}{2l_1}\right) + w_1 \frac{l_1}{2} + \frac{M_B}{l_1}$$

Similarly

$$R_C = w_b b \left(1 + \frac{b}{2l_2}\right) + w_2 \frac{l_2}{2} + \frac{M_B}{l_2}.$$

In all three cases, of course,

$$R_B = (w_a a + w_b b + w_1 l_1 + w_2 l_2) - (R_A + R_C),$$

and may be alternately found and checked by taking moments about either A or C.

When a graphical construction is used for the purpose of drawing the S.F. and B.M. diagrams for a given loading, a little consideration will show that, when the load-line is drawn to the *left* of the origin chosen for the polar diagram, the resulting funicular polygon giving the B.M. diagram becomes inverted, because drawn from a negative base. This accounts for the reversal in sign often apparent between S.F. and B.M. diagrams.

To avoid this inversion, clearly a *positive* base must be used in the polar diagram, so making

$$F = \frac{dM}{dx} \text{ at all points in the S.F. diagram.}$$

# LXXVIII. *A Simple Method for Determining the Orientation and Structure of Crystals with X-Rays.* By W. E. DAWSON, M.Sc., Assistant for Physics, Technische Hoogeschool, Delft (Holland) \*.

## 1. PRELIMINARY DISCUSSION.

THE principal object of the present experiments has been the devising of a simple method for determining the orientation and structure of crystals showing no well-developed faces, such, for example, as crystal fragments and metal crystallites.

For the purpose of defining the orientation, it is sufficient to define the directions of three non-parallel lines in the crystal, preferably the crystal axes, and to this end one may imagine the latter as radius vectors of a sphere, whose directions may then be given by the polar coordinates of their points of intersection with the surface.

A photograph taken with a single crystal rotating in a Debye-Scherrer camera will have two axes of symmetry, perpendicular and parallel respectively to the axis of rotation. The photographic spots produced by the reflected pencils fall thus into groups of four, each group arising from a single set of reflecting planes in the crystal, and yielding sufficient

\* Communicated by Prof. A. D. Fokker, Ph.D.

data to determine the inclination of the normal to these planes to the axis of rotation. If, in addition, the structure of the crystal be known, so also are the angles between the various normals, but in no case can the azimuth of a normal, measured from an arbitrary plane containing the axis of rotation, be determined.

In the case, then, of a rod containing several crystals of known structure, a Debye-Scherrer photograph is sufficient to determine the orientation of each with respect to an axis, but not the amount of its rotation about the latter. Their mutual orientations cannot thus be found unless separate exposures be made with the crystal rotating about three non-parallel axes, which in view of the time demanded and the restrictions imposed on the specimen, is not very convenient.

The present method has been devised to overcome this drawback, and is based upon the observation first made by Weissenberg\* that, if the rotation of the crystal be accompanied by a proportional movement of the recording film, the angle turned through by the crystal between successive reflexions may be obtained, and sufficient data are thus provided for determining uniquely the direction of the normal belonging to each set of atomic reflecting planes, and hence also the orientation and space-lattice of the crystal.

The arrangement used, which may also be called an X-ray goniometer, is depicted diagrammatically, though not to scale, in fig. 1. OA is the axis of rotation of a small crystal at C and of a wheel WHL. The latter bears against a photographic plate holder PP, which is constrained to move along a straight line perpendicular to OA. Thus as the crystal and wheel rotate together, the recording plate suffers a proportionate tangential displacement. IC, the incident pencil of X-rays, is perpendicular both to the axis OA and plane of the plate.

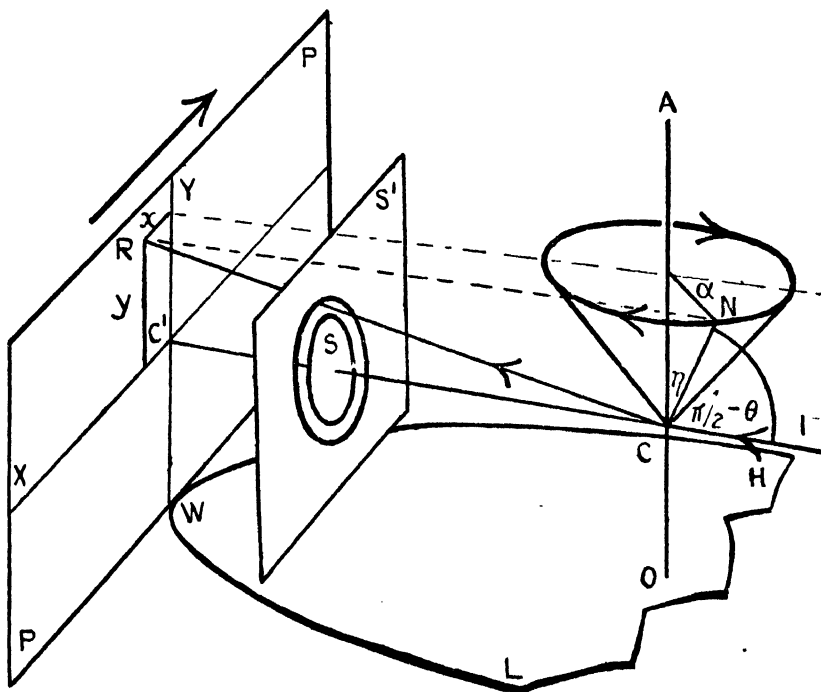
Let us suppose that CR is a reflected pencil of X-rays meeting the plate in R, and that CN is the normal to the set of atomic reflecting planes responsible for the reflexion. Let  $\eta$  be the co-latitude of the normal measured from OA, and  $\alpha$  its azimuth measured in the clockwise direction from the plane ACI (fig. 1) defined by the axis and the incident pencil. The direction of the normal is then defined by  $\alpha$  and  $\eta$ .

The incident beam produced meets the plate in C', and the lines C'X and C'Y through C', parallel and perpendicular

\* K. Weissenberg, *ZS. f. Phys.* xxiii. p. 229 (1924).

758 Mr. W.E. Dawson on a Simple Method for Determining  
 respectively to the axis of rotation, may be taken as axes  
 of reference for the photographic spots. If, then,  $x$  and  $y$  are

Fig. 1.



the coordinates of the spot produced at R by the reflected pencil CR, the following relations are deduced :—

$$\cos \eta = \frac{y}{l} \cdot \frac{\cos \theta}{\tan 2\theta}, \quad . . . . . (1)$$

$$\tan \alpha' = \frac{x}{l} \cdot \frac{\cot \theta}{\tan 2\theta}, \quad . . . . . (2)$$

$$x^2 + y^2 = l^2 \cdot \tan^2 2\theta, \quad . . . . . (3)$$

where  $l$  is the distance from crystal to plate,  $\alpha'$  is the value of  $\alpha$  when reflexion occurs, and  $\theta$  is the angle (measured from the reflecting plane) satisfying the Bragg reflexion

condition: viz.,

$$\lambda = 2d \cdot \sin \theta,$$

in which  $\lambda$  is the wave-length of the reflected X-rays, and  $d$  the spacing of the reflecting planes.

(1) and (2) are not independent, and, eliminating  $x$ ,  $y$ , and  $l$  with the aid of (3), we obtain

$$\tan^2 \alpha' = \left( \frac{\sin \eta}{\sin \theta} \right)^2 - 1 \quad . \quad . \quad . \quad . \quad (4)$$

For given values of  $\eta$  and  $\theta$ , (4) gives four real values of  $\alpha'$  or none, according as  $\eta$  is greater or less than  $\theta$ . Reflexion is obviously impossible in this latter case. If  $\eta$  is greater than  $\theta$ , and  $\alpha'$  is the smallest positive value of  $\alpha$  satisfying (4), then as the crystal rotates in the clockwise direction, successive reflexions will occur when the normal occupies positions determined respectively by the azimuths,

$$\alpha', \quad \pi - \alpha', \quad \pi + \alpha', \quad 2\pi - \alpha'.$$

Suppose, now, that the crystal makes one complete revolution. Two types of photograph are possible according to the initial position of the normal CN. These are shown in figs. 2 *a* and 2 *b*, which correspond, respectively, to the patterns to be expected when the normal begins with an azimuth given by

$$\alpha' > \alpha > -\alpha' \quad . \quad . \quad . \quad . \quad . \quad (5)$$

$$\text{or} \quad \pi - \alpha' > \alpha > \alpha' \quad . \quad . \quad . \quad . \quad . \quad (6)$$

Inverted the same figures would correspond to the normal starting from the diametrically opposite positions, given respectively by

$$\pi + \alpha' > \alpha > \pi - \alpha' \quad . \quad . \quad . \quad . \quad . \quad (7)$$

$$\text{and} \quad 2\pi - \alpha' > \alpha > \pi + \alpha' \quad . \quad . \quad . \quad . \quad . \quad (8)$$

The numbers indicate the order in which the reflexions occur when the plate moves in direction of the arrow. The upper and lower pairs correspond respectively to the azimuths  $\pm \alpha'$  and  $\pm (\pi - \alpha')$ .

The distance  $S$  separating the upper or lower pair of spots is expressed either by

$$S = 2\pi r - 2(r\alpha' + x) \quad . \quad . \quad . \quad . \quad (9)$$

$$\text{or} \quad S = 2(r\alpha' + x), \quad . \quad . \quad . \quad . \quad (10)$$

depending upon the initial conditions,  $r$ , representing the linear displacement of the plate per unit angular displacement of the crystal, or otherwise the effective radius of the wheel WHL. The distance separating the upper pair is in either figure given either by (9) or (10), according as the initial azimuth of the normal to the reflecting planes lies within or without the region of  $\alpha$  defined by the limits  $\pm \alpha'$ . The same is also true of the lower pair when we substitute for the limits  $\pm (\pi - \alpha')$ . In this latter case also, the value  $S$  given by (9) becomes negative when  $x > r (\pi - \alpha')$  and the numbers by the corresponding pair of spots need interchanging.

The difference of the abscissæ of spots 1 and 3 or 2 and 4 is in either figure equal to  $\pi r$ ; the linear displacement of the film accompanying half a revolution of the crystal. A means is thus afforded of determining the constant  $r$ . It may also be noted that the sum of the distances separating the upper and lower pairs in fig. 2 *a* amounts to  $2\pi r$ .

The lines joining the upper and lower pairs respectively stand at a distance  $2y$  apart. These joins have in fig. 2 *a* a common perpendicular bisector whose position on the photograph corresponds to that of the crystal in which the normal has the azimuths 0 or  $\pi$ , according as the distance separating the upper pair is identical with (9) or (10). This latter is easily ascertained since the two values of  $S$  are calculable,  $\alpha'$  being found from (4), and  $x$  from (2) or (3), in which  $r$  and  $y$  are obtained from the photograph, and  $\theta$  is calculated from the Bragg reflexion condition, or, in case the lattice dimension  $d$  is unknown, determined from an exposure with stationary plate.

A similar significance attaches to the perpendicular bisectors in fig. 2 *b*, the upper and lower ones corresponding respectively to the azimuths 0 and  $\pi$ .

The azimuthal angle of the normal measured from a plane containing the axis of rotation may therefore be found, and this in conjunction with the co-latitude  $\eta$ , given by (1), determines its direction completely.

Sufficient data are also obtained when the crystal performs only half a revolution, but in this case the interpretation of the photographs becomes somewhat more involved and the results less accurate, as only two spots are then recorded, the upper or lower pair or one member of each, according to the initial conditions.

When only the orientation of a crystal is desired, it is of course unnecessary to record all the reflexions rendered possible by the monochromatic radiation employed. In the

present experiments with aluminium crystals, for example, it was sufficient to record the reflexions arising from the cube faces ((100) planes). These determine the orientations of the cubic axes and so also that of the crystal. As in this case the other reflexions only serve to complicate the photograph, they were screened off by interposing between the crystal and plate two lead screens, S and S' (fig. 1)\*, the

Figs. 2a & 2b.

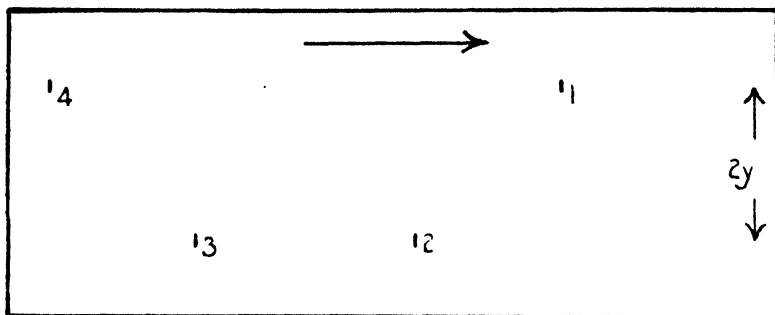


Fig 2a

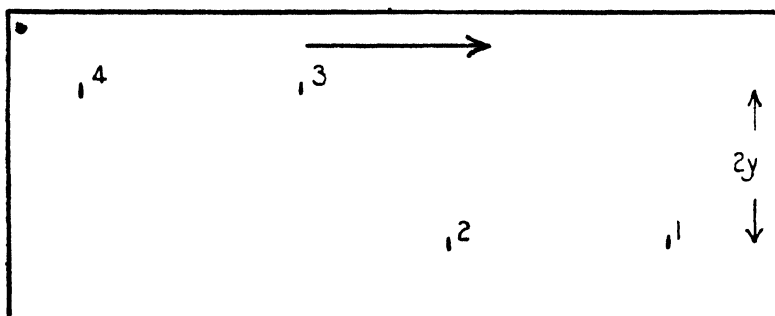


Fig 2b.

\* In the arrangement described by Weissenberg (*loc. cit.*), the reflected pencils are allowed to emerge only through an annular aperture concentric with the axis of rotation, and are recorded on a cylindrical film moving parallel to the latter. The reflexions photographed make thus a constant angle with the axis, determined by the dimensions of the aperture. Reflexions from planes having different indices may be simultaneously recorded, but then only one of the two possible pairs given by each set of reflecting planes. The elucidation of the photographs would, it seems, under these circumstances be somewhat more difficult than with the present arrangement, where the reflected pencils make a constant angle with the incident pencil, and proceed thus from atomic planes having the same indices.



one S, a circular plate, and the other S', a rectangular plate, having a concentric circular aperture of somewhat greater diameter. The disk S was further pierced centrally with a pin-hole which could be opened or closed at will by a small lead cover, and served both for making reference marks by allowing the incident pencil to fall directly on to the film and for setting the screens correctly in position, viz., so as to be traversed centrally and normally by the incident pencil\*. In this way the photographic plate was exposed only over a narrow annular region equidistant from the trace of the incident pencil and subtending at the crystal a circular cone of semi-vertical angle designed to admit only the second-order reflexions from the cube-faces. As is well known, the corresponding first-order reflexions are destroyed by interference owing to the face-centred structure of aluminium.

Under the above circumstances, a complete photograph should show twelve spots produced by the four reflexions arising from each of the three sets of (100) planes. If, however,  $\theta$  be greater than  $54^\circ 44'$ , no reflexions need occur, as the possibility exists of the normals to the reflecting faces simultaneously having co-latitudes  $\eta$  less than  $\theta$  (cf. (4)). Similarly, if  $\theta$  be less than  $54^\circ 44'$  but greater than  $45^\circ$ , only one set of (100) planes need reflect. In these cases, which indeed are improbable, either a new axis of rotation would have to be chosen, or reflexions from planes of different spacing would have to be recorded. When, finally,  $\theta$  is less than  $45^\circ$ , two sets of cube-faces are certain to reflect, and at least eight spots will appear in the resulting photograph. Just sufficient data are then provided for determining the orientation of the crystal. In the present investigation copper K $\alpha$  radiation was employed ( $\lambda = 1.537 \text{ \AA}$ ).  $\theta$  was therefore fixed at  $22^\circ 11'$ , and this being less than  $45^\circ$ , the sufficiency of the photographic material was ensured from the beginning. As a precautionary measure, however, a stationary plate,

\* Such screens may easily be prepared by cutting two pieces of cardboard to the same size and shape as the lead and pasting each to a sheet of good thin paper. For the sake of rigidity, the sheet bearing the disk may be furnished with a narrow cardboard frame. The lead screens are then superimposed on and fastened to the cardboard. When the two are mounted concentrically and parallel, a narrow ring of paper remains, transparent to X-rays. The angular aperture subtended by the ring at the crystal may be varied by displacing the screens with respect to the latter or each other, as the case may be. Reflexions from planes of given spacing may thus be recorded or eliminated according to choice.

which may be placed in front of the annular aperture and exposed simultaneously with the moving plate, serves to indicate all the available reflexions. Such a preliminary exposure is of course indispensable when dealing with crystals of unknown structure.

When, on the other hand, it is desired to determine the structure of a crystal, it would be more expedient to expose the plate over a considerable range, or even over the the whole range ( $\theta$  to  $\pi/2$ ) of  $\theta$ , at once.

## 2. EXPERIMENTAL.

In the arrangement employed, which was made throughout of brass, the photographic plate moved 20.33 cm. to a single revolution of the crystal, the coupling being effected by means of a toothed wheel engaging a toothed bar fixed to the plate-holder. The distance  $l$  from the axis of rotation to the plate was 3.28<sub>6</sub> cm., and, as appeared from the subsequent photographs, the effective radius  $r$  of the coupling-wheel was 3.23<sub>6</sub> cm. The plates themselves were 30 cm. long by 9 cm. wide. Obviously, if  $W = 2 \cdot l \cdot \tan 2\theta$  be the least permissible dimension of the plate parallel to the axis of rotation, the other dimension should be not less than  $W + 2 \cdot \pi \cdot r$ , or  $W + \pi \cdot r$  if only half a revolution be utilized, in order to ensure of no reflexions being missed.

The crystals were of aluminium in the form of cylindrical rods 1.5 mm. in diameter, prepared after the method due to Carpenter\*. They were rotated with a uniform angular velocity of one revolution in half an hour, and as a complete exposure occupied four hours, four revolutions were made in either direction, the reversing being performed automatically. Connexion between the goniometer and driving arrangement was made with a cardan coupling, enabling the former to be adjusted with respect to the X-ray beam. Provision was also made whereby the rod under examination could be given a pure displacement along its axis, either for the purpose of bringing a different crystal into the X-ray beam, or for allowing the latter to impinge directly on the photographic plate and produce reference marks.

X-rays were supplied by a Philips tube, having a water-cooled anticathode of metallic copper working under an

\* H. C. H. Carpenter, 'Nature,' cxviii. p. 266 (1920).

Figs. 3 a, 3 b & 4 a, 4 b.

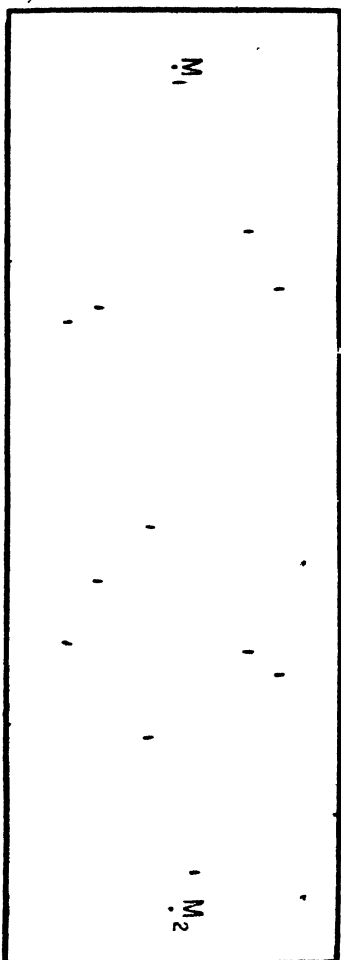


Fig 3a

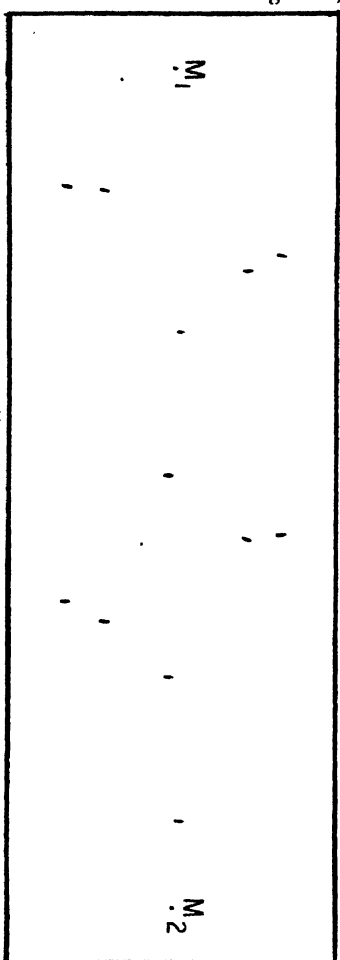


Fig 4a

Axis of Rotation

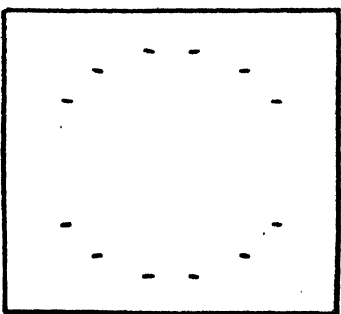
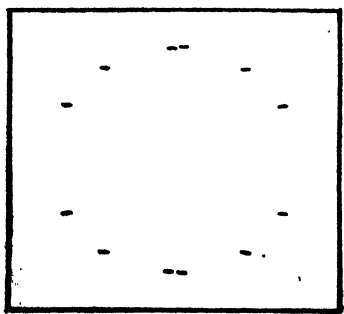


Fig 3b



-Fig 4b

alternating potential difference of 33 KV at 50 cycles, and taking a current of 8 mA. They were filtered through the aluminium window of the tube, 3 100 mm. thick, and a sheet of nickel 1/50 mm. thick, and were limited to suitable dimensions by passing through a cylindrical hole of circular cross-section, 4.5 cm. long and 1.5 mm. diameter, bored through a plug of lead. The intensity of the copper  $K\beta$  radiation was in this way so far reduced by selective absorption that only the reflexions arising from the copper  $K\alpha$ -radiation appeared in the photographs.

The specimen actually examined was a rod of aluminium 14 cm. long, comprising two single crystals which met at a point 6 cm. from one end of the rod.

Figs. 3*a* and 4*a* are scale drawings reduced to about one-half the original size of the photographs obtained. Each plate showed all twelve possible spots. Exposures made with the same crystals and stationary plates are similarly depicted in figs. 3*b* and 4*b* respectively. The upper photographs belong to the upper and shorter crystal as the specimen stood in the goniometer.  $M_1$  and  $M_2$  are reference marks, so chosen that, if the two figures be superposed, the  $M_1$ 's and  $M_2$ 's on each being made to coincide respectively, the resulting figure will represent the photograph to be expected when the two crystals are exposed simultaneously, as might be done by passing the X-rays through their junction. As follows from the foregoing discussion, and is to be seen from the figures,  $M_1 M_2$  is a screw axis of symmetry, characterized by a linear displacement of  $\pi r$  and a rotation of  $\pi$ . The spots are also seen to fall into groups of four, the members of the same group being equidistant from  $M_1 M_2$ . Each figure resolves thus into a superposition of three of the type of fig. 2*a*.

The only measurements which have to be made are the co-ordinates of the spots referred to a pair of axes parallel and perpendicular respectively to  $M_1 M_2$ , and the distance of the axis of rotation from the plate. In evaluating the measurements, the procedure followed consisted in first taking the difference  $2y$  of the ordinates of the upper and lower pairs in each group.  $\eta$  was then calculated from (1) and  $x'$  from (4). Next,  $x$  was obtained from either (2) or (3), and hence the values of  $2(\eta x' + x)$  in (10). Then, by inspection of the photograph, it was ascertained whether the latter values were identical with the distances separating the upper or lower pairs of the various groups, and so, too, whether the mid-point of a pair corresponded with a normal in

the position  $\alpha=0$  or  $\alpha=\pi$ . The azimuths of the normals reckoned from some plane common to the two crystals and containing the axis of rotation, *e.g.* that corresponding to  $M_1$  or  $M_2$ , were then determined. The results for the two crystals are exhibited in the following table, in which the azimuths are all reckoned from that of the first normal taken as zero.

*Upper Crystal.*

	<i>a.</i>	<i>η.</i>	<i>χ</i>
	$\begin{smallmatrix} \circ & ' \\ 0 & 0 \end{smallmatrix}$	$\begin{smallmatrix} \circ & ' \\ 54 & 51 \end{smallmatrix}$	$\begin{smallmatrix} \circ \\ (23) & 89 & 58 \end{smallmatrix}$
1 .....	0 0	54 51	(23) 89 58
2 .....	96 44	79 45	(31) 89 52
3 .....	200 40	36 50	(12) 89 32

*Lower Crystal.*

	<i>a.</i>	<i>η.</i>	<i>χ.</i>
	$\begin{smallmatrix} \circ & ' \\ 68 & 48 \end{smallmatrix}$	$\begin{smallmatrix} \circ & ' \\ 87 & 9 \end{smallmatrix}$	$\begin{smallmatrix} \circ & ' \\ (23) & 89 & 1 \end{smallmatrix}$
1 .....	68 48	87 9	(23) 89 1
2 .....	160 43	56 33½	(31) 89 34
3 .....	335 9	32 25	(12) 90 18

The interaxial angles  $\chi$  were also calculated with the aid of the well-known formula :

$$\cos \chi = \cos \eta_1 \cdot \cos \eta_2 + \sin \eta_1 \cdot \sin \eta_2 \cdot \cos (\alpha_1 - \alpha_2),$$

where the symbols have an obvious significance and their values are given in the last column. Their deviations from the theoretical value of  $90^\circ$  afford an estimate of their accuracy.

Denoting the axes 1, 2, 3, of the upper crystal by the symbols  $X_1$ ,  $Y_1$ ,  $Z_1$ , and those of the lower crystal by  $X_2$ ,  $Y_2$ ,  $Z_2$ , the angles included between the axes of the two crystals are shown below.

	$X_1$ .	$Y_1$ .	$Z_1$ .
	$\begin{smallmatrix} \circ \\ 71 \cdot 1 \end{smallmatrix}$	$\begin{smallmatrix} \circ \\ 28 \cdot 7 \end{smallmatrix}$	$\begin{smallmatrix} \circ \\ 111 \cdot 1 \end{smallmatrix}$
$X_2$ .....	71·1	28·7	111·1
$Y_2$ .....	109·1	62·7	34·5
$Z_2$ .....	27·8	97·3	63·3

On inspection of these figures, we observe that, among the nine angles, there seem to be three pairs of nearly equal angles: viz.,  $Y_1 X_2 = 28^\circ.7$  and  $X_1 Z_2 = 27^\circ.8$ ;  $Z_1 X_2 = 111^\circ.1$  and  $X_1 Y_2 = 109^\circ.1$ ; and  $Y_1 Y_2 = 62^\circ.7$  and  $Z_1 Z_2 = 63^\circ.3$ , where  $Y_1 X_2$  denotes the angle between  $Y_1$  and  $X_2$  etc. If these angles are in reality equal, it is seen that one crystal is the image of the other; and taking  $28^\circ$ ,  $110^\circ$ , and  $63^\circ$  as the mean values of the three pairs respectively, the symmetry plane is found to have the indices  $(4\bar{5}2)^*$ . The crystals form thus a kind of twin, though this may be accidental, since the most common twinning plane with cubic crystals is the  $(111)$ .

From the mode of preparation of these crystals, there is no obvious reason to suspect that they lie otherwise than at random. The data obtained from the two crystals here examined are scarcely sufficient to test this conclusion, but we may avail ourselves of the results found by F. Yoshida and K. Tanaka†. They prepared aluminium crystals after the same method, and determined their orientations by a modification of the Laue method, using a divergent pencil of heterogeneous X-rays. The results for the co-latitudes of the cubic axes measured from the axis along which stretching had occurred (identical in our case with the axis of rotation) are given in the first six columns of the following table, and our results in the last two columns. Their values for the azimuths are not available.

Crystal .....	1	2	3	4	5	6	7	8
	°	°	°	°	°	°	°	°
η {	87	87	85	88	89	89	80	87
	62	57	65	63	61	61	55	56.5
	29	34	26	27	28	30	37	32.5

The observation made by Yoshida and Tanaka, that these angles are for each crystal nearly the same and that each crystal has one axis nearly perpendicular to the direction of stretching, is more or less borne out. It may be pointed out, however, that, when the crystals are distributed at random, the latter circumstance is only to be

\* The actual values found for the indices are 4.00, -5.15, 2.00.

† N. Yoshida and K. Tanaka, 'Nature,' p. 913, Dec. 1926.

expected, since the average values of the greatest, intermediate, and least angles included between the cubic axes and an arbitrary line are respectively

$$81^{\circ}, 58^{\circ}5, \text{ and } 36^{\circ},$$

approximately. These values are found by actually taking averages for the directions of the arbitrary line given by all the indices between [600], [660], and [666]; *i. e.*, the directions obtained by substituting all possible combinations of the integers 0, 1, 2, 3 ... 6 for the two noughts in the first.

From the results of Yoshida and Tanaka, it is seen that the individual values, and hence also the averages, viz.

$$87^{\circ}5, 61^{\circ}5, \text{ and } 29^{\circ} \text{ respectively,}$$

show consistent deviations from the theoretical values (except for the angle  $57^{\circ}$  of crystal 2 in the table); and so it seems that the crystals are not orientated at random about the direction of stretching, which lends favour to the view that the crystals grow more readily when stretched in a certain direction.

This, again, is contradicted by the present results, where the deviations from the theoretical values seem more haphazard.

In conclusion, I should like to express my thanks to Professors A. D. Fokker and H. B. Dorgelo, the former for suggesting this research, and both for the interest they have shown during its progress. I am particularly indebted to Mr. P. van den Akker, chief of the workshop, for his skill and resourcefulness in constructing the apparatus.

The Physical Laboratories,  
College of Technology,  
Delft, Holland.

LXXIX. *A Theory of the Birefringence induced by Flow in Liquids.* By Prof. C. V. RAMAN, F.R.S., and K. S. KRISHNAN\*.

1. *Introduction.*

THAT a viscous liquid such as Canada balsam exhibits optical anisotropy when mechanically agitated appears to have been first observed by Clerk Maxwell. The subject was later pursued by other investigators, notably by Kundt and his pupils, whose work will be found well summarized in an article by G. de Metz†. An extensive series of observations on the subject has been made recently by Vorländer and Walter‡ with the arrangement, originally suggested by Maxwell, of placing the liquid in the gap between two coaxial cylinders and rapidly rotating the inner cylinder. A beam of plane-polarized light traversed the column of liquid in a direction parallel to the axis of the cylinders, and with the help of a suitable analyser and an auxiliary spectroscope, measurements were made of the birefringence exhibited by it. Vorländer and Walter examined in this way no fewer than 172 liquids, and have greatly extended our knowledge of the subject. An important outcome of their work is to show that mechanical birefringence is observable in numerous common liquids having a definite chemical composition, including several which do not possess an exceptionally high viscosity; they found also that careful purification and removal of suspended "colloidal" matter from the liquids studied, by vacuum distillation, leaves the birefringence unaffected. Their work obliges us to conclude that the power to exhibit birefringence under mechanical flow is just as much a characteristic of pure liquids as, for instance, the power of exhibiting birefringence when placed in an electrostatic field.

It is proposed in this paper to develop a molecular theory of mechanical birefringence in liquids based on ideas somewhat similar to those successfully employed by Langevin and Born to explain electric double-refraction in liquids. The birefringence is regarded as arising from the optical anisotropy of the molecules, taken together with a tendency for them to orientate under the mechanical stresses within

\* Communicated by the Authors.

† G. de Metz, *Scientia*, Gauthier-Villars, no. 26, Jan. 1906; see also Winkelmann's 'Handbuch der Physik,' Optik, pp. 1230-1236 (1906).

‡ D. Vorländer and R. Walter, *Zeits. Phys. Chem.* vol. cxviii. p. 1 (1925).



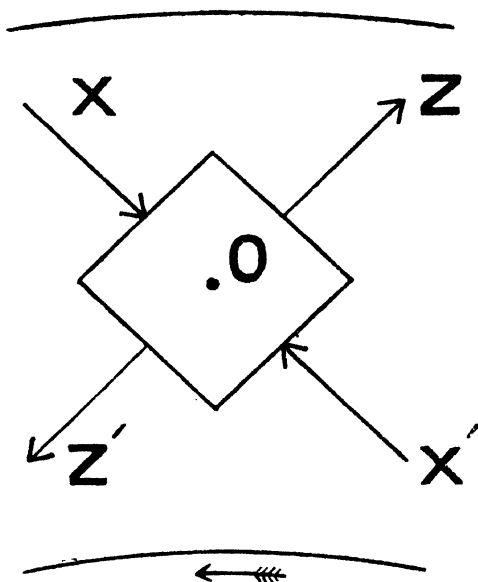
the fluid. The effective cause of such orientation is taken to be the non-spherical shape of the molecules.

It will be seen in the sequel that the theory succeeds not only in explaining the general features of the observed phenomena, but also in giving a value for the "Maxwell constant" in good agreement with observation.

## 2. Molecular Orientation in Flowing Liquid.

Stokes, in his memoir\* on the internal friction of fluids, discussed the character of the stresses arising from viscous flow, and showed that in the case of a simple sliding motion

Fig. 1.



parallel to a plane the tangential stresses acting along the plane may be replaced by two sets of stresses, one set consisting of tensions and the other set of pressures acting along two directions which are mutually perpendicular and inclined at  $45^\circ$  to the line of flow. The direction of the tensions is parallel to the axis of extension and of the pressures to the axis of compression (see fig. 1, which represents a section of the fluid between the two cylinders, perpendicular to their common axis). The inner cylinder is assumed to rotate in the direction of the arrow, the outer one remaining fixed. The tensions and pressures shown in the figure are

\* Sir George Stokes, Math. and Phys. Papers, Camb. Univ. Press, vol. i. p. 91.

each equal to  $\eta \frac{v}{c}$  per unit area, where  $\eta$  is the coefficient of viscosity and  $\frac{v}{c}$  is the radial velocity-gradient at O.

It is clear that if the molecules are highly asymmetrical in shape, the set of tensions and pressures pictured in fig. 1 would tend to cause them to orient in the fluid, in such manner that the longest dimension of a molecule lies along the axis of tensions and the shortest one along the axis of pressures. For such orientation would evidently result in the fluid (regarded as a densely-packed assemblage of molecules) expanding along the axis of  $z$  and contracting along the axis of  $x$ , the total volume remaining constant, thus allowing the system of stresses acting in the medium to do work. This orientative tendency of the molecules is, however, opposed by their thermal agitation, which tends to throw them into disarray. The resulting state of statistical equilibrium can be found by an application of the Boltzmann Principle.

In order to define the orientations of the molecules, we choose (see fig. 1) the direction of tension as the  $z$ -axis, the direction of pressure as the  $x$ -axis, and a direction perpendicular to these two (*i. e.* parallel to the common axis of the cylinders) as the  $y$ -axis, of a coordinate system  $x y z$  fixed in space. We also consider the principal geometrical axes of each molecule as the axes of another coordinate system  $\xi \eta \zeta$  fixed in it. Let the orientations of these axes with reference to the axes of the former system be given by the Eulerian angles  $\theta, \phi, \psi$ . Then the cosines of the various angles between the two sets of axes are as below :—

TABLE I.

	$x.$	$y.$	$z$
$\xi \dots\dots$	$\alpha_{11} = \cos \theta \cos \phi \cos \psi$ $\quad - \sin \phi \sin \psi.$	$\alpha_{12} = \cos \theta \sin \phi \cos \psi$ $\quad + \cos \phi \sin \psi.$	$\alpha_{13} = -\sin \theta \cos \psi.$
$\eta \dots\dots$	$\alpha_{21} = -\cos \theta \cos \phi \sin \psi$ $\quad - \sin \phi \cos \psi.$	$\alpha_{22} = -\cos \theta \sin \phi \sin \psi$ $\quad + \cos \phi \cos \psi.$	$\alpha_{23} = \sin \theta \sin \psi.$
$\zeta \dots\dots$	$\alpha_{31} = \sin \theta \cos \phi.$	$\alpha_{32} = \sin \theta \sin \phi.$	$\alpha_{33} = \cos \theta.$

For allowing the Principle of Boltzmann to be applied to our present problem, we require an expression for the

potential energy of each molecule in the fluid in terms of its orientation with respect to the fixed coordinate axes  $xyz$ . A suitable form of expression is suggested by the following considerations. The stress acting in the medium is, as we have seen,  $\eta \frac{v}{c}$ , and if we divide this by the number of molecules  $\nu$  per unit volume in the fluid, we obtain a quantity  $\eta \frac{v}{c} \cdot \frac{1}{\nu}$ , which has the physical dimensions of energy. It is therefore permissible to assume that the energy of each molecule, as determined by its orientation with respect to the axes of these stresses, is proportional to  $\eta \frac{v}{c} \cdot \frac{1}{\nu}$ , the coefficient of proportionality being a function of the angle-variables, which is physically dimensionless. Since by hypothesis the orientation of the molecules arises from their non-spherical shape, and since the positive and negative directions are necessarily equivalent, the potential energy of a molecule will remain unaffected if we rotate it through  $180^\circ$  round any of the  $\xi$ -,  $\eta$ -,  $\zeta$ -axes.

In view of what has been said above, and considering for the present only the effect of the *tensions* along the  $z$ -axis, we may assume the potential energy of each molecule to be given by the expression

$$u = -(\omega_1 \alpha_{13}^2 + \omega_2 \alpha_{23}^2 + \omega_3 \alpha_{33}^2) \cdot \eta \frac{v}{c} \cdot \frac{1}{\nu}, \quad (1)$$

where  $\omega_1, \omega_2, \omega_3$  are constants determined by the geometric form of the molecule, which will later be evaluated. Then, from Boltzmann's theorem, the number of molecules per unit volume whose orientations, when under thermal equilibrium, are given by the range  $\sin \theta d\theta d\phi d\psi$ , is equal to

$$C e^{-\frac{u}{kT}} \sin \theta d\theta d\phi d\psi, \quad (2)$$

where  $C$  is the constant given by the relation

$$\nu = C \int_{\theta=0}^{\theta=\pi} \int_{\phi=0}^{\phi=2\pi} \int_{\psi=0}^{\psi=2\pi} e^{-\frac{u}{kT}} \sin \theta d\theta d\phi d\psi. \quad (3)$$

In the orientated state the average potential energy per molecule in the medium is given by

$$u = \frac{\iiint e^{-\frac{u}{kT}} u \sin \theta d\theta d\phi d\psi}{\iiint e^{-\frac{u}{kT}} \sin \theta d\theta d\phi d\psi}.$$

the limits of integration being the same as in (3),

$$= -\frac{\omega_1 + \omega_2 + \omega_3}{3} \cdot \eta \frac{v}{c} \cdot \frac{1}{v} - \frac{2}{45kT} \left[ (\omega_1 - \omega_2)^2 + (\omega_2 - \omega_3)^2 + (\omega_3 - \omega_1)^2 \right] \cdot \left( \eta \frac{v}{c} \cdot \frac{1}{v} \right)^2 \quad (4)$$

If, on the other hand, the molecules are orientated entirely at random, then the average energy per molecule will be given by

$$\begin{aligned} u_0 &= \frac{\iiint u \sin \theta \, d\theta \, d\phi \, d\psi}{\iiint \sin \theta \, d\theta \, d\phi \, d\psi} \\ &= -\frac{\omega_1 + \omega_2 + \omega_3}{3} \cdot \eta \frac{v}{c} \cdot \frac{1}{v} \quad \dots \quad (5) \end{aligned}$$

The difference  $u_0 - \bar{u}$  multiplied by  $v$  gives the diminution of potential energy per unit volume in orientating the molecules contained in it, and is equal to

$$(\bar{u}_0 - u)v = \frac{2}{45kT} \left[ (\omega_1 - \omega_2)^2 + (\omega_2 - \omega_3)^2 + (\omega_3 - \omega_1)^2 \right] \cdot \left( \eta \frac{v}{c} \right)^2 \cdot \frac{1}{v} \quad (6)$$

### 3. The Optical Effect of Molecular Orientation.

We now proceed to find the double refraction which arises from this orientation of the molecules, here again confining our attention at first to the result of the tensions acting along the  $z$ -axis. Since the optic axes of the molecule will not, in general, coincide with its geometric axes  $\xi \eta \zeta$ , when a field (due to a light-wave) is incident along any one of these axes, say along the  $\xi$ -axis, the moment induced in the molecule will not be wholly along the  $\xi$ -axis, but will have components also along the  $\eta$ - and  $\zeta$ -axes. Thus for unit field actually acting on the molecule along the  $\xi$ -axis, let  $b_{11}$ ,  $b_{12}$ ,  $b_{13}$  be the moments induced in it along its  $\xi$ -,  $\eta$ -, and  $\zeta$ -axes respectively; and let  $b_{21}$ ,  $b_{22}$ ,  $b_{23}$ , and  $b_{31}$ ,  $b_{32}$ ,  $b_{33}$  be similar induced moments for unit field acting along the  $\eta$ - and  $\zeta$ -axes respectively:  $b_{ij} = b_{ji}$ . We have two special cases to consider.

*Case I.*—The electric vector of the incident light-wave lies along the  $z$ -axis—i. e., along the direction of the tension.

Let the optical field actually acting on each molecule in the same direction be denoted by  $E$ . Then the moments induced in the molecule under consideration along its axes,

when resolved along the direction of  $E$ , are together equal to

$$(b_{11}\alpha_{13}^2 + b_{22}\alpha_{23}^2 + b_{33}\alpha_{33}^2 + 2b_{12}\alpha_{13}\alpha_{23} + 2b_{23}\alpha_{23}\alpha_{33} + 2b_{31}\alpha_{33}\alpha_{13})E \quad (7)$$

$$= m_z E, \text{ say.} \quad (8)$$

Then the average value of  $m_z$  taken over all the molecules in the medium will be given by

$$\begin{aligned} \bar{m}_z &= \frac{\iiint e^{-\frac{u}{kT}} m_z \sin \theta d\theta d\phi d\psi}{\iiint e^{-\frac{u}{kT}} \sin \theta d\theta d\phi d\psi} \\ &= \frac{b_{11} + b_{22} + b_{33}}{3} + 2\Theta \eta_c \frac{v}{c} \cdot \frac{1}{v}, \quad (9) \end{aligned}$$

where

$$\begin{aligned} \Theta &= \frac{1}{45kT} [(\omega_1 - \omega_2)(b_{11} - b_{22}) + (\omega_2 - \omega_3)(b_{22} - b_{33}) \\ &\quad + (\omega_3 - \omega_1)(b_{33} - b_{11})]. \quad (10) \end{aligned}$$

*Case II.*—The light-vector lies along the  $x$ -axis.

Let us denote the actual field acting on each molecule along the  $x$ -axis by  $E$ . The moments induced in any molecule along its axes, when resolved along the  $x$ -axis, are together equal to

$$(b_{11}\alpha_{11}^2 + b_{22}\alpha_{21}^2 + b_{33}\alpha_{31}^2 + 2b_{12}\alpha_{11}\alpha_{21} + 2b_{23}\alpha_{21}\alpha_{31} + 2b_{31}\alpha_{31}\alpha_{11})E \quad (11)$$

$$= m_x E, \text{ say.} \quad (12)$$

The average value of  $m_x$  taken over all the molecules can be calculated as in the previous case, and comes out equal to

$$\bar{m}_x = \frac{b_{11} + b_{22} + b_{33}}{3} - \Theta \eta_c \frac{v}{c} \cdot \frac{1}{v}. \quad (13)$$

From (9) and (13)

$$\bar{m}_z - \bar{m}_x = 3\Theta \eta_c \frac{v}{c} \cdot \frac{1}{v}. \quad (14)$$

Hitherto we have considered only the effect of the tensions  $\eta_c \frac{v}{c}$  acting along the  $z$ -axis. The effect of the pressures of the same magnitude acting along the  $x$ -axis can be calculated in exactly the same way by considering them as tensions  $= -\eta_c \frac{v}{c}$  along the  $x$ -axis, and thus we get

$$\bar{m}_x - \bar{m}_z = 3\Theta \times -\eta_c \frac{v}{c} \cdot \frac{1}{v}.$$

Thus, when the two effects are superposed, as in the actual liquid, we get for the difference in the values of the mean induced moments, for directions of vibration of the incident light along the  $z$ - and  $x$ -axes, the expression

$$m_z - m_x = 6 \Theta \eta \frac{v}{c} \cdot \frac{1}{v}. \quad . \quad . \quad . \quad (15)$$

If we denote by  $n_z$  and  $n_x$  the refractive indices of the medium for light-vibrations along the  $z$ - and the  $x$ -axes respectively, by differentiating the well-known expression for refractivity

$$\frac{n^2 - 1}{n^2 + 2} = \frac{4\pi}{3} v \cdot m, \quad . \quad . \quad . \quad (16)$$

we have

$$\begin{aligned} n_z - n_x &= \frac{(n^2 - 1)(n^2 + 2)}{6n} \cdot \frac{\bar{m}_z - \bar{m}_x}{m} \\ &= \frac{(n^2 - 1)(n^2 + 2)}{n} \cdot \frac{\Theta}{m} \cdot \eta \frac{v}{c} \cdot \frac{1}{v}, \quad . \quad . \quad (17) \end{aligned}$$

where  $n$  is the refractive index and  $m$  is the mean moment induced in a molecule per unit field actually acting on it, in the randomly orientated state of the molecules. Obviously

$$m = \frac{b_{11} + b_{22} + b_{33}}{3}. \quad . \quad . \quad . \quad (18)$$

All the quantities in expression (17) for the birefringence of the medium are experimentally determinable, except  $\Theta$ , which involves, as is evident from (10), the optical constants of the molecule and the constants  $\omega_1, \omega_2, \omega_3$  appearing in expression (1) for the potential energy. We shall now proceed to consider how the quantities  $\omega_1, \omega_2, \omega_3$  may be connected with the geometric form of the molecules.

#### 4. *Molecular Shape and Molecular Orientation.*

Since, by hypothesis, the orientation of the molecules is the result of their non-spherical form, we may proceed to connect them in the following way. We idealize the molecules and consider them to have the form of ellipsoids with three unequal diameters,  $a_1, a_2, a_3$ . If we imagine the molecules to be arranged in contact with each other, their axes parallel, in the form of a rectangular parallelepiped having  $s$  molecules in each of its edges, the length of the latter would be  $sa_1, sa_2, sa_3$  respectively. This is an extreme case, which illustrates the general principle that the effect of any general tendency of the molecules to orientate in

specific directions is to cause the density of molecules per unit length in different directions to become different. It is difficult to express this principle with complete precision in a mathematical form, particularly in the case of liquids, where the molecules are not always necessarily in contact with each other. Considering, however, the fact that the density of the type of liquid with which we are concerned here is usually not very different from that in the solidified state, the error in considering the molecules to be in contact with each other all the time would not be serious in any event; and since we are only concerned with ratios, the inaccuracy involved can practically be eliminated by considering the "effective" dimensions of a molecule in the liquid to be slightly different from what they are in the solidified state. Subject to these remarks, we may assume that a molecule arbitrarily orientated contributes to the linear dimension of the aggregate measured along the  $z$ -axis a length equal to

$$a_1\alpha_{13}^2 + a_2\alpha_{23}^2 + a_3\alpha_{33}^2. \quad . \quad . \quad . \quad (19)$$

If the molecules are arbitrarily orientated, the average effective length of the molecule along the  $z$ -axis is simply

$$\frac{\iiint (a_1\alpha_{13}^2 + a_2\alpha_{23}^2 + a_3\alpha_{33}^2) \sin \theta \, d\theta \, d\phi \, d\psi}{\iiint \sin \theta \, d\theta \, d\phi \, d\psi} = \frac{a_1 + a_2 + a_3}{3}; \quad . \quad . \quad . \quad (20)$$

that is to say, the mean of the three diameters of the ellipsoid. Considering, however, the tendency of the molecules to orientate, due to the tensions along the  $z$ -axis in the fluid, we find the average length to be

$$\frac{\iiint e^{-\frac{u}{kT}} (a_1\alpha_{13}^2 + a_2\alpha_{23}^2 + a_3\alpha_{33}^2) \sin \theta \, d\theta \, d\phi \, d\psi}{\iiint e^{-\frac{u}{kT}} \sin \theta \, d\theta \, d\phi \, d\psi},$$

where  $u$  is given by expression (1),

$$= \frac{a_1 + a_2 + a_3}{3} + \frac{2}{45kT} [(\omega_1 - \omega_2)(a_1 - a_2) + (\omega_2 - \omega_3)(a_2 - a_3) + (\omega_3 - \omega_1)(a_3 - a_1)] \eta_c \cdot \frac{1}{\nu}. \quad (21)$$

The difference between (21) and (20) divided by (20) gives the effective expansion per unit length, along the  $z$ -axis, owing to the orientation of the molecules, as

$$\frac{2}{15kT} \cdot \frac{(\omega_1 - \omega_2)(a_1 - a_2) + (\omega_2 - \omega_3)(a_2 - a_3) + (\omega_3 - \omega_1)(a_3 - a_1)}{a_1 + a_2 + a_3} \times \eta \frac{v}{c} \cdot \frac{1}{\nu} \quad (22)$$

Multiplying this by the tension  $\eta \frac{v}{c}$  along the  $z$ -axis, we obtain the work done per unit volume resulting from the orientation of the molecules contained in it, an expression for which was obtained in an entirely different way in (6) above. Equating the two expressions, we have

$$\begin{aligned} & (\omega_1 - \omega_2)^2 + (\omega_2 - \omega_3)^2 + (\omega_3 - \omega_1)^2 \\ &= 3 \frac{(\omega_1 - \omega_2)(a_1 - a_2) + (\omega_2 - \omega_3)(a_2 - a_3) + (\omega_3 - \omega_1)(a_3 - a_1)}{a_1 + a_2 + a_3} \quad (23) \end{aligned}$$

The form of the equation immediately suggests as a solution

$$\frac{\omega_1 - \omega_2}{a_1 - a_2} = \frac{\omega_2 - \omega_3}{a_2 - a_3} = \frac{\omega_3 - \omega_1}{a_3 - a_1} = \frac{3}{a_1 + a_2 + a_3}, \quad (24)$$

which is readily seen to satisfy (23). For the special cases in which the molecule has the form of a prolate or oblate spheroid of revolution, the validity of (24) is rigorously demonstrable, and it seems justifiable to assume that it is generally true.

### 5. *Expression for the Maxwell Constant.*

Substituting (24) in (17) and (10) we obtain as the final expression for the birefringence

$$\begin{aligned} n_x - n_z &= \frac{(n^2 - 1)(n^2 + 2)}{5n \nu kT} \times \frac{(a_1 - a_2)(b_{11} - b_{22}) + (a_2 - a_3)(b_{22} - b_{33}) + (a_3 - a_1)(b_{33} - b_{11})}{(a_1 + a_2 + a_3)(b_{11} + b_{22} + b_{33})} \\ &\quad \times \eta \frac{v}{c} \quad (25) \end{aligned}$$

$$= \nabla \cdot \eta \frac{v}{c}, \quad (26)$$

where  $\nabla$  is the constant of mechanical birefringence in the fluid, which may appropriately be called the Maxwell



constant, in honour of the discoverer of the effect. It will be seen from the equation that the value of the constant depends jointly upon the optical anisotropy of the molecule and upon the anisotropy of its geometric form.

We shall now proceed to consider how the theory set out above compares with the phenomena as observed in their general features.

*Axes of Birefringence.*—The theory indicates in agreement with observation that the two principal directions of vibration are mutually perpendicular, and inclined at  $45^\circ$  to the plane of sliding within the liquid.

*Positive or Negative Birefringence?*—The theory indicates that the sign of the birefringence depends on whether the expression

$$[(a_1 - a_2)(b_{11} - b_{22}) + (a_2 - a_3)(b_{22} - b_{33}) + (a_3 - a_1)(b_{33} - b_{11})] \quad \dots \dots (27)$$

is positive or negative. It is easily seen that if  $a_1 > a_2 > a_3$  and  $b_{11} > b_{22} > b_{33}$ , the expression in question is positive and the birefringence is therefore positive, while if  $a_1 > a_2 > a_3$  and  $b_{11} < b_{22} < b_{33}$ , the birefringence will be negative. In other words, the sign of the double refraction depends on whether the optical constants of the molecule along its three axes follow the same sequence as the linear dimensions or follow the reverse order. If we can regard the chemical molecule as roughly equivalent to an ellipsoid of isotropic dielectric material, the former condition would be satisfied. It is thus readily understood why the great majority of the liquids examined by Vorländer and Walter exhibit positive birefringence. In fact, the only cases of negative birefringence contained in their table of results are the sodium and potassium salts of some of the higher fatty acids; the corresponding fatty acids themselves show positive birefringence.

*Influence of Speed, Viscosity, and Temperature.*—The theory indicates that the observed birefringence should be proportional to the speed of rotation. The experimental evidence appears to indicate that this is actually the case with most pure liquids. Where divergences appear, it seems not unlikely that they are due to disturbing causes, *e. g.*, departure from the assumed stream-line flow of the liquid, or a rise of the temperature of the liquid as a result of the rotation. The theory indicates a rapid fall of the birefringence with rising temperature, primarily because of the fall of the viscosity, the variation of the Maxwell constant itself with temperature being much less important. The experimental evidence fully supports this inference from theory.

*Influence of Molecular Form.*—The theory shows that, apart from the viscosity of the liquid, the birefringence should be specifically influenced by the form of the molecule, being greatest when the molecule is highly elongated and least when its form approaches spherical symmetry. The observations of Vorländer and Walter furnish ample evidence in support of this. They found that increasing the length of the chain in the fatty acid series increased the specific birefringence (or Maxwell constant as we call it), and introducing side-chains in the molecule diminishes it notably.

*Influence of Optical Anisotropy.*—The theory indicates that for molecules of given form the Maxwell constant should increase with increasing optical anisotropy and with increasing refractive index. Now it is known that organic liquids of the aromatic series exhibit in light-scattering a much higher degree of optical anisotropy than the aliphatic series, besides having usually a higher refractive index. On the other hand, the geometry of the benzene ring ensures a greater symmetry of form for simple benzene derivatives than for the aliphatic compounds. The two effects would thus set each other off to a considerable extent in the case of the simpler benzene derivatives. If, however, we consider long-chain compounds in which the benzene ring also appears, we may reasonably expect the increased optical anisotropy to manifest itself in an increased value for the Maxwell constant. Similarly it is known from observations on light-scattering that unsaturated carbon compounds show a high degree of optical anisotropy, and it follows that they should have a large Maxwell constant. Ample support for these inferences from theory is furnished by the observations of Vorländer and Walter.

*Dispersion of Double-Refraction.*—From our formula it will be seen that the wave-length does not appear explicitly in our formula. Since, however, the Maxwell constant is proportional to  $(n^2 - 1)(n^2 + 2)/n$ , where  $n$  is the refractive index, a not negligible degree of dispersion may be expected, as has indeed been observed in experiment.

#### 6. Absolute Value of Birefringence.

To calculate the Maxwell constant for any liquid, we require to know the refractive index of the liquid, its molecular weight and density, the optical anisotropy of the molecules and their geometric form. The optical anisotropy of the molecules can be completely determined from measurements of the light-scattering in the liquid if the molecule has an axis of symmetry, and can at least be estimated in other cases from such measurements. The geometrical form

of the molecules is known, at least approximately, from chemical considerations and from X-ray studies. It is thus possible to calculate the value of the Maxwell constant absolutely for any liquid for which the data referred to above are available. Unfortunately, few of the liquids for which the mechanical birefringence is known have been investigated for light-scattering. We may, however, test the theory in the following way. The range of variation of the quantities appearing in the expression for the Maxwell constant is well known. The refractive index of most organic liquids ranges between 1.4 and 1.7. The ratio of molecular weight to density for the type of compounds under consideration ranges between 80 and 240. The ratio of the longest to the shortest dimension of the molecule may of course range theoretically from 1 to large values, but practically it may be taken as lying between 2 and 5 for most compounds which are liquids and show an appreciable birefringence under flow. The ratio of the maximum and minimum polarizabilities of the molecule along its different axes is known from the extensive investigations on light-scattering carried on at Calcutta for different types of organic compounds. It is usually about 1.1 for aliphatic hydrocarbons and saturated cyclo-compounds, 1.5 for aliphatic compounds containing strongly refractive groups, 1.9 for simple benzene derivatives, and about 2.3 for very highly anisotropic compounds such as chloronaphthalene, quinolene\*, etc. We may group the data in such order as to have four representative classes, in which we have respectively very low, moderate, high, and very high values of the Maxwell constant as theoretically calculated. This has been done in Table II., in which, for simplicity of calculation, the molecule is assumed to have an axis of symmetry. The temperature assumed is  $293^{\circ}$  absolute.

For comparison with the values shown in Table II. we have analysed the data given by Vorländer and Walter in their paper. Of the 172 liquids studied, 37 were of very low viscosity and naturally did not yield any results. 15 other liquids having moderate or high viscosities also showed no indication of birefringence. This is not surprising in view of the fact that their optical arrangements did not permit a difference of path of less than 2 millimicrons to be detected. A liquid of moderately high viscosity, say 50 times that of water and having a Maxwell constant less than  $0.01 \times 10^{-9}$ , would have shown no detectable birefringence in their experiments. The limit of detectability would

\* These values give the *effective* anisotropies determined from observations of light-scattering in the liquid state.

be correspondingly larger for liquids of lower viscosity. It appears certain that an adequate explanation (*viz.*, a low viscosity, or an insufficient optical or geometric anisotropy

TABLE II.—Calculated values of the Maxwell constant.

Class.	Refractive index.	Ratio of molecular weight to density.	Ratio of geometric axes $a_1 = a_2$ $a_3$	Ratio of optic axes $b_{11} = b_{22}$ $b_{33}$	Maxwell constant $\times 10^9$ .
I.....	1.4	80	2	1.1	0.03
II.....	1.5	120	3	1.5	0.4
III.....	1.6	180	4	1.9	1.5
IV.....	1.7	240	5	2.3	3.7

of the molecules) would be forthcoming in most cases in which they failed to detect any effect. It must also be remembered that in the expression

$(a_1 - a_2)(b_{11} - b_{22}) + (a_2 - a_3)(b_{22} - b_{33}) + (a_3 - a_1)(b_{33} - b_{11})$  appearing in the Maxwell constant,  $b_{11}, b_{22}, b_{33}$  are the optical polarizabilities of the molecule, *not along its optic axes, but along its geometric axes*. Consequently, special cases may arise, if the optic and geometric axes are suitably inclined to each other, when the above expression will have very small values, even if the molecule possesses a large geometric and optical anisotropy.

Excluding the 52 liquids in which no effect was found, and the 12 compounds of potassium and sodium with the fatty acids which showed a negative birefringence, we have 108 liquids in which a normal effect was observed. From the dimensions of their apparatus (length of liquid column 4.68 cm., radii of the cylinders 1.15 cm. and 1.05 cm., and width of gap therefore = 0.10 cm.), and the known viscosity of water at 20° C., relative to which the values for the different liquids are expressed, and the specific birefringence as tabulated by them, the values of the Maxwell constant in C.G.S. units can be ascertained. In Table III. the observed values of the Maxwell constant have been grouped into five classes and are shown for comparison with the figures in Table II.

It appears highly significant that the observed values for the great majority of the liquids cluster round that calculated on the reasonable assumptions that the refractive index is about 1.5, the molecular weight about 120, the density about 1, the ratio of length of the molecule to its thickness

TABLE III.—Observed values of the Maxwell constant ( $\times 10^9$ ) for 108 liquids.

Observed values of $\nabla \times 10^9$ .	Below 0.03.	Between 0.03 and 0.4.	Between 0.4 and 1.5.	Between 1.5 and 3.7.	Above 3.7.
Number of aliphatic and hydro-aromatic liquids. }	12	44	12	—	—
Number of aromatic liquids. }	—	22	15	2	1

about 3, and the ratio of its maximum and minimum optical polarizabilities about 1.5. It is equally significant that all the low values of the Maxwell constant belong to the aliphatic or hydro-aromatic compounds, and all the high values to the aromatic compounds, and that the average values for the two sets of compounds differ just in the way we should expect in view of the greater refractive index and optical anisotropy of benzene and its derivatives.

Finally, as an example of the degree of quantitative agreement to be expected, we shall take the case of *n*-octyl alcohol. We may approximately consider this as a prolate spheroid whose major axis is 12.6 Å.U. and whose minor axis is 4.9 Å.U. Its refractive index is 1.430 and the molecular weight is 130.1.

The scattering of light in octyl alcohol has not been studied. We have, however, data for heptane and octane and also for ethyl, propyl, butyl, and amyl alcohols, and for all these compounds, assuming the optical ellipsoids of the molecules to be also prolate spheroids of revolution whose axes coincide with their respective geometric axes, the ratio  $b_{11} : b_{22}$  is equal to 1.15. We may therefore with confidence assume the same value for *n*-octyl alcohol. From these data we find the Maxwell constant for *n*-octyl alcohol to be

*Calculated value of  $\nabla = 0.125 \times 10^{-9}$ .*

From the measurements of Vörländer and Walter, taking the viscosity of octyl alcohol at 20° C. = 0.0895 (Landolt Tables),

*Observed value of  $\nabla = 0.13 \times 10^{-9}$ .*

### 7. Summary.

In this paper a theory is developed for the effect discovered by Maxwell—viz., that a liquid in a state of viscous flow exhibits birefringence. The state of stress in the fluid consists of tensions and pressures in directions perpendicular to each other and inclined at 45° to the plane of sliding.

When the molecules have an elongated form, these stresses tend to orientate them so that their direction of greatest length lies along the axis of tension, and that of shortest length along the axis of pressure. The tendency to orientation is, however, resisted by their thermal agitation, and the resulting state of statistical equilibrium may be found by the application of Boltzmann's Principle. The optical anisotropy of the molecules, taken together with the orientations referred to, causes the medium to become birefringent. The magnitude of the effect is proportional to the product of the viscosity and the velocity-gradient. The constant of proportionality, which is referred to as the Maxwell constant for the liquid, is evaluated in terms of the optical and geometrical anisotropies of the molecule, the refractive index, density, and molecular weight of the liquid, and Boltzmann's constant.

The data for 172 liquids recently obtained by Vorländer and Walter are critically discussed, and it is shown that the theory succeeds not only in giving an explanation of the general features of the phenomena observed, but also in giving quantitatively the observed values of the Maxwell constant.

210 Bowbazar Street,  
Calcutta, India.  
September 15, 1927.

---

LXXX. *Frequency Variations of the Triode Oscillator.* A Note on Mr. D. F. Martin's Paper. By Lieut.-Col. K. E. EDGEWORTH, D.S.O., M.C., A.M.I.E.E.\*

**I** HAVE just obtained a copy of the Phil. Mag. for November 1927 containing a paper by Mr. D. F. Martin on the Frequency Variations of the Triode Oscillator.

It is evident that the author has overlooked the paper which I read in December 1925 on the same subject before the Institute of Electrical Engineers (Wireless Section).

So far as they cover the same ground, the experimental results appear to be in agreement, and the explanations offered are substantially the same. The main cause of frequency variations is associated with damping of one sort or another in the grid circuit, and, other things being equal, the magnitude of the frequency variation is proportional to the amount of the damping. This type of frequency variation is referred to in my paper as a frequency variation of the first type.

My paper takes matters a good deal further, however. It is shown that the frequency variations of the first type are reversible; that is to say, the sign depends upon the direction of the coupling. With normal reactive coupling an increase

\* Communicated by the Author.

of filament current produces a decrease of frequency, but with reversed reactive coupling the opposite effect is produced. By employing resistance coupling the frequency variation of the first type can be eliminated altogether.

It is mentioned incidentally that, when the grid and anode circuits are tuned to different frequencies, the frequency of the oscillations approximates to the lower resonant frequency with normal coupling and to the higher frequency with reversed coupling.

The paper then proceeds to show that there are other sources of frequency variation which are irreversible; that is to say, they are independent of the direction of the coupling. They are usually much smaller than the frequency variations of the first type, but assume importance when the grid damping is made small enough.

When an oscillator is employed with an untuned grid circuit and heavy grid bias, the two types of oscillation may cancel out so that a circuit of constant frequency is obtained. It is suggested in the paper that these subsidiary variations are associated with the fact that the ordinary valve oscillator is single-acting, giving its impulses only during one-half of each cycle; but further research is undoubtedly required to place the matter on a proper footing.

The paper therefore discloses two types of constant frequency circuit; namely, the resistance coupled circuit and the untuned grid circuit with small grid current. Yet another type of constant frequency circuit is described by Fromy\*.

As regards the practical value of these constant frequency circuits, the untuned grid circuit with small grid current is undoubtedly the most convenient for wave-meters, and variations of frequency due to changes in the supply voltage can be reduced to less than one part in 10,000 without any particular difficulty. The necessary grid bias is most conveniently produced by means of a grid leak, as the oscillations are then self-starting. If a battery is used, some special expedient may be necessary for starting the oscillations.

The circuit is also suitable for master oscillators, but has received less attention than it deserves on account of the rapid development of oscillators employing crystal control.

The resistance coupled oscillator is a convenient circuit for small transmitters, and a number of transmitters working on this principle are now under construction for the Sudan Government.

Khartoum, 30th December, 1927.

---

\* 'L'Onde Electrique,' 1925 : 4e année, p. 433.

LXXXI. *Coefficient of Absorption in Lead of the  $\gamma$ -Rays from Thorium C'' and Radium C.* By L. BASTINGS, M.Sc., B.A., *The University, Durham* \*.

*Introduction.*

THE intensity of a beam of homogeneous radiation has in the past been regarded as reduced exponentially by its passage through an absorbing medium, the quality of the transmitted beam meanwhile remaining unaltered. Recently, however, Compton † has shown both theoretically and experimentally, that when the absorption of a beam of X-rays is accompanied by scattering, there is a definite change in the average quality of the beam, corresponding to an increase in the wave-length of the portion scattered. The magnitude of this increase is independent of the wave-length, and is determined only by the angle of scattering. Now, if the same phenomenon also occurs with  $\gamma$ -rays, the effect should be of relatively greater importance, since the increase in wave-length predicted by Compton's theory is comparable, in the  $\gamma$ -ray region, with the wave-length of the incident radiation.

Moreover, it is now generally accepted that in the X-ray region the absorption coefficient is a direct function of the cube of the wave-length; and Ahmad ‡ has furnished evidence to show that the same law is applicable to the  $\gamma$ -ray region.

If, then, a homogeneous beam of  $\gamma$ -rays is in part scattered in passing through a filter, the average wave-length of the emergent beam should be greater, and the absorption coefficient of the beam should also show an increase, which would be greater the larger the amount of scattered radiation included in the emergent beam considered. The absorption would not then be strictly exponential.

Now this quantum theory of Compton further involves a distribution of scattered radiation differing markedly from the classical prediction. The applicability of the theory to  $\gamma$ -rays has recently been tested by Ahmad §, who has found reasonable agreement with the formulæ obtained by Compton for the scattering; but the alteration in absorption coefficient

\* Communicated by Prof. Sir E. Rutherford, O.M., P.R.S.

† Compton, *Phys. Rev.* xxi. p. 483 (1923), xxii. p. 409 (1923); *Phil. Mag.* xlv. p. 897 (1923).

‡ Ahmad, *Roy. Soc. Proc. A*, cv. p. 507 (1924).

§ Ahmad, *Roy. Soc. Proc. A*, cix. p. 206 (1925).



in the scattered beam was not sufficiently pronounced to substantiate the theory.

Experiments with strictly homogeneous beams of  $\gamma$ -rays are unfortunately impracticable. It is now well established that the radiation emitted by radium in equilibrium, or by its emanation in equilibrium, consists of a number of homogeneous rays, stretching over a range of several octaves. The presence of a continuous background of  $\gamma$ -radiation has been suggested, but not definitely proved.

The case of thorium was believed to be similar: but recently Black\* has deduced evidence from  $\beta$ -ray spectra of an isolated  $\gamma$ -ray from Th C'' of very much higher frequency than that of any other monochromatic ray. As we shall see below, this  $\gamma$ -ray must carry a very considerable proportion of the total energy of the radiation, and the effect of filtering through large thicknesses of lead should be to increase very considerably the importance of this ingredient; so that eventually we might expect to produce a beam more nearly homogeneous than any other available. For this purpose it is obvious that a large source of Th C'' must be available.

#### *Previous Experiments.*

Although the literature on the absorption coefficient of radium is abundant, very little has been done with thorium. The first measurements were made by Russell and Soddy†, who determined  $\mu$  in lead, iron, and aluminium in two different experimental dispositions. In the first the absorber was placed next to the source and some distance from the ionization chamber. The values obtained were: in lead 0.462; and in aluminium 0.0916. In the second disposition the absorber formed the base of the ionization chamber, and the sources were placed some distance away. In this case  $\mu$  in lead was 0.408, and in aluminium 0.0971. In both cases the source was covered with from 6.4 to 10 mm. of lead to absorb the very soft radiation.

Next, Rutherford and Richardson‡, adopting the first disposition above, measured the coefficient in aluminium, and found that all the softer rays from a Th C source were absorbed in 2 mm. of the metal, and that the residual beam had a coefficient of 0.096 in aluminium of up to 9 cm. in thickness. This result is in approximate agreement with the earlier measurements.

\* Black, Roy. Soc. Proc. A, cix. p. 166 (1925).

† Russell & Soddy, Phil Mag. xxi. p. 130 (1911).

‡ Rutherford & Richardson, Phil. Mag. xxvi. p. 987 (1913).

No further experiments seem to have been made with Th C''.

The great amount of work done with radium shows clearly that the experimental disposition very considerably affects the results obtained. Most of the recent work in this field has been directed to distinguishing between the true absorption (photo-electric) and the apparent absorption due to scattering. Obviously, if the absorber is close to the ionization chamber, much of the radiation scattered in the forward direction will enter the chamber, and the observed coefficient will for this reason be smaller than when the absorber is removed to a distance, and so subtends a smaller solid angle at the chamber. This is confirmed in the case of thorium by the results of Russell and Soddy above, and in the case of radium by Ahmad\*.

In previous determinations of the coefficient over any considerable thickness of absorber, the method adopted has been to measure the ionization obtained through successively increasing thicknesses of absorber, plotting points representing logarithm of activity against thickness, and, if these are reasonably on a straight line, drawing the best such line through the points. From the slope of this line  $\mu$  is determined. This method entirely fails to detect any small change in  $\mu$  as the thickness of absorber is increased.

#### *Experimental Details.*

The method adopted in the present experiments consisted in measuring the absorption in a selected piece of material, of accurately known thickness, sufficiently great to reduce the ionization to about one-half. Other absorbers (or "filters") of less accurately measured thickness served, when required, to cut down the intensity of the beam. Thus the actual coefficient in the selected absorber is deducible with great precision for various thicknesses of filter. Since this absorber could be accurately replaced in a specified position, the results should clearly reveal any small change in  $\mu$  as the thickness of filter is increased.

Since the chief aim was to investigate a possible change in  $\mu$  due to the influence on the absorption of the rays scattered in the forward direction, the absorber was placed in immediate contact with the outside of the ionization chamber. The source was kept in a fixed position, and as close to the chamber as to allow just sufficient room for the insertion of the maximum thickness of filter employed. The

\* Ahmad, Roy. Soc. Proc. A, cvi. p. 507 (1924).

electroscope was completely covered externally with 3 mm. of lead. The absorber consisted of ten layers of sheet-lead ( $99\frac{1}{2}$  per cent. purity), aggregating 1.62 $\frac{1}{2}$  cm. in thickness and 13 cm. square. The source was enclosed in a sealed glass tube inserted in a cavity in a lead block so that the rays had to penetrate walls of minimum thickness 2.4 cm. The face of the block was placed 8.5 cm. from the outer surface of the electroscope, and two lead filters  $13 \times 13 \times 3.4$  cm. could be inserted between this and the standard absorber. Thus attention was concentrated on measuring the coefficient in this standard absorber when the rays were filtered in turn through 2.4, 5.8, and 9.2 cm. of lead.

### *The Sources.*

Two Th C'' sources have been used. Both were radiothorium preparations obtained from mesothorium by precipitation with ammonium hydroxide with the aid of a trace of added thorium. The precipitates were dried and sealed up in glass tubes about 6 mm. in diameter and 5 cm. long. The actual material occupied less than  $\frac{1}{4}$  c.c. and so they may be regarded as point sources. The precipitates, a week after being sealed up, had grown sufficient Th C'' to allow measurements to be made. The maximum  $\gamma$ -ray activity occurs about four weeks after preparation, and then falls off by about 0.07 per cent. per day. The first source (a) had a maximum activity about equal to that due to 5 mg. of radium in equilibrium (as measured through 3 mm. of lead), and had been precipitated as described a large number of times. It seemed unlikely, therefore, that it should contain any appreciable trace of mesothorium, and its behaviour indicated that it was reasonably pure. The second source (b) had a maximum activity of about 15 mg., and was prepared in the same way, but was precipitated only twice. In consequence there was a greater likelihood of its containing an appreciable amount of mesothorium. Its subsequent behaviour lent colour to this possibility; and some attempt was made to determine the amount of this contamination by following its curve of rise and decay, and also by the absorption-coefficient method of Bothe\*. This method is not at present very reliable for determining the mesothorium content of a radiothorium preparation, owing to our lack of accurate information on the absorption coefficient of pure mesothorium. The rise and decay method is of doubtful utility. Consequently a number of rather

\* Bothe, *Zeit. f. Phys.* xxiv. p. 10 (1924).

widely differing values for the proportion of mesothorium were obtained, ranging from 5 to 15 per cent. In consequence of this consideration, it was to be expected that the sources should give slightly different results for the absorption coefficient under similar conditions.

### *The Results.*

The absorption coefficient was invariably determined by making ten observations of the movement of the gold leaf, with and without the absorber, correcting for natural leak, and also, where necessary, for change in temperature and pressure of the air in the ionization chamber between sets of readings.

The values obtained with the two sources were not quite consistent, but the discrepancy is satisfactorily accounted for if we make the assumption, already shown to be highly probable, that source (b) owed some 5 per cent. of its maximum activity to mesothorium. With this adjustment, the average values of  $\mu$  were :—

0.417	through	2.4	cm. of lead,
0.419	„	5.8	„ „ „
0.425	„	9.2	„ „ „

with probable error of about 1 in 300.

Such an increase in  $\mu$  has not previously been recorded, either for Th C'' or for any other  $\gamma$ -ray product. A further discussion of this important result will be reserved till later.

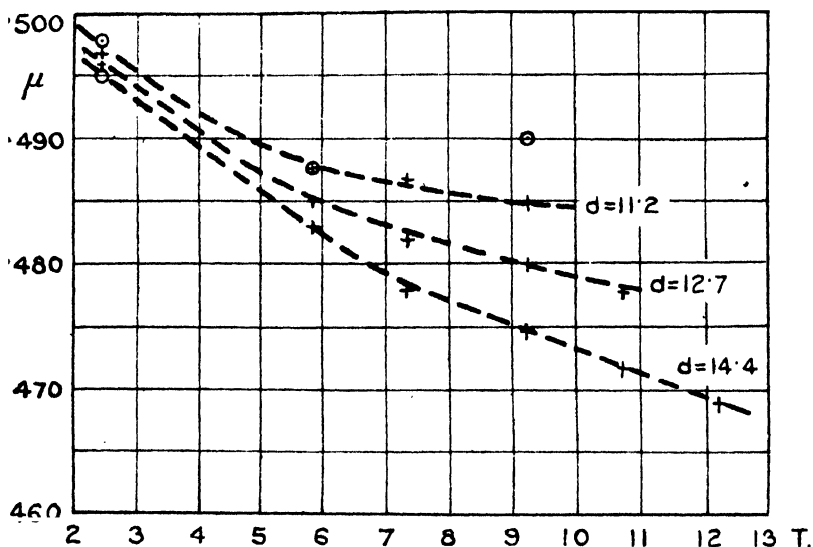
### *The Case of Radium C.*

At this stage it was thought advisable to re-examine the problem in regard to Ra C by the present method. Two large emanation sources were therefore prepared, the first initially of about 100 millicuries, the second about 300. They were contained in tubes as nearly as possible the same size and shape as in the thorium experiments.

As thicker filters were to be used in these experiments than in the previous ones, it was necessary to move the source further from the electroscope when these filters were employed; in consequence, the solid angle was different, as also the proportion of scattered radiation entering the absorber. Results at this stage will not therefore be strictly comparable with those for Th C''.

All the values obtained for  $\mu$  are represented in fig. 1. Results indicated by circles were obtained with some small radium sources; those indicated by crosses, with the emanation sources. The value obtained with a 15-mgm. radium source acting through 9.2 cm. of lead gives the only suggestion of an increase in  $\mu$  with distance: it is however based on very doubtful evidence, owing to the very small value of the ionization involved. All the remaining results show a consistent fall in  $\mu$  as the filter thickness is increased.

Fig. 1.



Variations of  $\mu$  with thickness of filter ( $T$ ) for various distances ( $d$ ).

But an examination of the figure shows that the decrease in  $\mu$  becomes more marked as the source distance is increased. This seems to suggest that if we could sufficiently reduce the source distance, and still obtain an extensive  $\mu$ - $T$  curve (as, *e.g.*, if an absorber and filter of much higher density were available), the curve might be found to bend upwards, at some stage, in somewhat the same way as the Th C'' curve has been shown to do above. The use of platinum, or even tungsten, might possibly elucidate this matter, but the quantity required would be almost prohibitive.

These data point, then, to the conclusion that in the case of Ra C, under the conditions actually investigated, the absorptibility of the  $\gamma$ -rays in lead does not increase with increasing thickness of absorber, as occurs in the case of Th C''.

*Discussion of Comparative Results.*

The difficulty in arriving at a just estimate of the value of these results in providing support for Compton's ideas depends partly on the complex nature of the beams of  $\gamma$ -rays employed, and partly on the even more complex sequence of events which probably occur during the scattering and the subsequent absorption. We may attempt to simplify the picture somewhat in the former respect by assuming the original beam to be composed of only a few monochromatic rays, and endeavouring to assign an effective wave-length and intensity to these. This may be attempted with sufficient accuracy for the present purpose if we divide the whole range of wave-lengths into three groups, and, having assigned relative intensities to the lines, we average the wave-lengths in each group with due regard to the intensities of the component lines. Now, Ellis & Wooster\* have recently outlined a valuable method for estimating these relative intensities, and their results for Ra C have been employed. Their method has also been extended to the case of Th C'' by operating on the data published by Black†. The conclusions are set out in Table I.

TABLE I.

Effective Wave-lengths and Energy of  $\gamma$ -Ray Groups.

Group.	No. of lines.	Range of $\lambda$ . (X.U.)	Average $\lambda$ . (X.U.)	Per cent. energy.	Approx. $\mu$ .
Ra C I.	4	21-9	12.5	21	} .50
II.	2	9.6	8.1	68	
III.	1	5.6	5.6	11	
Th C'' I.	6	59-42	45.1	2.3	} .42
II.	2	24-17	22.5	9.3	
III.	1	4.7	4.7	88.4	

Some of the low-frequency lines have been omitted in either case; their energy-content is negligible for the purpose in hand.

\* Ellis & Wooster, Proc. Camb. Phil. Soc. xxiii. p. 717 (1927).

† Black, Roy. Soc. Proc. A, cix. p. 166 (1925).

These conclusions, although based on data of only moderate accuracy, and deduced by a process of averaging of the roughest kind, are sufficiently valid to substantiate most unequivocally the difference between the two  $\gamma$ -ray products.

In the case of Ra C the rays are distributed over a moderate range of wave-lengths, with no outstanding gaps, or preponderating concentration of energy. But with Th C'' nearly 90 per cent. of the energy is resident in the high-frequency monochromatic wave, which is removed over two octaves from the centre of gravity of the next group. We are thus justified in our assumption that a Th C'' source approximates very closely to a monochromatic irradiator.

No account has here been taken of the continuous background of  $\gamma$ -radiation which may be present. The data available are inadequate to enable us to deal with it even as cursorily as we have done with the line spectrum. But it is unlikely to affect our conclusions materially, for Ellis and Wooster\* have shown that the continuous  $\gamma$ -ray spectrum is probably of weak intensity.

As has already been indicated, the total absorption has been shown by Ahmad† to be a function of  $\lambda$  of the form

$$AZ + B\lambda^3Z^4,$$

where A and B are independent of  $\lambda$ , and Z is the atomic number of the absorber. The relative importance of the two terms is not sufficiently established to justify accurate deductions. But Ahmad estimates that for  $\lambda = 20$  X.U. the two terms are comparable in magnitude. It is probable, then, that for waves two octaves below this,  $\mu$  is considerably smaller. The data in Table I. broadly support this conclusion.

It follows from these considerations that, in the absence of any further complexity, the passage of these hypothetical radiations through the same filter should result in a much greater proportionate concentration of the energy in the high-frequency group with Th C'' than with Ra C. The resulting coefficient for the Th C'' should thus fall more rapidly with increasing filter thickness than for Ra C.

But the further complexity—the change in quality on scattering, postulated by Compton—will act counter to this. The scattered portion of the beam suffers an increase in  $\lambda$ , and in consequence an increase in the average  $\mu$  which is measured. This effect will be at least twice as important for Th C'' III. as for Ra C III. under similar conditions.

\* Ellis & Wooster, Proc. Camb. Phil. Soc. xxiii. p. 717 (1927).

† Ahmad, Roy. Soc. Proc. A, cvi. p. 8 (1924).

The net effect which is observed will be determined by the relative importance of these two factors in each case.

This picture of the process involves very considerable simplifying assumptions; but still it seems sufficiently valid to indicate the reason for the difference in the behaviour of the two radioactive bodies. With Ra C the hardening effect under the experimental conditions outlined seems everywhere to be of greater importance than the Compton effect, and  $\mu$  to decrease continually in consequence; but with Th C'' the latter effect appears to be of greater importance, and the coefficient increases. The magnitude of the increase evidently depends on the experimental conditions, especially in so far as these control the proportion of scattered radiation which is included in the absorption measurements. But as the distribution of scattered radiation is again an uncertain and complex function of the wave-length, it is apparent that much more detailed information on all these matters and a much more elaborate analysis must be evolved before we can hope to obtain satisfactory quantitative agreement between this phase of Compton's theory and  $\gamma$ -ray absorption measurements.

#### *Summary.*

Careful measurements on the absorption of  $\gamma$ -rays in lead have shown that the coefficient increases with the thickness of lead penetrated in the case of Th C'', but decreases in the case of Ra C. The difference is shown to be in general agreement with the consequences of Compton's theory of scattering.

The important fact evolves that Th C'' acts almost as a monochromatic source of  $\gamma$ -radiation.

#### *Acknowledgments.*

I have much pleasure in recording my indebtedness to Sir Ernest Rutherford for his helpful interest during the prosecution of these measurements; also to Dr. J. Chadwick for advice, and especially for preparing and placing at my disposal the large Th C'' sources used.

The work was rendered possible through a grant from the Department of Scientific and Industrial Research, for which I am deeply grateful.

The University, Durham.  
July 28, 1927.



LXXXII. *Bubbles, Drops, and Stokes' Law.* (Paper 2.) By  
W. N. BOND, M.A., D.Sc., F.Inst.P., *Lecturer in Physics,*  
*University of Reading,* and DOROTHY A. NEWTON, B.Sc.,  
*a Senior Scholar, University of Reading* \*.

*Summary.*

IN a previous paper by one of the authors it was shown that spherical drops or bubbles surrounded by a more viscous fluid might have a terminal velocity as great as one and a half times that of a solid sphere of equal size and mass. The present paper shows experimentally and theoretically that the surface-tension of the surface of the drop or bubble decreases the terminal velocity. For any radii appreciably less than a certain critical value the drop or bubble behaves almost like a rigid sphere. After a fairly rapid transition, for all radii appreciably larger than the critical the effect of surface-tension is small. Experiments on the terminal velocity for air in water-glass, air in syrup, mercury in syrup, and water in castor-oil, all give critical radii of the order predicted; but the different media show appreciably mutual disagreement, the cause of which is not yet certain.

INTRODUCTION.

IN a previous paper by one of us †, Stokes' calculations for the slow rectilinear motion of a solid sphere through viscous fluid were extended, in the way he outlined, to the case where the sphere is composed of fluid. For a drop of radius  $a$ , and density  $\rho'$ , falling through an infinite extent of fluid of density  $\rho$  and viscosity  $\mu$ , the terminal velocity may be written

$$V_{\infty} = \frac{1}{k} \left\{ \frac{2(\rho' - \rho)ga^2}{9\mu} \right\}. \quad \dots \quad (1)$$

It was shown that, *if the surface of the drop did not itself exert any tangential force,*

$$k = \frac{2/3 + \mu'/\mu}{1 + \mu'/\mu}, \quad \dots \quad (2)$$

where  $\mu'$  is the viscosity of the fluid forming the drop.

\* Communicated by the Authors.

† Bond, Phil. Mag. (7) vol. iv. No. 24, pp. 889-898 (Nov. 1927).

According to this theory, if the fluid composing the drop has a very large viscosity compared with that of the surrounding fluid, the drop will behave as a solid sphere ( $1/k=1$ ); conversely, if the fluid of the drop be relatively very inviscous, the drop should move one and a half times as fast as a solid sphere of equal size and density ( $1/k=\frac{3}{2}$ ), there being now no tangential force at the surface of the sphere.

It was also recorded in the former paper \* that air-bubbles were found to rise in viscous liquid at a speed corresponding to  $1/k=1.43$ —almost that predicted. Fluctuations in the measurements, and the relatively small velocities obtained in the few experiments with water drops in castor-oil, were attributed to tangential forces exerted by the spherical surface that were then considered probably due to surface contamination. The present paper records an attempt to investigate this surface-effect further.

#### THEORY.

At first it might be thought that surface-tension, without contamination, would not influence the phenomenon, as the area and shape of the common surface are constant. But further consideration (as well as the experimental results) shows that surface-tension will itself have an effect.

The fluid just inside and outside the surface has, in general, a common tangential velocity. Because this velocity varies from zero at the two points on the axis of motion of the sphere to a maximum at points in (or near) the equatorial plane, the area of an element of the common surface must at first grow from zero, then attain a maximum, and finally decrease again to zero. This change in area will require a local supply or removal of energy, and will call into play tangential forces not considered in deriving equation (2). It appears likely that, as this effect becomes important,  $k$  will change from the value given by equation (2) towards unity (a rigid sphere).

Without making a detailed calculation, it may be assumed that one extra variable, the surface-tension,  $T$ , of the common surface, is all that need be considered (the conditions being sensibly isothermal). We then obtain dimensionally the most general form of relationship between the variables

$$f\left(\frac{a\mu V}{W}, \frac{\mu'}{\mu}, \frac{aT}{W}\right) = 0, \quad . \quad . \quad . \quad (3)$$

\* Bond, *loc. cit.*

where  $W$  is the apparent weight of the drop or bubble after allowing for buoyancy. This equation may be written

$$V_{\infty} = \left\{ \phi \left( \frac{\mu'}{\mu}, \frac{aT}{W} \right) \right\} \left\{ \frac{2}{9} \frac{(\rho' - \rho)ga^2}{\mu} \right\} \dots (4)$$

Thus  $1/k$  of equation (1) will be a function not only of  $\mu'/\mu$  as given by equation (2), but also of  $\frac{aT}{W}$ . For large drops or bubbles,  $\frac{aT}{W}$  is small, and  $1/k$  should approach the value given by equation (2), being a maximum ( $1/k = \frac{3}{2}$ ) when  $\mu'/\mu$  is also small. And for small drops or bubbles ( $\frac{aT}{W}$  large) it was suggested above that  $1/k$  should in all cases tend to unity (rigid sphere).

The surface-tension would probably become of moderate importance if  $\frac{aT}{W}$  were of the order unity\*. Or, changing to more convenient variables, we may define a critical radius,  $\bar{a}$ , near which the transition would be expected to occur, by

$$\bar{a} = \sqrt{\frac{T}{|(\rho' - \rho)| \cdot g}} \dots (5)$$

It might be thought that when surface-tension became of small importance ( $\frac{aT}{W}$  small) the large drops or bubbles would depart from the spherical form. It appears, however, from equation (4) of the previous paper † that, when there is no tangential force at the surface of the sphere (and when the kinetic energy of the fluid is negligible), the departure from sphericity is only due to the hydrostatic pressure being slightly different at the top and bottom of the drop, and is therefore very small.

#### EXPERIMENTS.

In order to investigate the effect of surface-tension on the terminal velocity, the viscosity of the fluid inside the sphere was kept very small compared with that outside.

\* For rapidly moving air-bubbles in water a change in effect has been found at a critical radius of about 0.165 cm. (O. Miyagi, Tôhoku Univ. Technol. Reports, (5) No. 3, pp. 1-33, 1925). This effect, also, seems to be due to surface-tension, and the order of the critical radius is given by equation (5) above.

† Bond, *loc. cit.*

The ratio of the terminal velocity to that of a solid sphere of equal size and density (*i. e.*,  $1/k$  defined by equation (1)) was then measured for various sizes of drop or bubble (*i. e.*, for various values of  $\frac{aT}{W}$ ). For no tangential force due to the surface of the sphere this ratio should be  $1/k = \frac{3}{2}$ , as given by equation (2) when  $\mu'/\mu$  is very small; but in general it might be less, being a function of  $\frac{aT}{W}$ ,  $\phi$  of equation (4).

Experiments were carried out with air in golden syrup, mercury in golden syrup, and water in castor-oil. Also the previous results on air in water-glass and air in golden syrup were analysed on the present basis. The velocities were in all cases such that the forces accelerating the liquid outside were negligible in comparison with those overcoming viscous resistance to relative motion (*i. e.*,  $V_{\infty} a \rho / \mu$  was small compared with unity). The temperature varied during the experiments between about 13° C. and 20° C.

The terminal velocities were found using a vertical brass box of internal cross-section 4.75 cm. square, containing about 13 cm. length of liquid column (as in the previous work). A pair of adjacent sides had plate-glass windows, and the drops or bubbles were viewed with a microscope, in front of a white background crossed by a number of horizontal dark lines. In some experiments on large water drops in castor-oil a glass cylinder was used (internal diameter 7.5 cm.; height 13½ cm.). To allow for the effect of the walls and ends, a curve was constructed for both vessels from observations of solid spheres of various sizes falling in golden syrup. As the size of sphere was increased, the correction began to exceed that given by Ladenburg's formula, being considerably in excess for the largest spheres.

The diameters of the slower drops and bubbles were found by measuring the time they took to move a distance equal to their diameter; the size of the larger mercury drops was found by previous weighing, and of the larger water drops by forming them from calibrated pipettes.

The viscosity of the surrounding liquid was found by measuring the terminal velocity of steel spheres before and after each experiment.

Since it was shown in the previous paper\* that the wall-correction for drops and bubbles is in general less than for a

\* Bond, *loc. cit.*

solid sphere (being closely proportional to  $k$ ), the unmodified wall-correction was first applied, yielding a first estimate of  $k$ . This was used to modify the wall-correction and obtain a second approximation to  $k$ . This again changes slightly the estimated wall-correction; and for large drops the approximation was carried out to three or four stages, the estimates being successively above and below the required value. The accuracy of this allowance for the wall-correction is confirmed by the agreement of the results, using two different containing-vessels (see Water in Castor-oil, fig. 1).

The surface-tension of the surface common to the two fluids was chiefly found by use of a large flat drop (Quincke's method), so as to have conditions nearly like those occurring during the main experiment.

#### DISCUSSION OF RESULTS.

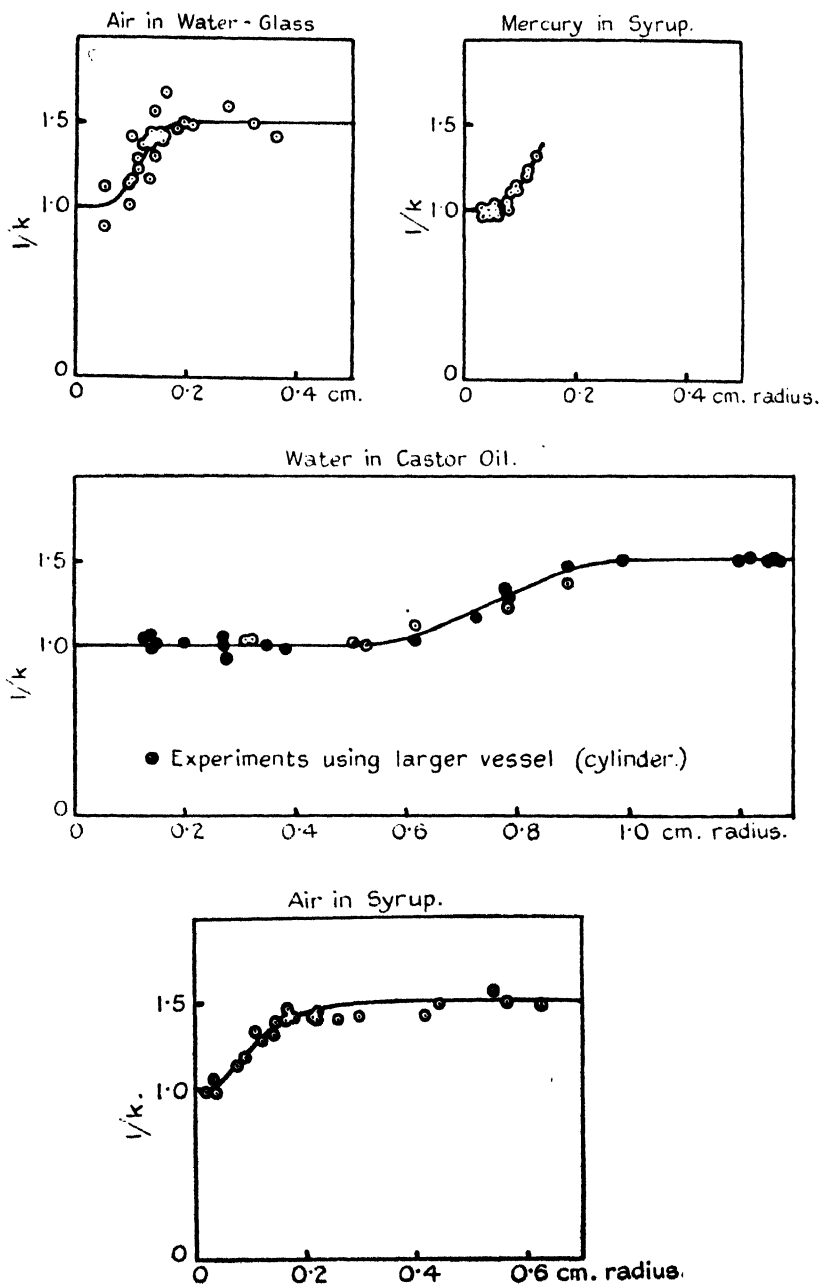
The values of  $1/k$  (defined by equation (1)) are plotted against values of the radius of the drop or bubble (fig. 1).

It is seen that in three cases  $1/k$  reaches the value  $\frac{3}{2}$  (given by equation (2) for  $\mu'/\mu=0$ ) for large drops or bubbles. In the case of the mercury, drops of radii larger than 0.13 cm. were not used, as they were non-spherical. This was evidently due to the large kinetic energy of the mercury in the drop, combined with the large difference in density between the mercury and the surrounding syrup. For the large water drops also,  $V_{\infty}a\rho'/\mu'$  was not small compared with unity. But in this case  $\rho$  and  $\rho'$  differed little, and the drops remained sensibly spherical for the largest diameters recorded. No obvious evidence of turbulence inside the drops was noticed, and for the largest drops the tangential forces required to circulate the inner fluid were evidently small, as  $1/k$  became very close to  $\frac{3}{2}$  in value.

For small diameters of drop or bubble the value of  $1/k$  approaches unity very closely (*i. e.*, Stokes' Law is obeyed). This is in general agreement with the predictions, assuming surface-tension to affect the problem. If there is very small velocity at the spherical surface, no appreciable work will be done in stretching the surface, and the problem reduces to that of a solid sphere. But the action of surface-tension has not been elucidated in detail.

Finally, let us consider the transition case (say  $1/k=1.25$ ). It is found that this occurs for a radius of the order predicted by equation (5) for the considerable range of values of  $T$  and  $(\rho'-\rho)$  covered by the experiments. The agreement

Fig. 1.



between the results for different fluids is not at all perfect, but there is enough evidence to show that surface-tension is the main cause of the departure from the value of  $1/k$  given by equation (2).

The values may be put in tabular form :—

	$\mu'/\mu$	T.	$\rho' - \rho$	$\bar{a} = \sqrt{\frac{T}{[(\rho' - \rho) \cdot g]}}$	Observed radius for $1/k = 1.25$ .
Air in water-glass...	$10^{-7}$	104	-1.69	0.25 cm.	0.10 <sub>5</sub> cm.
Air in golden syrup	$10^{-6}$	91	-1.48	0.25	0.11
Mercury in golden syrup.	$10^{-4}$	285	12.1	0.15 <sub>5</sub>	0.12
Water in castor-oil.	$10^{-3}$	18.0	0.037	0.70	0.77

The variation in the ratio of (observed radius for  $1/k = 1.25$ ) to ("critical radius,"  $a$ ) may be due to surface contamination. It seems impossible that it can be due to the conditions not being isothermal. The variation may also be due to the surface-tension changing with time. The surface-tension of water to castor-oil was found to decrease with time. Finally, the variation might possibly be due to the effect of the kinetic energy of the liquid inside the drops; or even, conceivably, to the ratio of  $\mu'$  to  $\mu$  being changed.

It is now clear that the variation in the values of  $1/k$  found in the previous work, and the low values found in some experiments at the start of the present work, were due to the action of surface-tension. Also surface-tension will cause Stokes' Law to be applicable in experiments such as those of J. J. Thomson and of Millikan, referred to in the former paper.

The authors would like to thank Professor Crowther, in whose laboratories the work was carried out, for his kind encouragement and interest in the work; thanks are also due to Mr. J. S. Burgess, the laboratory steward, for continued help in regard to apparatus.

Department of Physics,  
University of Reading,  
December 31st, 1927.

[The Editors do not hold themselves responsible for the views expressed by their correspondents.]

THE  
LONDON, EDINBURGH, AND DUBLIN  
PHILOSOPHICAL MAGAZINE  
AND  
JOURNAL OF SCIENCE.

---

[SEVENTH SERIES.]

---

SUPPLEMENT, MAY 1928.

---

LXXXIII. *The Secular Changes in Electronic Orbits in a Magnetic Field.* By W. M. HICKS, F.R.S.\*

THE use which has been made of Larmor's theorem to explain the Zeeman effect on the quantum basis is well known. On the supposition that the effect of  $H^2$  on the motion may be neglected, the motion of a single electron round a nucleus is compounded of an elliptic orbit in some plane inclined to  $H$  which at the same time regresses with angular velocity  $\omega = HE/2mc$ . Now, such an electron in orbits of atomic dimensions makes about a billion circuits in  $1/1000$  sec. Thus during the life even of an excited orbit there is time for secular effects to produce very large changes in the orbital constants. It is the purpose of the present investigation to determine these changes, and at the same time to find the conditions that  $H^3$  and higher powers may be neglected. Shortly, the principal results may be summarized as follows :—

(1) If the initial orbits are parallel or perpendicular to  $H$  their planes remain fixed, but the line of apses regresses.

\* Communicated by the Author.

*Phil. Mag.* S. 7. Vol. 5. No. 31. *Suppl. May* 1928. 3 F



(2) If the initial orbit be a circle, it will remain a circle, with the inclination of its plane unaltered, but the nodal line progredes at a constant rate of the second order of magnitude.

(3) In other cases the nodes, apsides, eccentricity, and inclination of plane all change. There are two categories of cases:

(3a) The apsides continually regrede. An orbit initially with its axis in the nodal line has its maximum inclination at that instant. As the axis moves back to a line perpendicular to the node, the inclination diminishes to a minimum at that stage. The nodal line progredes continuously and the eccentricity changes so that

$$(1 - e^2) \cos^2 a = \text{const.}$$

(3b) The apsides oscillate on either side of the line perpendicular to the node. The plane of the orbit swings up and down with its maximum and minimum inclinations now both when the apsidal line is perpendicular to the node. In the maximum position the axis is swinging in the same direction as the electron is moving (*i. e.* progredes), whilst in the minimum it is moving oppositely (regredes). No orbit can belong to this category whose inclination is less than

$$\sin^{-1} \sqrt{.8} = 63^\circ 26' 6''.$$

For numerical examples, see § 8.

The conclusion is drawn that, for orbits of  $10^{-8}$  cm. and  $H$  of the order of 30,000 gauss, we are justified in regarding  $H^2$  as a small disturbing effect, but not for those of  $10^{-6}$  or larger. The energy of the whole motion remains constant, also that of the standard portion if we regard  $-\omega^2 \rho$  as a force with potential  $-\frac{1}{2}\omega^2 \rho^2$ . The angular momentum round  $H$  of the standard portion remains constant, but that of the whole motion or of the regressive portion is not. If the field has been imposed on a previously existing orbit, the standard cannot possibly be the same as the original\*, and, in any case, its actual form would depend on the instant at which, and on the way in which, the field was imposed. The problem is considered only in its dynamical aspects, and no discussion is taken as to its application to various physical theories.

1. Taking fixed axes, with the axis of  $z$  along the field  $H$ , using cylindrical coordinates  $\rho$ ,  $\phi$ ,  $z$ , and denoting the

\* Larmor, 'Æther and Matter,' p. 348. Also see Nat. cxv. p. 978 (1925).

distance from the nucleus at the origin by  $r$ , the equations of motion are

$$\left. \begin{aligned} \frac{d^2\rho}{dt^2} - \rho \left( \frac{d\phi}{dt} \right)^2 &= -\frac{E^2\rho}{mr^3} + \frac{HE}{mc} \rho \frac{d\phi}{dt}, \\ \frac{d}{dt} \left( \rho^2 \frac{d\phi}{dt} \right) &= -\rho \frac{HE}{mc} \frac{d\rho}{dt}, \\ \frac{d^2z}{dt^2} &= -\frac{E^2z}{mr^3}. \end{aligned} \right\} \quad . \quad . \quad (1)$$

Write  $HE/(2mc) = \omega$  and  $E^2/m = p$ . Integrating the second gives

$$\rho^2 \frac{d\phi}{dt} + \omega \rho^2 = h.$$

Replacing  $\frac{d\phi}{dt} + \omega$  by  $\frac{d\theta}{dt}$ , the equations become

$$\left. \begin{aligned} \frac{d^2\rho}{dt^2} - \rho \left( \frac{d\theta}{dt} \right)^2 &= -\frac{p\rho}{r^3} - \omega^2\rho, \\ \rho^2 \frac{d\theta}{dt} &= h, \\ \frac{d^2z}{dt^2} &= -\frac{pz}{r^3}. \end{aligned} \right\} \quad . \quad . \quad . \quad (2)$$

The *form* of these equations is that of orbits referred to fixed axes, under the central attraction combined with one *towards* the axis of  $z$  proportional to  $\rho$ . Hence the actual motion is that of an orbit determined by equations (2) referred to fixed axes, which is at the same time subject to a uniform regression  $\omega$ . In determining the motion, therefore, we may pay no attention to the regressive part, whatever the magnitude of  $\omega$  may be. The orbit as determined by equations (2) we shall call the standard orbit. If  $\omega^2$  is negligible, the standard will be a plane elliptic orbit, and this regresses with angular velocity  $\omega$ . This is Larmor's theorem.

The energy of the whole motion is given by

$$\left. \begin{aligned} \frac{2p}{r} - \frac{2W}{m} &= \left( \frac{d\rho}{dt} \right)^2 + \left( \frac{dz}{dt} \right)^2 + \rho^2 \left( \frac{d\phi}{dt} \right)^2 \\ &= \left( \frac{d\rho}{dt} \right)^2 + \left( \frac{dz}{dt} \right)^2 + \rho^2 \left( \frac{d\theta}{dt} \right)^2 - 2\omega h + \omega^2 \rho^2, \end{aligned} \right\} \quad (3)$$

where  $W$  is the energy-defect of the whole motion, and  $W - m\omega h$  that of the standard.

Eliminating the time variable in the usual way and writing  $1/\rho = u$ ,  $z/\rho = zu = X$ , it is easily shown that

$$\left. \begin{aligned} \frac{d^2 u}{d\theta^2} + u &= \frac{p}{h^2(1+X^2)^{3/2}} + \frac{\omega^2}{h^2 u^3}, \\ \frac{d^2 X}{d\theta^2} + X &= \frac{\omega^2 X}{h^2 u^4}, \end{aligned} \right\} \quad \dots \quad (4)$$

and the energy equation becomes

$$\begin{aligned} \left(\frac{du}{d\theta}\right)^2 + \left(u \frac{dX}{d\theta} - X \frac{du}{d\theta}\right)^2 + u^2 \\ = \frac{2p}{h^2} \frac{u}{\sqrt{(1+X^2)}} - \frac{\omega^2}{h^2 u^2} + \frac{2\omega}{h} - \frac{2W}{mh^2}. \end{aligned} \quad (5)$$

2. If the effect of  $\omega^2$  is negligible, these give a fixed plane elliptic orbit. If the effect is not negligible but small, the standard motion may be regarded as taking place in an instantaneous ellipse whose constants are subject to continuous variation. The condition of negligibility, however, does not depend on  $\omega$  alone, but on the size of the actual orbit. This is evident from the fact that, if the orbit is very large, its form will depend almost wholly on  $H$ , whilst when it is sufficiently small, it depends chiefly on the electric forces. We shall assume here that  $\omega^3$  may be neglected, and determine later the conditions under which the assumption is permissible.

If  $l$  denote the semi-latus rectum of an orbit,  $lu$  is of order unity. Replacing  $lu$  for  $u$ , the disturbing terms in (4, 5) appear with the numerical coefficient

$$k = \frac{l^4 \omega^2}{h^2} = l^3 \frac{\omega^2}{p} = \frac{H^2}{4mc^2} l^3.$$

With a field of 30,000  $x$  gauss and an orbit of the order of  $10^{-8}$  cm. this becomes  $k = 2.7 \times 10^{-10}$ .

3. In fig. 1 let the plane of the orbit cut a spherical surface round  $O$  in the great circle  $PNA$ , the plane of  $xy$  in  $xNy$ , the radius vector to the particle in  $P$  and that to perihelion in  $A$ . Also let

- $a$  = inclination of orbital plane =  $PNm$ ,
- $b$  = nodal angle  $xON$ ,
- $c$  = angle from node to perihelion =  $NOA$ ,
- $\phi$  = angle  $PN^*$ ,
- $\theta$  = angle  $xOm$ .

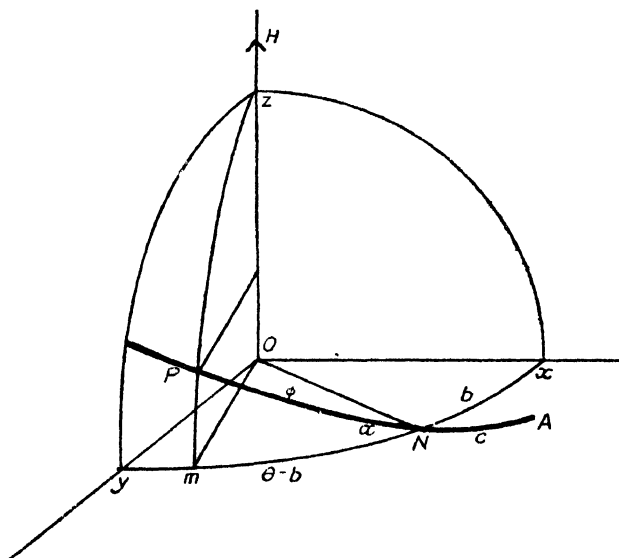
\* Not, of course, the  $\phi$  of § 1, which we shall no longer require.

The equation of the instantaneous ellipse in its own plane will be of the form

$$\frac{l'}{r} = 1 + e \cos (\phi + c).$$

Here  $l' = h_1^2/p$ , where  $\frac{1}{2}h_1$  is the rate of description of area in the plane of motion. The areal rate in the projection of the path on  $xy$  is the absolute constant  $\frac{1}{2}h$  of equation (2).

**Fig. 1.**



Hence  $h=h_1 \cos \alpha$ . Write  $h^2/p=l$ , also an absolute constant however  $\alpha$  may alter. Then

$$\frac{lu \cos Pm}{\cos^2 a} = 1 + e \cos \phi \cos c - e \sin \phi \sin c,$$

also

$$X = z/\rho = \tan P_m.$$

## Now

$$\tan P_m = \tan a \sin (\theta - b) ; \quad \tan (\theta - b) = \cos a \tan \phi.$$

Hence it is easy to show that

$$\left. \begin{aligned} \frac{lu}{\cos^2 a} &= \sqrt{1 + X^2} + e \left\{ \cos c \cos (\theta - b) - \frac{\sin c}{\cos a} \sin (\theta - b) \right\}, \\ X &= \tan a \sin (\theta - b). \end{aligned} \right\} \quad (6)$$

If, however,  $\omega^2$  be neglected—ON fixed—it is more convenient to express the relations in  $\phi$ , and then

$$lu\sqrt{Y} = 1 + e \cos(\phi + c) \quad . \quad . \quad . \quad (7)$$

with

$$Y = 1 - \sin^2 a \sin^2 \phi.$$

$$\cos(\theta - b) = \cos \phi / \sqrt{Y}; \quad \sin(\theta - b) = \sin a \sin \phi / \sqrt{Y}.$$

When  $\omega^2$  is small,  $a, b, c, e$  may be regarded as slowly changing. In settling these changes, equations (6) must be used, and not (7), which assumes  $a, b$  always constant. After, however, the variations of the orbital constants have been introduced into our equations,  $\phi$  may be regarded as a mere transformation of coordinates from  $\theta$ , and the corresponding expressions be used while integrating round a single orbit.

4. *Variation of X*, i. e. of  $a, b$ .—We shall denote throughout variations of the constants by the corresponding Greek letters. The equation in  $X$  is

$$\frac{d^2 X}{d\theta^2} + X = \frac{kX}{l^4 u^4}.$$

Multiply by  $\frac{dX}{d\theta}$  and integrate

$$\left(\frac{dX}{d\theta}\right)^2 + X^2 = 2k \int \frac{X dX}{l^4 u^4}.$$

In the small term on the right we may use values for the undisturbed motion, viz.:

$$X = \tan a \sin(\theta - b) = \sin a \sin \phi / \sqrt{Y},$$

$$\frac{dX}{d\phi} = \frac{\sin a \cos \phi}{Y^{3/2}}.$$

Hence, writing  $1 + e \cos(\phi + c) = D$ ,

$$\left(\frac{dX}{d\theta}\right)^2 + X^2 = 2k \frac{\sin^2 a}{\cos^3 a} \int \frac{\sin \phi \cos \phi}{D^4} d\phi.$$

In the disturbed motion let  $X$  become  $X + \xi$ ; then

$$\frac{dX}{d\theta} \frac{d\xi}{d\theta} + X\xi = k \frac{\sin^2 a}{\cos^3 a} \int \frac{\sin \phi \cos \phi}{D^4} d\phi.$$

Now  $\frac{d\theta}{d\phi} = \frac{\cos a}{Y}$ , whence

$$\cos \phi \sqrt{Y} \frac{d\xi}{d\phi} + \xi \cos^2 a \frac{\sin \phi}{\sqrt{Y}} = k \frac{\sin a}{\cos^6 a} \left( \dots \right)$$

$$\cos \phi \frac{d}{d\phi} (\xi \sqrt{Y}) + \sin \phi \xi \sqrt{Y} = \dots$$

It will be convenient to write  $\xi \sqrt{Y} = \lambda \zeta \sin a$ ,  $k = \lambda \cos^6 a$

$$P = \int \frac{\sin \phi \cos \phi}{D^4} d\phi, \quad Q = \int \frac{\sin^2 \phi}{D^4} d\phi.$$

Then

$$\cos \phi \frac{d\zeta}{d\phi} + \zeta \sin \phi = P, \quad \dots \dots \dots (8)$$

$$\frac{d}{d\phi} \left( \frac{\zeta}{\cos \phi} \right) = P \sec^2 \phi = P \frac{d}{d\phi} (\tan \phi),$$

$$\zeta = P \sin \phi - Q \cos \phi. \quad \dots \dots \dots (9)$$

Since

$$X = \tan a \sin (\theta - b),$$

$$\xi = \sec^2 a \sin (\theta - b) \alpha - \tan a \cos (\theta - b) \beta,$$

$$\xi \sqrt{Y} = \frac{\sin \phi}{\cos a} \alpha - \frac{\sin a}{\cos a} \cos \phi \cdot \beta.$$

Hence, comparing with equation (9),

$$\left. \begin{aligned} \alpha &= \lambda \sin a \cos a P, \\ \beta &= \lambda \cos a Q. \end{aligned} \right\} \quad \dots \dots \dots (10)$$

In the integrals,

$$D = 1 + e \cos (\phi + c) = 1 + e \cos \chi \text{ (say).}$$

If  $I_n$  denote  $\int \frac{d\chi}{D^n}$ ,

$$\int \frac{\cos \chi}{D^n} d\chi = -\frac{1}{n-1} \frac{d}{de} I_{n-1},$$

also

$$\int \frac{\sin \chi}{D^n} d\chi = \frac{1}{n-1} \frac{1}{e D^{n-1}}.$$

Let  $\Delta$  stand for the operator  $d/de$ . Then

$$P = \int \frac{\sin \chi \cos \chi \cos 2c - \sin c \cos c (2 \cos^2 \chi - 1)}{D^4} d\chi$$

$$= -\frac{1}{6} \cos 2c \Delta \left( \frac{1}{e D^2} \right) - \frac{1}{6} \sin 2c \Delta^2 I_2 + \sin c \cos c I_4,$$

so

$$Q = \frac{1}{6} \sin 2c \Delta \left( \frac{1}{e D^2} \right) - \frac{1}{6} \cos 2c \Delta^3 I_2 + \cos^3 c I_4.$$

As we require to find the changes in  $a, b$  after one revolution of the particle, the integration limits are  $\chi_0, \chi_0 + 2\pi$ . The first terms in the above for  $P, Q$  then disappear, and the  $I$  stand for the complete integrals. To find these we note that

$$e \Delta I_n = - \int n \frac{e \cos \chi}{D^{n+1}} = -n \int \left( \frac{1}{D^n} - \frac{1}{D^{n+1}} \right) = -n (I_n - I_{n+1}).$$

Thus

$$I_n = \left( \frac{1}{n-1} e \Delta + 1 \right) I_{n-1}.$$

The  $I_n$  depend then on  $I_1$ , viz. :

$$I_1 = \int \frac{d\chi}{1 + e \cos \chi} = \frac{2}{\sqrt{1-e^2}} \tan^{-1} \left( \sqrt{\frac{1-e}{1+e}} \cdot \tan \frac{1}{2} \chi \right).$$

It is easily seen that the indefinite  $I_n$  is of the form

$$A_n \tan^{-1}(\dots) + \left( \frac{B_1}{D} + \dots + \frac{B_{n-1}}{D^{n-1}} \right) \sin \chi.$$

These will give the complete values of  $\alpha, \beta$  at any point of the orbit. For our purpose, however,

$$I_1 = \frac{2\pi}{\sqrt{1-e^2}} = 2\pi Z \text{ (say).}$$

Here

$$e \Delta Z^n = n(Z^{n+2} - Z^n),$$

whence

$$\left. \begin{aligned} I_2 &= (e\Delta + 1)I_1 = 2\pi Z^3, \\ I_3 &= \left(\frac{1}{2}e\Delta + 1\right)I_2 = \pi(3Z^5 - Z^3), \\ I_4 &= \left(\frac{1}{3}e\Delta + 1\right)I_3 = \pi(5Z^7 - 3Z^5), \\ \Delta^2 I_2 &= 6\pi(5Z^7 - 4Z^5), \\ \Delta^3 I_1 &= 6\pi e(5Z^7 - 2Z^5). \end{aligned} \right\} \quad \dots \quad (11)$$

Substituting, it will be found that

$$\alpha = -\frac{5}{2}\pi\lambda \frac{\sin a \cos a}{(1-e^2)^{5/2}} \left( \frac{1}{1-e^2} - 1 \right) \sin 2c,$$

$$\beta = \pi\lambda \frac{\cos a}{(1-e^2)^{5/2}} \{1 + 5(Z^2 - 1) \sin^2 c\}.$$

We shall find in the next section that  $Z = C \cos a$ , where  $C$  is a constant. Hence, replacing  $\lambda$  by  $k/\cos^6 a$ ,

$$\left. \begin{aligned} \alpha &= -\frac{5}{2}\pi k C^5 \sin a (C^2 \cos^2 a - 1) \sin 2c, \\ \beta &= \pi k C^5 \{1 + 5(U^2 \cos^2 a - 1) \sin^2 c\}. \end{aligned} \right\} \quad (12)$$

5. *The eccentricity.*—In any elliptic orbit (major axis =  $2a$ ) the energy defect is given by  $W' = mp/2a$  and  $l' = a(1-e^2)$ , whence  $1-e^2 = 2W'l'/mp$ . In the present case the effective elliptic energy is not constant:

$$W' = W - m\omega h + \frac{1}{2}m\omega^2 \rho^2; \quad l' = l/\cos^2 a; \quad l = h^2/p.$$

Hence

$$\begin{aligned} (1-e^2) \cos^2 a &= 2(W - m\omega h) \frac{l^2}{mh^2} + \frac{l^2 \omega^2}{h^2 u^2} \\ &= \text{const.} + \frac{k}{l^2 u^2}. \end{aligned}$$

$$\therefore e\eta \cos^2 a = -(1-e^2) \sin a \cos a \cdot \alpha - \frac{k}{2l^2 u^2}. \quad (13)$$

Since  $l^2 \omega^2/(hu)^2$  is periodic, it follows that  $(1-e^2) \cos^2 a$  is unaltered after a complete revolution; or throughout the secular motion

$$(1-e^2) \cos^2 a = \text{const.} = (1-e_0^2) \cos^2 a_0,$$

where  $e_0, a_0$  are initial values. It is convenient to put the constant =  $\frac{1}{C^2}$ . Some interesting conclusions follow at once. *E.g.:*

(1) Since  $1-e^2$  is always  $< 1$ ,  $\cos^2 a > (1-e_0^2) \cos^2 a$ . Hence, even if  $a$  increases,  $a$  can never be greater than  $\cos^{-1} \{ \sqrt{(1-e_0^2)} \cos a_0 \}$ .

(2) If initially the plane of the orbit is parallel to  $H$ , it must always remain so, for then the constant is zero and  $(1-e^2) \cos^2 a = 0$  always, *i.e.* either  $\cos a = 0$  or  $e = 1$ , the latter denoting a line orbit. The same result also follows from the fact that, in this case, the areal rate projected on



the plane of  $xy$  is zero, and by equation (2) is constant and therefore zero always. This can only happen when the orbital plane remains perpendicular to  $xy$ .

(3) Any finite change in the inclination must involve simultaneous changes in the shape of the orbit, so that, if  $e$  denote the ratio of the axes,  $e \cos a$  is constant.

6. *The orientation of axis or c.*—Equation (5), the analogue of the energy equation, is

$$\begin{aligned} \left(\frac{du}{d\theta}\right)^2 + \left(u \frac{dX}{d\theta} - X \frac{du}{d\theta}\right)^2 + u^2 + \frac{2\omega}{h} + \frac{k}{l^2 u^2} \\ = \frac{2u}{l\sqrt{(1+X^2)}} - \frac{2W}{mh^2}. \end{aligned}$$

If the disturbed value of  $u$  is  $u + v$ ,

$$\begin{aligned} \frac{du}{d\theta} \frac{dv}{d\theta} + \left(u \frac{dX}{d\theta} - X \frac{du}{d\theta}\right) \left\{ u \frac{d\xi}{d\theta} - \xi \frac{du}{d\theta} + v \frac{dX}{d\theta} - X \frac{dv}{d\theta} \right\} + uv \\ - \frac{v}{l\sqrt{(1+X^2)}} + \frac{uX\xi}{l(1+X^2)^{3/2}} = - \frac{\dot{k}}{2l^4 u^2}. \end{aligned}$$

In this we may now transform to  $\phi$  with  $\frac{d\theta}{d\phi} = \frac{\cos a}{Y}$ . Now in general,

$$\begin{aligned} W \left( U \frac{dV}{d\phi} - V \frac{dU}{d\phi} \right) \\ = U \sqrt{W} \frac{d}{d\phi} (V \sqrt{W}) - V \sqrt{W} \frac{d}{d\phi} (U \sqrt{W}), \end{aligned}$$

whence, dashed letters denoting the corresponding letters  $\times \sqrt{Y}$ ,

$$\begin{aligned} \frac{du}{d\phi} \frac{dv}{d\phi} \frac{Y^2}{\cos^2 a} + \frac{1}{\cos^2 a} \left( u' \frac{dX'}{d\phi} - X' \frac{du'}{d\phi} \right) \\ \left( u' \frac{d\xi'}{d\phi} - \xi' \frac{du'}{d\phi} + v' \frac{dX'}{d\phi} - X' \frac{dv'}{d\phi} \right) \\ + uv - \frac{v'}{l} = - \frac{u' X' \xi'}{l} - \frac{k}{2l^4 u^2}. \end{aligned}$$

Now,

$$X' = X \sqrt{Y} = \sin a \sin \phi; \quad \frac{1}{1+X^2} = Y;$$

$$lu \sqrt{Y} = (1 + e \cos \chi) \cos^2 a;$$

∴ multiplying by  $l^2$ ,

$$\begin{aligned}
 l^2 \frac{du}{d\phi} \frac{dv}{d\phi} \frac{Y^2}{\cos^2 a} + \sin^2 a (D \cos \phi + e \sin \phi \sin \chi) \\
 \left( v' \cos \phi - \sin \phi \frac{dv'}{d\phi} \right) + l^2 uv - lv' \\
 = -\sin a \cos^2 a (D \cos \phi + e \sin \phi \sin \chi) \left( D \frac{d\xi'}{d\phi} + e \sin \chi \xi' \right) \\
 - \sin a \cos^2 a D \sin \phi \xi' - \frac{k}{2l^2 u^2}.
 \end{aligned}$$

Now,

$$\sqrt{Y} \frac{dv}{d\phi} = \frac{dv'}{d\phi} + \frac{\sin^2 a \sin \phi \cos \phi}{Y} v'.$$

The coefficient of  $l \frac{dv'}{d\phi}$

$$\begin{aligned}
 &= -eY \sin \chi + D \sin^2 a \sin \phi \cos \phi - \sin^2 a D \sin \phi \cos \phi \\
 &\quad - e^2 \sin^2 a \sin^2 \phi \sin \chi \\
 &= -e \sin \chi (1 - \sin^2 a \sin^2 \phi) - e \sin^2 a \sin^2 \phi \sin \chi \\
 &= -e \sin \chi;
 \end{aligned}$$

coefficient of  $lv'$

$$\begin{aligned}
 &= \frac{\sin^2 a \sin \phi \cos \phi}{Y} (-eY \sin \chi + D \sin^2 a \sin \phi \cos \phi) \\
 &\quad + D \sin^2 a \cos^2 \phi + e \sin^2 a \sin \phi \cos \phi \sin \chi + \frac{D \cos^2 a}{Y} - 1 \\
 &= D \sin^2 a \left( \frac{\sin^2 a \sin^2 \phi \cos^2 \phi}{Y} + \cos^2 \phi \right) + \frac{D \cos^2 a}{Y} - 1 \\
 &= D \frac{\sin^2 a \cos^2 \phi}{Y} + \frac{D \cos^2 a}{Y} - 1 = D - 1 = e \cos \chi.
 \end{aligned}$$

Hence the left-hand side of the equation is

$$-e \sin \chi \frac{d}{d\chi} (lv \sqrt{Y}) + e \cos \chi (lv \sqrt{Y}) = -e \sin^2 \chi \frac{d}{d\chi} \frac{lv \sqrt{Y}}{\sin \chi}.$$

The right-hand side :

$$\begin{aligned}
 &= -\lambda \cos^2 a \frac{Y}{2D^2} - \lambda \sin^2 a \cos^2 a \times \\
 &\quad \left\{ (\cos \phi + e \cos c) \left( D \frac{d\xi}{d\chi} + e \xi \sin \chi \right) + D \sin \phi \cdot \xi \right\}.
 \end{aligned}$$

Hence

$$\begin{aligned}
& \frac{e \sin^2 \chi}{\lambda \sin^2 a \cos^2 a} \frac{d}{d\chi} (lv \sqrt{Y}) \\
&= \frac{Y}{2D^2 \sin^2 a} + (\cos \phi + e \cos c + e \cos \phi \cos \chi + e^2 \cos c \cos \chi) \frac{d\zeta}{d\chi} \\
&\quad + \{e \sin \chi (\cos \phi + e \cos c) + \sin \phi (1 + e \cos \chi)\} \zeta \\
&= \frac{Y}{2D^2 \sin^2 a} + \cos \phi \frac{d\zeta}{d\phi} + \zeta \sin \phi \\
&\quad + e (2 \cos \phi \cos \chi + \sin \phi \sin \chi + e \cos c \cos \chi) \frac{d\zeta}{d\chi} \\
&\quad + e (2 \sin \phi \cos \chi + \sin c + e \cos c \sin \chi) \zeta \\
&= \frac{Y}{2D^2 \sin^2 a} + (1 + 2e \cos \chi) \left( \cos \phi \frac{d\zeta}{d\chi} + \zeta \sin \phi \right) \\
&\quad + e^2 \cos c \left( \cos \chi \frac{d\zeta}{d\chi} + \zeta \sin \chi \right) \\
&\quad + e \left( \sin \chi \frac{d}{d\chi} - \cos \chi \right) (\zeta \sin \phi).
\end{aligned}$$

Since

$\sin \chi \frac{d}{d\chi} - \cos \chi$  on  $\sin \phi$ ;  $\cos \phi$  produce  $\sin c$ ;  $-\cos c$

$\cos \chi \frac{d}{d\chi} + \sin \chi$  on „ „ „ „  $\cos c$ ;  $\sin c$

and (8, 9)

$$\cos \phi \frac{d\zeta}{d\chi} + \zeta \sin \phi = P, \quad \zeta = P \sin \phi - Q \cos \phi,$$

$$\cos \chi \frac{d\zeta}{d\chi} + \zeta \sin \chi$$

$$= \cos \chi \left( \sin \phi \frac{\sin \phi \cos \phi}{D^4} - \cos \phi \frac{\sin^2 \phi}{D^4} \right) + P \cos c - Q \sin c$$

$$= \int \frac{\sin \phi \cos \chi}{D^4} d\chi = P_1 \text{ (say);}$$

$$\therefore \frac{e \sin^2 \chi}{\lambda \sin^2 a \cos^2 a} \frac{d}{d\chi} \left( \frac{lv \sqrt{Y}}{\sin \chi} \right)$$

$$\begin{aligned}
&= e \sin^2 \chi \frac{d}{d\chi} \left( \frac{\zeta \sin \phi}{\sin \chi} \right) + \frac{Y}{2D^2 \sin^2 a} \\
&\quad + (1 + 2e \cos \chi) P + e^2 \cos c P_1.
\end{aligned}$$

Divide by  $\sin^2 \chi$  and integrate

$$\begin{aligned} & \frac{e}{\lambda \sin^2 a \cos^2 a} \frac{lv \sqrt{Y}}{\sin \chi} \\ &= \frac{e \zeta \sin \phi}{\sin \chi} - \left( \frac{Y}{2D^2 \sin^2 a} + P + e^2 \cos c P_1 \right) \cot \chi - 2eP \operatorname{cosec} \chi \\ &+ \frac{1}{2 \sin^2 a} \int \cot \chi \frac{d}{d\chi} \left( \frac{Y}{D^2} \right) d\chi \\ &+ \int \left\{ (\sin \phi \cos \phi + e^2 \cos c \sin \phi \cos \chi) \cos \chi \right. \\ &\quad \left. + 2e \sin \phi \cos \phi \right\} \frac{d\chi}{D^4 \sin \chi}. \end{aligned}$$

Now

$$\begin{aligned} & \int \cot \chi \frac{d}{d\chi} \left( \frac{Y}{D^2} \right) d\chi \\ &= \int \cot \chi \left( 2e \sin \chi \frac{Y}{D^3} - \frac{2 \sin^2 a \sin \phi \cos \phi}{D^2} \right) d\chi; \\ \therefore & \frac{elv \sqrt{Y}}{\lambda \sin^2 a \cos^2 a} \\ &= e \zeta \sin \phi - 2eP - \left( \frac{Y}{2D^2 \sin^2 a} + P + e^2 \cos c P_1 \right) \cos \chi \\ &+ \frac{e \sin \chi}{\sin^2 a} \left\{ \frac{Y \cos \chi}{D^3} d\chi + \sin \chi \int \frac{d\chi}{D^4 \sin \chi} \times \right. \\ &\quad \left[ -D^2 \cos \chi \sin \phi \cos \phi + \sin \phi \cos \phi \cos \chi \right. \\ &\quad \left. \left. + e^2 \cos c \sin \phi \cos^2 \chi + 2e \sin \phi \cos \phi \right] \right\}. \end{aligned}$$

Substituting  $D = 1 + e \cos \chi$  in the expression in [ ], gives

$$\begin{aligned} & 2e \sin \phi \cos \phi (1 - \cos^2 \chi) + e^2 \sin \phi \cos^2 \chi (\cos c - \cos \phi \cos \chi) \\ &= e \sin \chi (2 \sin \phi \cos \phi \sin \chi + e \sin^2 \phi \cos^2 \chi); \end{aligned}$$

$$\begin{aligned} & \frac{elv \sqrt{Y}}{\lambda \sin^2 a \cos^2 a} \\ &= e \zeta \sin \phi - 2eP - \left( \frac{Y}{2D^2 \sin^2 a} + P + e^2 \cos c P_1 \right) \cos \chi \\ &+ \frac{e \sin \chi}{\sin^2 a} \int \frac{\cos \chi}{D^3} d\chi \\ &+ e \sin \chi \int \left\{ -(1 + e \cos \chi) \sin^2 \phi \cos \chi \right. \\ &\quad \left. + 2 \sin \phi \cos \phi \sin \chi + e \sin^2 \phi \cos^2 \chi \right\} \frac{d\chi}{D^4} \\ &= \dots + e \sin \chi \int (\sin \phi \sin c + \sin \phi \cos \phi \sin \chi) \frac{d\chi}{D^4}. \quad (14). \end{aligned}$$

It is now necessary to express  $v$  in terms of the variations of the orbital constants. To do this we must use equation (6), which gives  $u$  in terms of  $\theta$ , viz. :

$$\begin{aligned}
 lu &= \cos^2 a \left\{ \sqrt{(1+X^2)} + e \left( \cos c \cos(\theta-b) - \frac{\sin c}{\cos a} \sin(\theta-b) \right) \right\}; \\
 \therefore lv &= \cos^2 a \left\{ -\frac{2D}{\sqrt{Y}} \tan a - e \frac{\sin a}{\cos^2 a} \sin c \sin(\theta-b) \right\} \alpha \\
 &\quad + \cos^2 a \left\{ \frac{X\xi}{\sqrt{(1+X^2)}} + \frac{\eta \cos \chi}{\sqrt{Y}} \right\} \\
 &\quad + \cos^2 a \left[ -e \left\{ \sin c \cos(\theta-b) + \frac{\cos c}{\cos a} \sin(\theta-b) \right\} \gamma \right. \\
 &\quad \left. + e \left\{ \cos c \sin(\theta-b) + \frac{\sin c}{\cos a} \cos(\theta-b) \right\} \beta \right].
 \end{aligned}$$

Transforming to  $\phi, \chi$

$$\begin{aligned}
 \frac{lv \sqrt{Y}}{\cos^2 a} &= \lambda \sin^2 a \sin \phi \cdot \xi - e \sin \chi \cdot \gamma \\
 &\quad + \eta \cos \chi + (-2D) - e \sin c \sin \phi \tan a \cdot \alpha \\
 &\quad + e \left( \cos c \cos a \sin \phi + \frac{\sin c}{\cos a} \cos \phi \right) \beta.
 \end{aligned}$$

Now

$$\alpha = \lambda \sin a \cos a \cdot P, \quad \beta = \lambda \cos a \cdot Q,$$

$$e\eta = -\frac{\lambda Y}{2D^2} - \lambda(1-e^2) \sin^2 a \cdot P \quad (\text{from 13}).$$

Hence

$$\begin{aligned}
 &\frac{elv \sqrt{Y}}{\lambda \sin^2 a \cos^2 a} \\
 &= -\frac{e^2 \sin \chi}{\lambda \sin^2 a} \gamma + e \xi \sin \phi - \frac{Y \cos \chi}{2D^2 \sin^2 a} - (1-e^2) P \cos \chi \\
 &\quad + e(-2D - e \sin c \sin \phi) P + e^2 \left( \frac{\sin \chi}{\sin^2 a} - \cos c \sin \phi \right) Q \\
 &= -\frac{e^2 \sin \chi}{\lambda \sin^2 a} \gamma + e \xi \sin \phi - \frac{Y \cos \chi}{2D^2 \sin^2 a} - 2eP \\
 &\quad + \{ -P + (-P \cos^2 c + Q \sin c \cos c) e^2 \} \cos \chi \\
 &\quad + e^2 \sin \chi \left\{ \frac{Q}{\sin^2 a} - P \sin c \cos c - Q \cos^2 c \right\}.
 \end{aligned}$$

Combining this with the former value for  $lv\sqrt{Y}$ , all the terms, except those in  $\sin \chi$ , cut out, since

$$-P \cos^2 c + Q \sin c \cos c = -P_1 \cos c,$$

and there results

$$\begin{aligned} \frac{e^2 \gamma}{\lambda \sin^2 a} &= e^2 \frac{Q}{\sin^2 a} - e^2 \cos c \int \frac{\sin \phi \sin \chi}{D^4} d\chi - \frac{e}{\sin^2 a} \int \frac{\cos \chi}{D^3} d\chi \\ &\quad - e \int (\sin \phi \sin c + \sin \phi \cos \phi \sin \chi) \frac{d\chi}{D^4}. \end{aligned}$$

As we require only the definite integral  $\chi_0$  to  $\chi_0 + 2\pi$ , odd powers of  $\sin \chi$  disappear and

$$\begin{aligned} \frac{e}{\lambda \sin^2 a} \gamma &= -\frac{1}{\sin^2 a} \int \frac{\cos \chi}{D^3} d\chi \\ &\quad + \frac{e}{\sin^2 a} \int \frac{\cos^2 c - \cos 2c \cos^2 \chi}{D^4} d\chi \\ &\quad - e \cos^2 c \int \frac{1 - \cos^2 \chi}{D^4} d\chi \\ &\quad + \sin^2 c \int \frac{\cos \chi}{D^4} d\chi - \cos 2c \int \frac{\cos \chi - \cos^3 \chi}{D^4} d\chi, \end{aligned}$$

whence

$$\begin{aligned} \frac{e}{\lambda \sin^2 a} \gamma &= \frac{1}{\sin^2 a} \left\{ \frac{1}{2} \Delta I_2 + e \cos^2 c I_4 - \frac{1}{6} e \cos 2c \Delta^2 I_2 \right\} \\ &\quad - e \cos^2 c \left\{ I_4 - \frac{1}{6} \Delta^2 I_2 \right\} - \frac{1}{3} \sin^2 c \Delta I_3 + \cos 2c \left\{ \frac{1}{3} \Delta I_3 - \frac{1}{6} \Delta^3 I_1 \right\}. \end{aligned}$$

Substituting the values of  $I$  from (11), it will be found that

$$\begin{aligned} \frac{e}{\lambda \sin^2 a} \gamma &= \frac{\pi e}{\sin^2 a} \{ 4Z^5 + 5(Z^7 - Z^5) \sin^2 c \} - 5\pi e Z^7 \sin^2 c, \\ \gamma &= \pi \lambda Z^5 \{ 4 + 5(Z^2 - 1) \sin^2 c - 5 \sin^2 a \sin^2 c Z^2 \} \\ &= \frac{\pi k}{\cos a} C^5 \{ 4 + 5(C^2 \cos^4 a - 1) \sin^2 c \}. \quad (15) \end{aligned}$$

Here  $\gamma$  gives the change of perihelion from the nodal line. It is therefore composite and measures the combined effect of the change of perihelion in space and the effect of the motion of the nodal line. In fig. 2 let the two successive orbital planes cut the sphere of reference in  $PN_1A_1$ ,  $PN_2A_2$ ,  $P$  denoting the projection of the particle at any instant.



The above equations give the change in  $a, b, c$ , whilst the particle makes one complete revolution in its orbit, say their annual variation. If  $2a$  denote the major axis of an ellipse, the period is

$$\frac{2\pi}{\sqrt{p}} a^{3/2} = \frac{2\pi}{\sqrt{p}} \left( \frac{l'}{1-e^2} \right)^{3/2} = \frac{2\pi l'^{3/2}}{\sqrt{p}} \{ (1-e^2) \cos^2 a \}^{-3/2} = \frac{2\pi l'^2}{h} C^3.$$

It is thus constant throughout the secular changes. The  $da, \dots$  are produced in this time. The final effect is the same as if these values are produced by continuous change during a period.

Now

$$\pi k C^5 l' \left( \frac{2\pi l'^2}{h} C^3 \right) = \frac{khC^2}{2l'^2} = \frac{1}{2} \omega^2 \frac{l'^2}{h} C^2 = \frac{1}{2} \omega \sqrt{k} C^2.$$

Hence we may write :

$$\left. \begin{aligned} \frac{da}{dt} &= -\frac{5}{4} \omega \sqrt{k} C^2 \sin a (C^2 \cos^2 a - 1) \sin 2c, \\ \frac{db}{dt} &= \frac{1}{2} \omega \sqrt{k} C^2 \{ 1 + 5(C^2 \cos^2 a - 1) \sin^2 c \}, \\ \frac{dc}{dt} &= \frac{1}{2} \omega \sqrt{k} \frac{C^2}{\cos a} \{ 4 + 5(C^2 \cos^4 a - 1) \sin^2 c \}, \end{aligned} \right\} \quad (17)$$

with  $\frac{da}{dc} = -\frac{5}{2} \frac{\sin a \cos a (C^2 \cos^2 a - 1) \sin 2c}{4 + 5(C^2 \cos^4 a - 1) \sin^2 c}.$

If  $\cos a = y$ ,  $\sin^2 c = x$ , the last may be written :

$$\frac{dy}{dx} = \frac{y(1-y^2)(C^2 y^2 - 1)}{4 + 5(C^2 y^4 - 1)x}.$$

These formulæ are valid for all the motions possible, except that they become nugatory when the orbital plane tends to become perpendicular to the plane of  $xy$ , for in this case the  $k$  tend to zero. The reason is that the constant areal rate  $h$  becomes zero and the actual orbits indeterminate. In fact,  $k = l'^4 \omega^2 / h$ , where  $l = l' \cos a$ ,  $h = h' \cos a$ ,  $l'$ ,  $h'$  being the values of  $l, h$  in the actual orbit. Hence  $k$  becomes

$l'^4 \omega^2 \cos^6 a / h'^2$ , which tends to zero as  $a \rightarrow \frac{\pi}{2}$ . But at the

same time  $C^5 \cos^5 a = (1-e^2)^{-5/4}$ . Hence, in the expressions for  $da, db, dc$ ,  $kC^5$  must be replaced by  $k' \cos a$ , where  $k' = l'^4 \omega^2 / h'^2$ , so that as the plane approaches parallelism to  $H$ ,  $a, b$  tend to become constant, i.e. the plane fixed,



as it clearly should be, since the disturbing force  $-\omega^2\rho$  lies in the plane, whilst the apse regression is given by

$$dc = \frac{\pi k'}{(1-e^2)^{5/2}}(4-5\sin^2 c). \quad . \quad . \quad (18)$$

This has also been verified by direct calculation.

The first conclusion we draw from the equations (16) is that, if ever  $\sin a=0$ ,  $\cos a=0$ , or  $C^2\cos^2 a-1=0$ , they maintain these values. For, writing  $da/dt=f(a)$ .  $F$ , where  $f=0$  has roots  $a_1, a_2 \dots$  and  $F$  and its differentials are finite,

$$\frac{da}{dt} = 0 \text{ for } a=a_1, \text{ or } a_2 \dots,$$

$$\frac{d^2a}{dt^2} = f(a) \frac{dF}{dt} + \frac{df}{dt} \frac{da}{dt} = 0 \text{ for } a=a_1 \text{ or } a_2 \dots,$$

and so on.

Thus  $(d/dt)^na=0$  for any root value. Consequently, if  $a=a_1$  or  $a_2 \dots$  at any instant, it will always retain that value. Here we have the three cases: A,  $\cos a=0$ ; B,  $\sin a=0$ ; C,  $C^2\cos^2 a-1=0$ .

A. This corresponds to a plane parallel to H. The motion of the apsides is given by equation (18). If  $c_0$  is the least value of  $\sin^{-1}\sqrt{8}$ ,  $dc=0$  when  $c=c_0, \pi-c_0, \pi+c_0, 2\pi-c_0$ . If initially  $c < c_0$ ,  $dc$  is positive and  $c$  grows asymptotically to  $c_0$ . If initially  $c > c_0$ ,  $dc$  is negative and  $c$  decreases back to  $c_0$ . Thus  $c_0$  is a stable position for the apsidal line. On the other hand,  $\pi-c_0$  is an unstable position, for if  $c$  is less,  $dc$  is negative, etc.; but  $\pi+c_0$  is again a stable position, giving the same apsidal position as  $c_0$ , but perihelion and aphelion reversed. The stable position is that in which the ellipse is tilted in the direction of the orbital motion. During a revolution the apsidal line makes small oscillations about this stable position.

B. Plane perpendicular to H. Here

$$\frac{da}{dt} = 0, \quad \frac{db}{dt} = \frac{1}{2}\omega\sqrt{kC^2}\left(1 + \frac{5e^2}{1-e^2}\sin^2 c\right),$$

$$\frac{dc}{dt} = \frac{1}{2}\omega\sqrt{kC^2}\left(4 + \frac{5e^2}{1-e^2}\sin^2 c\right).$$

These hold quite close up to the limit  $a=0$ , but when  $a=0$  they give the changes expressed in terms of a moving axis,

viz. an imaginary nodal line, without anything to show its relation to the motions in the plane. To express in terms of a fixed axis, recourse must be had to equation (16), which gives

$$\frac{db}{dt} = 0, \quad dc = 3\pi k C^5 \quad \text{or} \quad \frac{dc}{dt} = \frac{3}{2} \omega \sqrt{k} \frac{1}{1-e^2}.$$

This has been verified by direct calculation for this case.

C.  $C^2 \cos^2 a - 1 = 0$  corresponds to  $1/(1-e^2) = 1$  or  $e = 0$ , i. e. to a circular orbit. This gives the important result that, for every circular orbit, the inclination remains unchanged by secular variations. But the nodal line progresses at a constant rate  $= \frac{1}{2} \omega \sqrt{k} / \cos^2 a$ , or an annual rate  $\pi k / \cos^5 a$ . In other words, the Larmor regression  $\omega$  is decreased by this small amount. Also

$$\frac{dc}{dt} = \frac{1}{2} \omega \sqrt{k} \frac{4 - 5 \sin^2 a \sin^2 c}{\cos^3 a},$$

with the apparent paradox of a circle possessing a definite apse. To understand this, it must be remembered that we have been dealing with the complete changes produced after a single revolution in the orbit. If we take account of what goes on during a period, we never get the same instantaneous orbit persisting. It is only at certain instants that the true circle appears, and between these the orbit has been elliptic with its apse moving. The angle through which this has gone in a complete revolution is that given by the above equation. As the particle in a circle is always at an apse, it is to be supposed that the "apse" is at the point where the particle is at the moment of change, and is again in a circle after it has moved through  $2\pi - dc$ . This could be definitely settled by working out the details, but there is no interest in doing so.

Returning now to the consideration of the general case, we shall take a given initial orbit (i. e.  $e_0, a_0, c_0$ ) and trace the subsequent changes. In all cases these changes are symmetric on both sides of the nodal line as also of a line perpendicular to this. We may then confine the discussion to initial configurations between  $c=0$  and  $\frac{1}{2}\pi$ . Since  $C^2 \cos^2 a - 1$  is necessarily positive,  $-da, db$  are positive everywhere, so that within this region ( $\sin 2c$  positive)  $a$  continually decreases, and  $\cos a, b$  continually increase as  $c$  increases from 0 to  $\frac{1}{2}\pi$ .

Consider, first, that category of orbits in which during their secular changes their line of apses coincides at some

instant with the node. The rates of increase of  $a$  vanish at  $c=0$  and  $c=\frac{1}{2}\pi$ , increase up to a maximum at some point which depends on  $a_0$  and  $C$ , and then decrease up to  $c=\frac{1}{2}\pi$ . Starting from an initial value  $a_0$  at the node,  $a$  increases to some final value  $a_1$  at  $c=\frac{1}{2}\pi$ , which, again, is dependent on the  $C$  of the orbit as well as on  $a_0$ . This  $a_1$  will be less than  $\cos^{-1}(1/C^2)$ . This follows because if it ever attained this value it would continue in this state and the orbit remain a circle. Failing the integration of equations (17), the actual value of  $a_1$  cannot be given explicitly, but in any special case it can be determined to any desired degree of accuracy by numerical calculation (see § 8).

The course of the changes in  $c$  is not so simple, since for certain categories of orbits  $dc$  may become negative in certain regions.  $dc$  is necessarily positive at the start, since then  $\sin c$  is too small to make  $dc$  negative. If at the start  $C^2 \cos^4 a > 1$ , it will continue so,  $dc$  must always be positive, and  $c$  continually increase up to  $\frac{1}{2}\pi$ . If, however,  $C^2 \cos^4 a < 1$ ,  $dc$  depends on  $4 - 5(1 - C^2 \cos^4 a) \sin^2 c$ , and whether it ever becomes zero or negative depends on the relative changes in  $a$  and  $c$ . In any case, if  $\sin c$  reaches a value given by

$$5(1 - C^2 \cos^4 a) \sin^2 c = 4,$$

$dc=0$ ,  $\sin c$  is stationary, whilst  $1 - C^2 \cos^4 a$  goes on decreasing, and  $dc$  now again becomes positive. In such cases  $c$  rises to a stationary state at a certain value and then goes on again increasing to  $\frac{1}{2}\pi$ . Thus, for orbits in this category,  $dc$  can never become negative, or the line of apses always regresses.

Nevertheless, we can choose an orbit so that  $dc$  is negative. For this to happen we must have

$$\begin{aligned} C^2 \cos^4 a - 1 &< 0, & \cos^2 a &< 1 - e^2, & \sin a &> e, \\ 5(1 - C^2 \cos^4 a) &> 4, & \sin^2 a &> \cdot 8 + \cdot 2e^2, \\ \sin^2 c &> \frac{4}{5}(1 - C^2 \cos^4 a)^{-1}. \end{aligned}$$

Since  $\cdot 8 + \cdot 2e^2 > e^2$ , the second condition is sufficient as well as necessary. Orbits in this category, therefore, must have large inclinations  $> \sin^{-1} \sqrt{\cdot 8}$  or  $63^\circ 26' 6''$ . Also,  $\sin c$  cannot be  $< \sqrt{\cdot 8}$ , or  $c$  must be  $> 63^\circ 26' 6''$ . When these conditions for  $a, c$  are fulfilled,  $\sin c$  decreases, but this cannot continue up to  $\sin c=0$ , for, apart from the constantly increasing  $\cos a$ ,  $\sin^2 c$  at last reaches a point which contravenes the third of the above conditions. After

reaching this,  $dc$  again becomes positive,  $\sin^2 c$  now increases and is enabled to increase to 1 on account of the simultaneous increase of  $\cos a$ , which keeps  $dc$  positive. This is clear, since the longer  $\sin c$  exists, the larger becomes  $\cos a$  until  $C^2 \cos^4 a - 1 > 0$ , after which  $dc$  is necessarily positive. The point where  $\sin^2 c$  reaches its smallest value is given by  $dc=0$ , or

$$\sin^2 c_0 = \frac{4}{5} \frac{1-e^2}{\sin^2 a - e^2}.$$

In other words, if we choose as our initial configuration an orbit of eccentricity  $e$ , with inclination  $a > a_0$ , where  $\sin^2 a_0 = .8 + .2e^2$ , and with its axis at an angle given by the above value for  $\sin^2 c_0$ , the apses will move from  $c_0$  to  $\pi - c_0$ , and will never coincide with a nodal line.

The question arises: How did the orbit arrive at the configuration in question? To see this we trace back. Here  $\cos a$  decreases,  $dc$  is to be treated as positive, until at last  $\sin c$  becomes unity. In other words, we must start with the line of apses perpendicular to the nodal line, and the configuration of such a nature that  $dc$  is negative. This will be a position of maximum inclination with the apses progressing at their maximum rate. They reach a position  $c_0$  and then regrede, the inclination still decreasing and reaching its minimum when the apses are again perpendicular to the nodal line.

There are thus two categories of secular variations, distinguished as follows:—

I. The line of apses continually regredes, at a maximum rate, when they are perpendicular to the nodal line; the orbital planes swing up and down with the maximum inclination when the apses coincide with the nodal line and the minimum when perpendicular. The nodal line constantly progresses.

II. The line of apses oscillates about the line perpendicular to the nodal line; the orbital planes swing up and down with their maximum and minimum inclinations, both at instants when the apses are perpendicular to the nodal. The greatest inclination occurs when the apses are swinging from left to right in the diagram, *i. e.* when they are swinging in the same direction as that of the particle in its orbit. Again the nodal line constantly progresses.

The transition state between these two categories occurs

## 822 *Changes in Electronic Orbits in a Magnetic Field.*

for  $e=0$ . The orbit is then circular and inclined at the angle  $63^\circ 26' 6''$ .

8. The period of these secular variations will clearly be of the order of magnitude of the  $(\frac{1}{2}\omega\sqrt{kC^2})^{-1}$  of equation (16), say  $1/q$  of this. Thus the number of cycles per sec. =  $\frac{1}{2}q\omega\sqrt{kC^2}$ . Here

$$\sqrt{k} = \frac{\omega l^2}{h} = \frac{HE}{2mc} \times \frac{\sqrt{m}}{E} l^{3/2} = \frac{H}{2c\sqrt{m}} l^{3/2}.$$

$$\text{The electron year} = \frac{2\pi}{\sqrt{p}} a^{3/2} = 2\pi \frac{\sqrt{m}}{E} a^{3/2}.$$

These results may be expressed thus, with  $H=30000x$  gauss :—

$$\text{Electron years per sec.} \dots\dots\dots = 2.52 \times 10^8 a^{-3/2}$$

$$\text{Larmor cycles per year} \dots\dots\dots = 1.66x \times 10^7 a^{3/2}$$

$$\text{Sæcular cycles per Larmor} \dots\dots = 2.62 q C^2 x \times 10^8 l^{3/2}$$

$$,, \quad ,, \quad ,, \text{ electron year} = 4.35 q C^2 x^2 \times 10^{15} a^{3/2} l^{3/2}$$

As  $l=a(1-e^2)$ ,  $l, a$  are of the same order.

We are now in a position to make some estimate of the orders of magnitude of  $H$  and of “ $a$ ” below which we may treat their effects as small, *i. e.* for which we may neglect the effect of  $H^3$  and higher orders. Taking, as examples, the two cases of orbits of order  $10^{-8}$  and  $10^{-6}$ , we get the following table :—

	$10^{-8}$ .	$10^{-6}$ .
Electron years per sec. ....	$2.52 \times 10^{15}$	$2.52 \times 10^{12}$
Larmor cycles per year ....	$1.66x \times 10^{-8}$	$1.66x \times 10^{-2}$
Sæcular cycles per Larmor ...	$2.62 Ax \times 10^{-4}$	$2.62 Ax \times 10^{-1}$
,, ,, per year .....	$4.35 Ax^2 \times 10^{-9}$	$4.35 Ax^2 \times 10^{-3}$

Here  $A$  denotes  $qC^2$ , and  $H=30000x$  gauss. The sæcular change for the  $10^{-8}$  cm. orbit, or  $360^\circ$  per 1000 years, can certainly not be regarded as small. That for  $10^{-6}$  is well within this limit.

To illustrate the foregoing analysis, a numerical computation has been carried out for one example from each category. The inclinations and apsidal regressions have been calculated from equations (17) by steps of  $\frac{1}{2}\omega\sqrt{kC^2}t$  at successive

intervals = .1. The cases chosen are :

Cat. I.  $a = 45^\circ$  ;  $e = \sin 45^\circ$  when apse and node coincide.

„ II.  $a = 70^\circ$  ;  $e = \sin 32^\circ 26' = .5363$  ;  $c = 78^\circ 8'$  for stationary position.

These require  $C^2=4$  for I. and  $C^2=12$  for II. The results are :

- I. The orbital plane swings from  $45^\circ$  to  $25^\circ 55'$  in  $1.08/(\frac{2}{3}\omega\sqrt{kC^2}) = .108/(\omega\sqrt{k})$  seconds, whilst the apsidal line moves through  $90^\circ$ . Hence a complete cycle of one revolution of apse and two of the inclination takes place in  $.43/(\omega\sqrt{k})$  secs.
- II. The plane swings from  $72^\circ 15'$  through  $70^\circ$  to  $64^\circ 4'$  and the apsidal line has oscillated from  $90^\circ$  to  $78^\circ 8'$  and back to  $90^\circ$  in  $2.17/(\frac{2}{3}\omega\sqrt{kC^2}) = 11.9/(\omega\sqrt{k})$  sec. A complete cycle is twice this. The times from  $90^\circ$  to  $78^\circ 8'$  and back to  $90^\circ$  are in the ratio .98 : 1.19 , say 5 : 6.

The numerical values for  $10^{-8}$  and  $10^{-6}$  are :

	I.		II.	
	$10^{-8}$ .	$10^{-6}$ .	$10^{-8}$ .	$10^{-6}$ .
Secular per Larmor	$2.4x \times 10^{-4}$	$2.4x \times 10^{-1}$	$7.22x \times 10^{-4}$	$7.22x \times 10^{-1}$
„ „ year ...	$4x^2 \times 10^{-9}$	$4x^2 \times 10^{-3}$	$1.19x^2 \times 10^{-9}$	$1.19x^2 \times 10^{-2}$

**LXXXIV.** *On the characteristic Infra-Red Vibrations of certain Crystals of the Rock-Salt Type.* By L. G. CARPENTER, B.A., B.Sc., Lecturer in Physics, and L. G. STOODLEY, B.Sc., Research Student in Physics, University College, Southampton\*.

#### *Introduction.*

**I**N a recent series of papers† in the Proceedings of the Royal Society, J. E. Lennard-Jones has shown how the

\* Communicated by the Authors.

† Proc. Roy. Soc. A, cvi. pp. 441, 463, 709 (1924) ; A, cvii. pp. 157, 636 (1925) ; A, cix. pp. 476, 584 (1925) ; A, cxii. pp. 214, 230 (1926). These papers will be referred to below as Papers I. to IX.

force fields of certain atoms and ions may be deduced from one or more of the following data :—

1. The variation of viscosity of gases with temperature.
2. The equation of state of gases.
3. X-Ray measurements of interatomic distances in crystals.
4. Certain measurements of ionic refractivities by Wasastjerna.
5. The compressibility of certain crystals.

Lennard-Jones has classified the forces which occur between ions whose electronic structure is similar to that of the inert gases under four heads\* :—(1) electrostatic forces; (2) van der Waals' attractive forces; (3) intrinsic repulsive forces; and (4) forces due to polarization. In crystals of a high degree of symmetry, such as rock-salt, the polarization forces need not be considered; the van der Waals' attractive forces can also be neglected in comparison with the electrostatic forces. There remain, therefore, the electrostatic forces and the intrinsic repulsive forces. The electrostatic forces are of the inverse square type and depend on the valency of the ions concerned; while the intrinsic repulsive forces are known from the work of Lennard-Jones.

Lennard-Jones proceeds on the assumption that the intrinsic repulsive fields of the atoms and ions with which he deals may be regarded as spherically symmetrical, the field being represented by a formula of the type  $\lambda_n r^{-n}$ . This treatment of atomic and ionic fields on the basis of inverse power laws must be considered as approximate merely, to be replaced by more accurate methods when our knowledge of the disposition and motion of electrons in atoms is more complete †.

Born and Brody ‡ have shown that, for regular diatomic crystals of the rock-salt type, electrostatic cohesive forces, together with other forces, proportional to  $r^{-n}$  suffice for the explanation of expansion phenomena, elastic properties and infra-red frequencies. It is with these last that we are concerned here. Using density and compressibility data Born and Brody obtained values of  $n$  for the crystals dealt with, and calculated the frequencies of the characteristic infra-red vibrations. The values so obtained, when corrected by a method due to Försterling § for the difference

\* Paper IX.

† Paper I. p. 441.

‡ *Zeits. f. Phys.* (11) vi. p. 327 (1922).

§ *Ann. d. Phys.* (4) lxi. p. 577 (1920).

between characteristic frequencies and residual ray frequencies, are in good agreement with the experimental values obtained by Rubens.

It is the object of the present paper to point out that, using the data of Lennard-Jones, characteristic infra-red frequencies of the salts NaCl, KCl, KBr, and KI may be calculated which are in fair agreement with those obtained by Born and Brody from the compressibility and density of crystals. The method of treatment here given is a rough approximation; it will be seen that the agreement with the results of Born and Brody is, except in the case of NaCl, within about 10 per cent. Lennard-Jones has calculated the force constants for argon-like and neon-like\* ions without making use of data derived from the compressibility in the *solid* state. The values obtained in the present paper for the infra-red frequencies of NaCl and KCl are therefore also independent of compressibility measurements on solid crystals, and hence it is of especial interest to compare them with those obtained by Born and Brody.

In the case of xenon-like and krypton-like† ions Lennard-Jones has deduced values  $\lambda_n$  and  $n$  from the interatomic distances and compressibilities of solid crystals, together with the refractivity data of Wasastjerna. The infra-red frequencies of KBr and KI calculated in this paper are, therefore, dependent on these data also.

#### *Method of Treatment.*

We here calculate the frequency of the characteristic infra-red vibrations of NaCl, KCl, KBr, and KI on the following assumptions:—

1. In a crystal the two oppositely charged ionic lattices may be represented as vibrating as wholes relatively to one another.
2. The frequency of this vibration is identical with that of characteristic infra-red vibration of the crystal.
3. The oscillations are of sufficiently small amplitude to be taken as simple harmonic; *i. e.*, the restoring force is proportional to the first power of the displacement.

\* In Paper VI. page 485, he chose the model of Ne by comparison with the observed interatomic distance in NaF. In Paper VIII., however, he showed that the choice of this model was independently confirmed by the fact that it was the one which gave the best concordance between isotherm measurements and measurements of viscosity and thermal conductivity

† Paper VII.



4. The restoring force on an ion in a displaced lattice of one sign depends only on the presence of the 14 nearest ions in the lattice of the opposite sign, the effect of the remaining ions being neglected.

The frequency with which the positive lattice of mass  $M_1$  and the negative lattice of mass  $M_2$  oscillate relatively to each other is easily shown by simple dynamical reasoning to be

$$V = \frac{1}{2\pi} \sqrt{\frac{F_1(M_1 + M_2)}{M_1 M_2}}, \quad \dots \quad (1)$$

where  $F_1$  is the restoring force on one lattice per unit displacement relative to the other.

If there are  $N$  ions of each sign in the lattice, then

$$F_1 = Nf_1, \quad \dots \quad (2)$$

where  $f_1$  is the restoring force per unit displacement on one ion. This is evidently the case, since, by symmetry, all the ions are acted upon by similar forces, so that the total restoring force on the lattice is the arithmetic sum of the forces on individual ions. Similarly,

$$M_1 = Nm_1, \quad \dots \quad (3)$$

$$M_2 = Nm_2, \quad \dots \quad (4)$$

where  $m_1$  and  $m_2$  are the masses of the positive and negative ions respectively.

Hence the frequency of relative vibration of the lattices is

$$V = \frac{1}{2\pi} \sqrt{\frac{f_1(m_1 + m_2)}{m_1 m_2}}, \quad \dots \quad (5)$$

We therefore calculate  $f_1$  taking only the 14 neighbouring ions of opposite sign into account, and substituting in (5) deduce the corresponding frequency. It is convenient first to obtain a general expression for the restoring force per unit displacement on a displaced ion, due to another ion, for an inverse  $p$ th power law, the direction of displacement making any angle  $\theta$  with the line joining the centres of the two ions.

#### *Calculation of Restoring Force for Small Displacements.*

Let  $P$  be an ion at a distance  $e$  from another ion. Let the force between  $P$  and  $Q$  be represented by

$$F = \lambda_p e^{-p}.$$

Then the resolved part of this force in direction  $X'X$  is

$$\frac{\lambda_p}{\epsilon^p} \cos \theta.$$

Let  $P$  be displaced by an amount  $\Delta x$  (small compared with  $\epsilon$ ) in the direction  $X'X$ . Then, the restoring force

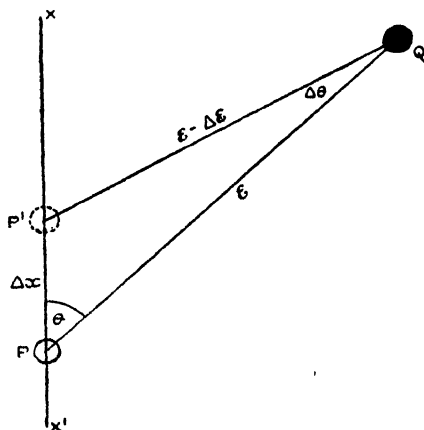
$$= -\Delta F,$$

where  $\Delta F = \frac{d}{dx} \left( \frac{\lambda_p}{\epsilon^p} \cos \theta \right) \Delta x,$

$$= \lambda \left[ \frac{-p d\epsilon}{\epsilon^{p+1} dx} \cos \theta - \frac{1}{\epsilon^p} \sin \theta \frac{d\theta}{dx} \right] \Delta x,$$

$$= \lambda_p \left[ \frac{p}{\epsilon^{p+1}} \cos^2 \theta - \frac{1}{\epsilon^p} \frac{\sin^2 \theta}{\epsilon} \right] \Delta x,$$

Fig. 1.



since  $\frac{\Delta\epsilon}{\Delta x} = -\cos \theta$  and  $\epsilon\Delta\theta = \Delta x \sin \theta,$

$$\therefore \frac{\Delta F}{\Delta x} = \frac{\lambda}{\epsilon^{p+1}} [p \cos^2 \theta - \sin^2 \theta] \dots (6)$$

Let fig. 2 represent the structure of crystals of the rock-salt type, the black and white points representing positive and negative ions respectively. Let  $\epsilon$  be the shortest distance between a positive and a negative ion. Calculate the restoring force per unit displacement of the ion  $P$  along the line  $AB$  parallel to the  $X-X'$  axis.

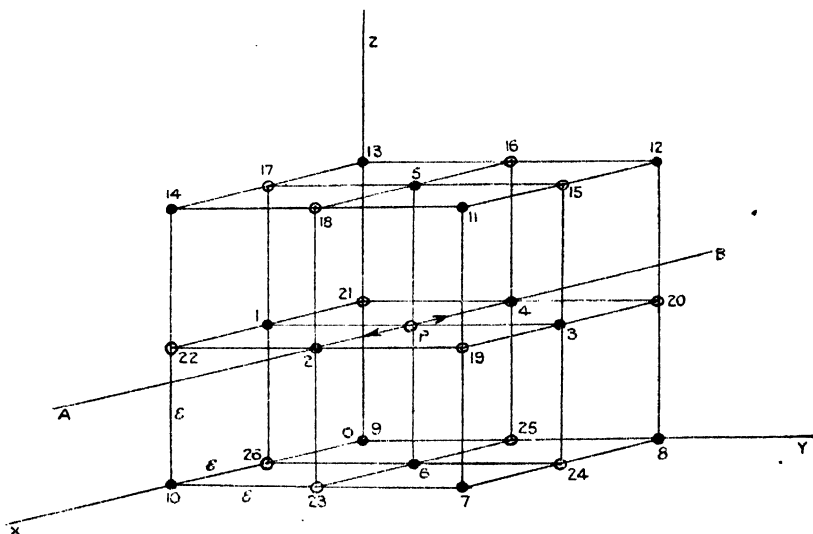
(a) In the case of ions 2 and 4,  $\theta = 0^\circ$  ;

$$\therefore \frac{\Delta F}{\Delta x} = \frac{2\lambda_p}{\epsilon^{p+1}} \cdot p \dots \dots \dots (7)$$

(b) In the case of ions 1, 5, 3, 6,  $\theta = 90^\circ$  ;

$$\therefore \frac{\Delta F}{\Delta x} = -\frac{4\lambda_p}{\epsilon^{p+1}} \dots \dots \dots (8)$$

Fig. 2.



(c) In the case of ions 7-14 consider the effect of ions 7, 8, 13, 14 on P ; (fig. 3),

$$\cos \theta = \frac{1}{\sqrt{3}},$$

$$\sin \theta = \sqrt{\frac{2}{3}},$$

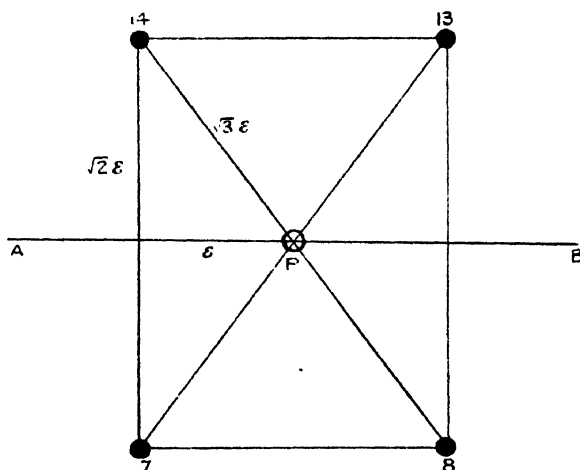
$$\therefore \frac{\Delta F}{\Delta x} = \frac{4\lambda_p}{(\sqrt{3}\epsilon)^{p+1}} \left[ p - \frac{2}{3} \right],$$

$$= \frac{4\lambda_p}{3^{\frac{p+3}{2}} \epsilon^{p+1}} [p-2].$$

The effect of the ions 9, 10, 11, 12 is precisely similar. Hence, for the ions 7-14, the total effect is given by

$$\frac{\Delta F}{\Delta x} = \frac{8\lambda}{3 \frac{r+3}{2} \epsilon^{p+1}} [p-2] \dots \dots \dots (9)$$

Fig. 3.



Hence, the total effect of the 14 nearest ions of one sign on an ion of the opposite sign is given by adding equations (7), (8) and (9), and  $f_1$ , the restoring force per unit displacement is given by

$$f_1 = \frac{2\lambda_p}{\epsilon^{p+1}} [p-2] \left[ 1 + \frac{4}{3 \frac{p+3}{2}} \right] \dots \dots \dots (10)$$

This equation is, of course, strictly true only for vibrations of infinitely small amplitude.

### Numerical Results.

The repulsive force constants ( $\lambda_n$ ), and the indices of the repulsive power law ( $n$ )\* for the four crystals considered,

\* Paper IX.

are given below in Table I., together with values of  $\epsilon$  the shortest distance between a positive and a negative ion as determined by X-ray measurements.

TABLE I.

	$\lambda n.$	$n.$	$\epsilon.$
N Cl .....	$2.12 \times 10^{-80}$	10	$2.814 \times 10^{-8}$
KCl .....	$1.59 \times 10^{-72}$	9	$3.13 \times 10^{-8}$
KBr .....	$1.95 \times 10^{-72}$	9	$3.285 \times 10^{-8}$
KI .....	$1.15 \times 10^{-79}$	10	$3.525 \times 10^{-8}$

From these are calculated, by means of equation (10), the corresponding values of  $f_1$ . It will be noticed that in equation (10),  $f_1$  vanishes when  $p=2$ . Hence, the contribution of the inverse square electrostatic attraction to the restoring force per unit displacement is zero within the body of the crystal. The charge on the ions affects the frequency through the effect on  $\epsilon$ .

The value of  $\frac{m_1 m_2}{m_1 + m_2}$  is calculated, taking the mass of the hydrogen atom as  $1.66 \times 10^{-24}$  gram. Substituting in equation (5), we obtain the frequency of the characteristic infra-red vibrations: the results are given in Table II.

TABLE II.

	$f_1.$	$\frac{m_1 m_2}{m_1 + m_2}$	$\nu.$
NaCl .....	$3.88 \times 10^4$	$2.30 \times 10^{-23}$	$6.54 \times 10^{12}$
KCl .....	$2.47 \times 10^4$	$3.06 \times 10^{-23}$	$4.52 \times 10^{12}$
KBr .....	$1.87 \times 10^4$	$4.32 \times 10^{-23}$	$3.32 \times 10^{12}$
KI .....	$1.77 \times 10^4$	$4.92 \times 10^{-23}$	$3.02 \times 10^{12}$

Finally, the results, converted to wave-lengths, are compared in Table III. with those of Born and Brody\*; the observations of the residual rays by Rubens are included in the third column.

TABLE III.

	Wave-lengths.		
	Calculated.	Born and Brody.	Residual rays.
NaCl .....	45.9 $\mu$	61.6 $\mu$	52.0 $\mu$
KCl.....	66.4	74.5	63.4
KBr .....	90.5	88.0	82.6
KI .. .....	99.5	108.3	94.1

The agreement with the calculations of Born and Brody is least satisfactory in the case of NaCl, for which the wave-length 45.9  $\mu$  is evidently too low; it is less than the wave-length of the residual rays.

The repulsive force constants determined by Lennard-Jones and used in the calculations of this paper are believed † to be accurate within about 10 per cent. The uncertainty from this cause in the values of the characteristic infra-red wave-lengths here deduced should therefore be about 5 per cent., since these wave-lengths are inversely proportional to the square roots of the force constants.

The wave-lengths of the characteristic infra-red vibrations are seen to differ from those of the residual rays, as indeed they should. The magnitude of the difference theoretically to be expected between the wave-lengths obtained by Born and Brody and those observed by Rubens has been calculated by Försterling ‡, who finds satisfactory agreement with experiment.

In conclusion, our thanks are due to Professor F. A. Lindemann and to Mr. F. G. Maunsell, with whom we have discussed the subject matter of this paper.

*Note added in proof.*—Since the above paper was written,

\* *Loc. cit.*

† Paper IX. p. 234.

‡ *Loc. cit.*

a paper \* by O. Reinkober has come to our notice, in which an experimental value of  $74\mu$  is given for the wave-length of the residual rays of rubidium chloride. Lennard-Jones has given the numerical data representing the repulsive force between a rubidium and a chlorine ion, and the crystal structure of rubidium chloride has been determined and is of the rock-salt type †. It is, therefore, of interest to calculate the wave-length of the fundamental vibration in the manner already described. The result is given in the table below :—

TABLE IV.

$\lambda u.$	$n.$	$c.$	$\rho.$	$\frac{m_1 m_2}{m_1 + m_2}$	Wave-length.	
					Calculated.	Residual Rays.
$2.1 \times 10^{-72}$	9	$3.267 \times 10^{-8}$	$2.13 \times 10^4$	$4.13 \times 10^{-23}$	$82.9 \mu$	$74 \mu$

It is seen that the wave-length of the fundamental vibration is greater than that of the residual rays, as it is in the case of the other crystals considered (except NaCl), and that if the residual ray wave-length be placed in numerical order between KCl and KBr in Table III., then the calculated fundamental wave-length lies between those of the same two salts.

LXXXV. *An Extension of Dulong and Petit's Law to Gaseous Compounds and Mixtures.* By Prof. A. PRESS ‡.

IN deriving the laws pertaining to adiabatic processes (see Phil. Mag., Dec. 1927), the writer deduced the following formulæ which held simultaneously

$$\left. \begin{aligned} p v \gamma &= \text{constant} \\ p v &= (\gamma - 1) \end{aligned} \right\} \dots \dots \dots (15)$$

\* *Zeits. f. Phys.* xxxix. 5-6, p. 437 (1926).

† Bragg, 'X-Rays and Crystal Structure,' 5th ed. p. 306.

‡ Communicated by the Author.

The latter were derived from the relation

$$\gamma = -\frac{v}{p} \cdot \frac{dp}{dv} = 1 + \frac{d(pv)^*}{dU} \quad . \quad . \quad . \quad (12)$$

It is easily checked that the latter amounts to proving that

$$p \cdot dv + dU = 0.$$

The anomalies of Thomson and Joule (see Birtwistle, 'Thermodynamics,' p. 76) have therefore to be accounted for on the basis that the  $\gamma$  components of specific heat varied during the process of the experiment.

Turning, then, to the second of (15), there is clearly a relation indicated with the usual equation of state,

$$pv = R\theta, \quad . \quad . \quad . \quad . \quad . \quad . \quad (8)$$

which, as known, applies rather well to all so-called fixed gases. We should therefore expect to find that, by equating the respective right-hand terms to each other, the following formula should hold, viz. :

$$(\gamma - 1)U = \alpha R\theta.$$

This would indicate at once by differentiating with respect to  $\theta$  that

$$\frac{\partial U}{\partial \theta} = \alpha \frac{R}{\gamma - 1}.$$

On the basis of Avogadro's law it is known that we have

$$R = 2 \text{ calories per gram-molecule.}$$

If, then, we substitute with  $M$  = molecular weight, as follows :

$$R = \frac{2}{M},$$

$$\left(\frac{\partial U}{\partial \theta}\right)_p = \text{specific heat} = s,$$

then it results that

$$2\alpha = (\gamma - 1) \cdot s \cdot M.$$

This formula is, of course, very much different from that of Leray, mentioned in Preston's 'Theory of Heat,' p. 295.

\* The error of sign, *i. e.*, should be corrected.



The constancy of the factor  $\alpha$  is indicated by the following tabulation :—

Substance *.	$\gamma$ .	$\gamma - 1$ .	$s$ .	M.	$2\alpha$ calc.
Air .....	1.4	.4	.238	28.8	2.74
Alcohol.....	1.136	.136	.453	46.06	2.84
Ammonia .....	1.31	.31	.523	17	2.78
Bromine .. .....	1.293	.293	.0553	159.9	2.59
CO <sub>2</sub> .....	1.3	.3	.201	44	2.65
CO .....	1.4	.4	.243	28	2.73
OS <sub>2</sub> .....	1.2	.2	.16	76.1	2.43
Chlorine .....	1.32	.323	.1125	71	2.58
Chloroform .....	1.106	.106	.149	119.4	1.89
Ether.....	1.029	.029	.456	74.1	.98
HCl .....	1.395	.395	.194	36.5	2.8
H <sub>2</sub> .....	1.41	.41	.3406	2	2.79
H <sub>2</sub> S .....	1.276	.276	.245	34.1	2.3
Methane .....	1.316	.316	.593	16.03	3.0
Nitrogen .....	1.41	.41	.244	28	2.8
Nitrous Oxide .....	1.291	.291	.221	44	2.82
SO <sub>2</sub> .....	1.26	.26	.7544	64.1	2.57
Steam .....	1.3	.3	.43	18	2.32
Argon .....	1.6	.6	.123	39.9	2.95
Oxygen .....	1.4	.4	.2175	32	2.78
Benzol .....	1.4	.4	.299	78	.936

\* Similarly, it can be shown that, taking provisionally that the specific heat of mercury vapour is .03 and  $\gamma = 1.6$ , we have  $2\alpha = .6 \times 200 \times .03 = 3.6$ .

Thus, the improved form of Dulong and Petit's formula is the following :

$$2\alpha = sM(\gamma - 1),$$

in which, of course, the expression  $2\alpha/(\gamma - 1)$  becomes, for solids,

$$\frac{2\alpha}{\gamma - 1} \equiv 6.4.$$

1314-18th St., N.W.,  
Washington, D.C., U.S.A.  
Dec. 24, 1927.

LXXXVI. *On Relativistic Cosmology.* By H. P. ROBERTSON, *Ph.D., National Research Fellow in Mathematics\**.

THE general theory of relativity considers physical space-time as a four-dimensional manifold whose line element coefficients  $g_{\mu\nu}$  satisfy the differential equations

$$G_{\mu\nu} = \lambda g_{\mu\nu} \quad . \quad . \quad . \quad . \quad . \quad (1)$$

in all regions free from matter and electromagnetic field, where  $G_{\mu\nu}$  is the contracted Riemann-Christoffel tensor associated with the fundamental tensor  $g_{\mu\nu}$ , and  $\lambda$  is the cosmological constant†. An "empty world," i. e. a homogeneous manifold at all points of which equations (1) are satisfied, has, according to the theory, a constant Riemann curvature, and any deviation from this fundamental solution is to be directly attributed to the influence of matter or energy. In considerations involving the nature of the world as a whole the irregularities caused by the aggregation of matter into stars and stellar systems may be ignored; and if we further assume that the total matter in the world has but little effect on its macroscopic properties, we may consider them as being determined by the solution for an empty world‡.

The solution of (1), which represents a homogeneous manifold, may be written in the form :

$$ds^2 = - \frac{d\rho^2}{1 - \kappa^2 \rho^2} - \rho^2 (d\theta^2 + \sin^2 \theta d\phi^2) + (1 - \kappa^2 \rho^2) c^2 d\tau^2, \quad (2)$$

where  $\kappa = \sqrt{\lambda/3}$ . If we consider  $\rho$  as determining distance from the origin (the measured distance being then  $\sin^{-1} \kappa \rho / \kappa$ ) and  $\tau$  as measuring the proper-time of a clock at the origin, we are led to the de Sitter spherical world; the astronomical

\* Communicated by Prof. A. S. Eddington, F.R.S.

† A. Einstein, "Die Grundlage der allgemeinen Relativitätstheorie," *Ann. d. Physik*, xlix. p. 769 (1916); 'Kosmologische Betrachtungen zur allgemeinen Relativitätstheorie,' Berlin, Sitzungsberichte, 1917, p. 142; W. de Sitter, "On Einstein's Theory of Gravitation and its Astronomical Consequences," *Monthly Notices*, R. A. S. lxxvi. p. 699, lxxvii. p. 155, lxxviii. p. 3 (1916-17). The notation here used is that of A. S. Eddington, 'The Mathematical Theory of Relativity,' Cambridge, 1923.

‡ This view, due to de Sitter, is an alternative to one proposed by Einstein in which the existing matter is considered uniformly spread throughout the world. The equations (1) are not applicable in this latter case, as terms involving the density must then be added to the right-hand side.

consequences of this interpretation have been discussed by de Sitter, Eddington and Weyl \*. Important among these is the prediction that the spectral lines in light from distant sources should be displaced toward the red; this would be interpreted as Doppler effect due to a larger motion of recession of the source, and seems to be in accord with the known facts concerning the radial velocities of spiral nebulae. The singularity  $\rho = \frac{1}{\kappa}$  of the line element creates the illusion of a

"mass-horizon" which recedes as we approach it and concerning which we can obtain no direct information, as light emitted from it never reaches us.

It is the purpose of this paper to replace (2) by a mathematically equivalent solution which is susceptible of a perhaps simpler interpretation and in which many of the apparent paradoxes inherent in (2) are eliminated; aside from this, it offers a convenient method of investigating the properties of the de Sitter form. The last paragraph will be devoted to a discussion of the analogous solution for a spherically symmetric mass.

1. *Kinematics*.—If we subject the de Sitter solution (2) to the transformation

$$\rho = re^{\kappa ct}, \quad \tau = t - \frac{1}{2\kappa c} \log(1 - \kappa^2 r^2 e^{2\kappa ct}),$$

we obtain

$$ds^2 = -e^{2\kappa ct}(dx^2 + r^2 d\theta^2 + r^2 \sin^2 \theta d\phi^2) + c^2 dt^2,$$

or, on changing to rectangular coordinates,

$$x = r \sin \theta \cos \phi, \quad y = r \sin \theta \sin \phi, \quad z = r \cos \theta,$$

$$ds^2 = -e^{2\kappa ct}(dx^2 + dy^2 + dz^2) + c^2 dt^2. \quad . \quad . \quad (3)$$

The space-time manifold, which is described in the de Sitter interpretation with the aid of the variable  $\rho$  with finite range  $0 < \rho \leq 1/\kappa$ , is here described with the aid of  $r$  with infinite range, and the singularity  $\rho = 1/\kappa$  is removed from the finite region.

Interpreting  $t$  as the proper-time of a clock at the origin, the distance, measured at time  $t$  with a rigid scale, from the origin to a point whose spacial coordinates are  $(r, \theta, \phi)$  is  $l = re^{\kappa ct}$ . The proper-times of all observers at points  $(r, \theta, \phi)$  = constant coincide with that of an observer at the origin,

\* De Sitter, *l. c.* (third paper); Eddington, *l. c.* chap. v.; H. Weyl, "Zur allgemeinen Relativitätstheorie," *Phys. Zeits.* xxiv. p. 230 (1923).

and such observers will be called *equivalent*. The line element (3) is "dynamical" in that its coefficients depend on the time  $t$ , whereas (2) is not. That the properties of the manifold are, however, independent of  $t$  may be seen by introducing a change of scale and time origin by means of the transformation

$$\bar{r} = re^{\kappa ct_0}, \quad \bar{t} = t - t_0.$$

A perhaps more serious objection is that the world is on this interpretation of infinite extent, but, as will be seen later, its closed character is maintained in the sense that the only events of which we can be aware must occur within a sphere of finite radius. In common with the special relativity world, and in contradistinction to the de Sitter world, the geometry of space is euclidean and the velocity of light is independent of its direction. The properties which distinguish the space-time defined by (3) from that of special relativity are thus to be sought in its kinematics.

The velocity of a point moving along the  $x$ -axis, measured by an observer at the origin, is

$$V_x = (x' + \kappa cx)e^{\kappa ct} = x'e^{\kappa ct} + \kappa cl_x \quad \left(x' = \frac{dx}{dt}\right),$$

the time rate of change of its measured distance  $l_x = xe^{\kappa ct}$ . An equivalent observer at  $x$ , whose coordinate velocity  $x'$  must by definition be zero, will thus have a measured velocity  $\kappa cl_x$  relative to 0, and light travelling along the  $x$ -axis, whose coordinate velocity is by (3)  $\gamma = ce^{-\kappa ct}$ , will have as measured velocity  $c(1 + \kappa l_x)$ . The measured velocity along the  $y$ - and  $z$ -axes may be similarly defined, and, by means of its three components, the motion of an arbitrarily moving point described. We shall usually refer to these quantities simply as distance and velocity, and it is to be remembered that they are measured with respect to some definite observer; the quantities  $x$  and  $x'$  will always be called the coordinate distance (or interval) and coordinate velocity.

2. *Geodesics*.—The geodesics of the manifold defined by (3), in terms of the time  $t$  as parameter, are obtained by minimizing the integral

$$\int_{t_0}^t F(tx'y'z') dt, \quad x' = \frac{dx(t)}{dt}, \text{ etc.,}$$

where

$$F(tx'y'z') = \frac{ds(t)}{dt} = \sqrt{-e^{2\kappa ct}(x'^2 + y'^2 + z'^2) + c^2}.$$

Since  $F$  does not depend on  $x$ , the Euler equation

$$\frac{\partial}{\partial t} \frac{\partial F}{\partial x'} - \frac{\partial F}{\partial x} = 0$$

yields immediately

$$\frac{x' e^{2\kappa ct}}{F(tx'y'z')} = \text{const.},$$

and the corresponding integrals for  $y$  and  $z$  are obtained in the same way. Solving for  $x'$ ,  $y'$ ,  $z'$ , and choosing the constants of integration in such a way that these quantities assume the values  $\delta_x$ ,  $\delta_y$ ,  $\delta_z$  at time  $t = t_0$ , we find

$$\begin{aligned} x' &= \delta \frac{e^{-2\kappa c(t-t_0)}}{\sqrt{1 - \left(\frac{\delta}{\gamma_0}\right)^2 (1 - e^{-2\kappa c(t-t_0)})}} \\ &= \delta_x \frac{\beta_0 e^{-2\kappa c(t-t_0)}}{\sqrt{1 + \left(\frac{\delta\beta_0}{\gamma_0}\right)^2 e^{-2\kappa c(t-t_0)}}}, \text{ etc.}, \quad (4) \end{aligned}$$

where  $\gamma_0 = c e^{-\kappa ct_0}$ , the initial coordinate velocity of light,

$$\delta^2 = \delta_x^2 + \delta_y^2 + \delta_z^2,$$

$$\text{and } \beta_0 = \left(1 - \left(\frac{\delta}{\gamma_0}\right)^2\right)^{-\frac{1}{2}}.$$

The coordinates themselves are, on integrating (4),

$$x - x_0 = \delta_x \frac{\gamma_0}{\kappa \delta^2} e^{\kappa - ct_0} \left(1 - \frac{1}{\beta_0} \sqrt{1 + \left(\frac{\delta\beta_0}{\gamma_0}\right)^2 e^{-2\kappa c(t-t_0)}}\right), \text{ etc.} \quad (5)$$

These are, according to the postulates of the general theory of relativity, the equations of motion of a free particle.

The minimal geodesics, giving the equations of motion of light, are

$$\left. \begin{aligned} x' &= \delta_x e^{-\kappa c(t-t_0)}, & \delta &= \gamma_0, \\ x - x_0 &= \frac{\delta_x}{\kappa \gamma_0} e^{-\kappa ct_0} (1 - e^{-\kappa c(t-t_0)}), \text{ etc.} \end{aligned} \right\} \quad (6)$$

Since

$$\frac{x - x_0}{\delta_x} = \frac{y - y_0}{\delta_y} = \frac{z - z_0}{\delta_z},$$

the motion of a free particle or light is rectilinear in the  $x, y, z$  coordinate space.

A particle, starting from  $(x_0, 0, 0)$  at time  $t=t_0$  with coordinate velocity  $(-\delta, 0, 0)$ , approaches the limiting position defined by

$$x_0 - \frac{\gamma_0}{\delta\kappa} e^{-\kappa\delta t_0} \left(1 - \frac{1}{\beta_0}\right);$$

so, unless the initial measured distance

$$l_0 = x_0 e^{\kappa\delta t_0} < L\left(\frac{\delta}{\gamma_0}\right) = \frac{1}{\kappa} \frac{\gamma_0}{\delta} \left(1 - \sqrt{1 - \left(\frac{\delta}{\gamma_0}\right)^2}\right),$$

it can never reach an observer at the origin. For a beam of light this becomes

$$l_0 < L(1) = \frac{1}{\kappa},$$

and since  $L(\zeta)$  is a monotonic increasing function of  $\zeta$ , it follows that all particles or light which reach an observer at the origin are initially within a sphere of measured radius  $R=1/\kappa$ . Hence the only events concerning which we can obtain any knowledge must occur within this sphere; it constitutes, therefore, our observable universe. According to recent evidence, celestial objects as distant as  $10^{26}$  cm. have been observed, so  $R$  must be greater than this—the interpretation given below of data concerning spiral nebulae indicates that it is of order between  $10^{27}$  and  $10^{28}$  cm. Considerations involving the whence and whither of celestial objects lead to results of a rather paradoxical nature—all matter and light within our observable universe must have started from the boundary and will be eventually lost to it;—but such long-time predictions cannot be taken too literally, as we have neglected their influence on the line element, an influence which undoubtedly plays an important role in such questions.

**3. Representation in Euclidean 5-Space. Transformations of Space-Time.**—Since the manifold defined by (3) has constant Riemann curvature, it must be possible to imbed it in euclidean space of five dimensions. This representation will be of value in finding the transformations relating the measurements of observers in relative motion—the analogue of the Lorentz transformations in special relativity.

We can, in fact, write (3) in the form :

$$ds^2 = -(d\alpha^2 + d\beta^2 + d\gamma^2) + d\zeta^2 - d\eta^2, \quad . \quad . \quad (7)$$

where

$$\left. \begin{aligned} \alpha &= x e^{\kappa \tau t}, & \zeta &= \frac{1}{\kappa} \sinh \kappa c t + \frac{1}{2} \kappa r^2 e^{\kappa \tau t}, \\ \beta &= y e^{\kappa \tau t}, & \eta &= \frac{1}{\kappa} \cosh \kappa c t - \frac{1}{2} \kappa r^2 e^{\kappa \tau t}, \\ \gamma &= z e^{\kappa \tau t}. \end{aligned} \right\} \quad \cdot \quad \cdot \quad (8).$$

The equation of space-time is then

$$\alpha^2 + \beta^2 + \gamma^2 - \zeta^2 + \eta^2 = \frac{1}{\kappa^2}, \quad \cdot \quad \cdot \quad \cdot \quad (9)$$

and it may therefore be considered as a hyper-sphere in the euclidean 5-space (7). A geodesic is the intersection of a (two-dimensional) plane through 0 with this hyper-surface.

Now, any rotation of this 5-space, *i. e.* any transformation under which (7) and (9) are invariant, will generate a transformation of the space-time variables which leaves (3) invariant. To obtain the explicit form of these latter it is only necessary to solve the equations:

$$\left. \begin{aligned} \alpha &= a_{11}\alpha + a_{12}\beta + \dots a_{15}\eta, \\ \bar{\beta} &= a_{21}\alpha + \dots \\ \vdots & \\ \bar{\eta} &= a_{51}\alpha + \dots a_{55}\eta, \end{aligned} \right\} \quad \cdot \quad \cdot \quad \cdot \quad (10)$$

defining the rotation of the 5-space, where  $\alpha, \beta$ , etc. are the functions of  $x, y, z, t$  given by (8), and  $\bar{\alpha}, \bar{\beta}$ , etc. are the same functions of the transformed space-time variables  $\bar{x}, \bar{y}, \bar{z}, t$ . But four of these five equations are independent, as the constants  $a_{ij}$  must be so chosen that

$$\bar{\alpha}^2 + \bar{\beta}^2 + \bar{\gamma}^2 - \bar{\zeta}^2 + \bar{\eta}^2 = \alpha^2 + \beta^2 + \gamma^2 - \zeta^2 + \eta^2,$$

and on substituting (8) this leads to an identity, so we have just enough equations to solve for  $\bar{x}, \bar{y}, \bar{z}, t$  as functions of  $x, y, z, t$ .

In order to effect the complete solution of this problem, we may consider the general transformation (10) as composed of ten elemental rotations, in each of which only the coordinates of one (two-dimensional) plane are involved. Because of the symmetry existing between  $\alpha, \beta, \gamma$ , this number can be reduced to four, say those in the  $(\beta, \gamma), (\zeta, \eta), (\alpha, \eta), (\alpha, \zeta)$  planes; in place of the third, however, it is found simpler to consider a rotation in a certain plane of the  $(\alpha, \zeta, \eta)$  3-space.

The first of these elemental transformations obviously leads to a rotation of the  $y$  and  $z$  axes. The second, which may be written

$$\begin{aligned}\bar{\zeta} &= \cosh \epsilon \zeta - \sinh \epsilon \eta, & \bar{\alpha} &= \alpha, & \bar{\beta} &= \beta, \\ \bar{\eta} &= -\sinh \epsilon \zeta + \cosh \epsilon \eta, & \bar{\gamma} &= \gamma,\end{aligned}$$

to

$$\bar{x} = x e^{\epsilon}, \quad \bar{y} = y e^{\epsilon}, \quad \bar{z} = z e^{\epsilon}, \quad \bar{t} = t - \frac{\epsilon}{\kappa c};$$

i. e., a change of time origin, with corresponding change of scale. The third rotation, defined by

$$\bar{\alpha} = \alpha - \epsilon \zeta - \epsilon \eta, \quad \bar{\beta} = \beta, \quad \bar{\gamma} = \gamma.$$

$$\bar{\zeta} = -\epsilon \alpha + \left(1 + \frac{\epsilon^2}{2}\right) \zeta + \frac{\epsilon^2}{2} \eta,$$

$$\bar{\eta} = \epsilon \alpha - \frac{\epsilon^2}{2} \zeta + \left(1 - \frac{\epsilon^2}{2}\right) \eta,$$

gives rise to a change of  $x$  origin. These three types are rather trivial, representing the transformations of euclidean 3-space with change of time origin. The most general rotation which can be built from them gives the relations between the coordinates of equivalent observers.

The only type remaining to be considered is a rotation in the  $(\alpha \zeta)$  plane:

$$\bar{\alpha} = \cosh \epsilon \alpha - \sinh \epsilon \zeta, \quad \bar{\beta} = \beta, \quad \bar{\gamma} = \gamma.$$

$$\bar{\zeta} = -\sinh \epsilon \alpha + \cosh \epsilon \zeta, \quad \bar{\eta} = \eta,$$

On solving for  $x, y, z, t$ , we find

$$\left. \begin{aligned}\bar{x} &= -\frac{1}{\kappa} \coth \frac{\epsilon}{2} \frac{1 - 2 \coth \epsilon \kappa x + \kappa^2 r^2 - e^{-2\kappa c t}}{\coth^2 \frac{\epsilon}{2} - 2 \coth \frac{\epsilon}{2} \kappa x + \kappa^2 r^2 - e^{-2\kappa c t}}, \\ \bar{t} &= t + \frac{1}{\kappa c} \log \left\{ \sinh^2 \frac{\epsilon}{2} \left( \coth^2 \frac{\epsilon}{2} - 2 \coth \frac{\epsilon}{2} \kappa x + \kappa^2 r^2 - e^{-2\kappa c t} \right) \right\}, \\ \bar{y} &= y e^{\kappa c (t - \bar{t})}, \quad \bar{z} = z e^{\kappa c (t - \bar{t})}.\end{aligned}\right\} \quad (11)$$

To interpret this transformation, we solve the first three of equations (11) for  $x, y, z$ , in terms of  $t$  when  $\bar{x}, \bar{y}, \bar{z}$  vanish, and find

$$x = \frac{1}{\kappa} \coth \epsilon \left\{ 1 - \sqrt{1 - \tanh^2 \epsilon (1 - e^{-2\kappa c t})} \right\}, \quad y = 0, \quad z = 0.$$

Comparing this with (5), it is seen that the point  $\bar{x}, \bar{y}, \bar{z} = 0$



describes a geodesic passing through the origin at time  $t=0$ , with initial coordinate velocity  $\delta=c \tanh \epsilon$ . Hence we may interpret  $\bar{x}$ ,  $\bar{y}$ ,  $\bar{z}$ , and  $\bar{t}$  as the spacial coordinates and proper-time of an observer in motion along the  $x$ -axis relative to the observer with coordinates  $x, y, z, t$ . We have thus found the analogue of the Lorentz transformations for the space-time here considered; here as there, the transverse measured distances are the same for both observers, since

$$\bar{y}e^{\kappa c \bar{t}} = ye^{\kappa ct}, \quad \bar{z}e^{\kappa c \bar{t}} = ze^{\kappa ct}.$$

We have arrived at an interpretation of the relations existing between the data of freely moving observers similar to that given by Minkowski for special relativity—that in our case they may be represented by the rotation of a hypersphere in flat 5-space\*. The transformations could, of course, be obtained directly by requiring that the transformation leave (3) invariant; but in this way we avoid the integration of rather cumbersome differential equations and obtain a more comprehensible view of the process.

4. *Parallax. Doppler Effect.*—The measured distances considered above, which are obtained by comparing the intervals involved with a rigid scale, are themselves ideal constructions when applied to celestial, or even large terrestrial, distances. Since, however, the path of light is rectilinear in the  $x, y, z$  coordinate space, the usual triangulation methods are valid; we can deduce the coordinate and, on multiplying by  $e^{\kappa ct}$ , the measured distances of objects not susceptible of direct measurement, provided we know the length of the base. The usual method of determining the parallax of celestial objects is then applicable if we know the mean distance of the earth from the sun; this is again reducible to a triangulation whose base is a measurable distance on the earth, provided we know the solution of the one-body problem. The latter is considered in the following section, and it suffices here to state that the required solution

\* This interpretation is valid not only for the particular space-time here considered, but also for de Sitter's or any other space-time of constant Riemann curvature. The relation between this interpretation and Minkowski's, which is applicable for the case  $\kappa=0$ , is seen from the fact that the equation (9) of the hyper-sphere, referred to origin at  $(0, 0, 0, 0, 1/\kappa)$ , becomes on letting  $\kappa \rightarrow 0$

$$x^2 + y^2 + z^2 - c^2 t^2 = 0.$$

This is the equation of the light "cone" in special relativity, and the rotations considered by Minkowski are the transformations of  $x, y, z, t$  space under which it is invariant.

and the data necessary for the measurement of the solar distances can be obtained.

The measurement of velocities can, in principle at least, be reduced to the measurement of distances. Transverse velocities of celestial objects are in practice determined in this way, but the measurement of the radial component offers more difficulty; in practice it is accomplished by means of the Doppler effect, so we must develop the theory of this effect for the space-time here considered.

The simplest case is that in which the light from a distant equivalent point-source is examined by an observer at the origin. Light emitted from the source in the time interval  $t_0, t_0 + dt_0$  arrives at 0 in the interval  $t, t + dt$ , and it can be shown with the aid of (6) above that

$$dt = \frac{dt_0}{1 - \kappa l_0}, \quad \dots \dots \dots (12)$$

where  $l_0$  is the measured distance of the source from 0 at time  $t = t_0$ . Since the proper-times of vibration of atoms situated at 0 and the equivalent point-source are the same (neglecting the Einstein effect due to mass), this leads to a shift  $\Delta\lambda$ , of a spectral line of wave-length

$$\frac{\Delta\lambda}{\lambda} = \frac{dt}{dt_0} - 1 = \frac{\kappa l_0}{1 - \kappa l_0} \dots \dots \dots (13)$$

This shift toward the red would be attributed in practice to the Doppler effect due to a velocity of recession  $v$  according to the formula

$$\frac{\Delta\lambda}{\lambda} = \sqrt{\frac{1 + \frac{v}{c}}{1 - \frac{v}{c}}} - 1. \quad \dots \dots \dots (13')$$

On comparing this with (13), it is seen that a velocity

$$v = \kappa l_0 (1 + O[\kappa]) \dots \dots \dots (14)$$

would be assigned as the cause of the shift; this velocity coincides to terms of first order in  $\kappa$  with the "measured" velocity  $\kappa l_0$  of the source.

In the more general case, where the source has a non-vanishing coordinate velocity, account must be taken of the fact that the proper-time of vibration of the moving atom is not the same as the time interval measured by a stationary observer. For this the transformation (11) must be used,

and it can then be shown that the shift is given by

$$\frac{\Delta\lambda}{\lambda} = \frac{1 + \frac{\delta_r}{\delta_0}}{\sqrt{1 - \left(\frac{\delta}{\delta_0}\right)^2}} \cdot \frac{1}{1 - \kappa l_0} - 1, \quad . \quad . \quad (15)$$

where  $\delta_r$  is the radial component of the coordinate velocity  $\delta$ , and  $\gamma_0$  is the coordinate velocity of light at time  $t_0$ . This shift would be attributed to a velocity  $v_r$ , where

$$\frac{\Delta\lambda}{\lambda} = \frac{1 + \frac{v_r}{c}}{\sqrt{1 - \left(\frac{v}{c}\right)^2}} - 1, \quad . \quad . \quad . \quad (15')$$

and on identifying the transverse component of  $v$  with the corresponding "measured" quantity, we find that the radial component  $v_r$  is

$$v_r = e^{\kappa c t_0} \delta_r + \kappa l_0 \left( 1 + O \left[ \left( \frac{\delta}{\delta_0} \right)^2 \right] \right) + O(\kappa^2). \quad . \quad (16)$$

Hence the ordinary interpretation of Doppler effect leads to a radial velocity which is to terms of order  $\kappa \left( \frac{\delta}{\delta_0} \right)^2$ , the same as the corresponding "measured" component, and may therefore for practical purposes be taken as measuring it.

If we assume that there is no systematic correlation of coordinate velocity with distance from the origin, we should expect that the Doppler effect would indicate a residual positive radial velocity of distant objects because of the term  $\kappa l_0$  in (16). Although we cannot, from Doppler effect alone, distinguish between proper motion and this distance effect, we should nevertheless expect a correlation

$$v \simeq c \frac{l}{R} \quad . \quad . \quad . \quad (17)$$

between assigned velocity  $v$ , distance  $l$ , and radius of the observable world  $R$ .\*

\* Weyl, *l. c.*, has deduced a similar relation on the de Sitter hypothesis, which is also given by (17) to first order, assuming that the geodesics concerned form a diverging pencil. L. Silberstein ('Nature,' March 8, April 26, June 7, 1924; Monthly Notices, R. A. S. lxxxiv. p. 368, lxxxv. p. 285, 1923-24, Phil. Mag. xlvii. p. 907, xlviii. p. 619, 1924-25) has supplemented this with a converging pencil, which allows him to write (17) for either positive or negative velocities, and he and K. Lundmark (Monthly Notices, R. A. S. lxxxiv. p. 747, 1924) have discussed the motion of various classes of celestial objects and arrived at the value of  $R$  of the order  $10^{28}$  cm. There is no possibility of introducing the negative sign in our case, unless we change the sign of  $\kappa$ , and then the positive sign could not appear!

Comparing the data given by Hubble \* concerning the value of  $l$  for the spiral nebulae with that of Slipher† concerning the corresponding radial velocities, we arrive at a rough verification of (17) and a value  $R=2 \times 10^{27}$  cm. This is somewhat lower than Hubble's value  $8.5 \times 10^{28}$  cm., which was obtained on Einstein's cosmology from the computed value of the mean density of matter; the fact that the two values do not differ more is rather remarkable, considering the radical difference in the methods by which they were determined.

5. *Central-symmetric Solution.*—The de Sitter line element (2) for an empty world can be obtained from the Schwarzschild solution

$$ds^2 = -\gamma^{-1} d\rho^2 - \rho^2 (d\theta^2 + \sin^2 \theta d\phi^2) + \gamma c^2 dt^2, \quad (18)$$

where

$$\gamma = 1 - \frac{2m}{c^2 \rho} - \kappa^2 \rho^2,$$

which represents the field of a spherically symmetric mass, on setting  $m=0$ . If the interpretation we have given for (3) is to have physical significance, it should be possible to derive it from a solution of the one-body problem by the same process. That such a solution exists can be shown by subjecting (18) to the transformation

$$\left. \begin{aligned} \rho &= r e^{\kappa c t} \left( 1 + \frac{m}{2c^2 r e^{\kappa c t}} \right)^2 \\ \tau &= t + 8 \frac{m^2 \kappa}{c^5} F \left( \frac{1 - \frac{m}{2c^2 r e^{\kappa c t}}}{1 + \frac{m}{2c^2 r e^{\kappa c t}}} \right) \end{aligned} \right\}, \quad \dots \quad (19)$$

where

$$F(\zeta) = \int \frac{d\zeta}{(1-\zeta^2) \left[ \zeta^2 (1-\zeta^2)^2 - 4 \frac{m^2 \kappa^2}{c^4} \right]};$$

\* E. Hubble, "Extra-galactic Nebulae," *Astrophys. Journ.* **lxiv.** p. 321 (1926).

† See Eddington, *l. c.* p. 162, for Slipher's Table of Radial Velocities.

whence

$$ds^2 = - \left( 1 + \frac{m}{2c^2 r e^{\kappa ct}} \right)^4 e^{2\kappa ct} (dr^2 + r^2 d\theta^2 - r^2 \sin^2 \theta d\phi^2) + c^2 \left( \frac{1 - \frac{m}{2c^2 r e^{\kappa ct}}}{1 + \frac{m}{2c^2 r e^{\kappa ct}}} \right)^2 dt^2. \quad (20)$$

On setting  $\kappa=0$  the usual isotropic form of the static Schwarzschild solution for the case  $\kappa=0$  is obtained †.

The observational tests of the general theory of relativity within the solar system (the advance of perihelion of Mercury, deflexion of light grazing the limb of the sun, and shift of spectral lines in the solar spectrum (mass effect)) are, in so far as the observational data are concerned, the same in the field defined by (20) as in Schwarzschild's. This can be most readily shown from the fact that the equations of the geodesics of (20) differ from those of (18) by terms of order  $\kappa ct$ , and for the tests under consideration this can at worst only lead to an insignificant correction. For this reason we do not attempt to give a full discussion of the rather complicated solar field. The rigorous discussion must be in terms of measured distances and proper-times; as an example of the method, we here derive the radial component of the measured distance and apply it to the advance of perihelion of a particle.

The radial component at coordinate time  $t$  of the distance between two points whose coordinates are  $r_0, r$  is

$$l(r e^{\kappa ct}) - l(r_0 e^{\kappa ct}),$$

where

$$l(\xi) = \int \left( 1 + \frac{m}{2c^2 \xi} \right)^2 d\xi = \xi + \frac{m}{c^2} \log \xi - \frac{m^2}{4c^4 \xi}.$$

This can obviously not be measured from the origin; but this difficulty can be avoided by measuring it from a surface

\* This solution was originally found by solving (1) for all dynamical manifolds expressible in orthogonal coordinates in which the velocity of light is isotropic (Trans. Amer. Math. Soc. xxix. April 1927). It was there shown that of the three solutions of the problem, (20) is the only one of physical significance. Furthermore, it is the simplest orthogonal isotropic form of (18).

† Eddington, *l. c.* p. 93.

$re^{kct} = \text{const. } \alpha$ , say that for which  $l(\alpha) = 0^*$ . An orbit, *i. e.* geodesic, of (18) will be an orbit of (20) on transforming its equations by (19), and its measured distance will be  $l(re^{kct})$ . As  $re^{kct}$  is a function of  $\rho$  alone, the directions  $\theta$ ,  $\phi$  of perihelion and aphelion, *i. e.* points at which the measured distance has an extremum, will be the same in both cases; in particular, leaving the numerical values of the constants of integration involved unchanged, the advance of perihelion will be the same here as in the Schwarzschild solution.

6. In conclusion, a system of cosmology based on (3), which is mathematically equivalent to that of de Sitter but differs from it in its physical interpretation, has been developed in which the "mass-horizon" and "arrest of time at the horizon" paradoxes do not occur, and in which space and the velocity of light are isotropic. In addition, it has the advantage of simplicity, since the geometry of space is euclidean, the motion of particles and light is rectilinear in coordinate space, and the proper-times of observers at relative rest in this coordinate space are the same. On the other hand,  $t$  appears explicitly in the line element, and consequently natural processes are not reversible, but space-time is isotropic in time in the sense that at any time the line element has the same form as at any other, provided the spacial scale is appropriately chosen. Although space is unlimited the observable world is not, and objects at an appreciable fraction of its radius should show a residual motion of recession; assuming that the known excess of recessional velocity of spiral nebulae is due to this cause, the radius of the observable universe is found to be  $2 \times 10^{27}$  cm.

The relations existing between observers in relative motion, the analogue of the Lorentz transformation, can be represented by the rotation of a hyper-sphere in a flat 5-space; and this is true for any cosmology in which space-time is considered as a manifold of constant Riemann curvature. Finally, the corresponding solution of the one-body problem is given, the predictions of which are indistinguishable from

\* The justification of this procedure consists in the fact that the circular orbits of the Schwarzschild field give, on applying (19), orbits  $re^{kct} = \text{const.}$  coplanar with 0. On choosing  $\theta = \frac{\pi}{2}$ ,  $\frac{d\phi}{dt}$  and  $\frac{ds(t)}{dt}$  are constant, and these orbits may be taken as the "circular" orbits of (20); on choosing one of them as origin of measured distance (considering a ring of particles travelling in it), the other circular orbits are at constant distance from it. The equation  $\phi = \sqrt{(m, l)}(t - t_0)$  for such orbits yields the analogue of Kepler's third law, and can be used for the determination of solar distances as required by (4) above.

those of Schwarzschild's (to which it is mathematically equivalent) within the solar system.

On replacing  $\kappa$  by  $-\kappa$  the solution (3) still satisfies Einstein's equations, as this is equivalent to the transformation  $t = -t$ . The consequences of this can be obtained from the foregoing by interchanging past and future; but the known facts concerning the spiral nebulae indicate that this is not desirable.

Göttingen, Germany.

LXXXVII. *The Resistance of Sputtered Films.*  
By RUSSELL STURGIS BARTLETT, Ph.D. (Yale) \*.

MANY observers† have remarked the peculiar electrical properties of thin metallic films on glass, whether deposited by chemical means, by cathode sputtering, or by evaporation and condensation. Many hypotheses have been advanced to explain these properties, though none has proved entirely satisfactory. It seems probable, however, that the true and complete explanation will include much that has already been suggested. The purpose of the present paper is to present some new experimental evidence, and to suggest a means, hitherto apparently overlooked, whereby many of the peculiarities can be explained.

It seems advisable, before proceeding further, to summarize briefly the peculiarities mentioned above. The specific resistance for the thinnest films is almost infinite, and decreases rapidly with increasing thickness up to a certain point. Beyond this point a further increase in thickness produces only a small change in the specific resistance. This critical thickness has been variously estimated by different experimenters, and appears to depend upon the rate of deposit and on the metal, but is in general in the neighbourhood of  $5 \times 10^{-7}$  cm., assuming normal

\* Communicated by Sir J. J. Thomson, O.M., F.R.S.

† Longden, *Phys. Rev.* xi. pp. 40, 84 (1900); Patterson, *Phil. Mag.* iv. p. 652 (1902); Kolschütter & Noll, *Zeits. Electrochem.* xviii. p. 419 (1912); Swann, *Phil. Mag.* xxviii. p. 467 (1914); King, *Phys. Rev.* x. p. 291 (1917); Kahler, *Phys. Rev.* xviii. p. 210 (1921); Koller, *Phys. Rev.* xviii. p. 221 (1921); Holmes, *Phys. Rev.* xxi. p. 386 (1923); Mackeown, *Phys. Rev.* xxiii. p. 85 (1924); and Reynolds, *Phys. Rev.* xxiii. p. 302 (1924) have worked with sputtered films. Stone, *Phys. Rev.* vi. p. 1 (1898); Vincent, *Ann. de Chimie et Phys.* (7) xix. p. 421 (1900); Grimm, *Ann. d. Physik*, (5) ii. p. 448 (1901); Weber & Oosterhuis, *K. Akad. Amst. Proc.* xix. p. 567 (1917); and Steinberg, *Phys. Rev.* xxi. p. 22 (1923) have dealt with evaporated or chemically deposited films.

density. The thinnest films have a negative temperature coefficient of resistance, changing through zero to a small positive coefficient for thicker films. Again, all show a permanent irreversible change in resistance with time, with heating, with passage of a heavy current, etc. This phenomenon, which is generally known as ageing, is usually an increase in resistance for very thin or high resistance films, and a decrease for thick and low resistance films. Bismuth always shows an increase of resistance with ageing, and always has a negative temperature coefficient. The presence of various gases or of vacuum affects the ageing in a rather irregular manner. Finally, the thermoelectric force, the change of resistance of bismuth in a magnetic field, and the photoelectric emission all show peculiarities.

### *Experimental Procedure and Results.*

The author has in general verified the results of previous experimenters, and has gone further to push the ageing process in certain cases to its ultimate limits. Gold films were used for the greater part of the observations; the subsequent considerations have shown that platinum would, perhaps, have been a more fortunate choice. However, some observations were made on sputtered films of platinum, palladium, copper, silver, bismuth, and tellurium.

The films were sputtered in a bell-jar in the usual manner. The electrode of the metal to be sputtered, in the form of a flat plate, was suspended horizontally near the top of the bell-jar. Beneath that, at a distance of from 2 to 4 cm., depending upon the metal used and other circumstances, was supported the glass plate for receiving the deposit. To ensure uniform thickness, the region of the plate to be used was always considerably smaller than the sputtering electrode. An unrectified current from a step-up transformer was used, with a variable resistance in the primary circuit to control the current. An aluminium electrode in the base of the bell-jar was sufficiently removed so that no sputtering from this could affect the metallic deposit at the top. The wax joints were carefully protected from the discharge, as previous experience had shown that muddy and dirty deposits were produced with grease or wax vapour in the bell-jar.

The thickness of the films was determined by weighing, a method which does not admit of great accuracy. But all methods are open to question in some way, and this one



seemed adequate. The absorption of light in the films was used also as a means of comparing thickness, and proved reasonably satisfactory.

But where it was desirable that two or more films should be identical, or nearly so, special precautions were taken. In some cases they were sputtered side by side, even on the same piece of glass. If this was impracticable, care was taken to maintain all conditions the same; and a good check on this was possible. The pressure, measured on a McLeod gauge, and the resistance in the primary of the transformer were maintained the same for two cases. If, then, the current in the primary and the size of the cathode dark space were also the same for both cases, it may be taken as a fair indication of identical conditions. Finally, the glass plates were similarly located, the sputtering continued for the same length of time, and the absorption of light in the two was found to be the same.

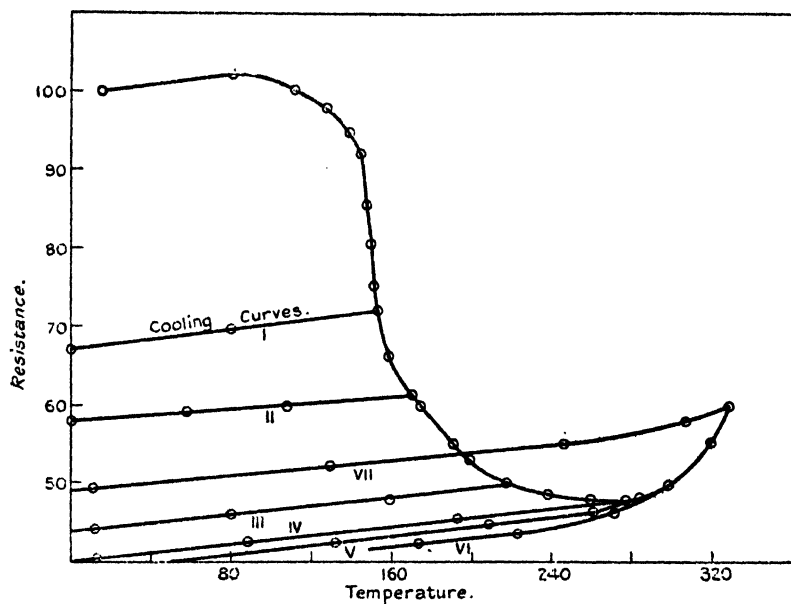
The ends were heavily sputtered to ensure good contact with brass clamps. In some cases the film was carefully ruled in a sort of gridiron pattern to increase the resistance, thus reducing the resistance of contacts and leads to a negligible factor. Both Wheatstone bridge and potentiometer methods were used to measure the resistance.

The films were placed in an electric oven and heated slowly, resistance measurements being made from time to time. At intervals during the ageing process the films were cooled again to room-temperature and sometimes to liquid-air temperature, and the temperature coefficient of resistance was measured.

It was found that, when a film was heated to a temperature above that which it had previously reached, the resistance changed rapidly at first, but more slowly as time went on, and appeared to approach a limiting value asymptotically. At any time a slight increase in temperature would increase the rate of change of resistance. It was also found that the temperature coefficient of resistance increased with ageing. There was no evidence of any sudden change in resistance at any temperature. Fig. 1 is a typical example of change of resistance with temperature, the temperature being maintained in so far as possible at a steady value till the resistance ceased to change.

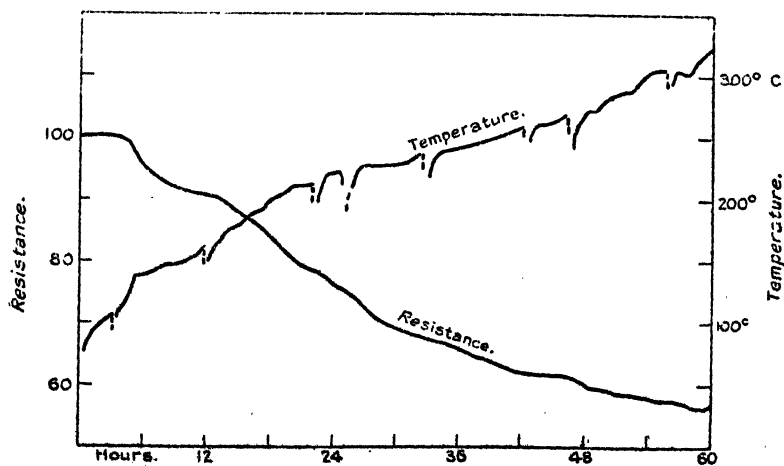
From measurements of the temperature coefficient of resistance at different stages of ageing, the readings were all reduced to resistances at room-temperature, 15° C. A typical example of variation of resistance with time, showing the corresponding temperatures, is given in fig. 2. From a

Fig. 1.



Changes of resistance with temperature of ageing.

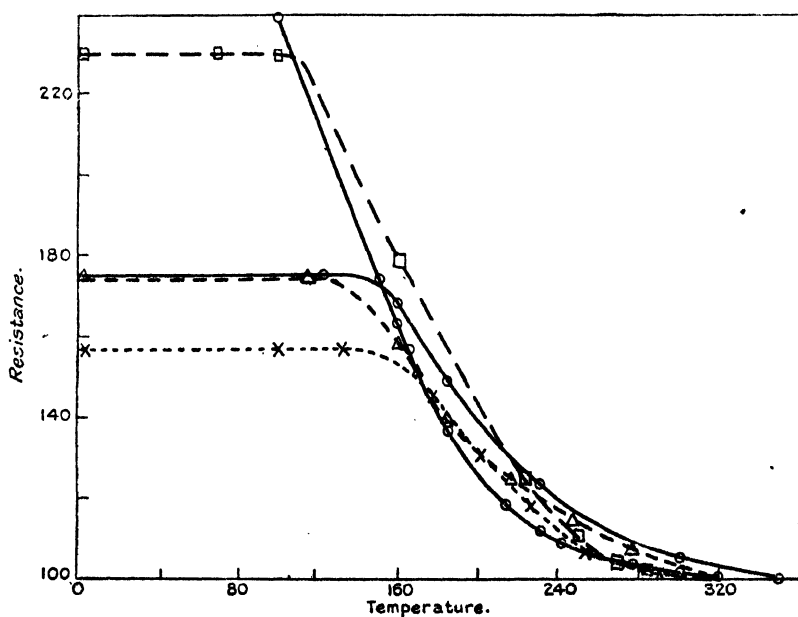
Fig. 2.



Changes of resistance with time, showing corresponding temperatures.

number of such curves it was possible to deduce the nature of the change of resistance with time at a given temperature, and thus to fix the limiting resistance reached after long ageing at any temperature. It was found that all films decreased in resistance with increasing temperature up to a certain point, where the resistance went through a minimum and began to increase with further increase in temperature. The temperature for this minimum resistance varied slightly with different films, but was in the neighbourhood of  $300^{\circ}\text{C}$ . for the films examined, varying in thickness from  $3 \times 10^{-6}$  up to  $7 \times 10^{-6}$  cm.

Fig. 3.



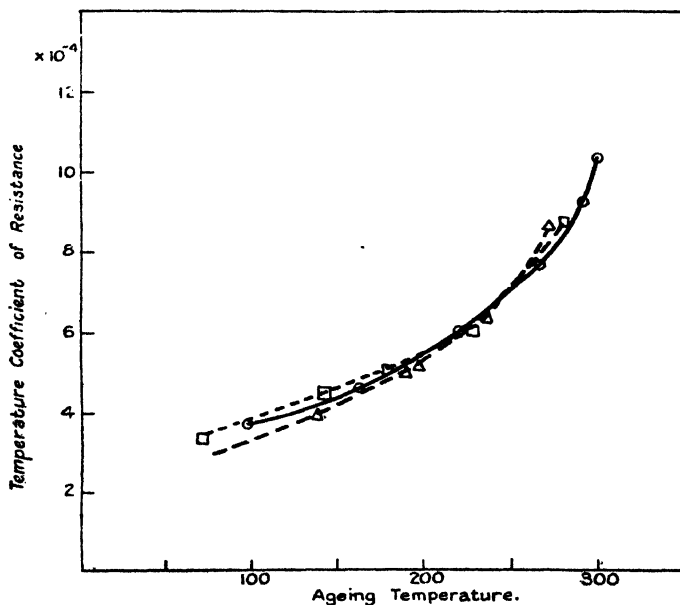
Resistances plotted as percentages of final value.

The specific resistance of these films cannot be fixed accurately because of the uncertainty as to the thickness, but it is worthy of note that for gold all reached nearly the same limiting value of  $8 \times 10^{-6}$  ohm per cm. cube, though starting with as widely differing values as  $18 \times 10^{-6}$  and  $12 \times 10^{-6}$  ohm per cm. cube. This suggested a means of comparison for a number of films. The resistances were plotted against temperature as before, but as percentages of the final value reached, which was assumed to be the same for all cases. These results are shown in fig. 3. It will be

observed that the curves for all films follow the same general course at higher temperatures, breaking away at various lower temperatures. These differences appear to depend upon the previous history of the film, temperature reached during sputtering, etc.

To determine, if possible, whether this ageing is caused by the escape of occluded gas, two films sputtered side by side were placed in the oven together, one in an evacuated tube and the other in air. The presence of air was found merely to retard the ageing process without having any effect on the final value reached. For temperatures above  $240^{\circ}\text{C}$ ., the films behaved in exactly the same manner.

Fig. 4.



Changes of temperature coefficient of resistance with temperature of ageing.

Fig. 4 shows the temperature coefficient of resistance for a number of films as a function of the ageing temperature. The agreement is fairly good for a short range. At higher temperatures very marked increases occur which are of particular interest, and will be discussed later. One curious point is that in general the absolute change of resistance per degree centigrade remained nearly the same during ageing, the change in the temperature coefficient being caused

almost entirely by the permanent decrease in resistance. As others have noted, once a film has been thoroughly aged at a given temperature, its behaviour below that temperature is reversible and reproducible.

The results of a few other attempts at ageing will be noted here. The instantaneous passage of a heavy current, of a current density of the order of  $3 \times 10^5$  amperes per square centimetre, reduced the resistance to 35.7 per cent. and 36.6 per cent. of its original value in two cases. A further increase of the current to double this value produced no appreciable change. In the case of heating externally, the greatest reduction observed was to 37.5 per cent. of the original value. And any increase in temperature beyond the optimum value caused a rapid increase in resistance. The question then arises whether the passage of a heavy current does not contribute to the ageing in some way besides the heating effect.

A film subjected to strong mechanical vibration during heating showed no more change than one similarly heated without the vibration. Another, heated in a discharge-tube by positive ion bombardment, showed no unusual change. And when the bombardment was increased sufficiently to produce appreciable sputtering, from a sputtered film, the change in resistance so produced did not indicate the ejection of appreciable chunks of metal from the film, but rather an evaporation, molecule by molecule or atom by atom.

#### *An Explanation of the Properties of Sputtered Films.*

Swann and King have suggested different theories of granular structure and incomplete covering to account for the high specific resistance of these films. Koller has shown that occluded gas is certainly a factor in ageing. He goes so far as to suppose that in sputtering small crystals are ejected from the cathode and deposited on the film. These are then kept from intimate contact by gas molecules which are gradually released. Kahler, from X-ray analysis, concludes that sputtered films are crystalline, identical with bulk metal, while evaporated films are amorphous. Steinberg does not agree with this, finding evaporated films identical in structure with bulk metal. Weber and Oosterhuis have shown that the granular structure of sputtered films may be quite as fine as that of evaporated films. There seems to be some difference of opinion as to the size of the granular structure, but this could be readily explained by differences in conditions of evaporation or sputtering.

One can point, then, confidently to occluded gas as the first cause of the peculiar properties of these thin films, particularly the ageing process. We can invoke Koller's granular structure held apart by gas-molecules. Or we can assume that the large amounts of gas in the metal increase its resistance in the same manner as the smaller quantities of gas in metal wires and foils, but to a much greater extent\*. In any case, it is the escape of this gas, with, perhaps, a settling together of the metal atoms, which causes the reduction in resistance known as ageing.

The granular or irregular structure, the second factor, is important, particularly in the variation of specific resistance with thickness; but it can also explain the negative ageing (increase of resistance) of high-resistance films. We do not need to suppose that crystals are deposited on the glass, though Longden's suggestion of crystallization at the edge of the cathode dark space would favour such an idea if the glass were far removed from the cathode (as it was for the films used in Kahler's X-ray analysis). For it is known that crystals of varying sizes may be produced in electrolysis by varying the rate of deposition. Electrolysis is not an exact parallel to condensation or sputtering deposition. But a similar arrangement of condensing atoms in groups is quite a probable occurrence, since the forces of attraction between two metal atoms are greater than between metal and glass. This is supported by the fact that, under suitable conditions, a sputtered film may be stripped from the glass and remain continuous. We may suppose, then, that metal atoms condense about those already on the glass, forming groups; and not until these groups have grown to a considerable size does the conductivity approach a reasonably steady value, at which point the glass is presumably completely covered. Further deposition adds to the thickness of the film irregularly, so that it will never be of a uniform thickness, and will always have a high specific resistance. Variation of the rate of deposition would vary the size and spacing of the aggregates, and thus cause the variations in the thickness at which the film shows a fairly constant specific resistance, as noted by different observers. One can go through mathematical calculations to justify these assumptions and obtain suitable values of specific resistance, but they would not carry much weight, and so will be omitted.

\* Fisher, *Ann. d. Physik*, xxi. p. 503 (1906); Kleine, *Zeits. f. Physik*, xxxiii. p. 391 (1925); Herrmann, *Ann. d. Physik*, lxxvii. p. 503 (1925); and Janitzky, *Zeits. f. Physik*, xxxi. p. 277 (1925), have all studied this phenomenon.

If a very thin film is heated, while still far from the melting-point, a rearrangement of the molecules begins, particularly towards the aggregates and massive centres of condensation, and away from the thinly-populated regions between. This may be aided by a variation with temperature of the cohesive forces of metal to metal and metal to glass; but increased thermal agitation could also be the cause of the rearrangement; and the result, of course, is a permanent increase in resistance. The same thing takes place for thicker films, but at a higher temperature. At first the out-gassing of the metal decreases the resistance, but at higher temperatures the other becomes effective, and the resistance finally increases. This probably combines with the tension effect noted below, though that is still effective when the film is of so great a thickness as to be sensibly uniform. Weber and Oosterhuis have noted that silver does not attain a constant specific resistance until much thicker than platinum or tungsten, which means that the silver aggregates are larger than those for the other metals. It is also notable that silver shows negative ageing at greater thicknesses, attributable to the same larger aggregates.

There is another factor, hitherto apparently overlooked, which should in most cases contribute towards several of the properties noted above. This factor is the difference in the coefficients of thermal expansion of the sputtered film and the material used to receive the deposit. A brief statement of the case will suffice to show what changes would be expected from this.

In most cases the coefficient of expansion of the metal is greater than that of the backing. When the film is cooled, its greater contraction produces a state of tension. Bridgeman\* has shown that most metals show an increase of resistance under tension, but the effect is so small as to be quite immaterial in the present instance. However, if we take the common case of gold films on glass, the tension on the gold is of the order of 5 kg./cm.<sup>2</sup> per degree centigrade of cooling; so that cooling of 100° would produce a tension as great as that applied by Bridgeman experimentally, and for a slightly greater range of temperature the elastic limit, or even the breaking-stress, of the gold would be exceeded. Taking into account the generally accepted hypothesis of a granular structure, we may justifiably suppose a process of opening or closing gaps in the film as the temperature falls or rises. This should produce an increase of resistance with

\* Bridgeman, Proceedings of the American Academy of Arts & Sciences, ix. p. 423 (Oct. 1925).

cooling, opposing the normal decrease, and resulting in the observed low or negative-temperature coefficient.

To test this hypothesis experimentally, gold was sputtered on three plates placed side by side in the discharge-tube, one of quartz crystal cut perpendicular to the axis, one of glass, and one of fused quartz. These have coefficients of expansion of about 13.7, 7.5, and  $0.42 \times 10^{-6}$  per degree centigrade respectively, whereas gold has a coefficient of about 13.9, almost identical with that of quartz crystal. A similar procedure was carried out for platinum, which corresponds roughly to glass in coefficient of expansion. The specific resistances of these films were then determined, and their temperature coefficients of resistance over the range from 15° C. to -185° C. The results are given below:—

Metal.	Backing.	$\Delta R/R_0(T_2 - T_1)$ .	Specific resistance.
Gold .....	Quartz crystal.	$7.06 \times 10^{-4}$	$19.8 \times 10^{-6}$
Gold .....	Glass.	6.38	21.6
Gold .....	Fused quartz.	5.27	28.6
Platinum .....	Glass.	4.41	75
Platinum .....	Fused quartz.	3.71	82

The figures in the first column, showing the lowest temperature coefficient of resistance where the difference in coefficients of expansion is greatest, are in accord with the above hypothesis. The data on specific resistance are necessarily inaccurate, but are useful for comparison, since the samples of gold were sputtered at the same time and in the same discharge-tube. If the film and backing are heated during sputtering, as is often the case, on cooling to room-temperature the tension should give rise to a high specific resistance, greatest where the greatest tension occurs. The figures in the last column show the expected differences, though somewhat larger than the observed differences in temperature coefficient would indicate. Reynolds has shown that films deposited on cold and on warm glass have markedly different properties, a fact which supports this view.

We may then point to the unequal coefficients of expansion of film and backing, with the attendant tension on the film, as a third factor contributing to the low-temperature coefficient of resistance, and probably, in some cases, to a part of the high specific resistance.

As noted above, consistent results are obtainable with



these films only at temperatures appreciably below those reached previously during sputtering or ageing, so that in most cases we are dealing with a stretched film. When a film is heated to a temperature in the neighbourhood of the highest previously reached, it will reach a state in which the gaps are all closed and the texture is fairly uniform. For a short range above this point the temperature coefficient of resistance should be more normal. Further increase in temperature should cause the film to buckle and heap up, giving rise, on cooling, to larger gaps than ever and an increased resistance. Fig. 1, typical of all the films examined, shows all these features. Over a short range the temperature coefficient of resistance was about 90 per cent. of that for bulk metal, whereas for the rest of the temperature range it was as low as 20 to 25 per cent.

Sputtered films of bismuth have in all cases a negative-temperature coefficient of resistance, a fact which can be attributed to its larger coefficient of expansion.

At 350° C., for gold in bulk, the specific resistance is about  $6 \times 10^{-6}$  ohm per centimetre cube, while for these films, when thoroughly aged, it was only 50 per cent. greater. If the abnormal temperature coefficient persisted, the specific resistance of the sputtered film would, at somewhat higher temperatures, be less than that of the bulk metal. But if we accept the effect of tension outlined above, this difficulty vanishes; for the abnormal temperature coefficient persists only to the previous temperature reached in sputtering or ageing, which was in the neighbourhood of 350° C. for most cases dealt with.

Much work has been done with films of platinum sputtered on glass, in which case the coefficients of expansion are nearly the same, and this reasoning would not apply; but the properties of platinum films on glass are closer to those of the metal in bulk than is the case for any other metal.

It appears that most of the discrepancies and disagreements between previous workers are caused by differences in the manner of obtaining deposits, both as to the rate of deposition, determining the size of the aggregates, and as to conditions, nature of gas and pressure, etc., affecting the gas-content of the metal. Experimental evidence on these points would be interesting, and would do much to prove or disprove the theories advanced. Deposits of platinum on glass, where the deposition is slow and the glass is heated from below, should be free from the tension troubles suggested above.

*Summary.*

The ageing of sputtered films is shown to depend on the temperature to which the film is raised. The resistance decreases to a minimum value and then increases as the temperature is further increased. The dependance of the temperature coefficient of resistance on degree of ageing and on temperature is shown. Other experimental evidence is brought forward in support of the theoretical considerations suggested below.

It is shown that the peculiar electrical properties of thin metallic films on glass may be attributed to three principal causes. Occluded gas contributes towards the high specific resistance, and particularly the decrease in resistance with ageing, brought about by the outgassing of the metal. A granular or irregular structure explains the dependance of specific resistance on thickness and the negative ageing of very thin films. A state of tension in the film, produced by unequal coefficients of expansion of film and backing, opens or closes gaps in the film as the temperature changes, giving rise to the low or negative-temperature coefficient of resistance and other peculiarities. Experimental evidence of the author and others is advanced to justify these proposals. The importance of the conditions of deposition in determining the properties of the film is pointed out.

Finally, the author wishes to acknowledge his indebtedness to Sir Ernest Rutherford and others at the Cavendish Laboratory for their kindness, and in particular to Sir J. J. Thomson for his interest and assistance in this work.

LXXXVIII. *Space-Charge Effects.* By E. W. B. GILL,  
*M.A., B.Sc., Fellow of Merton College, Oxford\*.*

1. **S**OME time ago † I described experiments with a three-electrode gas-free valve in which the current from the filament to the plate was investigated, the plate being kept at a few volts and the grid at from 20 to 30 volts positive to the filament. It was found that the space-charge between the grid and the plate had a considerable effect on the electric field in that region, and when the current was sufficiently increased discontinuous changes took place in the field. The theory which was given has recently been

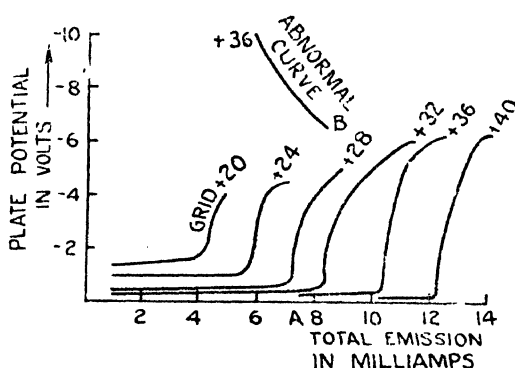
\* Communicated by Professor Townsend, F.R.S.

† Phil. Mag., May 1925, p. 993.

extended by Tonks \*. The present investigation comprises a further extension of the experiments to the case in which the plate is a little negative to the filament. Normally no electrons can reach the plate if it is negative to the filament, and another method is required to investigate the field.

2. The valve used was a modified Marconi MT 5 type, the same one as before. The spiral grid was 5 mm. and the plate 25 mm. in diameter. The plate lead was brought out at the top of the glass, and the insulation of this electrode is therefore much better than in an ordinary valve. No trace whatever of residual gas could be detected in the valve. In what follows the plate potential was measured by connecting it to a quadrant electrometer, the potential on insulating being the same as that of the negative end of the filament. This point will be taken as being at zero potential.

Fig. 1.



An experiment consisted in passing different currents through the grid kept at a fixed positive potential and observing the potential assumed by the plate, the plate being always earthed while the current was being varied. This variation of current was effected by adjustment of the filament heating. The plate current being zero, all the electrons set free from the filament must finally arrive at the grid, and the grid current, which was measured, represents the total electron emission from the filament.

The curves in fig. 1 represent the plate potentials thus obtained when the grid was kept at +20, +24, +28, &c.

\* Lewi Tonks, *Phys. Rev.*, Oct. 1927, p. 501.

volts plotted against the emission current. It will be observed that in all cases the plate acquires a small negative potential for the smaller currents, but a point is reached at which there is an abrupt increase in the value of this negative potential. The emissions at which this abrupt change occurs increase as the grid potential is increased. The curve for the grid at  $+36\frac{1}{2}$  volts labelled "abnormal curve" was obtained under conditions to be described later.

In order to explain the large abrupt increase of the plate potential the following questions may be considered :—

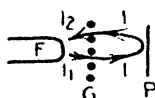
1. What is the distribution of the electric field between the grid and the plate?

2. How is this field initially set up?

3. As a preliminary it may be noted that no ionization or photo-electric effects can account for the curves. The amount of gas in the valve was, as stated, quite appreciable, but in any case the grid being positive to the plate no ionization or photo-electric effect can cause the plate to attain a negative potential.

The general current distribution inside the valve is indicated diagrammatically in fig. 2. The filament grid and plate are

Fig. 2.



represented respectively by F, G, and P; F and P are at the same potential and G positive to both of them. At any instant in the space between F and G a current  $i_1$  flows towards G; part of this current is collected by the grid, and the remainder  $i$  flows towards P. Since P and F are at the same potential, the electrons in the space between P and G return towards the grid, that is a current  $i$  also flows towards G, of which a part is collected on G and the remainder  $i_2$  flows towards F. As with the stream  $i$ ,  $i_2$  is reversed and forms part of  $i_1$ . The total current collected by the grid is  $i_1 - i_2$ , and this is the same as the emission current from the filament.

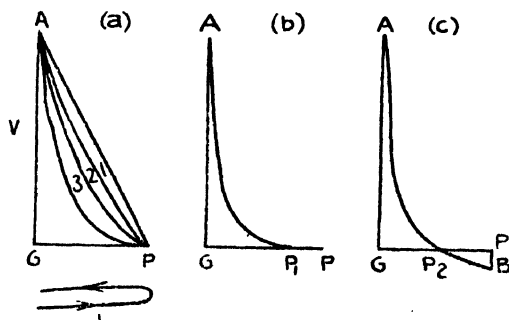
It is not possible to measure  $i$ ,  $i_1$ , and  $i_2$  separately with any accuracy, but only  $i_1 - i_2$ . The current  $i_1$ , and in many cases the currents  $i$  and  $i_2$  are larger than the total emission current  $i_1 - i_2$ , so that there is always the possibility with

this arrangement that there may be large space-charges in the valve even if the emission is comparatively small.

In the first part of the curves, where the ordinary small plate potential of about one volt is obtained, this potential is due to the velocity of emission of the electrons from the hot filament in addition to contact differences of potential between the plate and the filament. The plate potential is, however, measured from the negative end of the filament, while the fastest electrons come from about the middle of the filament whose potential alters as the filament current is varied. The reason for the curves not coinciding over this range is that in passing the grid the electrons are deviated and lose velocity in the direction normal to the plate, and this deviation increases with the voltage of the grid.

4. The abrupt increases in the negative potential of the plate are due to space-charge effects between the grid and

Fig. 3.



the plate. To simplify the explanation the grid and plate may be regarded as parallel planes, all electrons may be supposed to move at right angles to them, and the distribution to be uniform over any plane parallel to the electrodes. The velocities of emission and contact differences of potential will be neglected. The space-charges between the grid and plate are exactly the same as those due to a current  $2i$  carried by electrons leaving the plate with zero velocity and moving towards the grid, and the well-known results of Child and Langmuir can therefore be easily applied to this case.

Fig. 3 represents the distribution of potential between the plate P and grid G, the ordinates representing potentials at the different planes and the abscissæ the distances of the planes from the grid. The grid potential  $+V$  is represented by GA, the plate potential being zero.

When no current flows the straight line AP represents the potential distribution. A small current flowing in the space gives the potential distribution represented by curve 1, a larger current gives curve 2, and, finally, a current is reached which gives curve 3, in which GP is a tangent to the curve at P. This is the maximum current which can flow in this space provided that the electrons penetrate just to the plate before their direction of motion is reversed. Langmuir's equation for this saturation current gives  $2i = k \frac{V^{3/2}}{GP^2}$   $k$  being a constant.

If the current forced through the grid from the filament side exceeds this value, two different types of distribution are possible.

One of these is represented by the curve of fig. 3 (b), where the electrons penetrate as far as  $P_1$ , the space between the planes G and  $P_1$  carrying the maximum current, involving  $GP_1$  being the tangent to the curve at  $P_1$ . In this distribution the space between P and  $P_1$  has no charge, and all points in it are at zero potential.

As  $GP_1^2$  replaces  $GP^2$  in the denominator of Langmuir's equation, this distribution carries a larger current than that represented by curve 3 in fig. 3 (a).

The other possible distribution of potential is shown in fig. 3 (c). In this case the electrons only penetrate as far as  $P_2$ , where  $GP_2$  is less than  $GP_1$  and the space  $GP_2$  is not carrying its maximum current. The part of the curve from  $P_2$  to B is a straight line touching the curve at  $P_2$  since the electric force is continuous, and there is no charge in the space between the planes  $P_2$  and P. This distribution requires the plate to have a negative potential PB. It is evident that for a given current there are an infinite number of distributions of this type each with a different plate potential. The one actually set up depends on the amount of negative electricity which the plate can receive, which will be discussed in paragraph 5.

The curves of fig. 1 are explained by the distributions indicated by the curves of fig. 3. The early parts of the curves correspond to distribution (a) in which the plate potential remains constant; and the currents at which the discontinuities occur give distribution (a) 3, for which  $i$  is proportional to  $V^{1/2}$ . As explained, the current  $i$  is not the same as the total emission, but is probably roughly proportionate to it, and the emission currents at the points where the curves suddenly rise are within errors of experiment proportional to  $V^{1/2}$ .

The remainder of the curves in which the plate is negative corresponds to distributions of the type (c).

Distribution (c) is also an alternative to (a), which explains the abnormal curve in fig. 1 for the grid at 36 volts. Similar curves can be obtained for the other voltages by a method to be described later.

5. It remains to explain by what process the distribution represented by the curve fig. 3 (c) is set up, as it involves negative electricity from the filament reaching the plate to charge it to a negative potential. Under static conditions this is impossible, as no electron from the filament can reach an electrode at a potential negative to the filament.

If, however, there is any disturbance of the field, it is possible for the plate to receive negative charge. This will be seen from the following considerations:—If a small increase in the filament emission occurs when the current is

Fig. 4.



adjusted to the critical value giving the saturation distribution 3 (fig. 3 (a)) there is a sudden increase in the number of electrons entering the space between G and P. This space becomes momentarily super-saturated, and the field readjusts itself to something like fig. 3 (b). If this change is very sudden the electrons originally between P and P<sub>1</sub> are still in that space when the zero of potential moves to P<sub>1</sub>, and thus for an instant these electrons produce the potential distribution shown by the dotted part of the curve in fig. 4.

This distribution is unstable, and some of the electrons in it move on to the plate and charge it negatively. If the plate only goes slightly negative for this first disturbance so that in the distribution set up the space carrying the current is nearly saturated, further slight disturbances will cause more electrons to move to the plate, and the final potential of the plate depends on the total charge it has received.

The fact that distribution 3 (*c*) is always obtained instead of 3 (*b*) shows that the emission from a filament, though very steady, is not steady enough to prevent the above process occurring.

Even the stable distribution of the type *a*(1) can be changed to type *c*; the abnormal curve was obtained by establishing the normal field indicated by a point such as A (fig. 1) for a low emission, and then momentarily brightening the filament by shortening a few turns of the filament rheostat, the plate in this case being insulated. The electrometer at once showed a large negative deflexion to a point B which remained permanent when the emission returned to its original value.

The ease with which a static field can be upset by the minutest variation in the source of electrons constitutes a real danger in the interpretation of certain experiments. In the above experiments, if it had been assumed that the fields were always static, it would not have been possible to interpret the results in any other way than by saying that the electrons in their passage across the valve had picked up from other sources energies of several volts.

Although *V* is the greatest fixed potential difference in the system, some of the electrons attain an energy greater than  $eV$ .

Professor Townsend has given me much advice and criticism.

---

LXXXIX. *A Contribution to the Theory of Torsional Oscillations in Plastic Solids.* By JAMES P. ANDREWS, *M.Sc.*,  
*East London College* \*.

FROM time to time, explanations of the phenomenon of flow in solids have been attempted, various reasonable hypotheses being advanced to explain particular aspects. However different in other respects, these suggestions have one factor in common, namely, that during flow the solid possesses a certain fluidity which prevents parts of it from withstanding stress. The primary aim of this work is to embody that fact in an approximate equation of motion which will be of such a form as to allow specific hypotheses to be considered in some detail. A secondary aim is to demonstrate that the application of this theory leads to a

\* Communicated by the Author.



general explanation of the variation of logarithmic decrement with amplitude in torsional oscillations, even in cases where the amplitude is so small that the elastic limit is not surpassed.

This is not the first occasion upon which such an explanation has been put forward, for I have since found that Wiechert \* expressed similar fundamental ideas in a theory of the elastic after-effect, in which he has, however, restricted his attention to a particular hypothesis from the start; and Prof. Peddie † has developed a hypothesis as to the molecular alterations in a strained plastic substance, which has certain points nearly in common with the present theory. In this paper, however, a development not restricted to particular hypotheses is attempted.

Experimental results with which to compare this theory are almost entirely confined to the investigations of the logarithmic decrement, and a brief review of the chief conclusions is appropriate. Among the first investigators H. Streintz ‡ concluded that logarithmic decrement was independent of the amplitude of vibration, of the dimensions of the wire under observation—apart from the effect considered to be due to change of period,—and of the moment of inertia of the vibrating body suspended from the wire. For oscillations of longer period, the logarithmic decrement was smaller. This invariability of log. dec., although scarcely borne out by the contemporaneous work of Pisati §, agrees well with Boltzmann's theory of the after-effect ||. On the other hand, Prof. Peddie and his collaborators have given a definite law of variation of decrement with amplitude according to which, if  $y$  is the decrement and  $x$  the number of oscillations from the start,  $y^*(x+a)=b$ . Moreover, in some at least of their experiments, the motion was not simple periodic, motion outward being more rapid than motion inward. Similarly, we have the results of K. E. Guthe and L. P. Sieg ¶, which show that Platinum-Iridium and Bismuth wires—both brittle materials,—when oscillating with rather large amplitudes, exhibit a rapid decrease of both log. dec. and period as the oscillation dies down. Then

\* Wiechert, *Wied. Ann.* l. pp. 348 and 546 (1893).

† W. Peddie, *Proc. Roy. Soc. Edin.* p. 225 (1912-3).

‡ H. Streintz, *Wien. Ber.* lxx. p. 337 (1874), & lxxx. Abt. 2, p. 397 (1879).

§ G. Pisati, *Gaz. Chim. Ital.* t. vi. (1876), t. vii. (1877).

|| L. Boltzmann, *Abh.* i. p. 616.

¶ K. E. Guthe and L. P. Sieg, *Phys. Rev.* xxx. p. 132 (1910). L. P. Sieg, *Phys. Rev.* xxxi. p. 421 (1910).

Bouasse and Carrière \* have shown that an iron wire exhibits a clearly defined maximum decrement for a particular value of the amplitude. Kei Iokibe and S. Sakai † find again that the log. dec. decreases as the oscillation decays, but this time not for large amplitudes only; and, finally, G. Subrahmaniam and D. Gunnaiya ‡ show a variety of curves for different substances, where, even for small amplitudes, the log. dec. sometimes is constant, sometimes increases, but generally decreases at a decreasing rate, as the motion dies away. It appears fairly well established that the log. dec. varies in some cases in a rather complicated way, even for small amplitudes. We may perhaps conclude with G. Masing that the matter is not yet sufficiently unravelled to allow of a simple theory to include all cases. A little more generality is secured in this paper by avoiding hypotheses connected with the actual mechanism of the physical changes which occur.

Consider, then, a rod of the material of length  $l$ , and cross-section a circle of radius  $r_0$ . Let the upper end be maintained always at rest, and the lower end, to which is attached a body of moment of inertia  $I$ , let us suppose to be twisted through an angle  $\theta$  about the axis of the rod.  $I$  is to be so large that the moment of inertia of the rod itself about its axis is negligible in comparison. Let the whole be placed in an evacuated chamber.

Select a cylindrical element as in fig. 1, coaxial with the wire, of radii  $r$  and  $r + dr$ , and length unity. Its lower end is twisted through an angle  $\alpha_0$  relatively to the upper end, where, if we may assume as usual that the twist is uniform,  $\alpha_0 = \theta/l$  (fig. 1).

If no flow occurs, the shear stress on this element may be shown to be  $n\alpha_0 r$ , where  $n$  is the rigidity. If, however, flow has occurred,  $\alpha_0$  will be greater for a given couple than ordinary elastic theory would lead us to expect. Since  $\alpha_0$  is the actual angle of twist, we must therefore write for the stress called forth by the deformation  $n(\alpha_0 r - \psi_0)$  where  $\psi_0$  is (or may be) a function of  $\alpha_0$ ,  $r$ ,  $t$ , where  $t$  is the time. We shall take account later of forces elicited by the motion, or change of deformation. It is conceivable that if flow occurs, a straight line drawn in the material, as the radius

\* Bouasse and Carrière, *Ann. de Chem. et de Phys.* 8me ser. p. 190, t. 14.

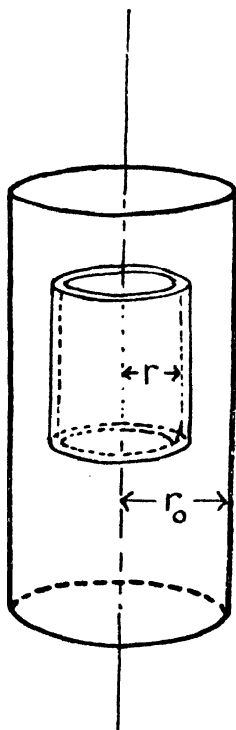
† Kei Iokibe and S. Sakai, *Phil. Mag.* xlii. p. 397 (1921)

‡ G. Subrahmaniam and D. Gunnaiya, *Phil. Mag.* xlix. p. 711 (1925).  
G. Subrahmaniam, *Phil. Mag.* l. p. 716 (1925).

of a section, will not remain straight; that is,  $\alpha_0$  may be a function of  $r$ . In any case, we have insufficient data to determine this function, and since we shall deal only with small oscillations, we shall take  $\alpha_0$  to be independent of  $r$ . The function  $\psi_0$ , related to  $\alpha_0$ , is also unknown; but a plausible and sufficiently general assumption is that

$$\psi_0(\alpha_0, r, t) = R \cdot \psi(\alpha_0, t),$$

Fig. 1.



where  $R$  is some function of  $r$  alone, and  $\psi$  does not contain  $r$ . On these assumptions, the restoring couple at any instant is

$$\begin{aligned} C &= \int_0^{r_0} 2\pi r^2 n(\alpha_0 r - \psi_0) dr \\ &= \frac{n\pi r_0^4 \alpha_0}{2} - n\psi(\alpha_0, t) \int_0^{r_0} 2\pi r^2 R dr. \end{aligned}$$

Now  $\int_0^{r_0} 2\pi r^2 R dr = \mu$ , is a constant whose value depends only on the radius of the rod, so that we may write

$$C = \frac{n\pi\alpha_0 r_0^4}{2} - n\mu\psi(\alpha_0, t). \quad (1)$$

Defining  $Q$  as  $\mu/R_0$ , where  $R_0$  is the value of  $R$  at  $r_0$ , again a constant depending only on the radius, we may write this equation

$$nQ(\alpha_0 r_0 - R_0\psi) + n\alpha_0 r_0 \left( \frac{\pi r_0^3}{2} - Q \right) = C,$$

$$\text{or} \quad nQ\phi + \frac{n\theta r_0}{l} \left( \frac{\pi r_0^3}{2} - Q \right) = C, \quad (2)$$

where  $\phi = (\alpha_0 r_0 - R_0\psi)^*$  is a convenient measure of the elastic strain in a particular wire; for it is the quantity to which the stress on the bounding element is proportional. We shall employ it later as a parameter with this meaning.

To obtain an idea of the possible magnitude of  $Q$ , let us imagine, as a rough test only, that  $R$  varies as the  $m$ th power of  $r$ . Then  $Q$  lies between 0 and  $\frac{2\pi r_0^3}{3}$ . This is sufficient to indicate that  $Q$  is of the same order as, or less than,  $\frac{\pi r_0^3}{2}$ .

Angular velocities are to be small, but the solution of this problem clearly depends in an important way upon the resistance due to motion, and it may not be sufficient to assume resistance proportional to velocity, even when  $\dot{\theta}$  is small. Let the resistance in the first case be  $\Omega\dot{\theta}$ , where  $\Omega$  is a function which may depend explicitly on the time. Then the equation of free motion of the suspended body may be written (see equation (1))

$$I\ddot{\theta} + \Omega\dot{\theta} + b\theta = A\psi \quad (3)$$

where  $A = n\mu$ .

The solution of the equation depends on the form of the functions  $\Omega$  and  $\psi$ , of which the latter is a measure of the flow. The following investigation shows, that if  $\Omega$  is not a constant and both  $\Omega$  and  $\psi$  are chosen to make the equation integrable, only by rather arbitrary assumptions can the solution be made to conform with experience. It was undertaken, however, at the suggestion of Prof. Lees, with

\* This is closely related to the "Katastasic" strain of Wiechert.

the object of tracing more accurately, if possible, the way in which the flow must enter the equations. Thus :—(1) If  $\Omega = \alpha/t$ , then the equation reduces to Euler's form

$$t\ddot{\theta} + \frac{\alpha}{t}\dot{\theta} + \frac{b''\theta}{t^2} = f(t)$$

provided  $A\psi = b\left(\theta - \frac{b'\theta}{t^2}\right) + f(t)$ , a not altogether unwarrantable assumption, where  $\alpha$ ,  $b'$ ,  $b''$ , are constants. Euler's form, however, for any reasonable assumption regarding  $f(t)$ , leads to a kind of oscillation in which the period very rapidly increases as the amplitude decreases. Nothing of this kind is known.

(2) Let  $\Omega = 1/t$ , and  $A\psi = \left(b - 1 + \frac{n^2}{t^2}\right)\theta$  where  $n^2$  is a constant. Then eqn. (3) may be written

$$t^2\ddot{\theta} + t\dot{\theta} + (t^2 - n^2)\theta = 0,$$

which is Bessel's equation of the  $n$ th order. We note first, that when  $t$  is fairly large, this becomes

$$\ddot{\theta} + \frac{\dot{\theta}}{t} + \theta = 0$$

which is Bessel's equation of zero order, the most general solution of which is

$$\theta = AJ_0(t) + BY_0(t),$$

where  $Y_0$  is Weber's function of zero order.

By choosing the origin of time suitably, we make  $B=0$  and the solution, using the asymptotic expansion is then

$$\theta = A_1 \frac{1}{\sqrt{t}} \cdot \cos\left(t - \frac{\pi}{4}\right).$$

Very clearly this is the right form of variation of amplitude. Unfortunately, the limiting value of the log. dec. is zero, as otherwise appears from the original equation, which becomes when  $t$  is very large,

$$\ddot{\theta} + \theta = 0,$$

the equation of undamped periodic motion. I know of no such case. This may, however, be circumvented by modifying  $\Omega$  and  $\psi$ .

$$(3) \text{ Let } \Omega = \left( \alpha + \frac{1}{t} \right), \text{ and } A\psi = \left( b + \frac{\alpha^2}{4I} + \frac{\alpha}{2t} + 1 \right) \theta.$$

Write  $\frac{\alpha}{I} = 2a$  where  $a$  is constant.

Then a particular solution to this equation is

$$\theta = A_0 e^{-at} J_0(t) = B \frac{1}{\sqrt{t}} e^{-at} \cos \left( t - \frac{\pi}{4} \right) \text{ approx.,}$$

and this will suffice as solution to this case, if we choose the origin of time correctly.

This represents a similar variation to that before obtained, but one which now gives us a log. dec.  $= \pi a$ , for infinitely small amplitudes. This is the type of variation most often found in practice, and this solution indicates that a decrease of the resistance with time (which has already been denoted "Accommodation" by early investigators), and an interdependence of the flow and the resistance of the kind indicated, can account for the variation of logarithmic decrement.

On the other hand, there is admittedly something very artificial about this method of searching for the solution, and a more simple method, if it will produce similar results, is clearly preferable. We therefore proceed with the exploration, after mentioning that many other equations have been tried without success, by putting  $\Omega = \text{constant}$ , as the simplest, and try likely functions for  $A\psi$ .

Forms to be tried are limited to those which will make the equation integrable, and the simplest may be tried first.

(1) Let  $A\psi = g\theta + ht$  where  $g$  and  $h$  are constants. This is the simplest way of allowing the time effect to continue increasing. It is equivalent to the notion of a flow which, once started, proceeds to relax the stresses at a constant pace until they are reduced to zero.

This leads without difficulty to the solution

$$\theta + H = Gt + Ae^{x_1 t} + Be^{x_2 t},$$

where  $G$  and  $H$  are formed from the constants of the original equation,  $A$  and  $B$  are arbitrary,  $x_1, x_2$  are

$$-\frac{\alpha}{2I} + \sqrt{\frac{\alpha^2}{4I^2} - \frac{b-g}{I}} \quad \text{and} \quad -\frac{\alpha}{2I} - \sqrt{\frac{\alpha^2}{4I^2} - \frac{b-g}{I}}.$$

In the periodic case this indicates an ordinary damped vibration of constant logarithmic decrement, but whose equilibrium position is drifting at a constant angular speed

in the positive or negative direction of  $\theta$ , according as  $g$  is less than, or greater than,  $b$ .

(2) Let  $A\psi = ct$  where  $c$  is a positive constant. This will have a similar interpretation to the last. It makes equation (3)

$$\ddot{\theta} + \frac{\alpha}{1} \dot{\theta} + \theta \left( \frac{b}{1} - \frac{ct}{1} \right) = 0.$$

With the substitutions  $\theta = ve^{-\frac{1}{2} \frac{\alpha}{1} t}$ , and  $y = h - kt$ , where  $h$  and  $k$  are constants, this becomes an alternative form of Riccati's equation, viz.,

$$\frac{d^2 v}{dy^2} + \frac{1}{k^2} y v = 0,$$

the solution of which in Bessel functions is \*

$$v = y^{\frac{1}{2}} \left[ A J_{\frac{1}{2}} \left( \frac{2}{3k} y^{\frac{3}{2}} \right) + B J_{-\frac{1}{2}} \left( \frac{2}{3k} y^{\frac{3}{2}} \right) \right],$$

where  $A$  and  $B$  are constants. The meaning being that, as the oscillation proceeds and the restoring force is gradually reduced to zero, the oscillation dies out: in a finite time however. After this, the solution will correspond to an unstable condition, in which  $\theta$  proceeds at an increasing rate in one direction only. Only the first part can we regard as approximating to any likely case.

Clearly, simplest assumptions regarding flow do not lead to very satisfactory solutions, and we may therefore proceed to the more complicated.

(3) Let  $A\psi = A_1 p \theta (1 - e^{-qt})$  where  $A$ ,  $p$ , and  $q$  are constants. This represents a flow, or at least an increase in the deformation, proportional to the angle of twist, reversing its direction with the twist; and also increasing independently with the lapse of time, from zero to a steady value, in such a way that the partial derivative with respect to time continually diminishes.

Equation (3) must now be written

$$I\ddot{\theta} + \alpha\dot{\theta} + b_1\theta = -B\theta e^{-qt}$$

where  $b_1 = (b - A_1 p)$ , and  $A_1 p = B$ .

The character of the solution is well brought out by successive approximations, commencing by neglecting the right-hand member of the equation, which is permissible if  $B$  is small. The solution thus obtained is then used to

\* Forsyth 'Differential Equations.'

evaluate  $-B\theta e^{-qt}$ , and a second approximation is made. After a few repetitions, it becomes clear that the solution may be expressed by an infinite series

$$\theta = \sum_{m=0}^{m=\infty} \left[ A_m e^{\left\{ -\left(\frac{a}{2l} + mq\right) + \sqrt{\frac{a^2}{4l^2} - \frac{b_1}{l}} \right\} t} + B_m e^{\left\{ -\left(\frac{a}{2l} + mq\right) - \sqrt{\frac{a^2}{4l^2} - \frac{b_1}{l}} \right\} t} \right]$$

in which the constant coefficients of the first two terms are arbitrary, the remainder related to them. Further

$$A_{r-1} > A, \quad B_{r-1} > B_r \text{ for all values of } r,$$

so that the coefficients form a convergent series. Clearly, we need only retain the first few terms of the series, since the higher terms are smaller, and decay more rapidly. If the motion is oscillatory, as we are to consider, the series may be written

$$\theta = \sum_{m=0}^{m=\infty} C_m e^{-\left(\frac{a}{2l} + mq\right)t} \cos(nt + \delta_m),$$

where  $\delta_m$  is a const. and  $n = \sqrt{\frac{b_1}{l} - \frac{a^2}{4l^2}}$ .

We may arrange initial conditions so that  $\delta_0 = 0$ , and it then follows that  $\tan \delta_1 = \frac{2n}{q}$ , and similarly for other  $\delta$ 's, so that in the event of  $q$  being large, we may write

$$\theta = \cos nt \sum_{m=0}^{m=\infty} C_m e^{-\left(\frac{a}{2l} + mq\right)t} \text{ approx.}$$

This type of solution is to be discussed in detail later (case 4), and it will be sufficient to say here that it represents an oscillation of nearly constant periodic time, whose logarithmic decrement diminishes as the amplitude decreases, in a manner very suggestive of certain experimental results. If, however,  $q$  is not large, we must replace  $\cos nt$  by  $\cos(nt + \delta)$  in the solution, where  $\delta$  is a function of the time, which reduces to a constant after a long time; the oscillation ending, as it dies out, as an ordinary damped vibration with a constant logarithmic decrement.

It is nevertheless very important to notice that both the periodic time and the log. dec. are related to the quantity  $n$ , which is a definite function of the dimensions of the wire.

(4) Let  $A\psi = A_2 e^{p\theta} (1 - e^{-qt})$  where  $A_2$ ,  $p$ , and  $q$  are positive



constants. This is merely a variant on the last, being mathematically rather simpler, but representing the flow as being non-symmetrical, since  $e^{p\theta}$  is not symmetrical with respect to  $\theta$ . This will resemble the case of a rod which has been twisted too far in one direction before the experiment began.

Equation (3) becomes

$$I\ddot{\theta} + \alpha\dot{\theta} + b\theta = A_2 e^{p\theta} (1 - e^{-q\theta}), \quad . \quad . \quad . \quad (4)$$

or, writing

$$\theta = \omega e^{p\theta}, \quad k_1 = p + \frac{\alpha}{2I}; \quad N^2 = p^2 + \frac{\alpha}{I} p + \frac{b}{I}; \quad A_1 = \frac{A_2}{I};$$

$$\ddot{\omega} + 2k_1\dot{\omega} + N^2\omega = A_3 - A_3 e^{-q\theta},$$

the solution of which by the ordinary rules is

$$\omega = A_3 \left( 1 - \frac{1}{B_2} e^{-q\theta} \right) + B_1 e^{(-k_1 + \sqrt{k_1^2 - N^2})t} + C_1 e^{(-k_1 - \sqrt{k_1^2 - N^2})t},$$

where

$$B_2 = q^2 - 2k_1q + N^2,$$

and where, if  $N^2 > k^2$ , the system oscillates in the manner given by

$$\omega = A_3 \left( 1 - \frac{1}{B_2} e^{-q\theta} \right) + E e^{-k_1 t} \cos (\sqrt{N^2 - k_1^2} t + \beta), \quad (5)$$

$E$  and  $\beta$  being arbitrary constants.

Whether the system oscillates or not, after a long time it returns to rest at a new position of equilibrium given by  $\omega = A_3$  or  $\theta = \text{constant}$ . This angular distance depends on the radius of the rod, and the moment of inertia of the suspended body.

Since  $\theta$  is always to be small,  $p\theta$  may be taken as a small quantity also, so that

$$\omega = \theta e^{-p\theta} = \theta (1 - p\theta + \frac{p^2\theta^2}{2} + \dots) \text{ approx.}$$

The solution in the form of equation (5) may then be interpreted to mean that the oscillations are not symmetrical, in such a way that excursions in the positive direction of  $\theta$  exceed the value given by

$$\theta = A_3 + E e^{-k_1 t} \cos (\sqrt{N^2 - k_1^2} t + \beta),$$

and on the negative side fall short of this value, by quantities which are roughly proportional to the squares of the amplitudes, if  $q$  is large enough.

The two roots of the approximate equation

$$p\theta^2 - \theta + A + E e^{-k_1 t} = 0$$

give us the equations to the two curves upon which the maximum and minimum values of  $\theta$  will lie. From these we may derive information concerning the decrement. It is easy to verify that if  $p$  and  $k$  are small, the decrement (and therefore the log. dec.) increases or decreases from one steady value to another as the amplitude diminishes, according as the constant  $E$  is positive or negative. The experimental results contain both kinds of variation.

It might be further pointed out that the conditions for oscillation in both cases (3) and (4) show that we may pass from the oscillatory to the aperiodic condition by changing the dimensions of the rod and of the vibrating body. No essential change is made by retaining  $\frac{A_3}{B_2} e^{-qt}$ .

## SECOND METHOD.

We may now try a method of expression in which the assumption as regards time is less arbitrary and the forms tried are more definite in meaning.

First, let  $\frac{d\psi_0}{dt} = f(\phi)$ , where  $\phi$  has the parametric meaning already assigned to it. This expresses the idea that the rate of flow depends on the elastic or "katastasic" part of the strain.

$$\text{Since} \quad \psi_0 = R\psi, \quad R \frac{d\psi}{dt} = f(\phi). \quad . \quad . \quad . \quad (6)$$

From (3) if  $\Omega = \alpha$ , a constant,

$$R_0 \psi = \frac{I}{nQ} \ddot{\theta} + \frac{\alpha}{nQ} \dot{\theta} + \frac{b}{nQ} \theta.$$

Hence

$$R_0 \dot{\psi} = \frac{1}{nQ} (I\ddot{\theta} + \alpha\dot{\theta} + b\theta) = f_0(\phi), \quad . \quad . \quad . \quad (7)$$

where  $f(\phi) = f_0(\phi)$  when  $R = R_0$ .

Also, since

$$\begin{aligned} \phi &= (\alpha_0 r_0 - R_0 \psi) \\ \phi &= - \left[ \frac{I}{nQ} \ddot{\theta} + \frac{\alpha}{nQ} \dot{\theta} + \theta \left( \frac{b}{nQ} - \frac{r_0}{l} \right) \right]. \quad . \quad . \quad (8) \end{aligned}$$

Also

$$f_0(\phi) = \frac{R_0}{R} f(\phi).$$

So that the problem is now to obtain a solution of the simultaneous differential equations (7) and (8) for  $\theta$ , after suitable assumptions as to  $f'(\phi)$  have been made. In general the equations are too complicated for exact solution, and recourse must be had to approximations, to reveal the character of the motion.

(5) Let  $f_0(\phi) = k\phi$  where  $k$  is a small positive constant.

This requires  $f(\phi) = \left(\frac{k \cdot R}{R_0}\right)\phi$ .

Our equation of motion then reduces to

$$\frac{1}{nQ} \ddot{\theta} + \ddot{\theta} \left( \frac{\alpha}{nQ} + \frac{kI}{nQ} \right) + \dot{\theta} \left( \frac{b}{nQ} + \frac{ak}{nQ} \right) + k\theta \left( \frac{b}{nQ} - \frac{r_0}{l} \right) = 0.$$

But if  $k$  is small enough, we may neglect the last term, whereupon, one integration gives

$$I\ddot{\theta} + (\alpha + kI)\dot{\theta} + (b + k\alpha)\theta = A \text{ where } A \text{ is constant,}$$

$$\text{or if} \quad \omega = \theta - \frac{A}{b + k\alpha},$$

$$I\ddot{\omega} + (\alpha + kI)\dot{\omega} + (b + k\alpha)\omega = 0,$$

the solution of which is

$$\omega = Be^{x_1 t} + Ce^{x_2 t},$$

$$\text{where} \quad x_1, x_2 = -\frac{\alpha + kI}{2I} \pm \sqrt{\left(\frac{\alpha + kI}{2I}\right)^2 - \frac{b + k\alpha}{I}},$$

(B and C are constants)

an ordinary damped motion, in which, if

$$b + k\alpha > \frac{\alpha^2}{4I^2} + \frac{k}{2} + \frac{k^2 I}{4},$$

the system performs damped oscillations about a position

$\theta = \frac{A}{b + k\alpha}$ , with constant period  $T = \frac{2\pi I}{b + k\alpha}$ , and constant log. dec.

$$\lambda = \frac{\pi(\alpha + kI)}{2(b + k\alpha)} \dots \dots \dots (9)$$

The interest of this result lies in the demonstration that a constant log. dec. is possible in the complete absence of

resistance or "internal friction" ; for if  $\alpha$  is put equal to zero in (9),  $\lambda_0 = \frac{\pi kI}{2b}$ , and the constant log. dec. would then determine  $k$ . The first assumption of this case is not unreasonable, since it merely implies that the rate of flow is proportional to the elastic stresses in those portions of the material which remain capable of withstanding them ; or, in short, the flow is proportional to the force producing it, if  $f(\phi)$  contains  $R$  as shown above.

(6) Let  $f_0(\phi) = p\phi^3$  where  $p$  is a positive constant, and not large.

This requires  $f(\phi) = \frac{pR}{R_0} \phi^3$ .

In this instance rate of flow is taken proportional to the cube of the forces producing it, to exemplify the law  $f(\phi) = p\phi^n$ . For symmetry,  $n$  must be odd.

A numerical example will be found helpful in this instance, and I have selected an aluminium wire and vibrating body, specified as follows :— $l = 100$  cm.,  $r = 0.5$  cm.  $n = 2.6 \times 10^{11}$  dynes/cm.<sup>2</sup>,  $I = 2 \times 10^5$  gram. cm.<sup>2</sup> ; so that  $b$  is about  $3 \times 10^4$  ; the approx. time of vibration  $T = 15$  sec. ; and if successive maximum amplitudes are reduced in the ratio 10 : 9, we may take  $\alpha$  to be  $5 \times 10^3$  (or less—see result of Case (5)). The value of  $Q$  may be roughly estimated in the way already indicated.

In (8) the first term has the largest coefficient, the third a coefficient of the order one tenth or less of the first, and the second a much smaller coefficient still. In order to obtain the essentials of the solution with moderate ease, we shall neglect the second and third terms in comparison with the first. The equation of motion may then be written

$$I\ddot{u} + au + bu = - \frac{pI^3}{n^2Q^2} (\dot{u})^3,$$

where  $u = \theta$ .

Now  $\frac{pI^3}{n^2Q^2}$  is, in general, small compared with the other coefficients, and the usual method of successive approximation may be used as in Case (1). The algebra, though laborious, is straightforward, and need not occupy space here. At every stage, very small terms are dropped, the numerical example helping in such selection. The results of the first

three approximations are as follows :—

$$\text{1st approx. } u_1 = B e^{-\frac{\alpha}{2I}t} \cos(\rho t + \delta),$$

$$\text{where } \rho = \sqrt{1 - \frac{\alpha^2}{4I^2}}.$$

$$\text{2nd approx. } u_2 = B e^{-\frac{\alpha}{2I}t} \cos(\rho t + \delta)$$

$$- 3E e^{-\frac{3\alpha}{2I}t} \cos(\rho t + \delta),$$

in which  $3E$  is small compared with  $B$ .

$$\text{3rd approx. } u_3 = u_2 + \text{a term much smaller still.}$$

Succeeding approximations merely add terms which are not only smaller in amplitude, but which die out quicker. We need only attend to the solution as given in  $u_2$ .

Let us now choose initial conditions so that  $\delta = 0$ , and we have, finally,

$$u = \left( B e^{-\frac{\alpha}{2I}t} - 3E e^{-\frac{3\alpha}{2I}t} \right) \cos \rho t,$$

and therefore

$$\begin{aligned} \theta - G = & -\frac{I\rho}{b} B \sqrt{1 + \frac{\alpha^2}{4I^2\rho^2}} e^{-\frac{\alpha}{2I}t} \cos(\rho t + \epsilon) \\ & - \frac{\rho}{b + \frac{2\alpha^2}{I^2}} 3E \sqrt{1 + \frac{9}{4} \frac{\alpha^2}{I^2\rho^2}} e^{-\frac{3\alpha}{2I}t} \cos(\rho t + \sigma), \end{aligned}$$

$$\text{where } \tan \epsilon = \frac{2I\rho}{\alpha} \text{ and } \tan \sigma = \frac{1}{3} \tan \epsilon.$$

In general,  $\tan \epsilon$  is large—near 40 in the numerical example, and is probably greater—and little error will therefore be made in the approximation if  $\epsilon$  is taken equal to  $\sigma$ , which indeed is probably correct to two or three per cent., and each of these equal to  $\frac{\pi}{2}$  so as to allow us to write, abbreviating the coefficients,

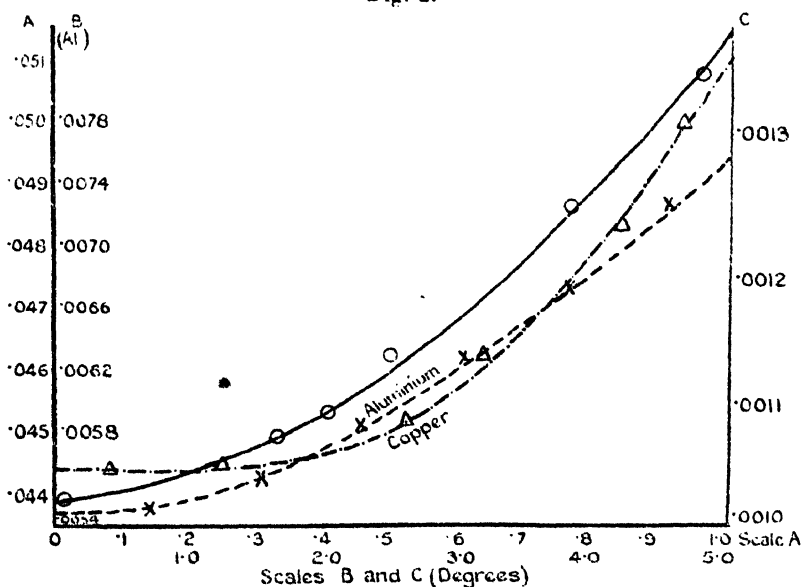
$$\theta - G = -\sin \rho t \{ H_1 e^{-\frac{\alpha}{2I}t} + H_2 e^{-\frac{3\alpha}{2I}t} \},$$

in which it appears that  $H_2$  is considerably smaller than  $H_1$ , both of them depending, however, on the arbitrary constant  $B$ , and  $H_2$  on the constant  $p$ ; both  $H_1$  and  $H_2$  are positive. The motion is clearly an oscillation whose amplitude decays in a rather complicated way. As this is an important case, a numerical example has been calculated by putting  $H_1 = 1$ ,  $H_2 = .1$ , other quantities being as laid down. The unbroken curve in fig. 2, to which scale A applies, gives the result of

this calculation, and the broken curves show the experimental results for aluminium and copper wires, from Subrahmanian. I have selected those curves which are in best agreement with the calculation. Scales B and C apply to these (fig. 2).

In this case the motion is clearly similar to that sometimes obtained practically, and it is suggested that the explanation of the variation of log. dec. is that given here. Case (4) clearly shows, however, that the magnitude of the log. dec. for infinitesimal amplitudes depends primarily on the resistance measured by  $\alpha$ , the flow being responsible for the rate

Fig. 2.



For the sake of a clear diagram, the curves in fig. 2 are drawn separated; but obviously, by a small adjustment of the scales, they could be made to lie more nearly along one another; the aluminium curve, indeed, would almost coincide with the calculated one. This last would present the same appearance whether drawn for large or small amplitudes, so that it is the shape only which is important.

of change of decrement. Now, many experiments have shown that when the dimensions of the wire are changed so that the period is increased, the log. dec. for a given amplitude is decreased. This indicates that  $\alpha$  is a function of the dimensions, which always diminishes for any change of dimensions which increases the period. For changes in the radius this is clearly the case; when the length increases

for a given angular velocity of the vibrating body, the relative angular velocity between the two ends of the element considered at the beginning is inversely proportional to the length of the wire. With this in view the condition may be fulfilled, and the theory is not in any way contradictory to practice.

*Other Cases.*—It becomes clear that the law  $A\psi = k(\phi)^{2m+1}$  will not lead to any fundamentally different kinds of motion, but will only introduce decaying terms in the amplitudes, whose rates of decrease will depend on other multiples of  $\alpha/2I$ . It is, however, possible that the phase angles such as  $\epsilon$ ,  $\sigma$ , in the above, will not be nearly equal. In such an event we must include a phase angle in the result, which phase angle will be a function of the time.

With this always allowable, we may conclude from the fact that our differential equations are linear (in the approximate method), that solutions found for various powers of  $\phi$  are additive, in the sense that if  $\theta = M$  is the solution when  $A\psi = k_m\phi^m$ , and  $\theta = N$  when  $\theta\psi = k_n\phi^n$ , then  $\theta = M + N$  when  $A\psi = k_m\phi^m + k_n\phi^n$ . Hence, except for a different rate of change of logarithmic decrement with amplitude, nothing new is introduced if we assume

$$A\psi = k_1\phi + k_3\phi^3 + k_5\phi^5 + \text{etc.},$$

all the constants being positive.

(Other trials could be made, but the calculations are sufficient to justify the hypotheses employed to explain those aspects of the phenomenon of flow dealt with here. It appears, too, that the assumption that flow is proportional to an odd power of the elastic stresses does lead to the prediction of a variation of logarithmic decrement which agrees with experiment. It is suggested that this affords an explanation of this effect, at least in some metals.

For encouragement and valuable advice during the course of the work, my thanks are tendered to Prof. C. H. Lees.

#### SUMMARY.

The equations of motion of a torsional pendulum whose suspension is a wire of plastic material, are worked out in two different forms which are kept as general as possible. The first form is employed to trace by trial the manner in which the flow varies with the time and the twist. With the second form, a definite hypothesis, that the rate of flow is proportional to an odd power of the elastic stresses, is developed, and is shown to lead at once to an explanation of the observed variation of logarithmic decrement with amplitude.

XC. *The Mobilities of the Positive Ions formed by Alpha Rays in Air, Hydrogen, and Helium.* By J. S. ROGERS, B.A., M.Sc., Senior Lecturer in Natural Philosophy, University of Melbourne\*.

#### INTRODUCTION.

THE mobility of positive ions has been shown to vary with the life of the ion by Erikson† and Wahlin‡. These authors have found that the mobility of the “normal” positive ion in air was 1·4 cm./sec. per volt/cm.; but if the mobility was measured in a very short time after the ion was formed (of the order of 1/50 sec.), the value obtained was 1·89 cm./sec., which is approximately the same as that of the negative ion. In addition to these values of the mobility, Nolan§ has reported evidence of many more types of positive ions—mobilities as high as 12·4 cm./sec. having been obtained. Later, Wahlin|| found mobilities of positive air-ions as low as ·970 cm./sec.

The dependence of the mobility of positive ions on their life has been investigated in air, hydrogen, and helium. The method employed was a modification of the original method of Rutherford¶, in which an alternating potential was produced by means of a commutator. The ionization was produced by alpha rays which, by means of a sectorised metal disk carried on the shaft of the commutator, were allowed to enter the mica window of the ionization vessel once only in every revolution. With the arrangement used the life of the ion could be measured accurately.

In addition, the apparatus was devised to examine helium for the presence of doubly-charged positive ions which had been reported by Millikan\*\* and Wilkins††.

#### DESCRIPTION OF THE APPARATUS.

The apparatus consisted of an ionization chamber and a compensating chamber, the upper insulated electrodes of each being connected to the same quadrant of a Dolezalek

\* Communicated by Sir E. Rutherford, O.M., P.R.S.

† Erikson, *Phys. Rev.* xx. p. 117 (1922).

‡ Wahlin, *Phys. Rev.* xx. p. 267 (1922).

§ Nolan, *Proc. Roy. Irish Acad.* xxxvi. p. 74 (1923).

|| Wahlin, *Phil. Mag.* xlix. p. 566 (1925).

¶ Rutherford, *Phil. Mag.* v. p. 95 (1903).

\*\* Millikan, *Phys. Rev.* xviii. p. 456 (1921).

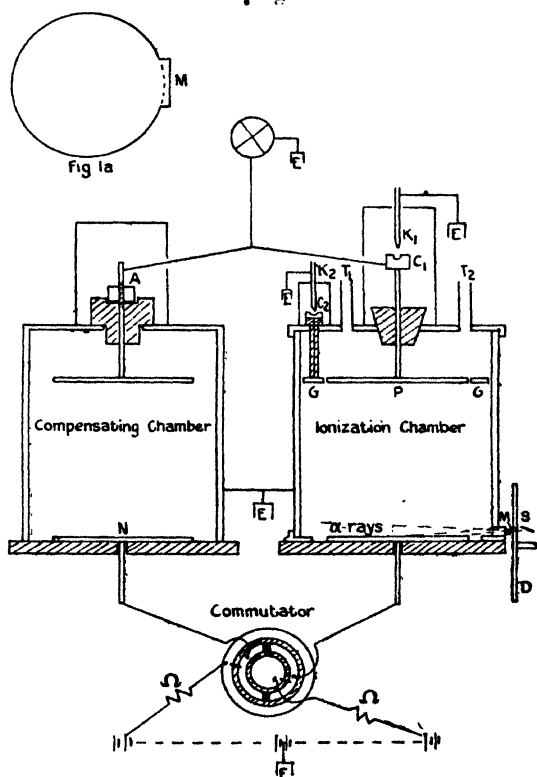
†† Wilkins, *Phys. Rev.* xix. p. 210 (1922).



electrometer. The sensitivity of the instrument was 600 mm. per volt when the needle potential was 200 volts and the lamp and scale 150 cm. from the electrometer.

The ionization vessel (see fig. 1) consisted of a hollow brass cylinder 10 cm. in diameter and 12 cm. high. The bottom of the vessel was made of ebonite 1 cm. thick. The curved side of the brass vessel fitted into a ring of brass

Fig. 1.



which was screwed down to the ebonite. This curved side was fastened to the ring with picein, while soft wax made the ring-ebonite joint air-tight. An insulated plate *L* about 8 cm. in diameter was placed on the ebonite, and connexion was made between this plate and the commutator by a lead which passed through the ebonite. The upper plate *P* of the ionization vessel and the guard-ring *G* were carried by the lid of the vessel. The lead to the plate passed through an amber stopper, and could be earthed by the key *K*<sub>1</sub>.

The guard-ring could be earthed by the key  $K_2$ . The source of  $\alpha$ -rays was polonium on a copper plate about 2 cm. long and 3 mm. wide, which was mounted with its long edges horizontal and with the other edges at an angle of  $30^\circ$  to the horizontal. This was so inclined to prevent the rays from the lower edge of the source, S, passing into the upper part of the chamber. The ideal ionizing beam for the work would have been a thin parallel horizontal one; but as this was not practicable, the beam of rays entered the chamber so that the majority of them grazed the lower plate L. The rays entered the chamber through a mica window M which had a stopping power of about 1.3 cm. of air. It was not possible to construct a window of thinner mica which would remain intact when the vessel was evacuated; in fact, there was considerable difficulty in supporting a mica window of the above thickness. It was possible to do so by soldering a flange on to the lower portion of the curved side where the mica was to be placed, as is indicated in fig. 1a. The openings in this flange consisted of three holes 4 mm. square side by side, the thickness of the metal between holes being 2 mm. The piece of mica for the window was then fastened by picein to a brass strip in the form of a grid, the holes in which corresponded to the holes in the flange. This strip, with the mica, was then fastened on to the flange with soft wax. As the melting-point of the soft wax is considerably lower than that of picein, it was possible to do this without disturbing the seal between mica and brass strip. This vessel, with the numerous wax joints, proved difficult to make gas-tight, and the difficulty was finally overcome by painting all the joints over with shellac dissolved in methylated spirits. Two brass tubes  $T_1$  and  $T_2$  were soldered on to the lid of the vessel, and glass tubes were passed into these and secured by picein. Through one of these tubes,  $T_1$ , the various gases were introduced, and through the other,  $T_2$ , the vessel was evacuated. For evacuation a Cenco Hyvac pump was used. The pressure attained by this was indicated by a discharge-tube connected to the apparatus. When the vessel was evacuated the alternative spark-gap between points was at least 2 cm., and on occasion exceeded 2 inches. After the vessel had been evacuated and left for several days, the cathode dark space was still found to be 1.5 cm., and from the colour of the discharge the gases present appeared to be vapours which arose from the various sealing agents used. The amount of these vapours was thus too small to affect seriously the purity of the gases employed.

*The Commutator.*

Difficulty was experienced in obtaining a suitable commutator. This difficulty was occasioned by two factors—first the uneven bearing of the brushes on the commutator, and second the presence of metallic dust, which caused short circuits between the insulated segments of the commutator.

All the commutators used were constructed on ebonite cylinders carried by an axial steel shaft which rotated within ball-bearings. The conducting strips were made of brass, the difference between the various commutators being merely in the nature of the end insulation separating the central segments.

In the first commutator the insulation between these central segments was of bakerlite 1.2 cm. wide, and brass brushes cut from strip .5 mm. thick were used. Four brushes were required; two bearing on the side brass cylinders were connected respectively to the positive and negative sides of the small storage-cells which provided the potential applied to the lower plate of the ionization vessel, and two diametrically opposite, bearing on the central segments, were connected to the lower plates of the ionization and compensating vessels. To protect the cells, megohms were inserted in the leads from the cells to the commutator.

The width of the insulation strip (1.2 cm.) introduced an uncertainty, for it was necessary to know how long the brush in contact with an insulating segment remained at the potential of the last conducting segment with which it had been in contact. This was ascertained by replacing the bakerlite strips with an air-gap 2 mm. wide; and by comparing readings obtained with these two commutators, it was concluded that the brush remained at the same potential the whole of the time it was in contact with the bakerlite insulation. The air-gap commutator was found to be useless for high speeds of rotation, for the brushes did not bear evenly on the commutator, and considerable irregularities were introduced into the readings.

In the final commutator the brass brushes were replaced by brushes of thin phosphor-bronze strip. The ends of these brushes, which touched the commutator, were cut with a fine saw, so that they resembled the tooth of a comb. This ensured a more even pressure on the commutator. These phosphor-bronze brushes produced a very much smaller quantity of brass dust than the brass brushes. The end insulation was here of mica, 1.7 mm. wide. This commutator proved to be much more satisfactory than any of

the previous types. The surface of the mica had, however, to be scraped lightly occasionally to remove traces of metallic dust.

To one end of the steel shaft of the commutator was attached the revolution counter, and to the other was a brass disk D (fig. 1) about 7 cm. in diameter, which moved between the source S and the mica window M. A sector of  $15^\circ$  was cut in this disk, and thus the rays could enter the ionization chamber only when the sector was between S and M. This disk was fastened by means of a screw to the steel shaft, and the position of the sector with regard to the remainder of the commutator could thus be varied. The purpose of this sector was to allow a beam of rays to be shot into the gas while the bottom plate was positively charged, and then only for a limited time. The commutator was rotated by a shunt-wound D.C. motor driven by large storage cells, and a sliding rheostat was placed in series with the motor. The rate of rotation could be maintained constant within 1 per cent. for a series of readings lasting for two hours. During every reading of the ionization current one reading at least was taken of the rate of rotation of the commutator.

#### *The Compensating Chamber.*

If the source of  $\alpha$ -rays was removed and L was charged positively (say to +200 volts), and the keys  $K_1$  and  $K_2$  raised, then the electrometer would register no charge.

If, now, the commutator were turned by hand until the potential of L were negative (—200 volts, say), the spot of light would be reflected completely off the scale, owing to the charge induced on the upper plate. The compensating chamber was used to overcome this; it was an earthed shielded vessel with the lower plate M connected to the commutator so that its potential was always opposite in sign to that of L and the upper insulated plate was connected to the electrometer. The distance between the upper and lower plates could be varied by means of the screw A, and when this vessel had the same capacity (electrostatic) as that of the ionization chamber, the reversal of the potential on L caused no deflexion of the electrometer. The actual experimental method employed was to turn the screw A until there was no deflexion on reversing the commutator. Whatever potentials were then applied to L and N, the whole apparatus remained compensated for induced charges. This adjustment was quite a sensitive one, as  $1/8$  of a turn of A could be readily detected. When the apparatus was compensated

and the commutator rotated by the motor, the earthing-keys could be raised and the electrometer was unaffected. The leads from the top plates of the ionization and compensation chambers passed through amber insulators within earthed tubes. All the insulation except the stopper at the top of the compensation chamber was of amber, the last being of sulphur. The electrostatic leak of the whole apparatus was very small; about 1 mm. in 5 min. near the zero, *i. e.* in the region where the final ionization was measured.

The potentials applied to the lower plates of the two chambers were supplied by 248 small storage-cells. One point of this battery was earthed. The potentials were measured by means of a Weston multi-range D.C. voltmeter.

#### PREPARATION OF GASES USED.

*Air.*—Before the air passed into the apparatus it was dried in a side-tube containing a tightly-fitting plug of phosphorus pentoxide. This plug occupied about one-third of the volume of the drying vessel. Before the air passed into the apparatus it was stored for at least an hour, and usually for very much longer, in this side-tube.

*Hydrogen.*—This was prepared by the electrolysis of water (plus a little sodium carbonate), nickel electrodes being used. An inverted burette was placed over the cathode, and the hydrogen as produced displaced the solution from this burette. The top of the burette was connected by a piece of pressure-tubing to the drying-tube of phosphorus pentoxide mentioned above. The hydrogen was stored in this tube for at least an hour, usually longer, before being passed into the apparatus. Hydrogen was passed through the apparatus several times before the sample, on which readings were taken, was introduced.

*Helium.*—The helium used was very generously sent to Australia by Sir Ernest Rutherford. When this arrived it was contained in a glass bulb with a drawn-out side-tube and contained nitrogen as an impurity. The tube was broken under mercury, and the helium was, by means of a mercury transfer-pump, passed backwards and forwards through finely broken-up coconut charcoal contained in a narrow tube immersed in liquid air until there was no further diminution in volume. The charcoal column was about 24 cm. long, and the charcoal had been carefully prepared and activated. During the process of the purification the charcoal was several times heated in a bath of boiling sulphur for some hours while the Hyvac pump was running.

The helium was then stored over mercury. For each experiment the helium was, on its path to the ionization chamber, again passed slowly through charcoal immersed in liquid air, and after each experiment the gas passed through the same purifier before being stored over mercury.

#### METHOD OF CALCULATING THE MOBILITY.

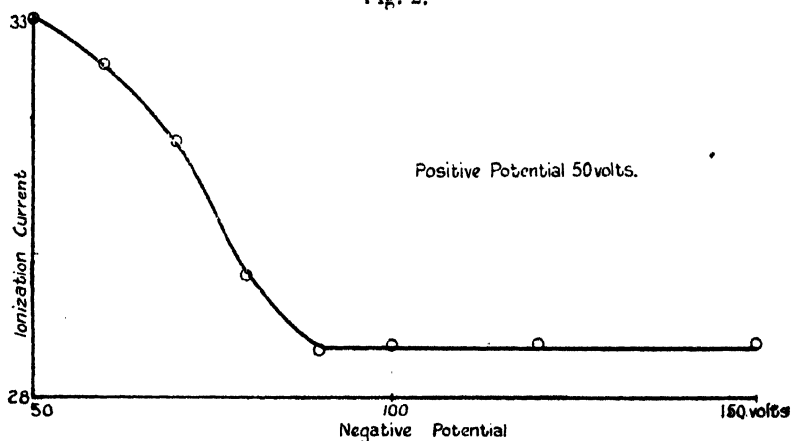
The method consisted in allowing a beam of rays to enter the chamber near the bottom plate when this plate was positively charged. The positive ions then proceeded towards the top insulated plate. If their velocity was sufficiently great, they would reach the latter plate before the potential of the lower plate changed in sign. On the other hand, if the velocity was insufficient, they would, on the reversal of the potential gradient, be drawn downwards to the lower plate. If  $x$  cm. is the distance between the plates, and  $X$  volts the potential applied to the lower plate when no charge is registered by the electrometer,  $p$  mm. the pressure of the gas, and  $K$  cm./sec. per volt/cm. the mobility at a pressure of 760 mm. of the fastest ion present in the gas, then  $\frac{x^2}{K} = \frac{760 X t}{p}$ , where  $t$  sec. is the interval elapsing from the instant when the last ions were formed by the  $\alpha$ -rays to that when the potential on the lower plate became negative. This quantity  $t$  is thus the *life of the ion*. It was determined by the product of two factors—the first was the rate of rotation of the commutator, and the second was what will subsequently be termed the reduction factor. This was obtained by dividing the circumference of the commutator into the distance that the positively-charged portion of the central part of the commutator moved under the brush connected to the ionization chamber (plus the width of the insulation strip) after the last  $\alpha$ -rays had entered the chamber. The reduction factor could be varied by changing the position of the rotating sector on the shaft of the commutator with regard to the rest of the commutator. The commutator was rotated in such a direction that the last  $\alpha$ -rays to enter the ionization chamber were those which grazed the lower plate.

#### INFLUENCE OF DIFFERENT VALUES OF NEGATIVE POTENTIAL.

The first point that was investigated after the compensation chamber had been adjusted was the influence that different values of the negative potential applied to one-half

of the commutator had on the readings when the positive potential applied to the other remained constant. A typical curve is shown in fig. 2. It was found that, as the negative potential was increased, the ionization current decreased to a certain value which then remained constant. This constant value was reached when the negative potential was approximately 25 per cent. greater than the positive. As the purpose of the negative potential was merely to sweep back to the lower plate those positive ions which were unable to reach the upper plate, it was arranged, in all readings described below, that the negative potential was at least 25 per cent. greater than the highest potential used.

Fig. 2.



It is considered the reason that a larger ionization current was obtained when the negative and positive potentials were equal was that either certain of the positive ions did not proceed directly between the plates, or else certain ions were formed in parts of the ionization chamber where the potential gradient had not its maximum value.

### EXPERIMENTAL RESULTS.

#### (a) *Method.*

After the gas had been introduced, and sufficient time had elapsed for the commutator to be rotating uniformly, readings of the ionization current were taken for different values of the positive potential applied to the lower plate of

the ionization vessel. Two consistent readings were made for each value of the positive potential. The ionization currents were then plotted against the positive potential, and the intercept of this curve on the potential axis gave the value of  $X$ . To find the reduction factor, the commutator was turned by hand until the  $\alpha$ -rays just failed to enter the ionization vessel. The distance that the positive portion of the central segment had still to run could then be readily measured.

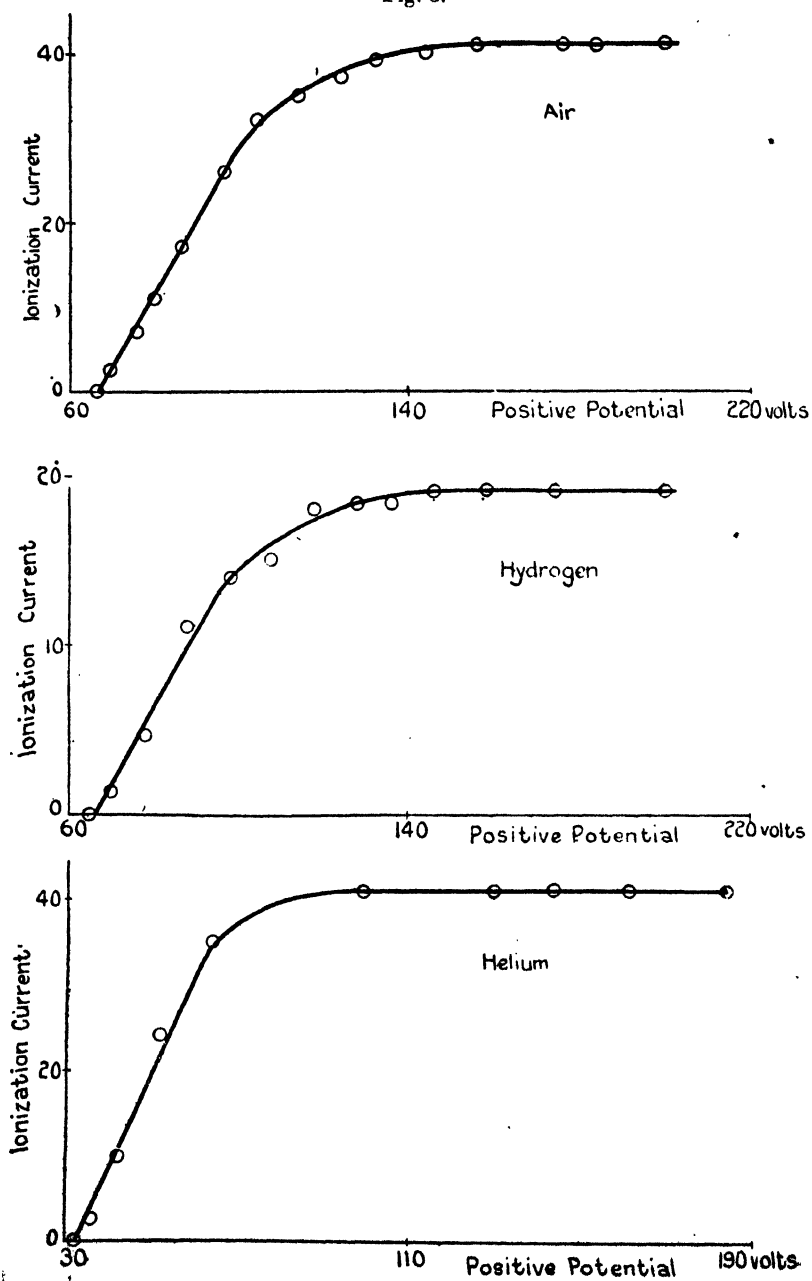
(b) *The Curves.*

Fig. 3 represents typical curves for air, hydrogen, and helium respectively. It will be noticed that for the higher potentials the curve runs parallel to the potential axis, showing that for such potentials all the positive ions were reaching the top plate. As the potential was further decreased, the curve began to slope off gradually, while the final portion is a straight line, and the intercept of the straight line on the potential axis gave the value of  $X$  mentioned above. Under ideal conditions for these experiments, after the straight horizontal portion of the curve the remainder would be a vertical descent to the potential axis. This cannot, however, be realized for the following reasons:—

Firstly, such a curve would be realized only when the ionizing beam was a thin, parallel, horizontal one which grazed the bottom plate of the ionization chamber. If the beam was not parallel, then the ions would be formed in the chamber at different distances from the top plate so that those which were produced near the bottom of the chamber would have greater distances to travel than those produced higher up. In consequence, as the positive potential was decreased, the "lower" ions would fail to reach the upper plate, while the "upper" ions still continued to do so. The source was so arranged that the majority of the rays were directed on this lower plate so that the ionization was limited to that portion of the chamber near the lower plate. It was impracticable with polonium sources to produce a parallel beam. The mica window, through which the rays entered the chamber, had to be equal to 1.3 cm. of air at least to withstand atmospheric pressure, and the  $\alpha$ -rays which entered the chamber had to have an emergent range over 1 cm. so that the source could not be placed further from the mica window than 1 cm. Even if a parallel beam of rays had been realizable, the ideal curve would not have



Fig. 3.



been obtained unless this beam were very thin, for a beam of finite thickness would produce ions at different vertical distances from the lower plate. In order that this effect should be as small as possible, the distance between lower and upper plates was made approximately 8 cm., so that the width of the beam would be small in comparison with the distance that the ions travelled in the chamber.

On the other hand, the thinner the beam of rays the less was the ionization current, and consequently either very intense sources were required or very sensitive detectors of the ionization current.

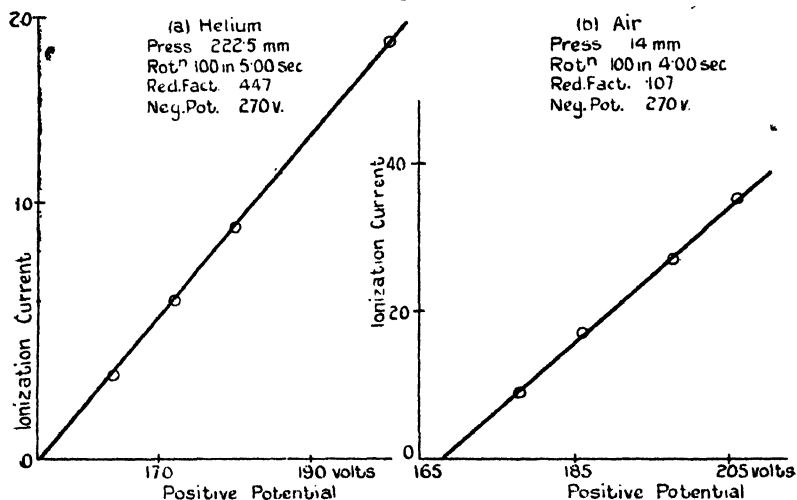
Secondly, in order to obtain the ideal curve the ionizing beam must enter the chamber momentarily once in each revolution. If the time in which the beam was present in the chamber was of any duration, those ions which were first formed would be moving towards the top plate before the last ones were formed. This could only be prevented by making the rotating sector of very small angle. Very small sectors necessitated, however, very intense sources if the ionization currents were to be appreciable. A compromise had thus to be arrived at between the ideal small-angled sector and one which would allow ionization currents to be measured in reasonable times.

If such ideal conditions could be realized, the presence of ions of more than one mobility in a gas could be readily shown. The existence of slower ions under the actual experimental conditions would be more difficult to show, as they would cause a somewhat slight discontinuity in the curves obtained. However, in the actual curves there was no definite evidence of ions of more than one mobility present at the same time.

In order to determine the mobilities of the ions when the life of the ion was very short, the whole curve was not obtained, but merely the last portion, *i.e.* that just before the ionization current disappeared. Sufficient points were obtained to allow the straight line to be drawn which determined the intercept.

Fig. 4 represents two end portions of the curves for helium and air respectively, and is typical of the type of curve obtained. The curves are quite straight, and thus show that there is only one type of ion present. The mobility obtained from (a) was 5.53 cm./sec. per volt/cm., and from (b) 1.65 cm./sec. Practically the whole of the curves were of this type, and thus represent the presence of one type of ion alone.

Fig. 4.

(c) *Values of the Mobilities.*

(i.) *Air.*—Table I. represents the results obtained with air. The table is arranged so that the life of the ion decreases as one reads down the table. It will be seen that, for lives between .138 and .0139 sec., the value of  $x^2/K$  remains constant within the limits of experimental error although the pressure varies between 98 and 22 mm., the rate of rotation of the commutator between 3.8 and 22 seconds for 100 revolutions, and the intercept on the potential axis between 15 and 164 volts. Further, these values were obtained with the three different commutators mentioned above.

For lives of ions between .00947 to .00675 sec. the value of  $x^2/K$  appears to be constant, so that these values have been bracketed, and the same applies to the values between .00428 and .00229 sec. The mobilities corresponding to the different values  $x^2/K$  are given in the last column. It was assumed that the value of the mobility corresponding to  $x^2/K = 47.8$  was that of the air-ion of mobility 1.36 cm./sec. per volt/cm. This is the mean of the values obtained by a great number of workers between whom there is fairly good agreement. (See Landolt-Börnstein Tabellen.) This value was assumed because it was difficult to measure the quantity  $x$ , which has to be measured twice as accurately as the other quantities, with the necessary precision. Further, with the

distance between the plates of the ionization vessel (*i. e.* approximately 8 cm.) there is reason to doubt that the potential gradient would be uniform throughout.

TABLE I.  
Mobilities of Positive Ions in Dry Air.

Life of Ion (sec.).	Press. (mm. Hg.).	Rotation. Time for 100 revs. (sec.).	Reduction Factor.	Intercept (volts).	$x^2/K$ .	Mean.	Mobility (K).
·1381	152	6·25	·461	70	48·3	47·8	<u>1·36</u> cm./sec./ volt/cm. (Value assumed.)
·0981	23·0	22·0	·446	15	48·3		
·0814	90	17·6	·461	68	46·9		
·0681	23	22·0	·310	20·7	46·7		
·0599	98	13·0	·461	106	49·3		
·0466	2	10·10	·461	83	48·1		
·0373	70·5	10·35	·348	117	46·8		
·0288	42·5	6·25	·461	95	49·0		
·0263	70·5	7·30	·348	164	46·5		
·0219	22·0	7·04	·310	64	48·5		
·0178	45	5·04	·352	157	47·0		
·0178	23·0	4·00	·446	79	46·7		
·0176	42·5	3·82	·461	147	46·3		
·0173	22·0	5·88	·310	76	48·1	44·2	<u>1·47</u>
·0158	22·0	5·10	·310	89	48·7		
·0139	22·0	4·50	·310	102	49·3		
·00947	21·5	3·06	·310	132	44·3		
·00939	27·5	3·03	·310	171	44·3		
·00676	22·0	3·10	·218	184	43·0	39·5	<u>1·65</u>
·00675	15·5	3·26	·207	136	45·0		
·00428	14·0	4·00	·107	169	39·3		
·00404	11·5	2·50	·169	138	38·7		
·00297	9·0	2·77	·107	162	40·2		
·00229	8·2	2·78	·0824	188	39·8		

*Note.*—In each of Tables I., II., and III. the values underlined in the sixth column with full lines were those obtained with air-gap of ·16 mm. between central segments of commutator; those underlined with dotted lines, with mica insulation ·17 cm. wide between segments; and all others with bakerlite insulation 1·2 cm. wide.

(ii.) *Hydrogen*.—The results are set out in Table II. In the first reading the ions were examined at a longer life than in the other gases. This necessitated a slow rotation of the commutator, and difficulty was experienced in securing the necessary uniformity of rotation. In consequence this result is not so reliable as the others, although the intercept was obtained from a straight line. The mobility of ions of lives between  $\cdot 261$  and  $\cdot 01363$  sec. appears to be constant and has the value  $5\cdot 30$ ; between  $\cdot 00913$  and  $\cdot 00644$  the value  $5\cdot 95$  holds, while between  $\cdot 00503$  and  $\cdot 00330$  the mobility is  $6\cdot 57$ . It will be noticed that when the life of the ion was  $\cdot 01152$  sec. a value of the mobility was obtained which lies between the first set of values and the second. Possibly this value should be included in the second set.

TABLE II.  
Mobilities of Positive Ions in Dry Hydrogen.

Life of Ion (sec.).	Press. (mm. Hg.).	Rotation, 100 revs. (sec.).	Reduction Factor.	Intercept (volts).	$x^2/K$ .	Mean.	Mobility.
$\cdot 442$	340	96.0	$\cdot 467$	13.0	13.62	.....	$4\cdot 78$
$\cdot 261$	244	56.0	$\cdot 467$	15.5	12.60	12.29	$5\cdot 30$
$\cdot 133$	307	27.5	$\cdot 486$	36.0	11.90		
$\cdot 1285$	307	27.5	$\cdot 467$	36.0	12.38		
$\cdot 0770$	209	16.75	$\cdot 461$	44	12.32		
$\cdot 0432$	188.5	9.40	$\cdot 472$	67	12.24		
$\cdot 1363$	101	3.00	$\cdot 453$	120	12.30		
$\cdot 01152$	81.5	3.04	$\cdot 379$	106	11.45	10.84	$5\cdot 99$
$\cdot 00913$	61.5	3.03	$\cdot 301$	94	11.05		
$\cdot 00894$	82.0	3.02	$\cdot 296$	130	11.00		
$\cdot 00832$	74.5	5.00	$\cdot 166$	126	10.70		
$\cdot 00667$	74.5	4.00	$\cdot 166$	156	10.60		
$\cdot 00503$	58.0	6.10	$\cdot 0824$	151	9.95	9.73	$6\cdot 67$
$\cdot 00412$	58.0	5.00	$\cdot 0824$	169	9.42		
$\cdot 00330$	44.5	4.00	$\cdot 0824$	177	9.97		

(iii.) *Helium*.—The results are set out in Table III. The mobility remains constant for lives between  $\cdot 1001$  sec. and  $\cdot 01095$  sec., and has the value of  $5\cdot 61$  cm./sec. per volt/cm.

When the life of the ion varies between  $\cdot 00795$  and  $\cdot 00679$  sec. the value of the mobility is  $6\cdot 12$ , while between  $\cdot 00528$  and  $\cdot 00290$  sec. the value is  $6\cdot 72$ .

TABLE III.  
Mobilities of Positive Ions in Helium.

Life of Ion (sec.).	Press. (mm. Hg.).	Rotation, 100 revs. (sec.).	Reduction Factor.	Intercept (volts).	$x^2/K$ .	Mean.	Mobility.
$\cdot 1001$	225	22.0	$\cdot 455$	34	11.50	11.56	5.61
$\cdot 0470$	222.5	10.50	$\cdot 447$	74	11.83		
$\cdot 0224$	222.5	5.00	$\cdot 447$	152	11.80		
$\cdot 0154$	92.5	4.00	$\cdot 384$	91	11.48		
$\cdot 0146$	97.7	3.28	$\cdot 446$	105	11.00		
$\cdot 0126$	92.5	3.28	$\cdot 384$	110	11.40		
$\cdot 01135$	100	5.00	$\cdot 227$	125	11.05		
$\cdot 01095$	90.5	3.28	$\cdot 333$	124	11.42	10.62	6.12
$\cdot 00795$	85.5	3.28	$\cdot 207$	152	10.79		
$\cdot 00779$	71.0	4.60	$\cdot 169$	130	10.80		
$\cdot 00686$	63.0	3.32	$\cdot 207$	128	10.60		
$\cdot 00679$	85.5	3.28	$\cdot 207$	171	10.30		
$\cdot 00528$	46.5	4.94	$\cdot 107$	110	9.51	9.69	6.72
$\cdot 00375$	30.5	3.50	$\cdot 107$	106	9.85		
$\cdot 00290$	30.5	2.70	$\cdot 107$	134?	9.73?		

One of the difficulties with helium was that a limit was imposed on the negative potential gradient that this gas would withstand before it became conducting (there being no external ionizing agent present). On one occasion, with the commutator at rest and when the pressure of the helium was 90.5 mm., it was found that when the lower plate on the ionization chamber was charged to  $-254$  volts the upper plate became charged negatively. When the negative potential was increased the rate of charge increased very rapidly. When the potential was decreased to  $-242$  volts, there was no such current, showing that the observed currents were not due to ionization caused by external sources, but that helium "broke down" (*i. e.* conducted) under quite small negative potential gradients. At times such clear demonstration of this breakdown was not possible, for, under much lower pressures and at potentials as high as  $-280$  volts,

the electrometer registered no negative charge. The effect was still present however, for when the negative potential was kept at  $-280$  and the positive adjusted to  $200$  volts, it was found that, when the commutator was rotated, the electrometer registered a negative instead of a positive charge; the positive charge was expected, since the gas was ionized while the lower plate of the ionization chamber was charged positively, and the pressure of the gas and rate of rotation of the commutator were such as would permit the positive ions to reach the top plate. When the negative potential was decreased and the positive decreased accordingly, this negative charge disappeared and the expected positive charge made its appearance. It is probable that, in the experiments last described, there were some minute traces of impurity present in the helium. When this phenomenon was first noted the coconut charcoal through which the gas passed had been evacuated while immersed in a bath of boiling sulphur just immediately previous to its being immersed in liquid air; and the fact that the breakdown was so readily demonstrated was due to the extreme purity of the helium.

There is another indication that the helium used was very pure. Franck and Gehlhoff\* stated that in pure helium the mobility of the negative ion was about  $500$  cm./sec. per volt/cm., while Franck and Pohl† had found that when slight traces of impurity were present this mobility was  $6.31$ . Accordingly the sector was adjusted on the commutator so that the mobility of the negative ions could be determined. Only one determination was made and a mobility of just over  $1000$  cm./sec. was found. It is intended to continue this examination of the negative ions later, this experiment being undertaken to demonstrate that the helium used was reasonably pure, even when the "breakdown" of helium under negative potentials did not occur.

As in the method which has been described for finding the mobilities of positive ions, the negative potential applied to the commutator was always greater than the positive, and as helium becomes conducting under certain negative potential gradients, the positive potentials that could be used with helium were limited if the gas was investigated at low pressures. In consequence of this, the mobilities of the helium positive ions have been investigated for as short lives as are possible with the present apparatus. In fact, the last reading (life  $0.00290$  sec.) merely shows that the mobility

\* *Vide Jahr. Rad.* ix. p. 250 (1912).

† *Verh. D. Phys. Ges.* ix. p. 194 (1907).

is not less than 6.72 cm./sec. per volt/cm., as it was impossible to vary the positive potential over a wide enough range to obtain the intercept with the necessary degree of accuracy.

## DISCUSSION OF RESULTS.

### *Comparison with Results obtained by other Investigators.*

An examination of the tables shows that, for the three gases investigated, the mobility of the positive ions depends on the life of the ion, and further that this dependence is not a continuous function of the life, but, for certain ranges of lives, the mobility remains constant. In each of the three gases investigated three different mobilities (four for hydrogen) have been found, and the change from one type to the next occurs for the three gases at very nearly the same lives. This is shown very clearly in Table IV. Probably the simplest type of ion investigated is that labelled third type, as the mobilities of these were measured in a very short time after their formation. If, however, the life of the ion is between 1/200 and 1/160 sec., the mobility of the ion in each case becomes less. There is a second change in the mobility at about 1/100 sec.

TABLE IV.

Collected Results for Air, Hydrogen, and Helium.

Gas.		First Type.	Second Type.	Third Type.
		Sec.	Sec.	Sec.
Air	{ Range of lives ...	·138-·0139	·00947-·00675	·00428-·00229
	{ Mobility .....	1.36	1.47	1.65
Hydrogen	{ Range .....	·261-·0136	·00913-·00664	00503-·00330
	{ Mobility .....	5.30	5.99	6.67
Helium	{ Range .....	·1001-·01095	·00795-·00679	·09528-·0029
	{ Mobility .....	5.61	6.12	6.72

This seems to suggest that whatever the mechanism is which causes the change from one type to another it is the same in the three gases; in other words, the ions in helium behave exactly similarly to those in the other two gases.

This investigation was undertaken originally to establish, if possible, the presence of doubly-charged helium ions. Millikan\* and his co-workers have shown that no gas other than helium when ionized by  $\alpha$ -rays showed any indication

\* Millikan, Gottschalk, and Kelly, *Phys. Rev.* xv. p. 157 (1920).



of doubly-charged ions. As in the above experiments no difference can be found between behaviour of helium ions and those in air and hydrogen, one is forced to the conclusion that there is no evidence under the experimental conditions here described of doubly-charged ions in helium. The reason that, while Millikan and Wilkins\* found evidence of doubly-charged helium ions, there is no evidence here, can be attributed to the different methods of experiment. In the method of Millikan a charged oil-drop was held suspended in the gas under examination while  $\alpha$ -rays passed very close to the drop. The interval of time between the formation of the ion and its arrival on the oil-drop (*i. e.* the life of the ion) was stated by Millikan to be "something like a ten-thousandth of a second." This life is much shorter than the shortest reached in these experiments (1/500 sec.). One is forced to the conclusion that the doubly-charged helium ion is converted very quickly to the singly-charged, in so short a time, in fact, that its increased mobility as a doubly-charged ion cannot be demonstrated experimentally by the method here employed.

In order to compare the results obtained with those of other experimenters, each gas will be dealt with separately.

(a) *Air* †.—Experiments by Erikson ‡ and Wahlin § had previously shown that the mobility of the positive ion in air depended on the life of the ion. In both of their investigations they were unable from the nature of their apparatus to give very accurately the life of the ion. Erikson used a modification of Zeleny's method, and he showed that while the ordinary mobility of the positive ion was 1.36, the mobility was 1.87 when the life of the ion was shorter. The transition of the higher value was estimated by Erikson to occur when the ion had aged for about 1/50 sec. In the method of Wahlin the ions were produced by polonium, and were forced into the chamber in which the mobility was measured by a small auxiliary field. Their mobility was then found by Franck's method, the alternating potential being supplied by a valve-oscillating circuit. His results substantiated those of Erikson in that he found a fast ion of mobility 1.80 and a slower one of mobility 1.35, and that the first changed to the second after a time between 1/75 and 1/120 sec.

Erikson advanced the following explanation to account for

\* Wilkins, *Phys. Rev.* xix. p. 210 (1922).

† All mobilities are expressed in cm./sec. per volt/cm.

‡ Erikson, *Phys. Rev.* xx. p. 117 (1922); *ibid.* xxiv. p. 502 (1924).

§ Wahlin, *Phys. Rev.* xx. p. 267 (1922).

his result :—The process of ionization consists in the removal of an electron from a molecule, and this electron at once attaches to a neutral molecule and forms the negative ion. The initial positive and negative ions thus both consist of a molecule, and if their mobility is at once measured it is the same for both. The negative ion remains unchanged, but the positive ion quickly attracts a neutral molecule to it. In consequence of the increased mass of the molecule its mobility decreases to the smaller value. Erikson states that his results suggest “that in any one gas the mobility is approximately proportional to the inverse square root of the mass of the ion.”

There are two objections to this rather simple theory. The first is that the mobility of an ion depends on the gas in which it is measured, and the mobility of any positive ion measured in air is the same as that of the air ion (the mobility for the air ion being the lower value 1.36)\*. The mobility in air has been measured for a large number of ions in which the mass of the ion has varied considerably—from hydrogen ( $M = 2$ ) to chloroform ( $M = 119$ ). The mass of the ion therefore does not appear to have very great effect on the mobility of the ion. The variation in the diameter of the ion, if we assume that it is composed of a single molecule, would be much less, but there should be some detectable difference between the mobilities if these depended directly on the diameter of the ion†, whereas Tyndall and Grindley find that the mobilities of the hydrogen, carbon dioxide, ether, and chloroform ions are the same to within 1 per cent. when measured in air.

The second objection is that Nolan and Wahlin (later) have obtained evidence of the presence of more than two types of positive air-ions. The experiments above have also shown three types of ions. Nolan has used two different methods ; in one he used an air-blast method and in the other the alternating field method in which ions were driven by an auxiliary field into the main chamber. In the last he took precautions to make the field, which draw back the ions which had not reached the plate connected to the electrometer, slightly greater than that of opposite sign which urged them towards the plate. The difference in the positive and

\* *Vide* Blanc, *Journ. de Phys.* vii. p. 825 (1908). Wellisch, *Proc. Roy. Soc.* lxxii. p. 500 (1909). Tyndall and Grindley, *Phil. Mag.* xlviii. p. 711 (1924). Erikson, *Phys. Rev.* xxvi. p. 465 (1925).

† Thus in Kaye and Laby's (1921) Tables, p. 35, the diameter of the hydrogen molecule is  $2.46 \times 10^{-8}$  cm., while the diameter of the  $\text{CO}_2$  molecule is  $3.81 \times 10^{-8}$  cm.

negative potentials, however, was of the order of two volts, and in view of fig. 2 (above) it is considered that the difference between the positive and negative potentials was inadequate for the purpose. He measured the mobilities of both the negative and positive ions. He has found more groups of mobilities than any other investigator, and, further, that the mobilities of positive and negative ions were the same throughout.

He obtained the values of the mobilities in both experiments by observed discontinuities in his ionization current-potential curves. Some of these discontinuities were very small, and the interpretation of them has been considerably criticized. Blackwood \* duplicated the apparatus used by Nolan in the air-current method, but failed to obtain a repetition of Nolan's curve. Loeb † has criticized the interpretation that Nolan places on his curves, and has pointed out that the electrometer readings would have to be extremely accurate before some of the discontinuities of Nolan could be regarded as definite evidence of different groups of ions.

In Wahlin's later determinations he again used the alternating field method, and from discontinuities in the ionization current-potential curve concluded that there were at least six types of positive air-ions. It must be pointed out that Wahlin took no precautions to make his negative potentials greater than his positive, as has been found necessary in this work.

The results of Nolan, Erikson, Wahlin, and the author are set out in Table V. (In his paper in the 'Physical Review,' Nolan ‡ mentions the presence of more ions than are given in this table—the values given here are those published in the 'Proceedings of the Royal Irish Academy.')

It would appear that the three types of ions found by the author correspond to three found by Wahlin and three by Nolan. The method used by the author has, however, the following advantages:—

1. The mobility values are found from straight-line intercepts on the potential axis and not from discontinuities in the curves.

2. The ions investigated are not produced in a subsidiary chamber, but directly in the chamber in which they are at once measured.

3. The ions are not entering the measuring-chamber continuously, but only for limited times (due to the sector wheel).

\* Blackwood, *Phys. Rev.* xx. p. 499 (1922).

† Loeb, *Journal Franklin Institute*, cci. p. 537 (1923).

‡ Nolan, *Phys. Rev.* xxv. p. 101 (1925).

4. Adequate precautions are taken to remove those positive ions which are approaching the top plate but which fail to reach it.

TABLE V.  
Mobility of Positive Air Ions.

Nolan.	Erikson.	Wahlin.	Rogers.
+ and -			
12.4			
6.6			
5.1			
4.31			
3.02			
2.04			
1.76	1.89	1.89	1.65
1.53	...	1.57	1.47
1.38	1.35	1.35	1.36
		1.20	
		1.10	
		.970	

No evidence has been found of any faster ions mentioned by Nolan, *i. e.* those of mobility (2) and greater, and if such exist they must have a life of less than  $1/500$  sec. Again, the curves show no evidence of any ions slower than 1.36, since there are no marked discontinuities in the curves when the ions of mobility 1.36 are being measured.

(b) *Hydrogen*.—The mobility of the positive ions in hydrogen has been previously investigated by Chattock\*, by Franck and Pohl†, by Zeleny‡, and Nolan§.

Chattock used an ingenious method in which he employed the point discharge in gases. His value of the mobility is 5.4. Although this value corresponds to that found below for ions of lives between .261 and .0136 sec., the life of the ions in Chattock's experiments would be very much shorter.

Franck and Pohl used a modification of the original Rutherford method in which the lower plate of their ionization chamber was connected to sinusoidal alternating potential of frequency about 55. The ions of the sign required

\* Chattock, Phil. Mag. xlvii. p. 401 (1899); *ibid.* i. p. 79 (1901).

Franck and Pohl, *Verh. Deut. Phys. Ges.* ix. pp. 67, 194 (1907).

† Zeleny, Phil. Trans. (A), cxcv. pp. 183, 193 (1900).

§ Nolan, Proc. Roy. Irish Acad. xxxvi. p. 74 (1923).

were introduced into the main field by a small auxiliary field. The life of ions was here approximately  $\cdot 009$  sec. The value of the mobility obtained by them,  $6\cdot 02$ , agrees very well with that found here,  $5\cdot 99$ , for ions of the same life.

The method of Zeleny consisted in deflecting the charged ions by an electric field at right angles to the direction in which they were moving in a current of gas. He measured the value of the mobility for a number of different lives and then extrapolated for zero life. His value was  $6\cdot 70$ , which is in good agreement with the value found here,  $6\cdot 67$  for the lives of ions between  $\cdot 00503$  to  $\cdot 00330$  sec.

The method of Nolan was the alternating field method, exactly the same as used by him for air. The values that he found were  $5\cdot 23, \begin{matrix} 5\cdot 68 \\ 6\cdot 15 \end{matrix} \}^*$  (mean  $5\cdot 83$ ),  $6\cdot 77, 7\cdot 93, 9\cdot 63$ .

The first three agree fairly well with those found by the author of  $5\cdot 30, 5\cdot 99, 6\cdot 67$ , but no evidence has been found of the latter types, and if they exist they must be of very short life.

(c) *Helium*.—The only previous determination of the mobility of the ions was by Franck and Pohl†, and by Franck and Gehlhoff‡. In these experiments they used the same method as for the hydrogen ions. The value that they obtained for the mobility of the positive ions was  $5\cdot 09$  cm/sec., a value which is considerably lower than their value for hydrogen. On the other hand, the values obtained in the above experiments for hydrogen were always less than those for helium.

There is a possible explanation of their lower value. The distance between the plates of their ionization chamber was about  $3\cdot 6$  cm. (*vide* their diagram on page 72 of vol. ix. of the *Verh. d. D. Phys. Ges.*). On page 195 of the same journal the effective values of the potentials used in helium were given as about 320 volts, and 275 volts on page 196. The maximum values of the potentials corresponding to these would be 450 and 390 volts, and the maximum potential gradients 125 and 108 volt/cm. resp.

Now, it has been mentioned above that when the pressure of helium was 90 mm. the gas "conducted" under a negative potential gradient of 30 volt/cm. It was thus possible in Franck's experiments that the helium conducted at the highest values of the negative potential, and hence the ionization current due to the positive ions alone would appear to cease for higher values of the positive potential than they actually did. Thus lower values of the mobility

\* The bracketing is that of Nolan. † *Loc. cit.* ‡ *Loc. cit.*

would be recorded than were correct. (*Note.*—Although the sparking potential of helium under negative gradients has not been exhaustively examined, it does not appear to be directly proportional to the pressure, for while the negative potential could not be raised above 240 volts when the pressure was 90 mm., a negative potential of 180 volts could be used when the pressure was 30.5 mm.)

#### CONCLUSION.

There is still no theoretical equation which will give satisfactorily the mobility of ions\*, but these experiments indicate that, whatever the ion is initially, after a very short time it has developed into some type of cluster. Loeb ascribes the ageing effects found by Erikson to small changes in the diameter of the ion. The ageing effects found here have probably the same explanation. The increase in the diameter can only be ascribed to neutral molecules being added to the ion as it ages. There is one property of ions which is however not explained by the increase in diameter, and this is, as illustrated by Tables I., II., and III., that the mobility does not appear to change gradually but in definite steps. If the changes in mobility were due to the gradual addition of neutral molecules, one would expect a gradual change in mobility with the life of the ion. If the ion starts as a single molecule, it will have a definite mobility, and each addition of a neutral molecule will cause a decrease in the mobility. If a series of measurements were taken on the mobility of the ion between the time of attachment ( $t'$ ) of one neutral molecule, the time of attachment ( $t''$ ) of the next and at longer times, it is obvious that after  $t''$  the measured mobility should gradually decrease; for, as the time exceeded  $t''$ , an increasing portion of the life of the ion would be spent in the latter state, i. e. that of the less mobility. There is, however, no such gradual change of mobility found either in these experiments or in those of Erikson, Wahlin, or Nolan.

This work was commenced while the writer held an 1851 Exhibition at Cavendish Laboratory, Cambridge. My thanks are due to Sir Ernest Rutherford, who suggested this method of investigation, and for his gift of helium, and also to the Australian Oxygen Company, Melbourne, for liquid air.

\* *Vide* Loeb, Journ. Frank. Inst. cci. p. 279 (1926).

XCI. *The Distribution of Temperature in Alternating Current Conductors* \*. By M. J. O. STRUTT, D.techn.Sc.†

ABSTRACT.

THE temperature in alternating current conductors of circular cross-section and infinite length is derived as a function of the distance from the centre for the case where the electric current is flowing along the axis, and for the case where the electric current is flowing in circles round the axis (inductive heating). In both cases very small and very high frequencies are considered. It is shown in the first case that for high frequency the highest temperature (in the centre) tends to one-half of the temperature when the same effective direct current is flowing through the conductor, the temperature of the surrounding medium being supposed to be zero. Herefrom it is deduced that by raising the frequency the temperature inside the conductor is decreased under the above circumstances. In the second case it is shown that, the temperature of the surrounding medium and the magnetic field outside the conductor being constant, the temperature inside the conductor increases everywhere with frequency. Some formulas are derived in four notes. A list of symbols is added.

---

I. *Introduction.*

THE purpose of the present paper is to investigate the temperature in the interior of alternating current conductors of circular cross-section and of infinite length.

Two cases will be considered separately. In the first place the electric current will be supposed to flow in the direction of the axis of the conductor. This problem relates to electric cables, lines, etc. In the second place the electric current will be assumed to flow in circles round the axis of the conductor. This problem occurs in the treatment of inductive heating.

\* Sections I. and II. of this paper form chapters of a thesis for the degree of Doctor in the Technical University of Delft, 1927.

† Communicated by the Author.

In both cases the temperature  $T$  is determined by the differential equation :

$$\Delta T = \frac{c}{K} \cdot \dot{T} - \frac{m_0}{K} \cdot S^2, \quad . \quad . \quad . \quad . \quad . \quad (1)$$

where

- $c$  = spec. heat per unity of volume,
- $K$  = heat conductivity,
- $m_0 = \alpha \cdot \rho$ ,
- $\alpha$  = constant, determined by the choice of units  
(with practical units equal to 0.239),
- $\rho$  = spec. electric resistance,
- $S$  = electric current density ;

and the boundary condition :

$$h \cdot (T - T_0) = - \frac{dT}{dn} \quad . \quad . \quad . \quad . \quad . \quad (2)$$

on the whole surface, where  $h$  is a constant depending on the surface of the conductor,  $T$  the temperature of the conductor surface, and  $T_0$  the temperature of the surrounding medium at the surface of the conductor.

Throughout this paper  $c$ ,  $K$ ,  $\rho$  will be treated as constants.

If the axis of the conductor coincides with the  $z$ -axis, and assuming symmetrical conditions round this axis, equations (1) and (2) assume the form :

$$\frac{\partial^2 T}{\partial r^2} + \frac{1}{r} \cdot \frac{\partial T}{\partial r} = \frac{c}{K} \cdot \frac{\partial T}{\partial t} - \frac{m_0}{K} \cdot S^2, \quad . \quad . \quad . \quad (1')$$

$$h(T - T_0) = - \frac{dT}{dr} \quad . \quad . \quad . \quad . \quad . \quad (2')$$

As the electric current density is assumed to be purely periodic with angular frequency  $\omega$ , it is seen from equation (1') that  $T$  will be a periodic function of time with frequency  $2\omega$ . Now  $T$  can be split up into a part independent of time, and a part varying with period  $2\omega$  :

$$T(r, t) = G(r) + L(r, t) \quad . \quad . \quad . \quad . \quad (3)$$

It is assumed that  $L$  is truly periodic, so that the stationary state has been arrived at.

As the conduction of heat may be compared with a process of diffusion, through which the variations of the temperature are everywhere diminished, we may expect that, already for moderate values of  $\omega$ , the part  $L$  of temperature will be small compared with  $G$ . Therefore, in this paper,  $G$  only will be considered.



II. *Electric Current Flowing along the Axis.*

In the first place,  $S$  is assumed to flow in the direction of  $z$ . In this case  $S$  is given by the expression :

$$S = (\text{real part of}) C \cdot I_0(m \cdot r \cdot \sqrt{-i}) \cdot e^{i\omega t}, \quad (4)$$

where

$$V^2 m^2 \cdot \rho = 4 \cdot \pi \cdot \mu \cdot \omega,$$

$$\mu = \text{permeability},$$

$$V = \text{velocity of light},$$

Gauss Units having been adopted. The constant  $C$  is determined by the total current amplitude  $I$  through the conductor :

$$|C| = \frac{I \cdot m_1}{\sqrt{2} \cdot \pi \cdot b \cdot [(\text{ber}' mb)^2 + (\text{bei}' mb)^2]}, \quad (5)$$

where

$$m = m_1 \cdot \sqrt{2},$$

$$b = \text{radius of conductor}.$$

From equations (1') and (4) we obtain for  $G$  :

$$\frac{1}{r} \cdot \frac{d}{dr} \cdot \left( r \cdot \frac{dG}{dr} \right) = - \frac{m_0}{K} \cdot \frac{C^2}{2} [\text{ber}^2 mr + \text{bei}^2 mr]. \quad (6)$$

So  $G$  may be found by double integration. The first integration gives (see Note 1) :

$$\frac{dG}{dr} = \frac{\gamma}{m} \cdot [\text{ber } mr \cdot \text{bei}' mr + \text{bei } mr \cdot \text{ber}' mr] + A, \quad (7)$$

where

$$\gamma = - \frac{m_0}{K} \frac{C^2}{2},$$

and  $A$  is a constant of integration. As the flow of heat through the centre of the wire must be zero,

$$\left( \frac{dG}{dr} \right)_{r=0} = A = 0.$$

We now proceed to consider equation (7) for two cases :

(a)  $m \cdot b \ll 1$  (small frequency),

(b)  $m \cdot b \gg 1$  (high frequency).

In case (a), equation (7) yields

$$\frac{dG}{dr} = \frac{\gamma}{m} \cdot \left( \frac{mr}{2} + \frac{(mr)^5}{2^3 \cdot 4^2} \right), \quad \dots \quad (7a)$$

and, by integrating,

$$G = \frac{\gamma}{4} r^2 \left( 1 + \frac{(mr)^4}{2^4 \cdot 3 \cdot 4} \right) + B, \quad \dots \quad (8a)$$

where B is a constant of integration.

Now, supposing the temperature  $T_0$  (equation (2)) of the medium surrounding the conductor to be zero, and the constant  $h$  (equation (2)) to be large, we get from equation (8a)

$$G = \frac{m_0 \cdot I^2}{8 \cdot K \cdot \pi^2 \cdot b^4} \left[ b^2 \left( 1 + \frac{(mb)^4}{2^4 \cdot 3 \cdot 4} \right) - r^2 \left( 1 + \frac{(mr)^4}{2^4 \cdot 3 \cdot 4} \right) \right], \quad \dots \quad (9a)$$

where the value of  $C$  has been inserted from equation (5). It is to be noted that, in equations (7a), (8a), and (9a), powers of  $mb$ , and therefore of  $mr$ , higher than the fourth have been neglected.

In the case of direct current we may easily solve equation (1), and find

$$T = \frac{m_0}{K} \cdot \frac{I_1^2}{4(\pi b^2)^2} (b^2 - r^2). \quad \dots \quad (10)$$

Comparing equations (10) and (9a), and bearing in mind that  $I$  is an amplitude which corresponds to an *effective* current  $I/\sqrt{2}$ , we easily verify that these equations coincide for the case that  $m=0$ .

Considering case (b) :

$$mb \gg 1,$$

we may write

$$\left. \begin{aligned} \text{ber } mr &= \frac{e^{m_1 r}}{\sqrt{2} \cdot \pi \cdot m \cdot r} \cdot \cos \left( m_1 r - \frac{\pi}{8} \right), \\ \text{bei } mr &= \frac{e^{m_1 r}}{\sqrt{2} \cdot \pi \cdot m \cdot r} \cdot \sin \left( m_1 r - \frac{\pi}{8} \right), \\ \text{ber}' mr &= \frac{e^{m_1 r}}{\sqrt{2} \cdot \pi \cdot m \cdot r} \cdot \cos \left( m_1 r + \frac{\pi}{8} \right), \\ \text{bei}' mr &= \frac{e^{m_1 r}}{\sqrt{2} \cdot \pi \cdot m \cdot r} \cdot \sin \left( m_1 r + \frac{\pi}{8} \right), \end{aligned} \right\} \quad \dots \quad (11)$$

where again

$$m_1 = \frac{m}{\sqrt{2}}.$$

Inserting these values into equation (7), we get

$$\frac{dG}{dr} = \frac{\gamma}{4 \cdot \pi \cdot m \cdot m_1} \cdot \frac{e^{2m_1 r}}{r}, \quad \dots \quad (7b)$$

from which we obtain by integration (see Note 2)

$$G = -\frac{m_0}{K} \cdot \frac{I^2}{2} \cdot \frac{1}{4 \cdot \pi \cdot m_1^2 \cdot \sqrt{2}} \text{Ei}(2m_1 r) + B, \quad \dots \quad (8b)$$

where  $\text{Ei}(2m_1 r)$  is the integral-logarithm of  $2m_1 r$ , and  $B$  a constant of integration.

Inserting the values of equation (11), we obtain from equation (5)

$$|G| = \frac{I \cdot m_1 \cdot \sqrt{m}}{\sqrt{\pi \cdot b} \cdot e^{m_1 b}} \cdot \dots \quad (5b)$$

Now again assuming the temperature  $T_0$  (equation (2)) of the surrounding medium to be zero, and combining equations (5b) and (8b), we obtain

$$G = \frac{m_0}{K} \cdot \frac{I^2 \cdot (2m_1 b)}{16 \cdot \pi^2 \cdot b^2 \cdot e^{2m_1 b}} [\text{Ei}(2m_1 b) - \text{Ei}(2m_1 r)]. \quad (9b)$$

It should be noted that equation (9b) is only valid for values of  $r$ , such that

$$mr \gg 1.$$

In order to find the temperature for  $r=0$ , we may proceed as follows. We may make  $r$  smaller and smaller, at the same time increasing  $m$  without limit :

$$r \rightarrow 0,$$

$$m \rightarrow \infty,$$

such that, during this whole process,  $mr$  retains a value large compared with unity. Carrying this out and replacing the function  $\text{Ei}(2m_1 r)$  by its values for large arguments (see Note 3), we obtain

$$G_{\left(\begin{smallmatrix} r \rightarrow 0 \\ m_1 \rightarrow \infty \end{smallmatrix}\right)} = \frac{m_0}{K} \cdot \frac{I^2}{16 \cdot \pi^2 \cdot b^2} \cdot \dots \quad (12)$$

Comparing this value with the one obtained in the case of direct current (equation (10)), we find the interesting result, that the highest alternating current temperature of a conductor, the frequency tending towards infinity, is equal to one-half of the highest direct current temperature of the same conductor. Here it is supposed that the effective currents are the same, and that the temperature of the surrounding medium is zero.

If the latter assumption is not fulfilled, we may apply our result to the differences of the temperatures in the conductor and that of the surrounding medium. Moreover, we have assumed the constant  $h$  from equation (2) to be large, which arises, *e. g.*, in the case where the conductor is surrounded by a liquid. From this result we deduce that, with constant total current and increasing frequency, the temperature decreases everywhere inside the conductor, the temperature at the boundary being kept constant.

### III. Electric Current flowing in Circles round the Axis.

This case occurs in the theory of inductive heating, the magnetic force having the direction of  $z$  and being given in the conductor (charge) by

$$H = (\text{real part of}) H_0 \cdot I_0(mr \sqrt{-i}) \cdot e^{i\omega t}, \quad (13)$$

where  $H_0$  represents a constant determined by the uniformly distributed magnetic force outside the conductor :

$$H_0 = \frac{H_1}{I_0(mb \sqrt{-i})}, \quad \dots \quad (14)$$

$b$  again being the radius of the conductor. From equation (13) the current density  $S$  is easily found to be

$$\begin{aligned} S &= (\text{real part of}) \sigma \cdot \frac{dH}{dr} \\ &= (\text{real part of}) \frac{V}{4\pi} H_0 m \cdot \sqrt{-i} I_0'(mr \sqrt{-i}) e^{i\omega t}, \end{aligned} \quad (15)$$

where  $\sigma = \frac{V}{4\pi}$ , adopting again Gauss Units and denoting the differentiation with respect to  $mr$  by an accent, as in the case treated before. Inserting the value (15) into equation (1'), we find for  $G$  the equation

$$\frac{1}{r} \cdot \frac{d}{dr} \left( r \cdot \frac{dG}{dr} \right) = - \frac{m_0}{K} \cdot \sigma^2 \frac{H_0^2}{2} m^2 \cdot [(\text{ber}' mr)^2 + (\text{bei}' mr)^2], \quad (16)$$

so that  $G$  may be found by double integration. The first integration gives (see Note 4)

$$\frac{dG}{dr} = \sigma^2 \cdot \frac{\gamma}{2} \cdot m \cdot (\text{ber } mr \cdot \text{ber}' mr + \text{bei } mr \cdot \text{bei}' mr), \quad (17)$$

$\gamma$  denoting  $-\frac{m_0}{K} \cdot H_0^2$ , the constant of integration being zero for the same reason as in equation (7).

By integrating equation (17) once again, we get

$$G = \frac{\gamma}{4} \sigma^2 (\text{ber}^2 mr + \text{bei}^2 rm) + B_1, \quad (18)$$

$B_1$  being a constant of integration, determined by the conditions at the surface of the conductor. Supposing, again, the temperature of the medium surrounding the conductor to be zero, and the constant  $h$  of equation (2) large, equation (18) yields

$$G = \frac{m_0}{K} \sigma^2 \frac{H_0^2}{4} \cdot (\text{ber}^2 mb + \text{bei}^2 mb - \text{ber}^2 mr - \text{bei}^2 mr). \quad (19)$$

From equation (14) we get

$$|H_0| = \frac{H_1}{[\text{ber}^2 mb + \text{bei}^2 mb]^{\frac{1}{2}}},$$

and inserting this value into equation (19), we find

$$G = \frac{m_0}{K} \cdot \frac{H_1^2}{4} \cdot \sigma^2 \cdot \left[ 1 - \frac{\text{ber}^2 mr + \text{bei}^2 mr}{\text{ber}^2 mb + \text{bei}^2 mb} \right]. \quad (20)$$

In the case that

$$mb \ll 1 \quad (\text{small frequency}),$$

we easily obtain from equation (20)

$$G = \frac{m_0}{K} \cdot \frac{H_1^2}{2^3 \cdot 4^2} \cdot \sigma^2 \cdot \left[ \frac{(mb)^4 - (mr)^4}{1 + \frac{(mb)^4}{32}} \right], \quad (20a)$$

powers of  $mb$  and of  $mr$  higher than the fourth being neglected.

As is to be expected,  $G$  vanishes with  $m$  (*i.e.* becomes equal to the temperature of the surrounding medium), a stationary magnetic field outside the conductor inducing no currents in it.

If we increase the frequency (and hence  $m$ ), keeping  $H_1$  constant, we see, from equation (20), that  $G$  increases in every point of the cross-section.

Hence from equation (20) we cannot explain the well-known phenomenon that, *e.g.* a disk placed in a longitudinal alternating magnetic field assumes a higher temperature at its circumference than at its centre. This phenomenon seems to depend essentially on the finite (and in fact rather small) length of the cylinder.

If we do not suppose the constant  $h$  from equation (2) to

be very large, we find for the temperature (that of the surrounding medium being zero) from equation (18)

$$G = \frac{m_0}{K} \cdot \sigma^2 \cdot \frac{H_1^2}{2} \left[ \frac{1}{2} + \frac{m}{h} \frac{(\text{ber } mb \cdot \text{ber}' mb + \text{bei } mb \cdot \text{bei}' mb)}{\text{ber}^2 mb + \text{bei}^2 mb} - \frac{1}{2} \frac{\text{ber}^2 mr + \text{bei}^2 mr}{\text{ber}^2 mb + \text{bei}^2 mb} \right]. \quad (21)$$

If we increase the frequency without limit, at the same time keeping the energy dissipated in the conductor constant, the induced currents and hence the temperature inside the conductor tend to zero, as is easily seen by expressing  $H_1$  in terms of the dissipated energy\*.

#### IV. Notes.

NOTE 1.—The integral wanted is

$$\int^r r \cdot (\text{ber}^2 mr + \text{bei}^2 mr) \cdot dr.$$

By the aid of the formulas :

$$\text{ber } mr = \frac{1}{2} [(I_0(mr \sqrt{-i}) + I_0(mr \sqrt{i})],$$

$$\text{bei } mr = \frac{1}{2i} [I_0(mr \sqrt{-i}) - I_0(mr \sqrt{i})],$$

$$\text{ber}^2 mr + \text{bei}^2 mr = I_0(mr \sqrt{-i}) \cdot I_0(mr \sqrt{i}),$$

we may write for this integral

$$\int r \cdot I_0(mr \sqrt{-i}) \cdot I_0(mr \sqrt{i}) dr.$$

Integrating by parts and denoting the differentiation with respect to  $mr$  by an accent, we get for this integral

$$\frac{r}{2im} [I_0'(mr \sqrt{-i}) \cdot I_0(mr \sqrt{i}) - I_0(mr \sqrt{-i}) \cdot I_0'(mr \sqrt{i})],$$

and by converting these functions into *ber* and *bei*, we obtain for the integral

$$\frac{r}{m} [\text{ber } mr \cdot \text{bei}' mr - \text{bei } mr \cdot \text{ber}' mr].$$

I have not succeeded in integrating equation (7) of section II. again.

\* *E. g.* Burch & Davis, *Phil. Mag.* (7) i. p. 768 (1926).

I finally remark that the previous integration could be avoided by regarding the physical meaning of the integral, *i. e.* the energy dissipated in a conductor of radius  $r$  times a constant, if we insert zero as lower limit of integration. The expression of this energy is well known \*, and thus may be used to check the above result. As the expression just mentioned may be calculated by the aid of Poynting's theorem †, the second method of evaluating the integral is, in fact, equivalent to the conversion of a surface-integral to an integral taken along a circumference, and so forms an application of Gauss's theorem.

NOTE 2.—The integral wanted is

$$\int \frac{r e^{2m_1 r}}{r^2},$$

for which we find, by expansion,

$$\ln(2m_1 r) + 2m_1 r + \frac{(2m_1 r)^2}{2 \cdot 2!} + \frac{(2m_1 r)^3}{3 \cdot 3!} + \dots.$$

Now, by definition ‡,

$$\begin{aligned} \text{Ei}(2m_1 r) &= \int_x^{-2m_1 r} \frac{e^{-u}}{u} \cdot du \\ &= \beta + \ln(2m_1 r) + 2m_1 r + \frac{(2m_1 r)^2}{2 \cdot 2!} + \dots, \end{aligned}$$

where  $\beta$  denotes the constant of Euler-Mascheroni :

$$\beta = 0.57721 \dots$$

By comparing the two expressions we easily derive equation (8) of the text.

NOTE 3.—Firstly, we notice that, for large values of  $2m_1 b$ , the expression  $\text{Ei}(2m_1 r)$  in equation (9 b) becomes negligible compared with  $\text{Ei}(2m_1 b)$ . Now, for large values of  $2m_1 b$  we may write §

$$\text{Ei}(2m_1 b) \sim \frac{e^{2m_1 b}}{2m_1 b},$$

and with this expression we easily obtain equation (12).

\* *E. g.* Jahnke & Emde, 'Funktions tafeln' p. 144.

† *E. g.* J. J. Thomson, 'Recent Researches,' p. 320.

‡ *E. g.* Jahnke-Emde, *l. c.* p. 19.

§ *E. g.* Jahnke-Emde, *l. c.* p. 9.

NOTE 4.—The integral wanted is

$$\int_0^r r [(\text{ber}' mr)^2 + (\text{bei}' mr)^2] dr.$$

By the aid of the formulas given in Note 1, we may write

$$\int_0^r r \cdot I_1(mr \sqrt{-i}) \cdot I_1(mr \sqrt{i}) dr,$$

and, integrating by parts, find

$$\frac{r}{2m} \cdot [I_0'(mr \sqrt{-i}) \cdot I_0(mr \sqrt{i}) + I_0(mr \sqrt{-i}) \cdot I_0'(mr \sqrt{i})],$$

from which equation (17) of the text is easily derived by inserting *ber* and *bei* functions again.

As to the evaluation of this integral, we may make the same remark as in Note 1, the integral with lower limit zero denoting the energy dissipated in a conductor of radius *r* times a constant. The known expression for this energy\* may be used to check the result obtained above.

### V. List of Symbols.

- b* radius of conductor.
- C* amplitude of current density (equation (4)).
- c* specific heat capacity per unit volume.
- Ei* integral logarithm (equation (8*b*) and Note 2).
- G* temperature in the conductor independent of time.
- H* magnetic force (equation (13)).
- H<sub>0</sub>* amplitude of magnetic force (equation (13)).
- H<sub>1</sub>* magnetic force outside conductor (equation (14)).
- h* constant depending on the nature of the surface of the conductor and of the surrounding medium (equation (2)).
- I* amplitude of total alternating current (equation (5)).
- I<sub>1</sub>* total direct current (equation (10)).
- K* specific heat conductivity.
- L* temperature inside conductor varying with time.
- m* alternating current constant (equation (4)).
- m<sub>0</sub>* = *α* · *ρ*.
- m<sub>1</sub>* = *m* /  $\sqrt{2}$ .
- n* normal direction at conductor surface.
- r* distance from centre of conductor.

\* Burch and Davis, *l. c.*



- S** amplitude of alternating current density (equation (1)).  
**T** temperature inside conductor.  
**T<sub>0</sub>** temperature of surrounding medium as the surface of the conductor.  
**V** velocity of light.  
 **$\alpha$**  constant depending on choice of units (equation 1)).  
 **$\beta$**  Euler's constant (Note 2).  
 **$\gamma$**   $= -\frac{m_0}{K} \cdot \frac{C^2}{2}$  (in section II.).  
 **$\gamma$**   $= -\frac{m_0}{K} \cdot H_0^2$  (in section III.).  
 **$\mu$**  permeability.  
 **$\omega$**  angular frequency of alternating current.  
 **$\rho$**  specific electric resistance.  
 **$\sigma$**   $= \frac{V}{4\pi}$ .

Physical Laboratory of  
 Philips's Glowlampworks, Ltd.,  
 Eindhoven, Dec. 1927.

**XCII. *The Problem of a Hidden Polarized Sphere.* By Prof. A. PETROWSKY, Hon. Member of Rori (The Russian Society of Radio Engineers) \*.**

**CONTENTS.**

- § 1. Zero curves of longitudinal electropfiles.
- § 2. Maxima curves of longitudinal electropfiles.
- § 3. Zero curves of transversal electropfiles.
- § 4. Maxima curves of transversal electropfiles.
- § 5. Zero curves of oblique electropfiles.
- § 6. Maxima curves of oblique electropfiles.

**PART II.**

*Properties of Zero Curves and Maxima Curves.*

**I**N Part I. † of this paper a general solution of differential equations was found, expressing a distribution of electric force, and general characteristics of electropfiles were given, obtained by observations on the plane of division.

\* Communicated by the Author.

† See Phil. Mag., Feb. 1928, p. 334.

In the present part we shall examine the following question:—

Let us suppose that the observer, wishing to determine the exact place of the hidden sphere, has chosen a certain arbitrary direction, has drawn in that direction a row of parallel equidistant lines, and has taken electrophiles along each of them. As we already know, he will obtain curves, each of them having two (or one) zero points and three (or two) maxima. Marking on the plan of the section under investigation the places of the zero points and maxima, and joining all the corresponding points with smooth curves, he will get five (sometimes three) geometrical loci. We shall now consider the particularities of these loci.

§ 1. Let us begin with Case A, when the electrophiles are taken parallel to the plane of polarization of the hidden sphere.

From formula (32), Part I., it follows that the zero points are defined by the equation:

$$3u \cos \alpha - (1 + v^2 - 2u^2) \sin \alpha = 0 \quad . \quad . \quad (1)$$

$$\text{or} \quad u^2 - \frac{1}{2}v^2 + \frac{3}{2} \cot \alpha \cdot u - \frac{1}{2} = 0. \quad . \quad . \quad (1')$$

This equation means the following:—

(a) In passing from one electrophile to another (parallel to the plane of polarization) the zero points shift along the branches A'A' and A''A'' of the hyperbola\* (fig. 1).

(b) The centre C of this hyperbola lies in the plane of polarization behind the place of position of the hidden sphere, at a distance from the projection of its centre equal to

$$\left. \begin{aligned} x_0 &= \frac{3}{4} \cot \alpha \cdot h, \\ y_0 &= 0. \end{aligned} \right\} . \quad . \quad . \quad (2)$$

(c) The real semi-axis of the hyperbola lies in the plane of polarization and has the length:

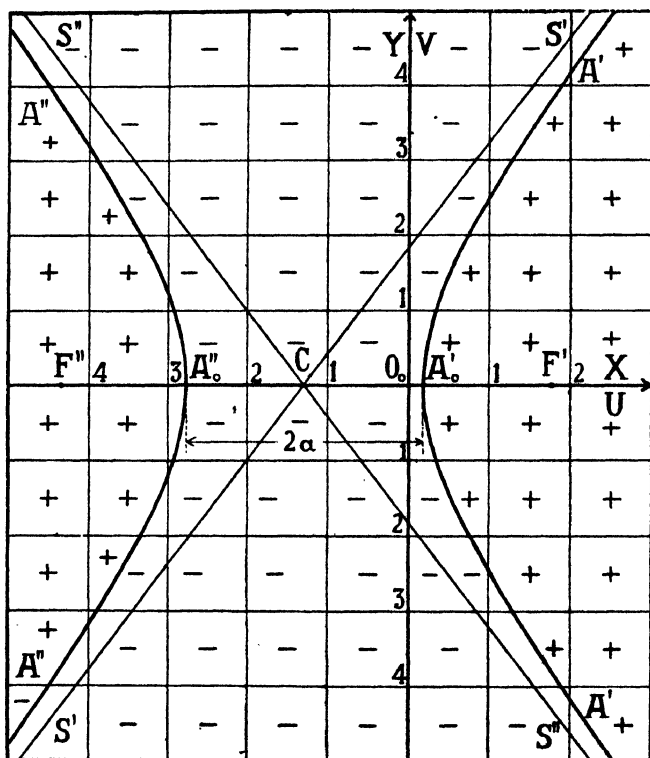
$$a \sqrt{\frac{1}{2} + \frac{9}{16} \cot^2 \alpha} \cdot h, \quad . \quad . \quad . \quad (3)$$

\* In fact the invariant of the equation is equal to  $+2 > 0$ , which corresponds to the hyperbola.

and the imaginary one is directed perpendicular to this plane and has the length \* :

$$b = \sqrt{2} \cdot a. \quad . \quad . \quad . \quad . \quad . \quad (4)$$

Fig. 1.—Curves presenting geometrical locus of zero points (O-curves) of an electrophile taken parallel to the plane of polarization (longitudinal electrophile).



\* As the equation contains neither the product  $uv$  nor the first power  $v$ , the hyperbola is symmetrical with respect to line  $U$ ; the direction of this line coincides with the direction of the real axis of the hyperbola; transforming the equation of the curve to the centre and to the axis, we obtain

$$u^2 - \frac{1}{2}v^2 = \frac{1}{2} + \frac{9}{16}\cot^2 \alpha \quad . \quad . \quad . \quad . \quad . \quad (5)$$

or

$$\frac{\frac{1}{2}u^2}{\frac{1}{2} + \frac{9}{16}\cot^2 \alpha} - \frac{v^2}{1 + \frac{9}{8}\cot^2 \alpha} = 1, \quad . \quad . \quad . \quad . \quad . \quad (5')$$

from which follow the expressions (8) and (4).

(d) The foci of the hyperbola are at distances from its centre equal to

$$c = \sqrt{3} \cdot a. \quad . \quad . \quad . \quad . \quad . \quad (6)$$

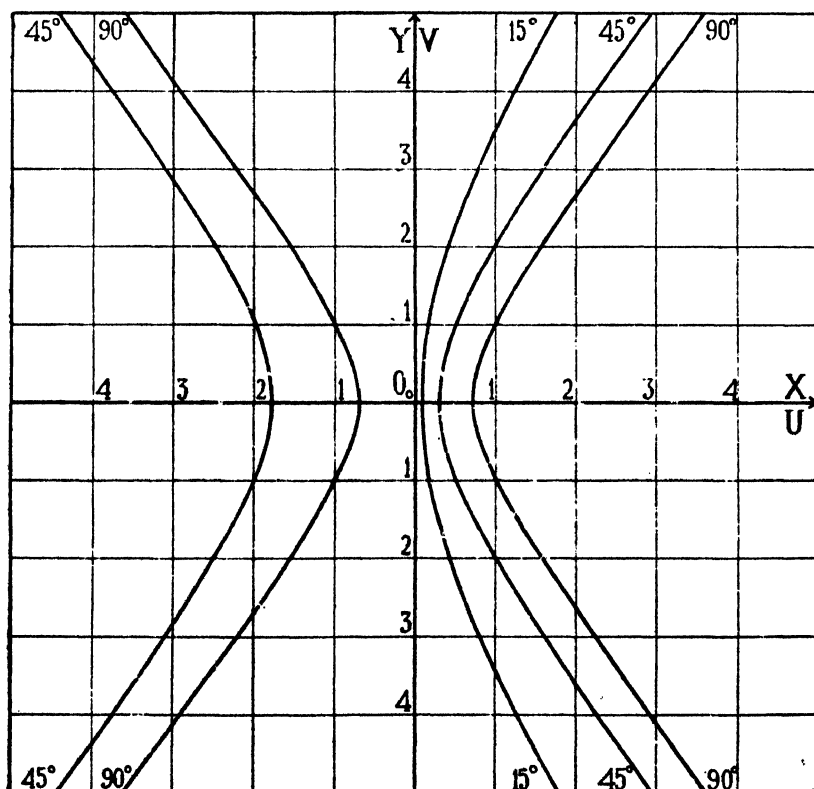
(e) The asymptotes  $S'S'$  and  $S''S''$  of the hyperbola are defined by the equations:

$$y = \sqrt{2}x, \quad . \quad . \quad . \quad . \quad . \quad (7')$$

$$y = -\sqrt{2}x; \quad . \quad . \quad . \quad . \quad . \quad (7'')$$

therefore they are inclined to the axis of abscissæ at angles equal to  $54^\circ 45'$ .

group of O-curves corresponding to  $\alpha = 15^\circ, 45^\circ$ , and  $90^\circ$ .



At different angles  $\alpha$  of inclination of the axis of polarization to the vertical the position of the above-mentioned hyperbola varies; and the differences are more marked for the front than for the rear branches, as is seen from fig. 2, on which are given hyperbolas obtained for  $\alpha = 15^\circ, 45^\circ$ ,

and  $90^\circ$ . [The rear branch of the hyperbola, corresponding to  $\alpha = 15^\circ$ , has no place already within the boundaries of the design; when  $\alpha = 0^\circ$  the hyperbola disappears, being reduced to one general point—the origin of the coordinates  $O_0$ .]

§ 2. Differentiating the formula (32), Part I., and equating the differential coefficient to zero, we obtain an equation defining the maxima of curve  $F_x$ :

$$1 + v^2 + 3 \tan \alpha \cdot (1 + v^2)u - 4u^2 - 2 \tan \alpha \cdot u^3 = 0 \quad (8)$$

$$\text{or} \quad 1 + v^2 = \frac{2u^2(2 + \tan \alpha \cdot u)}{1 + 3 \tan \alpha \cdot u} \quad (8')$$

This equation represents a curve of the 3rd order placed symmetrically with respect to the plane of polarization and consisting of three branches\* (fig. 3). The first branch  $M'M'$  is the geometrical locus of the front positive maximum, and lies between a certain value  $u = u'$  and  $u = +\infty$ ; the second branch is the geometrical locus of the middle negative maximum, and lies between  $u = -\frac{\cot \alpha}{3}$  and a certain negative value  $u = u''$ ; it has for asymptote the straight line  $T''T''$ , perpendicular to the plane of polarization, expressed by the equation:

$$u = -\frac{\cot \alpha}{3}; \quad (10)$$

\* The differential coefficient is

$$\frac{d(1+v^2)}{du} = \frac{2u}{(1+3 \tan \alpha \cdot u)^2} (4+9 \tan \alpha \cdot u+6 \tan^2 \alpha \cdot u^2). \quad (9)$$

It remains positive with positive values of  $u$ , passes through zero when  $u=0$ , and becomes negative with negative  $u$ :-

(1) By  $u = -\infty$  we have  $1+v^2 = +\infty$ : therefore  $v = \pm \infty$ ; by changing  $u$  from  $-\infty$  to a certain value  $u''' < -2 \cot \alpha$ , the value  $1+v^2$  diminishes to 1: therefore  $v$  changes till 0; these boundaries limit the rear branch of the M-curve.

(2) Further,  $1+v^2$  becomes less than 1: consequently  $v$  becomes an imaginary quantity till  $u = -\frac{\cot \alpha}{3}$ .

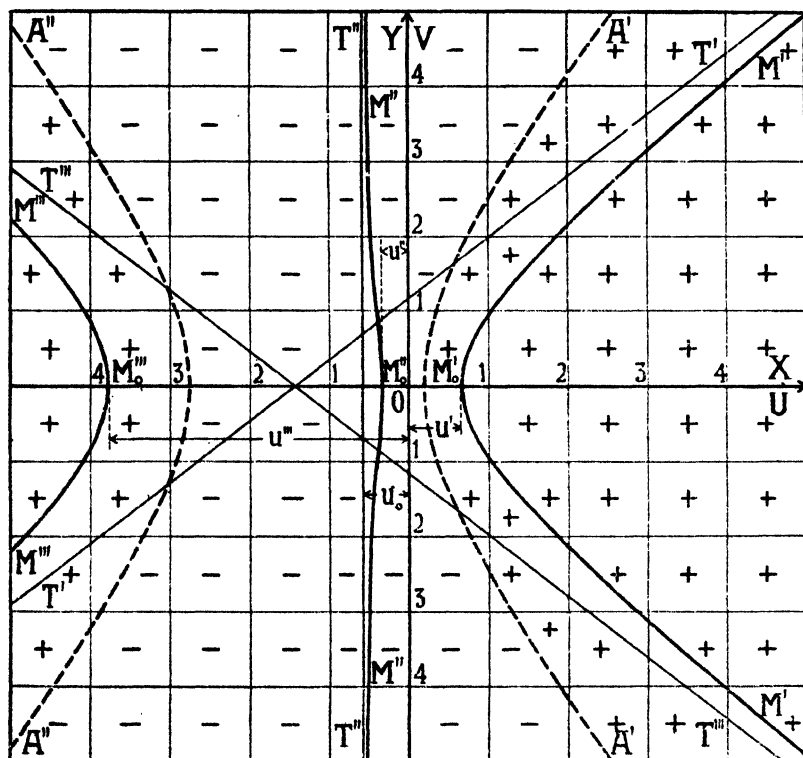
(3) When  $u = -\frac{\cot \alpha}{3}$  we have again  $1+v^2 = +\infty$ : therefore  $v = \pm \infty$ . In further change of  $u$  from  $-\frac{\cot \alpha}{3}$  to a certain value  $u'' < 0$  the value  $1+v^2$  diminishes to 1: therefore  $v$  again reaches 0; these boundaries limit the middle branch of the M-curve.

(4) Further,  $1+v^2$  becomes less than 1: therefore  $v$  once more becomes an imaginary quantity till  $u$ , passing through zero, takes a certain positive value  $u'$ .

(5) By  $u = u' > 0$  we have  $1+v^2 = 1$ ; by further change of  $u$  the value  $1+v^2$  increases, passing into infinity together with  $u$ : this region is occupied by the front branch of the M-curve.

the third branch  $M'''M''$  is a geometrical locus of the positive rear maximum, and lies between a certain negative

Fig. 3.—Curves representing geometrical loci of maxima (M-curves) of electrophiles taken parallel to the plane of polarization (transversal electrophile).



value  $u=u'''$  and  $u=-\infty$ . The first and third branches also have asymptotes; the last are expressed by equations:

$$v = \sqrt{\frac{2}{3}} \left[ x + \frac{5}{6} \cot \alpha \right], \quad . . . . (11)$$

$$v = -\sqrt{\frac{2}{3}} \left[ x + \frac{5}{6} \cot \alpha \right] . . . . (12)$$

The values  $u'$ ,  $u''$ , and  $u'''$ , expressing in a relative degree the shortest distance of the three above-mentioned geometrical loci from the projection of the place of the centre

of the sphere, may be obtained as roots\* of the cubic equation (8) by supposing  $v^2=0$ . Hence the equation :

$$u_m^3 + 2 \cot \alpha \cdot u_m^2 - \frac{3}{2} u_m - \frac{\cot \alpha}{2} = 0. \quad . \quad . \quad (13)$$

In view of the complexity of the functions expressing these roots, we do not state them.

We shall get the numerical value of each maximum by substituting in the expression  $F_x$  the value  $u_m$ , equal to the corresponding root of the equation (13) and the value  $v=0$ .

$$\begin{aligned} F_m &= Q \frac{3u_m \cos \alpha - (1 - 2u_m^2) \sin \alpha}{(1 + u_m^2)^{\frac{5}{2}}} \\ &= Q \frac{1 + 2u_m^2}{(1 + u_m^2)^2 \sqrt{1 + 4u_m^4}} \cdot \quad . \quad . \quad . \quad (14) \end{aligned}$$

With different angles  $\alpha$  of the inclination of the axis of polarization to the vertical, the distribution of M-curves is various: this difference is least perceptible in the middle branch  $M''$ , more so on the front branch  $M'$ , and most on the rear branch  $M'''$ .

This is well seen on fig. 4, in which are shown M-curves corresponding to  $\alpha=0^\circ$ ,  $15^\circ$ ,  $45^\circ$ , and  $90^\circ$ . The rear branches of the curves corresponding to  $\alpha=0^\circ$  and  $15^\circ$  are not placed on the chart; the middle branch of the curve corresponding to  $\alpha=90^\circ$  blends with the axis of ordinates.

§ 3. Let us now examine Case B; *i. e.*, when the electro-profile is taken perpendicular to the plane of polarization of a hidden sphere.

From formula (33), Part I., it follows that the zero points are defined by the equation :

$$v=0 \quad . \quad . \quad . \quad . \quad . \quad (15)$$

which corresponds to the straight line  $A'A'$  lying in the plane of polarization of the sphere, and by equation † :

$$\cos \alpha + u \sin \alpha = 0, \quad . \quad . \quad . \quad . \quad (16)$$

corresponding to the straight line  $A''A''$ , perpendicular to the plane of polarization and intersecting the latter in the point  $A_0''$ , for which

$$u''' = -\cot \alpha. \quad . \quad . \quad . \quad . \quad (17)$$

\* It is easy to ascertain that all three shown roots are real.

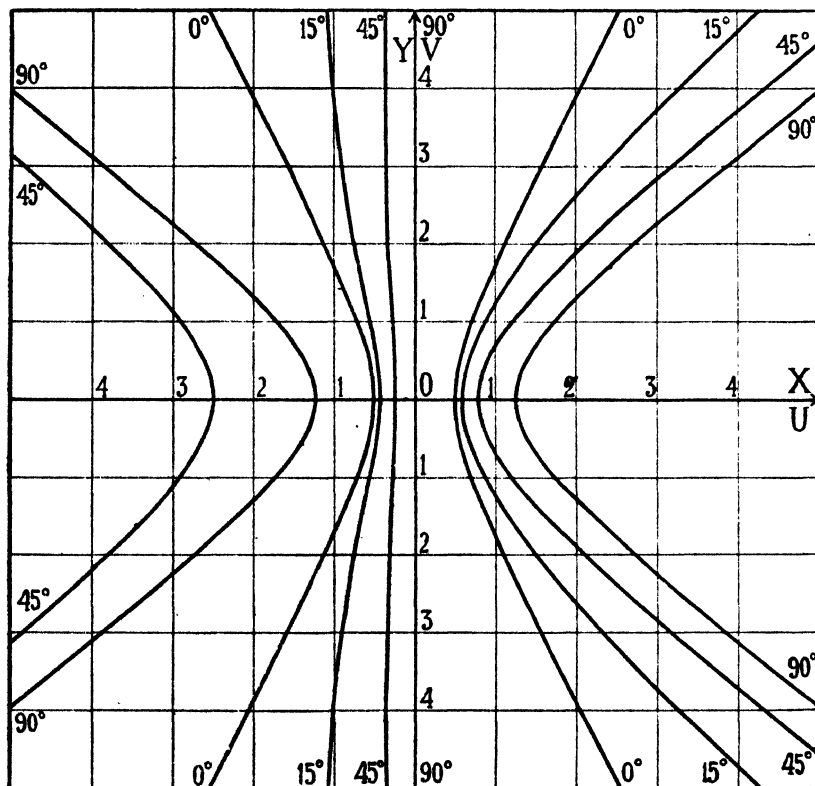
† The straight line defined by equation (16) is remarkable in that for points of this straight line, not only is the value  $F_y$  itself equal to zero, but also all differential coefficients of  $F_y$  by  $v$ , of any order whatever, also become zero.

§ 4. Differentiating formula (33), Part I., by  $v$ , and equating the differential coefficient to zero, we have the equation defining the geometrical locus of maxima :

$$1 + u^2 - 4v^2 = 0 \quad . \quad . \quad . \quad . \quad . \quad (18)$$

$$\text{or} \quad 4v^2 - u^2 = 1. \quad . \quad . \quad . \quad . \quad . \quad (18')$$

Fig. 4.—Group of M-curves corresponding to  $\alpha = 0^\circ, 15^\circ, 45^\circ$ , and  $90^\circ$ .



Hence we have the following :—

(a) According to the removal from one transversal electro-profile to another, the maxima remove along the lines of the hyperbola  $M'M'$ ,  $M'''M'''$  (fig. 5).

(b) The centre of this hyperbola lies exactly over the centre of the sphere.

(c) The real semi-axis of the hyperbola is perpendicular to



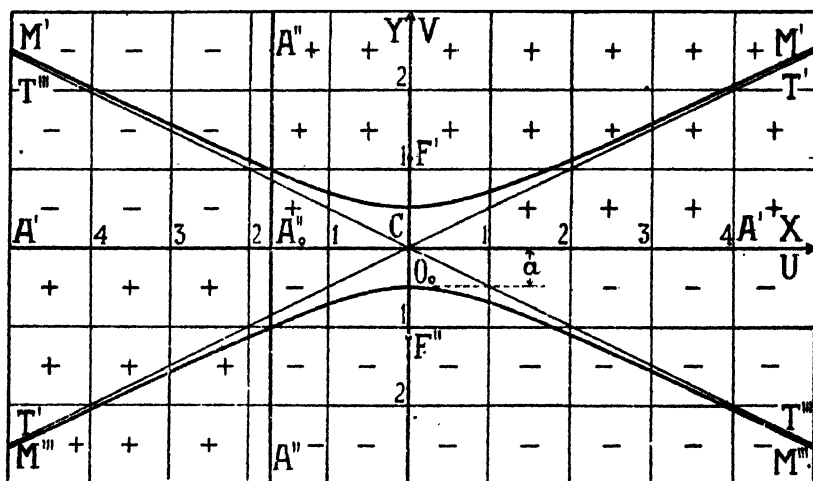
the plane of polarization, and is equal to the half depth of the centre of the hidden sphere :

$$a = \frac{h}{2}, \quad . . . . . (19)$$

but the imaginary semi-axis is in the plane of polarization and has a value equal to the depth of sphere ; *i. e.*, twice as much as the preceding one,

$$b = h. \quad . . . . . (20)$$

Fig. 5.—Geometrical loci of zero points and maxima of transversal electrophiles.



(d) The foci of the hyperbola  $F'$  and  $F''$  are at distances from the centre equal to

$$c = \frac{\sqrt{5}}{2}h. \quad . . . . . (21)$$

(e) The asymptotes  $T'T'$  and  $T''T''$  of the hyperbola are expressed by the equations :

$$u = -2v, \quad . . . . . (22')$$

$$u = +2v; \quad . . . . . (22'')$$

*i. e.*, are inclined to axis  $OX$  at angles of  $26^\circ 30'$ .

The value of the maxima is expressed by the formula :

$$(F_y)_m = \pm \frac{48Q(\cos \alpha + u \sin \alpha)}{25\sqrt{5}(1+u^2)^3} \quad . . . . . (23)$$

For different values of  $u$  this value is also different :

$$(\alpha) \text{ with } u = -\cot \alpha, \quad (F_y)_m = 0 ; \quad . \quad . \quad . \quad (24)$$

$$(\beta) \text{ with } u = -\frac{2}{3}\cot \alpha + \sqrt{\frac{4}{9}\cot^2 \alpha + \frac{1}{3}} \quad . \quad . \quad . \quad (25)$$

it takes the greatest value, equal to

$$(F_y)_m = \pm \frac{48Q}{25\sqrt{5}} \cdot \frac{-\frac{1}{3}\cos \alpha + \sqrt{\frac{4}{9}\cos^2 \alpha + \frac{1}{3}\sin^2 \alpha}}{\left[1 + \left(-\frac{2}{3}\cot \alpha + \sqrt{\frac{4}{9}\cot^2 \alpha + \frac{1}{3}}\right)^2\right]^2} ; \quad . \quad . \quad . \quad (26)$$

[Sign + corresponds to positive  $v$ , and sign - to negative  $v$ .]

$$(\gamma) \text{ with } u = -\frac{2}{3}\cot \alpha - \sqrt{\frac{4}{9}\cot^2 \alpha + \frac{1}{3}}, \quad . \quad . \quad . \quad (27)$$

it takes the greatest value, equal to

$$(F_y)_m = \mp \frac{48Q}{25\sqrt{5}} \cdot \frac{-\frac{1}{3}\cos \alpha + \sqrt{\frac{4}{9}\cos^2 \alpha + \frac{1}{3}\sin^2 \alpha}}{\left[1 + \left(-\frac{2}{3}\cot \alpha - \sqrt{\frac{4}{9}\cot^2 \alpha + \frac{1}{3}}\right)^2\right]^2} . \quad . \quad . \quad (28)$$

[Sign - corresponds to positive  $v$ , and sign + to negative  $v$ .]

§ 5. Let us examine now a general Case C, when the electrophile is taken at a certain angle  $\phi$  to the plane of polarization  $O_0X$  of the hidden sphere.

From formula (46), Part I., follows that zero points of the gradient of the field are defined by the equation :

$$3u' \cos \alpha - (1 + v'^2 - 2u'^2) \cos \phi \cdot \sin \alpha - 3u'v' \sin \phi \cdot \sin \alpha = 0 \quad . \quad . \quad . \quad (29)$$

$$\text{or} \quad u'^2 - \frac{1}{2}v'^2 - \frac{3}{2}\tan \phi \cdot u'v' + \frac{3}{2}\frac{\cot \alpha}{\cos \phi}u' - \frac{1}{2} = 0. \quad . \quad (29')$$

This equation shows the following :—

(a) According to the transition from one electrophile to another inclined at the same angle  $\phi$  to the plane of

polarization, the zero points remove along the branches  $A'A'$  and  $A''A''$  of the hyperbola\* (fig. 6).

(b) The centre  $C$  of this hyperbola has the coordinates:

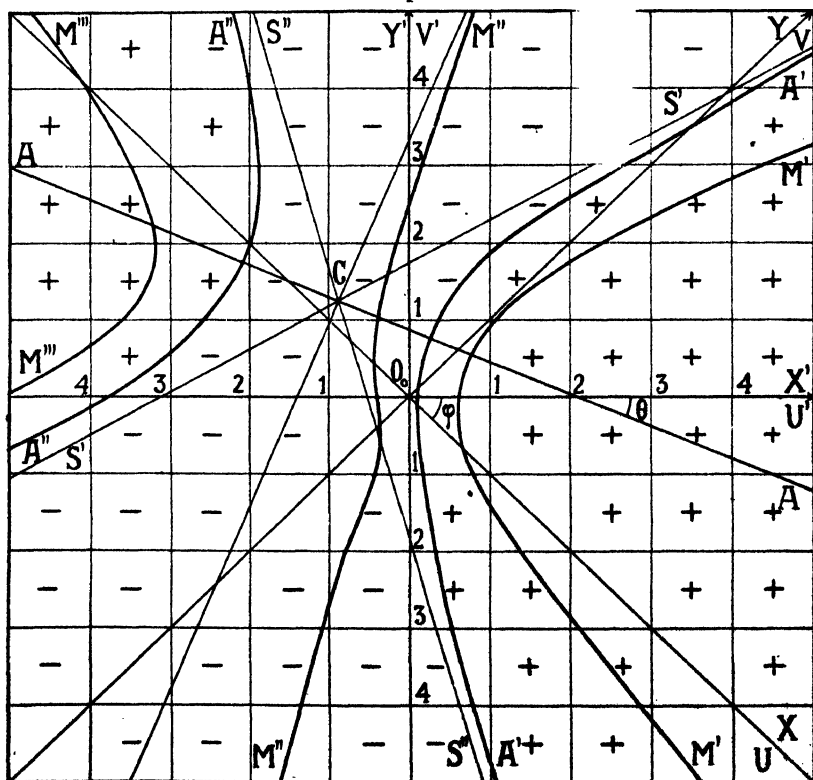
$$u_c' = -\frac{6 \cos \phi \cot \alpha}{8 + \sin^2 \phi}, \quad \dots \dots \dots (30)$$

$$v_c' = +\frac{9 \sin \phi \cot \alpha}{8 + \sin^2 \phi} \quad \dots \dots \dots (31)$$

or  $u_c = -\frac{3(2 + \sin^2 \phi) \cot \alpha}{8 + \sin^2 \phi}, \quad \dots \dots \dots (30')$

$$v_c = +\frac{3 \sin \phi \cos \phi \cot \alpha}{8 + \sin^2 \phi}; \quad \dots \dots \dots (31')$$

Fig. 6.—Geometrical loci of zero points and maxima of oblique electrophores.



\* In reality the invariant of equation (29') is

$$\Delta = \frac{9}{16} \tan^2 \phi + \frac{1}{2} > 0;$$

i. e., it presents a positive value corresponding to the hyperbola.

it does not lie any longer in the plane of polarization, and remaining behind the disposition of the centre of the sphere, removes to the same side from the plane of polarization to which the fore part of the line of survey has passed\*.

(c) The real semi-axis ACA of the hyperbola is inclined to the line of survey at an angle  $\theta$ , which is defined by the formula :

$$\tan 2\theta = -\tan \phi, \quad . \quad . \quad . \quad (33)$$

from which follows

$$2\theta = -\phi \quad . \quad . \quad . \quad (34)$$

$$\text{or} \quad \theta = -\frac{\phi}{2}; \quad . \quad . \quad . \quad (34')$$

in other words, the declination of the real semi-axis of the hyperbola from the line of survey takes place in a reverse direction and at half the angle.

(d) Transforming the equation of the hyperbola to the centre and to the axis, we obtain

$$\begin{aligned} & \left( \cos^2 \theta - \frac{1}{2} \sin^2 \theta - \frac{3}{2} \tan \phi \sin \theta \cos \theta \right) u'''^2 \\ & - \left( \frac{1}{2} \cos^2 \theta - \sin^2 \theta - \frac{3}{2} \tan \phi \sin \theta \cos \theta \right) v'''^2 \\ & = \frac{1}{2} + \frac{9 \cot^2 \alpha}{2(8 + \sin^2 \phi)}, \quad . \quad . \quad . \quad (35) \end{aligned}$$

from which one may find the values of the semi-axis and foci distances :

$$a = h \sqrt{\frac{2 \cos \phi \left( 1 + \frac{9 \cot^2 \alpha}{8 + \sin^2 \phi} \right)}{3 + \cos \phi}}, \quad . \quad . \quad (36)$$

$$b = h \sqrt{\frac{2 \cos \phi \left( 1 + \frac{9 \cot^2 \alpha}{8 + \sin^2 \phi} \right)}{3 - \cos \phi}}, \quad . \quad . \quad (37)$$

$$c = 2h \sqrt{\frac{3 \cos \phi \left( 1 + \frac{9 \cot^2 \alpha}{8 + \sin^2 \phi} \right)}{8 + \sin^2 \phi}}. \quad . \quad . \quad (38)$$

\* Transforming the equation of the hyperbola (29') to the centre, we obtain

$$u'''^2 - \frac{1}{2} v'''^2 - \frac{3}{2} \tan \phi \cdot u'' v'' - \left( \frac{1}{2} + \frac{9 \cot^2 \alpha}{2(8 + \sin^2 \phi)} \right) = 0. \quad (32)$$

(e) The asymptotes  $S'S'$  and  $S''S'$  of the hyperbola have the equations :

$$v' = \left( -\frac{3}{2} \tan \phi + \sqrt{\frac{9}{4} \tan^2 \phi + 2} \right) u' + \frac{3 \cot \alpha}{\sqrt{8 + \sin^2 \phi}}, \quad (39)$$

$$v' = \left( -\frac{3}{2} \tan \phi - \sqrt{\frac{9}{4} \tan^2 \phi + 2} \right) u' - \frac{3 \cot \alpha}{\sqrt{8 + \sin^2 \phi}}. \quad (40)$$

The angle between the asymptotes is defined by the equation :

$$\tan \omega = -\sqrt{8 + 9 \tan^2 \phi}; \quad . \quad . \quad . \quad (41)$$

therefore it depends only upon the angle  $\phi$  and lies between  $90^\circ$  and  $180^\circ$ .

§ 6. Differentiating the value  $F_x$  by  $u'$ , we obtain

$$\begin{aligned} \frac{\partial F_x}{\partial u'} = & \left[ 1 + \frac{3Q}{u'^2 + v'^2} \right]^{\frac{1}{2}} \{ \sin \alpha [ -2 \cos \phi \cdot u'^3 + 4 \sin \phi \cdot u'^2 v' \\ & + 3 \cos \phi \cdot u' v'^2 - \sin \phi \cdot v'^3 + 3 \cos \phi \cdot u' - \sin \phi \cdot v' ] \\ & - \cos \alpha [ 4u'^2 - v'^2 - 1 ] \}, \quad . \quad . \quad . \quad (42) \end{aligned}$$

from which follows that the curve of maxima is expressed by the equation :

$$\sin \alpha [ -2 \cos \phi \cdot u'^3 + 4 \sin \phi \cdot v' u'^2 + 3 \cos \phi \cdot v'^2 u' - \sin \phi \cdot v'^3 \\ + 3 \cos \phi \cdot u' - \sin \phi \cdot v' ] - \cos \alpha [ 4u'^2 - v'^2 - 1 ] = 0. \quad (43)$$

This is a curve  $M'M' M''M'' M'''M'''$  of the third order, which intersects the axis of abscissæ  $u'$  in three points, defined by the equation :

$$u'^3 + 2 \frac{\cot \alpha}{\cos \phi} u'^2 - \frac{3}{2} u' - \frac{\cot \alpha}{2 \cos \phi} = 0, \quad . \quad . \quad (44)$$

and the axis of ordinates  $v'$  in one point, defined by the formula :

$$v' = \frac{\cot \alpha}{\sin \phi}. \quad . \quad . \quad . \quad (45)$$

When  $\phi = 0$ , it passes into a curve expressed by equation (8), and when  $\phi = 90^\circ$  into the hyperbola expressed by the equation :

$$4u'^2 - v'^2 = 1, \quad . \quad . \quad . \quad (46)$$

which corresponds entirely to formula (18').

Examination of equation (43) shows that in observing the inequalities,

$$\left. \begin{aligned} 0 < \alpha < 90^\circ, \\ 0 < \phi < 90^\circ, \end{aligned} \right\} \dots \dots \dots (47)$$

the following hold :

- (a) The M-curve is asymmetric with respect to the line of removal and of its perpendicular ;
- (b) the M-curve has no centre of symmetry ;
- (c) the M-curve has no axis of symmetry ;
- (d) the M-curve has asymptotes whose equation is as follows :

$$v' = pu' + q, \dots \dots \dots (48)$$

and the angle coefficient is the root of the equation :

$$t^3 - 3 \cot \phi \cdot t^2 - 4t + 2 \cot \phi = 0, \dots \dots (49)$$

and the segment  $q$  is connected with the coefficient  $p$  by the correlation :

$$q = \frac{(p^2 - 4) \cot \alpha}{\sin \phi (3p^2 - 6 \cot \phi \cdot p - 4)} \dots \dots (50)$$

One may ascertain that the equation (49) always has three real roots, and consequently the M-curves have three asymptotes.

**XCIH. *The Problem of a Hidden Polarized Sphere.* By Prof. A. PETROWSKY, Hon. Member of Rori (The Russian Society of Radio Engineers) \*.**

**CONTENTS.**

- § 1. An analytical calculation of elements by data obtained by studying the longitudinal electrophiles.
- § 2. A graphical calculation.
- § 3. A calculation of elements obtained by studying transversal electrophiles.
- § 4. A general case of calculation.

**PART III.**

*Definition of Elements characterizing the Hidden Sphere.*

**S**TATEMENTS in the first two parts of this paper enable one to found the following method for defining elements characterizing a polarized hidden sphere by observations of electrophiles on the surface of division.

\* Communicated by the Author.

Having taken the electrophiles, and tracing on the plan the geometrical loci of zero curves and maxima curves, the observer will have one of three following cases, which we shall examine separately.

§ 1. CASE A.—The curves have the form, presented on fig. 1, characterized by the asymptote of the middle branch of the maxima curve being parallel to the imaginary axis of the zero hyperbola; hence we conclude that the profile has been taken along the lines parallel to the plane of polarization.

Further we proceed as follows.

(a) Drawing the asymptotes  $S'S'$  and  $S''S''$ , we find the centre  $C$  of hyperbola  $A'A'$ ,  $A''A''$  and its axis. The direction of the real axis presents the direction of the plane of polarization. The projection  $O_0$  of the sphere's centre is between the centre  $C$  of the hyperbola and its front branch  $A'A'$ , being at a distance from its centre equal to

$$x_c = \frac{3}{4} \cot \alpha \cdot h. \quad . \quad . \quad . \quad . \quad . \quad (1)$$

(b) Let us trace the asymptote  $T''T''$  to the curve of the second (negative) maxima. The point of intersection  $C_4$  of this asymptote,  $T''T''$ , and the real axis of the hyperbola lies behind the projection of the sphere's centre at a distance equal to

$$x_4 = \frac{1}{3} \cot \alpha \cdot h. \quad . \quad . \quad . \quad . \quad . \quad (2)$$

(c) Measure on the plan the distance  $CC_4$ . It is evidently to be equal to

$$d = \frac{5}{12} \cot \alpha \cdot h; \quad . \quad . \quad . \quad . \quad . \quad (3)$$

hence we find the distance of projection of the sphere's centre  $O_0$  from centre  $C$  of the hyperbola:

$$x_c = \frac{3}{4} \cot \alpha \cdot h = \frac{9}{5} d. \quad . \quad . \quad . \quad . \quad (4)$$

(d) Let us measure on the plan the real semi-axis of the hyperbola.

According to formula (3), Part II., its square member equals

$$a^2 = \frac{h^2}{2} + \frac{9}{16} \cot^2 \alpha \cdot h^2 \quad . \quad . \quad . \quad . \quad . \quad (5)$$

or

$$a^2 = \frac{h^2}{2} + \frac{81}{25} d^2 = \frac{h^2}{2} + x_c^2; \quad . \quad . \quad . \quad . \quad (5')$$

whence we find the depth of the sphere:

$$h = \sqrt{2a^2 - \frac{164}{25}d^2} \quad . \quad . \quad . \quad . \quad . \quad (6)$$

(e) We find the angle of inclination of the axis of polarization to the vertical by formula (3), substituting in it the value  $h$ :

$$\cot \alpha = \frac{12d}{5h} \quad . \quad . \quad . \quad . \quad . \quad (7)$$

(f) Measuring the distance  $x_m$  from the projection  $O_0$  of the sphere's centre to the point of intersection of any of the curves maxima with the real axis of the hyperbola (e.g., the distance from  $O_0$  to  $M_0'$ ), dividing it by value  $h$ , formula (6), we obtain

$$u_m = \frac{x_m}{h} \quad . \quad . \quad . \quad . \quad . \quad (8)$$

Substituting in expression (14), Part II., this value  $u_m$  and likewise the corresponding value of maximum  $F_m$  found from experiment, we find

$$Q = \frac{(1 + u_m^2)^{5/2} F_m}{3u_m \cos \alpha + (1 - 2u_m^2) \sin \alpha} \quad . \quad . \quad . \quad . \quad (9)$$

(g) Lastly, supposing  $E$  to be the greatest value of the electromotive force which is developed by the sphere, one may find the radius of the sphere:

$$r_0 = \sqrt{\frac{Qh^2}{E}} = h \sqrt{\frac{Qh}{E}} \quad . \quad . \quad . \quad . \quad (10)$$

§2. The calculation discussed in § 1, (c), (d), (e) may be made graphically. This is shown on fig. 1, and consists as follows:—

(c') Plot along  $Cv'$  from point  $C$  segment  $Ca$  and  $Cb$  in ratio 5:9, join  $a$  with  $C_4$ , and draw a line  $CO_0$  parallel to  $aC_4$ . Point  $O_0$  is the projection of the sphere's centre sought for.

(d') Draw a line  $O_0O$  parallel to  $Cv'$  and line  $O_0p$ , bisecting the angle  $UO_0O$ ; describe from point  $C$  as from a centre an arc  $A_0'n$  with radius equal to the real semi-axis of hyperbola  $a$ , up to the crossing of this arc with line  $O_0O$  in some point  $n$ ; then taking point  $O_0$  for the centre, describe an arc  $np$  up to the intersection with the bisecting





Calculating, according to the statements in (f) and (g), the value of the radius  $r_0$  of the sphere, and tracing with this radius the periphery from centre O, we get a full graphic representation of all correlations sought for.

§ 3. CASE B.—The curves have a shape represented on fig. 2, characterized by the fact that the zero lines represent two reciprocally-perpendicular straight lines A'A' and A''A'', and the curves of maxima the hyperbola M'M', M''M'', whose imaginary axis U coincides in direction with one of the zero straight lines A'A'. One may conclude that the profile is taken along the lines perpendicular to the plane of polarization. At the same time we act as follows :—

Tracing the asymptotes T'T' and T'''T''', we find the centre C of the hyperbola and its axis. The direction of its imaginary axis CU represents the projection of the plane of polarization. The projection O<sub>0</sub> of the sphere's centre is in the centre of the hyperbola.

(b) Measure the real axis of the hyperbola  $2a$ .

The depth of the sphere's centre is equal to

$$h = 2a. \quad . \quad . \quad . \quad . \quad . \quad . \quad . \quad (11)$$

(c) Let us measure the distance  $d$  between the centre of the hyperbola and the point of intersection of two zero lines. The angle of inclination of the axis of polarization is defined by the equality :

$$\cot \alpha = -\frac{d}{h} = -\frac{d}{2a}. \quad . \quad . \quad . \quad . \quad . \quad . \quad . \quad (12)$$

(d) Substituting the value  $\cos \alpha$  and the value  $(F_y)_m$ , found from experiment for line U=0 in the expression (23), Part II., find

$$Q = \frac{25 \sqrt{5}}{48 \cos \alpha} = \frac{25 \sqrt{5} \sqrt{4a^2 + d^2}}{48 d}. \quad . \quad . \quad . \quad . \quad . \quad . \quad . \quad (13)$$

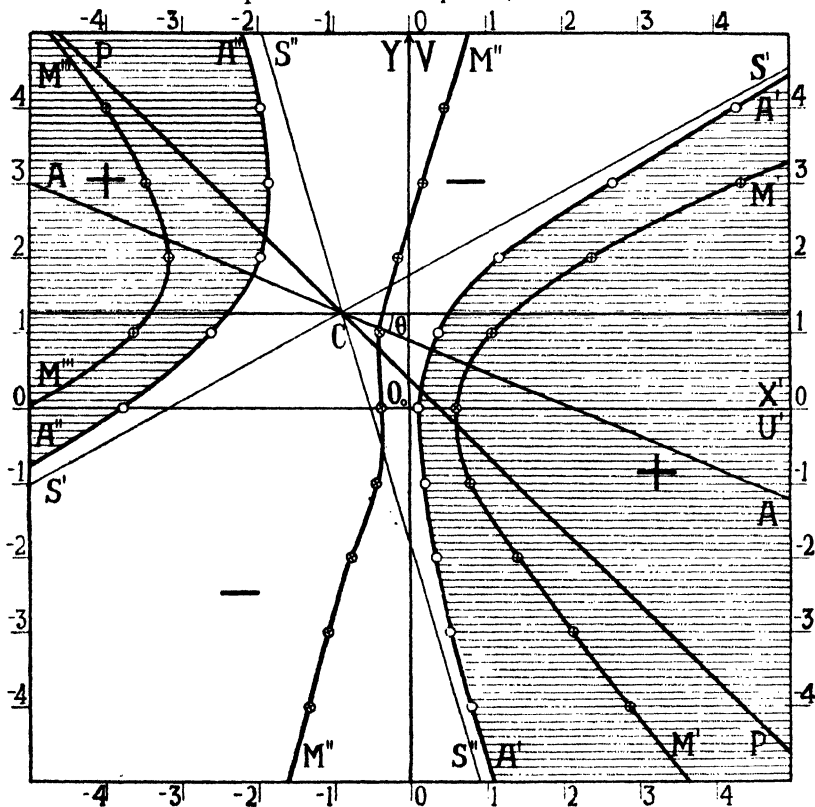
(e) Lastly, if E is the greatest value of the electromotive force developed by the sphere, one may find the radius of the sphere

$$r_0 = \sqrt{\frac{Qh^3}{E}} = h \sqrt{\frac{Qh}{E}}. \quad . \quad . \quad . \quad . \quad . \quad . \quad . \quad (14)$$



the observer repeats once more the survey of electrophile, taking it either parallel to the found plane or perpendicular

Fig. 3.—Graphical determination of the direction of the plane of polarization of the sphere (Case C).



to it, which leads the solution of the problem to Case A or Case B.

**XCIV. Oscillatory Motion of a Viscous Liquid in a long straight Tube.** By S. F. GRACE, *M.Sc.* (University of Liverpool)\*.

§ 1. **T**HE problem of the steady flow of a viscous liquid through a tube of circular section has been considered by Osborne Reynolds†; he finds that the critical

\* Communicated by the Author.

† "On the Dynamical Theory of Incompressible Viscous Fluids and the Determination of the Criterion," *Phil. Trans. A*, clxxxvi. p. 123 (1895) [Papers, ii. p. 535].

velocity, beyond which the flow becomes turbulent, varies directly as the kinematic viscosity and inversely as the radius of the tube. With regard to oscillatory motions, the laminar non-turbulent oscillations of a viscous liquid between two parallel plates are dealt with by Lamb\*, while in this paper the oscillations along a straight tube are considered and the velocity-distribution over a right section of a tube of uniform circular section is discussed in detail.

It is found that for very slow oscillatory motion along a uniform circular tube the velocity-distribution resembles that for steady motion along the tube, the velocity being in phase with the disturbing force. As the period of oscillation decreases, the magnitude of the velocity in the central portion of the tube tends to become uniform, the breadth of this central portion gradually increases, while the phase of the velocity tends to lag more and more behind that of the disturbing force. For comparatively short periods of oscillation, viz., less than 6 sec. for a tube of radius 1 cm., the velocity across a right section of the tube is approximately uniform, and has a phase-lag of  $\frac{1}{2}\pi$  behind the disturbing force, except near the walls of the tube. Here, proceeding radially inwards, the velocity increases rapidly from zero to a maximum, and then diminishes to the neighbourhood of the uniform value; the phase-lag meanwhile gradually increases to  $\frac{1}{2}\pi$ .

The object of the present paper is to draw attention to the difference in the velocity-distribution in the case of the oscillatory motion of a viscous liquid as compared with that which occurs when the liquid is in steady motion, and to raise the question as to what form the Osborne Reynolds criterion will take for oscillatory motion. The great difference in velocity-distribution produced by oscillation suggests the advisability of an examination of this criterion in the case of oscillatory motion from both theoretical and experimental view-points.

The author desires to express his thanks to Prof. J. Proudman for bringing the problem of the present paper to his notice.

## § 2. *Tube of General Section.*

Consider a uniform long straight tube of any section, and take rectangular axes  $Oxyz$ , with  $O$  at the centroid of a right section and  $Oz$  parallel to the length of the tube. Let the tube be filled with liquid, which is made to oscillate in the

\* Lamb, 'Hydrodynamics,' 5th ed., §§ 345-7.

direction of the length, and assume that the motion is everywhere axial; thus, if  $u, v, w$  are the components of velocity at  $(x, y, z)$ , then  $u=v=0$ , and the equation of continuity becomes

$$\partial w / \partial z = 0.$$

Hence, with the usual notation, the general hydrodynamical equations for a viscous liquid \* reduce to

$$\left. \begin{aligned} 0 &= X - \frac{1}{\rho} \frac{\partial p}{\partial x}, \\ 0 &= Y - \frac{1}{\rho} \frac{\partial p}{\partial y}, \\ \frac{\partial w}{\partial t} &= Z - \frac{1}{\rho} \frac{\partial p}{\partial z} + \nu \left( \frac{\partial^2 w}{\partial x^2} + \frac{\partial^2 w}{\partial y^2} \right). \end{aligned} \right\} \dots \dots (1)$$

Assuming that no external bodily forces act in the directions  $Ox$  and  $Oy$ , the first two equations of (1) give

$$\frac{\partial p}{\partial x} = \frac{\partial p}{\partial y} = 0,$$

so that  $p$  is a function of the variables  $z$  and  $t$  only.

Now let

$$Z - \frac{1}{\rho} \frac{\partial p}{\partial z} = C e^{i\sigma t},$$

where  $C$  is a constant depending upon the forces producing the oscillation of the liquid, and put

$$w = f(x, y) e^{i\sigma t}.$$

The third equation of (1) now becomes

$$i\sigma f = C + \nu \left( \frac{\partial^2 f}{\partial x^2} + \frac{\partial^2 f}{\partial y^2} \right)$$

or

$$\frac{\partial^2 f}{\partial x^2} + \frac{\partial^2 f}{\partial y^2} - \frac{i\sigma}{\nu} f = -\frac{C}{\nu} \dots \dots (2)$$

### § 3. Tube of Circular Section.

In the case of a uniform tube of circular section, the radius of which is  $a$ , the equation (2) is transformed into cylindrical polar coordinates  $r, \theta, z$ , where

$$r \cos \theta = x, \quad r \sin \theta = y,$$

\* Lamb, 'Hydrodynamics,' 5th ed., § 328.

936 Mr. S. F. Grace on *Oscillatory Motion of a*  
and the function  $f$  assumed to be independent of  $\theta$ . Thus

$$w = f(r)e^{i\sigma t},$$

where

$$\frac{d^2 f}{dr^2} + \frac{1}{r} \frac{df}{dr} - \frac{i\sigma}{\nu} f = -\frac{C}{\nu}.$$

This is Bessel's equation of zero order, and the solution is

$$f(r) = \frac{C}{i\sigma} \left[ 1 - \frac{J_0\{r\sqrt{(-i\sigma/\nu)}\}}{J_0\{a\sqrt{(-i\sigma/\nu)}\}} \right], \quad (3)$$

on the assumption that there is no slipping of the liquid at the surface of the tube, i. e., that  $f=0$  for  $r=a$ .

Taking  $\sigma/\nu$  small, it is seen, neglecting squares and higher powers of  $\sigma/\nu$ , that

$$f(r) = \frac{C}{i\sigma} \left\{ 1 - \frac{1 + \frac{1}{4}ir^2\sigma/\nu}{1 + \frac{1}{4}ia^2\sigma/\nu} \right\} = \frac{C}{4\nu} (a^2 - r^2).$$

This is the solution of the problem of the steady flow of liquid through the tube\*.

The functions  $J_0(x\sqrt{-i})$  which occur in (3) may be split up into their real and imaginary parts by means of the relations†

$$J_0(x\sqrt{-i}) = I_0(x\sqrt{i}) = \text{ber } x + i \text{bei } x,$$

and if  $f(r)$  is written in the form  $v_1 - iv_2$ , it is found that

$$\left. \begin{aligned} v_1 &= \frac{C}{\sigma} \cdot \frac{\text{bei } a\lambda \text{ ber } r\lambda - \text{ber } a\lambda \text{ bei } r\lambda}{\text{ber}^2 a\lambda + \text{bei}^2 a\lambda}, \\ v_2 &= \frac{C}{\sigma} \left\{ 1 - \frac{\text{ber } a\lambda \text{ ber } r\lambda + \text{bei } a\lambda \text{ bei } r\lambda}{\text{ber}^2 a\lambda + \text{bei}^2 a\lambda} \right\}, \end{aligned} \right\} \quad (4)$$

where  $\lambda$  has been written in place of  $\sqrt{(\sigma/\nu)}$ .

The values of  $\text{ber } x$  and  $\text{bei } x$  are tabulated for  $x=0$  to 10 at intervals of 0.1 in the British Association Report of 1912, and the values of  $\text{ber}^2 x + \text{bei}^2 x$  for the same values of  $x$  in the Report of 1916. With the aid of these tables the values of  $v_1$  and  $v_2$  have been found for values of  $r/a$  between 0 and 1 and for values of  $a\lambda$  equal to 1, 2, ..., 10 and the results exhibited graphically.

Since in practical applications one is usually concerned with an oscillation of definite magnitude rather than with the forces which produce this oscillation, the ratios  $v_1/V$  and  $v_2/V$  have been obtained and plotted against  $r/a$ ,  $V$  being

\* Lamb, 'Hydrodynamics,' 5th ed., § 331.

† Watson, 'Bessel Functions,' § 3.8.

the maximum velocity of the liquid along the axis of the tube—i.e.,  $V = \sqrt{(v_1^2 + v_2^2)}_{r=a}$ .

In diagrams I. and II. the variations of  $v_1/V$  and  $v_2/V$  are

Diagram I.

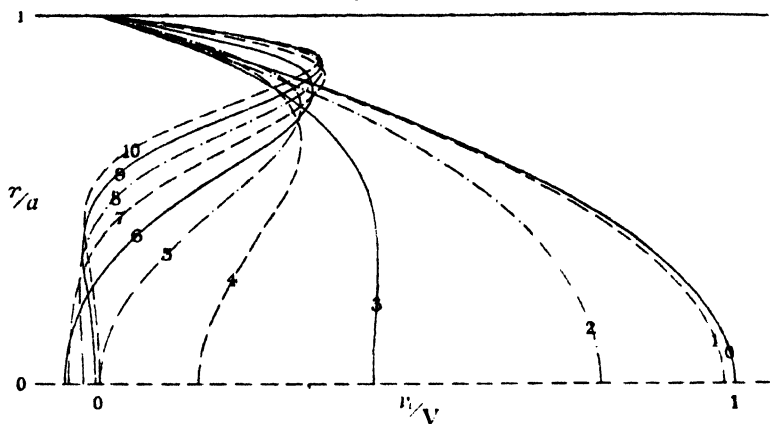
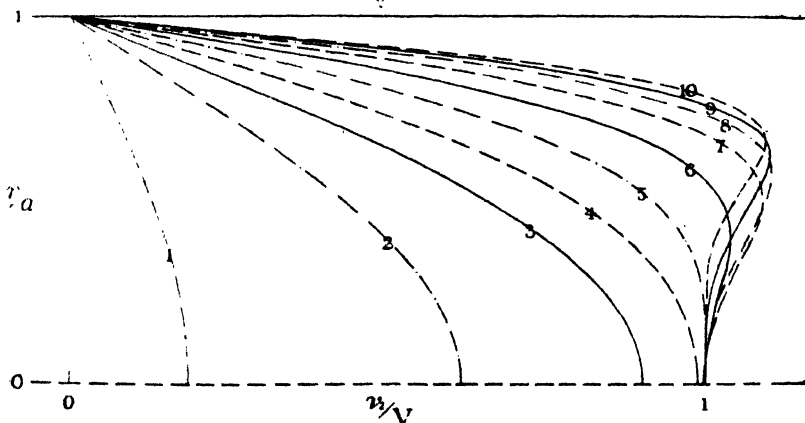


Diagram II.



shown for periods of oscillation of the liquid given by  $a\lambda = 1, 2, \dots, 10$ . For water at  $18^\circ\text{C}$ . oscillating in a tube of radius 1 cm., taking  $\nu = 0.0106$  gm./cm. sec., the periods (T) are given approximately by

$$a\lambda = 1, \quad 2, \quad 3, \quad 4, \quad 5, \quad 6, \quad 7, \quad 8, \quad 9, \quad 10$$

$$T = 593, \quad 148, \quad 66, \quad 37, \quad 24, \quad 16, \quad 12, \quad 9, \quad 7, \quad 6 \text{ sec.}$$



The curve marked 0 in diagram I. represents the velocity-distribution for steady motion along the tube.

#### § 4. *Asymptotic Formulæ.*

For large values of  $x$  (real) \*

$$\text{ber } x = (2\pi x)^{-\frac{1}{2}} e^{\alpha} \cos \beta, \quad \text{bei } x = (2\pi x)^{-\frac{1}{2}} e^{\alpha} \sin \beta,$$

$$\text{ber}^2 x + \text{bei}^2 x = e^{2\alpha} / 2\pi x.$$

$$\text{where} \quad \alpha = x / \sqrt{2}, \quad \beta = x / \sqrt{2} - \pi / 8.$$

If these asymptotic forms be substituted in the expressions for  $v_1$  and  $v_2$ , then, for large values of  $r\lambda$ , it is found that

$$\begin{aligned} v_1 &= \frac{C}{\nu \lambda^2} \left( \frac{a}{r} \right)^{\frac{1}{2}} e^{-\gamma} \sin \gamma; \\ v_2 &= \frac{C}{\nu \lambda^2} \left\{ 1 - \left( \frac{a}{r} \right)^{\frac{1}{2}} e^{-\gamma} \cos \gamma \right\}, \end{aligned} \quad (5)$$

$$\text{where} \quad \gamma = \lambda(a-r) / \sqrt{2}.$$

Comparing the values of  $v_1/V$ ,  $v_2/V$  obtained from these formulæ with those obtained from the expressions (4), it is found that for  $a\lambda = 5$  the formulæ (5) provide a good approximation for values of  $r$  between  $\frac{1}{2}a$  and  $a$ , the greatest error occurring for  $r = \frac{1}{2}a$ , and being here less than 1 per cent. For  $a\lambda = 10$ , either of the formulæ (4) and (5) may be used between  $r/a = 0.1$  and 1 for plotting the values of  $v_1/V$ ,  $v_2/V$  against  $r/a$  on paper 16 in.  $\times$  10 in., as in the original diagrams I., II., since the differences between the two sets of values are inappreciable.

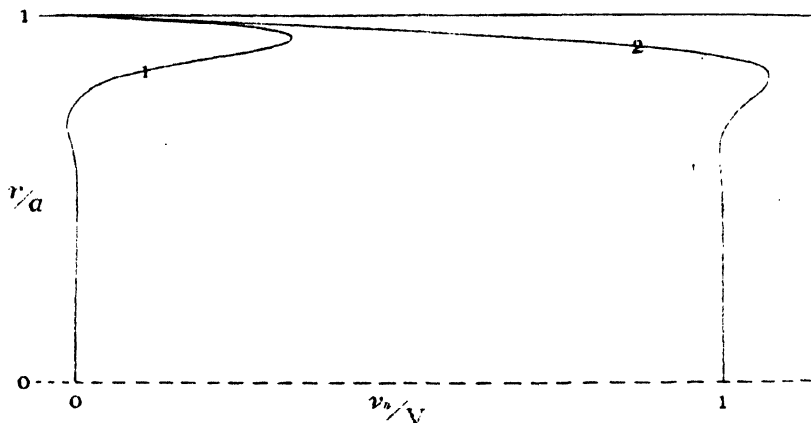
Consequently, for the purposes of the present problem, there is no need for further tabulation of the functions  $\text{ber } x$  and  $\text{bei } x$ ; the formulæ (4) are used for values of  $a\lambda$  between 0 and 10 and the formulæ (5) for larger values. Since these latter formulæ are only valid for  $r\lambda$  large, it follows that they cannot apply for small values of  $r$ —i. e., for points near the axis of the tube. However, a glance at the diagrams I. and II. shows that for  $\lambda$  large  $v_1$  is here approximately zero, while  $v_2$  is approximately equal to  $V$ .

Diagram III. shows the forms of the curves  $v_1/V$ ,  $v_2/V$  for large values of  $\lambda$ ; they are drawn for  $a\lambda = 20$ —i. e., for a period of oscillation of 1.5 sec. for water in a tube of radius 1 cm.

\* Watson, 'Bessel Functions,' § 7.24.

It will be noted that for large values of  $a\lambda$  and for  $r$  in the neighbourhood of  $a$  the distribution of  $v_1$  and  $v_2$  is

Diagram III.



practically independent of  $a$ , since only  $a-r$  and  $a/r$  occur in the expressions (5).

---

XCV. *A New Method of Conductivity Measurement by means of an Oscillating Valve Circuit.* By Professor E. F. BURTON and ARNOLD PITT, B.A., *Department of Physics, University of Toronto* \*.

### I. Introduction.

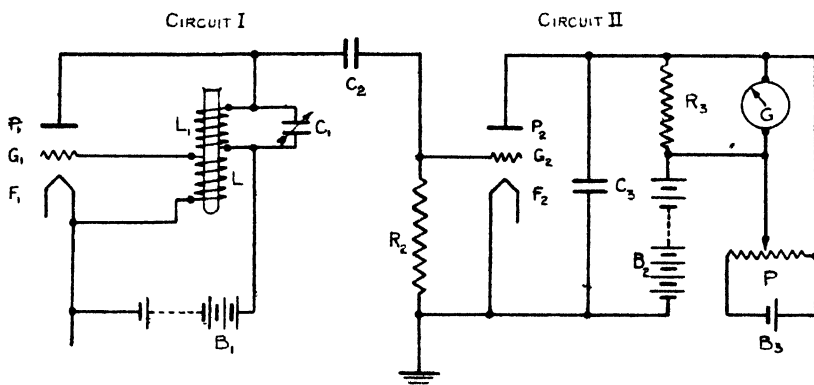
**I**N the course of setting up the apparatus for the measurement of the dielectric constant of conducting liquids by the use of the oscillations of a valve circuit, remarkable effects of the conductivity of the sample of liquid on the oscillating period, when the oscillations are in a peculiarly sensitive region, came to light unexpectedly. The extreme sensitivity to small changes in the conductivity of the purest conductivity water to which minute quantities of impurities are added indicates that the method herewith described offers something useful in this field.

The lay-out of the apparatus is very simple, but it requires considerable patience to master the conditions necessary to

\* Communicated by the Authors.

produce the sensitive region, but once it has been obtained it can be easily reproduced at will. Fig. 1 shows the arrangement: the left-hand portion of the figure represents an ordinary oscillating tube-circuit, for which the writers have used a Mullard tube; the coils  $L_1$  and  $L$  have coefficients of self-induction of 0.072 and 0.250 henries respectively, the condenser  $C_1$  has a range of 0.250 micro-microfarads, while the plate potential is 60 volts. The two  $L$  coils are placed closely end to end, and the sample, the conductivity of which is required, is inserted in the central core space; the position of maximum sensitiveness for the sample is within the core of  $L_1$ .

Fig. 1.



$P_1, G_1, F_1$ , elements of tube: Mullard D.F.A. 4.

$B_1$ , battery giving anode voltage of 60 volts.

$L_1$ , coil of self-induction, 0.072 henries, resistance 31.8  $\omega$ .

$L$ , coil of self-induction, 0.250 henries, resistance 124.8  $\omega$ .

$C_1$ , variable air-condenser, up to 250  $\mu\mu$  fd.

$C_2$  and  $C_3$ , fixed condensers, capacities 0.01  $\mu$  fd. and 1.0  $\mu$  fd., respectively.

$G$ , a sensitive aperiodic galvanometer, 1000  $\omega$  resistance (Ayrton-Mather type).

$R_2$ , grid leak of 3 megohms.  $R_3$ , adjustable shunt for  $G$ .

$P_2, G_2, F_2$ , element of U.X. 201 A tube.

$B_2$ , battery giving anode voltage of 70 volts.

$B_3, P$ , cell and potentiometer to adjust galvanometer.

The filament current is adjusted to about 0.2 ampere, the anode potential fixed at about 60 volts, the condenser adjusted so as to produce oscillations in the circuit, and the intensities of the voltage changes due to these oscillations as

impressed on the second circuit are measured by the galvanometer attached in this second circuit. The change of potential impressed on the grid of the second tube is rectified and amplified in the ordinary manner. The details of the second tube-circuit are indicated in fig. 1. The condenser  $C_2$  has a fixed capacity of  $0.01 \mu\text{fd.}$ , and a grid leak of 3 megohms is inserted. The condenser,  $C_3$ , has a fixed value of  $1 \mu\text{fd.}$  The filament voltage is 4 volts (current 0.21 ampere), and the anode voltage of this circuit is 70 volts.

When the circuits are operating the galvanometer is deflected off the scale owing to the steady plate current, but this deflexion is neutralized by the application of a contra-current from a potentiometer arrangement shown in the figure. Any succeeding deflexion of the galvanometer will measure the variation in plate current due to changes in the oscillating circuit caused by the insertion of the specimens in the L coils.

The sensitive region referred to in the first paragraph is obtained by adjusting the capacity of  $C_1$  so that it is near the value for which the oscillations stop: with the values of self-inductance, filament current, and plate voltage indicated above, the oscillations cease at a value of 90 micromicrofarads for  $C_1$ . If, for example,  $C_1$  is set at 100 micromicrofarads, the galvanometer is deflected and a zero re-established by the potentiometer voltage: the insertion of a sample of conducting material (liquid or solid) in the core of the coils L gives an additional deflexion of the galvanometer apparently due mainly to the influence of the conductivity of the material and not its magnetic permeability, as one might expect.

In the Tables which follow are shown results for the following series of substances:—(a) Samples of water of gradually increasing conductivities but all of quite small values; and (b) Samples of various organic liquids, purchased as C.P. but not specially re-purified.

(a) In Table I. are listed the results for measurements on aqueous solutions of very small conductivities. Beginning with doubly-distilled water of low conductivity, a series was prepared by using a standard KCl solution.

It is at once apparent that the apparatus is extremely sensitive to changes of conductivity between  $2 \times 10^{-6}$  and  $200 \times 10^{-6}$  for this setting of the condenser  $C_1$ , which was  $100 \mu\mu\text{fd.}$

(b) The capacity of  $C_1$  was then changed to  $95 \mu\mu\text{fd.}$ ,

which made the whole much more sensitive to extremely low conductivities, and the effects of samples of various

TABLE I.

Solution	Conductivity $k \times 10^6$ .	Deflexion of Galvanometer.
1.....	2.5 *	18.5 cm.
2.....	10.5	32.2
3.....	11.5	33.7
4.....	15.0	38.2
5.....	24.0	45.9
6.....	47.7	51.4
7.....	76.6	55.4
8.....	222.8	58.9
9.....	255.0	60.1
10.....	502.0	60.6
11.....	1225.0	62.0

\* The conductivity of this sample increased slightly, due to impurities in the experimental tube.

organic liquids were tried. These liquids were sealed hermetically into glass tubes which just fitted into the coils LL<sub>1</sub> projecting about 2 cm. from each end. Table II.

TABLE II.

*Organic Liquids.*

Liquid.	Formula.	Galvanometer Deflexion in cm. (corrected for effect of empty glass alone)
Carbon Tetrachloride ...	$\text{CCl}_4$	17.2
Chloroform .....	$\text{CHCl}_3$	42.5
Ether .....	$\text{C}_4\text{H}_{10}\text{O}$	32.3
Amyl Alcohol .....	$\text{C}_5\text{H}_{11}\text{OH}$	23.7
Butyl " .....	$\text{C}_4\text{H}_9\text{OH}$	71.4
Ethyl " .....	$\text{C}_2\text{H}_5\text{OH}$	77.2
Pentane.....	$\text{C}_5\text{H}_{12}$	8.8
Hexane .....	$\text{C}_6\text{H}_{14}$	6.8
Benzol .....	$\text{C}_6\text{H}_6$	18.0
Xylene (O. P.) } .....	$\text{C}_8\text{H}_{10}$	{ 15.3
Xylol (Com.) } .....		{ 11.8
Toluene (Com.) } .....		{ 14.0
Toluol (O. P.) } .....	$\text{C}_7\text{H}_8$	{ 15.1

shows the results for a series of organic liquids chosen, more or less, at random.

No attempt was made to measure the conductivity of the above liquids by any other method; these numbers are given merely to illustrate the way in which such slightly conducting liquids can be differentiated among themselves. Quantitative relations between the sensitivity of this arrangement and that used for results in Table I. were not obtained, as the purest water would have thrown the galvanometer image completely off the scale with the sensitivity used for organic liquids.

*Remarks.*

The purpose of the present paper is merely to draw attention to the occurrence of a rather striking phenomenon which opens out great practical possibilities in the measurement or testing of very small conductivities; along these lines further work is being carried on.

At the same time, the theoretical problems involved are very interesting, and it is hoped to prosecute this feature of the investigation. At present the writers are not in possession of sufficient data as to the influence of variation in the period of oscillations and other experimental conditions to justify embarking on this phase of the work here.

After the phenomenon noted here was first observed, the paper by Belz (*Phil. Mag.* (6) xliv. p. 479, 1922) on the magnetic effects of insertion of samples of various salts in coils of similar circuits was noticed. The conductivity effect seems to have escaped him, except for metallic wires, which, of course, also show a large effect in the above apparatus.

*Summary.*

A primary valve oscillating circuit and subsidiary measuring circuit have been developed which enable one to obtain remarkable indications of the conductivities of very dilute aqueous solutions and of various organic liquids.

The writers desire to express their thanks to the Director of the Physical Laboratory, Professor J. C. McLennan, for his generous support in the course of this work.

Department of Physics,  
University of Toronto,  
Toronto, Canada.

XCVI. *The Ultra-violet Absorption Spectrum of Cod-Liver Oil.*  
By JAY W. WOODROW, Ph.D.\*

SCHULTZ and his co-workers † have found absorption bands for a thin film of cod-liver oil at about  $328\ \mu\mu$  and  $279\ \mu\mu$ . Heilbron, Kamm, and Morton ‡, using a quartz spectrograph and rotating sector photometer, found three regions of abnormal absorption in the ultra-violet spectrum with a film of cod-liver oil about 0.1 mm thick. Almost complete absorption occurred for wave-lengths less than  $260\ \mu\mu$ , while a band was observed with its maximum at  $320\ \mu\mu$ , and another in the region from  $270\ \mu\mu$  to  $290\ \mu\mu$ . The latter was attributed to the small amount of ergosterol present. R. Pohl §, using a special type of photoelectric photometer has observed an absorption band at  $280\ \mu\mu$  for chlorestrol dissolved in alcohol.

In the experiments to be described briefly here, a photoelectric spectrophotometer was used to investigate the absorption spectrum of cod-liver oil between the wave-lengths  $255\ \mu\mu$  and  $320\ \mu\mu$ .

The photoelectric cell was made of pyrex glass with a quartz window sealed in by means of a graded quartz-to-pyrex seal. The cathode consisted of an aluminium cylinder with an opening immediately back of the quartz window, while the anode was a silver wire at the centre of this cylinder. The air-pressure within the cell was reduced until the maximum photoelectric current was obtained with a potential difference of about 350 volts between the wire and the cylinder. This gave a high sensitivity, as the current was large, due to ionization by collision. The current was measured by means of a quadrant electrometer, using an electrostatic balance with a potentiometer and a condenser.

The spectrometer was specially constructed in the laboratory for these experiments. It had a large quartz prism and a pair of large quartz lenses of long focal length, giving rather large dispersion in the ultra-violet. It was calibrated by means of a small direct-reading ultra-violet spectrometer. A spark between molybdenum terminals was used as the source of light, since this arrangement gave very strong

\* Communicated by Prof. J. S. Townsend, F.R.S.

† Schultz & Morse, Amer. J. Dis. Child. xxx. p. 199 (1925); Schultz & Ziegler, J. Biol. Chem. lxi. p. 415 (1926).

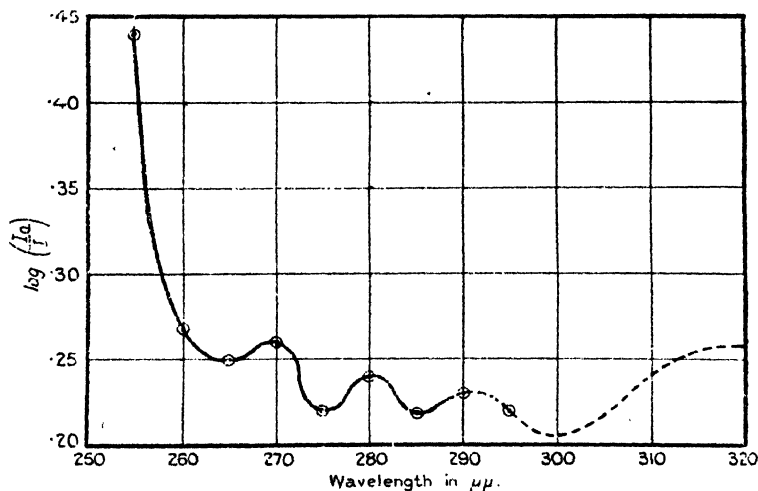
‡ Heilbron, Kamm, & Morton, Biochem. J. xxi. pp. 78 & 1279 (1927).

§ R. Pohl, *Nachrichten der Gesellschaft der Wissenschaften zu Göttingen, Mathematische-Physikalische Klasse*, 1926, Hefte 2, p. 142.

illumination in the region to be studied and remained very constant for the time necessary to take the readings.

The absorption cell consisted of two thin fused quartz plates separated by strips of metal foil about 0.04 mm. in thickness. After considerable difficulty at first, it was finally found possible to fill such a cell with the oil and have it free from air-bubbles. In all the readings, the absorption due to this cell was compared with that of another cell made in exactly the same way except that it contained no oil. These two cells were mounted together in such a way that either one could be brought accurately into place before the slit of the photoelectric cell. Trials were also made with the absorption cells in front of the slit of the spectrometer, giving the same results as in the other position.

Fig. 1.



The results of the experiments are given by the curve in the accompanying figure, where  $I$  and  $I_0$  represent the currents obtained for the cod-liver oil and the empty absorption cells respectively. It is seen that almost complete absorption occurred for wave-lengths less than 250  $\mu\mu$ . As the photoelectric cell was not very sensitive for wave-lengths greater than 290  $\mu\mu$ , the measurements were not so accurate in this region, and this part of the curve is shown by a broken line. However, the experiments indicated very definitely rather strong absorption in the neighbourhood of 320  $\mu\mu$ . There are also three narrow absorption bands with



maxima near 270, 280, and 290  $\mu\mu$  respectively. These coincide almost exactly with the absorption bands of ergosterol which Heilbron\* and his co-workers place at 270, 281.5, and 293.5  $\mu\mu$ . The magnitude of these absorption bands is not great, as is to be expected, since the amount of ergosterol present is small, but its effects are much larger than the experimental errors for the apparatus used.

Absorption cells of greater thickness were also tried, but it was found that the experimental errors were too great with the larger values of the ratio  $I_0/I$  for the absorption bands to show up clearly.

### *Summary.*

It has been shown that the characteristic ergosterol absorption bands can be observed in a thin film of cod-liver oil by means of a sensitive photoelectric spectrophotometer.

In conclusion, I wish to express my gratitude to Professor J. S. E. Townsend for furnishing the equipment for this investigation and for many helpful suggestions made during the progress of the work.

Electrical Laboratory,  
Oxford University,  
Oxford.

---

### XCVII. *Multiple Reactive Gears.* By E. K. SANDEMAN, *Ph.D. (London), B.Sc., A.C.G.I.†*

THE Multiple Reactive Gear follows as a logical outcome of the particular "Theory of the Torque Converter," which appeared in the October number of the Philosophical Magazine. In explaining the present modification of the principles, the same conventions and notation will be employed. It was there mentioned that certain advantages might result from employing, instead of a single mass, a mechanical reactive network containing a number of elements of mass or stiffness. Such a network can be made to have a reactance which changes with frequency (*e.g.* engine speed), in a much more flexible manner than the reactance of a pure mass; the use of a multiplicity of elements enables several performance conditions to be satisfied in the same gear.

In fig. 1*a* are shown two mechanical networks of the

\* Heilbron, Kamm, & Morton, *Biochem. J.* xxi. pp. 78 & 1279 (1927).

† Communicated by the Author.

Fig. 1 a.

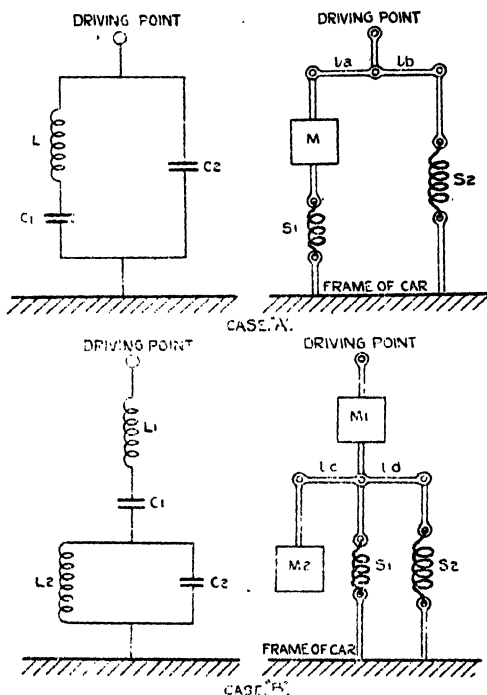
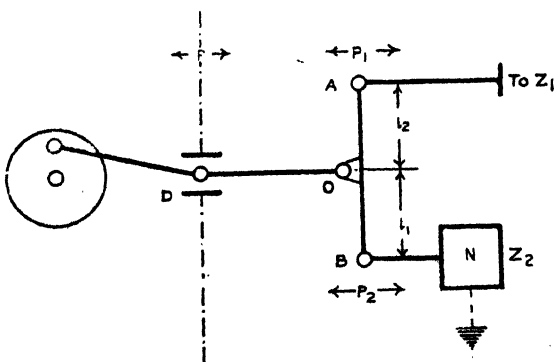


Fig. 1 b.



type contemplated, together with their equivalent electrical circuits. These networks are intended to have their driving-points connected to B (fig. 1 b). If  $l_a = l_b$  and  $l_c = l_d$ , then

in order that the impedances of the mechanical networks in pounds per foot per second shall be represented by the same numbers as the impedances of the electrical networks expressed in ohms, the equations relating the equivalent elements must be as below, where masses are expressed in pounds, stiffnesses in pounds per foot, inductances in henrys, and capacities in farads.

$$\begin{array}{ll} \text{Case A : } M = \frac{gL}{4}, & \text{Case B : } M_1 = gL_1, \\ S_1 = \frac{1}{4C_1}, & M_2 = \frac{gL_2}{4}, \\ S_2 = \frac{1}{4C_2}, & S_2 = \frac{1}{4C_2}, \quad S_1 = \frac{1}{C_1}, \end{array}$$

where  $g$  = the acceleration of gravity in feet per second per second.

The networks in fig. 1 are only types, it being possible to construct 2 two-element networks, 4 three-element networks, 11 four-element networks, etc. The values of the elements constituting one of these networks may be determined as follows :—

In equations (1), (11), and (13) of the above-mentioned paper the required resistance towards the engine is

$R_e$  = the real part of

$$\left( \frac{l_1}{l_1 \pm l_2} \right)^2 \frac{1}{Z_a} + \left( \frac{l_2}{l_1 \pm l_2} \right)^2 \frac{1}{Z_b}, \quad \dots \quad (1)$$

where  $Z_a$  is the load impedance and  $Z_b$  is the impedance presented by the network N at B (fig. 1).

Putting

$$\left( \frac{l_1}{l_1 \pm l_2} \right)^2 = A, \quad \left( \frac{l_2}{l_1 \pm l_2} \right)^2 = B, \quad \dots \quad (2)$$

let

$$Z_a = C + jD, \quad \dots \quad (3)$$

since the load resistance may be complex owing to the shunt stiffness ; and let

$$Z_b = jX, \quad \dots \quad (4)$$

since the network impedance is a pure reactance ; then

$$R_e = \text{real part of } \frac{1}{\frac{A}{C+jD} + \frac{B}{jX}} \quad \dots \quad (5)$$

$$= \text{real part of } \frac{jCX - DX}{jAX + BC - jBD}$$

$$= \text{real part of } \frac{(jCX - DX)(BC - jAX - jBD)}{B^2C^2 + (AX + BD)^2}$$

$$= \frac{CAX^2}{B^2C^2 + A^2X^2 + B^2D^2 + 2ABDX} \quad \dots \quad (5a)$$

$$\therefore (CA - R_e A^2)X^2 - 2R_e ABDX - R_e B^2(C^2 + D^2) = 0.$$

$$\therefore X = \frac{2R_e ABD \pm \sqrt{4R_e^2 A^2 B^2 D^2 + 4R_e B^2 (C^2 + D^2)(CA - R_e A^2)}}{2(CA - R_e A^2)} \quad \dots \quad (6)$$

If  $R_e > Z_a$ , then O must divide AB (fig. 1 b) internally, and the + signs in equation (2) are applicable. If  $R_e < Z_a$ , then O divides AB externally, and the - signs in equation (2) are applicable.

If  $R_e > Z_a$ , then

$$B = 1 - A. \quad \dots \quad (7)$$

Then from equation (5 a)

$$R_e = \frac{CAX^2}{(1-A)^2C^2 + A^2X^2 + (1-A)^2D^2 + 2A(1-A)DX}$$

$$\therefore (1-2A+A^2)C^2 + A^2X^2 + (1-2A+A^2)D^2 + (2A-2A^2)DX = \frac{1}{R_e} CAX^2.$$

$$\therefore C^2 - 2AC^2 + A^2C^2 + A^2X^2 + D^2 - 2AD^2 + A^2D^2 + 2ADX - 2A^2DX - \frac{1}{R_e} CAX^2 = 0$$

$$\therefore (C^2 + D^2 + X^2 - 2DX)A^2 + \left(2DX - 2C^2 - 2D^2 - \frac{1}{R_e} CX^2\right)A + C^2 + D^2 = 0.$$

$$2C^2 + 2D^2 + \frac{CX^2}{R_e} - 2DX$$

$$\pm \sqrt{\left(2DX - 2C^2 - 2D^2 - \frac{CX^2}{R_e}\right)^2 - 4(C^2 + D^2)(C^2 + D^2 + X^2 - 2DX)}$$

$$\therefore A = \frac{\pm \sqrt{\left(2DX - 2C^2 - 2D^2 - \frac{CX^2}{R_e}\right)^2 - 4(C^2 + D^2)(C^2 + D^2 + X^2 - 2DX)}}{2C^2 + 2D^2 + 2X^2 - 4DX} \quad (8)$$

Similarly, if  $R_e > Z_a$ , then

$$B = A - 1 \quad (9)$$

and

$$2C^2 + 2D^2 + \frac{CX^2}{R_e} + 2DX$$

$$\pm \sqrt{\left(2DX + 2C^2 + 2D^2 + \frac{CX^2}{R_e}\right)^2 - 4(C^2 + D^2)(C^2 + D^2 + X^2 + 2DX)}$$

$$A = \frac{\pm \sqrt{\left(2DX + 2C^2 + 2D^2 + \frac{CX^2}{R_e}\right)^2 - 4(C^2 + D^2)(C^2 + D^2 + X^2 + 2DX)}}{2C^2 + 2D^2 + 2X^2 + 4DX} \quad (10)$$

For the present purpose the positive value of the root will be taken.

Equation (6) gives the value of the impedance of the reactive network at any one power in order that a load resistance  $Z_a$  shall present a required impedance  $R_e$  towards the engine.

At any one power the values of  $R_e$  and  $Z_a$  are read respectively from the engine and load-resistance diagrams (figs. 2 and 3).

The value of  $R_e$  at each power is, on the engine diagram, the resistance corresponding to the point of intersection of the power line for the power concerned, with alternatively—

- (a) The upper curve of the limit of commercial performance when maximum car speed is required (*i. e.*, the engine delivers maximum power).
- (b) The curve of maximum economy when maximum economy is required.

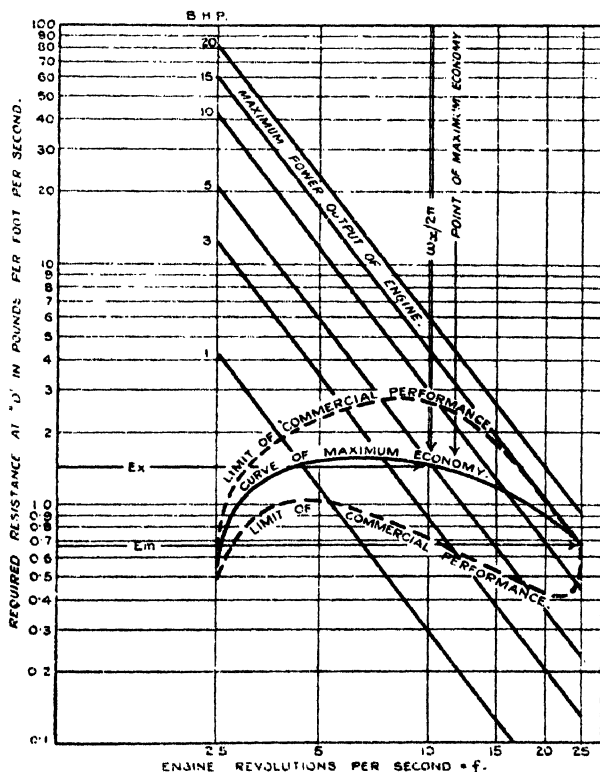
The value of  $Z_a^*$  at each power is, on the load diagram, the resistance corresponding to the point of intersection of

\* In the presence of shunt stiffness  $Z_a$  will be modified, as in equation (18) of previous article.

the power line for the power concerned, with alternatively—

- (c) The maximum gradient curve if maximum efficiency on hills is required.
- (d) The average resistance curve if the best average performance is required.

Fig. 2.



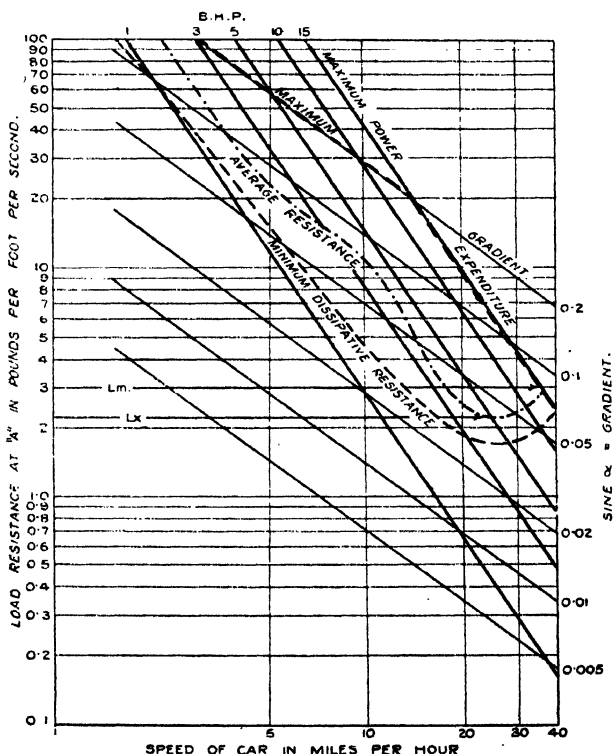
The above are chosen as examples of the type of criteria of performance which might be chosen, but other types can be chosen if desired.

Having chosen the type of engine performance required and the type of car performance (load performance) required, it is only necessary to adjust the lever ratio  $l_1/l_2$  and the reactance  $X$  so that at a number of chosen powers under load conditions specified by (c) or (d) the engine shall give a performance as specified by (a) or (b).

The value of  $l_1/l_2$  may be determined as follows:—

Let  $\hat{R}_e$  and  $\hat{Z}_a = \hat{C} + j\hat{D}$  be the values of  $R_e$  and  $Z_a$  at power  $p$  when the value of  $\frac{R_e}{Z_a}$  is a maximum. The shunt network is arbitrarily given a value which is as large as is practicably possible; let this value be  $\hat{X}$ . The corresponding

Fig. 3.



value of  $A = \frac{l_1}{l_1 \pm l_2}$  is given by substituting  $\hat{R}_e$ ,  $\hat{Z}_a$ , and  $\hat{X}$  in equations (8) or (10), according to whether  $\frac{R_e}{Z_a}$  is greater or less than unity. The value of B then follows from equation (9). Then by choosing suitable finite values of X at suitable powers other than  $p$ , exact impedance matching

at these powers may be obtained for conditions of load and engine performance corresponding alternatively to (a) or (b) and (c) or (d) above. The necessary value of  $X$  is given at each power by inserting the value of  $Z_a$  and  $R_e$  at that power, together with the values of  $A$  and  $B$ , in equation (6). The frequencies (engine speeds in revolutions per minute  $\times 60$ ) at which these powers are delivered are the frequencies corresponding to the points of intersection of the power-lines on the engine diagram with the curve of maximum economy, or the limit of commercial performance curve.

It is therefore required to construct a mechanical network which shall have certain known values of reactance  $X$  at a number of known frequencies. Formulæ for constructing an electrical network to accomplish this are given in 'Transmission Circuits for Telephone Communication,' by K. S. Johnson (van Nostrand Company), Appendix E, p. 296.

If the values of  $X$  calculated from equation (6), which are actually in pounds per foot per second, are imagined to be electrical ohms, then the Johnson formulæ will give a solution in terms of inductance  $L$  henrys and capacity  $C$  farads.

The type of formulæ to be used for conversion to masses in pounds, and to stiffnesses in pounds per foot, were given at the beginning of the present article.

In general, the network must be so constructed that while one effective network anti-resonance may occur at the limit of the range of frequencies (*i. e.* engine speeds) of importance, no resonance must occur in that range, or the load will be completely short-circuited. In particular cases this condition may be violated, since in practice, with the throttle open, the engine will rapidly accelerate from a speed at which network resonance occurs.

The networks shown are intended to have the driving-point connected to  $B$  (fig. 1) and the other end to the frame of the car, but networks may be used where no connexion is made to the frame of the car.

### Conclusion.

The Multiple Reactive Gear affords, among others, the following possibilities:—

If  $n$  elements are used in the network, by suitable adjustment of the fixed gear ratio (including the lever ratio), when the throttle is suitably adjusted, the engine may be made to give its most economical performance under average load conditions at  $(n + 1)$  chosen powers; or the engine may



be made to give its most economical performance under average load conditions at  $n$  chosen powers, and to deliver its maximum possible power on the heaviest gradient, or the engine may be made to give its maximum power under average load conditions at  $(n + 1)$  chosen engine speeds; or the engine may be made to attain any predetermined speed before it begins to exert an appreciable torque on the load. This last performance condition can be realized very simply by making the network anti-resonant at an engine speed just above the speed at which the engine is required to run. It is evident that the number of performance conditions may be multiplied indefinitely.

A number of modifications naturally suggest themselves which enable the impedance of the load to be further modified. Among these are the use of non-linear stiffnesses, *i. e.* springs whose stiffness increases as they are compressed; by this means the increasing stiffness brought into play by the large velocities flowing, as resonance is approached, may be made to prevent a condition of resonance ever being reached. Another device is a mechanical network presenting an impedance in series with the load.

#### APPENDIX.

##### *Solution of the Impedance looking into the Double-acting Ratchet.*

In the "Theory of the Torque Converter," published in the October number of the Philosophical Magazine, it was shown that  $R_E$ , the real part of the impedance looking into the double-acting ratchet, is approximately a pure resistance equal to the resistance looking into the ratchet-driven rotor.

It will now be shown how, in practice, an exact solution may be obtained. As a preliminary the case will be considered where a special type of ratchet is employed which is double-acting, and which maintains contact at each stroke during the whole time that the force in the rod between A (fig. 1) and the ratchet, *e. g.* compression or tension, is in the same sense. This is equivalent to a synchronous commutator in which commutation occurs at the time when the voltage has fallen to zero. In practice such a condition would be hard to realize exactly, but the results obtained from such an assumption indicate the magnitude and the type of the effect to be expected in the practical case, and, what is more important, it indicates how certain simple measurements can be made in practice to determine exactly the resistance to be

expected looking into any type of ratchet used, whether automatic or clutch-controlled.

It will now be shown that under the above conditions if  $R_L$  is the continuous velocity resistance of the ratchet-driven rotor then the resistance looking into the ratchet is practically given by

$$R_E = \frac{\pi^2}{8} R_L,$$

and that other effects introduced by the non-harmonic nature of the load are negligible.

In fig. 1*b* is shown the general arrangement of the multiple reactive gear, which is identical in principle with the torque converter except that the mass  $M$  attached to  $B$  is replaced by the network  $N$ .

In fig. 4 is shown an equivalent electrical circuit for the

Fig. 4.

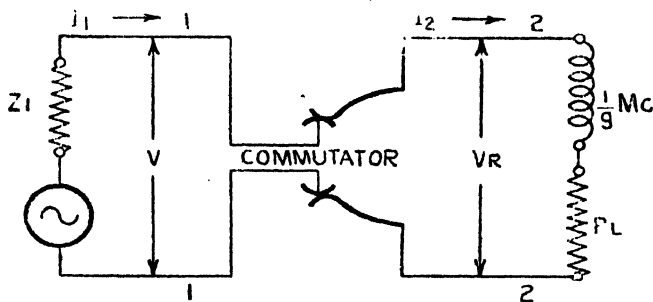
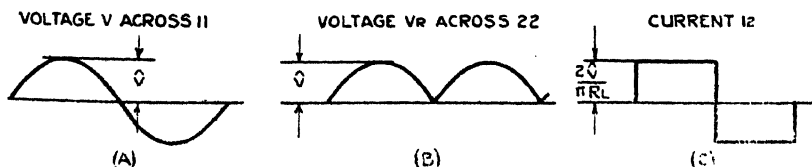


Fig. 5.



part of the gear to the right of A.  $Z_1$  is the impedance looking back from A towards the engine,  $M_C$  is the mass of the car in pounds, and  $R_L$  is the load resistance.

An e.m.f., as at A in fig. 5, occurring across 1, 1, therefore gives rise to an e.m.f.  $V_R$ , as at B in fig. 4, occurring

across 2, 2. By means of a Fourier expansion it may be shown that

$$V_R = \frac{2\hat{V}}{\pi} - \frac{4}{3} \frac{\hat{V}}{\pi} \cos \omega t - \frac{4}{15} \frac{\hat{V}}{\pi} \cos 4 \omega t - \text{etc.}$$

If  $Z_2$  has a very large impedance to alternating currents, as is the case in practice, then no alternating current flows through  $Z_2$ , but only direct current of magnitude

$$I_2 = \frac{2\hat{V}}{\pi R_L},$$

where  $R_L$  is the resistance component of the load defined by  $\frac{550 W}{x^2}$ ,  $W$  being the transmitted horse-power and  $x$  the peripheral speed of the ratchet-driven rotor.

The current through  $Z_1$  is therefore of the form shown at C in fig. 5. This is of the form

$$I_1 = A \sin \omega t + \frac{1}{3} A \sin 3\omega t + \frac{1}{5} A \sin 5\omega t + \text{etc.},$$

where

$$A = \frac{4}{\pi} \times \frac{2\hat{V}}{\pi R_L} = \frac{8}{\pi^2} \frac{\hat{V}}{R_L}$$

= the amplitude of the current of fundamental frequency.

The resistance, looking into the ratchet, is therefore

$$\frac{\pi^2}{8} R_L.$$

It is necessary here to show how the above condition of affairs (in  $Z_1$ ) can be imitated; in particular is this desirable in order to justify the use of an initial fictitious assumption of a sinusoidal voltage  $V$  across the output of  $Z_1$ .

If a circuit is set up, as in fig. 6, with two generators of e.m.f. as shown, the current in  $Z_1$  will be  $I_1$  as above, where the voltage of fundamental frequency across  $Z_1$  will be

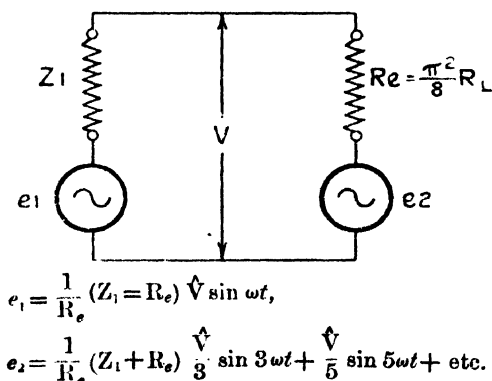
$$V = \frac{R_E}{Z_1 + R_E} e_1 = \hat{V} \sin \omega t.$$

There will be a series of voltages of multiple frequency across  $Z_1$ , but since  $Z_1$  is a pure reactance, no power will be delivered to it, and all the power generated by  $e$  will be absorbed in  $R_E$ . It can be imagined that part of the power delivered to  $R_E$  is used to drive a generator of e.m.f.  $e_2$ .

It therefore follows that one effect of the double-acting rectifier is to increase the effective load resistance presented towards the engine by the factor  $\frac{\pi^2}{8}$ . This follows from consideration of the forces of fundamental frequency.

The multiple frequency forces produce velocities which flow through the two alternative paths provided by the engine and the shunt network. In order that the engine speed shall not be appreciably altered by these velocities, and the wave-form of the velocity of the point D caused to depart very much from a sine-wave, the impedance looking into the engine must be large compared with the reactance network. In

Fig. 6.



practice this condition must also be satisfied in order that the reactive forces due to the network do not introduce undue fluctuations in engine speed. It is therefore true to say that the only appreciable effect of the forces of multiple frequency due to the ratchet is to cause relatively small velocities of multiple frequency to flow through the network.

#### *Measurements to be made in Practice.*

If it was not previously apparent, it is evident from the foregoing that by measuring at A (fig. 1) the force-wave in pounds and the velocity-wave in feet per second as functions of time, the impedance looking into the ratchet follows as the ratio

$$\frac{\text{Force component of fundamental frequency}}{\text{Velocity component of fundamental frequency}}.$$

Fortunately, the measurement of both these quantities is very simple. Two moving coils situated in radial magnetic fields are coupled through suitable mechanical reducing mechanisms, the one to the point A (fig. 1) and the other to point B (fig. 1). The two coils are connected through two resistance coupled amplifiers to the two ribbons of a twin oscillograph. The coils, amplifiers, and oscillographs are previously calibrated for velocity by being connected to a reciprocating part of known velocity. In this way the velocities of the points A and B are measured.

If at any frequency the reactance of the network is positive and  $= M\omega$ ,

$$\text{the force at B} = \frac{M}{g} \ddot{u}_b,$$

$$\text{the force at A} = \frac{l_1}{l_2} \times \text{the force at B.}$$

Hence by multiplying the slope of the velocity-curve for B by  $\frac{l_1 M}{l_2 g}$  the force-curve for A may be obtained. When the network reactance is elastic it may similarly be shown that the force is given by the product of the effective stiffness and the integral of the velocity-curve.

Fourier analysis then gives the force and velocity amplitudes of fundamental frequency. An alternative method, which is only practicable at high engine speeds (circa 2000 r.p.m.), is the use of amplifiers containing low pass filters to suppress all forces except those of fundamental frequency. This obviates the use of Fourier analysis.

It is evidently not practicable to make such measurements on a running car, but the inertia of the load may be simulated by a heavy flywheel and its energy dissipation by brake bands, or, better still, by the use of an hydraulic accumulator.

**XCVIII.** *On the Capillary Action of Mercury in the Absence of Gas-Grown Skins.* By J. J. MANLEY, M.A. (Research Fellow, Magdalen College, Oxford) \*.

[Plates XII.-XIV.]

**W**HILST removing the gas-grown skin from within a charged barometric tube, it was found that the curvature of the mercury lessened. First the normal

\* Communicated by the Author.

convexity dwindled until the surface appeared as a perfect plane: then as the skin became highly attenuated, the plane surface gradually gave place to one purely concave. Photographs of the unaided mercurial surface fail to show this progressive change with the requisite clearness. This difficulty was met by first attaching a strip of paper *p* to the posterior surface of the tube and directing the camera obliquely. As *p* was thus seen by reflexion, the form of its image at once revealed the form of the mercurial surface. The initial or normal curvature of the surface together with three successive phases in the transition, are respectively shown in  $\alpha$ ,  $\beta$ ,  $\gamma$ , and  $\delta$  of fig. 1 (Pl. XII.)\*. The experiment by which this complete inversion of curvature was effected was as follows:—

*Experiment A.*—First, the barometric tube was made chemically clean and dry and then highly evacuated. Next, its lower and sealed end was opened under pure mercury contained in a deep cistern and the tube thus charged. The tube was then set up between rotatable guides and rapidly driven up and down by a motor. During the ascent of the tube a feeble electric glow was produced within, and this was accompanied by a slow destruction of the gas-grown skin. At the conclusion of the experiment, when the mercurial surface was concave, the tube was inclined and a very small but quite appreciable bubble of gas representative of the destroyed and normal skin discovered. Other methods successfully used for the destruction of a gas-grown skin were the following:—

*Experiment B.*—The first additional experiment was made with a stationary barometric tube prepared and charged as for experiment A. Upon the upper portion of this tube was wound a spiral of wire the free end of which was joined to a coil yielding a 1 inch spark. The second terminal of the coil communicated with the mercury in the cistern. On activating the apparatus the vacuous space at first remained dark; but

\* These changes in curvature were, as will be seen from the following quotation, known to Young, who wrote:—"Professor Casbois, of Metz, has shown that the depression of mercury in glass tubes depends on the imperfection of the contact, and when it has been boiled in the tube long enough to expel all foreign particles, the surface becomes concave and the depression becomes an elevation. Perhaps this change may be the effect of the commencement of chemical action between the mercury and the component parts of the glass." (Thomas Young's *Collected Works*, vol. i. p. 425.) For this extract I am indebted to Prof. W. Ramsden. Since Young's day others have doubtless observed the same phenomena: but the explanation offered in this paper has not, I believe, been previously given.

after a short time a dull thud\* was heard, and this was instantly followed by a glow-discharge of the usual intensity. The discharge having been established, the mercurial surface soon lost its convexity, first becoming flat and then concave. The change in form was complete within 20 minutes. As in experiment A, free gas appeared in the tube; but in this instance the bubble was distinctly larger.

*Experiment C.*—The next experiment, C, was made with the apparatus shown in fig. 2 (Pl. XII.). The unseen portion of the barometric tube T was narrow; but the attached cylindrical vessel V had a diameter approximating 28 mm. After the latter had been more than half filled with pure mercury, it was placed in a sand-bath and enclosed with asbestos: the mercury was then boiled and so distilled. During the distillation, the apparatus functioned as a Sprengel pump and quickly produced a high vacuum. When but little mercury remained, the distillation was arrested and V allowed to cool. Finally, the mercurial surface was photographed, the result being that shown in  $\theta_1$  (fig. 2). For illustrating the entire reversal of the curvature of the surface, a photograph of a second tube  $\theta_2$  having the same diameter as  $\theta_1$ , but containing mercury in the presence of air, is also shown in fig. 2.

*Experiment D.*—The final experiment, D, was made to determine what effect the removal of the gas-grown skin might have upon the capillary height of the mercury. Accordingly the apparatus shown in fig. 3 (Pl. XIII.) was constructed. It differed from that of fig. 2 in that it possessed a narrow side-tube  $t$ . As for the preceding experiment C, so here pure mercury was introduced into the chemically clean and dry apparatus and then photographed ( $\lambda_1$ , fig. 3). Next the mercury was for a time rapidly distilled and a high vacuum produced. This done the flame was removed, the apparatus allowed to cool and a second photograph ( $\lambda_2$ , fig. 3) obtained. In  $\lambda_1$  we note the usual capillary depression of the mercury in the side-tube  $t$ . The internal diameter of  $t$  was 3 mm., and the measured depression 1.8 mm. After the distillation, both the wide and the narrow mercurial surfaces had, according to cathetometer measurements, one and the same level, the mercury in  $t$  being, as is clearly shown in  $\lambda_2$ , fig. 3, neither depressed nor elevated. The concavity of the surface of the residual mercury is demonstrated in fig. 4 (Pl. XIV.). A numerical value for the actual capillary effect

\* It would appear that the thud indicated a sudden and more or less complete rupture of the normal and resistant gas-grown skin.

common to both limbs of the apparatus was found by comparing the corrected length of the mobile mercurial column in the tube T with the mean of the reduced readings of two standard barometers. It was thus found that the mean standard barometer reading differed from that of the tube T by  $-3.12$  mm. Hence the ordinary and negative capillary effect of  $1.8$  mm. for the narrow limb  $t$  became, on the removal of the gas-grown skin, a positive one of  $3.1$  mm., a change totalling  $4.9$  mm. We conclude with some remarks upon the results obtained in the several experiments.

*Remarks.*—Elsewhere\* I have shown that at air-temperature a glass cylinder, even when maintained in a highly exhausted state for prolonged periods, still retains a gas-grown skin of unchanging density. Such a skin, which may quite appropriately be termed normal and permanent, is equivalent to an infinitely thin-walled tube which, as in the case of a standard barometric column, is interposed between the glass and the mercury. From the experiments A-C (*vide supra*), it seems abundantly clear that this barrier skin or film is initially responsible for the usual capillary depression of mercury. In general, liquids other than mercury instantly dissolve the skin and so come into intimate contact with and wet the glass: hence the familiar capillary elevation. Mercury, as we have seen, exhibits the same phenomenon so soon as the barrier skin has been either electrically erupted (exps. A & B), or destroyed by heat (exps. C & D). It will, however, be observed that the "wetting" of glass by mercury differs from that produced by other liquids: for on raising the tube  $\delta$  of fig. 1, the mercury drains completely from off the receding surface; with other liquids the glass retains a covering film.

The destruction of a gas-grown skin is gradual rather than instantaneous. This fact may be viewed in two ways:—

(1) If, as Langmuir and others have contended, the depth of the skin is represented by one molecule only, we reach the conclusion that upon the eruption of some of the molecules those remaining are re-arranged and form a more open type of skin or network. As the eruptive action progresses, the meshes of the molecularly constituted net continue to expand until, finally, the whole of the surface under consideration is left utterly bare.

(2) In opposition to Langmuir's views regarding the depth of the skin, we have the result of the preliminary measurement of a normal gas-grown skin alluded to above. That measurement appears to show quite conclusively that the

\* Proc. Phys. Soc. vol. xxxvi. pp. 288-290.



depth of a skin permanent at air-temperature and persisting in a high vacuum for nearly three years is most nearly represented by at least twenty strata of molecules. Under these circumstances it is reasonable to suppose that the destruction of the skin is commenced by the ejection of the upper stratum, and that the gradual attenuation is accomplished by the eruption of successive strata, the last to be thrown off being that nearest the glass. But, whatever view be accepted, the variations in curvature and also the growth in the capillary attraction of mercury observed during our experiments, are evidently largely dependent upon the mean thickness of the skin covering the glass.

The positive capillary attraction of 3.1 mm. obtained for mercury in experiment D is, when expressed in terms of water, approximately equal to 42 mm. This height is four times greater than that actually attained by water in a tube having a bore of 3 mm.

In conclusion, it may be stated that, with the object of still further testing the influence of a gas-grown skin, some measurements were made of the capillary attraction of "conductivity" water—(a) under usual conditions and (b) with tubes freed from gas-grown skins and situated within the highest attainable vacua. The differences noted in the two sets of data were negligible. Whence it appears that for liquids capable of dissolving gas-grown skins positive capillary attractions must invariably obtain.

XCI. *Apparent Irregularities in Experiments with heterogeneous X-ray Beams, with special reference to the J-Phenomenon.* By R. T. DUNBAR, M. A., Ph. D.\*

INTRODUCTION.

1. **S**INCE 1916, a number of papers have been published by Barkla and his collaborators, dealing with the results of their experimental researches on the properties of heterogeneous X-ray beams †. These papers deal with

\* Communicated by the Author.

† (1) Barkla & Janette Dunlop, *Phil. Mag.*, Mar. 1916.

(2) C. G. Barkla, 'Bakerian Lecture,' 1916.

(3) Barkla & Margaret White, *Phil. Mag.*, Oct. 1917.

(4) Barkla & Rhoda Sale, *Phil. Mag.*, April 1923.

(5) C. G. Barkla, 'Nature,' Nov. 17th, 1923.

(6) " " Nov. 22nd, 1924.

(7) Barkla & Khastgir, *Phil. Mag.*, Jan. 1925.

anomalies which the authors attribute to the existence of a new group of phenomena, to which they have given the name "J-Phenomena." For a full account of these the original papers must be consulted. For the present it will be sufficient to indicate their nature. They possess one remarkable property, that of appearing or not appearing under precisely the same physical conditions, so far as the observers have been able to discover. For example, Barkla writes [(8) p. 1036] : " We do not propose to give a description of the apparatus used in all experiments—they are far too numerous. And it is not easy to see that much would be gained, for the apparatus and arrangement used in experiments showing the J-phenomenon are identical with those in which the J-phenomenon did not occur." In one case, no fewer than three alternative results are to be expected : the experiment consists in comparing the X-radiations scattered at two different angles, by the method of observing the relative ionizations produced by the beams when successive equal sheets of Al (or other absorbing substance) are placed in their path. [(13) p. 550] " We have more recently obtained series of experimental results of both kinds—those showing a difference between the two beams by discontinuities and those showing a difference continuously, in addition to those showing no difference whatever between the two scattered beams."

2. To explain the phenomena, X-radiation is invested with certain new properties : heterogeneous beams are no longer to be looked upon as mere sums of harmonic constituents—they must be regarded as possessing other *additional* properties, which do not belong to any particular constituent or constituents, but to the beam as a whole. The beam is capable of suffering absorptions (additional to those associated with the photoelectric effect, and with scattering) in which every constituent loses the same fraction of its intensity. Such an absorption, it is clear, would

- 
- (8) C. G. Barkla, *Phil. Mag.*, May 1925.
  - (9) Barkla & Gladys Mackenzie, ' *Nature*, ' June 20th, 1925.
  - (10) Barkla & Khastgir, *Phil. Mag.*, Nov. 1925.
  - (11) " " ' *Nature*, ' Feb. 13th, 1926.
  - (12) C. G. Barkla, ' *Nature*, ' March 27th, 1926.
  - (13) Barkla & Gladys Mackenzie, *Phil. Mag.*, Feb. 1926.
  - (14) Barkla & Khastgir, *Phil. Mag.*, Sept. 1926.
  - (15) Barkla & Gladys Mackenzie, *Phil. Mag.*, Nov. 1926.
  - (16) Barkla & Watson, *Phil. Mag.*, Nov. 1926.
  - (17) C. G. Barkla, ' *Nature*, ' May 28th, 1927.
  - (18) Barkla & Khastgir, *Phil. Mag.*, Oct. 1927.

not modify the relative intensities of the components. Further, this J absorption, as they call it, *may or may not* take place—the deciding conditions have not been discovered,—and if it does, it may take place *continuously* or *discontinuously*, the total absorption in a sufficiently thick layer being the same in either case. The discontinuous condensations of energy are considerable, amounting to about 5 or 10 per cent. of the incident intensity, the thickness of the layer receiving the energy being, in the case of aluminium, probably considerably less than one-tenth of a millimetre.

3. To discuss whether these new hypotheses will fulfil their purpose, explaining the many irregularities and apparent inconsistencies observed, would be premature; for it is not yet clear, as it is hoped in this paper to show, that any modification of the well-established theories is required: much that has been described as conflicting with the existing theories is actually demanded by them. For the purpose of specifying the “quality” of a heterogeneous beam, the half-value mass-absorption coefficient \*, invariably used by experimenters in this field, must be described as quite inadequate and misleading, unless the radiations are well filtered; for, as will be illustrated in the sequel, different heterogeneous beams possessing the same  $\bar{\mu}/\rho$  will, according to the accepted theories, not necessarily give anything like the same experimental results when examined by Barkla’s methods. Consequently, such experiments are not only incapable of testing existing theory, but are liable to produce results which disagree among themselves. Barkla’s standpoint is different: the “irregularities” observed by him, assuming that  $\bar{\mu}/\rho$  defines the properties of the beam, have exhibited so pronounced a *regularity* that he has been led to conclude that he has been observing phenomena which depend only upon  $\bar{\mu}/\rho$  (rate of absorption as a whole), and not upon the constituent frequencies [(8) p. 1055]. The question of the existence of the J-phenomena is seen, therefore, to be concerned, not so much with the fact that discontinuities have been met with, but with the fact that the discontinuities have consistently appeared at the same points, and have exhibited other *regularities*.

4. The present paper contains an account of two experiments carried out by the author since his previous paper on

\* By trial a thickness  $x$  of substance, usually aluminium, is found which, when placed in the path of the radiation, absorbs 50 per cent. If  $I_0$  is the incident intensity, and  $I$  the transmitted intensity ( $I=0.5 I_0$  approx.),  $\bar{\mu}$  is calculated from  $I=I_0 e^{-\bar{\mu}x}$ , and if  $\rho$  is the density of the aluminium,  $\bar{\mu}/\rho$  is called the half-value mass-absorption coefficient of the heterogeneous beam in aluminium.

the J-phenomenon\*. Following this, an attempt is made to derive from theory the types of irregularity which are to be expected when working with heterogeneous beams as if they were nearly homogeneous; these show some resemblance to results which have been described as J-phenomena.

#### EXPERIMENTS.

5. The writer's experiments on the J-phenomenon commenced under the direction of Professor Barkla at Edinburgh, in 1919. At that time [see (2) and (3)], the anomalies were attributed to the existence of a J-series of characteristic radiations, for all the evidence was, without exception, in good agreement with this view. Experiments of another kind, conducted elsewhere, however, had begun to throw some doubt on Professor Barkla's interpretation of the results. Duane and Shimizu†, for example, were unable to find any evidence for the existence of J-characteristic rays using an anticathode of aluminium. The writer's experiments were therefore directed to extending the evidence already obtained for the existence of the J-series.

6. In these early experiments of the author's, the X-ray outfit provided consisted of a gas-filled tube, a 10 in. induction coil, and a mercury-gas interrupter. The tube was (apparently) self-rectifying, and the gas pressure within it was regulated by adjustment of the wires leading to the "softening" side-tube. Ionizations were measured by means of gold-leaf electroscopes of the well-known cubical box type. All the experiments which so far had given J-effects in the laboratory were performed with similar apparatus, except that the hammer-break replaced the mercury interrupter. After several months' experience with this simple apparatus, I had failed to obtain any reliable or satisfactory results from it. Irregularities were found, but could not be found consistently. The observational points when plotted had the appearance of being subject to an experimental error decidedly larger than could be accounted for by errors in reading the electroscopes. I suspected that the cause of the trouble was either that the rays were insufficiently filtered (*i.e.*, too heterogeneous) or that the tube's variations were more rapid than could be followed by the means at my disposal. To remove the latter possibility, the gas tube was replaced

\* R. T. Dunbar, *Phil. Mag.*, Jan. 1925.

† Duane and Shimizu, *Phys. Rev.* xiii. p. 288 (1919), and xiv. p. 389 (1919).

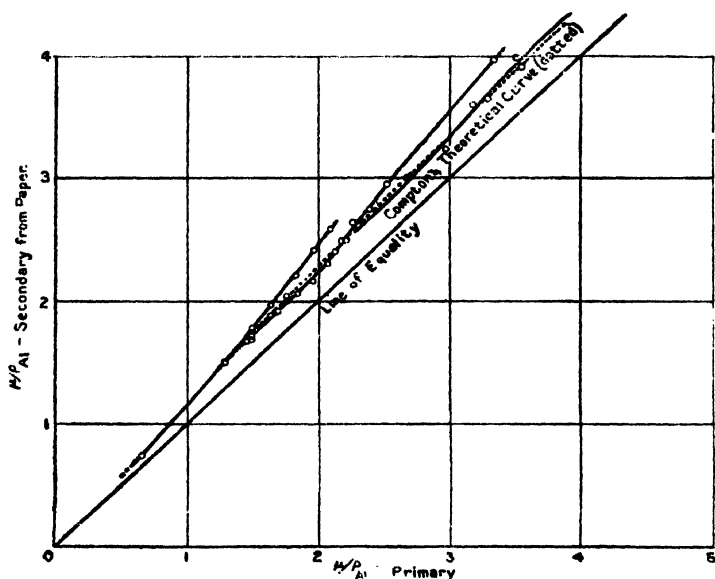
by a Coolidge tube, with tungsten anticathode; but the trouble persisted, suggesting that it arose from the radiations being too heterogeneous. The amount of filtering possible is limited in practice by the intensity of the rays and the sensitivity of the electrosopes. It was necessary, therefore, to increase one or both of these if comparatively homogeneous beams over the desired range of hardnesses were to be obtainable. The intensity was multiplied many times by the substitution of a Mammoth 16 in. coil for the small 10 in. one. With this apparatus consistency appeared for the first time. With the disappearance of inconsistency, however, all evidence of J-effects disappeared also, showing that the conditions necessary for the appearance of J-effects were removed by filtering in this particular set of experiments, and that it would be necessary to revert to the use of thin filters. I preferred to persist with the well-filtered beams, as more likely to give definite results, and with a view to finding whether any irregularities of any kind could be found with them. Some were found in ionization and scattering experiments, but they subsequently received a very satisfactory explanation when the Compton effect was discovered. These later experiments have already been described and discussed\*. That Barkla required heterogeneous beams to obtain his J-effects is indicated by the following quotation [(8) p. 1038]: "In many of the following experiments no attempt was therefore made to produce even approximately homogeneous beams, for these heterogeneous radiations provided us with the phenomenon which we wished to examine." It is to be noted that the facts mentioned in this paragraph are not inconsistent with the view that the effects arise from an inadequate description of the heterogeneous beam, for (1) *only well-filtered* beams with the same  $\bar{\mu}/\rho$  are sufficiently nearly alike to make a knowledge of the intensity distribution among the wave-lengths, for most practical purposes, superfluous, and (2) it is only with well-filtered beams that the J is definitely absent. So far as the writer's own experience is concerned, every shred of evidence favours this view; at no time has the radiation ever evinced any of the properties mentioned in § 2.

7. The last experiment carried out in Professor Barkla's laboratory by the author was a scattering experiment. This has been described elsewhere (*loc. cit.* p. 228 et seq.). In this experiment some 5 or 6 observations showed a departure from Compton's theory sufficient to indicate the possibility

\* *Loc. cit.*

of some J or other unrecognized effect being present. The indication was so slight that in ordinary circumstances it would probably have been either unobserved or put down to a result of some slight imperfection in the apparatus or method of measurement. Its possible association with the J-phenomenon was the only reason for drawing attention to it. The curve is reproduced here (fig. 1). The feature of the curve is an apparent "step" form, unduly emphasized by the drawing of lines through the observations. Without the lines (as frequently elsewhere) the pattern disappears.

Fig. 1.



These steps are, according to Barkla and Watson \*, J-discontinuities. "In Dunbar's experiments . . . the discontinuities certainly appeared, but the conditions were not sufficiently controllable, nor was the experiment itself of the kind which was later found most suitable to exhibit the phenomenon." The two experiments about to be described consist of (I.) a repetition of the above experiment under much improved conditions, (II.) an experiment of the kind which in Barkla and Watson's opinion is more suitable for exhibiting the J-phenomenon.

\* (16) p. 1122.

*Experiment I.*

8. Owing to the discrepancies which have appeared between the results of different observers, and even between the results of the same observer with the same apparatus, in experiments upon the J-phenomenon, rather a detailed description of the apparatus and procedure will be expected, and will therefore be given without apology. As the first experiment is merely a repetition of a previous one, and the latter has already been fully treated, it will be necessary to give only the points of difference between the two. For convenience the two experiments will be referred to as A and B, A being the one carried out at Edinburgh in 1923-24, and B recently at Cardiff. The changes adopted, which are for the most part refinements, are given in Table I.

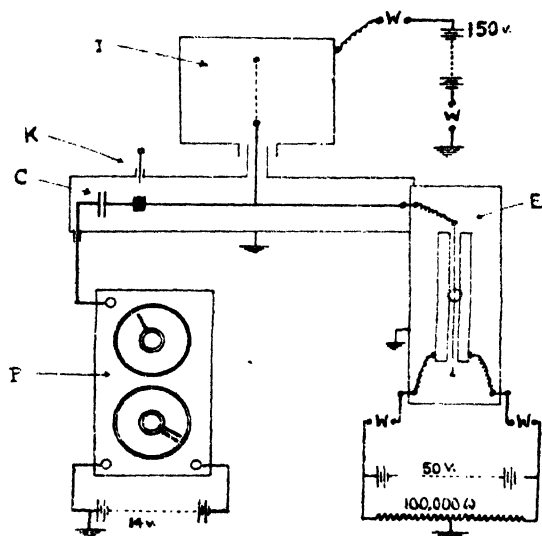
TABLE I.

EXPERIMENT A.	EXPERIMENT B.
Coolidge tube without rectifier.	Coolidge tube with mechanical rectifier on interrupter.
"Sanax" mercury - paraffin interrupter.	Gas-mercury jet interrupter.
Simple, untilted, gold-leaf electroscope on Secondary.	String electrometer on Secondary.
Secondary X-ray pencil about 4 cm. diameter.	Diameter reduced to 2 cm.
Diameter of ionization - chambers, 10 cm.	Diameter increased to 12.5 cm.
Saturation potential on Primary ion.-chr. 200 volts.	Increased potential to 350 volts.
Runs of tube from 3 to 15 minutes' duration.	Runs were from 2 to 9 minutes.
Recovery interval between readings (allowing tube to cool), 3 to 5 minutes.	Recovery interval 5 to 10 minutes.
Readings were seldom repeated.	Initial reading was, as a rule, repeated after every third or fourth reading, the absolute as well as the relative rates of leak being determined.

9. The method of measuring the relative ionizations in the primary and secondary ionization chambers in the repeated experiment (Expt. B) demands a more extended description. The feeble secondary requires a really sensitive electrometer. Also, the use of deflexion methods for *both* primary and

secondary is not to be recommended, for obvious reasons, if accuracy is aimed at. A string electrometer was used on the secondary, the connexions being depicted in fig. 2 (the Townsend method). The leak is determined in terms of a potentiometer reading. The insulated system of the secondary ionization chamber is connected to one plate of a small air-condenser of capacity 1 cm., approx., the other plate of which is connected to a Varley-Thomson potentiometer

Fig. 2.



- C - Air-Condenser, Capacity about 1 cm.
- E - String Electrometer.
- I - Secondary Ionisation Chamber.
- K - Earthing Key.
- P - Varley-Thomson Potentiometer.
- W - Water Resistance.

meter. During the incidence of the X-rays, the string of the electrometer is kept on the zero mark (zero potential) by adjusting the potentiometer. Thus, an equal charge to that picked up by the electrode is attracted into the condenser, and its magnitude, being accurately proportional to the change of potential of the other plate, is obtained from the initial and final readings of the potentiometer in arbitrary units. The arrangement was found to be remarkably simple to manipulate, and both sensitive and accurate. It possesses



all the advantages of a null method: (a) the readings are independent of the sensitivity and calibration curve of the electrometer: consequently, errors due to accidental variations in the field battery, tension of the fibre, etc., do not come in; (b) the sensitivity (*i. e.*, deflexion sensitivity) can be increased up to the limit of stability without in the least impairing the accuracy; (c) the insulated system is maintained, as nearly as may be, at zero potential, and leaks over insulating supports are therefore negligible; (d) the accuracy is much higher and the readings are dependent on the steadiness of fewer factors than in any deflexion method. In the actual experiment, the readings were estimated to be correct to at least one part in 1000. The error in measuring S/P (*i. e.*, secondary ionization/primary ionization) arose almost entirely from the reading of the primary ionization, for which a less accurate instrument was used.

10. A gold-leaf electroscope of the 3 in. cube type, carefully mounted and shielded from temperature changes, was connected to the primary ionization chamber. The reading microscope was mounted on a travelling carriage, which permitted an exact coincidence of the edge of the leaf with a scale division at the beginning of each run; the X-rays were switched off when the leaf was exactly coincident with another scale division, 12 removed from the first; the same pair of scale divisions was used for every run of the tube. This procedure entirely avoided errors due to (a) estimation of fractions of a division, (b) calibration of the eye-piece scale. The error in measuring the ratio S/P was calculated from some 40 determinations of the ratio with unintercepted radiations. By the method of least squares the probable error of a single determination was found to be one in 350. This accuracy is distinctly better than in Expt. A, in which two simple electroscopes were used, and the ratios determined by timing the "transits" of the leaf-edges across the scale divisions, using a split-seconds stop-watch. The accuracy in the corresponding experiments carried out by Professor Barkla's observers does not appear to have been stated, but from the graphs, and particularly from the information given by Barkla and Khastgir [(10) pp. 1131-2], the accuracy of measurement of ratios of ionizations in single experiments appear to have been approximately the same as in the author's present experiments.

11. The results of the experiment are shown in Table II. and in fig. 3. A comparison of figs. 1 and 3 will show that what has been described as a J-effect has been eliminated.

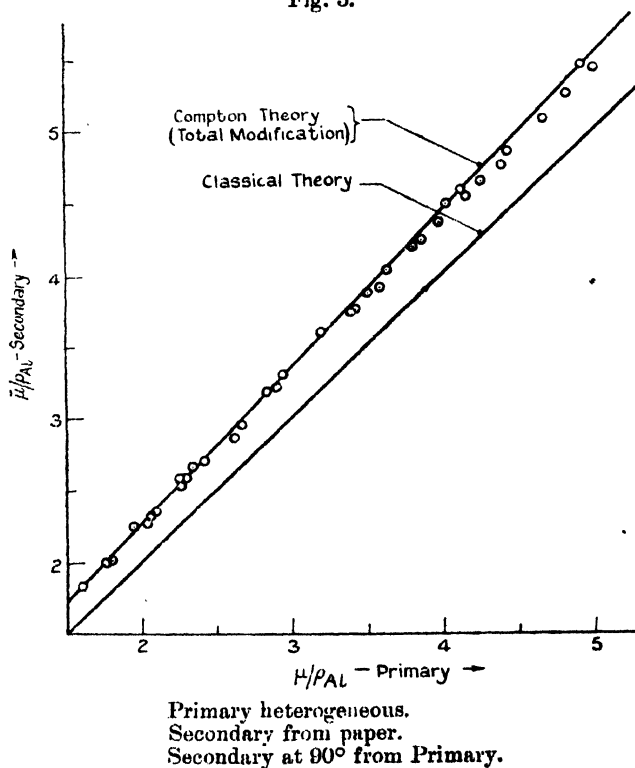
TABLE II.

Observed differences in the half-value mass-absorption coefficients for Aluminium, between Primary X-rays and the Secondary at 90° from Filter-paper.

	Filter-paper radiator.	Aluminium filtering incident beam.	Per cent. absorption for next columns.	Primary $\bar{\mu}/\rho$ (Al).	Observed $\delta\bar{\mu}/\rho$ (Al).	Theoretical $\delta\bar{\mu}/\rho$ (Al) (maximum).
	sheets.	mm.				
1	100	0.5	47	1.61	0.24	0.22
2	"	0.5	46	1.80	0.23	0.24
3	"	none	51	2.07	0.26	0.27
4	"	"	51	2.10	0.26	0.27
5	"	"	42	2.26	0.34	0.29
6	"	"	54	2.27	0.27	0.29
7	"	"	57	2.34	0.34	0.30
8	50	0.5	50	1.76	0.25	0.24
9	"	0.5	54	1.95	0.31	0.26
10	"	0.9	40	2.05	0.23	0.27
11	"	none	50	2.29	0.30	0.29
12	"	"	57	2.30	0.30	0.29
13	"	"	45	2.42	0.30	0.30
14	"	"	56	2.62	0.26	0.32
15	"	"	52	2.67	0.30	0.33
16	"	"	51	2.84	0.35	0.34
17	"	"	41	2.90	0.32	0.35
18	"	"	52	2.95	0.36	0.36
19	"	"	43	3.20	0.40	0.38
20	"	"	54	3.39	0.35	0.39
21	"	"	45	3.42	0.34	0.40
22	"	"	46	3.50	0.38	0.40
23	"	"	43	3.58	0.33	0.40
24	"	"	42	3.63	0.40	0.41
25	"	"	61	3.80	0.39	0.42
26	"	"	61	3.86	0.38	0.43
27	"	"	55	3.97	0.39	0.44
28	"	"	51	4.02	0.47	0.44
29	"	"	46	4.12	0.46	0.45
30	"	"	57	4.15	0.39	0.45
31	"	"	41	4.25	0.39	0.46
32	"	"	54	4.39	0.36	0.47
33	"	"	42	4.43	0.42	0.47
34	"	"	52	4.66	0.43	0.49
35	"	"	45	4.82	0.43	0.50
36	"	"	40	4.92	0.53	0.51
37	"	"	53	5.00	0.43	0.52

An examination of the differences between the two experiments, however, does not bring us any nearer to the origin of the J-phenomenon; it merely indicates that the effects, whatever they are, are removed by refining the measurements and the experimental procedure. The radiations were apparently quite as heterogeneous in the second as in the first case, judging by the thickness of the filters and of the scatterer. The whole point of repeating the experiment

Fig. 3.



was to verify the existence of the irregularities, which, if found again, would be a definite starting-point for an investigation of J-effects. Refinement was aimed at, without altering the conditions except in so far as to make them less variable. The negative result very strongly favours the view that the effects in the previous experiment were not fundamental. In the writer's opinion they arose from prolonged exposures and the presence of inverse current.

## Experiment II.

12. The second experiment, which is now about to be described, is one in which the two radiations, primary and secondary, are compared with each other, not by observing their half-value coefficients of absorption as in Experiment I. (which is done by intercepting the radiations with a single sheet), but by what would appear to be a more thorough method, namely, by observing the *relative* rates of extinction of the beams as a result of interposing a gradually-increased thickness of filter. This method was introduced by Barkla, and the experiment is one which has been repeated so often in his laboratory (altering the radiator, material of the absorbing sheets, angle of scattering, etc.) that it appears to represent something like half of the published experimental work on the J-phenomenon. It is the method which Barkla and Watson consider the most suitable for exhibiting the J-phenomenon.

13. The procedure is obvious and the theory (for homogeneous radiations) simple. Let  $S_0$  and  $P_0$  be the intensities of the unintercepted secondary and primary radiations, as measured (the only convenient way, though liable to misinterpretation) by ionization. If the same gas is used in the two ionization chambers, and they are identical in every respect and placed at the same distance from the scatterer, if, also, the gas has no characteristic radiation of wave-length in the neighbourhood of the wave-lengths used, nor any very appreciable amount of "recoil" ionization, it has been shown both by Compton's theory and by experiment (see, for instance, Dunbar, *loc. cit.* p. 233) that  $S_0/P_0$  is a constant, independent of the wave-length\*. If  $S$  and  $P$  are the intensities (ionizations) when a thickness of aluminium or other substance, equal to  $x$ , intercepts both beams, we have at once, assuming exponential absorption and that the radiation is completely modified in scattering,

$$\frac{S}{P} = \frac{S_0}{P_0} \cdot e^{-\delta\mu \cdot x} \quad . \quad . \quad . \quad . \quad . \quad (1)$$

for a single frequency constituent, the increase of whose absorption coefficient in the aluminium or other substance associated with the Compton effect is  $\delta\mu$ . For a continuous

\* To the first order of small quantities.

Consider only the radiation scattered at  $90^\circ$  here as elsewhere throughout the paper.

heterogeneous beam, it can be easily shown that the result is

$$\frac{S}{P} = \frac{S_0}{P_0} \cdot \frac{\int_0^\infty i(\lambda) e^{-(\mu + \delta\mu) \cdot x} d\lambda}{\int_0^\infty i(\lambda) e^{-\mu \cdot x} d\lambda}, \quad \dots \quad (2)$$

where  $i(\lambda) d\lambda$  is the intensity distribution of the primary beam and  $\mu$  is the absorption coefficient in Al of radiation of wave-length  $\lambda$ . For a beam consisting of lines of wave-lengths  $\lambda_1, \lambda_2, \dots$ , of intensities  $i_1, i_2, \dots$ , respectively, the corresponding result is

$$\frac{S}{P} = \frac{S_0}{P_0} \cdot \frac{\sum i_r e^{-(\mu_r + \delta\mu_r)x}}{\sum i_r e^{-\mu_r x}} \dots \dots \dots (3)$$

For unmodified scattered radiation—that is, if the radiation is scattered according to the classical theory—the relation between  $S/P$  and  $x$  degenerates into

$$\frac{S}{P} = \frac{S_0}{P_0} \dots \dots \dots (4)$$

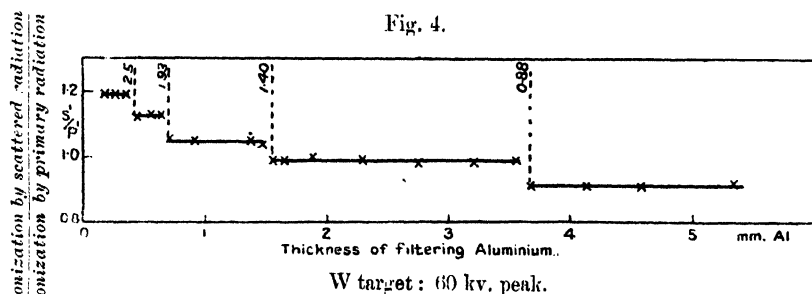
14. The curves obtained by experiment are to be compared with the above four theoretical relations. (1) is evidently a ratio which falls steadily (exponentially) with increasing  $x$ ; (4) will give a constant ratio—that is to say, a horizontal straight line—if the ratio is taken as ordinate and  $x$  as abscissa. The relation (2) I have been unable to work out, even for simple laws of distribution. (3), which is for a line-spectrum, is simple but lengthy in calculation, and a few examples have been worked out with a view to obtaining *first approximations* to the solutions for continuous distributions, which are, of course, the type of radiations we experiment upon. Rough solutions of the relation (2) have been arrived at in this way. These calculations will be discussed later.

15. The results obtained in Professor Barkla's laboratory are of three types, those in which  $S/P$  is constant for all values of  $x$ , indicating, as the authors presume, *unmodified* scattering; those in which the ratio falls steadily with increasing  $x$ , resembling relation (1), which is for homogeneous beams and Compton scattering; and, finally, an apparent combination of these two—the ratio is constant up to a certain value of  $x$  and then suddenly makes up for lost time, as it were, by falling to a lower value, at which it

remains constant for further increases of  $x$ , and so on [see fig. 4, reproduced from (16)]. The discontinuous changes in the third type are of the order of 5 to 10 per cent.

16. The first and second types (continuously constant and continuously falling) will be shown later to be *both* in conformity with the Compton effect, although the former has been very naturally interpreted as evincing unmodified scattering. It will appear that when the heterogeneous beam contains both very hard and very soft radiations of approximately equal intensities, the relation (2) (or more accurately (3)) shows that the ratio is almost accurately constant over a considerable range of values of  $x$ , in spite of the full Compton change of wave-length. The unexpected result is accounted for by the fact that filtering, which invariably transmits a more penetrating beam hardens up the secondary

Fig. 4.



(with heterogeneous rays) more rapidly than the primary, till, with certain beams at least, the secondary, originally the more absorbable, is more penetrating than the primary: this state of affairs does not persist however, for the primary in the long run is the more penetrating. For a considerable range of values of  $x$ , the two beams are almost exactly of the same penetrating power (though differently constituted). The third (discontinuous) type of result is in quite a different category. Discontinuous absorption of a heterogeneous beam cannot be accounted for on any theory which assumes that the beam is merely the sum of its constituents. This type will be considered later.

17. The author's experiment was carried out with exactly the same apparatus as in Experiment I. The procedure in taking the observations is the only point of difference. The interpretation of the results is not, however, quite so simple as would at first sight appear. The following

points are evidently to be considered before observations are taken :—

(1) The assumption is made that the same heterogeneous beam can be maintained unvaried for an hour or two. The 21 observations in fig. 4, for instance, taken from Barkla and Watson's paper, must have required from one to two hours of actual running of the tube. The intensity distribution in the X-ray beam depends on the temperature of the cathode if a Coolidge tube is used, and on the temperature of the tube itself if a gas-tube. It varies to a certain extent also as the coils of the transformer become warm. Variations are therefore to be expected, and some method of watching for changes devised. In the author's experiment, each reading was timed with an accurate stop-watch, and certain readings were repeated at intervals. Column 2, in Table III., gives the time in seconds for a leak of one division on the primary.

(2) The gas must be the same in both ionization chambers, and conform to the conditions stated in para. 13. Air must be ruled out as unsuitable, for this gas has been observed by the author to be subject to a marked increase of ionization relative to intensity of X-rays when the radiation is shortened in wave-length through the region of  $0.4 \text{ \AA}$  (*loc. cit.* p. 227), the increase being due to the recoil electrons. Such a characteristic would naturally produce a fold on the curve for S/P if the Compton modification were present—a fold, in fact, should appear for both oxygen and nitrogen, but the two would probably run into one. Sulphur dioxide would give a similar result on account of the *oxygen* it contains, but, as the latter gives only some 8 per cent. of the ionization of  $\text{SO}_2$ , the effect is negligible. The recoil ionization from *sulphur* does not appreciably affect the results within the range of these experiments, consequently  $\text{SO}_2$  was selected. That this selection was justified was proved by a control experiment in which the secondary from copper (almost entirely copper K, as tested by absorption in Al) was compared with the primary over the whole range of radiations to be used, the intensity being measured by  $\text{SO}_2$  ionization. The curve was smooth and only slightly sloped, showing that the primary (in which alone the wave-length was changing) was smoothly represented in intensity by the ionization it produced in  $\text{SO}_2$ .

(3) If any irregularity in the ratio S/P is observed, it must be possible to say whether it arises from a change in S, or in P, or in both. This can only be provided for by timing all observations. This was done. Actually no irregularities were observed which would not be covered by observational error and slight variations in the radiation.

In Barkla's experiments all irregularity is ascribed to the secondary, but it is not clear how this conclusion was arrived at. The point is of considerable consequence, for if the observations were timed, and the secondary was found to vary suddenly by some 5 to 10 per cent., *by time*, while the primary remained perfectly regular, the origin of the 5 to 10 per cent. J-discontinuity would justifiably be ascribed to some "post-scattering" process. Without the experimental data, however, the possibility must still remain that the irregularities arose from the source of most irregularities in X-ray work, the X-ray tube. A change in the incident X-rays would affect both P and S, but in general to different degrees. Such changes could be detected at once from the *absolute* rates of leak.

18. Table III. and fig. 5 contain the result of the author's experiment. The curves exhibit no discontinuities such as have been found in Barkla's experiments. There are minor irregularities in curvature, but these will be seen to be

TABLE III.

Comparison of Primary and Scattered (90°) by progressive absorption with aluminium sheets.

	Time per div. (P).	$\pi$ (Filter).	S/P.		Time per div. (P).	$\pi$ (Filter).	S/P.
1. $\bar{\mu}/\rho$ (Al) 4.7	sec.	mm.		3. $\bar{\mu}/\rho$ (Al) 4.2	13.3	nil	1.000
	17.1	nil	1.000		23.0	0.46	.948
	46.2	(0.88) *	1.000		24.6	0.55	.933
	?	0.19	.971		13.0	nil	1.000
	28.5	0.39	.946		27.0	0.65	.920
	35.4	0.58	.935		29.7	0.75	.923
2. $\bar{\mu}/\rho$ (Al) 4.2	17.0	nil	1.000	4. $\bar{\mu}/\rho$ (Al) 3.7	13.6	nil	.998
	13.2	nil	1.000		30.8	0.75	.923
	22.5	0.46	.950		28.8	0.65	.938
	34.0	0.91	.905		19.3	nil	1.000
	34.6	(0.91)	.990		21.5	0.10	.978
	34.5	0.91	.907		23.4	0.19	.965
	22.5	0.46	.940		25.8	0.29	.962
	13.5	nil	1.000		28.2	0.39	.954
					18.5	nil	1.002

\* Filters in brackets were placed in the path of the incident beam, otherwise they were in the paths of secondary and primary after incidence on the radiator, which consisted of 50 sheets of filter-paper.



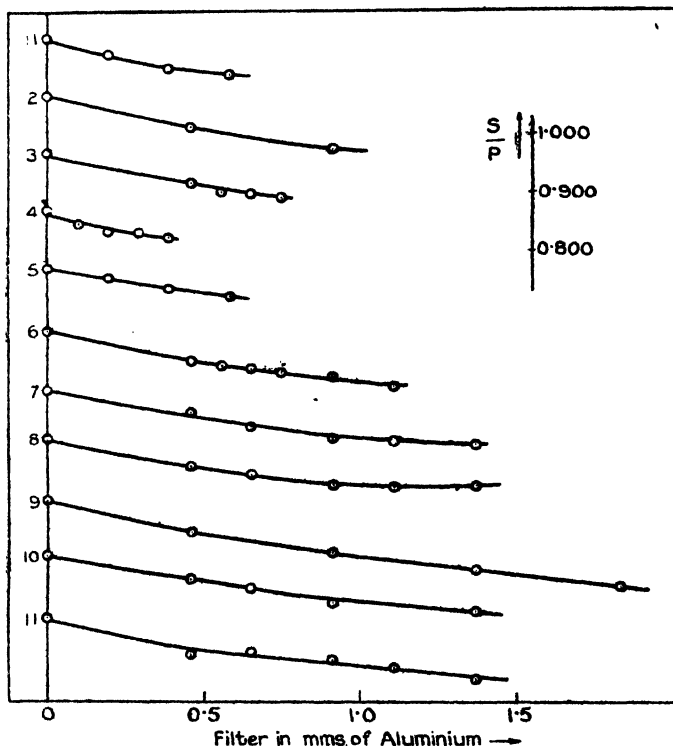
TABLE III. (*continued*).

Comparison of Primary and Scattered (90°) by progressive absorption with aluminium sheets.

	Time per div. (P).	$x$ (Filter).	S/P.		Time per div. (P).	$x$ (Filter).	S/P.
	sec.	mm.			sec.	mm.	
	14.0	nil	1.000		10.4	nil	.997
	16.8	0.19	.994		15.4	0.46	.945
	?	0.39	.966		9.7	nil	.997
5.	24.1	0.58	.958	9.	19.5	0.91	.905
$\mu/\rho$	13.6	nil	1.003	$\bar{\mu}/\rho$	25.6	1.36	.868
(Al)	23.7	0.58	.947	(Al)	32.8	1.82	.845
3.4	19.3	0.39	.967	3.0	9.7	nil	1.006
	16.3	0.19	.978		35.4	1.82	.859
	13.5	nil	1.003		28.9	1.36	.890
					22.7	0.91	.914
	?	nil	1.000				
	18.8	0.46	.942		12.0	nil	1.000
	11.7	nil	.990		16.7	0.46	.960
	19.5	(0.46)	.987				
	20.4	0.55	.934	10.	20.5	0.65	.946
6.				$\mu/\rho$	17.7	0.46	.965
$\mu/\rho$	21.9	0.65	.929	(Al)	24.7	0.91	.920
(Al)	23.3	0.75	.921	2.9	10.9	nil	1.008
3.4	12.0	nil	.995		21.4	0.91	.923
	27.5	0.91	.914				
	30.5	1.10	.898		27.3	1.36	.908
	29.8	(1.10)	.992				
	12.8	nil	1.000		11.8	nil	1.000
	19.3	0.46	.953		27.2	(1.36)	.998
	12.7	nil	.988		25.4	1.36	.884
	21.8	0.65	.929	11.	22.3	1.10	.910
7.	26.2	0.91	.908	$\bar{\mu}/\rho$	20.4	0.91	.924
$\bar{\mu}/\rho$				(Al)			
(Al)	30.4	1.10	.903	2.3	17.5	0.65	.936
3.0	12.7	nil	.990		15.2	0.46	.935
	30.2	(1.10)	.990		26.4	1.36	.896
	35.1	1.36	.896		10.8	nil	.989
	?	nil	.993				
	10.5	nil	1.000				
	17.7	0.46	.960				
	19.6	0.65	.945				
8.	21.9	0.91	.928				
$\bar{\mu}/\rho$	10.6	nil	1.017				
(Al)	23.3	1.10	.924				
3.0	26.8	1.36	.925				
	27.4	(1.36)	1.008				
	11.0	nil	1.008				

perfectly accounted for by the Compton theory in a later paragraph. Curves such as these are found amongst Barkla's results, and are not excluded by his "laws of the J-Phenomenon." Barkla, however, has hinted that where continuity is observed it is probable that the result is a statistical mean of discontinuities. Thus [(16), p. 1126], "... it would be expected that under variable conditions these

Fig. 5.



$P_1$  = Ionization by Primary (heterogeneous).

$S$  = Ionization by Secondary from paper,  $90^\circ$  from Primary.

The radiations are compared by progressive absorption.

discontinuities would be spread out and would show an apparently steady higher absorption of the scattered than of the primary radiation, such as has frequently been found in experiments on the progressive absorption of both beams. This suggests that all the apparent differences between scattered and primary radiations as shown by some absorption.

experiments may be fundamentally made up of such discontinuities." A comprehensive survey of the results obtained by all his observers, however, shows, on the average, a pronounced tendency for the results to be either *a* or *b*—i. e., either obviously smooth or obviously discontinuous. We cannot suppose that the conditions of running may be so neatly divided into two—that the steady can be differentiated from the unsteady with such certainty. In the author's curves, Nos. 1 to 7, fig. 5, the average difference between repeated readings in the rate of leak was only about two and one-half per cent., although the set of readings in each case was spread over a period of about two hours. It is hardly credible that there was sufficient unsteadiness present to mask so completely what with steady conditions would have been a set of "stepped" patterns, like (Barkla and Watson's) fig. 4. Curves 8, 9, 10, and 11, fig. 5, were obtained under much less steady conditions, the time variations between some of the repeated readings being as great as 15 per cent. The curves are arranged in the order of the absorptibilities, not in the order of observation. The unsteadiness is to be attributed therefore to some effect which appears when the penetrating power of the radiation exceeds a certain value. It will be shown later that there is some evidence that the tungsten K-lines were excited to an appreciable extent in these unsteady radiations, but not in the other cases. This would account quite naturally for the instability. It is worthy of remark that the curves include examples for both very steady and very unsteady conditions; nevertheless, there is little if anything to distinguish the smoothness of one set of curves from that of the other. It appears to be clear that the step pattern was not simply obscured—it was entirely absent.

19. The only other published results, outside of Professor Barkla's laboratory, on the examination of scattered radiations by the method of progressive absorption are, so far as I have been able to find, those of B. L. Worsnop\*, at King's College, London, and those of O. Gaertner†, at the Röntgen-Forschungsinstitut der Universität, Bonn. In both cases, in spite of the care and skill with which the experiments were evidently carried out, the discontinuities failed to appear. The fact that with Barkla's observers the search for J-effects has, more often than not, been successful while others have

\* B. L. Worsnop, *Proc. Phys. Soc.* xxxix. p. 305.

† O. Gaertner, *Phys. Zeit.*, 15th July, 1927.

consistently failed, is one for which a simple explanation ought to be forthcoming. Barkla has suggested that, if the J does not appear, one ought to keep on modifying the apparatus till it does appear (Brit. Assoc. 1927). Considering that his observers have found the J with almost every conceivable combination of apparatus, and that others have used transformers, induction-coils, and hot cathode tubes of different kinds without success, the necessary modifications would appear to be in the lesser details of apparatus regarding which we have so far received little information.

#### THEORETICAL.

20. The comparison of scattered and primary radiations by the method of progressive absorption gives a relation between the ratio, S/P, and the thickness of filter,  $x$ , placed in the path of both beams. If the object of the experiment is to find out which of the two processes of scattering is operating, the classical or the quantum, the theoretical consequences of both theories have to be calculated and the observed results compared with the theoretical. The method breaks down if the observed result is in agreement with *both* theories; and this appears to happen if the very absorbable components in the heterogeneous beams are incident upon the radiator and form an important part of the scattered intensity (as measured by ionization).

21. The theoretical result for heterogeneous beams in the case of classical scattering is simple; the ratio S/P is a constant independent of  $x$ , so long as the scattering coefficient of the material of the radiator is the same for all the wavelength constituents. The quantum theory (Compton) has been shown to give the results expressed in the relations (1), (2), and (3), in para. 13. Before applying these it has to be remembered that a certain amount of absorption subsequent to scattering is present even when  $x$  is zero—absorption by the radiator itself, by the atmosphere, and by the windows of the electroscopes. Allowance has to be made for this in calculating the  $\bar{\mu}/\rho$  which would be observed for the unintercepted radiation—the effect on the S/P curve is merely a slight shift of origin. It has been assumed in the following that the *equivalent* thickness of aluminium absorbing the P and S radiations, additional to the sheets,  $x$ , is 0.2 mm.

22. Assuming the relation  $\mu = \sigma + a\lambda^3$ , where  $\sigma$  is independent of  $\lambda$ , and  $a$  is a constant for the absorbing

material,  $\alpha$ , equal to about  $38.34 \text{ cm.}^{-1}$  for aluminium if the wave-lengths are in Ångström Units, I have calculated results for six cases, with each of which the  $\mu/\rho$  to be observed is exactly the same, making a comparison of the results all the more easy to interpret. The constituent radiations and their relative intensities are given in Table IV. and the curves for S/P appear in fig. 6. With each of these beams the  $\bar{\mu}/\rho$  to be

TABLE IV.

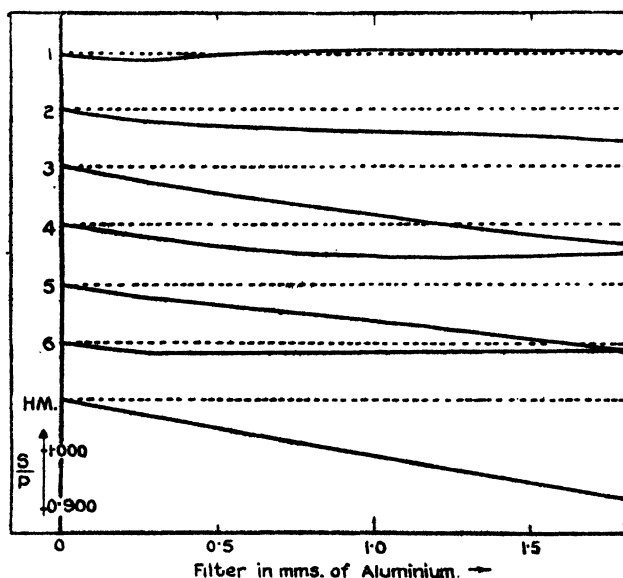
Wave-length Components and their Relative Intensities,  
from which the curves in fig. 6 were calculated.

No. of Curve.	0.20 Å.	0.35 Å.	0.50 Å.	0.70 Å.	0.85 Å.	1.00 Å.
	per cent.	per cent.	per cent.	per cent.	per cent.	per cent.
1 .....	32.9	—	—	—	—	67.1
2 .....	—	39.7	—	—	60.3	—
3 .....	—	—	46.5	53.5	—	—
4 .....	22.25	—	—	77.75	—	—
5 .....	—	—	59.8	—	—	40.2
6 .....	30	—	—	25	—	45

observed (with Al) is 3.2, which is the mass-absorption coefficient of homogeneous radiation of wave-length 0.6 Å. The results are obtained by using relation (3) in para. 13. They show at once that the result to be expected on Compton's theory depends very much on how the intensity is distributed amongst the wave-lengths. Curves 1, 2, and 3 give a first approximation to results for beams which are very broad, broad, and fairly narrow, respectively, for the wave-lengths they contain are far separated, well separated, and rather close together, respectively. The curves are seen to be intermediate between the classical and the Compton results for *homogeneous* radiation—1 is scarcely distinguishable from the classical result over a considerable range, while 3 is very nearly the Compton result for a *single* constituent. Curve 4 is for a beam with one constituent slightly more absorbable, and the other considerably more penetrating, than the pair together, while curve 5 is for the converse, one component slightly more penetrating and the other very absorbable. The latter is scarcely distinguishable from 3 and the curve

for homogeneous radiation. 4, however, after dropping regularly, rather suddenly changes its direction and runs horizontally. [This feature can be observed in some of the author's experimental curves in fig. 5. It possibly arises from the presence of K-tungsten radiation, from the anticathode, superposed on the general radiation. That the ratio S/P should tend to become constant after falling steadily was so unexpected a result that it caused considerable trouble at the time, repeating observations, and testing to see if anything had altered. It was only after these calculations

Fig. 6.



Theoretical curves to be compared with fig. 5. (The broken lines are merely horizontal rulings to aid the eye.)

Each beam has the same  $\bar{\mu}/\rho$  for Al (see Table IV.), the curve marked "HM." being for a homogeneous beam.

had been completed that it was seen that the result was quite in keeping with theory.]

23. It must be clear that by a proper selection of wavelengths and intensities, not restricted to two components only, it is possible to build up synthetically any curve whatever, within reason, lying between the classical and the quantum result for homogeneous rays. Curve 6 is a simple example.

It consists of three components: 0.2, 0.7, and 1.0 Å, with intensities in the ratio 6:5:9. It is a combination of curves 1 and 4 in the proportion of 2:1, very nearly. The values of S/P to be observed, as the thickness of absorbing aluminium is increased by steps of 0.2 mm. up to 3.8 mm., are, respectively: 0.975, 0.963, 0.959, 0.959, 0.959, 0.960, 0.961, 0.961, 0.962, 0.962, 0.961, 0.961, 0.960, 0.959, 0.958, 0.956, 0.954, 0.953, 0.951, 0.949. This constancy of ratio must be described as remarkable, for the rates of absorption of the corresponding constituents are very different, and it is only by a complicated process of *compensation* that the rates of absorption of the beams as a whole are so very nearly indistinguishable. Further, by adding more constituents in the proper proportion, the result may clearly be indefinitely improved upon. It seems possible that for a *continuous* beam, sufficiently broad, the result would be so perfect that absorption by aluminium subsequent to scattering would be quite incapable of distinguishing between classical and quantum scattering. [If this is true, and it has the appearance of being approximately so, it seems worthy of remark that this is a second, and independent, respect in which *compensation* appears to prevent absorption from distinguishing between quantum theory and classical theory; for, as pointed out originally by A. H. Compton, and frequently verified by experiment, the ratio of primary to secondary ionizations (for 90°, at least), with unintercepted radiations, is independent of wave-length whether the scattering is classical or quantum, the falling off of the *absolute* intensity of the secondary beam in the latter case with decrease of wave-length being, to the first order, exactly compensated for by the increased absorption by the gas, arising from the Compton increase in wave-length.]

24. The general conclusions to be drawn from fig. 6 are:

(a) The Compton effect, which requires an exponential fall in S/P with increasing  $x$ , for homogeneous beams, does not require such a fall if the beam is heterogeneous.

(b) The more widely the intensity is spread through the scale of absorbabilities—that is, the more heterogeneous the beam in the sense of absorbability (not necessarily in that of wave-length)—the closer apparently will the curve resemble that for classical scattering, a horizontal straight line.

(c) Very absorbable elements of the beam tend to produce an early flattening out of the curve, less absorbable elements produce the same effect later, while the presence of elements of all absorbabilities over an extended range, in the proper

proportion, would seem to give a horizontal curve over a correspondingly large range of values of  $x$ .

(d) The rate of fall of the curve is, on Compton's theory, influenced more by the degree of heterogeneity (in the absorbability sense) of the beam than by the half-value absorption-coefficient.

25. These conclusions invalidate a good deal of evidence that has been cited as disproving the existence of the Compton effect. For example ((17) paragraph 3), a systematic examination of the radiations scattered by different thicknesses of radiator showed that the difference in absorbability between secondary and primary was *steadily* diminished as the radiator was made gradually thinner. From this it was inferred that the change in absorbability was a gradual one brought about by the passage of the radiation through matter (the material of the radiator), and not a sudden one as visualised in the Compton effect. This, however, is exactly the result which the considerations above would lead us to expect. The incident radiation is, on the average, filtered by half the thickness of the radiator before it is scattered; consequently, a thick radiator would be expected to give a curve like 3, fig. 6, a thinner one a curve like 2, while a very thin radiator would give rise to a curve resembling 1, provided the X-ray beam in each case contained a considerable proportion of very soft elements. If for some reason the soft elements were absent—as, for instance, by wandering of the focal spot from an excrescence to a pit, and consequent filtering by the target—the Compton modification would appear to approximately the same extent, independent of the particular thickness of the radiator. This effect was observed by the same author, but was accounted for in a different way (*loc. cit.*).

26. A further illustration of how heterogeneous beams may give results which at first glance appear to contradict theory is afforded by the experiments described in (18), p. 738. A scattered radiation when tested by aluminium, copper, or gold was found to be a "modified" radiation, while the same scattered beam when tested by silver or tin (both of which substances have their K-absorption edge within the limits of the spectrum of rays tested) was found to be "unmodified"; that is, the former elements perceived a Compton change in the scattered beam, while the latter (silver and tin) found the scattered and primary radiations equally absorbable. This interesting



observation turns out to be a natural consequence of conclusion (b) arrived at above (paragraph 24), and is readily understood so soon as we perceive that the heterogeneity which masks the Compton effect is a heterogeneity in the sense of *absorbability* with respect to the testing substance, not necessarily in the sense of wave-length. What would be a comparatively homogeneous beam to Al, Cu, and Au, might well contain *extremes* of absorbability with Ag or Sn, if the bulk of the intensity were situated in the region of the K-absorption edge. In such a case, Compton's theory would predict that Al, Cu, and Au would find full modification, while Ag or Sn would show little if any evidence of modification. Now, let the intensity distribution be disturbed slightly—the proportion of intensity on the two sides of the absorption edge may well be sufficiently upset to give a "modified" curve with silver or tin. Such a change was observed by these authors.

27. The stepped curves obtained by Barkla and his observers will now be considered. A typical example is reproduced in fig. 4. The steps are from 10 to 20 times the probable error of experiment. This is not an isolated case : a considerable number of similar curves will be found in the works cited at the beginning of this paper. It must be clear that, although the curves in fig. 6 could account for irregularity in an observational curve as arising from slight variations in the X-rays delivered by the tube, the regularity exhibited by fig. 4 is not to be explained by such a fortuitous source of change. There can be but two possible explanations—either systematic error, arising from apparatus or procedure, or the existence of a new phenomenon ; no very obvious explanation in terms of systematic error seems to offer itself : an interpretation in terms of a phenomenon seems to present considerable difficulty also. Barkla's hypothesis of sudden condensations of radiant energy upon the absorbing sheets in the case of the scattered radiation seems to disregard the fact that the gas in the ionization chamber is also a "thin absorbing sheet," and that, according to his own observation in other experiments, the ratio S/P ought, therefore, to exhibit rising as well as falling steps on account of "sudden increases in ionization," associated with J-absorption by the gas ((12) para. 3). For this reason, an explanation in terms of an absorption process, subsequent to scattering, seems to be ruled out.

28. Finally, attention must be briefly directed to the

original J-experiments—those which indicated that there was a new series of characteristic radiations. It appears more than likely that the ionization irregularities [(2) p. 350] arose from “recoil” ionization, associated with the Compton effect. The results of the scattering experiments need not be considered [see (2) pp. 355–6]. The absorption experiments [see (3)] have been interpreted without taking into account the fact that the beams were not homogeneous. A 50 per cent. absorption of a heterogeneous beam by a light substance, such as aluminium or paper, gives a transmitted beam different to that which would be obtained by a 50 per cent. absorption by copper, for in the previous case a great part of the absorption is by *scattering*, which has little effect in quenching the longer wave-length constituents. In other words, *the lighter substance collects its 50 per cent. in a different way from the constituents to copper, and therefore the absorptions are not comparable.* In the case of homogeneous beams this objection does not arise. The magnitude of the error arising when absorption coefficients are compared, using heterogeneous beams and Barkla’s 50 per cent. test, will depend on how heterogeneous the beams are, and the disparity between the two absorbing substances as regards the relative values of scattering and true absorption. The error is invariably in the direction of giving the lighter relatively too high an absorption coefficient. The following calculated examples, using, as in a previous section, two wave-lengths instead of a continuous beam, will show that the error in practice is not one which may be ignored unless the radiations are well filtered. Here, as elsewhere, irregularities are to be expected, if the radiations are not well filtered. Irregularities have been found by Barkla, using lightly filtered beams; no irregularities were found by the author when thick filters were used (Dunbar, *loc. cit.* p. 217).

29. Each of the following pairs of wave-lengths, when taken in the proportions given, will, as a combined beam, have the half-value mass-absorption coefficient in copper, 6.0 \*. If heterogeneity did not matter, the corresponding  $\mu/\rho$  to be observed for aluminium would be 0.673 in each case. Calculation on the accepted views, that the phenomena of scattering and fluorescent absorption are concerned with the harmonic constituents only, and not

\* For these calculations, the numerical values have been taken from A. H. Compton’s ‘X-rays and Electrons,’ 1927, p. 185.

with the beam as a whole, gives the following very different values for  $\bar{\mu}/\rho$  in Al:—

43.2 per cent. of 1.1 Å	}	gives $\bar{\mu}/\rho$ , Cu=6.0; $\bar{\mu}/\rho$ , Al=1.26	
with			
56.8 „ „ 0.175	}	„ „ „ 0.807	
31.3 per cent. of 0.9 Å			
with	}	„ „ „ 0.798	
68.7 „ „ 0.25			
31.45 per cent. of 0.7 Å	}	„ „ „ 0.759	
with			
68.55 „ „ 0.25	}	„ „ „ 0.684	
32.45 per cent. of 0.60 Å			
with	}		
67.55 „ „ 0.25			
54.69 per cent. of 0.40 Å	}		
with			
45.31 „ „ 0.25			

Now, the value 6.0 for the  $\mu/\rho$ , Cu, was selected because it was at this point that Barkla and Miss White (3) observed a step in the curve, comparing the coefficients of Cu and Al. The extreme values of  $\mu/\rho$ , Al, observed by them were 0.707 and 0.766. It is suggested that the step corresponds simply to a marked difference in the degree of heterogeneity in the two cases, and that the irregularities in all the absorption-coefficient curves, ascribed by Barkla to the existence of a J-series at one time and to a J-transformation later, are intimately bound up with the fact that a heterogeneous beam is insufficiently specified by the half-value absorption coefficient.

#### SUMMARY.

(1) Two experiments are described which aimed at discovering the J-discontinuities in the absorption of scattered X-radiation (heterogeneous). The results were negative.

(2) The results obtained by Barkla and his collaborators are discussed. It is shown that much of the irregularity they observe is only apparent, that it possibly arises largely, if not altogether, from the assumption that a heterogeneous beam should give sufficiently nearly the same results as a homogeneous beam, the latter having an absorption-coefficient equal to the half-value absorption-coefficient of the former. The progressive absorption method, for instance, frequently used by them to test for the Compton effect, is not suitable

unless the radiation is homogeneous, or nearly so; for very heterogeneous beams it is unable to distinguish between classical and Compton scattering. It is suggested that the pronounced irregularities observed by the above authors are associated with the varying amounts of extremely soft radiation which may succeed in reaching the electroscopes.

In conclusion, I wish to thank the Royal Society for a grant towards the purchase of apparatus required for the experiments. I gladly take this opportunity also for expressing my great indebtedness to Professor H. Robinson, who has been keenly interested in this research and has been most helpful in many ways.

Viriamu Jones Laboratory,  
University College, Cardiff.

---

*C. On the Cause of the Loss of Thermionic Activity of Thoriated Tungsten Filaments under certain Voltage Conditions.* By ANN CATHERINE DAVIES, D.Sc., and RHODA N. MOSS, M.Sc.\*

**E**XTENSIVE investigations of the thermionic emission from thoriated tungsten filaments have been carried out by Langmuir†, whose conclusions in regard to the behaviour of such filaments may be briefly summarized as follows:—

The electron emission from a tungsten filament which contains a small amount of thorium and which has not been heated above a temperature of about 2600° K, is almost identical with that of a pure tungsten filament under similar conditions. Heating at temperatures above about 2600° K, however, reduces some of the oxide, and when the filament is subsequently maintained at lower temperatures the reduced thorium diffuses to the surface and, provided the temperature is not so high that the rate of evaporation of thorium from the surface exceeds the rate at which it diffuses to the surface, it accumulates until there is a complete layer of thorium of atomic thickness.

The thermionic emission at any temperature from such a filament is greater the greater the fraction of the surface covered with thorium, and when the emission at any

\* Communicated by Prof. Frank Horton, F.R.S.

† I. Langmuir, *Phys. Rev.* xxii. p. 360 (1923).

temperature has reached the steady state, there is a balance between the number of thorium atoms arriving at the surface per second from the interior (which depends on the coefficient of diffusion, and the radial concentration gradient of thorium in the wire), and the number of thorium atoms leaving the surface per second by evaporation. Langmuir distinguishes two types of evaporation, namely, ordinary temperature evaporation and "induced" evaporation. The latter type is explained as occurring because the thorium atoms in the surface are more loosely held by underlying thorium atoms than by tungsten atoms, so that a thorium atom diffusing from the interior and arriving just under a surface thorium atom causes the latter to leave the surface. He has shown that, in general, the condition of a thoriated tungsten filament can be expressed by the relation

$$N_0 \frac{d\theta}{dt} = DGf(\theta) - E \quad . \quad . \quad . \quad . \quad (1)$$

where  $\theta$  is the fraction of the filament surface which is thorium covered,  $N_0$  is the number of thorium atoms per  $\text{cm}^2$  in a complete monatomic adsorbed film ( $\theta=1$ ),  $t$  denotes time in seconds,  $D$  is the diffusion coefficient of thorium through tungsten at the particular temperature of the filament at any stage,  $G$  is the radial concentration gradient of thorium,  $E$  denotes the number of thorium atoms leaving a square centimetre of the surface per second, at the existing temperature of the filament, due to ordinary temperature evaporation, and  $f(\theta)$  is equal to  $1 - 0.82\theta - 0.18\theta^3$ . The last two terms in this expression represent the effect of induced evaporation. At temperatures above about  $2200^\circ \text{K}$  the rate of evaporation of thorium from a nearly completely covered surface exceeds the rate at which thorium atoms arrive at the surface, and the equilibrium condition corresponds to a surface only partially covered with thorium—i. e., not fully activated. For this reason temperatures above about  $2200^\circ \text{K}$  are referred to as deactivating temperatures, while temperatures between  $1900^\circ \text{K}$  and  $2200^\circ \text{K}$ , at which for most values of  $\theta$   $DGf(\theta)$  exceeds  $E$ , are known as activating temperatures. It is clear from equation (1) that, since  $D$  and  $E$  vary in a definite manner with temperature, while  $G$  depends on the previous history of the filament, there is some indefiniteness as to the dividing line between activating and deactivating temperatures.

Langmuir found that the large emission of an activated thoriated tungsten filament could only be maintained, at

any particular temperature, in a high vacuum. The presence of oxidising gases destroyed the activity, and in the presence of inert gases the application of large voltages caused the emission to fall off. This was attributed to the removal of thorium atoms from the surface through bombardment of the filament by positive ions \*.

In the use of thoriated tungsten for the filaments of dull-emitter valves it has been observed that the filaments only behave satisfactorily provided the voltage between the various electrodes, encouraging emission from the filament, is not made too large. The maximum safe voltage in each case differs in different types of valve, but four or five hundred volts or less applied for a few minutes at any of the ordinary working temperatures is, in general, sufficient to cause a considerable decrease in the maximum emission obtainable at such temperatures. The emission can, however, be restored to its normal value (corresponding to a completely thorium covered surface) by subjecting the filament to the usual heat treatment described by Langmuir, namely, by maintaining it for about half an hour or more at an activating temperature, *i.e.*, between  $1900^{\circ}$  K and  $2200^{\circ}$  K.

The object of the present investigation was to inquire more closely into the cause of the deactivation of thoriated tungsten filaments, in a high vacuum, by the application of voltage encouraging emission, at temperatures well below the minimum necessary to cause any decrease of emission due to the temperature alone. To this end a thorough investigation was first made of the way in which the emission from an activated thoriated tungsten filament varied with time during the application of various different arrangements of electric fields, at a series of different filament temperatures and concentration gradients of thorium in the filament. Valves of the type V. S. 8 B. were employed for this purpose. These are triode valves with cylindrical electrodes, the filament being enclosed by an open spiral grid of about 3 mm. diameter, and a cylindrical anode of about 1 cm. diameter and 2 cm. length.

*Method of estimating filament temperatures and relative concentration gradients.*

For many of the experiments accurate determinations of the actual temperature of the filament were not essential,

\* K. H. Kingdon & I. Langmuir, *Phys. Rev.* xx. p. 108 (1922); *ibid.* xxii. p. 148 (1923).

and it was sufficient to ascertain by trial what ranges of heating current corresponded to Langmuir's "activating," "deactivating" and "reducing" temperatures. The re-attainment of any particular temperature was effected by adjusting the heating current to the particular reading on a sensitive ammeter, the necessary fine adjustment being made by means of a suitable arrangement of rheostats in parallel. In some of the later work, however, it was necessary to have a fairly accurate estimate of the temperatures corresponding to particular heating currents. This was achieved by measuring its resistance when various heating currents were passing through the filament in question, and estimating the corresponding temperatures by reference to the results given by Jones\* showing how the resistance of a tungsten filament varies with temperature. This was done most satisfactorily by using the preliminary tests of activation, deactivation, and reducing heating current ranges, to locate approximately the correspondence between heating current and temperature for two or three definite temperatures. A check on these estimates was then obtained by comparing the ratio of the resistances at the heating currents corresponding to these temperatures, with the ratio of the resistances at the same temperatures in Jones's tables. At these relatively high temperatures the effect of the resistance of the leads to the filament was comparatively negligible, and sufficiently accurate estimates of corresponding temperatures and heating currents could be made without taking this into account. Though it is not claimed that the temperatures corresponding to different heating currents, thus estimated, have an accuracy greater than about  $\pm 20^\circ$ , the authors believe that the increment of temperature increase, produced by a given increment of heating current, cannot differ by more than a few per cent. from the values stated in the course of the paper.

A measure of the radial concentration gradient of thorium was obtained from observations of the rate at which the emission increased during the process of activation at the standard activating temperature employed in these experiments ( $1900^\circ \text{K}$ ). According to Langmuir, if  $i$  is the emission at any temperature when a fraction  $\theta$  of the surface is thorium covered,  $i_1$  the emission at the same temperature from a fully activated surface, and  $i_0$  the

\* H. A. Jones, *Phys. Rev.* xxviii. p. 202 (1926).

corresponding emission from a pure tungsten surface, then

$$\theta = \frac{\log i - \log i_0}{\log i_1 - \log i_0},$$

whence 
$$1 - \theta = \log\left(\frac{i_1}{i}\right) \cdot \log\left(\frac{i_0}{i_1}\right).$$

The value of  $\log\left(\frac{i_1}{i_0}\right)$  at  $1900^\circ \text{K}$  is  $3.7275^*$ . Langmuir found that the activation curves fitted a formula of the type  $\log(1 - \theta) = -kt$ , and he showed that the constant  $k$  is directly proportional to the concentration gradient. Hence by plotting  $\log\left[\log\frac{i_1}{i}\right]$  against the time a straight line is obtained, the slope of which to the time axis is proportional to the concentration gradient, if the activation observations are always taken at the same temperature. The relative values of the different concentration gradients employed in our experiments have been determined in this way, and similarity of the curves of emission against time, during activation, has been taken as the criterion for equal concentration gradients at different times.

#### *Statement and Discussion of Results of Preliminary Experiments.*

Most of the tests of the effects of the application of electric fields between the filament and the other electrodes were carried out at temperatures too low for any appreciable activation to occur. The condition of the filament after being subjected to any particular treatment was determined by measuring the emission which was obtained under arbitrary standard test conditions, namely, with a heating current corresponding to about  $1700^\circ \text{K}$  and with 40 volts applied between the filament and the other two electrodes joined together. The results of these preliminary experiments may be stated briefly as follows:—

1. The application of a potential difference of a few hundred volts between the filament as negative electrode, and either of the other electrodes, causes partial deactivation of the filament, the emission at once beginning to

\* This value is calculated from the values of the constants  $A$  and  $b$  of the equation  $i = AT^3e^{-b/T}$  for pure tungsten, and for a fully activated thoriated tungsten surface, given by Dushman & Ewald, *Phys. Rev.* **xix**, p. 857 (1927).



fall, and eventually becoming constant at some lower value than that obtained at the instant of application of the voltage. The emission under the test conditions falls also.

2. The extent of the deactivation, and the rate at which it occurs, for a given temperature and concentration gradient, increase with increase of applied voltage.

3. The extent of the deactivation, and the rate at which it occurs at a given voltage, increase as the temperature of the filament increases.

4. For a given voltage and a given temperature, the extent of the deactivation and the rate at which it occurs increase as the concentration gradient decreases.

5. For a given total electron emission, the extent of the deactivation for a given plate voltage is less the lower the grid voltage.

These results are in accord with equation (1) if we take into account an additional deactivating factor dependent on the number and energy of the thermionic electrons. If we assume that this factor causes  $P$  thorium atoms to be removed per second, per  $\text{cm}^2$ , the equation becomes :—

$$N_0 \frac{d\theta}{dt} = DGf(\theta) - E - P. \quad . \quad . \quad . \quad (2)$$

At the temperatures at which the experiments were carried out,  $DGf(\theta) - E$ , for a fully activated surface, is zero, and for a partially activated surface is very low.

Hence  $P$  would be the main factor controlling  $\frac{d\theta}{dt}$ . Starting

with the filament at any particular degree of activation, the emission continues to increase slightly as the potential difference increases, owing to the Schottky effect, and the energy of each electron increases also. Hence any factor to which the electron current gives rise, and consequently the deactivation caused by this factor, would be expected to increase as the voltage increased. Hence results 1 and 2 would follow immediately as soon as  $P$  became appreciable. So long as  $DGf(\theta) - E$  is very small it is clear that, in accordance with equation (2), the extent and rate of any deactivation caused by the extra factor must increase as the temperature increases owing to the increase in the thermionic current itself. Hence result 3 is accounted for. The fact that in these deactivation experiments the emission ultimately becomes constant and does not continue to fall until the pure tungsten value is reached, is accounted for because, as the emission decreases,  $P$  also decreases, and

$DGf(\theta)$  increases slightly, while  $E$  tends to decrease as  $\theta$  decreases. For high concentration gradients, an appreciable rate of activation occurs at temperatures which are not normally considered to be activating temperatures. This follows at once from equation (1) since the value of  $DGf(\theta) - E$  for given values of  $\theta$  and the temperature must depend upon  $G$  the concentration gradient. Bearing this in mind it becomes at once clear that result 4 quoted above is in accord with equation (2).

As regards the influence of grid-voltage upon deactivation, this is readily explained if we suppose the deactivating factor to be positive ion bombardment of the filament, for it follows that the lower the grid-voltage the greater the proportion of any positive ion current which must originate on the side of the grid remote from the filament, and the greater the proportion of this which will be stopped by the grid from reaching the filament. Hence the results of all the preliminary experiments on deactivation by voltage admit of explanation on the view that the thermionic electrons give rise to positive ions which in their turn bombard the filament, thereby removing thorium atoms and decreasing the fraction  $\theta$  of the filament surface which is thorium covered.

#### *Positive Ion Currents and the Setting in of Deactivation.*

It seemed desirable to make a direct determination of the order of magnitude of any positive ion currents which might be produced in the valves in circumstances similar to those in which deactivation tests had been made. This was done in the two following ways :—

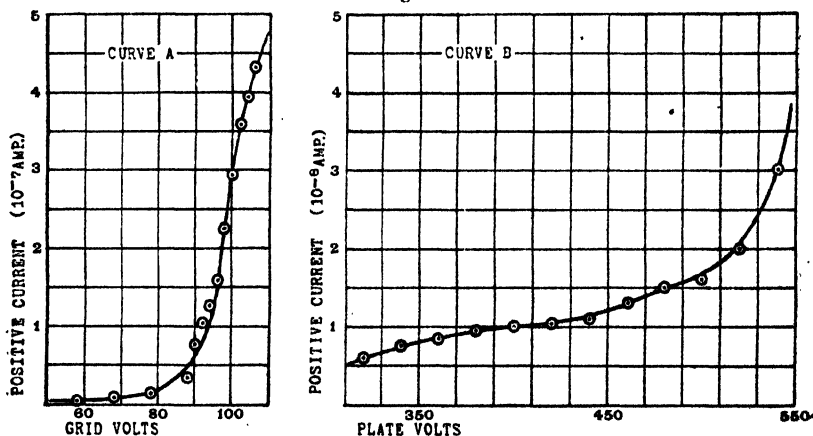
- (a) By making the plate sufficiently negative to the filament to prevent any thermions from reaching it, thus causing it to collect any positive ions produced in the space between it and the grid.
- (b) By making the plate positive to the filament so as to cause a considerable thermionic current to flow, at the same time making the grid sufficiently negative to prevent any of the electrons from being collected by it, and enabling it to collect only positive ions.

The positive currents were measured on a sensitive galvanometer, and by measuring the thermionic current simultaneously as the applied voltage was varied, it was possible to study the behaviour of the positive ion current at the stage when deactivation commenced; in this way some interesting points were revealed. With the fields

arranged as in (a) a positive current was first detected when the grid potential was between 30 and 40 volts, and this increased as the voltage was increased. Ultimately a stage was reached when the rate at which the positive current increased with the voltage became much larger (fig. 1, curve A), and a few volts beyond this stage both the emission current and the positive ion current began to fall off rapidly with time (fig. 2, A). With this arrangement, when the grid-potential had reached about 90 volts, and the emission current was 26 milliamperes, the positive ion current was of the order of  $10^{-7}$  amp. This is of about the same magnitude as the positive ion currents employed by Kingdon and Langmuir in their experiments.

With the fields arranged as in (b) much larger voltages

Fig. 1.

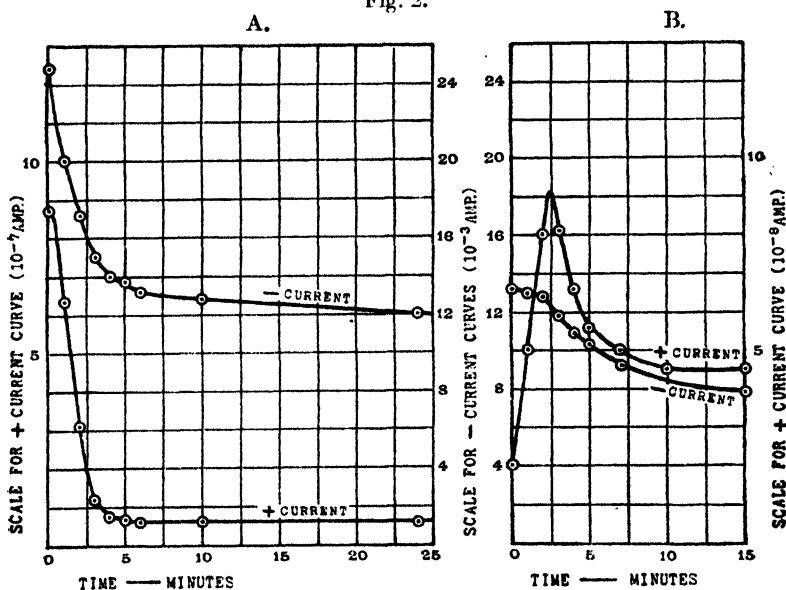


had, of course, to be employed to obtain thermionic currents of the same order of magnitude, and deactivation did not begin to be appreciable until much higher voltages than with the other arrangement, on account of the negative grid-potential. The positive ion currents were rather smaller in this case and increased much less rapidly with increasing potential difference, though the occurrence of a much augmented rate of increase of positive current just preceding the stage at which deactivation commenced was again consistently observed (fig. 1, curve B). With either arrangement, if the conditions corresponding to any stage beyond the bend in the positive ion current curve are established straight away, and readings of positive and negative currents taken at successive intervals, it is found that a certain

amount of deactivation occurs, a decrease in both currents taking place (fig. 2, A and B).

The question of the origin of the positive ions arises at this stage, and whether they can be accounted for by the ionization of residual gas distributed throughout the volume of the valves. The final stage of evacuation of the valves employed had been accomplished by using a magnesium getter, and under such conditions a pressure permanently less than  $10^{-7}$  mm. can be maintained\*. Some idea of the order of magnitude of the positive ion current to be expected

Fig. 2.



at such a pressure in valves of the type employed can be obtained from a consideration of the results yielded by certain forms of ionization gauge †, in which the dimensions of the electrodes and containers were comparable with those of the valves used in this research. It has been found that with an electron current of about 25 milliamps., with an anode voltage of 250, a positive ion current of about  $10^{-8}$  amp. can be obtained in argon when the pressure is  $7.5 \times 10^{-8}$  mm. of mercury, whence for pressures less than  $10^{-7}$  mm. the positive current for the same emission and the same voltage

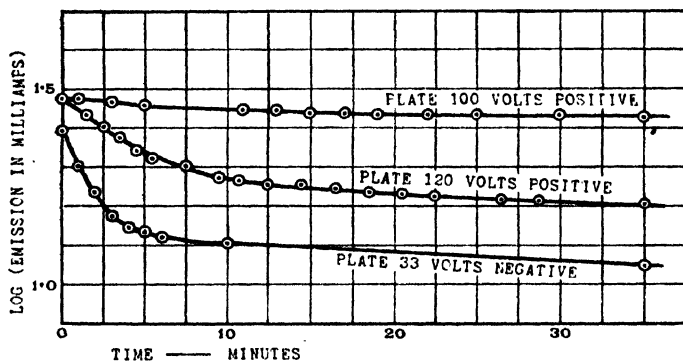
\* N. R. Campbell, *Phil. Mag.* vol. ii. p. 369 (1926).

† S. Dushman & C. G. Found, *Phys. Rev.* vol. xvii. p. 7 (1921).

would be  $1.33 \times 10^{-8}$  amp. If the residual gas were air or carbon dioxide, the ionization current at this pressure would be correspondingly lower. In our experiments with an electron current of 24 milliamps. and an anode voltage of 200, a positive ion current of  $2.1 \times 10^{-6}$  amp. was measured. Hence we cannot straight away attribute the observed effects to the presence of residual gas distributed throughout the volume of the bulb.

The variation of the positive ion current obtained in the present experiments, with variation of electron current at a constant anode voltage, and with variation of the anode voltage for a constant electron current, was investigated to see if it were in accordance with the variations to be

Fig. 3.



The curve for the plate 33 volts positive to the filament so nearly coincides with that for 120 volts, that to avoid confusion it has not been included in the figure.

The grid was 120 volts positive to the filament throughout the series.

expected if the positive current were due to ionization of residual gas. This was found not to be the case, the ionization current for a given emission increasing at a gradually increasing rate with increase of voltage, while the ratio of the positive current to the thermionic current increased steadily with increase of the latter instead of remaining constant, thus suggesting that there is some source of positive ions other than residual gas. This view obtains support from a consideration of the results represented in fig. 3. These curves show the variation with time of the logarithm of the emission current from a filament at a definite temperature, and concentration gradient of thorium, with a potential difference of 120 volts between the grid and the

filament, but with different voltages on the plate. The curves in the figure are typical of those obtained in several series of investigations of this kind. The potential difference of 120 volts between grid and filament was about the minimum voltage which produced appreciable deactivation in these valves. The logarithm of the emission current is plotted because, as has already been shown, this bears a linear relation to the fraction  $\theta$  of the filament surface which is thorium covered\*. The plate voltages employed in the investigations represented were such that in one case the grid and plate were at the same potential, in another the plate was negative to the filament, while in the third it was positive to the filament but negative to the grid. If positive ion bombardment of the filament is the sole cause of deactivation, and if residual gas distributed throughout the whole space between the electrodes were the main source of positive ions, one would expect the curves to be much the same for all cases in which the plate was at a negative potential with respect to the grid, because in these circumstances the positive ion current to the filament would be due to ionization of gas between the filament and the grid only, as all the positive ions produced between the grid and the plate would be urged by the electric field towards the plate. It is clear from fig. 3, however, that this is not the case, the deactivation being greatest when the plate is negative to the filament, and least when the plate is at a little lower potential than the grid.

Such a result can readily be explained if we assume that the positive ions, instead of being due mainly to residual gas, originate at the surfaces of the bombarded electrodes. In such a case one would expect the positive ion bombardment of the filament to be greatest when the largest proportion of the thermionic stream hits the inner surface of the grid, for the positive ions resulting from these impacts will travel directly to the filament. This occurs when the plate is negative to the filament. When the grid and plate are at the same potential, or when the plate is positive to the grid, the greater part of the electron current is to the plate, and of the positive ions originating from the bombardment of this, a certain proportion, depending on the grid potential, will be stopped by the grid. We have, therefore, to consider the factor  $P$  as consisting of  $P_g + P_A$  where  $P_g$  denotes the part of  $P$  which is due to positive ions originating at the surface of the grid, and  $P_A$  that part of  $P$  which is due to

\* The corresponding logarithm for pure tungsten ( $\theta=0$ ) is  $-2.0$ .

positive ions originating at the surface of the plate. When the plate is negative to the grid  $P_A$  becomes zero, since the electric field would draw positive ions back to the plate. We have seen that we should expect  $P_e$  to be greater the lower the plate potential. Hence we should expect least deactivation when the plate potential is less than that of the grid, but is considerably positive to the filament, and greatest deactivation when the plate is negative to the filament. The curves in fig. 3 show this to be the case and thus afford a certain amount of evidence in favour of the suggestion that positive ions are produced which have their origin in the bombardment of the surfaces of the electrodes.

The question now arises as to whether what occurs is a liberation of occluded gas due to heating up of the electrodes, under bombardment, or some more fundamental action. Suppose for a moment that liberation of occluded gas occurs. One would expect the amount of gas liberated to increase as the energy of bombardment of the electrode increased, *i. e.* to increase with the voltage for a given emission, and with the emission for a given voltage. Since the amount of ionization produced from a given quantity of gas will increase as the voltage increases, and also as the emission increases, it is clear that if liberation and subsequent ionization of occluded gas takes place under the electron bombardment, the positive current for a given voltage will increase more rapidly than in proportion to the emission, while the current for a given emission will increase more rapidly than in proportion to the voltage, *i. e.* the current will be expected to vary with these factors in much the manner it has been observed to do in practice. As the filament can be restored to give its original emission without difficulty, any gas evolved under bombardment of the electrodes can have no deactivating influence except when it exists in the form of positive ions which bombard the filament surface. When the emission has been restored the variation of positive ion current with voltage is found to agree with the variation obtained in the first place, showing that no permanent increase in residual gas pressure has taken place.

In connexion with the increased positive ion current at the deactivation stage the following considerations are of interest. If with the filament hot a voltage large enough to cause considerable deactivation is applied suddenly, the positive current obtained immediately is not as large as it eventually becomes, though the emission current at once attains a large value. It is found that 20 or more seconds after the voltage

has been applied, the positive ion current increases very considerably—up to 4 or 5 times its initial value—and either simultaneously, or immediately afterwards, the emission falls off rapidly, and the positive current then decreases rapidly too. This admits of explanation if the warming up of the electrodes under bombardment in any way facilitates the liberation of positive ions. That something of this kind occurs is borne out by the fact that if the voltage is switched off and on alternately, at suitably short intervals, even over such a period that the total time of application exceeds that in which very extensive deactivation occurs with continuous application, it is possible to maintain the large emission from the filament undiminished, while the positive current remains at a value comparable with that obtained when the voltage was first applied. If the electrons are being collected mainly on the grid, and if a sufficient voltage is applied between the filament and the grid to give, temporarily, a reasonably augmented positive current, the final equilibrium emission of the heated filament is fairly low and the ultimate positive ion current is always fairly small. If, however, the grid is made negative, and the plate 600 or 700 volts positive, the processes occur much more slowly and it is possible to maintain an augmented positive ion current for an appreciable interval. This is illustrated by the values given in Table I. below, in which the emission current and the

TABLE I.

Plate voltage.	Thermionic current $10^{-3}$ amp.	Positive current $10^{-9}$ amp.	Time Minutes.	Thermionic current $10^{-3}$ amp.	Positive current $10^{-9}$ amp.
580	7.4	12.5	0	12.0	25.0
600	8.8	14.5	1	11.8	32.5
620	9.6	16.0	2	11.6	50.0
640	10.0	19.0	4	11.0	60.0
660	10.7	20.0	6	10.1	55.0
680	11.3	21.0	8	9.2	50.0
700	12.0	25.0	10	8.2	50.0
			15	7.9	49.0
			20	7.2	45.0

positive ion current for gradually increased plate voltages are set out. When the applied voltage reached 700, it was observed that the emission current began to decrease. The



conditions were therefore kept constant and readings of the currents taken at regular time intervals. It will be seen that the positive ion current in these circumstances continued to increase for some time after the emission had begun to fall off. It would appear that the beginning of deactivation is to be attributed to the positive ions produced before the warming up of the electrodes had had time to augment the positive ion current, and that the subsequent increased rate of deactivation is to be attributed to the influence of the warming up of the electrodes in making possible the production of a larger positive ion current in spite of a smaller emission.

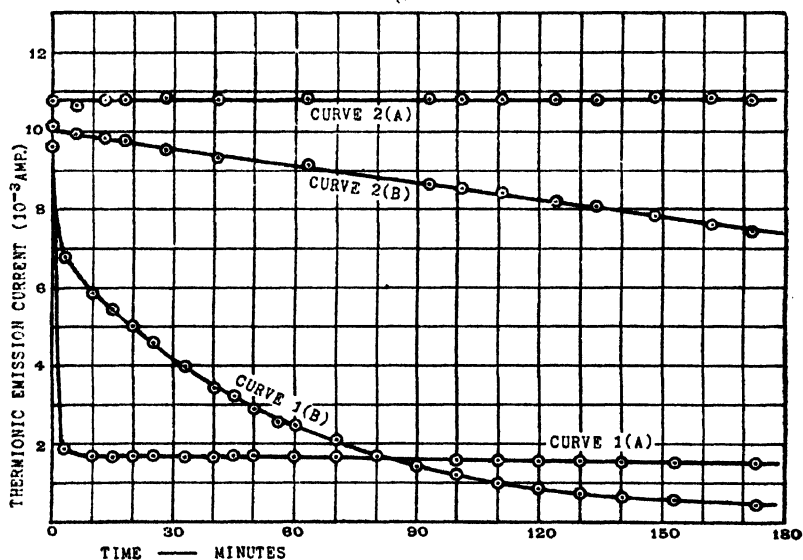
The possibility must, however, be borne in mind that positive ion bombardment may not be the main cause of deactivation of the filament, and that the peculiarities observed in the behaviour of the positive ion current at the stage when deactivation sets in may be merely the accompaniment of some other occurrence and not the primary cause of the reduced emission from the filament. A suggestion has been made that the reduced emission at large voltages is to be traced to an increased rate of evaporation of thorium from the surface of the filament, brought about in some way by the action of the electric field, this increased rate of evaporation causing the steady state of the filament to correspond to a surface less completely covered with thorium. Such an effect, if it occurred, would be expected to vary with different arrangements of electric fields in very much the manner in which the observed deactivation has been found to vary, and in many cases would account for the observed results equally well with the positive ion bombardment view, though it is difficult to see how the differences in the curves of fig. 3 could be explained on this view. However, if such an effect occurred, the increase of positive ion current immediately preceding deactivation might conceivably be a secondary consideration.

#### *Experiments with Two Filament Valves.*

To test the possibility of such an effect as this contributing to the observed deactivation, we had some valves specially constructed to be as nearly as possible the same as those hitherto employed, except that they contained two thoriated tungsten filaments instead of one, these being placed as close together as was consistent with there being no risk of contact between them, and as near as possible to the axis of the concentric grid and plate. In many of the experiments with these valves, the grid and plate were connected together

and various differences of potential were applied between this combined electrode and the filament which was heated to give the emission, the other filament being left unheated. Various electric fields were applied between the two filaments, the cold one being always negative, and the emission from each filament under the standard test conditions was measured at intervals during the application of the other electric fields. It was found that it was possible to arrange either so that both filaments became deactivated, or so that the cold one alone became deactivated while the hot one was unaffected. If the two filaments were at nearly the same potential, and if three or four hundred volts were applied

Fig. 4.



between the emitting filament and the grid and plate, the filament being negative, a reduction in the emission obtained from either under test conditions took place, the deactivation of the hot filament being more rapid and more extensive than that of the cold filament during the first few moments, though, eventually, an equilibrium condition was attained for the hot filament emission corresponding to a rather less completely covered surface, whereas the deactivation of the cold filament continued, the emission from it approaching more and more to the pure tungsten value. This is well illustrated by the curves 1(A) and 1(B), respectively of fig. 4. By having a potential difference of 150 volts or

more between the two filaments, and a potential difference not exceeding 120 volts between the emitting filament and the other two electrodes, it was possible to arrange so that the emission from the hot filament under working conditions, or under test conditions, remained unaffected, while the emission from the cold filament gradually fell off. This is illustrated by curves 2 (A) and 2 (B), respectively, of fig. 4. By a judicious selection of the electric fields any of the intermediate stages could be attained.

Observations were taken of the variation of the emission from the cold filament under test conditions, at intervals during the application of 120 volts between the hot filament and the grid, with the cold filament 320 volts negative to the hot filament, for the two following cases:—(a) with the plate at the same potential as the grid, (b) with the plate at the same potential as the cold filament. The total thermionic current was the same in the two cases, but in case (b) more electrons would strike the inner surface of the grid. The observations showed that the deactivation of the cold filament was very much more rapid in case (b) than in case (a), which agrees with the results obtained with the single filament valves, and therefore suggests that the main factor operative in causing deactivation is the same whether the filament is hot or cold.

It is clear that in these circumstances the deactivation of the cold filament cannot be due to an increased evaporation from the surface of the filament caused by a redistribution of the thorium vapour round it, brought about by the electric field, because the rate of evaporation is quite negligible in these circumstances. Hence the variation of the condition of the cold filament in these circumstances gives us a measure of the effect which can be definitely attributed to positive ion bombardment. The curves 1 (A) and 1 (B) of fig. 4 at first sight suggest that some other factor is operative as well, in the case of the hot filament, but it must be borne in mind that we do not know how the positive ion current directed towards the filaments divides itself between the two. It is quite possible, and even probable, that the hot filament receives more positive ions in these circumstances than the cold one does. Moreover, there exists the possibility that a given positive ion bombardment of a hot filament is more efficient in removing thorium atoms than the same positive ion bombardment of a similar cold filament.

*Filament Temperature and the Deactivation Efficiency  
of Positive Ion Bombardment.*

It was possible to make a test of this point by taking

series of observations for arrangements similar to those of curves 1 (A) and 1 (B) of fig. 4, for different temperatures of the hot filament. It was found that the ultimate steady value of the hot filament emission was lower, and that the deactivation of the cold filament occurred more rapidly, the higher the temperature of the hot filament. The following considerations show how the observations obtained from these experiments were utilized to test the point in question:—The condition of the filament at any instant is given by equation (2). The temperatures corresponding to the various heating currents employed were estimated in the manner already outlined as  $1800^{\circ}\text{K}$ ,  $1850^{\circ}\text{K}$ ,  $1900^{\circ}\text{K}$ , and  $1950^{\circ}\text{K}$ . At these temperatures  $E$  can be considered as negligible in comparison with  $DG^*$ , and with  $DGf(\theta)$ , so that the equation becomes

$$N_0 \frac{d\theta}{dt} = DGf(\theta) - P \quad \dots \quad (3)$$

When the steady state under positive ion bombardment is reached,  $P = DGf(\theta)$ , and using the observed final steady value of the hot filament emission under test conditions to calculate  $\theta$ , the final value of  $P$  can be obtained in terms of  $DG$  for the particular temperature and state in question. By taking observations of the rate of increase of the emission at a standard activating temperature, immediately after the completion of the particular deactivation observations in question, the value of  $\frac{DG}{N_0}$  corresponding to the state

\* From data given in Langmuir's paper (*loc. cit.*) we have the following relations:—

$$\log_{10} E = 31.434 - \frac{44,500}{T},$$

$$\text{and} \quad \log_{10} D = 0.44 - \frac{20,540}{T},$$

$$\therefore \log_{10} \frac{E}{D} = 31.39 - \frac{23,960}{T},$$

from which we obtain the following:—

$$\text{at } 1800^{\circ}\text{K}, \quad \log_{10} \frac{E}{D} = 18.08,$$

$$\text{at } 1900^{\circ}\text{K}, \quad \log_{10} \frac{E}{D} = 18.78,$$

$$\text{at } 2000^{\circ}\text{K}, \quad \log_{10} \frac{E}{D} = 19.41.$$

Now  $G$  is the order of  $10^{21}$ . Hence  $\frac{E}{DG}$  at temperatures from  $1800^{\circ}\text{K}$ — $1950^{\circ}\text{K}$  is negligible.

1006 Dr. Ann C. Davies and Miss Rhoda N. Moss on the  
of the filament at the activating temperature can be calculated,  
and by using Langmuir's equation  $\log_{10} D = \cdot 044 - \frac{20540}{T}$   
the value of  $\frac{DG}{N_0}$  in the actual deactivation experiment can  
be obtained. Hence the value of  $\frac{P}{N_0}$  at the final stage of  
the hot filament is known, and the value at any stage during  
the decrease can be calculated from equation (3) using the  
relation

$$\frac{d\theta}{dt} = \log \frac{i_0}{i_1} \cdot \frac{d}{dt} (\log i),$$

and obtaining  $\frac{d}{dt} (\log i)$  from the slope of the deactivation  
curve at the stage in question. For the cold filament, since  
 $DG$  and  $E$  are both negligible,  $P = N_0 \frac{d\theta}{dt}$ , and hence  $\frac{P}{N_0}$   
for any stage in the deactivation of the cold filament can be  
found from the slope of the curve for this filament. The  
actual observations obtained showed that by the time the  
emission from the cold filament under test conditions had  
reached the same value as the final emission from the hot  
filament under test conditions, the actual working emission  
from the hot filament in the deactivating experiment had  
reached a constant value.  $\frac{P}{N_0}$  was therefore worked out  
for both filaments for this stage in each of the series of  
observations at different heating currents. The results  
of the calculations are given in Table II. The final column  
gives the values of  $\frac{P}{N_0}$  for the hot filament divided by the  
actual working emission. The numbers show that in the

TABLE II.

Temperature during deactivation. Degrees K.	$\frac{P}{N_0}$ for hot filament.	$\frac{P}{N_0}$ for cold filament.	Thermionic current $i$ . $10^{-8}$ amp.	$\frac{P}{N_0 i}$ for hot filament.
1800	$1.97 \times 10^{-5}$	$1.93 \times 10^{-5}$	7.6	$2.59 \times 10^{-9}$
1850	$2.88 \times 10^{-5}$	$5.75 \times 10^{-6}$	8.8	$3.27 \times 10^{-9}$
1900	$4.44 \times 10^{-5}$	$5.47 \times 10^{-6}$	8.7	$5.11 \times 10^{-9}$
1950	$9.86 \times 10^{-5}$	$17.09 \times 10^{-6}$	10.0	$9.86 \times 10^{-9}$

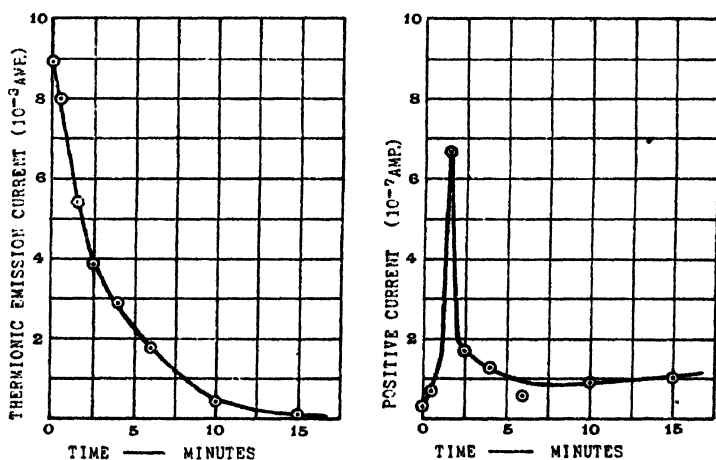
temperature region investigated, there is a rapid increase in the number of thorium atoms removed per unit emission as the temperature increases. The fact that the effects at  $1850^{\circ}\text{K}$  and  $1900^{\circ}\text{K}$  are as 3 : 5, although the thermionic currents are the same, shows that the increased effect with increasing temperature is not due mainly to the fact that the positive ion current increases more rapidly than in direct proportion to the thermionic current. In these two cases, the observations showed that the final rates of deactivation of the cold filament were practically the same, whence it may be concluded that the positive ion bombardment of the cold filament was the same in the two cases. As the actual final emission during the deactivation was the same for both, it is reasonable to suppose that the total positive ion current to the two filaments was equal in the two cases, and hence that the hot filament received the same final positive ion bombardment in these two cases. It therefore seems justifiable to conclude that the greater rate of removal of thorium atoms from the surface of the hot filament at  $1900^{\circ}\text{K}$  was due to its higher temperature. This may mean either that a given positive ion bombardment is more effective in removing thorium atoms the higher the temperature, or that there is some other factor contributing to the deactivation which increases with temperature, while the positive ion effect remains more or less constant.

Some evidence, which seems to show that the first-mentioned alternative cannot be ruled out, was obtained from experiments in which the cold filament was subjected to a definite treatment—first, with no current passing through it (the temperature therefore not being very different from, say,  $350^{\circ}\text{K}$ ), and then with a current passing through it such as would raise it to a temperature of about  $900^{\circ}\text{K}$ . In every such case it was found that the rate of removal of thorium atoms at the higher temperature was about twice as great as at the lower temperature. At neither of these temperatures does any appreciable evaporation occur. Considering these results in conjunction with the variation of  $\frac{P}{N_0^2}$  in the region  $1800^{\circ}\text{K}$ – $1950^{\circ}\text{K}$ , and the relative magnitudes of  $\frac{P}{N_0}$  for the hot and cold filaments set out in Table II., it seems reasonable to conclude that all the observed deactivation could be accounted for on the theory of positive ion bombardment.

The objection might be raised that the comparison of  $\frac{P}{N_0^2}$  at different temperatures has been made for the final

equilibrium condition of the hot filament, *i.e.* the state after deactivation has taken place, and that the arguments put forward do not therefore prove that no other factor contributes to the deactivation of the hot filament which occurs in the first few moments of application of the voltage. By carrying out certain experiments with the two filament valves, it was possible to obtain information which enables this contention to be met. The experiments referred to were based upon the fact that it was possible to arrange so that during the intervals when the deactivating factor was operative upon the cold filament, the positive ion current to this filament was measured. Then by switching over to test conditions at definite time intervals it was possible to observe

Fig. 5.



directly the effect of a known positive ion bombardment. With 120 volts applied between the grid and the plate joined and the hot filament, and with 200 volts between the two filaments, no deactivation of the hot filament occurred, and a steady positive ion current to the cold filament of  $10^{-8}$  amp. was measured. The resulting deactivation curve for the cold filament showed that this positive ion current gave a value of  $\frac{P}{N_0}$  of about  $3 \times 10^{-5}$ .

With the electric fields arranged a little differently, and with a larger thermionic current, deactivation of both filaments took place, and the curves in fig. 5 show the variation with time, of the positive ion current to the cold

filament, and the variation in the cold filament emission under test conditions. It may be observed that the positive ion current shows the initial increase to a larger value (about  $7 \times 10^{-7}$  amp.) which we associate with considerable deactivation of the hot filament. In many experiments the plate, instead of being connected to the grid, was maintained at the same potential as the cold filament, and the positive ion current to each was measured simultaneously. It was always observed that the two currents varied in a similar fashion, and the current to the cold filament was of the same order of magnitude as that to the plate, but was generally slightly smaller.

The mean values of  $\frac{P}{N_0}$  for the hot and cold filaments during the first minute of application of the deactivating conditions in each of the series of observations at the four temperatures,  $1800^\circ \text{K}$ ,  $1850^\circ \text{K}$ ,  $1900^\circ \text{K}$ , and  $1950^\circ \text{K}$ , have been calculated, and are tabulated in Table III. The values are calculated from  $\frac{d\theta}{dt}$ , i. e.  $\log \frac{i_0}{i_1} \frac{d}{dt} (\log i)$ , the values  $\frac{DG f(\theta)}{N_0}$  being negligible in comparison at this stage.

TABLE III.

Temperature during deactivation.	$\frac{P}{N_0}$ for cold filament.	$\frac{P}{N_0}$ for hot filament.
$1800^\circ \text{K}$	$5.55 \times 10^{-3}$	$9.56 \times 10^{-4}$
$1850^\circ \text{K}$	$4.90 \times 10^{-4}$	$27.43 \times 10^{-4}$
$1900^\circ \text{K}$	$10.09 \times 10^{-4}$	$25.78 \times 10^{-4}$
$1950^\circ \text{K}$	$8.52 \times 10^{-4}$	$39.36 \times 10^{-4}$

If we assume, as seems justified by Langmuir's experiments, that the rate of removal of thorium atoms is proportional to the bombarding positive ion current, we see that since  $10^{-8}$  amp. gives  $\frac{P}{N_0} = 3 \times 10^{-5}$ , the maximum value of positive ion current required to account for any of the above effects is about  $1.3 \times 10^{-6}$  amp. The curve in fig. 5 shows that it is not unreasonable to suppose that a current of this order of magnitude occurs for a short interval of time. Hence, bearing in mind the evidence already produced of the greater efficiency of a given positive ion bombardment of a hot filament, it seems clear that the positive ion currents



## 1010 *The Cause of the Loss of Thermionic Activity.*

to the filaments are sufficient to account for all the observed deactivation, and that the agency of no other factor need be evoked.

### *Tests for other Deactivating Factors.*

A direct attempt to test the extent to which any other factor might be operative in causing deactivation was made by arranging so that the positive ion current should be as small as possible, so as to reduce the removal of thorium atoms brought about in this way. This was done by arranging the electric fields so that the thermionic current from the hot filament could flow to the cold filament only. This being of much smaller surface area, and having previously been made very hot, it seemed likely that the yield of positive ions from it for a given electron bombardment would be much smaller than that obtained from the grid for the same bombardment. The actual thermionic current measured for a given applied accelerating potential difference was much smaller in these circumstances, doubtless on account of the repelling action of the field between the grid and the hot filament. Nevertheless, between the two filaments there should exist an electric field at least as intense as any existing with the other arrangements, and if this caused any increased evaporation of thorium to occur from the part of the filament subjected to it, one would expect to be able to detect it by a decrease with time in the emission measured in these circumstances. No such effect was observed, however, and the emission from each filament under test conditions remained unaffected even after the filaments had been subjected to this treatment for prolonged periods. There does not, therefore, appear to be any necessity for attributing any appreciable part of the observed deactivation to any factor other than bombardment of the filament by positive ions which originate in their turn from the electron bombardment of the grid and plate.

The authors desire to express their thanks to Professor F. Horton for his kind interest and advice throughout the course of this investigation, and to the Department of Scientific and Industrial Research for permission to publish this account of work which was carried out as part of the programme of the Radio Research Board.

*CI. Notices respecting New Books.*

*X-rays and Electrons—An Outline of Recent X-ray Theory.* By A. H. COMPTON, Professor of Physics in the University of Chicago. (Macmillan & Co., St. Martin's Street, London. Price 25s.)

NUMEROUS books on the subject of X-rays and atomic structure have appeared in recent years. Prof. Compton's work deals specifically with those aspects of the subject related to his own researches—the structure of the atom as deduced from the study of X-rays, their nature and properties. Evidence of this can be found in many of the chapters of the book; the investigations of other workers in this branch of physics are also recorded. 'X-rays and Electrons' gives a comprehensive and up-to-date account of the subject in two sections: the first dealing with X-rays and Electrodynamics, X-ray scattering, reflexion, refraction, and absorption; the second with X rays and the Quantum theory, including the Photo electric effect, X-ray spectra, and the Quantum theory of X-ray scattering, diffraction, and absorption. There are many valuable tables of indices of refraction and other data, and several appendices giving the results of the special theory of relativity, tables of wave-lengths of X-ray spectrum lines, and atomic and electronic constants.

*Kinetic Theory of Gases.* By L. B. LOEB. (McGraw Hill Publishing Co., 6-8 Bouverie Street, London, E.C. 4. Price 27s. 6d.)

PROF. LOEB has rendered signal service in placing his volume on this important branch of physics in the hands of students both elementary and advanced, serving the purpose of an introduction to the subject and a preparation for the study of the more advanced treatises and original papers.

The greater part of the volume gives a very complete and clear account of the Kinetic Theory: the equations of van der Waals, Dieterici and Reinganum; the relation of the theory to coefficients of viscosity, heat conduction and other problems; low-pressure phenomena and specific heats. Perhaps the two most important and interesting chapters are those having reference to the application of the Kinetic Theory of Gases to electrical and magnetic properties of molecules, especially the beautiful theory of Debye on the temperature variation of the dielectric constant with its experimental verification, the Bohr magneton and the classical experiments of Gerlach and Stern, and, finally, the relation to the conduction of electricity in gases, with Prof. Loeb's own contributions. At the end of each chapter there are references to original papers and treatises dealing with the special section of the subject: two useful indexes of authors and subjects are also given. Like Prof. Jellineck's 'Lehrbuch,' Prof. Loeb's volume is a mine of information and one likely to be accepted as a work of first-rate importance.

CII. *Proceedings of Learned Societies.*

## GEOLOGICAL SOCIETY.

[Continued from p. 672.]

December 14th, 1927.—Prof. E. J. Garwood, Sc.D., F.R.S.,  
Vice-President, in the Chair.

THE following communication was read:—

'The Lower Carboniferous Rocks of the Menaian Region of Carnarvonshire: their Petrology, Succession, and Physiography.'  
By Dr. Edward Greenly, V.P.G.S.; with Palæontological Notes by Dr. Stanley Smith, M.A., F.G.S.

The term Arvon is a convenient designation for the Menaian region of Carnarvonshire.

The Lower Carboniferous rocks of Arvon, like those of Anglesey, consist in the main of a limestone series with many beds of sandstone and shale. At the top of the series there is, as in Anglesey, a series of bedded cherts; but the Millstone Grit and Coal Measures are absent, being cut out by the unconformity at the base of the Red Measures. There is a Basement Conglomerate of the normal type, with rolled pebbles of the Mona Complex.

In Arvon, however, this is underlain by a singular formation, composed of yellow and red loams and breccias, which are studded with pisolites of göthite and kaolinite. The blocks in the breccias are angular, and the loams are unstratified. The loams are of alien, the blocks of local, derivation, the blocks not being derived from the same horizon of the Mona Complex as those in the overlying conglomerate. The extent of this formation seems to have been less than 6 square miles.

The limestones are rich in corals and brachiopoda, and are all in the Zone of *Dibunophyllum*, every division of which is present. The sandstones and shales of the Basement Series have yielded plants.

The structure is that of an asymmetrical synclinal infold, truncated by a great boundary-fault.

The Series rests with complete unconformity upon the Mona Complex and the Ordovician rocks; and there is rapid overlap in a west-north-westerly direction. From the direction of the overlap, and from the contents of the conglomerates, it is inferred that the region which is now Snowdonia was completely submerged in Lower Carboniferous times. The pre-Carboniferous land, which was a branch of the ancient uplands of Anglesey, was lofty. On its south-eastern slope, it steepened into a crag, against which the breccias accumulated. This ancient upland was largely composed of Ordovician shales, with a large inlier of rocks of the Mona Complex. Owing, however, to its height, combined with the effects of the tectonics of the Complex, the outcrops on the inlier were quite different from those on the Menaian Platform of the present day. During the subsidence, different horizons were presented to waste, thus accounting for the contrast between the breccias and the conglomerates.

At first, the climate seems to have been arid, with a large diurnal range of temperature; but, as the subsidence advanced, moist and genial conditions began to set in, persisting throughout the remainder of the period represented by the limestone series.

January 11th, 1928.—Dr. F. A. Bather, M.A., F.R.S.,  
President, in the Chair.

The following communication was read:—

‘The Geology of South-Eastern Arabia.’ By George Martin  
Lees, M.C., D.F.C., F.G.S.

South-Eastern Arabia consists of two separate tectonic and stratigraphic provinces:—(1) A foreland where, as at Dhofar, ancient gneiss is overlain by a ‘Nubian’ type of desert-sandstone. The first marine transgression took place in the Cenomanian; (2) An orogenetic zone of typical Alpine character. The presence of nappes is indicated by great overthrusts, klippen, and by the stratigraphic differences between adjacent units. The movement is of pre-Gosau age. Upper Cretaceous and Tertiary strata lie with strong, often vertical, unconformity on the older Mesozoic and Palæozoic rocks.

The stratigraphy of the orogenetic zone consists of:

- (i) A series of pre-Permian formations of unknown age.
- (ii) Permian dark-blue and black fossiliferous limestones. Near Jebel Rais limestones of a different facies appear as tectonic klippen; they are Crinoidal, Coral, Bryozoan, and *Neoschicagerina* limestones.
- (iii) Upper Triassic limestones, sandstones, and shales. The fauna consists of lamellibranchs and gasteropods; no ammonites have been found.
- (iv) Jurassic to Lower Cretaceous massive limestones.
- (v) ? Upper Jurassic to Lower Cretaceous shales, sandstones, and red and green radiolarites. This group probably belongs to a different tectonic unit from (iv).
- (vi) Hatat Schists. A series of calc- and sericite-phyllites of unknown age, probably Mesozoic, which appear as a tectonic window at Saih Hatat.
- (vii) Basic igneous series—lavas and intrusive rocks.
- (viii) Unconformable Upper Cretaceous to Miocene conglomerates, limestones, and marls. The Maestrichtian is exceptionally fossiliferous.

The relation of Oman to the Zagros arc is discussed. The characteristic zone with red and green radiolarites and shales and basic igneous rocks occurs again in Persia, and forms great tracts of country south-west of Kerman. Here also Upper Cretaceous rocks are strongly unconformable. One great branch of the Cretaceous orogenetic zone of Central Persia must, therefore, have passed southwards into Oman. The Upper Cretaceous-Tertiary geosyncline broke down across the older strike, and pursued an independent direction parallel to the present Persian Gulf-Mekran coast. The late Pliocene movements also followed this trend, the influence of the older tectonics only being shown in the marked swing of the strike between Bandar Abbas and Jashk. Such a complete independence of these two phases of Alpine movement is unique.

The Oman orogenetic zone may be followed through Masirah Island to Ras Madhraka, where it passes southwards into the

Arabian Sea. The Kuria Muria Islands belong already to the foreland.

A further movement, though of much less intensity, took place in Oman in post-Miocene time. South of Sur these folds strike north-west and south-east, and appear to pass out to sea at Ras al Hadd, independent of, and across, the older structures. Perhaps these folds form a continuous loop with the Kirthar Range of Sind, but no connexion can have existed between the latter and the Cretaceous orogen of Oman.

The Triassic, Lower, and Upper Cretaceous fossils are described. They include twelve new species.

January 25th, 1928.—Dr. F. A. Bather, M.A., F.R.S.,  
President, in the Chair.

The following communication was read :—

‘The Glacial Retreat from Central and Southern Ireland.’ By Prof. John Kaye Charlesworth, D.Sc., Ph.D., M.R.I.A., F.G.S.

The Newer Drift of Ireland is bounded on the south by a broad and well-developed kettle-moraine—the ‘South Irish End-moraine’—which runs from the vicinity of Wexford round the northern flanks of the Dublin hills and by way of Baltinglass, Bennettsbridge, Cahir, Tipperary, Charleville, and Newcastle West to the mouth of the Shannon, a distance of 310 miles from coast to coast.

Contemporaneous with this stage of the Ivernian Ice and the Irish-Sea Ice were the independent ice-centres in the Kerry and Wicklow Hills, the Comeraghs, Galties, Knockmealdown, and other mountain-clusters of the south. Their extent is likewise indicated by well marked outer moraines, and corresponds to a snow-line on northern and eastern slopes of about 1000 feet and on other slopes of approximately twice that altitude.

The Irish glacial fauna is restricted, with but few exceptions, to the region outside these moraines.

The ice-recession from the Dublin and Wicklow Hills is clearly shown by moraines and marginal drainage-features. These prove a pivoting of the ice on the northern slopes of the hills, immediately south of Dublin, and the sweeping of the ice-fronts to east and west, at successive stages of the retreat, in a series of curves which swing out of each other tangentially and northwards.

The dissolution of the Ivernian Ice-sheet caused the emergence of the higher hills, such as the Castlecomer Plateau, the Slieve Bloom and Keeper Hills, and the formation of large lobes protruded southwards down the intervening valleys. The moraines of the Barrow, Nore, Suir, Shannon, and other lobes are magnificently displayed, making possible the correlation from lobe to lobe and the delineation of the successive positions of the ice-margin across the country from coast to coast. The festooning of the moraines in the southern part of the country is governed by the relief, while their sinuous form in the northern region is to be ascribed to the break-up of the ice-sheet into separate lobes, flowing on roughly parallel lines.

The ice-sheet in its recession over Southern Ireland remained pivoted on the Dublin hills, and retreated over ever-widening strips of country as the ice-front is followed westwards; a withdrawal of 65 miles in the west is represented south of Dublin by but a few hundred yards.

The ice retreating over the Central Plain was dissected into three perfectly distinct lobes, which centred upon the mountains of Donegal, Leitrim, and Galway respectively. Their stages of recession are indicated by countless moraines, the 'eskers' of Irish Glacial literature. True esars occur subordinately, transversely within, and as integral parts of, the kettle-moraines.

February 22nd.—Prof. J. W. Gregory, D.Sc., President,  
in the Chair.

The following communication was read :—

'The Pre-Cambrian Complex and Associated Rocks of South-Western Lley (Carnarvonshire).' By Charles Alfred Matley, D.Sc., F.G.S. With a Chapter on the Petrology of the Complex, by Edward Greenly, D.Sc., F.G.S.

The pre-Cambrian Complex of Lley occupies the coastal strip from Nevin to Aberdaron and Bardsey Island, the geology of which was described by the Author in 1913, and is a detached 'region' (the Mainland Region) of the Mona Complex of Anglesey. Its age is definitely pre-Cambrian, and its special structures and metamorphism were impressed on it before Cambrian times. It is bounded on the east by a great thrust which has driven it over Ordovician strata and the Sarn granite.

Its members are now correlated with those of Anglesey. The Gneisses, several members of the Bedded Succession, the Plutonic Intrusions, and the 'Penmynydd Zone of Metamorphism' are all represented. The Holyhead Group is absent.

The Gneisses are always found near the boundary-thrust. Both their basic and their acid members are almost identical with those of Anglesey. Their crystallization and foliation are older than the deposition of the Bedded Succession.

Most of the region is occupied by the Gwna Group. On a low horizon of this are the laminated Abergeirch Phyllites, above which come alternating grit and phyllite, quartzites, and limestones. There is a strong development of ellipsoidal spilitic lavas, with tuffs, limestone, and jasper, and sills of albite-dolerite. All members of the group, except the Abergeirch Phyllites, are mostly in the condition of a schistose autoclastic mélange. Part of the group is in the anamorphic condition known in Anglesey as the Penmynydd Zone of Metamorphism, being now mica-schists, some of which may, however, be metamorphosed Fydllyn Beds.

Resting on the Gwna Beds are some 800 feet of quartz-albite dust-rocks (Gwyddel Beds). They may be a special facies of the Skerries Group of Anglesey, with a representative of the Tyfry Beds at their base.

The gabbros are akin to those of Anglesey, and are regarded as plutonic intrusions belonging to the Complex.

Arabian Sea. The Kuria Muria Islands belong already to the foreland.

A further movement, though of much less intensity, took place in Oman in post-Miocene time. South of Sur these folds strike north-west and south-east, and appear to pass out to sea at Ras al Hadd, independent of, and across, the older structures. Perhaps these folds form a continuous loop with the Kirthar Range of Sind, but no connexion can have existed between the latter and the Cretaceous orogen of Oman.

The Triassic, Lower, and Upper Cretaceous fossils are described. They include twelve new species.

January 25th, 1928.—Dr. F. A. Bather, M.A., F.R.S.,  
President, in the Chair.

The following communication was read :—

‘The Glacial Retreat from Central and Southern Ireland.’ By  
Prof. John Kaye Charlesworth, D.Sc., Ph.D., M.R.I.A., F.G.S.

The Newer Drift of Ireland is bounded on the south by a broad and well-developed kettle-moraine—the ‘South Irish End-moraine’—which runs from the vicinity of Wexford round the northern flanks of the Dublin hills and by way of Baltinglass, Bennettsbridge, Cahir, Tipperary, Charleville, and Newcastle West to the mouth of the Shannon, a distance of 310 miles from coast to coast.

Contemporaneous with this stage of the Ivernian Ice and the Irish-Sea Ice were the independent ice-centres in the Kerry and Wicklow Hills, the Comeraghs, Galtees, Knocknealdown, and other mountain-clusters of the south. Their extent is likewise indicated by well-marked outer moraines, and corresponds to a snow-line on northern and eastern slopes of about 1000 feet and on other slopes of approximately twice that altitude.

The Irish glacial fauna is restricted, with but few exceptions, to the region outside these moraines.

The ice-recession from the Dublin and Wicklow Hills is clearly shown by moraines and marginal drainage-features. These prove a pivoting of the ice on the northern slopes of the hills, immediately south of Dublin, and the sweeping of the ice-fronts to east and west, at successive stages of the retreat, in a series of curves which swing out of each other tangentially and northwards.

The dissolution of the Ivernian Ice-sheet caused the emergence of the higher hills, such as the Castlecomer Plateau, the Slieve Bloom and Keeper Hills, and the formation of large lobes protruded southwards down the intervening valleys. The moraines of the Barrow, Nore, Suir, Shannon, and other lobes are magnificently displayed, making possible the correlation from lobe to lobe and the delineation of the successive positions of the ice-margin across the country from coast to coast. The festooning of the moraines in the southern part of the country is governed by the relief, while their sinuous form in the northern region is to be ascribed to the break-up of the ice-sheet into separate lobes, flowing on roughly parallel lines.

The ice-sheet in its recession over Southern Ireland remained pivoted on the Dublin hills, and retreated over ever-widening strips of country as the ice-front is followed westwards; a withdrawal of 65 miles in the west is represented south of Dublin by but a few hundred yards.

The ice retreating over the Central Plain was dissected into three perfectly distinct lobes, which centred upon the mountains of Donegal, Leitrim, and Galway respectively. Their stages of recession are indicated by countless moraines, the 'eskers' of Irish Glacial literature. True osar occur subordinately, transversely within, and as integral parts of, the kettle-moraines.

February 22nd.—Prof. J. W. Gregory, D.Sc., President,  
in the Chair.

The following communication was read :—

'The Pre-Cambrian Complex and Associated Rocks of South-Western Lley (Carnarvonshire).' By Charles Alfred Matley, D.Sc., F.G.S. With a Chapter on the Petrology of the Complex, by Edward Greenly, D.Sc., F.G.S.

The pre-Cambrian Complex of Lley occupies the coastal strip from Nevin to Aberdaron and Bardsey Island, the geology of which was described by the Author in 1913, and is a detached 'region' (the Mainland Region) of the Mona Complex of Anglesey. Its age is definitely pre-Cambrian, and its special structures and metamorphism were impressed on it before Cambrian times. It is bounded on the east by a great thrust which has driven it over Ordovician strata and the Sarn granite.

Its members are now correlated with those of Anglesey. The Gneisses, several members of the Bedded Succession, the Plutonic Intrusions, and the 'Penmynydd Zone of Metamorphism' are all represented. The Holyhead Group is absent.

The Gneisses are always found near the boundary-thrust. Both their basic and their acid members are almost identical with those of Anglesey. Their crystallization and foliation are older than the deposition of the Bedded Succession.

Most of the region is occupied by the Gwna Group. On a low horizon of this are the laminated Abergeirch Phyllites, above which come alternating grit and phyllite, quartzites, and limestones. There is a strong development of ellipsoidal spilitic lavas, with tuffs, limestone, and jasper, and sills of albite-dolerite. All members of the group, except the Abergeirch Phyllites, are mostly in the condition of a schistose autoclastic mélange. Part of the group is in the anamorphic condition known in Anglesey as the Penmynydd Zone of Metamorphism, being now mica-schists, some of which may, however, be metamorphosed Fydllyn Beds.

Resting on the Gwna Beds are some 300 feet of quartz-albite dust-rocks (Gwyddel Beds). They may be a special facies of the Skerries Group of Anglesey, with a representative of the Tyfry Beds at their base.

The gabbros are akin to those of Anglesey, and are regarded as plutonic intrusions belonging to the Complex.



The tectonics and foliation of the Complex resemble in almost every detail those of the Complex in Anglesey. On the working hypothesis of recumbent folding adopted for Anglesey, Dr. Greenly is inclined to regard the Mainland Region as the lower uninverted limb of a recumbent fold (a Lleyrn Fold) belonging to a higher tectonic horizon than those now found in Anglesey.

The Arenig rocks at Aberdaron form a faulted syncline overridden on the west and north by the Complex, and faulted against it on the east. They probably occur as a 'window'. About 1000 feet of sediments belonging to the *D.-extensus* Zone and 200 feet of *D.-hirundo* Beds are exposed. They contain a thick sill of albite-dolerite, which transgresses a zone of fine-textured pyroclastic cherts containing abundant sponge-spicules.

Many basic dykes are exposed in the Complex, of which the great majority are Palæozoic (post-Llandovery and probably post-Silurian), but earlier than the great thrusting movements which took place after the close of Silurian time. Three Tertiary dykes have been found.

Many thrusts and shear-planes later than the Complex are found in the Complex itself, cutting across the foliation and the auto-clastic mélange, and disrupting the Palæozoic dykes. They were produced by minor movements during the general movement which drove the Complex of Lleyrn over the Ordovician strata. The boundary-thrust is certainly a great rupture, which shows no sign of dying out at either end of the exposed part of the Complex. The extent of its overdrive cannot be determined, but it should probably be measured in terms of miles, and may have been sufficient to sever the whole plexus of Palæozoic dykes in the Complex from their roots.

Dr. GREENLY compared the petrological characters of the several members of the succession in the Mona Complex with those found in Anglesey, showing that the correspondence, despite the distance, is singularly close. The Gwna Beds belong to the eastern facies. The fact that, despite the cover of Drifts and of frequent decomposition, the Acid Gneisses had been detected, was due to the minute mapping of Dr. Matley.

This region of the Complex does not appear to correspond to any of the region of Anglesey, and its prolongation is more likely to be buried beneath the Palæozoic formations between Bangor and the mountains.

The theory of recumbent folding has justified itself by furnishing consistent explanations of a number of anomalies, but ought not to be regarded as more than a good working hypothesis. The complexities of the visible structure are astonishing; and the speaker often wondered whether the key to these wonderful regions of crystalline schists might, after all, prove to be some principle whereof we have at present no idea whatever.

---

[The Editors do not hold themselves responsible for the views expressed by their correspondents.]

THE  
LONDON, EDINBURGH, AND DUBLIN  
PHILOSOPHICAL MAGAZINE  
AND  
JOURNAL OF SCIENCE.

[SEVENTH SERIES.]

MAY 1928.

CIII. *On the Purification of Radon.* By L. WERTENSTEIN,  
*Professor of Radiology at the Free Polish University,*  
*Warsaw* \*.

IT is often necessary in medical applications of radioactivity, and also in purely radioactive work, to prepare very small strong sources of radon. In order to compress 100 millicuries into a volume of 1 mm.<sup>3</sup>, which is a typical case, the preparation should contain 6·5 per cent. radon, and even this is not as easy as it would seem at first sight. For any work devoted to investigation of physical and chemical properties of radon, a much higher degree of purity is necessary.

During the course of some work on the determination of the volume of 1 curie of radon I have studied some methods of its purification.

My experiments were restricted to the case when radon is extracted from a solution of radium kept in an air-tight vessel and when at some stages of purification the contact of radon with organic substances is not excluded. The method of extracting radon from a finely-divided powder containing radium, described by Herschfinkiel † and Hahn ‡, seems very promising, and it is possible that it would, if properly used, yield radon of a high initial purity.

On the other hand, the purification of radon extracted from solutions could be made much easier if no organic

\* Communicated by Sir E. Rutherford.

† H. Herschfinkiel, *C. R.* cxlix. p. 275 (1909).

‡ Hahn u. Heidenhain, *Ber. d. D. Chem. Ges.* lix. p. 287 (1926).

substances were used in transfer pumps, etc., by means of which the operations with radon were performed. Owing to the fact, however, that in most laboratories radon is extracted under similar conditions to those mentioned in this paper and that a radical change in the method of storing radium is a very delicate operation, I think that the following remarks may be of some general interest.

The usual impurities of radon extracted from solutions by means of transfer pumps are: hydrogen, oxygen, carbonic dioxide, mercury, and water-vapour. The presence of hydrocarbons has not been definitely proved, but their formation under the influence of  $\alpha$ - and  $\beta$ -rays on organic substances is not unlikely. The removal of all these impurities is in principle very simple. In presence of heated copper and copper oxide, oxygen would combine with the copper, and hydrogen and hydrocarbons would burn to water-vapour and carbonic dioxide. With phosphorus pentoxide and potassium hydroxide used for absorbing these gases, the only impurity remaining would be the mercury vapour. This is immaterial in most cases and can be removed if necessary by the use of a convenient low temperature. In practice, however, things are not quite so simple. For ordinary chemical work the removal of gases by the use of convenient reagents may be considered as perfect. But it must be remembered that in a volume of ab. 50 c.c. the pressure due to 100 millicuries of radon is only 1.3 bar, so that, in order to obtain a good purification, the pressure of impurities should be brought down to a small fraction of 1 bar. In reality it is very difficult to reduce this pressure within a reasonable time to less than 20-30 bars, and in most cases the pressure, after the extracted radon has remained for one or two hours in presence of reagents, would be of the order of 100 bars. In some cases sparking instead of copper oxide is used, and then the residual pressure would be certainly much higher.

The incomplete purification of radon by chemical process is in itself no difficulty, provided the remaining gases do not condense at liquid-air temperature. A part of the purification apparatus may be cooled by liquid air and the uncondensed gases removed by putting the apparatus for a short time in connexion with a quickly working pump and repeating this operation four or five times.

The cooled part may be a slightly sloped tube of about 5 mm. inner diameter extending into a capillary tube. It should be made possible to separate this tube by mercury from the remaining apparatus. In this case the purified

radon, when released after removal of liquid air, can be compressed into the capillary tube. This tube sealed off through the mercury thread could constitute an appropriate source of radon. In some laboratories the cooled tube itself is sealed off while surrounded with liquid air, and radon is subsequently distilled into the capillary extension, which is sealed off in its turn. From the practical point of view both methods are equivalent, but if it is essential to know the degree of purity of radon, the first only can be used. Slight modifications of the above-described chemical methods have been used by different workers. Ramsay \* found that heated lime was more effective than potassium hydroxide for removing  $\text{CO}_2$ . Debiarne† has used heated lithium, which seems to remove even the last traces of gases. Rutherford ‡ obtained very good results by sparking the gaseous mixture and submitting it to the action of  $\text{KOH}$  and  $\text{P}_2\text{O}_5$ . Lind used lead chromate instead of copper oxide for the oxidation of hydrogen and hydrocarbons. All these physicists have succeeded in preparing very pure radon, as was proved by determinations of its volume and spectrum.

My experiments were in principle similar to those of Rutherford, with the difference that I have used copper oxide instead of sparking and that communications in my purification apparatus were obtained by means of mercury forks in order to avoid the evolution of  $\text{CO}_2$  from the tap grease, while in Rutherford's work this difficulty was overcome by greasing the taps with phosphorus pentoxide. In my first experiments roughly purified radon was introduced, by means of an ordinary gas transfer pump (provided with greased taps), into the apparatus, which could be evacuated by a Töpler pump and charcoal tube.

These experiments were unsuccessful, my preparations containing only 17 to 24 per cent. radon. It appeared evident that, in spite of a detailed description of the purification technique contained in the quoted papers, there were still some doubtful points left, and I decided therefore to study the details of the purification process.

As mentioned before, the pressure of radon is generally very small, and I have endeavoured, therefore, to build my purification apparatus according to the principles of high vacuum technique, and, in particular, to avoid the use of the transfer pump.

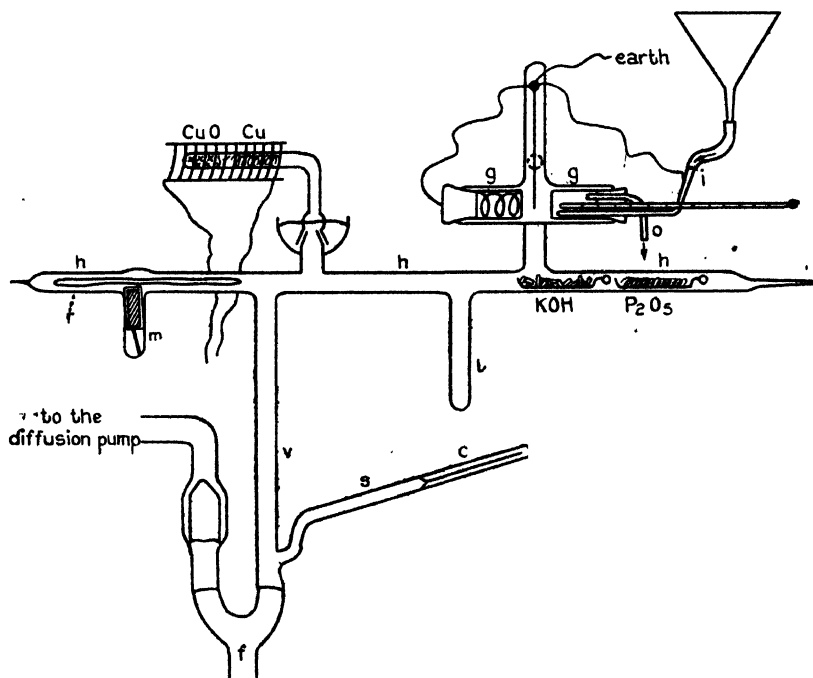
\* Ramsay and Gray, *Trans. Chem. Soc.* xcv. p. 1073 (1909).

† Debiarne, *C. R.* p. 1264 (1909).

‡ Rutherford, *Phil. Mag.* xvi. p. 300 (1908).

The purification apparatus based on these considerations is shown in fig. 1. Its essential part is a horizontal glass tube *h* of about 10 mm. diameter, ab. 40 cm. long, which could be evacuated through the fork *f* by means of a diffusion pump backed by a Töpler pump. The gases pumped off during purification could be collected in a tube over mercury, which was useful for testing loss of radon and for avoiding radioactive contamination of the laboratory. To the vertical

Fig. 1.



Purification apparatus.

tube *V* of ab. 30 cm. long leading to the fork was sealed a small tilted side tube *S* extending into a calibrated capillary *C*, into which the purified radon could be compressed by means of mercury.

The tube *h* contained the purifying agents.  $\text{KOH}$  and  $\text{P}_2\text{O}_5$  were introduced in glass boats. Copper oxide activated by heating to a high temperature with a few drops of palladium nitrate and copper gauze reduced by heating in a hydrogen stream were contained in a pyrex glass tube,

which communicated to the tube *r* by means of a ground joint surrounded with mercury.

Tube *l* is used for condensing radon in liquid air. GG is a calibrated Knudsen gauge of low sensitivity. Its moving part is an Al leaf of about  $4\mu$  thickness hanging between flat parallel surfaces. These surfaces form the ends of two vessels sealed into the tube *g*, which has the form of a double Dewar glass. The one vessel is closed by a cork provided with a thermometer and inlet and outlet tubes *i* and *o*. The inlet tube communicates to a funnel, and so the vessel can be filled alternatively with hot or room temperature water. In order to avoid electrostatic forces it was found sufficient to put a copper spiral in the empty vessel, a copper wire in the other vessel, and to connect spiral and wire with the leaf and the earth. The deflexion of the leaf is measured by a microscope with an eyepiece scale giving .1 mm. per division. The sensibility is about 2 divisions for 1 bar when the temperature of water is changed from *t*, the room temperature, to  $t + 10^\circ$ . This gauge is very convenient for the region of pressures used, and the readings can be taken very quickly.

Radon is admitted into the apparatus in the following way. A tube of about 5 mm. diameter, drawn at one end into a thin-walled capillary, was filled with partly purified radon; the total quantity of gas was .1 to .3 cm.<sup>3</sup> at atmospheric pressure. This tube was introduced into the tube *h* so that the thin-walled part lay over the tube *m*, which contained a cylindrical piece of iron in a sealed glass cylinder. After thorough evacuation of the purification apparatus and its separation from the diffusion pump, the capillary was broken by approaching an excited electromagnet to the part of *h* just over the tube *m*.

In order to find out the best conditions for using this apparatus, different gases which might be supposed to form an impurity of radon were introduced, and operations exactly identical to those used in purification of radon performed.

If the purification is efficient, these gases ought to disappear and give, after introducing and compressing them into the capillary, a negligibly small volume.

The quantity of each gas was of the order of a few tenths of 1 cm.<sup>3</sup> at atmospheric pressure. The investigated gases were: hydrogen, introduced by heating in a gas flame a palladium tube, not shown in the figure; carbonic dioxide prepared by heating pure magnesium carbonate, and coal-gas, which formed an extreme case of impurity owing to the large amount of hydrocarbons and carbon monoxide

contained in it. The coal-gas was introduced through a transfer pump sealed between the Töpler and the diffusion pump.

The operations were performed in the following order :—

1. The apparatus was thoroughly exhausted, the Knudsen gauge baked out, and other parts bombarded by an electrodeless discharge. The final pressure indicated by the Knudsen gauge was of the order of the vapour pressure of mercury.

2. Communication with the diffusion pump was cut off by raising mercury in the fork.

3. The gas to be investigated was admitted in the way described above (in the case of radon the thin-walled tube was broken magnetically).

4. Copper oxide was brought to about  $600^{\circ}$  for  $\frac{1}{2}$  hour.

5. Gas was allowed to stay in presence of reagents for a given time, one of the objects of the experiments being to find the shortest time necessary for an efficient purification.

6. Liquid air was put on tube *l*.

7. Uncondensed gases were pumped off by lowering mercury in the fork for a short time (ca. 10 secs.) and repeating this operation three or four times. The removal of these gases was considered as complete when the gauge showed a pressure of 2 bars, half of which at least was due to mercury vapour. The volume of the part into which condensable gases were to be transferred was about  $2\text{ cm.}^3$ , so that at a pressure of 1 bar the amount of uncondensed gases contained in this part corresponded to  $0.002\text{ mm.}^3$  at atmospheric pressure—a very small quantity compared with the amount of radon usually dealt with.

8. Liquid air was taken off and the tube reheated to room temperature.

9. Condensed gases were distilled into tube *S* by wrapping it with cotton-wool soaked in liquid air. The tube *S* was allowed to communicate with the remaining apparatus for 5–10 minutes.

10. Mercury was raised in the tube *V* separating gas collected on *S*.

11. Cotton-wool was taken off and the tube warmed up.

12. Released gas was compressed by raising mercury still higher into the capillary, its volume and pressure determined in the usual way allowing for the capillary correction.

Hydrogen was tried first. Its disappearance was quick and practically complete, as was to be expected. But carbonic dioxide gave some unexpected results, which it is worth while to describe in detail, because its behaviour explains all the difficulty of obtaining a good purification of radon.

When pure  $\text{CO}_2$  is admitted at an initial pressure of a few millimetres into the apparatus, its pressure, owing to absorption by the  $\text{KOH}$ , falls within 10–20 minutes to a fraction of a bar. If, however, we try to determine its residual amount by distilling the gas into the side tube and compressing it into the capillary, it will generally be found that its mass, measured by the product of volume and pressure, is many times greater than calculated. For instance, in one experiment I obtained, after 10 minutes' condensation,  $1 \text{ mm.}^3 \text{ CO}_2$  under a pressure of 200 mm. Hg. ( $pV = 250 \text{ cm.}^3 \times \text{bar}$ ), while its original pressure in a volume of ab.  $50 \text{ cm.}^3$  was  $\cdot 5$  bar.

When expanding the compressed gas in the purification apparatus, its pressure drops instantaneously to a value somewhat above the original and seems to diminish slowly afterwards. If we repeat in equal successive intervals the determination of  $\text{CO}_2$  by the capillary method, we shall find each time smaller values, but, as a rule, many hours are necessary before we get a " $pV$ " of the order of  $10 \text{ cm.}^3 \times \text{bar}$ . When we remember that the pressure of  $\cdot 1$  curie radon in  $10 \text{ cm.}^3$  is ab. 6.5 bars, we realize at once that effects of this kind may result in a complete failure of a purification experiment.

The only possible explanation of this curious behaviour of  $\text{CO}_2$  is that it is very strongly adsorbed by glass. During condensation gas is permanently given up by the glass walls, and the amount of it collected in the capillary in a given time depends on the rate of flow of  $\text{CO}_2$  and its pressure in the purification apparatus. Experiments have shown that this amount increases in the first half hour nearly linearly with the time, which proves that the free pressure of  $\text{CO}_2$ , and consequently the quantity adsorbed, diminishes very slowly during the distillation. It has been found in one experiment that the quantity of distilling gas was about  $20 \text{ cm.}^3 \times \text{bar}$  per minute, the rate of flow through the tube being about  $100 \text{ cm.}^3/\text{sec.}$  as calculated from its dimensions.



It results that the pressure of  $\text{CO}_2$  during distillation was about  $3 \cdot 10^{-3}$  bar. These figures illustrate well the importance of adsorption of  $\text{CO}_2$  in glass and the difficulty of getting rid of it. It is interesting to give an approximate evaluation of the total amount adsorbed. This amount could be estimated to be about  $2000 \text{ cm}^3 \times \text{bar}$ , i. e., ab.  $5 \cdot 10^{16}$  molecule. The total area of the walls of the purification apparatus amounted to about  $200 \text{ cm}^2$ , so that we get  $2 \cdot 5 \cdot 10^{14}$  molecules per  $\text{cm}^2$  or 25 per cent. of the amount necessary to form a mono-molecular layer. The above figures are given, of course, only as an estimate. Their order of magnitude is, however, surprising. From Langmuir's data we infer that an adsorption layer of  $\text{CO}_2$ , equivalent to the one found in my experiment, exists on mica at  $-80^\circ$  and at a pressure of 172 bars! \*

The adsorption effects on glass and on mica being of the same order of magnitude, we may safely deduce from Langmuir's experiments with mica at  $-80^\circ$ , that the equilibrium pressure for the same adsorption layer on glass at room temperature would be superior to 172 bars. In my experiments the pressure during the distillation was  $3 \cdot 10^{-3}$  bar, and before distillation, .5 bar.

The contradiction between mine and Langmuir's results is very striking. It is true that in Langmuir's experiments glass and mica were baked out completely and water-vapour kept off the adsorbing vessels, while in the experiments just described parts of the apparatus only could be heated to a really outgassing temperature, and some water-vapour, evolved by  $\text{KOH}$  and  $\text{P}_2\text{O}_5$ , was always present. But similar results, to be described more in detail in another paper, have been obtained with an apparatus which could be completely outgassed. It seems that the difference of results is rather due to the sensitivity of my method for detecting adsorption layers which give a very low equilibrium pressure.

It has been found recently † that glass treated by acids does not possess a smooth surface, so that its adsorbing area is certainly many times greater than calculated from its dimensions. Moreover, the corrosion products formed by the action of acids on glass form capillary spaces, and, therefore, the exchanges between the gas and the adsorbed layer take place more slowly than would be expected in a simple adsorption phenomenon. The behaviour of  $\text{CO}_2$  on glass can be easily explained on these assumptions. The sharp

\* Langmuir, Journ. Am. Chem. Soc. xl. p. 1361 (1931).

† Fraser, Patrick, & Smith, Journ. Phys. Chem. xxxi. p. 897 (1927).

fall of pressure when distillation sets in (from  $\cdot 5$  to  $\cdot 003$  bar) shows that gas is given up very slowly by the adsorbing layer, so that probably the rate of outgassing is given by the rate of escape of  $\text{CO}_2$  from the complicated capillary interstices on the glass surface. The partial irreversibility of the effects observed when the  $\text{CO}_2$  is expanded into the original volume is another proof that the effects cannot be due to an adsorption on a smooth surface, in which case a perfect reversibility is to be expected.

It would certainly be interesting to repeat these experiments with freshly blown glass, carefully kept out of contact with water-vapour, for in this case, according to the work of Fraser, Patrick, and Smith, the surface of the glass ought to be smooth.

This would be, of course, impossible in the purification work, owing to the formation of large quantities of water-vapour by the effect of  $\text{CuO}$  on hydrogen. It seems that a radical way of getting rid of the disturbing adsorption effects would be to keep the whole apparatus at a high temperature, except the part containing  $\text{KOH}$  and  $\text{P}_2\text{O}_5$ . This, however, would make the experimental arrangement very complicated.

It is much simpler and quite sufficient for purposes of purification to leave the gaseous mixture for a long time in contact with  $\text{KOH}$ . It will be remembered that this solution was found long ago by Rutherford, who stated that 24 hours were necessary for  $\text{KOH}$  to absorb the last traces of  $\text{CO}_2$ .

In this case  $\text{KOH}$  is acting like a pump which is extracting  $\text{CO}_2$  from the glass walls. As in the above condensation experiments, the rate of this extraction is really the rate of what could be called diffusion of  $\text{CO}_2$  through the adsorbing products of glass corrosion, and a period of the order of one day is just what would be expected for a process of this kind.

In comparing  $\text{KOH}$  to a pump for  $\text{CO}_2$  it is important to say a few words about its "efficiency" and its "limiting pressure."

Theoretically the limiting pressure is the dissociation pressure of  $\text{K}_2\text{CO}_3$ , which is negligibly small, and the efficiency, *i.e.* the number of  $\text{CO}_2$  molecules absorbed per unit time, is of the order of  $\frac{1}{4} N \Omega S$ , where  $S$  is the total area of  $\text{KOH}$ ,  $N$  is the number of molecules per  $1 \text{ cm}^3$ , and  $\Omega$  the mean velocity of  $\text{CO}_2$  molecules. But this is true only for a fresh  $\text{KOH}$  surface. If the "area" is to be taken in the macroscopic sense it would be generally of the order of

10 cm<sup>2</sup>., and a continuous layer of CO<sub>2</sub>K<sub>2</sub> would be formed on it after absorption of 10<sup>16</sup> molecules (.3 mm.<sup>3</sup> at atmospheric pressure). The amount of CO<sub>2</sub> introduced with radon is certainly many times more than this. We are led to expect that the process of removal of CO<sub>2</sub> would be very quick at first, being given by the rate of collisions of CO<sub>2</sub> molecules with KOH, and very slow at the end, being given by the rate of diffusion of CO<sub>2</sub>K<sub>2</sub> into KOH. This expectation is supported not only by my experiments, where it was found that after a sharp fall in pressure below 1 bar the further fall went on very slowly, but also by Debiere, who states that "apparently chemical reactions are extremely slow at very low pressures."

All the above considerations clearly point to the conclusion that it is impossible to obtain absolutely pure radon by use of chemical reagents only. All authors who have described the purification process state that the volume of radon immediately after compression into the capillary is generally greater than the one theoretically expected. The volume undergoes in most cases a marked contraction in the first few hours, remains afterwards stationary, and it is its final value which is assumed to be the volume of pure radon. These results will be discussed in another paper in connexion with my own results obtained by the same method. For the present it will be sufficient to say that the chemical method, at least in the form described in this paper, is not absolutely efficient in removing CO<sub>2</sub>.

When working with a quantity of radon of the order of 50-100 millicuries, the amount of CO<sub>2</sub> found with radon after a carefully conducted experiment will be, in general, about 20 to 50 per cent. of the total quantity of gas.

The important question is to know if CO<sub>2</sub> is the only impurity left with radon (with the exception of traces of water-vapour and of mercury-vapour, the presence of which is immaterial in capillary tubes when gas is compressed at atmospheric pressure, and also of traces of uncondensed gases, mostly hydrogen, due to an incomplete evacuation). *A priori* it does not seem improbable that some heavier hydrocarbons would behave in a similar way.

As it would be very difficult to investigate all hydrocarbons, I performed some experiments with coal-gas, which contains them in a great quantity and variety. The result was that, with an initial volume of about 5 cm.<sup>3</sup>, the volume immediately after oxidation by copper oxide was about 1 mm.<sup>3</sup>, but when gas was allowed to stay overnight with KOH this volume fell to about .005 mm.<sup>3</sup> (equal to the

volume of 8 millicuries of radon). As hydrocarbons are not absorbed by KOH this behaviour is obviously to be ascribed to the presence of CO<sub>2</sub> formed by the combustion of the coal-gas. We can conclude with some certainty that, in the method described in this paper, the only permanent gas which is concentrated with radon by use of liquid air is carbon dioxide.

[This work was performed during the years 1925/1926 and 1926/1927 in the Cavendish Laboratory.

It is a great pleasure for me to express my best thanks to Sir Ernest Rutherford for his kindness in receiving me in the Cavendish Laboratory, in placing at my disposal the large quantities of radon, and in showing a permanent interest in the progress of my work.

I am grateful to Dr. Chadwick for his help and interest.

I thank Mr. Crowe for the preparation of sources. My stay in England was made possible by a fellowship granted by the International Education Board. I wish to express my thanks to this Board.]

---

(IV. *Ranges of the Alpha-Particles of Uranium I. and II.\**.  
By GEORGE C. LAURENCE, *Department of Physics, Dalhousie University, Halifax, Canada* †.

I. *Introduction.*

NEARLY all the ranges of the alpha-particles emitted by the radioactive elements have now been measured accurately. The values, however, for uranium I., uranium II., and thorium may be considerably in error due to experimental difficulties resulting from their low activity. An accurate knowledge of the ranges of the latter elements is desirable for several reasons. Among these is the establishment of the validity of the Geiger and Nuttall Curve for elements of small decay constant. Apparent disagreement, moreover, between the ranges, as measured by Geiger and Nuttall in 1912 ‡, and as calculated from pleochroic

\* Carried out with the aid of a National Research Council of Canada Bursary.

† Communicated by Prof. G. H. Henderson, Ph.D.

‡ H. Geiger and J. M. Nuttall, *Phil. Mag.* xxiii. p. 439 (1912).

halo data \*, has led to a suggestion that there has been a gradual change in their ranges and decay constants throughout geological time.

A new determination of the ranges of uranium I. and II. has therefore been made, using the Wilson Chamber Method, which appeared likely to yield higher accuracy than the usual ionization and scintillation methods. The method consists essentially of photographing the tracks produced by the alpha-particles in a Wilson expansion chamber and measuring the photographs. The extremely small activity of the radioactive material made it necessary to make special modifications in the method, namely, to use a source of large area, to open the camera shutter by hand, and to operate the chamber without shutters to cut off the radiation before the completion of expansions.

## II. Apparatus.

The Wilson expansion chamber had a diameter of 6 cm. and a maximum depth of 1 cm. Its piston was operated by a lever, cam, and spring mechanism, so arranged that by turning a crank the piston was raised slowly and then quickly lowered, producing a practically adiabatic expansion. A fine bore mercury manometer connected to it provided for the measurement of the pressure inside, and a thermometer inserted between projecting flanges on the chamber indicated the temperature. The usual gelatin film kept the air in the chamber moist and served as an electrode for the field of 200 volts across the chamber.

The chamber was lighted from the side by a 10-ampere d.c. arc, the light from it passing through condensing lenses, and water to absorb heat radiation.

The camera had an f. 4.5 lens of focal length 7.5 cm., and was mounted 20 cm. above the chamber. Kodak Super-Speed Cine Film was used, being carried on reels in a box detachable from the back of the camera. Exposures of .4 to .6 sec. were used.

Although an electric device to operate the shutter automatically at the end of each expansion was made, it was found that the shutter could be operated by hand before the tracks diffused enough to affect results. Considerable saving of time and film was thus effected, as, on the average, only one expansion in eighty produced a track suitable for photographing.

\* J. Joly, Trans. Roy. Soc. A, 551, p. 51 (1917); B. Gudden, *Zs. f. Phys.* xxvi. p. 110 (1924).

### III. *Source.*

The radioactive source had to be such as to provide as many tracks as possible and at the same time cause little absorption of the alpha-particles. It had, therefore, to be of large area and very thin. The preparation of this source offered some difficulty, but it was finally accomplished by subliming uranium vapour on strips of mica. Small lumps of metallic uranium, supported on the ends of tungsten wires, formed the electrodes of an electric arc. The arc was struck in a pressure of a few millimetres of air, which was just sufficient gas to maintain it. The vaporized uranium deposited in a thin uniform film on the mica strips which were placed around the arc. A current of 10 amperes for a minute produced a film of the required thickness, 8 mg. per sq. cm., equivalent in absorption to 2 mm. of air. A strip thus prepared, 10 cm. long by .7 cm. wide, fastened to the side wall of the chamber with soft wax, served as the uranium source. About one-third of the glass wall remained bare to admit the light to illuminate the tracks.

The size of the source practically prohibited the use of shields and shutters to cut off the radiation before the expansions were complete. This difficulty was overcome by making the expansions very rapid. Thus more than 98 per cent. of the total number of tracks seen are formed at constant density after the expansion is complete and while the chamber is warming up to the temperature above which the vapour will no longer condense on the paths of the alpha-particles. The remaining, less than 2 per cent., which occur at slightly lower pressures, introduce a quite negligible error in the result. The fraction of the tracks which occur before the completion of expansion was here calculated from an approximate comparison of the time interval during which the expansions continue beyond the minimum value necessary to produce condensation on the tracks with the time it takes the average temperature in the chamber to rise until the condensation will no longer occur.

### IV. *Preliminary Experiments with Polonium.*

Thus modified, the method was applied to the alpha-particles of polonium as a check. For a source, small pieces of a glass tube which formerly contained radium emanation were used, being stuck to the walls of the chamber with wax. The photographs of the tracks were measured, corrected for the magnification of the camera, temperature, air and vapour pressure, and the obliquity of the tracks, as will

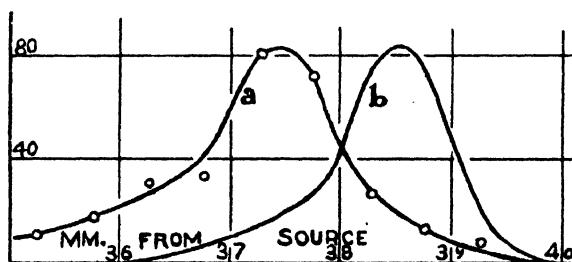
be described later. The range of polonium at  $15^{\circ}\text{C}$ . and 760 mm. was thus found to be 3.84 cm. The best recent values are :

Mlle I. Curie \*, 3.92 cm.

H. Geiger †, 3.925 cm.

The fact that our value is somewhat smaller than these is probably due to the penetration of the radioactive material into the glass by the recoil of Rn, RaA, and RaC'. A rough application of the correction for finite thickness of source (see subsequent section), to correct for the resulting absorption, brings the range up to 3.90 cm., in good agreement with the accepted value. The results of 164 tracks are shown in fig. 1, curve *a*, where the number of polonium tracks of length between .5 mm. less than and .5 mm. more

Fig. 1.



than the abscissa is plotted. Mlle Curie's curve is given for comparison (curve *b*). The fact that the straggling shown in our curve is not very much greater than in hers, obtained under the most favourable conditions, justified proceeding with the method.

### V. Uranium Measurements.

The experimental method was as follows: holding the cable shutter release in one hand and turning the crank which operates the piston with the other, the chamber was watched for the appearance of a cloud track. When a track was seen the camera was immediately snapped. The stop-cock connecting the manometer with the chamber was then opened, air-pressure and temperature read and recorded. The stop-cock was then closed and the film-reel given a turn

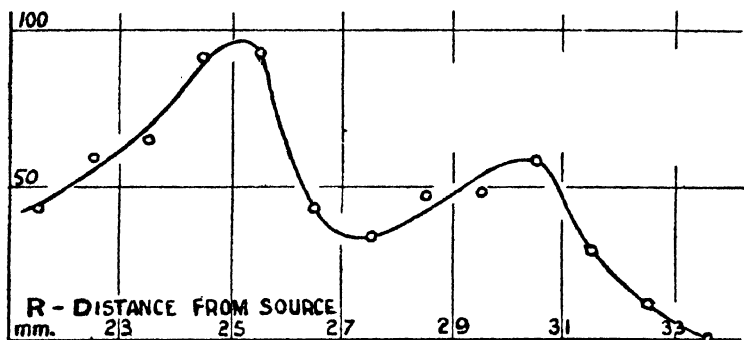
\* I. Curie, *Ann. de Phys.* iii. p. 299 (1925).

† H. Geiger, *Zs. f. Phys.* viii. p. 45 (1922).

ready for the next exposure. . About 1620 photographs of uranium tracks were taken. This required over 120,000 expansions. Poor photographs, and photographs of tracks whose length was less than 1.5 cm. or whose ends were indistinct, were discarded. The remaining 900 photographs of tracks were measured with the aid of a transparent scale and a small magnifying glass, and the lengths so obtained were multiplied by the magnification of the camera, which was determined by photographing lengths of fine glass tubing placed in the chamber. As the length of a path varies inversely as the density and the square root of the atomic weight of the gas, it was corrected for temperature, air and vapour pressure, to obtain the path-length in dry air at standard conditions.

The lengths of the tracks are plotted in figs. 2 and 3. In fig. 2 the ordinates represent the number of tracks having

Fig. 2.



a length lying between .05 cm. less than and 0.5 cm. more than the length indicated by the abscissa. In fig. 3 the ordinates represent the number of tracks of length greater than the abscissa. Only one track of length greater than 3.40 cm. was obtained. Its length, 3.67 cm., indicated it to be due to polonium contamination and it was therefore disregarded. The corrections discussed in § VI. and § VII. were applied in plotting fig. 2 and fig. 3.

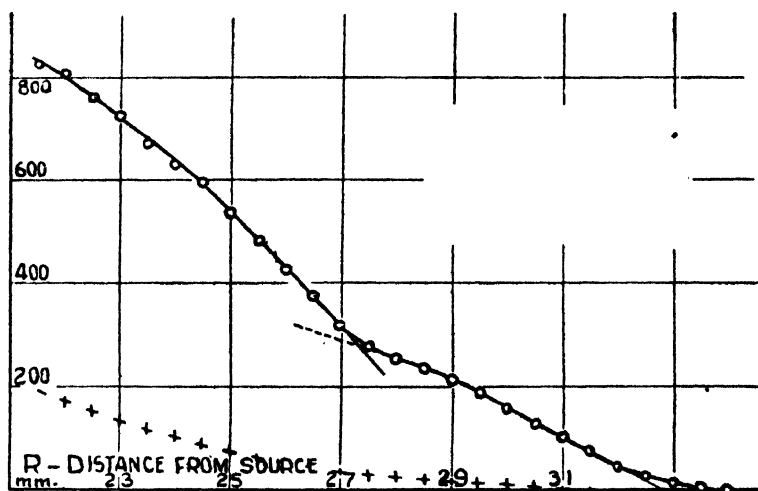
It will be seen that Curve 3 falls off rapidly to zero as the end of the range of uranium II. is reached. The range of uranium II. is obtained in the customary manner by extending the slope at the end of the curve to intersect the range axis. Superimposed on the curve representing the uranium II. tracks is another similar curve corresponding



to the shorter range uranium I. Producing the slope at the end of this curve to intersect the uranium II. curve extrapolated back (along the dotted curve in the figure) gave the range of uranium I.

While the photographs were being taken the source was changed, the apparatus taken apart and cleaned, and the gelatin layer renewed several times, and the pressure varied from 570 to 770 mm. of mercury. That such changes had practically no effect on the results was shown by dividing the tracks into groups representing different conditions and comparing the corresponding curves. These resembled each other as well as would be expected with such small groups of tracks.

Fig. 3.



### VI. Correction for Absorption by Source.

The range as determined in the manner described above depends slightly on the absorption of the radiation by the source itself. As it was not practical, because of the small activity of uranium, to use a source so thin as to cause negligible absorption, the effect of the absorption on the range will now be calculated and added as a correction to the range obtained from the curve.

Bohr\* and Flamm† have shown theoretically, and

\* Bohr, *Phil. Mag.* xxv. p. 10 (1913); xxx. p. 581 (1915).

† Flamm, *Wien. Ber.* cxxiii. p. 1393 (1914); cxxiv. p. 397 (1915).

I. Curie \*, Mercier †, Meitner and Freitag ‡, and others have verified experimentally, that the lengths of the tracks emanating from a very thin source are distributed about a mean value  $R$  according to the error law. That is, the fraction  $dz$  of the total number of tracks which has a range differing from this mean value by a distance  $+x$  is given by

$$dz = \frac{1}{a\sqrt{\pi}} e^{-\frac{x^2}{a^2}} dx, \quad . \quad (\text{Fig. 4, Curve } a)$$

where  $a$  is a parameter determining the extent of the straggling. The fraction of the tracks which are longer than  $R+x$  is therefore

$$z = \frac{1}{a\sqrt{\pi}} \int_x^\infty e^{-\frac{x^2}{a^2}} dx. \quad . \quad (\text{Fig. 5, Curve } a)$$

Since we are using a source of finite thickness, equivalent in absorption to  $m$  cm. of air, the measured ranges of those particles which come from a layer of the source at a depth  $v$  below the surface and of thickness  $dv$  (where  $v$  is measured in equivalent cms. of air) are shortened by a distance  $v$ . The fraction of the tracks having a range longer than  $R+x$  is therefore

$$\frac{dv}{m} \cdot \frac{1}{a\sqrt{\pi}} e^{-\frac{(x+v)^2}{a^2}} dx.$$

$v$  is so small that the change in  $a$  resulting from it may be neglected. So the fraction of the total number of tracks having a measured range greater than  $R+x$  is

$$\begin{aligned} dz_1 &= \frac{dx}{ma\sqrt{\pi}} \int_0^m e^{-\frac{(x+v)^2}{a^2}} dv, \\ &= \frac{dx}{ma\sqrt{\pi}} \int_x^{x+m} e^{-\frac{x^2}{a^2}} dx. \end{aligned} \quad (\text{Fig. 4, Curve } b)$$

Hence the fraction of the number of tracks whose measured length is greater than  $R+x$  is

$$z_1 = \frac{1}{ma\sqrt{\pi}} \int_0^\infty dx \int_x^{x+m} e^{-\frac{x^2}{a^2}} dx.$$

\* I. Curie, *Ann. de Phys.* iii. p. 299 (1925).

† I. Curie and P. Mercier, *Journ. de Phys.* (6), vii. p. 289 (1926).

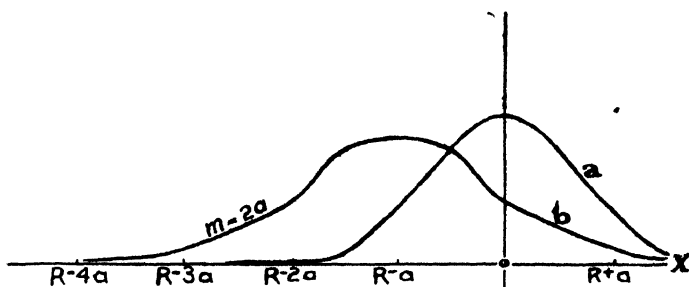
‡ L. Meitner and K. Freitag, *Zs. f. Phys.* xxxvii. p. 481 (1926).

This may be integrated by parts, yielding

$$z_1 = \frac{1}{ma\sqrt{\pi}} \left[ -x \int_x^{x+m} e^{-\frac{x^2}{a^2}} dx + m \int_{x+m}^{\infty} e^{-\frac{x^2}{a^2}} dx + \frac{a^2}{2} \left( e^{-\frac{x^2}{a^2}} - e^{-\frac{(x+m)^2}{a^2}} \right) \right]. \quad (\text{Fig. 5, Curve } b)$$

It is evident that if the tangents to the points of inflexion  $d$  and  $f$  (fig. 5) are produced down to intersect the range axis in the manner usual in determining the ranges, they will do so in two separate points,  $g$  and  $h$ . To obtain the ranges for a very thin source the distance  $gh$  must therefore be added to the measured range.

Fig. 4.



The point of inflexion is found by equating the second derivative of  $z_1$  to zero in the usual way. This gives  $x = -\frac{1}{2}m$ , which, when substituted in the equation of the curve, gives  $z_1 = \frac{1}{2}$ .

The slope at the tangent at this point is

$$\frac{dz_1}{dx} = \frac{1}{ma\sqrt{\pi}} \int_{-\frac{1}{2}m}^{+\frac{1}{2}m} e^{-\frac{x^2}{a^2}} dx = \frac{1}{m} \operatorname{erf} \frac{m}{2a},$$

where  $\operatorname{erf} \frac{m}{2a}$  represents the expression

$$\frac{2}{\sqrt{\pi}} \int_0^{\frac{m}{2a}} e^{-y^2} dy.$$

Hence the intersection of the tangent with the X-axis is

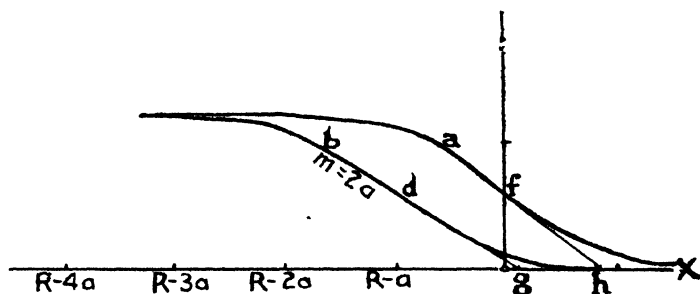
$$z_1' = x - \left( z_1 \frac{dz_1}{dx} \right) = -\frac{1}{2}m + m / (2 \operatorname{erf} (m/2a)).$$

When  $m$  approaches 0, as in Curve 5*a*, this expression reduces to  $z_1' = \frac{1}{2}a\sqrt{\pi}$ . So the required distance between the intercepts  $g$  and  $h$  is

$$\frac{1}{2}a\sqrt{\pi} + \frac{1}{2}m - m/(2 \operatorname{erf}(m/2a)). \quad (1)$$

As  $m$  increases, the value of this expression approaches  $\frac{1}{2}a\sqrt{\pi}$  and differs very little from  $\frac{1}{2}a\sqrt{\pi}$  for  $m$  greater than  $2a$ , and therefore need be known very accurately. This does not imply that  $m$  might just as well be quite large. Increasing it has the effect of flattening the slope of the curve and thereby making its intercept more difficult to determine accurately. It also causes the slopes corresponding

Fig. 5.



to the two uranums to overlap, making them difficult to distinguish.

Putting in the value of  $m$  and the value of  $a$  for the two uranums, the corrections are calculated to be  $+0.040$  cm. for uranium I. and  $+0.045$  cm. for uranium II.

## VII. Other Corrections.

Small corrections for the apparent shortening of the rays due to their obliquity to the photographic film must be added to the ranges. These corrections are derived as follows:—

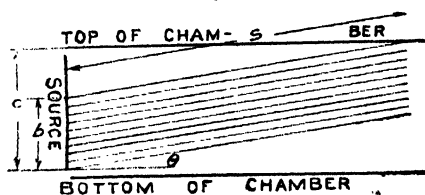
Let  $s$  be the average length of the tracks and  $c$  the depth of the chamber. Of the tracks whose angle of inclination to the horizontal is  $\theta$ , only those coming from a strip of width  $b = c - s \sin \theta$  along the bottom of the source will escape hitting the top or bottom of the chamber before the end of their path. Their number is therefore proportional to  $c - s \sin \theta$ . Their apparent length is  $s \cos \theta$ . See fig. 6.

Their average length is

$$\frac{2 \int_0^{\sin^{-1} c/s} (c - s \sin \theta) s \cos \theta d\theta}{2 \int_0^{\sin^{-1} c/s} (c - s \sin \theta) d\theta}$$

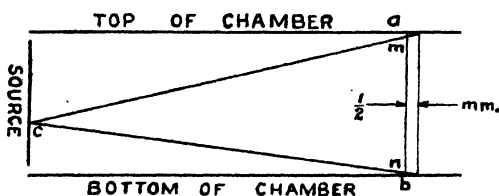
Solving and filling in the numerical values it is found that the ranges of uranium I. and II. are shortened by .016 cm. and .018 cm. respectively.

Fig. 6.



About 20 per cent. of the tracks have struck the top or bottom of the chamber. Their distribution is such, however, that they produce negligible effect on the range as determined above. Starting at 2.1 cm. from the source, we see from fig. 3 that there are 802 particles which travel farther than this. These all pass between  $a$  and  $b$ , fig. 7. Of this number,

Fig. 7.



only those passing between  $a$  and  $m$  and between  $n$  and  $b$  strike the top or bottom in the next half millimetre. Their number is proportional to the angle subtended at  $c$ , and since the angles are small, the fraction of the total number which strike the walls in the next half millimetre is  $(am + nb)/ab$ .

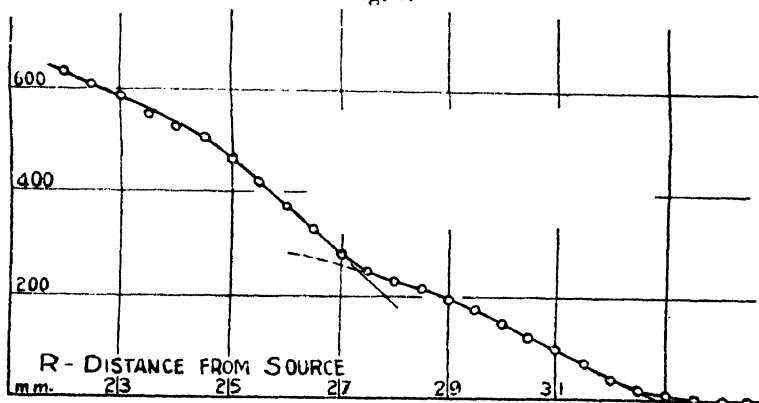
Continuing in this manner the number which strike the walls in each half millimetre is determined, and from these figures the dotted curve of fig. 3 is obtained, indicating the number of tracks of range greater than the abscissa which hit the top or bottom. Subtracting the ordinates of this curve from those of the solid line curve we get the curve of

fig. 8, showing the number of the tracks which have not hit the walls that are longer than the abscissa. If this curve is used in determining the ranges, the intercepts are found to fall on the same points as those of fig. 3 within the possible accuracy of plotting.

It may be noticed that in fig. 8 there are more uranium I. than uranium II. tracks. This is due to the shape of the chamber; short range particles have a larger solid angle in which they may be projected without hitting the walls.

The heating of the chamber by the radiation from the arc light was investigated by using the chamber and manometer as an air thermometer. Comparisons of the temperature measured in this manner with the reading of the thermometer

Fig. 8.



showed that the temperature of the chamber averaged  $\cdot 5$  degree above the thermometer during the time taken for a series of expansions. The corresponding correction of  $\cdot 005$  cm. was therefore subtracted from the ranges.

Possible sources of error not considered above are: the obliquity of the rays of light from the ends of the tracks to the axis of the lens, errors in measuring pressure, and in measuring the tracks themselves. These probably total less than  $\cdot 02$  cm. for most of the tracks.

### VIII. Results.

Applying the corrections discussed above the ranges in dry air at  $150^{\circ}$  C. and 760 mm. of mercury are

Uranium I. .... 2.73 cm.

Uranium II. .... 3.28 cm.

The error in these is probably less than 1 per cent.

## 1038 *The Ranges of Alpha-Particles of Uranium I. and II.*

Applying Geiger and Nuttall's law to the range 3.28 cm. gives for the decay constant of uranium II., which has never been measured,

$$1.7 \times 10^{-12} \text{ reciprocal seconds,}$$

making the half-life 13,000 years.

The range of uranium I. is about intermediate between Geiger and Nuttall's value and Gudden's value obtained from pleochroic halo data. Assuming that it has a half-life of  $4.67 \times 10^9$  years, the range of uranium I. calculated from the Geiger and Nuttall relation is 2.67 cm., slightly smaller than the present value. The range of uranium II. is considerably longer than the older values.

In a preliminary report on this work \*, based on less data, comprising 370 tracks, the ranges were given as 2.72 and 3.29 cm. respectively, differing very little from the final values.

### IX. *Summary.*

The ranges of the alpha-particles of uranium I. and II. were determined by the Wilson Cloud Chamber Method, with modifications made necessary by the small activity of the radioactive material.

The method was satisfactorily checked by its application to the range of polonium.

The ranges at 150° C. and 760 mm. of mercury were found to be

Uranium I. ....	2.73
Uranium II. ....	3.28

with a probable error of less than 1 per cent. From the range of uranium II. its decay constant was calculated to be  $1.7 \times 10^{-12} \text{ sec}^{-1}$ , or a half-life of 13,000 years.

The uranium metal for the source was kindly furnished by Dr. G. M. J. MacKay, of the General Electric Co., Schenectady, N.Y.

The author is gratefully indebted to Dr. G. H. Henderson for suggesting this problem and for his encouragement and advice. Mr. R. H. Fowler very kindly checked the calculations contained in Section VI., and the adoption of his suggestions added considerably to the clearness of that section.

\* G. C. Laurence, Trans. Nova Scotia Inst. of Sci. xvii. p. 108 (1927).

CV. *On the Primary Dark Space of a Geissler Discharge.*  
*By K. G. EMELEUS, M.A., Ph.D., Lecturer in Physics,*  
*and NORA M. CARMICHAEL, B.Sc., Musgrave Demonstrator,*  
*Queen's University of Belfast\*.*

### 1. *Introduction.*

THE cathode dark space of a glow discharge, although only relatively non-luminous, is actually separated from the cathode in some instances by a thinner intensely dark layer. This "primary dark space" was first noticed by F. W. Aston on an aluminium cathode in helium, hydrogen, and mixtures of helium with oxygen<sup>(1)</sup>, and the same appearance was subsequently found by Aston and Watson to be presented by discharges through all the inert gases, being clearest in helium and xenon<sup>(2)</sup>. Kossel made a detailed study of the primary dark space on an electrode of potassium in helium<sup>(3)</sup>, whilst Holst and Oosterhuis examined certain features of it in neon<sup>(4)</sup>. The present writers have observed it on a nickel electrode with argon containing some hydrogen. It does not appear to have been recorded up to the present in gases other than those mentioned.

Aston also found that striæ were present beyond the first dark space in helium<sup>(1)</sup>; these became less distinct as the negative glow was approached, but the differences in potential between them were approximately constant, so far as could be judged from rough estimates of the electric intensity. In neon, the primary dark space replaces the first of the dark negative striæ characteristic of the transition region between the normal glow discharge and simple ionization by collision, when the current is increased<sup>(4)</sup>. The difference in potential between the negative striæ is about the ionization potential of neon<sup>(4)</sup>, and the number of ions in the luminous parts is almost doubled at each fresh striation towards the anode<sup>(5)</sup>. By analogy, the fall of potential across the primary dark space should be the ionization potential of the gas, but this cannot be verified from the distribution of the electric field, which is unknown for the conditions under which the primary dark space can be seen. These are not much different from those occurring with a normal cathode fall of potential, for which a theory has been given by K. T. Compton and Morse<sup>(6)</sup>, but this again cannot be applied with certainty to the immediate neighbourhood of the cathode.

\* Communicated by Prof. W. B. Morton, M.A.



A theory of this dark space was proposed by Aston<sup>(1)</sup>, in which electrons from the cathode were supposed to move outwards to the negative glow, but to produce no visible effect until they had sufficient energy to ionize. The presence of striæ is an immediate consequence of this. It was shown subsequently by Güntherschulze<sup>(7)</sup> that it is also possible to explain in this way the apparent absence of the primary dark space in other gases, since, if the distribution of electric intensity found from the Stark effect for a strongly abnormal cathode fall is taken as an approximation to the state of affairs near the normal cathode fall, an electron starting at rest from the cathode would first produce radiation at a distance too small to be observed directly. The initial velocities of the electrons are probably small compared with the velocities required for ionization of the gases in question.

The experiments of Kossel, on the other hand, are not in complete agreement with this view. In helium, the main cathode dark space is blue-green, and the positive boundary of the primary dark space has a red rim. A closely similar light-structure can be produced within a hollow cathode built of mutually insulated sections, whose outer gauze surface is the main cathode of an ordinary glow discharge. The red rim can only be produced internally by an auxiliary electron-accelerating potential of not less than 21 volts. This is very close to a resonance potential of helium, which Kossel therefore concluded was the difference of potential between the faces. The energy of the electrons employed may, however, have been somewhat greater, since it had been shown that under somewhat similar conditions in hydrogen they left the cathode with initial energies equivalent to a maximum of about 2 volts, which has here to be diminished by the unknown work-function of the emitting surface. Moreover, the positive column of the main discharge was striated, which indicates that, although mercury was absent, other impurities may have been present, so that primary excitation of helium could have produced ionization by collisions of the second kind. In addition, the phenomena when hydrogen was used were less simple, and can be accounted for better on the ideas elaborated in § 2. However, even if Kossel's conclusion is correct, the general theory of the following section is not affected substantially, since the resonance potentials vary in much the same way as the ionization potentials.

It is not certain, nevertheless, that the relatively sharp outer boundary of the primary dark space is entirely due to the fact that the electrons lose practically no energy

until they make inelastic collisions. A cushion of light to the positive side of the primary dark space—the “cathode glow” \*—often persists even when the primary dark space cannot be detected, and exhibits certain features which seem to differentiate it from the remainder of the cathode dark space. The most obvious of these are :—

- (1) With strongly abnormal cathode fall, if not under all circumstances, some sections of it are electrically neutral or negative <sup>(8, 9)</sup>.
- (2) In hydrogen and oxygen, part of its light is due to positive rays <sup>(10)</sup>.
- (3) It is little affected by magnetic fields.

Experiments are in progress here on the characteristic curves of a collector in this part of the tube, and on the light from it, which it is hoped will give further information on this point, but it appears that the cathode glow is more nearly like the negative glow than is that part of the cathode dark space between the two glows. In the present paper, we propose to examine the consequences of supposing that the primary dark space is a positive ion sheath of the type studied by Langmuir in connexion with the use of cold exploring electrodes <sup>(11)</sup>. On this view, the flow of positive ions between the cathode and cathode glow is limited, as indeed elsewhere in the cathode dark space, by the positive space-charge which they produce, but a contributory cause to the absence of radiation will be that which is active at the surface of a negatively charged exploring electrode, in this case the cathode of the main discharge, rather than a specific inhibitory effect of free electrons, such as has been suggested by J. J. Thomson <sup>(12)</sup>. A simple theory of this type has already been tried by Ryde for the whole of the cathode dark space <sup>(13)</sup>. If this theory is correct, all the lines of force ending at the cathode start on positive ions in the primary dark space, and there must be a negative space-charge in part of the cathode glow to act as an effective negative electrode for the main cathode dark space, in agreement with Brose's observations, as far as the latter can legitimately be applied here <sup>(8, 9)</sup>. It may be significant that the outer rim of positive ion sheaths in regions of feeble ionization has an appearance very like the cathode glow, being markedly brighter than the main discharge, which is possibly partly due in both cases to a local accumulation of electrons repelled from the sheath.

\* Referred to in German literature as “Erste Kathodenschicht.”

The facts which have to be accounted for are <sup>(1)</sup> :—

- (a) That the primary dark space appears in only a limited number of gases.
- (b) That  $i_d$  is approximately constant, where  $i$  is the current density, and  $d$  the thickness of the primary dark space.
- (c) That  $d$  is independent of the pressure of the gas.
- (d) That  $Vd/D$  is constant for any one gas, where  $V$  is the cathode fall of potential, and  $D$  the thickness of the cathode dark space.

## 2. Space-Charge Theory.

The difficulties that have been encountered in attempts to form a theory of the cathode dark space, which arise chiefly from incomplete knowledge of the origin and paths of the cathode rays, are less important in the limited region now under consideration. In particular, the appearance of the primary dark space strongly suggests that ionization only occurs beyond its boundary, whilst relatively few collisions are made by electrons and ions in traversing it. The contribution of the electrons to the space-charge in the primary dark space will be neglected, but their contribution ( $i_e$ ) to the total current density ( $i$ ) must be taken into account. If  $i_p$  is the current density of positive ions,

$$i_e + i_p = i. \quad . \quad . \quad . \quad . \quad . \quad (1)$$

The maximum thickness of the primary dark space is about 0.1 cm., and the pressures at which it can be seen are of the order of 1 mm. Hg, so that the number of collisions made by an ion in traversing it will usually be decidedly less than 10. Their effect will be neglected, and Langmuir's solution of space-charge limited conduction for a plane electrode used <sup>(14)</sup>. This takes the form

$$i_p = \frac{2.34 \cdot 10^{-6} V_i^{3/2} \{1 + 0.025(T/V_i)^{1/2}\}}{\sqrt{1834M} d^2} \quad . \quad . \quad . \quad (2)$$

where  $V_i$  is the ionization potential of the gas (§ 1) and  $M$  is the molecular weight of the positive ions. The numerical constants correspond to current densities in amps./cm.<sup>2</sup> potentials in volts, and distances in cms. With sheaths of comparable thickness, it has been found that the most consistent results are obtained if the effects of collisions are completely ignored <sup>(15)</sup>. There is uncertainty as to the value of  $T$ , the temperature of the positive ions when they enter the sheath; Aston has given reasons for supposing that most

of the positive ions at low values of the cathode fall of potential should reach the neighbourhood of the cathode with approximately the energy obtained since the last collision with a gas-molecule<sup>(16)</sup>, but the electric field at the outer boundary of the primary dark space is unknown. If, however, the correcting factor in equation (2) is taken to be approximately constant, the formula contains the experimental relation (*b*) between current density  $i$  and thickness  $d$ , on the additional plausible assumption that the relative contributions of  $i_e$  and  $i_p$  to  $i$  are independent of the exact value of the latter. The fact that  $d$  is independent of pressure (*c*) is implicit in the assumption that the effect of collisions can be neglected.

The connexion between the thickness  $d$  and the nature of the gas is more complicated. Equation (2) shows that  $d$  is inversely proportional to  $M^{\frac{1}{2}}$ , so that hydrogen, where the mass of the positive carriers may be  $1(\text{H}^+)$ ,  $2(\text{H}_2^+)$  or  $3(\text{H}_3^+)$ , and helium, where it is 4, are the only two substances specially favoured by this factor. The distance  $d$  is also proportional to  $V_i^{\frac{1}{2}}$ , if the factor in brackets is neglected, which should single out from other gases helium, with an ionization potential of 24.6 volts, and neon, with one of 21.5 volts. Measurement of  $d$  in the case of neon is also facilitated by the peculiar ease with which optical phenomena can be seen in discharges through it, whilst the same is probably true of xenon, and to a less extent of argon and krypton.

These considerations alone are, however, inadequate to account completely for the failure of the primary dark space to appear in other gases, to do which the magnitude of  $i_p$ , equation (2), must be taken into account. The total current density across the primary dark space is the same as that across the cathode dark space, so that  $i_p$  enters into the equation as an empirical quantity dependent on  $i$ , which in turn has to be found by experiment in each case. The general nature of the variation of  $i$  from one gas to another will be seen from Table I., taken from Güntherschulze's data for a cooled platinum cathode<sup>(17)</sup>,  $i_n$  being the normal density at a pressure of 1 mm. Hg.

It will be seen that the current densities are smallest for the first four gases, and since  $d$  is inversely proportional to  $i^{\frac{1}{2}}$  (*b*), this factor, taken in conjunction with those already mentioned, can be taken to show that  $d$  should be particularly large in helium, neon, and hydrogen. The differences between the various gases will be less at lower pressures, since  $i_n$  is proportional to the square of the pressure, but the

primary dark space is then more diffuse and difficult to detect. Argon should be more comparable with the poly-atomic gases so far as the data of Table I. go.

TABLE I.

Gas.	He.	Ne.	A.	H <sub>2</sub> .	O <sub>2</sub> .	N <sub>2</sub> .
$i_n$ mA/cm. <sup>2</sup>	0.01	0.02	0.14	0.09	0.55	0.38
$i_p$ mA/cm. <sup>2</sup>	0.7	0.25	0.1	0.6	0.14	0.16
D <sub>n</sub> cm.	1.66	0.77	0.36	0.90	0.31	0.42

Krypton and xenon have been examined separately by G ntherschulze <sup>(18)</sup>, and the normal current densities for these gases, obtained with a massive iron cathode, are shown in Table II. Both values of  $i_n$  are small, which will partly compensate for their large atomic weights.

TABLE II.

Gas.	Kr.	Xe.
$i_n$ mA/cm. <sup>2</sup>	0.04	0.02
$i_p$ mA/cm. <sup>2</sup>	0.05	0.03
D <sub>n</sub> cm.	2.6	2.3

An exact quantitative test of equation (2) does not appear to be possible at present, both because of incomplete data in the literature on the primary dark space, and because of uncertainty as to the value of the bracketed factor. For the purpose of calculation, we shall assume that the latter has a constant value of 2, which is about what could be expected from Aston's analysis <sup>(18)</sup>. The current densities of positive ions against  $i_p$  in Tables I. and II. have been obtained in this way, and correspond to a primary dark space 0.1 cm. in thickness. In the case of nitrogen, where the positive ions are either N<sup>+</sup> or N<sub>2</sub><sup>+</sup>, with masses of 14 or

28, a mean value has been taken. A similar procedure has been adopted with oxygen. For hydrogen,  $M$  has been taken to be 1.5. The values of  $V_i$  for the diatomic molecules have been used.

For the last two gases of Table I. and argon,  $i_n$  and  $i_p$  are of the same order, the former being the larger of the two, in general agreement with the facts that the positive ions transport a considerable fraction of the current to the cathode, and that for these gases  $d$  is certainly less than 0.1 cm. The agreement in Table II. is closer than could be expected, as there is great latitude in the choice of current densities. For hydrogen,  $i_n$  is definitely less than  $i_p$ , which might be explained, following Kossel, as due to the presence of mercury, which would lower the value of  $V^{3/2}$  from about 64 to 36. In addition, no special precautions were taken to cool the cathode in Aston's experiments, and a rise in temperature has been shown to increase the value of the normal current density. It is unlikely, however, that these considerations explain the large values of the ratio  $i_p/i_n$  found for helium and neon, or that it is due to incomplete electrostatic shielding of the cathode by the primary dark space in these gases, and not in others. We would tentatively suggest that some such action as the following occurs.

If the current of positive ions is greater than the total current, a current of electrons must be flowing across the sheath against the electric field. This could take place either because of diffusion in a concentration gradient, or more probably because of the presence in the cathode glow of swift electrons moving in more or less random directions, and able to penetrate the sheath. We do not wish to lay stress on this point, because of the absence of exact data in support of it, but such electrons might give the secondary emission of electrons from the cathode which is usually attributed to impact of positive ions or a photoelectric effect, and so bring the discharge phenomena in line with the absence of secondary emission from outgassed electrodes bombarded with slow positive ions<sup>(19)</sup>. It would also partly explain why so great a fraction of the energy expended in the cathode fall space appears as heat at the cathode, by recombination of positive ions and electrons at the surface of the latter. It has been found by Mr. W. L. Brown and one of us (K. G. E.) in this laboratory, that electrons of the requisite energy are present in the negative glow, and certainly persist for some distance into the cathode dark space.

Given sufficient data, equation (2) gives ideally a means of finding the number of electrons which leave the cathode for

each positive ion received, by comparison of  $i$  with  $i$ , equation (1) <sup>(20)</sup>.

The relation (d) was used by Aston to calculate the ionization potentials of hydrogen and helium. This leads to certain discrepancies which have been pointed out by Kossel, and in addition  $Vd/D$  increases with atomic weight amongst the inert gases, whereas  $V_i$  decreases. The present theory is not concerned with  $V$  and  $D$ , but Aston's relation can be shown to be in agreement with another semi-empirical formula that he established, viz., that if  $p$  denotes the pressure,

$$iD^3pV^{-2} = \text{const.} \quad . \quad . \quad . \quad . \quad . \quad (3)$$

to a degree of approximation dependent on the gas used.

This can be regarded as derived from

$$Vpi^{-\frac{1}{2}} = \text{const.} \quad . \quad . \quad . \quad . \quad . \quad (4)$$

and

$$Dp = \text{const.} \quad . \quad . \quad . \quad . \quad . \quad (5)$$

which are approximate forms of the empirical relations

$$V = \text{const.} + K_1i p^{-1}, \quad . \quad . \quad . \quad . \quad . \quad (6)$$

and

$$D = K_2p^{-1} + K_3i^{-\frac{1}{2}} \quad . \quad . \quad . \quad . \quad . \quad (7)$$

where  $K_1$ ,  $K_2$ ,  $K_3$  are constants.

If  $p$  is eliminated between equations (4) and (5), on the grounds that the thickness of the primary dark space is independent of the pressure, we obtain,

$$VD^{-1}i^{-\frac{1}{2}} = \text{const.} \quad . \quad . \quad . \quad . \quad . \quad (8)$$

Both from the theory, equation (2), and experiment (b),

$$i^{\frac{1}{2}}d = \text{const.} \quad . \quad . \quad . \quad . \quad . \quad (9)$$

and hence from equations (8) and (9),

$$VdD^{-1} = \text{const.} \quad . \quad . \quad . \quad . \quad . \quad (10)$$

It is impossible to predict the relative accuracy with which equations (3) and (10) would be expected to be true.

Somewhat similar conditions determine both  $d$  and  $D$ , and the values of the latter at normal cathode fall on iron, at a gas pressure of 1 mm. Hg., are shown against  $D_n$  in Tables I. and II. The data are taken from various publications of Güntherschulze <sup>(21)</sup>. Those gases showing a primary dark space have in general the greatest values of  $D_n$ .

### 3. *General Considerations.*

The genesis of the primary dark space from the low current striæ has been mentioned in § 1, and its intimate connexion with the latter is indicated by the presence of striæ in the cathode dark space in helium. There is evidence that the space-charge is negative between the luminous parts of a low current discharge, but there is instability in the transition to the normal glow, both in appearance and in the characteristic curve<sup>(4, 22)</sup> which may well be associated with a change in electrical conditions similar to that which accompanies "blueing" in a thermionic diode containing gas<sup>(23)</sup>. The disappearance of the striæ at higher current densities may be due to causes similar to those which govern the transition from a striated positive column to the unstriated form. When the current density is so high that the primary dark space itself is not visible, it need not, nevertheless, be actually absent. On the contrary, it may play an important part in the change from a glow to an arc, since there is strong evidence that the cathode of the latter is covered with a sheath of positive ions<sup>(24, 25)</sup>, which may be generated from the primary dark space, rather than from the whole of the cathode dark space.

The discussion of § 2 is incomplete in several respects. In particular, it does not explain satisfactorily why a primary dark space is apparently absent in oxygen and nitrogen. It should be possible to detect it with more refined means of observation, if it is present, but very thin. It is possible that its presence is masked by radiation from excited molecules that have diffused into the sheath, although this is not the case with hydrogen, and with the mixtures of monatomic and diatomic gases in which it can be detected. Our main object has been to call attention to the fact that if the outer boundary of the primary dark space is at a definite potential relative to the cathode, then, on certain assumptions, space-charge equations of a simpler type than those holding in the main part of the cathode dark space can be applied to it, and that the results obtained in this way are, on the whole, consistent with those obtained by other means.

### 4. *Summary.*

The primary dark space on the cold cathode of a Geissler discharge is similar in appearance to the positive ion sheaths present on negative exploring electrodes. A number of its properties can be accounted for by application of the equations developed by Langmuir for the latter, but there are discrep-



ances between the observed and calculated current densities which indicate that the cathode is receiving fast electrons from adjacent parts of the discharge, which, in turn, could produce a secondary emission of electrons from the metal. The primary dark space may be the analogue in a glow discharge of the cathode sheath in an arc.

### References.

- (1) F. W. Aston, Roy. Soc. Proc. lxxx. p. 45 (1908).
- (2) Aston and Watson, Roy. Soc. Proc. lxxxvi. p. 168 (1912).
- (3) Kossel. *Jahrb. d. Radioakt.* xviii. p. 326 (1921).
- (4) Holst and Oosterhuis, *Physica*, i. p. 78 (1921).
- (5) Penning, *Zeit. f. Physik*, xl. p. 4 (1926).
- (6) K. T. Compton and Morse, *Phys. Rev.* xxx. p. 305 (1927).
- (7) Güntherschulze, *Zeit. f. Phys.* xxxiii. p. 810 (1925).
- (8) Güntherschulze, *Zeit. f. Phys.* xxxvii. p. 868 (1926).
- (9) Brose, *Ann. d. Phys.* lviii. p. 731 (1919).
- (10) Seeliger and Lindow, *Phys. Zeit.* xxvi. p. 393 (1925).
- (11) Langmuir, Journ. Franklin Inst. cxevi. p. 751 (1923).
- (12) J. J. Thomson, *Phil. Mag.* iv. p. 1128 (1927).
- (13) Ryde, *Phil. Mag.* xlv. p. 1149 (1923).
- (14) Langmuir and Mott-Smith, *Gen. Elect. Rev.* xxvii. p. 554 (1924).
- (15) Emeléus and Harris, *Phil. Mag.* iv. p. 49 (1927).
- (16) Aston, Roy. Soc. Proc. civ. p. 565 (1923).
- (17) Güntherschulze, *Zeit. f. Phys.* xx. p. 1 (1923).
- (18) Güntherschulze, *Zeit. f. Phys.* xxxiv. p. 549 (1925).
- (19) Jackson, *Phys. Rev.* xxx. p. 473 (1927).
- (20) Emeléus and Carmichael, 'Nature', Jan. 7, 1928.
- (21) See Bär, *Handb. d. Physik*, (Geiger-Scheele), xiv. p. 190.
- (22) Clarkson, *Phil. Mag.* iv. p. 849 (1927).
- (23) Compton, Turner, and McCurdy, *Phys. Rev.* xxiv. p. 597 (1924).
- (24) K. T. Compton, *Phys. Rev.* xxi. p. 266 (1923).
- (25) Slepian, *Phys. Rev.* xxvii. p. 407 (1926).

CVI. *Magnetism and the Structure of some Simple and Complex Molecules.* By D. M. BOSE, Ghosh Professor of Physics, Calcutta University\*.

**I**N the present paper it is proposed to discuss some recent theories on the structure of some simple and complex molecules in light of their magnetic properties. Before we can proceed further with our discussion, it will be necessary to give a short account of these theories.

### *Structure of diatomic molecules.*

The nature of the bond between the atoms of a diatomic molecule can be of two kinds, viz.: polar and non-polar or

\* Communicated by the Author.

contravalent and covalent. In the former by the transference of one or more electrons from one atom to the other, each is left with an outer configuration of eight electrons, with an excess or deficiency of negative charge. The two ions so formed are held together by electrostatic forces, and can be ionized in solution. In the case of the union of two atoms of the same type and other non-ionizable molecules, the nature of the forces holding the two atoms of the molecule is obscure, but it is assumed that two atoms, each of which is a few electrons short of a stable number, can share electrons in such a way that each of the latter is considered to be constituent of both the atoms, and thus form links which are not entirely due to electrostatic attractions and so cannot be ionized. Lewis showed that in a large class of non-polarizable compounds, the total number of electrons in the outer shells of the atoms taking part in them is even.

From this the conclusion is drawn that the chemical bond in them is due to pairs of electrons moving in binuclear orbits. Such bonds are known as covalent bonds. Recently a new theory of the distribution of valence electrons in diatomic molecules has been proposed by Mulliken, Birge, and Mecke\*, from their study of the band spectra of diatomic molecules.

The total energy of a molecule is made up of the electronic energy of the radiating electrons, the oscillatory energy of the atomic vibrations, and the energy of rotation of the molecule as a whole. We have now a more or less complete theory of the band spectra so far as the rotational and oscillatory energies of the molecule are concerned. In recent years a great deal of attention has been directed to the interpretation of that part of the band spectra which is due to the quantum jumps of the radiating electrons. From the recently acquired insight into the relation between spectral terms and the number and distribution of the emitting electrons in the different quantum orbits in an atom, it has been possible by the analysis of the electron part of the band spectra of molecules, to assign spectral terms to them, and from that to deduce the distribution of the electrons responsible for these terms, in different quantum orbits. Thus it has been found that spectra of diatomic molecules like BeF, BO, CN, show great similarity to that of Na, while CO gives a spectra similar to Mg, and so on. The

\* For references see Mecke and Guillery, "Report on Band Spectra," *Phys. Zeit.* xxviii. pp. 479, 514 (1927).

total number of electrons in the first group of diatomic molecules is thirteen, which, according to the hypothesis put forward by Birge and Mulliken, are distributed as follows—each of the nuclei retains its two K-electrons, of the remaining nine outer electrons, eight form an octet shell enclosing the two nuclei, while the ninth electron moves in a 3-quantum orbit, giving rise to a  $^2S$  term.

Thus we can arrange these diatomic molecules, according to the total number of outer electrons found in them, as follows (Table I.) :—

TABLE I.

Molecules.	Total No. of Outer Electrons.	No. of Electrons outside octet shell.		Expected ground terms.
		$l=0.$	$l=1.$	
BF, BeO, CN	9	1	—	$^2S$
N <sub>2</sub> , CO	10	2	—	$^1S$
NO	11	2	1	$^2P$
O <sub>2</sub>	12	2	2	$^3P, ^1D, ^1S$

If the analogy between these diatomic molecules and the corresponding atoms is to be maintained, it has to be shown that these molecules are capable of entering into chemical combination with a valency proportional to the number of electrons which lie outside the common octet shell. It will be seen later in what sense this expectation is realized.

When one of the combining atoms is hydrogen the molecules form non-metallic hydrides, the total number of electrons in their outer shell can be eight or fewer. These hydrides have been termed by Grimm\* as pseudo-atoms, with chemical properties similar to the atoms having the same number of electrons in the outer shells, as can be seen from the following Table II.

Band spectra of these hydrides show that round each hydrogen nucleus two electrons move in a closed orbit with zero impulse moment.

\* Geiger and Scheel, *Handbuch der Physik*, vol. xxiv. Grimm, *Atombau u. Chemie*, p. 512.

TABLE II.

Hydrides.	No. of Outer Electrons.	Corresponding Atoms.
OH, NH <sub>2</sub>	7	F
FH, OH <sub>2</sub> , NH <sub>3</sub> } CH <sub>4</sub>	8	Ne

*Coordination Compounds.*

The second class of molecules with which we have to deal are the so-called coordination compounds of Werner\*. A typical example is  $\text{Pt}(\text{NH}_3)_6 \cdot \text{Cl}_4$ . Here the Pt atom is capable of holding, not only the four Cl atoms by its electrovalency, but it can also further combine with six of such apparently stable molecules like  $\text{NH}_3$ . In solution all the four Cl atoms are found to be ionized, while the six ammonia molecules are found to be attached to the central atom by non-ionizable bonds. The characteristic properties of such complexes have been summarized by Sidgwick as follows :—

(1) Their structures appeared to be quite independent of the rules of valency, according to which the numerical value of the valency of an atom element was primarily determined by the group in the periodic table to which it belonged. In these compounds the structure was determined rather by the tendency of four or six atoms or groups to arrange themselves round a central atom.

(2) In them a univalent atom or group of atoms, such as Cl or NO, could be replaced by apparently saturated molecules like  $\text{H}_2\text{O}$  or  $\text{NH}_3$ , without affecting the stability of the complex.

(3) Such replacements are always accompanied by a change in the ionization of the molecule. Thus, taking the above complex compound  $\text{Pt}(\text{NH}_3)_6\text{Cl}_4$ , we find that the  $\text{NH}_3$  molecules can be replaced one by one, until  $\text{Pt}(\text{NH}_3)_2\text{Cl}_4$  is

\* I am indebted for the following account of Werner's theory of coordination compounds and Dr. Sidgwick's explanation of the origin of coordination links to the very interesting and suggestive address delivered by Dr. Sidgwick as President of the Chemistry Section of the B.A. Meeting, held at Leeds in September 1927. See 'The Advancement of Science,' 1927.

reached, which is not ionized at all. Here every molecule of  $\text{NH}_3$  in the complex group  $\text{Pt}(\text{NH}_3)_6^{++++}$  is replaced by a Cl atom with a consequent diminution of its positive charge. If, now, more  $\text{NH}_3$  are replaced ionization occurs again, but the complex has received a negative charge, and we finally have the double salt  $\text{K}_4\text{PtCl}_6$ .

Werner proposed to explain these phenomena by assuming that round the central atom of the complex there is a tendency for groups of atoms or molecules to attach themselves in definite numbers (usually six, sometimes four or eight). These groups occupy the first coordination sphere of combination of the central atom, and together with the latter form a coordination complex; the complex molecule might also contain other atoms or groups occupying a second sphere, which are less firmly attached, *e. g.*, in the above-mentioned compound, the  $\text{NH}_3$  molecules are attached to the first sphere of platinum and satisfy the coordination number six, while the four Cl atoms are attached to the second sphere. Experimentally the groups attached to the second sphere were distinguishable by the fact that they were ionized by water, while those forming part of the coordination complex were not. Recent X-ray analysis of the crystalline structures of some of these coordination compounds of platinum have confirmed Werner's theory of their structure\*.

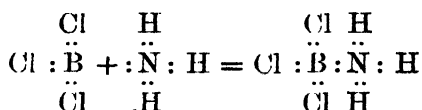
Werner himself has not given any picture of the nature of the forces which held the groups of atoms to the first coordination sphere. Kossel, who had successfully explained the formation of polar compounds by electrical forces, tried to apply the same ideas to explain the formation of complex molecules. But his views have not been generally accepted and we will not therefore go into the details of his theory.

Recently Sidgwick† has given a new interpretation of the nature of the bonds which hold atoms or atomic groups to the first coordination sphere of the central atom. According to modern electrical theories only two kinds of bonds are possible, *viz.*, electrovalent and the covalent, the one due to the transference and the other due to the sharing of electrons between two atoms—the former is ionizable, the latter is not. Sidgwick supposes that the coordination bonds being non-ionizable belong to the latter type. But they must arise in a way different from the ordinary covalent bonds, since their number is not related to the periodic group of the central atom, and they can combine with atoms

\* See Wycoff, 'The Structure of Crystals.'

† *Loc. cit.*

(like N in  $\text{NH}_3$  or O in  $\text{OH}_2$ ) which have already completed a stable number of electrons. In the normal covalency it is assumed that each of the two atoms contributed an electron to the link. Sidgwick extends the idea by supposing that both the electrons may be provided by one of the atoms. According to him the conditions for the formation of a coordination link are that we should have : (i.) one atom which has a pair of valency electrons to offer ; and (ii.) another which has room for one or more pair of electrons in its valency group. He calls the former atom which lend a pair of electrons the donor and the latter atom the acceptor. As an example of such formation he considers the combination of  $\text{NH}_3$  with  $\text{BCl}_3$ . In the former the N atom, which has five electrons in its valency group, of which three are shared with the three H atoms, leaving a pair of electrons to share, is the donor; in the latter the B atom which has all its valency electrons shared with the three Cl atoms, and has two vacant places in its valency group, is the acceptor. Their combination is represented as follows :



In this compound the atoms B and N assume a maximum covalency or coordination number of four, and round each an octet valency shell is completed.

Sidgwick extends this reasoning to the case of a regular coordination compound like  $[\text{Cr}(\text{NH}_3)_6]\text{Cl}_3$ . Here the Cr atom stripped of its three valency electrons forms the ion  $\text{Cr}^{+++}$  with a stable core of 21 electrons (of which three are in the  $\text{M}_3$  shell). It has no valency group left and the core is stable, as proved by the stability of the chromic salts. This ion can form a series of coordination links with  $\text{NH}_3$  molecules, by sharing the lone pair of electrons of the N atom. It is assumed that in the case of these types of compounds the stable size of the valency group is 12, as opposed to 8 in the previous case considered, and therefore 6 molecules of  $\text{NH}_3$  will be taken up. In case of one of the  $\text{NH}_3$  molecules being removed from the first coordination sphere, it takes away with it the two shared electrons which it contributed ; the Cl atom which replaces it moves from the second to the first coordination sphere. It can only supply one electron to the link, the other has to be supplied by the central atom. Thus the electrovalency of the latter is reduced by one, giving instead of  $[\text{Cr}(\text{NH}_3)_6]^{+++}$ , the ion

$[\text{Cr}(\text{NH}_3)_5\text{Cl}]^{++}$ , or the salt  $[\text{Cr}(\text{NH}_3)_5]\text{Cl}_2$ . The same change will occur for every replacement of a whole molecule in the complex by a univalent radicle. Thus the peculiar change of electrovalency noted by Werner in this class of compounds is explained. The chief assumption in the above theory is of the existence of a stripped atom with a stable core round which a *new valency shell* of 12 electrons can be formed by six stable molecules sharing pairs of electrons with it. In case one of the latter is replaced by a univalent radicle, one of the shared electrons is supplied by the central atom.

Besides  $\text{Cr}^{+++}$  other ions of elements belonging to the first transition group like  $\text{Fe}^{++}\text{Fe}^{+++}\text{Co}^{+++}\text{Ni}^{++}$ , etc., form stable coordination compounds. In all of them the  $M_3$  shell is incomplete, and the interesting question arises whether the 12 electrons which, according to Sidgwick, form a new valency group, lie entirely outside this  $M_3$  shell or some of them occupy vacant places in it. As these ions are paramagnetic and their moments depend upon the number of electrons in their  $M_3$  shell, it will be seen later that some definite information can be obtained by considering the magnetic moments of this class of coordination compounds. Further, in this class of compounds some of the groups of atoms or molecules which enter into coordination bond with the central atom are the following:  $\text{Cl}$ ,  $\text{OH}$ ,  $\text{OH}_2$ ,  $\text{NH}_3$ ,  $\text{CN}$ ,  $\text{CO}$ ,  $\text{NO}$ ,  $\text{O}_2$ , and  $\text{N}_2\text{H}_4$ —they represent types of molecules whose structures we have discussed in the first portion of this paper, in light of evidence obtained from band spectra. It will be seen from evidence presented later that  $\text{Cl}$ ,  $\text{OH}$ , and  $\text{CN}$  contribute only one electron to a coordination link,  $\text{OH}_2$ ,  $\text{NH}_3$ , and  $\text{O}_2$  contribute two,  $\text{NO}$  contributes one or three, and  $\text{N}_2\text{H}_4$  contributes four. We shall see later what relation there exists between the numbers of electrons contributed by these molecules, and their structures which have been suggested by the theories of Mulliken and Birge.

We will now proceed to test the above theories of Mulliken and Birge on the structure of diatomic molecules, and of Sidgwick on the nature of coordination links, by considering the magnetic properties of coordination compounds in which the central atom belongs to the first transition group of elements. It will be necessary here to interpose a short account of a theory of paramagnetism recently proposed by the writer\*, to account for the behaviour of atoms and ions of this group of elements.

\* *Zeit. f. Phys.* xliii. p. 864 (1927).

Hund\* has given a method of calculating the magnetic moments of atoms and ions from a knowledge of the number of electrons contained in any incomplete shell in the latter, and their quantum numbers. Every electron moving in a closed orbit is characterized by four quantum numbers,  $n$ ,  $l$ ,  $m_l$ , and  $m_s$ . For electrons belonging to the same shell, the values of  $n$  and  $l$  are the same, while the  $m_l$  and  $m_s$  are different. Here  $-l \leq m_l \leq l$  represents the orbital moment of an electron, and  $-\frac{1}{2} \leq m_s \leq \frac{1}{2}$  represents its spin moment. If there are  $z$  electrons in any incomplete shell, we have to take the sum of the orbital and spin moments separately, and thus get two numbers  $s = \sum_z m_s$  and  $\bar{l} = \sum_z m_l$ . The inner quantum number  $j$  is the vectorial sum of these two resultants, where  $|l - s| \leq j \leq l + s$ . The largest number of electrons which can occupy any shell is  $2(2l + 1)$ , and when  $z \leq 2l + 1$ , the value of  $j$  corresponding to the ground term is equal to  $|l - \bar{s}|$ , and for  $z \geq 2l + 1$  the corresponding value of  $j$  is  $l + \bar{s}$ .

The magnetic moment  $\mu$  of an ion with  $z$  electrons is given by  $\mu = jg$ , where

$$g = 1 + \frac{1}{2} \frac{j(j+1) + s(s+1) - \bar{l}(\bar{l}+1)}{j(j+1)}$$

is Lande's anomalous Zeeman effect factor. On going through the calculation it is found that if the magnetic moment of the ion is expressed in terms of Weiss's magnetons  $n_W$ , then

$$n_W = 4.97g \sqrt{j(j+1)}. \quad (1)$$

As has been shown in my paper†, that though Hund's formula gives a very good representation of the magnetic moments of the tri- and tetra-valent ions of the rare earth groups of elements, it fails entirely to account for the ions of the iron group. It has been shown there that a much better agreement with the experimentally determined values can be obtained, if in Hund's formula we put  $\bar{l} = 0$ , which interpreted physically means that only the spin moments of the electrons contribute to the magnetic moment of the ion. On making this substitution we get  $j = s$  and  $g = 2$ . The value of  $n_W$  now comes out to be

\* *Loc. cit.* xxxiii. p. 361 (1925).

† *Loc. cit.*



$$*n_w = 4.97 \sqrt{z(z+2)} \text{ for } z \leq 2l+1 \quad (2)$$

$$\text{and } = 4.97 \sqrt{z'(z'+2)} \text{ for } z \geq 2l+1 \text{ where } z' = 2(2l+1) - z. \quad (3)$$

The physical interpretation of the last formula is as follows: the maximum number of electrons which can occupy a shell with the azimuthal quantum number  $l$  is  $2(2l+1)$ . Of these the first  $2l+1$  electrons are free to align themselves in an external magnetic field. When the number of electrons  $z$  exceeds this value, then only  $z' = 2(2l+1) - z$  of them are free to align themselves, while the rest equal to  $z - z' = 2(l+1)$ , mutually neutralize one another in pairs and therefore are not influenced by any external field.

TABLE III.

$z$ .	$n_w$ (calc.)	$n_w$ (obs.)	
		Simple salt.	4-fold coord. comp.
1.....	8.6	V <sup>IV</sup> 8-9.1	
2.....	14.1	V <sup>+++</sup> 12.6 <sup>2</sup>	
3.....	19.2	Cr <sup>+++</sup> 18.3	
4.....	24.4	Cr <sup>++</sup> 24	
		Mn <sup>+++</sup> 25	
5.....	29.4	Mn <sup>++</sup> 29	
		Fe <sup>+++</sup> 29	
6.....	24.4	Fe <sup>++</sup> 26-27	24.1
7.....	19.2	Co <sup>++</sup> 25	21.3
8.....	14.1	Ni <sup>++</sup> 16-17	14.8
9.....	8.6	Cu <sup>++</sup> 9.1	

<sup>1</sup> Perrakis, *Compt. Rend.* clxxxv. p. 110 (1927).<sup>2</sup> Bose and Bhar, to be published shortly.

In Table III. are given the calculated and experimentally determined values of  $n_w$  corresponding to the different number of electrons  $z$  in the  $M_s$  shell of the ions belonging

\* If the magnetic moments are expressed in terms of Bohr's magnetons  $\mu_B$ , then

$$n_B = z \text{ for } z \leq 2l+1$$

$$= 2(2l+1) - z \text{ for } z \geq 2l+1.$$

to the elements of the first transition group. The theoretically calculated values of  $n_w$  are obtained by means of equations (2 & 3) proposed by me. The experimentally determined values are mostly taken from Stoner's book. In the last column are given the values of  $n_w$  for the fourfold coordination compounds of these elements, and are taken from some recent measurements made by Messrs. P. Ray and H. G. Bhar. On looking through the table it will be found that there is fairly satisfactory agreement between the calculated and experimentally determined values of  $n_w$  for ions in which the number of electrons  $z$  in the  $M_3$  shell is less than or equal to  $2l+1$ , viz. (5). But for values of  $z$  greater than this, there is serious discrepancy between the two sets of values; there is considerably better agreement, however, between the calculated values of and those found for the fourfold coordination compounds of these ions.

In Table IV. I have given the number of magnetons contained in certain fourfold compounds of Fe, Co, Ni, and Cu, and compared them with the values to be theoretically expected from the number of electrons in the  $M_3$  shell of the central atom of the complex.

TABLE IV.

Compounds.	$n_w$ (obs.)	$n_w$ (calc.)
$[\text{Fe}(\text{N}_2\text{H}_4)_2]\text{Cl}_2$	24.1	24.4
$[\text{Co}(\text{N}_2\text{H}_4)_2]\text{SO}_3, \text{H}_2\text{O}$	21.3	19.1
$[\text{Co}(\text{N}_2\text{H}_4)_2](\text{CH}_3\text{COO})_2$	22.6	
$[\text{Co}(\text{N}_2\text{H}_4)_2]\text{Cl}_2$	24.4	
$[\text{Co}(\text{O}_2\text{H}_5\text{N})_4](\text{SCN})_2$	24.0	
$[\text{Ni}(\text{N}_2\text{H}_4)_2]\text{SO}_3$	14.96	14.1
$[\text{Ni}(\text{N}_2\text{H}_4)_2](\text{NO}_2)_2$	14.76	
$[\text{Ni}(\text{NH}_3)_4]\text{SO}_4^1$	13.00	
$[\text{Cu}(\text{NH}_3)_4](\text{NO}_3)_2^1$	9.00	8.6

Rosenbohm *loc. cit.*

All these compounds with the exception of the last two have been prepared in the Science College by Messrs. P. Ray and H. G. Bhar, with whose permission their results are given here. It has been found that the Hydrazine compounds give values for the magnetic moments which approach most

closely the theoretically expected values. That the agreement is not always good is evident from the table. In these fourfold compounds, each  $N_2H_4$  group is assumed to contribute two pairs of coordination links to the central atom. Due to the presence of these four coordination links the magnetic moments of the central ion remain either unaltered or are brought up to values which we should expect when the spin moments of the electrons on the  $M_3$  shell are alone effective. I have taken this as a magnetic test of a satisfactory coordination linkage, viz., when the magnetic moment of the complex compound—corrected for diamagnetism—approaches very nearly the value to be expected from the number of electrons on the  $M_3$  shell of the central atom. We conclude therefore that in a fourfold coordination compound the central atom, stripped of its valency electrons, is attached to the atomic groups forming the complex by four pairs of coordination electrons. These electrons form an octet shell which lies outside the  $M_3$  shell of the central atom. The structure of these compounds is similar to that of the  $CH_4$  molecule.

#### *Sixfold Coordination Compound.*

We proceed next to consider the six-fold coordination compounds—which differ from the fourfold compounds in having two extra pairs of coordination bonds of four electrons. We shall show that these four extra electrons can under circumstances occupy, either the vacant places in the  $M_3$  shell of the central atom, or orbits which lie quite outside the latter.

In Table V. are given a number of sixfold compounds of Cr, Fe, Co, and Ni. In columns 2 and 3 are given the principal valency of the central atom and the corresponding

TABLE V.

Complex compound.	Simple ion.	$z_1$ .	$n_w$ (obs.)	$n_B$ (calc.)	$z_2$ .
$[Cr^{+++}(NH_3)_6](NO_3)_2$	$Cr^{+++}$	3	20.0	3(19.2)	7
$K_4[Fe^{++}(CN)_6]$	$Fe^{++}$	6	dia.	0	10
$K_3[Fe^{+++}(CN)_6]$	$Fe^{+++}$	5	10	1(8.6)	9
$[Co^{+++}(NH_3)_6]Cl_3$	$Co^{+++}$	6	dia.	0	10
$[Ni^{++}(N_2H_4)_3]Cl_2$	$Ni^{++}$	8	13.97	2(14.1)	8+4
$[Ni^{++}(N_2H_4)_3]SO_3, H_2O$	$Ni^{++}$	8	13.6	2(14.1)	8+4

number of  $z_1$  of electrons in their  $M_3$  shells. In column 4 the experimentally determined number of Weiss' magnetons contained in these compounds are given, the corresponding number of Bohr's magnetons  $n_B$  are to be found in column 5. Knowing the value of  $n_B$  the number of electrons actually present in the  $M_3$  shell of the central atom is calculated according to the formula

$$n_B = z' = 2(2l + 1) - z_2 = 10 - z_2, \quad . \quad . \quad . \quad (3)$$

their values are given in column 6. From the above we see that in every sixfold compound, with the exception of those of nickel, the number of electrons in the  $M_3$  shell of the coordinating atom is greater by four than that in the corresponding simple ion.  $Ni^{++}$  has already 8 electrons in its  $M_3$  shell and there is no room for four extra electrons which we assume to move in orbits lying entirely outside the  $M_3$  shell. This keeps the magnetic moment of the nickel salt unaltered by the addition of six coordination bonds. Another such example of a cobalt compound is given in Table VI. We therefore conclude that in a sixfold compound, four pairs of the electron links form an octet shell whose orbits lie entirely outside the  $M_3$  shell of the central atom; the four electrons of the remaining two links may occupy the  $M_3$  shell or not, according as there is room for all of them there or not. The results we have obtained confirm on the whole Sidgwick's theory of the formation of a fresh valency group by the coordination electrons, but give a more detailed picture of how they are distributed, viz., eight of them form an octet shell round the central ion and the remaining four try to fit themselves in the  $M_3$  shell of the latter, if there is room for all of them; otherwise they move in orbits outside the  $M_3$  shell and their resultant magnetic moment is null.

### *Structure of Diatomic Molecules.*

We now turn to the second part of our investigation, which is to find out what information we can get from a study of these coordination compounds, of the structure of diatomic and similar molecules.

A number of coordination compounds, in which the atomic groups  $NH_3$ ,  $N_2H_4$ ,  $OH$ ,  $OH_2$ ,  $CN$ ,  $CO$ , and  $O_2$  are attached to the primary coordination spheres, are given in Table VI. In column 2 are given the number of Bohr's magnetons contained in them. In column 3 are given the atomic groups whose contribution of coordination electron

are placed in the last column. Every one of the coordination compounds satisfies our magnetic test, viz., they have magnetic moments which are very nearly multiples of Bohr's anagnetons. Wherever possible only such compounds are

TABLE VI.

Coordination Comp.	$n_B$	Atomic group.	Contribution to coordination.
$[\text{Co}(\text{NH}_3)_6]\text{Cl}_3^1$	0	$\text{NH}_3$	2
$[\text{Co}(\text{NH}_3)_5\text{Cl}]\text{Cl}_2^1$	0	Cl	1
$[\text{Co}(\text{NH}_3)_5(\text{NO})]\text{Cl}_2^2$	0	NO	1
$[\text{Co}(\text{NH}_3)_5(\text{NO})(\text{NO}_3)_2]^2$	2	NO	3
$[\text{Co}(\text{NH}_3)_4(\text{OH})(\text{OH}_2)]\text{SO}_4^1$	0	$\text{OH}_2$	2
$[\text{Co}(\text{NH}_3)_5(\text{OH})(\text{NO}_3)_2]^1$	0	OH	1
$\left( \begin{array}{c} \text{Co}(\text{NH}_3)_5 \\   \\ \text{O}_3 \\   \\ \text{Co}(\text{NH}_3)_5 \end{array} \right) \text{SO}_4$	0	$\text{O}_2$	2
$[\text{Ni}(\text{NH}_3)_6]\text{Cl}_2^1$	2	$\text{NH}_3$	2
$[\text{Ni}(\text{N}_2\text{H}_4)_2]\text{Cl}_2$	2	$\text{N}_2\text{H}_4$	4
$\text{Fe}(\text{CO})_5^4$	0	CO	2
$[\text{Fe}(\text{CN})_6]\text{K}_4^5$	0	CN	1
$[\text{Fe}(\text{CN})_5(\text{NO})]\text{Na}_2^3$	0	NO	3

<sup>1</sup> Rosenbohm, *Zeit. f. phys. Chem.* xciii. p. 693 (1919).

<sup>2</sup> P. Ray & H. Bhar to be published shortly.

<sup>3</sup> Feytis, *C. R.* clii. p. 708 (1911).

<sup>4</sup> Oxeley, *Proc. Camb. Phil. Soc.* xvi. p. 102 (1911).

<sup>5</sup> Welo, 'Nature,' cxvi. p. 359 (1925).

selected for which  $n_B=0$ , i. e. they are diamagnetic. From the value of  $n_B$  it is at once possible to find out what is the number of electron links supplied by each of the atomic groups.

Starting with a hexamine compound of cobalt, we find that each  $\text{NH}_3$  molecule supplies two electrons to the central atom. In the next compound, a  $\text{NH}_3$  molecule has been replaced by a Cl atom without altering the magnetic moment of the compound; the electrovalency of the complex has been reduced by unity, from which we conclude that the Cl atom contributes only one electron to a coordination link, the other is supplied by the Co atom. In

the third compound the Cl atom inside the complex has been replaced by a NO molecule without in any way disturbing the complex. We thus conclude that here the NO molecule supplies only one electron to a coordination link. The fourth compound, though exactly similar to the third, contains two Bohr's magnetons. This behaviour can only be explained on the assumption that here the NO molecule supplies three electrons to the coordination links instead of one, as in the previous case. This can be explained as follows:—The central atom Co is divalent in this compound, and therefore contains 7 electrons in its  $M_3$  shell. The five  $NH_3$  molecules associated with it contribute 10 shared electrons and if the NO molecule only contributed one electron there would altogether be  $7+10+1=18$  electrons moving in the outer orbits of which 10 would be in the  $M_3$  shell and the other 8 would form into an octet shell. Such a distribution would make the complex diamagnetic, which it is not. On the other hand, if NO contributes three electrons, the total number of outer electrons becomes  $7+3+10=20$ , which can only be distributed in the following way:—8 electrons on the  $M_3$  shell, and the remaining 12 electrons in 6 pairs of orbits which lie outside the latter. With such a distribution the magnetic moment of the complex comes out to be  $10-\epsilon_2=10-8=2$ , as is found experimentally. This conclusion is supported by considering the nitroso-compound of iron which is placed last in the table. To make a compound like  $K_4[Fe(CN)_6]$  diamagnetic, it is necessary to assume that each CN group contributes one electron each to a coordination link, the other six are made up by the central atom contributing two, and the four K atoms contributing one each. On replacing a CN by a NO group inside the complex, it is found that the magnetic moment of the latter remains unchanged, while its electrovalency is reduced by two, which can only be accounted for by supposing that the NO molecule contributes three electrons to the coordination links. Thus we see that a NO molecule can contribute either one or three electrons to coordination links. The contributions to coordinate links made by the remaining atomic groups like OH,  $OH_2$ , CO,  $O_2$ , and  $N_2H_4$ , can be inferred without difficulty from the table.

The relation between the structure of these molecules and the number of coordination links they contribute is summarized in Table VII. In column 2 the total number of electrons in the outer shells of the combining atoms are shown distributed amongst the different quantum levels according to the structure of such molecules proposed by

Mulliken and Birge. In column 3 are given the distribution of the actual number of electrons which are available for the formation of coordination links; we obtain this number by subtracting from the number of electrons in the

TABLE VII.

Atomic groups.	No. of electrons in outer orbits.		No. of electrons available for sharing.				Actual contribution to coord. links.
	$n=2$ .	$n=3$ .	$n=2$ .		$n=3$ .		
			$l=0$ .	$l=1$ .	$l=0$ .	$l=1$ .	
Cl	7	—	2	5			1
OH	7	—	2	3			1
NH <sub>2</sub>	7	—	2	1			
N <sub>2</sub> H <sub>4</sub>	7+7	—	2+2	—			4
OH <sub>2</sub>	8	—	2	2			2
NH <sub>3</sub>	8	—	2	0			2
CN	8	1			1	—	1
CO	8	2			2	—	2
NO	8	3			2	1	3, 1
O <sub>2</sub>	8	4			2	2	2

valency shell of the molecule, those which have already taken part in a covalent bond, *e. g.*, in the case of NH<sub>3</sub>, the 3H atoms form covalent bonds with three of the five outer N electrons, so that only two of the latter are available for coordination links.

In the last column the actual contributions made by these atomic groups are given. Leaving for the present the N<sub>2</sub>H<sub>4</sub> group, we can divide the other atomic groups into the following classes :—(i.) Those in which the total number of outer electrons is less than 8, with them the tendency is to form covalent bonds with the central atom, so as to complete their own octet configurations; (ii.) those in which the outer electrons form an octet, but some of the electrons have entered into covalent bonds, they contribute a pair of electrons to the central atom, all of which come either from the shell  $l=1$  or  $l=0$ ; (iii.) those in which the number of outer electrons exceed eight; the surplus electrons are

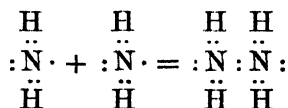
assumed to move in three quantum orbits with  $l=0$  and  $l=1$ . Some or all of these electrons can take part in co-ordination links, so as to leave the number of unshared electrons in the shell  $l=0$  either two or zero.

We infer that besides the octet shell, the two electrons in the shell  $l=0$  form a stable configuration similar to what occurs in atomic distributions. There is, however, this difference that the valency electrons of such molecules are not detachable, and they cannot therefore give rise to polar bonds. Coming back to the consideration of the atomic group  $N_2H_4$ , it can be regarded as due to the combination of two  $NH_2$  groups. The structure of the latter can be

$$\begin{array}{c} \text{H} \\ \vdots \\ :\ddot{\text{N}}\cdot \\ \vdots \\ \text{H} \end{array}$$

represented graphically as follows :

such groups will give rise to a new one



in which each of the N atoms has eight electrons in its valency shell of which six take part in covalent links. There are therefore  $2+2=4$  electrons in the  $N_2H_4$  molecule available for taking part in coordination links, and this is the actual number of electrons they supply to a coordinating atom.

We thus find that the model of diatomic and similar non-polar molecules inferred from the study of Band Spectra can satisfactorily account for the number of coordination links which these atomic groups can supply.

In this connexion it will not be out of place to consider the criticism of the Birge-Mulliken structure of diatomic molecules which has recently been made by Stoner in an interesting paper\* entitled "Magnetism and the Structure of Molecules." The principal point in Stoner's criticism is the failure of these models to account for the experimentally determined values of the magnetic moments of NO and  $O_2$ . The following Table VIII., taken from his paper, gives a comparison between the calculated and experimentally determined values of  $n_w$  for these molecules based on Hund's theory. In the last line I have given the values to be

\* Phil. Mag. iii. p. 351 (1927).



expected on the modification of Hund's theory which has been put forward by me.

TABLE VIII.

Molecule.		NO.		O <sub>2</sub> .				
<i>n<sub>w</sub></i> (obs.)		9.20		14.12				
Theoretical ground terms.		<sup>2</sup> P		<sup>3</sup> P		<sup>1</sup> D		<sup>1</sup> S
		<sup>2</sup> P <sub>1</sub>	<sup>2</sup> P <sub>2</sub>	<sup>3</sup> P <sub>0</sub>	<sup>3</sup> P <sub>1</sub>	<sup>3</sup> P <sub>2</sub>	<sup>1</sup> D <sub>2</sub>	<sup>1</sup> S <sub>0</sub>
<i>n<sub>w</sub></i> (calc.)	Hund	2.9	13.8	0	10.6	18.2	12.2	0
	Bose	8.6		14.2				

The assumption that only the spin moment of the electrons in the outer valency shell of these molecules leads to values for their magnetic moments which are in excellent agreement with the experimental values. This furnishes another proof of the validity of this assumption.

### *Discussion.*

It will be useful here to sum up the results we have obtained up till now. We started with the assumption that the paramagnetic moments of the compounds of the elements belonging to the first transition group are due only to the spin moments of the electrons present in their incomplete shells. On comparing the values of the magnetic moments calculated according to this assumption with those found experimentally, it was found that up to manganese the agreement was satisfactory, but the simple salts of the ferromagnetic elements gave values of magnetic moments considerably larger than the expected ones. This deviation seems to be associated with the addition of the sixth, seventh, and the eighth electrons to the M<sub>s</sub> shell of these atoms, where, according to Pauli's equivalence theorem, they begin to form neutral doublets with an equal number of electrons out of the first five already present on the shell. If it is supposed that the alignments of the newly added electrons to form neutral doublets is not perfect, then the deviations

noted can be accounted for. This surmise is strengthened by the discovery that certain fourfold coordination compounds of these elements have magnetic moments which are in good agreement with the theoretical values. According to the conception of Sidgwick, in a fourfold coordination compound, a new octet shell of valency electrons is formed round the core of the central atom, and this helps to stabilize the electron orbits on the outer core of the central atom. We are not in a position to say why all the fourfold coordination compounds of, say, cobalt, have not the theoretically expected magnetic moments. Further investigations on this point are being carried out.

In the case of the sixfold coordination compounds, according to Sidgwick, the size of the valency shell formed round the core of the central atom was increased to accommodate twelve instead of eight electrons. Magnetic evidence, however, points to the interpretation, that where there is room for all the four extra electrons in the  $M_3$  shell of the central atom, the octet shell is not disturbed but the extra electrons are accommodated in the  $M_3$  shell. Where there is no accommodation for all of the four in the  $M_3$  shell, these four move in orbits outside the latter. It is found, however, that in the latter case the compounds are not very stable.

In connexion with the coordination compounds, two further questions arise to which no satisfactory answer can be given at present. The first is what limits the number of coordination groups that can be associated with a central atom? Sidgwick seems to think with Main Smith that it is the quantum number of the outer electrons of an element is the determining factor, *e. g.*, the maximum covalency of hydrogen is 2, of the elements of the first period (Li to F) is 4, of the elements of the second short period (Na to Cl) and of the first long period (K to Br) is 6, and of the later elements is 8.

The other view is of Kossel who supposes that the number depends on the atomic volume and the charge on the central ion—these two determine the number of molecules which can cluster round the central atom.

This brings us to the second question, *viz.*, whenever a definite number of molecules cluster round the central core, is there a sharing of electrons between the latter and each of the former? It can be shown that in certain cases no such coordination links exist, *e. g.*, the compound  $\text{FeSO}_4 \cdot 7\text{H}_2\text{O}$ , has exactly the same magnetic moment as the anhydrous salt  $\text{FeSO}_4$ . The former, which can be written as  $[\text{Fe}(\text{H}_2\text{O})_6]\text{SO}_4 \cdot \text{H}_2\text{O}$ , was considered by Werner to be a

true coordination compound, and as such it ought to have been diamagnetic;  $[\text{Ni}(\text{NH}_3)_6]\text{Br}_2$  has been found by Rosenbohm to have 16 Weiss's magnetons, the same as that contained in the simple salts. According to our theory the magneton number ought to have been about 14, as is the case with a similar compound  $[\text{Ni}(\text{N}_2\text{H}_4)_3]\text{Cl}_2$ . Here it seems doubtful whether the  $\text{NH}_3$  molecules are in coordination link with the central atom. We can think of other kinds of forces which can hold the  $\text{NH}_3$  molecules to the central atom, viz., the latter stripped of its valency electrons is left with a positive charge. Molecules with large dipole moments like  $\text{H}_2\text{O}$ ,  $\text{NH}_3$  can be attracted to form clusters round such a charged ion, and the maximum number that can be attached depends upon the atomic volume of the latter. Blitz\* has calculated the heat of reaction which is given out by the addition of a varying number of  $\text{NH}_3$  molecules in the space lattice of a simple salt. The original salt lattice is expanded to accommodate  $n\text{NH}_3$  molecules, and suppose  $E$  is the work done. If  $A'$  is the energy set free by the association of  $n$  molecules of  $\text{NH}_3$  round each salt molecule, then  $\phi_n = A' - E$ , where  $\phi_n$  is the heat of reaction due to this process. It is found, for example, that the value of  $\frac{A'}{n}$  for the association of  $\text{NH}_3$  molecules to a

simple alkali-halogen compound with univalent cation and 8 outer electrons is 14 calories per gm. mol.; when the cation has a double charge it is 28 calories. On the other hand, for the small  $\text{Li}^+$  ion with two outer electrons, the value is 21 calories. These numbers give an approximate idea of the forces between dipole molecules and charged ions. It may be that forces of this type attract the atomic groups to cluster round the core of the coordinating atom, and later on, in certain cases, a further linkage is introduced by the sharing of electrons between the atomic groups and the core.

### *Summary.*

1. In this paper the recent theories of the structure of diatomic molecules proposed by Birge and Mulliken, and of the nature of coordination links in Werner's coordination compounds, proposed by Sidgwick, have been tested by the investigation of the magnetic properties of the coordination compounds of the elements belonging to the first transition group.

\* Blitz, *Zeit. f. anorg. Chemie*, vol. cxxx. p. 93 (1923).

2. Sidgwick has proposed to account for the linkage of the six atomic groups to the central atom in a sixfold compound by supposing that in general each of the atomic groups contributes two electron orbits to the latter; all of them taken together form a valency group of twelve electrons round the core of the central atom, which has been stripped of its own valency electrons. From magnetic evidences it is concluded that if there are vacancies in the  $M_3$  shell of the central atom for four electrons, then four out of the twelve shared electrons occupy the  $M_3$  shell, while the remaining eight form an octet shell round the core. When the  $M_3$  shell of the core cannot accommodate all of the four electrons, they move in orbits outside the latter. In the case of fourfold compounds the valency shell of eight electrons contributed by the four atomic groups form an octet shell outside the core of the central atom.

The atomic groups which are usually found in coordination compounds include, amongst others, the following:  $OH$ ,  $OH_2$ ,  $NH_3$ ,  $CN$ ,  $CO$ ,  $NO$ ,  $O_2$ , and  $N_2H_4$ . Birge and Mulliken have, from Band Spectra evidence, given a new theory of the structure of diatomic non-polar molecules like those included in the above group. It is shown that the number of coordination bonds contributed by these groups can be satisfactorily accounted for on their structures proposed by the new theory.

London,  
February 1928.

---

*CVII. On the Positions of X-Ray Spectra as formed by a Diffraction Grating.* By ALFRED W. PORTER, D.Sc., F.R.S., F.Inst.P., Professor of Physics in the University of London\*.

**I**N the calculation of the positions of X-ray spectra as formed by a diffraction grating, it is customary to consider them as Fraunhofer spectra, such as are obtained with gratings in ordinary spectroscopy. In such cases the incident light is a parallel bundle, and so also is the diffracted bundle which is afterwards brought to a point (or line) by a lens. But when X-rays are used, there is no means of producing this parallelism; the incident beam is always divergent, and the diffracted beam that reaches any one

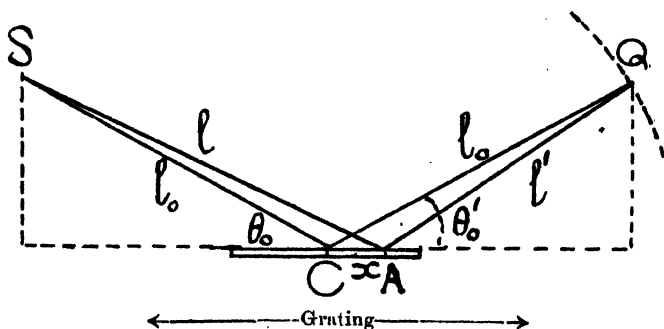
\* Communicated by the Author.

point is convergent. For ordinary measurements this is of small importance; but when we consider the extreme accuracy with which X-ray spectral measurements are now being made, the question arises as to what will be the consequence of the lack of parallelism.

The object of this paper is to find a first approximation to the correction which the usual formula needs.

Let S be the source and Q the point on the screen on which the spectra will be formed. For simplicity (and to fit in with common practice) let  $SC=CQ$ , where C is the central point of the grating. The ray SAQ is a neighbouring ray reaching the same point. The phases of the effects

Fig. 1.



at Q can be obtained by calculating the sum of the lengths  $SA=l$  and  $AQ=l'$ . Putting  $CA=x$ , we have

$$l = \sqrt{l_0^2 + x^2 + 2l_0x \cos \theta_0}$$

$$\text{and} \quad l' = \sqrt{l_0'^2 + x^2 - 2l_0'x \cos \theta_0'}.$$

The sum  $l+l'$  can be written approximately equal to

$$a_0 + b_0x + c_0x^2 + g_0x^3,$$

where

$$a_0 = 2l_0,$$

$$b_0 = \cos \theta_0 - \cos \theta_0',$$

$$c_0 = \frac{1}{2l_0} (\sin^2 \theta_0 + \sin^2 \theta_0'),$$

$$\text{and} \quad g_0 = -\frac{b_0}{2l_0^2} [1 - \cos^2 \theta_0 - \cos \theta_0 \cos \theta_0' - \cos^2 \theta_0'].$$

The range of retardations for the complete grating of length  $X$  is

$$X(\cos \theta_0 - \cos \theta'_0) \left[ 1 - \frac{X^2}{8l_0^2} (1 - \cos^2 \theta_0 - \cos \theta_0 \cos \theta'_0 - \cos^2 \theta'_0) \right];$$

the range of phases is obtained by multiplying this by  $2\pi/\lambda$ ; the corresponding coefficients we will represent by  $a$ ,  $b$ ,  $c$ , and  $g$ .

Now in the Fraunhofer case the maximum of order  $P$  occurs when

$$\frac{2\pi}{\lambda} (\cos \theta_0 - \cos \theta'_0) = PN \cdot 2\pi,$$

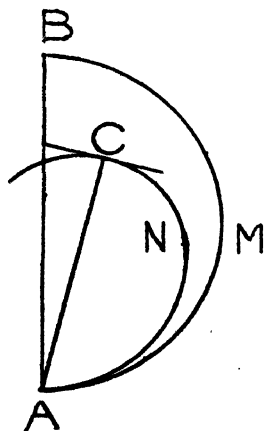
where  $N$  is the total number of "lines" on the grating; or, if  $r$  is the grating-interval, when

$$r(\cos \theta_0 - \cos \theta'_0) = P\lambda.$$

We can get some idea of the correction required by calculating also the factor in brackets. If the incidence is nearly grazing, we can write each of the cosines in the *small* term equal to unity, and consequently the range of phases becomes

$$X(\cos \theta_0 - \cos \theta'_0) \left[ 1 + \frac{X^2}{4l_0^2} \right].$$

Fig. 2.



If we could still take a range of phases  $2\pi NP$  as determining a maximum, the correcting factor to the wave-length as usually calculated would be  $1 + \frac{X^2}{4l_0^2}$ .

Although this must give the right order, it is in excess of the true value. Reference to a vibration diagram, in which AMB is the curve for the Fraunhofer case, with its maximum at B, shows that when the curve, such as ANC, is of increasing curvature from A to C, the maximum chord does not correspond to a phase difference of  $\pi$ , but is at a point C such that the tangent thereat is at right angles to the radius vector AC.

We will now obtain a more accurate value.

Taking the middle point C of the grating as origin, the two halves of the grating lie symmetrically on the two sides if the centre of one opening coincides with C. With the exception of this one opening (which need not concern us when the number  $n$  on each side is large), the openings can be divided into pairs, so that the vibration due to the  $\kappa$ th pair is

$$\begin{aligned} & \cos(pt + a + \kappa br + \kappa^2 cr^2 + \kappa^3 gr^3) \\ & + \cos(pt + a - \kappa br + \kappa^2 cr^2 - \kappa^3 gr^3) \\ & = 2 \cos(\kappa br + \kappa^3 gr^3) \cos(pt + a + \kappa^2 cr^2). \end{aligned}$$

This is very nearly (because  $\kappa^2 cr^2$  is very small compared with  $a$ ) a simple vibration of amplitude

$$2 \cos(\kappa br + \kappa^3 gr^3),$$

or approximately

$$2 \cos \kappa br_1 - 2 \kappa^3 gr^3 \sin \kappa br_1.$$

Summing for all the  $n$  pairs, the intensity is

$$4 \left[ \sum_{\kappa=1}^{\kappa=n} \cos \kappa br - \sum_{\kappa=1}^{\kappa=n} \kappa^3 gr^3 \sin \kappa br \right]^2.$$

The maximum occurs when the differential coefficient of this with regard to  $br$  is zero, or

$$\sum \kappa \sin \kappa br + gr^3 \sum \kappa^4 \cos \kappa br = 0.$$

We are only concerned with the value of  $br$  in the immediate neighbourhood of a principal maximum for which  $br = 2\pi P$ , where  $P$  is the order of the maximum. Put, therefore,

$$br = 2\pi P + \alpha;$$

then the condition becomes

$$\sum \kappa \sin \kappa \alpha + gr^3 \sum \kappa^4 \cos \kappa \alpha = 0,$$

or, because  $\alpha$  is small,

$$\sum \kappa^3 \alpha + gr^3 \sum \kappa^4 = 0,$$

i. e.,

$$\frac{n(n+1)(2n+1)}{6}\alpha + gr^3 \frac{n(n+1)(2n+1)(3n^2+3n-1)}{30} = 0;$$

or, when  $n$  is large,

$$\alpha = -\frac{3gr^3}{5}n^2 = -\frac{3}{20}gr^3N^2,$$

where  $N$  is the total number of elements.

Now for nearly grazing incidence

$$g = \frac{b}{l_0^2},$$

and for a maximum

$$\begin{aligned} br &= 2\pi P - \frac{3}{20}gr^3N^2 \\ &= 2\pi P - \frac{3}{20}br \cdot \frac{N^2r^2}{l_0^2}, \end{aligned}$$

and we obtain

$$br \left[ 1 + \frac{3}{20} \frac{X^2}{l_0^2} \right] = 2\pi P$$

or

$$r[\cos \theta_0 - \cos \theta_0'] \left[ 1 + \frac{3}{20} \frac{X^2}{l_0^2} \right] = P\lambda.$$

Assuming nearly grazing incidence, the wave-lengths, calculated in the usual way, require therefore to be multiplied by the factor  $1 + \frac{3}{20} \frac{X^2}{l_0^2}$  in order that their true values may be obtained. The following table shows the values of this correcting factor in various cases:—

$\begin{array}{c} X. \\ \diagup \\ l_0. \end{array}$	5 cm.	10 cm.	20 cm.
1 mm.	1·00006	1·000015	1·000004
5 mm.	1·0015	1·000375	1·000094
1 cm.	1·006	1·0015	1·000375



CVIII. *The Electronic Theory of Valency* \*.—Part V. *The Molecular Structure of Strong and Weak Electrolytes: (a) Complete Ionization.* By T. MARTIN LOWRY †.

1. *The Theory of Complete Ionization.*

THE theory of complete ionization had its origin in a physico-chemical study of the properties of solutions; but it was very soon adopted by physicists as an explanation of the high symmetry of the crystal-structures revealed by the X-ray analysis of metallic salts, since this could not be accounted for on the traditional theory that the ions of the salt were united into molecules. The new theory has had a large measure of success in both fields of study, since, on the one hand, the conductivity of solutions of ordinary metallic salts has been calculated for the first time by means of a rationally deduced formula, which is valid up to a concentration of perhaps  $N/100$ ; on the other hand, many of the physical properties of crystals, such as their linear dimensions and angles, heat of formation, elasticity, refractive index, and infra-red absorption, have been calculated successfully on the assumption that the crystals are aggregates of ions of varying degrees of "hardness," which are drawn together by the electrostatic attraction between their opposite charges, but are also repelled from one another with a force varying inversely as (say) the 6th to the 35th power of the distance. On the other hand, the theory of complete ionization fails to cover the behaviour of those weak electrolytes which obey Ostwald's dilution law, just as completely as the latter law failed to cover the behaviour of highly-dissociated metallic salts. Again, although many of the properties of solid ionic aggregates, such as rock salt or calcite, have been predicted successfully from fundamental data, all attempts to predict the dimensions and behaviour of the carbonate ion itself have failed, since this does not behave as a mere aggregate of carbon and oxygen ions. The object of the present paper is therefore to determine the boundaries of the region within which the theory of complete ionization is valid, to find out the factors which make it inoperative in so many cases, and in particular to study the chemical significance of the classification of electrolytes as "strong" and "weak." The applications of similar

\* Parts I, II, and III. *Phil. Mag.* xlv. p. 1105 (1928), xlv. p. 946 (1918); Part IV. *Phil. Mag.* xlvii. p. 1021 (1924).

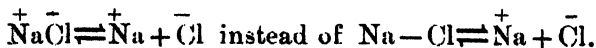
† Communicated by the Faraday Society.

considerations to the study of crystal-structure will form the subject of a subsequent communication.

In both cases the principal argument put forward will be that, although the ions of a salt are generally prevented from neutralising their opposite electric charges by factors which find their simplest expression in the "octet" rule, there are many cases in which this inhibition does not operate, with the result that the ions can be converted into real molecules, as distinguished from mere aggregates of ions, by the neutralisation of their opposite charges with formation of a chemical "bond." These two groups of compounds correspond broadly with the "strong" and "weak" electrolytes; but the two methods of classification cannot be expected to lead to identical results. Thus, on the one hand, a salt which consists entirely of ionic aggregates may be placed under conditions which are so unfavourable to the independent migration of the ions as to bring it within the group of "weak electrolytes"; and, on the other hand, the bond which holds the positive and negative radicles together in a covalent molecule may be so weak as to interfere but little with the disruption of the molecule into ions, with the result that a compound of the second type may exhibit the behaviour of a strong electrolyte.

## 2. *Electrolytic Dissociation of Strong Electrolytes.*

A "strong electrolyte" means, in the first instance, nothing more than a substance which has a high electrolytic conductivity, *e. g.*, in aqueous solutions. In the language of Arrhenius's theory, such a substance was said to have a large "coefficient of ionization"; but this term has no longer any real meaning when applied to a salt which is 100 per cent. ionized even in the solid state. We can, however, still interpret the decrease of equivalent conductivity in strong solutions as being due, at least in part, to the formation of electrically-neutral doublets, which play the part of molecules, just as in the vapour of the salt. We need, therefore, only modify Arrhenius's equation to the extent of writing



The "degree of dissociation" of the doublets then has still a perfectly definite physical meaning, even if it cannot be calculated directly, as was formerly supposed, from the simple equation  $c = \Lambda/\Lambda_{\infty}$ . Moreover, since the readiness with which neutral doublets of oppositely charged ions are

formed by the mutual attraction of their electrostatic charges must vary with the linear dimensions of the ion, with the dielectric constant and other properties of the solvent, and with the extent to which the naked ion becomes hydrated or solvated in solution, as well as with the temperature at which the association and dissociation of the ions takes place, there is ample scope, even in the theory of complete ionization, for variations in the "degree of dissociation" of different salts, either in solution or in the fused state.

(a) *Ionization of Strong Electrolytes in Solution.*—Is it possible, then, for a completely ionized salt to behave as a "weak electrolyte" and exhibit a low "coefficient of ionization" or, more accurately, a low "degree of dissociation" of the pre-existing ions? The answer is undoubtedly "Yes," provided always that the conditions under which this effect is theoretically possible can be realized in practice.

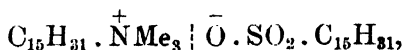
Of these conditions the most obvious has reference to the nature of the solvent. Thus Hartley\* has shown that, in the case of N/500 KI, the ratio  $\Lambda/\Lambda_\infty$  falls from 0.98 in water to 0.90 in methyl alcohol, 0.81 in ethyl alcohol and 0.77 in acetone, although his solutions were all so dilute that  $1-\alpha$  was still proportional to the square root of the concentration as required by the theory of complete ionization. If, then, we accept the general validity of Walden's rule, that *a dissolved salt gives a definite value for  $\Lambda/\Lambda_\infty$  at a dilution which is inversely proportional to the cube of the dielectric constant of the solvent*, it follows that we should be able to repress the dissociation of the ions to any desired extent by dissolving the salt in a medium of low dielectric-constant.

At this point, however, a fresh difficulty presents itself, since the majority of metallic salts are insoluble except in media which possess marked ionizing properties; in particular, most of these compounds are completely insoluble in media, such as benzene or cyclohexane, where the dielectric constant is low enough to compel the salt to behave as a weak electrolyte. Walden has, indeed, put forward a definite rule, according to which *the coefficient of ionization of a salt is approximately constant for saturated solutions in any anhydrous solvent*. Thus in the case of tetraethylammonium iodide, we should not expect to find any solution in which the "degree of dissociation" is much below 50 per cent., since saturated solutions in a dozen different solvents (but excluding water

\* 'Nature,' cxix. p. 323 (Feb. 26, 1927).

and all other solvents in which the solubility is more than 1 gram-molecule in 2500 c.c.) gave values for  $\alpha = \Lambda/\Lambda_\infty$  which were almost constant at 0.48. We may therefore conclude that only in exceptional cases will it be possible to prepare a solution of a strong electrolyte in which the degree of dissociation is so small as to be negligible, and that this effect, when it occurs, will probably be due to some special chemical relationship between the solvent and the solute, which enables the solute to dissolve, but without any marked disruption of the ions.

Such an effect might be looked for in Reychler's trimethyl-cetylammonium cetylsulphonate



in which the single polar valency in the middle of so long a chain of atoms might very well remain almost undetected. Thus, whilst the 30 carbon atoms in the two hydrocarbon chains should suffice to make the compound soluble in hydrocarbon solvents, these solvents need not necessarily be so drastic in their action as to tear the two ions apart. Fortunately, however, this phenomenon can be observed in much simpler compounds. Thus, sodium oleate at a dilution of 100 litres gives the following equivalent conductivities in water and in methyl, ethyl, and amyl alcohols:—

$\text{H}_2\text{O}$	$\text{CH}_3\text{OH}$	$\text{C}_2\text{H}_5\cdot\text{OH}$	$\text{C}_5\text{H}_{11}\cdot\text{OH}$
$\epsilon = 81.7$	$\epsilon = 35.4$	25.4	15.9
$\Lambda_{100}^{18} = 30.09$	$\Lambda_{100}^{25} = 0.0052$	0.0018	0.0002

When sodium oleate is dissolved in *water*, the “hydrophilous” sodium ion compels the “anhydrophilous” oleate ion to follow it into aqueous solution, where it functions as the “ionic micelle” of a “colloidal electrolyte.” In the alcohols, on the other hand, and especially in amyl alcohol, the oleate radicle appears to drag a reluctant sodium ion into solution in an *organic solvent*, in which the salt behaves for all practical purposes as a *non-electrolyte*.

Walden, however, has gone a great deal further in studying the abnormal conductivities of salts in hydrocarbons and in their halogen derivatives. Thus, by a suitable choice of radicles, in salts such as  $\overset{+}{\text{N}}(\text{C}_5\text{H}_{11})_4\bar{\text{I}}$ , he has been able to obtain solutions of reasonable strength in a dozen of the least promising solvents, including benzene and toluene, methyl iodide, methylene and ethylene chlorides, chloroform and carbon tetrachloride. In every case, the salt-solution

showed an appreciable conductivity, the values for  $\Lambda_{20}^{25}$  varying from 0.0140 in carbon tetrachloride to 1.57 in chloroform and 9.51 in methylene chloride; but the equivalent conductivities were abnormal in that they generally fell to a minimum value at some intermediate dilution, from which there was not only the usual increase on dilution, but an equally striking increase on passing to more concentrated solutions. The "degree of dissociation" was obviously small and in some cases almost negligible, so that the "salt" was behaving quite clearly as a "weak electrolyte" in all these solvents. Neutralization of the ionic charges, however, would appear to be even more difficult than usual, in view of the fact that the positively-charged nitrogen of the tetra-amyllumonium ion is separated from the negatively-charged halogen ion by a permanent hydrocarbon "atmosphere" containing 20 atoms of carbon. The small conductivity of these solutions then suggests that the salt must be present predominantly in the form of neutral ionic doublets, rather than as freely dissociated ions. The formation of these doublets also appears to afford a sufficient explanation of the different absorption-coefficients which Hantzsch observed\* when quaternary ammonium salts of this type were dissolved in organic solvents instead of in water, since we need not suppose that the absorption-coefficients of the ionic doublet must necessarily be identical with those of the aqueous ions.

Attention may also be directed to the fact that, whilst solutions of phosphorus pentabromide and antimony pentabromide in liquid bromine exhibit a marked conductivity†, the equivalent conductivity decreasing with dilution just as in the case of the "abnormal" conductivities cited above, potassium bromide and tetramethylammonium iodide, as well as tribromacetic acid, behave as insulators in this solvent (Walden).

(b) *Ionization of Fused Salts.*—Since considerations of limited solubility do not apply in the case of fused salts, it is of special interest to inquire what is known in reference to the magnitude of the "degree of dissociation" under these conditions. It has been generally assumed that the calculation of these coefficients is impossible, since it cannot be done either by Arrhenius's method, which depends on measuring the conductivity of the salt at different stages of dilution with a solvent, or by van't Hoff's method, which implies

\* *Ber.* lii. p. 5444 (1919).

† Plotnikow, *Z. physikal. Chem.* xlviii. p. 228 (1904).

a knowledge of the osmotic pressure of the salt in solution. A formal solution of the problem is possible, however, in the case of fused silver chloride at 600° C., for which the relevant data are all known, namely,

Molecular weight .....	$M=143.34$ .
Density.....	$\delta=5.267-0.0092t=4.715$ at 600°.
Specific conductivity .....	$\kappa=4.48$ at 600°.
Viscosity .....	$\eta=0.01606$ at 603°.

The normality of the fused salt is  $4715 \div 143.34 = 32.9N$ ; and the equivalent conductivity is therefore  $\Lambda = 4.48 \div 0.0329 = 136$ . The limiting value for the conductivity at infinite dilution in aqueous solution is given by the sum of the ionic mobilities as  $54 + 65 = 119$ ; if, therefore, a proportional allowance is made for an increase of viscosity from 0.01056 to 0.01606, the corresponding limiting value for the fused salt would be  $\Lambda_{\infty} = 119 \times 0.01056 \div 0.01606 = 78$ . The equivalent conductivity of a completely ionized salt can, however, also be calculated, without making use of the value for aqueous solutions, by means of Walden's relation,  $\Lambda_{\infty} \eta_{\infty} \sqrt{M} = 11.15$ , which has been verified for six salts in 29 non-aqueous solvents, as well as for two "anhydrous" salts in aqueous solution: For silver chloride this relation gives  $\Lambda_{\infty} = 11.15 \div 0.01606 \div 12 = 58$ .

These two methods of calculation concur in giving a maximum conductivity for completely dissociated silver chloride,  $\text{AgCl} \rightarrow \overset{+}{\text{Ag}} + \bar{\text{Cl}}$ , which is only about half as great as the values found experimentally. It has been suggested, and the idea has found widespread acceptance, that the

exceptional mobility of the ions  $\overset{+}{\text{H}}$  and  $\text{OH}^-$  in aqueous solutions is due to the fact that they are *the ions of the solvent*. This idea is at least plausible in the case of water, where it might be supposed that the exceptional mobility of

$\overset{+}{\text{H}}$  (in the form of  $\text{OH}_3^+$ , since  $\overset{+}{\text{H}}$  cannot persist as a separate entity), depended in part on the transfer of a naked proton from one complex to another, without necessarily involving the migration of the whole of the oxonium ion; but it is not valid, even in the closely-related case of liquid ammonia,

where  $\overset{+}{\text{H}}$  (in the form of  $\text{NH}_4^+$ ) and  $\bar{\text{N}}\text{H}_2$  are less mobile than  $\overset{+}{\text{K}}$  and  $\overset{+}{\text{Tl}}$ ; and there is no reason why it should be true in the case of a completely ionized salt, where it is

difficult even to suggest a theoretical justification for it. It therefore appears more likely that the high conductivity of fused silver chloride may be due to the presence of something analogous to the "ionic micelle" in a colloidal electrolyte, *i. e.*, to complex aggregates of ions carrying multiple electric charges, since these would have the effect of increasing both the viscosity and the electrolytic conductivity of the melt. Such aggregates might be formed by an incomplete destruction of the crystal lattice, and it may be supposed that the conductivity of a fused salt is determined very largely by the character of the aggregates that persist when the crystalline salt is melted.

From this point of view it is of interest to notice that all fused salts are not good electrolytes, even when the theory of valency indicates that they must be completely ionized. Thus, leaving out weak electrolytes such as  $\text{SnCl}_4$  and  $\text{HgCl}_2$ , where covalent molecules appear to be formed from the metal and the halogen, the values

$$\Lambda^{70} = 0.0009, \Lambda^{100} = 0.0050$$

recorded by Walden for the molten hydrobromide of dimethyl-aniline, present a remarkable contrast with the values

$$\Lambda^{600} = 4.48, \Lambda^{800} = 4.98$$

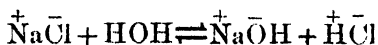
for silver chloride. In this compound we must either suppose that the fused solid breaks up into electrically neutral doublets,  $[\overset{+}{\text{N}}\text{HPhMe}_2 \cdot \overset{-}{\text{Br}}]$ , in which the oppositely-charged ions cling together, just as they must do in a salt-vapour of normal vapour-density, and, therefore, do not migrate in opposite directions under the influence of a small electromotive force; or we must postulate the existence of some subtle type of bond, which binds the ions into a molecule of such an unstable character that it is unable to persist in aqueous solution\*. Until, however, the existence of such molecules has been proved, it is simpler to admit that a salt, even if it is completely ionized in the crystalline state, will not become a good electrolyte when fused, unless the lattice is resolved into oppositely-charged fragments. If the cleavage of the lattice on fusion tends predominantly to produce neutral ionic aggregates like those which are formed on vaporization, the conductivity of the fused salt may be reduced to such an extent as to give rise to the properties of

\* Compare Hantzsch's hypothetical pseudo-ammonium halides; also Ulich, *Trans. Faraday Soc.* 1928.

a typical "weak electrolyte." This effect, it is clear, is most likely to appear in salts which are easily vaporized, *i. e.*, which break down readily into volatile neutral doublets.

### 3. Hydrolysis.

It is an interesting and novel feature of the theory of complete ionization that it very largely destroys the meaning of the term "hydrolysis." Thus an equation such as

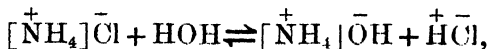


becomes a mere paraphrase of the equation



unless we admit that the theory of complete ionization breaks down in the case of one or both of the products.

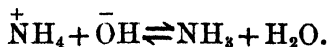
This can always be admitted in the case of the acid, since all hydrogen compounds exist predominantly in a covalent form. A more curious case is afforded by ammonium chloride,



where the *acid* is so strong that the proportion of covalent hydrogen chloride is too small to produce an appreciable vapour-pressure, but where the *base* is quite weak, so that hydrolysis must depend on the conversion of ammonium hydroxide into a covalent compound. This may take place, as Latimer and Rodebush have suggested\*, through the weak linkage of a bivalent hydrogen atom



A more familiar, but less effective, method is by eliminating the hydroxyl ion as a covalent molecule of water,



In the latter case the *hydrolysis* of the salt of a weak ammonium base (which would then be a thermal dissociation into which water does not enter directly,

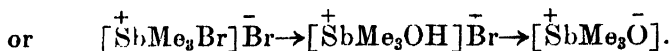
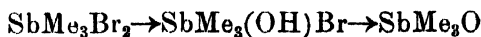


would actually depend on a *dehydration* of the hydroxide.

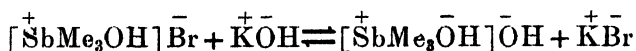
\* J. Am. Chem. Soc. xlii. p. 1431 (1920); cf. Moore & Winmill, J. Chem. Soc. ci. p. 1675 (1912).



A similar example of "hydrolysis by dehydration" is afforded by the quinquivalent compounds of phosphorus, arsenic, and antimony\*. Thus trimethylstibine dibromide can be hydrolysed in two stages as follows:—



In the first stage, hydrolysis can take place in the normal way, by an interchange of Br and OH, since the hydroxylion of the base can be fixed by the quadricovalent antimony, giving rise to a product which can be isolated in the form of an oxy-bromide,  $\bar{\text{Br}}[\overset{+}{\text{SbMe}_3}.\text{O}.\overset{+}{\text{SbMe}_3}]\bar{\text{Br}}$ ; but, since the equation



has no meaning, from the point of view of the theory of complete ionization, the second stage of the hydrolysis must depend on a direct removal of HBr, giving rise to an oxide, which can be isolated without difficulty, instead of to a dihydroxide.

### *Summary.*

(a) Compounds in which neutralization of the ionic charges is prevented by the laws of valency generally behave as "strong electrolytes" in solution. Badly-conducting solutions can, however, be obtained by dissolving a salt in a medium with a low dielectric constant, when abnormal variations of conductivity with dilution are generally observed.

(b) Many fused salts are good conductors, giving values for the "coefficient of ionization" which may be above 100 per cent., perhaps as a result of the formation of multiple-charged ionic aggregates. Other fused salts, however, are poor conductors, probably because the crystal lattice breaks down into neutral ionic doublets on fusion.

(c) The term "hydrolysis" has no significance, from the point of view of the theory of complete ionization, unless the hydrogen or hydroxyl ion of water can be fixed by one of the ions of the salt, with formation of a covalent compound.

\* Hantzsch & Hibbert, *Ber.* xl. p. 1513 (1909).

CIX. *Note on the Diffusion of Hydrogen through Iron.*

By W. EDWARDS DEMING\*.

THE diffusion of gases through metals has called forth no little theoretical and experimental work, chiefly since 1904, with the impetus given by the brilliant papers of Richardson<sup>(1)</sup>, and Richardson, Nicol, and Parnell<sup>(2)</sup>. In the former is derived an expression for the rate of flow for a gas through a slab of thickness  $x$  and with gas pressures  $P_1$  and  $P_2$  on its sides. When the gas does not combine chemically with the material through which it is passing, this expression is the sum of two terms, one proportional to  $(P_2 - P_1)x^{-1}$ , and the other to  $(P_2^{1/n} - P_1^{1/n})x^{-1}$ , i.e., to the concentration gradients of the undissociated and of the dissociated gas. ( $n$  is here the number of atoms into which one molecule of the gas dissociates, according to  $X_n \rightleftharpoons nX$ ). It was expected that in metals the former term would be inappreciable compared with the latter, one reason being that in these substances dissociation of a gas into atoms is believed to be readily accomplished. An abundance of experimental work has confirmed this expectation; for example, Richardson, Nicol, and Parnell<sup>(2)</sup>, and more recently Lombard<sup>(3, 4, 5)</sup> found that the diffusion rate of hydrogen through iron and other metals is proportional to  $P^{\frac{1}{2}}$  (the pressure being zero on the low-pressure side). Substantially the same is concluded by Borelius<sup>(6)</sup>, whose work will be mentioned later in another topic. But through rubber and fabric, Edwards and Pickering<sup>(7)</sup> found the rate of diffusion of any gas to be proportional to its partial pressure if the total pressure remains constant.

The conclusions of experimenters, that the amount  $m$  of hydrogen passing through an iron (or other metal) slab of thickness  $x$  in a time  $t$  is proportional to  $P^{\frac{1}{2}}$ , are quite unanimous, but, owing to the fact that the pressure on the low-pressure side has in every experiment (as far as the writer can ascertain) been zero, it is impossible to tell whether their data confirm

$$m = K_1 A t \frac{(P_2^{1/n} - P_1^{1/n})}{x^{a_1}}, \quad \dots \quad (1)$$

or

$$m = K_2 A t \frac{(P_2 - P_1)^{1/n}}{x^{a_2}}, \quad \dots \quad (2)$$

because both of these reduce to  $m \propto P^{1/n}$  when  $P_1 = 0$  and  $x$  is kept constant.

\* Communicated by the Author.

Nearly all experimenters on the subject have investigated the variation of the diffusion rate with pressure and temperature, few its variation with thickness. The writer wishes to show that experiments on the variation of diffusion rate with respect to thickness of a metal will enable us to decide between these two equations, for, as will be proved shortly,  $\alpha_1$  must be unity and  $\alpha_2$  must be  $1/n$ . Hence the fact that Lombard<sup>(4)</sup> found the diffusion rate of hydrogen through metals to vary inversely as the thickness is experimental proof not only that  $m \propto x^{-1}$ , but also decides in favour of  $m \propto (P_2^{1/n} - P_1^{1/n})$  rather than  $m \propto (P_2 - P_1)^{1/n}$ . On the other hand, the fact that Edwards and Pickering<sup>(7)</sup> found  $m \propto x^{-1}$  for hydrogen passing through rubber was to be expected, because if  $n=1$ , as their conclusion  $m \propto P$  for rubber indicates, then (1) and (2) become identical.

To investigate  $\alpha_1$  and  $\alpha_2$ , imagine a plane slab of homogeneous material of thickness  $a$  with pressures  $P_1$  and  $P_2$  on its sides. Let the two faces of an infinitesimal slice be distant  $x$  and  $x + dx$  from the side whose pressure is  $P_1$ , and let the pressures with which these two faces are in equilibrium when the steady state is reached be  $y$  and  $y + dy$ . (1) demands that

$$\frac{(y + dy)^{1/n} - y^{1/n}}{(dx)^{\alpha_1}} = \frac{y^{1/n} - P_1^{1/n}}{x^{\alpha_1}}$$

$$\frac{d(y)^{1/n}}{(dx)^{\alpha_1}} = \frac{y^{1/n} - P_1^{1/n}}{x^{\alpha_1}}.$$

Clearly  $\alpha_1$  must be unity, because  $dy^{1/n}$  and  $dx$  are the same order of infinitesimals. With  $\alpha_1 = 1$ , this integrates to

$$y^{1/n} = (P_2^{1/n} - P_1^{1/n})x/a + P_1^{1/n};$$

and, more important, (1) yields for the amount  $dm$  of hydrogen diffusing through an area  $A$  of thickness  $dx$ , with pressures  $P$  and  $P + dP$ ,

$$dm = K_1 A \nabla P^{1/n} dt, \quad \dots \dots \dots (3)$$

in time  $dt$ . So, if experimenters using  $P_1 \neq 0$  and  $P_2 \neq 0$  find either  $m \propto (P_2^{1/n} - P_1^{1/n})$  or  $m \propto x^{-1}$  for a plane slab, then (1) is established and (3) would be the differential equation to be applied to any problem of diffusion through walls of any shape, plane slab, cylindrical shell, spherical shell, etc., in the steady state.

By similar reasoning with (2),  $\alpha_2$  must be  $1/n$ , and at any point  $x$  in the slab

$$y = (P_2 - P_1)x/a + P_1,$$

(2) yields

$$dm = K_2 A (\nabla P)^{1/n} dt. \quad \dots \dots \dots (4)$$

Now if it is found either that  $m \propto (P_2 - P_1)^{1/n}$  or that  $m \propto x^{-1/n}$ , then (2) would be established and (4) would be the proper differential equation for the steady state.

Borelius<sup>(6)</sup> finds the amount of hydrogen absorbed or in solution in metals to be proportional to the square root of the pressure to which the metal is subjected. He substantiates this with some theory. If his result is correct, then equation (3) means that the amount of hydrogen diffusing normally through any (small) area would be proportional to the concentration gradient at that point, a logical supposition. Lombard<sup>(6)</sup>, working with a slab of electrolytic iron at 300° C., thickness 0.0162 cm.,  $P_2=1$  atmosphere,  $P_1=0$ , found  $dm/dt$  to be 5.62 c.c. of hydrogen (S.T.P.) per hour, whence  $K_1=0.091$ , and  $K_2=0.715$  in the same units. Dr. E. P. Bartlett, of this Laboratory, has recently extended his pressure, volume, and temperature relations<sup>(8)</sup> to 400° C. For this work he employed a chrome vanadium steel pipet seven inches long and having internal and external radii  $\frac{1}{8}$  inch and  $\frac{9}{8}$  inch. At  $P_2=1000$  atmospheres and  $P_1=0$ , he observed 0.5 c.c. of hydrogen (S.T.P.) diffusing through the walls per hour. Equation (3) applied to a seven-inch portion of an infinitely long cylinder (the end correction being an unnecessary refinement) yields the result 2.5 c.c. of hydrogen (S.T.P.) per hour, and equation (4) yields 25 c.c. per hour, using  $K_1=0.091$  and  $K_2=0.715$ . Naturally one would expect the  $K_1$  or  $K_2$  to be several times less for chrome vanadium steel than for electrolytic iron, so it may be concluded from this that equation (3) gives fairly good results up to very high pressures, and that equation (4) is not valid.

Adopting (3), and with Borelius taking the solubility proportional to the square root of the subjecting pressure, it is easy to extend the equation to apply at any time, whether the steady state obtains or not.

$$\frac{dP^{1/n}}{dt} = \frac{K_1}{c} \nabla^2 P^{1/n}, \quad . \quad . \quad . \quad . \quad . \quad (5)$$

$c$  is the amount of gas absorbed per unit volume under unit pressure. In the steady state,  $dP^{1/n}/dt=0$ , and under this condition, equation (3) is a first integral of (5).

In dealing with the conduction of heat, we write

$$d\theta/dt = h^2 \nabla^2 \theta,$$

which is exactly in the same form for  $\theta$  as (5) is for  $P^{1/n}$ . Thus problems in the diffusion of a gas through metals become the problems in the conduction of heat, whose solutions are now classic.

It is a pleasure to thank Dr. P. H. Emmett, of this Laboratory, for several suggestions for the presentation of these ideas.

### References.

- (1) Richardson, Phil. Mag. vii. p. 266 (1904).
- (2) Richardson, Nicol, Parnell, Phil. Mag. viii. p. 1 (1904).
- (3) V. Lombard, *Comptes Rendus*, clxxvii. p. 116 (1923); clxxxii. p. 463 (1926).
- (4) V. Lombard, *Ibid.* clxxxiv. p. 1327 (1927).
- (5) V. Lombard, *Ibid.* clxxxiv. p. 1557 (1927).
- (6) G. Borelius, *Ann. Physik*, lxxxiii. p. 121 (1927).
- (7) J. D. Edwards and S. F. Pickering, Sci. Papers, Bureau of Standards, No. 387, pp. 327-362 (1923); Chem. & Met. Eng. xxiii. pp. 17-21 and pp. 71-75 (1920).
- (8) E. P. Bartlett, Journ. Am. Chem. Soc. xlix. pp. 687, 1955 (1927); and extensions of this work to appear in the May number of the same journal.

Bureau of Chemistry and Soils,  
U.S. Department of Agriculture,  
Washington, D. C.

CX. *The Emission of Particles from Hot Platinum in Air at Atmospheric Pressure.* By WILLIAM D. FLOWER, B.Sc.\*.

[Plate XV.]

**M**EASUREMENTS of the mobility of ions emitted by hot wires at atmospheric pressure have disclosed that the emission consists initially of normal ions and uncharged nuclei. Since in the presence of ions these nuclei can pick up charges, the nature and rate of their growth is a matter of some interest, as it might lead ultimately to information on the variation of mobility with the size of the ion. It was felt that an ultra-microscopic survey of air containing these nuclei might throw some light upon the problem. Such a study of the large ions from a bunsen flame had already been made by De Broglie<sup>(2)</sup>, who described the sample as nearly optically empty. Nolan and Enright<sup>(3)</sup>, however, were led to the conclusion that the radius of large ions from a flame is greater than  $1.0 \times 10^{-6}$  cm., and De Broglie<sup>(4)</sup> himself, from his measurements of Brownian motion in gases, deduced a value of the order  $0.5 \times 10^{-6}$  cm.

\* Communicated by Prof. A. M. Tyndall, D.Sc.

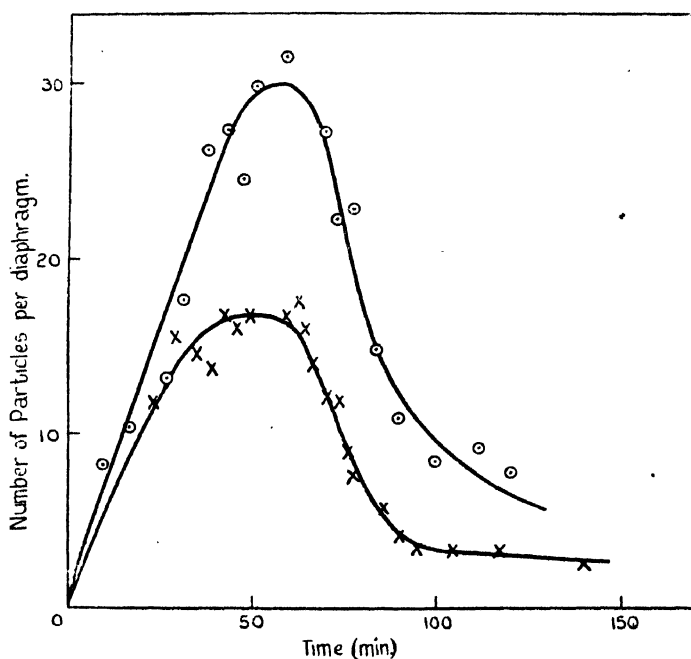
Particles of this size should be visible in the ultra-microscope. While it is conceivable that the reason for the approach to optical emptiness of the sample was that the large ions consisted of a loose grouping of molecules too diffuse to give an ultra-microscopic image, yet it might be possible to detect a greater number by improvement of the optical system. For this reason, as a preliminary, some experiments on the gases from a bunsen flame were carried out, using the ultra-microscopic method developed by Whytlaw-Gray<sup>(5)</sup> for the examination of aerosols. The apparatus used was essentially the same as that described by him, except that bilateral illumination from two 1000-c.p. pointolite lamps was used. To obtain a supply of large ions and nuclei a bunsen burner was placed in the large chamber and the atmosphere in the latter was then rendered dust free. The bunsen was lighted by an incandescent platinum spiral placed above it and allowed to burn for a few minutes. A sample of the dispersoid was then drawn off and examined in the ultra-microscope. A large number of particles, exhibiting violent Brownian movement, were observed. The same result was obtained when the coal-gas supplied to the bunsen was filtered. It was reasonable to conclude from this that with the optical arrangements described large ions were visible in the ultra-microscope.

The apparatus was then adapted for examining the emission from a hot wire by replacing the bunsen flame by a spiral of platinum wire which had been previously cleaned in acid, washed in distilled water, and dried. After the wire had been heated to a dull red heat for twenty minutes the examination of a sample showed the existence of particles, smaller in number, however, than in the preceding case.

It might be expected that the phenomenon of coagulation in aerosols would have a counterpart in these systems. To test this the following procedure was adopted. The nuclei were generated by passing a known current through the spiral for four minutes. In later work this time of generation was varied to other values and in some cases was reduced to twenty seconds. The current was switched off, the air in the chamber kept in constant circulation by a small propeller, and a very slow flow of dispersoid maintained through the observation chamber. Counts in uninterrupted succession were made of the number of particles seen through the eyepiece stops. Some typical results are shown in fig. 1 of the variation of number with time over a period of about two hours for two different values of the heating current and therefore of the temperature of the wire.

As will be shown later, the numbers recorded must be corrected because of the possibility of the inclusion in the counts in certain cases of particles lying outside the beam, but sufficiently illuminated by light scattered from particles inside the beam to be recorded as present. This, however, does not alter the general shape of the curve with its definite rise to a maximum at about one hour and its subsequent fall. The higher the temperature of the wire, the higher the maximum value becomes. It was found, however, that successive

Fig. 1.



curves for the same temperature did not repeat one another, but progressively decreased in height, indicating that the ability of the wire to emit these particles decreased with use. Further, after prolonged heating for about twelve hours, the appearance of the particles in the field of view was different from that after initial heating. The brightness of the disks decreased with succeeding curves until eventually only faint points in intense Brownian movement were observed and even these only under the best conditions. By passing

through the wire a current higher than that previously used or by heating the fatigued wire in a bunsen flame for a short time, its power of emission was temporarily restored.

This effect is analogous to the behaviour of the positive ion emission from a hot filament, but as the two phenomena were not studied simultaneously, it is not possible to say whether they are in any way related.

It is possible to explain the general form of the curve in a simple manner. It may be assumed that at emission the particles, whether they are atoms, molecules, or minute particles of metal, are too small to be seen at all and therefore nothing countable is perceived in the ultra-microscope at the time when a heating current of short duration is cut off. By coagulation with one another with time they grow in size and become visible. Some grow more rapidly than others and these are seen first. At the same time it should be mentioned that the actual process of collision and coalescence of two particles was never visually observed in the field of view of the microscope.

From the quantitative side there seemed to be little hope of carrying the matter any further on these lines unless it was possible in some way to make all the particles visible at all times. If, however, one assumes that each of the particles, whatever its age, can act as a nuclei for condensation when supplied to a Wilson expansion chamber this result can be achieved.

The form of apparatus used was such that the observation cell formed part of the expansion chamber and is shown diagrammatically (fig. 2). A given height of the piston corresponded to a certain expansion ratio which could be determined by calibration. It was found unnecessary to use an expansion ratio greater than 1.3, since there was no increase in the number of particles seen when a greater ratio than this was used.

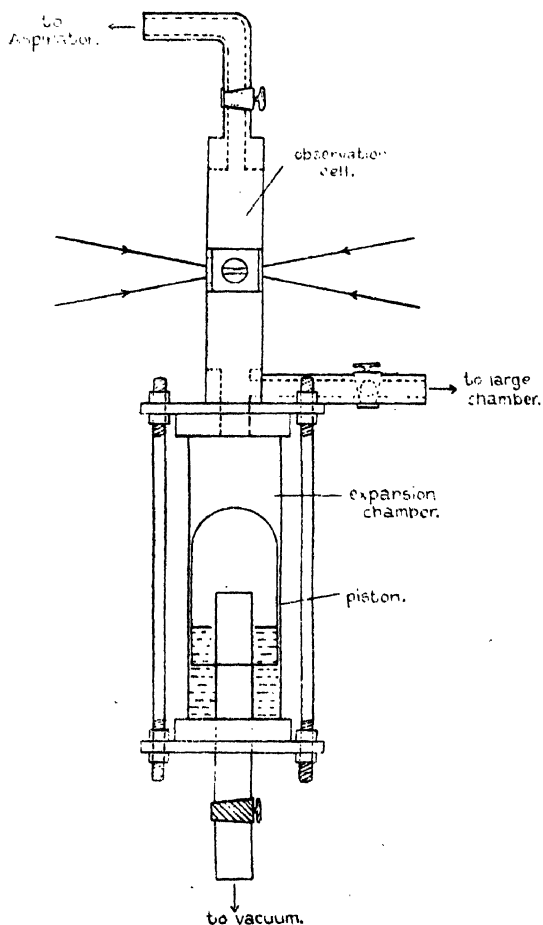
In the following experiments the nuclei were produced in exactly the same manner as before. In order to determine the number of nuclei per unit volume the number of particles seen in the eyepiece stop of the microscope, directly after producing an expansion, was noted. Owing to the fact that the cloud formed fell rapidly, under the action of gravity, considerable practice was required in estimating the number of particles seen. Typical results obtained by this method are shown graphically in fig. 3 for two experiments.

It will be seen from curves  $A_1$ ,  $A_2$ , that the number of



particles is now shown to be a maximum at zero time and to diminish subsequently along a hyperbolic curve. This is shown by plotting the particulate volume with time, curves  $B_1$ ,  $B_2$ .

Fig. 2.

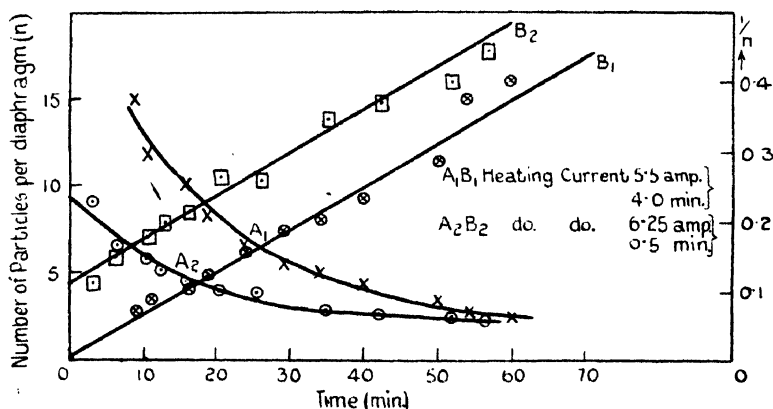


It would appear at first sight that it would be a simple matter to express these results quantitatively in terms of the number of particles per unit volume, provided that the depth of the illuminated beam is known, but, as Whytlaw-Gray has pointed out, the difficulty is found in this form of

observation cell \* in making accurate measurements of the depth of the beam since the edges of the beam were not clearly defined owing to the light scattered or reflected from particles inside the beam illuminating them outside. An error was thus introduced in calculating the absolute number per unit volume. Further, as the system aged, the number of particles in the field of view decreased and it became necessary to change from one eyepiece stop to another. It was found that the number counted was not proportional to the change in area, the number with the larger stop being smaller in proportion than with the smaller one.

At this stage the writer was brought into touch with Mr. Green, who was working on similar lines on the coagulation of smoke particles, and from this point the work was

Fig. 3.



continued in consultation with him. He had experienced the same difficulties on the quantitative side and in order to overcome them had developed a photographic method in conjunction with a continuous action Wilson apparatus<sup>(7)</sup>. In this method a photograph was taken of the contents of the cell immediately after an expansion and the resulting negative counted under a reading microscope. Mr. Green kindly allowed his apparatus to be used by the writer and with it a series of experiments was carried out. The results for two experiments are collected below, Table I., and shown graphically in fig. 4.

\* In later work by Whytlaw-Gray<sup>(6)</sup> this has been avoided by using a different type of cell.

TABLE I.

Experiment B3.		
Heating Current .....	6.53 amp.	
Duration of Heating Current .....	2.0 min.	
Time T min.	No. of Nuclei per c.c. N.	Particulate Volume I/N.
1.50	30.80 $\times 10^4$	3.25 $\times 10^{-6}$
4.25	28.55	3.52
8.25	25.10	3.98
13.60	24.30	4.12
15.20	21.30	4.59
17.20	22.18	4.54
20.75	21.70	4.61
29.25	19.20	5.21
33.00	18.00	5.56
36.50	15.92	6.30
40.20	17.10	5.85
44.50	15.32	6.54
48.25	14.73	6.82
50.50	14.49	6.99
56.35	14.20	7.04
59.35	12.90	7.75
63.40	11.33	8.87
66.00	11.70	8.55
71.50	11.33	8.87
74.80	10.33	9.73
79.00	9.52	10.50
81.10	10.55	9.57
89.00	9.32	10.72

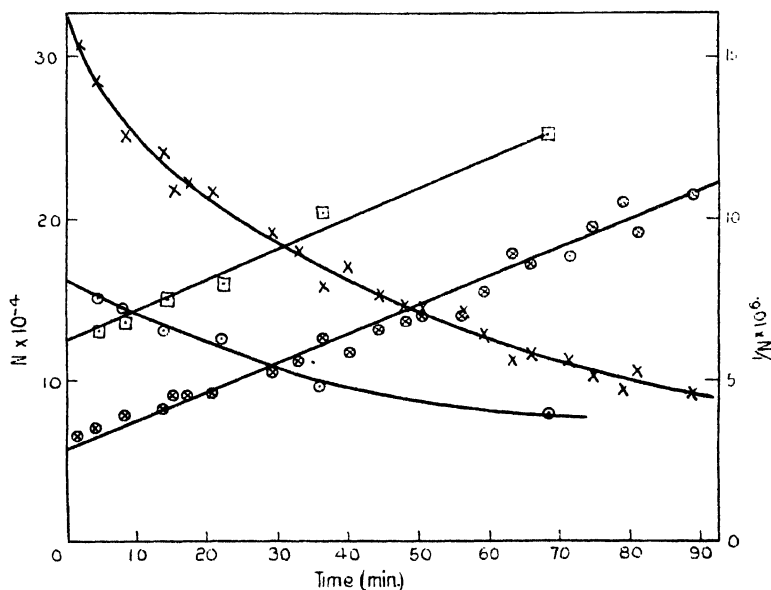
Experiment B4. <sup>1</sup>		
Heating Current .....	7.0 amp.	
Duration of Heating Current .....	2.0 min.	
4.5	15.10	6.6
8.0	14.50	6.9
14.0	13.08	7.6
22.0	12.50	8.0
36.0	9.78	10.2
68.5	7.95	12.6

<sup>1</sup> Enlargements from photographs taken during Experiment B4 are given on Plate XV.

To test whether these nuclei were charged a cylindrical ionization chamber was introduced between the observation cell and the metre chamber. The electric field and the rate of flow through the ionization chamber were so adjusted

that only ions of mobility less than  $3.5 \times 10^{-5}$  cm./sec./volt/cm., could pass through to the cell. It was found that in an aerosol of nuclei emitted from a hot platinum wire the majority of particles were initially uncharged but that more charged particles made their appearance during the stages of coagulation so that after a period of about sixty minutes half of the total number of nuclei present were charged.

Fig. 4.



#### *The Accuracy of the Observations.*

The question of the probable error in the observations has been considered on the same lines as has been done by Green, and suggests that the irregular variations shown by the departure of many of the points from the mean straight line is consistent with a random distribution of the nuclei.

#### *Discussion of Results.*

The number-time curves showing the variation of the total number of nuclei with time, for both the visual and photographic methods, exhibit certain characteristics in common. They all show a decrease in number of nuclei

with time in accordance with a hyperbolic law. This may be clearly seen by plotting the reciprocal of the number of nuclei with time when a straight line is obtained. If  $n_0$  = number of nuclei present initially,  $n$  = number of nuclei present at any subsequent time  $t$ , the following relation must hold :—

$$1/n - 1/n_0 = kt \text{ or } \frac{dn}{dt} = -kn^2$$

where  $k$  is a constant.

This relation has the same form as that found by Kennedy<sup>(8)</sup> to apply to the decrease in number of large ions and nuclei from a bunsen flame.

The values of the constant  $k$  deduced from the results obtained by the photographic method are given in Table II.

TABLE II.

Duration of Emission in minutes.	Heating Current amp.	Number of particles per c.c. initially.	$k$ cm. <sup>3</sup> /sec.	Mean $k$ cm. <sup>3</sup> /sec.
2.0	5.7	$0.98 \times 10^5$	$0.15 \times 10^{-8}$	$0.15 \times 10^{-8}$
2.0	7.0	1.10	0.16	
2.0	6.5	3.28	0.14	
2.0	7.0	1.62	0.16	
4.0	5.6	2.78	0.13	
2.0	4.8	1.88	0.13	
4.0	6.4	1.79	0.16	

If in the visual method the assumption is made that the depth of beam through which observations are made is actually the "depth of focus" of the viewing microscope, and from this calculate the number of particles per unit volume it is found that the value of  $k$  by this method is  $0.10 \times 10^{-8}$  cm.<sup>3</sup>/sec. Since this number is of the same order it may be regarded as a reasonable confirmation of the value given by the photographic method.

It is interesting to compare this value with that obtained by Kennedy for the decrease in number of large ions and nuclei from a bunsen flame with time. Kennedy used an Aitken Dust-Counter and obtained the value  $0.13 \times 10^{-8}$  cm.<sup>3</sup>/sec. The agreement for these two sources is satisfactory.

The only theoretical formula relating to coagulation appears to be the one derived mathematically by Smoluchowski<sup>(9)</sup> for

the coagulation of sols. In this formula  $n = n_0/(1 + kt)$  where  $n$ ,  $n_0$ ,  $t$ , and  $k$  have the same meanings as before. Also  $k = 4\pi DR_a$ , where  $D$  and  $R_a$  are respectively the diffusion constant and radius of the sphere of action for the same particle.

The application of the formula to the problem is only strictly justified if  $k$  is independent of  $n_0$ . Evidence of this is given in fig. 4, where the values of the particulate volume,  $1/n$ , are plotted against time for two experiments and the two straight lines are seen to be approximately parallel.

Whytlaw-Gray has shown from the formula that  $k = 1.46 \times 10^{-10} (1 + 9 \times 10^{-6} r^{-1}) R_a r^{-1}$  cm.<sup>3</sup>/sec. It is necessary to apply the Cunningham correction to the term for the mobility of the particles involved in the diffusion constant, though this makes  $k$  a function of the initial radius of the particle. No evidence of this exists in the present experiments, though it might appear if it had been possible to study the coagulation over shorter and longer time: while therefore there is no real justification for deducing the radius of the initial nucleus from the above expression and the observed value of  $k$ , it may be of interest to note that the radius obtained in this way,  $2.2 \times 10^{-6}$  cm., lies between the value suggested by De Broglie<sup>(4)</sup> and that suggested by Nolan and Enright<sup>(3)</sup>.

### *Summary.*

An ultra-microscopic study of air containing large ions and nuclei emitted by a hot platinum wire has been made. After the source of nuclei had been removed the number visible increased to a maximum and then diminished. This is explained if at emission the nuclei are too small to be seen but subsequently coagulate.

Reliable results on the rate of coagulation of these nuclei were obtained by using them as nuclei for condensation and photographing the droplets formed.

The equation of the coagulation time-curves are hyperbolic and is given by  $\frac{dn}{dt} = -kn^2$  where  $n$  is the number present and  $k$  is a constant equal to  $0.15 \times 10^{-8}$  cm.<sup>3</sup>/sec. This value is in reasonable agreement with the value  $0.13 \times 10^{-8}$  cm.<sup>3</sup>/sec. obtained by Kennedy for large ions and nuclei from a bunsen flame.

The application of the coagulation theory of Smoluchowski to these results is discussed.

In conclusion I wish to express my indebtedness to Professor A. M. Tyndall both for proposing the research and for the interest he took in the progress of the work, and to Mr. H. L. Green for the use of his apparatus in the latter part of the investigation.

### References.

- (1) Tyndall, A. M., and Grindley, G. C., *Phil. Mag.* xlvii. p. 701 (1924).
- (2) De Broglie, *C. R.* cxlviii. p. 1317 (1909).
- (3) Nolan, J. J., and Enright, J., *Proc. Roy. Irish Acad. A*, vi. p. 105 (1923).
- (4) De Broglie, *loc. cit.* p. 1317.
- (5) Whytlaw-Gray, R., and others, *Proc. Roy. Soc. A*, cii. p. 600 (1923).
- (6) Whytlaw-Gray, R., Nonhebel, G., and others, *Proc. Roy. Soc. A*, cxvi. p. 540 (1927).
- (7) Green, H. L., *Phil. Mag.* ser. 7, iv. No. 25, p. 1046 (1927).
- (8) Kennedy, H., *Proc. Roy. Irish Acad. A*, xxxiii. p. 66 (1916).
- (9) Von Smoluchowski, *Zeit. f. Phys. Chem.* xcii. p. 129 (1918).

## CXI. *A Note on the Predicted Ionization Potential of Niton.*

By SUSHIL CHANDRA BISWAS, *M.Sc.\**

**I**ONIZATION potentials of elements of the same family are in general found to diminish almost in a linear way with progressing atomic number. On a closer scrutiny, however, it is found that elements in the P-shell, viz. (79) Au, (80) Hg, (81) Tl, (82) Pb, etc., indicate an appreciable increase in their ionization values. This is shown in Table I.

TABLE I.  
Ionization Potentials (Volts) †.

N Shell.	O Shell.	P Shell.
29. Cu—7.691	47. Ag—7.542	79. Au—9.25
30. Zn—9.35	48. Cd—8.95	80. Hg—10.39
31. Ga—5.8	49. In—5.76	81. Tl—6.08
32. Ge—	50. Sn—	82. Pb—7.93
33. As—11.54	51. Sb—8.0	83. Bi—8.0±.5
36. Kr—15.3	54. Xe—11.5	86. [Nt—14.0±0.5] (cal.)

\* Communicated by Prof. S. N. Bose, M.Sc.

† Foote & Mohler, 'Origin of Spectra,' 1922. Franck & Jordan, 'Anregung Von Quantensprungen,' 1926.

It thus seems that Glockler's\* and Struwe's† extrapolated value of (86) niton (8-10) volts, calculated on the assumption that the same relation which holds for the first five rare gases may be extended to all six of them, and thus the ionization potential of niton must be less than that of xenon (54), may be far from truth.

*Calculation of the Ionization Potential.*

Moseley's Law  $\nu_R = \left(\frac{z'}{n}\right)^2$  can be written as

$$\frac{I}{I_H} = \left(\frac{z'}{n}\right)^2, \quad . \quad . \quad . \quad . \quad . \quad (1)$$

where  $I$  represents the ionization potential of an element,  $I_H$  that of a hydrogen atom, " $n$ " representing the total quantum number, and  $z'$  effective nuclear charge for the given element.

As, according to Sommerfeld, the energy of an electron orbit can be determined by two quantum numbers  $n$  and  $k$  (radial and azimuthal quantum numbers respectively), such that the ratio between the semi-major and semi-minor axes

$$\frac{a}{b} = \frac{n}{k},$$

it can be shown that the radius of a hydrogen-like ( $n, k$ ) orbit (circular) about an effective nuclear charge  $z'$

$$a = \frac{n^2}{z'} \cdot a_H,$$

where  $a_H$  represents the radius of a (1, 1) hydrogen orbit.

Thus

$$b = \frac{n \cdot k}{z'} \cdot a_H.$$

Now, following as according to Stoner ('Magnetism and Atomic Structure,' pp. 97, 304, 1926), the mean areal velocity of the elliptic orbit

$$\frac{\pi \cdot ab}{\tau} = \frac{\pi \cdot \bar{r}^2}{\tau}$$

$$\text{or} \quad \bar{r}^2 = k \cdot n \cdot \frac{n^2}{z'^2} \cdot (a_H)^2 = 0.283 \cdot k \cdot n \cdot \left(\frac{n}{z'}\right)^2, \quad . \quad . \quad (2)$$

where  $\bar{r}^2 \cdot (\text{A.U.})^2$  represents the mean square radius of ( $n, k$ )

\* Glockler, *Phil. Mag.* l. p. 997 (1925).

† Struwe, *Zeits. f. Phys.* xxxvi. p. 410 (1926); xxxvii. p. 859 (1926).



orbit and ( $a_H = 0.532$  A.U.) as the radius of the normal atom of hydrogen has been substituted.

By combining (1) and (2) and substituting for  $I_H = 13.54$  volts,

$$I_{(\text{volts})} = \frac{k \cdot n}{r^2} \times 3.83. \quad . \quad . \quad . \quad . \quad . \quad (3)$$

For elements of the same family of Mendeleef's Table, " $k$ " remains the same, and hence it follows that the ionization potentials of elements of the same family will be inversely proportional to the square of the radius and directly to the quantum number " $n$ ."

Table II. contains atomic radii as determined from their crystal data. These indicate for elements in P-shell a noticeable diminution in their values of radii. It may also be seen that the radii of elements of the same series in O- and P-shells are very nearly the same.

TABLE II.\*

## Atomic radii (A.U.).

N Shell.	O Shell.	P Shell.
Cu—1.42	Ag—1.62	Au—1.60
Zn—1.33	Cd—1.52	Hg—1.41
Ga—1.26	In—1.46	Tl—1.42
Ge—1.21	Sn—1.36	Pb—1.36
As—1.25 †	Sb—1.44 †	Bi—1.55 §
Kr—1.985	Xe—2.07	Nt—2.05

The radii for the rare gas elements are those as obtained by A. F. Scott ||, who, according to Simon ¶ and Von Simson's determination of solidified argon structure to be face-centred cubic, assumed all other inert gases to have the same structure and then computed their atomic volumes from the densities at absolute zero according to Hertz's \*\* calculation.

\* Huggins, *Phys. Rev.* xxviii. (ii.) p. 1024 (1926).

† Brandt, *Phil. Mag.* xlvii. p. 657 (1924).

‡ James and Tunstall, *ibid.* xl. p. 233 (1920).

§ James, *ibid.* xlii. p. 193 (1923), recalculated by McKeehan, *Journ. Frank. Inst.* cxcv p. 159 (1923).

|| A. F. Scott, *Journ. Phys. Chem.* xxx. (i.) p. 580 (1926).

¶ Simon and Von Simson, *Naturwissenschaften*, xi. p. 1015 (1923).

\*\* Hertz, *Zeits. Anorg. Chemie*, cv. p. 171 (1919).

*Radius of Niton.*

From the well-known ionization potentials of rare gases, the radii as calculated by equation (3) are entered in column ii. Table III. For comparison, atomic radii, determined by Rankine \* from viscosity measurements, and those of Chapman † from van der Waals' "b," after correcting for the recent value of Loschmidt number ( $2.705 \times 10^{19}$ ), are given in columns iii., iv. Radii from crystal data are also included in column v.

TABLE III.  
Radii (A.U.).

i. Gases.	ii. Ionization volts.	iii. Viscosity.	iv. Van der Waals' "b."	v. Crystal data.	vi. Differences (v.-ii.).
Ne .....	0.84	1.18	1.188	—	—
Ar .....	1.20	1.43	1.42	1.89	0.67
Kr .....	1.52	1.60	1.62	1.99	0.47
Xe .....	1.83	1.76	1.77	2.07	0.24
Nt .....	(1.81 ± .03)	(1.81—1.84)‡	1.84	2.05	0.24

Indefiniteness as to the nature of the term atomic radius even for such simple monatomic gases, becomes apparent as a comparison is made of the radii for these gases by different methods. Though the radii by any two methods are not found to agree for any element, there is in general an agreement in the results of the same series by the same method, and one series of results offers parallelism with those of other methods.

The radius of niton, as calculated by Rudolf § from the critical temperature and pressure of the gas, indicates an increase in its value from that of xenon. On the other hand, the radius of niton (column v., Table III.) determined from crystal data gives a value less than that of xenon.

Though it may thus appear doubtful to extrapolate the radius of niton which may fall along the radii of other rare gases calculated from their ionization values, clearly enough the radius of this element cannot lie very far from that of xenon. It has already been noted that the radii for elements

\* Rankine, Proc. Roy. Soc. A, xcvi. p. 360 (1920).

† Chapman, Phil. Trans. A, ccxvi. p. 279.

‡ Struwe, *loc. cit.*

§ Rudolf, *Zeits. f. Electro-Chemie*, xv. p. 748 (1909).

in O- and P-shells are very nearly the same, which means that, according to equation (3), the ionization values of chemically similar elements in O- and P-shells will bear a ratio as the ratio of quantum numbers 5:6. This is approximately satisfied from the data of ionization potentials Table I. More than that, the radius of niton is expected to be smaller than that of xenon, even from a superficial study of the radii and ionization potentials of elements in O- and P-shells (*vide* columns ii. and iii. of Tables I. and II.).

If the radius of niton is taken as 1.81 A.U., the error cannot exceed 0.03 A.U., as appears from viscosity or from critical data. Hence the calculated ionization potential of niton, taking the external electron at (6, 2) orbits is  $(14.0 \pm .5)$  volts.

Turner\*, on the assumption that linear relationship subsists between the atomic numbers and quantum defects when Bohr's quantum numbers are increased by integral amounts, calculated the ionization value of niton to be  $(27.5 \pm 1.5)$  volts (given the quantum number 10), but taking ( $n=11$ ); the value turned so low as  $(4.66 \pm .11)$  volts. Though no satisfactory purpose is served by Turner's enumeration of quantum number, it may be seen that for ( $n=10$ ), the ionization value of niton does not exceed (24.0) volts, and goes on increasing with the increase of quantum number.

Physics Department,  
University of Dacca,  
Bengal, India.

CXII. *The Shadowgraph Method as applied to a Study of the Electric Spark.* By HARVEY A. ZINSZER, M.A., Ph.D.,  
*Professor of Physics, Hanover College, U.S.A.* †

[Plates XVI. & XVII.]

### *Introduction.*

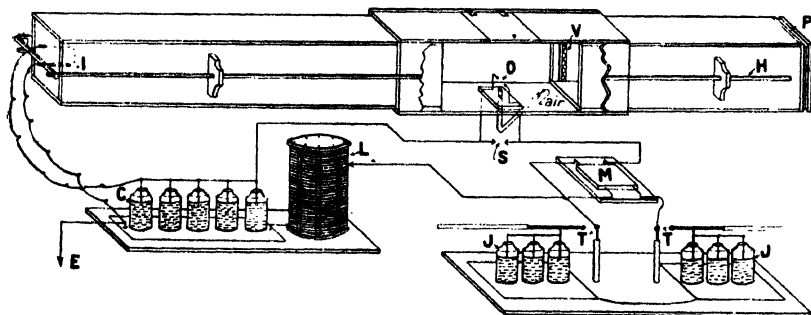
EVER since Henry<sup>(1)</sup> prophesied the oscillatory character of the leyden-jar discharge, a great deal of work has been done with regard to the electric spark, both from a theoretical and an engineering standpoint, and various theories of the phenomena involved in the electric spark resulting from a condensed discharge have been propounded.

\* Turner, Phil. Mag. xlviii. p. 1010 (1924).

† Communicated by the Author.

Apart from the work of Fëdderson<sup>(2)</sup> and Boys<sup>(3)</sup>, who succeeded in photographically showing the actual oscillations in an electric spark discharge—the former by means of a rotating mirror, the latter by the use of a rotating lens system,—little work has been reported on instantaneous photographic studies of the electric-spark discharge. But as early as 1867, Toepler<sup>(4)</sup> devised the so-called “schlieren methode,” a method of instantaneous photography by which he and, later, Mach<sup>(5)</sup> and Wood<sup>(6)</sup> made kinematographic demonstrations of the evolution of reflected wave-fronts resulting from spark-discharges. While their work involved the photographing of the spark itself, they were more concerned with the sound-pulse than a life-history of the spark. Moreover, their method called for a lens system which tends to mask some of the finer details of the spark

Fig. 1.



owing to the smallness of the image and the concentration of light upon the photographic plate by the lens system. In view of these facts, it was thought worth while to make a further investigation of the electric-spark discharge in order to obtain, if possible, a more complete life-history of it, and to compare the more recent theories of the spark-discharge with the photographs thus obtained.

### *Apparatus.*

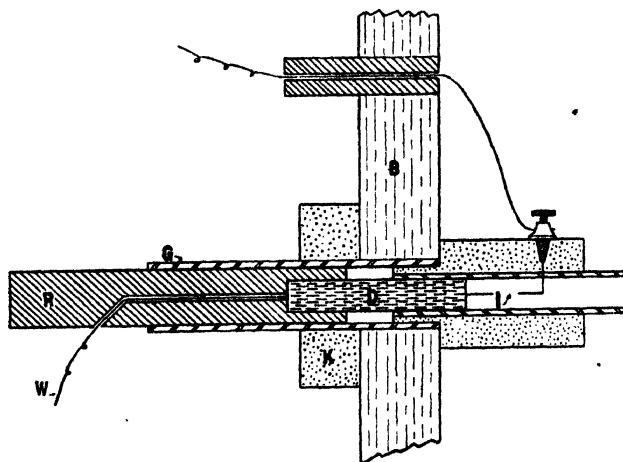
The apparatus employed in this investigation, and the operation thereof, was essentially the same as that devised by Foley and Souder<sup>(7)</sup> in their work, “A new Method of Photographing Sound-waves.” The general arrangement of the apparatus in this experiment is shown in fig. 1.

The charge which produced the electric spark was generated by a Wagner static induction machine consisting of four

mica plates, 77 cm. in diameter, driven by a variable-speed motor. Three leyden-jars of about two gallon capacity were used on each side of the static machine. The spark-gap, O, under investigation was located in a long, collapsible, light-tight wooden box, one end of which contained the illuminating gap, I, and the other the plate-holder, P. The overall length of the box was about 3 metres and the middle section measured  $40 \times 40$  cm. in cross-section. It was constructed of inch boards and painted black inside. Numerous tin vanes, V, about 3 cm. wide and 28 cm. long, were provided to eliminate reflexion.

The spark-gaps, O and I, were connected in series with a variable inductance, L, through a reversing switch, M, to

Fig. 2.



the terminals, T, of the static machine. A retarding capacity, C, was connected in multiple with the illuminating gap, I. A temporary micrometer gap, S, in multiple with the object gap, O, was located outside of the dark-box. The system was earthed as shown in the figure.

Fig. 2 shows a sectional view of the illuminating gap, I. In this figure, D is a cadmium cylinder, into one end of which is wedged a short piece of #24 magnesium wire, the latter forming one of the terminals of the illuminating gap, I. The cadmium cylinder is in turn fastened to the end of a hard rubber rod, R. The rod, R, slides snugly in a 2.5 cm. glass tube, G, which is held in the wall, B, of the dark-box by means of a cork support, K. The gap distance of I is

adjusted from the plate end of the dark-box by means of a long lever, H, shown in fig. 1.

The capacity of the leyden-jars used in this work was found to be approximately 1430 e.s.u. The inductance consisted of a helix of 25 turns of #00 copper wire wound on a framework 25 cm. in diameter and 35 cm. in length; its resistance was 0.0131 ohm and its self-inductance measured approximately 340.5 microhenrys.

The theory of this method, which is sometimes called the point-source shadow method, is based on the phenomenon of refraction. The light from a point-source is allowed to fall directly upon a photographic dry plate several metres distant from the source. About half-way between the illuminating source and the plate-holder is placed an object consisting of a fluid stream or an electric discharge. The object differing in density from the air about it causes the light from the point-source to be refracted, with the result that a shadow of the refracting object is cast upon the photographic dry plate.

#### *Observations.*

The following photographic investigations were made of the electric-spark discharge at O, using the arrangement of apparatus as exhibited in fig. 1 :—

(a) *Variable Capacity*.—With no inductance, L, in the circuit and with the side-gap, S, eliminated, the effect of varying the retarding capacity, C, was investigated. The latter was varied two leyden-jars at one time, going from one to fifteen jars inclusive for all values of the gap-distance, I. Whenever good shadows appeared on the ground-glass at P, a dozen plates were exposed for a single adjustment of the apparatus. With this disposition of apparatus, it was found that for low values of C a shadow showing the spark in its streamer or brush stage was obtained, while for high values of C the later stages of the spark appeared.

(b) *Variable Inductance*.—The second part of this investigation involved the introduction of inductance, L, into the circuit as shown in fig. 1. The inductance was varied five turns at one time for constant values of retarding capacity, C. Hence a considerable number of adjustments were necessary to adequately cover this field. The inductance was inserted between the static machine terminal, T, and the retarding capacity, C, as shown in fig. 1. Here it was found that for relatively low values of inductance a

large part of the life-history of the spark could be satisfactorily obtained. The capacity,  $C$ , was varied four leyden-jars at one time through a range of one to thirteen jars inclusive, and for any one value of  $C$  the inductance,  $L$ , was varied throughout its entire range, five turns, or about 70 microhenrys, at one time.

(c) *Parallel Gap*.—Since some of the shadowgraphs representing the spark in its infancy showed streamer effects resembling a heavy brush discharge, it occurred to the writer that, by arranging a temporary micrometer gap outside the dark-box, as shown in fig. 1, extremely early sparking conditions might be photographed, from the faintest spark discharge to probably a very late stage. This supposition was not unfounded, as the plates of this paper will show. In this particular phase of the study the retarding capacity,  $C$ , was again varied from one to thirteen leyden-jars, four at one time. Furthermore, various types of object-gaps were constructed and used in this particular phase of the work. The gaps were: (i.) point to point; (ii.) point to vertical wire, #30; (iii.) point to disk; (iv.) disk to vertical wire, #30; and (v.) blade to blade.

(d) *Air-Draft*.—Having read with interest the work done by Hemsalech<sup>(8)</sup> on an electric spark taking place between two electrodes inclined one to the other while a strong air-blast was directed into the gap-space, it was thought that instantaneous shadowgraphs of a similar arrangement might disclose some new results. The air-pressure was varied from four to ten pounds per square inch in steps of two pounds at one time. The orifice of the air-tube projecting through the base of the object-gap,  $O$ , had an inside diameter of 8 mm., and extended to within 5 cm. of the gap-space. The air-draft yielded the best results when used in connexion with the parallel gap,  $S$ .

### *Discussion of Results.*

Of the 1264 photographic dry plates exposed to the spark discharge during this investigation, 886 have been catalogued. Four prints of the latter appear herewith showing various possible stages of exceeding interest through which a spark discharge may pass. However, it is not to be supposed that any one spark will necessarily pass through all these stages. Based upon Professor Foley's<sup>(9)</sup> figures for velocities of sound near its source, the exposures of these prints have been calculated to approximate 3 microseconds.

Fig. 3 (Pl. XVI.) represents a brush discharge of a weak spark. Apparently the energy of the spark has been spent. The configuration near the negative terminal most probably represents diffusion of hot air through which the discharge previously took place. A brush and a glow discharge persist at the positive terminal.

Fig. 4 (Pl. XVI.) represents the "pilot" spark of Trowbridge<sup>(10)</sup>. According to Schuster and Hemsalech<sup>(11)</sup>, the air lines are now being replaced by metallic lines, the vapour of which is beginning to diffuse into the gap-space.

Fig. 5 (Pl. XVII.) may represent the breaking-up of Trowbridge's<sup>(12)</sup> "charred hole," or, perhaps, the projection of globules or molecular aggregations<sup>(13)</sup> from the electrodes into the gap-space.

Fig. 6 (Pl. XVII.) represents the striation stage of the spark discharge. Paalzow<sup>(14)</sup> discovered that when an electric discharge took place under reduced pressure, striations would result for critical values of resistance. A lantern-slide of this print shows the striations most beautifully.

### *Summary.*

1. Optimum conditions for studies of the early stage of the spark discharge and also of sound-pulses were discovered, the former by the use of an auxiliary gap, the latter by the use of a low variable inductance.

2. The findings of Trowbridge<sup>(15)</sup> and of Schuster and Hemsalech<sup>(16)</sup> as to the diffusion of metallic vapour into the gap-space are verified by instantaneous photography.

3. Photographic life-histories of various spark discharges have been obtained, parts of which are reproduced herein.

4. A new method for determining the lag of a needle-gap, for the study of steep wave-front impulses, for the study of vortex rings and explosions is herewith suggested.

This investigation was carried out in the physical laboratory of Indiana University under the direction of Prof. A. L. Foley, to whom the author wishes to express his gratitude for the aid extended and for the facilities placed at his disposal.

### *References.*

- (1) 'The Scientific Writings of Joseph Henry,' i. p. 201 (Washington, D.C.).
- (2) Feddersen, *Pogg. Ann.* ciii. p. 69 (1859); cxiii. p. 437 (1861); cxvi. p. 132 (1862).
- (3) Boys, *Proc. Phys. Soc. Lond.* xi. p. 1 (1890).
- (4) Toepler, *Pogg. Ann.* cxxxi. p. 33 (1867); cxxxiv. p. 194 (1868).
- (5) Mach, *Sitz. d. Wien. Akad.* xcvi. p. 1333 (1889).



- (6) Wood, *Phil. Mag.* xlviii. p. 218 (1899); 1. p. 148 (1900).
- (7) Foley & Sounder, *Phys. Rev.* xxxv. p. 374 (1912).
- (8) Hemsalech, *Comptes Rendus*, cxxx. p. 898 (1900); cxxxii. p. 917 (1901); cxl. p. 1105 (1905); *Journ. de Phys.* 1. p. 76 (1902).
- (9) Foley, *Phys. Rev.* xvi. p. 449 (1920).
- (10) Trowbridge, *Phil. Mag.* xxxvi. p. 343 (1893).
- (11) Schuster & Hemsalech, *Phil. Trans.* xciii. p. 189 (1899); *Proc. Roy. Soc. Lond.* lxiv. p. 331 (1899).
- (12) Trowbridge, *loc. cit.*
- (13) *Vide* Author's discussion on the "Mechanism of the Condensed Spark Discharge," *Proc. Indiana Acad. of Sci.* 1927.
- (14) Pualzow, *Pogg. Ann.* cxii. p. 567 (1860); cxviii. p. 178 (1863).
- (15) Trowbridge, *loc. cit.*
- (16) Schuster & Hemsalech, *loc. cit.*

CXIII. *On the Presence of Charges at an Electrode Surface.*  
*By* WILLIAM CLARKSON, *Ph.D.*, *M.Sc.*, *A.Inst.P.*, *International Education Board Fellow*, *Physical Institute of the University of Utrecht* \*.

#### I. INTRODUCTION.

**T**HE paper describes experiments made to determine whether at any time after an electrical discharge

- (1) an electrode gives up a charge ;
- (2) there is an electric field within some distance of the surface.

They form part of a series of experiments on electrode surface effects as demonstrated by "build-up" lag variations, contact potential variations, and variations of the sparking potential. These effects are invariably present in discharge systems, and are of great significance in their study.

The particular phenomena being heterogeneous, many explanations have been advanced. The changes selected for investigation here may be shown to occur under pure as well as impure conditions, to be reversible and to decay with time. They are ascribable to temporary unstable modifications of the gas-electrode interface; this suggests a change in the work of extraction of an electron.

The most generally applicable hypothesis will be shown to be that of double layers—a potential introduced at the electrode surface ; but other explanations deserve consideration. As direct experiments on residual charges might be expected to throw light on this problem, even negative results being of significance, the following experiments were made.

\* Communicated by Professor Ornstein.

## II. PRELIMINARY EXPERIMENTS.

### 1. *General Methods.*

The following description of experiments made to determine whether a charge is given up by an electrode shows the development of the problem.

Condenser discharges in discharge-tubes of great purity<sup>(1)</sup>, and later unidirectional sparks in air, were employed. The effects of merely applying a field were also studied.

The general experimental scheme was as follows: one electrode, X, was connected to a charge-measuring device; this system could be (a) earthed or (b) insulated. The other electrode, Y, could be (a) connected to a suitable source of potential, or (b) earthed, in conjunction with this source. A switch permitted the rapid performance of the following sequence of operations: (a) X to earth, Y to voltage supply, *i.e.* a discharge, (b) Y and potential source earthed, *i.e.* entire system at earth potential, and (c) X released. If X now acquired a charge, this must have been derived from some part of a metal system initially at the one potential.

The whole system was screened as completely as possible from all additional influences likely to cause deflexions.

An electroscope proving unsuitable a string-electrometer was employed. It exhibited no appreciable leak and had a limit of sensitivity consistent with stability of 1/100 volt. Its capacity was some cms.

### 2. *Discharge-tubes.*

In the case of discharge-tubes the electrometer showed a deflexion when insulated any time within a minute or two of a discharge. It was equivalent to several volts when the time-interval was of the order of 1/5 sec., and decreased as the time-interval was increased. The sign of the charge was opposite to that of the electrode, and was determined by the direction of the last discharge preceding observation.

It was found, however, that these effects were not due to the electrodes themselves, but to the leakage of charge from the insulating walls of glass; any electrode effects were completely masked. (See Section IV.)

The alternative was to discard discharge-tubes in favour of a spark system in air, as this permitted the problem of insulators to be attacked, but in so doing the advantage of working under pure conditions was lost.

### 3. *Spark-Gaps.*

Work on spark-gaps with a wide variety of arrangements merely showed that all observable effects could still be

attributed to charges induced on the insulators; radiations from the discharge were particularly troublesome.

These effects being eliminated, no residual charges could be detected.

#### 4. *Improvements.*

These were directed to the following ends: (1) to attain maximum sensitivity—this meant minimising the capacity; (2) to screen all insulators completely; and (3) to minimise the time-interval between the discharge and release.

(1) Instead of small pieces of metal, the mounts of the electrometer wire were made of a minimum length of fine wire mounted in glass. The lead was reduced to 3 cm. of 1/10th-mm. wire. All contacts were soldered.

It was necessary to keep the electrometer system easily accessible so that frequent calibration was possible.

(2) With small light electrodes the insulator was correspondingly small; screening was thus greatly facilitated.

(3) The cycle of operations was made automatic. It was necessary to avoid the transmission of vibrations to the electrometer, these tending to cause a shift in zero.

### III. FINAL METHODS.

#### 1. *Charge given up by an Electrode.*

By effecting the refinements suggested, the time-interval between discharge and release was reduced to 1/1000 sec. without loss of sensitivity.

A. *Apparatus.*—The electrode was a fine needle mounted in well-screened amber. Hinged, interlocking jaws of brass gave perfect earthing and completed the screening of the insulator. The needle-point was situated within a thick brass screen at the other side of which was the second electrode. A brass slide could be drawn before the hole, *i. e.* between the electrodes, to complete the earthed screening. A projecting lug was so attached to this that on the hole being covered the jaws were wedged open just sufficiently to release the needle.

The slide was attached to a sliding contact actuated by a falling weight. The impact of the weight occasioned the following sequence of events: (*a*) the contact was made for a short time; (*b*) it was then broken and the slide drawn, the needle now being quite isolated; and (*c*) the needle was released.

B. *Observations.*—With the time-interval small appreciable deflexions—up to 1/20 volt—were generally observed. They were very erratic in value and were always negative.

They were not due to vibrations or insulation, and were not associated with the discharge, as they occurred in its absence with an average value the same as that when the needle was anode or cathode. Further, sensitizing<sup>(2)</sup> or fouling the needle was without influence.

Previous experience suggested the cause, the release of the needle by the jaws. With needle and jaws freshly cleaned the effects were negligible.

The results of the experiment thus were entirely negative.

## *2. Field near Electrode Surface.*

A. *Method.*—A circular disk electrode rotating at high speed was employed. The discharge passed at a point on the edge, and a collecting needle was placed as near as was practicable to the opposite end on the diameter. With the needle at the potential of the electrode the presence of a field—presumably attendant on a surface-charge—would be detected by a charging-up of the needle, *i. e.* the electrometer string. Rotation would provide for maintenance of the field.

B. *Apparatus.*—The electrode consisted of a knife-edge ridge round the middle of a light, hollow, brass cylinder,  $3 \times 2\frac{1}{2}$  cm. This revolved axially, without vibration, in a metal frame. The side of the drum nearest the discharge was earthed along its whole length by stranded brushes, and the spindle and frame were also earthed. The whole system was then connected to the electrometer case. The drum also served as an earthed screen between the discharge and the collecting point.

The air-gap between the needle and the electrode was 1/10 mm. Tests under working conditions showed that the needle rapidly acquired the potential of the revolving drum.

Speeds up to 200 revs. per second were attainable, *i. e.* 1/400 sec. between discharge and needle; since the discharge was drawn out by the rotation, this figure may be reduced to 1/600 sec.

A continuous discharge not being attainable, a transformer fed by an alternative source of 520 periods per second was used; the discharge lasted throughout most of each period. Generally, unidirectional sparks some 4 mm. long were employed. The electrodes were made symmetrical.

C. *Observations.*—It was found that inconstant deflexions of about 1 volt, positive or negative, were obtained, the positive being about 10 per cent. the greater. The sign was opposite to that of the rotating electrode.

Apart from the effects sought for, these possibly could be

due to two other causes : (1) imperfect earthing of the drum, (2) charged gas being carried round from the discharge. They could not be traced to insulators.

It was sought to remove (2) : firstly, by blowing a jet of air across the electrode between the discharge and the collecting needle, and, secondly, by inserting metal or other screens between them. On this being done, it was found that (a) the positive and negative deflexions were now equal at about the mean of their former values ; (b) they were independent of whether the screening was a strong or weak current of air, a metal plate or a pad of felt bearing on the electrodes ; and (c) they occurred independently of the kind of spark or whether it passed at the middle or the edge of the drum, but increased with the discharge intensity and when the drum contacts became worse. Impurities had no effect.

From this it was concluded that the deflexions were certainly not due to a residual charge on the electrodes, but were attributable to a fall of potential in the drum contacts. The former negative results were thus fully confirmed.

#### IV. EXPERIMENTAL CONCLUSIONS.

The results of the foregoing series of experiments may be summarized as follows : with (a) a detecting system of some few cms. capacity and a sensitivity of 1/100 volt ; (b) discharges in air from brush-discharges to sparks of several mm. or alternating fields ; and (c) electrodes, polished or rough, sensitized, clean or impure, it is found that

1. No detectable charge is given up by a steel needle after a 1/1000-sec. interval ; and
2. No field can be detected by a point 1/10 mm. distant from a sharp brass edge after a 1/600-sec. interval.

These results show that there is no appreciable free charge persisting at an electrode surface for a longer period after a discharge than that stated.

Charges amounting to several volts, even with large electrodes, were recovered, however, when the insulator was exposed to the slightest influence of varying fields or of radiations from the discharge. The effect depended on the time-interval, but might last for minutes. Breaking contact might also give rise to a charge.

Results neglecting these possibilities must be received with caution as, in general, the effects are identical with those sought for. In discharge-tubes the effects are great and inevitably present, but it has yet to be shown that they need necessarily help to determine the conditions of discharge.

Discussion.

A general idea of the phenomena of temporary polarization may be derived from a study of preceding work. Further, the results will be applicable to the present case, even though, as just stated, some experiments are open to criticism.

Contact-potential measurements show that polarizations of several volts are detectable in an X-ray discharge-tube several seconds after the cessation of a discharge, or even an applied field<sup>(3)</sup>. Spark-gaps exhibit similar phenomena<sup>(4)</sup>. It is stated that a residual charge corresponding to a large fraction of the quantity transferred by the discharge is recoverable<sup>(4)</sup>.

Sparking-potential measurements show that effects of similar magnitude are observable even in pure discharge-tubes<sup>(5, 1)</sup>; in spark-gaps<sup>(6, 10)</sup> and  $\alpha$ -particle counters<sup>(7, 10)</sup> they are many times greater.

A lag of several per cent. of the applied voltage (400) with a life of at least 1/50 second has been recorded for the mass-spectrograph<sup>(8)</sup>.

Without claiming any relation between these effects, or proving that they are due to surface-charges, it may certainly be stated that if in any way charges were involved, they could not have failed to be detected in the present experiments, save on one condition *that, with respect to electrical charges, the system responsible for polarization, whether reversible or irreversible, must be a closed one.*

By assuming that reversible polarization is due to a *charged layer at the cathode surface*, however, we are provided with an explanation not only of contact-potential variations<sup>(4)</sup>, but of sparking-potential variations<sup>(5)</sup>, build-up lag variations<sup>(1)</sup>, and the effect of radiations on these<sup>(5, 1)</sup>, for all these may be correlated with variation of the emissivity of the cathode surface.

Grease layers<sup>(3)</sup>, layers of oxide<sup>(7)</sup> or chemical compounds<sup>(2, 8)</sup>, thick<sup>(10)</sup> or monomolecular<sup>(4, 5)</sup> layers of condensed gas, whether native or an impurity, may all be postulated for particular cases. Temporary, reversible, polarization, however, would appear to be a general property of all discharge-systems irrespective of conditions; and if, as has been shown, a closed system of charged layers must be postulated, we must conclude that *reversible polarization is a manifestation of "double-layers" at the cathode surface.* The phenomena mentioned in the preceding paragraph will be but other manifestations of the same influence.

Such layers, whatever the actual mechanism involved, represent dynamic equilibrium of the gas and electrode at

## 1110 *The Presence of Charges at an Electrode Surface.*

their interface. They will be influenced by electric fields, radiations, and particularly by such an active process as a discharge, where radiations are intense and the gas is abnormally active. On the active agent being removed or reduced, they will be left in unstable equilibrium; their recovery could conceivably be slow enough to account for the facts cited above.

### *Summary.*

The possibilities of a charge or field existing at an electrode surface after a discharge are investigated.

It is shown that with brass in air no field greater than 1/100 volt was present 1/10 mm. distant after a spark, and no charge as great as 1/100 volt for a capacity of some cms. was given up by a steel needle after 1/1000 second. Impurities etc. caused no appreciable change.

A *résumé* is given of related work, and it shows that if charges actually are involved they must be immeasurably greater than those detectable here. From this it is concluded that, with respect to electrical charges, the system responsible for polarization, whether reversible or irreversible, must be a closed one.

When this conclusion is applied to the charged cathodic layers which are shown to correlate and explain contact potential, sparking potential, and lag variations, it follows that reversible polarization, like them, is a manifestation of "double-layers" at the cathode surface.

Such layers may be expected to attend dynamic equilibrium of the gas-electrode interface.

"Wall" and insulator effects are discussed.

The writer has pleasure in expressing his great obligation to Professor Ornstein and to the International Education Board.

### *References.*

- (1) Clarkson, *Phil. Mag.* iv. p. 121 (1927).
- (2) Kovarik, *Phys. Rev.* xiii. p. 272 (1919).
- (3) Compton and Ross (also Ratner etc.), *Phys. Rev.* iii. p. 207 (1915).
- (4) Gaede, etc., etc., *Ann. d. Phys.* xiv. p. 669 (1904).
- (5) Taylor, *Utrecht Dissertation*, Sept. 1928.
- (6) Peek (also Züber etc.), 'Dielectric Phenomena,' New York, 1915.
- (7) Gorton and Warburg (also Geiger etc.), *Ann. d. Phys.* xviii. p. 28 (1905).
- (8) Aston, *Proc. Roy. Soc. A*, cxv. p. 487 (1926).
- (9) See discussion, *Proc. Phys. Soc.* i. p. 13 (1926).
- (10) Zelany, *Phys. Rev.* xvi. p. 102 (1920); xix. p. 556 (1922).

CXIV. *On the Fine Structure of the Spectrum Lines of Thallium in the Ultra-violet.* By WALI MOHAMMAD, M.A. (Punjab), B.A. (Cantab.), Ph.D. (Göttingen), Professor of Physics, Lucknow University, and S. B. L. MATHUR, M.Sc.\*

### I. Introduction.

THE work under report forms the third instalment of the investigation undertaken by the authors on the fine structure of the spectrum lines in the ultra-violet. The authors' results on cadmium have been published in the Phil. Mag. of July, 1927 while those on zinc are under publication.

### II. Previous Work.

Some of the thallium lines appear to have been among the first to be investigated for fine structure.

Michelson<sup>1</sup>, Fabry and Perot<sup>2</sup>, and Janicki<sup>3</sup> determined the structure of  $\lambda$  5351, while Barnes<sup>4</sup> investigated  $\lambda$  5439. Back<sup>5</sup>, in course of his researches on the Zeeman effect of certain lines, has dealt with the structure of the lines  $\lambda$  5351,  $\lambda$  3776, and  $\lambda$  2767. These appear to be the only four lines of thallium of which the fine structure has been attempted.

### III. Experimental Arrangement.

The experimental arrangement was the same as described previously. Briefly stated, light from an arc in vacuum consisting of a Wehnelt oxy-cathode of platinum and the anode of thallium was rendered parallel by means of a quartz lens, and allowed to fall on a Hilger Quartz Lummer-Gehrcke plate (13 cm. long, 0.46 mm. thick). The interference fringes from the upper face of the L-G. plate were focussed on the slit of a Hilger E<sub>2</sub> quartz spectrograph and photographed on Ilford Special Rapid plates. The wavelength of the satellites was calculated from von Baeyer's formula. As a control the cadmium line  $\lambda$  4800, which has been examined by several investigators, was photographed and its structure determined. The agreement between the observed values of other experimenters and our own was sufficiently close to show that the Lummer plate was giving satisfactory results.

\* Communicated by the Authors.



IV. *Difficulties.*

Among the difficulties met with in working out the photographs, the following are worth mentioning :—

(a) Absence of a means of eliminating a ghost if one is present. The performance of the given plate showed it to be almost free from ghosts, but another plate or, still better, a crossed plate arrangement would have been more desirable.

(b) The fringes are not always sharp—some components are well defined, while others are somewhat diffuse. This makes accurate measurement difficult.

V. *Results.*

The results of the investigation are given below. The wave-lengths are taken from Exner and Haschek, and the figures in brackets indicate the intensity as estimated from the photographs.

(1) *Line 3775·89 (500).*

This line shows six satellites as follows :—

$$+0\cdot054 (5), \quad +0\cdot042 (5), \quad +0\cdot017 (9), \quad 0\cdot000 (10), \\ -0\cdot020 (9), \quad -0\cdot035 (6), \quad -0\cdot052 (5).$$

It will be noted that the satellites are situated more or less symmetrically about the principal line.

This is an interesting line, as the recent experiments of Grottrian<sup>6</sup> and Carroll<sup>7</sup> have indicated that the ground orbit of the valence electron is  $1, \pi$  orbit and not  $1, \sigma$  orbit as in the case of other metals. Narayan<sup>8</sup> and his co-workers found that the absorption band  $\lambda 3775$  is distinctly asymmetrical, being sharply defined on the wave-length side, but with increasing density of the vapour gradually spreads out towards the red end. They concluded that this line shows the existence of anomalous dispersion. Back, using a concave grating, found the following structure :—

$$+0\cdot058 (3), \quad 0\cdot000 (10) \text{ double?}, \quad -0\cdot101 (8).$$

It should be noted that Back suspects the principal line itself to be double, but gives no clue to its structure.

(2) *Line 3529·52 (100).*

The line appears to have the following structure :—

$$0\cdot000 (10), \quad -0\cdot027 (6).$$

There is some doubt about the sign of this satellite. In some photographs the satellite appears to be negative, while

in others it appears to be positive. In two of the photographs a very faint satellite appears at  $+0.044$ , and in four others another satellite at  $-0.047$ . Combining all these values, we get the following structure:—

$$+0.044, 0.000, -0.027, -0.047.$$

(3) *Line* 3519.38 (500).

This line shows the following structure:—

$$+0.043 (8), +0.026 (6), 0.000 (10), -0.015 (9), \\ -0.029 (6), -0.044 (6).$$

(4) and (5) *Lines* 3229.89 (20) and 3230.7 (1).

This is a doublet consisting of two lines of unequal intensity, the one of longer wave-length being very faint indeed. Its close proximity to the line 3229.89 makes it very difficult to differentiate a satellite from the weak principal line. The structure of line 3229.89 is as follows:—

$$0.000 (10), -0.019 (5).$$

There is a suspicion of another satellite at  $-0.038$ , but it may be due to a ghost.

(6) *Line* 2921.66 (20).

This line shows only one satellite:—

$$+0.016 (9); 0.000 (10).$$

(7) *Line* 2918.42 (100).

This line also only shows one satellite:—

$$+0.027 (9); 0.000 (10).$$

Two photographs on two different plates show another satellite situated at  $-0.019$ .

(8) *Line* 2826.45 (10).

This line also shows one satellite:—

$$+0.023 (5); 0.000 (10).$$

(9) *Line* 2767.87 (20).

This line was found by the authors to possess three satellites clustered together about the principal line. But the satellites were not well resolved and could not be measured. Back gives the following structure of this line:—

$$2767.913 (5), \\ \cdot 882 (4), \\ \cdot 852 (3), \\ \cdot 833 (3).$$

(10) and (11) *Lines* 2710·74 (5) and 2709·33 (20).

This again, is a close doublet. Both the lines appear to be simple, but, on account of the faintness of the images on the photographs, this cannot be decided with certainty.

(12) *Line* 2580·25 (3).

This line appears simple. As in the former case, on account of the faintness of the image, the conclusion is not definite.

## VI. Summary.

Thallium is not very rich in lines. According to Exner and Haschek there are 21 lines between 6550·15 and 2580·25. Out of these, 11 are very weak, having an intensity less than 4 (maximum intensity 500) and thus, except 2580·25, these could not be photographed. The structure of the remaining lines has been determined for the first time. Further work on the structure and the energy-levels is in progress.

## References.

- (1) Michelson, *Phil. Mag.* (5) xxxiv. pp. 280-299 (1892).
- (2) Fabry and Perot, *Comptes Rendus*, cxxvi. pp. 407-410 (1898); also *Ann. de Chim. et Phys.* xvi. pp. 115-144 (1899).
- (3) Janicki, *Ann. de Physik*, xix. pp. 36-79 (1906); *ibid.* xxix. pp. 856-857 (1909).
- (4) Barnes, *Astrophys. Journ.* xix. pp. 190-211 (1904); *Phil. Mag.* (6) vii. pp. 485-503 (1904).
- (5) Back, *Ann. de Physik*, lxx. pp. 333-372 (1923).
- (6) Grotrian, *Zeits. f. Physik*, vols. ii., iii., & iv. pp. 218-31 (1922).
- (7) Carroll, *Proc. Roy. Soc. A*, vol. ciii. pp. 334-339 (1923);
- (8) Narayan, *Proc. Roy. Soc. A*, cvi. p. 596 (1924).

CXV. *On a Curious Optical Theorem and its Geometrical Basis.* By ALFRED A. ROBB, Sc.D., F.R.S.\*

THE following curious theorem, though purely geometrical in its character, is most simply understood from an optical illustration; and, indeed, it was from this standpoint that the writer originally arrived at the result.

Let us imagine a shell exploding in free space into  $n$  particles, which fly off in various directions with various velocities, and suppose that, after the explosion, a flash of light starts out from particle 1 at any instant P and goes to particle 2, thence to particles 3, 4...  $n$  in succession, and finally back to particle 1, where it arrives at an instant Q.

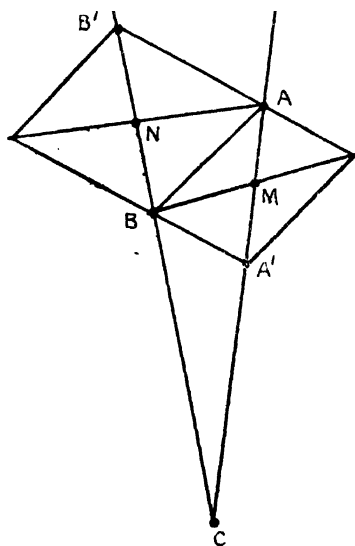
\* Communicated by the Author.

Further, suppose a second flash of light starts out from particle 1, also at the instant P, and makes a circuit of the particles in the reverse order; that is to say, it goes first to particle  $n$ , thence to particle  $n-1$ , and so on in succession back to particle 1; then the theorem asserts that it will also arrive at the instant Q.

The assumptions are that the  $n$  particles start from simultaneous contact and move with uniform velocities.

The result is very simply deduced on the basis of the author's 'Theory of Time and Space,' but may also be proved in other ways.

Fig. 1.



Let CA and CB be two intersecting inertia lines, and let AB be an optical line intersecting both, so that B is *after* C and A is *after* B.

Let the second optical line through A in the plane of ABC intersect CB in B', and let the second optical line through B in the plane intersect CA in A'.

If  $M$  be the centre of an optical parallelogram of which  $A'$ ,  $B$ , and  $A$  are three corners, we know that  $BM$  is normal to  $A'A$ .

Similarly, if  $N$  be the centre of an optical parallelogram of which  $B$ ,  $A$ , and  $B'$  are three corners, we have  $AN$  normal to  $BB'$ .

Let us denote the lengths: CB by  $a$ , CA by  $b$ , MA by  $g$ , BN by  $h$ , and let the hyperbolic angle BCA be denoted by  $C$ . Then we have:

$$\frac{a+h}{b} = \cosh C = \frac{b-g}{a}.$$

Thus

$$h = b \cosh C - a$$

$$\text{and} \quad g = b - a \cosh C.$$

Also, since  $A'B$  and  $AB'$  are parallel, we have:

$$\frac{2g}{2h} = \frac{b-2g}{a}.$$

Thus

$$\frac{b-a \cosh C}{b \cosh C - a} = \frac{2a \cosh C - b}{a}$$

$$\text{or} \quad a^2 + b^2 - 2ab \cosh C = 0.$$

Thus

$$\cosh C = \frac{a^2 + b^2}{2ab} = \frac{1}{2} \left( \frac{b}{a} + \frac{a}{b} \right).$$

Comparing this with the formula

$$\cosh C = \frac{1}{2}(e^C + e^{-C}),$$

we find for the absolute value of  $C$ ,

$$C = \log \frac{b}{a},$$

$$\text{since} \quad b(b-2g) = a^2,$$

and therefore  $b > a$ .

Thus, if we have two particles separating from contact, and moving with uniform velocity with respect to one another, and we measure "local times" from the instant of contact; then, if a flash of light starts out from the one at "local time"  $a$ , and arrives at the other at "local time"  $b$ , we shall have

$$C = \log \frac{b}{a},$$

where  $C$  is what I have elsewhere called the "rapidity" \* of the one particle with respect to the other.

\* The rapidity is defined thus:

$$\text{rapidity} = \tanh^{-1} \frac{v}{V},$$

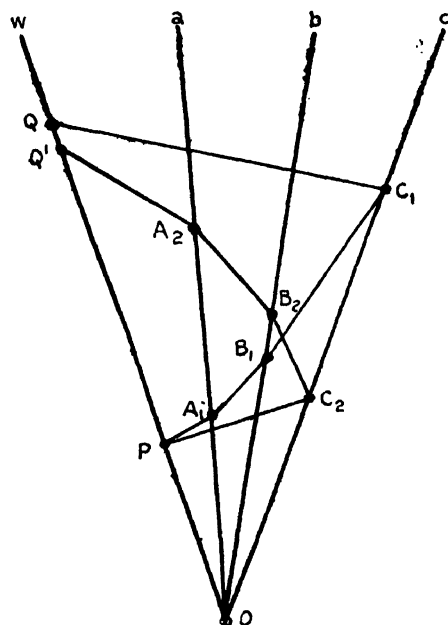
where  $v$  is the velocity of the one particle with respect to the other and  $V$  is the velocity of light.

In order now to prove the theorem, let  $Ow, Oa, Ob, Oc, \dots$  be a set of inertia lines all intersecting in  $O$ .

For the sake of definiteness suppose that we have just four, though the method of proof obviously applies to any number.

Take any element  $P$  in  $Ow$  which is *after*  $O$ .

Fig. 2.



Let $A_1$	be the first element in $Oa$	which is <i>after</i> $P$ ,
„ $B_1$	„ „ „ $Ob$	„ „ „ $A_1$ ,
„ $C_1$	„ „ „ $Oc$	„ „ „ $B_1$ ,
„ $Q$	„ „ „ $Ow$	„ „ „ $C_1$ .

Similarly,

let $C_2$	be the first element in $Oc$	which is <i>after</i> $P$ ,
„ $B_2$	„ „ „ $Ob$	„ „ „ $C_2$ ,
„ $A_2$	„ „ „ $Oa$	„ „ „ $B_2$ ,
„ $Q'$	„ „ „ $Ow$	„ „ „ $A_2$ .

Then  $PA_1, A_1B_1, B_1C_1, C_1Q$  are all optical lines.

Similarly  $PC_2, C_2B_2, B_2A_2, A_2Q'$  are all optical lines.

Thus, using our formula for the hyperbolic angle, we see that

$$\frac{OA_1}{OP} = \frac{OQ'}{OA_2},$$

$$\frac{OB_1}{OA_1} = \frac{OA_2}{OB_2},$$

$$\frac{OC_1}{OB_1} = \frac{OB_2}{OC_2},$$

$$\frac{OQ}{OC_1} = \frac{OC_2}{OP}.$$

Thus, multiplying corresponding sides, we get

$$\frac{OQ}{OP} = \frac{OQ'}{OP}$$

$$\text{or} \quad OQ = OQ',$$

and, since Q and Q' are each *after* O, it follows that Q' must be identical with Q, as was to be proved.

A similar result will obviously hold if we suppose that the particles are all approaching simultaneous contact and the flashes of light start out *before* the instant of contact.

Apart from Time-Space theory, the theorem has an interpretation in ordinary three-dimensional geometry and also in Euclidean geometry of any higher number of dimensions. We shall state the theorem as it holds for the case of three dimensions.

Referring to fig. 2, suppose that we have any number  $n$  of straight lines all intersecting in a point O, and such that they all lie inside a certain quadric cone having O as vertex.

Now if, for convenience of reference, we call one half of the cone the "upper half" and the other the "lower half," and, taking a point P on the first of the set of straight lines and lying (say) inside the upper half of the cone, let the upper half of a similar and similarly situated cone having P as vertex intersect the second line in a point  $A_1$ .

Again, let the upper half of a similar and similarly situated cone having  $A_1$  as vertex intersect the third line in a point  $B_1$ .

Proceeding thus round the whole set of straight lines, we arrive at last at a point Q in the first line.

The theorem then asserts that, starting again at P, and making the circuit of the lines in the reverse order, we arrive again at the same point Q.

Any line passing through the origin and whose equations are

$$\frac{x}{l} = \frac{y}{m} = \frac{z}{n},$$

will lie within the cone

$$\frac{z^2}{c^2} - \frac{x^2}{a^2} - \frac{y^2}{b^2} = 0, \quad . \quad . \quad . \quad (1)$$

provided that

$$\frac{n^2}{c^2} - \frac{l^2}{a^2} - \frac{m^2}{b^2} > 0. \quad . \quad . \quad . \quad (2)$$

The cone (1) is asymptotic to the system of hyperboloids of two sheets :

$$\frac{z^2}{c^2} - \frac{x^2}{a^2} - \frac{y^2}{b^2} = K^2. \quad . \quad . \quad . \quad (3)$$

If now we consider the region inside one half of the cone (1), the position of any point in the region may be determined if we know the direction cosines of the radius vector from the origin through the point, together with the value of K for the particular hyperboloid of the system which passes through the point. Thus, if the point lies in the line

$$\frac{x}{l} = \frac{y}{m} = \frac{z}{n} = r,$$

we shall have

$$\left( \frac{n^2}{c^2} - \frac{l^2}{a^2} - \frac{m^2}{b^2} \right) r^2 = K^2 \quad . \quad . \quad . \quad (4)$$

for the point in question.

Consider now any two lines passing through the origin and satisfying condition (2), say

$$\frac{x}{l_1} = \frac{y}{m_1} = \frac{z}{n_1} = r$$

and

$$\frac{x}{l_2} = \frac{y}{m_2} = \frac{z}{n_2} = r,$$

and let  $(x_1, y_1, z_1, r_1)$  be any point on the first line which lies within the selected half of the cone (1).

The equation of a cone similar and similarly situated to cone (1), but having its vertex at this point, will be

$$\frac{(z - n_1 r_1)^2}{c^2} - \frac{(x - l_1 r_1)^2}{a^2} - \frac{(y - m_1 r_1)^2}{b^2} = 0. \quad . \quad (5)$$



If this cone intersects the second line in a point  $(x_2, y_2, z_2, r_2)$ , we shall have

$$\frac{(n_2 r_2 - n_1 r_1)^2}{c^2} - \frac{(l_2 r_2 - l_1 r_1)^2}{a^2} - \frac{(m_2 r_2 - m_1 r_1)^2}{b^2} = 0.$$

This may be written in the form

$$\left(\frac{n_2^2}{c^2} - \frac{l_2^2}{a^2} - \frac{m_2^2}{b^2}\right) r_2^2 - 2\left(\frac{n_2 n_1}{c^2} - \frac{l_2 l_1}{a^2} - \frac{m_2 m_1}{b^2}\right) r_2 r_1 + \left(\frac{n_1^2}{c^2} - \frac{l_1^2}{a^2} - \frac{m_1^2}{b^2}\right) r_1^2 = 0.$$

If now  $K_1$  and  $K_2$  be the values of the  $K$ s for the points  $(x_1, y_1, z_1, r_1)$  and  $(x_2, y_2, z_2, r_2)$  respectively, this last result may be written in the form

$$K_2^2 - 2 \frac{\left(\frac{n_2 n_1}{c^2} - \frac{l_2 l_1}{a^2} - \frac{m_2 m_1}{b^2}\right)}{\sqrt{\left(\frac{n_2^2}{c^2} - \frac{l_2^2}{a^2} - \frac{m_2^2}{b^2}\right)} \sqrt{\left(\frac{n_1^2}{c^2} - \frac{l_1^2}{a^2} - \frac{m_1^2}{b^2}\right)}} K_2 K_1 + K_1^2 = 0.$$

Now it is to be observed that this equation is symmetrical with respect to the two lines  $(l_1, m_1, n_1)$  and  $(l_2, m_2, n_2)$ , so that we can make the substitution  $\left(\frac{l_2 m_2 n_2 l_1 m_1 n_1}{l_1 m_1 n_1 l_2 m_2 n_2}\right)$  without altering it. Also we can interchange  $K_2$  and  $K_1$  without altering the equation.

It may be proved that, under the conditions

$$\left(\frac{n_1^2}{c^2} - \frac{l_1^2}{a^2} - \frac{m_1^2}{b^2}\right) > 0 \quad \text{and} \quad \left(\frac{n_2^2}{c^2} - \frac{l_2^2}{a^2} - \frac{m_2^2}{b^2}\right) > 0,$$

the roots of this equation (regarded as an equation for  $K_2$  in terms of  $K_1$ ) are always real, and only become equal when the lines  $(l_1, m_1, n_1)$  and  $(l_2, m_2, n_2)$  coincide.

Further, if  $K_2'$  and  $K_2''$  be the two roots, we have  $K_2' K_2'' = K_1^2$ , so that one of them (say  $K_2''$ ) is greater than  $K_1$ , while the other (say  $K_2'$ ) is less than  $K_1$ .

But we know that a line which is parallel to any line which would lie within a cone will itself intersect the cone in two points, one of which lies on one half of the cone and the other on the other half; so that  $K_2''$  will correspond to a point on one half of cone (5), while  $K_2'$  will correspond to a point on the other half.

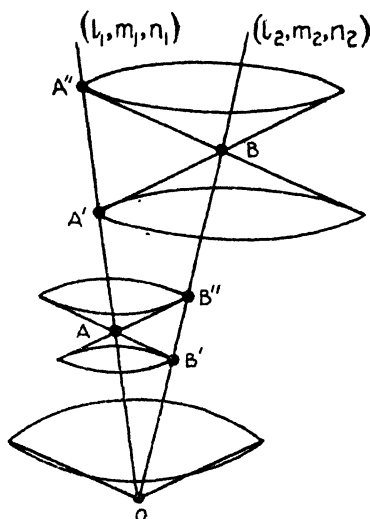
If, then, for convenience of reference, we refer to the halves of these similar and similarly situated cones as "upper" halves and "lower" halves, and suppose that the

point  $(x_1, y_1, z_1, r_1)$  lies inside the upper half of cone (1), then it is easy to see that the point corresponding to  $K_2''$  lies on the upper half of cone (5), while the point corresponding to  $K_2'$  lies on the lower half of cone (5).

Thus the ratio  $\frac{K_2''}{K_1}$  will be the larger root of the equation

$$\left(\frac{K_2}{K_1}\right)^3 - 2 \frac{\left(\frac{n_2 n_1}{c^2} - \frac{l_2 l_1}{a^2} - \frac{m_2 m_1}{b^2}\right)}{\sqrt{\frac{n_2^2}{c^2} - \frac{l_2^2}{a^2} - \frac{m_2^2}{b^2}} \sqrt{\left(\frac{n_1^2}{c^2} - \frac{l_1^2}{a^2} - \frac{m_1^2}{b^2}\right)}} \left(\frac{K_2}{K_1}\right) + 1 = 0 \quad (6)$$

Fig. 3.



and this is a perfectly definite number which is independent of the actual position of the point  $(x_1, y_1, z_1, r_1)$  on the line  $(l_1, m_1, n_1)$ .

In the same way, if we take a cone similar and similarly situated to cone (1), and having its vertex inside the selected half of cone (1) on the line  $(l_2, m_2, n_2)$ , we shall arrive at the same quadratic equation for the ratio of the  $K$  of a point of intersection of this cone with the line  $(l_1, m_1, n_1)$  to the  $K$  of the vertex of the cone.

Also the larger root of the equation will be the ratio of the  $K$  of the point of intersection of the line  $(l_1, m_1, n_1)$  with the upper half of the cone to the  $K$  of the vertex.

Thus, provided we confine ourselves to the upper halves of the cones, we get the same ratio for the  $K$  of the point of intersection to the  $K$  of the vertex, no matter which of the two lines the vertex lies in, and no matter where it lies in either line. Thus, if we denote the  $K$  coordinate of a point  $A$  by  $K(A)$ , our results, as illustrated in the figure, are as follows:—

$$\frac{K(B'')}{K(A)} = \frac{K(A'')}{K(B)},$$

no matter where  $A$  may be situated on the line  $(l_1, m_1, n_1)$  or where  $B$  may be situated on the line  $(l_2, m_2, n_2)$ , provided that  $A$  and  $B$  lie inside the upper half of the cone whose vertex is  $O$ .

Also

$$\frac{K(B')}{K(A)} = \frac{K(A')}{K(B)}.$$

Further,

$$K(B') \cdot K(B'') = \{K(A)\}^2$$

$$\text{and} \quad K(A') \cdot K(A'') = \{K(B)\}^2.$$

Similar results hold, of course, if  $A$  and  $B$  lie inside the lower half of the cone whose vertex is  $O$ .

Making use of these  $K$  coordinates, we are now in a position to prove the theorem in a manner exactly analogous to that in which we proved it for the Time-Space case.

Thus, referring again to fig. 2, we have

$$\frac{K(A_1)}{K(P)} = \frac{K(Q')}{K(A_2)},$$

$$\frac{K(B_1)}{K(A_1)} = \frac{K(A_2)}{K(B_2)},$$

$$\frac{K(C_1)}{K(B_1)} = \frac{K(B_2)}{K(C_2)},$$

$$\frac{K(Q)}{K(C_1)} = \frac{K(C_2)}{K(P)}.$$

Thus, multiplying corresponding sides, we get

$$\frac{K(Q)}{K(P)} = \frac{K(Q')}{K(P)}$$

$$\text{or} \quad K(Q) = K(Q'),$$

and therefore  $Q'$  and  $Q$  lie on the same hyperboloid and on the same sheet of it.

But  $Q'$  and  $Q$  also lie on the same line through the origin, and so it follows that  $Q'$  must be identical with  $Q$ , as was to be proved.

It is clear that a similar result holds if, instead of taking the points of intersection of the various lines with the upper halves of the cones, we always take the points of intersection with the lower halves.

In considering the extension of this theorem to space of more than three dimensions, there are several points which have to be observed.

In the first place the equation of any proper cone in three dimensions may always be put in the form

$$\frac{x^2}{a^2} + \frac{y^2}{b^2} - \frac{z^2}{c^2} = 0.$$

If we make a second square negative, we get a cone of the same general type. If, on the other hand, we consider cones in more than three dimensions, things are rather more complicated.

Thus in four dimensions we should have two essentially different types of cone whose equations might be put in one of the forms

$$\frac{x^2}{a^2} + \frac{y^2}{b^2} + \frac{z^2}{c^2} - \frac{w^2}{d^2} = 0,$$

and

$$\frac{x^2}{a^2} + \frac{y^2}{b^2} - \frac{z^2}{c^2} - \frac{w^2}{d^2} = 0.$$

Only the first of these can be divided into two halves by a single point, and this is the type of cone to which the theorem directly applies.

In general, for a larger number of dimensions than three, say for  $m$ , the equation of the cone, when expressed as the sum of  $m$  squares equated to zero, must be such that all the squares *with one exception* are of the same sign.

Under these circumstances it may be proved that the roots of the quadratic equation for  $K_2$  in terms of  $K_1$  are always real under conditions analogous to those which we gave when considering the three-dimensional case.

There is a limiting case of this theorem in which the  $n$  straight lines are all parallel instead of meeting in a point, but are such that any one of them would lie within a quadric cone of given form and orientation, having its vertex on the line. It may hardly be regarded as necessary to give

1124 *A Curious Optical Theorem and its Geometrical Basis.*

a separate proof of this, since we have proved that it must hold for the case of lines all passing through one point, however distant the point may be and however small the angles between them. As, however, the actual method of proof breaks down for the case of parallel lines, the following hints as to the mode of procedure may prove useful.

Let the system of lines be

$$\frac{x-\bar{x}}{l} = \frac{y-\bar{y}}{m} = \frac{z-\bar{z}}{n} = r,$$

where 
$$\frac{n^2}{c^2} - \frac{l^2}{a^2} - \frac{m^2}{b^2} > 0 \quad \text{as before,}$$

and, for convenience, let the points  $(\bar{x}, \bar{y}, \bar{z})$  be always selected, so that

$$\frac{l\bar{x}}{a^2} + \frac{m\bar{y}}{b^2} - \frac{n\bar{z}}{c^2} = 0,$$

which is always possible provided that

$$\frac{l^2}{a^2} + \frac{m^2}{b^2} - \frac{n^2}{c^2}$$

be not zero, as is here the case.

Proceeding as before, we find that

$$\left(\frac{n^2}{c^2} - \frac{l^2}{a^2} - \frac{m^2}{b^2}\right)(r_2 - r_1)^2 = \left\{ \frac{(\bar{x}_2 - \bar{x}_1)^2}{a^2} + \frac{(\bar{y}_2 - \bar{y}_1)^2}{b^2} - \frac{(\bar{z}_2 - \bar{z}_1)^2}{c^2} \right\}.$$

It may be proved that the expression on the right can never be negative, provided that

$$\frac{l^2}{a^2} + \frac{m^2}{b^2} - \frac{n^2}{c^2} < 0$$

and

$$\frac{l(\bar{x}_2 - \bar{x}_1)}{a^2} + \frac{m(\bar{y}_2 - \bar{y}_1)}{b^2} - \frac{n(\bar{z}_2 - \bar{z}_1)}{c^2} = 0,$$

(as is here the case), and it can only be zero when

$$\bar{x}_2 - \bar{x}_1 = \bar{y}_2 - \bar{y}_1 = \bar{z}_2 - \bar{z}_1 = 0^*.$$

Since the above equation for  $(r_2 - r_1)$  is unaltered when we make the substitution

$$\begin{pmatrix} \bar{x}_2 & \bar{y}_2 & \bar{z}_2 & \bar{x}_1 & \bar{y}_1 & \bar{z}_1 \\ \bar{x}_1 & \bar{y}_1 & \bar{z}_1 & \bar{x}_2 & \bar{y}_2 & \bar{z}_2 \end{pmatrix},$$

we may prove our theorem in a manner analogous to that

\* A similar result holds for  $n$  dimensions.

previously employed, except that we use differences instead of ratios, and add instead of multiply.

In the optical problem the analogous state of things would be that in which the  $n$  particles remained at constant distances from one another, and one would hardly be surprised, in this case, that the light should take the same time to make the circuit in one order as it does in the reverse order.

---

CXVI. *An Optical Method of Measuring Small Vibrations.*  
By H. A. THOMAS, M.Sc., and G. W. WARREN, B.Sc. (of  
the National Physical Laboratory)\*.

SUMMARY.

AN interferometer method of measuring small mechanical vibrations, such as those encountered in telephone diaphragms and structures, is described, and its application to the measurement of the vibration of a stiff reed is considered. Substantial agreement between the theory of such a vibration is obtained, and its use for the study of the vibration of light moving systems is suggested.

---

*Description of Method.*

THE essential principle of operation is that of an interferometer in which one plate is attached to the vibrating system and the other plate is fixed. Referring to fig. 1(A), a small glass plate 0.5 cm. square and 1 mm. thick optically plane was ground on one side so as to be non-reflecting. This block A was gummed to a vibrating reed B, actuated by the magnet mechanism C. This reed and magnet was a standard cone loud speaker movement.

Above this block a second sheet of glass D was supported by the brass carriage E, which was capable of adjustment by means of three screws F. These screws served to adjust the plate D until it was parallel to A, and were tapped into a rigid block G fixed to the stationary portion of the magnet mechanism.

A quartz mercury vapour lamp H and lens J gave a parallel beam, and a monochromatic filter K permits only the mercury green ray of wave-length  $0.5461 \times 10^{-3}$  mm. to be admitted to the interferometer. The glass prism L gave

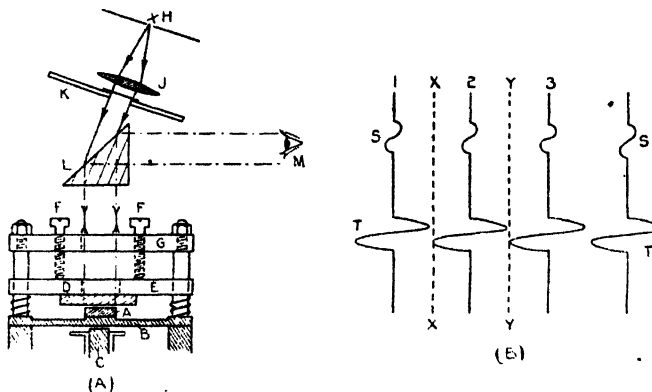
\* Communicated by Sir J. E. Petavel, K.B.E., F.R.S.

a reflexion of the reflected beam from A, which can, therefore, be observed by the eye at M.

With the block A stationary, interference fringes are observed at M, as shown in fig. 1 (B), and if the block A moves  $\frac{\lambda}{2}$ , where  $\lambda$  is the wave-length of the light, the fringes will shift once, *i. e.*, fringe 1 will shift to position 2, 2 will shift to position 3, and so on.

Now let the reed vibrate a very small amount, and assume that its vibrations are sinusoidal in form, then all the fringes will execute a simple harmonic motion about the original stationary position and always parallel to that position.

Fig. 1.



This is illustrated at S, and it is clear that the fringes will disappear, but if the amplitude is now increased till the peak value of the reed movement is  $\frac{\lambda}{4}$ , we shall get a peak move-

ment of each fringe equal to half the distance between successive fringes, as shown at T, and since the fringes 1 and 2 remain longest along the line X, a fringe will appear due to the persistence of vision. Similarly a fringe Y will appear, and therefore when the amplitude of vibration reaches a maximum value of  $\frac{\lambda}{4}$ , a new set of fringes will appear equally spaced as before, but shifted by half the distance between a pair of the original fringes.

If the amplitude is still further increased, the fringes will

again disappear and will reappear when the maximum amplitude is  $\frac{\lambda}{2}$ , and so on. In this way we see that we get no fringes at maximum amplitudes of  $\frac{\lambda}{8}$ ,  $\frac{3\lambda}{8}$ ,  $\frac{5\lambda}{8}$ ,  $\frac{7\lambda}{8}$ , etc., or in general  $\frac{\lambda}{8} + \frac{n\lambda}{4}$  where "n" is an integer, and fringes at amplitudes of  $\frac{\lambda}{4}$ ,  $\frac{2\lambda}{4}$ ,  $\frac{3\lambda}{4}$ , etc., or in general  $\frac{n\lambda}{4}$ .

Since the rapidity of movement is greatest for a large amplitude, the visibility of the fringes gets poorer as "n" is increased, but it was found possible to count the reappearances up to 30 shifts. The point of disappearance was more definite than the point of maximum fringe intensity, and the accuracy with which this disappearance could be detected was found to be 1 per cent. of one wave-length of the light used. This corresponds to 1 per cent. of  $0.5 \times 10^{-4}$  cm. =  $0.5 \times 10^{-6}$  cm.

#### *Application to the Study of a Vibrating Reed.*

The loud speaker reed used for the preceding vibrating object was examined at various audible frequencies and amplitudes.

The relation between movement and current at various frequencies is shown in fig. 2, from which it will be noticed that the amplitude is very nearly proportional to the current. Plotting amplitude against frequency for two values of current, viz., 1 milliampere and 0.5 milliampere, we obtain fig. 3, which shows the resonance of the reed at a frequency of 1060.

It is interesting to compare the shape of this response characteristic with constant input current with the theory of a vibrating reed with fixed supports at both ends.

The general law of motion for a reed with a forcing vibration of sinusoidal form can be expressed as

$$\ddot{x} + b\dot{x} + \frac{\mu}{m}x = \frac{F}{m}\cos \omega t,$$

where

$\omega = 2\pi \times \text{frequency},$

$F = \text{Maximum value of the applied force},$

$m = \text{Mass of moving body},$

$\mu = \text{an elastic constant},$

$b = \text{a damping constant}.$



Fig. 2.

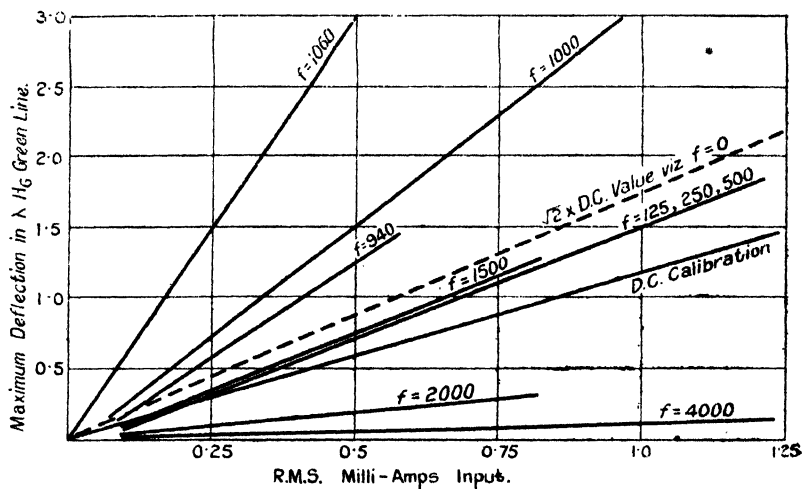
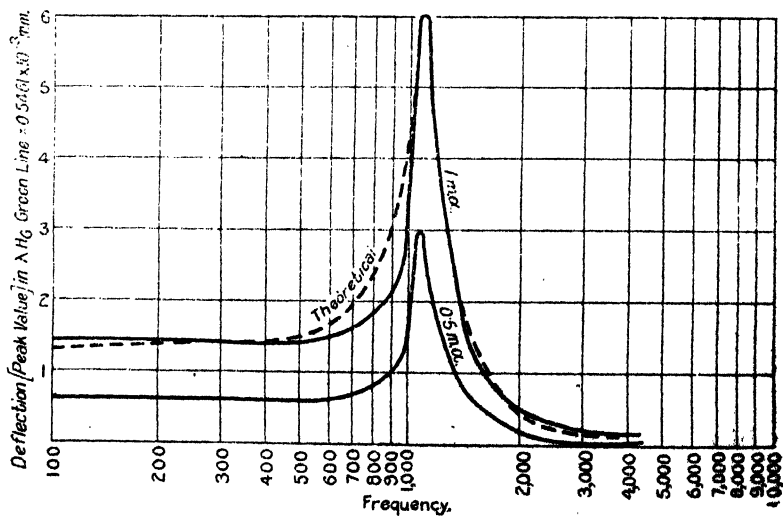


Fig. 3.



The particular solution of this differential equation is of the form

$$x = \frac{F}{m \sqrt{\left(\frac{\mu}{m} - \omega^2\right)^2 + b^2 \omega^2}} \cos(\omega t - \phi),$$

where

$$\tan \phi = \frac{b\omega}{\left(\frac{\mu}{m} - \omega^2\right)},$$

and the maximum displacement at a frequency  $f = \frac{\omega}{2\pi}$

$$\hat{x} = \frac{F}{m \sqrt{(\omega_0^2 - \omega^2)^2 + b^2 \omega^2}},$$

where  $\omega_0$  is  $2\pi \times$  the natural frequency of the reed

$$\omega_0 = \sqrt{\frac{\mu}{m}} \text{ and so at resonance } \hat{x} = \frac{F}{mb\omega},$$

and at a frequency far removed from resonance

$$\hat{x} = \frac{F}{m(\omega_0^2 - \omega^2)}.$$

In general

$$\hat{x} = \frac{A}{\sqrt{(f_0^2 - f^2)^2 + \frac{b^2 f^2}{4\pi^2}}},$$

where  $f_0$  = the natural frequency of the reed,

$f$  = the applied frequency,

and  $A$  is a constant.

Taking the measured value of  $\hat{x}$  at resonance in our case and substituting, we get

$$\frac{A}{b} = \frac{3180}{2\pi},$$

and substituting the measured value of  $\hat{x}$  at a frequency of 50 cycles per second obtained by exciting the magnet from a 50 cycle alternator, we get

$A = 0.672 \times 10^6$ , a constant of the reed,  
and  $b = 1.33 \times 10^3$ , the damping constant.

Using these values, we can now calculate the amplitude at any other frequency. This theoretical curve is shown in fig. 3, and comparative agreement with the experimental results is noticed.

The resonance value of the vibration amplitude with an input of 1 milliampere was only  $\frac{3}{1000}$  mm. When the reed is loaded by a loud speaker diaphragm, this resonance peak will be seriously reduced and so we see that the movement of a cone type of loud speaker with good signal intensity, corresponding to a current of 1 milliampere, is of the order of  $0.75 \times 10^{-3}$  mm. at frequencies below the natural resonance of the reed, and above this resonance frequency, the amplitude is of the order of  $0.1 \times 10^{-3}$  mm. At an amplitude of this value the accuracy of measurement is 5 per cent.

With a movement of  $10^{-3}$  mm. the accuracy is 0.5 per cent., and at the maximum movement which can be measured at present, due to poor visibility at large amplitudes, viz.,  $4 \times 10^{-3}$  mm., the accuracy is 0.12 per cent.

The method can readily be adopted to measure small vibrations of light systems, since the necessary reflecting surface attached to the vibrating system can be obtained in various ways which would introduce no appreciable loading effect.

A thin metal film could be sputtered on to the surface, as it is not necessary to have a perfectly flat surface. If the fringes are not straight, the same shifting effect will occur and the accuracy will in no way be affected.

CXVII. *Note on the Construction of a Valve Oscillator for use in Conductivity Measurements.* By J. W. WOOLCOCK, B.A., and D. M. MURRAY-RUST, B.A.\*

A valve oscillator similar to that described by Ulich † has been constructed by the authors and applied to the measurement of the conductivity of dilute solutions of acids and salts in non-aqueous solvents. Excellent minima are obtained even with resistances as high as 100,000 ohms, provided that not only the resistances but also the capacities in the bridge circuit are accurately balanced. The purpose of this note is to describe how such an instrument may conveniently be made from components sold in this country for the construction of broadcast receivers. Experiments with other types of valve oscillator gave far less satisfactory

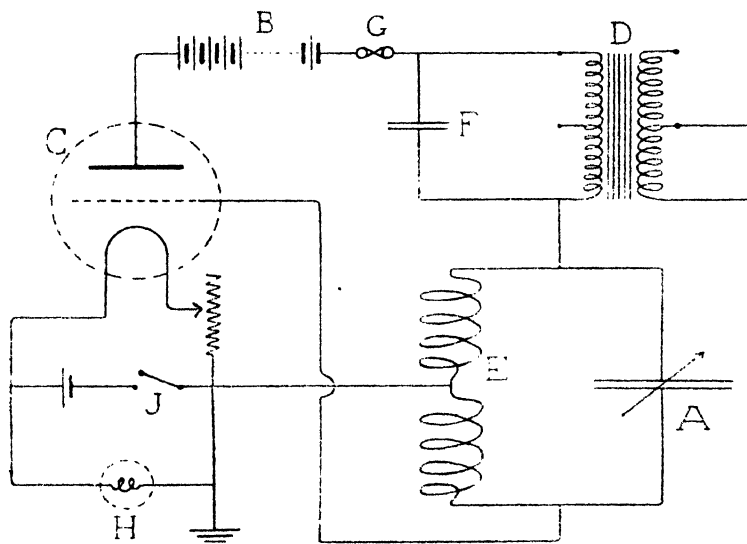
\* Communicated by Sir Harold Hartley, F.R.S.

† *Zeits. physikal Chem.* cxv. p. 377 (1926).

results than those obtained with the apparatus described here.

As the diagram shows, the circuit is of the auto-coupled type. The instrument consists of the oscillator unit, the variable condenser A, the dry cells B supplying the high tension, and a 2-volt accumulator to supply the filament current, the whole being enclosed in a galvanized iron box.

A condenser variable in steps of 0.002 mf. up to 0.2 mf. could have been built up from good quality Mansbridge condensers; in the instrument described a condenser box



made by the Cambridge Scientific Instrument Company is in use.

The valve C and transformer D were mounted on a wooden box provided with an ebonite panel. The two "1500-turn" Igranic coils E were mounted in an adjustable coil holder. The valve used is of the dull-emitter type designed for resistance capacity coupling, having an impedance of 70,000 ohms and an amplification factor of 35. The "Multi-ratio" transformer made by Radio Instruments Ltd. was connected in the plate circuit so that the voltage applied to the bridge could be varied. To maintain the oscillation when the connexion to the bridge was broken a 0.01 mf. condenser F was placed in parallel with

the primary. A fuse G was inserted in the high tension lead.

The iron box containing the instrument acted as an efficient shield; as an additional precaution the box was placed at a distance from the bridge and the connexion made by two lead-covered wires, the casing of which was connected to the box and to earth. The flash-lamp bulb H, mounted on the outside of the box, showed when the switch J was closed.

At high resistances the conductance of the cell due to the capacity between the plates is appreciable compared with the conductance of the electrolyte regarded as a pure resistance; the true minimum can only be obtained if the capacities as well as the resistances are balanced by connecting a variable condenser of about 0.002 mf. across the resistance box. It is also convenient to connect a small condenser across the cell for making the final adjustment, since very accurate balancing of the capacities is necessary in order to secure a sharp minimum with high resistances.

Instead of the single Bell telephone frequently employed a pair of Brown A-type head-telephones were used, and no satisfactory results were obtained until the connexions to one ear-piece had been removed and joined together leaving only the other in circuit. If both are connected in series, as supplied, it is impossible to obtain complete silence at the null-point, the setting of the condensers is not sharp and the minimum is difficult to read. This is due to the fact that the body of the observer has a large capacity to earth.

In order to obtain a good wave-form free from harmonics the coupling between the coils should be as loose as possible. Oscillations of the right strength with a frequency of 1000 cycles were obtained with the coils almost at right angles, using 1.8 volts low tension, 160 volts high tension, a capacity in the oscillating circuit of 0.09 mf. and the 1:1 ratio of the transformer. The introduction of grid bias was found to be unnecessary.

When the condensers in the bridge circuit have been adjusted, the minimum is found to be as sharp and easy to read at 100,000 ohms as at 1000 ohms, and perfect silence is obtained at the null-point over the whole range of resistance. In order to show that the minimum so obtained was the true one, the frequency of the oscillator was varied, and no alteration in the position of the minimum was observed; in every case the minimum was perfectly symmetrical. The same minima, but less easy to read, were obtained from the improved bridge circuit when the source of alternating

current was the Siemens' alternator previously in use in this laboratory.

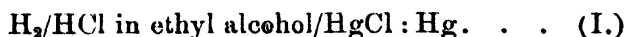
We wish to express our thanks to Dr. Ulich for a detailed description of his apparatus and much valuable advice, and to Mr. C. E. G. Bailey of Balliol College for assistance with the mathematical theory of the apparatus.

The Physical Chemistry Laboratory,  
Balliol College and Trinity College,  
Oxford.  
March, 1928.

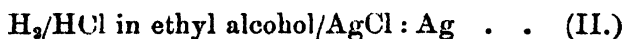
---

CXVIII. *The Activity Coefficients of Hydrogen Chloride in Ethyl Alcohol.* By J. W. WOOLCOCK, B.A., and Sir HAROLD HARTLEY, M.A., F.R.S., Balliol College, Oxford\*.

THE activity coefficients of hydrogen chloride in ethyl alcohol have been determined by Danner† and by Harned and Fleyscher‡. Danner measured the electromotive force of the cell



over the range of concentration 0.011 to 0.38 m. at 25° C., and Harned and Fleyscher that of the cell



between 0.001 and 3.62 m. The results were shown by Harned and Fleyscher to agree in the range 0.01 to 0.1 m. if 0.0350 volt is subtracted from Danner's results "to account for the difference in potential between the calomel and silver-silver chloride electrodes." This difference is, however, independent not only of the concentration but also of the solvent, provided that the solubilities of silver chloride and calomel are negligible compared with the concentration of the electrolyte, and has been shown to be 0.0467 volt in water§ and in methyl alcohol||. If this value is employed there exists a discrepancy of about 12 millivolts between

\* Communicated by the Authors.

† *Journ. Amer. Chem. Soc.* xlv. p. 2822 (1922).

‡ *Loc. cit.* xlvii. p. 82 (1925).

§ Linhart, *loc. cit.* xli. p. 1175 (1919). Horsch, *ibid.* p. 1790.

|| *Phil. Mag.* l. p. 729 (1925).

1134 Mr. J. W. Woolcock and Sir H. Hartley : *The Activity*  
the data of Danner and those of Harned and Fleysher, as  
has already been pointed out by Scatchard \* and by  
Nonhebel and Hartley †.

In order to derive the numerical values of the activity  
coefficients from measurements of the electromotive force of  
cell (II.) it is first necessary to find the value of  $E_0$  in the  
equation

$$E = E_0 - 0.1183 \log f.c \dots \dots (1)$$

where  $f$  is the mean activity coefficient of the ions, and  $c$  is  
the concentration of the electrolyte in equivalents per litre.  
When accurate results are available in dilute solutions, it is  
possible to obtain  $E_0$  without the aid of any auxiliary  
assumptions by plotting the function  $E_0'$ , defined by the  
equation

$$E_0' = E + 0.1183 \log c \dots \dots (2)$$

against  $c^{1/2}$  and extrapolating to infinite dilution.

The results of Danner extend only to 0.011 m., and those  
of Harned and Fleysher are stated by the authors to be  
unsuitable for direct extrapolation. The accuracy of the  
activity coefficients deduced by them must therefore depend  
on the validity of the auxiliary assumptions made in  
deducing  $E_0$ .

In the present investigation the electromotive force of  
cell (II.) has been redetermined at 25° C. in the concentration  
range 0.0003 to 1.2 m., with a view to obtaining values of  
the activity coefficient based on a value of  $E_0$ , arrived at by  
direct extrapolation. The data also serve to explain the  
discrepancy between the results of Danner and those of  
Harned and Fleysher.

### *Experimental.*

The method employed was that used by Nonhebel ‡ in  
very dilute aqueous solutions, in which values of the  
electromotive force corresponding to a series of concen-  
trations were obtained every time the cell was set up. This  
was done by starting with a known weight of pure  
alcohol in the cell and making successive additions of a  
solution of hydrogen chloride from a weight pipette. This  
type of cell is called a "dilution cell" to distinguish it from

\* Journ. Amer. Chem. Soc. xlvii. p. 2098 (1925).

† Phil. Mag. i. p. 729 (1925).

‡ Phil. Mag. ii. p. 1085 (1926).

the ordinary H-cell which is filled with solution of known strength, and gives only one value every time it is set up. Each experiment is referred to as a "run."

Dilution cells have the advantage with aqueous solutions that the risk of contamination of the solutions by atmospheric impurities is decreased and several values are obtained in each run; it is therefore possible to recognize a faulty run by the lack of concordance among the points and lack of agreement with other runs in the range in which the concentrations overlap. For dilute solutions of non-aqueous solvents the dilution cell has the important additional advantage that it is possible to distinguish errors due to the presence of small traces of water from those due to other causes, since with these cells the amount of water does not change during the run, and consequently random errors due to faulty electrodes can be detected. The position of each set of values will show at once whether the alcohol contained any appreciable quantity of water, since 0.08 per cent. by weight of water raises the electromotive force of the cell by 8 millivolts at 0.01 m., and the effect increases with dilution.

Measurements of the viscosity were used as a routine method of detecting the presence of water in each sample of alcohol. The agreement of the results (0.01078 at 25° C.) with those of Goldschmidt and Aarflot\* (0.01084 at 25° C.) and the concordance of the values for samples subjected to repeated purification indicated that only very small traces of water were present. This was confirmed by the agreement of the values obtained for the conductivity of solutions of hydrogen chloride with those of Goldschmidt†, and further evidence is to be found in the general concordance of the values of the electromotive force obtained by the authors and their agreement with those of Danner.

The method used for purifying the alcohol is based on the work of McKelvy‡; the details have been worked out in this laboratory by Mr. E. D. Copley. The alcohol was first refluxed with freshly burnt lime and distilled through a Hempel column of the type described by Hartley and Raikes§. After treatment with aluminium amalgam, it was again distilled and a final distillation was made from a few grams of anhydrous copper sulphate in a current of

\* *Zeits. phys. Chem.* cxxii, p. 371 (1926).

† *Loc. cit.* lxxxix, p. 129 (1915); *ibid.* cxiv, p. 1 (1924).

‡ *Bull. Bur. Standards*, xi, no. 3.

§ *Journ. Chem. Soc.* cxxvii, p. 524 (1925).



pure air. Its average specific conductivity was  $0.005 \times 10^{-6}$  reciprocal ohms.

The solutions were made by passing hydrogen chloride, generated by the action of strong sulphuric acid on pure dry sodium chloride, into ethyl alcohol. The apparatus used was constructed entirely of glass, and included a spray trap between the generator and absorber. The concentration of the solutions was determined by weight titration against baryta, methyl red being used as indicator ; the baryta was standardized against constant boiling aqueous hydrochloric acid \*. The more dilute solutions were obtained by weight dilution.

If any esterification had taken place the effect of the water produced would have been more important than the change of concentration. The measurements of Kailan † of the rate of esterification of hydrogen chloride dissolved in ethyl alcohol show, however, that this cannot affect the results, provided that solutions are made up immediately before each experiment.

The cells were Jena flasks of 250 c.c. capacity, two of which (A and B) were employed in each run. A fully assembled cell is shown in fig. 1. The cells were cleaned, dried, closed with a ground glass stopper, weighed and re-weighed after filling with alcohol to just below the neck. The iridized gold hydrogen electrodes and the silver chloride electrodes were prepared in the manner described by Nonhebel and Hartley. The electrodes usually came rapidly to equilibrium with the solution, and the results of the run then showed good internal concordance ; on the other hand, in certain runs when equilibrium was attained slowly, the results were irregular and were rejected. In runs 9-12 satisfactory equilibrium values were never reached, and it was found necessary to remove completely the coating of iridium from the gold and to use a new iridium solution for plating the electrodes, when concordant results were again obtained.

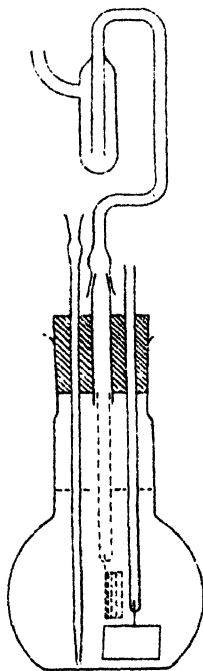
A hydrogen electrode and two silver chloride electrodes, which had stood in alcohol for 20 minutes, were inserted in a rubber bung which also held the hydrogen inlet and exit tubes. The rubber bungs had been freed from uncombined sulphur by treatment with caustic soda. The stopper of the

\* Foulk and Hollingsworth, Journ. Amer. Chem. Soc. xlv. p. 1220 (1923).

† *Monatsh.* xxviii. p. 559 (1907).

Jena flask was removed and the rubber bung carrying the electrodes was at once inserted. The two cells A and B were mounted on a wooden frame, together with hydrogen saturators of the type described by Lewis, Brighton, and Sebastian\*, and placed in a paraffin thermostat regulated to  $25 \pm 0.02^\circ \text{C}$ . A stream of hydrogen generated electrolytically, freed from oxygen and dried by phosphorus pentoxide, was passed through the saturators into the cells.

Fig. 1.



The "Dilution" Cell.

Additions of solution were made by temporarily removing the hydrogen exit bubbler. Readings were begun two hours after the first addition of acid; after each addition the cell was left until an electromotive force constant to 0.1 millivolt had been maintained for at least one hour.

In order to make concordance between runs as valuable a criterion of accuracy as possible, every run was carried out

\* Journ. Amer. Chem. Soc. xxxix. p. 2245 (1927).

1138 Mr. J. W. Woolcock and Sir H. Hartley : *The Activity* with a different sample of alcohol, a separately standardized solution of hydrogen chloride and freshly prepared electrodes.

### *Results.*

Seventeen runs in all were carried out ; of these two were rejected on account of the presence of moisture in the alcohol, four failed owing to the poisoning of the iridium mentioned above, and two gave irregular results. The values of the electromotive force of the cells are given in Table I., the data for each run being grouped together. The number of the run, the cell, and the number of the point are shown in the first column ; for example, 2 A 1. indicates that this point was the first obtained from cell A in run 2. The second column gives the concentration in mols per 1000 grams of solvent. The third column gives the electromotive force of the cell corrected to 760 mm. pressure of hydrogen. The vapour pressure of ethyl alcohol solutions at 25° C. was taken as 59.0 mm.

Since dilution cells are not adapted for use at high concentrations, five determinations were carried out with two H-cells described by Nonhebel and Hartley, using solutions stronger than 0.1 m. ; these are distinguished by the letter H in the first column.

The results, together with those of Danner and Harned and Fleysher, are shown in fig. 2, where  $E$  is plotted against  $\log m$ . It will be seen that there is substantial agreement between our results and those of Danner except that the latter's two most dilute points are rather higher. Harned and Fleysher's value at 1.0 m. coincides with that obtained by us, but at higher dilutions their values are higher by as much as 10 millivolts at 0.1 m., 17 millivolts at 0.01 m. and 15 millivolts at 0.001 m. This supports the view of Scatchard that the alcohol used by Harned and Fleysher was not sufficiently dry, since the effect of water in raising the electromotive force increases in dilute solution.

In the second and third columns of Table II. the values calculated for  $\alpha^\dagger$  and  $E_0'$  are given for points more dilute than 0.037 m. arranged in order of concentration. These data are plotted in fig. 3 together with similar values obtained by Danner and Harned and Fleysher in this range of concentration.

It will be seen that the relation between  $E_0'$  and  $\alpha^\dagger$  is

approximately linear for values of  $c^{\frac{1}{2}}$  less than 0.06; the value of  $E_0$  obtained by direct extrapolation being  $-0.0883 \pm 0.0003$  volt.

TABLE I.

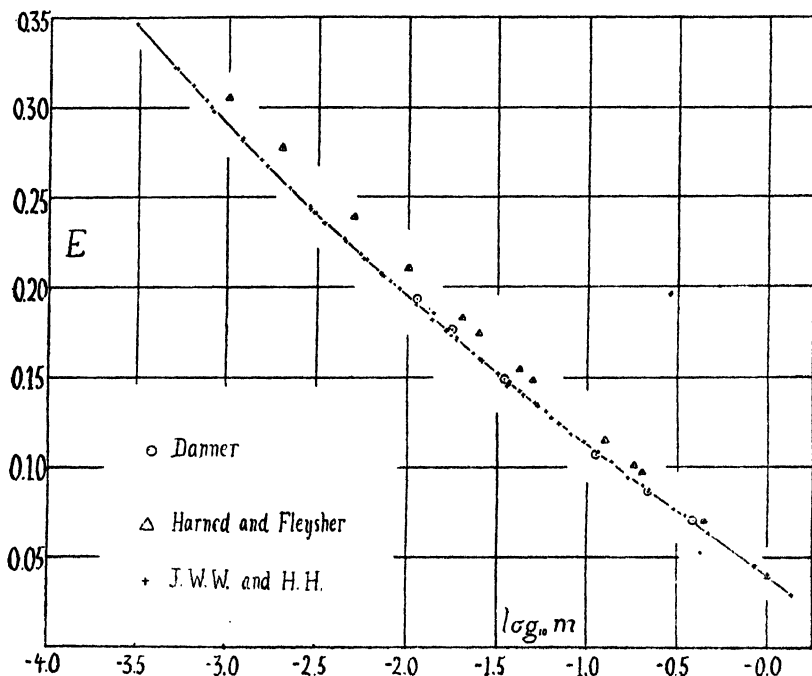
No.	$m$ .	E.	No.	$m$ .	E.
2A 1 .....	0.002861	0.2447	8A 1 .....	0.03621	0.1450
2A 2 .....	0.007909	0.2034	8A 2 .....	0.08100	0.1185
2B 1 .....	0.005442	0.2185	8A 3 .....	0.1677	0.0946
2B 2 .....	0.01382	0.1856	8B 1 .....	0.06342	0.1273
2B 3 .....	0.02537	0.1601	8B 2 .....	0.1147	0.1090
2B 4 .....	0.05339	0.1345	8B 3 .....	0.2031	0.0906
3A 2 .....	0.007243	0.2067	13A 1 .....	0.0004965	0.3221
3A 3 .....	0.01673	0.1762	13A 2 .....	0.001531	0.2710
3B 1 .....	0.002963	0.2412	13A 3 .....	0.003036	0.2417
3B 2 .....	0.007103	0.2070	13A 4 .....	0.004499	0.2252
3B 3 .....	0.01643	0.1760	13B 1 .....	0.0007990	0.3001
3B 4 .....	0.02329	0.1636	13B 2 .....	0.001190	0.2820
3B 5 .....	0.03204	0.1522	13B 3 .....	0.002193	0.2550
4B 1 .....	0.0008175	0.2977	13B 4 .....	0.003429	0.2357
4B 2 .....	0.002862	0.2431	16A 1 .....	0.04330	0.1404
4B 3 .....	0.005613	0.2163	16A 2 .....	0.06934	0.1248
6A 1 .....	0.004401	0.2270	16A 3 .....	0.1351	0.1032
6A 2 .....	0.01872	0.1710	16A 4 .....	0.2189	0.0880
6A 3 .....	0.03703	0.1473	16A 5 .....	0.3476	0.0734
6A 4 .....	0.05165	0.1359	16A 6 .....	0.4732	0.0636
6B 1 .....	0.007007	0.2080	16B 1 .....	0.09501	0.1146
6B 2 .....	0.01379	0.1820	17A 1 .....	0.0006297	0.3119
6B 3 .....	0.02615	0.1594	17B 1 .....	0.0003045	0.3466
6B 4 .....	0.04246	0.1425	17B 2 .....	0.0005158	0.3216
7A 1 .....	0.005852	0.2156	17B 3 .....	0.0007510	0.3040
7A 2 .....	0.008863	0.1995	17B 4 .....	0.001198	0.2827
7A 3 .....	0.01114	0.1905	17B 5 .....	0.001639	0.2677
7A 4 .....	0.01749	0.1731	H 1 .....	1.3427	0.0292
7A 5 .....	0.02848	0.1552	H 2 .....	1.0000	0.0405
7B 1 .....	0.01875	0.1716	H 3 .....	0.8429	0.0453
7B 2 .....	0.03715	0.1477	H 4 .....	0.8388	0.0451
7B 3 .....	0.05188	0.1356	H 5 .....	0.3000	0.0769
7B 4 .....	0.05905	0.1311			

In non-aqueous solvents it is often more convenient to work in terms of weight normality than of volume normality, in which case the absence of density data will make it impossible to convert the results to a volume basis if the density of the solution differs appreciably from that of the

pure solvent. It is therefore simpler to use an activity coefficient corresponding to a concentration expressed in mols per 1000 grams of solvent; this is usually denoted by  $\gamma$ . Nonhebel and Hartley calculated values of  $\gamma$  from their values of  $f$  by the relation

$$cf = a = m\gamma$$

Fig. 2.



where  $a$  is the activity referred to a standard state corresponding to the value of  $E_0$  defined by the equation

$$E = E_0 - 0.1183 \log cf.$$

This convention has the disadvantage that the limiting value of  $\gamma$  in dilute solution is numerically equal to the density of the solvent, while the limiting value of  $f$  is unity, since in such solutions  $c/m = d$ , where  $d$  is the density of the solvent. It is therefore preferable to define  $\gamma$  in terms of a standard state determined by the equation

$$E = E_0^m - 0.1183 \log m\gamma.$$

4

*Coefficients of Hydrogen Chloride in Ethyl Alcohol.* 1141

The coefficients  $\gamma$  and  $f$ , which express the deviation of the properties of the solution from those of an ideal solution, will then both approach unity in the limit. In aqueous solutions the two standard states will be almost identical, but in other solvents the values of  $E_0$  and  $E_0^m$  will differ by  $0.1183 \log d$ .

TABLE II.

No.	$c^{\frac{1}{2}}$ .	$E_0'$ .	No.	$c^{\frac{1}{2}}$ .	$E_0'$ .
17B 1 .....	0.01546	0.0818	7A 1 ... ..	0.06778	0.0610
13A 1 .....	0.01974	0.0812	6B 1 .....	0.07416	0.0593
17B 2 .....	0.02012	0.0797	3B 2 ... ..	0.07466	0.0596
17A 1 .....	0.02224	0.0792	3A 2 .....	0.07540	0.0589
17B 3 .....	0.02428	0.0780	2A 2 .....	0.07879	0.0577
13B 1 .....	0.02505	0.0788	7A 2 .....	0.08341	0.0558
4B 1 .....	0.02534	0.0800	7A 3 .....	0.09353	0.0530
13B 2 .....	0.03057	0.0764	6B 2 .....	0.1040	0.0506
17B 4 .....	0.03067	0.0753	2B 2 .....	0.1041	0.0489
13A 2 .....	0.03467	0.0745	3B 3 .....	0.1135	0.0475
17B 5 .....	0.03588	0.0742	3A 3 .....	0.1146	0.0464
13B 3 .....	0.04148	0.0720	7A 4 .....	0.1171	0.0472
2A 1 .....	0.04739	0.0686	7B 1 .....	0.1212	0.0451
4B 2 .....	0.04740	0.0702	6A 2 .....	0.1212	0.0458
3B 1 .....	0.04823	0.0703	3B 4 .....	0.1352	0.0420
13A 3 .....	0.04883	0.0686	2B 3 .....	0.1411	0.0411
13B 4 .....	0.05189	0.0683	6B 3 .....	0.1432	0.0402
6A 1 .....	0.05878	0.0642	7A 5 .....	0.1496	0.0400
13A 4 .....	0.05943	0.0649	3B 5 .....	0.1585	0.0370
4B 3 .....	0.06331	0.0624	6A 3 .....	0.1705	0.0345
2B 1 .....	0.06537	0.0618	7B 2 .....	0.1797	0.0339

Table III. gives the molal activity coefficients at round concentrations calculated in this way for solutions of hydrogen chloride in water, methyl alcohol, and ethyl alcohol.

Table IV. gives the values of the free energy of transfer of hydrogen chloride from ethyl and methyl alcohol to water calculated from the above data.

It is of interest to see whether the values obtained for the activity coefficient of hydrogen chloride are in agreement with the theory of Debye and Hückel \*, which in very dilute solutions leads to the limiting equation

$$-\log f = A c^{\frac{1}{2}}$$

\* *Phys. Zeits.* **xxi.** p. 185 (1923); **xxv.** p. 97 (1924).

Fig. 3.

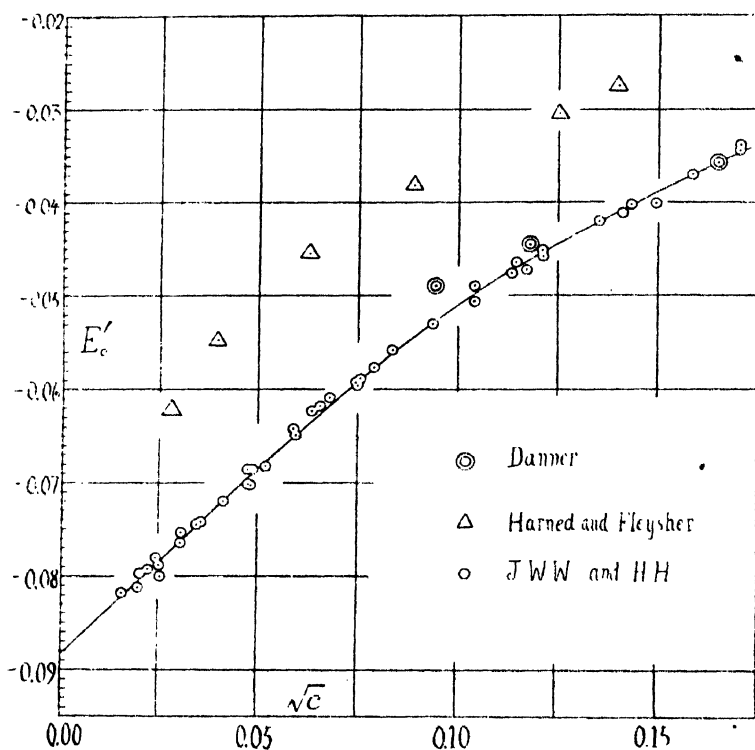


TABLE III.

<i>m.</i>	Ethyl alcohol.	Methyl alcohol.	Water.
0.0005	0.851	0.953	0.981
0.001	0.800	0.912	0.973
0.002	0.731	0.867	0.962
0.005	0.622	0.813	0.942
0.01	0.518	0.745	0.919
0.02	0.426	0.664	0.889
0.05	0.317	0.541	0.841
0.1	0.253	0.461	0.807
0.2	0.198	0.386	0.779
0.5	0.140	0.289	0.768
1.0	0.103	...	0.822

TABLE IV.

The Free Energy of Transfer of HCl from  
Alcohol to Water.

<i>m</i> in both solutions.	-Δ <i>F</i> (in calories).	
	EtOH to H <sub>2</sub> O.	MeOH to H <sub>2</sub> O.
0.001	6683	5256
0.01	6209	5076
0.1	5521	4670
0.5	4855	4253
1.0	4434	.....

where *A* is a constant depending on the temperature, the dielectric constant of the solvent and certain universal constants. For hydrogen chloride in ethyl alcohol, as in water and methyl alcohol, the curve obtained by plotting the values of  $-\log f$  against  $c^{\frac{1}{2}}$  becomes linear in dilute solutions in conformity with the theory. This can be seen in fig. 3, for since

$$E_0' = E + 0.1183 \log c,$$

$$\text{and} \quad E = E_0 - 0.1183 \log cf,$$

$$E_0' = E_0 - 0.1183 \log f,$$

and therefore as  $E_0'$  has a linear relationship to  $c^{\frac{1}{2}}$  the same is true of  $-\log f$ .

The value of *A* calculated from the Debye theory at 25° C is for water 0.505, for methyl alcohol 2.10, and ethyl alcohol 2.79. The observed values of *A* in water and methyl alcohol are 0.39 and 1.485, which agree more closely with the coefficient of Milner\* than of Debye. Scatchard†, however, points out that the experimental results can be reconciled with the Debye value of *A* if the complete Hückel‡ equation

$$-\log f = \frac{Ac^{\frac{1}{2}}}{1 + \alpha c^{\frac{1}{2}}} - Bc$$

is used to obtain  $E_0$ . This equation contains two additional

\* Phil. Mag. xxiii. p. 551 (1912); xxv. p. 743 (1913).

† Phil. Mag. ii. p. 577 (1926).

‡ Phys. Zeits. xxvi. p. 98 (1925).



## 1144 *The Activity Coefficients of Hydrogen Chloride.*

constants  $\alpha$  and B, of which  $\alpha$  is proportional to the radius of the ions and B is a function of the change of dielectric constant with concentration. In practice  $\alpha$  and B are evaluated empirically. In ethyl alcohol the experimental value of A is 3.40, which is larger than the Debye theory predicts. The use of the Hückel equation would only make the lack of agreement more pronounced, unless a negative value were given to  $\alpha$ , corresponding to a negative ionic radius.

The basic assumption of the Debye-Hückel theory is complete dissociation, and the most probable explanation of the discrepancy in the value of A in the case of ethyl alcohol is that even in dilute solutions an appreciable quantity of hydrogen and chlorine ions are associated to form molecules. Evidence for this is seen in the much lower values of the activity coefficient in solutions in ethyl alcohol than in solutions in water or methyl alcohol, and in the larger vapour pressure of hydrogen chloride in ethyl alcohol solutions. Experiments in progress in this laboratory on the conductivity of salts and acids in ethyl alcohol afford additional evidence that dissociation may not be complete even at very high dilutions.

### *Summary.*

1. The activity coefficients of solutions of hydrogen chloride in ethyl alcohol have been obtained by measurements of the electromotive force of the cell  $H_2/HCl/AgCl:Ag$  at 25° C.

2. A comparison has been made with the results obtained by Danner and by Harned and Fleysher.

3. The equation  $-\log f = 3.40c^{\frac{1}{2}}$  has been found to represent the course of the activity coefficient in the range 0.0003 m. to 0.004 m., the value of the coefficient being greater than that demanded by the Debye theory. It is suggested that this is due to incomplete dissociation.

Physical Chemistry Laboratory,  
Balliol College and Trinity College,  
Oxford.  
March 1928.

---

[The Editors do not hold themselves responsible for the views expressed by their correspondents.]

THE  
LONDON, EDINBURGH, AND DUBLIN  
PHILOSOPHICAL MAGAZINE  
AND  
JOURNAL OF SCIENCE.

[SEVENTH SERIES.]

JUNE 1928.

CXIX. *Fluorescent Secondary X-Radiation and the J-Phenomenon.* By W. H. WATSON, M.A., Ph.D., Lecturer in Natural Philosophy, University of Edinburgh \*.

*Introduction.*

THE study of the absorption of the secondary X-radiation from light substances has hitherto been the most successful means of investigating the J-phenomenon. It is obviously desirable that this study should be extended to the secondary radiation from substances whose characteristic radiation of K-series is excited by the primary beam. Some years ago † measurements were, in fact, made to determine the absorption coefficients in copper and aluminium of the whole characteristic radiation from a series of elements, the exciting primary beam being adjusted in hardness so as to produce the optimum emission of characteristic radiation (K-series) from the radiator. The results of the experiments were inconclusive, and actually it appears from recent work that the method of experiment adopted then is not the most suitable to exhibit "J" absorption effects.

In a recent paper on the J-phenomenon ‡, experiments were described in which the difficulties of control were surmounted sufficiently well to allow of consistent measurements which exhibited the "J" absorption effect in the transmission of the secondary radiation from paraffin-wax

\* Communicated by Prof. C. G. Barkla, F.R.S.

† W. H. Watson, Ph.D. Thesis, 1925.

‡ C. G. Barkla and W. H. Watson, *Phil. Mag.*, Nov. 1926.

through aluminium. Some further experiments of the same nature have since been made, and the results are put on record here, although the main investigation to be reported is concerned with the use of radiators of higher atomic number.

### 1. *Experimental Control.*

The main requirements for adequate control of the X-ray tube were stated in the paper referred to \* :

- (1) The peak voltage applied to the Coolidge tube should be maintained constant; and
- (2) The current through the X-ray tube should be kept steady.

When radiators of silver and tin were first employed about a year ago, it became clear that, even if the above conditions were carefully maintained, consistent results were obtained only when the X-ray tube was run into a steady state before measurements were made, and throughout the experiment was allowed to function continuously, the X-rays being shut off when desired by means of a shutter in the primary beam.

*It should be clearly understood, therefore, that in the experiments to be described the results recorded here were obtained consistently, only when the X-ray tube was employed as a constant source of radiation, and that when this method of procedure was departed from, the only type of consistent result obtained was that got by making readings in a definite time order.*

The arrangements for the control of the Coolidge X-ray tube are made clear in the diagrams. In fig. 1*a* the rheostat  $R_1$ , operated by means of an insulating handle, is used to adjust the filament current when the tube is working. The power for high tension is supplied from the direct current mains (230 volts) through a rheostat  $R_2$  (fig. 1*b*) to a rotary converter (2 kw., 50 cycles), from which the alternating current is passed through an auto-transformer tapped suitably to operate the high-tension transformer (Watson & Sons, Ltd.; 2 kw. 60 kv.). The secondary of the H.T. transformer is earthed in the middle, and there the high-tension current passes through a shunt-type resistance of 1 ohm. The potential across this shunt is measured by means of a direct-reading potentiometer in millivolts, so if there is no leakage, the milliamperage

\* Barkla and Watson, *loc. cit.*

through the tube is known. The rheostat  $R_1$  is adjusted when necessary, so that the galvanometer in the potentiometer circuit remains undeflected: by this means the current through the tube is maintained constant within 1 per cent. The peak voltage is kept steady by employing the rheostat  $R_2$ , in conjunction with the voltmeter  $V$ , across the input to the converter, so that the reading on the voltmeter varies, under favourable circumstances, no more

Figs. 1 a & 1 b.

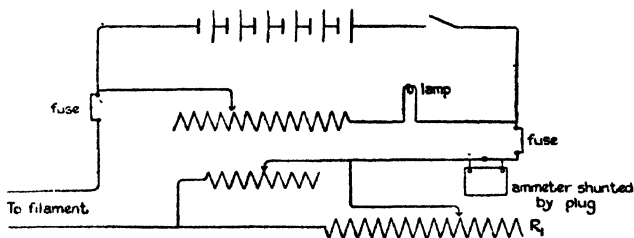


Fig 1a

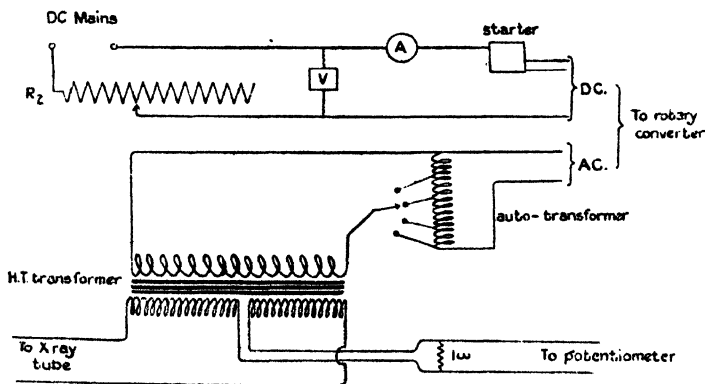


Fig 1b

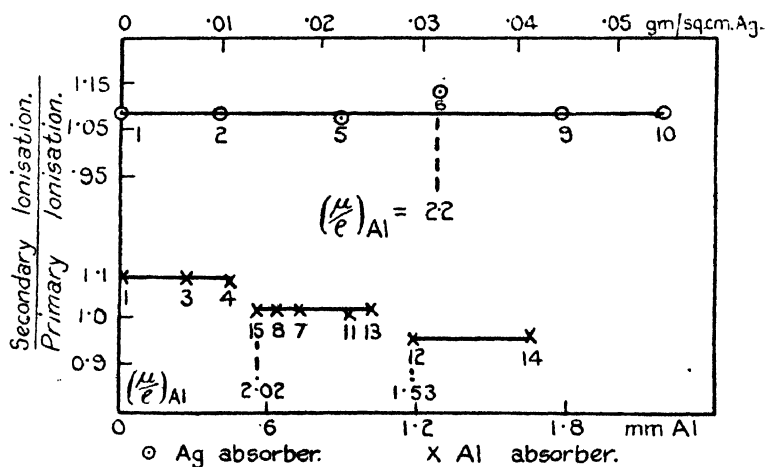
than half a volt. On account of the fact that the D.C. supply frequently falls below 230 volts, the constant reading maintained on the voltmeter is 225 volts, and this figure has been used throughout in the experiments.

## 2. Experiments on the Secondary Radiation from Paraffin-Wax.

The absorption of the secondary radiation at right angles to the exciting primary has been compared with that of the

primary by the method previously employed \*. The former results with aluminium absorbing sheets have been confirmed when a plate of paraffin-wax was substituted for the cylindrical radiator, and measurements have also been made with silver and copper as absorbing materials. Equal thicknesses ( $x$ ) of absorbing material were placed in the paths of the secondary and the primary beams, and the ratio of the ionizations in air was measured for different values of  $x$ . The figures 2 and 3 show the type of result obtained with Ag and Cu, compared with that with Al, measurements with absorbers of Al and Ag or Cu being made alternately.

Fig. 2.



There is a slight indication in the case of silver that the K-absorption occurs with less filtering material in the primary beam than in the secondary; this is shown by the tendency, which showed itself not only in one case, for the ratio of secondary ionization to that produced by the primary to have a slightly higher value when the mean hardness of the transmitted radiation was about that of silver K-radiation †. This is what is expected on account of the Compton effect, which causes in the scattering process a displacement of some of the energy in the spectrum

\* Barkla and Watson, *loc. cit.*

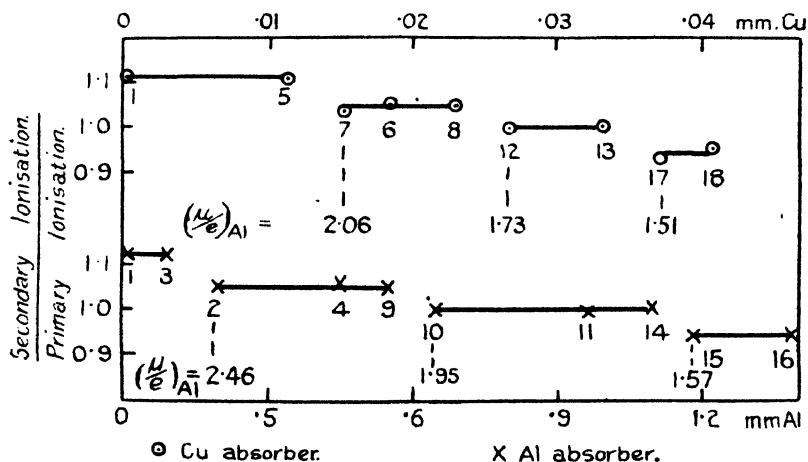
† See Barkla and Khastgir, *Phil. Mag.* iv. p. 735 (Oct. 1927).

of the heterogeneous beam into the longer waves. Absorption by silver in this way will not, in general, be sensitive enough to show the resulting difference in penetrating power between the primary and secondary except when the average wave-length of the heterogeneous radiation is very close to the K-absorption edge of silver.

The results for Cu and Al, on the other hand, seem to point to there being no difference in the rate of absorption of the primary and secondary beams except where the J-discontinuities occur in the secondary.

With a heterogeneous primary, a comparison of the absorption of the secondary and primary beams *over a limited thickness of absorbing material* may not necessarily be

Fig. 3.

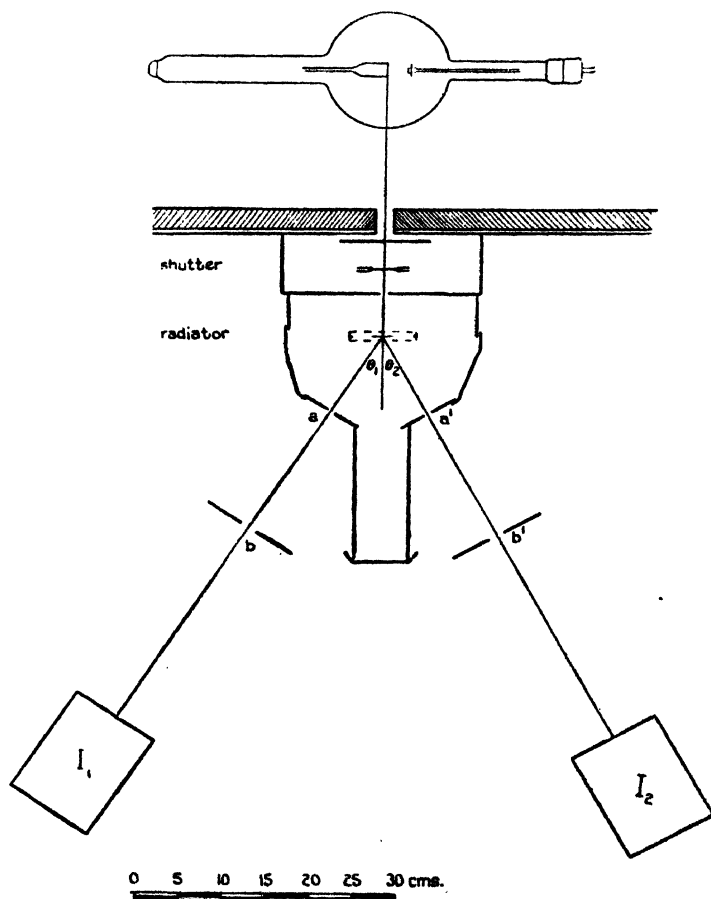


a sensitive method of testing the occurrence of the Compton effect. Factors are known which might compensate the effect of wave-length change on the absorbability of the whole beam. If the compensation were exact, the experiments would not show the Compton effect in a difference of the rates of absorption of primary and secondary radiations. It is difficult to believe that the exact compensation takes place in all these experiments so that the latter show only the occurrence of the J-phenomenon, the relation of which to the Compton effect is still obscure. This distinction of the two phenomena will be made obvious when we consider what happens when a thin fluorescent radiator is employed.

3. *Experiments with Fluorescent Radiators.*

When a thin sheet of silver or tin (about  $\cdot 001$  cm. say) is placed in the path of a beam of X-rays just sufficiently penetrating to excite its K-series characteristic radiation,

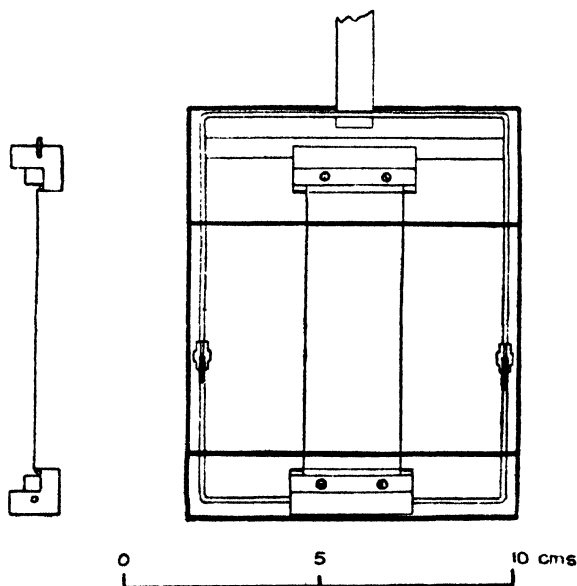
Fig. 4.



the secondary radiation contains only a small proportion (generally not more than 2 or 3 per cent.) of general radiation; the K-series characteristic is the main secondary emission. In order to obtain in ionization measurements a sensitive means of showing J-absorption effects when material is placed in the path of the secondary beam, it is

necessary to set up two ionization chambers to receive secondary radiation in different directions from the radiator. The ratio of the ionization currents in the two chambers is then measured when equal thicknesses of material are placed in the two beams. If identical processes take place in both beams, the ratio of the ionizations should remain constant as the thickness of absorbing material is increased, and any alteration of the ratio observed will indicate differences between the two secondary beams studied.

Fig. 5.



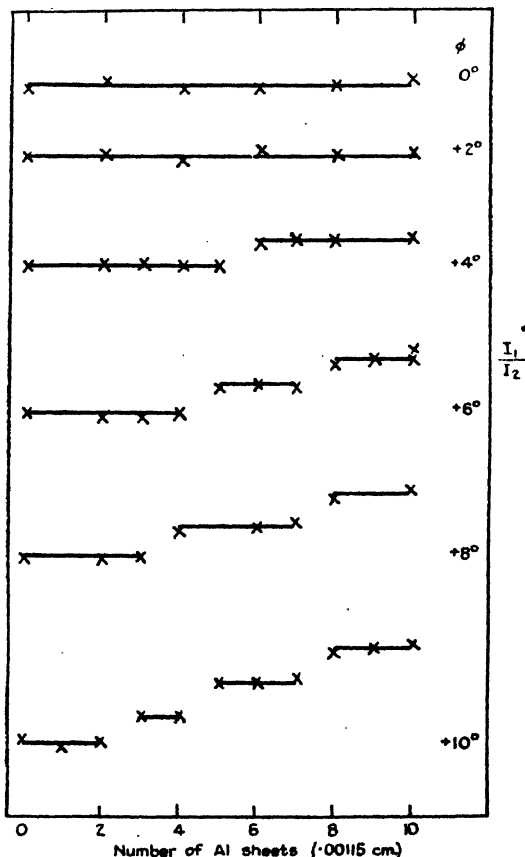
The arrangement of apparatus used with a copper radiator will be described, and the same figure (4) will serve for reference to the experiments with a tin radiator.

The Coolidge tube, with a molybdenum anticathode face set at right angles to the cathode stream, produced X-rays in a lead box; a pencil of these passed through an adjustable vertical slit 4 cm. long and 4 mm. wide, and then encountered a lead shutter supported between brass slides 3 cm. apart. When the shutter was raised, the rays passed through a second slit to the radiator, which consisted of a sheet of copper approximately .001 cm. thick. This sheet was stretched flat in a frame of brass (see fig. 5) protected by a



lead sheath. The frame was rigidly attached to a spindle 35 cm. long fitted axially to the vernier arm of a graduated circle, so the plane of the radiator could be set at any desired angle with respect to the direction of the primary X-ray beam. The rays which passed straight through the radiator

Fig. 6.



The ordinates are  $\frac{I_1}{I_2}$  (reduced to same initial value 1).

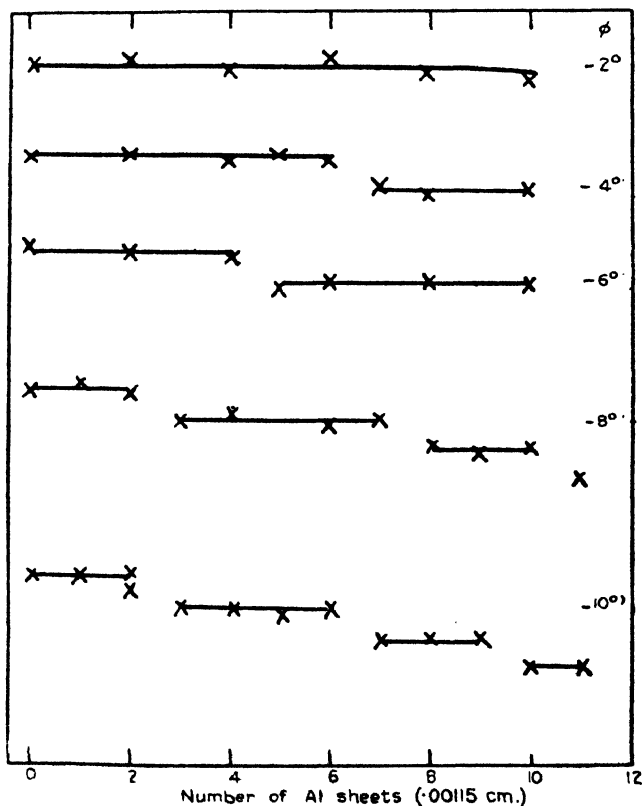
The scale is obtained from the discontinuities which are on the average 7 per cent.

$\phi$  is the radiator angle (see text).

were trapped in a lead tunnel which was sufficiently long to eliminate stray effects due to secondary radiation from the end striking the radiator.

The secondary radiation from the copper sheet was allowed to pass, through slits  $a$ ,  $b$ , and  $a'$ ,  $b'$ , along two directions making  $\theta_1$  and  $\theta_2$  with the primary beam, to cylindrical ionization chambers containing air and provided with Al windows 0.0012 cm. thick. The chambers were lined with aluminium 0.7 mm. thick and with six thicknesses

Fig. 6 (continued).



(For legend see p. 1152.)

of filter paper, the former to eliminate fluorescent X-rays from the walls of the chambers and the latter to prevent  $\beta$ -rays from the Al lining from reaching the air in the chamber. The electrodes were Al rings supporting wide mesh gauze, and sufficiently large to prevent the radiation entering the chambers from striking them; they were connected to tilted electroscopes of the Wilson type, which

were employed usually at a sensitivity of 40 divisions to the volt, and adjusted so that the deflexion of the gold leaf was sufficiently nearly linearly dependent on the leaf potential. Absorbing material was placed in equal amounts at  $b$  and  $b'$ , and the ratio of ionizations was obtained by observing the deflexion in one electroscope in the period during which the shutter was raised, while the other showed a deflexion of 10 divisions. The error of reading, therefore, should not exceed 1 or 2 per cent. Many measurements have been made with the above arrangement of apparatus. We shall quote in detail a set of results which are typical.

The X-ray tube was operated throughout at 40 kv. (peak), and passed 1.8 milliamps., while the filament current was 3.52 amps. The directions of secondary emission examined were

$$\theta_1 = 24^\circ 30', \quad \theta_2 = 25^\circ.$$

A series of curves (see fig. 6) was plotted, for each of which the radiator was set at a different angle with the primary beam. We shall refer to the position of the Cu radiator in which its plane was perpendicular to the direction of the primary beam of X-rays as zero setting and reckon angles of rotation of the radiator which are in the clockwise sense in fig. 4 as positive, those in the contrary sense as negative.

In the graphs plotted in fig. 6 the abscissæ are "number of absorbing sheets of Al" (each .00115 cm. thick), and the ordinates are the ionization ratio  $I_1/I_2$  reduced so that the unintercepted ratio has the same value in each case. This has been done, since it was advantageous to adjust the actual value of the ratio for the unintercepted beams by altering the electroscope sensitivity or slit width in order to ensure accuracy of measurement. This adjustment was found by repeated trial not to affect the results appreciably.

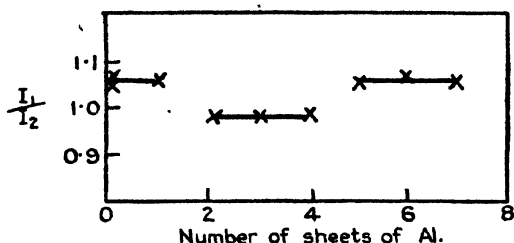
A study of these results leads to the following observations :—

- (1) When the radiator was nearly normal to the primary X-ray beam there was practically no change in the ionization ratio when increasing equal thicknesses of aluminium were placed in the beams.
- (2) At other settings of the radiator the only changes in the ratio were sudden changes of about 7 per cent. When tested these were found to be due to a decrease in the ionization produced by the secondary beam which made the larger angle with the normal to the radiator.

- (3) The effect of turning the radiator from zero setting in either sense was to bring one of these discontinuities gradually into the range of observation. This process was followed by making measurements at settings of the radiator intermediate between those for which the results are given in fig. 6. At greater angles a second and a third discontinuity appeared.

It may be pointed out, further, that, while the effects in the two beams seem to be separated from each other (*i. e.*, in no case in the results quoted above is there direct evidence of the appearance of discontinuities in both beams for one setting of the radiator), some other experiments have shown the simultaneous separate occurrence of two compensating discontinuities. An example of this is given in fig. 7.

Fig. 7.



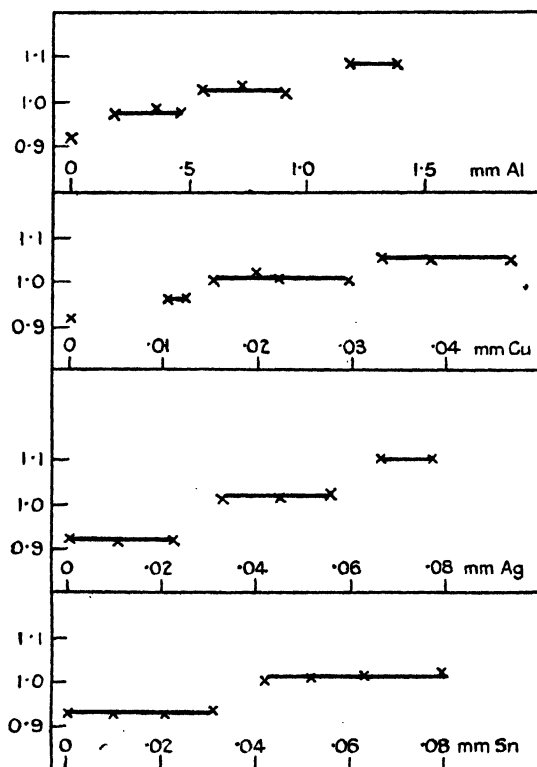
Moreover, a discontinuity may be observed when the radiator is normal to the X-ray beam, if the angle  $\theta_1$  or  $\theta_2$  is increased. It is then found, in accordance with the statement (2) above, that the ionization due to the beam making the increased angle with the normal to the radiator is reduced at the discontinuity.

In conformity with the law now well known as one of the characteristics of the J-phenomenon, the amount of absorbing material required to show a discontinuity is decreased when the peak voltage on the tube is increased.

The above measurements were made with aluminium as the most suitable absorbing substance for the soft copper K-radiation. Some other measurements, of a preliminary nature, have also been made with the secondary radiation from a sheet of tin, the absorbing substances being Al, Cu, Ag, and Sn. In fig. 8 are shown the values of the ionization ratio  $I_1/I_2$ , when equal thicknesses of absorbing material are

placed in two secondary beams ( $\theta_1 = 90^\circ$ ,  $\theta_2 = 25^\circ$ ) from a tin radiator .00267 cm. thick. The radiator was set so that it made nearly equal angles with the two directions along which the secondary was observed. At the apertures  $a$ ,  $a'$  (see fig. 4) in each beam was placed a sheet of silver about .001 cm. thick. This acted as a filter to reduce the intensity

Fig. 8.

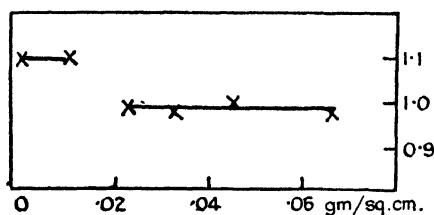


The ordinates are  $\frac{I_{90}}{I_{25}}$  for Sn radiation when filtered with Al, Cu, Ag, Sn.

of the  $K\beta$  relative to the  $K\alpha$  component of the characteristic radiation from the tin radiator, and, on the whole, tended to reduce the amount of general radiation in the secondary beams studied. A logarithmic curve of the absorption by

aluminium gave 1.81 as a mean value of  $\left(\frac{\mu}{\rho}\right)_{\text{Al}}$  for the secondary: this agrees very well with Richtmyer's value 1.78 for homogeneous radiation of the same wave-length as Sn K $\alpha$  (mean of  $\alpha_1$  and  $\alpha_2$ ). With regard to the amount of scattered radiation present in the secondary beams, it was found that a number of sheets of paper of the same total mass per unit area as the tin radiator yielded only 1.2 per cent. of the whole secondary effect from tin. Allowing for the difference in scattering power between paper and tin, it is estimated that the secondary radiation examined must have contained not more than 4 or 5 per cent. of general scattered radiation. This estimate does not take account of the selective transparency of the silver filters which reduces the percentage of general radiation except in the case of the hardest rays, 0.2 to 0.3 Å.U. These rays,

Fig. 9.



The ordinates are  $\frac{I_1}{I_2}$  for Sn radiation ( $\theta_1 = 26^\circ$ ,  $\theta_2 = 23^\circ 30'$ ) when transmitted through silver.

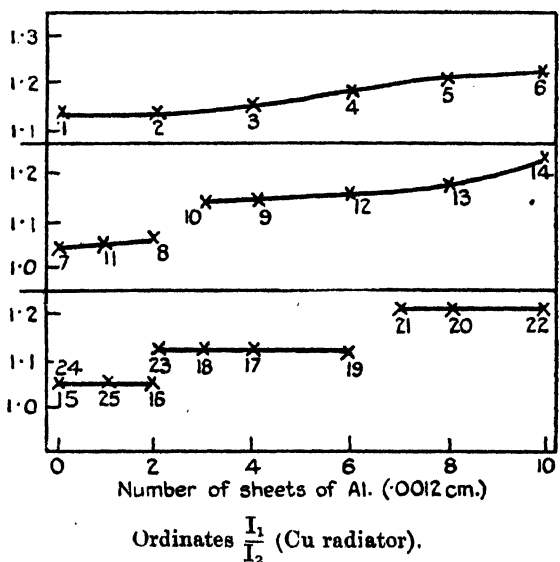
however, are less efficiently scattered by the tin radiator. We are certainly justified in concluding that the filtered radiation examined was composed of over 90 per cent. Sn K $\alpha$  radiation.

Finally, fig. 9 shows a result with the secondary from tin in conditions similar to those which obtained with the copper radiator. Silver was employed as absorbing material, and the directions of secondary emission compared were  $\theta_1 = 26^\circ$  and  $\theta_2 = 23^\circ 30'$ , the radiator being nearly perpendicular to the X-ray beam. It will be seen that these preliminary experiments on the secondary radiation from tin show discontinuities in the absorption by all the substances tested; it is hoped to supplement these results by a complete investigation.

#### 4. *Effect of Continued Running of the X-ray Tube.*

All the results quoted above were obtained only when the X-ray tube was run into a steady state. Let us now consider what happens during the establishment of that state. In fig. 10 have been plotted all the measurements of a series taken with the copper radiator and commenced just after the tube began to function. The number attached to each point denotes the order of its observation; the time taken for the observations 1 to 6 was about 25 minutes.

Fig. 10.



The effects of running the tube are exhibited by the figure:—

- (1) The values of the ratio  $I_1/I_2$  are not steady until the tube has run for nearly an hour.
- (2) Discontinuities appear in the relation between  $I_1/I_2$  and the number of absorbing sheets placed in the beams.

It does not seem that the process of stabilization is accompanied by displacement of a discontinuity (*i. e.*, alteration of the amount of material required to produce it) and that the results obtained at the beginning of the series are a consequence of "smudging" due to changing conditions during

measurement, but rather it seems that, to use an analogy, the discontinuities "crystallize"—*i. e.*, they are not present until conditions are sufficiently steady. Moreover, the discontinuities occurring at greater thickness of absorbing material seem to require a longer period before they are observed.

In the attainment of a steady state a very important factor was the heating of the anticathode. It was found that stabilization was expedited by preliminary rapid heating of the anticathode, the tube being operated for 7 or 8 minutes at 60 kilovolts before the commencement of measurements at 40 kilovolts. In many cases this preliminary heating was sufficient to produce a steady state quite quickly, but in others—and in these it was noted that the tube had been idle for some days previously—it was also necessary to run at 40 kilovolts for 20 minutes before steady results were obtained.

These facts suggest that a water-cooled target should be employed and that the vacuum in the tube must be maintained steady. This latter condition may be quite easy to attain in a tube which is connected to a pump when it is operating. It is desirable, however, to attempt to introduce some such control in experiments on the J-phenomenon, and, indeed, to give serious attention to all devices to ensure steady operation of the X-ray tube.

### *5. Constitution of the Beams.*

In the constitution of the beams compared we have to consider :—

- (1) The ratio of the intensities of the  $\alpha$  and  $\beta$  components of the characteristic K-series emission, and
- (2) the intensity and character of the non-characteristic secondary radiation.

Differences between the beams with respect to (1) may be ignored, as the direct cause of detectable changes in the ionization ratio measured. Simple calculation shows that if the primary beam is changed in wave-length from that just required to excite copper K-radiation to 0.3 Å.U. (the shortest wave-length excited by 40 kv.), the ratio  $I(K\alpha) : I(K\beta)$  does not alter by more than 3 per cent., and that a similar limit may be set to the variation of this ratio when the radiator is turned from zero setting through an angle  $\phi \leq 10^\circ$ . This means that the difference in the relative intensity of  $K\alpha$  to  $K\beta$  in the beams compared cannot exceed



10 per cent. ; and even when ten sheets of aluminium (each .0012 cm. thick) are placed in each beam the ionization ratio measured cannot be affected, in virtue of that difference, to the extent of 1 per cent.

With regard to the second factor, only strong crystal reflexion of some constituent of the primary beam into one of the directions along which the secondary is observed could produce measurable differences in the ionization ratio. The ionization due to the ordinary scattered radiation cannot, in the present experiments, exceed 1 per cent. of that due to the characteristic radiation, even when the latter has been reduced to a quarter of its original intensity by the absorbing aluminium placed in the path of the secondary beam. Consequently, the effect of absorption in the radiator on the character of this weak secondary radiation may be ignored. The calculation which determined the above figure of 1 per cent. took into account absorption of the characteristic radiation in the radiator, excess scattering in directions making angles less than  $30^\circ$  with the primary, and the relative ionization coefficients given by Barkla's work many years ago ; it was carried out for several wave-lengths in the primary spectrum. The shortest wave-length in the primary, of course, fixed the upper limit.

We have now to consider the effects of X-ray reflexion by the crystals of the copper sheet. On account of the rolling of the latter, it is likely that the individual crystals will not be orientated at random, and quite strong reflexion may be expected along certain directions. The lattice constant for copper is  $3.61 \text{ \AA.U.}$ , so that the longest waves which can be diffracted through  $25^\circ$  are of wave-length  $1.56 \text{ \AA.U.}$  These rays are approximately of the same wave-length as  $\text{CuK}\alpha$ , but in the second-order reflexion the wave-length is  $0.78 \text{ \AA.U.}$ , and although these harder rays are only one-tenth as efficient as the characteristic Cu radiation in producing ionization in air (and any other diffracted rays are, of course, less efficient), it must be noted that even 5 per cent. of this radiation in the secondary (intensity determined by ionization in air) will produce a 14 per cent. change in the ionization ratio measured when .012 cm. of aluminium is placed in the beams. According to the ordinary laws of absorption the presence of secondary radiation due to crystal reflexion should show itself by making the ionization ratio change exponentially with increase in absorbing material in the path of the beams. The experimental results do not show this progressive change in the ratio, but only discontinuous changes when

definite amounts of aluminium are placed in the beams. Hence the ordinary laws of absorption fail to explain the results, whether there is strong crystal reflexion or not.

### 6. *The J-Phenomenon.*

The discontinuities in the ratio observed here are of the same order of magnitude as those hitherto obtained in experiments on the J-phenomenon. Moreover, in all the latter experiments, the introduction of any influence which rendered the radiation more penetrating on the whole, caused a discontinuity to appear when less absorbing material was placed in the beam. It will be noticed that the turning of the copper radiator from zero setting in the present investigation has just that effect on the secondary beam, making the larger angle with the normal to the radiator, *i. e.*, as the angle is increased the discontinuity occurs when less absorbing aluminium is placed in the beam. In addition, if the radiator is not moved and one of the angles  $\theta_1$  or  $\theta_2$  is increased, a similar effect takes place. We conclude, therefore, that fundamentally the origin of the discontinuities observed in the present investigation is very probably in the same process which determines the occurrence of the J-phenomenon.

It must be noted, however, that the absorption coefficient of the whole beam which, to a first approximation, has appeared in many experiments as one of the critical factors in determining J-absorption with heterogeneous X-radiation, is not, in the present experiments, the factor controlling the occurrence of the J-absorption discontinuities. For here,  $\frac{dI}{dx}$  is practically unchanged when a number of thin absorbing sheets is placed in the beam; the large proportion of Cu K-radiation quite outweighs the other harder secondary radiation in determining this quantity.

In the second place, while it may be that the occurrence of the discontinuities requires the presence of, at least, a small amount of hard radiation, it is quite certain that the discontinuities cannot be explained by assuming that this hard radiation itself experiences J-discontinuities, and that, on account of a sensitive state induced in the absorbing material by the J-absorption of the hard radiation, the soft characteristic radiation suffers a sudden extra absorption in passing through the specially absorbing layer. This hypothesis might explain one discontinuity: it will not explain the occurrence of two and three in a thickness of material

which scarcely affects the character of the hard secondary radiation. The experiments in which Sn K-radiation has been transmitted through silver absorbing sheets may be cited to the same effect. Thus, in general, the soft characteristic radiation itself plays a primary rôle in determining the occurrence of a discontinuity.

Thirdly, the fact that absorption coefficient is inadequate to describe the condition of the radiation from a thin fluorescent radiator, suggests that, under the conditions of former experiments, showing a series of discontinuities, the progressive change of the absorption coefficient of the whole radiation (as measured) is associated with the periodic recurrence of a condition in the radiation favourable to specially great absorption in a thin layer of absorber. This possibility suggested itself at the time of the experiments on scattered radiation in which it was shown that the absorption coefficient at the discontinuity is dependent on the current through the X-ray tube\*. It was even noticed that the critical absorption coefficients formed a very approximate arithmetic series. In the present experiments it seems that a periodic variation of the conditioning factor takes place unaccompanied by a measurable change in the absorption coefficient. There is, of course, a progressive change in the relative intensity of the two characteristic components, and the possibility of greater absorption of the shorter wave component at the discontinuity. This would, of course, lead to periodic recurrence of conditions.

The conditioning factor must be latent in the emission and absorption history of the whole radiation passed through the absorber, and it will influence observable effects in a periodic way only if there is interaction between the Fourier constituents of the beam in its passage through matter. It is therefore essential to control the source of radiation very carefully, and it seems likely that experiments on the J-phenomenon which do not employ a constant source of X-radiation are not the proper experiments to investigate the phenomenon.

So far, the only mechanism that has been suggested to describe interaction between the constituents of a coherent heterogeneous beam of X-rays in its passage through matter is that X-radiation is propagated by wave-motion and that in matter the simple additive law of superposition breaks down. If the principle of the conservation of energy is to be retained, this idea encounters difficulties which have proved insurmountable in the past—it is absolutely necessary to

\* Barkla and Watson, *loc. cit.*

have concentration of energy into particles in the radiation. On the other hand, Barkla \* has shown, with the aid of experimental evidence, that the conception (which was already open to serious philosophical objection) of independent quantum particles corresponding to all monochromatic constituents in a heterogeneous X-radiation is untenable. It is natural, therefore, to suggest, following quantum wave-theory, that there are particles in a heterogeneous X-radiation which, in a narrow beam, are all approximately the same, but that the wave-system of each particle possesses the spectrum of the whole beam. It is possible that the remarkable features of the J-phenomenon may be suitably described in terms of a conception of this kind.

In conclusion, I have to thank Professor Barkla for suggesting that the secondary radiation from fluorescent radiators should be studied, for his interest and helpful advice and criticism throughout the work, and for the apparatus he has set at my disposal. To the Trustees of the Moray Fund of Edinburgh University I am grateful for the use of the Coolidge X-ray tube and for the high-tension batteries required for the ionization measurements.

#### *Summary.*

The ionizations produced by two secondary beams from a radiator whose K-characteristic X-radiation was excited, have been compared with equal amounts of absorbing material in the paths. Under the proper conditions of tube control, the ratio of the ionizations did not alter continuously when the amount of absorbing material ( $x$ ) was increased, but exhibited discontinuities in its relation with  $x$ , which seem identical with the J-absorption discontinuities observed in former experiments.

It is shown that, except for the effects of crystal reflexion in the radiator, the radiation studied is composed almost entirely of the K-characteristic radiation of the radiator. The effect of changing the orientation of the radiator with respect to the primary beam is to displace a discontinuity, so that a different amount of absorbing material is required to produce it.

The results show that the J-phenomenon may recur periodically in absorption without appreciable change in the absorption coefficient of the beam in its passage through the absorber.

\* C. G. Barkla, 'Nature' (March 27, 1926); see also Barkla & Khastgir, Phil. Mag. vol. ii. p. 666 (1926).

CXX. *Note on Modified Scattered X-Radiation and Super-Position. The J-Phenomenon* (Part VIII.). By Professor C. G. BARKIA, F.R.S. \*

**I**N previous notes it has been shown that the absorption of an X-radiation (either heterogeneous or comparatively homogeneous) and its action upon the substance in which absorption occurs depend to quite a considerable extent upon factors which had been regarded as of no significance. The properties of a heterogeneous scattered X-radiation, for instance, depend, in a very remarkable way, upon the whole atmosphere of that heterogeneous beam, and not upon independent constituents.

With a certain type of radiation or sequence of radiations, it is necessary only to slightly change the average frequency of the radiation by (1) a change in the potential applied to the X-ray tube, or by (2) a change in the proportion of the various constituents such as is produced by filtering the complex radiation, or by (3) combinations in various proportions of (1) and (2), or by (4) superposing radiations of higher, or (5) of lower frequency on the beam experimented upon in order to show the sudden change in the level of its activity which we have described as the J-discontinuity †. These changes in the level of activity, dependent not upon any particular wave-length but on some kind of average measured to a first approximation by an average absorption coefficient, have been observed hundreds of times in this laboratory; records of many typical experiments have been published.

On the other hand, there are radiations or sequences of radiations of the same average frequency which do not show this J-discontinuity; that is, a further factor is involved which is less easily measured or even identified. All the evidence goes to show that this essential factor is some condition of the whole complex radiation, or sequence of radiation, as, for instance, possibly a degree of continuity or of superposition in the stream of radiation. But whatever this factor is, it is certain that the conditions showing discontinuities are separated by only a very narrow margin from those not showing such discontinuities. This critical condition then itself involves a discontinuity. Such a discon-

\* Communicated by the Author.

† (4) and (5) are, of course, changes in reverse order; (5) has been obtained in collaboration with Mr. Sen Gupta.

tinuity, produced when the average frequency (or the average absorption coefficient) remains constant, occurs

- (1) in a scattered radiation with a change in the thickness (or mass) of the scattering substance ;
- (2) in a scattered radiation with a change in the angle of scattering ;
- (3) in a scattered radiation with a change in the frequency of interruption of the primary current in an exciting induction-coil ;
- (4) in a scattered radiation (and less frequently in the primary) with some quite accidental change of an apparently trifling nature in the excitation of rays in the X-ray tube ;
- (5) in the region between the state of a primary and of a scattered radiation, for a scattered radiation shows the discontinuities when the primary does not ;
- (6) in a primary X-radiation when the angle it makes with the cathode stream is changed ;
- (7) in a characteristic radiation from an element with some change, apparently in the primary radiation exciting it ;
- (8) it also occurs in a very homogeneous beam during transmission through absorbing substances (W. H. Watson, unpublished).

All of these, then, are discontinuities of the same magnitude as the other discontinuities occurring when the average frequency (or "temperature") of the radiation remains practically constant. They are produced by a change in some other governing factor, which, so far as we can see at present, can only be identified with the large scale structure of the radiation.

The significance of two factors has, of course, been recognized from the earliest experiments on the subject. [This is in some way analogous to the manner in which the discontinuities involved in the change from the vapour to the liquid state of matter are dependent on temperature and density—within certain limits a discontinuity may be brought about by a change either of temperature or of density alone. Also the critical temperature, that is, the temperature at which the discontinuity occurs, is dependent on the density.] While there is no consistent evidence that the second factor in the case of the J-phenomenon is density (or intensity) of radiation as usually measured, there does seem to be the possibility that this is due to the fact that we can only measure an average energy density for large

volumes of radiation, while localized energy density is the important factor. Indeed, superposition definitely is of primary importance.

Confining ourselves now to a comparison of primary and scattered heterogeneous X-radiations, we can generalize by saying:—The absorbability in aluminium of the radiation scattered from very light elements in a direction perpendicular to the primary radiation is either very accurately the same as that of the primary radiation, or differs from it by a considerable amount. These are “unmodified” and “modified” scattered radiations as shown by ionization-absorption methods with heterogeneous beams. It is the step from one to the other which is the striking feature of our experimental results. We do not find such scattered radiations either more penetrating than the primary, or even slightly more absorbable—only equally absorbable, within a small possible error, or considerably and consistently more absorbable. Either of these may persist throughout experiments lasting for months ; anything between is rare and transitory.

Many examples of the abrupt change from ‘unmodified’ scattered radiation to a modified scattered radiation (due, that is, to a change in the level of activity) have already been given and can be multiplied. We have not, however, hitherto systematically studied the development of the modified radiation from the unmodified, except by passing the complex radiation through one of the “critical temperatures” and so observing the J-discontinuity. The following note shows the manner in which, with a suitable radiation, the modified scattered radiation may be developed from the superposition of unmodified scattered radiations. In other words, the transformation from unmodified scattered radiation is obtained, not by passing beyond a certain critical average frequency, but by changing the structure of the radiation while the same constituent frequencies are maintained in nearly the same proportion. This is a change in the second variable, which we have tentatively called the structure of the complex radiation.

When using a certain primary X-radiation excited in a Coolidge tube by an induction coil with mercury interrupter, it was found that the scattered radiation from air was an unmodified radiation, *i. e.*, a radiation with accurately the same absorbability as the primary radiation exciting it. This was shown by the fact that the ratio of the ionizations produced in two ionization chambers by the scattered and primary radiations ( $S/P$ ) was precisely the same as the ratio  $S'/P'$  for the two beams when these were both intercepted by

sheets of aluminium cutting off a large proportion of the two beams. The radiation scattered from thick sheets of paper or paraffin-wax was, however, quite definitely a "modified" scattered radiation, or contained a modified radiation, *i. e.*, differed considerably in absorbability from the primary radiation. In this case  $S'/P'$ , when the intercepting aluminium was .145 cm. thick, was 9-10 per cent. less than  $S/P$ , the ionizing effect of the scattered radiation having thus been diminished much more than that of the primary. The two radiations scattered from paper and from paraffin-wax were found to be equally modified within a small possible error. Such a result has frequently been obtained in this laboratory, *i. e.*, an unmodified scattered radiation from a gas or thin solid radiator and a modified scattered radiation from a thicker solid. In many experiments made by Mrs. Sale, for instance, the results of which are unpublished, the radiation scattered from twenty sheets of paper was an unmodified radiation, while that scattered from fifty sheets was definitely modified, as measured by these ionization-absorption methods. The result was at that time so inexplicable that we withheld it for further investigation and confined our statement of conclusions to the comparatively simple ones obtained with thin scattering sheets which yielded simple and unmistakable results\*.

In our more recent experiments we made a systematic investigation of the radiation scattered from various thicknesses of scattering substance. It was found that when the sheet of paper or paraffin-wax was made gradually thinner, the difference between  $S/P$  and  $S'/P'$ , that is, the difference between scattered and primary radiations, became smaller, and ultimately almost vanished, indicating very definitely a vanishing difference for an infinitely thin layer of the scattering material.

In fig. 1 a measure of the difference between the absorptions of primary and scattered radiations, or of the transformation by scattering, is plotted against the number of sheets of paper used as the scattering substance. (The radiation scattered from air had an intensity about equal to that from one sheet of paper.) The ordinate is  $\left(\frac{S/P - S'/P'}{S/P}\right) \times 100$ , that is, the percentage change in the ratio of ionizations produced when both beams were intercepted by .145 cm. of Al. Thus if the magnitude of this transformation is  $y$ , the ionization produced by the intercepted scattered radiation is  $y$  per cent. less than would be the case if the scattered

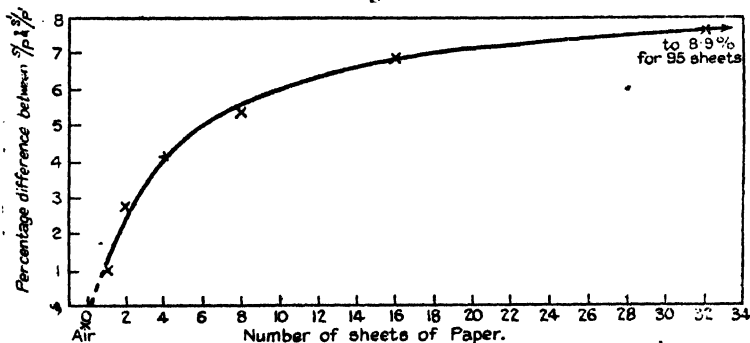
\* Barkla and Sale, *Phil. Mag.*, April 1923.



radiation had been absorbed precisely like the primary. Thus from air alone the percentage of change was zero, within the possible error ; from air and one sheet of paper it was about 1.0 per cent. ; from air and two sheets of paper nearly 3 per cent. and so on approaching a definite limit of a 9 to 10 per cent. change for the radiation from thick layers of paper. The values actually obtained for  $y$  were  $-0.4$ ,  $1.0$ ,  $2.8$ ,  $4.2$ ,  $5.4$ ,  $6.9$ ,  $7.6$ , and  $8.9$  for the radiations from air, air and 1, 2, 4, 8, 16, 32, and 95 sheets of paper respectively.

Paraffin-wax when used as the scattering substance showed precisely similar results, but equal degrees of transformation were obtained from very much greater masses of scattering paraffin. That is the curves were similar, but a much more intense radiation from paraffin was necessary to give the

Fig. 1.



same degree of transformation. Thus fig. 2 indicates the degree of modification of the scattered radiation plotted against mass per unit area (gm. per sq. cm.) of the scatterer, for both paraffin-wax and paper. (As in previous experiments, the face of the scattering slab was inclined at  $45^\circ$  to both primary and scattered radiations.)

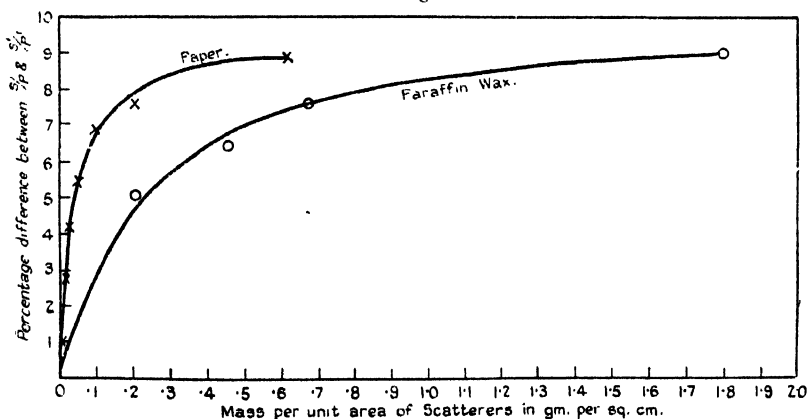
It will be seen that the maximum amount of modification was shown much earlier for a paper- than for a paraffin-wax scatterer, but the two measures of modification were finally equal—appearing as a limiting amount of modification by scattering.

The possibility of the measured difference between scattered and primary radiations being affected in some way by mere variation in the intensity of the ionization occurring in the electrosopes was quite easily disposed of by making considerable variations in the output of the Coolidge tube. Taking the most sensitive portion of the curve and using

two scattering sheets of paper, it was found that quadrupling the intensity of the radiation in this manner was entirely without influence on the measured ratio of ionizations in the two electroscopes.

But, quite independently of this, fig. 2 illustrates the same point, and perhaps much more effectively, for, as indicated, corresponding changes in the scattered radiations from paper and from paraffin-wax occurred for very different intensities of the scattered radiation, the scattered beam from paraffin-wax being seven or eight times as intense as that from paper when the same degree of modification was observed. The degree of modification appeared thus to depend upon a quality of radiation distinct from wave-length and intensity as usually measured, yet associated with superposition.

Fig. 2.



In order to study the effect of isolating the last sheet of a bundle of sheets of paper for which the scattered radiation was considerably modified, it was first observed that the modification in the radiation scattered from thirteen sheets of paper was indicated by a value of  $y$  of about 6.5 per cent. Then twelve of these sheets were moved nearer to the X-ray tube in such a position that the secondary ionization chamber and the absorbing sheets placed in the scattered beam received no radiation from them, but the primary beam still had to traverse these before falling on the thirteenth sheet. That is, the thirteenth sheet was now exposed to the same primary radiation as in the first experiment, but it alone sent secondary radiation through the absorbing sheet into the measuring electroscope. It was then found that the scattered radiation differed only very slightly from the

primary, the amount of modification being as it was in previous experiments when the other twelve sheets were completely removed. The actual figures were 0.7 and 0.9 per cent. respectively. Thus the thirteenth sheet when its radiation was examined alone emitted a radiation which was only very slightly modified; whereas this radiation, along with that from twelve other sheets, gave something approaching the full modified radiation \*.

Such results were obtained for a considerable time, and were quite easily verified. It was our intention to investigate the secondary radiation further when it was in this sensitive state. After the apparatus had been left for a period of about ten days in the Easter vacation of 1927, we returned to these experiments and found that after a few experiments the unmodified radiation from air and from thin paper and paraffin-wax had been replaced by the fully modified radiation. The radiations from these substances (air, paper, and paraffin-wax) were all similar, *i. e.*, were equally modified (within the error of experiment). The critical state in which the development of the modified scattered radiation from the unmodified scattered radiation could be observed had disappeared, and we were compelled for the time to pursue other investigations †.

If any portion of such results should be regarded with greater scepticism than the other as an indication of fundamental processes, it is the modification observed with thicker layers of scattering substance, rather than the absence of modification from the thinner layer. These results, however, are not isolated; they fit consistently into a system of experimental results obtained throughout an enormous range of conditions; one result is as real as the other. Further, this degree of modification was later given by the thin sheets and even by air itself; it cannot, therefore, be attributed to disturbing effects of absorption or to any generally recognized property of radiation.

A fuller discussion can only profitably be given in a paper in which all the experimental results are summarized. This will shortly follow.

\* The maximum measure of modification observed.

† We hope shortly to conduct experiments with apparatus giving a constant high tension instead of the intermittent and varying potentials applied by an induction coil or by a transformer. In the meantime, however, we have found the means for securing this critical state in another absorbing substance and have further confirmed the conclusion that the difference between the results with thin and thick radiators was not in the transmitted primary radiation, but in the different properties of the radiations scattered from these radiators.

*Summary.*

The results given in this note exhibit the change from "unmodified" to "modified" scattered radiations, not by passing through a certain critical average frequency as measured by an average absorption coefficient (illustrated previously by many examples of the J-discontinuity)—but by a change in the other factor involved. (See earlier papers.) In this case it was produced by the superposition of radiations of the same frequencies, and in almost exactly the same proportions. An unmodified radiation was found from air or thin paper, but the degree of modification as measured by absorption methods rapidly developed with increasing thickness of the scattering substance, and approached a limiting value.

The experiments appear to link up the classical and the quantum results, though it may be only by a combination of the two in various proportions dependent on the relative duration of two processes in the time required for an experiment.

The modification, however, depends on some kind of coherence of the whole radiation. What this means fundamentally is not yet apparent: it may, as previously suggested, depend on a certain degree of continuity or of superposition in the whole stream of radiation.

---

CXXI. *Cohesion and Intermolecular Repulsion.* By R. KENWORTHY SCHOFIELD, M.A., Ph.D., Lecturer in Physics in the University of Durham\*.

FIG. 1 represents diagrammatically the variation of the mutual force with distance for the rigid-sphere type of molecule postulated by numerous theorists. These molecules are regarded as spherical, and the force is an attractive one which increases steadily as their centres approach one another. The curve ends abruptly at a distance equal to twice the molecular radius, since the molecules, being supposed absolutely rigid, cannot be closer than this.

Fig. 2 similarly represents the force between two molecules whose fields are of the complex type postulated many years ago by Young and Rayleigh, and recently subjected to mathematical treatment by Lennard-Jones<sup>(1)</sup>. Here also, for the sake of simplicity, the field is regarded as having spherical symmetry with respect to a centre. In this case, as the

\* Communicated by Prof. J. E. P. Wagstaff, D.Sc.

centres approach one another, the mutual attraction increases to a maximum, falls to zero, and then changes to a repulsion which increases very rapidly.

In a liquid or compressed gas, consisting of molecules of the rigid-sphere type, the cohesion would increase continuously with reduction in volume. With molecules of the complex-field type, however, the cohesion might be expected to rise to a maximum, and then become less with further reduction in volume. With this idea in mind, the author calculated the cohesion in a number of gases and liquids at a series of volumes from the data of Amagat <sup>(2)</sup>. The interest

Fig. 1.

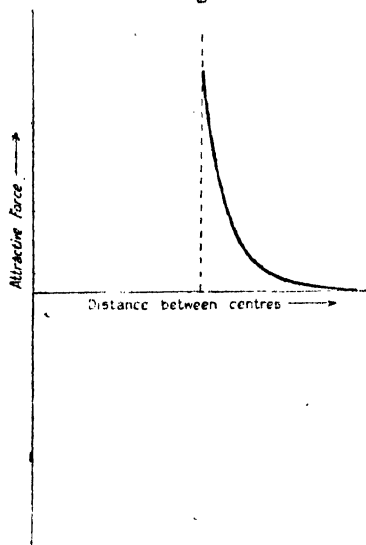
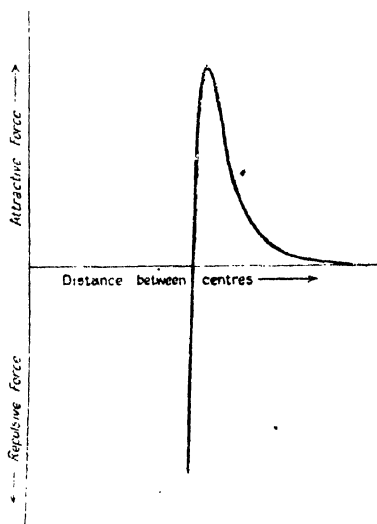


Fig. 2.



of the results obtained seems sufficient to warrant their publication.

#### *Determination of Cohesion.*

As there is no universally accepted method for evaluating cohesion, it is necessary to explain and, it is hoped, justify the one used.

The heat  $dQ$ , taken up by a fluid during a reversible expansion  $dv$ , goes partly to the performance of external work  $p dv$ , against the external pressure  $p$ , and partly to increasing the internal energy  $U$ . Thus

$$dQ = \left( \frac{dU}{dv} \right)_T dv + p dv.$$

But, by the Clapeyron-Claussius relation,

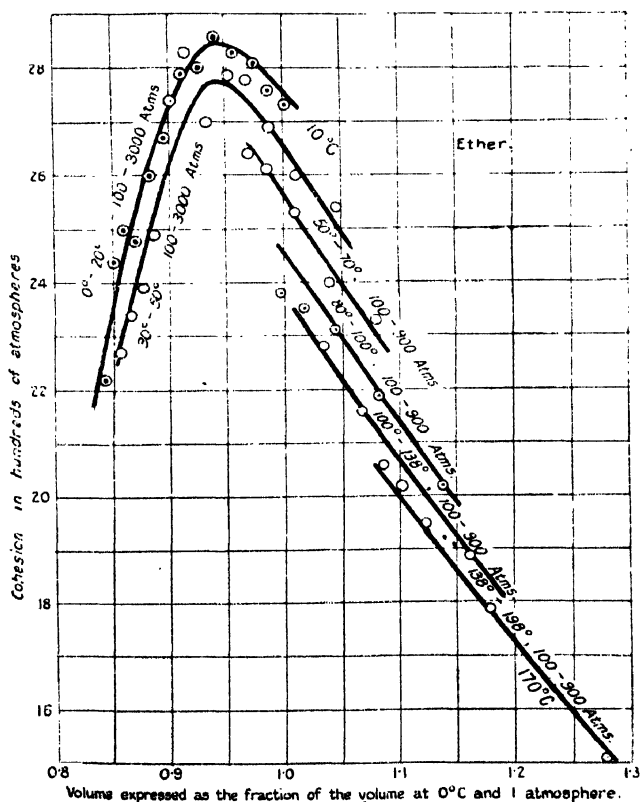
$$dQ = T \left( \frac{dp}{dT} \right)_v dv.$$

Hence

$$\left( \frac{dU}{dv} \right)_T = T \left( \frac{dp}{dT} \right)_v - p,$$

a well-known thermodynamic relation.

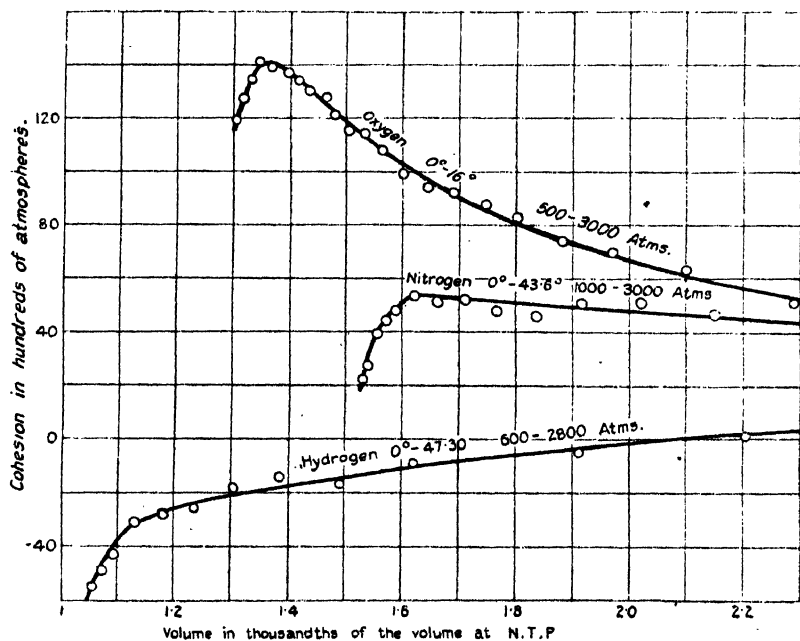
Fig. 3.



$(dU/dv)_T$  has the dimensions of a pressure. In forming an idea of its significance, it is necessary to distinguish between the case where molecular encounters sometimes lead to temporary chemical union, and the case where this does not occur. The possibility of chemical union is not taken account of in either of the molecular theories under consideration. Hence discussion of the case where chemical

unions occur is not germane to the present inquiry. Where no chemical unions occur, the number of molecules (*i. e.* the number of entities taking part in thermal agitation) will not be affected by a change in volume. Hence an isothermal expansion  $dv$  will not affect the total translational kinetic energy (the K. E. associated with the movements of the centres of mass of the molecules), and so the increase in internal energy  $(dU/dv)_T dv$  is the direct outcome of the mutual separation of the molecules consequent upon the expansion. Thus  $(dU/dv)_T dv$  is the energy that must be

Fig. 4.



supplied in order to effect the necessary separation of the molecules, and therefore it seems reasonable to give the name cohesion to  $(dU/dv)_T$ . In using this word, no restriction upon the form taken by the ingoing energy is implied, except that it is not chemical and not translational kinetic.

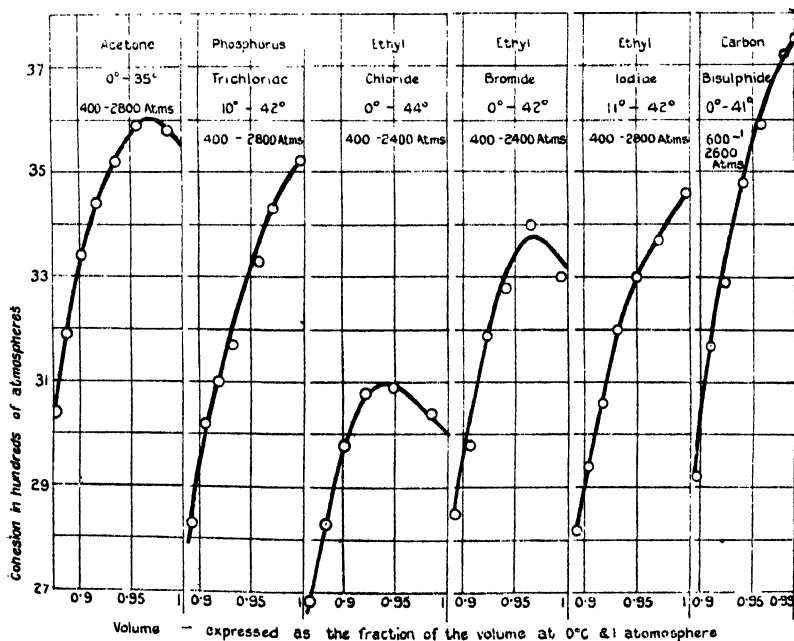
#### *Discussion of the Curves.*

Curves showing the variation of cohesion with volume are given in figs. 3, 4, and 5. These cover all the substances investigated by Amagat, with the exception of water and

four alcohols which have been excluded because molecules of these substances are believed to associate chemically. The most striking feature of the curves for the remaining substances is the final decrease in cohesion with decrease in volume which occurs in every case—this gives emphatic support to the complex-field, as opposed to the rigid-sphere theory.

The curves\* for ether form a link between the oxygen curve and those for the liquids. They are also important in showing that, for this substance, the cohesion at a given

Fig. 5.



volume decreases with temperature (over the volume and temperature range of Amagat's experiments)†. The data

\* It was found best to obtain  $(dp/dT)_v$  as the product of  $(dv/dT)_p$  and  $-(dp/dv)_T$  calculated from Amagat's figures for the volumes at two neighbouring temperatures and at a series of pressures. These two temperatures are stated for each curve; the cohesion will presumably be that for the mean temperature. A certain amount of straying of the points from the smooth curve is to be expected, especially when the two temperatures are not very different.

† There is evidence from the data of Young<sup>(8)</sup> that, at rather larger volumes (i. e. just less than the critical volume) and at higher temperatures, the cohesion increases with temperature.



for the three gases only permit of determination of the sign of the temperature variation of the cohesion as far as  $p = 1000$  atmospheres ( $v =$  about 18), but thus far it is the same in all three cases as for ether. It is possible, therefore, that the curves for oxygen, nitrogen, and hydrogen are typical of the stages through which the curves for the other substances would pass at sufficiently high temperatures.

The quantitative interpretation of the cohesion in terms of the forces between individual molecules is obviously an exceedingly complex problem in statistical mechanics, seeing that the relative position of the molecules is constantly changing on account of their thermal movements. Yet it will be seen in a general way that the more violent the thermal agitation, the more deeply will the molecules (considered to be of the complex field type) penetrate into the inner (repulsive) parts of each other's fields. Thus the ratio of the time that molecules repel each other to the time that they attract each other increases with the temperature. This may account for the temperature variation of the cohesion, and its negative value in hydrogen at  $24^{\circ}\text{C}$ .

In conclusion, I gladly take this opportunity of expressing my gratitude to Professor Masson for the interest he has taken in this work and for several very helpful suggestions.

### *Summary.*

The cohesion in a number of highly compressed liquids and gases has been calculated over a wide pressure range. As the volume is reduced the cohesion first increases to a maximum and then decreases.

The results cannot be reconciled with the view that molecules resemble rigid spheres, but are readily accounted for on the view that the force between two molecules is repulsive when they are very near together, and attractive when they are further apart.

### *References.*

- (1) Lennard-Jones, Proc. Roy. Soc. A. cvi. p. 463 (1924), & cxii. p. 214 (1926). Faraday Soc. Trans. xxiv, p. 100 (1928).
- (2) Amagat, *Annales de Chimie et de Physique*, series 6, p. 29 (1893).
- (3) Young, Phil. Mag. 5, xxiii. p. 485 (1887); Proc. Phys. Soc. xiii. p. 602 (1895); Phil. Mag. p. 47 (1899).

CXXII. *The Velocity of Sound in Liquids at High Frequencies by the Sonic Interferometer.* By PROF. J. C. HUBBARD (Johns Hopkins Un.) and A. L. LOOMIS\* (Communication No. 3 from the Loomis Laboratory, Tuxedo Park, N.Y.)\*

*Introduction.*

THE method of measuring the velocity of sound in liquids herein described, has been developed for its purpose of securing results of high precision with employment of relatively minute quantities of liquid. From the results it is possible to deduce the adiabatic compressibility, and when the specific heat at constant pressure is known, the isothermal compressibility, difference of specific heats, increase of internal energy with volume at constant temperature, and so forth. The method is, therefore, capable of furnishing information of thermodynamic importance. The precision attainable is such that the instrument promises, like the refractometer or pycnometer, to be of use to physicists and chemists for empirical analysis.

The measurement of the velocity of sound in liquids by methods hitherto used is beset with peculiar difficulties, either of experiment or of interpretation. The velocity is of such magnitude that the direct method necessarily has been restricted in application to large bodies of water. Most painstaking effort has been expended in securing data on salinity and temperature with the object of specifying these quantities for the velocity found. Resonance methods at audible frequencies have been tried by a number of observers. Such methods call for large-size apparatus and a large quantity of liquid, restricting measurements to commoner and more easily purified substances. These methods, moreover, involve a serious correction factor owing to the influence of the materials and dimensions of the apparatus upon the wave-length. The interesting experiments of Dörsing† and others, using resonance methods, have yielded a large number of values of the velocity of sound in different liquids, in most cases for temperatures between 15° and 20° C. Owing to the different correction formulæ used and to different means of approximation

\* Communicated by Prof. R. W. Wood.

† K. Dörsing, *Ann. d. Phys.*, xxv. pp. 227-251 (1908). See also *Handbuch der Physik*, viii. Akustik, p. 641; W. Busse, *Ann. d. Phys.* lxxv. pp. 657-664 (1924).

employed by various observers, the results, where comparable, are in serious disagreement. The latest and probably the best of the experiments by the resonance method at audible frequencies are those by Pooler\*, who has measured the velocity of sound in distilled water as a function of the temperature. He has made use of a correction formula developed for special application to his experiments by Gronwall†.

Langevin made use of the piezoelectric property of quartz for the purpose of generating a beam of high-frequency sound-waves for the detection of submarines. Wood and Loomis‡ have made an extensive study of the effects of such waves and have described a number of phenomena depending upon standing wave systems produced in a vessel of oil containing a quartz plate driven at high frequencies. They were able to estimate the half wave-length in oil by the observation of a number of effects, and the work of the present paper makes use of these experiments as the starting point.

Boyle§ has published a series of studies of beams of sound-waves produced by a piezoelectric plate in a large tank. He has produced standing wave systems in water and in castor oil, and gives the velocity of sound in these liquids at a number of frequencies. These values are significant within one per cent, but are restricted to the neighbourhood of a single temperature. Boyle does not find any sensible dependence of velocity upon frequency within the range of his experiments.

Preliminary results by the method described in the present paper have been published by the authors||. The present paper summarizes all the results of value obtained at the Loomis Laboratory, Tuxedo Park, during the summer of 1927.

### *Apparatus and Method.*

The sonic interferometer for liquids consists of a cylindrical chamber containing the liquid to be studied, in which plane compressional waves are produced by a piezoelectric

\* L. G. Pooler, *Phys. Rev.* xxxi. pp. 157-158 (1928) (Abstract).

† T. H. Gronwall, *Phys. Rev.* xxx. pp. 71-83 (1927).

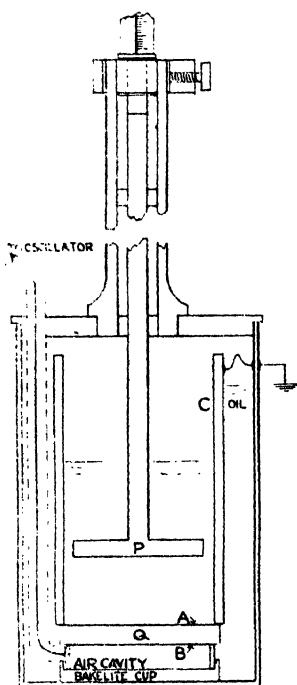
‡ R. W. Wood and Alfred L. Loomis, *Phil. Mag.* iv. pp. 417-436 (1927). See also W. T. Richards and A. L. Loomis, *Journ. Am. Chem. Soc.* xlix. pp. 3086-3099 (1927).

§ R. W. Boyle, *Trans. Roy. Soc. Can.* iii. p. 141 (1923); pp. 159, 191, 197 (1925); p. 79 (1927). See also 'Nature,' cxx. p. 476, Oct. 1 (1927).

|| J. C. Hubbard and A. L. Loomis, 'Nature,' cxx. p. 189, Aug. 6 (1927); *Phys. Rev.* xxxi. p. 155 (1928) (Abstract).

plate maintained in forced vibration by connexion of one of its electrodes with a point on the coil of a high-frequency oscillating electrical circuit, the other electrode of the plate being in contact with the liquid and grounded. The waves are reflected by a movable piston, which may be displaced by a micrometer screw so as to be set at successive positions for the production of standing waves. The frequency of oscillation is so high that the wave-length in the liquid is

Fig. 1.



short in comparison with the diameter of the plate. (We have used quartz plates of 50 mm. diameter, the wave-length in the liquid being in the neighbourhood of 3 mm.) Under these conditions our experiments have shown that the effect of the walls of the vessel may be entirely neglected when the piston is within a few cm. of the plate.

In fig. 1, let Q be the quartz plate, A and B the electrodes, the latter connected to the coil of the oscillating electrical system and the former closing the end of the cylinder and

serving as a diaphragm for the transmission of the vibrations of the quartz plate to the liquid. The diaphragm A as well as the cell C and the piston P are all grounded. In the experiments about to be recorded, the results for water and for salt solutions were obtained with instruments exactly as here described, except that an outer chamber filled with oil was provided to serve as a temperature bath. All parts exposed to the liquid being studied were gold-plated. In the experiments with mercury the cell C consisted of a small pyrex beaker, the bottom of which was ground plane inside and out. The beaker rested upon a thin foil serving as the grounded electrode on the upper side of the quartz. The piston in this case was cut from the bottom of a pyrex beaker and fused to a pyrex rod, the piston afterwards being ground plane. Owing to the fact that part of the piston rod is in an unhomogeneous temperature field when working with temperatures in the liquid chamber far from that of the room, the rod should have a small coefficient of expansion. The rods used with all substances except mercury were of quartz or of invar. The piston is displaced vertically by a Brown and Sharp micrometer screw, the head of which is divided into hundredths of a millimetre. Since the results reported in this paper were obtained, great improvements have been made in the design of the interferometer, so as to prevent loss of vapour of the liquid and to render the instrument suitable for deep immersion in a thermostat or in a Dewar flask. The various forms of instruments which we have devised will be the subject of a paper which will appear in another place. It remains to be said that the one requirement for successful operation is that there be no air or gas bubbles between the quartz plate and the liquid in which it is desired to produce waves. Mechanical coupling between the quartz and the liquid is secured by the use of a transformer oil, a few drops being placed upon the quartz plate before it is put in contact with the diaphragm. Similarly in case a glass vessel is to replace the cell C, there must be an oil film between the plane bottom of the vessel and the electrode.

The electrical circuit which is used to drive the quartz plate is of the usual type of oscillator; it is provided with a variable condenser, and the frequency is adjusted so as to be somewhat removed from the natural frequency of the quartz plate in order to avoid distortion of wave-form. In nearly all the experiments recorded here a vernier condenser was also provided for a purpose that will appear below.

As the piston is displaced through the liquid, the tuning of the liquid column varies, passing through successive resonance points. The impedance of the liquid varies through a cycle, causing a corresponding variation in the reaction of the liquid on the quartz plate, and through the inverse piezoelectric effect a corresponding reaction is produced in the electrical circuit. This variation produces a number of effects, any one of which may be used as a basis of measurement of the half wave-length of the compressional wave in the liquid. Among these cyclic variations are: plate current of oscillator observed by means of a milliammeter; voltage variation in the coil, measured by voltage amplifier (designed for us by Dr. A. W. Hull); voltage variation in the coil indicated by a neon lamp, so placed as to be extinguished at the instant of passage through resonance; variation in frequency of oscillation which may be detected by the cyclic changes of reading of the milliammeter of a wave-meter which is loosely coupled to the oscillator; variation of heterodyne beat with a second oscillator of constant frequency; variation in current in high-tension lead to the quartz plate indicated by vacuum thermocouple and galvanometer. For the purpose of most precise measurement and by means of which all the results here reported were measured, we have used a double heterodyne method, similar in principle to that used by Whiddington in his "ultra-micrometer." By this method the frequency is automatically held constant and the half wave-length to be determined is thus invariable.

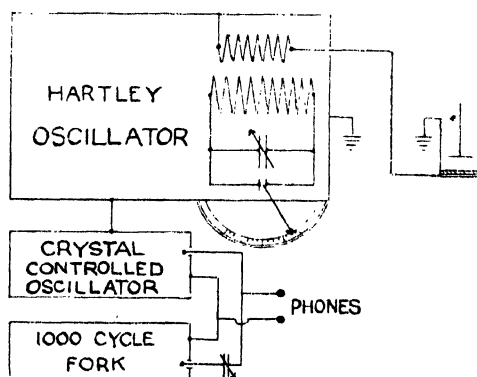
The main oscillator (fig. 2) is loosely coupled to a crystal-controlled oscillator of known frequency. The heterodyne beat note thus produced is then tuned by means of a vernier condenser to unison with a tuning fork, the frequency of which is 1000 cycles per second. The frequency of oscillation of the main oscillator and thus of the interferometer plate is accordingly that of the piezoelectric oscillator, plus or minus 1000 cycles per second.

In some of the experiments we have used, in the crystal-controlled oscillator, a crystal ground to 501,000 cycles  $\pm$  0.01 per cent., so that with a beat note of 1000 cycles the main oscillator is kept at exactly 500,000 cycles. As a result, the velocity of sound in metres per second has the same numerical value as the half wave-length in the liquid in thousands of a millimetre, and accordingly may be read directly from the screw.

As the piston is advanced through the liquid column, the reaction on the main oscillator is such as to require a cyclic

variation of the vernier condenser in order to maintain unison of the heterodyne note with the fork. If we plot vernier condenser readings as ordinates and screw readings as abscissæ we may take as the half wave-length in the liquid the difference in screw readings corresponding to two adjacent similar mean points on the curve. In practice, the reaction is so sharp at the node that settings may be made by ear within a few thousandths of a millimetre. Usually we have determined the position of three successive settings nearest the diaphragm, then of three successive positions about 2 cm. beyond. Under usual conditions the precision obtainable in the value of the half wave-length

Fig. 2.



from such readings is about one part in five thousand. The following illustrate the magnitudes of quantities involved and the variations in their measurement.

Mercury.  $t = 20^{\circ}0$  C.

Setting.	Screw, cm.	Difference.	Setting.	Screw, cm.	Difference.
1 .....	·4445		12 .....	2·2695	
2 .....	·6105	·1660	13 .....	2·4368	·1673
3 .....	·7772	·1667	14 .....	2·6034	·1666
Mean ...	·6107		Mean ...	2·4866	

Displacement for 11 half wave-lengths, 1·8259 cm.

$\lambda/2 = 16582$  cm.

$f = 437,600$  cycles/sec.

$u = 1451\cdot3$  metres/sec.

The following results, from similar measurements, include all those found for mercury at 20.0° C.:—

$\lambda/2$ , cm.	$u$ , m./sec.
·16579	1451.0
·16576	1450.7
·16570	1450.2
·16580	1451.1
·16583	1451.4
·16580	1451.1
·16582	1451.3

Mean  $u = 1451.0$  m./sec.

Average deviation,  $\pm 0.3$  m./sec.

### *Thermodynamic Relationships.*

The velocity of sound in a liquid is given by

$$u = (1/\beta_{\phi}\rho)^{\frac{1}{2}} = (k/\beta_T\rho)^{\frac{1}{2}}, \quad . \quad . \quad . \quad (1)$$

where  $\beta_{\phi}$  and  $\beta_T$  are respectively the adiabatic and isothermal compressibilities of the liquid,  $\rho$  is the density, and  $k$  the ratio of specific heats,  $c_p/c_v$ . Using the relations

$$c_p - c_v = -T \left( \frac{\partial v}{\partial T} \right)_p^2 / \left( \frac{\partial v}{\partial p} \right)_T \quad . \quad . \quad . \quad (2)$$

and

$$\alpha = \frac{1}{v} \left( \frac{\partial v}{\partial T} \right)_p; \quad \beta_T = -\frac{1}{v} \left( \frac{\partial v}{\partial p} \right)_T, \quad . \quad (3 \text{ \& } 4)$$

we have

$$c_p - c_v = T\alpha^2/\beta_T\rho = T\alpha^2u^2/k \quad . \quad . \quad . \quad (5)$$

and

$$k = 1 + T\alpha^2u^2/c_p \quad . \quad . \quad . \quad (6)$$

For purposes of calculation it is more convenient to use, in place of  $\alpha$ , the quantity  $\alpha_0 = (\partial v/\partial T)_p/v_0$ , which may be found for a number of substances from data in standard tables. Equations (5) and (6) then take the form

$$c_p - c_v = \frac{T\alpha_0^2u^2}{k} \cdot \frac{\rho^2}{\rho_0^2} \quad . \quad . \quad . \quad (5')$$

and

$$k = 1 + \frac{T\alpha_0^2u^2}{c_p} \cdot \frac{\rho^2}{\rho_0^2} \quad . \quad . \quad . \quad (6')$$

From (6') it is thus possible to calculate the ratio of specific heats of a liquid for which the specific heat at constant pressure is known. Since in most cases  $\alpha_0$ ,  $\rho$ , and  $\rho_0$ , and, as it is hoped the present paper will show,  $u$ , may be deter-



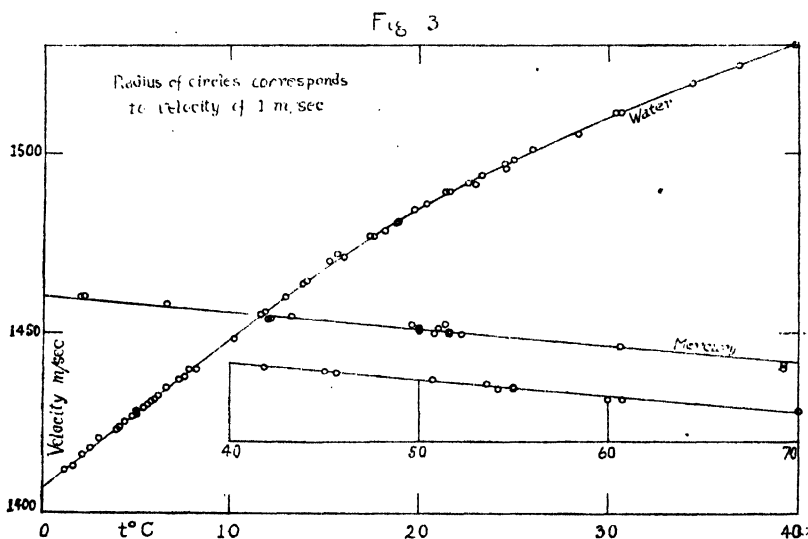
mined to a high order of accuracy, the computed value of  $k$  is limited in precision at present only by the limitations of existing data on  $c_p$ .

Having determined  $k$ ,  $c_p - c_v$  may be found from (5'). Other coefficients of especial interest are :

$$\left(\frac{\partial v}{\partial p}\right)_T = \frac{k}{v^2 \rho^2} \quad \dots \quad (7)$$

and

$$\left(\frac{\partial E}{\partial v}\right)_T = \frac{\rho_0}{\alpha_0} (c_p - c_v) - v \quad (8)$$



### Results.

The velocity of sound has been measured in the manner described for water from zero to 40° C. ; for mercury from zero to 70° C. ; for five solutions of NaCl ; two of NaI ; and one of KCl. Data were obtained for CS<sub>2</sub>, chloroform, toluene, and acetone, which were of use in suggesting improvements in the design of the instrument, especially in respect of insuring against liability to absorption of water-vapour from the atmosphere ; but these data are not included here, as contamination was quite possible with the instrument as used.

Fig. 3 represents in graphic form the results for water and for mercury. The points on the water-curve were

obtained with three different instruments, using a four-fold variation in wall-thickness of measuring vessel, a number of different modes of attachment of diaphragm, and both with and without a surrounding oil-bath for temperature control. The oil-bath, when used, was immersed in a larger water thermostat. The intensity of the electrical vibration was varied from that which produced a barely perceptible heating effect to a value so small that it was just possible to detect nodes. It was found that a most gratifyingly large margin for use in measurements exists in the power which may be employed between the value which will produce sensible error due to heating and the smallest value that will permit a precise definition of nodes. The procedure has been to draw a smooth curve through the points, and from the smooth curve to read off values at intervals of  $5^\circ$  for computation of thermodynamic quantities. Table I. presents these quantities for water.

TABLE I.—Water.

$t^\circ \text{C.}$	$u, \text{m./sec.}$	$k.$	$c_p - c_v \frac{\text{cal.}}{\text{gr. deg.}}$	$\left(\frac{\partial v}{\partial p}\right)_T \times 10^{10}.$	$\left(\frac{\partial E}{\partial v}\right)_T 10^{-7}.$
0 ...	1407.0	1.0005847	.0005872	.5056	-36.53
5 ...	1427.7	1.00003438	.00003448	.4906	+ 8.943
10 ...	1448.8	1.001086	.001086	.4772	51.82
15 ...	1467.5	1.003357	.003345	.4667	92.86
20 ...	1484.2	1.006556	.006506	.4586	131.82
25 ...	1498.1	1.010583	.010454	.4529	169.6
30 ...	1509.9	1.01525	.01499	.4492	205.6
35 ...	1520.6	1.02037	.01992	.4466	239.7
40 ...	1530.3	1.02575	.02505	.4449	271.5

The coefficients of expansion of water are calculated from the formulæ of Chappuis. The values of  $c_p$  are taken from 'Handbuch der Physik,' x. p. 323.

It is interesting to compare the value for  $c_p - c_v$ , .0079 at  $22^\circ$  and zero pressure obtained by Bridgman\* for water, with the value .008004, calculated from the velocity of sound,  $u = 1490.2 \text{ m./sec.}$  at  $22^\circ$ . F. A. Schulze† gives for  $c_p - c_v$  the values .0005 and .006 respectively at  $0^\circ$  and  $20^\circ \text{C.}$  The other quantities are in similar agreement with published data. It will be observed, however, that the values recorded

\* P. W. Bridgman, Proc. Am. Acad. of Arts & Sciences (1912). 1792.9

† F. A. Schulze, Phys. Zs. xxvi. p. 155 (1925).

in the present paper may be regarded, in the case of quantities proportional to  $c_p - c_v$ , as having four significant figures, and that the decimal part of  $k$  also has four significant figures.

Corresponding data for mercury are given in Table II.

TABLE II.—Mercury.

$t^\circ \text{C.}$	$u, \text{m./sec.}$	$k.$	$c_p - c_v \frac{\text{cal.}}{\text{gr. deg.}}$	$\left(\frac{\partial v}{\partial p}\right)_T \times 10^{13}.$	$\left(\frac{\partial^2 v}{\partial v^2}\right)_T \times 10^{-7}.$
0 ...	1460.2	1.1371	.004034	.2885	1264
10 ...	1455.6	1.1415	.004132	.2925	1294
20 ...	1451.0	1.1457	.004228	.2965	1322
30 ...	1446.4	1.1499	.004322	.3006	1350
40 ...	1441.7	1.1539	.004412	.3047	1377
50 ...	1437.1	1.1579	.004501	.3089	1404
60 ...	1432.4	1.1618	.004587	.3131	1429
70 ...	1427.7	1.1655	.004670	.3173	1454

Bridgman\* gives .0544 gram calories for the difference  $c_p - c_v$  for 13.596 grams of mercury at  $0^\circ \text{C.}$  From the above table we obtain, for comparison,  $.004034 \times 13.596 =$

.05484. Bridgman gives values of  $\left(\frac{\partial v}{\partial p}\right)_T$ , which in c.g.s.

units reduce to  $.286 \times 10^{-12}$  and  $.297 \times 10^{-12}$  for  $0^\circ$  and  $22^\circ$  respectively, as compared with  $.2885 \times 10^{-12}$  and  $.2973 \times 10^{-12}$  obtained from the above results for the same respective temperatures. The value of  $k$  for mercury at  $0^\circ \text{C.}$  is frequently taken to be 1.14 (see, for example, Planck, 'Thermodynamik'). So far as we can find, there is no previous record of any measurements of the velocity of sound in mercury.

One phenomenon of marked interest was observed in the measurements with mercury. If the power supplied by the oscillating circuit is not reduced greatly below any value at which heating of the mercury can be observed, the indication of resonance is at once destroyed. That is, as the piston advances through the mercury, a resonance-point is reached, only to disappear immediately, no further movement of the piston indicating a resonance-point for some seconds. It seems probable that, in view of the very high absorption

\* Bridgman, Proc. Am. Acad. Arts & Sciences, xlvii. p. 383.

observed by Wood and Loomis (*loc. cit.*) for high-frequency waves in mercury, we may expect a heating at nodes causing a heterogeneity of the medium and destroying the plane-wave system. To guard against this phenomenon, the amplitude of oscillation was reduced until the heterodyne beat note, the vernier condenser being unchanged, varied by not more than ten or twelve vibrations per second from the pitch of the fork as the piston was advanced from node to node. A second difficulty in these measurements with mercury arose from the fact that, owing to the improvised nature of the glass cell in which the measurements were made, the vibrating quartz plate was separated from the mercury by a glass wall which was not accurately plane-parallel, and which had several visible flaws in it. Probably, owing to this cause, some of the measurements deviate more widely than is the case with any other substance which we have tried. All the points obtained are shown in fig. 3.

Five solutions of sodium chloride were studied. Table III. presents the values of the velocity of sound obtained. The concentration is expressed in weight per cent. NaCl. The values given for the three solutions of lower concentration are reduced from the values reported by the authors in 'Nature,' it being found that, owing to a curvature of the carriage-guides carrying the piston-support used in those measurements, the results were all too high by approximately 0.6 per cent.

TABLE III.—NaCl Solutions.

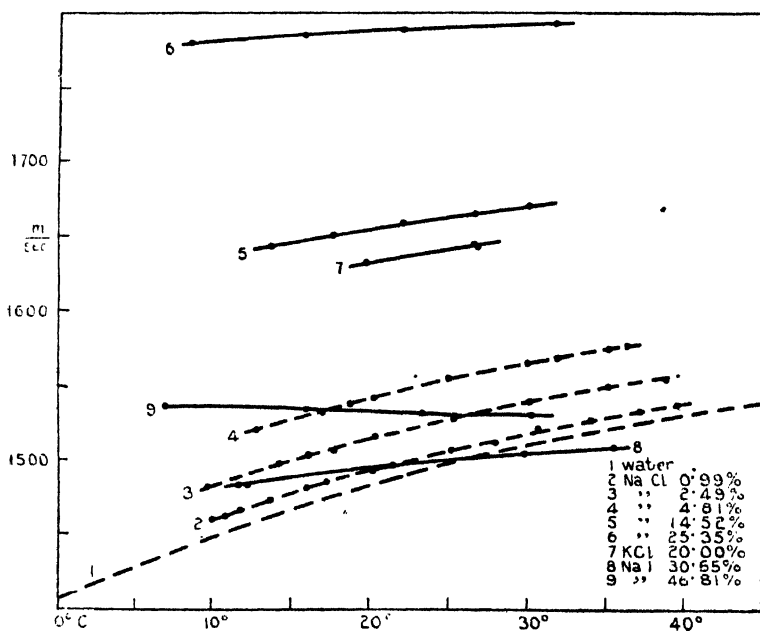
$t^{\circ}\text{C.}$	.99 per cent. NaCl.	2.49 per cent. NaCl.	4.81 per cent. NaCl.
	$u$ , m./sec.	$u$ , m./sec.	$u$ , m./sec.
10 .....	1460	1483	
20 .....	1492	1515	1542
30 .....	1517	1538	1565
40 .....	1538	1556	1583

14.52 per cent. NaCl.		25.35 per cent. NaCl.	
$t^{\circ}\text{C.}$	$u$ , m./sec.	$t^{\circ}\text{C.}$	$u$ , m./sec.
13.8 .....	1644.1	8.25 .....	1780.2
17.6 .....	1650.9	15.8 .....	1786.0
22.0 .....	1658.5	22.05 .....	1789.3
26.7 .....	1665.6	31.8 .....	1792.9
29.2 .....	1669.4	31.95 .....	1792.9

Smooth curves have been drawn through the points plotted,  $u$  being ordinates and  $t$  abscissæ. These are indicated in fig. 4, curves 2, 3, 4, 5, and 6. To show the effect of concentration of the salt upon the velocity of sound, the values of  $u$  have been taken from large-scale plots at the respective temperatures of  $16^{\circ}$  and  $30^{\circ}$  C. Fig. 5 shows  $u$  as a function of the weight per cent. of NaCl. It is interesting to note that the values of the velocity of sound in NaCl solutions at a given temperature are almost exactly linear

Fig. 4.



with the percentage of salt. We have chosen the value of  $t=16^{\circ}$  C. for comparison with the data summarized in the 'Handbuch der Physik,' vol. viii. p. 642. The curves there shown are reproduced as curves B, D, and V in fig. 5. Curve B is computed from measurements of O. Tait (1889) on the compressibility of salt solutions. Curve D shows three points obtained for the velocity of sound in salt solutions at  $16^{\circ}$  C. by Dörsing (1907). Curve V shows values of  $u$  obtained at the same temperature by Veenekamp (1922). The Handbuch should be consulted for additional

discussion of these values. Our measurements indicate a slight departure from linearity with concentration, but do not indicate any obvious effect of dissociation.

Table IV. gives the results for the one solution of KCl which was studied. This case shows a marked similarity to that of NaCl in the same region of velocities (fig. 4, curve 7).

Fig. 5.

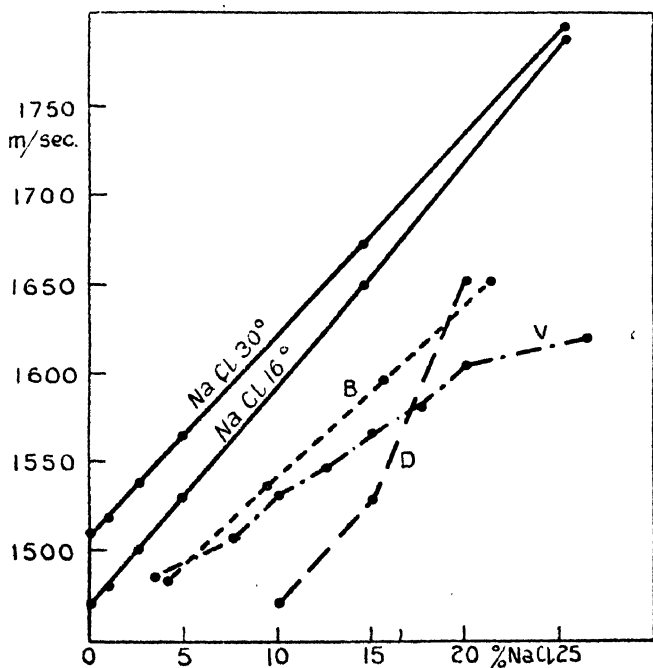


TABLE IV.

KCl, 20.00 per cent. : Water, 80.00 per cent.

$t$ .	$u$ , m./sec.
19.8 .....	1632.5
26.6 .....	1643.4
26.7 .....	1648.7

Table V. shows the values of  $u$  which have been found for two solutions of NaI in water.

TABLE V.

30.55 per cent. NaI.		46.81 per cent. NaI.	
<i>t.</i>	<i>u</i> , m./sec.	<i>t.</i>	<i>u</i> , m./sec.
11.6 .....	1484.3	7.0 .....	1536.3
12.2 .....	1484.5	16.0 .....	1534.5*
21.5 .....	1497.0	23.4 .....	1531.9
29.9 .....	1503.8	30.4 .....	1530.8
35.5 .....	1508.9		

These values are shown in fig. 4, curves 8 and 9. These solutions are of especial interest, showing above 25° C. an actual decrease in the velocity of sound as compared with pure water for moderate concentrations, and an increase to values greater than for pure water at higher concentrations. Mr. E. B. Freyer, working at Johns Hopkins University with one of the authors, has confirmed these results, and has observed a similar behaviour for solutions of potassium iodide.

#### *Summary.*

In the foregoing paper is described a new method of measuring the velocity of sound in liquids at high frequencies. A circular plate of quartz two inches in diameter, with plane-parallel faces, is caused to vibrate piezoelectrically at such frequencies that the compressional waves produced by it in a column of liquid are of short length as compared with the diameter of the plate and of the liquid column. Under these conditions it is found that the velocity of sound, measured by resonance, is independent of the materials or dimensions of the vessel containing the liquid; the method is thus free from the troublesome corrections that have hitherto been necessary when measuring the velocity of sound in tubes by resonance. Sound-velocities are reported for a number of temperatures for water and for mercury, and for a number of concentrations, each at several temperatures, of solutions of sodium chloride. One concentration of potassium chloride and two of sodium iodide at several temperatures are reported. Several thermodynamic coefficients for water and for mercury have been computed from the results, and good agreement has been found with the work of Bridgman.

A more detailed description of the instrument and its theory will be published in another place.

CXXIII. *On Changes that may take place in the Inter-atomic Internal Energy according to Thermodynamics, and Catalytic Action.* By R. D. KLEEMAN, B.A., D.Sc.\*

§ 1. *The Form of the Equation of State of a Perfect Gas according to Thermodynamics.*

ON allowing a liquid to evaporate the external work  $w$  done is given by

$$w = p(v_2 - v_1) = \int_{v_1}^{v_2} p \cdot \partial v, \quad . \quad . \quad . \quad (1)$$

where  $p$  denotes the pressure and  $v_1$  and  $v_2$  the volumes of the liquid and vapour respectively. The internal heat of evaporation  $L$  at the absolute temperature  $T$  is obtained by multiplying the well-known thermodynamical equation

$$\left(\frac{\partial U}{\partial v}\right)_T + p = T \left(\frac{\partial p}{\partial T}\right)_v \quad . \quad . \quad . \quad (2)$$

by  $\partial v$  and integrating it between the limits  $v_1$  and  $v_2$ , giving

$$U_2 - U_1 + p(v_2 - v_1) = L + w = T \int_{v_1}^{v_2} \left(\frac{\partial p}{\partial T}\right)_v \cdot \partial v, \quad . \quad (3)$$

where  $U_2$  and  $U_1$  denote the internal energies in the vaporous and liquid states respectively. On differentiating equation (1) with respect to  $T$  at constant volume, it may be written

$$\left(\frac{\partial w}{\partial T}\right)_v = \left(\frac{L + w}{T}\right) \quad . \quad . \quad . \quad (4)$$

by means of the foregoing equation. Now the writer has shown† that the adiabatic of zero entropy corresponds to  $T=0$ . Therefore, when  $T=0$ , we have

$$\frac{L + w}{T} = 0, \quad . \quad . \quad . \quad (5)$$

\* Communicated by the Author.

† Phil. Mag. iv. p. 261 (1927).



1192 Prof. R. D. Kleeman: *Changes in the Inter-atomic*  
and equation (4) under these conditions may be written

$$\left(\frac{\partial w}{\partial T}\right)_v = \frac{\partial}{\partial T} \{p(v_2 - v_1)\} = \left[\frac{\partial}{\partial T}(pv_2)\right]_v = 0, \quad (6)$$

since  $v_2$  is infinitely large in comparison with  $v_1$  \*.

A substance by definition is in the state of a *perfect gas* when its volume is infinitely large. In certain cases, however, a gas may behave as a perfect gas over a region of finite volumes. Let us write the equation of a perfect gas in the form

$$pv = M\xi RT, \quad (7)$$

where  $M$  denotes the mass of the gas in mols, and  $\xi$  a quantity whose nature remains to be determined. On substituting for  $pv_2$  from this equation in the preceding equation, it becomes

$$\left(\frac{\partial w}{\partial T}\right)_v = M\xi R + MRT \left(\frac{\partial \xi}{\partial T}\right)_v = 0 \quad (8)$$

It follows from this equation that  $\xi$  is a function of  $T$  which becomes zero when  $T=0$ . We will show presently that it is also a function of the volume  $v$ , and that its functional form depends on the nature of the substance.

## § 2. *The Gas Scale and Thermodynamical Scale of Temperature.*

The temperature  $T$  in equation (2) refers to the absolute thermodynamical scale of temperature, which is fundamentally defined by the equation

$$\frac{Q_1}{T_1} = \frac{Q_2}{T_2}, \quad (9)$$

which refers to a reversible cycle in which  $Q_1$  denotes the heat energy taken in at the temperature  $T_1$ , and  $Q_2$  the heat energy given out at the temperature  $T_2$ . Hence  $T$  in equation (7) also refers to that scale. The scale based on the perfect gas thermometer for which it has been assumed

\* Since the result expressed by equation (6) is very important, subsidiary evidence of the truth of equation (5) would be welcome. In a paper that will appear in the May number of the 'Journal of the Franklin Institute,' it is shown that since  $T=0$  in equation (5) it follows from the calculus that  $L=0$ . This result, it is then shown, can also be deduced from Clapeyron's well-known equation referring to the evaporation of a liquid.

that  $pv = MRT$  holds exactly, and the foregoing thermodynamical scale will therefore *not coincide exactly* according to equation (7), but the difference will evidently be negligible except close to the absolute zero.

§ 3. *The Change in Inter-atomic Internal Energy on Change of Volume of a Chemically Non-Interacting Gas.*

On substituting for  $p$  in equation (2) from equation (7), it becomes

$$\left(\frac{\partial U}{\partial v}\right)_T = \frac{MRT}{v} \left(\frac{\partial \xi}{\partial T}\right)_v \dots \dots (10)$$

Thus  $\left(\frac{\partial U}{\partial v}\right)_T$ , the change in internal energy per unit change in volume of a perfect gas, is not zero as is usually supposed.

On multiplying the equation by  $\partial v$  and integrating it between the limits  $\infty$  and  $v$ , supposing that the gas law is obeyed between these limits and that  $\xi$  is independent of  $v$ , we obtain

$$U_\infty - U_v = MRT \left(\frac{\partial \xi}{\partial T}\right)_v \{\log \infty - \log v\}, \dots (11)$$

where  $U_\infty$  and  $U_v$  denote the internal energies at the volumes  $\infty$  and  $v$  respectively. The right-hand side of the equation is infinite, and hence the gas would undergo, if the supposition made is true that  $\xi$  is independent of  $v$ , an infinitely large change in internal energy on increasing its volume till it is infinitely large. But this is manifestly absurd, and hence  $\xi$  must be a function of  $v$  besides of  $T$ , and of a form which would make the right-hand side of the equation finite. Its value when  $v$  has not very large values will evidently not differ appreciably from unity. But for very large values of  $v$  it must differ considerably from unity, otherwise the value of  $U_\infty - U_v$  would not be rendered finite.

This result has an important and interesting bearing on the kinetic theory of gases. The pressure according to kinetic theory is given by

$$p = \frac{1}{3} \frac{M}{v} V^2, \dots \dots (12)$$

where  $V$  denotes the average velocity of translation of a molecule. From this equation and equation (7) we have

$$\xi RT = \frac{1}{3} V^2, \dots \dots (13)$$

from which it follows that *the kinetic energy of a molecule is not exactly proportional to  $T$ , and that it also depends on the*

1194 Prof. R. D. Kleeman: *Changes in the Inter-atomic volume of the gas, especially when it is large.* The physical significance of this will be discussed in a subsequent paper.

Let us next determine how this change in internal energy on change of volume is produced. Equation (10) may be written

$$\left(\frac{\partial U}{\partial v}\right)_T = CRT\left(\frac{\partial \xi}{\partial T}\right)_v, \quad \dots \quad (14)$$

where  $C$  denotes the concentration in mols. Thus the change in internal energy  $\partial U$  depends on the molecular concentration  $C$ , or on the average distance of separation of the molecules, and hence it depends on molecular interaction. We may, therefore, also write the equation

$$\left(\frac{\partial U}{\partial v}\right)_T = knT\left(\frac{\partial \xi}{\partial T}\right)_v, \quad \dots \quad (15)$$

where  $n$  denotes the number of times per second each of the molecules in unit volume gets within a distance  $r$  of another molecule, and  $k$  is a constant. Such an event will be called a chemical collision. Now it will be evident on reflexion that  $\partial U$  could only depend on  $n$  if a molecule during a chemical collision undergoes a change in internal energy which is not permanent but changes with time. Its average internal energy will then depend on the interval between two collisions, or on  $n$ . The distance  $r$ , it now appears, is the largest distance two molecules may be separated from each other and still affect each other's internal energy.

The average change in internal energy of a molecule during a collision will evidently depend on its nature, and hence the functional form of  $\xi$  of a gas, or the constants it contains, depends on the nature of the molecules. It is, therefore, convenient to write equation (15)

$$\left(\frac{\partial U}{\partial v}\right)_T = n \cdot \psi(n, T, A), \quad \dots \quad (16)$$

where  $A$  is a quantity depending on the nature of a chemical collision, and  $\psi$  a function of  $n$ ,  $T$ , and  $A$ .

#### §4. *The Change in Internal Energy on Change of Volume of a Chemically Non-Interacting Gaseous Mixture.*

If we consider two isolated non-interacting gases  $a$  and  $e$ , whose volumes are equal, we have

$$\left(\frac{\partial U_a}{\partial v}\right)_T = n_a \cdot \psi(n_a, T, A_a), \quad \dots \quad (17)$$

$$\left(\frac{\partial U_e}{\partial v}\right)_T = n_e \cdot \psi(n_e, T, A_e), \quad \dots \quad (18)$$

from equation (16), where the suffixes  $a$  and  $e$  refer to the substances  $a$  and  $e$  respectively. If the gases are mixed and the volume of the mixture is equal to that of either of the constituents before mixing, it follows from equation (16) that

$$\begin{aligned} \left(\frac{\partial U}{\partial v}\right)_T &= n_a \cdot \psi(n_a, T, A_a') + n_e \cdot \psi(n_e, T, A_e') \\ &\quad + n_{ae} \cdot \psi(n_{ae}, T, A_{ae}), \quad \dots \quad (19) \end{aligned}$$

where  $n_{ae}$  denotes the number of chemical encounters of the molecules  $a$  with the molecules  $e$  in unit volume per second, and  $A_{ae}$  a quantity depending on the nature of an encounter. The quantities  $A_a'$  and  $A_e'$  in this equation are not the same as the quantities  $A_a$  and  $A_e$  in equations (17) and (18), since what now happens when two molecules  $a$  chemically encounter each other depends on their previous encounters with molecules  $e$ , and hence on previous encounters of molecules  $e$  with each other, besides on the previous encounters of the

molecules  $a$  with each other. Thus  $\left(\frac{\partial U}{\partial v}\right)_T$  of a gaseous mixture is not an additive property of the constituents, in other words they affect each other's internal energy. This result, we shall see presently, is very important.

The equation of state of the mixture of gases is

$$pv = (M_a + M_e) \xi_{ae} RT, \quad \dots \quad (20)$$

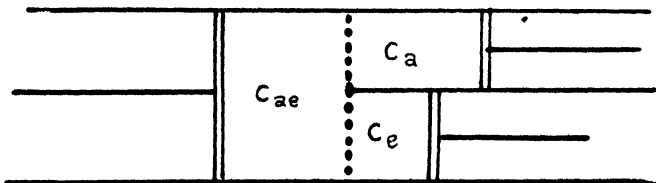
where  $(M_a + M_e) \xi_{ae}$ , according to the foregoing result, is not equal to the sum of  $M_a \xi_a$  and  $M_e \xi_e$  referring to the constituents in the isolated state. It may be mentioned here that it will be shown in a separate paper that at the absolute zero of temperature, however,

$$(M_a + M_e) \xi_{ae} = M_a \xi_a + M_e \xi_e \quad \dots \quad (21)$$

### § 5. Changes in Internal Energy that Substances undergo on being brought into Contact.

The effect the constituents of a mixture exert on each other's internal energy may be further studied by means of the apparatus shown diagrammatically in the figure. It consists of a chamber  $C_{ae}$  separated from the chambers  $C_a$  and  $C_e$  by membranes permeable to the substances  $a$  and  $e$  respectively, the volumes of the chambers being varied by means of pistons. Suppose that the chamber  $C_{ae}$  contains a mixture of non-interacting molecules or atoms  $a$  and  $e$ . The constituents

may be separated from each other by passing them into the chambers  $C_a$  and  $C_e$ , keeping the pressures in the chambers constant during the process. The constituents will not undergo a change in internal energy during separation since the nature of the mixture in the chamber  $C_{ae}$  remains unchanged. Now suppose that the constituents are separated in this way and the volume in each case then increased by  $v_1$ . Next suppose that the foregoing process is varied by first increasing the volume of the chamber  $C_{ae}$  by  $v_1$ , and then separating the constituents similarly as before, in which case the same final volumes are obtained. Now the change in internal energy of the isolated molecules  $a$  in the first case on changing the volume from  $v$  to  $v_1$  is not equal to the change in internal energy that takes place on changing the volume of the mixture, according to the investigation of the previous Section, or the substance  $a$  in the two final states in these processes will not possess the same internal



energies, and the same holds for the final states of the substance  $e$ . From this it follows that a substance may permanently change the internal energy of another substance by contact when both are in the perfectly gaseous state. When the substances are not in the perfectly gaseous state the effect is likely to be much more pronounced. Since a change in the internal energy of an atom must be accompanied by a change in its nature, *it follows that the nature of matter is constantly changing*, these changes being, however, as far as we know, immeasurably small, at least in most cases. An atom would accordingly bear the impression of all its previous history.

### § 6. *Contact Catalytic Action.*

If substances undergoing chemical interaction are brought into contact with another substance, a change in the inter-atomic energies of the interacting substances, we have seen, takes place. The latter substance for convenience may be

in the solid state but exhibiting a large surface, which obtains when the substance is in a finely divided state. This change in internal energy will have the effect of increasing or retarding the rapidity of the interaction, since what happens to two atoms or molecules when they come together evidently depends on their internal energy. *Contact catalytic action, the kind that does not involve a chemical change of the catalysing agent, is thus shown to be physically possible, and a consequence of the Laws of Thermodynamics.* This result should give confidence in the effectiveness of contact catalysing agents and extend their use.

It may be mentioned in this connexion that in a previous paper\* the writer has shown that the constant of mass-action  $K$  of a gaseous reaction is given by

$$K = \frac{k_1 \kappa_1}{k_2 \kappa_2}, \quad . \quad . \quad . \quad . \quad . \quad (22)$$

where  $k_1$  and  $k_2$  are quantities depending on the chances of molecular collision, and  $\kappa_1$  and  $\kappa_2$  quantities depending on the state of the molecules during collision. This state is determined by the previous molecular encounters and therefore depends on the volume of the gas and the masses of the constituents. In the light of the present investigation it appears that *the interacting substances themselves have a catalytic action upon each other*, which is expressed by the quantities  $\kappa_1$  and  $\kappa_2$ .

In a subsequent paper it will be shown that when the catalytic agent undergoes a chemical change itself a special kind of catalytic effect exists.

#### § 7. *The Use of Equation (7) in Determining the Functional Nature of the Constant of Mass Action.*

In a previous paper\* the writer showed that the constant of mass-action  $K$  is in general a function of the volume of the interacting gas and the masses of the constituents besides of the temperature. In a subsequent paper† the writer gave the differential equations by means of which the functional nature of the constant of mass-action may be determined. Using the orthodox gas equation  $pv = MRT$  it was shown that in some cases  $K$  is a function of the temperature only. It appears now that strictly equation (7) should be used.

\* Phil Mag. v. p. 263 (1928).

† Phil. Mag. v. p. 620 (1928).

Since  $\xi$  in the equation is a function of  $v$  (but whose exact form is not yet known), it appears that in the foregoing cases  $K$  will now be obtained as a function of the volume and the masses of the constituents, but appreciable only when the volume is very large. In exceptional cases only it appears, which may even not exist, may  $K$  be *strictly* a function of the temperature only.

---

CXXIV. *The Crystal Structure of  $\alpha$ -Manganese.* By G. D. PRESTON, B.A., *The National Physical Laboratory* \*.

[Plates XVIII. & XIX.]

*Introduction.*

THE crystal structure of the allotropes of manganese has been the subject of three investigations. The  $\alpha$ -modification, stable at room temperatures, has been examined by the powder method by Bradley† and by Westgren and Phragmén‡. The latter investigators found that the lines of a powder X-ray photograph could be accounted for by a cubic structure of side  $a = 8.894 \pm 0.005$  Å., the unit containing 56 atoms giving a density  $7.21$  g./cm.<sup>3</sup> as compared with a figure  $7.39$  g./cm.<sup>3</sup> given by Kaye and Laby.

In a subsequent paper Bradley and Thewlis§ have shown that the number of atoms associated with the unit is 58, and, using the intensity of the reflexion as observed by Westgren and Phragmén, they have given values for the parameters which fix the positions of the atoms within the unit.

The present paper contains an account of experiments which have been done using single crystals of manganese. In a structure of such complexity it appeared very desirable to supplement the results of the powder method by the Laue and oscillating crystal methods. The results of the experiments to be described are in agreement with the structure proposed by Bradley and Thewlis, and are now offered as an experimental verification of the deductions from the powder method.

\* Communicated by Dr. W. Rosenhain, F.R.S.

† Bradley, *Phil. Mag.* vol. 1. p. 1018 (1925).

‡ Westgren and Phragmén, *Zeit. f. Phys.* vol. xxxiii. p. 777 (1925).

§ Bradley and Thewlis, *Proc. Roy. Soc. A*, vol. cxv. (1927).

*Material.*

The material used for the X-ray investigation has been made available by the development of a method of purifying manganese by distillation\*. The sublimate consists of small lumps of manganese† which can be broken up and the fragments examined by the Laue method to ascertain if they are single crystals. After several trials a suitable specimen was obtained.

*Laue Photograph.*

The Laue photograph obtained from the specimen finally selected is shown in fig. 1 (Pl. XVIII.). The crystal has been oriented so that the incident beam of X-rays is parallel to an axis of tetragonal symmetry. Rotation through  $90^\circ$  about the proper axis produced a similar photograph, and a photograph showing trigonal symmetry was obtained when the crystal was set at the calculated angles. These photographs show that the material has cubic symmetry. The photographs also show that the specimen consists of more than one crystal, the reflexions from which interfere with the symmetry of the picture to some extent. In spite of this complication all the photographs obtained from different specimens during the search for the one finally selected have shown symmetry of the type  $O_h$ , which places the crystal in one of the groups  $T_d$ ,  $O$ , or  $O_h$ .

*Oscillating Crystal Method.*

The presence of more than one crystal complicated the application of this method. To eliminate the reflexions from the crystals not under examination the following scheme was used. Eight photographs in all were taken, the axis of oscillation being (001). In the first photograph the (100) direction oscillated through a range from  $0^\circ$  to  $12^\circ$  from the incident beam of X-rays. In the fifth photograph the range of oscillation of (100) was  $0^\circ$  to  $-12^\circ$  from the X-ray beam. Owing to the symmetry of the crystal the right-hand side of the first photograph should be identical with the left-hand side of the fifth as far as reflexions from the crystal under examination are concerned. The other crystal or crystals with a random orientation will give reflexions which, if they appear in the left-hand side in the first photograph, will not appear on the right-hand side of the fifth. Denoting the left hand-side of the first photograph by 1 L and the

\* M. L. V. Gayler, Journ. Iron and Steel Inst. vol. cxv. p. 393 (1927).

† *Ibid.* p. 408, pl. xxxv. fig. 4.



right-hand side by 1 R, the following scheme shows the ranges of oscillation and the correspondence between the photographs:—

Range of Oscillation.	Photo.		Photo.	Range of Oscillation.
0° to 12° .....	1 L	identical with	5 R	0° to -12°
	1 R	" "	5 L	
10° to 22° .....	2 L	" "	6 R	-10° to -22°
	2 R	" "	6 L	
20° to 32° .....	3 L	" "	7 R	-20° to -32°
	3 R	" "	7 L	
30° to 42° .....	4 L	" "	8 R	-30° to -42°
	4 R	" "	8 L	

As an example of the sort of photograph obtained Nos. 4 and 8 are reproduced in fig. 2 (Pl. XIX.). Assuming that the unit cube has a side of 8.89 Å., as found by Westgren, the planes ( $hkl$ ) which should appear on the different photographs were determined by the method described by Bernal \*. No reflexions were observed on the photographs which could not be accounted for by a cube of this size. Had a wrong choice been made reflexions would have appeared when not expected, so that the results confirm the fact that the unit has a side approximately 8.89 Å. No reflexions were observed other than those for which  $h+k+l$  is even, indicating that the lattice is body-centred. Westgren and Phragmén, in the work already referred to, recorded a weak reflexion corresponding to the plane (320), but no trace of this could be found on the photographs 1 L, 5 R, 2 L, 6 R, 3 R, or 7 L where it should have appeared. With this exception the values of ( $h^2+k^2+l^2$ ) recorded by Westgren and Phragmén are all even, in agreement with the results of the present investigation.

The results of a careful comparison of the pairs of photographs are given in Table I., from which, for the sake of brevity, values of ( $hkl$ ) which make  $h+k+l$  odd have been omitted. In the first column are given the values of  $h^2+k^2+l^2$ , in the second the corresponding values of ( $hkl$ ). In the third the appropriate value of  $\sin\theta$ , the angle of reflexion, calculated for the  $K_\alpha$  radiation of iron ( $\lambda=1.932$  Å.) and a cube of side 8.89 Å. The  $K_\beta$  radiation of iron is strongly absorbed by manganese, and reflexions arising from it are not observed on any of the films. The next eight columns of the table correspond with the eight photographs. Each of these eight columns is subdivided into three, the first of which contains a figure 0, 1, 2, 3, or 4, giving the value of the index

\* Bernal, Proc. Roy. Soc. A, vol. cxiii. p. 117 (1926).







$l$  which determines the "layer" line on which the reflected spot is calculated to fall. An entry in this column means that a reflexion is to be expected on the corresponding photograph. The next two columns contain figures which give the intensity of the observed spots on each of a pair of corresponding photographs. A rough estimation of the intensity is all that has been attempted. For this purpose a photographic plate was exposed under a sheet of lead in which ten small holes had been drilled. These holes were covered with 0, 1, 2 . . . 9 sheets of copper 0.05 mm. thick. The diffraction spots on the X-ray photograph were then compared with this arbitrary intensity scale, and the figures are those entered in the columns under 1 R, 5 L, etc., in Table III. The following Table shows approximately the relation between the intensity and the number given in Table I. :—

No.....	10	9	8	7	6	5	4	3	2	1
Intensity.....	200	140	100	70	50	40	30	25	20	15

The means of the observed intensities have been entered in the last column of Table I. In the majority of cases the agreement between different photographs is tolerably good, but where doubt arises the larger figures have been chosen, because it appeared more probable that a reflexion should be too weak than too strong. This arises from two causes:—the crystal may come into the reflecting position near the end of its nominal range of oscillation and a small error in setting might prevent the reflecting position ever being attained; for instance, this has been the cause of the small intensity of (332) in photograph 6 L and of the absence of (431) in 5 L. The possibility of a plane being absent from this cause has been indicated by a question mark after the figure giving the value of  $l$  in the table. Again, the intensity may be weakened by the obstruction to the passage of X-rays offered by the small crystals associated with the one under examination.

For the most part, however, there is not much doubt about the order of intensity. Of the 53 planes recorded in the table doubt exists as to the intensity of four, namely (510), (741), (743), and (752).

Before proceeding to make use of the intensity of reflexions to place the atoms within the unit it is necessary to fix the number of atoms within the cell. For this purpose the density ( $\rho$ ) and side ( $a$ ) of the unit must be determined. These quantities are connected by the relation

$$\frac{nM}{a^3} = \rho,$$

where  $M$  is the weight of the manganese atom in grammes and  $n$  is the number of atoms associated with the cell.

### *Density and Parameter of Unit.*

The density was determined by weighing the powder in a specific-gravity bottle, the liquid used being  $\text{CCl}_4$ , as the powder oxidizes rapidly in contact with water. About 50 g. of distilled manganese were ground in an agate mortar and passed through a sieve of 200 meshes to the inch. The determination of density was made in the usual way: the weighed powder in the specific-gravity bottle of about 11 c.c. capacity having been covered with  $\text{CCl}_4$  was placed in a receiver, which was then exhausted until the liquid boiled. The bottle was then filled with the liquid in a thermostat at  $25.0^\circ \text{C}$ . As the cap on the bottle did not fit sufficiently tightly to prevent evaporation, weighings were taken at 5 min. intervals and the true weight was determined by extrapolation. The loss of weight due to evaporation was quite small, amounting to about 0.1 mg. per minute. Owing to the small amount of material available it was not possible to make the determination to more than three figures. The results of two determinations were 7.445 and 7.437 g./cm.<sup>3</sup>, whence it may be inferred that the density is not less than 7.44 g./cm.<sup>3</sup> since the errors are likely to lead to too small a value.

The parameter of the lattice was determined from an X-ray photograph of powdered material. The camera was of the Seeman focussing type, and its constants had been previously determined by a calibration photograph of powdered rock-salt. The mean value of the parameter was found to be  $8.894 \pm 0.002 \text{ \AA}$ ., as shown in Table II., in agreement with the value given by Westgren and Phragmén in the paper already referred to.

TABLE II.

$\log \sin \theta$ .	$h^2 + k^2 + l^2$ .	$\lambda$ .	$a$ .
9657	72	$a_2$	8.802 Å.
9645	...	$a_1$	8.896
9521	68	$a_1$	8.896
9456	66	$a_1$	8.896
9330	62	$a_2$	8.896
9321	...	$a_1$	8.894
9177	58	$a_1$	8.893
9099	56	$a_1$	8.897
9022	54	$a_1$	8.893
8855	50	$a_1$	8.892

Mean  $a = 8.294 \pm .002$

Taking the atomic weight of manganese to be 54.93 ( $O = 16$ ) and the weight of the hydrogen atom to be  $1.663 \times 10^{-24}$  g. with the atomic weight of hydrogen equal to 1.008 ( $O = 16$ ), the above values of the density and parameter give

$$n = \frac{\rho a^3}{M} \leq 57.7,$$

or within the limits of accuracy to which  $\rho$  is known,  $n = 58$ .

To complete the solution of the structure we have now to assign positions to the 58 atoms within the unit so as to account for the observed intensities of the reflexions of the oscillating crystal photographs. The Laue photograph shows symmetry of the type  $O_h$ , so that the crystal has the symmetry of one of the point groups  $T_d$ ,  $O$  or  $O_h$ . The oscillating crystal photographs show reflexions from planes ( $hkl$ ) only when  $h+k+l$  is even. The lattice is, therefore, body-centred. Of the space-groups isomorphous with these point-groups only six, viz.,  $T_d^2$ ,  $T_d^6$ ,  $O_8$ ,  $O_8$ ,  $O_h^8$  and  $O_h^{10}$  are constructed on a body-centred lattice.

Reference to Wyckoff ('The Analytical Expression of the Results of the Theory of Space Groups') shows that the groups  $T_d^6$ ,  $O_8$ , and  $O_h^{10}$  may be eliminated. In the case of  $T_d^6$ , for instance, the equivalent positions contain 12, 16, 24, or 48 points, so that the number,  $n$ , of atoms within the unit must be expressed by

$$n = 12p + 16q + 24r + 48s,$$

where  $p$ ,  $q$ ,  $r$ , and  $s$  are integers or zero. It follows that  $n$  must be a multiple of 4, and in the case under consideration we know that  $n = 58$ , which is not a multiple of 4. An exactly similar argument excludes the possibility of  $\alpha$ -manganese belonging to either of the groups  $O_8$  or  $O_h^{10}$ .

According to the tables of Astbury and Yardley\*, the group  $T_d^6$ , in addition to the halving of the spacing when  $h+k+l$  is odd, is characterized by the spacing  $hhl$  being quartered if  $l$  is odd, normal if  $l = 2x$  ( $x$  odd) and halved if  $l = 2x$  ( $x$  even or zero). The last condition is not fulfilled by the X-ray spectra of  $\alpha$ -manganese, because 330 and 550 and 114 are all very intense. The same objection arises in the case of  $O_h^{10}$ , so that on these grounds also these groups must be rejected. We have, therefore, to place the atoms in the unit in positions in accord with the symmetry requirements of one of the groups  $T_d^2$ ,  $O_8$ , or  $O_h^8$ .

\* Phil. Trans. Roy. Soc. A, vol. ccxiv. p. 255.

Bradley and Thewlis place the crystal in the group  $T_d^3$ , the 58 atoms being divided into four sets, two of 24, one of 8, and one of 2 atoms. The coordinates within the unit are as follows:—

24 Equivalent positions:

$$\begin{array}{llll} u & u & v & \bar{u} & u & \bar{v} & u + \frac{1}{2} & u + \frac{1}{2} & v + \frac{1}{2}, \text{ etc.} \\ v & u & u & \bar{v} & \bar{u} & u & & & \\ u & v & u & u & \bar{v} & u & & & \\ u & \bar{u} & \bar{v} & \bar{u} & \bar{u} & v & & & \\ \bar{v} & u & \bar{u} & v & \bar{u} & \bar{u} & & & \\ \bar{u} & \bar{v} & u & \bar{u} & v & \bar{u} & & & \end{array}$$

8 Equivalent positions:

$$\begin{array}{llll} u & u & u & u + \frac{1}{2} & u + \frac{1}{2} & u + \frac{1}{2}, \text{ etc.} \\ \bar{u} & u & \bar{u} & & & \\ u & \bar{u} & \bar{u} & & & \\ \bar{u} & \bar{u} & u & & & \end{array}$$

2 Equivalent positions:

$$0 \ 0 \ 0 \quad \frac{1}{2} \ \frac{1}{2} \ \frac{1}{2}.$$

The values of the coordinates given by Bradley and Thewlis expressed in degrees are

$$\begin{array}{ll} 24 \ (1) & u_1 = 128 \quad v_1 = 15 \\ 24 \ (2) & u_2 = 32 \quad v_2 = 100 \\ 8 & u = 114. \end{array}$$

Prior to the publication of the paper by Bradley and Thewlis an almost identical result had been obtained from the intensities of the photographs given in Table I. The values found for the coordinates were

$$\begin{array}{ll} 24 \ (1) & u_1 = 125^\circ \quad v_1 = 20^\circ \\ 24 \ (2) & u_2 = 33^\circ \quad v_2 = 101^\circ \\ 8 & u = 115^\circ \end{array}$$

in very close agreement with the results of Bradley and Thewlis. The values of the coordinates given by Bradley and Thewlis afford a somewhat better account of the intensities, so the "structure factor" has been computed for these values for the planes recorded in Table I. The intensity of reflexion  $I$  is given by

$$I = k(A^2 + B^2),$$



where  $k$  is some function of the angle of reflexion, and

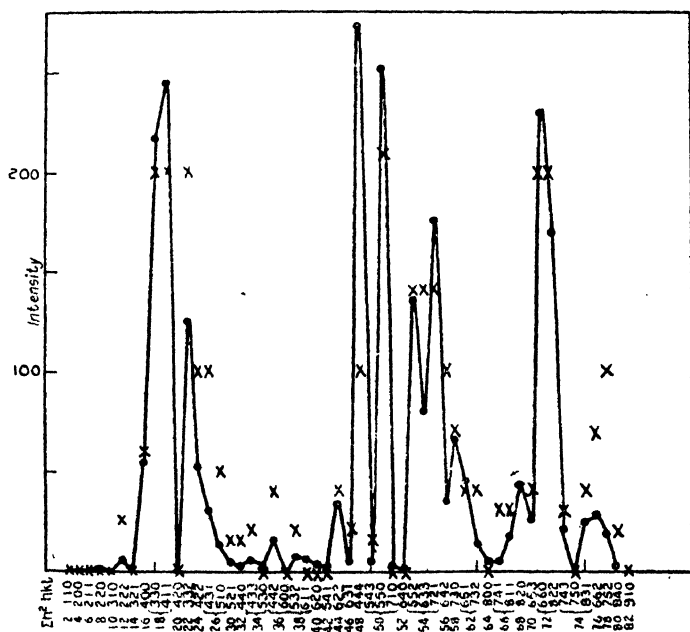
$$A = \sum \cos 2\pi(hx_s + ky_s + lz_s),$$

$$B = \sum \sin 2\pi(hx_s + ky_s + lz_s),$$

$(x_s, y_s, z_s)$  being the coordinates of the  $s$ th atom within the unit. The contribution to  $A$  from 24 atoms whose coordinates are fixed by the parameters  $(uvw)$  reduces to

$$8 (\cos 2\pi uh \cos 2\pi uk \cos 2\pi vl + \cos 2\pi uh \cos 2\pi vk \cos 2\pi ul \\ + \cos 2\pi vh \cos 2\pi uk \cos 2\pi ul),$$

Fig. 3.



while the contribution from 8 atoms whose position is fixed by the parameter  $u$  is

$$8 \cos 2\pi uh \cos 2\pi uk \cos 2\pi ul,$$

with similar expressions involving sines for the contributions to the factor  $B$ .

The quantities  $A$  and  $B$  having been computed from the above expressions,  $A^2 + B^2$  is plotted on an arbitrary scale as shown in fig. 3, the calculated points being joined by a continuous line. The intensities as observed are marked in

the same figure with a cross. It will be seen that there is a very general agreement as to the order of intensity; where the calculated intensity is great the observed intensity is also great, the agreement extending over a wide range of values of  $(hkl)$ . In view of the very rough nature of the estimation of the intensity, the agreement is quite as good as can be expected. No attempt has been made to integrate the intensity, so that a reflexion such as 444 appearing in the fourth layer line and covering a comparatively large area on the film would appear too weak. The values of  $A^2$  and  $B^2$  vary so rapidly, especially for large values of  $h$ ,  $k$ , and  $l$ , that it is possible to choose values of the parameters within one or two degrees which give the best representation of the observed intensities, even when these are only approximately known.

As regards the possibility of the crystal belonging to either of the groups  $O^6$  or  $O_A^3$ , it has not been found possible to account for the observed intensities by any set of equivalent points characteristic of these groups. The values of the variable parameters fixing the positions of the atoms for any group of equivalent points is limited by the consideration that the centres of atoms cannot approach one another too closely. It has been assumed that the "diameter" of the manganese atom is not less than  $2A^\circ$ , and subject to this assumption  $T_d^3$  is the only group that has been found to afford an explanation of the observed intensities.

### *Summary.*

Laue photographs of  $\alpha$ -manganese show that this material crystallizes in the cubic system. The oscillating crystal method shows that the lattice is of the body-centred type, and a powder photograph gives the side of the cube as  $8.894 \pm 0.002 \text{ \AA}$ . The density is determined to be  $7.44 \text{ g./cm.}^3$ , requiring 58 atoms to be associated with the unit. The observed intensities of reflexion of the oscillating crystal photographs are satisfactorily accounted for by placing the crystal in the space group  $T_d^3$ .

The author desires to express his thanks to Dr. Marie L. V. Gayler for supplying the material which made the work possible, and to Dr. Rosenhain for his continued interest in and encouragement of the research.

CXXV. *The Crystal Structure of  $\beta$ -Manganese.* By G. D. PRESTON, B.A., *The National Physical Laboratory* \*.

[Plate XX.]

*Introductory.*

X-RAY examinations of the structure of the allotropic modifications of Manganese have been carried out by Bradley† and by Westgren and Phragmén‡. Bradley demonstrated the existence of two different forms of Manganese, and Westgren and Phragmén, whose work was published at the same time as Bradley's, showed that the lines of the powder photograph of  $\beta$ -manganese could be accounted for by a cubic structure of side  $6.289 \pm 0.004$  Å. The presence of three weak lines on their photographs led them to suppose that, if these lines were due to the manganese and not to some impurity, the parameter might be double the above figure, the number of atoms associated with the unit being 20 or 160, according as the smaller or larger figure is the correct one.

In the present investigation an attempt has been made to supplement the information derived from the powder method by that obtained from the Laue and the oscillating crystal methods. The results have made it possible to assign the crystal to its space group and to place the atoms within the unit.

*Material.*

The material used for the Laue and oscillating crystal methods was similar to that used in the investigation of the structure of  $\alpha$ -manganese §. Some of the distilled material, consisting of the  $\alpha$ -modification, was annealed at a temperature of  $975^{\circ}$  C. and quenched in water. This treatment preserves the  $\beta$ -modification by suppressing the change which on slow cooling would take place at  $742^{\circ}$  C.|| The material so obtained is somewhat ductile, and attempts to obtain single crystals by breaking small lumps in an agate mortar were useless, as the crystals became deformed in the process. It was found that deformation of the crystals could

\* Communicated by Dr. Walter Rosenhain, F.R.S.

† Bradley, *Phil. Mag.* **1** p. 1018 (1925).

‡ Westgren & Phragmén, *Z. für Phys.* **xxxiii.** p. 777 (1925).

§ *Supra*, p. 1198.

|| M. L. V. Gayler, *J. Iron and Steel Inst.* **cxv.** p. 303 (1927).

be avoided by etching small pieces of the quenched metal in dilute hydrochloric acid. After a few minutes' treatment in the acid the lumps could be crumbled between the fingers, and specimens so obtained yielded satisfactory Laue photographs, showing no serious signs of deformation. It was not possible by this means to obtain a specimen consisting of one crystal only, so that the information yielded by the oscillating crystal photographs was not so complete as would otherwise have been the case. In spite of this they yielded valuable information, to be described below. The search for a suitable specimen to be subjected to X-ray analysis is exceedingly laborious, much time having been expended in isolating the specimen, the results obtained from which will now be described.

#### *The Laue Method.*

A small specimen exposed for two hours in a beam of X-rays from a Coolidge tube with a tungsten target operated at 70 k.v. and 3 m.a., yielded the photograph shown in fig. 1 (Pl. XX.) after the necessary adjustment in orientation had been made. A similar photograph was obtained when the specimen was rotated through  $90^\circ$  about the proper axis. Both photographs show that the X-ray beam is parallel to an axis of tetragonal symmetry, proving that the crystal is cubic and belongs to one of the space-groups isomorphous with the points groups  $T_d$ ,  $O$ , or  $O_h$ . It is evident from the photograph that the specimen consists of more than one crystal.

#### *The Oscillating Crystal Method.*

The same specimen was used in an attempt to apply the oscillating crystal method to determine the structure of the crystal. The method described in the account of the structure of  $\alpha$ -manganese was applied to eliminate the effects of the crystals associated with the one under examination, but, unfortunately, the extra crystals were in this case too numerous to allow the method to be employed with complete success. As in the case of  $\alpha$ -manganese, radiation from an iron target was used, the range of oscillation in each photograph being  $12^\circ$  and the exposure  $3\frac{1}{2}$  hours, with a current of 8 to 10 m.a. passing through the tube. The presence of the crystals not under examination led to the appearance of a large number of reflexions on all the photographs. The values of  $\sin \theta$  for all these reflexions, however, correspond to those to be expected from a cubic structure of side

6.29 Å. No reflexions have been found on any of the photographs which would necessitate the choice of a larger unit, particular attention having been paid to the possibility of the occurrence of the three reflexions recorded by Westgren and Phragmén, which do not agree with the results to be expected from the smaller unit. No trace of these could be found on any of the photographs. It may here be pointed out that of these lines the one for which  $\sin^2 \theta = 0.214$ \* corresponds exactly with a line observed by the same authors in the spectrum of  $\alpha$ -manganese to which the corresponding value of  $\Sigma h^2$  is 13. This last line has been found by Bradley and Thewlis† to be spurious, and was not observed in the oscillating crystal photographs of  $\alpha$ -manganese. There is, therefore, reason to doubt the existence of one of these lines, and careful search has failed to reveal any trace of either of the others on the oscillating crystal photographs of  $\beta$ -manganese. The presence on these photographs of reflexions due to crystals other than the one under examination adds to the possibility of finding any of these reflexions if they existed. There is no reason for ascribing to the unit a side greater than 6.29 Å. so far as can be ascertained by an inspection of the oscillating crystal photographs. A complete analysis of each photograph, on the lines adopted in the case of  $\alpha$ -manganese, has been attempted, but many of the reflexions to be expected are absent, because the reflected beam has been absorbed in the stray crystals. In spite of this, much useful information has been obtained from the photographs and is recorded in Table I., column 4. The information of greatest use is that obtained in cases of such planes as (300) and (221), for which  $h^2 + k^2 + l^2$  is the same. On the powder photograph the lines due to reflexions from these planes are superposed, and it is impossible to tell how the intensity is distributed between the two planes. With the oscillating crystal method this is not the case, and in the present instance it is found that (221) is very strong and no reflexion is observed from (300). This fact, by itself, would hardly be sufficient evidence on which to base the conclusion that reflexion from (300) is absent, but when the photograph on which it should appear is examined, it is found that the reflexions to be expected\* from (410), (520), and (301), to mention no more, are observed. There is, therefore, some evidence to show that the absence of reflexion from the (300) plane is not due to the obstruction of the reflected ray by other

\* See Table 3, p. 78, *loc. cit.*

† Proc. Roy. Soc. A, cxv. p. 458 (1927).

TABLE I.

$\Sigma h^2$ .	$hkl$ .	$\sin \theta$ .	Oscillating Crystal.		Powder.				
			I.	$A^2+B^2$ .	$\frac{N(A^2+B^2)}{\Sigma h^2}$ .	W. & P.	Calc. I.	Observed.	Calc. II.
1	100	0.1535	—	0	0	—	—	—	—
2	110	0.217	w	0.4	2.4	—	26	—	21
3	111	0.266	—	1.0	27	vw	25	—	22
4	200	0.307	—	0	0	—	—	—	—
5	210	0.343	mw	1.9	9.1	m	18	—	17
6	211	0.376	—	0.4	1.6	—	30	—	28
8	220	0.435	w	1.6	2.4	—	26	—	27
9	{ 300 221	0.461	—	0	} 27.0	s	1	1	1
10	310	0.486	vs	102.0		—	—	—	—
11	311	0.509	s	67.8	163.0	s	2	4	2
12	222	0.532	—	0.5	89.6	s	5	6	5
13	320	0.554	w	1.1	0.3	—	32	—	32
14	321	0.575	ms	8.4	.20	w	28	9	29
16	400	0.614	—	0	28.8	s	12	—	13
17	{ 410 322	0.633	w	2.8	0	—	—	—	—
18	{ 330 411	0.652	—	0.0	} 4.0	w	22	—	25
			s	0.3		m	11	9	12
				22.7	30.5	—	—	—	—

19	.....	331	0.670	—	ms	0.3	0.4	—	31	—	31
20	.....	420	0.687	—	ms	23.8	28.6	—	13	—	14
21	.....	421	0.704	—	—	0.8	1.8	—	29	—	30
22	.....	332	0.721	w	w	4.7	5.1	w	21	—	23
24	.....	422	0.752	ms	ms	9.1	9.1	—	18	—	20
25	.....	{ 430	0.768	m	m	10.1	9.7	w	16	—	19
	.....	{ 500		—	—	0					
26	.....	{ 431	0.783	vs	vs	67.6	142.2	vs	3	3	3
	.....	{ 510		ms	ms	18.6					
27	.....	{ 333	0.798	—	s	1.6	25.3	m	14	11	15
	.....	{ 511		—	—	27.9					
28	.....	{ 432	0.827	vs	vs	46.1	127.2	vs	4	2	4
	.....	{ 520		vs	vs	61.5					
30	.....	521	0.841	ms	ms	24.3	38.9	m	7	11	11
32	.....	440	0.869	—	—	7.4	2.8	—	24	—	26
33	.....	{ 522	0.882	—	—	0.5	3.6	—	23	—	24
	.....	{ 441		—	—	4.5					
34	.....	{ (433)*	0.896	—*	—*	10.4	9.3	—	17	—	18
	.....	{ 530		mw	mw	2.7					
35	.....	531	0.908	vs	vs	26.4	36.2	—	8	8	10
36	.....	{ 442	0.922	vvs	vvs	77.1	51.4	—	6	5	6
	.....	{ 600		—	—	0					
37	.....	610	0.934	vs	vs	51.9	33.6	—	9	13	9
38	.....	{ (532)	0.946	—*	—*	18.9	32.3	—	10	13	8
	.....	{ 611		ms	ms	13.3					
40	.....	620	0.972	ms	ms	12.2	7.3	—	20	—	16
41	.....	{ (443)*	0.984	—*	—*	5.8	19.1	—	15	7	7
	.....	{ 540		—	—	1.9					
	.....	{ 621		ms	ms	12.5					

\* Outside limits of film in oscillating crystal photographs.

crystals. The remaining planes of the structure have been dealt with in the same way and the result entered in the table, the intensities being denoted by very strong (vs), strong (s), medium strong (ms), medium (m), and weak (w).

With the exception of the three planes mentioned above, the results of the present investigation are in good agreement with those of Westgren and Phragmén, as is seen by comparison of columns 4 and 7 of Table I. The latter column contains the intensities of the lines observed by Westgren and Phragmén up to the plane (521), the limit imposed by the use of radiation from a chromium target. Some further information as to the intensities of planes up to  $h^2 + k^2 + l^2 = 41$  is given by the use of iron radiation. In fixing the position of the atoms within the unit it is planes with large values of  $h$ ,  $k$ , and  $l$  which are the most sensitive in determining the values of the parameters.

#### *Number of Atoms in the Unit.*

There are no available data as to the density of  $\beta$ -manganese, but it seems certain that on cooling the material undergoes a marked contraction on changing into the  $\alpha$ -modification. The density must, if this is the case, be less than  $7.45 \text{ g./cm.}^3$ , which is known to be the figure for  $\alpha$ -manganese. If there are  $n$  atoms of mass  $M$  within a cubic unit of side  $a$ , then the density  $\rho$  is given by

$$\rho = \frac{nM}{a^3}.$$

In the present case

$M = 54.93 \times 1.65 \times 10^{-24} \text{ g.}$  and  $a = 6.29 \times 10^{-8} \text{ cm.,}$   
so that

$$\rho = 0.3645 n \text{ g./cm.}^3$$

The most probable value for  $n$  is 20, giving a density of  $7.29 \text{ g./cm.}^3$ . These atoms have to be arranged within the unit so as to satisfy the symmetry requirements of one of the cubic space-groups and so as to afford an account of the observed intensities of reflexion.

#### *Determination of the Space-Group.*

The results of the oscillating crystal method and of the powder method show that the lattice is of the simple cubic type, for the fact that the planes (310) and (311) give first



order reflexions excludes the possibility of the lattice being either face-centred or body-centred. Reference to the tables of Astbury and Yardley \* show that the only possible groups which will yield a Laue photograph of full  $O_h$  symmetry and have a simple cubic lattice are  $T_d^1$ ,  $T_d^4$ ,  $O^1$ ,  $O^2$ ,  $O^6$ ,  $O^7$ ,  $O_h^1$ ,  $O_h^2$ ,  $O_h^3$ , and  $O_h^4$ . The same tables show that the groups  $T_d^4$ ,  $O_h^2$ , and  $O_h^3$  are impossible because they are characterized by the absence of odd order reflexions from planes  $(hh\bar{l})$  when  $l$  is odd, but the plane 113 is observed.  $O_h^4$  is excluded because the spacing  $(hko)$  should be halved if  $h+k$  is odd, but (320) and (500) or (430) are observed, as reference to Table I. will show. The choice of space-group is, therefore, reduced to one of  $T_d^1$ ,  $O^1$ ,  $O^2$ ,  $O^6$ ,  $O^7$ , or  $O_h^1$ . It was not found possible to account for the intensities of reflexion by any permissible choice of coordinates for the group  $T_d^1$ . On the other hand, the group  $O^7$  (or  $O^6$ , which differs from it only in having an opposite sense of rotation of its screw axes) provides a satisfactory account of the observed reflexions. Reference to Wyckoff † shows that a possible arrangement of 20 atoms in this group is in two sets, one of 12 and the other of 8, whose positions in the unit are as follows:—

12 atoms.

$$\begin{aligned} \frac{1}{2} - u, u, \frac{2}{3} &: \frac{1}{2} - u, \frac{1}{3} - u, \frac{2}{3} &: u + \frac{1}{2}, u + \frac{1}{3}, \frac{1}{3} &: u + \frac{1}{2}, \bar{u}, \frac{1}{3} \\ \frac{2}{3}, \frac{2}{3} - u, u &: \frac{2}{3}, \frac{1}{2} - u, \frac{1}{3} - u &: \frac{2}{3}, u + \frac{1}{2}, u + \frac{1}{3} &: \frac{2}{3}, u + \frac{2}{3}, u \\ u, \frac{2}{3}, \frac{2}{3} - u &: \frac{1}{2} - u, \frac{2}{3}, \frac{1}{2} - u &: u + \frac{1}{2}, \frac{2}{3}, u + \frac{1}{2} &: \bar{u}, \frac{2}{3}, u + \frac{2}{3} \end{aligned}$$

8 atoms.

$$\begin{aligned} v, v, v &: v + \frac{1}{2}, \frac{1}{2} - v, \bar{v} &: \bar{v}, v + \frac{1}{2}, \frac{1}{2} - v &: \frac{1}{2} - v, \bar{v}, v + \frac{1}{2} \\ \frac{2}{3} - v, \frac{2}{3} - v, \frac{2}{3} - v &: v + \frac{1}{2}, \frac{1}{2} - v, v + \frac{2}{3} &: \frac{1}{2} - v, v + \frac{2}{3}, v + \frac{1}{2} &: v + \frac{2}{3}, v + \frac{1}{2}, \frac{1}{2} - v. \end{aligned}$$

The choice of values for  $u$  and  $v$  has now to be made so as to satisfy the observed intensities. The group  $O^7$  is characterized by the quartering of the (100) spacing. Reference to the list of observed intensities of the oscillating crystal method shows that no reflexion is observed from any of the first six orders of (100). The utility of the method is here well illustrated, because in the powder method reflexions are observed at the required values of  $\sin \theta$  for (300), (500), and

\* Phil. Trans. Roy. Soc. A, cccxiv. p. 225.

† 'Analytical Expression of the Results of the Theory of Space-Groups,' pp. 137, 104 and 105.

(600), but the oscillating crystal method shows that these reflexions are in reality due to the planes (221), (430), and (442) respectively. With the exception of (400) all the reflexions from (100) automatically disappear in this group, so that a choice of  $u$  and  $v$  must now be made so that (400) also is of small intensity, because this plane has not been observed in either the powder or the oscillating crystal photographs.

The intensity of reflexion from the plane ( $hkl$ ) is given by

$$I = k(A^2 + B^2),$$

where  $k$  is a function of the angle of reflexion ( $\theta$ ), and

$$A = \sum \cos 2\pi(hx_s + ky_s + lz_s),$$

$$B = \sum \sin 2\pi(hx_s + ky_s + lz_s),$$

( $x_s, y_s, z_s$ ) being the coordinates of the atoms in the unit. For the plane (400)

$$A_{400} = 8 (\cos 2\pi 4u + \cos 2\pi 4v - \frac{1}{2}), \quad B_{400} = 0.$$

The possible values of  $u$  are limited by the fact that the centres of the atoms cannot approach one another too closely. In  $\alpha$ -manganese neighbouring atoms are separated by distances varying from 2.24 Å. to 2.96 Å. Since the density of  $\beta$ -manganese is less than that of  $\alpha$ -manganese, it is reasonable to assume that the minimum distance of approach of atoms is not less than 2.25 Å. The distance between the atoms ( $u, \frac{1}{2}, \frac{1}{2} - u$ ) and ( $\frac{1}{2}, u + \frac{1}{2}, u + \frac{1}{2}$ ) is

$$2r = a \{2(u - \frac{1}{2})^2 + (2u - \frac{1}{2})^2\}^{1/2} = a(\frac{1}{2} - u) \sqrt{6},$$

where  $a = 6.29$  Å. When  $u = 0$ ,  $2r = 1.93$  Å. and  $r$  diminishes as  $u$  increases from zero. Consequently, a small negative value of  $u$  is required to make  $2r$  exceed 2.25 Å. The minimum numerical value of  $u$  is about 0.021, giving  $2\pi u = -7.5^\circ$ ; the value of  $2\pi v$  required to make  $A_{400}$  very small is about  $28^\circ$  with this value of  $u$ . Consider, now, the intensity of the line (311), which is observed to be fairly intense. For this plane,  $B = -A$  and the 12 atoms contribute to  $A$  a quantity  $-3\sqrt{2} \sin 2\pi \cdot 2u$ , while the contribution from the 8 atoms to  $A$  is

$$\begin{aligned} & \cos 2\pi 5v + 2 \cos 2\pi 3v + \cos 2\pi v \\ & - \sin 2\pi 5v + 2 \sin 2\pi 3v - \sin 2\pi v. \end{aligned}$$

The former of these expressions is positive if  $u$  is negative, and increases with  $u$ ; the latter is also positive and increases as  $v$  diminishes. Trial showed that the above minimum value of  $u$  and maximum value of  $v$  gave too small an intensity for (311), so the intensities of all planes have been computed for the following values of  $u$  and  $v$  chosen to make  $A_{400}$  very small:—

	$2\pi u.$	$2\pi v.$
(1)	$-12^\circ$	$25^\circ$
(2)	$-16$	$22$
(3)	$-20$	$20$

Arrangement (2) gave results definitely in better agreement with observation than either (1) or (3). For instance, both (1) and (3) make  $A^2 + B^2$  for (222) too strong in comparison with the value for (320), the former plane being absent from the photographs and (320) giving a weak reflexion. The values of  $A^2 + B^2$  for arrangement (2) are given in Table I., column 5, and may be compared directly with the results of the oscillating crystal photographs in column 4. The agreement is very good.

As regards the powder photographs, the observed intensity may be compared with the quantity  $N(A^2 + B^2)/(h^2 + k^2 + l^2)$ , the values of which are given in column 6 of the table. Here  $N$  is the number of planes ( $hkl$ ) in the crystal. In the seventh column are entered the intensities as given by Westgren and Phragmén. The agreement is again very good, and is even better than comparison of columns 6 and 7 would indicate. For instance, the lines due to  $K\alpha$  radiation for which  $\Sigma h^2$  is 9, 10, and 11, are recorded as "strong" by Westgren and Phragmén, while the  $K\beta$  reflexions are recorded as strong, medium, and weak respectively, the order of fall of intensity agreeing with the fall of the calculated values. Again, no reflexion is recorded for the plane 422, which, judging by the calculated values of the neighbouring lines, should have been weak. There is recorded however, a reflexion (Table 3 of the paper referred to) for which  $\sin^2 \theta = 0.800$ , so that  $\sin^2 \theta / 24 = 0.03333$  if the reflexion is ascribed to (422) ( $\Sigma h^2 = 24$ ). For the other  $K\alpha$  reflexions recorded by Westgren and Phragmén, the mean value of  $\sin^2 \theta / \Sigma h^2$  is 0.03331, so that the  $\alpha$  reflexion of (422) coincides with the  $\beta$  reflexion from (432) and (520), and is not separately recorded.

The last three columns contain a comparison between the calculated order of intensity and that observed. For this purpose a powder photograph was taken with iron radiation which was filtered through a screen of manganese oxide ( $Mn_2O_4$ ) to absorb the  $K\beta$  radiation and so diminish the fogging of the film due to scattering. The observed lines have been entered in column 9 of the table in order of intensity, 1 being the most intense and 13 the least. In the eighth column is given the order in which the values of  $N(A^2 + B^2)/h^2 + k^2 + l^2$  fall. It will be seen that there is a very general agreement between the two columns. The last line recorded in the table is observed to be stronger than the calculation would indicate, but no allowance has been made in the calculation for the fact that at small and large angles of reflexion the reflected energy is distributed over the surface of a cone of small angle. To make allowance for this, the last column of the table is the order in which the values of

$$\frac{N(A^2 + B^2)}{(h^2 + k^2 + l^2) \sin 2\theta}$$

fall. This alteration has the effect of increasing the calculated figures at the beginning and end of the spectrum, and effects an improvement in agreement between theory and observation in the case of the lines for which  $\Sigma l^2$  is 30 and 41, without affecting the remaining lines appreciably. The agreement is quite as good as is to be expected. It is, perhaps, worth while remarking that the calculated intensity of the most intense line is 272, and of the 7th most intense line is 38.9, while the 14th is 25.3. The most we can expect, then, of a comparison between theory and experiment is that lines 7 to 14 should have about the same intensity, which is, in fact, the case.

The above somewhat lengthy discussion of the intensity of the lines has been rendered necessary by the difficulty of obtaining a single crystal of the material capable of yielding an oscillating crystal photograph that could be relied on, but it leaves little doubt that the structure proposed accounts for the observed intensity of reflexion. A drawing of the unit cube is shown in fig. 2, the numbers attached to the atoms corresponding to those given in Table II., which includes a list of the coordinates of the atoms expressed in degrees, and shows that the groups  $O^6$  and  $O^7$  cannot be distinguished by X-rays although they are physically different, being related

TABLE II.—Coordinates of Atoms.

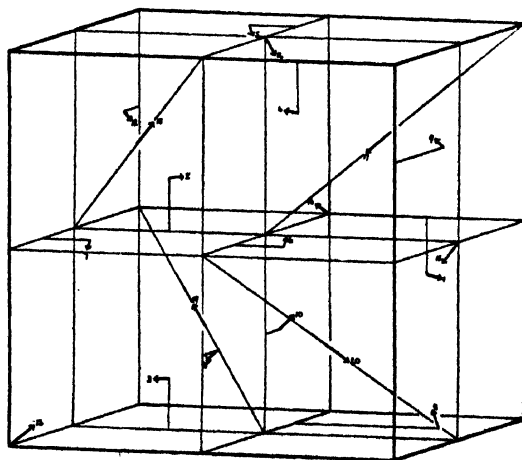
$O_6$ .												$O_7$ .											
$2\pi u = -16^\circ$ .												$2\pi v = -16^\circ$ .											
$12g$ .												$12r$ .											
1	.....	$u + \frac{1}{2}$	$\bar{u}$	$\frac{3}{2}$	$16$	$-135$	$74$	$16$	$-135$	1	.....	$\frac{3}{2}$	$-u$	$u$	$\frac{3}{2}$	$135$	$-74$	$-16$	$135$				
2	.....	$u + \frac{1}{2}$	$\frac{3}{2}$	$164$	$135$	$-106$	$-106$	$164$	$135$	2	.....	$\frac{1}{2}$	$-u$	$\frac{3}{2}$	$106$	$-135$	$106$	$-164$	$-135$				
3	.....	$\frac{3}{2}$	$-u$	$-74$	$-45$	$-74$	$-74$	$-45$	$-45$	3	.....	$u + \frac{1}{2}$	$\frac{3}{2}$	$74$	$164$	$45$	$74$	$164$	$45$				
4	.....	$u$	$u$	$106$	$16$	$106$	$106$	$16$	$45$	4	.....	$u + \frac{1}{2}$	$\bar{u}$	$-106$	$16$	$-45$	$-106$	$16$	$-45$				
5	.....	$u + \frac{1}{2}$	$\bar{u}$	$-135$	$74$	$-135$	$-135$	$74$	$16$	5	.....	$\frac{3}{2}$	$-u$	$u$	$135$	$-74$	$-135$	$-74$	$-16$				
6	.....	$u + \frac{1}{2}$	$\frac{3}{2}$	$135$	$-106$	$164$	$135$	$-106$	$164$	6	.....	$\frac{1}{2}$	$-u$	$\frac{3}{2}$	$106$	$-164$	$106$	$-164$	$-164$				
7	.....	$\frac{3}{2}$	$-u$	$-45$	$-74$	$-164$	$-45$	$-74$	$-164$	7	.....	$u + \frac{1}{2}$	$\frac{3}{2}$	$45$	$74$	$164$	$45$	$74$	$164$				
8	.....	$u$	$u$	$45$	$106$	$-16$	$45$	$106$	$-16$	8	.....	$u + \frac{1}{2}$	$\bar{u}$	$-45$	$-106$	$16$	$-45$	$-106$	$16$				
9	.....	$u + \frac{1}{2}$	$\bar{u}$	$16$	$-135$	$74$	$16$	$-135$	$74$	9	.....	$\frac{3}{2}$	$-u$	$\frac{3}{2}$	$135$	$-74$	$-135$	$-74$	$-74$				
10	.....	$u + \frac{1}{2}$	$\frac{3}{2}$	$164$	$135$	$-106$	$164$	$135$	$-106$	10	.....	$\frac{1}{2}$	$-u$	$\frac{3}{2}$	$106$	$-135$	$106$	$-135$	$106$				
11	.....	$\frac{3}{2}$	$-u$	$-164$	$-45$	$-74$	$-164$	$-45$	$-74$	11	.....	$u + \frac{1}{2}$	$\frac{3}{2}$	$164$	$45$	$74$	$164$	$45$	$74$				
12	.....	$u$	$u$	$-16$	$45$	$106$	$-16$	$45$	$106$	12	.....	$\frac{3}{2}$	$-u$	$u$	$16$	$-45$	$-16$	$-45$	$-106$				
$2\pi v = -22^\circ$ .												$2\pi v = 22^\circ$ .											
$8j$ .												$8k$ .											
13	.....	$v$	$v$	$158$	$-22$	$-22$	$-22$	$-22$	$-22$	13	.....	$v$	$v$	$22$	$22$	$22$	$22$	$22$	$22$				
14	.....	$v + \frac{1}{2}$	$\bar{v}$	$158$	$-158$	$22$	$158$	$-158$	$22$	14	.....	$\frac{1}{2}$	$-v$	$-158$	$158$	$-22$	$-158$	$158$	$-22$				
15	.....	$\frac{1}{2}$	$-v$	$22$	$158$	$-158$	$22$	$158$	$-158$	15	.....	$v + \frac{1}{2}$	$\frac{1}{2}$	$22$	$-22$	$-158$	$-22$	$-158$	$158$				
16	.....	$v + \frac{1}{2}$	$\bar{v}$	$-158$	$22$	$158$	$-158$	$22$	$158$	16	.....	$\bar{v}$	$v + \frac{1}{2}$	$158$	$-22$	$-158$	$-22$	$-158$	$158$				
17	.....	$\frac{1}{2}$	$-v$	$112$	$112$	$112$	$112$	$112$	$112$	17	.....	$\frac{1}{2}$	$-v$	$112$	$-112$	$-112$	$-112$	$-112$	$-112$				
18	.....	$v + \frac{1}{2}$	$\bar{v}$	$-112$	$-68$	$68$	$-112$	$-68$	$68$	18	.....	$v + \frac{1}{2}$	$\frac{1}{2}$	$68$	$-68$	$-68$	$-68$	$-68$	$-68$				
19	.....	$\frac{1}{2}$	$-v$	$68$	$68$	$68$	$68$	$68$	$68$	19	.....	$v + \frac{1}{2}$	$\frac{1}{2}$	$68$	$-68$	$-68$	$-68$	$-68$	$-68$				
20	.....	$v + \frac{1}{2}$	$\bar{v}$	$-68$	$-112$	$-68$	$-112$	$-68$	$-68$	20	.....	$\frac{1}{2}$	$-v$	$-112$	$112$	$112$	$112$	$112$	$112$				
$2\pi v = -22^\circ$ .												$2\pi v = 22^\circ$ .											
$8j$ .												$8k$ .											
13	.....	$v$	$v$	$158$	$-22$	$-22$	$-22$	$-22$	$-22$	13	.....	$v$	$v$	$22$	$22$	$22$	$22$	$22$	$22$				
14	.....	$v + \frac{1}{2}$	$\bar{v}$	$158$	$-158$	$22$	$158$	$-158$	$22$	14	.....	$\frac{1}{2}$	$-v$	$-158$	$158$	$-22$	$-158$	$158$	$-22$				
15	.....	$\frac{1}{2}$	$-v$	$22$	$158$	$-158$	$22$	$158$	$-158$	15	.....	$v + \frac{1}{2}$	$\frac{1}{2}$	$22$	$-22$	$-158$	$-22$	$-158$	$158$				
16	.....	$v + \frac{1}{2}$	$\bar{v}$	$-158$	$22$	$158$	$-158$	$22$	$158$	16	.....	$\bar{v}$	$v + \frac{1}{2}$	$158$	$-22$	$-158$	$-22$	$-158$	$158$				
17	.....	$\frac{1}{2}$	$-v$	$112$	$112$	$112$	$112$	$112$	$112$	17	.....	$\frac{1}{2}$	$-v$	$112$	$-112$	$-112$	$-112$	$-112$	$-112$				
18	.....	$v + \frac{1}{2}$	$\bar{v}$	$-112$	$-68$	$68$	$-112$	$-68$	$68$	18	.....	$v + \frac{1}{2}$	$\frac{1}{2}$	$68$	$-68$	$-68$	$-68$	$-68$	$-68$				
19	.....	$\frac{1}{2}$	$-v$	$68$	$68$	$68$	$68$	$68$	$68$	19	.....	$v + \frac{1}{2}$	$\frac{1}{2}$	$68$	$-68$	$-68$	$-68$	$-68$	$-68$				
20	.....	$v + \frac{1}{2}$	$\bar{v}$	$-68$	$-112$	$-68$	$-112$	$-68$	$-68$	20	.....	$\frac{1}{2}$	$-v$	$-112$	$112$	$112$	$112$	$112$	$112$				

to one another in the same way as an object and its mirror image. Table III. gives a list of the distances between neighbouring atoms.

TABLE III.  
Interatomic Distances.

From	To	Å.	From	To	Å.
13	1, 5, 9	2.675	1	13, 17	2.675
13	3, 7, 11	2.671	1	15, 19	2.671
13	4, 8, 12	2.530	1	16, 20	2.530
13	18, 19, 20	2.365	1	6, 11	2.615
			1	7, 8, 10, 12	2.659

Fig. 2.



### *The Impossibility of Other Atomic Groups.*

It has been shown above that an atomic grouping of the type  $O^7$  (or  $O^6$ ) gives a good account of the observed X-ray spectrum. It remains to be shown that no selection of coordinates for the atoms from the groups  $T_1^1$ ,  $O^1$ ,  $O^2$ , or  $O_1^1$  can give the observed X-ray spectrum.

The possible positions of atoms in the group  $T_d^1$  are as follows\* :—

Equivalent Positions.	Coordinates.				
1 .....	{	1(a)	(ooo)		
		1(b)	( $\frac{1}{2}\frac{1}{2}\frac{1}{2}$ )		
3 .....	{	3(a)	( $\frac{1}{2}\frac{1}{2}o$ )	( $\frac{1}{2}o\frac{1}{2}$ )	( $o\frac{1}{2}\frac{1}{2}$ )
		3(b)	( $\frac{1}{2}oo$ )	( $o\frac{1}{2}o$ )	( $oo\frac{1}{2}$ )
4 .....		4(a)	(uuu)	( $u\bar{u}\bar{u}$ )	( $\bar{u}u\bar{u}$ ) ( $\bar{u}\bar{u}u$ )
6 .....	{	6(a)	(uoo)	(ouo)	(oou)
			( $\bar{u}oo$ )	( $o\bar{u}o$ )	( $oo\bar{u}$ )
		6(d)	( $\frac{1}{2}u\frac{1}{2}$ )	( $\frac{1}{2}\frac{1}{2}u$ )	( $u\frac{1}{2}\frac{1}{2}$ )
			( $\frac{1}{2}u\frac{1}{2}$ )	( $\frac{1}{2}\frac{1}{2}u$ )	( $\bar{u}\frac{1}{2}\frac{1}{2}$ )
12 .....	{	12(f)	( $uo\frac{1}{2}$ )	( $\bar{u}o\frac{1}{2}$ )	( $u\frac{1}{2}o$ )
			( $\frac{1}{2}uo$ )	( $\frac{1}{2}\bar{u}o$ )	( $ou\frac{1}{2}$ )
			( $o\frac{1}{2}u$ )	( $o\frac{1}{2}\bar{u}$ )	( $\frac{1}{2}ou$ )
	{	12(g)	( $uv\bar{v}$ )	( $\bar{u}\bar{v}v$ )	( $\bar{u}v\bar{v}$ )
			( $vuv$ )	( $\bar{v}u\bar{u}$ )	( $\bar{v}u\bar{u}$ )
			( $uvu$ )	( $\bar{u}\bar{v}u$ )	( $\bar{u}v\bar{u}$ )

The arrangements 1(a), 1(b), 3(a), and 3(b) can occur only once in the unit because there are no variable parameters in these arrangements. Subject to the assumption that the centres of atoms must be separated by a distance not less than 2.25 Å., arrangement 4(a) may occur three times. It cannot occur five times, and if four groups of 4(a) are included in the unit, the remaining four atoms must include one of the arrangements 1(a) or 1(b), thus placing five atoms on each cube diagonal of length 10.9 Å. The arrangements 6(a) can occur only once, because it places two atoms on the side of the cube. A second group of 6(a) would thus put four atoms in a length of 6.29 Å. For the same reason 6(d) can occur only once. As there are only twenty atoms in the unit, 12(f) and 12(g) can each occur only once.

Subject to these restrictions there are twenty-six possible ways of putting twenty atoms in the unit. The following scheme shows how these arrangements arise :—

\* The notation 1(a), 3(a), etc., is that used by Wyckoff in 'The Analytical Expression of the Results of the Theory of Space Groups,' and has been retained to facilitate reference to that work.

TABLE IV.

Number of Atoms.

	12.	6.	4.	3.	1.
1 .....	<i>f</i>	<i>a</i>	—	—	<i>ab</i>
2 .....	<i>f</i>	<i>d</i>	—	—	<i>ab</i>
3 .....	<i>f</i>	—	<i>aa</i>	—	—
4 .....	<i>f</i>	—	<i>a</i>	<i>a</i>	<i>a</i>
5 .....	<i>f</i>	—	<i>a</i>	<i>a</i>	<i>b</i>
6 .....	<i>f</i>	—	<i>a</i>	<i>b</i>	<i>a</i>
7 .....	<i>f</i>	—	<i>a</i>	<i>b</i>	<i>b</i>
8 .....	<i>f</i>	—	—	<i>ab</i>	<i>ab</i>
9 .....	<i>g</i>	<i>a</i>	—	—	<i>ab</i>
10 .....	<i>g</i>	<i>d</i>	—	—	<i>ab</i>
11 .....	<i>g</i>	—	<i>aa</i>	—	—
12 .....	<i>g</i>	—	<i>a</i>	<i>a</i>	<i>a</i>
13 .....	<i>g</i>	—	<i>a</i>	<i>a</i>	<i>b</i>
14 .....	<i>g</i>	—	<i>a</i>	<i>b</i>	<i>a</i>
15 .....	<i>g</i>	—	<i>a</i>	<i>b</i>	<i>b</i>
16 .....	<i>g</i>	—	—	<i>ab</i>	<i>ab</i>
17 .....	—	<i>ad</i>	<i>aa</i>	—	—
18 .....	—	<i>ad</i>	<i>a</i>	<i>a</i>	<i>a</i>
19 .....	—	<i>ad</i>	<i>a</i>	<i>a</i>	<i>b</i>
20 .....	—	<i>ad</i>	<i>a</i>	<i>b</i>	<i>a</i>
21 .....	—	<i>ad</i>	<i>a</i>	<i>b</i>	<i>b</i>
22 .....	—	<i>a</i>	<i>aaa</i>	—	<i>ah</i>
23 .....	—	<i>a</i>	<i>aa</i>	<i>ab</i>	—
24 .....	—	<i>d</i>	<i>aaa</i>	—	<i>ab</i>
25 .....	—	<i>ad</i>	<i>aa</i>	<i>ab</i>	—
26 .....	—	—	<i>aaa</i>	<i>ab</i>	<i>ab</i>

A number of these arrangements may be rejected by considering what pairs of groups place atoms too close together. The arrangements 6(*a*) and 1(*a*) place three atoms on the cube edge of length 6·29 Å., and the arrangements 6(*d*) and 1(*b*) place three atoms in the same length. Both *u* and 1-2*u* cannot exceed one-third, *i.e.* the interatomic distance must be less than 2·1 Å. contrary to hypothesis. This eliminates arrangements 1, 2, 9, 10, 18, 19, 20, 21, 22, and 24.



The pair of arrangements 6(*a*) and 3(*b*) cannot occur together because the distance from the point (*uoo*) to ( $\frac{1}{2}oo$ ) must exceed 2.25 Å., i. e.  $u < 0.145$ , while, if the distance (*uoo*) to (*ouo*) is to exceed 2.25 Å.,  $u > 0.25$ . The same argument applies to the pair of groups 6(*d*) and 3(*a*). Arrangements 23 and 25 are therefore excluded. Arrangement 26 places five atoms on the cube diagonal which is not possible.

The pair of arrangements 12(*f*) and 3(*a*) is impossible. For the value of *u* in 12(*f*) is fixed within the limits  $0.32 > u > 0.25$ , but if the distance ( $\frac{1}{2}\frac{1}{2}o$ ) to ( $\frac{1}{2}uo$ ) is to exceed 2.25 Å.,  $u < 0.145$ . Similarly, if the distance ( $\frac{1}{2}oo$ ) ( $\frac{1}{2}uo$ ) is to exceed 2.25 Å.,  $u > 0.355$ . Accordingly, 12(*f*) cannot occur with either 3(*a*) or 3(*b*), thus eliminating arrangements 4, 5, 6, 7, and 8. So far as consideration of space goes, the remaining groups—namely, 3, 11, 12, 13, 14, 15, 16, and 17—are possible. They must be considered individually to ascertain if they can account for the observed intensities.

*Arrangement 3.* 12(*f*), 4(*a*<sub>1</sub>), 4(*a*<sub>2</sub>).—The intensity factor *A* for the planes *hoo* for this grouping is

$$A_{hoo} = 4(2 + \cos 2\pi uh + \cos 2\pi a_1 h + \cos 2\pi a_2 h),$$

and the *B* term vanishes. Now the parameter *u* fixing the position of the atoms 12(*f*) must lie between 0.32 and 0.25, i. e.  $115^\circ > 2\pi u > 90^\circ$ ; the parameter  $2\pi a_1$  must exceed  $45^\circ$ , while  $a_2$  may be about  $135^\circ$ ,  $-45^\circ$ , or  $-135^\circ$ . For the fourth order reflexion to be small we must have  $2\pi u = 115^\circ$ ,  $2\pi a_1 = 45^\circ$ ,  $2\pi a_2 = -45^\circ$  or  $+135^\circ$ . The values of *A* for the first six orders of *hoo* are then

	<i>A.</i> $2\pi a_1 = 45^\circ$	<i>A.</i> $2\pi a_2 = 135^\circ$
100 .....	11.9	6.3
200 .....	5.4	5.4
300 .....	6.2	11.8
400 .....	-0.7	-0.7
500 .....	-0.9	4.7
600 .....	11.5	11.5

As no reflexion from any of the first six orders of (*hoo*) is observed, this arrangement is impossible.

Arrangements 11 to 16 all include the group 12(*g*), the contribution from which to the intensity term of (*hoo*) is

$$A = 4(2 \cos 2\pi uh + \cos 2\pi vh) \quad \text{and} \quad B = 0.$$

Consideration of the distance between (*uvv*) and ( $\bar{u}\bar{u}v$ ) shows that  $u > 0.125$ , and of the distance between (*uvv*) and ( $1-u, 1-u, v$ ) that  $u < 0.378$ . Hence  $135^\circ > 2\pi v > 45^\circ$ . Also  $u-v > 0.251$  from consideration of the distance (*uvv*) to (*uvu*), or  $2\pi u - 2\pi v > 90^\circ$ ,  $u$  and  $v$  being both positive and less than 0.5. Table V. shows the value of  $2 \cos 2\pi uh$  for different values of  $u$  within these limits, and for values of  $h$  from one to six.

TABLE V.

	$u = 50$	60	70	80	90	100	110	120	130
1 ...	1.28	1.0	0.68	0.35	0	-0.35	-0.68	-1.0	-1.28
2 ...	-0.35	-1.0	-1.53	-1.88	-2.0	-1.88	-1.53	-1.0	-0.35
3 ...	-1.73	-2.0	-1.73	-1.0	0	1.0	1.73	2.0	1.73
4 ...	-1.88	-1.0	0.35	1.53	2.0	1.5	0.35	-1.0	-1.88
5 ...	-0.68	1.0	1.97	1.53	0	-1.5	-1.97	-1.0	0.68
6 ...	1.0	2.0	1.0	-1.0	-2.0	-1.0	1.0	2.0	1.0

*Arrangement 11.* 12(*g*), 4( $a_1$ ), 4( $a_2$ ).—The values of  $2\pi a_1$ ,  $2\pi a_2$  are between  $45^\circ$  and  $135^\circ$ , so that the contribution of these eight atoms to  $A_{200}$  is always negative or zero. From the table it is seen that the value of  $2 \cos 2\pi uh$  is also negative or zero when  $h=2$ . To make the intensity of 200 small we must have  $a_1$  and  $a_2$  approximately  $45^\circ$  or  $135^\circ$ , and then either  $45^\circ < u < 60^\circ$  and  $145^\circ < v < 180^\circ$ , or  $120^\circ < u < 135^\circ$  and  $0^\circ < v < 35^\circ$ . Considering now the case of (100), it seems that we must put  $a_1=45$  and  $a_2=135$ . A for 100 and 200 will now be small, but the contribution of every term except  $\cos 2\pi vh$  is negative for (400) and is positive for (600). This arrangement is, therefore, impossible.

*Arrangement 12.* 12(*g*), 4(*a*), 3(*a*), 1(*a*).—The contribution to  $A_{h00}$  from the atoms 1(*a*) and 3(*a*) is  $2(1 + \cos \pi h) = 4$  or 0, according as  $h$  is even or odd. We now have:

$$A_{h00} = 4(2 \cos 2\pi uh + \cos 2\pi vh + \cos 2\pi ah) + 2(1 + \cos \pi h),$$

where  $2\pi a$  lies between  $45^\circ$  and  $135^\circ$ , and  $2\pi u$  is now confined within the limits  $50^\circ < u < 90^\circ$ , the corresponding limits of  $2\pi v$  being  $140^\circ < v < 180^\circ$ . The values of  $A$  for  $(hko)$  and  $(hhh)$  are

$$A_{hko} = 4(\cos^2 2\pi uh + 2 \cos 2\pi uh \cos 2\pi vh + \cos^2 2\pi ah) \\ + 2(1 + \cos \pi h),$$

$$A_{hhh} = 12 \cos^2 2\pi uh \cos 2\pi vh + 4 \cos^2 2\pi ah + 4.$$

Now, when  $h=2$ ,  $\cos 2\pi vh$  is positive; so to make  $A_{222}$  small, we must put  $a=20$  and  $u=50$ , with  $140^\circ < v < 180^\circ$ , which makes  $A_{220}$  quite large, and is otherwise inconsistent with the observed intensities.

The expression  $A_{hko}$  and  $A_{hhh}$  for the arrangements 13, 14, and 15 are the same as those for arrangement 11, so that these groups are also impossible.

*Arrangement 16.*  $12(g)$ ,  $3(a)$ ,  $3(b)$ ,  $1(a)$ ,  $1(b)$ .—The values of  $A$  are now

$$A_{hoo} = 4(2\cos 2\pi uh + \cos 2\pi vh) + 4(1 + \cos \pi h),$$

$$A_{hko} = 4(\cos^2 2\pi uh + 2 \cos 2\pi uh \cos 2\pi vh) + 4(1 + \cos \pi h),$$

$$A_{hhh} = 12 \cos^2 2\pi uh \cos 2\pi vh + 4(1 + \cos \pi h).$$

In order that  $A_{111}$  may be small,  $2\pi u=90^\circ$ , and therefore  $2\pi v=0^\circ$  or  $180^\circ$ ; but this makes  $A_{400}$  very large and also places the atoms too close together, and is, therefore, impossible.

*Arrangement 17.*  $6(a)$ ,  $6(d)$ ,  $4(a_1)$ ,  $4(a_2)$ .—The parameter  $a$ , fixing the position of the atoms  $6(a)$ , lies within the limits  $115^\circ > 2\pi a > 90^\circ$ ; while  $d$ , fixing  $6(d)$ , lies within  $90^\circ > 2\pi d > 64^\circ$ . The only possible arrangement of  $4(a_1)$  and  $4(a_2)$  is  $2\pi a_1=90^\circ$  and  $2\pi a_2=-90^\circ$ , with  $2\pi a=134^\circ$  and  $2\pi d=65^\circ$ . Even now the atom centres come slightly within the limits we have supposed possible. But in any case, we have

$$A_{hoo} = 2(2 + \cos 2\pi ah) + 2(2 \cos \pi h + \cos 2\pi dh) \\ + 4 \cos 2\pi a_1 h + 4 \cos 2\pi a_2 h,$$

which is large when  $h=4$  and  $2\pi a_1$ ,  $2\pi a_2$  are nearly  $90^\circ$ . The arrangement is, therefore, impossible.

There is, then, no combination of positions for atoms in the group  $T_2^2$  which can account for the observed X-ray spectrum and at the same time keep the distance between atoms in excess  $2.25 \text{ \AA}$ .

O<sup>1</sup>.

The possible positions of atoms in this group are :

$$\begin{array}{lll}
 1(a) & 1(b) & \\
 3(a) & 3(b) & \\
 6(a) & 6(d) & \\
 6(b) & (\frac{1}{2}uo) & (o\frac{1}{2}u) \quad (uo\frac{1}{2}) \\
 & (\frac{1}{2}\bar{u}o) & (o\frac{1}{2}\bar{u}) \quad (\bar{u}o\frac{1}{2}) \\
 6(c) & (ou\frac{1}{2}) & (\frac{1}{2}ou) \quad (u\frac{1}{2}o) \\
 & (o\frac{1}{2}) & (\frac{1}{2}ou) \quad (o\frac{1}{2}u) \\
 8(c) & = 4(a) \text{ and } 4(-a) & \\
 12(m) & = 12(g) \text{ with } v = o & \\
 12(n) & = 12(g) \text{ with } v = \frac{1}{2} & 
 \end{array}$$

The only new cases arising are those involving 6(b) and 6(c). Neither of these groups can be combined with either 3(a) or 3(b), so the only new series are: (1) 6(b), 6(c), 8(c), which is very similar to arrangement 3 of Table IV.; (2) 6(a), 6(b), 8(c); and (3) 6(d), 6(b), 8(c). In the first of these new arrangements, the parameters  $b$  and  $c$  defining the positions of the atoms 6(b) and 6(c) must lie between  $65^\circ$  and  $115^\circ$ , and if  $b > 90^\circ$ ,  $c < 90^\circ$ . Consideration of the fourth order of (100) necessitates  $b = 66^\circ$ ,  $c = 114^\circ$ , and  $c^1 = 45^\circ$  (or 135) when  $c^1$  defines the positions 8(c). But this arrangement makes (200) and (300) too strong. Similar arguments exclude the remaining two cases.

O<sup>2</sup>.

The possible positions are as follows:—

$$\begin{array}{ll}
 2(a) & = 1(a) \text{ and } 1(b) \\
 4(d) & = 4(a) \text{ with } a = \frac{1}{2} \\
 4(e) & = 4(a) \text{ with } a = \frac{3}{4} \\
 6(e) & = 3(a) \text{ and } 3(b) \\
 6(f) & = 6(b) \text{ with } b = \frac{1}{2} \\
 6(g) & = 6(c) \text{ with } c = \frac{1}{2} \\
 8(d) & = 4(a) \text{ and } 4(a_2) \quad a_2 = \frac{1}{2} - a \\
 12(a) & = 6(a) \text{ with } 6(d) \quad d = a + \frac{1}{2} \\
 12(i) & = 6(b) \text{ with } 6(b_2) \quad b_2 = b_1 + \frac{1}{2} \\
 12(j) & = 6(c_1) \text{ with } 6(c_2) \quad c_2 = c_1 + \frac{1}{2} \\
 11(o) & \text{ and } 12(p)
 \end{array}$$

The only new cases are those involving 12(o) and 12(p). The coordinates of the equivalent positions 12(o) are :

$$\begin{array}{cccc} (u & \frac{1}{2} - u & \frac{1}{4}) & (u & u + \frac{1}{2} & \frac{3}{4}) & (\bar{u} & \frac{1}{2} - u & \frac{3}{4}) & (\bar{u} & u + \frac{1}{2} & \frac{1}{4}) \\ (\frac{1}{4} & u & \frac{1}{2} - u) & (\frac{3}{4} & u & u + \frac{1}{2}) & (\frac{3}{4} & \bar{u} & \frac{1}{2} - u) & (\frac{1}{4} & \bar{u} & u + \frac{1}{2}) \\ (\frac{1}{2} - u & \frac{1}{4} & u) & (u + \frac{1}{2} & \frac{3}{4} & u) & (\frac{1}{2} - u & \frac{3}{4} & \bar{u}) & (u + \frac{1}{2} & \frac{1}{4} & \bar{u}) \end{array}$$

The contribution to  $A_{h00}$  from these atoms is

$$A_{h00}^o = 4 \cos \frac{\pi h}{2} + \cos 2\pi u h (1 + \cos \pi h).$$

Consideration of space shows that  $2\pi u$  lies between  $0^\circ$  and  $36^\circ$ . The possible combinations of 6(e), 6(f), or 6(g) with 2(a) to give eight more atoms, all contribute 8 units to  $A_{400}$ . With  $u < 36$ ,  $A_{400}$  is too large. The only possible arrangement is 12(o) with 8(d) or with 4(d) and 4(e). The latter will make  $A_{400}$  large. With the former arrangement the values  $2\pi u = 15^\circ$ ,  $2\pi d = 45^\circ$  make  $A_{400} = 0$  and  $A_{200}$  small but not small enough.  $A_{600}$  is also too large. With these values of  $u$  and  $d$ , however,  $A_{222} = -9$ , which is much too large. This arrangement is therefore, not possible, and 12(p) leads to a similar result.

#### $O_1^1$ .

This group contains no case which has not already been examined and rejected.

There are, therefore, no possible arrangements in any of the groups  $T_d^1$ ,  $O_1^1$ ,  $O_2^1$ , or  $O_3^1$ . The crystal must belong to  $O^6$  or  $O^7$ , and the only possible arrangement is that already described.

#### Summary.

THE  $\beta$ -modification of manganese stable above  $742^\circ$  C. has been examined at room temperatures by the Laue oscillating crystal and powder methods. The results show that the material crystallizes in the cubic system  $O^7$  (or  $O^6$ ), the unit having a side of  $6.29 \text{ \AA}$ . and containing 20 atoms. The groups  $O^6$  and  $O^7$  are enantiomorphous and indistinguishable by X-ray methods. It is also shown that these two groups are the only possible ones which can account for the observed intensities of reflexion.

I am indebted to Dr. Marie L. V. Gayler for supplying the material for X-ray examination, and to Dr. W. Rosenhain, F.R.S., for his interest in the work.

CXXVI. *Tesla Luminescence Spectra of the Halogens.*—  
 Part I. *Iodine.* By S. S. BHATNAGAR, D.Sc., D. L.  
 SHRIVASTAVA, M.Sc., K. N. MATHUR, M.Sc., and R. K.  
 SHARMA, M.Sc.\*

[Plate XXI.]

**I**ODINE and bromine have been examined spectroscopically by many investigators. As early as 1898 Konen<sup>(1)</sup> examined the emission spectra, and gave the positions of several bands and lines in both the visible and the ultra-violet region. The fluorescence spectra have been largely investigated by Wood<sup>(2)</sup>, and later by McLennan<sup>(3)</sup> and by Oldenburg<sup>(4)</sup>. Much of the work on the emission spectra has been stimulated by the discovery by Steubing<sup>(5)</sup>, in the case of iodine, of a region of continuous emission ending sharply on the long wave-length side at  $4800 \pm 15 \text{ \AA}$ . and its explanation by Franck<sup>(6)</sup> on the basis of the electron affinity of the halogen. Recent work by Gerlach and Gromann<sup>(7)</sup>, Noyes<sup>(8)</sup>, Ludlam and West<sup>(9)</sup>, Mecke<sup>(10)</sup>, Cario and Oldenburg<sup>(11)</sup> and others has been mainly directed towards the elucidation of this view.

Attention has been called by several experimenters<sup>(12),(13),(14)</sup> to differences that occur in emission spectra as a result of the form of excitation. McVicker, Marsh, and Stewart<sup>(13)</sup> working with organic vapours have found remarkable differences with Tesla frequencies. Swindler<sup>(15)</sup>, working with chlorine and other gases, has found that at low pressures the high-frequency spectra differ widely from 60-cycle spectra with gases containing nitrogen as an impurity. Bloch and Bloch<sup>(16)</sup>, employing high-frequency oscillatory discharge, have been able to obtain several successive stages of ionization. In the present investigation, iodine and bromine have been studied under a high-frequency discharge from the secondary of a Tesla coil excited by a powerful 50-cycle A.C. transformer. In order to avoid all complications due to the presence of electrodes, the discharge was made electrodeless, and to obtain an intense discharge a scheme of connexions rather different from that employed by previous workers was adopted after making a number of trials. The arrangement of McVicker, Marsh, and Stewart<sup>(13)</sup> consisted in connecting the internal electrode of their discharge-tube to the secondary of an air-insulated

\* Communicated by the Authors.

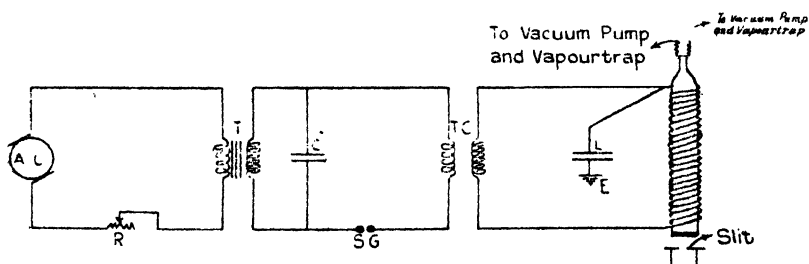
Tesla coil having a directly-coupled primary and using four big Leyden jars, an 18-inch induction coil being used as the source of current. The other electrode, which consisted of tin-foil coating over the entire length of the tube, was earthed along with the other end of the Tesla secondary.

Robertson<sup>(17)</sup> caused electrodeless discharge in a bulb 12 cm. in diameter by suspending it inside a coil of a few turns of stout copper wire, which was connected to two Leyden jars excited by a transformer.

### *Experimental.*

The arrangement adopted by the authors is shown in fig. 1. Current from a 50-cycle A.C. generator coupled to a D.C. motor was fed to the primary of a dental X-ray

Fig. 1.



transformer T made by the General Electric Company<sup>(18)</sup> of America, through a regulating rheostat R. The secondary of this was connected to the primary of the Tesla coil TC with a condenser C and a spark-gap as shown. The secondary of the Tesla coil was connected to a solenoid wound on the discharge-tube. The Tesla coil used was made in the laboratory, and had 14 turns of stout bare copper wire for the primary. The secondary had a single layer of 155 turns of 22 S.W.G. D.C.C. wire wound on a thin ebonite former. The space between the ebonite former and the primary coils was filled with paraffin-wax. This gave a fairly tight coupling for the high-frequency circuit. The spark-gap consisted of two adjustable brass knobs 1.3 cm. in diameter. The condenser C was made up of four thin zinc plates of  $20 \times 15$  cm., with a projection on one side for connexions, separated by 0.6 cm. thick plate glass, size  $30 \times 25$  cm. Previous to making up, the glass

plates were cleaned and thoroughly dried. The whole of the block was then set in good paraffin-wax. The capacity of this condenser was thus about 370 cm. During the course of preliminary investigation we employed Leyden jars as used by McVicker, Marsh, and Stewart (*loc. cit.*), but we found them very unsatisfactory with long hours of continuous working. Similarly we had also tried two other forms of Tesla coil. One had a primary of four turns over a long secondary of about a thousand turns or more, the two being air-spaced; the other was simply made by connecting together the two ends of the solenoid over the discharge-tube and winding over it a few turns of copper wire separated by a large air-distance and connected to the Tesla secondary. In both these cases the intensity of discharge becomes very feeble. The air-spaced coupling cannot work satisfactorily, because at the high potential employed there is always a vigorous corona discharge.

The discharge-tube used by us consisted of a glass tubing 2.5 cm. in diameter and 30 cm. long. One end was finely ground so that a quartz plate (as supplied by Adam Hilger Ltd. for Baly absorption-tube) could be cemented on it. The other end was drawn out and suitably narrowed for taking a joint of thick rubber tubing. The whole of the tube, excepting about 2 cm. from either end, was wound over with 250 turns of insulated 22 S.W.G. copper wire, which was well varnished with shellac. The two ends of this solenoid were joined to the secondary of the Tesla coil. One of these ends was also joined to the knob of a Leyden jar whose outer coating was earthed. This considerably increased the intensity of discharge, due no doubt to the capacity putting this circuit in better tuning with the primary oscillating circuit of the Tesla.

A wash-bottle filled with suitable absorbing substances was included between the discharge-tube and the vacuum pump to catch the halogen vapours. A Cenco Hyvac pump was used for exhausting. The instrument used for photographing the spectra was a quartz spectrograph, size E 3, made by Adam Hilger Ltd. It gives a spectrum about 200 mm. in length between  $\lambda$  2100 and 7000 Å. The wave-lengths were measured by the scale mounted in the instrument. This scale was further standardised by comparing it with standard copper lines. The error of reading, as shown by our copper spectrum, is 1 Å. for  $\lambda$  2200, increasing to about 10 Å. for  $\lambda$  7000. Wellington Spectrum plates were used throughout and found very suitable; both as regards the speed and freedom from halation. The



maker's metol-hydroquinone formula was adopted for development.

### *Iodine.*

Merck's extra pure resublimed iodine was carefully resublimed again, and the sample thus obtained was used for the experiments. A sufficient quantity of the crystals was then spread throughout the length of the discharge-tube. The quartz window was then cemented, using Everett's hard vacuum wax, and connexion was made with the vacuum pump through an absorption-trap. At a pressure of 3 mm. the discharge has a beautiful bluish glow throughout the entire length of the tube. An exposure of half-an-hour was found sufficient with the discharge-tube about 3 cm. from the spectrograph slit.

### *Results.*

An examination of the iodine spectrum shows the following peculiarities:—

(a) A continuous background beginning from  $\lambda$  4800 and ending at  $\lambda$  2130. Both the edges at  $\lambda$  4800 and  $\lambda$  2130 are sharp.

(b) A number of emission bands superposed on the continuous background.

(c) A few of the iodine emission lines. These are visible only outside the region of continuous emission.

(d) An almost complete absorption of radiation in the region  $\lambda$  4800 to  $\lambda$  5650.

A narrow continuous background with its maximum wave-length limit at  $\lambda$  4800 was first observed by Steubing<sup>(5)</sup>. The extension of the continuous emission up to  $\lambda$  2130 has not been previously observed.

The emission bands (b) with their positions are given on p. 1232. Some of these bands have been previously located, but we have been able to note many new bands further in the ultra-violet.

Wood and Kimura<sup>(19)</sup> give a long list of closely-spaced iodine lines between  $\lambda$  4632 and  $\lambda$  6585. Of these, Pl. XXI. shows  $\lambda\lambda$  4835, 4865, 5200, 5650, 6200, 6450 only. These coincide with their lines within the accuracy of our readings. Wood and Kimura were able to change gradually from band to line spectra by varying the capacity in the circuit or by heating. They were thus led to conclude that the line spectrum is due to the atoms, and that the dissociation of the iodine molecule results from an elevation of temperature.

St. Landau-Ziemecki<sup>(30)</sup>, applying a formula of Bodenstein and Stark<sup>(21)</sup>, calculates that at 500° C. and 1/4 mm. pressure the degree of dissociation of iodine molecule is 0.1. In our experiments the pressure was 3 mm., and the rise of temperature, even with prolonged exposures, could not be appreciably higher than 25° C. The degree of dissociation should thus be of the order of  $10^{-11}$ . This is evidently too small a dissociation to show any of the lines ascribed to atomic iodine. We thus think that in our tube the discharge itself was responsible for the dissociation of the molecular into atomic iodine, irrespective of temperature. This accords with Franck's<sup>(22)</sup> view that the halogens belong to the class of molecules that are able to take up so much oscillation energy through absorption that they dissociate into a normal and an excited atom.

Wood and Kimura have also observed the spectrum of electrically-excited iodine vapour as being made up of a fluted band spectrum between wave-lengths  $\lambda$  5200 and  $\lambda$  7000 and a continuous band between wave-lengths 4300 and 4800 Å. The former has been shown by them to exhibit, under high dispersion, a structure comparable to that of the absorption spectrum. In our plate we find an almost complete absorption of radiations (with the exception of three atomic lines mentioned above) between the wave-lengths  $\lambda$  4800 and  $\lambda$  5650. Mecke<sup>(10)</sup> has investigated the band-absorption spectra of iodine. His results show a long series of absorption bands stretching in the direction of short wave-lengths and having a real convergence limit at  $\lambda$  5000, followed by a region of strong continuous absorption. The band limit  $\lambda$  5000 has been taken by Franck<sup>(22)</sup> to represent the energy absorbed by a molecule for dissociation and the excitation of one of its atoms. The absence of any radiation in our plate between  $\lambda$  4800 and  $\lambda$  5650 is undoubtedly due to the fact that, as the coils in our discharge-tube were not wound completely up to the end of the tube facing the slit, the region (about 2 cm. long), which was only under a weak stimulus, acted as the absorbing layer for all the bands to be found within this spectral region.

We give below tables of the bands systems observed by us. The stronger of these had been previously observed chiefly by St. Landau-Ziemecki. We have here the band system starting from  $\lambda$  4800 and going up to  $\lambda$  2130, with a continuous background throughout. The most prominent of these bands are those stretching between  $\lambda\lambda$  4300-4170,  $\lambda\lambda$  3440-3360<sup>(25)</sup>, and  $\lambda\lambda$  2640-2600.

An examination of the bands shows three well-defined and one weak systems. These have their heads approximately at

- (A)  $\lambda$  4320,
- (B)  $\lambda$  3440,
- (C)  $\lambda$  2710,
- (D)  $\lambda$  2481.

The system A is made of a number of very intense but diffuse bands. These are given in Table I. below :—

TABLE I.

Long wave-length. Edge of bands.	Short wave-length. Edge of bands.	Wave-number for long wave-length edge.
4320.0	4169.0	23148
4096.3	4014.8	24414
3994.2	3933.3	25037
3890.0	3850.0	25707
3812.0	3780.0	26232
3749.0	3720.0	26673
3685.0	3670.0	27137
3640.0	3610.0	27470
3598.0	3569.0	27793
3540.0	—	28248

Owing to their diffuseness and low dispersion of the quartz spectrograph in this region, it has not been possible to find any regularity in these so far.

There are a few bands between  $\lambda$  4800 and  $\lambda$  4320 which do not seem to belong to any of these systems. Their long wave-length edges are situated at  $\lambda$  4750,  $\lambda$  4680,  $\lambda$  4610,  $\lambda$  4480,  $\lambda$  4390 (line).

The system B consists of a large number of bands, systematically placed and having a very peculiar intensity distribution.

The heads of these bands are given within the limits of our accuracy of reading by a formula of the usual electronic band type,

$$\nu = 29078 + (710n' - 8n'^2) - (213.7n'' - .6n''^2),$$

where, adopting the accepted notation,  $n'$  refers to the

1232 Messrs. Bhatnagar, Shrivastava, Mathur, and Sharma :  
initial electronic state of the emission process and  $n''$  to the final state, and  $\nu_0 = 29078$  is the head of the first band with  $\Delta n = 0$ .

In Table II. below we give the observed wave-numbers and those calculated by the formula. Again the diffuseness of the bands forbids precise measurements; but within these limitations the agreement is perfect.

TABLE II.

Wave-length limits of bands. $\text{\AA}$ .	Estimated intensity.	Wave-number of head.		Values of vibrational quantum number. $n', n''$ .
		Observed.	Calculated.	
3480	1	28735	28727	1, 5
3440—3360	10	29070	{ 29078 29567	0, 0 1, 1
3307	2	30239	30253	2, 1
3283—3070	5	30460	{ 30466 30500	2, 0 3, 3
3258—3243	8	30694	30711	3, 2
3237—3218	8	30893	{ 30923 30945	3, 1 4, 4
3214—3197	8	31114	{ 31136 31154	3, 0 4, 3
3190—3176	8	31348	31365	4, 2
3168—3160	3	31566	{ 31577 31583	4, 1 5, 4
3144—3140	3	31807	{ 31790 31792	4, 0 5, 3
3124—3113	8	32010	32003	5, 2
3108—3093	7	32175	{ 32205 32215	6, 4 5, 1
3085—3080	1	32415	{ 32414 32428	6, 3 5, 0
3066—3051	6	32616	{ 32602 32625	7, 5 6, 2
3048—3033	7	32830	{ 32811 32837	7, 4 6, 1
3024—3020	1	33069	{ 33050 33020	6, 0 7, 3
3008—2995	6	33245	33231	7, 2
2989—2981	7	33456	33443	7, 1
2972—2966	1	33647	{ 33656 33610	7, 0 8, 3
2958—2944	7	33807	{ 33821 33789	8, 2 9, 5
2938	2	34037	34033	8, 1
2920	0	34246	34246	8, 0
2908	2	34388	34395	9, 2

TABLE II. (cont.).

Wave-length limits of bands. Å.	Estimated intensity.	Wave-number of head.		Values of vibrational quantum number. $n', n''$ .
		Observed.	Calculated.	
2880—2863	5	34698	{ 34607 34742 34840	9, 1 10, 3 9, 0
2850—2842	3	35087	{ 34953 35165	10, 2 10, 1
2827—2813	3	35373	{ 35378 35495	10, 0 11, 2
2798—2790	0	35740	{ 35707 35811	11, 1 12, 3
2770—2760	1	36023	36021	12, 2
2748	1	36390	{ 36232 36320	12, 1 13, 3
2739	1	36509	36531	13, 2
2728	1	36657	36743	13, 1

The values calculated above are only for the heads of the various vibrational bands. Each of these bands has a definite thickness due to the associated rotational levels.

In the above analysis it will be seen that large values of  $n'$  are the most favoured ones. This was, indeed, anticipated by Franck from the peculiar intensity distribution of the fluorescence spectrum.

The wave-lengths of the systems (C) and (D) are given in Tables III. and IV. respectively.

TABLE III.

Long wave-length. Edge of the bands.	Wave-numbers.	Estimated intensity.
2729	36643	0
2709	36913	2
2693	37133	2
2683	37271	2
2672	37425	0
2601	38446	1 (very diffuse)
2590	38610	1
2582	38729	1
2565	38982	0
2555	39138	0
2532	39494	1

TABLE IV.

Long wave-length. Edge of the bands.	Wave-numbers.	Estimated intensity.
2480	40322	2 b. d.
2462	40617	0
2450	40816	0
2430	41151	0
2410	41493	0
2390	41841	1 b. d.
2350	42553	1 b. d.
2328	42964	0
2306	43365	0

Most of the bands of Table III. have the appearance of thick lines, except one very diffuse band. The general character of bands in Table IV. is very hazy. All of these are of very low visibility against a continuous background, which made readings very difficult and uncertain. The bands indicated by letters b. d. are very broad and diffuse. The system (D) might be stretching a little further than  $\lambda$  2306, but it is not possible to locate bands any further. The continuous background, however, extends up to  $\lambda$  2130, as indicated before.

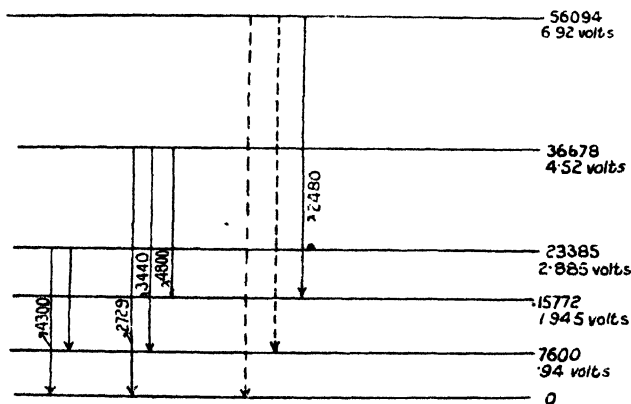
#### Discussion.

All the heads of the band systems observed by us can be represented within the limits of our accuracy by an energy-level diagram as shown in fig. 2. The numbers on the right-hand side indicate the various term values with equivalent values in volts written below. It will be seen that the first excited state of the molecule differs from the stable state by 0.94 volt. This is the same as the value found by Turner<sup>(24)</sup> by measuring the recurring doublet separation of the iodine spectrum in the far ultra-violet region. These are the stable and the meta-stable states of the iodine atom, and were first indicated by Franck<sup>(25)</sup> as  $2p_2$  and  $2p_1$  states. The level above the  $2p_1$  state is 1.005 volt higher, while the next higher is again 0.94 volt higher. It seems here as if the  $2p_2$  and  $2p_1$  states have undergone a repetition. This is followed by two levels still higher at 4.52 and 6.92 volts respectively. It is significant that transitions from the latter level to the stable and the

meta-stable states gives us two prominent lines of the atomic spectrum of iodine. These are indicated in our diagram by broken lines, and the values of these have been taken from Turner's measurements.

Thus, of our bands the system A is indicated as a transition from 2.885 volts to the normal state, and the system B as a transition from 4.52 volts to the meta-stable  $2p_1$  state, while a transition from this same level to the stable  $2p_2$  state gives us the system C. The system D is given by a transition from 6.92 volts to 1.945 volts level. Transitions from this same level to the  $2p_2$  and  $2p_1$  states gives the two atomic lines of iodine. Besides the above four systems a

Fig. 2.



transition from 4.52 volts to 1.945 volts gives us the edge  $\lambda$  4800.

It is noteworthy that the line at  $\lambda$  2062 has been noted by Turner and others as more intense than  $\lambda$  1876 line. From our diagram it would appear that the latter is the real resonance line. This is also the view of Turner and Compton<sup>(25)</sup>, who regarded  $\lambda$  2062 as the line terminating on a level 0.545 volt above the normal. Our evidence indicates that it terminates on a 0.94 volt level. The greater intensity of  $\lambda$  2062 will then mean that the probability of a change,  $6.92 \rightarrow 0.94$  volt, is much greater than  $6.92 \rightarrow 0$ : that is, the atom first tends to assume the meta-stable rather than the stable orbit. This will also explain the greater intensity of the band system B ( $4.52 \rightarrow 0.94$ ) over the system C ( $4.52 \rightarrow 0$ ). But this will not explain the great intensity of system A. Indeed, our only justification for creating the level 2.885

has been the peculiar wide separation of the bands most unlike the systems associated with  $2p_1$  level. Similarly the edge at  $\lambda 4800$  which on our diagram is associated with the excited levels  $4\cdot52 \rightarrow 1\cdot945$  defies complete explanation. Gerlach and Gromann<sup>(7)</sup> have shown that at higher temperatures and lower pressures the band at  $\lambda 4800$  decreases in intensity while that at  $\lambda 3440$  increases in intensity. As these conditions will favour a greater proportion of iodine vapour in the atomic state, they will also, we might suppose, favour the meta-stable state. Thus, clearly the chances for transitions to the  $2p_1$  state will be much increased, and consequently the intensity of the band at  $\lambda 3440$ <sup>(26)</sup>. If, however, we follow the same argument for  $\lambda 4800$ , we find that, as its terms are higher still, it should also be strengthened. A way of escape from this difficulty is found if we assume that the transitions responsible for  $\lambda 3440$  are possible both in the atomic as well as the molecular state, while those responsible for  $\lambda 4800$  are possible only for the molecular state, and are forbidden on the selection principle in the atomic state. Franck has pointed out that for homopolar molecules like  $I_2$ , which are bound together by van der Waals's forces, the electron orbits of the individual atoms still exist, though in a more or less disturbed state. Such molecules can be separated adiabatically into normal atoms, and on excitation by light an electron of one of the atoms passes to a higher quantum orbit, and the corresponding absorption frequency will be almost identical with a frequency found in the spectrum of the constituent atom. Now, several investigators have called attention to the appearance of "forbidden" lines in the molecular spectra. We might thus be justified in assuming that the transitions responsible for  $\lambda 4800$  are only possible in the molecular state, and thus under those conditions of temperature and pressure which favour a greater amount of atomic iodine this band must be necessarily weakened, while that at  $\lambda 3440$  is strengthened. But this does not explain the observations of Steubing and others that even under large dispersion it remains unresolved.

It should be pointed out here that the bands  $\lambda 4800$  and  $\lambda 3440$  are the so-called electron-affinity spectra of iodine. Franck suggested the former while Gerlach and Gromann, Ludlam and West, and others have been leading evidence in favour of the latter. If such a spectrum exists at all for iodine, we would agree with Gerlach<sup>(27)</sup> and attribute  $\lambda 4800$  to the affinity of the iodine molecule.

Referring to our analysis of the band system B involving a number of vibrational levels associated with the electronic



levels 4.52 and 0.94 volts, it will be seen that the final term of the formula

$$\nu = 29078 + (710n' - 8n'^2) - (213.7n'' - .6n''^2)$$

is the same as given by Kratzer and Sudholt<sup>(28)</sup> and corrected by Kemble and Witmer<sup>(29)</sup> from analysis of the resonance series of iodine. The presence of this term shows that in the above transitions the final state of the molecule is that of the excited  $2p_1$  condition. That is, contrary to the usual belief that the vibrational levels of the resonance spectra ( $213.7n'' - .6n''^2$ ) are associated with the unexcited normal molecule, we find that even in fluorescence the final level of the emission process is the excited  $2p_1$ . We also notice that in the system B for all those transitions for which the final vibrational quantum number  $n''=0$ , the observed bands are very much feebler. That is as it should be, for, as pointed out before, the end of our discharge-tube facing the slit was under a comparatively feeble stimulus, and consequently must necessarily have a great preponderance of molecules in the excited  $2p_1$  state. These will act as a partially absorbing layer for all the transitions involving  $n''=0$ .

On our energy-level diagram the highest value of the electronic energy absorbed by the molecule before it dissociates is  $(6.92 - 1.94) = 4.98$  volts. If, now, the molecule dissociates, it will absorb the energy necessary for its dissociation, the rest being evolved as a quantum of light. Referring again to the band at  $\lambda$  3440, it will be noticed that its great intensity and breadth is not wholly explained by its being the head of the system. The most intense part of this lies at  $\lambda$  3410, and we consider that this is due to the light-quantum evolved on dissociation of the molecule. Thus, since  $\lambda$  3410 is equal to 3.62 volts, the energy required for the dissociation of the molecule would be

$$4.98 - 3.62 = 1.36 \text{ volts.}$$

This is slightly lower than the chemically-calculated value 1.5 volts, but is in excellent agreement with the value of Foote and Mohler<sup>(30)</sup>. The former workers have found a resonance potential in iodine vapour at  $2.34 \pm 0.2$  volts. If from this we subtract 0.94 volt as the energy required for exciting one of the atoms to the meta-stable state, we get the value  $1.40 \pm 0.2$  volts, which agrees with our value within the limits of the accuracy.

Following, again, the contention of Franck and Dymond<sup>(31)</sup> that the result of the dissociation of iodine when produced by light-absorption is one stable atom and one meta-stable

1238 Messrs. Bhatnagar, Shrivastava, Mathur, and Sharma :

atom, if we take the excited molecule at 4.98 volts to dissociate as above, the energy absorbed would be

$$1.36 + .94 = 2.30 \text{ volts,}$$

and the emitted light-quantum should have the value

$$4.98 - 2.30 = 2.68 \text{ volts.}$$

We should expect a band terminating in this region. We have actually a fairly intense band from  $\lambda\lambda$  4610-4550. This agrees well.

As already pointed out, the continuous spectrum from  $\lambda\lambda$  4800-2130 forms a strong background throughout. This seems to be a continuation of the narrow continuous spectrum at  $\lambda$  4800 of Steubing<sup>(5)</sup>. An explanation of this will probably be a special case of the general theory of retardation spectra, which is as yet very little understood. For the present, however, we might adopt the views of Wright<sup>(32)</sup> and of Crew and Hulburt<sup>(33)</sup> in conjunction with the idea of electron affinity.

Franck, in explaining Steubing's results, conceived the idea of electron affinity spectra as being due to the capture of an electron by the iodine atom because of the tendency of the latter to form a stable octet in its outermost shell. Thus

$$W_i - W_f = h\nu_0,$$

where  $W_i$  = energy in the initial state and  $W_f$  in the final state and  $\nu_0$  the wave-number of emitted quantum, would give the position of the edge; but since initially the captured electron might possess any velocity, this sharp edge would be followed by a continuous spectrum, that is

$$h\nu = W_i - W_f + \frac{1}{2}mv^2 = h\nu_0 + \frac{1}{2}mv^2.$$

$\nu_1$  will thus depend on  $v$ , the velocity with which the captured electron was moving. It is clear, however, that this velocity cannot be large, for then the electron will penetrate the atom and escape. If, now, the atom (or the molecule in the case of homopolar compounds like iodine, where the atoms more or less maintain their separate entity) is already in an excited state when the electron is captured, then along with molecular bands we should find associated a continuous spectrum. That is, in the above equation each excited quantized state of value  $W_i$ , giving a band head will also form the head of a continuous spectrum linked up with it. The sharp high-frequency edge at  $\lambda$  2130 will then mean the maximum velocity  $v_{\text{max}}$  of the electrons which can be captured by molecular iodine. With a greater value of any

of these, either the molecule dissociates or the electron escapes. A similar edge, but at  $\lambda$  2125, is shown by bromine.

### Summary.

Iodine has been examined spectroscopically by excitation under electrodeless Tesla discharge. The spectrum obtained has a bright continuous background from  $\lambda$  4800 to  $\lambda$  2130 with a number of electronic emission bands superposed on it. Four different systems of bands have been located. One of these systems has been analysed and shown to confirm to the equation

$$\nu = 29078 + (710n' - 8n'^2) - (213 \cdot 7n'' - 0 \cdot 6n''^2),$$

where 29078 is the wave-number of the head of the system. The presence of the fluorescence term  $(213 \cdot 7n'' - 0 \cdot 6n''^2)$  has been shown to indicate that this system is given in emission as the molecule returns from a higher excited state to the meta-stable  $2p_1$  state. A brief discussion is given of the bands at  $\lambda$  4800 and  $\lambda$  3440, which have been frequently called the "electron affinity" bands. An attempt has also been made to explain the continuous background.

### References.

- (1) Konen, *Ann. d. Physik*, lrv. p. 265 (1898).
- (2) Wood, 'Researches in Physical Optics.'
- (3) McLennan, *Proc. Roy. Soc. A*, lxxxviii. p. 289 (1913); xci. p. 231 (1915).
- (4) Oldenburg, *Z. Physik*, xxv. p. 136 (1924).
- (5) Steubing, *Ann. d. Physik*, lxiv. p. 673 (1921).
- (6) Franck, *Z. Physik*, v. p. 428 (1921).
- (7) Gerlach & Gromann, *Z. Physik*, xviii. p. 239 (1923).
- (8) Noyes, *J. Amer. Chem. Soc.* xlv. p. 337 (1923).
- (9) West & Ludlam, *Proc. Roy. Soc. Edin.* xlv. p. 185 (1924).
- (10) Mecke, *Ann. d. Physik*, lxxi. p. 104 (1923).
- (11) Cario & Oldenburg, *Z. Physik*, xxxi. p. 914 (1925).
- (12) Merton, *Proc. Roy. Soc. A*, lxxxix. p. 447 (1912).
- (13) McVicker, Marsh, & Stewart, *J. Chem. Soc. (England)*, cxxiv. p. 642 (1923).
- (14) Foley, *Proc. Ind. Acad. ser. 34*, p. 185 (1924).
- (15) Swindler, *Phys. Rev.* xxviii. p. 1136 (1926).
- (16) Bloch & Bloch, *Comptes Rendus*, t. clxxx. p. 1740 (1925).
- (17) Robertson, *Phys. Rev.* xix. p. 470 (1922).
- (18) Our thanks are due to Prof. J. M. Benade for the kind loan of this.
- (19) Wood & Kimura, *Astrophysical Journ.* xlv. p. 189 (1917).
- (20) St. Landau-Ziemecki, *Phil. Mag.* xlv. p. 651 (1922).
- (21) Bodenstein & Stark, *Zeits. f. Electrochemie*, xvi. p. 961 (1910).
- (22) Franck, *Trans. Faraday Soc.* xxi. p. 536 (1926).
- (23) This band has been given by Ludlam and West at  $\lambda$  3450 and by Gerlach and Gromann as lying between  $\lambda$  3460-3340. In our case we are certain that the boundaries of this band do not extend much beyond  $\lambda$  3440-3360.

- (24) Turner, *Phys. Rev.* xxvii. p. 404 (1926).  
 (25) Turner & Compton, *Phys. Rev.* xxv. p. 747 (1925).  
 (26) This band comes out at  $\lambda 3440$  in our spectrograms. It has been shown by Cario and Oldenburg (*loc. cit.*) to possess a fine structure.  
 (27) Gerlach, *Phys. Z.* xxiv. p. 417 (1923).  
 (28) Kratzer & Sudholt, *Zeits. f. Physik*, xxxiii. p. 144 (1925).  
 (29) Kemble & Witmer, *Phys. Rev.* xxviii. p. 637 (1926).  
 (30) Foote & Mohler, *Phys. Rev.* xxi. p. 382 (1923); also 'Origin of Spectra.'  
 (31) Dymond, *Zeits. f. Physik*, xxxiv. p. 553 (1925).  
 (32) Wright, 'Nature,' cix. p. 810 (1922).  
 (33) Crew & Hulburt, *Phys. Rev.* xxviii. p. 936 (1926).

University Chemical Laboratories,  
 University of the Punjab,  
 Lahore, India.

## CXXVII. *The Measurement of Sound-absorption in a Room*\*.

By VERN O. KNUDSEN, *Ph.D., Assoc. Prof. of Physics,*  
*University of California at Los Angeles*†.

### I. Introduction.

THE fundamental differential equation for the distribution of sound in a room is ‡

$$V \frac{\partial I}{\partial t} + \frac{1}{2} vaI = E, \quad . . . . . (1)$$

where  $V$  is the volume of the room,  $I$  the average density of sound energy in the room,  $v$  the velocity of sound,  $a$  the total absorption of the room and its contents, and  $E$  the uniform rate of emission of sound energy from the sound source. The solution of (1) yields two equations which suggest practical methods for the determination of  $a$ . The first and simpler of these equations, which applies to the steady state when the rates of emission and absorption are equal, is

$$a = \frac{4E}{vI_0} t, \quad . . . . . (2)$$

\* A part of this investigation was presented to the American Physical Society, March 5, 1927. (See Abstract, *Phys. Rev.* xxix. p. 753 (May 1927).)

† Communicated by the Author.

‡ G. Jaeger, "Zur Theorie des Nachhalls," *Akad. Wiss. Wien, Sitzungsberichte*, May 1911, p. 120. (See also E. A. Eckhardt, "Acoustics of Rooms," 'Journal of the Franklin Institute,' June 1923, p. 799; and E. Buckingham, "Theory and Interpretation of Experiments in the Transmission of Sound through Partition Walls," *Scientific Papers of the Bureau of Standards*, No. 506, May 26, 1925.)

where  $I_0$  is the average maximal steady state value of the density of sound energy in the room. The second of these equations, which applies to the decay of sound in a room after the source has been stopped, is

$$I = I_0 e^{-\frac{va}{4V}t} \dots \dots \dots (3)$$

The somewhat similar equation for the growth of sound in a room is also serviceable but not so convenient as the one for the decay. Equation (3), which gives the rate of decay of sound in a room, suggests two methods for determining  $a$ : (1) measurement of oscillograms of the decadent sound, or (2) measurement of the time required for a sound to be reduced to a known fraction of its initial steady state value. This latter method is the one chosen and developed by W. C. Sabine, and it has been used almost exclusively by all subsequent investigators. It is customary to use the ear as the detector in these measurements. The observer stops a tone of predetermined intensity (usually about one million times the minimal audible intensity) and measures the duration of audibility.

## II. *Advantages and Limitations of the Different Methods for Measuring a.*

The simplicity of equation (2) makes it appear as a direct and an attractive means for determining  $a$ . It is necessary to measure only  $E$  and  $I_0$ , and substitute their values in (2). This is similar to the determination of electrical resistance by the voltmeter-ammeter method—the rate of sound emission corresponds to the e.m.f., and the average intensity  $I_0$  corresponds to the current.

It is easy to modify (2) into a more useful form for laboratory measurements. Thus, by making two sets of measurements in the room, one with the room as it is to be tested and another with a known amount of absorption added to the room, it becomes unnecessary to know the rate of emission of the source, provided it remain constant for the two sets of measurements. The equations for these measurements are obtained from (2). Suppose measurements of  $I_0$  be made in the room as it is to be tested. Then

$$a = \frac{4E}{vI_0}.$$

Now suppose a known amount of absorption  $a'$  has been  
*Phil. Mag. S. 7. Vol. 5. No 33. June 1928.* 4 L

added to the room, by opening windows or by other means. Then

$$a + a' = \frac{4E}{vI_0'},$$

where  $I_0'$  is the resulting steady state intensity of sound in the room. Whence,

$$a = \frac{a'}{I_0'/I_0 - 1} \dots \dots \dots (4)$$

with  $I_0$  and  $a$  known,  $E$  can be determined from (2) and its value used in all subsequent measurements, either in the same room or in other rooms, provided, of course, that  $E$  remain constant.

This method of determining the absorption of a room has a number of obvious advantages:—

1. The measurements are all instrumental, and thus independent of the ear of an observer.
2. The error in determining the absorption of a room is the same as the error in measuring the average intensity of sound in the room, and with suitable apparatus it should be easy to reduce this error to one per cent. or less.
3. The disturbing effect of residual noise in a room can be made negligible. If the intensity of the test tone be one thousand times as great as the intensity of the residual noise in the room, the noise introduces an error of only one-tenth of one per cent. It is an easy matter to produce test tones of this required intensity in an average room. Elaborate sound insulation, or the making of the measurements during the quiet part of the night, is thus obviated.

The method of measurement appears simple and precise, and, indeed, would be, were it not for the difficulties encountered in determining the average value of  $I_0$ . These difficulties were set forth lucidly by W. C. Sabine in one of his early lectures given at the Sorbonne in the spring of 1917\*. The difficulties are of two sorts: first, the reflexions from the walls produce an interference pattern in the room with pronounced maxima and minima; and second, the rate of emission of the sound source is influenced

\* W. C. Sabine, 'Collected Papers,' pp. 277-279. This is a free translation from notes which he prepared for one of the lectures.

by the interference pattern. If the vibrating source is situated at a maximum, it will experience difficulty in imparting any additional motion to the surrounding air. Or, if the vibrating source be situated at a minimum, it will impart an excessive motion. Sabine cites an instance in which the introduction of a large amount of acoustic felt in a room actually increased the loudness of the test tone; whereas, according to expectations from equation (2), the intensity should have been reduced to one-third of its initial value. Other workers in the field of sound, including the writer, have experienced similar "anomalies" in sound-intensity measurements. It is necessary, therefore, to thoroughly "mix" the sound in a room if reliable measurements of average intensity are to be made. W. C. Sabine introduced a large rotating steel vane into the sound chamber, which continuously shifts the sound interference pattern. This suffices for reverberation measurements. Eckhardt and Chrisler,\* at the Bureau of Standards Sound Laboratory, use a rotating variable-frequency source of sound. Such devices help greatly to provide a uniform distribution of sound in a room, but even under these conditions it is necessary to make many measurements in all parts of the room in order to determine the average intensity of sound. The difficulties in making these measurements have been realized by Sabine and his successors, and for that reason practically all measurements of the sound-absorption of a room have been made by the reverberation method. The difficulties, however, do not seem insurmountable, and the simplicity and directness of utilizing such intensity measurements for the determination of the sound-absorption of a room have always appealed to the writer. Just what success may be anticipated from the use of this method will be indicated by the experimental part of this paper.

Equation (3), which expresses the law of decay of sound in a room, indicates that the absorption of a room can be determined by measuring the rate of decay. Perhaps the most obvious method for determining the rate of decay is to obtain oscillograms of the decadent sound. Suppose the curve in fig. 1 be the envelope of a typical oscillogram. If the ordinates in fig. 1 be measured for successive intervals of time,  $t'$ , the ratios of corresponding ordinates separated by the same time-intervals will be constant. Let  $I'_0/I'$  represent the constant ratio of any ordinate to a successive

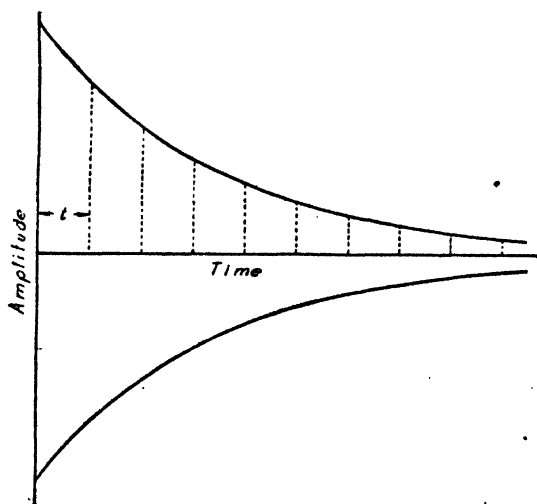
\* 'Scientific Papers of the Bureau of Standards,' No. 526, April 28, 1926.

one  $t'$  seconds later; then the absorption of the room is given by

$$a = \frac{4V}{vt'} \log_e \frac{I'_0}{I'} \dots \dots \dots (5)$$

In the actual oscillograms the ordinates will represent the pressure-amplitude of the sound and not the intensity  $I$ , which is proportional to the square of the amplitude.  $I'_0/I'$  is therefore the square of the corresponding ordinates measured on the oscillogram.

Fig. 1.



Curve giving an ideal representation of how sound dies away in a room. The rate of decay furnishes a means of determining the total absorbing power of the room.

The advantages of this method of determining the absorption of a room are :—

1. The measurements are made from a photographic film, and can be made as slowly and accurately as desired. The oscillogram is thus a compact, permanent record, which can be filed for future reference.
2. The error in determining the absorption is proportional primarily to the logarithm of the intensity ratio  $I'_0/I'$  and therefore should be very small.
3. It is an absolute method, and no calibrating is required.



There are two limitations to this method for determining  $\alpha$ . First, the decay is not uniform. The interference pattern in the room is pronounced and is in a state of rapid change; successive maxima and minima are presented to the detector, and consequently the oscillogram is a complicated record of the decay of sound. After the source of sound has been stopped the residual sound becomes more and more uniform, but the successive maxima and minima are not completely eliminated.

The second limitation to this method comes from the interfering effect of any noise in the room. Since the residual decadent sound in the room becomes more and more uniform, the terminating portion of the oscillogram is best adapted for measurements. Hence any extraneous noise in the room would be superposed upon the decadent sound. This requires a relatively quiet room.

The two methods for determining  $\alpha$  which have just been outlined have probably been considered by W. C. Sabine and subsequent workers, but have been abandoned because of the inherent difficulties arising from the sound-interference pattern in a room. These difficulties have been discussed, and, as will be shown later, special devices must be used to overcome them.

Sabine's investigations led him to adopt a third method for determining  $\alpha$ . This is known as the reverberation method. It is necessary to have a source of sound, the rate of emission of which,  $E$ , can be varied by a known ratio. Then, if the duration of audibility of the residual sound for two values of  $E$  be determined,  $\alpha$  can be calculated. Thus, let  $E_1$  and  $E_2$  be the rates of emission of the source, the ratio  $E_2/E_1$  being known. (Sabine used one and four identical organ-pipes, separated from each other sufficiently to neglect mutual coupling, so that the four pipes emitted four times as much energy as one pipe. A suitable loudspeaker, actuated by a filtered oscillator current, can be used to advantage.) Let  $t_1$  and  $t_2$  be the durations of audibility of the two sources having rates of emission of  $E_1$  and  $E_2$ , respectively; and let  $I_m$  be the minimal audible intensity for an observer in the room. Then, since the intensity ratio,  $I_2/I_1$ , for the steady state, is equal to the ratio of the rates of emission of the source,  $E_2/E_1$ , it follows from (3) that

$$I_m/I_1 = e^{-\alpha a/4V \cdot t_1} \quad \text{and} \quad I_m/I_2 = e^{-\alpha a/4V \cdot t_2}.$$

Whence, by division and solving for  $\alpha$ ,

$$\alpha = \log_e E_2/E_1 \cdot 4V/v(t_2 - t_1). \quad (6)$$

In the organ-pipe experiments of Sabine,  $E_2/E_1$  is usually four, the number of pipes used. In experiments using a loud-speaker as the source,  $E_2/E_1$  can and should be at least one hundred. The only measurements necessary, besides  $V$ , the volume of the room, and  $v$ , the velocity of sound, are  $t_1$  and  $t_2$ , which can be determined by the ear and a suitable chronograph. It is an advantage to have  $E_1$  and  $E_2$  as large as possible, as this increases the accuracy in measuring  $t_1$  and  $t_2$ . It is an even greater advantage to have the ratio  $E_2/E_1$  large, since this will reduce the error in the difference  $t_2 - t_1$ . This method for determining  $a$  will yield fairly accurate results, provided a large number (at least fifty) of measurements of  $t_1$  and  $t_2$  are taken, and provided further that the test-room be completely free from noise.

The reverberation method has the following advantages:—

1. The decadent sound in the room, after the source has been stopped, becomes more and more mixed up as time goes on, so that near minimal audibility the intensity is nearly uniform in all parts of the room.
2. The pertinent measurements consist simply of time-measurements, usually of two or more seconds duration.
3. The apparatus requirements are simple—a standard source of tone, with means for adjusting the intensity, and a suitable chronograph comprise the necessary apparatus.

There are, however, a number of limitations to the reverberation method, and some of them are objectionable or difficult to control. There is an inherent error in judging just when the sound has reached minimal audibility. Two elements contribute to this error: first, the poor sensibility of the ear to small changes of intensity near the threshold of audibility; and second, the actual fluctuation of intensity resulting from the interference pattern in the room. Under ideal conditions, the smallest discernible change of intensity near minimal audibility is approximately 30 per cent\*. Under actual working conditions, a change of about 50 per cent. would be nearer the practical limit. This would appear, on first thought, to be a serious source of error; but for a tone of usual intensity, that is one having an intensity of one million times the minimal audible intensity, the error in the measurement of  $t$  would be approximately 5 per cent.

\* V. O. Knudsen, "Sensibility of the Ear to Small Differences of Intensity and Frequency," *Phys. Rev. (ser. ii.)* xxi. p. 84 (1923).

The actual fluctuation of intensity resulting from the ever-changing interference pattern also introduces an error in the observer's judgment of minimal audibility, the magnitude of which depends upon the nature of the room and the experimental equipment. The rotation of a large reflecting surface in the room, as is used by Paul E. Sabine in the Riverbank Laboratories, minimizes this error. However, measurements of  $t$  in an ordinary room, without a rotating reflector or other means for "mixing" the decadent sound, would be subject to an error of 5 per cent. or more. The errors arising from the poor sensibility of the ear and the interference pattern will be regularly distributed, and therefore, by taking an appropriate average of a large number of separate measurements (as many as fifty are usually made), satisfactory results can be obtained.

A more serious limitation to the reverberation method for measuring  $\alpha$  is the necessity for absolute quiet in the test-room. The masking effect of any slight residual noise upon a feeble tone approaching minimal audibility is sufficient to introduce objectional errors in the measurement of  $t^*$ . Since a noise comprises almost a continuous spectrum of all audible frequencies, it is capable of producing a masking effect upon a tone of any pitch. Even a very feeble noise of only 5 to 10 S.U.† would be sufficient to introduce an error of nearly 10 per cent. in the measurement of  $t$ . Noises of this loudness are prevalent in many rooms which are regarded as practically quiet. The limitations resulting from noise can be removed by providing a sound-proof test-room, or by choosing the quiet hours of the night, if there be any, as was done by W. C. Sabine. But the rooms in which absorption measurements are to be made are not always sound-proofed, and the task of making routine measurements between midnight and 4 A.M. is not attractive.

Another objection to the reverberation method is the use of the observer's ears as a most important part of the apparatus. Although a trained observer becomes adept at judging

\* See article on "Auditory Masking of One Pure Tone by Another and its Probable Relation to the Dynamics of the Inner Ear," by R. L. Wegel and C. E. Lane, *Phys. Rev.* xxiii. p. 266 (Feb. 1924).

† This unit of loudness, proposed by telephone engineers, is gaining prestige among acoustic investigators. The loudness of a sound is expressed in S.U. by the formula:

$$\text{S.U.} = 10 \log_{10} \frac{I}{I_m}.$$

$I$  is the intensity of the sound and  $I_m$  is the intensity at the threshold of minimal audibility.

just when the decadent sound has reached his minimal threshold of audibility, he is not infallible. There are a number of factors, such as judgment, attention, fatigue, reaction time in closing or opening the key associated with the chronograph, and actual change of hearing-sensitivity, all of which introduce errors in the measurement of  $t$ . The human element in the reverberation method for measuring the absorption of a room is probably its greatest weakness. Confidence in the accuracy of any measurements is increased if they can be made independently of fallible judgments of the sense organs. Anyone who has made reverberation measurements is certain to realize the limitations imposed by the use of his ear in judging just when a sound has reached minimal audibility, especially if there be any disturbing noise in the room.

The reverberation method, besides having the limitations mentioned, is laborious and slow, and requires the utmost care and patience on the part of the observer.

Finally, the method becomes very inaccurate in rooms having a short time of reverberation. For example, attempts to measure  $t$  in a theatre with carpeted floors and upholstered seats, in which  $t$  may be less than 1.5 sec., are most unsatisfactory.

But in spite of these limitations, the reverberation method is capable of yielding very useful results, accurate to about 1 per cent. under the most favourable conditions, and about 5 per cent. under conditions more commonly met with in the average room. The most fundamental data and principles in the field of architectural acoustics have been obtained by this method, and in the past it has afforded the only means for investigating the important problem of reverberation in auditoriums.

### III. *Experimental Methods and Results.*

The object of the experimental part of the present investigation is to develop a simple and accurate method for determining the absorption of a room; a method which will be free from the objectionable limitations of the reverberation method. Specifically, this investigation aims to determine whether the first two methods for determining  $\alpha$ , discussed in the previous section, can be developed into practical laboratory methods. The main effort has been directed toward the development of the first method, that is, the determination of  $\alpha$  by intensity measurements. For brevity, this method will be called the intensity method.

The method depending on measurements of oscillograms of the decay of sound in a room will be called the oscillograph method. The method depending upon measurements of duration of audibility will be called the reverberation method.

The experimental results presented in this paper are only of a preliminary nature, but they seem to indicate conclusively that there is at least one method of measuring  $\alpha$  which can be freed from the limitations of the reverberation method, and which also can be made simple and accurate.

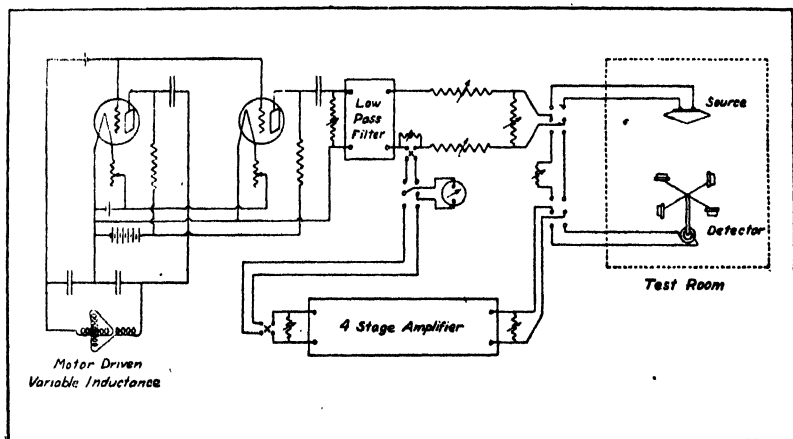
The first experiments on the intensity measurements, which were begun more than three years ago, indicated the nature of the difficulties described by W. C. Sabine in his 1917 Sorbonne lectures. Measurements were attempted using a loud speaker as a source of sound, and an electromagnetic telephone receiver and an amplifier as a detector. A single frequency of 512 d.v. was used. It was anticipated that an average value of the intensity would be obtained by taking a sufficiently large number of measurements, provided both the source and the detector were successively moved to representative parts of the room. For every position of the source a series of intensity measurements was obtained. The method indicated some promise of accuracy, but was abandoned because it was so laborious.

These initial experiments suggested the desirability of "mixing" or "stirring up" the sound in the room so that the interference pattern at any point in the room would shift between extreme limits of maxima and minima, and shift rapidly and continuously. All such devices as a rotating source, a rotating or oscillating detector, the use of as many as fifty detectors, distributed throughout the room, and a continuous change of frequency between two frequency limits, were employed in various combinations. The arrangement which worked most satisfactorily can be described by referring to fig. 2, which is a schematic diagram of the apparatus and electrical connexions. The oscillator is a Colpitts' circuit with a variable rotating inductance in the tuned circuit. With properly chosen values of inductance and capacitance in the tuned circuit, the oscillator generates an alternating current the frequency of which varies continuously with the rotation of the inductance, between 408 and 629 d.v. per second. The movable coil of the inductometer rotates at a constant speed of about two revolutions per second, so that the frequency periodically varies from 408 to 629 d.v. and back again to 408 d.v. A low-pass filter in the output of the oscillator is used to

eliminate the undesirable harmonics, and the current, thus purified, goes to a measuring circuit and thence either to the loud-speaker\* in the test room, for producing the source of sound, or to the input of an amplifier, for calibrating the amplifier.

Two different types of detector were used. One, indicated in fig. 2, consisted of four electromagnetic telephone receivers, suitably mounted on a vertical shaft which was rotated by means of a phonograph motor. The receivers, mounted at different levels, thus are made to rotate in circles of about 4 feet diameter, with a speed of about 40 r.p.m. A second detector consisted of a single condenser trans-

Fig. 2.



Schematic diagram of the circuit and apparatus used for determining the average intensity of sound in a room.

mitter, rotated as a conical pendulum, with a swivel arrangement which eliminated all moving contacts.

The e.m.f. generated by either detector is amplified (four stages were used with the four receivers as detector, but

\* Both the electromagnetic and the electrodynamic types of loud speaker have been used for the sound source. Davis & Fleming (Phil. Mag. ii. p. 51, July 1926) have shown that the electrodynamic type is the better suited for producing a constant source. This agrees with the findings of the writer. However, in most of the tests, a Western Electric electromagnetic cone type was used. This was used to avoid the resonant effects of horns associated with the available electrodynamic loud speakers. The constancy of the sound source with both types of loud speaker was maintained by frequent calibrations of the set-up under identical conditions.

three stages were sufficient with the condenser transmitter) and then measured with a thermo-couple and galvanometer. In order to eliminate errors arising from any possible changes of the amplification constant of the amplifier, the latter is calibrated for every measurement of the acoustically generated e.m.f.\* The amplifier, the input leads, and the detector are shielded so as to prevent stray induction from reaching the amplifier.

The periodic variation of the frequency of the source and the rotation of the detector provide a satisfactory means of obtaining an average value of sound intensity at a certain locality in the room not too near the source. The variation of frequency serves the double purpose of "mixing" the sound pattern near the detector and also near the source. The latter is necessary to assure a constant rate of emission from the loud speaker. Since the frequency changes more than 50 per cent., the interference pattern at any point in the room will pass through all phases of intensity from local maxima to local minima.

The loud-speaker is located near the ceiling of the test room. A screen is placed between the source and the detector in order to shield the detector from the direct radiation from the source. In each series of measurements the detector is placed successively at eight different stations in the room. Four of these stations are about 4 feet above the level of the floor and near the four corners of the room. The other four stations are elevated about 7 feet above the floor. The separate measurements at the eight different stations, for a given condition of the room, do not differ among themselves by more than 10 per cent. The average of the eight measurements is taken to represent the average intensity of sound in the room. When the room is tested again with a different amount of absorption in it, the detector is placed in the same eight positions or stations.

The test room in which most of the measurements have been made is a reinforced concrete sound laboratory, 18 ft.  $\times$  18 ft.  $\times$  16 ft. high, furnished through the kindness of the Calacoustic Corporation of Los Angeles. The room has no windows and only one door. The loud-speaker and detector were the only equipment in the test room. The oscillator, the amplifier, and the measuring apparatus were in a separate room.

\* The method of measurement is essentially the same as that used by the Bureau of Standards. See Bureau of Standards Scientific Paper No. 526, "Transmission of Sound of Some Building Materials," by E. A. Eckhardt and V. L. Chrisler.

*Measurements by the Intensity Method using an Electromagnetic Cone Type Loud-Speaker as Source and Four Rotating Electromagnetic Receivers as Detector.*—In these tests the absorption in the room was supplied by an acoustic plaster applied to the walls and ceiling. Tests were begun in the room with all four walls and the ceiling plastered. Then the acoustic plaster on two walls was stripped off and the room again tested. This was repeated with the acoustic plaster removed from all four walls. Finally, the room was tested with all of the acoustic plaster removed, that is, with walls, floor, and ceiling in concrete. The total absorption in the room, under each of the four different conditions, was determined both by the reverberation method\* and by the intensity method. Many separate measurements of the absorption of the empty room, using the reverberation method with a tone of 512 d.v., had been made in previous work, and it was felt, therefore, that this absorption (25.0 units†) should be used as the most accurately known datum. All other calculations of  $a$ , by the intensity method, are based upon the assumed correctness of this datum. A summary of the results of the tests is given in Table I.

TABLE I.

Condition of Room.	$a$ by Reverberation Method (512 d.v.).	Square of Input e.m.f. (in m.v.) <sup>1</sup> .	$a$ by Intensity Method (408–629 d.v.).	Percentage Difference.
Walls and ceiling concrete .....	25.0 units	.851	25.0	
Two walls plastered .	48.2 „	.458	46.4	3.8
Four walls plastered .	105.8	.205	103.8	1.9
Walls and ceiling plastered .....	152.0 „	.144	148.0	2.7

<sup>1</sup> The actual intensity in the room was approximately  $10^7$  times minimal audibility.

\* V. O. Knudsen, "Measurement of Reverberation using the Thermionic Tube Oscillator as a Source," Jour. Op. Soc. & Rev. Sc. Inst. xlii. pp. 609–612 (1926).

† A unit is 1 square foot of perfectly absorbing surface, as an open window. All units in this paper are based on the British System because of the general use of these units in buildings among English-speaking people.



The agreement between corresponding values of  $a$  is very satisfactory, and is of the order of the probable experimental error.

Two other similar determinations of different amounts of absorption in a room, one in the same test room and another in a smaller test room at the University, both gave good agreement between the values of  $a$  obtained by the reverberation method and by the intensity method. In the first instance the percentage difference was 3.0 per cent., and in the second .8 per cent.

*Measurements by the Intensity Method using an Electro-dynamic Loud-Speaker as Source and a Condenser Transmitter as Detector.*—In these tests the absorption in the room was controlled by placing on the floor different amounts of patented acoustic tile. The total absorption of the empty room and its equipment, but with no absorbing material on the floor, was now 28.3 units, as determined by the reverberation method for a tone of 512 d.v. The increased absorption of the room (it was only 25.0 units in the former series of tests) is accounted for by the presence of additional equipment for supporting and rotating the condenser transmitter. The coefficient of absorption of the patented acoustic tile was determined both by the reverberation and the intensity methods. The coefficients obtained by the two methods differed by only 2.0 per cent., the average value being .433. With the use of these two data, 28.3 units for the absorption of the empty room and .433 for the coefficient of absorption, measurements were made to determine the relation between the average intensity of sound in the room and the total absorption in the room, the activity of the source remaining constant. Different amounts of absorbing material, from 4 sq. ft. to 127 sq. ft., were brought into the test chamber, and the average sound intensity determined for each condition of the room\*. The results of the measurements are given in Table II. The first column in the table gives the amount of absorbing material in the room. The second column gives the total absorption of the room obtained by adding the amount contributed by the absorbing material (the area  $S$  of the acoustic tile multiplied by the difference between the coefficients of the acoustic tile and the concrete it covered) to the absorption of the empty room. The third column gives the deflexion of the galvanometer connected with the thermocouple in the output of the

\* The apparatus was sufficiently delicate to detect readily the addition to the empty room of a single square foot of the absorbing material.

TABLE II.

Absorption Material in Room (S).	$\alpha$ calculated from $\alpha=28.3$ + $S(433-.014)$ (512 d.v.).	Average Galvanometer Deflexion on Output Thermocouple.	Average Sound Intensity in Room.	$\alpha$ by Intensity Method (408-629 d.v.).	Percentage Difference in values of $\alpha$ .
Room Empty .....	28.3 units	14.25	$5.00 \times 10^7$	28.3 units	
4 sq. ft. ....	30.0 "	13.34	4.68 "	30.2 "	+ .7
16 " " .....	35.0 "	11.13	3.91 "	36.2 "	+ 3.4
36 " " .....	43.3 "	9.25	3.25 "	43.6 "	+ .7
49 " " .....	48.8 "	8.19	2.88 "	49.2 "	+ .8
64 " " .....	55.1 "	6.99	2.46 "	57.5 "	+ 4.5
81 " " .....	62.3 "	6.42	2.25 "	62.8 "	+ .8
100 " " .....	70.2 "	5.61	1.97 "	71.9 "	+ 2.4
127 " " .....	82.1 "	5.05	1.77 "	79.8 "	- 2.8

amplifier. The calibration curve of the amplifier showed that this deflexion was accurately proportional to the square of the a.c. voltage input of the amplifier. It follows that these deflexions are proportional to the energy density of the sound in the test chamber, provided the amplification factor of the amplifier remain constant. The amplification factor decreased about 2 per cent. during this series of measurements, but the change was a gradual one. The recorded deflexions in the third column have been corrected for this slight change, and hence these numbers give a relative measure of the sound intensity in the room. The fourth column gives the actual average intensity of sound in the room, expressed in terms of minimal audibility. The intensity was determined in the case of the empty room by reducing the current through the loud-speaker to the point of inaudibility. All other values of intensity were obtained by assuming the intensity proportional to the deflexions given in the third column. The total absorption of the room, as recorded in the fifth column, is calculated from equation (2). The last column gives the percentage difference between the corresponding values of  $a$  in the second and fifth columns.

The results recorded in Table II. are shown graphically in fig. 3. The first point on the curve was obtained by plotting the sound intensity in the empty room, measured by the galvanometer deflexion, against the absorption of the empty room. Thus, from Table II., it can be seen that the ordinate of this point is 14.25 and the abscissa is 28.3. The other points on the curve were determined by assuming that the sound intensity in the room was proportional inversely to the total absorption of the room for a tone of 512 d.v. The curve, therefore, is a rectangular hyperbola. The actual observed intensities for different amounts of absorption in the room are indicated by the small circles.

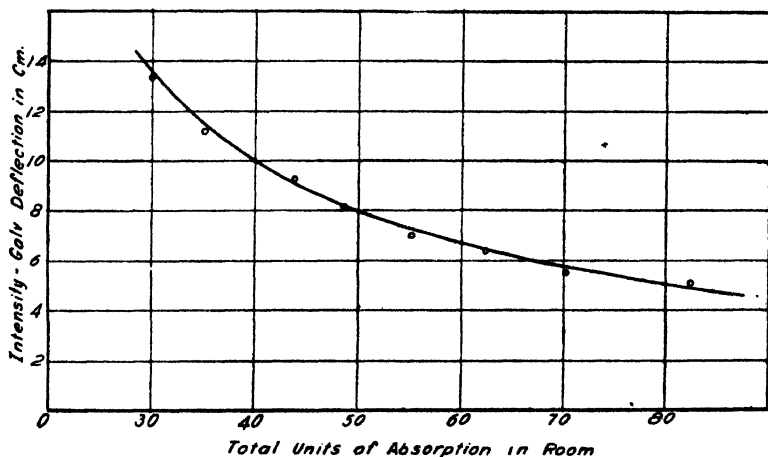
The close agreement between the observed intensities and the hyperbolic curve seems to support the general validity of the equation for the steady state of sound in a room, namely, that the average density of sound energy in a room is inversely proportional to the total absorption of the room.

In general, the measurements obtained with the electrodynamic loud-speaker as source and the condenser transmitter as detector were subject to smaller variations, and were altogether more satisfactory than those obtained with the electromagnetic loud-speaker as source and the four electro-

magnetic receivers as detector. The electrodynamic loud-speaker supplied a more nearly constant source of sound than the electromagnetic loud-speaker, and the condenser transmitter as a detector was both more sensitive and more nearly uniform in its sensitivity characteristic than the electromagnetic receivers.

The results obtained to date indicate that the intensity method can be utilized for accurate work in the determination of the absorption of a room or the coefficient of absorption of acoustic materials. The writer is at present designing a laboratory for testing purposes which will utilize this method. By reducing the size of the test

Fig. 3.



Curve showing how the average intensity of sound in a room depends upon the total absorbing power of the room. The curve gives the theoretical values of intensity, based upon the intensity being inversely proportional to the absorption of the room. The small circles indicate the measured values of intensity.

chamber and increasing the number of microphone units in the detector, it is believed that the absorption of the test chamber can be determined from a single reading of the galvanometer deflexion in the output of the amplifier. In future work it is also planned to design the oscillator so as to give a wide band of frequencies near 128 d.v. and another near 2048 d.v. Thus it will be possible to determine, both accurately and expeditiously, coefficients of absorption of acoustic materials for low, medium, and high frequencies. This is all that is necessary for most practical purposes.

*Measurements by the Oscillograph Method.*—Considerable work has been done in an effort to develop the oscillograph method for measuring  $\alpha$ . The initial work began with a single frequency of 512 d.v. The oscillograms obtained indicate that the decay is very irregular, owing to the shifting interference pattern surrounding the detector. Measurements of the rate of decay on such oscillograms led to inaccurate results. They indicated only the order of magnitude of the absorption in the room, giving errors as great as 50 to 100 per cent. The best decay curves were obtained with the variable frequency source, 408 to 629 d.v., and the detector at rest. Oscillograms obtained in this manner gave values of  $\alpha$  which differed approximately 10 per cent. from corresponding values obtained by the reverberation method. The results of two sets of measurements are given in the following table :—

TABLE III.

Condition of Test Room.	$\alpha$ by Reverberation Method.	$\alpha$ by Oscillograph Method.	Percentage Difference.
Empty.....	25.0 units	22.0 units	12.8 %
Floor covered with hairfelt, celotex, etc. ....	102.0 units	111.0 units	8.5 %

These preliminary results indicate that the oscillograph method probably could be developed into a precise and convenient method for measuring the absorption of a room. It appears necessary only to improve the technique of "mixing" the sound in the room so that the detector at every instant of the decay will respond to the average intensity of sound in the room. A more rapid fluctuation of the frequency of the source and a larger number of units in the detector should give more satisfactory oscillograms. This and other possible improvements will constitute a part of future work.

In conclusion, the writer gratefully acknowledges the co-operation of W. A. Munson and Lewis Delsasso in the experimental part of this work. He also wishes to record his thanks to the Calacoustic Corporation of Los Angeles for the use of the test chamber and for the labour of preparing the room for some of the measurements.

CXXVIII. *Cavitation in Screw Propellers.**To the Editors of the Philosophical Magazine.*

GENTLEMEN,—

**I**N the paper by Mr. J. Tutin, published in your July 1927 issue, there appears to be an error in equations (6) and (7) on page 21.

Taking equation (6), there are two ways of obtaining a momentum equation. First, we may consider the whole volume bounded by the curved lines in fig. 1. The inflow area is greater than  $A$ , say  $A'$ , so that the left-hand side of (6) should be  $p_0 A' - pA$ . Further, the pressures on the curved sides should be included.

Alternatively, we may consider a cylinder whose section is that of the disk and with generators parallel to the central line of flow. In the momentum equation the left-hand side of (6) is now correct; but on the right a term should be added expressing the momentum of the fluid entering the cylinder through its sides due to the obliquity of the flow.

In either case, equation (6) is clearly incorrect, and by similar methods equation (7) can also be shown to be defective. The remainder of the paper is founded on these two equations, and, in my opinion, the author's conclusions are therefore erroneous.

Yours faithfully,

L. WOOLLARD.

Naval Construction Dept.,  
Admiralty, London, S.W.1.

CXXIX. *Notices respecting New Books.*

*The Problem of Physico-Chemical Periodicity.* By E. S. HEDGES and J. E. MYERS, with a foreword by Prof. F. G. DONNAN. (Edward Arnold: London. Price 7s. 6d.)

**I**N this work, the authors give an extensive and connected account of periodic phenomena in chemistry and physics. They have collected a considerable amount of information bearing on this important and interesting subject, and from an examination of the data and from their own researches, put forward the suggestion that periodicity in chemical reactions is associated with surfaces in a metastable state.

Many examples of these periodic phenomena are cited in the text, *e. g.*, Dr. Holker's beautiful experiment on the periodic opacity of Wassermann "antigen" with sodium chloride as the electrolyte, the periodic decomposition of hydrogen peroxide, and the parallel periodicity of electropotential and the evolution of hydrogen by the dissolution of metals.

The bibliography and author index include nearly three hundred references to researches, from those of Fechner, Joule, and Quincke to the most recent contributions in the *Kolloid Zeitung* and other magazines, and the authors' papers in the 'Journal of the Chemical Society.'

*Recent Advances in Organic Chemistry.* By ALFRED W. STEWART, D.Sc. Fifth Edition. Vol. i. pp. xiv + 387; vol. ii. pp. xiv + 382. (London: Longmans, Green & Co. 1927. Price 21s. net each.)

THE fifth edition of Prof. Stewart's well-known account of recent advances in organic chemistry has been expanded into two volumes, an indication of the enormous amount of research which is in progress in this subject. In previous editions, a balance has been maintained between those portions of the subject on which general agreement has been reached and the newer lines of research. With the rapid development of the subject, some of the older material has had to be discarded in the preparation of new editions. The expansion into two volumes now allows some of this material—such as the chapters on addition reactions and unsaturation—to be included again.

The balance between the older and newer fields of organic chemistry is maintained by devoting one volume to each. The first volume, which is complete in itself, contains a survey of numerous fundamental problems of organic chemistry and is intended to cover the requirements of third-year students. It forms an introduction to the second volume, which contains an account of the most recent work in several well-selected fields which are of general interest. This volume is intended for Honours students and post-graduate workers. The subjects discussed include carbohydrate constitutions, the sesquiterpenes, rubber, the alkaloids, the anthocyanines, the chlorophyll problem, the depsides, abnormal valency, and applications of electronics. Several of the chapters are entirely new; the remainder have been revised or rewritten.

The first volume is prefaced by a historical chapter summarising the development of the subject up to the end of the nineteenth century. The second volume is prefaced by a similar chapter continuing the account up to the present time.

The output of original research in organic chemistry is so extensive that workers in and students of the subject will find Prof. Stewart's summaries of some of the more important problems invaluable both for study and for reference.

*Spherical Harmonics. An Elementary Treatise on Harmonic Functions with Applications.* By T. M. MACROBERT, M.A., D.Sc. Pp. xii+302 with 20 diagrams. (London: Methuen & Co. 1927. Price 15s. net.)

AN account of the elements of the theory of spherical harmonics, in so far as it is required for applications to mathematical physics, is given in this volume. The treatment is sufficiently elementary for students with a good working knowledge of the calculus, but without knowledge of the theory of functions. The conditions for convergence of infinite series and for change in the order of terms are stated, but proofs of these conditions are not given. The use of spherical harmonics, Legendre functions, and associated Legendre functions, are illustrated by numerous applications to potential theory and to electrostatic problems. One chapter is devoted to Clerk Maxwell's theory of spherical harmonics.

Additional chapters are devoted to Fourier series, with illustrative applications to problems connected with the conduction of heat, and the vibrations of strings and membranes; and to Bessel functions with application to cylinder problems.

The volume contains all that will normally be required by the physical investigator, and the treatment is straightforward and elementary. It can be recommended to the student both for study and for reference.

*The Measurement of Air Flow.* By E. OWER, B.Sc., Hons. I., A.C.G.I. Pp. vii+199 with 73 figures. (London: Chapman & Hall. 1927. Price 15s. net.)

THE author in the course of his work at the National Physical Laboratory has experienced the need for a text-book on the subject of air-flow measurements, which frequently present serious practical difficulties to engineers. The volume under review has been written as a first step in the direction of meeting this need, and is intended to serve both as a text-book for students and as a work of reference for engineers engaged on matters such as fan engineering and the ventilation of mines and buildings.

With the practical needs in mind, the treatment is primarily of a practical nature. Mathematical discussions, where necessary, are of a sufficiently elementary nature to be followed without difficulty by those with a slight knowledge of the calculus. The design of Pitot and static tubes is discussed in detail, and the detailed dimensions of tubes which will record correct velocities without calibration are given. The use of Pitot-static tubes, as well as the plate orifice, Venturi tube and shaped nozzle for the measurement of the flow of air in pipes are described. Other methods of measuring air flow, by means of the vane anemometer (the theory of which is discussed in a very complete manner), the rate of cooling of heated wires, etc., are explained, and a chapter is devoted to a description of various types of manometer for the accurate measurement of small pressure-differences.



*History of Science Teaching in England.* By D. M. TURNER, M.A.  
B.Sc. Pp.x+208. (London: Chapman & Hall. 1927. Price  
7s. 6d. net.)

THE introduction of science teaching into the Universities and into the schools, both secondary and primary, in England is of comparatively recent date, and was not achieved without considerable opposition from those who regarded science as a purely utilitarian subject without cultural value. The volume under review gives an interesting account of the gradual growth of the scientific spirit in England and of its reaction on the system of education, leading by slow stages to the present system in which the teaching of science is definitely incorporated, together with practical instruction.

It is of interest to note that the demand for science teaching resulted, in the first half of the nineteenth century, in the establishment of the Mechanics Institutes and night schools in which science teaching of a kind was given long before it was adopted as a general subject in the school or University Curriculum and before any discussion had been given to the question why science should be taught. The author discusses in an interesting manner different views which have been held as to the reasons for teaching science.

All students of pedagogy or of the history of science will find much to interest them in this volume.

# CXXX. *Proceedings of Learned Societies.*

## GEOLOGICAL SOCIETY.

[Continued from p. 1016.]

March 7th, 1928.—Prof. J. W. Gregory, D.Sc., F.R.S.,  
President, in the Chair.

THE following communication was read:—

‘The Major Intrusions of South-Eastern Iceland.’ By Hilda Kathleen Cargill, M.Sc., F.G.S., Leonard Hawkes, D.Sc., F.G.S., and Julia Augusta Ledebøer, M.Sc., F.G.S.

The main plutonic intrusions into the Tertiary plateau-basalts of Iceland were discovered some forty-five years ago in the south-east of the island, but little is known of their field-relations or petrology—and the present paper is a summary of the results obtained in the course of several summer visits to the more accessible localities.

The outcrops are scattered; the largest one (the Slaufudal Stock) is elongate in plan, and its area covers  $1\frac{1}{2} \times 4\frac{3}{4}$  miles. The relationship of intrusives to country-rocks (splendidly ex-

hibited in a series of cliff- and deep valley-sections) is a discordant one, the intrusions being stocks with steep-sided walls and domed roofs (not laccoliths as formerly suggested). The elongation of the stocks is parallel to the strike of the regional dykes, and intrusion clearly took place under, and was facilitated by, crustal tension. All intrusions are multiple: the common association is that of gabbro and granophyre. A horizontal layered structure of granite and granophyre is visible in the Slaufudal stock, which seems to have grown by the injection of successive sills with intermittent subsidence of the replaced block.

The rocks belong to the calc-alkaline suite, and comprise in the order of differentiation gabbro-peridotite, gabbro, diorite, granodiorite, granophyre, granite, quartz-vein. This sequence may be correlated with the order of crystallization, which in the colourless minerals is:—plagioclase, potash feldspar, potash feldspar and quartz, quartz. No true orthoclase has been detected in the rocks—the 'potash feldspars' are shown by analysis to contain about 40 per cent. of orthoclase. The plagioclase of the most basic rocks (gabbro-peridotites), which are poor in feldspar, is more acid than that of the less basic and feldspar-rich gabbros.

Eight new analyses are given. The suite, with the addition of granodiorite, is similar to that of the main plutonic intrusions of Tertiary age in Scotland. Comment is made on the absence of alkaline types in a region of 'Atlantic' tectonics.

The acid rocks exhibit two extreme textures—the graphic and the granitic, with intermediate varieties (semi-granophyres). The granophyres are richer in plagioclase and poorer in quartz than the granites which are quartz and potash-feldspar rocks with 1 to 5 per cent. of hornblende. In the semi-granophyres the last residuum to crystallize shows granitic texture, and this is correlated with the fact that the granites are a later differentiate than the granophyres. The failure of the graphic intergrowth is ascribed to a diminished magmatic viscosity due to an increased content of volatile substances, with a consequent wider spacing of the centres of spontaneous crystallization, which inhibits the formation of the graphic fret.

The composition of the fret approximates to Vogt's 'granite eutectic', and the granophyres are considered to be eutectics, the excess of quartz in the granite residues being due to the presence of water.

In the whole Icelandic area intermediate rocks are relatively unimportant in bulk, the extrusives are dominantly basic, and the intrusives dominantly acid: this may be related to the superior mobility of the basic magma.

The absence of a sedimentary 'floor' in Iceland is noted, and in harmony with J. Barrell's hypothesis that the collapse of the North Atlantic basaltic plateau resulted from the intrusion of a basic magma, it is suggested that the preservation of the Iceland-Faeroes remnant is due to the intrusion beneath it of an acid magma.

March 21st, 1928.—Horace W. Monckton, Treas.L.S.,  
Vice-President, in the Chair.

The following communication was read:—

‘The Geological Structure of the Central Mendips.’ By Francis Brian Awburn Welch, Ph.D., B.Sc., F.G.S.

The Central Mendips comprise a rectangular area roughly measuring 80 square miles, lying between the towns of Shepton Mallet and Cheddar on the east and west respectively. This area has been mapped on the 6-inch scale, applying the late Dr. A. Vaughan’s zones for the purpose of investigating the structure.

As a whole, the Mendips consist of a west-north-westerly to east-south-easterly ridge, the structure being that of four periclines arranged en échelon. The cores of these periclines are of Old Red Sandstone age, with the Carboniferous Limestone Series succeeding.

The Central Mendips include the North Hill, the Pen Hill, and part of the Beacon Hill periclines. Of these, North Hill and Pen Hill are more or less anticlinal in structure; but the Pen Hill pericline has been much disturbed by extensive earth-movements. The pericline itself is overfolded, and its eastern portion is thrust northwards against the eastern end of the North Hill pericline, north-and-south faults bounding the thrust-block. Overfolding combined with thrusting appears to explain the non-appearance of *Cleistopora* Beds along the north side of the pericline.

A large syncline, which extends from Cheddar to Wells, has been thrust from the south against the southern limb of the North Hill pericline, while at one point a ‘window’ occurs in this syncline, revealing beds of the main hill-mass beneath the thrust. Parallel to this thrust, at Ebbor, a second great thrust is developed, isolated remnants of which are seen in the small hills north of Wells.

The inliers of Carboniferous Limestone age in the plain on the south point to considerable disturbance; but, owing to the covering of Triassic strata, relationship to the main hill-mass is not clear.

Earth-movements seem to have been directed mainly from the south, at first producing the ridge with periclines en échelon, and separated one from the other by normal synclines. Pressure continued, and appears to have been greatest in the Pen Hill region, where overfolding was developed. Finally overthrusting resulted, and large blocks of beds bounded by extensive north-and-south faults, formed at the time of the thrusting, were driven northwards.

---

[The Editors do not hold themselves responsible for the  
views expressed by their correspondents.]

## INDEX to VOL. V.

- ACOUSTICS** of strings struck by a hard hammer, on the, 547.
- Aerofoil** sections, on vortices behind, 449.
- Air**, on the mobilities of the positive ions in, 881; on the emission of particles from hot platinum in, 1084.
- Alcohol**, on the magnetic rotary dispersion of methyl and propyl, 593; on the activity coefficients of hydrogen chloride in ethyl, 1133.
- Alpha particles**, on the ranges of the, of uranium I. and II., 1027.
- **rays**, on the mobilities of the positive ions formed by, in air, hydrogen, and helium, 881.
- Alternating current conductors**, on the distribution of temperature in, 904.
- Aluminium**, on the energy distribution among secondary electrons from, 367.
- Amalgams**, on the conductivities of some dilute, 271.
- Ammonium sulphate**, on the crystal structure of, 354.
- Andrews (J. P.)** on the theory of torsional oscillations in plastic solids, 865.
- Angular velocity of a rigid body**, on the, 289.
- Arcs**, on the lowest natural frequency of circular, 400.
- Argon**, on the diamagnetic susceptibility of, 380.
- Arkell (W. J.)** on the stratigraphical distribution of the cornbrash, 224.
- Atomic magnetism**, on an extension of Langevin's theory of, 536.
- Auto-electronic discharge**, on the, 574.
- Bangham (Dr. D. H.)** on chemical dynamics in a rigidly coherent phase, 737.
- Barkla (Prof. C. G.)** on modified scattered X-radiation and the J-phenomenon, 1164.
- Bartlett (Dr. R. S.)** on the resistance of sputtered films, 848.
- Bastings (L.)** on the coefficient of absorption in lead of the gamma-rays from thorium C" and radium C, 785.
- Baxter (J. P.)** on the combustion of carbonic oxide, 82.
- Beams**, on the torsion-flexure oscillations of a system of two connected, 97.
- Benham (W. E.)** on the rectification efficiency of thermionic valves, 323; on the internal action of thermionic systems, 641.
- Beutler (H.)** on double excitation of upper levels in the mercury atoms, 222.
- Bhatnagar (Prof. S. S.)** on an extension of Langevin's theory of atomic magnetism, 536; on the Tesla luminescence spectra of the halogens, 1226.
- Biotite**, on the formation of pleochroic halos in, 444.
- Birefringence**, on the, induced by flow in liquids, 769.
- Bisacre (F. F. P.)** on the relativistic rule for the equipartition of energy, 639.
- Biswas (S. C.)** on the ionization potential of niton, 1094.
- Bond (Dr. W. N.)** on bubbles, drops, and Stokes' law, 794.
- Books, new**:—The Nature of the World of Man, 223; Abstracts of Theses. Science Series, 448; Ince's Ordinary Differential Equations, 668; Doig's An Outline of Stellar Astronomy, 669; Compton's X-Rays and Electrons, 1011; Loeb's Kinetic Theory of Gases, 1011; Hedges and Myers's The Problem of Physico-Chemical Periodicity, 1258; Stewart's Recent Advances in Organic Chemistry, 1259; MacRobert's Spherical Harmonics, 1260; Ower's The Measurement of Air Flow, 1260; Turner's History of Science Teaching in England, 1261.

- Bosanquet (C. H.) on the capillary rise of liquids in wide tubes, 296.
- Bose (D. M.) on magnetism and the structure of some simple and complex molecules, 1048.
- Bromwich (Dr. T. J. I.A.) on the problem of the mass of a moving electron, 636.
- Brooks (W. H.) on sign conventions applied to flexing problems, 749.
- de Bruyne (N. A.) on the auto-electronic discharge, 574.
- Bubbles, drops, and Stokes' law, on, 795.
- Burton (Prof. E. F.) on a method of conductivity measurement by an oscillating valve circuit, 939.
- Cadmium, on the spectrum of, excited by active nitrogen, 375.
- oxide particles, on oscillatory ionization currents from clouds of, 561.
- Cæsium sulphate, on the crystal structure of, 354.
- Calcium, on the spectrum of, excited by active nitrogen, 378.
- Capillary action of mercury in the absence of gas-grown skins, on the, 958.
- rise of liquids in wide tubes, on the, 296.
- Carbonic oxide, on the combustion of, 82.
- Cargill (Miss H. K.) on the major intrusions of South-eastern Iceland, 1261.
- Carmichael (Miss N. M.) on the primary dark space of a Geissler discharge, 1039.
- Carpenter (L. G.) on the infra-red vibrations of crystals of the rock-salt type, 823.
- Catalytic action, on, 1191.
- Cathode rays in the electrodeless ring-discharge, on, 446.
- Cavitation in screw propellers, on, 1258.
- Chambers (Miss F. M.) on the resonances of a violin, 160.
- Chapman (Prof. S.) on approximate theories of diffusion phenomena, 630.
- Charges, on the existence of, smaller than the electron, 225; on the presence of, at an electrode surface, 1104.
- Charlesworth (Dr. J. K.) on the glacial retreat from Central and Southern Ireland, 1014.
- Chemical dynamics in a rigidly coherent phase, on, 737.
- Clarkson (Dr. W.) on the presence of charges at an electrode surface, 1104.
- Cod-liver oil, on the ultra-violet absorption spectrum of, 944.
- Cohesion and intermolecular repulsion, on, 1171.
- Colloidal test-bodies, on the resistances of, 225.
- Condenser, on the parallel-plate, 545.
- Conduction of heat, on problems in the, 701.
- Conductivity measurements, on a new method of, by an oscillating valve circuit, 939; on a valve oscillator for use in, 1130.
- Conductors, on the distribution of temperature in alternating current, 904.
- Copper, on the conductivities of dilute amalgams of, 279; on the energy distribution among secondary electrons from, 367.
- Corona discharge in helium and neon, on the, 721.
- Cosmology, on relativistic, 835.
- Crystal structure of the sulphates of potassium, ammonium, rubidium, and cæsium, on the, 354.
- Crystals, on a method for determining the orientation and structure of, with X-rays, 756; on the infra-red vibrations of, of the rock-salt type, 823.
- Davies (Dr. A. C.) on the loss of thermionic activity of thoriated tungsten filaments, 989.
- Dawson (W. E.) on a simple method for determining the orientation and structure of crystals with X-rays, 756.
- Dean (W. R.) on the stream-line motion of fluid in a curved pipe, 673.
- Deming (W. E.) on the diffusion of hydrogen through iron, 1081.
- Den Hartog (J. P.) on the lowest natural frequency of circular arcs, 400.

- Dhawan (C. L.) on an extension of Langevin's theory of atomic magnetism, 536.
- Diamagnetic susceptibilities of gases at low pressures, on the, 380.
- Differential equations, on Hamilton-Jacobi's, 79; on formulæ for the numerical integration of, 392; on the, of a reacting mixture, 620.
- Diffraction grating, on the positions of X-ray spectra as formed by a, 1067.
- Diffusion phenomena, on approximate theories of, 630.
- Disks, on the periods of, 39.
- Donaldson (R. H.) on electrodeless discharges, 178.
- Douglas (Dr. J. A.) on the stratigraphical distribution of the corn-brash, 224.
- Drane (Dr. H. D. H.) on making sensitive helical springs from quartz fibre, 559.
- Drops, bubbles, and Stokes' law, on, 795.
- Dulong and Petit's law, on an extension of, to gaseous compounds and mixtures, 832.
- Dunbar (Dr. R. T.) on apparent irregularities in experiments with heterogeneous X-ray beams, 962.
- Eagle (A.) on the Fourier constants of a periodic function and the coefficients determined by harmonic analysis, 113.
- Earth's crust, on the thermal instability of the, 662.
- thermal history, on the, 208, 215.
- Edgeworth (Lt.-Col. K. E.) on the frequency variations of the triode oscillator, 783.
- Ehrenhaft (Prof. F.) on the existence of charges smaller than the electron, 225.
- Electric properties of monatomic gases, on the, 695.
- resistance of sputtered films, on the, 848.
- spark, on the shadowgraph method as applied to the study of the, 1098.
- Electricity, on the emission of positive, from hot tungsten in radio valves, 67.
- Electrode surface, on the presence of charges at an, 1104.
- Electrodeless discharges, on, 178, 446.
- Electrolytes, on the equivalent conductivity of strong, 199; on the molecular structure of strong and weak, 1072.
- Electronic isomers, on an extension of Langevin's theory of atomic magnetism to molecules constituting, 536.
- orbits, on the saecular changes in, in a magnetic field, 801.
- theory of valency, on the, 1072.
- Electrons, on waves associated with moving, 191; on the existence of charges smaller than, 225; on the energy distribution among secondary, from nickel, aluminium, and copper, 367; on the mass of moving, 636.
- Emeléus (Dr. K. G.) on the primary dark space of a Geissler discharge, 1039.
- Energy, on the relativistic rule for the equipartition of, 629.
- distribution of secondary electrons, on the, 367.
- Entropy, on the absolute zero of the controllable, of a substance, 668.
- Ethyl alcohol, on the activity coefficients of hydrogen chloride in, 1133.
- Evans (Dr. E. J.) on the conductivity of some dilute amalgams, 271; on the magnetic rotary dispersion of methyl and propyl alcohols, 593.
- Explosions, on the radiant heat emitted during gaseous, 301.
- Fage (A.) on the structure of vortex sheets, 417.
- Fagerberg (S.) on interference between grating-ghosts, 204.
- Films, on the resistance of sputtered, 848.
- Flexing problems, on sign conventions applied to, 749.
- Flow of liquids through orifices, on the, 1.
- Flower (W. D.) on the emission of particles from hot platinum in air at atmospheric pressure, 1084.
- Fluid, on the stream-line motion of, in a curved pipe, 673.

- Forbidden multiplets, on the intensities of, 106.
- Fourier constants of a periodic function, on the relations between the, and the coefficients determined by harmonic analysis, 112.
- Gallium amalgams, on the conductivities of dilute, 278.
- Gamma-rays from thorium C" and radium C, on the absorption in lead of the, 785.
- Ganguli (R.) on the acoustics of strings struck by a hard hammer, 547.
- Gaseous compounds and mixtures, on an extension of Dulong and Petit's law to, 832.
- explosions, on the radiant heat emitted during, 301.
- Gases, on the diamagnetic susceptibilities of, at low pressures, 380; on the electrical properties of monatomic, 695; on the rate of sorption of, 737.
- Gates (S. B.) on the torsion-flexure oscillations of a system of two connected beams, 97.
- Gears, on multiple reactive, 946.
- Geissler discharge, on the primary dark space of a, 1039.
- Geological Society, proceedings of the, 224, 670, 1261.
- Geometry, on Riemannian null-, 241.
- Germanium amalgams, on the conductivities of dilute, 276.
- Geyser theory, on the, 441.
- Gill (E. W. B.) on space-charge effects, 859.
- Glass, on the sorption of gases at a surface of, 737.
- Grace (S. F.) on the oscillatory motion of a viscous liquid in a long straight tube, 938.
- Grating-ghosts, on interference between, 204.
- Green (Dr. G.) on some problems in the conduction of heat, 701.
- Greenly (Dr. E.) on the lower carboniferous rocks of Arvon, 1012; on the petrology of South-western Lley, 1016.
- Halogens, on the Tesla luminescence spectra of the, 1226.
- Halos, pleochroic, on the action of heat on, 182; on the formation of, in biotite, 444.
- Hamada (H.) on metallic spectra excited by active nitrogen, 372.
- Hamilton-Jacobi's differential equation in dynamics, on, 79.
- Hartley (Sir H.) on the activity coefficients of hydrogen chloride in ethyl alcohol, 1133.
- Hawkes (Dr. L.) on the major intrusions of South-eastern Iceland, 1261.
- Heat, on problems in the conduction of, 701.
- Helical springs, on making sensitive, from quartz fibre, 559.
- Helium, on the corona discharge in, 721; on the mobilities of the positive ions in, 881.
- lines, on the reversal of, 141.
- Herzberg (Dr. G.) on cathode rays in the electrodeless ring-discharge, 446.
- Hicks (Prof. W. M.) on the saecular changes in electronic orbits in a magnetic field, 801.
- Hirst (Miss D. M.) on the parallel-plate condenser in two dimensions, 545.
- Howland (R. C. J.) on the calculation of the periods of circular membranes and disks, 39.
- Hubbard (Prof. J. C.) on the velocity of sound in liquids, 1177.
- Hume-Rothery (Dr. W.) on the classification of metallic substances, 173.
- Huxley (L. G. H.) on the corona discharge in helium and neon, 721.
- Hydrogen, on the mobilities of the positive ions in, 881; on the diffusion of, through iron, 1081.
- chloride, on the activity coefficients of, in ethyl alcohol, 1133.
- Infra-red vibrations of crystals of the rock-salt type, on, 823.
- Integration, on formulæ for the numerical, of differential equations, 392.
- Interferometer, on the sonic, 1177.
- Intermolecular repulsion, on cohesion and, 1171.
- Internal energy, on changes in the interatomic, 1191.
- Iodine, on the Tesla luminescence spectrum of, 1226.
- Ionization by collision, on, 445.

- Ionization currents from clouds of cadmium-oxide particles, on, 561.  
 — potential of niton, on the, 1094.
- Ions, on the emission of, from hot platinum, 1084.
- Iron, on the diffusion of hydrogen through, 1081.
- Irons (E. J.) on the effect of constrictions in Kundt's apparatus and the end corrections of a partially-stopped tube, 580.
- J-phenomenon, on the, 962, 1145, 1164.
- Jeffreys (Dr. H.) on the earth's thermal history, 208.
- Johansen (F. C.) on the structure of vortex sheets, 417.
- Johns (A. L.) on the conductivity of some dilute amalgams, 271.
- Johnson (Dr. C. H.) on the radiant heat emitted during gaseous explosions, 301.
- Joly (Prof. J.) on the earth's thermal history, 215.
- Jones (D. O.) on the magnetic rotary dispersion of methyl and propyl alcohols, 593.
- Joseph (B.) on double excitation of upper levels in the mercury atoms, 222.
- Kar (Dr. K. C.) on the acoustics of strings struck by a hard hammer, 547.
- Kleeman (Dr. R. D.) on the constant of mass action, 263: on the differential equations of a reacting mixture, 620; on the absolute zero of entropy and internal energy, 668; on changes in inter-atomic internal energy, and catalytic action, 1191.
- Knudsen (Prof. V. O.) on the measurement of sound-absorption in a room, 1240.
- Krishnan (K. S.) on light-scattering in liquids, 498; on the birefringence induced by flow in liquids, 769.
- Kundt's apparatus, on the effect of constrictions in, 580.
- Kunz (Prof. J.) on Hamilton-Jacobi's differential equation in dynamics, 79.
- Laha (S. C.) on the acoustics of strings struck by a hard hammer, 547.
- Langevin's theory of atomic magnetism, on an extension of, 536.
- Laurence (G. C.) on the ranges of the alpha-particles of uranium I. and II., 1027.
- Lead, on the absorption in, of the gamma-rays from thorium C' and radium C, 785.
- Ledeboer (Miss J. A.) on the major intrusions of South-eastern Iceland, 1261.
- Lees (G. M.) on the geology of South-eastern Arabia, 1013.
- Lewis (T.) on the results of classical wave mechanics obtained by using the methods of relativity mechanics, 408.
- Light-scattering in liquids, on the theory of, 498.
- Liquids, on the flow of, through orifices, 1; on the capillary rise of, in wide tubes, 296; on the theory of light-scattering in, 498; on the properties of dry, 609; on the birefringence induced by flow in, 769; on the motion of viscous, in a long straight tube, 933; on the velocity of sound in, 1177.
- Loomis (A. L.) on the velocity of sound in liquids, 1177.
- Lowry (Prof. T. M.) on the electronic theory of valency, 1072.
- MacCallum (S. P.) on the electrical properties of monatomic gases, 695.
- McConnell (A. J.) on Riemannian null-geometry, 241.
- McCurdy (W. H.) on the fine structure of mercury lines, 386.
- Magnesium, on the spectrum of, excited by active nitrogen, 376.
- Magnetic rotation of methyl and propyl alcohols, on the, 593.
- Magnetism and the structure of some simple and complex molecules, on, 1048.
- Mali (Prof. S. B.) on the properties of dry liquids, 609.
- Manganese, on the structure of  $\alpha$ -, 1198; of  $\beta$ -, 1207.
- Manley (J. J.) on the capillary action of mercury in the absence of gas-grown skins, 958.
- Mass of a moving electron, on the, 686.



- Mass action, on the constant of, 263.  
 Mathieu's equation, on the stability of the solutions of, 18.  
 Mathur (K. N.) on the Tesla luminescence spectra of the halogens, 1226.  
 Mathur (S. B. L.) on the fine structure of the ultra-violet lines of thallium, 1111.  
 Matley (Dr. C. A.) on the Pre-Cambrian complex of South-western Lley, 1015.  
 Membranes, on the periods of circular, 39.  
 Mercury, on the spectrum of, excited by active nitrogen, 375; on the capillary action of, in the absence of gas-grown skins, 958.  
 — atoms, on double excitation of upper levels in the, by collisions of the second kind, 222.  
 — lines, on the fine structure of, 386.  
 Metallic points, on the influence of charged, on the spark discharge, 513.  
 — substances, on the classification of, 173.  
 Methyl alcoholic solutions, on the equivalent conductivity of, 199.  
 Micromagnet, on the, 225.  
 Milne (Prof. E. A.) on the angular velocity of a rigid body, 289.  
 Mitra (P. K.) on the emission of positive electricity from hot tungsten, 67.  
 Mixture, on the differential equations of a reacting, 620.  
 Mohammad (Prof. W.) on the fine structure of the ultra-violet lines of thallium, 1111.  
 Molecules, on magnetism and the structure of some simple and complex, 1048.  
 Morton (Prof. W. B.) on the parallel-plate condenser in two dimensions, 545.  
 Moss (Miss R. N.) on the loss of thermionic activity of thoriated tungsten filaments, 989.  
 Multiple reactive gears, on, 946.  
 Multiplets, on the intensities of forbidden, 166.  
 Murray-Rust (D. M.) on a valve oscillator for use in conductivity measurements, 1130.  
 Mushketov (Prof. D. I.) on the geology of the Alai and Trans-Alai chains, 670.  
 Neon, on the corona discharge in, 721.  
 Newman (Prof. F. H.) on the spectrum of ionized sodium, 150.  
 Newton (Miss D. A.) on bubbles, drops, and Stokes' law, 794.  
 Nickel, on the energy distribution among secondary electrons from, 367.  
 Niton, on the ionization potential of, 1094.  
 Nitrogen, on metallic spectra excited by active, 372; on the diamagnetic susceptibility of, 380.  
 Null-geometry, on Riemannian, 241.  
 Ogg (Dr. A.) on the crystal structure of the isomorphous sulphates of potassium, ammonium, rubidium, and caesium, 354.  
 Okubo (J.) on metallic spectra excited by active nitrogen, 372.  
 Optical method of measuring small vibrations, on an, 1125.  
 — theorem, on an, 1114.  
 Orifice flow, on operational factors in, 1.  
 Oscillating valve circuit, on a new method of conductivity measurement by an, 939.  
 Osman (C. W.) on the granites of the Scilly Isles, 671.  
 Parallel-plate condenser, on the, 545.  
 Paris (Dr. E. T.) on sound-absorption measured by the reverberation method, 489.  
 Periodic function, on the relation between the Fourier constants of  $a$ , and the coefficients determined by harmonic analysis, 113.  
 Petrowski (Prof. A.) on the problem of a hidden polarized sphere, 334, 914, 927.  
 Photographic exposure, on the theory of, 464.  
 Pipe, on the stream-line motion of fluid in a curved, 673.  
 Pitt (A.) on a method of conductivity measurement by means of an oscillating valve circuit, 939.  
 Plastic solids, on torsional oscillations in, 865.  
 Platinum, on the emission of particles from hot, 1084.

- Pleochroic halos, on the action of heat on, 132; on the formation of, in biotite, 444.
- van der Pol (Dr. B.) on the stability of the solutions of Mathieu's equation, 18.
- Polarized sphere, on the problem of a hidden, 334, 914, 927.
- Poole (Dr. H. H.) on the thermal instability of the earth's crust, 662.
- Poele (Dr. J. H. J.) on the action of heat on pleochroic halos, 132; on the formation of pleochroic halos in biotite, 444; on the thermal instability of the earth's crust, 662.
- Porter (Prof. A. W.) on the positions of X-ray spectra as formed by a diffraction grating, 1067.
- Positive ions, on the mobilities of the, in air, hydrogen, and helium, 881.
- Potassium, on the spectrum of, excited by active nitrogen, 377.
- chloride, bromide, and iodide, on the infra-red vibrations of, 825.
- sulphate, on the crystal structure of, 354.
- Press (Prof. A.) on an extension of Dulong and Petit's law, 832.
- Preston (G. D.) on the structure of  $\alpha$ -manganese, 1198; of  $\beta$ -manganese, 1207.
- Primary dark space of a Geissler discharge, on the, 1039.
- Quartz fibre, on making sensitive springs from, 559.
- Radiant heat emitted during gaseous explosions, on the, 301.
- Radio valves, on the emission of positive electricity from hot tungsten in, 67.
- Radium C, on the absorption in lead of the gamma-rays from, 785.
- Radon, on the purification of, 1017.
- Raman (Prof. C. V.) on light-scattering in liquids, 498; on the birefringence induced by flow in liquids, 769.
- Ratchet, on the impedance looking into the, 954.
- Rayleigh disk method for measuring sound-intensities, on a modification of the, 615.
- Rectification efficiency of thermionic valves, on the, 323.
- Relativistic cosmology, on, 835.
- rule for equipartition of energy, on the, 639.
- Relativity mechanics, on the methods of, applied to the results of classical wave mechanics, 408.
- Remes (E.) on approximate formulæ for the numerical integration of differential equations, 392.
- Resonances of a violin, on the, 160.
- Reverberation method, on the coefficient of sound-absorption measured by the, 489.
- Riemannian null-geometry, on, 241.
- Rigid body, on the angular velocity of a, 289.
- Rings, on the lowest natural frequency of, 400.
- Robb (Dr. A.) on a curious optical theorem, 1114.
- Robertson (Dr. H. P.) on relativistic cosmology, 835.
- Rogers (J. S.) on the mobilities of the positive ions formed by alpha-rays in air, hydrogen, and helium, 881.
- Rubidium sulphate, on the crystal structure of, 354.
- Saecular changes in electronic orbits in a magnetic field, on the, 801.
- Sandeman (Dr. E. K.) on multiple reactive gears, 946.
- Schofield (Dr. R. K.) on cohesion and intermolecular repulsion, 1171.
- Screw propellers, on cavitation in, 1258.
- Shadowgraph method as applied to the study of the electric spark, on the, 1098.
- Shafts, on whirling speeds and torsional oscillations in, 47.
- Sharma (R. K.) on the Tesla luminescence spectra of the halogens, 1226.
- Shrivastava (D. L.) on the Tesla luminescence spectra of the halogens, 1226.
- Sign conventions applied to flexing problems, on, 749.
- Silberstein (Dr. L.) on the theory of photographic exposure, 464.
- Silver amalgams, on the conductivities of dilute, 280.
- Sivian (L. J.) on a modification of the Rayleigh disk method for measuring sound-intensities, 615.

- Soderberg (C. R.) on the application of the theory of vibrations to systems with several degrees of freedom, 47.
- Sodium, on the spectrum of ionized, 150; on the spectrum of, excited by active nitrogen, 376.
- chloride, on the infra-red vibrations of, 825.
- Sound, on the velocity of, in liquids, 1177.
- absorption, on the coefficient of, measured by the reverberation method, 489; on the measurement of, in a room, 1240.
- apparatus, on the effect of constrictions in Kundt's, 580.
- intensities, on a modification of the Rayleigh disk method for measuring, 615.
- Space-charge effects, on, 859.
- Spark, on the shadowgraph method as applied to the study of the electric, 1098.
- discharge, on the influence of charged metallic points on the, 513.
- Spectra, on metallic, excited by active nitrogen, 372; on the positions of X-ray, as formed by a diffraction grating, 1067.
- Spectrograph, on interference between the ghosts in a, 204.
- Spectrum, on the, of helium, 141; on the, of ionized sodium, 150; on the mercury arc, 386; on the ultra-violet absorption, of cod-liver oil, 944.
- Sphere, on the problem of a hidden polarized, 334, 914, 927.
- Springs, on making sensitive, from quartz fibre, 559.
- Stream-line motion of fluid in a curved pipe, on the, 673.
- Strings, on the acoustics of, struck by a hard hammer, 547.
- Stokes' law, on bubbles, drops, and, 795.
- Stoodley (L. G.) on the infra-red vibrations of crystals of the rock-salt type, 823.
- Strutt (M. J. O.) on the stability of the solutions of Mathieu's equation, 18; on the distribution of temperature in alternating current conductors, 904.
- Suga (T.) on the reversal of helium lines, 141.
- Swift (H. W.) on operational factors in orifice flow, 1.
- Synge (Prof. J. L.) on Riemannian null-geometry, 241.
- Takamine (Dr. T.) on the reversal of helium lines, 141.
- Taylor (Dr. J.) on the intensities of forbidden multiplets, 166; on ionization by collision, 445.
- Tesla luminescence spectra of the halogens, on the, 1226.
- Thallium, on the spectrum of, excited by active nitrogen, 377; on the fine structure of the spectrum lines of, in the ultra-violet, 1111.
- Thermionic activity, on the loss of, of thoriated tungsten filaments, 989.
- systems, on the internal action of, at moderately high frequencies, 641.
- valves, on the rectification efficiency of, 323.
- Thomas (H. A.) on an optical method of measuring small vibrations, 1125.
- Thomson (J.) on the influence of charged metallic points on the spark discharge, 513.
- Thomson (Sir J. J.) on waves associated with moving electrons, 191.
- Thorium "C", on the absorption in lead of the gamma-rays from, 785.
- Thorkelsson (T.) on the geyser theory, 441.
- Torsion-flexure oscillations of a system of two connected beams, on the, 97.
- Torsional oscillations in plastic solids, on, 865.
- Townsend (Prof. J. S.) on electrodeless discharges, 178; on the electrical properties of monatomic gases, 695.
- Triode oscillator, on the frequency variations of the, 783.
- Tube, on the end corrections of a partially-stopped, 580; on the motion of a viscous liquid in a long straight, 933.
- Tungsten, on the emission of positive electricity from hot, in radio valves, 67.

- Tungsten filaments, on the loss of thermionic activity of, 989.
- Tyler (E.) on vortices behind aerofoil sections and rotating cylinders, 449.
- Ultra-violet spectrum of cod-liver oil, on the, 944: of thallium, on the, 1111.
- Uranium I. and II., on the ranges of the alpha-particles of, 1027.
- Vaidyanathan (V. I.) on the diamagnetic susceptibilities of gases at low pressures, 380.
- Valency, on the electronic theory of, 1072.
- Valve oscillator for use in conductivity measurements, on an, 1130.
- Vogel (I.) on the equivalent conductivity of strong electrolytes, 199.
- Vibrations, on the periods of, of circular membranes and disks, 39; on the application of the theory of, to systems with several degrees of freedom, 47; on the lowest natural frequency of, of circular arcs, 400; on an optical method of measuring small, 1125.
- Violin, on the resonances of a, 160.
- Viscous liquid, on the motion of a, in a tube, 933.
- Vortex sheets, on the structure of, 417.
- Vortices behind aerofoil sections and rotating cylinders, on, 449.
- Walmsley (H. P.) on oscillatory ionization currents from clouds of cadmium-oxide particles, 561.
- Warren (G. W.) on an optical method of measuring small vibrations, 1125.
- Wasser (Dr. E.) on the existence of charges smaller than the electron, 225.
- Watson (Dr. W. H.) on fluorescent secondary X-radiation and the J-phenomenon, 1145.
- Wave mechanics, on the results of classical, obtained by using the methods of relativity mechanics, 408.
- Waves, on, associated with moving electrons, 191.
- Welch (Dr. F. B.) on the structure of the Central Mendips, 1263.
- Wells (Prof. D. A.) on energy distribution among secondary electrons from nickel, aluminium, and copper, 367.
- Wertenstein (Prof. L.) on the purification of radon, 1017.
- Wolf-note phenomenon, on the, 160.
- Woodrow (Dr. J. W.) on the ultra-violet absorption spectrum of cod-liver oil, 944.
- Woolcock (J. W.) on a valve oscillator for use in conductivity measurements, 1130; on the activity coefficients of hydrogen chloride in ethyl alcohol, 1133.
- Woollard (L.) on cavitation in screw propellers, 1258.
- X-radiation, on fluorescent secondary, 1145: on modified scattered, 1164.
- X-ray beams, on apparent irregularities in experiments with heterogeneous, 962.
- spectra, on the positions of, as formed by a diffraction grating, 1067.
- X-rays, on a method for determining the orientation and structure of, crystals with, 756.
- Zinc, on the spectrum of, excited by active nitrogen, 376.
- Zinszer (Prof. H. A.) on the shadow-graph method as applied to a study of the electric spark, 1098.

END OF THE FIFTH VOLUME.

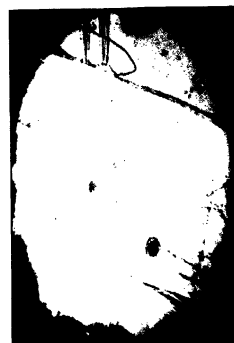




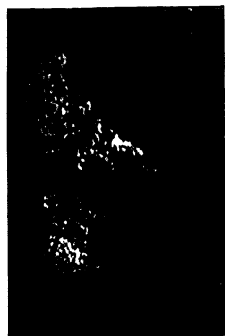
565°C.



435°C.



15°C.



615°C.



640°C.



620°C.



640°C.



585°C.



15°C.



480°C.



450°C.



15°C.



15°C.



505°C.



590°C.



515°C.

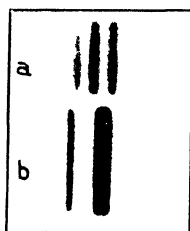


485°C.



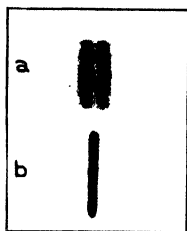


FIG. 1.



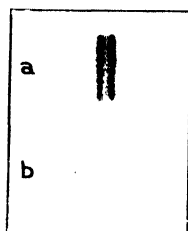
$\lambda 5876$

FIG. 2.



$\lambda 6678$

FIG. 3.



$\lambda 5016$

FIG. 7.

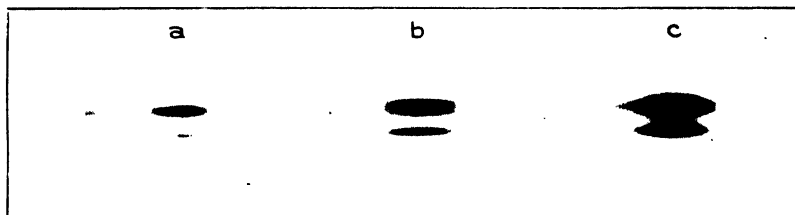


FIG. 8.

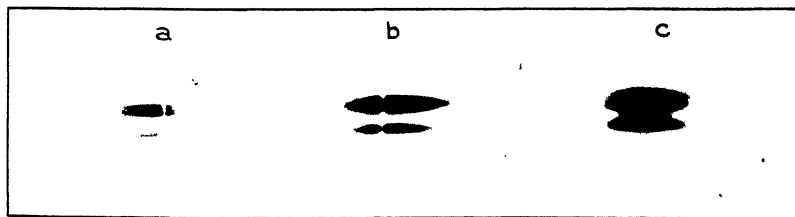
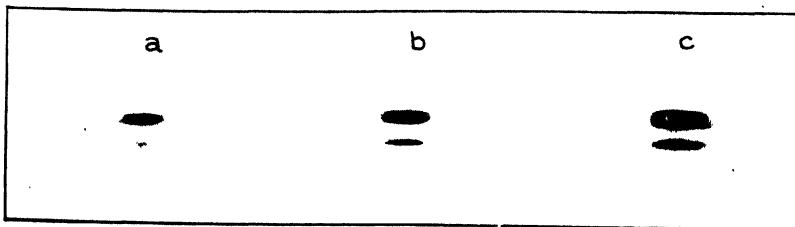
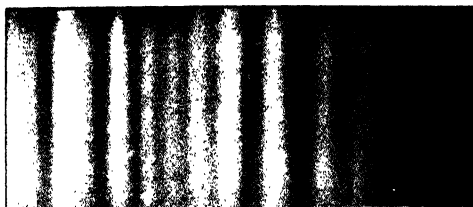


FIG. 9.



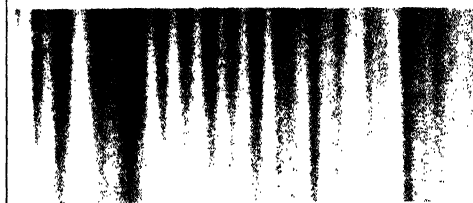


A



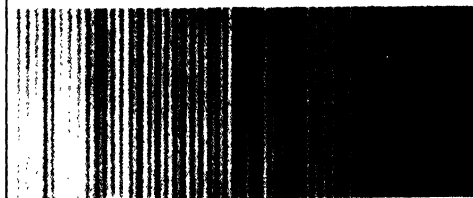
Principal line alone.

B



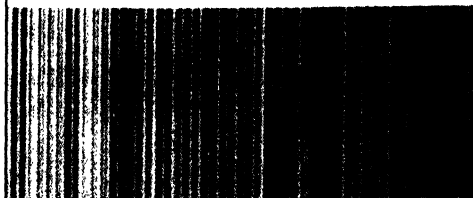
Ghost of first order  
alone.

C



Principal line and  
ghost of first order.

D



Principal line and  
ghosts of first and  
second order.

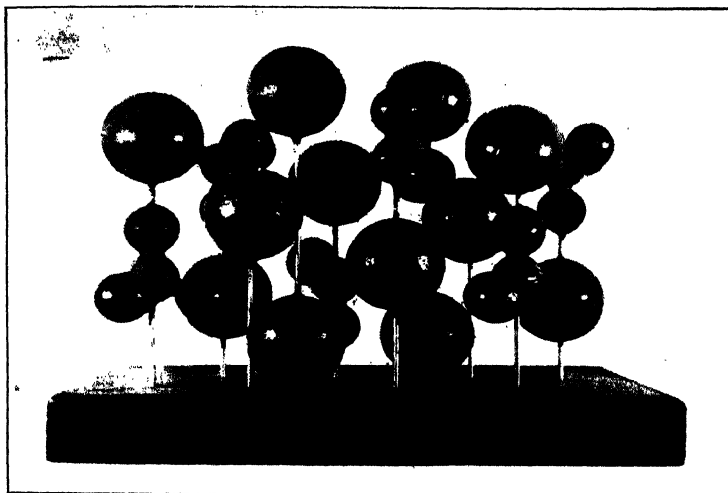
E



Principal line and  
four ghosts.

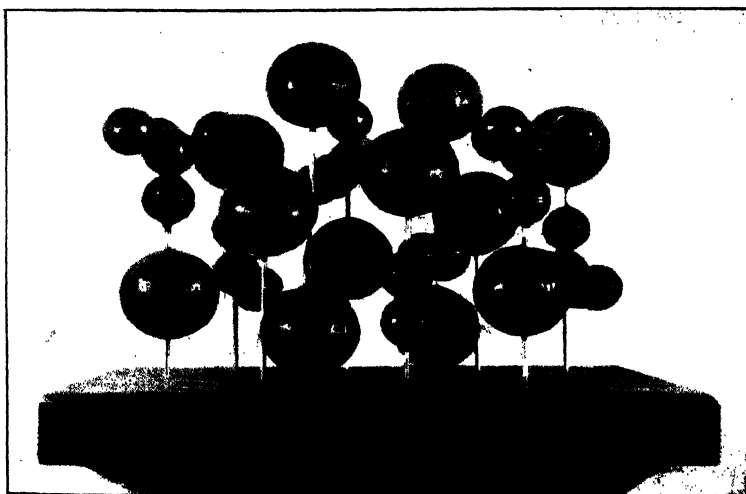


FIG. 5 A.



$K_2SO_4$  (100).

FIG. 5 B.



$K_2SO_4$  (100).



FIG. 6 A.

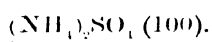
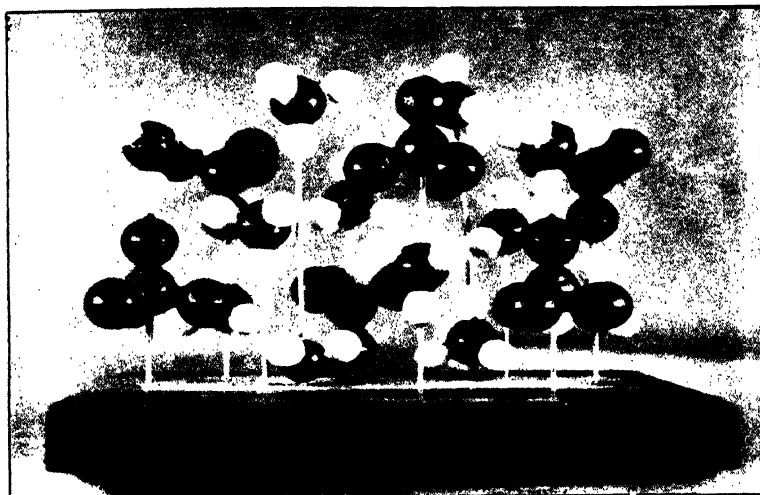
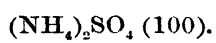
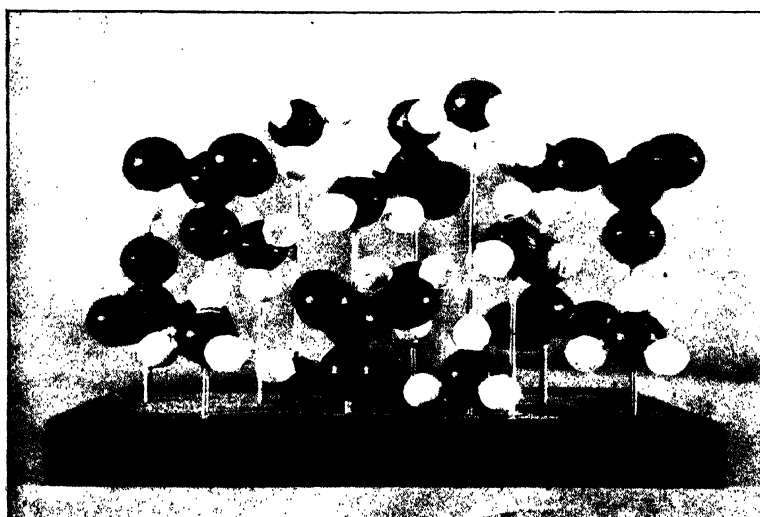
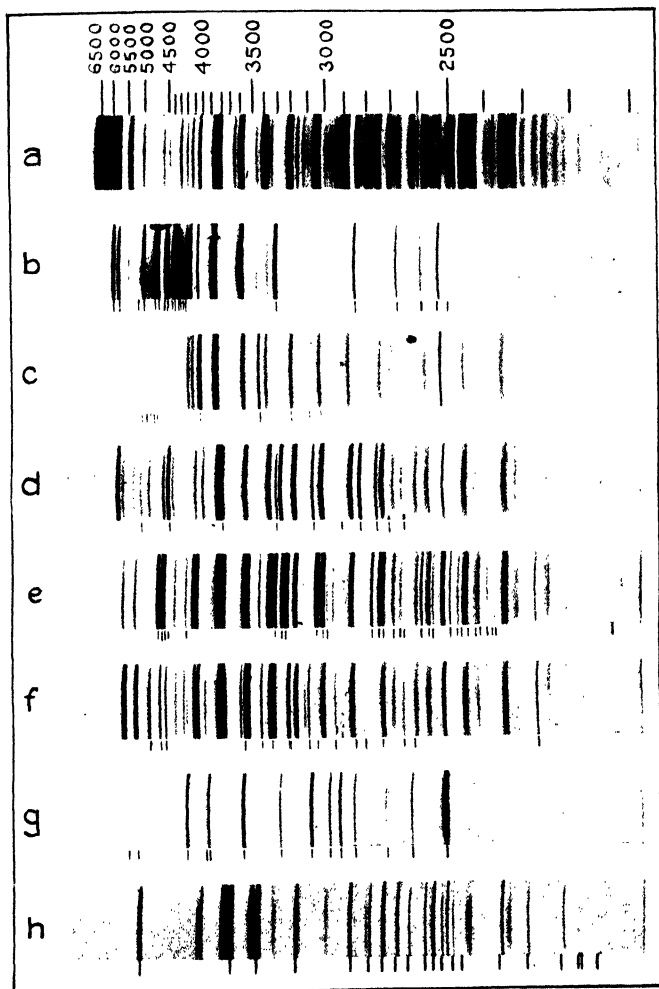


FIG. 6 B.









*a.* Active Nitrogen. *b.* Sodium. *c.* Potassium. *d.* Magnesium.  
*e.* Zinc. *f.* Cadmium. *g.* Mercury. *h.* Thallium.



FIG. 1.

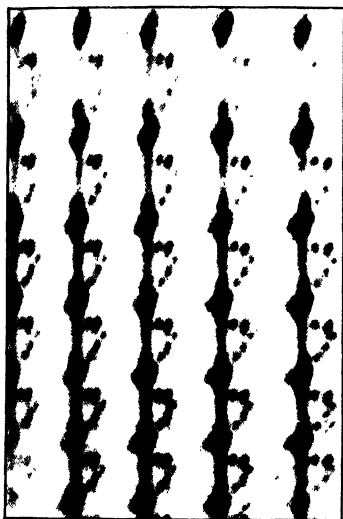


FIG. 2.

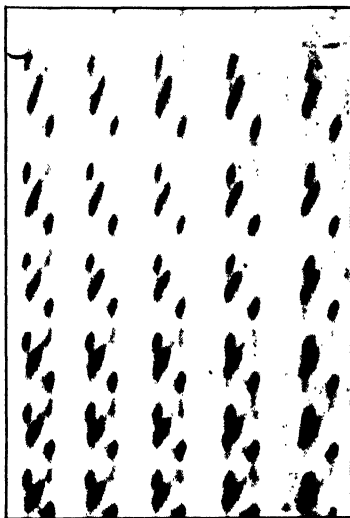


FIG. 3.

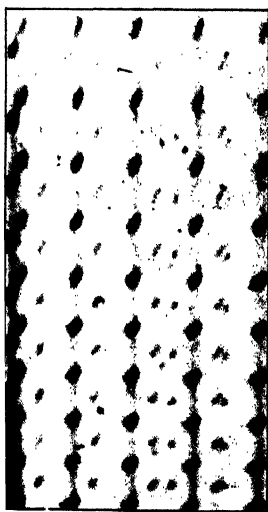


FIG. 4.

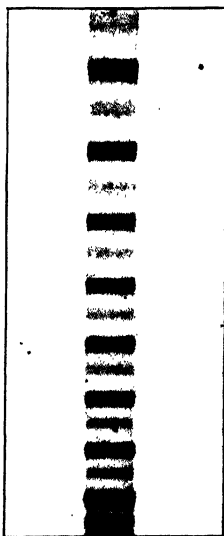


FIG. 5.

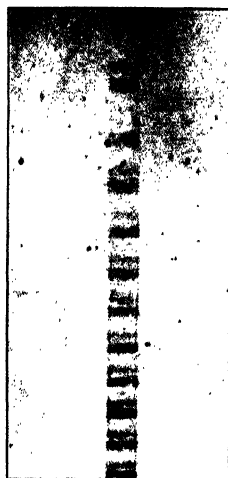




FIG. 3.

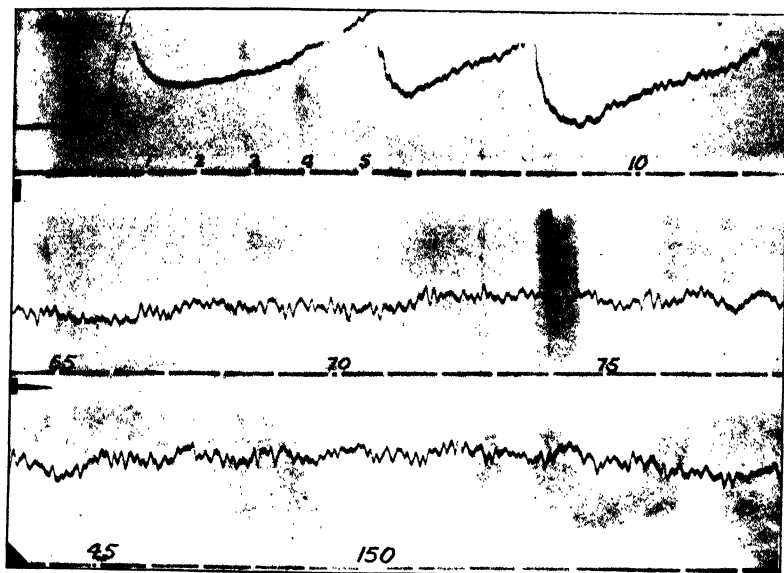


FIG. 4.

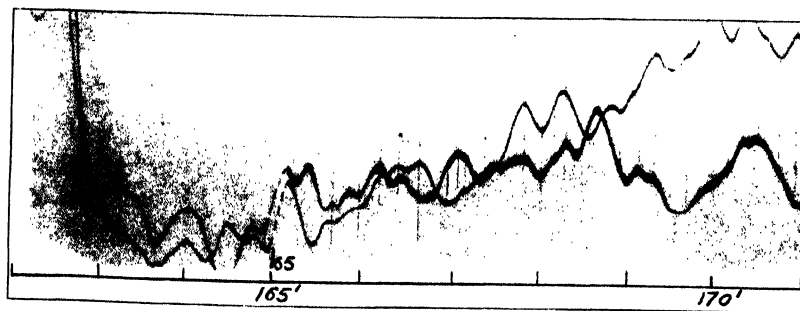




FIG. 2.

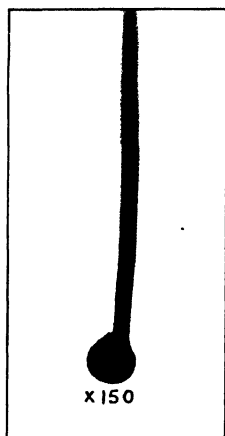


FIG. 3.

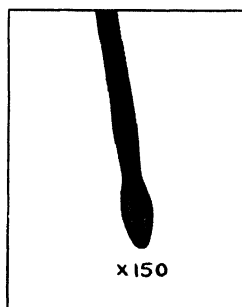






FIG. 5.

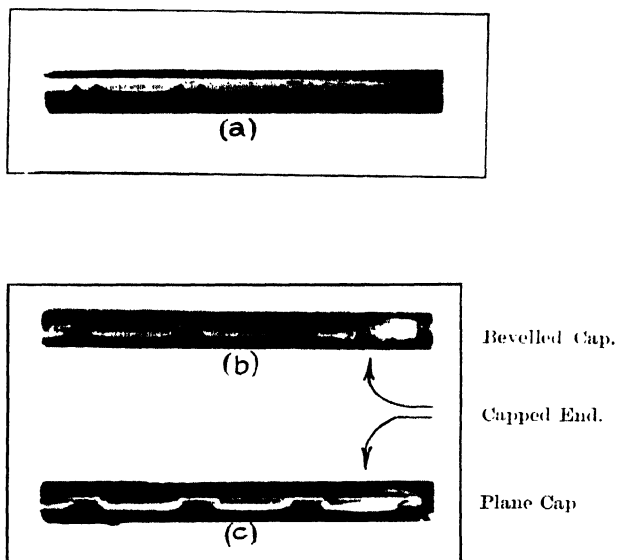




FIG. 1.

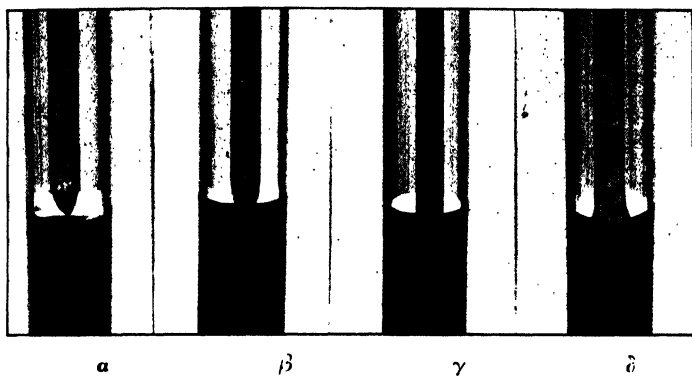


FIG. 2.

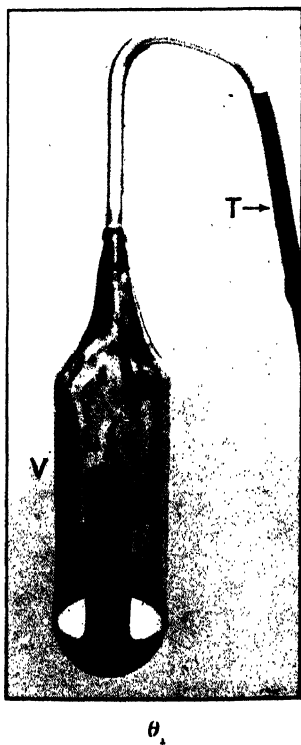
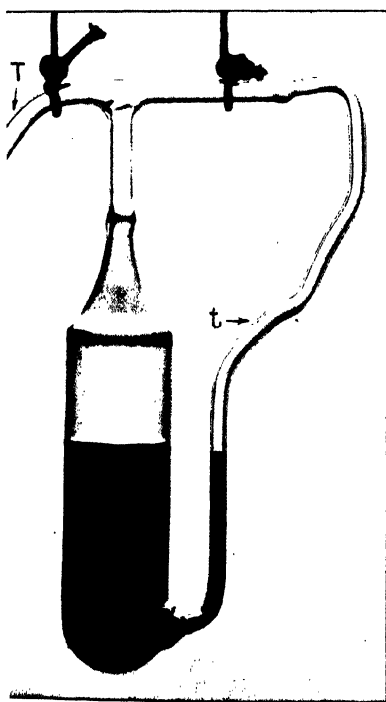
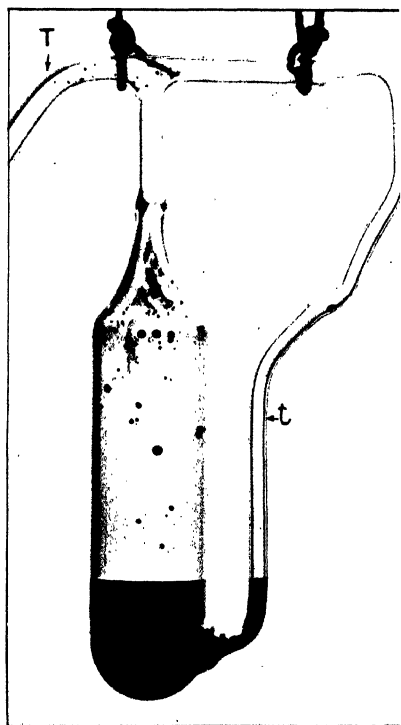




FIG. 3.



$\lambda_1$



$\lambda_2$



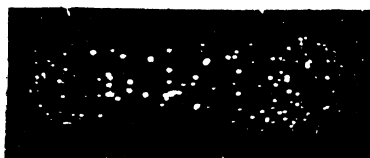
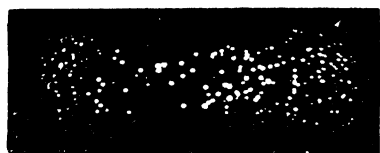
FIG. 4.







Droplets formed by Condensation on Nuclei emitted  
by a hot Platinum Wire.



$14.5 \times 10^3$  nuclei per c.c.



$7.95 \times 10^3$  nuclei per c.c.

Total magnification  $\times 13$ .



FIG. 3.

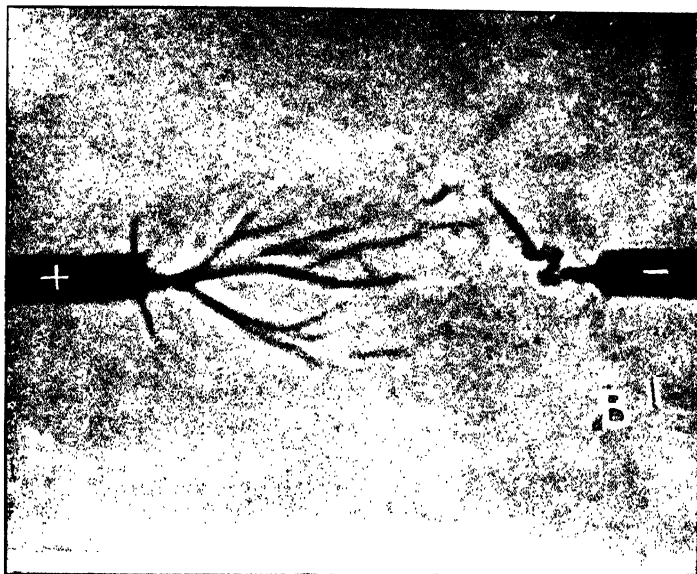


FIG. 4.

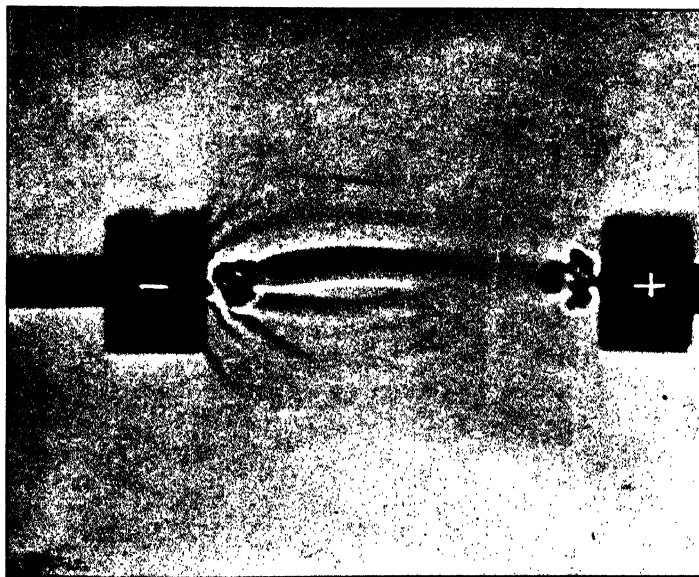




FIG. 5.

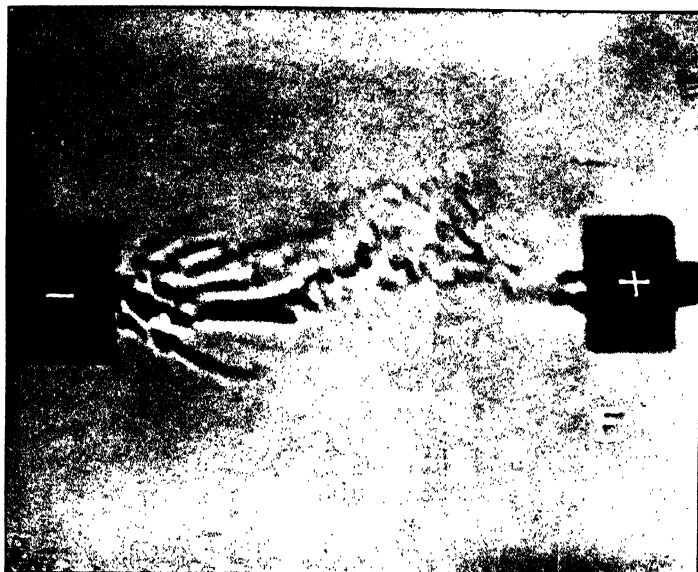


FIG. 6.

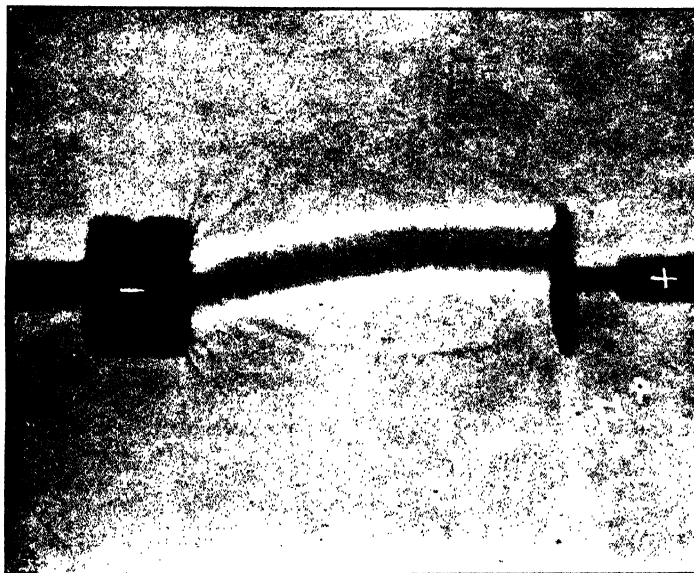
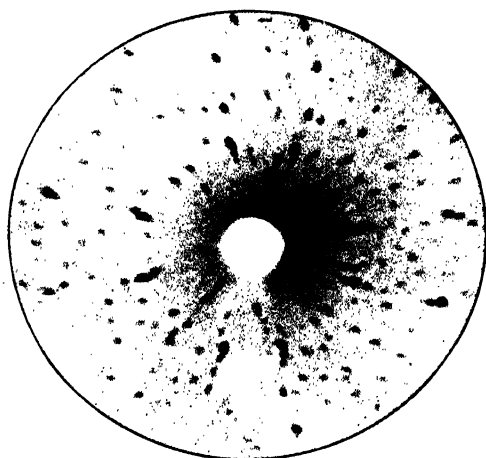




FIG. 1.

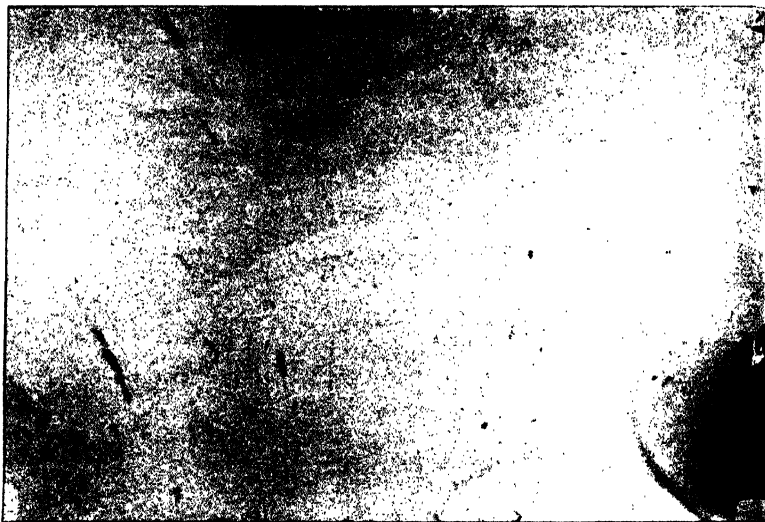


Laue Photograph of  $\alpha$ -Manganese.

PRESTON. 2

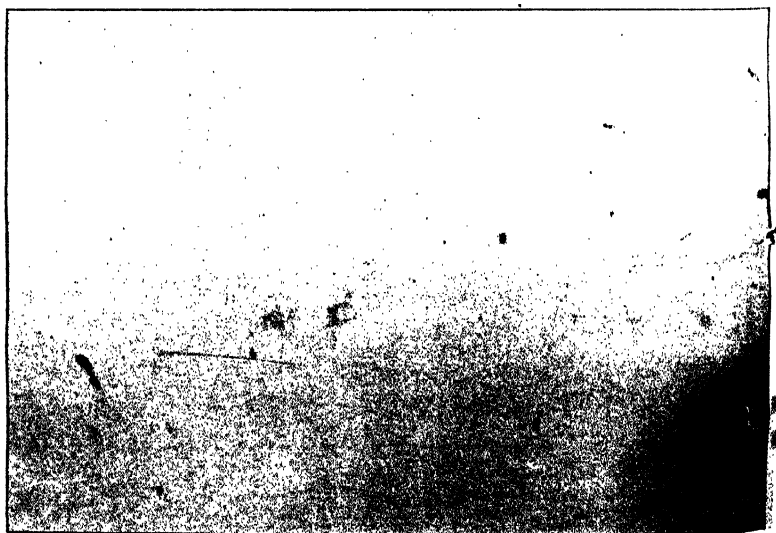
Mn1

4L



Mn1

8R



Oscillating Crvstal Pl



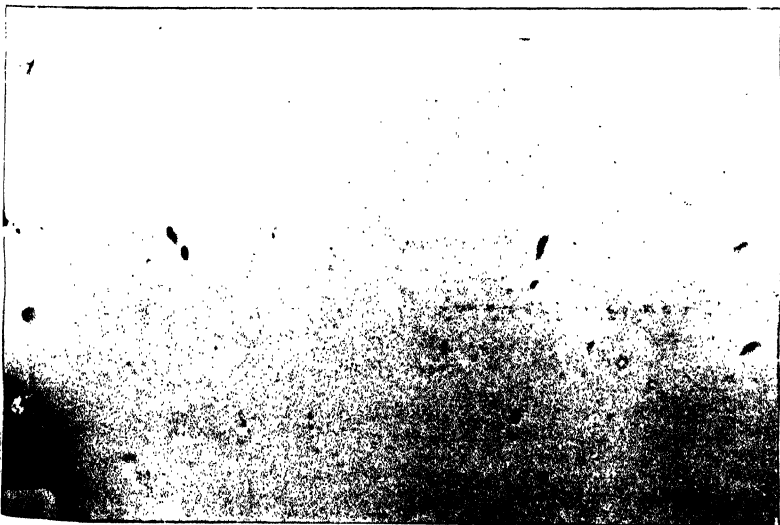
MnI

4R



MnI

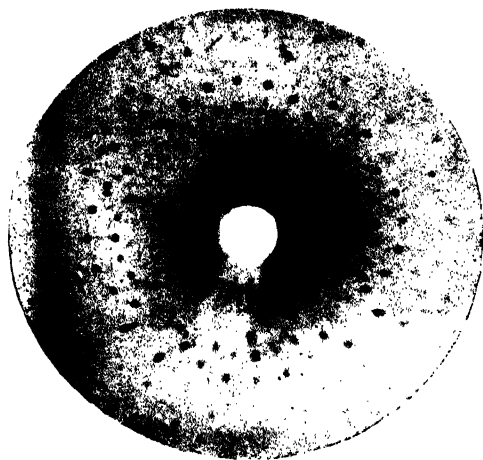
SL



aphs of  $\alpha$ -Manganese.

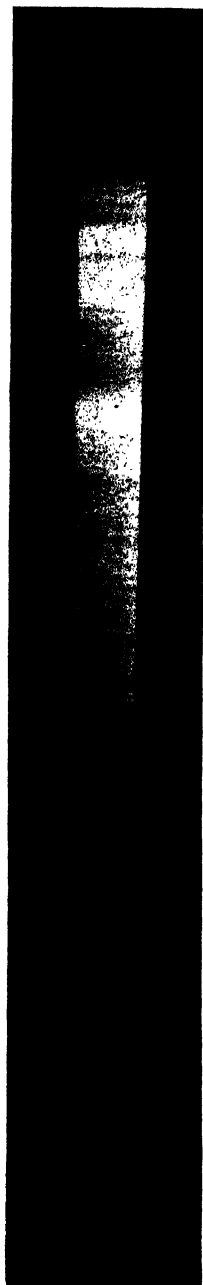


FIG. 1.



Laue Photograph of  $\beta$ -Manganese.





TESLA LUMINESCENCE SPECTRUM OF IODINE.



IMPERIAL AGRICULTURAL RESEARCH  
INSTITUTE LIBRARY  
NEW DELHI.

[illegible]